

Astrophysics and Space Science Library 386

Mauro D'Onofrio
Paola Marziani
Jack W. Sulentic
Editors

Fifty Years of Quasars

From Early Observations and
Ideas to Future Research

AS
SL

 Springer

Fifty Years of Quasars

For further volumes:
<http://www.springer.com/series/5664>

Astrophysics and Space Science Library

EDITORIAL BOARD

Chairman

W. B. BURTON, *National Radio Astronomy Observatory, Charlottesville, Virginia, U.S.A. (bburton@nrao.edu); University of Leiden, The Netherlands (burton@strw.leidenuniv.nl)*

F. BERTOLA, *University of Padua, Italy*

J. P. CASSINELLI, *University of Wisconsin, Madison, U.S.A.*

C. J. CESARSKY, *Commission for Atomic Energy, Saclay, France*

P. EHRENFREUND, *Leiden University, The Netherlands*

O. ENGVOLD, *University of Oslo, Norway*

A. HECK, *Strasbourg Astronomical Observatory, France*

E. P. J. VAN DEN HEUVEL, *University of Amsterdam, The Netherlands*

V. M. KASPI, *McGill University, Montreal, Canada*

J. M. E. KUIJPERS, *University of Nijmegen, The Netherlands*

H. VAN DER LAAN, *University of Utrecht, The Netherlands*

P. G. MURDIN, *Institute of Astronomy, Cambridge, UK*

F. PACINI, *Istituto Astronomia Arcetri, Firenze, Italy*

V. RADHAKRISHNAN, *Raman Research Institute, Bangalore, India*

B. V. SOMOV, *Astronomical Institute, Moscow State University, Russia*

R. A. SUNYAEV, *Space Research Institute, Moscow, Russia*

Mauro D'Onofrio • Paola Marziani
Jack W. Sulentic
Editors

Fifty Years of Quasars

From Early Observations and Ideas
to Future Research



Springer

Editors

Mauro D'Onofrio
Dipartimento di Astronomia
Università di Padova
Padova
Italy

Paola Marziani
Osservatorio Astronomico di Padova
Istituto Nazionale di Astrofisica (INAF)
Padova
Italy

Jack W. Sulentic
(IAA-CSIC)
Instituto de Astrofisica de Andalucia
Granada
Spain

ISSN 0067-0057

ISBN 978-3-642-27563-0

ISBN 978-3-642-27564-7 (eBook)

DOI 10.1007/978-3-642-27564-7

Springer Heidelberg New York Dordrecht London

Library of Congress Control Number: 2012941739

© Springer-Verlag Berlin Heidelberg 2012

This work is subject to copyright. All rights are reserved by the Publisher, whether the whole or part of the material is concerned, specifically the rights of translation, reprinting, reuse of illustrations, recitation, broadcasting, reproduction on microfilms or in any other physical way, and transmission or information storage and retrieval, electronic adaptation, computer software, or by similar or dissimilar methodology now known or hereafter developed. Exempted from this legal reservation are brief excerpts in connection with reviews or scholarly analysis or material supplied specifically for the purpose of being entered and executed on a computer system, for exclusive use by the purchaser of the work. Duplication of this publication or parts thereof is permitted only under the provisions of the Copyright Law of the Publisher's location, in its current version, and permission for use must always be obtained from Springer. Permissions for use may be obtained through RightsLink at the Copyright Clearance Center. Violations are liable to prosecution under the respective Copyright Law.

The use of general descriptive names, registered names, trademarks, service marks, etc. in this publication does not imply, even in the absence of a specific statement, that such names are exempt from the relevant protective laws and regulations and therefore free for general use.

While the advice and information in this book are believed to be true and accurate at the date of publication, neither the authors nor the editors nor the publisher can accept any legal responsibility for any errors or omissions that may be made. The publisher makes no warranty, express or implied, with respect to the material contained herein.

Cover illustration: Giacomo Balla, *Scienza contro oscurantismo* (Science against obscurantism). Glazed gouache and oil on wood, 1920. Roma, Galleria Nazionale d'Arte Moderna. Reproduced by kind permission of the Ministero per i Beni e le Attività Culturali.

Printed on acid-free paper

Springer is part of Springer Science+Business Media (www.springer.com)

*To all people who dedicated most of their
lives to understanding quasars*

Foreword

It's good, on occasion, to reflect on the fact that science is fundamentally a very human endeavor. The essential principles of the scientific method, drummed into us at an early age, are that science is dispassionate, objective, and self-correcting: none of which are virtues that humans necessarily come by naturally. But this view of how science works reflects an ideal to which we aspire and not necessarily the world in which we live. Scientists are in fact passionate about their work, sometimes with the result that it's difficult to achieve true objectivity. On the other hand, science is indeed self-correcting—but usually at a much slower pace than we'd like, and with consequential forays down wrong paths while the facts get sorted out. Unfortunately, the false steps are just an inevitable part of a long process.

When we attempt to examine the present state of a vibrant scientific field, we see a mixture of things that are going to be very important in the final assembly of the puzzle, things that will turn out to be of lesser importance, and some things that will turn out to be misleading, and perhaps even wrong. At any given time, however, distinguishing among these possible outcomes is not easy. But it's entertaining to try.

The editors of this volume recognized that the fiftieth anniversary of the discovery of quasars presented an interesting opportunity to open a discussion on both the current state of an exciting field of research and how it got to where it is now. The latter is actually manageable as quasars have almost no “pre-history,” notwithstanding the birth of radio astronomy, which led to identification of the first quasars, and limited work on the bright nuclei of local spiral galaxies beginning with Seyfert twenty years earlier. Fifty years is long enough for the field to have reached some level of maturity, but short enough that many of the pioneers of quasar studies are still with us, and some of them have contributed their insights and recollections to this book.

In some sense, it's surprising how slow progress has been, given that the correct basic physics was recognized by Zel'dovich and Novikov, Salpeter, and Lynden-Bell within a few years of Schmidt's interpretation of the redshifted spectrum of 3C 273 in 1963. But over at least the first two decades of quasar research, the question that dominated discussion was whether quasars were indeed at the cosmological distances implied by their redshifts! This problem was resolved definitively (or at

least to my personal satisfaction), first, with the identification of normal galaxies in close proximity to and at the same redshift as relatively low-redshift quasars by Stockton in 1978, and then with the detection of host galaxy starlight in the spectrum of 3C 48 by Boroson and Oke in 1982 in one of the first uses of an astronomical CCD detector. Another similar diversion was the nearly universal assumption that the UV-optical-IR continuum radiation of quasars was synchrotron radiation: that the continuum shortward of one micron is thermal emission from an accretion disk was suggested by Shields in 1978 and that the near-IR continuum is reradiation by dust was posited by Rieke the same year. But these points were not broadly appreciated until the optical work of Malkan and Sargent in 1982 and the near-IR study of Sanders, Phinney, Neugebauer, Soifer, and Mathews in 1989. It was only around 15 years ago that the supermassive black hole paradigm achieved any kind of consensus, even though Rees had convincingly argued as early as 1984 that supermassive black holes in galactic nuclei are inevitable. As recently as 1992, Blandford noted that “it remains true that, even by the lax standards of astronomy, there is no *proof* that black holes exist in AGN, or indeed anywhere else.¹” But within only a few more years, solid detection of supermassive black holes at the center of the Milky Way, M87, and NGC 4258 shifted the paradigm once again, and the question was no longer “are quasars powered by accretion onto supermassive black holes?” but instead became “why are some supermassive black holes active (i.e., accreting matter) and others are not?”

So after 50 years of efforts to understand quasars, where are we currently, how did we get here, and where do we think we are headed next? That, in essence, was what the editors of this volume asked 50 quasar researchers (one for each year, it seems). Except for a short contextual introduction and a summary chapter, the book is formatted as a series of epistolary interviews: questions from the editors are phrased as letters to each of the 50 quasar researchers, with each researcher being asked to address a restricted set of questions covering topics selected by the editors.

As an active researcher in the field for 35 years, I find this to be fascinating reading: this is not a formal history, but rather it has elements of collected individual memoirs. It’s not a consensus view of the state of the field either, but rather the specific points of view of individual researchers looking at the overall field of quasar research, each from his or her own vantage point, in answer to particular questions addressed to them. For me, the most interesting aspect was hearing the opinions of fellow quasarphiles on what things they believe are important now and what are the most promising directions for future research. One of the current themes in quasar research is that quasars are not only tracers of the evolution of galaxies, but agents of galactic evolution through energetic feedback processes: will this currently popular view hold up to continued scrutiny or it is another massive diversion? Will we ever understand the dichotomy between radio-loud and radio-quiet quasars? And what

¹Blandford, R.D., 1992 in *Relationships Between Active Galactic Nuclei and Starburst Galaxies*, ed. A.V. Filippenko, ASP Conf. Series Vol. 31, p. 455.

surprises will come with future facilities like ALMA and, we hope, with *JWST* and the next generation of ground-based telescopes?

This book won't answer these questions. But it will give you some things to think about.

Columbus, OH, USA

Bradley M. Peterson

Preface

On a cold day in January 2010, the three Editors of this book were sitting together during a lunch break in front of a warm cup of coffee discussing the completion of the just-published *Questions of Modern Cosmology—Galileo’s Legacy*. That book was intended to celebrate the International Year of Astronomy and the 400 years that had passed since Galileo’s discoveries announced in *Sidereus Nuncius*.

Several people had expressed appreciation of the editorial approach to the book edited by Mauro D’ Onofrio and Carlo Burigana. Interviews with experts who had discussed the major topics in Cosmology and Fundamental Physics. Questions and answers offered a great freedom of possibilities and made the book accessible to a broad audience interested in scientific issues. While sipping her cup of coffee Paola distractedly said: “. . . it would be nice to have a similar book for quasars . . .” Probably the suggestion would have passed without consequences had not Mauro promptly shouted: “Why not? We are approaching the anniversary of the discovery of quasars!” and Jack promptly added “Of course! What a great idea!” The present book was born in this way.

Fifty years have indeed passed since quasar discovery. Fifty years are an ample time lapse when even human beings are led to take a breath and make a balance of their previous existence. Where did fifty years of quasar studies lead to? We would like to gain a broad view of where we stand now elucidating what we know and especially what we do not know yet. The last half-century has seen formidable achievements during which quasars never ceased to be one of the hot topics in astrophysics. Many conferences have been hosted and many textbooks and popular books about quasars have been written since 1962. Textbooks however reflect the view of a single, or a few, authoritative researchers. Since so many important questions about quasars remain open and debated we wanted to give voice to a variety of opinions that reflect different research paths as well as different views about the nature of quasars. At the same time we wanted to create a book that is readable and accessible to students and other people with an interest in Astronomy. The book on Cosmology demonstrated that this approach was feasible. So we contacted many of the most active and/or influential researchers working on quasars and most of them immediately expressed their interest for this project. Some of

them were very enthusiastic and provided us with advice that helped improve the book in the course of its development—our special thanks go to Martin Gaskell, Deborah Dultzin, Martin Elvis, Hagai Netzer, and Julian Krolik. We warmly thank all contributors and Ramon Khanna, the Editor of Springer Verlag, for having believed in this project since its inception.

Venezia

Mauro D’Onofrio
Jack W. Sulentic
Paola Marziani

Acknowledgements by Contributors and Editors

H. Arp: I would like to acknowledge the time and effort of Dr. Christopher Fulton in the writing and organization of this contribution. For most of the past decade, Chris has been a close collaborator and co-author.

M. Elvis: I thank my old friends Mike Watson, Andy Lawrence, Martin Ward and Ian McHardy, for careful readings that significantly improved this paper.

D. Hutsemékers: I thank Dominique Sluse for his careful reading of Sect. 5.4.

S. Lipari: I want to thank the collaboration of the members of our Team of Study of Evolution of Galaxies and QSOs (since the results presented in this review were obtained mainly by our Team): R. Terlevich, Y. Taniguchi, S. Sanchez, W. Zheng, M. Bergmann, M. Pastoriza, H. Dottori, B. Punsly, L. Colina, D. Golombek, M. Giavalisco, Z. Zvetanov, J. Acosta Pulido, K. Janke, Ch. Bonatto, C. Winge, T. Storchi-Bergmann D. Merlo, A. Ahumada, J. Ahumada, R. Sistero, G. Carranza, M. Paz, R. Diaz.

I. Marquez-Perez: I would like to thank my collaborators, especially J. Masegosa and O. González-Martín. I am also grateful to JM for her encouragement, careful reading and feedback of the manuscript, that help to improve it. Financial support is acknowledged from the Spanish grant AYA2010-15169 and Junta de Andalucía TIC114 and the Excellence Project P08-TIC-03531.

J.V. Narlikar: The author thanks IUCAA for secretarial assistance.

G. Richards: I'd like to thank Mike Eracleous, Sarah Gallagher, Pat Hall, Paul Hewett, Karen Leighly, Daniel Proga, and Yue Shen for their contributions to the work discussed herein.

I. Shlosman: I thank my collaborators and colleagues who made research such an enjoyable endeavour and at the same time so challenging. I am grateful to Copernicus Astronomical Center in Warsaw for hospitality during the time this text has been largely written up, to Marek Sikora for numerous discussions about accretion

processes and for support, Moshe Elitzur for commenting on the first draft, and to Frederic Chopin for making this visit possible.

The Editors want to thank all contributors for having accepted the challenge posed by this book. The Editors also want to thank Ramon Khanna and the staff of Springer Verlag for their support in all phases of the work. PM would like to thank her friend Giovanni Candeo for sensible support in the last few years.

Contents

Acronyms	xxvii
Contributions by all authors	
Web pages	xxxii
Contributions by all authors	
1 An Introduction to 50 Years of Research on Quasars	1
<i>Paola Marziani, Jack W. Sulentic, and Mauro D’Onofrio</i>	
1.1 The Roaring Sixties	1
1.2 An Operational Definition of Quasars?	4
1.3 Outline of the Book	6
References	9
2 Quasars in the Life of Astronomers	11
Contributions by <i>Mauro D’Onofrio, Paola Marziani, Jack W. Sulentic, Suzy Collin, Giancarlo Setti, Martin Gaskell, Joe Wampler, Martin Elvis, Iraidia Pronik, Vladimir Pronik, Sergey Sergeev, Aleksander Volvach, Julian Krolik, Hagai Netzer, Alfonso Cavaliere, Paolo Padovani, Halton Arp, and Jayant Narlikar</i>	
2.1 Quasars seen from Europe	13
2.2 Quasars in the Early Radio Sky	18
2.3 Recollections of a US Astronomer	24
2.4 The Development of a New Instrument	35
2.5 Seyfert Galaxies as X-Ray Sources	41
2.6 AGN Astrophysics in the USSR at the Time of Quasar Discovery and Afterward	45
2.7 Early Modelling Attempts	51
2.8 The Interpretation of Quasar Spectra	53
2.9 Quasars in a Cosmological Context	55
2.10 The Affirmation of a Unified View	59

2.11	Challenging the Standard Paradigm	61
2.12	Alternative Views and Ideas	73
	References	81
3	Quasars: The Observational Perspectives	91
	Contributions by <i>Mauro D’Onofrio, Paola Marziani, Jack W. Sulentic, Greg Shields, Martin Gaskell, Todd Boroson, Ari Laor, Michael Hawkins, Vladimir Pronik, Sergey Sergeev, Deborah Dultzin, Dirk Grupe, Gordon Richards, Raffaella Morganti, Aleksander Volvach, Sebastian Zamfir, Heino Falcke, Elmar K�rding, Martin Elvis, Tracey Jane Turner, Ajit Kembhavi, Luigi Foschini, Yuri Neshpor, and Alberto Franceschini</i>	
3.1	Optical Phenomenology of Quasars	94
3.2	Techniques of Discovery	101
3.3	Organizing Quasar Broad-Line Diversity	106
	3.3.1 More on the Importance of Eigenvector 1	112
3.4	Variability	114
3.5	A Photometric Monitoring Campaign	118
3.6	Micro-Variability and Its Anecdotes	120
3.7	Quasar Spectral Energy Distributions	124
3.8	Inferences from the Quasar UV Spectrum	125
	3.8.1 The Baldwin Effect	125
	3.8.2 Quasars’ Internal Emission-Line Shifts	128
3.9	Radio Properties of Quasars	131
	3.9.1 Radio Variability and Its Implications	138
	3.9.2 Radio Jets	139
	3.9.3 Radio Quiet and Radio-Loud	142
	3.9.4 Microquasars: Inclusion of Stellar Mass Black Holes	150
	3.9.5 Radio Loudness and a Unified View of Black Holes	151
3.10	X-Rays Properties of Quasars	154
	3.10.1 Discovering Quasars in the X-ray Domain	159
	3.10.2 X-Ray Emission and Absorption Lines	164
	3.10.3 Blurred Reflection and Absorption	169
	3.10.4 More on X-ray Absorption: The “Warm Absorber”	173
	3.10.5 More on the Fe K α Line	178
3.11	The γ Ray Domain	184
3.12	Observations at Infrared Wavelengths	190
	3.12.1 Evidence of a Thick Torus	190
	References	192

4 Quasars Classes and Their Relationships	217
Contributions by <i>Mauro D’Onofrio, Paola Marziani, Jack W. Sulentic, Deborah Dultzin, Yuri Efimov, Martin Gaskell, Marianne Vestergaard, Damien Hutsemékers, Alberto Franceschini, Ari Laor, Dirk Grupe, Sebastian Lipari, Begoña García Lorenzo, Evencio Mediavilla, Todd Boroson, Mike Eracleous, Isabel Marquez-Perez, Elmar Körding, and Heino Falcke</i>	
4.1 BL Lacs and Blazars	219
4.2 Unobscured and Obscured Quasars: Where are They?	222
4.3 Phenomenology of Absorption Lines in Quasars	223
4.3.1 The Broad Absorption Lines QSOs	224
4.4 Type-2 AGNs	230
4.4.1 Dust Obscuration	235
4.5 Narrow-Line Seyfert-1 Nuclei	240
4.6 The ULIRG–QSO Connection	248
4.7 Double-Peaked Emitters and the Greater AGN Population	255
4.8 LINERs	258
4.9 Quasars and Microquasars	266
4.9.1 Black Hole X-Ray Binaries	266
4.9.2 The Fundamental Plane of Black Hole Activity	267
References	272
5 From Observations to Physical Parameters	287
Contributions by <i>Mauro D’Onofrio, Paola Marziani, Jack W. Sulentic, Greg Shields, Shai Kaspi, Paolo Padovani, Damien Hutsemékers, Ross McLure, Ari Laor, Marianne Vestergaard, Bozena Czerny, Krzysztof Hryniewicz, and Deborah Dultzin</i>	
5.1 Chemical Abundances	288
5.2 Reverberation Mapping	290
5.2.1 Size–Luminosity Relation	291
5.2.2 Stratification and Keplerian Kinematics of the BLR	292
5.3 An Alternative Method to Estimate the BLR Radius	293
5.4 Microlensing	295
5.5 Black Hole Mass Estimation	297
5.5.1 Difficulties and Uncertainties	298
5.5.2 Supermassive Black-Holes and the Host Galaxy Bulge	307
5.6 The Eddington Ratio	319
5.7 Narrow-Line Seyfert-1 as Extreme Radiators	323
5.8 Orientation Effects on Emission Lines	325
References	328

6 Models of Quasars 337

Contributions by *Mauro D’Onofrio, Paola Marziani, Jack W. Sulentic, Julian Krolik, Martin Gaskell, Suzi Collin, Hagai Netzer, Bozena Czerny, Krzysztof Hryniewicz, Luigi Foschini, Michael Eracleous, Daniel Proga, Paolo Padovani, Serguei Komissarov, Isaac Shlosman, and Martin Elvis*

6.1 The Formation of Optical–UV Emission Lines and the AGN Structure 339

6.2 BLR and NLR Properties 349

6.3 Radiation Pressure and Irregular Line Profiles 354

6.4 Line and Continuum Emission from an Accretion Disk 360

6.4.1 The Accretion Disk–BLR Relationship 362

6.4.2 Double-Peaked Profiles and Accretion Disk Line Emission 364

6.5 Origin of the Continuum 368

6.5.1 Accretion Disk Structure and Continuum Emission 370

6.6 QSO Outflows 373

6.6.1 Three Main Driving Mechanisms 374

6.6.2 The Quasar Outflows 375

6.6.3 Line-Driven and Magnetic Disk Winds 377

6.7 Interpretation of Radio Emission 381

6.7.1 Superluminal Motions 381

6.7.2 Blandford–Znajek Mechanism 390

6.7.3 Where is the Jet Launched? 395

6.8 Mechanisms of Black Hole Accretion 397

6.8.1 Accretion Drivers: Small Scales 398

6.8.2 Accretion Drivers: Large Scales 400

6.9 Modes of Disk Accretion 403

6.10 Relativistic Accretion Disk Theory 406

6.10.1 The Nature of Internal Stress in Disks 406

6.10.2 Stress at the ISCO? 408

6.11 The Obscuring Torus 410

6.12 A Quasar Model 414

6.12.1 Parsing the Torus, Dissecting the Donut 417

References 420

7 Quasars in the Cosmic Environment 439

Contributions by *Mauro D’Onofrio, Paola Marziani, Jack W. Sulentic, Deborah Dultzin, Gordon Richards, Johan Knapen, Isaac Shlosman, Raffaella Morganti, Renato Falomo, Mike Hawkins, Alfonso Cavaliere, Ross McLure, Greg Shields, Hagai Netzer, Daniel Proga, Alberto Franceschini, Xiaoui Fan, and Martin Elvis*

7.1 The Environment Around Quasars and AGNs 441

7.2	The Observational Evidence of Infall from the Circumnuclear Environment	448
7.3	Evidence of Feedback	459
7.3.1	Interplay Between Radio Jet and the Environment	459
7.3.2	Feedback Due to Quasar Winds	462
7.4	Quasars from Well Dressed to Naked.....	464
7.5	Quasar Birth and Evolution	471
7.6	Black Hole Growth and Extremely Large Black Holes	478
7.6.1	Primordial (Seed) Black Holes	478
7.6.2	Black Hole Growth Through Galaxy Evolution	482
7.7	Dust-Enshrouded Quasars	484
7.8	High-Redshift QSOs.....	486
7.9	The Optical Luminosity Function of QSOs and Its Evolution.....	490
7.10	QSO Large-Scale Environment and Clustering	493
7.11	What Are Quasars Telling Us on Structure Formation?	495
7.12	QSOs as Cosmological Probes	499
	References	505
8	The Future of Quasar Studies	521
	Contributions by <i>Mauro D’Onofrio, Paola Marziani, Jack W. Sulentic, Suzy Collin, Alberto Franceschini, Martin Elvis, Shai Kaspi, Marianne Vestergaard, Paolo Padovani, Johan Knapen, and Isaac Shlosman</i>	
8.1	The Past Achievements.....	522
8.2	Future Observational Prospects	524
8.2.1	Visual–Near IR	524
8.2.2	IR–mm Domain	526
8.2.3	X-Ray	528
8.3	Reverberation Mapping	531
8.3.1	Two-Dimensional Reverberation Mapping and Structure of the BLR.....	533
8.3.2	Dust Reverberation Mapping	536
8.3.3	X-Ray FeK α Reverberation Mapping.....	536
8.4	Digital Observatories	537
8.5	The Detection of Infalling Matter and the Accretion Scenario	542
	References	543
9	Fifty Years of Quasars: Current Impressions and Future Perspectives	549
	Contributions by <i>Jack W. Sulentic, Paola Marziani, and Mauro D’Onofrio</i>	
9.1	Summary of Achievements.....	549
9.2	Areas of Major Achievements	551
9.2.1	A Large Population of Quasars and Unification.....	551
9.2.2	A Universe Filled with Quasars	551

- 9.2.3 Probing Deep 552
- 9.2.4 Self-Similarity of Accretion Processes 553
- 9.3 The Weak Points or Some Questions That Remain for
the Editors and Probably Many Readers as Well 553
 - 9.3.1 The Nature of Radio Jets and the RL–RQ Dichotomy ... 553
 - 9.3.2 The Origin of Continuum Emission in
Radio-Quiet Quasars 554
 - 9.3.3 The Broad-Line-Emitting Region(s) 555
 - 9.3.4 Feedback and the Joint Evolution of Quasars
and Their Host Galaxies 556
- 9.4 Areas Supported by Partial or Inconclusive Evidence 557
 - 9.4.1 The Quasar Environment 557
 - 9.4.2 The Smoking Gun of Infall 557
 - 9.4.3 Is It Really a Black Hole? 558
 - 9.4.4 The Quest for an H–R Diagram 558
- 9.5 The Future: Peering into the First of the Next 50 Years 559
 - 9.5.1 Do We Really Need to Find More Quasars? 560
 - 9.5.2 Toward a Deeper Physical Understanding 563
 - 9.5.3 The New Redshift Frontier 564
 - 9.5.4 Moore’s Law in Quasar Astronomy 566
 - 9.5.5 Quasars, the Foundations of Cosmology and
Fundamental Physics 567
- References 567
- Index** 571

Contributors

Halton Arp Max Planck Institut für Astrophysik, Karl Schwarzschild Str. 1, Postfach 1317, D-85741 Garching bei München, Germany, arp@mpa-garching.mpg.de
Author's contribution in: Chap. 2, Sect. 2.11, p. 61.

Todd Boroson National Optical Astronomy Observatory, Tucson, AZ, USA, tyb@noao.edu
Author's contribution in: Chap. 3, Sect. 3.2, p. 101; Chap. 4, Sect. 4.7, p. 255.

Alfonso Cavaliere Dipartimento di Fisica, Università di Tor Vergata, via Ricerca Scientifica 1, 00133 Roma, Italy, cavaliere@roma2.infn.it
Author's contribution in: Chap. 2, Sect. 2.9, p. 55; Chap. 7, Sect. 7.5, p. 471.

Suzy Collin LUTH, Observatoire de Paris-Meudon, Section de Meudon, 92195 Meudon, France, suzy.collin@obspm.fr
Author's contribution in: Chap. 2, Sect. 2.1, p. 13; Chap. 6, Sect. 6.1, p. 344; Chap. 6, Sect. 6.4, p. 360; Chap. 8, Sect. 8.1, p. 522.

Bozena Czerny Copernicus Astronomical Center, Bartycka 18, 00-716 Warsaw, Poland, bcz@camk.edu.pl
Author's contribution in: Chap. 5, Sect. 5.6, p. 321; Chap. 6, Sect. 6.4.1, p. 362; Chap. 6, Sect. 6.5.1, p. 371.

Mauro D'Onofrio Dipartimento di Astronomia, Università degli Studi di Padova, Vicolo Osservatorio 3, I35122 Padova, Italy, mauro.donofrio@unipd.it
Co-editor of the book.

Deborah Dultzin Instituto de Astronomia, Universidad Nacional Autónoma de México (UNAM), Apt.do postal 70-264, México, D.F., México, deborah@astroscu.unam.mx
Author's contribution in: Chap. 3, Sect. 3.6, p. 120; Chap. 4, Sect. 4.1, p. 219; Chap. 5, Sect. 5.8, p. 325; Chap. 7, Sect. 7.1, p. 441.

Yuri Efimov Crimean Astrophysical Observatory, 98409, Ukraine, Crimea, Nauchny, yseyse@mail.ru

Author's contribution in: Chap. 4, Sect. 4.1, p. 221.

Martin Elvis Harvard Smithsonian Center for Astrophysics, Cambridge MA02138, USA, elvis@cfa.harvard.edu

Author's contribution in: Chap. 3, Sect. 3.10, p. 154, 155, 158; Chap. 6, Sect. 6.12, p. 414; Chap. 7, Sect. 7.12, p. 504; Chap. 8, Sect. 8.2.3, p. 528.

Mike Eracleous Department of Astronomy and Astrophysics and Center for Gravitational Wave Physics, The Pennsylvania State University, 525 Davey Lab., University Park, PA 16802, USA, mce@astro.psu.edu

Author's contribution in: Chap. 4, Sect. 4.7, p. 256; Chap. 6, Sect. 6.4.2, p. 364.

Heino Falcke Radboud Universiteit Nijmegen, Dept. Astronomy, IMAPP, The Netherlands

ASTRON, Dwingeloo, The Netherlands

Max-Planck Institut für Radioastronomie, Bonn, Germany, h.falcke@astro.ru.nl

Author's contribution in: Chap. 3, Sect. 3.9.3, p. 147; Chap. 4, Sect. 4.9.1, p. 266.

Renato Falomo INAF-Osservatorio Astronomico di Padova, Vicolo Osservatorio 2, I35122 Padova, Italy, renato.falomo@oapd.inaf.it

Author's contribution in: Chap. 7, Sect. 7.4, p. 464.

Xiaoui Fan Steward Observatory and Department of Astronomy, University of Arizona, 933 N. Cherry Avenue, Tucson 85721, Arizona, USA, fan@as.arizona.edu

Author's contribution in: Chap. 7, Sect. 7.8, p. 486; Chap. 7, Sect. 7.11, p. 496.

Luigi Foschini Istituto Nazionale di Astrofisica (INAF) - Osservatorio Astronomico di Brera, Via E. Bianchi, 46 - 23807 - Merate (LC) - Italy, luigi.foschini@brera.inaf.it

Author's contribution in: Chap. 3, Sect. 3.11, p. 184; Chap. 6, Sect. 6.5.1, p. 372.

Alberto Franceschini Dipartimento di Astronomia, Università degli Studi di Padova, Vicolo Osservatorio 3, I35122 Padova, Italy, alberto.franceschini@unipd.it

Author's contribution in: Chap. 3, Sect. 3.12, p. 190; Chap. 4, Sect. 4.4, p. 230; Chap. 7, Sect. 7.7, p. 484; Chap. 8, Sect. 8.2.2, p. 526.

Begoña García-Lorenzo Instituto de Astrofísica de Canarias, E-38200 La Laguna, Tenerife, Spain, garcialorenzo@iac.es

Author's contribution in: Chap. 4, Sect. 4.5, p. 245.

Martin Gaskell Departamento de Física y Astronomía, Facultad de Ciencias, Universidad de Valparaíso, Av. Gran Bretaña 1111, Valparaíso, Chile, martin.gaskell@uv.cl

Author's contribution in: Chap. 2, Sect. 2.3, p. 24; Chap. 3, Sect. 3.1, p. 97, Sect. 3.8.1, 125; Chap. 4, Sect. 4.2, p. 223; Chap. 6, Sect. 6.1, p. 341.

Dirk Grupe The Pennsylvania State University, 525 Davey Lab., University Park, PA 16082, USA, grupe@astro.psu.edu

Author's contribution in: Chap. 3, Sect. 3.7, p. 124; Sect. 3.10.1, p. 159; Chap. 4, Sect. 4.5, p. 240.

Michael Hawkins Institute for Astronomy (IfA), University of Edinburgh, Royal Observatory, Blackford Hill, Edinburgh EH9 3HJ, UK, mrsh@roe.ac.uk

Author's contribution in: Chap. 3, Sect. 3.4, p. 114; Chap. 6, Sect. 7.4, p. 470; Chap. 6, Sect. 7.12, p. 503.

Krzysztof Hryniewicz Copernicus Astronomical Center, Bartycka 18, 00-716 Warsaw, Poland, krhr@camk.edu.pl

Author's contribution in: Chap. 5, Sect. 5.6, p. 321; Chap. 6, Sect. 6.4.1, p. 362; Chap. 6, Sect. 6.5.1, p. 371.

Damien Hutsemékers F.R.S. - FNRS, Institute of Astrophysics and Geophysics, University of Liège, Allée du six août 17, B5c, B-4000, Liège, Belgium, hutsemekers@astro.ulg.ac.be

Author's contribution in: Chap. 4, Sect. 4.3.1, p. 224, 227; Chap. 5, Sect. 5.4, p. 295.

Shai Kaspi School of Physics and Astronomy and the Wise Observatory, The Raymond and Beverly Sackler Faculty of Exact Science, Tel-Aviv University, Tel-Aviv 69978, Israel, shai@wise.tau.ac.il

Author's contribution in: Chap. 5, Sect. 5.2, p. 290; Sect. 5.5, p. 297; Sect. 5.5.1, p. 299; Chap. 8, Sect. 8.3, p. 531.

Ajit Kembhavi The Inter-University Centre for Astronomy and Astrophysics, Pune, India, akk@iucaa.ernet.in

Author's contribution in: Chap. 3, Sect. 3.10.4, p. 173; Chap. 3, Sect. 3.10.4, p. 179.

Johan Knapen Instituto de Astrofísica de Canarias, E-38200 La Laguna, Tenerife, Spain

Departamento de Astrofísica, Universidad de La Laguna, E-38205 La Laguna, tenerife, Spain, jhk@iac.es

Author's contribution in: Chap. 7, Sect. 7.2, p. 449; Chap. 8, Sect. 8.5, p. 542.

Seguei Komissarov School of Mathematics, University of Leeds, Leeds, L529JT, UK, serguei@maths.leeds.ac.uk

Author's contribution in: Chap. 6, Sect. 6.7.1, p. 384.

Elmar K rding Radboud Universiteit Nijmegen, Dept. Astronomy, IMAPP, The Netherlands, elmar.koerding@astro.ru.nl

Author's contribution in: Chap. 3, Sect. 3.9.3, p. 147; Chap. 4, Sect. 4.9.1, p. 266.

Julian Krolik Dept. of Physics and Astronomy, Johns Hopkins University, 3400 N. Charles Street, Baltimore, MD 21218-2686, USA, jhk@jhu.edu

Author's contribution in: Chap. 2, Sect. 2.7, p. 51; Chap. 6, Sect. 6.1, p. 339; Chap. 6, Sect. 6.5, p. 368; Chap. 6, Sect. 6.10, p. 406.

Ari Laor Technion - Israel Institute of Technology Physics Department, Technion City, Haifa 32000, Israel, laor@physics.technion.ac.il

Author's contribution in: Chap. 3, Sect. 3.3.1, pp. 112, 127; Chap. 4, Sect. 4.4.1, p. 237, Sect. 4.8, p. 258; Chap. 5, Sect. 5.5.1, p. 306.

Sebastian Lipari Observatorio Astronómico de la Univ. Nac. de Córdoba, Laprida 854, X5000BGR, Córdoba, Argentina, and CONICET, Argentina, lipari@oac.uncor.edu

Author's contribution in: Chap. 4, Sect. 4.5, p. 245.

Paola Marziani INAF, Osservatorio Astronomico di Padova, Vicolo Osservatorio 5, IT35122 Padova, Italy, paola.marziani@oapd.inaf.it

Co-editor of the book.

Ross McLure Institute for Astronomy, Royal Observatory Edinburgh, Blackford Hill, Edinburgh EH9 3HJ, UK, rjm@roe.ac.uk

Author's contribution in: Chap. 5, Sect. 5.5.1, p. 300; Chapter 5, § 5.6, p. 319.

Evencio Mediavilla Instituto de Astrofísica de Canarias, E-38200 La Laguna, Tenerife, Spain, mediavilla@iac.es

Author's contribution in: Chap. 4, Sect. 4.5, p. 245.

Raffaella Morganti Netherlands Institute for RadioAstronomy (ASTRON), Postbus 2, 7990 AA, Dwingeloo, The Netherlands

Kapteyn Astronomical Institute, University of Groningen, P.O. Box 800, 9700 AV Groningen, The Netherlands, morganti@astron.nl

Author's contribution in: Chap. 3, Sect. 3.9, p. 132; Chap. 7, Sect. 7.3.1, p. 459.

Jayant V. Narlikar Inter-University Centre for Astronomy and Astrophysics Post Bag 4, Ganeshkhind, Pune 411007, India, jvn@iucaa.ernet.in

Author's contribution in: Chap. 2, Sect. 2.12, p. 73.

Yuri Neshpor Crimean Astrophysical Observatory, 98409, Ukraine, Crimea, Nauchny, yneshpor@mail.ru

Author's contribution in: Chap. 3, Sect. 3.11, p. 188.

Hagai Netzer School of Physics and Astronomy, Tel Aviv University, Tel Aviv 69978, Israel, netzer@wise.tau.ac.il

Author's contribution in: Chap. 2, Sect. 2.8, p. 53; Chap. 6, Sect. 6.2, p. 349.

Paolo Padovani European Southern Observatory, Karl-Schwarzschild-Str. 2, D-85748 Garching bei München, Germany, ppadovan@eso.org

Author's contribution in: Chap. 2, Sect. 2.10, p. 59; Chap. 5, Sect. 5.3, p. 293; Chap. 6, Sect. 6.7.1, p. 381; Chap. 8, Sect. 8.4, p. 537.

Isabel Marquez Pérez Instituto de Astrofísica de Andalucía (CSIC), Granada, Spain, isabel@iaa.es

Author's contribution in: Chap. 4, Sect. 4.8, p. 259.

Daniel Proga Department of Physics and Astronomy, University of Nevada, Las Vegas 4505, South Maryland Parkway, Las Vegas, Nevada 89154-4002, USA, dproga@physics.unlv.edu

Author's contribution in: Chap. 6, Sect. 6.6, p. 373.

Iraida Pronik Crimean Astrophysical Observatory, 98409, Ukraine, Crimea, Nauchny, ipronik@mail.ru

Author's contribution in: Chap. 2, Sect. 2.6, p. 45; Chap. 2, Sect. 2.6, p. 47;

Valdimir Pronik Crimean Astrophysical Observatory, 98409, Ukraine, Crimea, Nauchny, vpronik@mail.ru

Author's contribution in: Chap. 2, Sect. 2.6, p. 45; Chap. 2, Sect. 2.6, p. 46; Chap. 2, Sect. 2.6, p. 47; Chap. 3, Sect. 3.5, p. 118.

Gordon Richards Drexel University, Department of Physics, 3141 Chestnut Street, Philadelphia, PA 19104 USA, gtr@physics.drexel.edu

Author's contribution in: Chap. 3, Sect. 3.8.2, p. 128; Chap. 7, Sect. 7.2, p. 448.

Sergey Sergeev Crimean Astrophysical Observatory, 98409, Ukraine, Crimea, Nauchny, sergeev@crao.crimea.ua

Author's contribution in: Chap. 2, Sect. 2.6, p. 46.

Giancarlo Setti INAF-Istituto di Radioastronomia, Via P. Gobetti, 101 40129 Bologna Italy, setti@ira.inaf.it

Author's contribution in: Chap. 2, Sect. 2.2, p. 18.

Greg Shields Department of Astronomy, University of Texas, Austin, TX 78712-0259, USA, shields@astro.as.utexas.edu

Author's contribution in: Chap. 3, Sect. 3.1, p. 94, Chap. 5, Sect. 5.1, p. 289, Chap. 7, Sect. 7.12, p. 500.

Isaac Shlosman Department of Physics and Astronomy, University of Kentucky, Lexington, KY 40506-0055, USA, shlosman@ps.uky.edu

Author's contribution in: Chap. 6, Sect. 6.8, p. 397; Chap. 7, Sect. 7.2, p. 455; Chap. 8, Sect. 8.5, p. 543.

Massimo Stiavelli Space Telescope Science Institute, 3700 San Martin Drive Baltimore, MD 21218, USA, mstiavel@stsci.edu

Author's contribution in: Chap. 7, Sect. 7.10, p. 493; Chap. 8, Sect. 8.2.1, p. 524.

Jack W. Sulentic Instituto de Astrofísica de Andalucía (CSIC), Granada, Spain, sulentic@iaa.es

Co-editor of the book.

Tracey Jane Turner UMBC, 1000 Hilltop Circle, Baltimore MD 21250, USA, tjturner@umbc.edu

Author's contribution in: Chap. 3, Sect. 3.10.1, p. 160; Chap. 3, Sect. 3.10.5, 178.

Marianne Vestergaard The Dark Cosmology Centre, The Niels Bohr Institute, University of Copenhagen, Juliane Maries Vej 30, 2100 Copenhagen 0, Denmark

Steward Observatory and Department of Astronomy, University of Arizona, 933 N. Cherry Avenue, Tucson 85721, Arizona, USA, vester@dark-cosmology.dk
Author's contribution in: Chap. 4, Sect. 4.3, p. 223, Chap. 5, Sect. 5.5.2, p. 307; Chap. 8, Sect. 8.3.1, p. 533.

Aleksander Vol'vach Radio Astronomy Laboratory of Crimean Astrophysical Observatory, 98688, Ukraine, Crimea, Yalta, Katsively, RT-22, volvach@crao.crimea.ua
Author's contribution in: Chap. 2, Sect. 2.6, p. 51; Chap. 3, Sect. 3.9.1, p. 138.

E. Joseph Wampler 330 Llama Ranch Lane, Santa Cruz, California CA 95060, USA, jwampler@cruzio.com
Author's contribution in: Chap. 2, Sect. 2.4, p. 35.

Sebastian Zamfir University of Wisconsin-Stevens Point, 1848 Maria Dr Stevens Point, WI 54481-1957, USA, szamfir@uwsp.edu
Author's contribution in: Chap. 3, Sect. 3.9.3, p. 142.

Acronyms

Contributions by all authors

2MASS	Two Micron Sky Survey
3CR	Third Cambridge Catalogue
4DE1	Four dimensional eigenvector 1
AAO	Anglo Australian Observatory
AAS	American Astronomical Society
ACIS	Advanced CCD Imaging Spectrometer
ADAF	Advection dominated accretion flow
ADIOS	Advection dominated inflow–outflow solution
ADS	Astrophysics Data System
AGB	Asymptotic giant branch
AGN	Active galactic nucleus
ASP	American Society of the Pacific
BAL	Broad absorption line
BAT	Burst Alert Telescope
BE	Baldwin effect
BELR	Broad emission line region
BH	Black hole
BLR	Broad line region
BPT	Baldwin, Phillips, Terlevich
BQS	Bright Quasar Survey
CCD	Charge coupled device
DRn	Data release n
CD	Core dominated
CDAF	Advection dominated accretion flow
CMB	Cosmic microwave background
CrAO	Crimean Astrophysical Observatory
CSS	Compact-steep-spectrum
DQE	Detective quantum efficiency
EGRET	Energetic Gamma-ray Experiment Telescope
ELAIS	European Large Area ISO survey
EPIC	European Photon Imaging Camera

EV1	Eigenvector 1
EVLA	Expanded Very Large Array
EW	Equivalent width
EXIST	Energetic X-ray Imaging Survey Telescope
FIR	Far infrared
FIRST	Faint Images of the Radio Sky at Twenty-Centimeters
FRI	Fanaroff–Riley type I
FR II	Fanaroff–Riley type II
FSRQ	Flat Spectrum Radio Quasar
FWHM	Full width half maximum
GPS	Gigahertz-peaked-spectrum
GRB	Gamma ray burst
HDF	Hubble deep field
HEG	High energy grating
HERG	High excitation radio galaxy
HETG	High energy transmission grating
HIL	High ionization line
H–R	Hertzsprung–Russell
HST	Hubble Space Telescope
IAU	International Astronomical Union
IUE	International Ultraviolet Explorer
IDS	Image Dissector Scanner
IDV	Intra day variability
INOV	Intra night optical variability
IPCS	Image Photon Counting System
IR	Infra-red
IGM	Inter galactic medium
ISCO	Innermost stable circular orbit
ISM	Inter stellar medium
IXO	International X-ray Observatory
LBQS	Large Bright Quasar Survey
LERG	Low excitation radio galaxy
LETG	Low energy transmission grating
LIL	Low ionization line
LINER	Low ionization nuclear emission-line region
LISA	Laser Interferometer Space Antenna
LLAGN	Low luminosity active galactic nucleus
LOFAR	Low frequency array
MACHO	Massive compact halo object
MAGIC	Major Atmospheric Gamma-ray Imaging Cherenkov
MAXIM	Micro-Arcosecond X-ray Imaging Mission
MBH	Massive black hole
MEG	Medium energy grating
MERLIN	Multi-Element Radio-Linked Interferometer
MOS	Metal oxide semi-conductor
NASA	National Aeronautics and Space Administration
NED	NASA Extragalactic Database
NFS	National Science Foundation
NGC	New General Catalogue

NIR	Near infra-red
NLR	Narrow line region
NLSy1	Narrow line Seyfert-1
NRAO	National Radio Astronomy Observatory
OM	Optical microvariability
PCA	Principal component analysis
PG	Palomar-Green
Pan-STARRS	Panoramic Survey Telescope & Rapid Response System
PKS	Parkes radio source
PSF	Point spread function
PAH	Polycyclic aromatic hydrocarbon
QSG	Quasi stellar galaxy
QSO	Quasi stellar object
QSS	Quasi stellar source
RASS	ROSAT All Sky Survey
RGS	Reflection grating spectrometer
RIAF	Radiatively inefficient accretion flow
RIQ	Radio intermediate quasar
RL	Radio loud
RQ	Radio quiet
RLQ	Radio loud quasar
ROSAT	Röntgensatellit
RQQ	Radio quiet quasar
RXTE	Rossi X-Ray Timing Explorer
SAI	Sternberg Astronomical Institute
SAS	Small astronomy satellite
SDSS	Sloan Digital Sky Survey
SEC	Secondary electron conducting
SED	Spectral energy distribution
SINFONI	Spectrograph for INtegral Field Observations in the Near Infrared
SKA	Square kilometer array
SMBH	Super massive black hole
SPIE	Society of Photo-Optical Instrumentation Engineers
SSI	Sky Survey Instrument (Ariel V)
ULIRG	Ultra-luminous infra-Red galaxy
UV	Ultraviolet
VHE	Very high energy
VLA	Very large array
VLBA	Very long baseline array
VLBI	Very long baseline interferometry
VLT	Very Large Telescope
VLTI	Very Large Telescope Interferometer
VSOP	VLBI Space Observatory Program
XMM	X-ray multi-mirror mission, XMM- <i>Newton</i>
XBONG	X-ray bright optically normal galaxy
XRb	X-ray binary
WFXT	Wide-field X-ray telescope
WWII	World War II

Web pages

Contributions by all authors

2QZ	2dF QSO Redshift Survey http://www.2dfquasar.org/
ALMA	Atacama Large Millimeter Array http://www.eso.org/sci/facilities/alma/
ASKAP	Australian Square Kilometre Array Pathfinder http://www.atnf.csiro.au/projects/askap/
<i>Chandra</i>	http://chandra.si.edu/
E-ELT	European Extremely Large Telescope http://www.eso.org/sci/facilities/eelt/
EMU	Evolutionary Map of the Universe http://www.atnf.csiro.au/people/morris/emu
eROSITA	http://www.mpe.mpg.de/heg/www/Projects/EROSITA/main.html
<i>Euclid</i>	http://sci.esa.int/euclid/
IVOA	International Virtual Observatory Alliance http://ivoa.net
JWST	James Webb Space Telescope http://www.stsci.edu/jwst/
Gravitas	http://www.mpe.mpg.de/gravitas/workshop_2010/workshop.php
GMT	Giant Magellan Telescope http://www.gmto.org/
LBQS	Large Bright Quasar Survey http://heasarc.gsfc.nasa.gov/W3Browse/galaxy-catalog/lbqs.html
LSST	Large Synoptic Survey Telescope http://www.lsst.org
NASA	National Aeronautic and Space Administration http://www.nasa.gov
NED	NASA Extragalactic Database http://ned.ipac.caltech.edu
PAN-STARRS	Panoramic Survey Telescope and Rapid Response System http://pan-starrs.ifa.hawaii.edu/

SDSS	Sloan Digital Sky Survey http://www.sdss.org
SKA	Square Kilometer Array http://www.skatelescope.org
TMT	Thirty Meter Telescope http://www.tmt.org/
VO-tools	Virtual Observatory tools http://www.euro-vo.org/pub/fc/software.html
WISE	Wide-field Infrared Survey Explorer http://wise.ssl.berkeley.edu/
WFXT	Wide Field X-ray Telescope http://wfxt.pha.jhu.edu/

Chapter 1

An Introduction to 50 Years of Research on Quasars

Paola Marziani, Jack W. Sulentic and Mauro D’Onofrio

1.1 The Roaring Sixties

We are approaching the 50th anniversary of the discovery of quasars. Those old enough to have been cognizant of astronomy in 1962–1963 can remember the sense of excitement connected with this finding. There was talk of a major new constituent of the universe. The excitement of the discovery was palpable even to one of us (the most senior of the editors) who was then a high school teenager.

The early history of quasar discovery is, ironically, based on determination of accurate positions for radio sources. Ironic because around 90% of quasars are now known to be radio quiet. But, perhaps, it was not so surprising in the 1960s when a few people (e.g., Rudolf Minkowski and Walter Baade [3, 14]) were finding strange and energetic things connected with recently discovered radio-loud galaxies. Quasar discovery occurred in a period when many thought that we had a reasonably complete picture of the the major constituents of the universe as well as their distribution and their motions. Galaxies were the basic building blocks and appeared to be quiescent aggregates of stars, gas, and dust in this pre-dark matter era. Carl Seyfert had found evidence in the early 1940s for some spiral galaxies with active nuclei but this discovery had not yet taken hold [21]. The optical jet in the elliptical galaxy Messier 87 had been known since 1917 [6]. The Abell and Zwicky catalogues

P. Marziani

INAF, Osservatorio Astronomico di Padova, Vicolo Osservatorio 5, IT35122 Padova, Italy
e-mail: paola.marziani@oapd.inaf.it

J.W. Sulentic (✉)

Instituto de Astrofísica de Andalucía (CSIC), Granada, Spain
e-mail: sulentic@iaa.es

M. D’Onofrio

Dipartimento di Astronomia, Università degli Studi di Padova, Vicolo Osservatorio 3,
I35122 Padova, Italy
e-mail: mauro.donofrio@unipd.it

of galaxies and galaxy clusters (late 1950s and early 1960s [1, 26]) revealed that the distribution of these building blocks was clumpy and the concept of an underlying homogeneous “field” slowly faded away. This complex distribution of galaxies appeared to be superimposed on a smooth Hubble expansion flow. A quiet universe (except for supernovæ connected with stellar death). There was nary a whisper of dissent about this picture.

The changes of the 1960s were the cause of the excitement and radio astronomy was the major conduit. The late 1950s had already revealed the first double-lobed radio sources which lead inescapably to the conclusion that galaxies were capable of extremely energetic phenomena. Slowly, it was realized that the lobes were a nonthermal phenomenon powered by relativistic jets (e.g., [17, 22]). People started to go back and look at the optical galaxies producing these radio outflows (Messier 87, Cygnus A, Centaurus A), and it became clear that these were not quiescent systems. As radio positions improved in this period, it became clear that some apparently starlike objects were also strong radio sources. This result leads to the discovery of quasars.

By 1959, three catalogues of radio sources had been published by the Cambridge group of radio astronomers. The last one [7] proved instrumental to the discovery of quasars; however, due to the still poor resolution of the Cambridge interferometer, a lunar occultation (observed from the Parkes radio telescope in Australia) was needed to determine the position of the radio source 3C 273 (see Fig. 1.1) with accuracy good enough to make possible identification with an optical counterpart [11]. Identification of stellar-appearing optical counterparts to strong radio sources motivated spectroscopic observations by Maarten Schmidt and Jesse Greenstein (3C273—[19]; 3C48—[9]). The most surprising thing about these sources involved their redshifted broad emission-lines that implied enormous distances and enormous energies. The first two sources showed relatively modest (but high for the time) redshift values of $z = c(\Delta\lambda/\lambda) = 0.16$ and 0.37 , respectively (where c is the speed of light, λ the rest wavelength of an observed line, and $\Delta\lambda$ the difference between rest and redshifted wavelengths for that line). Values of redshift as high as 2.2 were found shortly thereafter [2]. That paper reported detection of both broad emission and absorption lines with measurably different redshifts in the same spectrum.

The first summary of quasar properties and issues was provided by Margaret and Geoff Burbidge with their book in 1967 [4]. Clearly, these quasi-stellar sources were a mystery, and resolution of that mystery was impossible without knowledge of their distances. The redshift-distance relation had been accepted for decades, so the most direct interpretation of the quasar redshifts placed them at the edge of the then known universe. Quite exciting. This did not satisfy everyone. People who believed in an infinite universe (steady-state cosmology) did not like the implication that the distant universe (the past) was filled with quasars, while locally, no such hyper-energetic sources were found. In fact, the discovery of quasars led Fred Hoyle to abandon the steady-state model [13]. Seyfert-1 galaxies that are found in the local universe were radio quiet and showed optical luminosities several dex lower than the quasars. Seyferts were enough different from quasars that it took some time for a link with quasars to be widely accepted; after all, even a supernova in the Milky Way

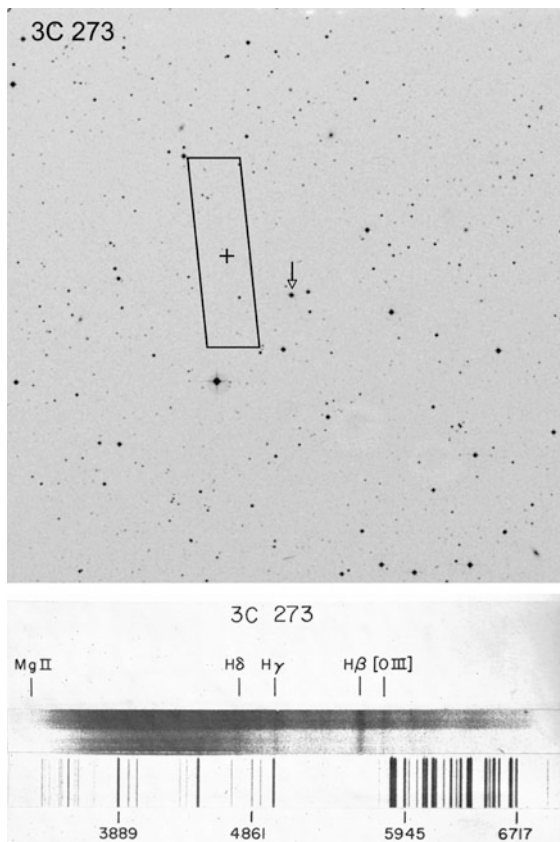


Fig. 1.1 *Top*: 3C 273, the first quasar, as it appears on the POSS digitized plates. Superimposed on the optical image is the position uncertainty box for the Cambridge radio interferometer used to produce the third Cambridge (3C) survey of radio sources, drawn following the prescription of [7]. *Bottom*: an optical spectrum of 3C 273 obtained in the early 1960s and showing the redshifted Balmer lines, reported by [10]. The telescope had been moved to let the quasars “walk” along the slit; the upper half of the spectrum was obtained with an exposure three times as long as the one of the lower half. A “comparison” spectrum of hydrogen, helium, and neon was also recorded on the lower half of the plate

can show broad emission lines. The discovery of quasars with spectra showing lines with different redshifts also likely contributed to doubts about the direct application of the redshift-distance relation. The idea that quasars were hosted by galaxies was yet to take hold.

Another almost simultaneous surprise involved the discovery that these sources were variable in intensity and on small timescales (weeks/months) implying very small (light-months \sim a few 10^3 Schwarzschild radii) emitting volumes [10]. The possibility that the high redshifts were of gravitational origin was ruled out contemporaneously (the emitting region was likely small but not *that* small), and

there were no redshift gradients in the spectra. No clusters of like redshift galaxies were immediately found around the quasars although the image of 3C 48 was fuzzy and 3C 273 showed a faint jet reminiscent of the one in Messier 87. Since redshifts of galaxies were more widely accepted as distance indicators (i.e., the Hubble law), discovery of galaxies near a quasar with the *same* redshift would have been tantamount to proof of the redshift distance of the quasar—pieces of a puzzle. There were the low-redshift Seyfert galaxies with active nuclei showing broad emission lines. Were quasars truly compact sources (i.e., naked) or the nuclei of conventional, but currently active, galaxies? In 1968, Steward Observatory hosted the first conference devoted to Seyfert galaxies, soon after the discovery of quasars. The University of Arizona astronomy graduate students produced a souvenir for the occasion: an auto bumper sticker showing a spiral galaxy and proclaiming “Seyfert Galaxies Cause Cancer.” The former high school student, now a UA undergraduate, was following the excitement from the back of the conference room even succeeding to obtain this souvenir after some machinations.

By 1966, the excitement had reached the mainstream media. Shortly thereafter, a television was marketed under the brand name “Quasar.” In the words of a 1966 TIME magazine article:

Fast & Far. Quasars were first recognized as astronomical curiosities when, unlike the ordinary stars they resemble, they showed up as the sources of enormous amounts of radio energy. Then Dr. Schmidt studied spectrograms of their light and demonstrated that it had shifted far toward the red wave lengths – proof positive that quasars are not only incredibly far-off but are speeding away still farther, carried along by the rapid expansion of distant parts of the universe.

With every new observation, the mystery deepened. Quasars turned out to be by far the most brilliant objects in the universe, shining with the light of from 50 to 100 galaxies, each containing 100 billion stars as bright as the sun. Where did all the energy come from?

It is interesting and fascinating to remember that quasars were discovered at a time when: (1) 2m telescopes were considered “large,” (2) CCDs were still 20 years away, (3) very few observations existed outside the radio and optical domains (e.g. the UV line $\text{MgII}\lambda 2,798$ had only been observed in the Sun but was now seen in many redshifted quasar spectra), and (4) computing power was one step beyond the rapidly appearing electronic calculators (mechanical ones were still in wide use).

1.2 An Operational Definition of Quasars?

It is often difficult to look back 50 years and understand why it took so long to unify the quasar phenomenon with Seyfert and radio galaxies under the active galactic nuclei (AGNs) umbrella. All or part of the difficulty was due to the lack of an operational definition of what is a “quasar.” The 1964 definition would have involved a “quasi-stellar radio source” (quasar) which could be defined optically as a stellar (or quasi-stellar) object with a UV excess and capable of erratic fluctuations in intensity. Spectroscopically, the sources showed broad permitted emission lines and

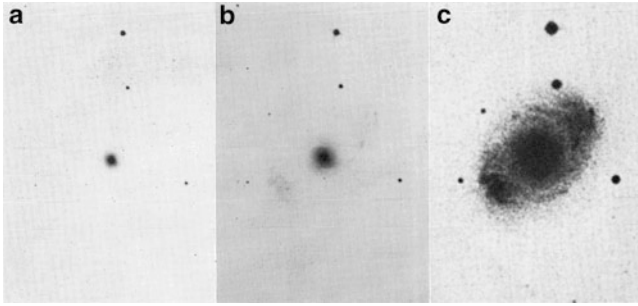


Fig. 1.2 Three exposures of the Seyfert-1 galaxy NGC 4151. In the shortest one (on the *left*), only the active nucleus is visible, giving the source a starlike appearance; in the *middle one*, the inner spiral structure of the host galaxy becomes visible; in the *deepest one*, the nucleus is saturated, and the host galaxy becomes well visible (reproduced from [15])

narrow permitted and forbidden emission lines. And, of course, they showed strong radio emission. Take any part of that definition, and within a few years, exceptions and contradictions to that first attempt at an operational definition were known. Quasars were radio-emitting stellar sources, Seyfert galaxies were radio-quiet spiral galaxies, and low-redshift radio galaxies like Messier 87, which does not show broad emission lines, were hosted in elliptical galaxies. By the mid-1960s, Allan Sandage [16] made it obvious that many sources, otherwise identical to quasars, were radio quiet (today 90% of known broad-line emitters). In succeeding years, sources otherwise thought to be quasars/Seyfert galaxies/radio galaxies were found showing only narrow lines or no lines at all. That is why this chapter devotes so many questions and so much space (Chaps. 2 and 3) to issues of unification.

All of this did not hamper the slow acceptance of a *unification in source luminosity* that nowadays is often unspoken of and that remains in the shadow of topics debated in the various chapters. Decades of observations with ever-improving instruments show that the emission-line spectrum and spectral energy distribution of quasars are similar over a very wide range of luminosity. There is a continuity between QSOs and bright nuclei of relatively nearby active galaxies such as Seyfert galaxies (the left panel of Fig. 1.2 shows the stellar appearance of the nucleus of a nearby active galaxy). Among radio-loud sources, a similar luminosity continuity exists between quasars and low- z radio galaxies. There is no discontinuity among source luminosities in the most comprehensive catalogue of AGNs [25]. The once canonical distinction between Seyfert galaxies and QSOs at absolute blue magnitude $M_B = -23$ is now mainly of historical importance. As long as the physical processes are the same at low and high luminosity, some extrapolation is possible from the analysis of nearby AGNs to the most distant sources. Is this extrapolation always possible? Has it been abused because of the scarce information about the most distant and faintest sources? Self-similarity does not imply that every quasar is identical to all others even if they are observed at the same viewing angle. There is an obvious spread of spectral properties for unobscured quasars in even

a narrow luminosity range. The existence of two major classes of quasars—radio quiet and radio loud—still lacks a convincing explanation. Nor do we know why radio-loud quasar represent a minority of only $\approx 10\%$ of all quasars.

So overarching questions in this book beyond “What are quasars?” could be: how much has the field advanced since the supermassive black hole/accretion disk/obscuring torus (SMBH-AD) paradigm became widely accepted around 1970? How have the myriad technological advances aided those advances? What do we know about quasars today that we did not know in 1970 or when Virginia Trimble and Lodewijk Woltjer reviewed the first 25 years of quasar discovery [24]? Perhaps, quasars should not be described today as a new constituent of the universe but rather a new insight into the evolution of galaxies and interactions with their environment. We suggest that this anniversary does not warrant another monograph but an attempt to solicit as wide a range as possible of empirical results and theoretical ideas. A great challenge involves organizing the subject matter into some kind of logical flow since every datum is related to all the other data. In the end this book is intended as a resource for results and ideas in order to define, and defend, what we know about these fascinating sources.

1.3 Outline of the Book

Before starting to outline the book content, we have to consider that the cosmological scenario underlying quasar studies has changed significantly since the 1960s. We are now living in the widely accepted Λ CDM cosmological scenario. Not only the Hubble constant value is now estimated as $H_0 \approx (72 \pm 8) \text{ km s}^{-1} \text{ Mpc}^{-1}$ [8, 23], while in the late 1950s and early 1960s, its values ranged between 50 and $100 \text{ km s}^{-1} \text{ Mpc}^{-1}$, but the entire Universe is now believed to accelerate rather than decelerate or flow at a constant rate. The reader might ask whether such important changes have had consequences for our understanding of quasars and for the derivation of physical parameter like luminosity and mass. The left panel of Fig. 1.3 shows that this is not the case for the majority of quasars known as of today at $z < 4$ since the comoving radial distance of quasars in the case of a flat universe and in the preceding scenario with deceleration parameter $q_0 = 0.1$ (considered the observationally supported case until 1997) are only slightly different. On the right panel, we report the lookback time, i.e., the time needed for light emitted by a quasar at redshift z to reach us. We show these diagrams because the contributors to this book often use redshift as a distance indicator, and it might not be easy to grasp the meaning of redshift in terms of distance or lookback time and age of the universe.

The book adopts a different format from classical conference proceedings and graduate textbooks. Astrophysicists and astronomers were interviewed with questions aimed first at highlighting the basic aspects of quasar phenomenology and interpretation. Other questions focus on contentious areas and presently unclear aspects of our understanding of quasars. Given the abundance and scope of present-

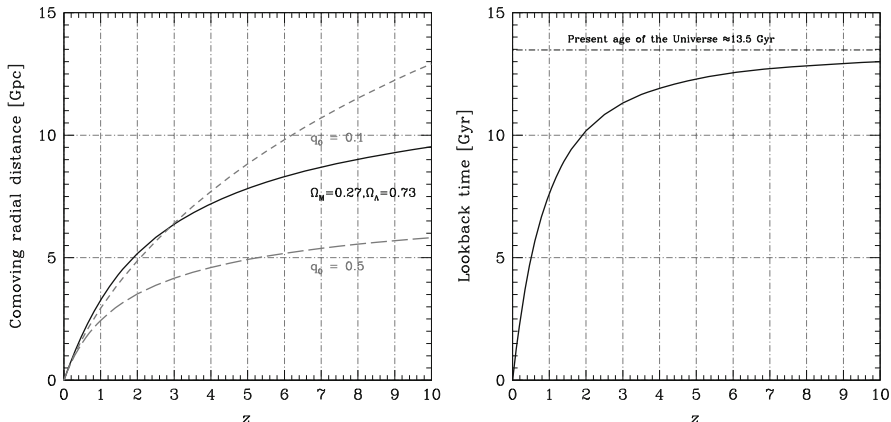


Fig. 1.3 *Left:* radial comoving distance as a function of redshift z for $\Lambda = 0, q_0 = 0.1$ (short-dashed line); $\Lambda = 0, q_0 = 0.5$ (long-dashed line); and $\Omega_\Lambda = 0.73, \Omega_M = 0.27$ (filled line), in units of Gpc. *Right:* Lookback time in units of Gyr for the case $\Omega_\Lambda = 0.73, \Omega_M = 0.27$. The Hubble constant is assumed $H_0 = 72 \text{ km s}^{-1} \text{ Mpc}^{-1}$

day observations along with the refinement of current models, it is of special interest to follow how major ideas emerged and developed during the first years of quasar research.

Chapter 2 (“Quasars in the Life of Astronomers”) offers 15 recollections of astronomers that were active during or shortly after the discovery of quasars. These range from descriptions of instrument development during this time as well as a wide range of observational and theoretical recollections. Quasar discovery came at a time when the world was split into two major blocs, and relatively, little dialog occurred between them. Soviet studies of quasars and nearby AGNs were in many ways parallel to the ones of Western astronomers and led to many interesting discoveries, as recounted here by several astronomers from the Crimean Astrophysical Observatory. Contributors were encouraged to recall how much of the current paradigm was already in place around 1970. A vigorous debate erupted in the 1960s over the cosmological interpretation of redshifts. Although most of the contributors started within the framework of what is now called the standard model, voices of dissent played an inspiring role for those who wanted to investigate the universe beyond theoretical assumptions and prejudices. Enduring voices remind us about still unsolved conundrums of the quasar view.

Chapter 3 (“Quasars: The Observational Perspectives”). Given the different techniques employed in various spectral ranges, observational astronomers were in the past—and often remain today—specialized in some window of the electromagnetic spectrum. Optical, radio, and X-ray data are produced by astronomers working in different communities. For example, radio astronomers are not always cognizant of interesting discoveries made by optical and UV spectroscopists and viceversa. These facts grounded in the historical development of astronomical research justifies our attempt to review major observational achievements across the electromagnetic

spectrum with the various spectral ranges ordered according to a rough sequence of historical development. The visual and UV are considered first. Thanks to the high redshifts, the UV spectra of quasars were known well in advance of the launch of the first spaceborne UV telescope. The optical/UV spectral phenomenology remains a (often confusing) part of the operational definition of a quasar.

As customary in other fields of astronomy, there are nearby and bright objects that are deeply and frequently studied. Quasars are variable sources, and several have been monitored over past decades. These sources prove to be pivotal to our understanding of the larger population. Even the most elusive form of photometric variability—microvariability—provides valuable information on the accretion process. A broader view is however achieved by the statistical analysis of large samples of quasars, often labeled as flux-limited (an unspoken acknowledgement that the samples are much affected by the Malmquist bias). A major boost for these studies came from the *Sloan Digital Sky Survey* (SDSS [20])—but also Large Bright Quasar Survey [12], 2QZ [5], and others). Is it possible to organize spectroscopic diversity found in large samples of quasars or are quasars essentially clones of each other? Hence our questions about eigenvector techniques.

Chapter 4 (“Quasar Classes and Their Relationships”). The previous chapter reviews results of multiwavelength observations. This chapter reflects the need to interpret these observations within the context of different unification schemes. Unification is a potentially powerful framework within which to organize various aspects of quasar phenomenology. Orientation unification is a good example of a special challenge facing quasar (but not stellar) astronomers. First attempts at unification date back to the early 1970s. The pioneering scheme of Scheuer and Readhead [18] is now abandoned: radio-quiet sources are very unlikely to be misaligned radio-loud quasars (well justified at the time). A consolidated unification scheme for radio-loud AGNs is now supported by developments in interferometric radio astronomy. What physical processes form the basis of unification schemes? Are Unification schemes a framework (if not a theory) with predictive power? Do they really apply to all sources?

Chapter 5 (“From Observations to Physical Parameters”). The next logical step is to ask how observations might be connected to theoretical models. Editorial biases may be unavoidable here as we concentrate mainly on what can be derived from optical and UV spectroscopy. There is strong focus on approaches that have become widespread in the past 10 years and that will likely be pursued with a broader scope in the coming years. They are aimed at obtaining the two most important physical parameters of quasars interpreted as accreting systems: the mass of the central black hole and the accretion rate. Many questions are directed at learning how we measure these parameters and estimate their accuracy.

Chapter 6 (“Models of Quasars”). Modern astronomers can still be described as observers or theorists. While this distinction is not a rigid one—many are involved in both observations and theoretical studies—this is the way it has been for the past 50 years. In this chapter, theorists were given free rein to talk about the most advanced and recent theoretical ideas and computations. Can observations lead to models in a convincing way?

Chapter 7 (Quasars in the cosmic environment). Quasars, viewed today as accreting supermassive black holes, likely accrete a large amount of matter to sustain their extreme luminosities. Infall of gas toward the center of a quasar host galaxy is crucial to this accretion process. The birth and evolution of quasars is believed to be influenced by the host galaxy and by its environment. No gas—no quasar. The discovery of high-redshift quasars ($4 < z < 6$) since the early 1990s indicate that quasars (or better, seed black holes in the center of protogalaxies) must have formed at a very early epoch. How early? Perhaps, too early to be consistent with Big Bang cosmology? Summarizing the response of the contributors in this chapter, we will try to find a “reassuring” answer to this very provocative question. On the other hand, the enormous amount of energy released by a quasar is believed to affect the host galaxy evolution in a complex interplay of radiative and mechanical process that is hotly debated at present.

Chapter 8 (“The Future of Quasar Studies”). Our final contributor chapter focusses on future developments that will come from planned ground and space-based instrumentation as well as from the expected discovery of many more quasars. Large aperture, wide-field telescopes that are expected to become operational in the next decade will almost certainly discover an enormous number of quasars. How many will be found at redshifts higher than six? How will “digital observatories” built from the archived observations of planned instruments with enormous multiplexing ability affect our knowledge?

Chapter 9 (“Fifty Years of Quasars: Current Impressions and Future Perspectives”). In this chapter, we take editorial license to give some interpretations and conclusions that we have drawn from the varied and fascinating contributions. It will be the questionable privilege of the editors (who cannot shake off an uncanny feeling of appearing wrong or naïve in due time) to carry out the developments described in Chap. 8 a bit further ahead in time, speculating on how our knowledge of quasars might improve in the coming decades, even if not as far as 50 years ahead from now. Looking back at how different the world was 50 years ago, and not only in astronomy, makes us realize that guessing 50 years in advance is really beyond our imagination.

Now that we have introduced our motivations, we think it is now time to leave the floor to the many contributors and to their varied life and research experiences.

References

1. Abell, G.O.: The distribution of rich clusters of galaxies. *Astrophys. J. Suppl.* **3**, 211 (1958)
2. Arp, H.C., Bolton, J.G., Kinman, T.D.: A quasi-stellar object with a redshift of 2.22 and an unusual absorption spectrum. *Astrophys. J.* **148**, L165 (1967)
3. Baade, W., Minkowski, R.: Identification of the radio sources in cassiopeia, Cygnus a, and Puppis a. *Astrophys. J.* **119**, 206 (1954)
4. Burbidge, G.R., Burbidge, E.M.: *Quasi-Stellar Objects*. Freeman, San Francisco (1967)
5. Croom, S.M., Smith, R.J., Boyle, B.J., Shanks, T., Loaring, N.S., Miller, L., Lewis, I.J.: The 2dF QSO redshift survey – V. The 10k catalogue. *MNRAS* **322**, L29–L36 (2001)

6. Curtis, H.D.: Descriptions of 762 nebulae and clusters photographed with the crossley reflector. *Publ. Lick Obs. (University of California Press)* **13**, 31 (1918)
7. Edge, D.O., Shakeshaft, J.R., McAdam, W.B., Baldwin, J.E., Archer, S.: A survey of radio sources at a frequency of 159 Mc/s. *Mem. R. Astron. Soc.* **68**, 37–60 (1959)
8. Freedman, W.L., et al.: Final results from the hubble space telescope key project to measure the hubble constant. *Astrophys. J.* **553**, 47–72 (2001)
9. Greenstein, J.L., Matthews, T.A.: Redshift of the radio source 3C 48. *Astron. J.* **68**, 279 (1963)
10. Greenstein, J.L., Schmidt, M.: The quasi-stellar radio sources 3c 48 and 3c 273. *Astrophys. J.* **140**, 1 (1964)
11. Hazard, C., Mackey, M.B., Shimmins, A.J.: Investigation of the radio source 3C 273 by the method of lunar occultations. *Nature* **197**, 1037–1039 (1963)
12. Hewett, P.C., Foltz, C.B., Chaffee, F.H.: The large bright quasar survey. 6: Quasar catalog and survey parameters. *Astron. J.* **109**, 1498–1521 (1995)
13. Hoyle, F.: *Galaxies, Nuclei and Quasars*. Heinemann, London (1966)
14. Minkowski, R., Greenstein, J.L.: The power radiated by some discrete sources of radio noise. *Astrophys. J.* **119**, 238 (1954)
15. Morgan, W.W.: A comparison of the optical forms of certain seyfert galaxies with the n-type radio galaxies. *Astrophys. J.* **153**, 27 (1968)
16. Sandage, A.: The existence of a major new constituent of the universe: The quasistellar galaxies. *Astrophys. J.* **141**, 1560 (1965)
17. Scheuer, P.A.G.: Models of extragalactic radio sources with a continuous energy supply from a central object. *MNRAS* **166**, 513–528 (1974)
18. Scheuer, P.A.G., Readhead, A.C.S.: Superluminally expanding radio sources and the radio-quiet QSOs. *Nature* **277**, 182–185 (1979)
19. Schmidt, M.: 3C 273: A star-like object with large red-shift. *Nature* **197**, 1040 (1963)
20. Schneider, D.P., et al.: The sloan digital sky survey quasar catalog. IV. Fifth data release. *Astron. J.* **134**, 102–117 (2007)
21. Seyfert, C.K.: Nuclear emission in spiral nebulae. *Astrophys. J.* **97**, 28 (1943)
22. Shklovskii, I.S.: Application of the special-relativity principle to an interpretation of some sources of cosmic radio waves. *Soviet Astron.* **12**, 730 (1969)
23. Spergel, D.N., et al.: Three-year Wilkinson microwave anisotropy probe (WMAP) observations: Implications for cosmology. *Astrophys. J. Suppl.* **170**, 377–408 (2007)
24. Trimble, V., Woltjer, L.: Quasars at 25. *Science* **234**, 155–161 (1986)
25. Véron-Cetty, M.-P., Véron, P.: A catalogue of quasars and active nuclei: 13th edition. *Astron. Astrophys.* **518**, A10 (2010)
26. Zwicky, F., Herzog, E., Wild, P.: *Catalogue of Galaxies and of Clusters of Galaxies, vol. I*. California Institute of Technology (CIT), Pasadena (1961)

Chapter 2

Quasars in the Life of Astronomers

Contributions by Mauro D’Onofrio, Paola Marziani, Jack W. Sulentic, Suzy Collin, Giancarlo Setti, Martin Gaskell, Joe Wampler, Martin Elvis, Iraida Pronik, Vladimir Pronik, Sergey Sergeev, Aleksander Volvach, Julian Krolik, Hagai Netzer, Alfonso Cavaliere, Paolo Padovani, Halton Arp, and Jayant Narlikar

M. D’Onofrio

Dipartimento di Astronomia, Università degli Studi di Padova, Vicolo Osservatorio 3,
I35122 Padova, Italy
e-mail: mauro.donofrio@unipd.it

P. Marziani

INAF, Osservatorio Astronomico di Padova, Vicolo Osservatorio 5, IT35122 Padova, Italy
e-mail: paola.marziani@oapd.inaf.it

J.W. Sulentic (✉)

Instituto de Astrofísica de Andalucía (CSIC), Granada, Spain
e-mail: sulentic@iaa.es

S. Collin

LUTH, Observatoire de Paris-Meudon, Section de Meudon, 92195 Meudon, France
e-mail: suzy.collin@obspm.fr

G. Setti

INAF-Istituto di Radioastronomia, Via P. Gobetti, 101 40129 Bologna, Italy
e-mail: setti@ira.inaf.it

M. Gaskell

Departamento de Física y Astronomía, Facultad de Ciencias, Universidad de Valparaíso,
Av. Gran Bretaña 1111, Valparaíso, Chile
e-mail: martin.gaskell@uv.cl

J. Wampler

330 Llama Ranch Lane, Santa Cruz, California CA 95060, USA
e-mail: jwampler@cruzio.com

M. Elvis

Harvard Smithsonian Center for Astrophysics, Cambridge MA02138, USA
e-mail: elvis@cfa.harvard.edu

I. Pronik · V. Pronik · S. Sergeev

Crimean Astrophysical Observatory, 98409, Nauchny, Crimea, Ukraine
e-mail: ipronik@mail.ru; vpronik@mail.ru; sergeev@crao.crimea.ua

A. Volvach

Radio Astronomy Laboratory of Crimean Astrophysical Observatory, 98688, Ukraine, Crimea,
Yalta, Katsively, RT-22
e-mail: volvach@crao.crimea.ua

In this chapter, we collect reminiscences and experiences about the early days of quasar astronomy. The recollections of two of the major pioneers who have recently passed away, Geoffrey Burbidge and Allan Sandage, can be found in two Annual Review papers [38, 197]. Others have given their experiences at earlier times [34, 201]. Our contributors involve mostly astronomers who entered the field around or in the decade after the time of the discovery, living both in different Western countries and in the Soviet Union. These authors provide insight into the state of experimental and theoretical astrophysics largely in the period from 1965 to 1980. Questions addressed include early developments in detectors (the pre-CCD times). Specific goals were to discover when it was realized that Seyfert galaxies and quasars were part of the same phenomenon as well as when the black hole—accretion disk paradigm became widely accepted. We also try to catch the flavor of the debate about the nature of the redshift which was provoked by the discovery of the quasars. The first sections consider the discovery of quasars. They are intended to reflect the state of extragalactic astrophysics in the early 1960s with a focus on the hottest issues and the instrumental and computing capabilities of the time. Questions will deal with the early development of radio astronomy, the unexpected discovery of hyper-luminous radio galaxies, and subsequently, extragalactic X-ray emission. There are some questions about early assessments of the physical problems entailed with the discovery of quasars that eventually led the standard paradigm and unification.

J. Krolik

Department of Physics and Astronomy, Johns Hopkins University, 3400 N. Charles Street,
Baltimore, MD 21218-2686, USA
e-mail: jhk@jhu.edu

H. Netzer

School of Physics and Astronomy, Tel Aviv University, Tel Aviv 69978, Israel
e-mail: netzer@wise.tau.ac.il

A. Cavaliere

Dipartimento di Fisica, Università di Tor Vergata, via Ricerca Scientifica 1, 00133 Roma, Italy
e-mail: cavaliere@roma2.infn.it

P. Padovani

European Southern Observatory, Karl-Schwarzschild-Str. 2, D-85748 Garching bei München,
Germany
e-mail: ppadovan@eso.org

H. Arp

Max Planck Institut für Astrophysik, Karl Schwarzschild Str. 1, Postfach 1317, D-85741 Garching
bei München, Germany
e-mail: arp@mpa-garching.mpg.de

J. Narlikar

Inter-University Centre for Astronomy and Astrophysics Post Bag 4, Ganeshkhind,
Pune 411007, India
e-mail: jvn@iucaa.ernet.in

2.1 Quasars seen from Europe

Dear Suzy (*Collin*), what attracted you to this research field? When you entered the field, did you find a paradigm (e.g., supermassive black hole, accretion disk, obscuring torus) already fixed in place? If not, what ideas about, and interpretations of, the quasar phenomenon were in vogue?

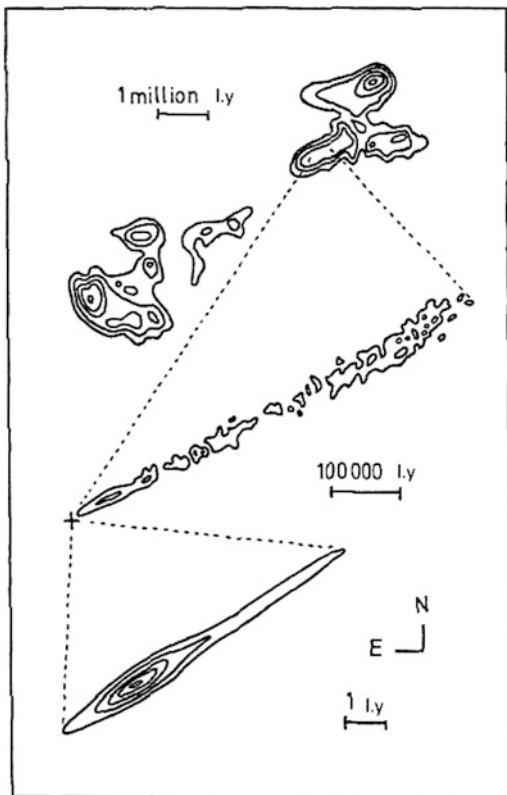
I began to work on Seyfert galaxies in 1965, 2 years after the discovery of the first quasars. I was previously preparing a thesis on solar flares—thesis could take up to 8 or 10 years in France in the 1960s—when I discovered the paper by Greenstein and Schmidt [101] where they concluded that the only possible explanation for the redshifts of the recently discovered quasars 3C 273 and 3C 48 was the Hubble law, which led to attribute them the power of hundreds of galaxies. And almost at the same time, came the discovery that 3C 273 was variable in timescales of weeks! I decided to change the subject of my thesis (my adviser, Evry Schatzman, often incited his students to follow their own preferences). I chose quasars because, having worked a little on solar flares, I was attracted by energetic phenomena. I was also aware of the papers on radio galaxies by Burbidge [37] who noticed, on the basis of simple considerations of energy equipartition, that the intensity of synchrotron radiation implied an enormous amount of energy in magnetic field and relativistic particles, corresponding to the transformation of 10^6 – $10^8 M_{\odot}$ into radiation for instance in Cygnus A (the uncertainty is due to the fact that one does not know how much energy in protons is associated with relativistic electrons).¹ I have the impression that very few people realized the importance of this result.

Finally, I preferred to work on the galaxies discovered by Carl Seyfert 20 years before [209] which were much less “fashionable” than quasars in 1965. Few weeks before the discovery of quasars, Burbidge et al. [40] have indeed published a long paper entitled “Evidence for the Occurrence of Violent Events in the Nuclei of Galaxies” which was a prefiguration of quasars from the energetic point of view. Thus, after the quasar’s discovery, Seyfert galactic nuclei were immediately suspected to have some relation with them because of their bright blue nucleus and intense broad spectral lines. It was quite premonitory since after all, quasars were proved to be active galactic nuclei (AGNs as we call them now) only when the first “host galaxies” were unambiguously identified with large telescopes in the 1980s. For radio galaxies, one can consider that their relation with nuclei of galaxies was demonstrated only by the first observation of the jet linking the compact radio nucleus to the big radio lobes in NGC 6251 [187] (cf. Fig. 2.1).

When I began to work on the subject, there were almost no studies of Seyfert nuclei since that of Seyfert himself, except two by Woltjer [237] and by Burbidge et al. [36] published in the same ApJ issue, whose conclusions were in total conflict. Burbidge et al. studied the rotation curve of the Seyfert galaxy NGC 1068 and

¹Actually, he underestimated the energy by an order of magnitude because he used an old value of the Hubble constant.

Fig. 2.1 This radio map of NGC 6251, as published by [187], shows that a small jet of 5 light-years long located in the galactic nucleus is aligned with a larger jet of 600,000 light-years, itself aligned with the direction of the radio lobes, separated by 9 million light-years



deduced that the gas giving rise to the emission lines should be ejected from the nucleus. While Woltjer, discussing the properties of the line emission in six Seyfert galaxies, concluded that it should be gravitationally confined by a massive body. Woltjer was right, but with wrong arguments, because he overestimated the mass of the ejected gas (which he assumed to be homogeneous) and concluded that it could not be ejected unless the whole galaxy would have been emptied rapidly. Burbidge et al. were right because NGC 1068 is a peculiar Seyfert (we call it now a Seyfert-2), whose emission lines are formed at a much larger distance than in the other Seyfert galaxies and are partly outflowing, while the others were mainly what we call now Seyfert-1 galaxies. From the rotation curve, Burbidge et al. deduced a central mass of $3 \times 10^{10} M_{\odot}$ which was basically correct, corresponding to an escape velocity of 450 km s^{-1} , and since the lines indicated a velocity spread of $1,450 \text{ km s}^{-1}$, the gas was clearly not gravitationally bound. I think it is unfortunate that Burbidge et al. were studying just this galaxy, which led them to conclude that what occurs in Seyfert nuclei is related with the phenomenon taking place in radio galaxies, that is, ejection of plasma and relativistic particles, and to generalize this result. It was the first aspect of the controversy on “anomalous redshifts” which lasted for 20 years (and is even lasting now).

I observed the most brilliant Seyfert nuclei at the Haute-Provence Observatory, with the help of Dr. Yvette Andrillat who was specialized in the observations of novae and planetary nebulae. We used an old 120-cm Cassegrain telescope, to which were attached several low-dispersion spectrographs from the near UV (3800 Å) to the infrared (9000 Å), necessary for our study. We used photographic plates because at this time, there was only one electronic device in France, the so-called “electronic camera” which could be used only for relatively bright objects like the M31 nucleus [133]. We had to go through a complex reduction process, implying in particular the measure of a comparison star located on the sky close to the galaxy, whose absolute flux as a function of wavelength was known. Moreover, since the sensibility of the detectors was so low, the exposure times were very long in order to get not too noisy spectra, and it was a real challenge to maintain by eye the slit exactly on the nucleus. All reductions were made with pencil and paper, and the equivalent widths of the lines were measured with a planimeter.

In 1968, when I published my thesis (in French, as it was common at this time [216] and [217]), a paper appeared also on Seyfert nuclei by Dibai and Pronik [70]. We came to the same conclusion that there were two different emission regions, one made of dense and small clouds emitting broad lines (the “broad-line region” or BLR as it was called), and one made of dilute and large clouds emitting narrow lines (the “narrow-line region” or NLR). The “narrow lines” were actually mainly forbidden lines, like the [OIII] lines at 4959–5007 Å.² Their presence implies that the medium is very dilute and therefore extended. The second type of spectral lines (like the Balmer or the Lyman series of hydrogen) are “permitted”, because their upper level has a short lifetime, and line photons are very easily emitted. As already mentioned, the line widths in Seyfert nuclei were (and are still now) attributed to Doppler motions. But the permitted and the forbidden lines are not broadened similarly, except in NGC 1068. The widths of the forbidden lines correspond to velocities of a few hundreds km s⁻¹, while those of the permitted lines correspond to velocities of a few thousands km s⁻¹. It means that they come from two different regions, which must have different densities: in the region emitting the forbidden lines, the density must be smaller than 10⁶ cm⁻³, and in the region emitting the permitted lines, the density must be larger than 10⁶ particles cm⁻³ to explain why no forbidden lines are observed (from the study of the line intensities, one deduces that it is in fact at least 10¹⁰ cm⁻³). In the 1970s, one begun to make a distinction between two types of Seyfert nuclei: type-1 Seyfert, with both broad and narrow lines, and type-2 Seyfert, with only narrow lines.

From the temperature found in the dilute clouds, I deduced that they were photoionized by an intense UV continuum, contrary to the widely accepted opinion

²When they were discovered in planetary nebulae at the beginning of the twentieth century, these lines were attributed to an unknown element called “nebulium”—not expected by Mendeleiev table!—and their nature was understood only 30 years later. The same story happened for a line observed during solar eclipses and attributed to an unknown element called “coronium”; it is actually also a forbidden line, this time of highly ionized iron, also present in the spectrum of Seyfert galaxies.

that they were heated and ionized by suprathermal particles (as proposed by [168]). Besides, Andrillat and myself [3] found evidences for variations of the profile of the broad $H\beta$ line in the nucleus of NGC 3615 since Seyfert's 1943 observations. Owing to the difficulty of the measurements (in particular we feared to have moved the slit during long observations and to have therefore observed circumnuclear regions), we went on observing carefully this nucleus during several years, and we confirmed the variation in a timescale of a few years, but I think that the result was not accepted before other people confirmed our finding (though it was quite predictable, owing to the small size of the emitting region). I must add that I wrote to the referee of our paper that "if we were not women and French, he would have accepted our paper without discussion!" One knows that such variations have been extensively monitored since 1985 within the "AGN Watch", and have led to the determination of the masses of about forty black holes in active nuclei. It is why I am always paying attention to ideas which are not in the main stream.

During the 1960s, there was no single paradigm concerning the origin of the energy radiated by quasars. On the contrary, many explanations were proposed, and they almost all involved stars: front collisions of stars with high velocity, chain explosions of supernovae, "flares" at the galactic scale, etc. The most popular was a "supermassive star" energized by nuclear reactions or by pulsations leading to gravitational release. The reason was certainly because stellar studies had been very successful during the previous decade, and some of their eminent promoters (the Burbidges, Hoyle, Fowler) were active in the quasar and AGN field. This was illustrated during the meeting held in 1971 in Cambridge for the 60th birthday of Hoyle, "supermassive objects," which was devoted mainly to quasars. After the discovery of the first pulsars in 1968, "supermassive rotators" were also privileged, because massive stars are highly unstable and can be stabilized by rotation. However some people have guessed immediately the correct explanation: Salpeter [194] and Zel'dovich [240] suggested independently that a massive black hole (MBH) was present in these objects, and Salpeter proposed that the matter and angular momentum was transported, thanks to a turbulent viscosity (as one knows, this is the presently most accepted view). But nobody took this idea seriously, except general relativity specialists. Lynden-Bell was the first to reiterate their suggestion [138], and again, the year after at the famous Vatican conference on "Nuclei of Galaxies."³ Apparently, almost none of the 25 well-known astronomers that were attending it paid due attention to this model. Instead, most were attracted by "non-cosmological redshifts", which were still largely discussed at this time.

You attended the first focussed meeting on Seyfert galaxies held at the Steward Observatory in 1968. What kinds of observations and ideas were presented at that conference? Was it already established that Seyfert galaxies and quasars were different luminosity manifestations of the same phenomenon?

³These meetings in the Vatican take place from time to time, and it was the first devoted to astrophysics. They gather a few of the best scientists in a given science, to discuss some fundamental issue on which experts have contradictory opinions.

I attended the meeting on “Seyfert nuclei and related objects” in Tucson (1968), which was indeed the first one on Seyfert nuclei. “Related objects” were actually mainly quasars and radio galaxies (at this time, often called “N-galaxies”). There were already several books published on quasars and radio galaxies, but none on Seyfert nuclei. When reading the introduction (by Minkowski) and the conclusions (by Woltjer and Osterbrock), I am amazed of how many things were not understood in spite of the available observations, but of course, these were limited to radio and to the optical and near-infrared bands. The meeting was mainly observational, with only a few theoretical papers. In particular, the idea that the ionization and heating of the gas could be due to UV radiation was stressed by myself and by Williams and Weymann. The following topics were among those debated in Tucson:

- It was not clear at all that quasars were galactic nuclei like the Seyfert ones, owing to the enormous gap in luminosity between the two classes (Barnothy’s suggestion that quasars could be gravitationally lensed, Seyfert nuclei was statistically not tenable). This is strange since Schmidt [200] had already proved that quasars undergo a big cosmological evolution in luminosity and/or in number, but this result was not extended to the present time. We think now that there is a continuous transition between quasars and Seyfert galaxies along the cosmic time, Seyfert galaxies being very low luminosity quasars, the only ones which can be activated presently.
- Concerning Seyfert nuclei, the difference between Seyfert-1 and 2 was not pointed out (and a fortiori not understood). It was thus difficult to understand the diversity of the spectra and the line broadening (which was attributed also to electron scattering).
- Synchrotron radiation was assumed to be responsible for the blue continuum of Seyfert galaxies and radio-quiet quasars, presumably by analogy with radio galaxies. This idea prevailed during almost 20 years, and it certainly did much damage to the black hole model. It was dismissed by Shields [212] who proposed instead that the radiation was of thermal origin, due to the accretion onto the black hole.
- Coronal lines were attributed to a very hot gas, by analogy with the solar corona. It is mostly believed now that they are formed in a warm gas photoionized by X-rays, but at this time, one could certainly not imagine that the bolometric luminosity could be dominated by a “big blue bump.”
- A density larger than 10^8 cm^{-3} for the BLR was not accepted, and this is why a long discussion (without any solution) was devoted to the “Balmer decrement” problem. One knows now that the large Balmer decrement, as well as the small $L\alpha/H\beta$ ratio put into evidence by Baldwin [20], are due to the combined effects of a large optical thickness and a high density (larger than 10^{10} cm^{-3} cf. Netzer [160] and subsequent papers).
- The problem of the affiliation of several classes of objects to Seyfert nuclei was not clear at all (and one understands now why, in particular thanks to the Unified Scheme).
- The bulk of the luminosity was assumed to be in the near infrared.
- etc, etc...

Clearly, at the time of the Tucson meeting, there was a lack of key observations, in particular in the UV and X-ray range, and also a great need for a theoretical model. Then, during the 10 following years, progress was relatively slow, as is always the case when a theoretical background is not ready at the time of a discovery (contrary for instance to what happened for pulsars or for the cosmic radiation), and when the observations are sparse and not statistically significant. The breakthrough came only at the end of the 1970s, when Rees proposed an astrophysical context for the MBH model with his “flow chart” [185]. Then immediately after, “accretion onto a massive black hole” was widely accepted and became a paradigm.

Thank you Suzy for your recollection of the debate that took place soon after quasar discovery. We now would like to hear the point of view of a radio astronomer about the early developments that were pivotal for that discovery.

2.2 Quasars in the Early Radio Sky

Dear Giancarlo (*Setti*), please share with us your impressions about the first years after the discovery of quasars.

The 1960s will be remembered as the *mirabilis* decade of astronomy for the string of major discoveries that took place at an impressive rate (extrasolar X-ray astronomy, quasars, the CMB, and pulsars), a revolution in cosmology, and the foundation of high-energy astrophysics. Second, in the string of discoveries, the quasars immediately attracted much attention not only among astronomers but also in the physics community and in the media, to the extent that the name became part of the common language. On this last point, I recall the headlines on newspapers reporting the suggestion of some Russian radio astronomers that the strong variability on short timescales of the compact radio source CTA 102, then identified with a quasar ($z \sim 1$), could be evidence of the broadcasting station of a very advanced extraterrestrial civilization. As a young researcher attending the 2nd Texas Symposium on Relativistic Astrophysics (Austin, December 1964), I was impressed and almost scared by the extremely qualified list of participants including, among a large number of well-known physicists and astronomers, Paul Dirac, a Nobel laureate in physics. A large part of the symposium was dedicated to the radio galaxies and quasars of which only a handful were known, and so everybody was eagerly waiting for new observations which could possibly constrain the field of theoretical speculations. Obviously, the nature of the redshifts, was central to the discussion. I was particularly impressed by the lucid exposition of Maarten Schmidt, based on a paper [101] just published in *The Astrophysical Journal* in collaboration with Jesse Greenstein of Caltech. From the analysis of the optical spectra of the quasars 3C 48 and 3C 273, he concluded that the gravitational origin of the redshifts was not viable because the differential redshifts would have washed out the lines and proposed, in the framework of the cosmological hypothesis, a simple quasar model consistent with all available data as an HII region of parsec

scale size and a patchy gas distribution, encapsulating a central power source of the optical continuum. After half a century, I still consider the Greenstein–Schmidt paper as a classic contribution to the subject. Thus, the question of the redshifts remained confined to the possible choice between a Doppler shift as opposed to the cosmological interpretation.

In the first years after their discovery, did you think that the quasars might be a largely radio phenomenon?

The quasi-stellar galaxies (QSG) were proposed by Allan Sandage [196] as a major new constituent of the universe with optical properties very similar to the quasars, but with no evidence of radio emission. The paper appeared in *The Astrophysical Journal* in mid-1965, just about 6 months after the 2nd Texas Symposium. As I recall it, no explicit mention about them was made by Sandage at that meeting; instead, he reported on an ongoing project in collaboration with Philippe Véron, aiming at selecting blue stellar objects that he called “interlopers,” by a two-colour photographic technique to ease the finding of quasars by comparison with radio source positions. However, what mostly struck me reading Sandage’s paper was the large number of QSGs compared to the estimated number of quasars, almost a factor 1,000, meaning that perhaps the radio emission was a transition phenomenon or, may be, something else to be identified. But to me, the basic characteristics of the quasars, aside from the discovery’s history, as of a starlike appearance, large redshifts, optical variability, broad emission lines, nonthermal continua, and UV excess were all present in the QSG of Sandage. On the other hand, a similar situation was already known for the Seyfert’s galaxies characterized by compact bright nuclei with optical spectra similar to those of the quasars, but with a relatively weak radio emission. So it was natural to speculate that perhaps the QSGs represented the very bright end of the Seyferts’ luminosity function and that together with the quasars, they combined in forming a unique class of quasi-stellar objects (QSOs) representative of the extreme energetic events taking place in galactic nuclei.

As a matter of fact, I thought that this picture was indirectly supporting a coherent cosmological scenario. Therefore, my answer to the first question is negative.

But “natural” and “speculate” as used above are very imprecise terms that must be substantiated by observational evidence. It was tempting to think that radio-loud quasars with diffuse radio structures very similar to the strong radio galaxies could be the expression of the activity in the nuclei of giant elliptical galaxies. But the morphologies of the putative host galaxies were completely outshined by the quasar luminosities. It was only after many years that Woltjer and I [207] tried a first approach to the problem by looking for possible similarities in the optical spectra of quasars with those of radio and Seyfert galaxies. For instance, by examining a small sample of low-redshift QSOs, for which good optical spectra were available, we noticed that similarly to the broad-line radio galaxies, all radio-loud quasars with steep radio spectra ($\text{flux} \propto \nu^{-\alpha}$; $\alpha > 0.7$) and extended radio lobes did not show the presence of the iron line $\text{FeII}\lambda 4570$ and generally presented a strong Balmer decrement, at variance with the Seyfert galaxies (mostly spirals). So one

could argue that this type of quasars is the active nuclei of giant elliptical galaxies. The sample contained too few radio-quiet quasars to reach any statistically valid conclusion. Much work has since been done on the emission-line properties of QSOs starting from the classic work of Boroson and Green [28], and I am sure some other author in this volume will report on this very important but extensive subject.

In 1966 (and also in 1973 at the 6th Texas Symposium), you and Lo Woltjer discussed the local hypothesis for the quasars. What led you to rule this out?

At the 2nd Texas Symposium, Geoffrey Burbidge strongly argued against the cosmological nature of the quasars' redshifts, mainly on energetic grounds. He estimated that if placed at the large distances implied by their redshifts, the total energy involved in the acceleration of the relativistic particles and in the magnetic fields filling the radio volume of a typical quasar was equivalent to the rest mass energy of ten billion solar masses, that is, about 10% of the mass of a sizable galaxy like the Milky Way, which he deemed to be unrealistic. Therefore, he favored a "local" interpretation of the quasars and a Doppler nature of their redshifts, objects ejected at high speeds in explosive phenomena occurring in galaxies such as, for instance, the radio galaxies. An immediate problem with this hypothesis was the absence of observed blue shifts, as would be expected in random ejection phenomena unless very contrived scenario were assumed. Early on, James Terrell had advanced an easy way out of this dilemma by proposing that the quasi-stellars were small objects, light days across on the basis of the detected time variability, ejected by the Milky Way at speeds close to the light velocity. Burbidge and Hoyle argued that a better candidate could be the relatively nearby radio galaxy NGC 5128 (Cen A). Remember that the basic argument put forward in support of a local hypothesis was the large source energy budget under the cosmological interpretation of the redshifts. What Woltjer and I [204] did was to show that the local hypothesis for the origin of the QSOs required minimum energies by far larger than those associated to the high-energy phenomena manifest in our Galaxy and Cen A. This would still hold if one considers the QSS population only which represents about 10% of the overall QSO population. Therefore, the local hypothesis did not seem to ease the energy problem, on the contrary.

One of the argument frequently raised against the cosmological hypothesis was the apparent lack of the Hubble relationship, that is, the progressive weakening of the observed luminosities with increasing redshifts or distances of the QSOs. What Woltjer and I [205] pointed out was that the Hubble diagram could be completely blurred by the mix of various types of quasars. To this end, we subdivided the overall quasars' population known at that time into three categories according to their radio properties: quasars with steep ($\alpha > 0.7$) radio spectra and extended radio structures typical of the strong radio galaxies, quasars with flat ($\alpha < 0.6$) radio spectra and compact radio structure, and optically selected quasars with no detectable radio emission. It was found that steep radio spectra quasars did follow the Hubble relationship: the plot of the redshift vs. the visual magnitudes of the objects showed a clear upper envelope sloping upward with increasing redshift in

agreement with the cosmological interpretation of the redshifts. The somewhat large dispersion could be easily accounted for in terms of a broad luminosity function. The sample included quasars with well-separated double radio structures for which a systematic decrease of the angular diameters with increasing redshift had already been established. As a consequence, it appeared that quasars with steep radio spectra did comply with the two basic tests for the cosmological interpretation of the redshift. As a corollary, it was conjectured that this type of quasars, similarly to the strong radio galaxies, could be associated to the giant elliptical galaxies, basically the same objects.

On the other hand, the Hubble diagrams for the two distinct samples of flat radio spectra and radio-quiet quasars did not show any systematic behavior with the redshift. Although no definite conclusions could be reached as to the nature of their redshifts, however the close similarity of the object distributions in the redshift-V magnitude plane with that of the steep radio spectra quasars pointed to a most likely interpretation of the absence of redshift correlations in terms of broader luminosity functions.

But perhaps the strongest evidence against any possible local hypothesis was suggested by Woltjer and myself [206] already several months before the 6th Texas Symposium in a paper, summarizing the possible contributions of different classes of objects to the extragalactic X-ray background. At that time, 3C 273 was the only quasar detected in X-rays in the 2–10-keV band. By assuming a constant ratio of optical to X-ray luminosity for all QSOs and integrating over the available QSO counts down to the 19.4 blue magnitude, we estimated a 13% contribution to the X-ray background and possibly much greater (up to 2/3) by applying a still somewhat uncertain extrapolation of the optical counts down to the 23rd magnitude. As a consequence, any “local” hypothesis involving an association of the bulk of the QSOs with our Galaxy or other galaxies within a distance corresponding, to be generous, to a redshift of 0.1 would have by far violated the limit imposed by the X-ray background, unless we were placed in a very special region of the universe or, alternatively, unless 3C 273 was exceptionally bright in X-rays, a possibility we considered unlikely. It is remarkable that our conjecture, based on one object, maintained its basic validity as new data on the optical and X-ray properties of QSOs accumulated. I may just add that present knowledge indicates that the contribution of the QSOs to the X-ray background at the reference energy of 1 keV is just over 30% of which about 1/3 due to radio-loud quasars [98].

For the sake of completeness, I may also add that the same argument might be applied in the γ -ray regime, although restricted to a subgroup of the overall quasar population. Following the discoveries made with the EGRET instrument onboard the NASA Gamma Ray Observatory, we pointed out [208] that a large fraction of the extragalactic γ -ray background above 100 MeV could be accounted for by the integrated observed emission of flat spectra radio quasars. Indeed, present evidence with the NASA *Fermi* gamma ray satellite indicates that these objects contribute about 16% of the extragalactic γ -ray background measured by *Fermi*. Again, if the radio-loud quasars would be “local” objects, then the background would be largely exceeded.

Did you favor any version of the standard model at that time?

As it normally happens following a major discovery, and in the absence of sufficient observational constraints, quite a number of models were immediately proposed to explain the quasars. One type, that I would collectively call the “many stars” models, involved at least a few hundred million Sun-like stars packed in a parsec scale galactic nucleus—energetic star collisions, self-triggered chain of supernovae explosions, and so on—or many millions of ordinary massive stars distributed in relatively dense nuclei of 100 parsec size giving rise to random supernova explosions, about 100 at any time, during the quasars’ lifetime. Soon, this type of models ran into difficulties in explaining the observed brightness variations both at optical and radio wavelengths, and in particular long term variability. The other type of models was concerned with the presence of single massive bodies, such as the hypothetical new class of supermassive stars suggested by Hoyle and Fowler [111].

I liked this model because of its simplicity: a pulsating massive star energized by nuclear burning and supported by radiation pressure, a mass of up to 10^8 solar masses to meet the energy budget of a typical quasar, a sufficient amount of angular momentum, and an embedded dipolar magnetic field, which could help in understanding the axial symmetry shown by the associated radio source—to me, these were essentially all the basic ingredients one needed to explain the optical and radio emission of quasars. However, the detailed model was much more complex and, in particular, it was not possible to account for the energy stored in relativistic particles and magnetic fields in the extended radio volumes. The discovery of pulsars in 1968 and the successful application of the magnetic oblique rotator model to the very efficient workings taking place in the Crab Nebula, together with the observed variability of the quasar 3C 345 with a period of about 200 days, inspired the idea that perhaps an upscaled version of the pulsar model could represent the powerhouse of quasars. Several papers on this type of model, that is, a centrifugally supported, very massive rotating object with a large scale magnetic field, appeared in the literature at about the same time, included one that I coauthored [46]. For instance, by applying the well-known formulae of the pulsar electrodynamics, one could easily derive that the required luminosity, meaning the total energy output of a typical quasar, would require a massive rotator of about one billion solar masses contained within 0.01 pc (unlike the case of a pulsar where the mass is that of a neutron star, here, one had to make some assumptions about the value of the magnetic field, e.g., in [46], we adopted a value corresponding to a typical magnetic field of the interstellar medium). In a way, these models were closely related to the above-mentioned model of Hoyle and Fowler, except that here, the massive rotators were made of cold nonrelativistic matter. Unlike the polytrope of index 3 objects of Hoyle and Fowler, which could provide the required optical luminosity, in the cold massive rotators, one had to adjust the parameters (such as the magnetic field configuration and the likely presence of differential rotation, the particle acceleration, and so on) in order to account for the observed emission properties via nonthermal mechanisms.

So in answer to your question, I would say that at that time, I was clearly in favor of a massive rotator model as a most likely interpretation of the quasar properties. However, the same year of our work, Lynden-Bell [138] published a paper showing that the main properties of a quasar could be understood in terms of mass accretion onto a MBH. I thought this was providing a simpler and energetically more attractive scenario, also because a main difficulty with the massive rotator model was how to halt the contraction of the accreting mass before reaching the relativistic regime.

How did the Italian astronomical community react to the discovery of quasars? What was the contribution of Italian astronomers who attempted to find new quasars using optical and radio surveys?

My recollection is that the quickest and most felt reactions came from the Bologna group involved in the construction of the “Northern Cross” radio telescope, a large instrument of a sufficient angular resolution and surface area to survey the radio sky at a frequency of 408 MHz in order to discover and locate radio sources down to a limiting sensitivity not yet achieved. Indeed, the strongest scientific motivation behind this project was to make a solid contribution to the extragalactic research and cosmology. Clearly, the discovery of quasars opening unforeseen research possibilities was received with great excitement by the Bologna group lead by the particle physicist Marcello Ceccarelli, all members being very young and some still attending a last year course in physics.

The “Northern Cross” was inaugurated in November 1964, and its 600-m length and about 20,000-square meter surface collecting area of the E–W arm (the N–S arm still under construction) were promptly used to survey the sky. Data from the directions of 15 QSG in the Sandage–Véron list of “interlopers” were collected: none was individually detected, but it was found that by stacking the recorded fluxes in the direction of each object, an average signal of about 0.1 flux units could be present [30]. This corresponded to a radio luminosity at least a factor 50–100 lower than the average radio luminosity of the quasars at the same frequency of 408 MHz. Not a bad result for new comers in experimental radio astronomy! Now, we know that at the reference frequency of 5 GHz, the radio luminosities of radio-quiet quasars are a factor 100–1,000 lower than those of the radio-loud ones and show radio structures similar to those found in the nuclear regions of Seyfert-1 galaxies (e.g., [136]). With the completion of the “Cross” N–S arm, a large program of radio surveys started leading in the early 1970s to the well-known B2 catalogue of about 10,000 sources complete down to 0.2 Jy and to an associated extensive optical identification work with the discovery of many quasars.

On the optical side, the most important earlier contribution was made by Alessandro Braccesi of the Bologna group—by taking into account the typical non-thermal spectra of the QSOs, he had the bright idea of extending the two-colour procedure of Sandage–Véron to look for a combined infrared excess. This represented a major advancement in separating QSO candidates from the stars. The Braccesi and collaborators list of 175 QSOs on a 6.5×6.5 deg² field to the 19.4 blue magnitude has remained for years a most important reference catalogue [31].

Obviously, the Northern Cross project has been the driver for the very early interest of the Bologna group in quasars research. It was only at the beginning of the 1970s that serious work started in other astronomical groups in Italy. In combination with the development of X-ray astronomy, the investigations on quasars and AGNs have since become one of the major fields of research of the Italian astronomical community.

Thank you, Giancarlo. The reader might realize that we have first interviewed two European astronomers—even if they were not involved firsthand in the discovery of quasars. Their answers show that European astronomers were immediately ready to be involved in important quasar research, both on the theoretical and observational side. We now ask a US astronomer who was a graduate student with a very influential group that in the early 1970s carried out the most advanced research in optical spectroscopy.

2.3 Recollections of a US Astronomer

Dear Martin (*Gaskell*), you are a representative of the “Lick Observatory school” which made many pioneering contributions to AGN research—one of the few groups that focussed on high S/N optical spectroscopy.

I think we should call this the “IDS school” because it was the image-dissector scanner (IDS) of Lloyd Robinson and Joe Wampler [190] that made Lick Observatory the center of AGN spectroscopy in the 1970s. Because Joe worked on AGNs, the very first IDS paper published [189] included observations of an AGN, PKS 2251+11.

The IDS revolutionized astronomy. When I was in grad school, it dominated Lick Observatory in general and my life in particular. Joe Wampler was my thesis advisor, and I also worked for a while as a research assistant to Lloyd Robinson, investigating and turning the IDS into a true two-dimensional detector. The obvious thing the IDS did was let one readily get spectra of fainter objects than had hitherto been observable. This was the aspect of the IDS that Joe Wampler immediately utilized. Joe, Lloyd, and Joe’s graduate student Jack Baldwin had their names in the Guinness Book of Records for a decade for having discovered the most distant known object in the universe [232]. Furthermore, when observers at the Anglo-Australian Observatory (AAO) finally beat the Lick Observatory record [174], they did so using an IDS that Joe and Lloyd had taken to the AAO.

Not only could the IDS get spectra of faint objects, but one could just as easily rapidly obtain very high signal-to-noise ratio (S/N) spectra of bright objects on a linear flux scale. The only other competing device at the time, the IPCS [25], was limited to low count rates. High S/N IDS spectroscopy of AGNs began immediately in 1971–1973 with the observations for Jack Baldwin’s thesis [19]. The IDS not only obtained high S/N spectra on a linear scale, but, equally importantly, it could obtain them consistently and repeatedly. Sandy Faber utilized these strengths of the IDS



Fig. 2.2 Martin Gaskell at work in the summer of 1977

for a major program measuring stellar absorption line strengths in elliptical galaxies and related objects—what have come to be called the “Lick indices.” When Don Osterbrock moved to Lick Observatory in 1973, he began a program of systematic high S/N ratio spectroscopy of low-redshift AGNs. Although Joe Wampler was my thesis advisor, Don Osterbrock and his group of graduate students and postdocs were an important influence on me, and Don served on my Ph.D. committee. Don’s group was one of the few groups that focussed on high S/N spectroscopy. Over the years, I have kept coming back to those superb datasets that they acquired (Fig. 2.2). The ability of the IDS to get repeatable high signal-to-noise ratio spectra also meant that it could be used for spectropolarimetry [153].

What motivated you to enter this new research area?

In my last year as undergraduate in the Astronomy Department at Edinburgh University, there was a very stimulating extragalactic astronomy course taught by Ray Wolstencroft. Ray is someone who has worked on a wide range of topics, and he introduced us to many of the then-current topics in galaxy formation and evolution, and AGNs. We looked at the questions of the relationship between galaxies and nuclear activity.

Stimulated by Ray’s course, I had definitely decided that I wanted to go into extragalactic astronomy when I came to Santa Cruz as a graduate student. The question that interested me most at the time was as follows: how did galaxies and clusters of galaxies get to be the way they are now? I began working with Sandy Faber. At Sandy’s suggestion, I initially worked on what proved to be the frustrating task of trying to get bulge parameters of early-type galaxies using photographic plates. At that time, the CCD revolution was still a couple of years in the future—perhaps, I was the last person to attempt getting bulge parameters using photographic plates! At the start of my second year, Joe Wampler returned to Lick Observatory from being the first director of the AAO. Joe invited me to

help him observe on the Lick 3-m, and that was the start of my AGN career. For a while I worked with both Sandy, on the Lick indices of absorption-line strengths (see [43] and [75]), and with Joe on high-redshift AGNs. Ultimately, of course, I had to choose which area to work in for my thesis, and I chose high-redshift AGNs.

Looking back with over 3 decades of hindsight, the odd thing about this time in Santa Cruz was that the connection between AGNs and normal galaxies—something much discussed nowadays and one of the things that had got me interested in extragalactic astronomy through Ray Wolstencroft’s course—was not being made.

Did you focus mainly on low-luminosity Seyfert galaxies in the early days?

No—quite the opposite. I focused on high-luminosity, high-redshift AGNs. In the 1970s, there was a significant separation between people who studied “quasars” (bright, high-redshift AGNs) and those who studied low-luminosity Seyfert galaxies.

When was it realized that Seyferts were likely the low-redshift/low-luminosity manifestations of the quasar phenomenon?

That is a fascinating question, and one that I suspect future historians of science will have an interesting time debating. The question has many dimensions to it. There is “when *should* it have been realized?” and “when *was* it realized?” When one asks “when was it realized?” one has to ask “by whom?” I think the answer varies from country to country, from institution to institution, and person to person.

One answer to the question of “when was it realized?” is to say that it *still* has not been realized by some people! Unfortunately, this is not a joke. One still hears people use the word “quasar” as though a quasar were something fundamentally different from a lower-luminosity AGN. A distinction between “quasars” and “active galactic nuclei” has been maintained by the famous AGN catalogues of the Vérons where AGNs are arbitrarily divided up by luminosity into two separate tables. One still finds this in their recent 13th edition [226]. If you use this catalogue, you can find yourself wondering why some well-known AGNs does not seem to be in it, until you realize you are looking in the wrong table! In the days of searchable online databases this might be less of a problem, but the Sloan digital sky survey (SDSS) has propagated the idea of a quasar/AGN distinction by having had special criteria for targeting quasars and producing lists of quasars. This sort of artificial distinction sometimes leads both to misconceptions and misleading results. For example, Boroson and Lauer [29] did an elaborate search of the SDSS “quasar” database and found that objects with strong, asymmetric, displaced BLR peaks seemed to be extremely rare (about one or two in 17,000). However, their most extreme case is similar to an example I had published in 1983 (see [86,87]) without having had the benefit of the SDSS. AGNs with strong displaced peaks are thus *not* really rare. The reason why they seem to be so in the SDSS quasar database simply lies in how the SDSS makes an artificial distinction between “quasars” and galaxies.

As John Faulkner and I put it in our report on the 1978 Santa Cruz AGN meeting [78], AGN research back then was “bedevilled... by the terminology used to describe the vast subclasses of objects observed.” This was a problem for a long time and remains something of a problem. When you attach different classifications to things, it is all too easy to get convinced that they *are* different things. This would happen within the same research group. Don Osterbrock’s group provided a good illustration. They published important papers separately on radio galaxies (e.g., [166]) and Seyfert galaxies (e.g., [164]).

The idea that Seyferts are low-redshift/low-luminosity manifestations of the quasar phenomenon is really an old idea. The evidence for AGN activity goes back over a century to the first spectroscopy of Seyfert galaxies at Lick Observatory [77]. However, it was not clear at first that the excitation of the emission lines in Seyferts was not due to stars. In fact, people are *still* vigorously discussing the relative roles of stellar and nonstellar excitation. The first clear signs that something was going on in the nuclei of galaxies in addition to familiar stellar processes was the discovery of radio galaxies in the 1940s. In a paper submitted in 1962, Hoyle and Fowler [112] made the important point that the energy in a powerful radio source exceeded the binding energy of a galaxy. From this, they argued for the existence of compact supermassive objects with masses of 10^5 – 10^8 solar masses in the centers of galaxies. In a sequel paper in *Nature*, Hoyle and Fowler [111] showed that such supermassive objects must collapse to what we now call a black hole (I will use our modern name for simplicity—the term “black hole” had not yet been coined), and they pointed out the “decisive importance” of gravitational energy. They considered the width of the broad lines in Seyfert galaxies to be support for the existence of black holes. From the probable lifetime of AGN activity, they argued that every large galaxy had undergone such activity multiple times and hence that there would be dormant black holes in such galaxies. They noted that from imaging at Lick Observatory in 0.5 arcsec seeing Lallemand et al. [133] had estimated the mass within 7.4 pc of the center of M31 to be 1.7×10^7 solar masses.

The date of publication of the Hoyle and Fowler *Nature* paper is significant: it was only a few weeks before the publication in the same journal of the discovery of high-redshift quasars [99, 199]. All the key theoretical pieces were thus in place *before* this discovery: i.e., that radio galaxies and Seyfert galaxies are powered by the release of gravitational potential energy of matter accreting onto black holes, that black hole masses of AGNs are of the order of 10^5 to 10^8 solar masses, that every galaxy (meaning galaxies like our Milky Way or more massive) has gone through at least one AGN phase, and that dormant black holes can be found in nearby inactive galaxies. I should also add that radio source counts [193] had been showing for some time that that there was strong cosmological evolution and that luminous AGNs were much more numerous at early times.⁴

⁴I consider this discovery by the Cambridge radio astronomers that the universe was changing (contrary to the “steady-state” theory) to be one of the great cosmological discoveries. Unfortunately, because of initial problems with source confusion, it was not a clean discovery. Despite this problem, the conclusion of Ryle and Scheuer was shown to be correct [192].

The discovery of bright high-redshift “quasars” [99, 199] not only generated enormous interest in AGNs, but also created confusion for a long time. The high redshifts and the high luminosities implied were a surprise. This led to the so-called redshift controversy in which several prominent astronomers argued that the redshifts observed were not the result of Hubble expansion but of some unknown process. How the redshift controversy arose is another topic for future science historians to enjoy. The result of the controversy was that while nobody doubted that radio galaxies and Seyfert galaxies were the active nuclei of galaxies, many people were reluctant for a long time to lump “quasars” together with other AGNs because of the redshift controversy. The confusion in nomenclature did not help.

The confusion was regional. The clearest idea of the unity of activity in galaxies seems to have been among Soviet astronomers. This can be seen in the introductory lecture by Ambartsumian at the 1966 Byurakan conference [1]. The growth in the numbers of abstracts in the NASA Astrophysics data system (ADS) is shown in Fig. 2.3 for various terms in the abstracts. There are two things to note. The first is that even after over half a century, those of us who study AGNs are still in a rapidly growing field! The second is the shift in terminology. The term “radio galaxy” goes back to the 1950s, notably in usage by Ambartsumian, Shklovskii, and Ginzburg in the Soviet Union. The terms “quasar” or “QSO” (derived from “quasi-stellar object”) appear suddenly in the mid-1960s. The words “active galactic nuclei” (unifying the whole phenomenon) appear only gradually around 1970. The early uses of the term were predominantly by Soviet astronomers. The acronym AGN does not appear in an abstract in the ADS until 1980 and not in a paper title until 1982. One can see that the designation “active galactic nuclei” or AGN has now become the most widely used term, but it is interesting that the QSO/AGN distinction is still being maintained by the new generation of AGN researchers.

My own memories match the story the numbers from the ADS tell. It is my recollection that by 1977–1978, the realization that Seyfert galaxies and quasars were one and the same was strongly gaining ground. This change was perhaps clearest at the 2-week long 1978 Lick Observatory workshop on AGNs. Unfortunately, there were no proceedings from this, but John Faulkner and I published a summary in *Nature* [78]. Our (punning) title was “Astronomers licked by QSOs and active galactic nuclei,” but we stated that “there did seem to be a tacit assumption [among those attending the workshop] that all QSOs and AGNs are indeed manifestations of varying degrees of the same phenomenon.”

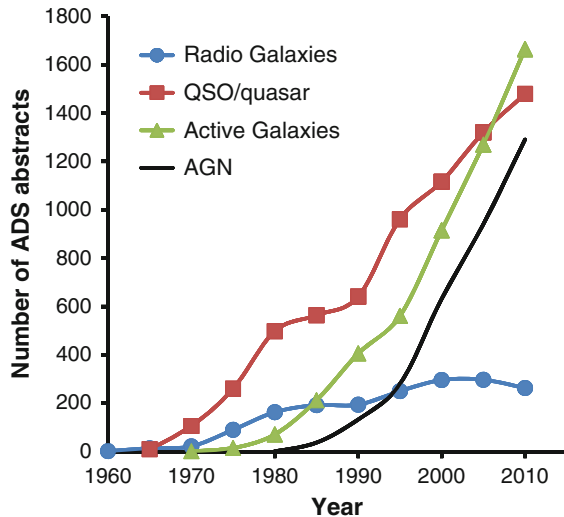
Did you make use of linear detectors for your first spectroscopic work in this pre-CCD era?

Yes. All my thesis work was done using the Lick IDS.

How were optical spectra handled? Which kind of measurements were routinely carried out?

Spectra were taken, reduced, and analyzed on DEC PDP-8 computers. When I arrived in Santa Cruz in 1975, these only had 8 KB of memory! By the time I got my Ph.D. in early 1981, the PDP-8s had been upgraded to 40k. Most of

Fig. 2.3 Number of abstracts in the NASA Astrophysics data system (ADS) shown by terminology as a function of time. “Active galaxies” includes the abbreviation “AGN.” Many papers use more than one term (e.g., “quasars and active galaxies”)



the programming was done in a very easy-to-use interpretive BASIC-like language called FOCAL. Obviously, massive computing power is not necessary for producing good data. However, good reduction software is. Joe Wampler and Lloyd Robinson introduced a lot of now standard procedures into astronomy for the first time on a regular basis: flat fielding, wavelength calibration, sky subtraction, and adding spectra. Joe commented to me once that the revolution brought about by the IDS was not really due to its higher quantum efficiency but to the linear digital data produced which allowed accurate sky subtraction and the addition of spectra.

Almost all the observational graduate students in Santa Cruz used the IDS. What made Lick Observatory so outstandingly successful in the 1970s and early 1980s was not just the existence of the IDS, but what I can only describe as the “IDS culture.” There was excellent user feedback at every stage of the process. This included the data reduction software and Joe Miller’s design of the Cassegrain spectrograph for the IDS that made observing so easy. When you have the same users using the same equipment and doing the same reductions over and over again, and you have some of these same people writing the software, the irritations that occur in many modern data reduction software packages are quickly eliminated from the process. As well as to Joe Wampler, Lloyd Robinson, and Joe Miller, credit for the highly efficient Lick Observatory “IDS factory” was also due to the electronics shop headed by Terry Ricketts, to programmer Bob Kibrick, to Rem Stone who calibrated the standard stars, to the mountain staff who did the instrument changes and kept things running, and to the graduate students who developed data reduction software. The latter included Jack Baldwin, Alan Koski, Mark Phillips, Steve Hawley, Dave Burstein, and Howard French.

One unique analysis program was a deblending program which allowed one to experiment with iteratively and interactively subtracting blends of lines in complex blends. An important application of this was Mark Phillips’ study of Fe II

emission [175]. Thanks to the high-quality IDS spectra taken by Don Osterbrock’s group, Mark was able to measure individual Fe II line strengths in I Zw 1. This provided the first evidence that the optical depths in the partially ionized zone of the BLR were far higher than had hitherto been realized [176]. This is now a standard part of BLR models, but such high optical depths had not been considered yet.

What was your preferred picture or interpretation about the physical nature of AGNs around the time of your graduation from Santa Cruz?

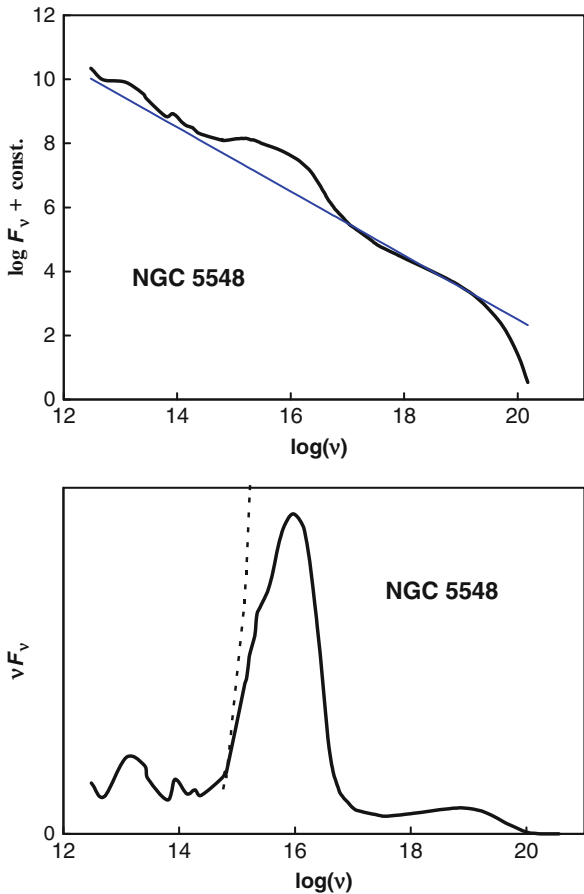
That is a great question. When I think about it, I now realize that much of the picture I had of the nature of AGNs back then was wrong! Actually, at that time and even into the twenty-first century, I did not adhere strongly to any particular picture because I was uncomfortable with the problems, contradictions, and uncertainties I was aware of. I believe things are a lot clearer now, so I am a lot more confident of the nature of AGNs.

One wrong idea I and essentially everyone in the field at that time shared was that the IR–optical–UV continuum was nonthermal synchrotron radiation. However, the first published spectral energy distribution (SED) of an AGN [137] showed a rise in the UV which Johnson and Low attributed to a then unexplained *thermal* component; 13 years later, Greg Shields, probably unaware of Low and Johnson’s paper, pointed out that there was an excess in the UV above the presumed synchrotron power law, and he proposed [212] that this was due to thermal emission from an accretion disk. The wrong idea we all had was that this thermal emission was a perturbation on the dominant nonthermal continuum. In fact, it is quite the other way round: the energetically dominant thing is the *thermal* continuum. The wrong impression arose because everyone was plotting SEDs on log–log scales (what else does a good astronomer do?). This makes the accretion disk contribution (what we now call the “big blue bump”) appear to be insignificant. A log–linear scale shows things correctly because the areas under the curve correspond to energy [44]. I have illustrated this in Fig. 2.4.

The idea of any accretion disk emission being just a small perturbation on a dominant nonthermal spectrum extending from the radio to X-ray regions was also a result of the belief that the spectrum the disk produced would go as $F_\nu \propto \nu^{+1/3}$ in the IR to UV [178, 210]. In fact, the spectral shape is very sensitive to the temperature structure in the disk, and the introduction of a modest amount of thermal reprocessing of radiation from the inner regions drastically changes the disk spectrum (see [88]).

I have always been most at home at the interface of theory and observation. The two AGN theorists in Santa Cruz were Bill Mathews and George Blumenthal. They have always been wonderful people to discuss ideas with, and they influenced my thinking a lot. Just before I came to Santa Cruz, George and Bill had published an influential paper on radiative acceleration of BLR clouds [24], and they continued to work on this throughout my time in Santa Cruz. There was a lot of evidence in favor of their model. The outflow of gas from an AGN had been discovered at Lick Observatory back in the 1930s [149]. Three decades later, a major high-velocity outflow was discovered in the bright high-redshift AGN PHL 5200 [194]. There was

Fig. 2.4 The top frame shows the spectral energy distribution of NGC 5548 (*thick curve*) and a ν^{-1} power law (*thin line*). The lower frame shows the same SED (*solid line*) plotted on a log-linear scale and the spectrum of an idealized $F_\nu \propto \nu^{+1/3}$ accretion disk (*dotted line*). (Figure adapted from [88]; data from [91])



thus clearly outflow. When George and Bill showed that radiative acceleration of clouds produced “logarithmic” line profiles that beautifully fit the newly obtained high-quality line profiles produced by Jack Baldwin, it seemed that the observational case for the BLR being a radiatively driven outflow was solid. The alternative of randomly moving clouds had theoretical problems because the mean free path between clouds was short, and the velocities were high, so there would be frequent hypersonic collisions. These would destroy clouds and heat them to the virial temperature.

Sometimes erroneous conclusions in one area lead to wrong conclusions in another. Another important reason in the 1970s for believing that the BLR was outflowing was that the alternative—gravitational domination of BLR motions—was thought to give unreasonably large black-hole masses. There was no problem if the BLR was a wind instead. The problem was that the size of the BLR had been overestimated by an order of magnitude. At first, BLR sizes could only be estimated from photoionization arguments [69]. The luminosity in a line depends on

the volume of the emitting region and the emissivity. If you know the line luminosity and emissivity, then you know the volume, and hence the size of the emitting region. The emissivity, however, depends on the square of the density. Because of the presence of strong C III] λ 1909, the density was thought to be significantly less than 10^{10} cm^{-3} [163]. In the early 1970s, Victor Lyutyi and Analoly Cherepashchuk of the Sternberg Astronomical Institute (SAI) in the Soviet Union introduced what is now called “reverberation mapping” whereby the size of the BLR is estimated from the reverberation time in response to continuum variability [49, 139]. Unfortunately, this pioneering work, which found smaller than expected BLR for NGC 4151 and NGC 3516, got ignored in the west. It was especially unfortunate that it was ignored at Lick Observatory because the IDS with its high repeatability was the ideal instrument for reverberation mapping. Bill Mathews recognized the importance of studying line variability in high S/N spectra. I remember Bill saying to me that “the observers should get really high-quality line profiles and then lock them away” for a long time (I think he had waiting 5 or 10 years in mind). That did not sound very appealing to the observers, and I do not think that any of the senior people took the idea seriously. It was left to two of my fellow Santa Cruz graduate students, Ski Antonucci and Ross Cohen, to carry out the first reverberation-mapping campaign with an IDS [4]. Roger Blandford and Chris McKee, who gave us the name “reverberation mapping” in the title of their 1982 paper [22] were unaware of the earlier Soviet work. In the mid-1980s, inspired by the papers of Lyutyi and Cherepashchuk, Linda Sparke and I (then both postdocs in Cambridge) introduced the interpolation cross-correlation technique for determining the reverberation time delay [93], and we showed that BLR were more than an order of magnitude smaller than had hitherto been thought. As we stated in our conclusions, “the good news for observers (particularly writers of NSF grants and Ph.D. theses, etc.) is that significant results can be obtained in less than one observing season!” This began the reverberation-mapping industry which has continued to the present day.

At the time of finishing my Ph.D. thesis, I was convinced that at least the high-ionization BLR gas was outflowing. In my thesis, I discovered that the peaks of the high-ionization BLR lines in AGNs were systematically blueshifted by of the order of $1,000 \text{ km s}^{-1}$ relative to the low-ionization lines [89]. This required two things: some sort of opacity and radial motions. The model I proposed for this was the “disk–wind” model. The high-ionization lines came from outflowing clouds, as in the Blumenthal and Mathews picture, but the accretion disk was blocking our view of the high-ionization clouds receding on the far side. The low-ionization lines were arising in a different region, perhaps further out, and did not suffer as badly from the blocking by the disk. This disk–wind explanation has become very popular, but it always had major problems, and I no longer believe it is the correct explanation for the blueshifting effect.

In the mid-1980s, I introduced velocity-resolved reverberation mapping. To my great surprise, velocity-resolved reverberation mapping of the high-ionization CIV line [90] completely failed to show the outflow I had been confidently expecting! The BLR motions were gravitationally dominated with a slight inflow. My first Ph.D. student, Anuradha Koratkar, and I confirmed this for more lines in more

AGNs [127, 128]. The good news was that black hole masses and Eddington ratios could be estimated from the BLR [129], but the bad news was that a simple disk-wind model of the blueshifting effect was untenable.

Another thing wrong with the picture I had of AGNs when I left Santa Cruz was that, like pretty much everybody up to that point, I thought that the BLR as spherically symmetric. In fact, until 1978, there was a widespread general assumption in the AGN community that not only the BLR but almost *everything* about AGNs was spherically symmetric. The only obvious exception was the radio jets. Greg Shields (with whom I was collaborating in my last year at Santa Cruz) had proposed that the BLR could arise from the accretion disk [211], but as Greg himself pointed out the following year [213], there were serious problems with this (Stephanie Snedden and I have reviewed the early history of ideas of a disk contributions to the BLR in [92]), and Greg quickly accepted the outflow picture. A major problem was that disks were not expected to produce nice logarithmic line profiles.

I believed that BLR emission came from dense clouds of gas in pressure equilibrium with a hotter, lower density medium. I believed that the number of clouds was enormous ($\gg 10^{11}$) because I was sure that the clouds could not be too much bigger than a few Strömgren lengths, and the Strömgren length, which is a well-known quantity, was very small. In talks, I referred to the BLR as being “like a mist.”

Although I held to a spherical BLR when I graduated (and it is still often depicted in cartoons of AGNs), I already knew that the *outer* parts of AGNs were *not* spherically symmetric. The paradigm shift away from spherical symmetry began with a landmark paper presented by Roger Blandford and Martin Rees at the 1978 Pittsburgh conference on BL Lacs [23]. They suggested that BL Lac objects were the result of Doppler boosting from the jets being aimed straight at us. I did not go to the Pittsburgh conference, but the Blandford and Rees paper was *the* thing being talked about by everyone from Santa Cruz who attended. The paradigm-changing proposal of Blandford and Rees was not immediately accepted. As John Faulkner and I put it in our above-mentioned report on the Santa Cruz AGN meeting (the Santa Cruz meeting occurred a few months after the Pittsburgh one), the Blandford and Rees idea initially “met with firm opposition from the observers on whom these jets were supposedly aligned.”

Opposition to the Blandford and Rees beaming idea soon evaporated, and there was much discussion of how far the idea could be carried. The discussion centered on differences in radio properties (see [2] for a review). There seemed to be differences in the radio properties of type-1 and type-2 Seyfert galaxies. In a seminar series taught in Santa Cruz by a visiting lecturer, Wayne Stein, we discussed the possibility of relativistic beaming, and hence orientation effects, in Seyfert galaxies. One day after the seminar, my fellow graduate student Bill Keel suggested a straightforward way of doing checking for relativistic beaming effects in Seyfert galaxies—measuring the axial ratios of host galaxies with a hand lens. I thought this was a great idea (I particularly liked the low-tech hand lens approach!) and encouraged Bill to go for it. Bill spent a Saturday afternoon in the Sky Survey

room poring over the prints. With a big smile on his face, he reported back to me that Seyfert-1 galaxies were preferentially face on. There was not an obvious effect for Seyfert-2 galaxies. Bill had thus shown that orientation was a factor in the detectability of type-1 AGNs and hence in the difference between type-1 and type-2 Seyferts. He proposed that this was a consequence not of relativistic beaming, but of dust very close to the nucleus. The paper resulting from this, [122], is the seminal paper on Seyfert orientation. (Due to an oversight, it did not get mentioned in Ski Antonucci’s review 13 years later.)

To summarize, the picture I had of the structure of AGNs when I left Santa Cruz was thus of a black hole with a spherical mist of outflowing BLR clouds, an accretion disk (which I thought was necessary to explain the blueshifting), and a surrounding flattened distribution of dust (which we now called the “torus”). The NLR had to be outside the torus (because Bill Keel had not found any orientation dependence for Seyfert 2s). One thing I was quite agnostic about was where the BLR came from. Many ideas were being floated about at the time. I did not think that the flattened distribution of dust had anything to do with the BLR.

Interestingly, something very close to what I now believe to be the correct picture of the BLR—a thick, rotating, highly turbulent disk—had already been proposed by Don Osterbrock when I was a graduate student [169]. Don had taken Greg Shields (1977) model and arbitrarily added a substantial amount of turbulence in order to explain the line profile statistics. The problem with this was that it required gravitational domination of the motions rather than the radial outflows favored at the time, so Don Osterbrock’s turbulent BLR disk model got relatively little attention. I considered it to be a much less likely possibility than radiative acceleration.

There was yet another wrong idea I and many others had when I was a graduate student. Despite Ray Wolstencroft’s undergraduate course, I thought that AGNs and their black holes had little connection to “normal” galaxies. Like essentially everybody in the west, I was unaware of the work of Anatoly Zasov and Ernst Dibai, showing that the luminosities of AGNs and their host galaxies were correlated [239]. When Dibai showed in his important 1977 paper on obtaining black hole masses from the BLR (a modification of his method is now the most widely used method of obtaining black hole masses) that for the same galaxies, the black hole masses were correlated with the AGN luminosity [66], Zasov and Dibai’s result now meant that black hole masses were correlated with galaxy luminosity. This got ignored for over a decade and a half until 1993 when John Kormendy discovered that black hole masses and bulge masses were correlated [130].

Back in the 1970s, I just thought that there were some weird galaxies that, due to some unusual circumstances in their past, now found themselves with giant black holes in their centers. This attitude prevailed until near the end of the twentieth century. During that time, there were innumerable NASA press releases saying in effect “NASA discovers black hole in a galaxy.” What should have been recognized early on (and indeed was pointed out by Hoyle and Fowler back in 1963) was that *every* galaxy would have gone through an active phase and would thus have a black hole.

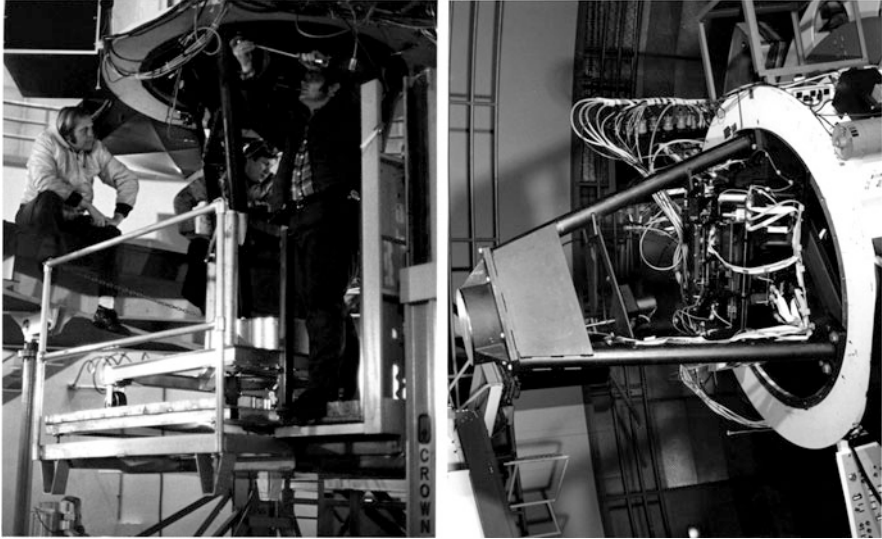


Fig. 2.5 *Left panel:* Wampler and Fred Mueller, who had primary responsibility for the spectrograph's design, watch as Ron Laub, chief of mountain operations, attaches the new spectrograph to the telescope. *Right panel:* The new spectrograph that replaced the Yerkes spectrograph mounted on Lick's 3-m telescope, shown before a light proof shroud was installed and rotated by 90°

Thank you, Martin. From your words, we understand that the development of linear detectors was very important for progressing in the analysis of quasar spectra, so that we now talk to an astronomer that actually build one of the first linear detectors employed in astronomy.

2.4 The Development of a New Instrument

Dear Joe (Wampler), what were the principal observational techniques used to study quasars in the pre-CCD era? You and Joe Miller had perhaps the most innovative instruments of that era. What were some of the observational breakthroughs or revelations that you participated in? For example, were your observations of strong FeII emission in the spectra of many quasars a surprise?

Maarten Schmidt's [199] discovery of the extragalactic nature of 3C 273 in the spring of 1963 came at a time when the detectors used by astronomers to record astronomical spectra were just starting a 20-year revolution that replaced photographic plates which had about 0.1% detective quantum efficiency (DQE) with photoelectric cathodes which had up to 20% DQE to solid-state CCD detectors that not only achieved DQE values near 100% but also surpassed all previous detectors in both mechanical and electrical stability.

Following WW II, electron-multiplying phototubes (aka photomultipliers) were used as the detector of choice for measuring the brightness of stars in broadband colors. But photomultipliers were able to measure only one spectral band and one star at a time. Light falling outside the chosen band was rejected either by spectral filters, or by spectral masks placed in the focal plane of a spectrograph. And because photomultipliers were rather large, several centimeters in diameter, it was difficult to pack detector arrays into the confined space of telescope focal planes. The photographic plate, because it was able to record the light at many different focal positions simultaneously, was still very widely used for photometry despite its low DQE, poor dynamic range, and inability to be accurately calibrated. But for some research needs, the deficiencies of the photographic process were so serious that increasingly complex scanning spectrophotometers with photomultiplier detectors were also in demand. Advances in transistor electronics for photomultipliers at national and university physics departments and some observatories led to single-photon counting photomultiplier arrays and semiautomatic digital control and sequencing of spectrophotometers.

In the fall of 1963, I arrived as a fresh postdoctoral fellow at Lick Observatory. I was interested in studying the interstellar medium and in particular the unidentified shallow diffuse interstellar bands that were sometimes seen in photographic spectra of reddened stars. Because these bands were wide and shallow, it was important to observe them with an instrument that was linear and could be accurately calibrated. With the guidance and support of the observatory director, Albert Whitford, I undertook the design and construction of a compact two-channel automated spectrophotometer (scanner) that could be used at the prime focus of both the Observatory's 120-in. Shane telescope and the much smaller 36-in. Crossley telescope. The mechanical parts were constructed in the Lick Observatory shops, and I assembled the electronic parts myself in the Observatory electronics room. I was greatly assisted in the electronic design by the experts at the University of California's Lawrence Radiation Laboratory (as it was known then) in Berkeley. The scanner was designed as a two-channel instrument with one channel recording the light from the target star plus a small portion of the surrounding sky, while the other channel simultaneously recorded the light from a similar patch of nearby blank sky. This permitted an easy correction for any contaminating sky background. As the instrument proved to be successful, similar instruments were also constructed for the National Observatories at Kitt Peak and Cerro Tololo. There, they were known as the "Danziger scanners" after John Danziger, who adapted the Lick Observatory design for the National Observatory telescopes and supervised their construction.

When Maarten Schmidt discovered the redshift of the quasar 3C 273, he noted that there were broad, low-intensity emission bands in the spectra which he was unable to explain. Bev Oke suggested that I scan the spectrum of 3C 273 with the new Lick Observatory spectrophotometer and see if I could suggest a good identification for the features. Oke thought that perhaps one feature near rest wavelength $\lambda 5300$ might be a forbidden $\lambda 5303$ line of iron-stripped of 13 electrons [Fe XIV]. This line is a strong feature in the spectrum of the solar corona. Oke also suggested that I compare the spectrum of 3C 273 with those of nova and supernova

to see if there might be spectral similarities. When a good scanner spectrum of 3C 273 was compared to that of Nova Herculis 1934, it was immediately apparent that the broad emission bands seen by previous observers could be identified with permitted transitions of singly ionized iron (Fe II) [231]. Because the Lick scanner produced a spectral intensity profile that could be accurately calibrated, the relative strengths of individual Fe II features could be determined. And these agreed well with the expected oscillator strengths of the FeII lines. A search for forbidden iron lines or high-ionization iron lines did not reveal any likely alternative candidates for the observed features. In particular, [Fe XIV] did not seem to be present. While it was satisfying to identify the broad emission lines in the spectrum of 3C 273, I would not say that at the time, I was particularly surprised that FeII was present; since in those days, the mere existence of 3C 273 was already sufficiently shocking.

Although the FeII lines in 3C 273 are unusually strong for a quasar, permitted FeII lines have now been observed in the spectra of many quasars—in both emission and absorption. Recent discussions of the iron spectra in quasars are given in papers by Shields et al. [214], Kovacević et al. [131], and Ferland et al. [80]. And Boroson and Green [28] show that FeII anti-correlates with the strength of the forbidden narrow doubly ionized oxygen lines near $\lambda 5000 \text{ \AA}$. For 3C 273, the lines earlier identified with doubly ionized oxygen turned out to be mostly due to Fe II multiplet 42. The physical processes underlying the Fe II emission lines are still uncertain. Two principle contenders are ionizing radiation from the central quasar engine and turbulent/shock heating.

In these early days, a second achievement of the two-channel scanner was a proof that the steep hydrogen Balmer decrement seen in Seyfert galaxy spectra was due to dust reddening. This had long been suspected, but because other processes, such as collisional excitation of the hydrogen levels, can also lead to steep Balmer decrements, the case for dust reddening had not been firmly established. As the Lick Observatory scanner was equipped with both visible light and infrared-sensitive photomultipliers, it could measure the relative strengths of forbidden S II spectral lines that originated from the same upper level of singly ionized sulfur, one group in the near UV at $\lambda 4010 \text{ \AA}$, the other in the infrared near $1.06 \mu\text{m}$. The relative strengths of these lines are determined only by atomic transition probabilities, and any deviation from the predicted ratios would establish the presence of dust in Seyfert galaxy nuclei. Comparing the scanner observational results with Miller's theoretical values [152], Wampler [228] showed that dust reddening caused the steep Balmer decrement in Seyfert nuclei.

As noted above, the two-channel scanner used for the 3C 273 observations was mounted at the prime focus of the 120-in. telescope at Lick Observatory. This focus position conserves photons as there is only one mirror between the instrument and the sky, but the observer's cage, located in front of the primary mirror, is very cramped and, in the winter, very cold. The long hours spent observing at the telescope's prime focus give ample opportunity for considering alternative possibilities. By the late 1960s, Westinghouse had developed a highly sensitive television-camera tube with a so-called secondary electron conducting (SEC) target

that could be run in a mode with very slow framing speeds. To “freeze” the the readout image at the end of an integration, the camera was coupled to a frame-storage device that could hold and replay at normal TV scan rates what would ordinarily be the camera tube’s single readout flash. The Westinghouse SEC TV camera was greatly superior to the human eye in detecting faint-star images when the framing speed was set to be slower than 0.1 s/frame. (The dark-adapted human eye is actually quite sensitive to optical light, but it can only collect light photons for about 0.1 s before it refreshes itself.) The development of the SEC vidicon by Westinghouse, with its ability to detect and image *fainter* stars than could be seen by the human eye was key to moving the astronomical observer from the telescope focus into a control room.

In late 1968, I purchased an SEC vidicon from Westinghouse with Lick Observatory research funds, and after a few tests, I was confident of its sensitivity and general usefulness for telescope guiding. At this time, a decision was made to implement the Cassegrain focus of the 120-in. telescope. And it was decided to remove the observer from the telescope dome and fully control the new focal position from a control room. Fortunately, Dr. Lloyd Robinson, an expert in exactly the type of computer control systems’ need by an automated telescope, was able to transfer from Berkeley’s Lawrence Radiation Laboratory to the staff at Lick Observatory in the spring of 1969. Also, in the summer of 1969, Dr. John McNall, another computer expert from the University of Wisconsin’s Pine Bluff Observatory, joined us for a sabbatical. The Lick Observatory technical group now had the expertise to equip the 120-in. telescope Cassegrain focus with a suit of automated instruments that could be controlled by a computer-assisted observer in a human-friendly control room.

As the implementation of the Cassegrain focus proceeded, the three of us decided to test an idea of mine that the phosphor screens of military image tubes could be used as a volatile memory element. These tubes were used by the military in the Vietnam War for night vision applications and were available in the Saigon black market, but were still classified in the United States. However, Dr. Charles Towns, who was then at the University of California, Berkeley, was able to persuade the military lead agency at Fort Detrick, in Frederick, Maryland, to declassify the tubes so that they would be available for civilian use. A second important ingredient was an ITT photomultiplier, similar to the detectors used in the 120-in. prime focus scanner, but with the addition of an electron imaging front section that had a slot in its electron image plane. With a magnetic deflection yoke mounted externally to the tube, it was possible to rapidly move an electron image of the tube’s photocathode across the image plane slot and rapidly sample different portions of the photocathode. ITT called this tube an image-dissector photomultiplier. By coupling the ITT image dissector to the output phosphor screen of the image tube, one could easily sample the entire output image of the image tube during the decay time (about 4 ms^{-1}) of the phosphor screen. Thus, it was possible to detect single photons arriving anywhere in the spectral image of a star.

This was the principle of the Lick Observatory IDS. Of course, the detection was a statistical process, and the brightness of single-electron flashes were also

subject to statistical variation, so there was a loss of perhaps a factor of $\sqrt{2}$ in the signal-to-noise ratio when compared to a perfect multichannel photometer. But for the first time, it was possible to envisage a rugged, photon-counting detector with hundreds of independent channels and a very high dynamic range. A “breadboard” version of the IDS was attached to a spectrograph that my thesis advisor, Albert Hiltner of Yerkes Observatory, had given us. The IDS detector was controlled by the third important part of the system, a PDP-8 computer which sorted the photon detections into their correct image positions and displayed the accumulating spectrum in real time on the computer monitor. After we had assembled a prototype of the IDS in the Lick Observatory shops, we moved it into the adjacent parking lot one night to see if it could detect the nighttime sky. We soon had a fine spectrum of the night sky, and as we were celebrating this achievement, we attracted the suspicion of a university campus policeman who was only satisfied that we were not thieves after telephoning the Lick Observatory director to clear our activity. This policeman was not the only one suspicious of our gadgeteering. One Lick Observatory colleague suggested that we should “stop developing new gadgets and do some real astronomy,” and another agreed that while the IDS was an interesting device, it was likely that having a computer in the telescope dome would be too distracting. And, finally, our first attempt to publish our results met with a referee who asserted that image tubes were incapable of quantitative results. Fortunately, our work was strongly supported by Bob Kraft, who by then had succeeded Whitford as director of Lick Observatory.

I think that the most impressive aspect of the development of the IDS was that the technology just seemed to “fall into place.” In other words, we had little difficulty in turning our ideas into a working instrument that was soon in regular operation at the new Cassegrain focus of the 120-in. telescope (Fig. 2.5). We never had to backtrack the design because some concept did not work. While the many subcomponents required careful design and sometimes delicate assembly, they all worked from the beginning. Very few parts had to be remanufactured, and any needed rework was usually the result of missed manufacturing tolerance.

The fact that the IDS could easily detect the nighttime sky in the parking lot of the Lick Observatory shops showed that it was sensitive enough to detect faint stars. A few months later, in the fall of 1969, a two-channel (star+sky and sky alone) version of the IDS with the Yerkes spectrograph was installed at the new Cassegrain focus of the 120-in. telescope. Because this IDS spectrograph had more than 200 photon-counting spectral elements in each channel, it was more than 10 times faster than previous electronic systems in acquiring calibrated astronomical spectra of faint stars. Later, Dr. Joseph Miller aided in constructing a new folded spectrograph that provided a better match to both the IDS detector, and the telescope was constructed and replaced the Yerkes spectrograph at the 120-in. telescope. Then the Yerkes spectrograph, with a second IDS system, was moved to the smaller observatory telescopes. The new spectrograph at the 120-in. telescope also provided remote grating and order-separating filter changes which further increased the observing efficiency [153].

It is worth pointing out that even though the IDS represented an advance in astronomical detector instrumentation, the success of the 120-in. telescope largely resulted from an integrated observing system. The remotely controlled Cassegrain focus, the sensitive SEC vidicon centering and guiding system, an efficient spectrograph with remote configuration control that could be programmed in advance of the actual observations and called up when needed by the sequencing computer were all necessary parts of an efficient observing campaign. This is now called “end-to-end” engineering. At the time, no other observatory had automated its observing facility as extensively as Lick Observatory. As a result of these changes, the Lick Observatory facilities came under heavy demand from the University of California astronomers. In 1975, a copy of the IDS was taken to the AAO where it was used as a popular commissioning instrument. And a modified copy of the IDS was also used at the ESO in Chile. An unexpected consequence of the heavy use of these IDS systems was that a Robinson and Wampler, paper [190] describing the IDS system was frequently cited by astronomers when they published papers using IDS data. As a result, this became the most cited paper by a factor of 2 published by the PASP, and it was selected by the University of Pennsylvania’s Garfield Library for inclusion in their “Citation Classic,” series [191].

Examples of major quasar programs undertaken at Lick Observatory using the IDS include the studies of the AGN phenomenon by Osterbrock [165,167]. Polarization observations of obscured AGNs by Miller and his student, Antonucci [5, 165], that showed that the narrow-line AGNs were frequently normal broad-lined objects with their BLR obscured by a dusty disk. A thesis study by Baldwin [79] showed an inverse correlation between the equivalent width of the quasar $\lambda 1550$ broad emission line and the strength of the local continuum flux. In 1983, Martin Gaskell, then a doctoral student at UCSC, showed that the high-ionization lines in quasars were systematically blueshifted with respect to the low-ionization lines and the local standard of rest [85]. Using the IDS, Baldwin, Burbidge, Hazard, Robinson, and Wampler undertook an extensive radio-quasar survey and one of the objects in this survey, OQ 172, [232] for a number of years held the record for the highest redshift quasar. A second quasar source in the survey, Q1548+115, proved to be the first instance of a pair of very close quasar images with discordant redshifts [230]. This may be a case of a foreground quasar gravitationally imaging a background quasar. Wampler [229] later found that, given the sky density of quasars, there are too many cases of close quasar pairs with discordant redshifts for the pairing to be simply random coincidences. Studies of gravitational lenses in which the quasar is the lens rather than the lensed object is a subject that has had little investigation, but Courbin et al. [59] have recently shown that quasars can be gravitational lenses by finding an unambiguous case in which a $z = 0.12$ quasar is imaging a $z = 0.640$ galaxy.

The heavy demand for the IDS system at Lick Observatory continued throughout the 1970s and into the early 1980s when the new solid-state CCD detectors replaced it. Although the IDS was an advance over photographic plates and scanning spectrophotometers using photomultipliers, it had substantial deficiencies when compared to CCD detectors: the IDS was bulky; its image tubes not only required very high voltages, but for image stability, they had also to be shielded from

field changes caused by variations in the instrument's orientation to the Earth's magnetic field. The image plane had severe pincushion distortion, the intensity of the phosphor screen output was slightly nonlinear, and the number of independent resolution elements achievable with these image tubes was far fewer than for CCDs.

Thank you, Joe. The appreciation that Seyfert nuclei and quasars were powerful X-ray emitters came years later than their discovery. Radio interferometry caused a takeover unprecedented in the history of astronomy, surpassing the spatial resolution of optical instruments in the 1970s. Instrumental advances in different bands have not been concomitant since quasar discovery. Instruments in the X-ray domain have only recently achieved spatial resolution comparable to the one typical of seeing limited observations in the optical. Martin Elvis had the opportunity to follow the impressive achievement in X-ray astronomy since the times when only a few nearby AGNs were detected.

2.5 Seyfert Galaxies as X-Ray Sources

Dear Martin (Elvis), could you tell us about the discovery of Seyfert galaxies as X-ray sources?

When I arrived, along with Mike Watson, at Leicester University (UK) in 1974, as a fresh Ph.D. student of Ken Pounds in X-ray astronomy, I had no real idea what X-ray astronomy was, or that I was lucky enough to be arriving at a moment of explosive growth. I was in awe of an older, wiser, postdoc, Richard Griffiths, who had read *every* paper ever published in X-ray astronomy, and had a card file entry for each one. At this point, there were just 3 X-ray-emitting AGNs: 3C 273, NGC 4151, and Cen A. There were upper limits for a few others [123], and people were debating the differences between “X-ray” AGNs and “non-X-ray” AGNs.

This was at the very end of the heroic “rocket man” era of X-ray astronomy, where each student got to build a payload, that then flew on a rocket to get 5 min of data. As someone with a knack for making smoke come out of electronics, it was lucky for me, and for rocketry, that I just missed that era.

Instead, the era of X-ray satellites was beginning. The fabulously successful *Uhuru* satellite [95], with monthslong datasets, had discovered eclipsing, pulsing, X-ray binaries, made a good case for black holes in binaries, and found powerful extended emission from clusters of galaxies, among other discoveries. The main satellite experiment that Leicester was involved in, on the UK's Ariel V satellite, seemed rather modest by comparison: 100 cm² vs. 800 cm², limited telemetry (1,024 bytes per 90 min orbit, Fig. 2.6, center), and almost no time resolution. Yet the Ariel V Sky Survey Instrument (SSI, Fig. 2.6, left), launched on October 15, 1974, the same month I arrived, unknowing, turned out discovery after discovery in the next few years, including my thesis topic: that Seyfert galaxies were luminous X-ray sources.

Ariel V was spin-stabilized, and all the experiments used this spin to advantage. The SSI scanned a set of collimated proportional counters around the sky. Two sets of detectors had their collimators canted at opposite angles, so that when they passed over a source, two “lines of position” were formed, and where they crossed was the X-ray source. Unfortunately, one half of the detectors failed soon after launch, due to corrosion of the windows at the seaborne launch site. Thereafter, we could only locate a source by changing the scan direction. The collimators were 10° long, but only half a degree wide, so crossing several “lines of position” gave locations on the sky (“error boxes”) that were a fraction of a square degree. The Ariel V SSI advantage turned out to be this narrow collimation plus longevity. The full *Uhuru* operations only lasted about 8 months, after which, it lost its star tracker, forcing it into a more limited mode.

That meant that the 3U catalogue [96] had an effective flux limit closer to 5 mCrab, while the SSI 2A catalogue reached closer to 1 mCrab [58]. Many of the *Uhuru* error boxes were a square degree or so. That left them with many “UHGLS”—“unidentified high galactic latitude sources,” or “X-ray galaxies” [18,97]. UHGLS were a mystery that promised to explain the cosmic X-ray background. As Ariel V gathered months of data, we started to find new sources appearing as “stars” of lines of position on our maps (Fig. 2.6, right). The bright galactic sources were prominent, but there were some fainter high-galactic latitude sources too. As the only two Ph.D. students on the SSI, Mike and I had to decide who would do what. So, emulating in miniature Pope Alexander VI, who divided the New World between Portugal and Spain, we divided the X-ray sky: Mike took the galactic sources; I took the faint high-latitude sources. I was more intrigued by the idea of finding something wholly new, I suppose. We wanted to identify these new X-ray sources with optical objects.

Mike and I had just come from an astronomy Masters program at Sussex University, and that gave us a modest advantage over most of the Ariel V team, who had more of a physics instrumentation background. We knew something about galaxies and quasars, for example, and knew a few people to ask when we did not know enough. This turned out to be crucial for the discovery of Seyfert galaxies.

For example, Mike and I knew about the Palomar prints, but Leicester did not have a copy, and I remember making a rare and expensive international phone call to California to order a set from the Caltech Bookstore. Before the Palomar plates arrived, we started collecting catalogues of whatever likely sounding objects we could find. The Abell catalogue of clusters of galaxies was an obvious one. For active galaxies, I asked Richard Bingham of the Royal Greenwich Observatory, with whom I had done my Masters’ thesis project, if he knew of a list of Seyfert galaxies, and he duly supplied his own. It only had a few dozen, at most, objects on it. But as the brightest active galaxies in the sky, they seemed like a good bet.

At the time, the *Uhuru* team had just published upper limits for some Seyferts which appeared to show they were not generally strong X-ray sources [123]. But we plotted the Seyfert galaxy positions on our maps anyhow. I was showing Jean Eilek around our high-tech computer room where the SSI data was first processed to make maps, when one of the first large area maps came off the CalComp line plotter.

As the plotter drew one line after another, it was clear that we had a really obvious source and, almost obscured by the thick lines, was the name “NGC 3783.” “It looks like we have a Seyfert galaxy,” I told Jean. And we had! And I had a thesis topic.

Collaborating with Mike Penston and his student, Martin Ward, who was on the same Sussex M.Sc. course with Mike and me, but stayed on there to do a Ph.D., and Tommaso Maccacaro, then a student visiting from Milano (Italy), we wrote it up [57]. Soon afterward, a Seyfert was found in an X-ray error box—the first time one was discovered via X-rays—MCG 8-11-11, and we published that [233]. The Monthly Notices referees soon got tired of seeing one source at a time and asked, rather firmly, when we were going to publish a real catalogue. That had Brin Cooke put us on the path to the “2A” catalogue [58] and in the process, the discovery of another dozen or so Seyferts [73]. With such poor positions, how did we know the identifications were correct? Luckily, Ian McHardy had just joined Leicester as a temporary lecturer. He came from Martin Ryle’s Cambridge radio astronomy group, where they had learned to take statistics seriously. We adopted their technique of randomizing the positions (actually slipping them in Galactic longitude by 15°) and redoing the identifications. The peak at small optical–X-ray offsets went away, confirming the Seyferts’ X-ray emission. The UHGLS were Seyferts, you see.

Almost simultaneously, the SAS-3 X-ray satellite started finding Seyfert galaxies with its rotation modulation collimator. They had no ambiguity about the identifications as they had arc minute locations, which bolstered the case for Seyfert galaxies as X-ray sources [202], but they could not cover the whole sky.

The distinction between type-1 and type-2 Seyferts had just been introduced [124], and we were only getting detections of type-1 Seyferts. Type 2s were clearly less luminous in X-rays. Instead, Mike Penston and Martin Ward started finding “narrow emission line galaxies” in, and often just outside,⁵ our new high-latitude error boxes [234]. Some had weak broad H-alpha emission (e.g., NGC 526a), some did not (e.g., NGC 7582). Reddening became the likely explanation quite soon. The link with X-ray obscuration came with spectra from Ariel V “experiment C” [198], and the new HEAO-1 A-2 experiment [154]. Andy Lawrence (another Ariel V Ph.D. student) and I put this together a few years later in a paper proposing a “unified scheme” of active galaxies using obscuration [135].

The SSI discovered several other classes of X-ray source, but Seyferts were special. They really were the key to the X-ray background. I foolishly removed the short section by Mike Penston from our discovery paper, that said the luminosity function we had made (thanks to Cesare Perola) would integrate up to the X-ray background if extrapolated. Of course, others soon pointed that out for us [17]. This taught me a good lesson.

⁵This became a standing joke: “That’s where most of the area is.” Yet the identifications were all correct. [Update: Mike Watson points out that the most probable distance to find an identification is at 1σ ; just differentiate the Rayleigh function (a two-dimensional Gaussian multiplied by the annular area) and find the maximum. Neat.]

Quasars had to wait another year. They were optically fainter and X-ray fainter, so it took the imaging *Einstein Observatory* to detect them [221]. I was lucky enough to have moved to Giacconi's Einstein Observatory team by then and could join in the fun. Kellogg et al. had been unlucky in that *Uhuru* did not have enough exposure to detect many Seyferts, but also they chose to look at the *nearest* Seyferts, not the *brightest*. It turns out that going for the brightest is usually a winning strategy in astronomy.

Thank you, Martin. In parallel with European and American Astronomers, quasars and active galaxies were subjects of much observational and theoretical investigations. One of the most impressive among the early survey was carried out by Benjamin Markarian, yielding to a widely used series of lists of active galaxies since 1967 [148]. Viktor Ambartsumian put forward an original interpretation of quasars.

2.6 AGN Astrophysics in the USSR at the Time of Quasar Discovery and Afterward

Dear Vladimir and Iraida (*Pronik*), what were the most widely debated issues among Russian astronomers just before the quasars were identified?

Before the discovery of quasars, Russian astronomers widely debated a report by V. A. Ambarzumian at the Solvay Conference (1958), where he introduced his ideas on activity in galaxy nuclei: continuous medium ejection, jets, and blue compact galaxies ejection [1]. The strong linear file of small blue galaxies pointed out from the nucleus of massive galaxy, undoubtedly evidence in favor of this file connection with the active nucleus of massive galaxy. Most of astronomers did not hold his opinion, as well as his idea about a prestellar D-body in the nuclei which can provide the activity of nuclei. The most widely issue among Russian astronomers was a single body must explain AGNs and quasi-stellar sources (QSS). It was obvious that an active nucleus is not "a thousand Orion nebulae," but a gas formation with a single source of ionizing radiation [102]. A large role was attributed to magnetic fields. L. M. Ozernoy considered a magnetoid for the AGN central body [170].

What motivated you to enter quasar research?

Jointly with E. A. Dibaj, we started spectral investigations of AGNs after Maarten Schmidt had identified two broad emission lines with significant redshift in spectra of two bright quasars (3C 273 and 3C 48). The line profiles resembled analogous lines in spectra of Seyfert galaxy nuclei (AGNs) which Shklovskii [215] named miniquasars (AGN luminosity is lower than quasar luminosity). Thus, investigating AGN spectra, we were sure that the obtained results would be true for quasars as well. Dibaj and us already knew that quasars were variable objects in optical light, but we were not sure whether (Seyfert) galaxy nuclei were also optically

variable. Optical variability of the active nucleus in NGC 5548 was first discovered by Pulkovo astronomer Dejch [64] which he reported at the Byurakan conference in May 1966.

When you entered the field did you find a quasar paradigm already fixed in place?

The modern paradigm of active galaxy nucleus—MBH with a very hot accretion disk—is a great achievement of scientific thought. The model was developed during my activity, but I am unrelated to it. I do not know whether Dibaj took part in the creation of the modern paradigm of AGNs or not. But I know that A. Cherepashchuk was one of the creators of this paradigm.

Dear Vladimir (*Pronik*) and Sergey (*Sergeev*), what were the main observational facilities used during the discovery period? How did linear detectors impact the investigation of quasars and AGN?

Our observational facilities were very poor. The 2.6-m telescope at CrAO was already operating but more important projects, from the point of view of the direction, being pursued there. Jointly with Dibaj, we used a 1.2-m telescope which belonged to the Crimean Laboratory of the SAI. We constructed a high-transmission spectrograph in the mechanics workshop of the Crimean Laboratory of SAI. The photographic films, despite their high sensitivity, had very dark background (Soviet emulsion, made in Kazan). A number of papers were written at Crimean Astrophysical Observatory (CrAO) (Chuvaev K.K., Pronik I.I., Pronik V.I.) based on observed data obtained with an image intensifier constructed in the USSR and a home-made high-transmission spectrograph operating at the Nasmyth focus of the 2.6-m telescope. When all the detectors at 2.6-m telescope had been changed to CCDs, the level of science increased significantly.

The CrAO was a pioneer of CCD observations among the astronomical institutes of the Soviet Union. Spectral observations with the Astromed-2000 CCD [117] were started at the 2.6-m Shajn telescope in 1985. AGN observations with this telescope were initiated by V.I. Pronik who had developed a Cassegrain focus spectrograph for this purpose (the Pronik's spectrograph). The first CCD spectra of AGNs were acquired in February 1988 (Fig. 2.7) by V.I. Pronik and S.G. Sergeev. During the next several years CCD observations of AGNs continued on a regular basis (usually one set of 2–3 nights per month). The main target was the NGC 4151 nucleus (e.g., [203]). By 1987, the first CrAO software to process CCD spectra was developed by I. Ilyin. The experience of these first AGN observations allowed us to identify the key sources of uncertainty in the CCD data (such as the seeing effect, the effect of atmospheric dispersion, etc.) as well as difficulties with the observational technique. As a result, CCD observation techniques were developed in the early 1990s for CCD observation of AGNs and processing of their spectra which have not changed significantly up to the present. And of course, the quality of the CCD spectra became much higher than the first CCD spectrum shown in Fig. 2.7. Intensive spectral monitoring over more than 13 years were carried out with the Astro-550 CCD (see [21] for the specification of this CCD). NGC 4151, NGC 5548, NGC 7469,

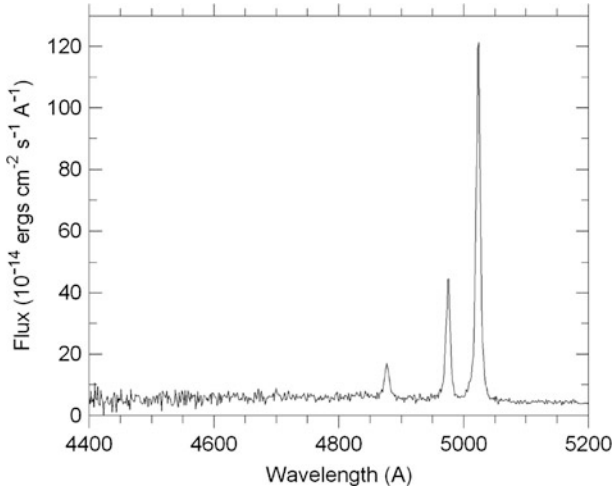


Fig. 2.7 The first CCD spectrum of the NGC 4151 nucleus obtained at the CrAO in February 26, 1988 when it was in a low activity phase

Mrk 6, Arp 102B, 3C 390.3, and some other AGNs were studied by K. Chuvaev, Yu. Malkov, V. Pronik, and S. Sergeev. A database containing more than 2,500 CCD spectra of AGNs was created.

Thank you, Vladimir and Sergey.

Dear Iraida and Vladimir, what were the major lines of research carried out after the discovery of quasars?

Spectral study of AGNs at CrAO was started in 1963. The large cosmological distance $z = 0.16$ and high apparent magnitude of 3C 273 indicated an extremely high luminosity for this source requiring a physical explanation. Dibaj and Pronik [67,68] began their studies of physical conditions in nuclei of Seyfert galaxies (SG) in 1964. Their works were pioneer at that time with observations carried out using a high-speed spectrograph at the 1.2-m telescope of the Crimean Station of SAI. Analysis of the spectra allowed them to make a conclusion about the presence of two subsystems (two zones) of gas in the nuclei of Seyfert galaxies: zone 1 emitting narrow lines in a more extended region (tens to hundreds parsecs) with low electron density ($10^3\text{--}10^4$) cm^{-3} and low velocity dispersion (300–500) km s^{-1} . Zone 2 emitting broad lines is a small (fraction to several pc) inner region with high electron density ($10^6\text{--}10^7$) cm^{-3} and high velocity dispersion of several 1,000 km s^{-1} . The two regions were subsequently called: the NLR and BLR, respectively. Both regions were assumed to be the result of successive explosions in the nuclear source. Since 1971, Pronik and Chuvaev [184] started photographic spectral monitoring of AGN variability. The image-tube spectrograph at the 2.6-m telescope of the Crimean Observatory was used. Markarian 6 was the first Seyfert galaxy for which the analysis of systematic spectroscopic observations was carried out. The authors

presented the first long-term $H\beta$ line flux curve for an AGN. They were also the first to introduce the now widely used technique of calibration of AGN spectra by assuming constancy of [OIII] line flux. A variable component in the blue wing of $H\beta$ line profile in the Markarian 6 nucleus spectrum was investigated. Changes of Seyfert type were first revealed.

K.K. Chuvaev continued monitoring AGN spectra with the image-tube spectrograph during about 20 years up to 1991. The archive of spectral data created by Chuvaev includes photographic spectra of Seyfert and Markarian galaxies. More than 20 of them were observed during the 20-year period. The results of long-term observations of $H\beta$ and [OIII] line profiles and their intensities in NGC 7469, NGC 5548, NGC 4151, NGC 1275, 3C 120, and others were published in a series of papers by Chuvaev [52–54]. Doroshenko [71] compiled results on investigations of AGNs NGC 7469, Mkn 509, Akn 120, and Mr 6, obtained from 1972 to 1992 using spectra from Chuvaev's archive. Spectral observations of AGNs by Chuvaev were described in a special paper by Pronik [183]. Using the image-tube spectrograph at 2.6-m telescope of CrAO. Kopylov et al. [125, 126] obtained spectra for dozens of Markarian galaxies and revealed 17 new Seyfert galaxies. Seyfert type changes were observed for the nuclei of Mrk 6 by Pronik and Chuvaev [184], NGC 3227—by Pronik [179], NGC 4151—by Lyutyj et al. [140] and NGC 7469—by Chuvaev et al. [55]. Two reviews on variability of emission lines were published by Lyutyj and Pronik [141] and by Pronik [180].

When did photometric brightness monitoring begin?

Photoelectric monitoring of AGNs was first performed with the 1.25-m telescope of CrAO in 1982. Observations of NGC 1275 were carried out over the period from November 12, 1982 to October 23, 1987 by N.I. Merkulova and I.I. Pronik using the photon-counting scanning spectrometer ASP-38. A differential photometric technique was employed. During 35 nights, a total of 379 series of observations of $H\beta$ [OIII] 4949, 5007 Å, and continuum fluxes were obtained. A continuum measure was taken 100 Å redward from the [OIII] doublet. The direct dependence between $H\beta$, [OIII], and continuum fluxes was obtained with time resolution of 0.5 h in each spectral region [150].

Figure 2.8 shows the obtained dependences of nightly averaged fluxes in the units of comparison star fluxes. One can see that variation of the emission lines $H\beta$ and [OIII] fluxes during 5 years was about factor of 4 [182]. It was shown that the histogram of continuum flux distribution has two-hump form like that of radio emission fluxes in 8-mm and 2.6-cm wavelengths. This fact do not contradict to the thesis that radio sources of AGNs strongly influences their optical appearance: optical structure of AGNs consists of two components, one of them generally aligned along the radio jets.

E.A. Dibaj and V.F.Esipov obtained spectra of NGC 1275 in optical in autumn of 1967. The profiles of emission lines $H\beta$, [OIII] 4959, 5007 Å, $H\alpha$, [NII] 6563 Å measured by Dibaj [65] are shown on Fig. 2.9. One can see that all profiles are asymmetrical. The redshift of the main peak of the profiles is equal to the redshift of NGC 1275 star formations. Blue component shifted from the main one on -10 Å

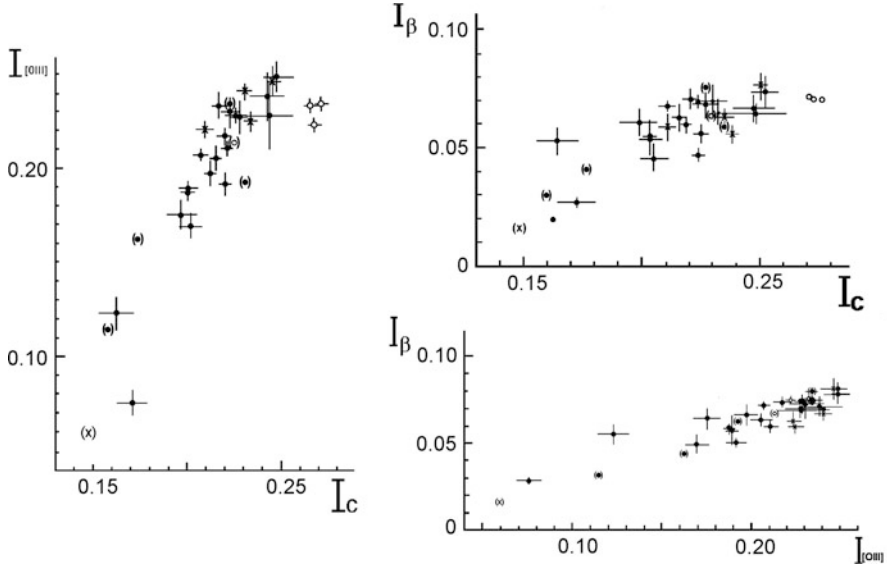


Fig. 2.8 The dependences of nightly averaged fluxes of $H\beta$, $[OIII] 4959, 5007 \text{ \AA}$ emission lines and continuum in the units of comparison star fluxes, obtained by Pronik et al. [182] in 1982–1987 for the NGC 1275 nucleus

or -600 km s^{-1} . It was assumed that in the nucleus of NGC 1275, there are two gas clouds, one of them is in the nucleus of the galaxy, and another one moves to observer with the velocity -600 km s^{-1} . E.A. Dibaj supposed that the last one is a jet from the galaxy nucleus. All these data permit to suppose that fluxes of emission lines and continuum obtained by us in 1984–1987 (Fig. 2.8) consist of two components. One of them corresponds to the nuclear gas, and another one to the jet which is observed in radio region. Part of the jet in the observed fluxes was essential as in BL Lac objects.

Since 1989, simultaneous UBVRI observations of selected Seyfert galaxies were carried out with the 1.25-m telescope at CrAO by N.I. Merkulova and L.P. Metik using the five-channel double image chopping photometer–polarimeter developed by Prof. Piirola. The character of the flux variability was found to be different for different sources. Up to 1,500 measurements were obtained simultaneously in the UBVRI bands for each galaxy nucleus NGC 1275, NGC 4151, NGC 5548, NGC 7468 over the period 1982–1998. Intranight observations lasted up to 8 h [181]. The structure functions (SFs) was computed for characterizing the flux variability. The SF parameter b can be defined as $b = 2 \log(\text{SF}) / \log(\Delta t)$ and interpreted as a characterization of the energy output rate or power of the emitting source. SF parameter b for intranight (dots) and internight (circles) UBVRI variations for four galaxies obtained using all massive observations are shown in Fig. 2.10. The figure shows that values of the b parameter for intranight variations are higher than those of internight variations over 5–8-years span. These data provide evidence for

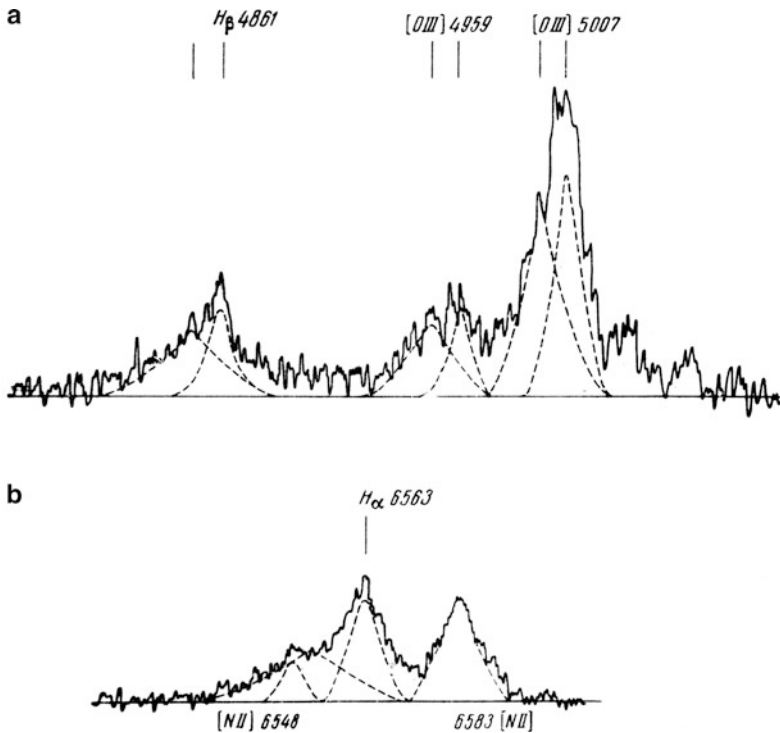


Fig. 2.9 Profiles of emission lines $H\beta$, $[OIII]$ 4959, 5007 Å and $H\alpha$, $[NII]$ 6563 Å obtained by Dibaj using spectra observed in autumn 1967 [65]

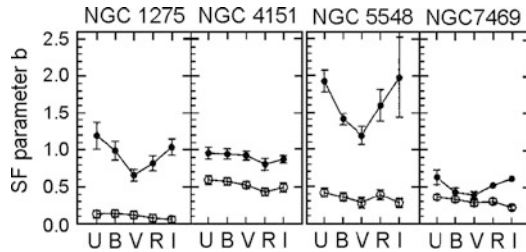


Fig. 2.10 SF parameter b for intranight (*dots*) and internight (*circles*) UBVR variations for four galaxies obtained using the massive observations over 5–8 years in 1982–1998

more powerful sources of intranight variations than for internight variations for all nuclei. It was suggested that the origin of intranight and internight variations is different for investigated galaxy nuclei.

Near Ultraviolet. Since 1983, space station “Astron” developed at CrAO operated for about 10 years beginning in 1983. N.I. Merkulova, L.P. Metik, V.I. Pronik, I.I. Pronik discovered that the 1600–3500-Å SED of circumnuclear regions in AGNs shows an excess of regions of recent star formation compared to the central regions

of normal galaxies. Variability of Mrk 573 Seyfert nucleus was observed in the UV region with an amplitude 0.75^m during about 2.5 years. Mini-Seyfert nuclei of NGC 598 (M 33) and NGC 5236 (M 83) showed a UV amplitude of about 1^m . The first source exhibits flares, but the second one shows drops of brightness in comparison with the normal state. Results obtained by Merkulova et al. were published in series of papers, one of them in 1990 [151].

Thank you, Iraida and Vladimir.

Dear Aleksander (Volvach), can you please tell us about the early days of AGN radio astronomy at CrAO?

The 22-m radio telescope RT-22 of the Radio Astronomy Laboratory of CrAO is located at the foot of Mount Koshka (“the cat”) on the shore of the Black Sea near Simeiz (20 km west from Yalta). Radio astronomical station “Simeiz” was founded in 1965 with single-dish observations of AGNs made beginning 1966. The first Very Long Baseline Interferometric (VLBI) observation was made in 1969. The “Simeiz” station was included in the VLBI network beginning in 1980. Several hundreds of AGNs were studied over the past years with VLBI. It was found that they have similar core-jet type structures with relativistic motions detected in components of the jets. Radio observations of AGNs have been performed at RAL CrAO since 1967 by Moiseev and Efanov [72]. Millimeter wave observations of extragalactic radio sources were started on the 22 m of RAL CrAO in 1973. Since 1973, over 25,000 observations of some 200 sources have been obtained. Extensive monitoring data for several dozen sources were combined with other observations at cm and mm waves to derive separate quiescent and flare spectral components that are crucial for understanding the structure and evolution of compact radio sources [227].

Thank you, Aleksander. We now ask people involved in the interpretation of observational results and in the definition of the main physical processes thought to occur in quasars. We will ask first about the observational support and then about the “engineering” of quasar models.

2.7 Early Modelling Attempts

Dear Julian (Krolik), in the 1970s, consensus formed around the idea of accretion onto black holes as the prime mover of quasars (and other AGNs) largely by a process of elimination of competing ideas. Is there now any positive evidence in support of this idea?

Although it is very difficult to demonstrate directly that any object is a black hole, that is, an object with an event horizon, there are now quite a number of observations that point strongly in that direction.

Of these, the most direct is our ability to detect the signature of matter orbiting deep in a relativistic gravitational potential. The $K\alpha$ fluorescence line of Fe has an energy that varies from 6.4 (in neutral Fe) to 6.9 keV (in H-like Fe). When

X-rays of energy at least 7.1-keV strike Fe atoms, they can remove electrons directly from the K-shell of Fe, and in 35% of these events, the atom relaxes by emitting a $K\alpha$ fluorescence photon. Because quasars radiate large quantities of hard X-rays, these $K\alpha$ lines are very frequently seen in their spectra. Since 1995 [220], X-ray telescopes have had the sensitivity and spectral resolving power both to detect these line features and to measure their profiles. Remarkably, they often show line widths $\Delta E/E \sim O(1)$ [32, 155]; in other words, if interpreted in terms of Doppler shifts due to line-of-sight motions, the atoms radiating them must exhibit a relativistic range of velocities.

A particularly easy way to understand matter with relativistic speeds is, of course, to suppose that it orbits in a relativistically deep potential. But the evidence that the matter responsible for these lines is orbiting around a black hole is stronger than this plausible qualitative guess: the detailed shape of the line profiles corresponds rather specifically to just that situation. To first order in v/c , special relativistic Doppler shifting due to circular motion by an orbiting ring of gas produces a line profile that is sharply peaked at the largest offsets and lower in the middle. The separation of the peaks grows with shrinking radius ($\propto r^{-1/2}$ in the Newtonian regime) and growing inclination of the orbital plane to our line of sight ($\propto \sin i$), but remains symmetric. When the radiating material is spread over a range of radii, these contributions add according to the relative power produced by each annulus. Special relativistic beaming also compresses the angular distribution of radiation, focusing it into the direction parallel to the orbital motion. General relativity breaks the spectral symmetry because, to second order in v/c , there is a systematic gravitational redshift. In addition, general relativistic effects bend photon trajectories. When all these contributions to the line profile are assembled, one expects a line profile with a sharp edge to the blue of the line peak and a much broader red wing. This is, in fact, the characteristic shape of observed lines. Detailed model fits have been made to the X-ray spectra of objects with the best-quality data, and they are generally well described by models in which the matter follows circular orbits in a common plane whose surface brightness rises steeply inward to a radius as small as a few gravitational radii ($r_g \equiv GM/c^2 = 1.5[M/M_\odot]$ km for central mass M) [32].

A less direct argument also points toward black holes as the prime movers of quasars: their near-ubiquitous presence at the centers of all good-sized galaxies. In the overwhelming majority of cases, these black holes are extremely faint, e.g., the luminous power of the black hole at the center of our own galaxy radiates only $\sim 100\times$ as much light as the Sun does. However, their masses can be measured by their effect on the orbits of nearby stars. By this means, we have found that dark objects with mass $\sim 10^6\text{--}10^9 M_\odot$ and sizes less than a few parsecs are commonly found in the centers of galaxies [103].

When these inferred black hole masses are compared with the properties of their host galaxies, strong correlations emerge. With scatter of only factors of a few, the dark masses in galactic nuclei have masses $\simeq 10^{-3}$ of the host’s stellar bulge mass [103, 144]. In this context, “bulge mass” means the mass of the spherical stellar structure near the center of a disk host galaxy, and the total stellar mass when

the host is an elliptical galaxy. Moreover, these inferred black hole masses also correlate strongly with the velocity dispersion of the stellar bulge, the characteristic magnitude of its stars' orbital velocity [81, 94, 103].

Applying these correlations to a large-scale census of the numbers of galaxies with bulges of a given mass or dispersion leads to an estimate of the total mass density in black holes in galactic nuclei [147, 238]: $3\text{--}5 \times 10^5 M_{\odot} \text{Mpc}^{-3}$. Assuming that all these black holes were once active quasars, one can estimate the total amount of energy that might have been released in their construction. Although there is much uncertainty about the details of this process, the relativistic character of black hole accretion means that one can expect a significant fraction of the accreted mass's rest-mass energy to be released. For a "radiation efficiency" $\eta = 0.1$, this argument predicts a total energy density of quasar light in the universe.

This prediction can be checked by direct measurement. All we need to do is add up the light from the quasars found in a small region of sky and multiply by the ratio between 4π and the solid angle of the survey. To determine the radiated light density produced per unit, comoving volume requires a further multiplication by $(1+z)$ to correct for how much the photons have been, on average, reduced in energy by cosmological expansion since they were made. To the degree that quasar light may have been absorbed between its source and us, this estimate is only a lower bound.

When one goes through this exercise, the result is a quasar light density remarkably close to the number arrived at by local measurement of the comoving mass density of black holes in galactic nuclei and assuming $\eta \simeq 0.1\text{--}0.2$. Conversely, it is very hard to imagine how the quasar light could have been made any other way. If the energy-generation process were the same as for stellar light, nucleosynthesis, η could be at best somewhat less than 0.01.

Thank you, Julian.

2.8 The Interpretation of Quasar Spectra

Dear Hagai (Netzer), you entered the field in the mid-1970s or about 10 years after the discovery of quasars. Did you find a paradigm already fixed when you entered the field and, if not, what sort of ideas were circulating about the physical nature of these sources? One area that you pursued involved the variability of these sources. What sort of variability timescales were discovered and what did this tell us about the physical nature of the quasars?

The idea of an accreting black hole (BH) as the main powerhouse of AGNs was in place in 1970 and even earlier. It was clear, right from the beginning, that no other mechanism can supply the observed luminosity while keeping with the extremely small dimensions inferred from the short timescale variations. Exotic alternatives, like super massive stars and even "white holes," have popped out, occasionally, but mostly from physicists who were interested in the new physics rather than astronomers trying to explain their observations. In this respect, there was no need

for a paradigm shift. There was, however, an urgent need to convert the basic idea to reality by finding the mechanisms that explain how this huge amount of radiation is actually emitted, what is the origin of the observed variable continuum, what is behind the unusual SED, and what is the origin of the unique emission-line spectrum.

The first variability studies were launched right after the discovery of quasars. For bright sources, these are relatively simple observations, especially the broad band photometric monitoring of luminous sources. Short timescales were immediately recognized as indications for small dimensions, but their origin was not understood. The search for periodicity, or other regular patterns, was always considered as the ultimate goal, but it took some time to realize that this is not going to be found so easily. In fact, the nature of AGN variability is still not very well understood today. Thus, while the main ideas of massive BHs, rapid but irregular accretion and small dimension, were recognized very early on, the real physical ingredients, and the modern AGN picture of today, took years to develop. The search for these ingredients can be described in terms of the main spectral components of AGNs: the multiwavelength continuum and the broad and narrow, large equivalent width (EW) emission lines. The idea of a nonthermal continuum was the one I have encountered first. This was thought to be the dominant process at all wavelengths. In fact, several of the very early variability studies focused on color changes, e.g., the change in $B - V$ during variations, in attempt to discover the changes in the spectral index of a synchrotron sources. I was involved in such studies, as an undergraduate student in Israel, in 1971. The thermal origin of the optical–ultraviolet (UV) continuum was suggested, seriously, only in the late 1970s. This was motivated by the understanding that a big part of the optical–ultraviolet (UV) continuum cannot be described as a simple power law in energy. This led to the study of the actual accretion mechanism, rather than the general concept, and involved accretion disks. The concept of accretion through “geometrically thin optically thick” accretion disks was known since the 1960s. It was formulated, in great detail, by Shakura and Sunyaev in 1973 [210] but took about 15 more years to reach the stage that detailed comparison with real AGN observations could be used to validate it and to infer the disk properties. Milestones along this way are the suggestions by Shields in 1978 [212] Malkan and Sargent in 1982 [145, 146] that some of the blue observed continuum is due to such disks. It is only in the late 1980s that such ideas turned into semi-realistic models, starting with the simple collection of blackbodies, or the combination of stellar spectra (e.g., [219]), continuing with the inclusion of electron-scattering atmosphere [60], and ending with the more detailed work of Laor and Netzer [134] that included a treatment of the opacity in the disk atmosphere and the general relativistic effects. The 1970s have also seen major improvements in the observations of low- and high-redshift AGNs, their classification, and the understanding of the observed broad emission-line spectrum. A heroic effort by Don Osterbrock, his students and postdocs, resulted in beautiful spectra, first-class measurements, and detailed classification of dozens of nearby type-1 and type-2 AGNs (e.g., [164]). This work provided the first benchmark for testing the emission-line models developed at the same time. The addition of many

rest-wavelength UV lines, collected from observations of high-redshift sources, took a few more years (work by J. Wampler, W. Sargent, A. Boksenberg, and others).

The first detailed realistic models of the BLR and the broad emission lines, go back to the work of Davidson in 1972 [63] and also McKee and Tarter [143], McAlpine in 1972 [142], and others. The early work of Davidson introduced the concept of ionization parameter, adopted from other areas of astronomy, that is being used, almost in the same way, until today. He published the first scalable emission-line models and realized that conditions in sources with different luminosities scale with L/r^2 . The density estimated for the emission-line gas was already close to what we know today, and the typical BLR size inferred from these conditions was larger by a factor of 5–10 compared with the known size of today. Such realistic models were essential to understand, later on, that something was missing in these models. This was hinted by several unusual line ratios that were never observed in other emission-line nebulae. This discrepancy is what led me to suggest, in 1975 [160], that the physics of the broad emission lines is very different than what was suggested until that time.

Thank you, Hagai. It is now important to ask how we came to understand (even if not yet fully) quasar birth and evolution and their place in the Cosmos.

2.9 Quasars in a Cosmological Context

Dear Alfonso (*Cavaliere*), what was your preferred model of the universe at the time the quasars were discovered?

As in the late 1960s, I entered astrophysics from plasma physics, cosmology was the realm of few data and many speculations. The cosmological origin of the microwave background radiation, not yet pronounced CMB, was still doubted at times; in fact, its blackbody nature was still argued against, as the Wien spectral maximum was at best looming out in the data at $\lambda \approx$ a few mm. On the other hand, the cosmic abundances of He and D were still blurred by considerable observational uncertainties. So the very Big Bang picture was still challenged at times by supporters of the steady-state view of the universe.

As to specific cosmological models, a number of mathematical and sometimes farfetched possibilities were still entertained. Many workers in extragalactic astronomy and astrophysics were of course adopting the classic Friedmann–Robertson–Walker models for the expanding cosmic scale; but then both key parameters ranged widely in the current usage, H_0 from 50 to 100 km s⁻¹ Mpc⁻¹, and $\Omega_0 = 0, 1$ at the empty or the critical value.

On my side, with inspiration from the neat formulations and sharp discussions by Weinberg in his 1971 book “Gravitation and Cosmology” [235], I had been conquered at once by the Big Bang picture, so adroit in extending the cosmic expansion back to cosmic times of order $t \sim 10^{-43}$ s (then inflation was still to come) and so clever in linking whatever data were available about current density and CMB temperature with the values suitable for cooking up the light elements at $t \sim 3$ min.

Specifically, the flat critical model with $H_0 = 75 \text{ km s}^{-1} \text{ Mpc}^{-1}$ was winning with me on grounds of uniqueness and simplicity and tolerable mismatch with lower bounds (then loose) on the universe’s age. So with no hesitation, I adopted this as the best available space-time arena to embed the specific evolutions of quasars and clusters of galaxies that were central to my research interests.

It so happened that the advent in the years 2000s of the flat, dark energy and dark matter dominated cosmology with $\Omega_M \approx 0.27$ and $H_0 \approx 71 \text{ km s}^{-1} \text{ Mpc}^{-1}$ implying the universe age $t_o \approx 13.7 \text{ Gyr}$ now standard (despite its still unfathomed heart of darkness), in practice, required little revision of my own scales of distance and time, especially for $z > 0.5$.

What were the prevailing cosmological ideas at that time when the largest known quasar redshifts were a few tenths and before the advent of concepts, such as, supermassive black holes, mergers, dark matter, and dark energy that play such important roles today?

It is worth stressing that the assessment of the cosmological framework was predated by a number of cosmogonical concepts concerning the populations of normal galaxies and of the so-called peculiar sources. For one, by the beginning of the 1970s, the excess number counts of radio sources down to a given flux had been accepted as proof of cosmological source “evolution,” that is, of more and/or brighter sources long ago and far away in the universe.

In addition, the first z -resolved luminosity functions were emerging also for radio-quiet quasars. Here, complete samples were slower to come, but the glaring redshifts were clear markers of epochs, and warranted empirical models privileging either “density” or “luminosity” evolution.

On the upside, these observational marks of evolving populations disagreed with the overall steady-state view, soon put to a final rest by closer CMB spectral measurements. On the downside, the extended and smooth luminosity functions soon recognized in quasars frustrated all attempts to pick a standard candle for charting directly the expanding cosmic framework. Moreover, the evolution intrinsic to quasars soon appeared to be strong enough as to overwhelm any difference in expansion envisaged by sensible cosmological models.

Once again, Weinberg’s book nailed this down in the form of a neat theorem, to the effect that efforts at deriving the cosmological model from the counts were doomed to fail in the absence of a firm grasp of the intrinsically evolving luminosity functions.

All that motivated us to tackle the quasar demography [45]. To that aim, we wrote a “continuity equation”:

$$\partial N / \partial t + \partial(\dot{L} N) / \partial L = S \quad (2.1)$$

for the change in cosmic time t of the (differential) luminosity function $N(L, t)$. This is treated as a hydrodynamical flow of source density spreading or converging over the $L - t$ plane, with L playing the role of a one-dimensional coordinate.

The flow takes place with velocity $\dot{L}(L, t)$ given by average brightening or fading of the sources, once they are given birth according to the source function $S(L, t)$. These two functions are to embody the essence of the physical processes governing the source demographics.

By way of relevant examples, sources undergoing a density or a luminosity evolution are described by particular solutions of (2.1). The former evolution corresponds to $\dot{L} = 0$, and implies a rising normalization of the luminosity function with no change in shape; the simple instance with $S = N/\tau$ yields for $N(L, t)$ an exponential rise in look-back time on the scale τ . The latter evolution corresponds to $S = 0$ with $\dot{L} \neq 0$, and implies $N \dot{L} = \text{const}$, that is, a shift to higher L with no change in the integrated source number. More structured evolutions obtain from combining these into a general solution. Thus, (2.1) provides a handle to bridge the gap from empirical fitting formulae to astrophysical processes.

In one of your first papers, you used the term “active galactic nuclei.” Was it already commonly used then? Did you think that all high-redshift quasars were likely hosted by galaxies or were you, and others, open to the idea of naked quasars?

I think the notion, if not the term, was around by then. In fact, Seyfert galaxies harbored the first bunch of “peculiar” nuclei singled out in 1943 by C. Seyfert; these were physically discussed by Woltjer [237] who based on line widths and nuclear compactness combined into a virial-like relation $M \sim v^2 r/G$ to estimate the binding masses at $M \sim 10^8 M_\odot$. Then came the radio galaxies and eventually, the quasars since 1962–1963 as recounted elsewhere in this book.

Strong similarities between these source classes had been recognized, and were discussed at length in the book [39]. These features included high and compact nuclear brightness, narrow and broad emission lines, and in some cases, nonthermal radio emissions.

Thus, by the late 1960s, the ground was tilled for grouping all these sources together. The straight implication—though one not always held by the latter authors themselves—pointed to quasars being scaled-up versions of Seyferts from under $L \sim 10^{45} \text{ erg s}^{-1}$ into the range $10^{46} \div 10^{48} \text{ erg s}^{-1}$, but similarly hosted in galactic nuclei.

However, the formation and evolution of the galaxies themselves was much in a floating state until Press and Schechter [177] derived their hierarchically evolving mass function. With all its sweeping and long-debated simplifications, this constitutes another case of clever and winning adroitness in capturing the basic thread that connects the sequential formation of all cosmic structures of increasing masses.

Yet, for a long while, this went nearly unnoticed, to be eventually corroborated by the advent of the cold dark matter paradigm (see Peebles [172] and references therein). This was soon followed by the other paradigm describing the development of cosmic structures in the specific terms of repeated mergers, perhaps more striking in numerical simulations [236] than on the real sky. To my knowledge, the paper [48]

marked the first use—due to soon expand into a commonplace in the 1990s—of Press and Schechter in the quasar context to substantiate the birth function S in (2.1) and explicitly link—with some delay—QSO shining with galaxy forming.

So then, what stance in this context take the AGNs: fading embers of once flaming sources, to imply negative \dot{L} fading down on timescales of several Gyrs or small fires rekindled or kindled anew in closer galaxies, to imply a source function S prolonged down to low z ? Surely, a telling sign (argued by [47]) would be provided by the relic masses left over in galactic nuclei as fossils of a sort from a flaming past. On average, these would be far more massive under the former activity pattern; however, at the time, only tentative estimates and upper limits were available. We may take up the issue and some related developments later on in this volume.

On the other hand, naked quasars are conceivable if rare in both scenarios as a result, e.g., of slingshot effects caused by multiple galaxy encounters and deep mergers; in fact, tens of quasar pairs have been observed by now, sufficiently close as to provide credible candidates for a further encounter to unbind a source. The other issue, however, concerns how long quasar-like luminosities can be sustained from a naked object.

Your earliest papers (1969–1970) suggest that you had already adopted the idea of a compact massive object in connection with quasars. Was this motivated by experimental or theoretical considerations?

Perhaps, the main motivation in that pioneering era was pretty empirical: pulsars/neutron stars had just been discovered, and provided glaring—if scaled down to stellar masses—prototypes of compact objects that deliver not thermonuclear but rather rotational/gravitational energy with high efficiency [46]. On the theoretical side, the role of gravitation had to be overwhelming at mass scales $10^8 M_\odot$ or larger, considering the energy and compactness associated with the quasar engines.

In fact, sources that produce in excess of 10^{60} ergs (as often gauged) from masses $M \sim 10^8 M_\odot$ can release under a moderate efficiency $\eta \approx 10^{-1}$ more binding energy $G M^2/2r$ erg as they gather to sizes $r < \text{light-day}$ (indicated especially in blazar-type quasars by intraday flares and by the presence of narrowly collimated jets) than possibly obtained from nuclear reactions at their upper yield $0.008 M c^2$.

The gravitational efficiency is estimated at $\eta \approx r_s/12r \lesssim 0.08$ when the size approaches the last stable orbit around a black hole at $r_s \sim 3GM/c^2 \sim \text{light-hours}$. Full general relativity focuses the value to $\eta \approx 0.06$ for a non-rotating hole at r_s , and up to nearly 0.4 for a maximally rotating one.

All that squared well with the picture of accreting supermassive black holes (SMBH) as pioneered by Salpeter and Zel’dovich et al. [138, 194, 241] and tackled by Rees [186]. The latter stressed their role as stable endpoint configurations behaving as an attractor, as it were, for diverse paths of development including growth from seeds in the range $M_{\text{BH}} \sim 10^2 \div 10^5 M_\odot$ left over by early massive or supermassive stars. This convincing paradigm splits the roles: the SMBH provides the gravitationally active mass with high efficiency, while the output $L = \eta c^2 dm/dt$

is fueled by accretion at a rate dm/dt from a surrounding stockpile holding a gas mass $m \sim 10^{10} M_{\odot}$. Part of this accrues to the SMBH and constitutes a relic of all past activities in a fossil form, as it were.

It follows that in the presence of a rich gas supply, as likely occurs at quasar birth in a collapsing galactic halo, the accretion is only self-limited by the radiation pressure exerted mainly via Thomson scattering. This leads to the classic Eddington luminosity, a combination of microscopic fundamental constants yielding values $L_E = 1.3 \cdot 10^{46} M/10^8 M_{\odot} \text{ erg/s}$ that (despite geometrical simplifications) remarkably suit the observed QSO outputs. The related accretions $dm/dt = L_E/\eta c^2 \approx$ a few M_{\odot}/year cause the holes to exponentiate their masses on the common timescale $\eta t_E = 40 \text{ Myr}$, taking some 600 Myr to grow from 10^2 to $10^8 M_{\odot}$.

Thus, the SMBHs grow up rapidly in mass and activity, but as their reservoirs are exhausted, they fall asleep and remain dormant, waiting for any next fueling to come. This will be supply-limited, thus sparing and possibly intermittent, depending critically on specific accretion drivers.

Thank you Alfonso. So many quasars have been discovered since the 1960s—and many classes and types have been defined. Some classification schemes are now defunct; however, the existing terminology can be confusing if not framed in a simpler conceptual scheme.

2.10 The Affirmation of a Unified View

Dear Paolo (Padovani), can you help us unify the main types of AGNs? Is there any subtype that does not fit into the major unification schemes?

The prevailing picture of the physical structure of AGNs is inherently axisymmetric and includes an accretion disk, which produces optical/ultraviolet and soft X-ray radiation, fast moving clouds giving rise to the broad lines observed in AGN spectra, gas and dust, possibly in a flattened configuration (the so-called “torus”), absorbing this radiation along some lines of sight and re-emitting it in the infrared, and slower moving clouds beyond the obscuring material producing narrower lines. Outflows of energetic particles can occur along the poles of the disk or torus, escaping and forming collimated jets and sometimes giant radio sources when the host galaxy is an elliptical, but forming only very weak radio sources when the host is a gas-rich spiral. The plasma in the jets, at least on the smallest scales, streams outward at very high velocities, beaming radiation relativistically in the forward direction [225]. This model implies a radically different AGN appearance at different aspect angles. In practice, AGNs of different orientations will therefore be assigned to different classes. Unification of fundamentally identical but apparently disparate classes is an essential precursor to understanding the underlying physical, intrinsic properties of AGNs.

Based on a variety of arguments related to their intrinsic, isotropic properties, Seyfert-2 galaxies, which show only narrow lines, have been “unified” with Seyfert-

I galaxies, which display broad lines, in the sense that the former are thought to be the same objects as the latter with the central nucleus obscured by the torus [2]. On the same vein, low-luminosity (so-called Fanaroff-Riley type I [FR I]) and high-luminosity (FR II) radio galaxies have been unified with BL Lacs and radio quasars, respectively [2, 225]. In other words, BL Lacs are thought to be FR I radio galaxies with their jets at relatively small ($\lesssim 20\text{--}30^\circ$) angles w.r.t. the line of sight. Similarly, we believe flat-spectrum radio quasars (FSRQs), defined by their radio spectral index at a few GHz ($\alpha_r \leq 0.5$, $f_\nu \propto \nu^{-\alpha}$), to be FR II radio galaxies oriented at small ($\lesssim 15^\circ$) angles, while steep spectrum radio quasars ($\alpha_r > 0.5$) should be at angles in between those of FSRQ and FR IIs ($15^\circ \lesssim \theta \lesssim 40^\circ$). Blazars, which include BL Lacs and FSRQs, whose main difference is the absence in the former class of strong, broad lines, are then a special class of AGNs, which we think have their jets practically oriented toward the observer.

This relatively simple scenario has survived basically unchanged for the past 30 years or so, which does suggest that overall, it is a reasonable representation of reality. One open issue was the apparent absence of the obscured versions of the high-power equivalent of Seyfert-1 galaxies, radio-quiet quasars, the so-called QSO 2s. This was not only a problem for unification, as such sources were needed to explain the X-ray background [98]. It has now been realized that these objects are selected against by (classical) optical searches, tuned to find AGNs with strong (and unabsorbed) nonstellar optical–UV continua. Seyfert-2 galaxies are relatively easy to find locally where selection is based on host galaxy properties, but at higher redshifts, one needs to move to bands less affected by absorption, like the IR and hard X-ray ones. Indeed, many examples of X-ray- and IR-selected QSO 2s are now known (e.g., [83, 171, 218]).

A few refinements and additions to unified schemes have come up recently. These include (a) the fact that obscuration toward the nuclei of FR Is appears to be much smaller than in FR IIs (e.g., [50, 74]), which indicates that a standard torus might be present only in the latter class (and therefore obscuration plays a small role, if any, in the FR I–BL Lac unification); (b) a separation of radio galaxies on the basis of their nuclear activity into high-excitation (HERGs) and low-excitation (LERGs) radio galaxies shows that, while most FR Is are LERGs and most FR IIs are HERGs, there is a population of FR II LERGs as well [132]. These cannot be radio quasars seen at large angles [105], and their weak IR emission [161] suggests that, like FR Is, they lack a torus. Therefore, the “proper” unification might be of LERGs with BL Lacs and HERGs with radio quasars; (c) the addition of accretion rate as another possible “axis” of AGN unification, with sources accreting at less than 1% of the Eddington luminosity being unobscured and yet lacking a BLR [223], which also fits with the lack of a torus in FR Is discussed above; (d) the likely random alignment between the torus and the accretion disk or a very small torus covering factor (both contrary to expectations), given the presence of almost edge-on disks among quasars [188]. Finally, low-ionization nuclear emission-line regions (LINERs), originally identified in otherwise normal spiral galaxies showing potential evidence for AGN, have long been known to be a rather mixed bag. Recent work suggests that many LINERs are simply galaxies that have stopped forming stars and are ionized by their

old stellar populations. This would mean that many LINERs have no role in unified schemes of AGNs, despite the fact that they are often counted as AGNs in optical surveys [56].

Thank you, Paolo. We now move to an entirely different view of quasars, and in many ways to a different universe. Not everyone back in the 1960s accepted at once that quasars were “fast and far.” Several astronomers suggested that quasars were not at the distances implied by their redshift. In the course of time, some of them pointed out “oddities” in the standard scenario, e.g., connections between nearby galaxies and distant quasars or periodicity in the redshift distribution. We now ask two of the most eminent critics of the standard interpretation to report their supporting observational evidence and their alternative views on quasars.

2.11 Challenging the Standard Paradigm

Dear Halton (*Arp*), what were the most widely debated issues in astronomy just before the quasars were discovered? What drew you into quasar research? You changed from globular cluster H–R diagrams to quasars just after the initial quasar discovery period. What attracted you to the quasar field? Did this discovery motivate the *Atlas of Peculiar Galaxies*? When you entered the field, did you find a paradigm already fixed in place? Did you subscribe to the standard paradigm for some time or had you already abandoned standard approaches and solutions? What observations motivated this abandonment?

The most widely debated issue in astronomy just before the discovery of quasars in 1962–1963 was the Hubble constant, sometimes referred to as “cosmology in search of a number.” Observers competed strongly over the value of the expansion velocity of the universe. I was eager but busy doing globular cluster color-magnitude diagrams because Hubble and Baade wanted to improve the accuracy of the local distance scale. When the unprecedentedly high redshifts of the quasars were discovered, however, there was a rush to find more quasars, and particularly, to announce record high redshifts. It became clear that positions of quasar candidates were not freely available, so I chose to use my allotted telescope time to study critical examples of active nuclei and morphologically disturbed galaxies. My major interest had always been the birth and evolution of galaxies. In an ironic turn of events, as soon as the “*Atlas of Peculiar Galaxies*” [6] was finished, I reported that a fairly complete catalogue of peculiar galaxies showed physical interaction with radio sources and quasars associated with disturbances in the galaxies. As more and more radio, and now X-ray and ultraviolet, studies showed, quasars were ejected from galaxies, evolving from plasmoids of modest luminosity into smaller companion galaxies with smaller, but quantified, non-Doppler redshifts. I will attempt to communicate these results.

In the course of assembling the *Atlas of Peculiar Galaxies* [6], it was noticed that 3C 273 was situated in the central region of the Virgo Cluster, forming an aligned

pair with 3C 274 (M87) across the central galaxy of the cluster, the largest galaxy NGC 4472 (3C 275). The chance of accurate alignment of these two very bright active nuclei with the central galaxy was 1 in one million. This requires these three objects forming a physical association, and being at the same distance from the earth in spite of having very different redshifts.

Meanwhile, the Burbidges and Hoyle, in informal discussions with colleagues, put forward the idea of quasar redshifts being a consequence of intense gravity fields in quasars. This model would have produced enormously broad emission lines, and for this reason, the model was discarded. Therefore, a model involving conventional physics to explain these intrinsic redshifts was not possible.

It was already known at that time that in a large number of radio galaxies, the two lobes of the radio emission were symmetrically located with respect to the central optical galaxy. It had been reluctantly accepted that the two radio lobes were the result of symmetrical ejections of plasma from the central galaxy. So there existed direct observational evidence of ejection of plasma clouds from a compact central object (the nucleus of the radio galaxy). We propose that we are seeing the same phenomenon in quasars paired with respect to a galaxy and that we are observing the time evolution of these plasmoids as they are ejected in different stages.

The important parameter in this model is the high-energy plasma states, which produce the synchrotron energy in the nucleus of the ejecting galaxies. These plasma states are expected to oscillate and produce quasars at different redshifts. The plasma energy density oscillations could occur in arcs. This could be the explanation for the nearly concentric luminous arcs seen around some galaxies. The best example is Arp Atlas number 227.

The operational definition of quasar-like objects is the large amount of high-energy radiation observed as synchrotron radiation, mostly in the optical, UV, and X-rays. The intrinsic redshift decreases with time because the mass of the particles increases with time. The intrinsic redshift of the quasars and of the galaxy nucleus from which they come can be calculated. It is found that the intrinsic redshifts match very closely the Karlsson peaks. This coincidence with the peaks together with the frequent occurrence of symmetrical pairs make it certain that the quasar–galaxy juxtapositions are not accidental.

After almost 50 years, quasars are still mandated to be the most luminous objects in the universe because their high redshifts are widely interpreted to be velocities of recession in an expanding universe—implying that they are very distant objects. That is the essence of the standard paradigm. Below, we summarize major points of historical and current evidence that cannot be reconciled by this paradigm.

What defines a quasar?

QSR, QSO, quasar, compact galaxy, N (compact nucleus) galaxy, and Seyfert galaxy are all variations on a class of compact, high surface brightness objects that were intensely investigated starting about 1963 motivated by their surprisingly high redshifts. The loose usage of “quasar” signifies a high surface brightness object

(showing a near stellar image ~ 1 arcsec). If the redshift is greater than $z \sim 0.30$, then we can adopt usage of the term “quasar.”

However, even this loose definition carries its own refutation because the first discovered and most famous quasars, 3C 273 and 3C 48, are eliminated from the class: the first shows a redshift of only $z = 0.158$, and both violate the compact image stricture showing size greater than $12''$ radius (see [7] pp. 56–58). Actually, even if we specify exactly the constraints, it is not possible to organize a rigorous taxonomy for quasars. The elements of the subject are not operationally defined. For one, the luminosity is taken from the redshift/distance relation, which is a theory, and not a universally accepted one. For another, the calculated luminosity shows an arbitrary value of $M_V = -23.1$ mag. The respected Harvard physicist Percy Bridgman emphasized the importance in science of dealing only with operational definitions [33]. The challenge then becomes if it is possible to design a meaningful definition for a quasar? One place to start is with the radio sources discussed in the introductory comments above.

Radio Sources. It is accepted that radio sources are ejected from galaxies, that is, the famous double-lobed radio sources centered on some galaxies. High surface brightness nuclei and morphological disturbances usually describe the galaxies from which objects are ejected. The basic pattern is one of pairing of ejecta across the nucleus. This alignment signals conservation of linear momentum as the objects emerge from a galaxy. Recently, particularly well-aligned pairs of sources have been discovered, herein described, that can be assumed to be traveling with equal velocities toward and away from the parent galaxy. Only these pairs show redshifts different from the galaxy that lies between them. For the first time, we attempt to measure an ejection velocity separately from what we assume to be the largely intrinsic (i.e., non-Doppler) redshift [84]. The similar placement of pairs of higher redshift radio quasars across lower redshift AGNs were already long ago (e.g., 1969) a strong indication that at least some quasars lie at distances comparable to nearby galaxies.

Nonthermal Radiation. Galaxies or parts of galaxies can, e.g., be ionized at an early stage of their formation, or as part of an ejection process. One way galaxies can lose energy is by nonthermal radiation due to acceleration and deceleration of charged particles. On the other hand, thermal radiation from heated matter is not the controlling factor in the evolution of ejected matter. Nonthermal radiation, which is the defining characteristic of newly formed matter, dominates the overall form of the spectra of newly ejected objects. We suggest that the UV excess and nonthermal emission are due to particle mass being a function of time.

What do you believe is the main evidence in favor of intrinsic quasar redshifts?

There is substantial evidence that quasar redshifts are discretized and/or periodic [118–121]. Such observed properties argue against acceptance of quasar redshifts as indicative of recession velocities. The alternate interpretation is that extragalactic redshifts are intrinsic. In [156, 158], and [7] the redshifts are interpreted as related to the age of a source. In this view, the youngest matter shows the largest redshifts. Regardless of what causes the intrinsic (non-velocity) redshift, however, there

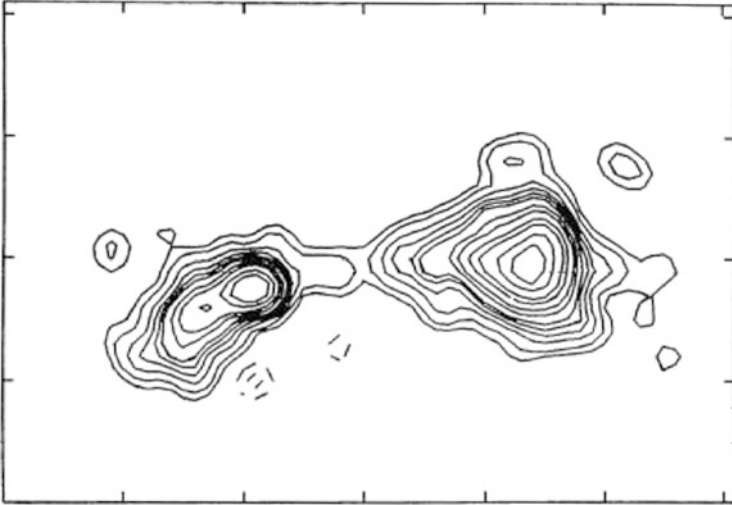


Fig. 2.11 1.6 GHz radio map of 3C 343.1 [76]. Separation of the two sources is $0.25''$. Note the opposite ejections from the radio galaxy with the western one leading directly into the quasar. The compression of radio contours on the west side of the quasar suggests motion directly away from the galaxy

may be a small positive or negative velocity component that contributes to the overall redshift. We present below details of the elucidation of several galaxies with associated quasars.

3C 343.1. When the nucleus of an active galaxy is observed spectroscopically, it will most likely show emission lines at the redshift of the rest of the galaxy and superposed on a nonthermal continuum. In the case of the M87, jet we only observe this nonthermal component. The nucleus is sometimes variable in brightness [224]. Only rarely reported is an object with more than one set of lines with different redshift values. A notable exception was one of four radio quasars observed in the early operation phase of the 10 m Keck telescope. This object, 3C 343.1, showed a set of lines which gave a redshift of $z = 0.34$ and another set which gave a redshift of $z = 0.75$. The separation of the two objects/components was only 0.25 arcsec and required a high-resolution radio map to reveal the radio connection between the two [76]. Figure 2.11 shows radio isophotes that establish ejection in opposite directions from the galaxy/quasar. Compression of the isophotes at the head of the western quasar attests to its motion outward which has left a trail back to the lower redshift galaxy of origin. Using data from more recent studies [14] have computed a conservative probability of $\sim 1 \times 10^{-8}$ that the superposition of the two objects is accidental.

One might ask what is the probability of accidentally finding this strong radio source quasar in the background within $0.25''$ of an arbitrary position on the sky ($P = 3 \times 10^{-11}$ [10]). If we further consider the unlikely coincidence that radio tails would point toward each other, the combined probability of random occurrence

is $P \leq 10^{-14}$. We also found that the redshift values of the two objects fulfilled the previous prediction of Karlsson for quantization of quasar redshifts. (For references to the derivation of these peaks see [10, 13, 42].) The peak redshifts in the present range are: $z_K = 0.06, 0.30, 0.60, 0.96, 1.41$.

The galaxy/quasar at $z = 0.344$ is close to the $z = 0.30$ value, and the quasar at $z = 0.750$ is midway between two preferred values. The solution to this apparent discrepancy is to remember that we should calculate the redshift of the ejected quasar *as seen from the ejecting galaxy!* In this case, the $z = 0.75$ quasar in the $z = 0.344$ reference frame is: $(1+z_0) = (1+z_Q)/(1+z_G) = 1.750/1.344 = 1.302$

So what was an apparent violation of Karlsson's quantization peaks becomes another strong confirmation at 0.302. It is important to note that testing Karlsson peaks must be done with attention to criteria composed of classes of active parents.

Properties of active galaxies can be quantified by strong radio, X-ray, or disturbed morphological characteristics. A test plotting all quasars and all galaxies over an area of the sky will likely give a negative result. (Also, high surface brightness, nearness, alignment, connections, jets, and generally, signs of disturbances mark candidate parent galaxies.) The quiescent galaxies then form a control sample for the ejecting galaxies with the many nonequilibrium features connected with the latter. The importance of validating the Karlsson peaks is that just by themselves, they represent repeatable evidence for non-velocity redshifts. As argued subsequently, they also establish an ejection origin for quasars (is there any other way for the quasars to get out of the nucleus?). Finally, Karlsson peaks allow us to see the quasars at the very beginning of their evolution into new galaxies. And over it all hangs the mystery of what causes the periodicity in the Karlsson values. Is there a connection between that series with implications of population dynamics or frequency as the smallest matter node under musical control?

IC 1767. Figure 2.12 schematizes the environment of the disturbed galaxy IC 1767. The bracketing pair of quasars is so optically bright (magnitudes 17 and 18), radio bright and X-ray bright that it obviates the need to calculate a probability of random occurrence for the configuration.

We summarize additional properties that demonstrate the likelihood that the quasars have been ejected from IC 1767. When the quasar redshifts are transformed to the frame of reference of the central galaxy, they become $z_0 = 0.64$ and 0.58 (an average of $z_0 \sim 0.6$, a major Karlsson peak).

AM 2230-284. During study of the relation between quasars and galaxies in the 2dF field, a concentration of quasars was found [84]. The most striking aspect was the redshift similarity of 14 central quasars (around a mean $z = 2.149$) with a range of only ± 0.019 . The cluster in spite of its high redshift subtends an area of diameter $D = 2.3^\circ$. At the conventional redshift distance, this diameter corresponds to 180 Mpc [15]. AM 2230-284 is diagrammed in Fig. 2.13.

The conventional assumption that redshift indicates distance in an expanding universe yields a size for this cluster of quasars, 180 Mpc, that is unrealistically large. Our interpretation of the redshift within an ejection scenario would reduce the distance and hence size of this configuration.

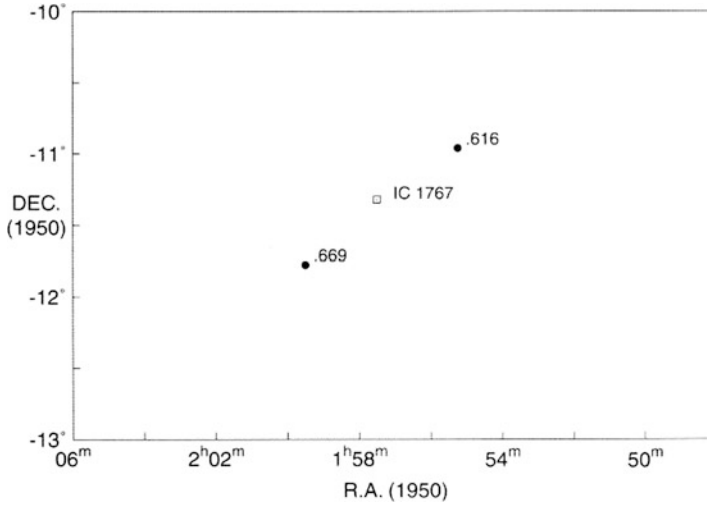


Fig. 2.12 Radio quasars paired across disturbed galaxy IC1767 [10]. The pair with corrected $z = 0.6$ and $z = 0.6$ are aligned across the galaxy with $z = 0.018$

In Fig. 2.14, we show residual redshifts about the mean cluster redshift for the innermost 14 quasars. Note that seven quasars have slightly higher redshifts than the mean and seven have slightly lower—this is the evidence of ejection. This is exactly what one would expect from the empirical evidence for ejection of *oppositely directed pairs from parent galaxies and AGNs*.

You mentioned that quasars appear to having been ejected by nearby active galaxies. Can you please illustrate a few ejection examples that you consider most convincing?

NGC 3628 (Fig. 2.15, panel (a)) is a starburst galaxy with a low-level active nucleus that has been extensively observed at X-ray, optical, and radio wavelengths. I with my collaborators [12] identified numerous indications of ejection activity associated with the quasars. Most notably, there is a quasar pair along the minor axis with nearly identical redshifts ($z = 0.99$ and 0.98). A narrow X-ray and optical filament extends out from the galaxy nucleus and passes through the nearer quasar in the pair. It terminates at a third quasar with $z = 2.15$. These quasars are likely ejected especially considering that they all lie within 6 arcmin of the galaxy.

NGC 2639 (Fig. 2.15, panel (b))—optical spectrophotometry [35] measured two blue stellar objects located at the centers of compact X-ray sources bracketing NGC 2639, a LINER/Seyfert-2 galaxy. Both objects were identified as quasars with similar spectra and measured redshifts of $z = 0.03$ and 0.32 (suggesting association of the quasar pair with NGC 2639).

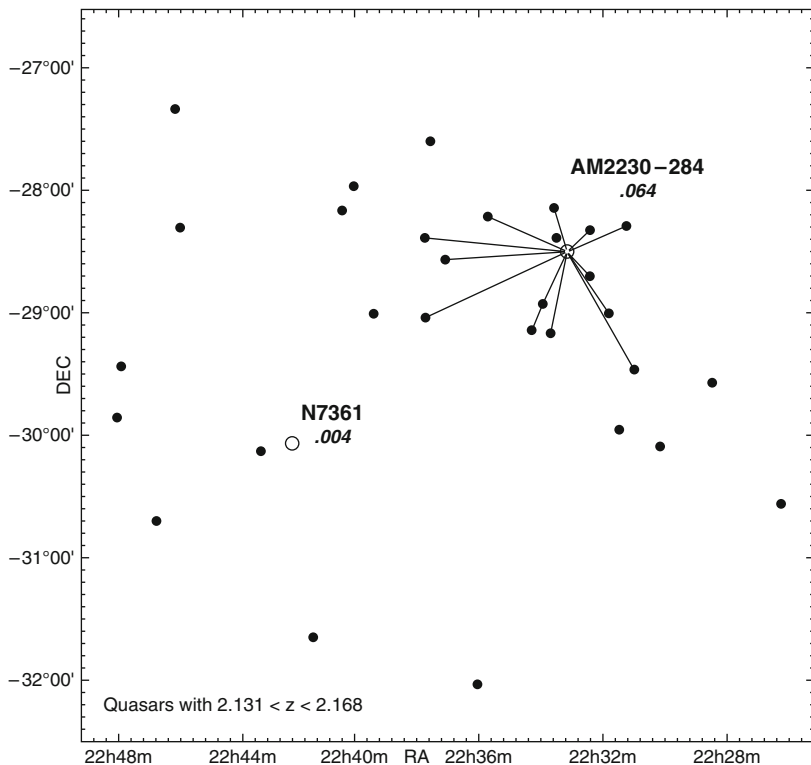


Fig. 2.13 Plot of catalogued quasars $2.131 < z < 2.168$. The central 14 quasars are shown connected to the assumed parent galaxy

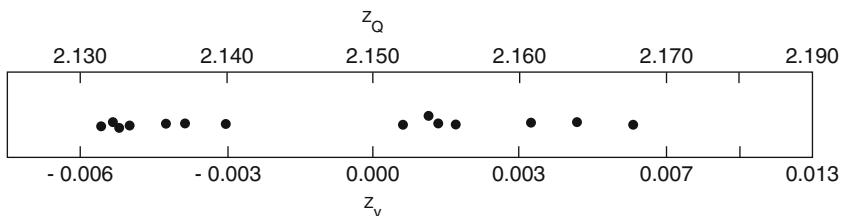


Fig. 2.14 The Redshifts (z_Q) of the 14 QSOs within 70 arcmin of AM 2230-284. Their mean is $z = 2.148$

NGC 3516 [51] and NGC 5985 [9] are both Seyfert galaxies with 11 quasars aligned along their minor axes (Fig. 2.15, panels c and d). Ten of these clearly associated quasars fell close to Karlsson quantized redshift values (see [7] p. 244, pp. 284–285). Most recently, Burbidge and Napier [42] tested the periodicity yet again with three different samples of quasars and found the fit to be significant at the 10^{-5} level.

Fig. 2.16 M 87 jet from John Biretta via William Keel (<http://www.astr.ua.edu/keel/agn/m87jet.html>)

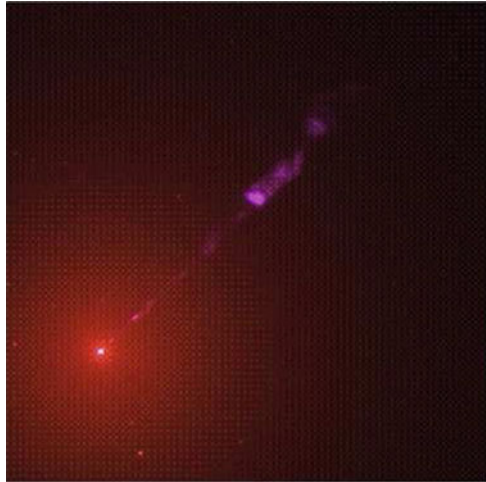


Table 2.1 Evidence of intrinsic quasar redshifts

Evidence of intrinsic redshift	3C 343.1	AM 2230-284	IC 1767	NGC 3628	NGC 2639	NGC 3516
(1) Concentration on sky	*	*	✓	✓	✓	✓
(2) Brighter than average						
(a) Optical	✓		*	✓		✓
(b) Radio	*	✓				
(c) X-ray		✓		✓	✓	*
(3) Similar redshifts		✓	*	✓	✓	
(4) Alignment	✓✓	✓✓	*	✓	✓	✓
(5) Karlsson periods	✓	*	*	✓	✓	*
(6) Balanced separations	✓	*	*		*	
(7) Ejection	*	*	*	*	✓	*
(8) Fits age-morphology-redshift relation	*	*	*	*		✓

* outstandingly strong property

✓✓ from large numbers, readily recognizable as an association

✓ readily recognizable as an associations

actually seen ablating against the side of the boundary between the ambient medium and the environment inside the jet.

Table 2.1 uses the *symmetry* in the numerical value of the redshifts that reflects the production of the quasars in pairs and their initial alignment. The observations

tend to support this scenario. Asymmetrical arrangements, as postulated, are produced by delays in plasmoids working their way out through the parent medium. Regarding “concentration on the sky,” note that in the context of the current discussion, *even two or three quasars constitute a concentration*.

Spectra were obtained of four “radio source” quasars around 3C 343.1 with the 10-m Keck telescope. One of the quasars shows two redshifts at $z = 0.344$ and $z = 0.750$ within a circle of radius $0.1''$. In a standard model, they must involve two discrete sources at much different distances although the probability of such an alignment is very small.

In 3C 343.1, the most significant *experimentum crucis* to date, the result conclusively rejects an accidental association because—in the essentially complete 3C catalogue there are about 50 radio quasars. Assuming 23,000 square degrees to Dec. -5° covered by the 3C survey, we compute 2.2×10^{-3} such quasars per square degree. This gives a probability of 3×10^{-11} of accidentally finding the $z = 0.75$ quasar within $0.125''$ of the $z = 0.344$ galaxy.

The question arises as to whether it is possible to test quasars in a group around a candidate parent galaxy against control fields or by Monte Carlo methods. It turns out there is, by the simple expedient of transforming redshifts to the rest frame of the presumed parent galaxy and then varying the redshift of that parent. We have done that here by transforming the quasar redshifts for NGC 2639 to z_0 by means of the redshift of the central galaxy, then computing z_v , the component of velocity needed to explain its deviation from the nearest, exact Karlsson redshift value. We then compute the same z_v values after transforming the observed redshifts to a large range of different parent redshifts.

The results are shown in Fig. 2.17. Plotted as dots are the mean of the absolute values of the residuals, $|z_v|$, from the periodicity formula. Plotted also are the mean values of the residuals, $|z_v|$, with plus for a positive and minus for a negative residual. What we see in Fig. 2.17 is that the scatter for the absolute values of the residuals remains large throughout the tested range. But at a low redshift, about that of the parent, $z = 0.02$ – 0.03 , the scatter reduces to about 0.03 – 0.04 , and the residuals then start a smooth convergence, systematically positive, reducing toward zero and then increasing negatively on the other side of a sharply defined position where the receding and approaching ejection velocities are at a minimum and exactly balanced between plus and minus.

A word should be mentioned about the plus and minus signs between minima. When the transformed z values transit from one Karlsson redshift to the next, their residual is at a maximum but suddenly changes sign, affecting the mean strongly. It is not until the residuals are all small, that the plus and minus z_v values accurately measure the convergence of balanced plus and minus ejection velocities. The absolute value of the residuals has a shallow minimum no more than $|z| \geq 0.03$, suggesting that it is the average projected ejection velocity which then must average to near zero in pairs of oppositely ejected quasars. That average projected velocity is comparable with the measured outflow velocity of ionized material close to AGN quasars, e.g., outflows of 0.08 – $0.10c$. It is also apparent that there is a secondary minimum for a parent at $z = 0.062$, not quite as good as the $z = 0.305$ but very similar and exactly one Karlsson redshift away from $z = 0.305$.

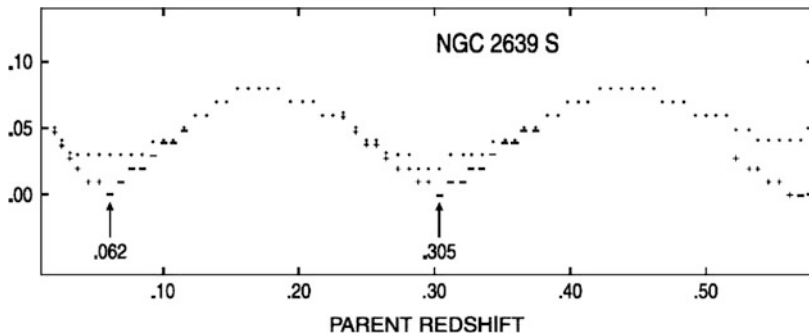


Fig. 2.17 Minimum residual analysis for NGC 2639 when it is taken as the ejecting parent of nine quasars in with $50'$ of the galaxy. When transformed to the rest frame of galaxies having a wide range of fictitious redshifts, the residuals from the nearest Karlsson redshifts (measured as z_v) assumes a deep minimum just at $z = 0.305$. Therefore, the association is extremely unlikely to be by chance. The standard periodicity is thus fitted with great accuracy by this group of quasars discovered in 1980. A secondary minimum at $z = 0.062$ is exactly at the next Karlsson redshift lower. The residuals are given near the minima as *plus* and *minus* symbols. The absolute values of the residuals are given as *dots*

With all the possible values of measured redshifts from 0.06 to 2.64, why do the redshifts of the associated companions fall near Karlsson values of 0.30, 0.60, and 0.96?

The most important result here is: we have established that, at least in some cases, the observed redshift is related to the ejection from an active galaxy. At any given time, there is a source of nonthermal radiation in the center of the galaxy. That source explodes episodically and sends out quasars in opposite directions. In some cases the quasars explode and form companion galaxies—the natural end of the evolution. In some other cases, a quasar collides with local clouds and diminishes in luminosity and becomes unobservable.

We have established non-velocity redshifts and the only way to understand them is to allow mass to be variable with time. This possibility has been explored and developed by Hoyle and Narlikar and others in this group [11, 82]. This calls for news physics.

What are your ideas on the origin of quasars?

The above calculation emphasizes the low probability of such a close pair being accidental. As for physical relation and/or evolution/origin of this double redshift quasar, we can look at the radio isophotes in Fig. 2.11. They suggest a scenario beginning with the densest, slightly extended Eastern isophotes (high-redshift radio quasars had been discovered in many associations [41]). It should be noted that some authors have shown that galaxies with redshifts near $z = 0.30$ are either ejecting quasars or are continuing their own evolution. The transition region in evolution is not perfectly smooth from galaxy to galaxy. The eastern galaxy/quasar in Fig. 2.11 shows a radio isophote extension to the western quasar. *Here, we may be seeing the*

ejection of a quasar from a compact galaxy nucleus. This fits well the dominant form of ejection of radio, X-ray, and optical material from the nuclei of active galaxies. The initially low-mass particles of the plasma would be flowing outward with the gas condensing into atomic matter, which subsequently evolves into galaxies.

Alignments and Balance. The concept of ejection was forced upon us in the late 1960s by the resolution of radio galaxies into double (actually, triple if we include emission from the central parent)-lobed sources. It was virtually obvious that the plasma clouds were ejected in opposite directions manifesting linear momentum conservation. When some were found to contain optical objects with much higher redshifts, it should have been clear that these radio quasars were discrete synchrotron emitting objects with intrinsic redshifts.

When we observe a pair of discrete objects, we can attempt to estimate their ejection velocities. The remainder is then the intrinsic redshift, a fundamental property of matter about which there is still no general acceptance or understanding.

Observation of a pair of quasars bracketing a galaxy with an active nucleus is a strong argument for interpreting those quasars as physical companions of the galaxy. Data presented in [7] (p. 87) indicates that quasars most likely to be associated with galaxies fall within $\pm 20^\circ$ of a line through the parent galaxy minor axis.

When the ejecting nucleus coincides with the center of the alignment, we can say that the ejecta started off from that nucleus. How else but by ejection could the quasar material escape from the galaxy nucleus? And how else could it exit with the same velocity in the opposite direction? We refer to that symmetry as *balance*. If the intrinsic redshift component is to be explained, then we must rely on low-mass charged particles to generate magnetic plasma, and, at 90° , the matter forming mechanism—low mass, fragile plasmoids [158].

Do you think that some alternative fundamental physics could help explain the quasar phenomenon?

One of the main results of this investigation of quasars is that their redshifts cannot be caused by the Doppler effect nor can they be explained by frequency resonances. Is the redshift periodicity found here a form of plasma oscillation? $m \sim (1/t^2) \sim v^2$.

It is necessary to fit matter in different states by means of models such as the one of Hoyle and Narlikar where the mass of an object is a function of age/time. One direction which might be explored is to ask whether Bose–Einstein quantum states are large enough to affect processes that build galaxies. Is the pre-galactic medium cool enough to carry all the information necessary to create a new galaxy? The results presented here may have uncovered fundamental physics processes which would change the hot Big Bang into cold little bangs. Perhaps, even more satisfying is the opportunity to observe growth and maturation of the basic elements of the universe.

Thank you, Halton for your considerations. Since the above discussion involves unconventional theories, interested readers may look at the more extended presentation in Halton Arp's book [7].

2.12 Alternative Views and Ideas

Dear Jayant (*Narlikar*), we would really like to hear your personal account of the events that led to the discovery of quasars.

As a research student of Fred Hoyle, I was fortunate in having a ringside seat for the unfolding events that led to the discovery of quasars. Later, as a skeptic of the “standard model,” I was associated with alternative explanations for these remarkable objects. These are briefly mentioned here as well as current conundrums which have not yet been adequately addressed by the standard model.

The Early Days. One spring morning in 1961, Fred Hoyle walked into the hut and came to my desk, which was one among eight in the large room at the back of the building. The “hut” was a small cottage-like building off Downing Street, just outside the Cavendish. It had been acquired by George Batchelor to house the astrophysics students from his department. That day, Fred had a message for me: “Hanbury Brown has replied. He has invited us to Jodrell to look at his data.” What was more, the hospitable radio astronomer had offered to put us up for the night if we found that convenient.

This offer was in stark contrast to the attitude of the Cambridge radio astronomers. Fred Hoyle had been drawn into a fierce controversy with Martin Ryle and the Cambridge group over their claim that their latest counts of extragalactic radio sources disproved the steady-state cosmology (SSC) of which Fred Hoyle was one of the three authors [27, 108]. On that occasion, I had been drawn into the argument since Fred and I worked together to show that with realistic modeling based on inhomogeneities on the scale of ~ 50 Mpc, one could explain Ryle’s steep counts within the framework of the SSC. But Fred had all the while been concerned as to the nature of radio sources. Were they all galaxies emitting in the radio waveband? More importantly, what bothered him was the doubt; how can one draw conclusions on the counts of objects that one did not know the nature of? Hanbury Brown’s studies of radio sources brought in information of their angular sizes, and such morphological information was bound to be useful for understanding radio sources.

So taking him up on his offer, Fred and I went over to Jodrell Bank in Fred’s sports car, the Austen Healy Sprite. I recall it as a fine warm day when traveling in the open car was a real pleasure. But driving in the pre-motorway England was an exercise requiring patience amidst traffic jams. Nevertheless, Fred managed to get us there for the proverbial English teatime when Hanbury was expecting us. He took us to his work area and brought out charts and sheets of paper containing information which perhaps only he could interpret.

The sum and substance of his findings was that the then data on radio sources indicated a mixture of two populations: the regular extended sources like Cygnus A and another family of compact sources much smaller in size than the regular ones. Were these radio stars? Hanbury did not think so. Indeed, I recall the words in which he put the question bothering him: “We have to find out what are these little chaps.”

This was the question unanswered that day, and worrying over that homework we returned to Cambridge the following morning.

Supermassive Stars. For Fred’s fertile brain, however, the solution did not take long to figure out. For there was a possible scenario that he and Willy Fowler had been working on which held the clue, a scenario that had been inspired by a letter from Geoffrey Burbidge that had arrived in the aftermath of the Hoyle–Ryle controversy.

Indeed, Fred had shown me the letter a few weeks back when I had walked into Fred’s house at 1 Clarkson Close at 10 a.m., his favorite time for discussion. “Look at this letter from Geoff: he has gone crazy” he said. Coming from a person known for highly original, even outlandish ideas, the adjective of “crazy” suggested something really unconventional. And it was. Noting that there was increasing supernova activity as one approaches the galactic center, Burbidge had suggested a sequence of outbursts in which the greater proximity toward the center made one supernova trigger another neighboring star into a supernova explosion. Such a sequence of events, Geoff had argued, could explain the output of so much energy as seen in a radio source.

It may be recalled that Geoff had been the first to draw attention to the energy crunch faced by radio sources. Assuming that synchrotron emission was the mechanism for the radio emission, Burbidge had demonstrated that even in the optimum situation, the energy budget of a strong radio source demanded a storehouse of 10^{60} erg. The then popular interpretation that colliding galaxies were involved in generating this energy had been proved inadequate, and so a new source of so much energy preferably in a concentrated form was required. Burbidge’s letter suggested that triggering supernovae might do the trick.

Although dubbed “crazy,” the Burbidge idea made sense to Fred in a modified form: instead of a sequence of supernovae, think of all of them together as parts of a supermassive supernova. And this led Hoyle and Fowler to think of a supermassive star, say of a million solar masses evolving to be a “supersupernova” [112]. And then came the realization that the nuclear furnace in such a star is not powerful enough to resist the strong inward gravitational pull of the superstar. A rough argument describing this scenario has the nuclear force $\propto M$, while the gravitational force is $\propto M^2$, M being the mass of the object. For a star of mass 1–100 solar masses, the two forces may be comparable, but for higher masses, gravity dominates because of its higher power dependence on mass.

Indeed, this was the stage at which Hoyle and Fowler realized that general relativity may become relevant, and with the onset of gravitational collapse, gravity may become the dominant force. Their paper in *Nature* in January 1963 is very likely the first one to suggest strong gravity as a source of energy in compact objects like Hanbury Brown’s little chaps [111].

3C 273: Position by Lunar Occultation. In 1962, Fred Hoyle visited Australia, and while there, he sent me the position coordinates of one of the little chaps measured by Cyril Hazard et al. using the technique of lunar occultation [107]. It was a very accurate determination, probably the best one in radio astronomy till then.

Fred realized its importance for optical identification. For, the feeling was “seeing is believing”: that the true understanding of the radio source should wait till we see what optical object it corresponds to.

The observers were also aware of the potential significance of their data, and they took extraordinary precautions to ensure its safety. As described by Fred: “Several tons of metal were sawed off the telescope to permit observation at a lower angle of elevation than the normal operational range. For hours before the occultation all local radio stations broadcast repeated appeals: that no one should switch on a radio transmitter during the critical period of the observation. All roads leading anywhere near the telescope were patrolled to make sure that no cars were in motion in the vicinity. A final, somewhat macabre touch: after the observation Hazard and Bolton carried duplicate records back to Sydney on separate planes.”

The optically identified object looked like a star and had a magnitude ~ 13 . Maarten Schmidt at Caltech studied its spectrum, and discovered that it had emission lines. This was an unusual feature, and what was more, the identification of those lines with $H\alpha$, $H\beta$, $H\gamma$ led to the conclusion that they were redshifted by $z = 0.158$. In the early 1960s, a redshift of this magnitude was a significant one and in any case, led to a preliminary diagnosis that the object was outside the Galaxy and its redshift cosmological.

The magnitude of the “star” being as bright as 13^m , at its Hubble distance, its estimated luminosity was as high as 10^{47} erg s $^{-1}$. So here was a powerful emitter of radiation with luminosity exceeding that of our Galaxy but all of it coming from a very compact region, which turned out later to be no bigger than the solar system. Was this the kind of compact object conjectured by Hoyle and Fowler?

With all the fanfare it received, 3C 273 was not the first object of its kind. Another similar object from the 3C (-Third Cambridge) Catalogue had been known (3C 48). It had been optically identified with a starlike object by Allan Sandage and Thomas Matthews in 1960 using interferometry [195]. In 1963, Jesse Greenstein and Matthews found its redshift to be 0.367 [100].

Thus, 1963 had two little chaps of Hanbury Brown identified and classified differently from radio galaxies. They looked starlike but their redshifts far exceeded anything found in the Galaxy. They were given the name “Quasi-Stellar Radio Source,” a rather long name that was shortened to “Quasar.” And the discovery was suggesting that as Hoyle and Fowler had argued, these were compact massive objects, whose strong gravitational field warranted the use of general relativity. In short, astrophysicists needed the help of general relativists in modeling and interpreting the quasars.

The Dallas Symposium. The interdisciplinary nature of quasars led to the organization of an interdisciplinary conference to which astronomers and relativists were invited. The meeting was organized in Dallas in December 1963, by Alfred Schild, Ivor Robinson, and Engelbert Schucking. The organizers were all professional relativists, but they did a good job in getting the relevant astronomers to the meeting, apart from the general relativists. Fittingly, the opening talk was given by J. Robert

Oppenheimer whose 1939 paper with Snyder [162] had discussed the problem of gravitational collapse of a massive object.⁶

Oppenheimer's introductory speech at the symposium was followed by talks by Hoyle and Fowler. Hoyle set the tone of the meeting by highlighting the strong gravity aspect of gravitational collapse of a supermassive object. He also held out the possibility of a "creation field": a scalar field of negative energy density and negative stresses which facilitates creation of matter and also prevents the space-time singularity that awaits an object undergoing gravitational collapse [113]. Although these ideas were considered speculative in the 1960s, the concept of a scalar field with negative stresses was used by Alan Guth [104] in the formulation of the inflationary model of the universe in 1981. Also, the presently popular "phantom fields" are recognized to be no different than the C-field of Hoyle and Narlikar [115]. The first singularity theorem that Roger Penrose came up with in 1965 [106, 173] mentions the C-field as an exception to the energy conditions, leading to a singularity.

Fowler [113] elaborated on the physical descriptions of supermassive stars, highlighting their equilibrium conditions. In particular, he highlighted the different behaviors of the binding energy of a shrinking object in the Newtonian and relativistic cases. While the rest of the presentations were largely observational in character, inviting theoreticians to explain them, the work presented by Hoyle and Fowler can be seen in retrospect as setting the scene for today's model of a quasar powered by a black hole.

The Dallas meet admirably served the purpose of bringing together scientists from different fields so as to arrive at an appreciation of the challenge posed by quasars. It was decided to have such meetings biennially under the title of "Texas Symposium." This series of symposia continues today, but the expectation of interaction between scientists of different disciplines is hardly seen. The symposium program has one discipline a day. Thus, on a day when all X-ray data are presented the X-ray astronomers will come and go, followed the next day by, say, the optical astronomers.

You have developed a skeptical view of the standard model. What do you believe are the most relevant alternative idea for quasars? Are there still open issues that have not been addressed by the standard model?

Since the above-mentioned symposium, quasars have been extensively studied in different wavelengths. By 1966, it became clear that not all quasars are radio sources: perhaps, 10% of them may be so. On the other hand, optical and X-ray emission may be more generic among them. Thus, instead of calling them "quasi-stellar radio sources," it is now more usual to call them "quasi-stellar objects" or QSOs. The shorter name "quasar" has also stayed.

⁶As an aside, it is worth mentioning that a year earlier than Oppenheimer and Snyder, an Indian relativist Datt had published a paper [62] in the German journal *Z. Phys.* with similar analysis as in the Oppenheimer–Snyder paper. However, little information is available about this scientist to date.

Over the years, it is generally believed that a quasar is powered by a central black hole, and models of the internal constitution of a quasar are constructed. It is claimed that such a model works well enough to serve as a starting point for understanding this “little chap.”

Although the standard scenario of a massive (a billion solar masses, say) black hole is commonly used as the central powerhouse of a quasar, it would be optimistic to argue that we are close to completing our understanding of these objects. There are several points where criticism has been forthcoming. The major ones are briefly summarized below:

1. Very large efficiency is assumed in conversion of gravitational energy to optical, X-ray, etc. A more realistic efficiency $\ll 1$ will raise the required mass of the black hole to very high values.
2. The dynamics of conversion is more the hand-waving kind lacking details.
3. The black hole when formed may end with a large angular momentum.
4. In a compact region, the synchrotron process may not work as required by the observed radiation [110].

It is fair to say that we have something to look forward to in the next 50 years to some revolutionary idea which may well be needed to bring our understanding of quasars to the same level as our current understanding of stars.

The Nature of Redshifts. The above difficulties with the standard model of quasars are based on the commonly made assumption that their redshifts are cosmological. The cosmological hypothesis, however, has its doubters. In the early days, Terrell had argued that the redshift is Doppler with all quasars ejected from the Galactic Center [222]. Later, Hoyle and Burbidge made a case for AGNs like NGC 5128 emitting quasars, with their redshifts being Doppler [109]. The major problem against this hypothesis is that we ought to see some blueshifts. It could be argued that these are not found because they have not been looked for seriously. Nevertheless, the absence of any blueshift is a problem for this option.

Hoyle and Fowler [114] also investigated the possibility that redshifts might be gravitational. Here, one needs to counter a result obtained by Hermann Bondi [26] to the effect that if an object has a physically reasonable equation of state, then its maximum surface redshift is no more than 0.62. Hoyle and Fowler therefore assumed that the redshift is of light coming from the deep interior of the quasar. This requires the quasar to have a body that is optically thin. Looking for realistic objects, Das showed that redshifts of the order of 2–2.5 may be obtainable this way [61]. Nevertheless, a central gravitational redshift demands the rather unusual physical condition of transmitting coherent radiation from the center of an astronomical object through its main body.

Given these problems, these alternative explanations of redshifts have fallen by the wayside, and the majority of astronomers have taken the remaining option of cosmological redshift to be the correct option for quasar redshifts. However, as reviewed by Narlikar [157], even this option experiences problems in specific cases. The problem cases are typified by the following examples:

1. The Hubble diagram for quasars is a scatter diagram, thus the signal of a “Hubble law” is not obvious from the data.
2. There are many cases of crowding of high-redshift quasars around a low-redshift (mostly NGC) galaxy.
3. There is filamentary connection between a low-redshift main galaxy and a companion of significantly higher redshift.
4. There are cases where quasars of nearly equal redshifts are positioned in opposite directions from the central galaxy.
5. The redshifts of such “anomalously redshifted” quasars often show a periodicity.

Apart from dismissing the anomalous cases as “freaks” or “artefacts” how does one deal with them? Extensive studies of these cases might well result in concluding that the claims were wrong, and the Hubble law stands strengthened. Or these studies may confirm the anomalous behavior claimed. Either way, the topic of quasars will receive a big boost. Unfortunately, the quasar establishment tends to ignore these findings. For a detailed compendium of such anomalous cases, see Arp [7, 8].

We may write the redshift z of a quasar as a composition of three components:

$$(1 + z) = (1 + z_C)(1 + z_D)(1 + z_I), \quad (2.2)$$

where the three suffixes denote redshifts from cosmology, Doppler effect, and an unexplained part called the intrinsic redshift. We will suggest a new formula for the intrinsic component.

The Variable Mass Hypothesis. We describe briefly another explanation for redshift, arising out of Mach’s principle as interpreted by Hoyle and Narlikar [116]. The basic feature of Mach’s ideas on inertia was that it arises only if matter is present in a non-empty universe. Hoyle and Narlikar (HN in brief) gave a mathematical formulation of how this happens, and later, one of us (JVN) considered a special circumstance when new matter is created. The build up of inertia of a newly created particle starts to grow as it gets in touch with “other matter” in the universe, which happens with the speed of light [156].

Whenever new matter is created, it starts with zero inertia, since at the time of creation, it has not had time to interact with the whole of the universe. Since the interaction that conveys and contributes to inertia of new matter travels with the speed of light, its effect on the mass of the new matter gradually builds up. As the created matter ages, it comes in contact with more and more of the universe, and so its inertia builds up. In short, we have new matter having mass that does not stay constant but increases with time. For this reason, this idea is referred to as the variable mass hypothesis.

This theory therefore leads to a new source for redshift. How? The answer to this question can be understood by imagining an atom of hydrogen, in which the electron and proton both have half the masses that they are known to have in a typical hydrogen atom in the laboratory. We know from atomic theory that the frequencies of the atomic lines like, say of the Lyman series, are proportional to the Rydberg

constant which is proportional to the mass of the electron. Calculations of atomic theory applied to this atom will therefore tell us that the wavelengths of light emitted in its spectrum will be twice the wavelengths of the same lines in a normal laboratory atom. This is an example of the general rule that the younger the piece of matter, the longer the wavelengths of the characteristic lines in its spectrum.

Consider now an observer O in a static universe with the Minkowski space-time metric, observing a galaxy G at a distance r . If the universe was created at $t = 0$, the age of the observer in its present time coordinate t while the galaxy is seen to be at age $t - r/c$. Thus, the hydrogen atoms in the galaxy will have a smaller mass compared to the masses of the same atoms in the vicinity of O. By our rule, the light emitted by the former will have longer wavelength than that emitted by the latter. Hence, O will conclude that light from G is redshifted.

How much is the redshift? A simple calculation, shows that the mass of a particle in the above static universe will be given by

$$m = \alpha t^2, \quad (2.3)$$

where the constant α is related to the density of the universe (assumed here to be quite homogeneous). Hence, the redshift of the galaxy z_G is given by

$$1 + z_G = t^2/(t - r/c)^2. \quad (2.4)$$

It is clear that this formula delivers the linear Hubble law for nearby galaxies with the Hubble constant given by

$$H(t) = 2/t. \quad (2.5)$$

This formula gives essentially the same results as the standard Einstein–de Sitter model. The Hoyle–Narlikar theory is conformally invariant, and so a conformal transformation will transform the above flat space-time model into the expanding universe model. So what has been gained by going into this new formulation? The answer lies in that this new theory is capable of being extended in order to explain anomalous redshifts.

How can we explain the redshift anomalies of the kind described above? Imagine that at time t_1 , the galaxy there creates new matter that is ejected in the form of a quasar. The HN gravity theory allows for creation of new matter. The mass of a particle in this quasar increases with age as

$$m = \alpha (t - t_1)^2. \quad (2.6)$$

Notice that the mass of a similar particle in the galaxy as given by (2.3), will be greater than this because it is older. Correspondingly, the redshift of the quasar will be higher than that of the galaxy. A simple calculation shows that the observer O will see a quasar redshift z_Q given by

$$1 + z_Q = t^2/(t - t_1 - r/c)^2. \quad (2.7)$$

The presumption here is that the atom studied in the laboratory is old and has a larger mass than a newly created atom. So if we imagine an old galaxy creating and ejecting a quasar, the wavelengths of the spectral lines of the quasar will be longer than the spectral lines of the galaxy. So whatever the redshift of the galaxy, the quasar will show a higher redshift. The extra redshift that the quasar has is the anomalous component that we have been discussing here. And, from the above argument, the younger the quasar, the larger the anomalous redshift.

This hypothesis was applied by Prashanta Das and the author [159] in 1980, to a number of quasar–galaxy associations as well as to galaxy–galaxy associations. The observed features tallied very well with the theoretical descriptions. Later work by Chip Arp showed that when one sees a number of quasars ejected by the same galaxy, one finds that the farther quasar has the lower anomalous redshift. This happens because as the quasar ages, it moves farther from the parent galaxy, and so it has reduced anomalous redshift [158].

In this picture, an ejected quasar may move farther and farther from the parent galaxy if the force of its ejection were greater than a critical limit. Such quasars may be identified with those that seem isolated with no galaxy nearby to relate to. If the ejection force is less than the critical limit, the quasar comes to a halt and returns close to the galaxy, finally going round it in smaller and smaller orbits. As it ages, its mass grows and it evolves into a galaxy. Thus, a companion galaxy close to a main galaxy like NGC 7603, say, can be seen as an “older version” of the typical quasar–galaxy association. The companion galaxy in such cases has anomalous redshift but it is small.

The variable mass hypothesis therefore seems able to provide a basic explanation of what has been described so far. However, the story does not end here! There are even more weird observations relating to redshifts that pose challenges even to this hypothesis. We will come to those next. They suggest a quantization effect operating on a large scale which is certainly hard to fit into the conventional Hubble law-based paradigm.

Quantized Redshifts? In 1977, Karlsson [120] spotted a strange pattern. He found that the redshifts of quasars show a bunching at certain values which display periodicity. Thus, if the sequence of redshifts so found is $\{z_0, z_1, z_2, \dots, z_n, \dots\}$, then

$$(1 + z_n) = \alpha^n(1 + z_0), \quad (2.8)$$

where $\alpha = 1.227$ and z_0 is 0.06. This effect is seen even more clearly in bigger samples, with the proviso that if the quasar is associated with a galaxy, then first, the galaxy redshift is factored out by using (2.2).

This effect is hard to understand. In terms of the VMH, all we can say for the present is that the epochs when quasars are created and ejected by galaxies are quantized. With a discrete set of creation epochs, one can understand why the periodicity appears. However, further work is needed to understand why such discretization occurs.

In conclusion, despite considerable progress in probing a quasar, it continues to remain a mystery. On the one hand, we have to understand its source of energy and the mechanism of delivering it. On the other side, it is necessary to resolve the anomalous redshift cases. The quantized redshifts then present another (higher) level of difficulty. In short, we have still to answer the question that Hanbury Brown posed that day: what are these little chaps?

Thank you, Jayant.

References

1. Ambartsumian, V.A.: On the activity of galactic nuclei (introductory lecture). In: Non-stable Phenomena in Galaxies, Proc. IAU Symp. No. 29, Byurakan, 4–12 May 1966, p. 11. Armenian Acad. of Sci. (1968)
2. Antonucci, R.: Unified models for active galactic nuclei and quasars. *Ann. Rev. Astron. Astrophys.* **31**, 473–521 (1993)
3. Andriillat, Y., Souffrin, S.: Variations du spectre du noyau de la galaxie de seyfert NGC 3516. *Astrophys. Lett.* **1**, 111 (1968)
4. Antonucci, R.R.J., Cohen, R.D.: Time development of the emission lines and continuum of NGC 4151. *Astrophys. J.* **271**, 564 (1983)
5. Antonucci, R.R.J., Miller, J.S.: Spectropolarimetry and the nature of NGC 1068. *Astrophys. J.* **297**, 621 (1985)
6. Arp, H.: Atlas of peculiar galaxies. *Astrophys. J.* **14**, 1 (1966)
7. Arp, H.: *Seeing Red*. Apeiron, Montreal (1998)
8. Arp, H.: *Quasars, Redshifts and Controversies*. Interstellar Media, Berkeley (1987)
9. Arp, H.: A QSO 2.4 arcsec from a dwarf galaxy – the rest of the story. *Astron. Astrophys.* **341**, L5–L8 (1999)
10. Arp, H.: *Catalog of Discordant Redshift Associations*. Apeiron, Montreal (2003)
11. Arp, H.: Research with Fred. *Astrophys. Space Sci.* **285**, 451–457 (2003)
12. Arp, H., Burbidge, E.M., Chu, Y., Flesch, E., Patat, F., Rupprecht, G.: NGC 3628: Ejection activity associated with quasars. *Astron. Astrophys.* **391**, 833 (2002)
13. Arp, H., Burbidge, G., Hoyle, F., Narlikar, J.V., Wickramasinghe: The extragalactic universe – an alternative view. *Nature* **346**, 807 (1990)
14. Arp, H., Burbidge, E.M., Burbidge, G.: The double radio source 3C 343.1: A galaxy-QSO pair with very different redshifts. *Astron. Astrophys.* **414**, L27 (2004)
15. Arp, H., Fulton, C.: The 2dF redshift survey II: UGC 8584 – redshift periodicity and ring. arXiv:0802.1587v1 (2008)
16. Arp, H., Roscoe, D., Fulton, C.: Periodicities of quasar redshifts in large area surveys. arXiv:0501.090v1 (2005)
17. Avni, Y.: On the contribution of active galactic nuclei to the diffuse X-ray background. *Astron. Astrophys.* **66**, 307 (1978)
18. Bahcall, J.N., Bahcall, N.A.: The unidentified high galactic latitude X-ray sources – bright galaxies or rich clusters 1975. *Astrophys. J.* **19**, L89 (1975)
19. Baldwin, J.A.: Spectrophotometry of low-redshift quasi-stellar objects. *Astrophys. J.* **201**, 26 (1975)
20. Baldwin, J.A.: The $Iy\alpha/H\beta$ intensity ratio in the spectra of QSOs. *Mon. Not. R. Astron. Soc.* **178**, 67P (1977)
21. Berezin, V.Y., Zuev, A.G., Kiryan, G.V., Rybakov, M.I., Khvilivitskii, A.T., Ilin, I.V., Petrov, P.P., Savanov, I.S., Shcherbakov, A.G.: CCD array for astronomical observations. *Soviet Astron. Lett.* **17**, 405 (1991)

22. Blandford, R.D., McKee, C.F.: Reverberation mapping of the emission line regions of seyfert galaxies and quasars. *Astrophys. J.* **255**, 419 (1982)
23. Blandford, R.D., Rees, M.J.: Some comments on radiation mechanisms in Lacertids. In: Pittsburgh Conference on BL Lac Objects, Pittsburgh, PA, 24–26 April 1978, Proceedings, pp. 328–341. University of Pittsburgh, Pittsburgh, PA (1978)
24. Blumenthal, G.R., Mathews, W.G.: Theoretical emission line profiles in QSOs and seyfert galaxies. *Astrophys. J.* **198**, 517 (1975)
25. Boksenberg, A.: Performance of the UCL image photon counting system. In: Proceedings of ESO/CERN conference on auxiliary instrumentation for large telescopes, pp. 295–316 (1972)
26. Bondi, H.: Massive spheres in general relativity. *Proc. R. Soc. A.* **282**, 303 (1964)
27. Bondi, H., Gold, T.: The steady-state theory of the expanding universe. *Mon. Not. R. Astron. Soc.* **108**, 252 (1948)
28. Boroson, T.A., Green, R.F.: The emission-line properties of low-redshift quasi-stellar objects. *ApJ. Suppl.* **80**, 109–135 (1992)
29. Boroson, T.A., Lauer, T.R.: Exploring the spectral space of low redshift QSOs. *Astron. J.* **140**, 390 (2010)
30. Braccesi, A., Fanti, R., Giovannini, C., Vespignani, G.: Radio emission from quasi-stellar galaxies. *Astrophys. J.* **143**, 603 (1966)
31. Braccesi, A., Formigginini, L., Gandolfi, E.: Magnitudes, colours and coordinates of 175 ultraviolet excess objects in the field 13h + 360. *Astron. Astrophys.* **5**, 264 (1970); Erratum: *Astron. Astrophys.* **23**, 159 (1973)
32. Brenneman, L.W., Reynolds, C.S.: Relativistic broadening of iron emission lines in a sample of active galactic nuclei. *Astrophys. J.* **702**, 1367–1386 (2009)
33. Bridgman, P.: Reflections of a Physicist. Philosophical Library, New York (1950)
34. Burbidge, E.M.: Quasi-stellar objects. *Ann. Rev. Astron. Astrophys.* **5**, 399 (1967)
35. Burbidge, E.M.: Spectra of two X-ray-emitting quasi-stellar objects apparently ejected from the seyfert galaxy NGC 2639. *Astrophys. J.* **84**, 99 (1997)
36. Burbidge, E.M., Burbidge, G.R., Prendergast, K.H.: Mass distribution and physical conditions in the inner region of NGC 1068. *Astrophys. J.* **130**, 26 (1959)
37. Burbidge, G.R.: Electromagnetic phenomena in cosmical physics. B. Lehnert (Ed.). Cambridge University Press, IAU Symp. 6, 222 (1958)
38. Burbidge, G.: An accidental career. *Ann. Rev. Astron. Astrophys.* **45**, 1–41 (2007)
39. Burbidge, G., Burbidge, M.: Quasi-Stellar Objects. Freeman, San Francisco (1967)
40. Burbidge, G.R., Burbidge, E.M., Sandage, A.R.: Evidence for the occurrence of violent events in the nuclei of galaxies. *Rev. Modern Phys.* **35**, 947 (1963)
41. Burbidge, G., Hewitt, A.: The redshift peak at $z = 0.06$. *Astrophys. J.* **359**, 33 (1990)
42. Burbidge, G., Napier, W.M.: The distribution of redshifts in new samples of quasi-stellar objects. *Astron. J.* **121**, 21 (2001)
43. Burstein, D., Faber, S.M., Gaskell, C.M., Krumm, N.: Old stellar populations. I – A spectroscopic comparison of galactic globular clusters, M31 globular clusters, and elliptical galaxies. *Astrophys. J.* **287**, 586 (1984)
44. Carleton, N.P., Elvis, M., Fabbiano, G., Willner, S.P., Lawrence, A., Ward, M.: The continuum of type-I seyfert galaxies. II – Separating thermal and nonthermal components. *Astrophys. J.* **318**, 595 (1987)
45. Cavaliere, A., Morrison, P., Wood, K.: On quasar evolution. *Astrophys. J.* **170**, 223–231 (1971)
46. Cavaliere, A., Pacini, F., Setti, G.: Rotating collapsed objects, quasars and supernova remnants. *Astrophys. Lett.* **4**, 103 (1969)
47. Cavaliere, A., Padovani, P.: The connection between active and normal galaxies. *Astrophys. J.* **340**, L5–L8 (1989)
48. Cavaliere, A., Szalay, A.S.: Primeval QSOs. *Astrophys. J.* **311**, 589–594 (1986)
49. Cherepashchuk, A.M., Lyutyi, V.M.: Rapid variations of H alpha intensity in the nuclei of Seyfert galaxies. NGC 4151, 3516, 1068. *Astrophys. Lett.* **13**, 165 (1973)

50. Chiaberge, M., Macchetto, F.D., Sparks, W.B., Capetti, A., Allen, M., Martel, A.R.: The nuclei of radio galaxies in the ultraviolet: The signature of different emission processes. *Astrophys. J.* **571**, 247–255 (2003)
51. Chu, Y., Wei, J., Hu, J., Zhu, X., Arp, H.: Quasars around the seyfert galaxy NGC 3516. *Astrophys. J.* **500**, 596 (1998)
52. Chuvaev, K.K.: The spectrum variations of the galaxy 3C 120. *Pis'ma v Astron. Zhurnal* **6**, 323–328 (1980)
53. Chuvaev, K.K.: The NGC 1275 nucleus – some results from an 11-year spectroscopic program *PAZh.* **11**, 803–810 (1985)
54. Chuvaev, K.K.: Multiyear spectral observations of active galactic nuclei in the optical range. I – The galaxy NGC 1275 *IzKry* **81**, 138–148 (1990)
55. Chuvaev, K.K., Lyutyj, V.M., Doroshenko, V.T.: Rapid brightness and spectrum variations of the nucleus of the seyfert galaxy NGC 7469. *Pis'ma v Astron. Zhurnal* **16**, 867–876 (1990)
56. Cid Fernandes, R., Stasińska, G., Schlickmann, M.S., Mateus, A., Vale Asari, N., Schoenell, W., Sodré, L.: Alternative diagnostic diagrams and the 'forgotten' population of weak line galaxies in the SDSS. *Mon. Not. R. Astron. Soc.* **403**, 1036–1053 (2010)
57. Cooke, B.A., Elvis, M., Ward, M.J., Fosbury, R.A.E., Penston, M.V., Maccacaro, T.: NGC 3783 – a possible X-ray emitting seyfert galaxy. *Mon. Not. R. Astron. Soc.* **177**, P121 (1976)
58. Cooke, B.A., Ricketts, M.J., Maccacaro, T., Pye, J.P., Elvis, M., Watson, M.G., Griffiths, R.E., Pounds, K.A., McHardy, I., Maccagni, D., et al.: The ariel V /SSI/ catalogue of high galactic latitude /absolute value of B greater than 10 deg/X-ray sources. *Mon. Not. R. Astron. Soc.* **182**, 455 (1978)
59. Courbin, F., Tewes, M., Djorgovski, S.G., Sluse, D., Mahabal, A., Rérat, F., Meylan, G.: First case of strong gravitational lensing by a QSO: SDSS J0013+1523 at $z = 0.120$. *Astron. Astrophys.* **516**, 12 (2010)
60. Czerny, B., Elvis, M.: Constraints on quasar accretion disks from the optical/ultraviolet/soft X-ray big bump. *Astroph. J.* **321**, 305–320 (1987)
61. Das, P.K.: Physical properties of collapsed objects with large central gravitational redshifts. *Mon. Not. R. Astron. Soc.* **177**, 391 (1977)
62. Datt, B.: Über eine klasse von lösungen der gravitationsgleichungen der relativität. *Zeit. Phys.* **108**, 314 (1938)
63. Davidson, K.: Photoionization and the emission-line spectra of quasi-stellar objects. *ApJ* **171**, 213 (1972)
64. Dejach, A.N.: Determination of photographic magnitudes of galaxy nuclei. In: *Non-Stable Phenomena in Galaxies, Proceedings of IAU Symp. 29, held in Byurakan, 4–12 May 2663*, pp. 130–133 (1966)
65. Dibai, E.A.: Certain properties of the nucleus of the radiogalaxy NGC 1275 (perseus-A). *Astron. Zhurn.* **46**, 725–729 (1969)
66. Dibai, É.A.: The masses of central bodies in active galactic nuclei. *Soviet Astron. Lett.* **3**, 1 (1977)
67. Dibai, E.A., Pronik, V.I.: Spectrophotometric investigation of the nucleus of NGC 1068. *Astrophysics* **1**, 54–69 (1965)
68. Dibai, É.A., Pronik, V.I.: A spectrophotometric study of Seyfert-Galaxy nuclei. *Astron. Zhurnal* **44**, 952 (1967)
69. Dibai, É.A., Pronik, V.I.: A spectrophotometric study of Seyfert-Galaxy nuclei. *Soviet Astron.* **44**, 952 (1967)
70. Dibai, É.A., Pronik, V.I.: A spectrophotometric study of Seyfert-Galaxy nuclei. *Soviet Astron.* **11**, 767 (1968)
71. Doroshenko, V.T.: Investigation of seyfert galaxies using the spectra obtained by K.K. Chuvaev with the 2.6-m telescope of crimean astrophysical observatory in 1972–1992. *Izv. Krymsk. Astrofiz. Obs.* **104**, 114 (2008)
72. Efanov, V.A., Moiseev, I.G., Nesterov, N.S.: Extragalactic radio sources survey at 1.35 cm wavelength. *Izvest. Crim. Astrifiz. Obs.* **60**, 3 (1979)

73. Elvis, M., Maccacaro, T., Wilson, A.S., Ward, M.J., Penston, M.V., Fosbury, R.A.E., Perola, G.C.: Seyfert galaxies as X-ray sources. *Mon. Not. R. Astron. Soc.* **183**, 129 (1978)
74. Evans, D.A., Worrall, D.M., Hardcastle, M.J., Kraft, R.P., Birkinshaw, M.: Chandra and XMM-newton observations of a sample of low-redshift FR I and FR II radio galaxy nuclei. *Astrophys. J.* **642**, 96–112 (2006)
75. Faber, S.M., Friel, E.D., Burstein, D., Gaskell, C.M.: Old stellar populations. II – an analysis of K-giant spectra. *Astrophys. J. Suppl.* **57**, 711 (1985)
76. Fanti, C., Fanti, R., Parma, P., Schilizzi, R.T., van Breugel, W.J.M.: Compact steep spectrum 3CR radio sources – VLBI observations at 18 cm. *Astron. Astrophys.* **143**, 292 (1985)
77. Fath, E.A.: The spectra of some spiral nebulae and globular star clusters. *Lick Obs. Bull.* **5**, 71 (1909)
78. Faulkner, J., Gaskell, M.: Astronomers licked by QSOs and active galactic nuclei. *Nature* **275**, 91 (1978)
79. Ferland, G., Baldwin, J.A.: Quasars and cosmology. ASP Conference Series, vol. 162. ASP, San Francisco (1999)
80. Ferland, G.J., Hu, C., Wang, J.-M., Baldwin, J.A., Porter, R.L., van Hoof, P.A.M., Williams, R.J.R.: Implications of infalling Fe II-emitting clouds in active galactic nuclei: Anisotropic properties. *Astroph. J.* **707**, L82–L86 (2009)
81. Ferrarese, L., Merritt, D.: A fundamental relation between supermassive black holes and their host galaxies. *Astrophys. J. Lett.* **539**, L9–L12 (2000)
82. Field, G.B., Arp, H.C., Bahcall, J.N.: The Redshift Controversy. *Frontiers in Physics*, pp. 294–314. W.A. Benjamin, Reading (1973)
83. Fiore, F., Brusa, M., Cocchia, F., Baldi, A., Carangelo, N., Ciliegi, P., Comastri, A., La Franca, F., Maiolino, R., Matt, G., et al.: The HELLAS2XMM survey. IV. Optical identifications and the evolution of the accretion luminosity in the universe. *Astron. Astrophys.* **409**, 79–90 (2003)
84. Fulton, C.: Analyses of the 2dF deep field. PhD Thesis, University of Western Australia (2010)
85. Gaskell, C.M.: PKS 0119-046 and the origin of infalling absorption-line systems in quasars. *Astrophys. J. Lett.* **267**, L1–L4 (1983)
86. Gaskell, C.M.: Quasars as supermassive binaries. In: *Proc. 24th Liège Int. Astrophys. Colloq., Quasars and Gravitational Lenses*. Univ. Liège, Coïnte-Ougree, p. 473 (1983)
87. Gaskell, C.M.: Close supermassive binary black holes. *Nature* **463**, E1 (2010)
88. Gaskell, C.M.: Accretion disks and the nature and origin of AGN continuum variability. *Rev. Mexicana Astron. Astrof. Conf. Ser.* **32**, 1 (2008)
89. Gaskell, C.M.: A redshift difference between high and low ionization emission-line regions in QSOs – evidence for radial motions. *Astrophys. J.* **263**, 79 (1982)
90. Gaskell, C.M.: Direct evidence of gravitational domination of the motion of gas within one light-week of the central object in NGC 4151 and the determination of the mass of the probable black hole. *Astrophys. J.* **325**, 114 (1988)
91. Gaskell, C.M., Klimek, E.S., Nazarova, L.S.: NGC 5548: The AGN energy budget problem and the geometry of the broad-line region and torus. *Astrophys. J.* arXiv:0711.1025 (2007) submitted
92. Gaskell, C.M., Snedden, S.A.: The optical case for a disk component of blr emission. In: *Structure and Kinematics of Quasar Broad Line Regions*. ASP Conference Series, vol. 175, p. 157 (1999)
93. Gaskell, C.M., Sparke, L.S.: Line variations in quasars and seyfert galaxies. *Astrophys. J.* **305**, 175 (1986)
94. Gebhardt, K., Bender, R., Bower, G., Dressler, A., Faber, S.M., Filippenko, A.V., Green, R., Grillmair, C., Ho, L.C., Kormendy, J., Lauer, T.R., Magorrian, J., Pinkney, J., Richstone, D., Tremaine, S.: A relationship between nuclear black hole mass and galaxy velocity dispersion. *Astrophys. J. Lett.* **539**, L13–L16 (2000)
95. Giacconi, R., Gursky, H.: X-ray astronomy. Dordrecht, Reidel (1974)

96. Giacconi, R., Murray, S., Gursky, H., Kellogg, E., Schreier, E., Matilsky, T., Koch, D., Tananbaum, H.: The third UHURU catalog of X-ray sources. *Astrophys. J. Suppl. Ser.* **237**, 37 (1974)
97. Giacconi, R., Murray, S., Tananbaum, H., Kellogg, E., Gursky, H.: X-ray galaxies. *Bull. Am. Astron. Soc.* **3**, 477 (1971)
98. Gilli, R., Comastri, A., Hasinger, G.: The synthesis of the cosmic X-ray background in the chandra and XMM-newton era. *Astron. Astrophys.* **463**, 79–96 (2007)
99. Greenstein, J.L.: Red-shift of the unusual radio source: 3C 48. *Nature* **197**, 1041 (1963)
100. Greenstein, J.L., Matthews, T.A.: Redshift of the radio source 3C 48. *Astron. J.* **68**, 279 (1963)
101. Greenstein, J.L., Schmidt, M.: The quasi-stellar radio sources 3c 48 and 3c 273. *Astrophys. J.* **140**, 1 (1964)
102. Gudzenko, L.I., Ozernoy, L.M., Chertoprud, V.E.: Quasar nucleus: Is it a star cluster or a single body? *Nature* **215**, 605 (1967)
103. Gültekin, K., Richstone, D.O., Gebhardt, K., Lauer, T.R., Tremaine, S., Aller, M.C., Bender, R., Dressler, A., et al.: The M- σ and M-L relations in galactic bulges, and determinations of their intrinsic scatter. *Astrophys. J.* **698**, 198–221 (2009)
104. Guth, A.: Inflationary universe: A possible solution to the horizon and flatness problems. *Phys. Rev. D.* **23**, 347 (1981)
105. Hardcastle, M.J., Evans, D.A., Croston, J.H.: The X-ray nuclei of intermediate-redshift radio sources. *Mon. Not. R. Astron. Soc.* **370**, 1893–1904 (2006)
106. Hawking, S.W., Ellis, G.F.R.: *The Large Scale Structure of Space Time*. Cambridge University Press, Cambridge (1973)
107. Hazard, C., Mackey, M.B., Shimmins, A.J.: Investigation of the radio source 3C 273 by the method of lunar occultations. *Nature* **197**, 1037 (1963)
108. Hoyle, F.: A new model for the expanding universe. *Mon. Not. R. Astron. Soc.* **108**, 372 (1948)
109. Hoyle, F., Burbidge, G.R.: On the nature of the quasi-stellar objects. *Astrophys. J.* **144**, 534 (1966)
110. Hoyle, F., Burbidge, G.R., Sargent, W.L.W.: On the nature of the quasi-stellar sources. *Nature* **209**, 751 (1966)
111. Hoyle, F., Fowler, W.A.: Nature of strong radio sources. *Nature* **197**, 533 (1963)
112. Hoyle, F., Fowler, W.A.: On the nature of strong radio sources. *Mon. Not. R. Astron. Soc.* **125**, 169 (1963)
113. Hoyle, F., Fowler, W.A.: Nature of strong radio sources. In: Schild, A., Robinson, I., Schucking, E. (eds.) *Proceedings of the First Texas Symposium on Relativistic Astrophysics*, p. 441 (1965)
114. Hoyle, F., Fowler, W.A.: Gravitational red-shifts in quasi-stellar objects. *Nature* **213**, 373 (1967)
115. Hoyle, F., Narlikar, J.V.: Mach's principle and the creation of matter. *Proc. R. Soc. A* **270**, 334 (1962)
116. Hoyle, F., Narlikar, J.V.: *Action at a Distance in Physics and Cosmology*. W.H. Freeman, San Francisco (1974)
117. Huovelin, J., Poutanen, M., Tuominen, I.: Helsinki University of Techn., Radio Lab. Report VS **166**, 18 (1986)
118. Karlsson, K.G.: Possible discretization of quasar redshifts. *Astron. Astrophys.* **13**, 333 (1971)
119. Karlsson, K.G.: Quasars – selection effects and the nature of redshifts. *Nat. Phys. Sci.* **245**, 68 (1973)
120. Karlsson, K.G.: On the existence of significant peaks in the quasar redshift distribution. *Astron. Astrophys.* **58**, 237 (1977)
121. Karlsson, K.G.: Quasar redshifts and nearby galaxies. *Astron. Astrophys.* **239**, 50 (1990)
122. Keel, W.C.: Inclination effects on the recognition of seyfert galaxies. *Astron. J.* **85**, 198 (1980)
123. Kellogg, E.M.: Extragalactic X-ray sources. In: Giacconi, R., Gursky, H. (eds.) *X-ray Astronomy*, Dordrecht, Reidel (1974)
124. Khachikian, E.Y., Weedman, D.W.: An atlas of Seyfert galaxies. *Astrophys. J.* **192**, 581 (1974)

125. Kopylov, I.M., Lipovetskii, V.A., Pronik, V.I., Chuvaev, K.K.: Spectral observations of markarian galaxies. *Astrofizika* **10**, 483–491 (1974)
126. Kopylov, I.M., Lipovetskij, V.A., Pronik, V.I., Chuvaev, K.K.: Spectral observations of markarian galaxies. II. *Astrofizika* **12**, 189–194 (1976)
127. Koratkar, A.P., Gaskell, C.M.: Emission-line variability of fairall 9: Determination of the size of the broad-line region and the direction of gas motion. *Astrophys. J.* **345**, 637 (1989)
128. Koratkar, A.P., Gaskell, C.M.: Structure and kinematics of the broad-line regions in active galaxies from IUE variability data. *Astrophys. J. Suppl.* **75**, 719 (1991)
129. Koratkar, A.P., Gaskell, C.M.: Radius-luminosity and mass-luminosity relationships for active galactic nuclei. *ApJ. Lett.* **370**, L61 (1991)
130. Kormendy, J.: A critical review of stellar-dynamical evidence for black holes in galaxy nuclei. In: Beckman, J., Colina, L., Netzer, H. (eds.) *The Nearest Active Galaxies*, p. 197. Consejo Superior de Investigaciones Científicas, Madrid (1993)
131. Kovačević, J., Popović, L.Č., Dimitrijević, M.S.: Analysis of optical Fe II emission in a sample of active galactic nucleus spectra. *ApJS* **189**, 15–36 (2010)
132. Laing, R.A., Jenkins, C.R., Wall, J.V., Unger, S.W.: Spectrophotometry of a complete sample of 3CR radio sources: Implications for unified models. *The Physics of Active Galaxies. ASP Conference Series*, vol. 54, pp. 201–208 (1994)
133. Lallemand, A., Duchesne, M., Walker, M.F.: The rotation of the nucleus of M 31. *Publ. Astron. Soc. Pac.* **72**, 76 (1960)
134. Laor, A., Netzer, H.: Massive thin accretion discs. I – calculated spectra. *Mon. Not. R. Astron. Soc.* **238**, 897–916 (1989)
135. Lawrence, A., Elvis, M.: Obscuration and the various kinds of seyfert galaxies. *Astrophys. J.* **256**, 410 (1982)
136. Leipski, C., Falcke, H., Bennert, N., Hüttemeister, S.: The radio structure of radio-quiet quasars. *Astron. Astrophys.* **455**, 161 (2006)
137. Low, F.J., Johnson, H.L.: The spectrum of 3C273. *Astrophys. J.* **141**, 336 (1965)
138. Lynden-Bell, D.: Galactic nuclei as collapsed old quasars. *Nature* **223**, 690 (1969)
139. Lyutyi, V.M., Cherepashchuk, A.M.: Rapid variations of H alpha intensity in the nuclei of seyfert galaxies NGC 4151, 3516, 1068. *Astron. Tsirk.* **688**, 1 (1972)
140. Lyutyj, V.M., Oknyanskij, V.L., Chuvaev, K.K.: NGC 4151 – a seyfert-2 in a deep photometric minimum. *Pis'ma v Astron. Zhurnal* **10**, 803–807 (1984)
141. Liutyi, V.M., Pronik, V.I.: Optical variability of the nuclei of seyfert galaxies. *IAU Symp.* **67**, 591–604 (1975)
142. MacAlpine, G.M.: Photoionization models for the emission-line regions of quasi-stellar and related objects. *Astrophys. J.* **175**, 11 (1972)
143. McKee, C.F., Tarter, C.B.: Radiation pressure in quasar clouds. *Astrophys. J.* **202**, 306–318 (1975)
144. Magorrian, J., Tremaine, S., Richstone, D., Bender, R., Bower, G., Dressler, A., Faber, S.M., Gebhardt, K., Green, R., Grillmair, C., Kormendy, J., Lauer, T.: The demography of massive dark objects in galaxy centers. *Astron. J.* **115**, 2285–2305 (1998)
145. Malkan, M.A.: The ultraviolet excess of luminous quasars. II – Evidence for massive accretion disks. *Astrophys. J.* **268**, 582–590 (1983)
146. Malkan, M.A., Sargent, W.L.W.: The ultraviolet excess of seyfert-1 galaxies and quasars. *Astrophys. J.* **254**, 22–37 (1982)
147. Marconi, A., Risaliti, G., Gilli, R., Hunt, L.K., Maiolino, R., Salvati, M.: Local supermassive black holes, relics of active galactic nuclei and the X-ray background. *Mon. Not. R. Astron. Soc.* **351**, 169–185 (2004)
148. Markarian, B.E.: Galaxies with an ultraviolet continuum. *Astrofizika* **3**, 24–38 (1967)
149. Mayall, N.U.: The spectrum of the spiral nebula NGC 4151. *Publ. Astron. Soc. Pac.* **46**, 134 (1934)
150. Merkulova, N.I., Pronik, I.I.: The results of photoelectric observations of the continuous and emission-line spectrum of the nucleus of the galaxy NGC 1275 observed with the AZT-11 telescope. *Izvestiia Krymskaia Astrofizicheskaia Obs.* **77**, 135–143 (1987)

151. Merkulova, N.I., Metik, L.P., Pronik, V.I., Pronij, I.I.: Comparison of UV fluxes determined for 19 galaxies by means of the astron astrophysical station with results of ground-based photometry – UV flux variability of certain galactic nuclei. *Astron. Zhurnal* **67**, 449–462 (1990)
152. Miller, J.S.: The use of [S II] lines to determine interstellar reddening. *Astrophys. J. Lett.* **154**, L57–L59 (1968)
153. Miller, J.S., Robinson, L.B., Schmidt, G.D.: The remote-controlled spectrograph, area scanner, and spectropolarimeter for the lick 3-m telescope. *Publ. Astron. Soc. Pac.* **92**, 702 (1980)
154. Mushotzky, R.F., Marshall, F.E., Boldt, E.A., Holt, S.S., Serlemitsos, P.J.: HEAO 1 spectra of X-ray emitting seyfert-1 galaxies. *Astrophys. J.* **235**, 377 (1980)
155. Nandra, K., O’Neill, P.M., George, I.M., Reeves, J.N.: An XMM-newton survey of broad iron lines in seyfert galaxies. *Mon. Not. R. Astron. Soc.* **382**, 194–228 (2007)
156. Narlikar, J.V.: Two astrophysical applications of conformal gravity. *Ann. Phys.* **107**, 325 (1977)
157. Narlikar, J.V.: Noncosmological redshifts. *Sp. Sci. Rev.* **50**, 523 (1989)
158. Narlikar, J.V., Arp, H.: Flat spacetime cosmology – a unified framework for extragalactic redshifts. *Astrophys. J.* **405**, 51 (1993)
159. Narlikar, J.V., Das, P.K.: Anomalous redshifts of quasi-stellar objects. *Astrophys. J.* **240**, 401 (1980)
160. Netzer, H.: Physical conditions in active nuclei-I. The balmer decrement. *Mon. Not. R. Astron. Soc.* **171**, 395–406 (1975)
161. Ogle, P., Whysong, D., Antonucci, R.: Spitzer reveals hidden quasar nuclei in some powerful FR II radio galaxies. *Astrophys. J.* **647**, 161–171 (2006)
162. Oppenheimer, J.R., Snyder, H.: On continued gravitational contraction. *Phys. Rev.* **56**, 455 (1939)
163. Osterbrock, D.E.: Excitation of C III 1909 and other semiforbidden emission lines in QSOs and nebulae. *Astrophys. J.* **160**, 25 (1970)
164. Osterbrock, D.E.: Spectrophotometry of seyfert-1 galaxies. *Astrophys. J.* **215**, 733 (1977)
165. Osterbrock, D.E.: Observations of broad emission-line regions. In: Miller, J.S. (ed.) *Astrophysics of Active Galaxies and Quasi-Stellar Objects*, pp. 111–155. University Science Books, Mill Valley (1985)
166. Osterbrock, D.E., Koski, A.T., Phillips, M.M.: Broad balmer emission lines in radio galaxies. *Astrophys. J. Lett.* **197**, L41 (1975)
167. Osterbrock, D.E., Mathews, W.G.: Emission-line regions of active galaxies and QSOs. *Ann. Rev. Astron. Astrophys.* **24**, 171–203 (1986)
168. Osterbrock, D.E., Parker, R.A.R.: Physical conditions in the nucleus of the seyfert galaxy NGC 1068. *Astrophys. J.* **141**, 892 (1965)
169. Osterbrock, D.E.: Observational model of the ionized gas in seyfert and radio-galaxy nuclei. *Proc. Nat. Acad. Sci.* **75**, 540 (1978)
170. Ozernoy, L.M.: About the mechanism of variable radiation and a nature of quasi-stellar objects. In: *The Proceedings of Symposium The problems of stellar evolution and the variable stars held in Moscow, 24-27 November 1964*. Nauka, p. 140–155 (1967)
171. Padovani, P., Allen, M.G., Rosati, P., Walton, N.A.: Discovery of optically faint obscured quasars with virtual observatory tools. *Astron. Astrophys.* **424**, 545–559 (2004)
172. Peebles, P.J.E.: *Principles of Physical Cosmology*. Princeton University Press, NJ (1993)
173. Penrose, R.: Gravitational collapse and space-time singularities. *Phys. Rev. Lett.* **14**, 57 (1965)
174. Peterson, B.A., Savage, A., Jauncey, D.L., Wright, A.E.: PKS 2000-330 – a quasi-stellar radio source with a redshift of 3.78. *Astrophys. J. Lett.* **260**, L27 (1982)
175. Phillips, M.M.: Permitted Fe II emission in seyfert-1 galaxies and QSOs. I. Observations. *Astrophys. J. Suppl.* **38**, 187 (1978)
176. Phillips, M.M.: Permitted Fe II emission in seyfert-1 galaxies and QSOs. II. The excitation mechanism. *Astrophys. J.* **226**, 736 (1978)

177. Press, W.H., Schechter, P.: Formation of galaxies and clusters of galaxies by self-similar gravitational condensation. *Astrophys. J.* **187**, 425 (1974)
178. Pringle, J.E., Rees, M.J.: Accretion disc models for compact X-ray sources. *Astron. Astrophys.* **21**, 1 (1972)
179. Pronik, I.I.: Variability of emission line spectrum of the nucleus of the seyfert galaxy NGC 3227 bull. Crimean Astrophys. Obs. **68**, 75 (1983)
180. Pronik, I.: Emission lines variations in the spectra of seyfert galaxies nuclei. *Observational Data IAUS* **121**, 169 (1987)
181. Pronik, I.I.: Flows and shocks in seyfert galaxy nuclei. In: Gaskell, G.M., Hardy, I.M.M., Peterson, B.M., Sergeev, S.G. (eds.) *AGN Variability from X-rays to Radio Waves*. ASP Conference Series, vol. 360, pp. 245–249 (2006)
182. Pronik, I.I., Merkulova, N.I., Metik, L.P.: On the H β , [OIII] lines and continuum variability character in the nucleus of seyfert galaxy NGC 1275. *Astrophys. Space Sci.* **171**, 91–95 (1990)
183. Pronik, V.I.: *Izv. Krymsk. Astrofiz. Obs.* **104**, 3–4, 80 (2008)
184. Pronik, V.I., Chuvaev, K.K.: Hydrogen lines in the spectrum of the galaxy markaryan 6 during its activity. *Astrophysics* **8**, 112–116 (1972)
185. Rees, M.J.: Dissipative processes, galaxy formation and ‘early’ star formation. *Phys. Scripta* **17**, 371 (1978)
186. Rees, M.J.: Black hole models for active galactic nuclei. *Ann. Rev. Astron. Astrophys.* **22**, 471–506 (1984)
187. Readhead, A.C.S., Cohen, M.H., Blandford, R.D.: A jet in the nucleus of NGC6251. *Nature* **272**, 131 (1978)
188. Risaliti, G., Salvati, M., Marconi, A.: [O III] equivalent width and orientation effects in quasars. *Mon. Not. R. Astron. Soc.* **411**, 2223–2229 (2011)
189. Robinson, L.B., Wampler, E.J.: The spectra of two galaxies near PKS 2251+11. *Astrophys. J. Lett.* **171**, L83 (1972)
190. Robinson, L.B., Wampler, E.J.: The lick observatory image-dissector scanner. *Publ. Astron. Soc. Pac.* **84**, 161–166 (1972)
191. Robinson, L.B., Wampler E.J.: An electronic detector for astronomy. *Eng. Tech. Appl. Sci.* **5**, 18 (1990)
192. Ryle, M., Clarke, R.W.: An examination of the steady-state model in the light of some recent observations of radio sources. *Mon. Not. R. Astron. Soc.* **122**, 349 (1961)
193. Ryle, M., Scheuer, P.A.G.: The spatial distribution and the nature of radio stars. *R. Soc. Lond. Proc. Ser. A* **230**, 448 (1955)
194. Salpeter, E.E.: Accretion of interstellar matter by massive objects. *Astrophys. J.* **140**, 796 (1964)
195. Sandage, A.R.: First True Radio Star? *Sky and telescope* **21**, 148 (1961)
196. Sandage, A.: The existence of a major new constituent of the universe: The quasistellar galaxies. *Astrophys. J.* **141**, 1560 (1965)
197. Sandage, A.: The first 50 years at palomar: 1949–1999 the early years of stellar evolution, cosmology, and high-energy astrophysics. *Ann. Rev. Astron. Astrophys.* **37**, 445–486 (1999)
198. Sanford, P.W., Ives, J.C.: Ariel results on extragalactic X-ray sources. *Proc. R. Soc. Lond. A* **350**, 491 (1976)
199. Schmidt, M.: 3C 273: A star-like object with large red-shift. *Nature* **197**, 1040 (1963)
200. Schmidt, M.: Space distribution of quasi-stellar radio sources. *Publ. Astron. Soc. Pac.* **79**, 437 (1967)
201. Schmidt, M.: Quasistellar objects. *Ann. Rev. Astron. Astrophys.* **7**, 527 (1969)
202. Schnopper, H.W., Davis, M., Delvaile, J.P., Geller, M.J., Huchra, J.P.: Contribution of intermediate luminosity X-ray galaxies to the background – anon 0945-30. *Nature* **275**, 719 (1978)
203. Sergeev, S.G.: Gas kinematics: Estimation of the broad-line region size and the central source mass from the profile variability of the H α line in NGC 4151. *Astron. Rep.* **38**, 162–171 (1994)

204. Setti, G., Woltjer, L.: On the local hypothesis for the quasi-stellar objects. *Astrophys. J.* **144**, 838 (1966)
205. Setti, G., Woltjer, L.: Hubble diagram for quasars. *Astrophys. J.* **181**, L61 (1973)
206. Setti, G., Woltjer, L.: Extragalactic X-ray sources and their contribution to the diffuse background. In: Bradt, H., Giacconi, R. (eds.) *Proc. COSPAR-IAU Symp. No. 55*, p. 208. D. Reidel Publ., Dordrecht (1973)
207. Setti, G., Woltjer, L.: Quasar number counts and the X-ray background. *Astron. Astrophys.* **76**, L1 (1979)
208. Setti, G., Woltjer, L.: The gamma-ray background. *Astroph. J. Suppl.* **92**, 629 (1994)
209. Seyfert, C.K.: Nuclear emission in spiral nebulae. *Astrophys. J.* **97**, 28 (1943)
210. Shakura, N.I., Syunyaev, R.A.: Black holes in binary systems. Observational appearance. *Astron. Astrophys.* **24**, 337 (1973)
211. Shields, G.A.: The origin of the broad line emission from seyfert galaxies. *Astrophys. Lett.* **18**, 119 (1977)
212. Shields, G.A.: Thermal continuum from accretion disks in quasars. *Nature* **272**, 706 (1978)
213. Shields, G.A.: Physical conditions in the emission-line regions of BL lac objects and QSOs. In: *Pittsburgh Conference on BL Lac Objects*, Pittsburgh, PA, 24–26 April 1978, p. 257. University of Pittsburgh, Pittsburgh, PA (1978)
214. Shields, G.A., Ludwig, R.R., Salvander, S.: Fe II emission in active galactic nuclei: The role of total and gas-phase iron abundance. *Astrophys. J.* **721**, 1835–1842 (2010)
215. Shklovsky, I.S.: Quasi-stellar objects in seyfert galaxies. *Astron. Zhurnal* **42**, 893 (1965)
216. Souffrin, S.: Étude des noyaux des galaxies de seyfert. *Annales d’Astrophysique* **31**, 569 (1968)
217. Souffrin, S.: Study of seyfert galaxies. III. Ionization Mechanism. *Astron. Astrophys.* **1**, 414 (1969)
218. Stern, D., Eisenhardt, P., Gorjian, V., Kochanek, C.S., Caldwell, N., Eisenstein, D., Brodwin, M., Brown, M.J.I., Cool, R., et al.: Mid-infrared selection of active galaxies. *Astrophys. J.* **631**, 163–168 (2005)
219. Sun, W.-H., Malkan, M.A.: Fitting improved accretion disk models to the multiwavelength continua of quasars and active galactic nuclei. *Astrophys. J.* **346**, 68 (1989)
220. Tanaka, Y., Nandra, K., Fabian, A.C., Inoue, H., Otani, C., Dotani, T., Hayashida, K., Iwasawa, K., Kii, T., Kunieda, H., Makino, F., Matsuoka, M.: Gravitationally redshifted emission implying an accretion disk and massive black hole in the active galaxy MCG-6-30-15. *Nature* **375**, 659–661 (1995)
221. Tananbaum, H., Avni, Y., Branduardi, G., Elvis, M., Fabbiano, G., Feigelson, E., Giacconi, R., Henry, J.P., Pye, J.P., Soltan, A., Zamorani, G.: X-ray studies of quasars with the einstein observatory. *Astrophys. J.* **234**, L9 (1979)
222. Terrell, J.: Quasi-stellar objects: Possible local origin. *Science* **154**, 1281 (1966)
223. Trump, J.R., Impey, C.D., Kelly, B.C., Civano, F., Gabor, J.M., Diamond-Stanic, A.M., Merloni, A., Urry, C.M., et al.: Accretion rate and the physical nature of unobscured active galaxies. *Astrophys. J.* **733**, 60 (2011)
224. Ulrich, M.-H., Maraschi, L., Urry, C.M.: Variability of active galactic nuclei. *Ann. Rev. Astron. Astrophys.* **35**, 445 (1997)
225. Urry, C.M., Padovani, P.: Unified schemes for radio-loud active galactic nuclei. *PASP* **107**, 803–845 (1995)
226. Véron-Cetty, M.-P., Véron, P.: A catalogue of quasars and active nuclei: 13th edition. *Astron. Astrophys.* **518**, A10 (2010)
227. Volvach, A.E.: RT-22 CrAO long-term monitoring of extragalactic radio sources at 22 and 37 GHz. *SDP Conf. Ser.* **360**, 133–136 (2006)
228. Wampler, E.J.: Reddening in the nuclei of seyfert galaxies. *Astrophys. J. Lett.* **154**, L53–L56 (1968)
229. Wampler, E.J.: Do quasars lens quasars? *Astrophys. J. Lett.* **476**, L55–L58 (1997)
230. Wampler, E.J., Baldwin, J.A., Burke, W.L., Robinson, L.B., Hazard, C.: A double quasistellar object. *Nature* **246**, 203–205 (1973)

231. Wampler, E.J., Oke, J.B.: The emission-line spectrum of 3c 273. *Astrophys. J.* **148**, 695–704 (1967)
232. Wampler, E.J., Robinson, L.B., Baldwin, J.A.: Redshift of OQ 172. *Nature* **243**, 336–337 (1973)
233. Ward, M.J., Wilson, A.S., Disney, M.J., Elvis, M., Maccacaro, T.: A seyfert galaxy in an X-ray source error box. *Astron. Astrophys.* **59**, L19 (1977)
234. Ward, M.J., Wilson, A.S., Penston, M.V., Elvis, M., Maccacaro, T., Tritton, K.P.: Optical identifications of extragalactic X-ray sources. *Mon. Not. R. Astron. Soc.* **223**, 788 (1978)
235. Weinberg, S.: *Gravitation and Cosmology*. Wiley, New York (1971)
236. White, S.D.M.: Simulations of merging galaxies. *Mon. Not. R. Astron. Soc.* **184**, 185–203 (1978)
237. Woltjer, L.: Emission nuclei in galaxies. *Astrophys. J.* **130**, 38–44 (1959)
238. Yu, Q., Tremaine, S.: Observational constraints on growth of massive black holes. *Mon. Not. R. Astron. Soc.* **335**, 965–976 (2002)
239. Zasov, A.V., Dibai, É.A.: Some properties of seyfert-galaxy nuclei and the integrated parameters of the galaxies. *Soviet Astron.* **14**, 17 (1970)
240. Zel'dovich, Ya.B.: *Dokl. Akad. Nauk SSSR* **155**, 67. English translation in *Sov. Phys. Dokl.* **9**, 195 (1964)
241. Zel'dovich, Ya. B., Novikov, I.D.: Mass of quasi-stellar objects. *Sov. Phys. Dokl.* **9**, 834–837. In Russian original **158**, 811–814, 1964 (1965)

Chapter 3

Quasars: The Observational Perspectives

Contributions by Mauro D’Onofrio, Paola Marziani, Jack W. Sulentic, Greg Shields, Martin Gaskell, Todd Boroson, Ari Laor, Michael Hawkins, Vladimir Pronik, Sergey Sergeev, Deborah Dultzin, Dirk Grupe, Gordon Richards, Raffaella Morganti, Aleksander Volvach, Sebastian Zamfir, Heino Falcke, Elmar K rding, Martin Elvis, Tracey Jane Turner, Ajit Kembhavi, Luigi Foschini, Yuri Neshpor, and Alberto Franceschini

M. D’Onofrio
Dipartimento di Astronomia, Universit  degli Studi di Padova, Vicolo Osservatorio 3,
I35122 Padova, Italy
e-mail: mauro.donofrio@unipd.it

P. Marziani
INAF, Osservatorio Astronomico di Padova, Vicolo Osservatorio 5,
IT35122 Padova, Italy
e-mail: paola.marziani@oapd.inaf.it

J.W. Sulentic (✉)
Instituto de Astrof sica de Andaluc a (CSIC), Granada, Spain
e-mail: sulentic@iaa.es

G. Shields
Department of Astronomy, University of Texas, Austin, TX 78712-0259, USA
e-mail: shields@astro.as.utexas.edu

M. Gaskell
Departamento de F sica y Astronom a, Facultad de Ciencias, Universidad de Valpara so,
Av. Gran Bret a 1111, Valpara so, Chile
e-mail: martin.gaskell@uv.cl

T. Boroson
National Optical Astronomy Observatory, Tucson, AZ, USA
e-mail: tyb@noao.edu

A. Laor
Technion - Israel Institute of Technology, Physics Department, Technion City,
Haifa 32000, Israel
e-mail: laor@physics.technion.ac.il

M. Hawkins
Institute for Astronomy (IfA), University of Edinburgh, Royal Observatory, Blackford Hill,
Edinburgh EH9 3HJ, UK
e-mail: mrsh@roe.ac.uk

V. Pronik · S. Sergeev · Y. Neshpor
Crimean Astrophysical Observatory, 98409, Nauchny, Crimea, Ukraine
e-mail: vpronik@mail.ru; sergeev@crao.crimea.ua; yneshpor@mail.ru

D. Dultzin
Instituto de Astronomia, Universidad Nacional Autonoma de Mexico (UNAM),

Apt.do postal 70-264, Mexico, D.F., Mexico
e-mail: deborah@astroscu.unam.mx

D. Grupe
The Pennsylvania State University, 525 Davey Lab., University Park, PA 16802, USA
e-mail: grupe@astro.psu.edu

G. Richards
Drexel University, Department of Physics, 3141 Chestnut Street, Philadelphia, PA 19104, USA
e-mail: gtr@physics.drexel.edu

R. Morganti
Netherlands Institute for RadioAstronomy (ASTRON), Postbus 2, 7990 AA, Dwingeloo,
The Netherlands

Kapteyn Astronomical Institute, University of Groningen, P.O. Box 800, 9700 AV Groningen,
The Netherlands
e-mail: morganti@astron.nl

A. Volvach
Radio Astronomy Laboratory of Crimean Astrophysical Observatory, 98688, Ukraine, Crimea,
Yalta, Katsively, RT-22.
e-mail: volvach@crao.crimea.ua

S. Zamfir
University of Wisconsin-Stevens Point, 1848 Maria Dr Stevens Point, WI 54481-1957, USA
e-mail: szamfir@uwsp.edu

H. Falcke
Radboud Universiteit Nijmegen, Department of Astronomy,
IMAPP, The Netherlands

ASTRON, Dwingeloo, The Netherlands

Max-Planck Institut für Radioastronomie, Bonn, Germany
e-mail: h.falcke@astro.ru.nl

E. Körding
Radboud Universiteit Nijmegen, Department of Astronomy, IMAPP, The Netherlands
e-mail: elmar.koerding@astro.ru.nl

M. Elvis
Harvard Smithsonian Center for Astrophysics, Cambridge MA02138, USA
e-mail: elvis@cfa.harvard.edu

T.J. Turner
UMBC, 1000 Hilltop Circle, Baltimore MD 21250, USA
e-mail: tjturner@umbc.edu

A. Kembhavi
The Inter-University Centre for Astronomy and Astrophysics, Pune, India
e-mail: akk@iucaa.ernet.in

L. Foschini
Istituto Nazionale di Astrofisica (INAF) - Osservatorio Astronomico di Brera,
Via E. Bianchi, 46 - 23807 - Merate (LC) - Italy
e-mail: luigi.foschini@brera.inaf.it

The empirical basis of quasar astronomy can be overawing especially in the twenty-first century. A first source of intricacy involves the nomenclature that has evolved to label the multifold phenomenological manifestations now united under the umbrella of active galactic nuclei (AGNs). A further complication involves observations of the many subclasses with the observations now spanning the electromagnetic spectrum.

The number of quasars satisfying the original discovery definition (blue optical point sources showing (a) broad redshifted emission lines spectroscopically, (b) manifesting frequent optical variability, and (c) those redshifted less than a few tenths almost always found in the centers of galaxies) has long ago passed $n \sim 10^5$. Our questions begin with this definition but quickly branch out into subclasses and wavelengths little imagined in 1962–1964. We will address the photometric and spectroscopic properties of quasars from radio to γ -ray, their variability, the unification scheme, as well as the most important correlations involving quasar properties.

Observational capabilities changed dramatically since the time of quasar discovery. Radio interferometry caused a takeover unprecedented in the history of astronomy, surpassing the spatial resolution of optical instruments in the 1970s. The X-ray and especially the γ ray domain are the ranges where substantial and perhaps the most impressive achievements have been obtained most recently. X-ray instruments were able to detect quasars relatively late, as in the early 1970s, only three sources were known. However, since relatively recent times (the late 1990s), spaceborne X-ray observatories like ASCA, *Chandra*, and XMM-*Newton* have provided a wealth of imaging and spectroscopic data that is comparable to the one provided by the optical ground-based observatories. The iron $K\alpha$ lines whose photons are probably the ones closest to the central black hole (a few gravitational radii). The unique closeness of this emission line to the very heart of a quasar merits the huge observational effort occurred in the last 20 years. No doubt the IR that has been penalized in the past will play an increasingly important role, as the Ly α emission line along with the strongest UV emission lines is shifted into the IR for quasars of $z \gtrsim 6$. Largely optical in the past, discovery techniques—quasars are to be found among a myriad of stellar objects that can be of similar brightness but of somewhat different *color* are now benefitting of new multifrequency abilities. How many quasars did we miss relying on optical color selection? Is it possible that new classes of quasars are awaiting for discovery? Perhaps, when we will pass the new “redshift frontier” at $z \approx 6$ –7?

Given the different instrumental approaches in the various spectral ranges, observational astronomers were in the past—and often remain today—specialized in a defined range of the electromagnetic spectrum. Optical, radio, and X-ray data

A. Franceschini

Dipartimento di Astronomia, Università degli Studi di Padova, Vicolo Osservatorio 3,
I35122 Padova, Italy

e-mail: alberto.franceschini@unipd.it

are produced by astronomers working in different communities. For example, radio astronomers are not always cognizant of interesting discoveries made by optical and UV spectroscopists and vice versa. These facts grounded in the historical development and in the organization of astronomical research convey the need to review major observational achievements across the electromagnetic spectrum, with the various spectral ranges ordered according to a sequence of (rough) historical preeminence. The visual and UV are considered first (thanks to the redshift, the quasar UV spectrum has been known much in advance of the launch of the first spaceborne UV observatories) since, until present time, to confirm that a quasar is a quasar has meant to take an optical spectrum. Therefore, the optical/UV spectral phenomenology is still the birthmark that allows the recognition of a quasar.

3.1 Optical Phenomenology of Quasars

Dear Greg (*Shields*), early work involving spectra stressed the similarity between the spectra of Seyfert galaxies and quasars and those of planetary nebulae. They also stressed many differences between the spectra of active nuclei and the spectra of regions photoionized by hot stars i.e., the HII regions. Of course, these are very different sources, but they share the common property that lines are mainly emitted by photoionized gas. Can you please summarize the main difference between the line-formation processes in these sources? Can the results reached on Seyfert nuclei spectra straightforwardly extended to quasars?

The earliest studies of emission-line nuclei of galaxies noted similarities to ionized nebulae in our Galaxy. In fact, when [157] discovered nuclear emission lines in NGC 1068, he was observing the spectra of galaxies to see if they had emission-line spectra like galactic nebulae or continuous spectra as expected for a collection of stars. The emission lines in NGC 1068 were familiar ones in the spectra of galactic emission nebulae. Hubble [238] noted that spiral galaxies with stellar nuclei show emission lines resembling those of planetary nebulae.

In his systematic study of galaxies with stellar nuclei, Seyfert noted that NGC 1068 and NGC 4151 showed “all the stronger emission lines . . . in planetary nebulae like NGC 7027” [460]. Seyfert’s reference to NGC 7027 is significant. This is a prototype for high-excitation planetary nebulae, which have a wide range of ionization stages in their emission-line spectra, from [OI] to [NeV]. This naturally suggested that photoionization of gas in the galactic nucleus by a central continuum source might be responsible for the observed emission lines, by analogy to planetary nebulae ionized by a hot central star. The presence of high-ionization stages of some elements then implies ionizing radiation extending up to high frequencies. For NGC 1068, Seyfert found that the line intensities were similar to those in NGC 7027 “except that the [OII], [SII], [NII], and [FeVII] lines are considerably stronger in NGC 1068.” This simple remark contains a variety of implications for AGN

emission-line regions, from the spectrum of the ionizing radiation to the chemical abundances in the gas.

An important difference between the spectra of AGNs and nebulae is the presence of strong emission lines of a wider range of ionization in AGNs. The difference is most extreme in comparing AGNs to HII regions. AGNs typically show substantial intensity in narrow lines from [OI] to [FeVII] (and sometimes higher) in the optical and broad lines up to OVI or higher in the ultraviolet. Galactic HII regions ionized by O-stars rarely show high-ionization lines like HeII or [NeV] that are common in AGN spectra. This reflects a cutoff in the ionizing spectrum of the exciting stars beyond the He II photoionization edge at 4 Rydbergs photon energy. Planetary nebulae such as NGC 7027 having high-temperature ionizing stars ($\sim 10^5$ K) show strong HeII and [NeV]. However, AGNs are distinguished from high-excitation planetary nebulae by the simultaneous presence of strong lines of low-ionization stages such as [OI]. This wide range of ionization was on the minds of the first workers to construct photoionization models of AGNs [504, 554]. In these models, X-rays produce a wider H^+ to H^0 transition zone than occurs in nebulae ionized by stars. This gives greater strength to the low-ionization emission lines.

The line emission processes in AGNs and ionized nebulae have much in common [398]. Ionizing photons eject photoelectrons from hydrogen and other elements, while radiative recombination returns the atoms to lower stages of ionization. In AGNs and nebulae, this generally leads to a photoionization equilibrium in which hydrogen is strongly ionized. The photoelectrons add thermal energy to the gas, while a variety of processes convert this energy to line and continuum photons that carry the energy away and thus cool the gas. These processes include radiative recombination, bremsstrahlung, and collisional excitation of bound levels by electron impact. The balance of heating and cooling leads to an equilibrium temperature typically around 10,000 K. The ionization equilibrium is governed by the intensity and spectrum of the ionizing radiation and the density of the gas. A key quantity is the “ionization parameter” U that expresses the ratio of ionizing photon flux to gas density, higher U , giving a higher degree of ionization. Also, critical is the progressive absorption of the ionizing radiation as it flows outward from the central source through the gas. At some point, the ionizing photons are exhausted, and the gas becomes neutral, the transition typically being fairly abrupt in relation to the radius of the nebula (“Strömgren sphere”). Different frequencies are absorbed to different degrees as one goes out in radius. For AGNs and high-excitation planetary nebulae, the resulting ionization structure is characterized by an inner “He⁺² zone” surrounded by a zone dominated by H^+ , He^+ , and O^{+2} . Ions such as O^+ and N^+ are found closer to the transition zone, which is the site of [OI] emission.

Differences between AGNs and ionized nebulae arise not only from the ionizing continuum shape and but also from the gas density and ionizing continuum intensity. The classic AGN spectrum consists of a continuum with a roughly power-law shape and superimposed emission lines. The forbidden lines such as [OIII] $\lambda\lambda$ 5007, 4959 have narrow widths (around 500 km s⁻¹FWHM), whereas the permitted lines have widths of around 4,000 km s⁻¹. These are understood to arise in distinct physical regions, the “narrow-line region” (NLR) and the “broad-line region” (BLR). The

NLR has a radius of about 100 pc, whereas the BLR has a radius of about 0.1 pc, depending on the luminosity of the AGN. The NLR consists of clouds or filaments with an internal electron density of order $n_e \approx 10^4 \text{ cm}^{-3}$, whereas the BLR has $n_e \approx 10^{10} \text{ cm}^{-3}$. The physical conditions, including U , n_e , and T in the NLR resemble those in high-excitation planetary nebulae, and the line emission processes are largely the same. However, the high density and intense ionizing flux in the BLR lead to a more complicated situation. The absence of forbidden line emission results from the high electron density, which causes collisional deexcitation of the metastable levels that give rise to these transitions. The high density in turn requires a small BLR radius in order for the ionization parameter to be consistent with the ions present in the broad-line spectrum.

Another important difference from nebulae is the large optical depth in many of the permitted lines and the importance of thermalization. Optical depths in the Lyman- α line in nebulae are roughly 10^4 . In the partially ionized zone of AGN, they can be considerably higher. During the many scatterings of $L\alpha$ as it escapes the emission region, the high density in the BLR gives a substantial probability of collisional de-excitation, suppressing the emergent intensity compared to a simple nebular Case B prediction. A similar process can affect the resonance lines of the heavier elements, affecting their intensities. Observational evidence for this was found in some AGN that show approximately thermalized doublet ratios for some of the ultraviolet lines in AGN [288]. Optical depths and collisional excitation in the Balmer lines can be significant in high-density nebulae and in the NLR and are very important in the BLR. An important discovery was that the intensity of broad $H\alpha$ and $H\beta$, relative to $L\alpha$, is several times larger than expected for nebular Case B [29]. This stimulated studies involving photoionization models incorporating complex treatments of the level populations and optical depths in the hydrogen lines [282, 333]. Also, complicated is the FeII emission from the BLR. Strong bands of emission in the optical and ultraviolet come from blended multiplets of FeII. This can be explained qualitatively in models incorporating collisional excitation, line and continuum fluorescence, and radiative transfer [555]. However, models have had difficulty giving the large strength of FeII emission observed in some AGN.

A striking fact about AGN is how similar the emission-line spectra are over several orders of magnitude in luminosity, from luminous quasars to feeble Seyfert nuclei. The presence of broad and narrow lines, and the relative intensities of the lines, are substantially the same. A consequence of this is to frustrate the search for luminosity indicators that would allow AGN to be used as standard candles for cosmology (see discussion by Martin Elvis in this volume). The equivalent widths of some emission lines, in particular the ultraviolet CIV line, decrease with increasing continuum luminosity, in a statistical sense [32]. However, no convincing cosmological results based on such methods have been achieved. The uniformity of the emission-line ratios among AGN suggests that some physical processes lead to a similar density and ionization parameter in the BLR and in the NLR. The leading suggestion for this regulatory mechanism is the “locally optimally emitting cloud” model [30]. This picture postulates that gas is present over a wide range of

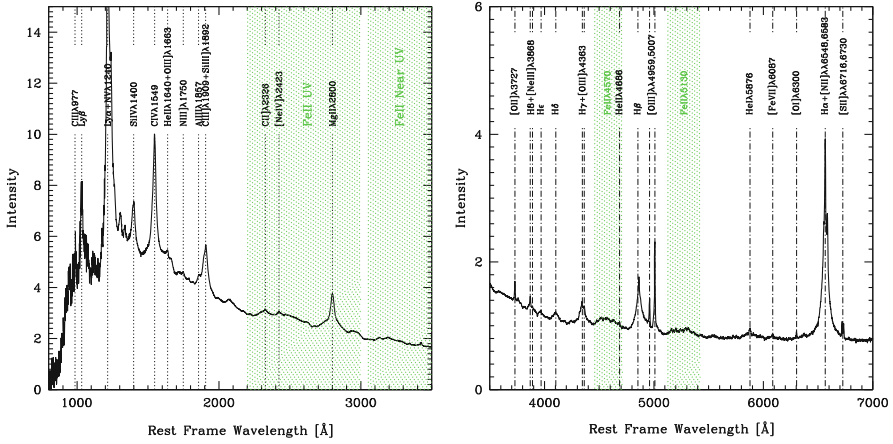


Fig. 3.1 SDSS composite spectrum, in the UV (*left panel*) and in the optical spectral range (*right panel*). Major features are identified; regions with strong emission blends of Fe II are shaded [534]

radii with a wide range of densities. A particular emission line comes from those combinations of density and ionization parameter that give the strongest emission in that line. Different lines come from different zones in this structure, but the total emission summed over the entire region has a fairly robust spectrum that resembles the observed line intensities. So it appears that similar processes are at work in Seyfert galaxies and QSOs.

Thank you, Greg. We now look into more detail at the emission-line spectrum of quasars. A composite spectrum obtained from combining about 2,200 SDSS spectra reveals the richness of emission features (Fig. 3.1) and can serve as reference for the discussion that follows.

Dear Martin (Gaskell), please give us an overview of the optical/UV emission-line spectra of type-1 AGNs

Probably, all AGNs have forbidden lines with line widths comparable to the stellar velocity dispersions of the galaxies in which they are located. These lines are hard to detect in some AGNs (if there is a bright jet aimed at us in a BL Lac object or if an AGN is very heavily obscured), but probably, still there. Optical spectra of AGNs can be classified into two broad groups: type-1 and type-2 [262]. If only the forbidden lines can be seen in the optical, the AGN is called a “type-2.” If we also see broad permitted or inter-combinational lines then we call an AGN “type-1.” We see both narrow and broad lines from a wide range of ionization. These range from low-ionization lines such as Ca II to very highly ionized lines of Fe seen in the X-ray region.

The broad permitted lines have FWHMs ranging from a few hundred km s^{-1} (as narrow as the forbidden lines) up to several percent of the speed of light. The

strongest broad lines in AGN spectra are the hydrogen recombination lines. We also see recombination lines of HeII and HeI in both the broad-line and narrow-line spectra. The other strong broad and narrow lines are collisionally excited lines. The strongest of these come from low levels with high collision strengths from among the dominant ionization degrees of the most abundant elements. The broad lines can be substantially stronger than the corresponding narrow lines.

When the broad lines are fairly narrow (up to a FWHM of $3,000 \text{ km s}^{-1}$ or so), their profiles are well fit by “logarithmic” profiles with flattened tops. The widths of the lines generally increase with ionization potential. As the lines get broader, double-peaked profiles are seen. One peak is blueshifted and the other redshifted. The peaks are unequal in intensity, and either one of the displaced peaks can be strongest.

How many distinct emitting components can we identify in the strongest well-studied lines like $H\beta$ and C IV?

The most fundamental separation is into the *broad-line region* (BLR) and the *narrow-line region* (NLR). This clear distinction was first recognized back in the 1960s by the Soviet AGN pioneers Ernst Dibai and Vladimir Pronik (see [119]). Dibai and Pronik recognized that what they called the “nebular region” and the “hydrogen region” are very distinct both spatially and kinematically and that the latter had a much higher density. Since there was hydrogen emission from both regions, it was clearly better to label the lines as simply “broad” and “narrow.” Calling the two region the BLR and NLR was firmly entrenched by the mid-1970s. We now know that the BLR ranges from light-hours to light-years across, depending on the luminosity of the AGN (an order of magnitude smaller than Dibai and Pronik thought), while the NLR can be a hundred to a thousand times larger. The NLR can often readily be resolved in nearby AGNs, while the BLR is the small enough not to be resolved directly yet.

The number of components of *broad* lines is controversial and will probably remain so for a long time. I have always been worried by attempts to fit multiple components to any line profile. Just because a component can be fit in IDL or IRAF does not mean that it has any physical meaning. The same goes for principal component analyzes. In practice, anything can be fit with orthogonal functions. Having software packages readily available that will fit gaussians means that a lot of gaussians get fit. There is a very real danger that question “how many distinct emitting components can we identify?” becomes “how many distinct emitting components can we make up?” We need to remember the words of Aristotle, “the superiority *ceteris paribus* of the demonstration which derives from fewer postulates or hypotheses” (*Posterior Analytics*, Chap. 25, Sect. 1), and following [492], to ask whether a component we are adding is “a region *praeter necessitatem*”.

Unlike the BLR/NLR separation, I do not think that *the observations themselves* force us to separate the BLR into meaningful separate components. I think it is theoretical ideas that have motivated the separation. My views on how many BLR components there are have changed. Back in the 1960s and 1970s most people were modeling BLR clouds as single clouds, and we thought of different lines as arising

from different parts of the same clouds. This is still a widely accepted picture. In the mid-1980s, I proposed that there were instead two distinct components to the BLR [179]. I labeled the components “BLR I” and “BLR II.” Collin-Souffrin and Lasota [102] labeled them the “HIL BLR” (high-ionization-line BLR) and “LIL BLR” (low-ionization-line BLR). I think the latter labels are better. Although there was some observational support for proposing that there were two components, I think our motivation was again largely theoretical, and we were influenced by “disk–wind” models. It is certainly very clear that there is a disk component. However, there is a problem that there is too much of a continuity in the change of properties with velocity and the widths of the “disk” and “wind” components are not independent. Reverberation mapping ([180]; see [181] for a review) resoundingly rules out winds as a significant contributor to BLR emission.

This leads me back to now believing in a single-component BLR. This single component is the thick turbulent disk proposed by Osterbrock [397]. I believe that this explains the many observational constraints very well [182].

In 1982, you presented evidence for a systematic blueshift of some or all of the higher ionization lines. Is this an ubiquitous phenomenon or do some quasars not show this blueshift?

It varies from AGN to AGN. The effect is strongest in AGNs with the highest accretion rates (the so-called “narrow-line Seyfert 1s” or NLSy1s). As I have mentioned already, I proposed in [178] that the blueshifting was due to outflow and obscuration in a “disk–wind” model, but velocity-resolved reverberation mapping now rules out a significant wind contribution to the BLR. We now believe that the blueshifting is due to scattering of photons off material with a net inflow [183]. We believe that the effect is strongest in NLSy1s because the scattering depends on the product of the optical depth and the inflow velocity, and together, these are related to the relative accretion rate.

Do all broad lines show velocity shifts and asymmetries?

I think the answer is “yes,” but whether they are detectable or not is another matter. We need to separate out *systematic* velocity shifts and asymmetries from *random* ones. I believe that these have quite different causes. The strongest systematic effect is the blueshifting of high-ionization lines [178]. This is a significant and sometimes spectacular shift that includes the line peak. Another systematic effect is the presence of broad redshifted shelves to broad Balmer lines [495]. In contrast to *systematic* effects, we get *random* effects which, as discussed above, I believe are the result of off-axis illumination which causes highly asymmetric disklike profiles (see Fig. 6.3 in Chap. 6). In an individual AGN at a given moment, it is hard to separate out the random asymmetries and shifts from the systematic ones. All shifts and asymmetries are harder to see in the narrower-line AGNs.

When we speak of line shifts, how do we estimate the local quasar rest frame against which to measure the shifts?

It depends on how concerned one is with accuracy. The stars give the ultimate local reference frame, but the narrow-line region is a good proxy for this. The low

ionization narrow lines are a better indicator of the rest frame than higher ionization lines like [OIII] because the latter can be asymmetric and blueshifted.

Do we see any evidence that a given broad line changes width, shift, or shape as a function of redshift?

Comparing things at different redshifts is dangerous because we are usually not selecting the same sorts of objects at different redshifts. At low redshift, the detectable low-mass black hole AGNs are accreting at high Eddington ratios. They are hard to detect if they are not. Among the high-mass black holes at low redshift, high accretion rates are rare. The high-mass black holes are in high-mass galaxies, and these tend to be “red-and-dead” galaxies that are not actively forming stars. There is not much gas around, and their relative accretion rates are low. At high redshift, massive black holes are still in galaxies with plenty of gas, and they can have high relative accretion rates. Since emission-line properties are correlated with relative accretion rate and black hole mass, we *see* differences in the emission-line properties. It is not clear to me that when we allow for differences in black hole mass, relative accretion rate, orientation, and dust/gas content that significant changes with redshift will remain.

If a stellar or compact extragalactic source shows broad emission lines in its spectrum, is it “by definition” a quasar?

This is a really interesting question. Obviously, just having broad lines does not make an object an AGN—Wolf Rayet stars and supernovae have broad lines, e.g., but are not AGNs. We clearly have to be careful with definitions and classifications. We do not want to create unnecessary problems through our classifications by putting unrelated phenomena together, and we do not want to exclude things unnecessarily. I tell students that classification is one of the first step in science. As science progresses, however, I believe that we need to move toward physically meaningful classification schemes as soon as possible. To achieve this, we need to be willing to modify our definitions, or else we can impede progress.

Should the presence of broad optical/UV FeII emission be added as an additional part of the definition for type-1 AGNs?

I think the key word here is “additional.” Strong optical FeII emission is certainly not a *necessary* criterion for defining an object as a type-1 AGN, but it is an interesting parameter [484], and it is useful for recognizing a BLR. A notable example was the historic discovery by Ski Antonucci and Joe Miller at Lick Observatory of the hidden BLR in the polarized spectrum NGC 1068 [23]. Not only did the polarized light show broad Balmer lines, but it also showed broad FeII emission.

Thank you, Martin. After having discussed the SED and the main emission features of quasars, we now consider how the quasar spectral properties can be turned into a tool for picking them up from an anonymous field of stellar objects.

3.2 Techniques of Discovery

Dear Todd (*Boroson*), what are the principal search techniques employed by quasar hunters at low redshift? How efficient is/was the UV excess techniques that has been employed since the early days? Can one technique find all of the quasars that exist in any given volume? Can you compare for us the results of Palomar-Green (PG) and SDSS searches for quasars brighter than $B \sim 16$?

Search techniques for quasars have gone through a number of stages, as technology and our understanding of quasar characteristics have advanced. Initially, of course, quasars were identified as radio sources—as stellar (or point-like) objects, showing optical emission lines, at the positions in the sky of strong radio emission (detected in surveys such as 3C, 4C, Tonantzintla, Ohio, Parkes). After it was realized that most quasars are radio quiet, the unusual optical features, strong broad emission lines and a continuum that turns up in the UV, led to two types of searches, UV excess surveys, such as the Bright Quasar Survey [200, 459], also known as the Palomar-Green (PG) survey, and grism or objective prism surveys, such as the University of Michigan Curtis Schmidt survey. UV excess surveys identified objects which appeared brighter through an ultraviolet filter than through a blue filter. The grism or objective prism surveys actually dispersed the light from each object and found those with excess flux at the ultraviolet end or with strong emission lines. These search techniques, which took maximal advantage of the most dramatic features of quasars, were well suited for photographic plates, which could cover a large area, but which were limited in the signal to noise that they could achieve. The advent of larger CCDs and CCD mosaics, i.e., digital detectors, led to the development of techniques such as that used by the Sloan Digital Sky Survey (SDSS) [1, 570], in which quasar candidates are all objects that lie significantly off the stellar locus in a multicolor space. Finally, as the physics of quasars have come to be understood better, we have realized that there are a substantial fraction that do not show optical properties that differentiate them strongly from inactive galactic nuclei because of obscuration. These are found through their mid-IR emission which is where the obscuring material reradiates its absorbed energy or by their X-ray emission, which is able to penetrate the obscuring material.

So, let us focus on the UV excess technique and try to understand how well it works. There are two questions here: (1) what fraction of objects that the UV excess method should have found were actually found, i.e., how many were missed and why? and (2) what fraction of true quasars cannot be found by the UV excess method? For the first questions, reasons for missing objects might include observational “errors,” i.e., uncertainty in the measured colors, or variability, when colors were derived from observations made at different times. Of course, there is also the possibility of picking the wrong color threshold to define a set of candidates. These will all lead to objects that should have been in a UV excess defined sample being missed.

For the second part, we run smack into the definition of quasars. It is generally believed that (a) some type of obscuring material exists in some, if not all, quasars

and (b) that material has a geometric distribution that divides similar objects into three general classes. These classes are (1) those in which we see all the way to the center, and so the hot continuum and broad lines are visible; (2) those in which the very center is obscured, but the more extended narrow-line region is still visible to us, so we see a high-ionization narrow emission-line spectrum; and (3) those in which all the activity is hidden, e.g., the so-called XBONGs (X-ray bright optically normal galaxies). While it is clear that these three classes of objects do exist, it is not obvious that their isotropic characteristics are identical. That is, when one searches for objects with strong UV continua and broad emission lines, what one finds are objects with minimal obscuration, while when one searches for objects with strong mid-IR excesses, what one finds are objects with maximal obscuration. There are also more subtle effects. For instance, as we look at objects of different redshift, the emission lines move through the filter passbands and affect the apparent colors, so it is possible for two objects with the same redshift to have different colors if one has much stronger emission lines than the other.

One of the best studies to draw on for an understanding of these effects is the paper titled, “The Sloan Digital Sky Survey View of the Palomar-Green Bright Quasar Survey” (BQS) [247]. These authors are able to quantify—using modern digital data—the limits and limitations of the much older PG survey. I start by describing the two surveys.

The PG survey [200, 459] was supposed to find all objects in a 10,668-square degree region in the north galactic cap, having B magnitudes brighter than 16.16 and $U - B$ colors bluer than -0.46 . The discovery films were taken with a small telescope; the plate scale (220 arcsec/mm) precluded distinguishing between stellar and slightly extended objects. The objects in this UV excess sample were observed spectroscopically to classify them. The survey produced a sample of 114 quasars (with one object in the original list removed as a starburst galaxy and one object added in the later paper). Of these, 88 have redshifts less than 0.5, and these range in absolute magnitude (using the published $q_0 = 0.1$ numbers [459]) from $M_B = -20.75$ to -27.09 . Limiting magnitudes varied from field to field, but the average limiting magnitude, $B = 16.16$, corresponds to an absolute B magnitude of $M_B = -26.09$ at a redshift of 0.5 for a current cosmological model ($H_0 = 71 \text{ km s}^{-1} \text{ Mpc}^{-1}$). Thus, the sample is not complete for any, but the highest luminosity objects (nine quasars have $z < 0.5$ and $M_B < -26.09$).

Of these 88 low-redshift active galactic nuclei, 21 are classified as Seyfert galaxies and 67 as quasars, depending on their appearance (stellar for quasars, fuzzy for Seyfert galaxies) on the Palomar Sky Survey plates. This distinction adds another level of complication since this is not a quantitative measurement.

Of course, one of the principal limitations of the bright quasar survey (BQS) is that it was carried out on photographic film, and so there are significant variations and uncertainties in the sensitivities and the transformations. Studies that compared the BQS to other surveys that went fainter over smaller areas [195, 562], but also using photographic methods, found incompleteness in the BQS by a factor of 2–3.

The Sloan Digital Sky Survey (SDSS) Legacy Survey [1, 570] was an imaging survey in five colors of 8,400 square degrees in the northern sky, together with a

spectroscopic survey of almost one million galaxies, 120,000 quasars, and about 225,000 stars in that region. Within the galaxy and quasar spectroscopic samples, there are subsets that represent complete samples: every object within some well-defined set of constraints was observed. The quasar sample was intended to be complete to a limiting magnitude of $i = 19.1$. The SDSS used digital detectors, CCDs, for both imaging and spectroscopy. Not only are these detectors much more sensitive than photographic plates, they can be calibrated to a few percent. The comparison of these two surveys, the PG survey and an preliminary version of the SDSS (DR3), which includes about half of the final sample, forms the basis for the paper by Jester et al. [247]. They found the following: (1) The photographic PG magnitudes are systematically too faint at the bright and faint ends; objects brighter than $B = 14$ and fainter than $B = 16$ are actually a few tenths of a magnitude brighter than the PG numbers. (2) There is a significant offset in the $U - B$ colors. This results in the finding that the best approximation to the red color limit for the PG sample is $U - B < -0.71$ rather than the value of -0.44 that is quoted in BQS. Thus, substantial numbers of quasars that are redder than the true $U - B$ limit may have been missed. No dependence on magnitude was seen for this offset. (3) There was significant variation in both the limiting magnitude and the limiting $U - B$ color from field to field. And (4) no other property was found to have influenced the selection of the PG sample, including radio properties. The resulting picture is that the BQS is significantly incomplete as the actual limiting $U - B$ color is close to the mean $U - B$ color for low-redshift quasars but that that incompleteness is random with respect to magnitude, redshift, and radio properties.

Given the availability now of the SDSS, we can ask, if one were to create a sample based on the intended BQS properties, what would that sample look like? This is quite simple, if one adopts a set of criteria that translates the BQS properties to the SDSS measurements. Using the transformations derived by Jester et al. between UBV and the SDSS *ugriz* filter system, we can search the DR7 database for all objects that satisfy the constraints that they derived for the BQS sample. We limit our search to objects with redshifts less than 0.5.

We do not distinguish between stellar and extended objects (as classified by SDSS) in our search, but we toss out objects if their PSF magnitude (representative of a point-like measurement) is more than 0.5 magnitudes fainter than their “model” magnitude (representative of the entire object). We judge that these would be noticeably extended. This search turns up 45 objects from the 8,032 square degrees covered by the Legacy survey spectroscopic observations in Data Release 7. To this number, we must make three corrections. First, SDSS did not obtain a spectrum of any object that had a magnitude in the r band brighter than 15. There are 11 such saturated objects in the PG sample that are also in the SDSS region. We assume that the BQS is complete at this bright level, and so we add these 11 objects to the SDSS DR7 total. Second, we note that some objects that should have been targeted for spectroscopy by SDSS were not for various reasons, most commonly if there were defects or blends in the image. While it has been estimated [535] that this only affects about 4% of the objects, we find that for the PG objects, seven of the objects in the DR7 region were mixed. This implies a missed fraction of 14%.

So we multiply the number found, 56, by $1/0.96$ (58) or $1/0.86$ (65) for these two cases. Finally, we note that DR7 includes spectroscopy over 8,032 square degrees as compared with the BQS coverage of 10,714 square degrees. When we multiply this factor, we obtain a number of quasars expected for the BQS of 78–87 objects. This is actually surprisingly close to the 67 quasars with $z < 0.50$ found by BQS and suggests that the incompleteness in BQS is only at the 20–30% level.

How can we reconcile this with the claims, based on deeper surveys over smaller areas that the BQS is much more incomplete? The answer is that the BQS agreement with our SDSS number is, at some level, a coincidence. It is a consequence of the variation of limiting magnitude from field to field and the fact that there are very few quasars in this magnitude range with $U - B$ colors bluer than the actual $U - B$ limit of the BQS (as opposed to the intended limit). As the luminosity function rises steeply with decreasing luminosity, there are many more fainter objects included in the BQS than brighter objects lost. Thus, the studies that find more PG-like quasars in deeper surveys over a small part of the BQS field can only make the claim that that the BQS is incomplete in that area. They cannot discover that the BQS is “over-complete” in other areas. Thus, conclusions drawn from the total number of objects found in the BQS are not far wrong.

Why did PG find so many radio louds ($2 \times$ the canonical fraction of $\sim 8\%$)? If we have found so many ($> 10^5$) quasars, why do we search for more?

Most quasars are radio quiet. It has taken quite a while to understand the radio characteristics of quasars in detail because much of the early work depended on samples in which quasars had been discovered by their radio emission. Thus, these samples were not representative.

The radio-loudness statistics of the PG sample are particularly interesting, and I have done some additional work, based on the SDSS analysis of the optical properties of the PG sample, to understand these statistics. Several studies [196,345] have pointed out that the fraction of radio-loud quasars among the most luminous (in the [OIII] emission line) objects in the low-redshift part of the PG sample is surprisingly large, about 50%. Consequently, one wonders whether this is (1) indicative of evolution in the radio-loud fraction (a decrease with increasing redshift), (2) due to a unexpected and unrecognized selection effect in the sample, or (3) a flaw in the PG sample in that previously known, radio-loud objects were preferentially included. This question was explored a bit by the Jester et al. study, which attempted to construct a comparison sample from SDSS with similar properties to the subset from which previous studies drew their conclusion. This sample of 13 objects yields 3 radio-loud objects, which is not statistically significantly different from the 6.5 expected, though is suggestive of a discrepancy.

Of course, if one wants to look at the evolution of properties, one would not limit the sample by [OIII] luminosity as it might well be the case that a significant fraction of the [OIII] emission is due to the radio source. I think there are two questions here: first, are the radio statistics of the PG sample misleading us? and second, what is the fraction of radio-loud quasars as a function of true physical parameters, e.g., black hole mass, accretion rate, and redshift? I think, to answer these questions

in a confident way, we have to be very careful about how samples are constructed and compared.

Starting with the first question, the PG sample, as described above, has 67 quasars and 21 Seyfert galaxies with redshift, $z < 0.50$. I consider only the quasars here. Using the Schmidt and Green [459] M_B luminosities (calculated for a cosmology with $q_0 = 0.1$), the quasars range in luminosity from -20.30 to -27.09 .

These objects have all been very well observed at a number of radio frequencies, so there is little question about their radio characteristics. There are two approaches to “radio-loudness.” One can look at radio luminosity density (i.e., Watts per Hz) at a given frequency, or one can look at a ratio of radio flux density to optical flux density. I prefer to use the straight radio luminosity, measured at a low frequency. Not only do the optical brightnesses vary, but both high-frequency radio emission and optical emission may be enhanced by relativistic “beaming” or other orientation effects. Thus, I adopt $L > 10^{26.5} \text{ W Hz}^{-1}$ at 325 MHz as the definition of a luminous radio source. I find that 11 of the 67 PG objects, 16.4%, are radio luminous by this definition. However, the choice of definition makes little difference; if one uses $R = f(5 \text{ GHz})/f(4400 \text{ \AA}) > 100$ as is often done, one gets one additional object, which has a log luminosity at 325 MHz of 26.43, i.e., just barely under the cutoff.

We can compare this result with the PG-like sample extracted from SDSS. Examination of the radio data for this sample of 45 objects shows that six of them are radio luminous by our adopted criterion, giving a fraction of 13.3%. If we add in the saturated objects (11), which include one radio-luminous object (3C 273), we derive a fraction of 7/56, or 12.5%.

It is pretty clear that these are not wildly discrepant, but even if they were, the samples are too small to make a comparison meaningful. Even had we derived a radio luminous fraction of 9%, say 5/56, the different fractions in the two samples represent only an 89% probability rejection of the hypothesis that they are the same. Thus, the statistics of the BQS sample itself prevents the conclusion that radio-loud quasars are overrepresented to a significant degree.

This brings us to the second question. Why are quasar searches valuable, even when we now have samples of more than 100,000? There are two answers. The first is that we wish to understand the properties of quasars and their evolution as a population of objects in the universe. In order to do this, we have to understand the numbers and characteristics of complete sample. That is, if we believed that we were missing half the objects because our search techniques were defective, we would want to figure out how to find those missing objects. While I have argued that UV and color searches are effective for the objects that they are supposed to find, we still may be missing large numbers of quasars that do not have obvious UV excesses or non-stellar colors. As I noted above, these may be the objects in which the central engine is hidden, but we still see narrow emission lines (type-2 quasars), or they may be objects in which all the activity is hidden.

A second reason for continuing to search is to find those particular objects that are special, in the sense that they provide some particular insight into the physics of quasars. The quasar zoo has quite a few types that only occur a small percentage of the time: radio-luminous objects, double-peaked emission lines, and objects in

which the broad lines are barely broader than the narrow lines. Each of these types allows us a slightly different view of the relationships among properties. The SDSS sample is rich with such objects. Almost a decade after the first release of SDSS data, new examples of rare phenomena are still being found in the database.

Thank you, Todd. Until the early 1990s, correlation analysis of quasar spectral properties was carried out on small sample and with a limited scope. Results were partial, often confusing or contradictory. The PCA analysis of Boroson and Green changed all of this and for the first time, made it clear that quasar spectral properties can be organized in a meaningful way that is conducive to physical interpretation.

3.3 Organizing Quasar Broad-Line Diversity

Dear Todd (*Boroson*), you (and Richard Green) were among the first to analyze quasar spectroscopic properties in a systematic way. Your principal component analysis of the correlation matrix of observed properties for Palomar-Green bright quasars allowed us to identify “first and second eigenvectors” of quasars. Your first two eigenvectors carry a significant fraction of the variance with the exact value, depending on sample and on spectral parameters included in the correlation matrix. However, the fraction does not exceed 70%. Can you explain how one could account for the residual variance?

The Boroson and Green (BG92) [66] study of low-redshift quasar spectra was our attempt to quantify the correlations among the most obvious spectral properties. Previous studies had come to conflicting conclusions about things like whether radio-loud and radio-quiet quasars had different spectral characteristics, whether FeII was stronger in objects with narrower emission lines, etc. There was the need for a comprehensive study of a well-defined sample. Our study of 87 objects was about as large as we could manage with the instruments available at that time. The two novel things that we did were (1) to figure out a way to measure and remove the very complex FeII spectrum so that we could make good measurements of the other features and (2) to use a mathematical technique called principal component analysis to try to make sense of the entire ensemble of measurements. The results of that study showed that much (though not all) of the range of measurements could be grouped into two sets of linked correlations, which we termed eigenvector 1 and eigenvector 2.

When Richard and I began that project, I had the naive hope that we would find a set of correlations that would not only account for all variance but would be interpretable in terms of obvious physical parameters, black hole mass, and accretion rate, for instance. Looking back, I think it is more surprising that we found correlations that accounted for even a significant fraction of the variance. I think that one reason that these correlations are not as few and simple as we would like is that the processes and the number of parameters is large. A second reason is a bit like the difference between weather and climate; we see continuum fluxes change,

lines change shape, and even appear and disappear over timescales that correspond to short-lived events. These changes may mimic long-term changes, or they may look different, but in either case, they add “noise” to the variance of properties, and to the extent that they do not mimic the long-term changes, they add noise to the correlations as well.

Another caution to keep in mind is that principal component analysis is a purely mathematical technique; there is no physics involved. All it does is create a new set of “properties” that are (a) linear in the original properties, (b) orthogonal, and (c) represent the largest fraction of the remaining variance. There is no guarantee that the eigenvectors correspond to single physical parameters that can be identified. One consequence of this is that different samples or different methods will turn up somewhat different sets of properties as the first eigenvector. This is seen in a dramatic way in studies that have done “spectral” principal component analysis, in which the properties are replaced by the actual spectral pixels. Since many more pixels are representative of the behavior of the continuum than of the lines, the variation of continuum shape will seem to be more important in explaining the variance. Also, sample selection effects will affect the outcome of PCA. A luminosity lower limit translates to a lower limit on accretion rate, but some properties may be driven more directly by that rate expressed as a fraction of the Eddington limit, which is proportional to black hole mass. Thus, for objects with relatively low-mass black holes, the lower Eddington fraction objects will be excluded. These sorts of sample selection effects will determine which observed properties dominate the variation in any given sample, and thus will determine the precise outcome of a principal component analysis.

Another difficulty is the precision of the measurements themselves or the “purity” of the property that one has chosen to measure. Of course, there is noise in the measurements, especially in cases where the measurement process is complex. For instance, the procedure that we used in the BG92 paper was to first subtract the FeII emission and then subtract the narrow component of $H\beta$ before measuring the full width at half maximum (FWHM) of the broad $H\beta$ line. Every step has an uncertainty, and in particular, the FeII subtraction and the narrow $H\beta$ subtraction were done by a subjective technique, in which we determined the best result by when it looked smoothest. Then, there is the choice of measuring the FWHM as the property to characterize the line width. As the broad lines have various shapes (which perhaps even change in a systematic way with other properties), the FWHM may be an imperfect way to characterize the true line width, but the degree to which it is imperfect will be different in different objects. This will add scatter to the correlations.

Is it reasonable or useful to regard correlation diagrams between properties involved in, e.g., the first eigenvector, as surrogate H–R diagrams for quasars? How and why might that analogy with the stellar H–R diagram break down?

The Hertzsprung–Russell (H–R) diagram is a two-dimensional graph in which stellar luminosity or absolute magnitude is plotted on the ordinate and stellar temperature or color or spectral type is plotted on the abscissa. It demonstrates the relationship between two easily measured characteristics of stars (brightness

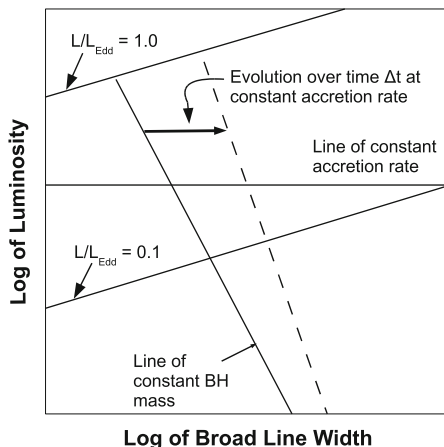
and color) and the two most fundamental physical parameters, mass and age. It is calibrated through models of stellar structure and stellar atmospheres, and it is verified (and was discovered) through the fact that clusters of stars represent an ensemble with a common age and distance. That is, only one parameter, mass, varies from object to object.

I have spent a lot of time thinking about what would correspond to an H–R diagram for quasars. The stellar H–R diagram comes about as a result of the simplicity of stellar structure and the gross behavior of stellar properties. It is notable because (a) an ensemble of coeval stars with a range of mass occupies a well-defined locus, and (b) a single star of a given mass moves along a well-defined track with time. Moreover, these two fundamental parameters—mass and age—express themselves in distinct ways in the H–R diagram. The fact that the two axes of the H–R diagram, luminosity and temperature in the theoretical regime, turn into two observables that are easy to measure—(absolute) magnitude and color—in the observational regime, is an additional benefit, but not essential. The implication of the simplicity of the behavior of stars in the H–R diagram is that there is relatively little coupling between these gross properties and all the other “minor parameters” such as spin, abundances, or magnetic fields that also affect the structure and appearance.

Our model of the processes that produce the objects that we call quasars has a lot of potential complications compared to stars. First, we have more properties that might be important. Specifically, we have a black hole with a mass and a spin. We have accretion of material, which has a rate and a geometrical structure. The material may have motion that we characterize as infall, outflow, rotation, and turbulence. Those motions, as well as the geometric structure, change with radial distance from the black hole and may also be different for different accretion rates. And worst of all, we see these processes at a large range of radii, not just at an outer spherical surface, as is the case for stars. Similarly, the observables of quasars appear to be much more complex and variable than those of stars. We have luminosities and SEDs that vary over many timescales. We have broad and narrow emission lines over ranges of widths and strengths, both relative to each other and to the continuum or in an absolute sense. We have host galaxies and radio sources with cores, jets, and lobes. Finally, we have only a very simplistic view of how the properties and the observables are linked. All of this makes the potential utility of an H–R-like diagram for quasars both very large, but the likelihood that such a thing exists very small.

What would an H–R diagram for quasars look like? Let us start with a theoretical approach involving just the two most important physical parameters. These are arguably black hole mass and accretion rate. We know that the luminosity of a quasar is proportional to its accretion rate, and that its black hole mass is proportional to a function of luminosity and the width of its emission lines. Thus, we can construct a very simple, conceptual diagram (Fig. 3.2) that relates two observables—luminosity and line width—to two fundamental physical parameters—black hole mass and accretion rate. However, this approach has three obvious drawbacks. First, all we have done is represent the known relationships with lines in a plot; the plot does not tell us anything that the formulae did not. Second, although some regions might be

Fig. 3.2 A simple H–R diagram for quasars based on a theoretical perspective. This diagram uses known relationships to define a space in which one could predict how different points would be related in terms of fundamental physical parameters



excluded, we do not expect that real quasars are restricted to a well-defined locus; it is not apparent that you could find any kind of “sequence” using this diagram. Third, we have only included luminosity and line width. When we explore the characteristics of quasars, these represent only a small fraction of the variation from object to object.

Alternatively, we can take an empirical approach. A different way to think of an H–R diagram is that it is a plot in which objects measurements fall in a well-defined and limited region and that it shows separation between objects that we classify as distinctly different—think red giants and white dwarfs. Classification tends to be based on the characteristics that show the most obvious variation within a set of objects. This perspective relates most directly to the principal component analysis approaches, including both the BG92 study discussed above and the work that Sulentic, Marziani, Dultzin, and collaborators have done over the past 10 years. These studies have found the correlations between observed characteristics of quasars and the relationships between those correlations. For instance, their 4DE1 (four-dimensional eigenvector 1) space has axes that represent broad-line width, relative strength of the Fe II emission lines, soft X-ray photon index, and the velocity shift of the broad C IV line from its systemic location. Shown in Fig. 3.3 is one projection of that space onto the first two axes [499, 577]. Measurements of individual objects with different radio properties are plotted as different symbols in this diagram. It can be seen that the objects concentrate in a sequence that drops from the upper left and then extends to the right along the bottom and that there is some separation between the different radio types. This approach, too, has obvious drawbacks. First, we have not produced a diagram in which the locus of object measurements is highly constrained. It is clear that to do that, our diagram would have to have many more dimensions, and even so, it would be unlikely to account for all the variance (see discussion above). Second, we do not know what this sequence represents in terms of real physical parameters.

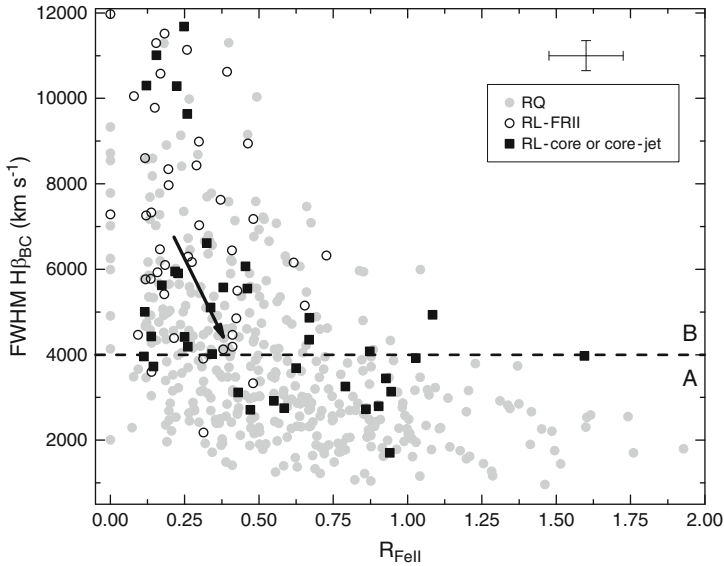


Fig. 3.3 The optical plane of the 4DE1 populated by $N \sim 470$ bright SDSS quasars, based on data from [499, 577]. The two populations A and B are separated at $4,000 \text{ km s}^{-1}$ for clarity. The vector indicates the shift in median (x,y) position between RL-FRII and RL-CD sources; estimated 2σ error bars are displayed for both axes. This is an empirical approach to an H–R diagram for quasars. Note that objects are confined to a limited region, and objects with different radio properties are somewhat separated

Part of the problem is that we do not have a sample in which variation is limited to a single property, as star clusters are for stars. Abundances and age are approximately uniform in a cluster; only mass is a variable. Similarly, theorists have been quite successful at making models of stellar interiors and stellar atmospheres and producing isochrones, tracks in which the mass is a constant but the age changes. If we could define a sample in which all objects had the same black hole mass, accretion rate, or orientation, perhaps we could learn something from these plots.

Probably, we will not uncover anything so useful as an H–R diagram for quasars, but the efforts to understand the correlations between observable properties and their relationships to the physics is a good way forward.

The above eigenvector discussion focused on properties of the broad lines. However, type-1 quasars also usually show a narrow-line spectrum as well, including the well-studied $[\text{OIII}]\lambda\lambda 4959, 5007$ lines near $H\beta$. Type-2 AGNs show only narrow lines. Are there differences in the narrow-line properties of radio-quiet and radio-loud sources? Do all low z type-1 AGNs show narrow lines? Do luminous high z quasars show narrow-line properties similar to those

of the low-redshift AGNs? How can one exploit narrow lines to improve our understanding of BLR structure and kinematics?

Actually, the eigenvector analysis did include narrow lines as well as broad lines. One has the impression that the narrow lines are simpler because the broad lines have such obvious dispersion in their line profiles, but the narrow lines are almost as complex. They are often asymmetric and offset from their systemic position, indicating that we are seeing effects of radial motion and nonuniform obscuration. There is also the likelihood that some fraction of the narrow-line emission—especially the lower ionization level lines—comes from processes other than the quasar. Excitation by hot stars and shocks (including those driven by radio jets) can enhance the narrow-line emission produced by the excitation by the nonthermal continuum.

I have long had the impression that the most luminous radio sources have stronger [OIII] lines than other quasars. There are a few exceptions; 3C 273 comes to mind, but that is a compact flat-spectrum radio source, and so its true, isotropic luminosity is unknown. Now that I have looked at spectra of a lot more objects, though, I think that it is just that the weak (narrow-)lined objects are missing from the luminous radio sources. The radio-quiet objects range all the way from objects like PG1700+518 in which the [OIII] is vanishingly weak to objects like PG1427+480, which has very strong narrow lines. This difference, however, has not been quantified with a large well-defined sample, and this study could be done now with the SDSS DR7 quasars.

Almost all type-1 quasars show narrow lines. Most of the narrow lines are from forbidden transitions ([OII], [OIII], [NII], [SII]) that only arise in low-density material. This implies two things: (1) the low-density material is further away from the central engine than is the high-density material that emits the broad lines, and (2) there is a large volume of low-density material since many atoms are needed to make strong lines. The correlation expressed in (1) even goes further. In studies of high-resolution spectra of quasars, it is often the case that as one looks at lines of higher ionization level (and/or critical density), one measures larger widths to the lines.

As I said above, the narrow lines are not necessarily simple, just because they are narrow. In many objects, the higher ionization narrow lines show offsets to the blue from the systemic velocity, as derived either from the low-ionization narrow lines or from stellar absorption lines [68, 576]. Also, in many objects, the blue wings of these lines are extended; we see more material moving toward us than away. This means that we are seeing either the front side of an outflow or the back side of an inflow. Since the material is of low density, the outflow explanation is preferred.

So, what is this material? Some of it must be torn off the accretion flow and accelerated outward by radiation pressure from the central engine. However, the bulk of it may be quiescent gas in the interstellar medium of the host galaxy, being excited by radiation from the quasar. The volumes implied by the density limits and the emission-line luminosities correspond to radii of hundreds to thousands of parsecs, and these numbers are consistent with imaging studies of the nearest active nuclei. The line widths are comparable to stellar velocity dispersions in normal

galaxies. This is the basis for using the widths of the narrow lines as a surrogate for stellar velocity dispersions in studies of black hole masses. However, it must be remembered that the shifts and asymmetries mean that some fraction of the emitting gas is coming from an outflow, not material in equilibrium with the gravitational potential.

If a substantial fraction of the narrow-line emission comes from the interstellar medium of the host galaxy, one might wonder about those objects that show no narrow lines. The cause of this is unlikely to be the availability of gas in the galaxy as these objects also have extreme broad-line properties, i.e., relatively narrow broad lines and very strong (broad) FeII emission.

Thank you, Todd.

3.3.1 More on the Importance of Eigenvector 1

Dear Ari (*Laor*), are all quasar broad emission-line spectra basically the same? “The same” would imply that the average of e.g., ten thousand random quasar spectra would yield a composite spectrum (better) representative of the entire type-1 population. The same question might be put to stellar spectroscopists. Can we gain physical insights by indiscriminately averaging OBAFGKM stellar spectra together? One difference between quasars and stars involves evidence that source orientation influences spectra of quasars. If we could correct ten thousand spectra for the effects of orientation, would their average spectrum yield better physical insights or is there too much spectral diversity among the quasars?

AGN spectra change from type-1 to type-2 with inclination, but do the type-1 spectral features also change with inclination? The strongest case for that is the relation of the $H\beta$ FWHM with core to extended radio flux density ratio, R , in radio-loud AGNs [556]. High R value AGNs are interpreted as face-on AGNs. They have $H\beta$ FWHM $< 5,000 \text{ km s}^{-1}$, consistent with a near face-on view of a disk structure for the BLR. However, there is a difficulty with the low R values AGNs. These are expected to provide a side view of AGNs, and the $H\beta$ should generally be broad. The observed $H\beta$ FWHM in low R values ranges from 2,000 to 15,000 km s^{-1} , and they are not preferentially broad, as would be expected for a side view of AGNs. The seminal study of [66] has cast significant doubt on the inclination interpretation. The $H\beta$ FWHM is significantly correlated with a number of emission properties, including the strength of [OIII] and the optical FeII emission, the so-called eigenvector 1 (EV1) correlations. The main problematic point for the inclination interpretation is that there is a sequence along EV1, with radio-quiet AGNs on one end, in particular NLSy1s at the extreme of EV1, then core-dominated flat-spectrum radio-loud AGNs, and at the other extreme of EV1, lobe-dominated steep-spectra radio-loud AGNs. Since RL AGNs are not RQ AGNs seen at different inclination, EV1 cannot be inclination driven. Also, it was later realized that the

$H\beta$ FWHM provides a reasonable estimate of M_{BH} , based on its correlation with the host bulge mass, as in the Magorrian relation, as shown in Fig. 5.5 (Sect. 5.5.1) taken from [290] (see also [334,392]). This correlation precludes a strong inclination effect on the $H\beta$ FWHM, as it will produce a large scatter in the Magorrian relation. Furthermore, we now know that radio-loud AGNs are preferentially more massive, and reside in luminous ellipticals [51,291] which may explain why the most radio-loud AGNs, which tend to be lobe dominant, reach the highest $H\beta$ FWHM. Beamed RL AGNs are intrinsically less luminous in the radio and may tend to reside in less massive BHs. These trends may be responsible for the $H\beta$ FWHM vs. R relation found by [556]. On the other hand, the BLR most likely resides in a thick disk or torus-like configuration, and some inclination dependence for the $H\beta$ FWHM should exist. Various recent studies try to disentangle the mass and inclination effects on the $H\beta$ FWHM, which is also important as a mean to obtain a more accurate estimate of M_{BH} from the $H\beta$ FWHM.

What is the physical property associated with EV1? Since the $H\beta$ FWHM is a major component of EV1, the likely underlying physical properties are M_{BH} and L/L_{Edd} . What is then the physical mechanism which drive the EV1 emission properties? A high optical FeII EW could be driven by a high Fe abundance [34]. A high metallicity has been derived from the NV/CIV line ratio [211], and appears to be associated with a high L/L_{Edd} [465], which may be associated with a high star formation rate in the host galaxy, which produces the high metallicity. Alternatively, there is evidence that the metallicity may be driven by M_{BH} [330,550]. This relation may result from the M_{BH} vs. bulge luminosity relation, together with the observed metallicity–luminosity relation in galaxies. Thus, either L/L_{Edd} or M_{BH} may underlay the EV1 correlations. Apart from the metallicity, there may be other BLR properties which affect the observed emission lines, like mean density, ionization parameter, column density, and non-isotropic emission. The column density may be driven by L/L_{Edd} [162], but there is no clear physical mechanism which can drive a systematic change in the mean density, ionization parameter, or the emission isotropy along EV1.

Thank you, Ari. Variability is a powerful tool to probe the structure of any emitting region. It is a very common property of quasars, and we believe that even all of most luminous quasars, in due time, will be found to be variable. The subject is immense, as variability patterns differ in different wavebands. We refer to the excellent review by Marie-Helene Ulrich and collaborators [524] that collects all major results achieved until the mid-1990s. Here, Mike Hawkins will address the major aspects of variability with a report on more recent results. Later on, Vladimir Pronik and Sergey Sergeev will inform on the photometric monitoring campaigns carried out in Crimea over tens of years. Last, Deborah Dultzin will discuss the most elusive form of variability — microvariability — that however provides valuable information on the accretion processes occurring in nearby AGNs.

3.4 Variability

Dear Michael (*Hawkins*), quasars are variable sources. Can you review the current phenomenology of quasar photometric variability? Which are thought to be the most relevant physical mechanisms behind quasar variability? Are there differences between quasar types? What aspects of the best and most recent variability studies lend support to the standard model? Are there results that are difficult to reconcile with the standard paradigm?

When quasars were first discovered in the 1960s, one of their key defining properties was their variability. Substantial variations in brightness over a few weeks put an upper limit to the size of the emitting region of about one light-month. This, combined with the great luminosity inferred from the high redshift, posed a major challenge to modeling the energy source. The standard model which emerged, including a central supermassive black hole, accretion disk, dusty torus, and broad- and narrow-line emission regions has survived relatively little changed for a number of years now.

After the success of defining the size of the emitting region, it was hoped that variability studies would shed further light on the emission process. Early quasar monitoring programs typically lasted several years and were designed to look for correlations between parameters such as amplitude or timescale of variation with luminosity and redshift. Analysis of light curves of such short duration was made harder by the degeneracy between amplitude and timescale, in the sense that both amplitude and measurements of timescale tended to increase with the length of the survey. It seems fair to say that the only correlation about which there was some consensus among different groups was an anti-correlation between luminosity and amplitude, such that more luminous quasars varied with smaller amplitude. There was, however, some debate over whether this could be interpreted as an anti-correlation between timescale and luminosity, such that luminous quasars took longer to achieve a given luminosity.

A much sought-after correlation was that between timescale of variation and redshift. This effect, known as time dilation, is predicted for an expanding universe and is a fundamental consequence of the Big Bang theory. Observing time dilation is made more difficult by the degeneracy between redshift and luminosity in magnitude-limited samples of quasars. The high-redshift quasars in the sample tend to be the more luminous ones, and so the correlation between luminosity and amplitude could masquerade as a correlation between timescale and redshift. In the event, no convincing evidence emerged confirming the presence of time dilation, and it was clear that larger samples covering a wider range of redshift and luminosity and a longer timescale would be required before further progress could be made.

Over the last 20 years or so, quasar light curves have been studied in considerable detail, and a number of properties have emerged. Firstly, the debate over the correlation between luminosity seems to be settled. The left-hand panel of Fig. 3.4 shows the combined SED for a large sample of light curves from [209]. The SED has a power-law shape toward high frequencies (short timescales) and peaks at a timescale

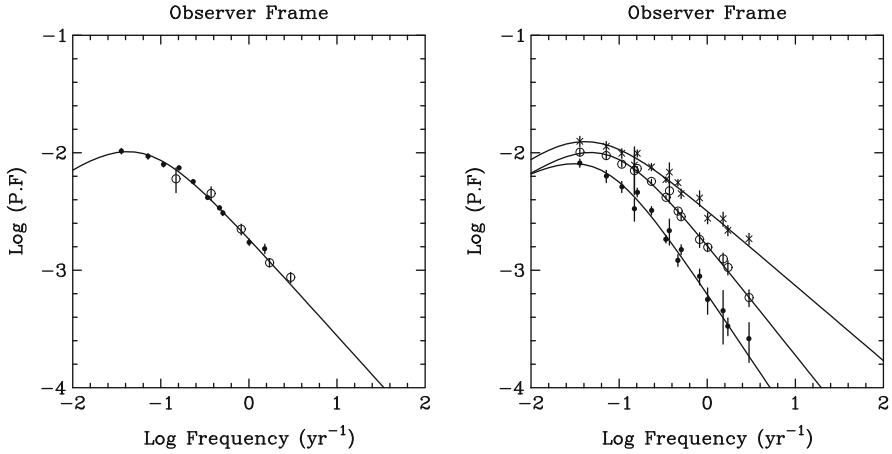


Fig. 3.4 The *left-hand panel* shows SEDs of light curves in the observer frame for quasars from the Field 287 survey (*filled circles*) and from the MACHO project (*open circles*). The *solid line* is the best fit model curve. The *right-hand panel* shows the same data divided into three magnitude ranges. In this case, *filled circles*, *open circles*, and *stars* represent high-, medium-, and low-luminosity bins, respectively. *Solid lines* are fits to the data as for the left-hand panel

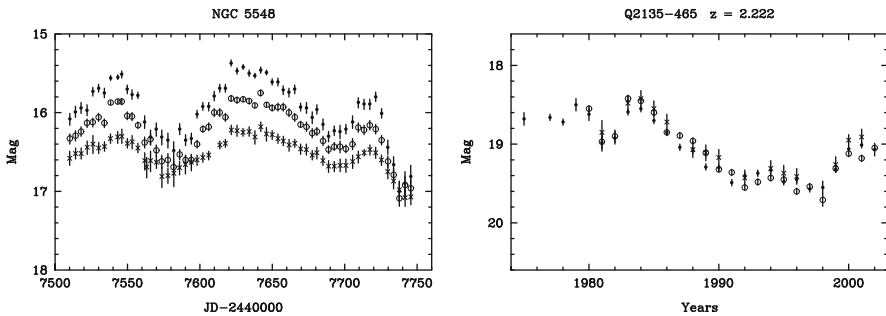
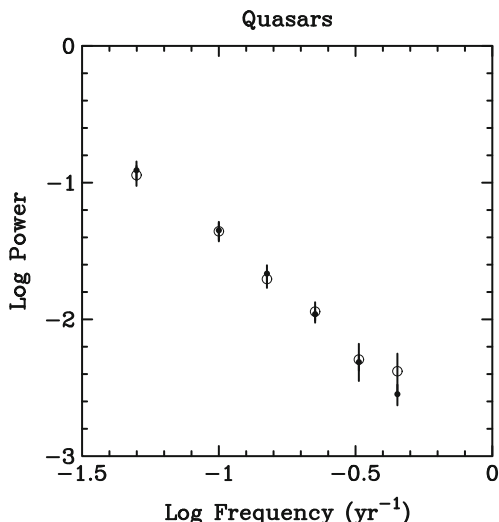


Fig. 3.5 The *left-hand panel* shows continuum ultraviolet light curves for the Seyfert galaxy NGC 5548 from the IUE satellite. The wavelength bands are centered on $\lambda 11350$ (*crosses*), $\lambda 11840$ (*filled circles*), and $\lambda 12670$ (*open circles*). The *right-hand panel* shows optical light curves for a high-redshift quasar from the Field 287 survey. The wavelength bands are *U* (*crosses*), *B_J* (*filled circles*), and *R* (*open circles*)

of around 20 years. The right-hand panel shows the same data split into three luminosity bins, and here we see that at all timescales, there is a decrease in power (or amplitude) with luminosity. This circumvents the degeneracy described above, and establishes that the anti-correlation between amplitude and luminosity is real.

An important diagnostic of quasar variation is the change of color associated with variation in flux. The extensive observations of Seyfert galaxy nuclei as part of reverberation mapping programs have established that as a nucleus increases in brightness, it becomes bluer. This is illustrated in the left-hand panel of Fig. 3.5

Fig. 3.6 Fourier power spectra for a sample of 75 quasar light curves in B_J (filled circles) and R (open circles). The sample limits are $z > 1.5$ and $M_B < -26$

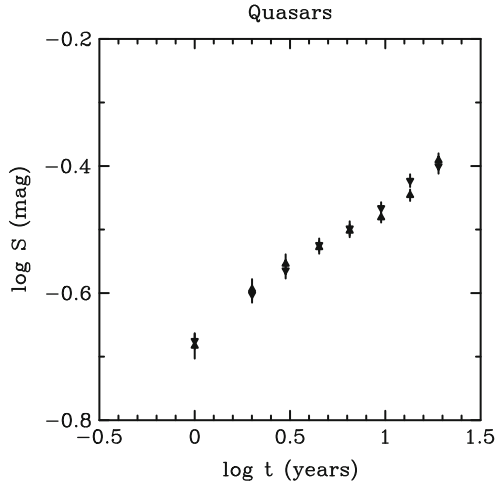


which shows a light curve in three different passbands for the Seyfert galaxy nucleus NGC 5548. For quasars, the situation is more complicated. For most observations of quasar light curves, the light of the host galaxy cannot be separated from the nuclear light, and given that the host galaxies are usually very much redder than the nuclei, there is a tendency for the combined quasar light to redden as the nucleus fades. However, for sufficiently luminous quasars, the nuclear light dominates, and in this case, color changes do not occur, as illustrated in the right-hand panel of Fig. 3.5. This achromatic variation is illustrated for a large sample of luminous quasars in Fig. 3.6, which shows Fourier power spectra for red and blue light curves. It will be seen that the power in both passbands is the same for all timescales, implying no change in color.

An interesting aspect of quasar variation concerns the time symmetry of the light curves. One way to look at this is to ask whether the direction of time can be established by examining the spectrum of variations. Kawaguchi et al. [257] devised a straightforward way to test this using a modified structure function of the light curves, such that the power of increasing and decreasing luminosity could be compared on different timescales. Figure 3.7 shows such modified structure functions for a large sample of quasar light curves, and it can be seen that the power is essentially the same for all timescales implying that within the errors, the light curves are statistically symmetrical.

During the 1990s, three broad mechanisms for quasar variability emerged. Accretion disk instability was perhaps the most straightforward explanation, and considerable effort was put into modeling the statistical properties of the resulting variations. Although most models were not published in a form which could readily be compared to observations of quasar light curves, an interesting exception was the work of [257]. They published structure functions of simulated light curves

Fig. 3.7 Time asymmetric structure functions for a sample of 366 quasar light curves. Functions for increasing and decreasing brightness are shown by upward- and downward-pointing triangles, respectively. The sample limits are $z > 1.5$ and $M_B < -23$



from their cellular-automaton disk-instability model which could be compared with structure functions of observed quasar light curves. The second candidate mechanism for explaining quasar variability was supernova bursts. The idea was that a stochastic series of supernova explosions in the nuclear regions of quasars could produce variability of the type observed. The main problem with this idea is that the large numbers of supernovae needed to make up the average quasar luminosity cannot easily reproduce the size of the variations seen in quasar light curves. The third possibility was that the observed variations were not intrinsic to the quasars, but the result of gravitational microlensing by a population of compact bodies along the line of sight to the quasar.

Kawaguchi et al. [257] concluded that the evidence favored the accretion disk-instability model over the supernova model. Hawkins [222] used structure functions of a sample of several hundred quasar light curves to compare with model predictions and also found that the structure functions from these data did not fit the supernova model. The disk accretion model provided an adequate fit to the structure functions for Seyfert galaxy variations, but for quasars, it did not fit the data, and the microlensing model provided the best fit.

The variability of Seyfert galaxies has been studied in considerable detail as part of the monitoring programs for reverberation mapping. Here, there is no doubt that the nucleus is varying in brightness and that the broad-line region responds to the changes a few weeks later. For quasars, the situation is not so clear, and it seems likely that variation results from both accretion disk instability and microlensing.

One situation where the effects of both disk instability and microlensing can be observed is in multiply lensed quasar systems. In these systems, it is well established that the individual quasar images vary partly synchronously with a short time gap and partly independently. The variations which are seen in both images are taken to be associated with intrinsic variations of the quasar nucleus, and the time difference is a measure of the difference in path length between the two images. With a suitable

lensing model, this can then be used to measure the Hubble constant. In practice, there are a number of difficulties to be overcome in obtaining a reliable value of H_0 . Firstly, the measurement of the time lag is not usually straightforward in the face of poor signal to noise. Secondly, there now seems to be a good case that the time lag is not a constant, presumably due to small changes in the effective path length, and thirdly, the result depends on how accurately the lensing configuration can be modeled. This can be quite a challenge as the lensing galaxy is usually very faint at the high redshift of most quasars, and the dark matter distribution can only be guessed at.

In most quasar systems, the individual quasar images are seen to vary independently, especially over timescales of several years. This has generally been interpreted as being due to microlensing, where the paths to each image are microlensed in different ways. The source of the microlensing bodies has generally been attributed to stars in the lensing galaxy, but the feasibility of this mechanism has not so far been established. If quasars in general are being microlensed by dark matter in the form of compact bodies, then the microlensing seen in multiple quasar systems would be a manifestation of this microlensing.

The mechanism for intrinsic variation in quasars is still surrounded by much uncertainty. If it is assumed that the observed quasar variability is dominated by the intrinsic variation, then any viable model must be able to account for the key properties described above which have been observed in quasar light curves. The situation is made more complicated by the evidence suggesting that these properties are not the same for low-luminosity Seyfert nuclei as for luminous quasars. Although there has been much work on accretion disk instability and the resulting flux variations, it seems fair to say that so far, the models are not able to make predictions for the shape of the SEDs, characteristic timescale, color changes, or time symmetry of the variations which are sufficiently precise to be usefully compared with observations.

There is a case that much of the photometric variation observed in quasars is the result of gravitational microlensing. This mechanism makes reasonably precise predictions about the properties of the light curves listed in the previous paragraph, which broadly coincide with the observations. The area of debate in this case focuses on the population of compact bodies required to produce the microlensing. They must be nonbaryonic and sufficient to make up the dark matter, and there is so far no consensus that such bodies exist.

Thank you, Mike.

3.5 A Photometric Monitoring Campaign

Dear Vladimir (Pronik) and Sergey (Sergeev), what are the main results from the extensive photometric monitoring of AGNs?

Since 2001, CCD BVRI photometric observations of about 50 AGNs, including BL Lac objects, have been made using the AP7p CCD camera at the 70-cm AZT-8



Fig. 3.8 A view of the 70-cm telescope and of the CCD photometer at CrAO

Telescope of CrAO. The observations have been carried out by Merkulova N.I., Doroshenko V.T., Sergeev S.G., and some others. The CCD was mounted at the prime focus ($f = 282$ cm) of the telescope. The CCD array has a size of 512×512 pixels, giving a field of view of “ 15×15 ”. The camera has a set of B , V , R , $R1$, and I filters, where the filter designated $R1$ closely resembles the Cousins I filter and the other filters closely resemble the standard Johnson filters (see [122] for more details). The filters and their positioning system (the wheel with a stepper motor) were manufactured in the CrAO. A general view of the 70-cm telescope and our CCD photometer are shown in Fig. 3.8. The telescope was upgraded in the early 2000s [462]. It has become much easier to control the telescope, and the efficiency of the observations has increased significantly. Photometric monitoring of the AGN sample is intended to study multicolor variability of AGNs and to support spectral observations as well as for concurrent observations in other bands (HST, RXTE, etc.).

Our photometric light curves revealed interband lags between variations in the B band and in the V , R , and I bands for a sample of 14 AGNs. The lag scales with luminosity as $\tau \propto L^b$, where $b \approx 0.4 \div 0.5$ [461]. These results were interpreted in terms of the reprocessing model in which optical emission is mainly reprocessed emission that arises in the accretion disk heated by an X-ray source above the disk. In several more papers, the properties of the optical and X-ray variability of AGNs have been compared [95, 123, 124]. The Crimean photometric data were used to construct a reprocessing model which is able to reproduce the observed optical light curve from the X-ray light curve in Mrk 79 and NGC 4051 [74, 75]. Our data were also used as a support for spectral observations in reverberation mapping studies (e.g., [116, 125, 463]).

Thank you, Vladimir and Sergey.

3.6 Micro-Variability and Its Anecdotes

Dear Deborah (*Dultzin*), the question of quasar microvariability has been around for quite some time with much skepticism surrounding the earliest claims. You are one of the pioneers in this area. Can you give us the current state of our knowledge?

Optical microvariability (OM), also called intranight optical variability (INOV) is defined as minute-to-hour fluctuations in optical brightness with very small amplitudes (typically tenths and even hundredths of magnitude). These variations are now well known to occur—at other wavelengths such as the X-rays but with amplitudes substantially larger (e.g., [409]). Thus, the variations are also called intra-day variability (IDV), as they can be detected at any time. The detection of this kind of optical variability is as old as the discovery of quasars themselves and yet, no one believed in it. I use the word “believe” on purpose because in science, it is often not enough to show something, others have to be convinced as well, and for this to happen, others have to be interested, and more observations have to be pursued (and even allowed to be pursued, meaning having telescope time). I do want to cite textually from a paper by [332] which was way ahead of its time:

Optical photometry of 3C continued sporadically during 1961... The most striking feature of this data is that the optical radiation varies! The only evidence for short term fluctuations is the data obtained on October 11/12, 1961, where the observations listed were made in a time interval of 15 minutes. We believe the observed difference in intensity between these times is probably real because the local standard star D was observed after each of the 3C 48 observations. The differences between the measurements of D were only $\Delta V = 0.007$, $\Delta(B - V) = 0.007$, and $\Delta(U - B) = 0.10$, whereas the 3C 48 differences are $\Delta V = 0.044$, $\Delta(B - V) = 0.053$, and $\Delta(U - B) = 0.24$.

OM was detected right away after their discovery in two BL Lac objects: the prototype BL Lac [421], and OJ 287 [134]. Of course, skepticism continued until [87] reported an OM event in OQ 30 that was observed simultaneously in two observatories. Also, they used CCDs. By the way, I want to notice that we, the extragalactic community, very much tend to reject “old” techniques and consider them inaccurate. Differential photoelectric photometry has been used for decades by astronomers working on stellar variability to detect very small and rapid light fluctuations (typical for example of Delta Scuti-type stars). My colleagues working on stellar photometry assure me that it is even more accurate than CCD photometry. Anyway, these results lead people to believe OM could also be detected in quasars. Further down, I shall address the discussion about radio-loud vs. radio-quiet quasars.

The case for Seyfert galaxies has been even more debatable due to the possible contamination of the underlying galaxy, but mainly due to bad sampling. With respect to the first “problem,” it is often related once again to mistrust on photoelectric photometry although accurate techniques to subtract the possible contamination of the underlying galaxy have been extensively described [126, 312]. Systematic photoelectric UBV observations of rapid variability in AGNs were begun at the Crimean Laboratory in 1986. Optical microvariability was detected in each of the

three galaxies monitored. In the case of NGC 7469, OM was later confirmed by [126], and in the case of NGC 5548 by [311]. Negative results are not reported here. OM in Seyfert galaxies was definitively established by simultaneous optical–infrared–X-ray observations of NGC 4051 reported by [121]. More recent results can be found in, e.g., [339].

Why is OM so important? OM can provide insight into the innermost regions of the AGN. To this day, it is not clear which phenomena are involved, for the moment, let us say it is probably due to instabilities in the innermost part of the accretion disk, in the jet, or both. I will be much more specific below. Optical variability on intra-night timescales was recognized as a well established phenomenon for Blazars (see references above). The relationship of OM to long-term variability remains unclear. Some authors report association to high brightness states (e.g., [227]), others find it associated to flux level transition states (e.g., [127, 312]). Its relationship with color (spectral energy distribution) and radio loudness are also open questions. I shall address recent results [423] below. All of these investigations are crucial to obtain information of the physical processes involved in the emission.

A real technical advancement has been the possibility to correlate OM with fluctuations in other spectral bands, from radio to X-rays. The first reports on optical and radio (e.g., [546]) simultaneous IDV showed that also in radio frequencies, micro-variability is an intrinsic property of Blazars, not due to scintillation. Today, we have results on simultaneous monitoring at radio, infrared, optical, soft and hard X-ray, and γ -ray frequencies, from flares to IDV. Recent observation of 3C 66A [9] show that in order to explain IDV, an external (to the jet) radiation field is needed to produce the inverse Compton scattering.

Now, I want to address a special kind of OM which is particularly interesting as well close to my heart: periodic micro-variations. The first report on periodic OM or rather IDV, as it was reported simultaneously in radio, was for the Blazar OJ 287 [88, 531]. This gives me the opportunity to include a juicy scientific anecdote. I met Esko Valtaoja in the first IAU General Assembly I attended (not even as a member yet) in Petra (Greece). We became good friends almost immediately as he is a very nice person with an incredible sense of humor. As it usually happens, our bond became stronger with collaboration. He gave a talk on blazars, which were relatively recently discovered intriguing objects. He told me about a case where he and his colleagues at Metsahovi radio observatory, who had been monitoring blazars, found evidence of periodic microvariability with 20-min. period. They sent a letter to Nature, but it was not accepted because the referees “doubted the reality of the observations.” I must mention that this object has also long-term variations of very large amplitude also periodic [469, 470] which are attributed to the presence of a binary supermassive black hole in its nucleus. This makes it one of the most interesting objects in the universe and one of the best tests for general relativity [299, 532, 533].

When I came back to Mexico, OJ 287 was in its brightest state: 12th magnitude, and thus it could be monitored even with our 1-m telescope at Tonantzintla Observatory, nearby Mexico City. My only problem was that I had never before done photometric observations. I told my colleague Luis Carrasco, and he was also

interested. We got all the nights we wanted. We monitored all night for weeks, and suddenly, there it was. Even without reduction, the light curve looked periodic. After careful reduction and Fourier analysis, we calculated a periodicity of ~ 15 min. There was no internet at the time, and thus we phoned Esko to Finland: “we found it.” We estimated the size of the innermost boundary of the disk, etc., wrote the paper as quickly as we could and submitted it as a letter to Nature together with our colleagues from Metsahovi who decided to resubmit their earlier rejected letter. This time, referees believed all of us, and both letters were published in the same number of Nature [88, 531]. The anecdote is that Valtaoja and collaborators had sent the first rejected draft to Marek Abramowicz, who immediately wrote a letter to Nature with a model on instabilities in the inner border of a thick accretion disk which could periodically be occulted by the disk itself if viewed at small inclination [10]. The theoretical model was published 3 years before the observations of Valtaoja et al., which were cited as a preprint! And then, there are theoreticians who claim that it is “easy to publish observations” Ha!

Today, our paper has more than 60 citations, 10 of them from the last 2 years. Periodic and/or quasi-periodic OM is a well-established fact with the shortest period reported of 15 min (e.g., [427] and references therein). This kind of periodicity can give us valuable information on the structure of accretion disks. It is also a transient phenomenon, and thus, in order to detect it, you have to look for it. How? By having dedicated small-size (1–1.5 m) telescopes monitoring during many nights and many hours.

The current “state of art” for the origin of OM is amply reviewed in [423, 425] (references therein). For a number of years, there has been a search of OM in radio-quiet quasars (RQQs) in order to compare its incidence in radio-quiet with radio-loud quasars (RLQ). The main purpose has been to identify the source of OM and try to constrain the most probable models: accretion disk and/or jet emission (see e.g., [58, 91, 188, 197, 198, 275, 317, 320, 321, 419]). Recent studies indicate that OM in quasars does not depend on the radio properties of quasars (see [114, 208, 425, 481]). However, the mechanism responsible for OM has not been fully characterized. When I say “in quasars,” I explicitly mean to stress that I exclude blazars. This last consideration is very important, because it has been the source of much debate in the literature. Results have often been biased due to the inclusion of blazars in RLQs samples (see, e.g., [208, 425, 481]).

In a recent paper, Ramirez et al. [423] developed a method to discriminate between thermal and nonthermal processes in the innermost parts of quasars during an OM event, by means of color changes during the event. They show that even in the case of RLQs, the broadband spectral variation may require to assume the presence of a second component, of thermal origin, and vice versa: in RQQs, a nonthermal origin may be required. This result agrees with the discovery of small relativistic jets in RQQs [61]. If a disk–jet relationship exists (e.g., [150]), more complex variations can be produced by perturbations in the disk that are propagated to the jet (e.g., [553]).

In the case of blazars, this study shows that in BL Lacs, some OM events have been detected in which the object turned bluer when it increases its brightness

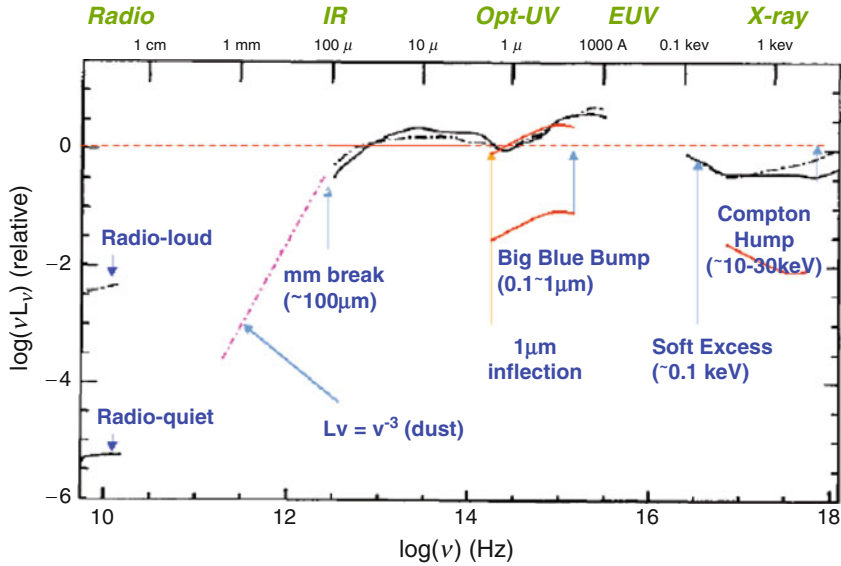


Fig. 3.9 The quasar spectral energy distribution (courtesy of Martin Elvis). Abscissa is frequency in Hertz, ordinate is relative luminosity

(e.g., [99, 237, 376, 404, 480, 537]). These variations should be generated by a non-thermal component (e.g., [184, 237, 328, 421, 530, 537]). On the other hand, the spectral changes in FSRQ seem to be larger than in BL Lac objects, because the latter have not a remarkable contribution from the thermal component [204, 424]. Then, a difference between the two blazar types (BL Lacs and FSRQ) may arise: the thermal component and its influence on spectral changes.

The main recent result is thus the possibility to distinguish between thermal and nonthermal origin of an optical micro-variation event in quasars. Also, the fact that there is not such a clear-cut dichotomy between thermal and nonthermal contributions to the instabilities that produce OM. Recently, Chand et al. [93] have suggested that if the OM is produced by processes related to the jet, then it is expected a smaller FWHM of the emission lines in quasars with positive detection than in those without OM detection. These authors found no such behavior (see also [422]). With respect to blazars, multiwavelength monitoring from radio to γ rays has yielded extremely few data for IDV. However, in order to explain these few events, an external radiation field seems to be required to account for the inverse Compton scattering [9, 434] needed to explain the SED variations.

Thank you, Deborah. We now turn our attention to the multifrequency behavior of quasars. Before considering a detailed discussion of each waveband, a bird's-eye view of the spectral energy distribution (SED) might be helpful to better frame the subject. In Fig. 3.9, we provide the spectral energy distribution of a typical quasar.

3.7 Quasar Spectral Energy Distributions

Dear Dirk (*Grupe*), can you describe a synoptical view of the quasar continuum multifrequency spectrum?

AGNs are really multiwavelengths objects which spectral energy distribution (SED) ranges from the radio to gamma rays. As for the SED in the radio, we distinguish between radio loud and radio-quiet AGNs. This is defined by their ratio of the flux density at 5 Ghz and in the B-band, following the definition by [258]. About 10% of all AGNs appear to be radio-loud. The other parameter typically used to describe the SED of AGNs is the optical to X-ray spectral slope α_{ox} . This spectral slope was originally proposed by Tananbaum et al. [503] to describe the fluxes at 2500 Å and 2 keV. It has been found that this parameter is strongly dependent on the luminosity of the AGNs (e.g., [193, 203, 249, 489, 536, 573, 574]). AGNs with higher luminosity appear to be X-ray weaker. It has also been found by Grupe et al. [203] and Lusso et al. [309] that AGN with higher L/L_{Edd} show larger α_{ox} . In other words, NLSy1s which are typically high L/L_{Edd} AGNs appear to be X-ray weaker than BLS1s.

Which are the major differences between radio-loud and radio-quiet AGN concerning their SEDs?

While generally radio-loud and radio-quiet AGN show very similar SEDs in the optical to X-ray regime, they deviate dramatically at radio and γ -ray energies. While the optical/UV to X-ray part of the SED is dominated by thermal emission from the accretion disk, the radio and γ -ray part of the SED is nonthermal emission from a jet. The radio to UV part of the SED is dominated by synchrotron radiation. Radio-loud AGN are characterized by a high-energy bump in the MeV/GeV range which is caused by inverse Compton and synchrotron self-Compton effects.

Can a reasonable bolometric correction be computed for quasars?

Bolometric corrections are needed to convert a luminosity at one wavelength into the bolometric luminosity. For example, Elvis et al. [132] gave relations with $L_{\text{bol}} = 5.6 \times L_{2500\text{\AA}}$ and $L_{\text{bol}} = 13.2 \times L_{\text{V}}$. For a large number of AGN, not to say for the majority of them, it is impossible to determine the bolometric luminosity directly because large parts of the SED are not observable or too faint. With bolometric corrections, however, the bolometric luminosity of an AGN can be estimated. As we have seen before, one of the most important drivers in an AGN is the Eddington ratio L/L_{Edd} .

As long as we can assume that the general AGN phenomenon is the same for low- and high-redshift AGN, bolometric corrections can be computed for quasars. While the often-used relations given by Elvis et al. [132] are based on nonsimultaneous data, the bolometric corrections given by Vasudevan and Fabian [536] and Grupe et al. [203] are calculated from SEDs based on simultaneous optical/UV and X-ray data taken by *XMM-Newton* and *Swift*. AGN, especially high L/L_{Edd} AGN, is highly variable at all wavelengths. This produces additional scatter in the bolometric corrections if the data are not taken simultaneously.

Obtaining L/L_{Edd} from bolometric corrections is one aspect. The other one is that we can also get an estimate of the black hole masses of high-redshift quasars if we assume that they accrete close to their Eddington limit.

What is the main difference between the bolometric correction for quasars and stars?

While the SEDs of AGN at least in the optical to X-ray regime are somewhat uniform, for stars, this is quite different. Stars have blackbody spectra, and the peak of their spectrum is, according to Wien's law $\lambda_{\text{peak}} \approx 2,900/T \mu\text{m}$, temperature dependent. The peak of the spectrum shifts toward smaller wavelengths (or higher energies) with increasing temperature. In other words, the SED and therefore the bolometric correction of a star depends on its spectral type. For quasars, generally speaking, we do not have this problem. This is why we can apply bolometric corrections that have been found for low-redshift AGN to quasars at high redshift. However, keep in mind that bolometric corrections can be luminosity dependent as suggested by Marconi et al. [319] or as shown by Vasudevan and Fabian [536] the bolometric correction for at least the 2–10 keV luminosity depends on L/L_{Edd} .

Thank you, Dirk. We now focus on the different spectral ranges, starting from the UV range as it is in the quasar rest frame. A major discussion involved one of the strongest lines in that range, C IV. This and other high-ionization lines apparently showed an anti-correlation with quasar luminosity that became known as the Baldwin effect after [30]. The importance of the Baldwin effect stems from a search of line parameters that correlate with luminosity. To find just one would be an enormous feat in quasar astrophysics. However, the Baldwin effect has been a highly contentious issue. We feel obliged to hear two independent opinions on this topic.

3.8 Inferences from the Quasar UV Spectrum

3.8.1 The Baldwin Effect

Dear Martin (Gaskell), in the late 1970s, there were claims of a remarkable inverse correlation between quasar luminosity and C IV $\lambda 1549$ equivalent width. This so-called ‘‘Baldwin Effect’’ was later found for many other lines. The Baldwin effect was originally thought to have cosmological significance. Is that still true?

Since quasars could be seen to high redshifts, it was recognized that it would be a major breakthrough in observational cosmology if a way could be found to calibrate their luminosities. As I have mentioned, Jack Baldwin's 1974 thesis was the first study to use high-quality spectra taken with a detector with a linear response to study a sample of AGNs. It was very highly cited in the 1970s and 1980s. Joe Wampler had wanted Jack to look for luminosity effects, but Jack did not find anything in his

thesis. After Jack finished his thesis, he had a staff position at Lick Observatory for a couple of years before going to Cambridge. During this time, he discovered that the equivalent width of CIV *was* correlated with luminosity. In [156], we called this “the Baldwin effect,” a name that readily caught on. There was a danger that the Baldwin effect was due to a selection effect because faint, weak-lined AGNs could have been left out. Joe Wampler therefore initiated a program of observations of complete homogeneous samples of flat-radio-spectrum AGNs. We confirmed the Baldwin effect for CIV and found a Baldwin effect for MgII [31]. Despite our efforts to avoid selection effects, I had a suspicion at the time that they remained a significant factor in making the Baldwin effect look tighter than it really was. Further observations with larger samples have indeed shown that the scatter is large. In [31], we also made an estimate of the cosmological deceleration parameter, q_0 . I believe this was the first attempt to get q_0 using high-redshift data ($z > 1$). Bill Burke, the Santa Cruz relativist, realized when we were writing the paper that the formulae given in the standard books for apparent magnitudes for cosmological models had all been derived from power-series expansions in z or $z/(1+z)$. The books had not expected observations to be made $z > 1$. So we gave new exact formulae valid for all redshifts.

Our AGN observations favored $q_0 \approx +1$ [547]. However, supernova observations now show that the universe is accelerating, and hence $q_0 < 0$. So where did we go wrong? The problem was, as Kinney et al. [265] showed, that because of the large scatter in the Baldwin effect, attempts to find q_0 diverge to large positive values. (Kinney et al. derive a completely unphysical formal value of over a hundred thousand.). It is possible that the scatter in the Baldwin effect can be reduced, but as Jack Baldwin ruefully put it, this was being done “just in time to be told that cosmology has been ‘solved’ by other types of measurements” [33].

Is the Baldwin effect extrinsic or intrinsic to a quasar?

There have been a lot of ideas about the underlying cause of the Baldwin effect. I think that the safest thing to say at this stage is that the Baldwin effect is not yet understood. The Baldwin effect differs for different lines (FeII, e.g., shows an “inverse Baldwin effect;” [271]). The Baldwin effect is only one of a number of correlations between properties of AGNs discovered from the Lick Observatory spectroscopy of AGNs in the mid-1970s. The high-quality AGN spectra of Don Osterbrock’s group revealed a set of correlations between optical FeII strength, [OIII] strength, line width, and radio properties [395, 396]. This set of correlations is commonly called “eigenvector 1” since they make up the first eigenvector in the principal component analysis of Boroson and Green [66], but the main correlations had all been identified earlier from Don Osterbrock’s group’s data. Steiner [484] showed that there was a strong connection between AGN luminosity, the OIII/H β ratio, and optical FeII strength. Steiner thus showed that the Baldwin effect is associated with what we now call “eigenvector 1.”

The Baldwin effect clearly involves the continuum and the broad-line region. My view over the years has been that to understand the Baldwin effect, the correlations of eigenvector 1, and other correlations, we first needed to pin down the basics of the nature of the continuum emission and the structure and kinematics of the broad-line

region. Once we have those things straight, we have a framework for understanding the various intercorrelations of AGN properties. I think we are approaching that point now.

Thank you, Martin.

Dear Ari (Laor), in the early 1980s, there were claims of a remarkable inverse correlation between quasar luminosity and CIV $\lambda 1549$ equivalent width. This so-called Baldwin effect (BE) was later found for many other lines. It was originally thought to have cosmological significance. Is that still true?

Both cosmology and studies of AGN have evolved significantly since Baldwin's [30] discovery that the EW of CIV decreases with increasing luminosity. We now know that this relation has a much larger scatter than initially thought [394]. More importantly, cosmology is now in the so-called precision era [479], and the Baldwin relation is now completely irrelevant as a distance measurement tool for cosmology.

Is the BE extrinsic or intrinsic?

Since the continuum emission of quasars most likely originates in an accretion disk, it is likely to be inclination dependent. The BLR needs to cover $\sim 10\text{--}20\%$ of the ionizing source sky, it therefore cannot reside in a thin disk, it must form a thicker configuration, and is likely to be more isotropic. As we view an AGN at a higher inclination, the continuum luminosity will go down, but the BLR luminosity will remain constant, thus leading to a decreasing line EW with increasing continuum luminosity, i.e., to the BE [383, 384, 444]. However, there is a significant problem with the inclination (i.e., extrinsic) interpretation. Different lines show significantly different slopes for the EW vs. luminosity relation. The Balmer lines in particular show no BE, and the slope gets steeper with increasing ionization energy (Fig. 3.10, [120, 137]). This rules out inclination, which is a purely geometric effect, as the main mechanism for the BE. A likely significant mechanism is an ionizing SED which gets softer with increasing luminosity (as accretion disk models predict). The NV line is an exception as it shows no BE, despite the high-ionization energy. This is interpreted as a metallicity effect. The increasing metallicity with luminosity apparently compensates for the decrease in the NV producing photons, as the SED gets softer with increasing luminosity. Also, the CIV EW shows a stronger relation with L/L_{edd} [27, 40] and is actually part of the EV1 correlation [500]. A summary of the recent results on the BE is given in [467].

Thank you, Ari. We will now deal with another fundamental aspect of emission lines in quasars. Once the effect of cosmological redshift has been removed (and this is usually obtained measuring the redshift of narrow forbidden and permitted lines), and a quasar rest frame defined, there remain residual shifts between broad lines. These "internal" line shifts have played (and are still playing) an important role in constraining the geometry and kinematics of the emitting regions.

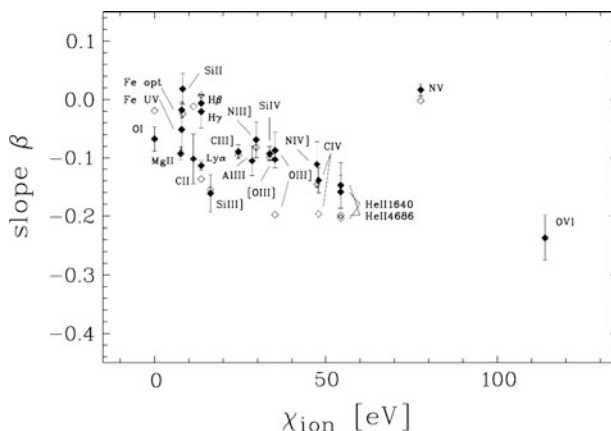


Fig. 3.10 Figure 9 from [120]. This figure shows the slope of the BE as a function of ionization energy of the various detectable lines. The slope gets steeper with increasing ionization energy, suggesting that the BE relation is driven by a softening of the ionizing SED of AGNs with increasing luminosity. Note that the Balmer lines, and other low-ionization lines, have a slope of zero, i.e. they show no BE. The large offset of the NV line suggests the BE is also affected by metallicity and a relation of metallicity with luminosity

3.8.2 Quasars’ Internal Emission-Line Shifts

Dear Gordon (Richards), the line of triply ionized carbon at $\lambda 1549 \text{ \AA}$ has been used by several authors as representative of high-ionization lines. You studied this line in a large sample of intermediate/high-redshift SDSS quasars and found that 75% show profiles that are blueshifted/blue asymmetric. Why are the blueshifts so common? What is the interpretation of the blueshifting of CIV $\lambda 1549$?

It is perhaps best to answer these questions together. Following up on our previous work [438], our current thinking [441] is that the blueshifts are the result of an outflowing component of the broad emission-line region (BELR). Not only are the black holes in the centers of massive galaxies not completely black—their accretion disks shine more than $1,000 \times$ brighter than the rest of their host galaxy, but also instead of swallowing everything in their vicinity, black holes can blow matter *away* from them in the form of an *accretion disk wind*.

The theory of accretion disk winds has a long history [59], but really gained hold in the late 1990s in a series of publications by N. Murray and collaborators [362–364]. This was supported by a phenomenological picture by [133] and further theoretical work by [414], among others. The basic idea is that in the “atmosphere” of the accretion disk, there is partially ionized material, including triply ionized carbon. Many of these atoms have electronic transitions in the UV part of the spectrum. At the radius where emission from the accretion disk peaks in the UV part of the spectrum, there are lots of photons with energies comparable to these

transitions. These photons will excite the electrons in the atoms and as a result, will exert a pressure on the whole atom itself, which we refer to as “radiation line driving.”

The result is that a wind can be blown from the accretion disk in a small annulus where there is sufficient UV radiation to accelerate the atoms in the atmosphere of the accretion disk. This process is very efficient (more than Thomson scattering) so long as the atoms are not completely ionized by high-energy photons from the central engine. If that happens, then there are no electrons left in the atoms to produce radiation pressure from spectral lines. Thus, the wind is sensitive to the ratio of the UV to X-ray continuum, which makes investigations of the relationship between the UV luminosity and the optical-to-X-ray flux ratio, α_{ox} particularly relevant to this discussion [25, 249].

This wind is thought to be optically thin, and those electrons will eventually return to their ground state—emitting UV photons (including C IV $\lambda 1, 549$) in the process. The wind then represents one source of BELR photons. Since the wind has a significant radial velocity (with respect to our line of sight), the mean wavelength of the emission feature is shifted blueward in quasars [178, 557] with a significant wind component of the BELR. As such, the ubiquity of the blueshifts [438, 441, 494] is taken as a sign that most (perhaps all) quasars have a significant wind [178, 301].

Our own work [441] has shown that it may be possible to use the combination of the C IV equivalent width and the C IV blueshift to place quasars along a continuum of wind properties; see Fig. 3.11. Those quasars with SEDs relatively rich in UV photons as compared to the X-ray are consistent with having strong radiation line-driven winds. These objects have large C IV blueshifts but are also weak in C IV overall. This weakness may occur as a result of the wind filtering ionizing photons from the continuum before they strike the outer accretion disk, which we take as the location of a second source of BELR photons [103, 301]. Indeed, quasars that are intrinsically stronger in the X-ray continuum may over-ionize the atoms that would have been in the wind. For such objects, more ionizing flux reaches the outer accretion disk, and the “disk” component of the BELR dominates over the wind component. These objects have very strong, more symmetric C IV lines with little, if any, blueshift.

Is the absence of blueshifts restricted to a particular subset of quasars? Do the radio louds in your sample also show a blueshift/blueward asymmetry?

As can be seen in Fig. 3.12, the blueshifts are essentially ubiquitous. However, very large blueshifts do seem to be restricted to a particular subset of quasars. In particular, we find that large C IV blueshift quasars also have weak C IV emission lines (but not all quasars with weak C IV emission lines have large blueshifts). In [441], we used the behavior of the C IV line coupled with the Si IV, He II, and C III] line complexes to argue that highly blueshifted quasars are consistent with having a weak ionizing SED. This finding is borne out by an examination of the α_{ox} parameter [279, 566], specifically, large blueshift quasars are relatively weaker at X-ray fluxes. These relationships are particularly interesting given the well-known anti-correlation between UV luminosity and C IV EW (the BE [30]) and the

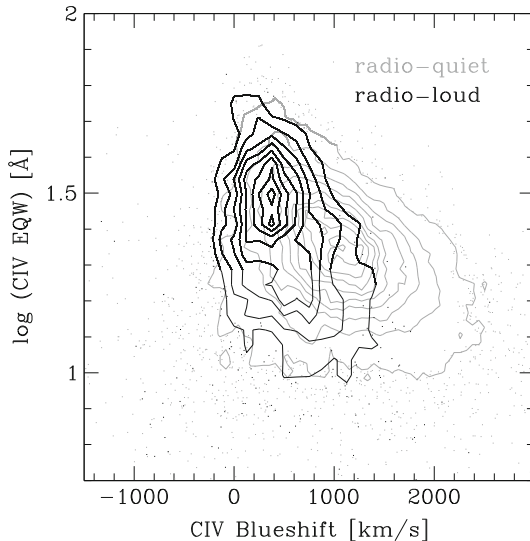


Fig. 3.11 Joint W(CIV)—blueshift distribution for 9438 $z > 1.5$ radio-quiet (*gray contours/dots*) and 593 radio-loud (*black contours/dots*) quasars from the Sloan Digital Sky Survey [458]. Only objects with spectral S/N > 10 are included; heavily reddened quasars are also excluded. Noteworthy are the lack of quasars with both strong lines and large blueshifts and also the relative isolation of radio-loud quasars in one section of the parameter space occupied by radio-quiet quasars. Similar findings have been observed in other lines for low- z quasars [500]

above-mentioned relationship between the UV luminosity and the optical-to-X-ray flux ratio. In particular, high-blueshift quasars appear to be relatively weaker than average at X-ray wavelengths as compared to UV wavelengths. Such a SED is exactly what is needed to produce a strong radiation line-driven accretion disk wind. Although they are also more luminous on average, we find that it must be the shape of the SED and not the overall flux level that is the crucial parameter. Sulentic and collaborators [493, 500], using the “eigenvector 1” parameter [66] space (defined largely by the FWHM of $H\beta$ and the ratio of the FeII EW to the EW of $H\beta$) have termed these objects “Population A” objects. Our work suggests that the most extreme (in terms of CIV blueshift and/or FeII EW) might instead be described as “soft-spectrum” quasars [279].

The radio-loud quasars on the other hand have relatively small blueshifts suggesting that they may have weaker (or no) wind components to their BELRs. Again, we found that an exploration of the SiIV, HeII, and CIII] line complexes revealed that quasars with small blueshift and large equivalent widths are consistent with having a strong ionizing continuum [441]. These objects also have “harder” values of α_{ox} , which is consistent with the X-ray flux over-ionizing the wind and/or insufficient UV flux to drive a strong wind (at least through radiation line pressure). Curiously, we found little difference between radio-loud and radio-quiet quasars in the upper left corner of the CIV EW-blueshift parameter space shown in Fig. 3.11. It may be

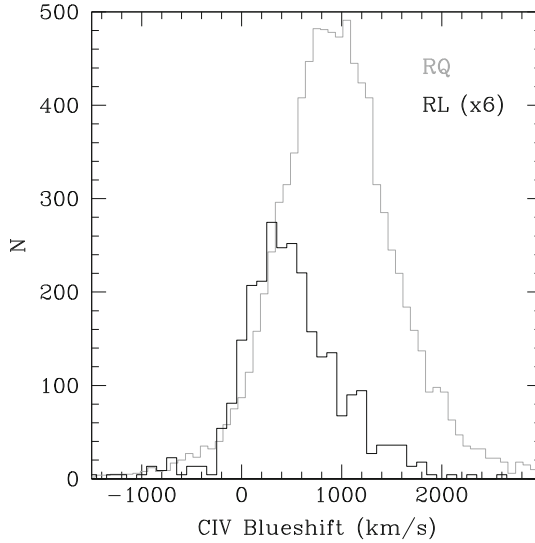


Fig. 3.12 Histogram of C IV blueshifts for the radio-quiet and radio-loud objects in Fig. 3.11. While the blueshift has a luminosity dependence like the Baldwin effect, the vast majority of quasars have their C IV emissions that peak blueward of the expected laboratory wavelength. Even radio-loud quasars, while having much smaller blueshifts on average, are not all consistent with having zero blueshift. It may be then that all quasars have some outflowing (wind) component to their BELRs, but in some objects, radiation line driving is particularly effective and causes significant blueshifts

then that both radio-loud quasars and some radio-quiet quasars have SEDs that are not conducive to driving a strong line pressure wind and instead have a “disk”-dominated BELR. These objects have been designated as Population B [493, 500]; however, could also be considered as “hard spectrum” quasars [279].

Thank you, Gordon. In the next interviews, we will discuss radio observations and the constraints they put on the origin of radio jets. We remark again that the observational abilities in this waveband are nowadays unparalleled in terms of spatial resolution. However, the ultimate origin of radio emission is still an unsolved issue. A related problem is the existence of two quasar populations, radio quiet (but not radio silent) and radio loud. What is at the origin of this differentiation, assuming that we can truly distinguish quasars on the basis of their radio-to-optical power ratio?

3.9 Radio Properties of Quasars

Dear Raffaella (Morganti), if human eyes were sensitive to radio waves, we would see a very different sky. The strongest sources would be powerful

extragalactic radio sources like Cen A, Pic A, and Pers A. that are kin to radio-loud quasars.

Radio emission is one of the many manifestations of an active nucleus, and it is also an ideal tracer for pinpointing AGN at high redshift (see review [343]). Historically, AGN have been divided in radio-loud and radio-quiet (although not necessarily radio silent) based on the ratio between the radio emission at 5 GHz and the optical flux in the B-band (see [258]). The reason for this dichotomy is still a matter of debate: as you will read through this chapter, the dilemma between nature and nurture is certainly still unsolved. It is probably worth repeating here that radio-quiet objects include Seyfert galaxies and radio-quiet quasars where most of their radio emission is confined to the inner kpc of the host galaxy. Members of the radio-loud group include BL Lac objects, radio galaxies, and radio-loud quasars, and they will be the main focus of this conversation. So, how radio AGN relates to the other type of nuclear activities covered by this book? To first order, one can at least say that the most radio-loud AGN are typically host by early-type galaxies, and for some of these galaxies, radio emission is the only sign of activity from the nucleus. Thus, the radio view of AGN is essential if one wants to get a complete picture of the nuclear activity.

Can you please review the typical radio morphologies of AGN and of quasars? Are there differences in the corresponding optical spectroscopic properties?

For low radio powers (i.e., for radio-quiet objects, $P_{1.4\text{GHz}} < 10^{22}$ W/Hz), the radio emission can be originated by either nonthermal synchrotron radiation from the AGN or synchrotron radiation from relativistic electrons accelerated by supernova remnant and free–free emission from HII regions, therefore probing recent star formation or a combination of all this [104]. This can be a source of confusion and problems as it is often not straightforward to separate these different contributions. The presence of radio jets, and the presence of nuclear radio emission unresolved on the parsec scales or radio fluxes deviating from the far-IR–radio correlation [104] are all signatures of radio emission connected to an active black hole. For example, in the case of Seyfert galaxies, we know that, although they can have a complex structure on large scale, they often show radio jets [176], suggesting the coexistence of radio emission tracing star formation in the host galaxy and a radio AGN. Many Seyfert galaxies contain compact nuclear radio components with brightness temperatures $\gg 10^7$ K (see the extensive work of, e.g., [360, 526], and they harbor compact components moving in a jetlike structure typically showing nonrelativistic motion, unlike their more powerful cousins (e.g., [342, 528] and references therein). The inner region of the well-studied Seyfert galaxy NGC 4151 is shown in Fig. 3.13 and clearly illustrates the presence of radio jets, although not so collimated and well defined as in more powerful radio sources (see below).

But why are the radio sources in Seyfert galaxies small, weak, and slow compared to those in radio-loud objects? Various answers to this question have been proposed (see, e.g., [342]), involving either “intrinsic” differences in the central engine or “extrinsic” differences in the surrounding medium. The structure and the subrelativistic velocities of the jet components may be related to the galactic

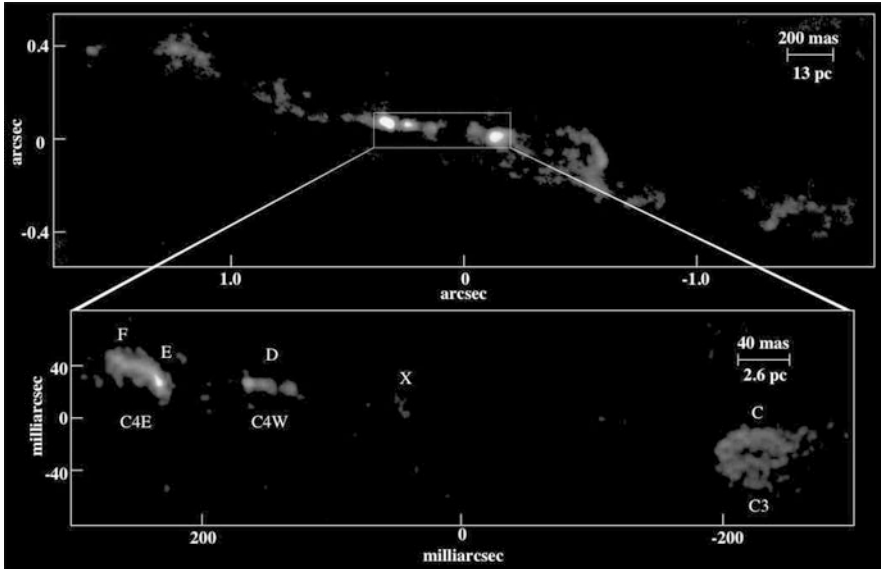


Fig. 3.13 This figure has been taken from the detailed study of the Seyfert galaxy NGC 4151 by [361]. The *upper panel* shows the inner part of the jet (about 3 arcsec in length) imaged with a resolution of 25 mas (1.6 pc). The *lower panel* shows a zoom in of the structure of the jet at higher resolution (5 mas corresponding to 0.33 pc or 1.1 lt-year). More details about the components labeled in the figure can be found in [364] and [526]. The jet appears less collimated and defined than those in powerful radio galaxies, compare, e.g., with Fig. 3.15

environment, with Seyfert galaxies mainly being hosted by spiral galaxies where even initially relativistic jets can be affected by a rapid deceleration by collisions in a dense surrounding broad-line region or ISM. Intrinsic differences include lower masses or spins of the central BH or differences in the characteristics of the jet. It has been proposed that the jets in Seyfert galaxies, unlike the collimated relativistic jet in radio-loud sources, could be formed by buoyant plasmons that bubble up through the density gradient of the narrow-line region, or they have a larger thermal plasma fraction.

At higher radio power (above $P_{1.4\text{GHz}} \sim 10^{23}$ W/Hz), the radio is undoubtedly dominated by emission produced by the AGN. The fraction of galaxies that host radio-loud AGNs in this range of radio power is a strong function of stellar and black hole (BH) mass, reaching up to 30% of early-type galaxies being radio loud for stellar masses $5 \times 10^{11} M_{\odot}$ [51]. This is different from what found for optical AGN and suggests a difference in the way these two kinds of activities are triggered and fueled ([51] and references therein).

While considering the occurrence of radio-loud AGNs, one should not forget that their radio emission can be a recurrent phenomenon in the life of their host galaxy. The typical lifetime for a radio source is estimated, from spectral index considerations, to be relatively short (10^7 – 10^8 year). However, in a number of cases

(see [448] for a review), relics of radio emission are observed (e.g., in the form of diffuse, low surface brightness, and steep-spectrum radio emission), likely due to previous activity. Although we do not know what are the exact conditions that make the restarting of the activity possible, the existence of some cases suggests that perhaps a large fraction of early-type galaxies may actually have gone through a radio phase in the past (see also [51]).

In connection with this question, we ask what are FRI and FR II radio galaxies? Why is FRI radio morphology so rare among broad emission line type-1 quasars? How are FRI and FR II radio galaxies likely related?

Although a signature of the presence of an AGN is the detection of jets, the morphology of a radio source associated to galaxies and quasars can be quite varied. In the 1970s, Fanaroff and Riley [154] introduced a simple distinction in two morphological types. This classification separates the extended radio sources on the basis of where the brighter part of their radio emission is located. Edge darkened Fanaroff–Riley type I (FRI) have bright jets rising from the nucleus, becoming fainter as they expand farther away from the core, and ending up in plumes or diffuse low surface brightness lobes (see Fig. 3.14). Reality is, unfortunately, more complicated than this. It can already be seen in the two examples given in Fig. 3.14 that very different types of sources exist under the classification FRI. Edge brighter Fanaroff–Riley type II (FR II) have typically faint (or invisible) jets that end in bright hot spots, representing the interaction between the jet and the interstellar medium (see Fig. 3.15 for an example). Diffuse lobes are visible around the jets. The interesting result that [154] pointed out is that this classification actually corresponds to a separation in radio power around $P_{480\text{MHz}} \sim 10^{25}$ W/Hz, with the FR II galaxies being the most powerful one, while FRI represent the “low-luminosity” end of radio-loud objects.

The reasons for the differences in the morphological properties of the radio emission between FRI and FR II sources are still a matter of debate. Also, in this case, as for radio-quiet vs. radio-loud objects, both intrinsic differences as well as differences in the interaction with ISM/IGM have been proposed and explored. The effects of interaction between the radio source and the ISM are clearly seen in some young radio sources. This suggests that already, the first phase in the life of a radio source can be crucial for its evolution. Indeed, not all the sources that we see in their initial stage of activities are likely to reach their maturity in an FRI or FR II extended radio source (see, e.g., [118] and references therein). However, the different relation between radio source and properties of the AGN at other wavelengths (see below) suggests that some intrinsic differences must play a role. Thus, the separation may be due to differences in the properties of the central supermassive black hole (SMBH), e.g., accretion rate, accretion mode, or black hole spin [44, 508].

Following the work of [154], other differences between the two classes of sources were pointed out. From optical spectroscopy, it is clear that the majority of FRIs have low-ionization spectra with weak emission lines (e.g., [82, 428, 505] and references therein, see also Fig. 3.16). Furthermore, the study of obscuration toward the central regions of these galaxies (in particular, the lack of X-ray absorption and



Fig. 3.14 Two examples of sources classified as Fanaroff–Riley type I. It is already clear from these examples the broad variety of morphology even inside this class. Images courtesy of NRAO/AUI. *Left:* 3C 31, Investigator(s): R. Laing, A. Bridle, R. Perley, L. Feretti, G. Giovannini, and P. Parma. *Right:* Fornax A, investigator(s): E. Fomalont (NRAO), R. Ekers (ATNF), W. van Breugel and K. Ebner (UC-Berkeley). Radio/optical superposition by J. M. Uson

the frequent presence of optical cores; see, e.g., [35, 216, 563] and refs therein) has shown that the nuclear disks—if present—in these galaxies are geometrically and optically thin. This suggests that the *standard pc-scale geometrically thick torus is not present* in these low-luminosity radio galaxies. For the FR II sources, the

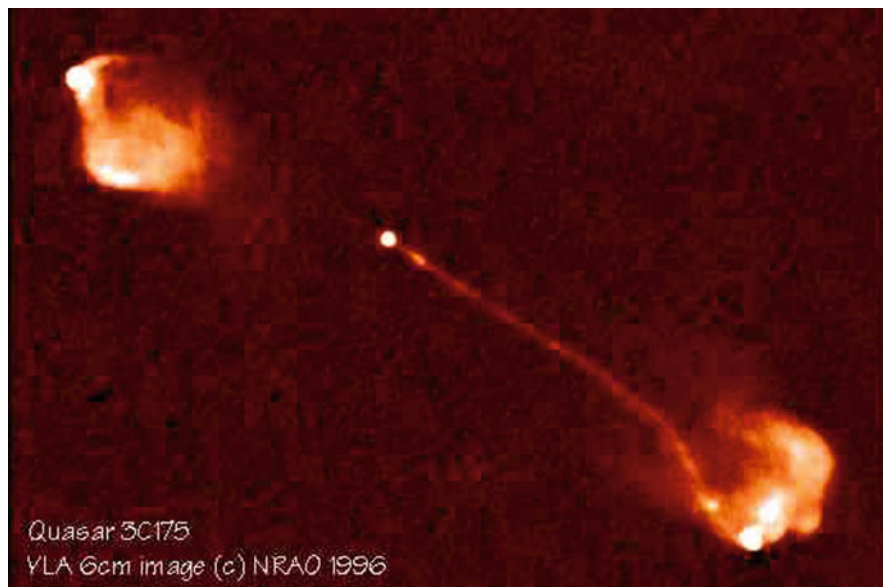


Fig. 3.15 An example of Fanaroff–Riley type II radio emission from the quasar 3C175, the overall linear size of the radio structure is about 200 kpc, note the highly collimated main jet and an almost invisible due to Doppler boosting, counter-jet. Image courtesy of NRAO/AUI, Investigator(s): A. Bridle, D. Hough, C. Lonsdale, J. Burns, and R. Laing

situation is less defined: in most cases, they show strong, high-ionization lines as well as a clear correlation between luminosity of the lines and radio power [506]. However, a substantial group of FR II galaxies have “low-excitation” emission lines. Because of this, the separation is now often made on the basis of the optical lines (high- and low-excitation radio galaxies, HERGs and LERGs, respectively; see [82, 217] and references therein) instead of the radio morphology.

The differences mentioned above suggest that not all the AGNs (in particular, radio sources without strong emission lines like FRIs or the LERGs) can be explained with the conventional picture in which the accretion of cold matter onto the central supermassive BH proceeds via an accretion disk that provides the radiation field to photoionize the broad- and narrow-line regions. A possible explanation for these differences is that HERGs are powered by cold gas accretion (e.g., provided by a recent merger), with the cold gas flowing to the central region of the AGN (see [225]), while LERGs are fueled by accretion of, e.g., hot gas in a radiatively inefficient way (i.e., via Bondi accretion; [18, 36, 110, 217]) as shown for central cluster galaxies. The high temperature of this hot gas would prevent the formation of the “cold” structures (e.g., the broad-line region and the torus). This hypothesis would explain the non-detection of broad lines in the vast majority of LERGs and also their X-ray properties. If this is the case, one may have to consider some revision in the unified scheme model that seem to work quite well for powerful radio galaxies.

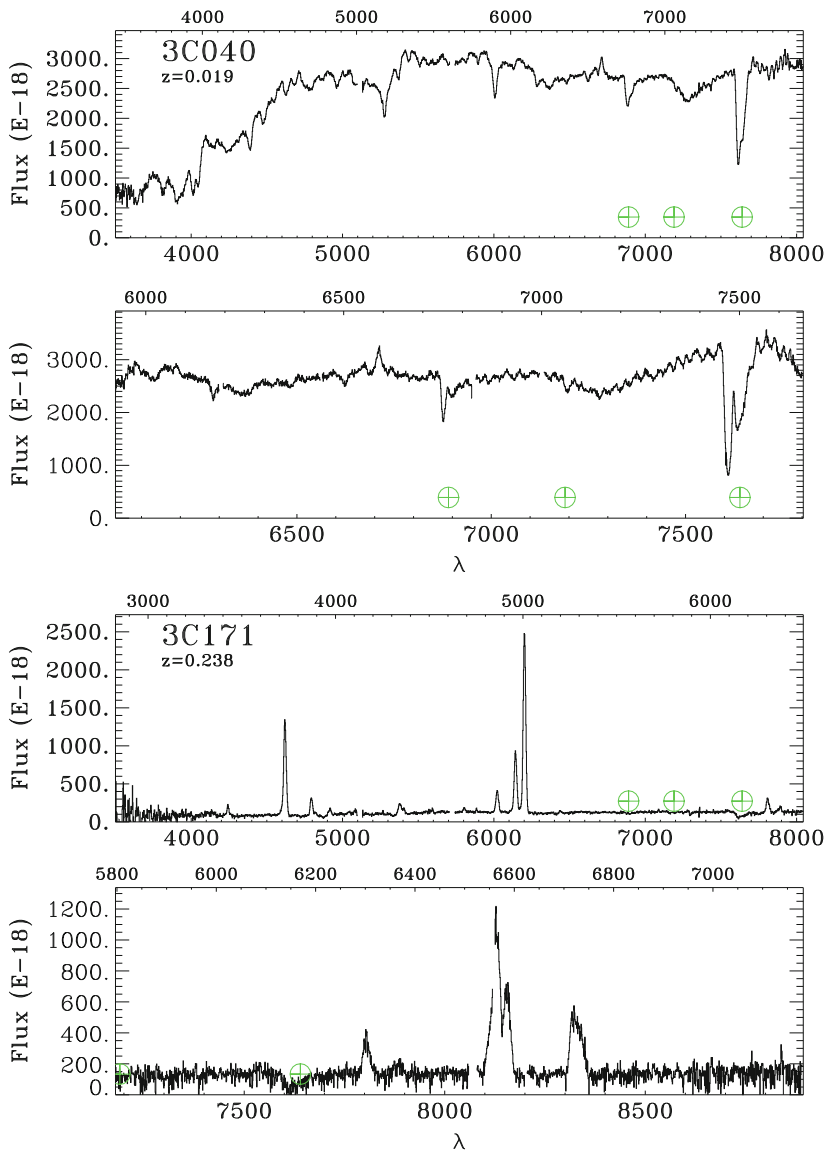


Fig. 3.16 Example of the difference in optical spectra between LERGs and HERGs (3C 40 and 3C 171, respectively), taken from [82]

Whether cold gas can also provide a source of fuel, it is still unclear but see the case of NGC 315 [357]. It is known since the work of [225] that sign of merger/interaction are found in the majority of the FRII radio galaxies if deep images are available. A more recent work has shown that interaction and merger cannot be excluded also for FRI although this appears present in a smaller number

(27%) compared to the large fraction (85%) of FRII [426]. Thus, this is consistent with the suggestion that the former are more commonly fueled by Bondi accretion of hot gas but, in a nonnegligible number of FRI gas can also be accreted. The study of [426] is also showing that the fueling is happening at different stages of the merger. This, of course, further complicates the quest for the origin of the morphological dichotomy.

3.9.1 Radio Variability and Its Implications

Dear Aleksander (Volvach), what are the main results from the extensive campaign of radio observations carried out at the Crimean Astrophysical Observatory?

Radio flux variations in AGN over various timescales (decades to a year) were analyzed using long-term monitoring data at five frequencies from 4.8 to 36.8 GHz. Spectral analysis of the flux curves reveals the presence of periodic components. These data are used to construct kinematic models for AGN using values for the orbital and precessional periods of supermassive black hole binary systems [544].

Second, a model for the energy release in AGN that is not associated purely with accretion onto supermassive black holes was proposed. As is the case for other active members of the AGN family, estimates of the lifetime of the binary black hole system in 3C 454.3 suggest that this object is in a stage of its evolution that is fairly close to coalescence. The energy that is released as the companion of the central black hole loses orbital angular momentum is sufficient to explain the observed AGN phenomena. The source of primary energy release could be heating of the gas behind shock fronts that arise due to the friction between the companion black hole and the ambient gaseous medium. The orbit of the companion could be located at the periphery of the accretion disk (apocenter) associated with the central body and plunge more deeply into the accretion disk at its pericenter, inducing multi-wavelength flares. The proposed model assumes omnidirectional radiation of the medium in the presence of a magnetic field. The radiation corresponding to the minimum flux level (base level) could represent omnidirectional radiation due to the orbit of the moving companion. The fraction of the energy that is transferred to jets is small, comprising 1–2% of the total energy released from loss of orbital angular momentum by the companion [542].

We proposed a model of localization of emitting regions in the jet at different wavelengths during the development of flare phenomena that identifies the developmental delay effects between different wavelengths. The dependence of delay phenomena in flares from gamma to radio bands, which obeys a logarithmic law and saved from flare to flare, are installed. The companion orbital period in a black hole binary system, the duration of flare phenomena in optical and radio wavelengths, and the characteristics of the ionized medium around the central region of AGNs are estimated [545].

The observational data are used to construct kinematic models for AGNs using values for the orbital and precessional periods of binary systems consisting of supermassive black holes. The derived speeds of the companions in their orbits lie in the narrow range 3,000–4,000 km s⁻¹. The orbital radii for the binary black holes also lie in a narrow range, 10^{17±18} cm, providing evidence that observed prominent examples of AGNs are fairly close binary systems. The parameters of the medium in which the components of the binary systems are moving are estimated, as well as the rates at which the systems are losing orbital angular momentum and their lifetimes to coalescence [544]. The combined analysis of integral flux density variations and milliarcsecond scale structures was performed for radio sources. It is found that for a number of sources, the flux density bursts at high frequencies are not accompanied by emerging new VLBI jet component, while for some objects, the flux density changes occur quasi-simultaneously at different frequencies, and the bursts are accompanied by new (ejected) VLBI components. Observations of a sample of sources from the preliminary “Radioastron” space mission catalogue were obtained on the RT-22. We have plotted the log $N - \log S$ dependence down to flux levels of about 0.1 Jy using the survey data around 22 GHz, where there is reduction in the density of cosmological sources in relation to not evolving Euclidean universe [543].

Thank you, Aleksander.

3.9.2 Radio Jets

Dear Raffaella (*Morganti*), radio jets have been known since the first days of quasars. Subsequently, superluminal motions were discovered in many of the jets associated with the radio-loud quasars. How many superluminals are now known? Please give us a summary of their properties.

The study of radio jets has concentrated on a number of aspects that are worth to be mentioned here. Apart from the study of the superluminal motions, the structure of jets in low-power FRI radio sources is another aspect that I think should be considered here together with the results from very high-resolution observations (high-frequency VLBI) that are starting to disclose the structure at the base of the jet, just a few Schwarzschild radii from the BH. The study of jets has also benefited from a major improvement in the quality and availability of data at high energy (like X-ray (*Chandra* and *XMM*) and more recently, γ -ray *Fermi* data, see [5, 564]).

There are significant differences between the structures of the jets in FRI and II sources. The jets in FRI sources often flare close to the nucleus and have large opening angles, whereas their equivalents in FRII sources are highly collimated out to the hot spots [73]. Jets in FRI are initially relativistic but decelerate on kiloparsec scales. The relativistic motions of jet knots on kpc scales have been observed in a number of cases, e.g., M 87 and Cen A. This regime is followed by

a rapid deceleration that occurs over distances of 1–10 kpc. It is likely that FRI jets decelerate as a result of entraining matter, either by injection of mass lost from stars within the jet volume or by ingestion of ambient gas from the surrounding IGM via a mixing layer (see [285, 286] for an overview).

FRII jets are also spectacular objects. They remain relativistic until they terminate, which assume that the jet flows are essentially laminar. Kellermann et al. [260] summarized the efforts done so far by the main multi-epoch programs to trace evolution and speed of these jets. After many years of monitoring, there are now more than hundred cases of well-studied jets for which their evolution and velocities have been followed (see the reviews of [260] and [322]). An example of superluminal jet that has been monitored for 12 years is shown in Fig. 3.17 (from [322]). One of the largest collection of jet followed up with multi-epoch VLBI observations has been presented in [304]. They derive that the observed maximum speed distribution is peaked at $\sim 10c$, with a tail that extends out to $\sim 50c$.

However, as summarized in [260], a number of issues complicate the analysis of the jet speed, including the fact that features do not remain stable with time but may break up into subcomponents, while other features may merge into a single complex feature, e.g., [250].

The bright knots that appear to move superluminally down the jets (see, e.g., Fig. 3.15) must represent regions of higher relativistic electron density and/or magnetic field compared to the ambient jet. Although these structure could represent “blobs” of turbulent plasma with electrons accelerated, the explanation most favored is that they are coherent structures, such as propagating shock waves caused by surges in the energy density or velocity injected into the jet at its origin near the central engine (see [322]). Interestingly, quasars detected by *Fermi* in γ -ray have significantly faster apparent jet speeds and higher core brightness temperatures than undetected quasars [272, 305].

One of the main open question in AGN is what are the conditions that give rise to the formation of radio jets. The best way to address this is via VLBI observations at high frequencies, able to achieve a very high spatial resolution. Although very challenging, they are now starting to give impressive results. These observations are necessary to studying jet acceleration and collimation on sub-parsec scales. The most accepted theory is that the formation of AGN jets by magnetic fields threading an accretion disk around a supermassive black hole (SMBH). The resulting jet structure is expected to show a large opening angle near the base and tighter collimation on larger scales ([338] and references therein). The most impressive case is the jet in M87 (see [310] and references therein) shown in Fig. 3.18. This observation indicates that the jet must form within 30 Schwarzschild radii of the black hole with an opening angle of at least 60° .

To conclude, it is perhaps relevant to mention that radio astronomy is going through a “*new golden age*” with a number of new facilities being constructed or upgraded. Some of the radio studies of AGN are now limited by the sensitivity and/or field of view of present-day radio telescopes, and this will change dramatically in the near future. Actually, it is already changing now. For example,

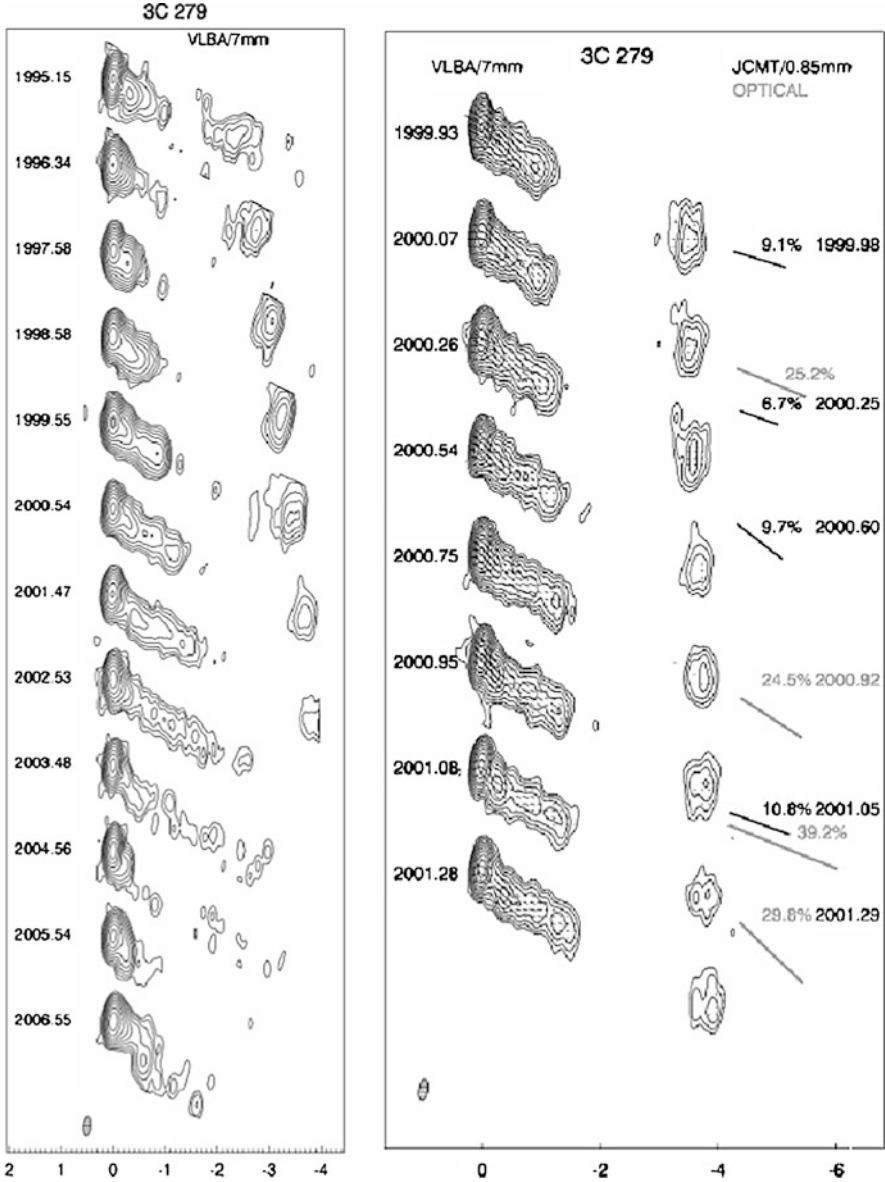


Fig. 3.17 Twelve-year sequence of annual VLBI images of the quasar 3C 279 at 43 GHz taken from [322]. At the redshift of the quasar, 1 mas = 6.3 pc. The feature at the narrow end of the jet, closest to the supermassive black hole, is referred to as the “core” and is assumed to be stationary. The motion of the outlying knot has an apparent superluminal speed of $\sim 10 c$. Note the change in direction of the innermost jet with time

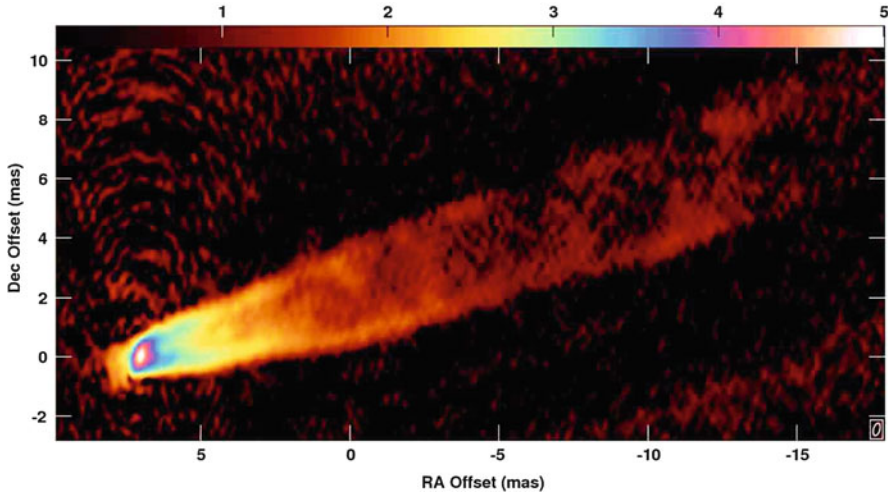


Fig. 3.18 Image courtesy of NRAO/AUI (see also <http://www.aoc.nrao.edu/~cwalker/M87> and [310]). VLBA image at 7mm (43GHz) of the very central regions of the jet in M 87. This image shows that M 87s jet is formed within a few tenths of a light-year of the galaxy’s core. In the formation region, the jet is seen opening widely, at an angle of about 60 degrees, nearest the black hole, but is squeezed down to only 6 degrees a few light-years away (0.43 by 0.21 mas, at the distance of M 87: 1 mas = 0.078 pc)

the upgrade of the EVLA already promises us unprecedented sensitivity for radio continuum.

Furthermore, the Low Frequency Array (LOFAR, [447]) that is now coming on-line and operates between 10 and 200 MHz, will allow detections of relic structures (perhaps also in galaxies that are not currently radio-loud), thus providing insight on the duty cycle of radio activity. All this will offer great opportunities for the study of AGN (both radio loud and radio quiet), their distribution in redshift and their properties, e.g., the presence of gas, etc. Furthermore, the picture of low-radio-power AGN is getting even more confused as radio telescopes become more sensitive and fainter radio sources are detected, the investigation of faint AGN is becoming more elaborated (see, e.g., [400] and references therein).

Ultimately, the Square Kilometer Array (SKA, [295]) will provide a major step forward by allowing a complete census of, e.g., H I in radio sources (including the weak ones), detailed studies of the kinematics of the gas close to the nucleus, with the possibility of looking for outflows in weaker sources [358].

Thank you, Raffaella.

3.9.3 Radio Quiet and Radio-Loud

Dear Sebastian (Zamfir), how does one objectively define a radio-loud quasar?

There is no unique definition of a radio-loud (RL) quasar currently adopted by researchers. A couple of zero-order criteria are employed in the literature to assign a quasar the status of “radio loud.” The first one is based upon the radio power (e.g., the luminosity $L(6\text{cm}) > 10^{25} \text{ W Hz}^{-1} \text{ sr}^{-1}$; [344]); the second one is geared by a radio/optical flux density ratio (e.g., $R_K \equiv f(6\text{ cm})/f(B - \text{band}) > 10$; [258]). It is still an open question whether one criterion is more relevant or more justified than the other. While some argue in favor of the radio luminosity as a more fundamental discriminator (e.g., [344]), others favor a measure that relates the radio to other energy regimes output and offers in some sense a scaling of nonthermal and thermal mechanisms at work within the quasar. The adopted definition should always be determined by and adapted to the specific outline of the problem one addresses. For example, if the goal is to search for a (statistically) bimodal distribution of sources in a radio-loudness measure then R_K may be more troublesome when the samples are flux-limited in both optical and radio.

We also point out a few other cautionary aspects mostly pertaining to the potential choice of R_K as a defining criterion for quasar radio loudness: (1) in the literature, there are various surrogate definitions of R_K involving on one hand radio measures at wavelengths other than 6 cm and on the other hand, optical i-band, UV, or even X-ray measures (e.g., [239, 246, 247, 488, 509, 548]); (2) R_K tends to be luminosity dependent ($R_K \sim L^{-0.5}$; [292]), and a fixed radio-loud/radio-quiet (RL/RQ) boundary of $R_K = 10$ (proposed by Kellermann et al. [258] for luminous samples $M_B \sim -26$) may not be a valid choice for lower luminosity sources (e.g., [233]); (3) the quantitative distinction RL/RQ should not be evaluated on R_K alone but should rather be based on R_K as a function of Eddington ratio [471]; (4) different nominal R_K limits should be considered for radio steep- and radio flat-spectrum sources [149]. Thus, not only do we see a complicated framework for comparing different studies, but we also could face the conundrum of qualifying the same object as RL based on one criterion/definition and as RQ when judged by an alternate measure.

A significant improvement to the definition of an RL quasar is provided by incorporating the classical radio morphology as a criterion. Double-lobed Fanaroff–Riley (FR II; [154]) radio morphology is typically associated with broad-line emitting quasars, while Fanaroff–Riley I (FRI) morphology is very rare among such broad-line emitters (e.g., [61, 226]). Thus, the FR II’s should be considered the parent population of RL quasars (e.g., [37, 244, 393, 455, 507]), which is also supported by the recent confirmation that the shape of the luminosity functions of FR II radio galaxies and RL quasars are basically the same [306]. Sulentic et al. [496] thus consider that the radio-weakest FR II sources should determine the empirical boundary between RL and RQ quasars: $\log[L(6\text{ cm})] > 32 \text{ erg s}^{-1} \text{ Hz}^{-1}$ or alternatively $R_K > 70$. More recently, Zamfir et al. [577] find that the radio-weakest FR II quasar corresponds to $\log[L(1.4\text{ GHz})] \sim 31.6 \text{ erg s}^{-1} \text{ Hz}^{-1}$ by cross-correlating a large sample of bright Sloan Digital Sky Survey (SDSS) quasars with NVSS (NRAO VLA Sky Survey¹) and FIRST (Faint Images of the Radio Sky

¹ <http://www.cv.nrao.edu/nvss/>, see also [106].

at 20 cm^2) radio surveys. Core-dominated (CD) RL sources are interpreted as FRII sources seen along the jet’s axis (e.g., the simple orientation–unification scenario summarized by [529]. Figure 3.3 (based on the data from [577] and shown on page 110 within the contribution of Todd Boroson) shows a clear separation between FRII sources and the CD RL’s within the optical plane of four-dimensional eigenvector 1 parameter space (4DE1; [325, 326, 493, 494, 500]); median FWHM($H\beta$) is $6,750 \text{ km s}^{-1}$ for FRII’s and $4,400 \text{ km s}^{-1}$ for CD’s, respectively. This difference can be interpreted as a manifestation of source orientation (see also [67, 117, 445, 496]). The CD counterparts of any FRII population would be, on average, more radio luminous due to relativistic boosting effects (e.g., [37, 244, 393, 455]).

What is the current best evidence for a phenomenological boundary between radio-loud and radio-quiet quasars?

Although a clear boundary between RL and RQ active galactic nuclei (AGN) is still elusive, there are clear phenomenological differences between the two classes of objects:

- Spectroscopic studies of quasars in the 4DE1 seem to clearly indicate that RL quasars occupy a restricted regime within the optical plane FWHM($H\beta$) vs. $R_{\text{FeII}} \equiv W(\text{FeII } 4570\text{\AA})/W(H\beta)$ compared to most RQ quasars (see Fig. 3.3). The large majority of RL quasars belong to the so-called Population B that show FWHM($H\beta$) $> 4,000 \text{ km s}^{-1}$ [496, 577]; however, we should note that Population B is a mixture of RL and RQ quasars, very similar to each other in terms of optical spectra alone. Still in the context of the 4DE1 space [27], compare the UV C IV $\lambda 1549\text{\AA}$ emission line (HST spectra) in subsamples of RL and RQ sources that occupy the same bin within the optical plane FWHM($H\beta$) vs. R_{FeII} , namely, $4,000 \text{ km s}^{-1} < \text{FWHM}(H\beta) < 8,000 \text{ km s}^{-1}$ and $R_{\text{FeII}} = 0 \div 0.5$. They find an excess of narrow-line components and redshifted C IV broad emission line in the RL subsample. Similar conclusions regarding the broad emission lines are also found in [438] (based on composite SDSS spectra) and most recently [418] (and references therein).
- The report of Punsly [418] presents a significant correlation between the spectral index from 10 GHz to 1350\AA and the amount of excess luminosity in the red wing of the broad C IV emission line for RL quasars, but not for RQ sources. They also find that RQ quasars tend to show an excess of blueshifted C IV profiles (e.g., [41, 79, 324, 500, 557]), probably associated with an accretion disk [327], but RL sources tend to show a red excess in the C IV broad emission line. The distribution of C IV asymmetry is in fact bimodal. This excess is tied to the presence of a powerful jet and seems increasingly dominant as the observer’s line of sight approaches the jet’s axis and the radio core emission appears to dominate. A similar conclusion is presented by [578] relative to the $H\beta$ broad emission line (see their Fig. 19).

²<http://sundog.gtsci.edu/>, see also [47].

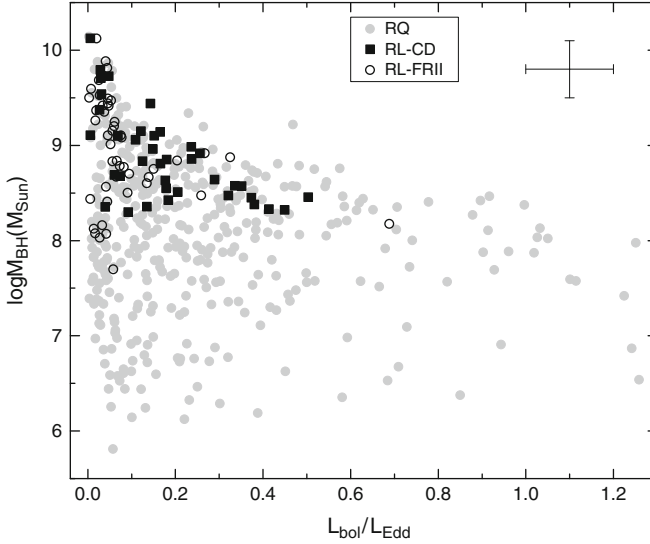


Fig. 3.19 Considering the same sample as in Fig. 3.3; RL FRII and CD are shown together with the RQ quasars in the plane defined by BH mass and the Eddington ratio; estimated 2σ error bars are displayed for both axes

- Using $\text{FWHM}(\text{H}\beta)$ and optical continuum luminosity measures around 5400\AA to estimate black hole masses M_{BH} [253, 255] and Eddington ratios (which involve bolometric and Eddington luminosities, $L_{\text{bol}}/L_{\text{Edd}}$), one can clearly see again a restricted domain for RL quasars compared to RQ sources (see Fig. 3.19 based on SDSS quasars from the sample used in [577]): (a) RL quasars are found only above $M_{\text{BH}} = 10^8 M_{\odot}$ (with a strong concentration in the range $3 \times 10^{8-9} M_{\odot}$; see also [326, 498], and (b) Eddington ratios $L_{\text{bol}}/L_{\text{Edd}}$ are less than 0.3 for most RL quasars. The majority of RQ quasars generally show smaller values of M_{BH} and larger values of $L_{\text{bol}}/L_{\text{Edd}}$ (e.g., [67, 128, 326, 335, 341]).
- Steep-spectrum RL quasars show no evidence for polycyclic aromatic hydrocarbon (PAH) emission, either in individual or averaged spectra [174]. Moreover, *Spitzer* observations of powerful Third Cambridge Catalogue (3CR; [284]) of radio galaxies and quasars show only weak or undetectable PAH emission [98, 214, 390, 466], indicative of a very low level of star formation compared to quasars from Palomar-Green (PG; [459]) and Two Micron Sky Survey (2MASS; [112]) samples (only 18% of 3CR quasars/radio galaxies show detectable PAH emission compared to 40% in the PG and 2MASS quasars at $z < 0.5$). RQ quasars tend to follow the radio–far infrared (FIR) correlation [213, 280, 478], which is driven by star-formation processes.
- Optical analysis of nearby AGN [84, 85] shows that virtually all RLs are hosted by giant core ellipticals (i.e., elliptical galaxies whose surface brightness profile shows light deficit in the nuclear region relative to the extrapolated outer radii profile; [270]). RQ AGNs reside in less massive, coreless ellipticals (i.e.,

elliptical galaxies whose surface brightness profile shows light excess in the nuclear region relative to the extrapolated outer radii profile; [270]). A recent report [212] reinforces these findings from a different direction. It suggests that a combination of accretion rate and host scale determines whether a given elliptical galaxy could host a RL or a RQ quasar. The high X-ray luminosity ($L(0.5keV) > 10^{44.5} \text{ erg s}^{-1}$) sources tend to be RL, while among the low luminosity ones, only the larger ones (half-light radius in optical light $r_e > 10 \text{ kpc}$) are RL, the rest being RQ. The $r_e = 10 \text{ kpc}$ appears to be similar to the boundary between core and coreless elliptical galaxies.

These empirical results may provide substantial support that the RL and RQ quasars are tied to different evolutionary paths of their hosts (mergers, interactions, etc.).

Do we see a dichotomy? Irrespective of whether a real dichotomy exists, should we see a dichotomy?

In the literature of the last 10–15 years, one can find a large array of results regarding a dichotomy for *RL/RQ* quasars. Studies of large samples of SDSS quasars reveal a bimodal distribution of sources in terms of radio/optical (UV) ratios [239, 552]. White et al. [552] find a significant dip at $R_K \sim 30\text{--}40$ (see their Fig. 15), after the luminosity dependence of R_K is being taken into consideration. A similar conclusion is proposed by [307] from the distribution of orientation-corrected R_K measures for a smaller and heterogeneous sample of quasars. They find a *RL/RQ* separation in the region $\log(R_K) = 1.5\text{--}2.0$. On the other side, there are numerous studies that challenge the reality of a bimodal distribution in radio-loudness measures (e.g., [80, 96, 97, 149, 283]). Some authors propose the existence of a radio-intermediate (RI) population that bridges the gap between RL and RQ sources.³

The apparently contradictory results regarding the dichotomy are not a surprise considering (1) the lack of a unified or standardized definition of a RL quasar coupled with (2) the luminosity dependence of R_K (e.g., [292]), (3) the inherent use of radio and optical flux-limited samples of sources which leads to unavoidable selection biases, and (4) the fact that the fraction of RL sources is a strong function of redshift and optical luminosity (e.g., [196, 235, 246, 344, 399, 405, 538]). Any direct search for a quasar *RL/RQ* dichotomy involves some kind of luminosity dependence, thus one faces the aforementioned pitfalls.

Sampling only the bright end of the quasars’ optical luminosity function (e.g., [70, 109, 439, 440]), an *RL/RQ* dichotomy is apparent even in luminosity-dependent diagrams (e.g., L_{bol} vs. $L(1.4\text{GHz})$ in Fig. 6 of [577]). The two populations seem to follow separate correlations. However, the inclusion of fainter quasar samples allows also for an increasing number of RQ sources that fill the initially evident

³Zamfir et al. [577] define a population of RI quasars with $\log[L(1.4\text{GHz})] = 31.0 - 31.6$ ($\text{erg s}^{-1} \text{ Hz}^{-1}$) in order to test whether they show a restricted domain occupation in the optical plane $\text{FWHM}(H\beta)$ vs. R_{FeII} of the 4DE1 space. Their conclusion is that RI and RQ sources are statistically indistinguishable.

separation between RL and RQ sources, effectively quenching the dichotomy (see Fig. 7 of [577]).

In order to circumvent such strong luminosity effects, one must be able explore a potential dichotomy in a context that has no obvious dependence on radio properties and no dependence on source luminosity. 4DE1 parameter space has these advantages (e.g., [326, 493, 497]). As we mentioned before, such an analysis yields hints that the dichotomy is real, RL sources occupying a restricted domain of the optical plane $\text{FWHM}(\text{H}\beta)$ vs. R_{FeII} compared to the majority of RQ quasars. Nonetheless, 4DE1 does not remove entirely the degeneracy between RL and RQ Population B sources. Other physical parameters may play a key role, among which the properties of the host galaxy (mentioned previously; see also [471]), the environment (e.g., [256]), the BH spin (e.g. [27, 177, 337, 356, 508, 541, 560]), and accretion mode [248, 267, 268, 313].

Thank you, Sebastian. This issue has been hotly debated in the last several years, so that we think it proper to hear a second opinion, the one of Heino Falcke and Elmar K rding.

Dear Heino (Falcke) and Elmar (K rding), a subject of considerable debate over past years involves the possibility of a dichotomy in properties between radio-loud and radio-quiet quasars. Do you think that there is evidence for a dichotomy? How does one objectively define a radio-loud quasar? What is the current best evidence for a phenomenological boundary between radio-quiet and radio-loud quasars? Do we see a dichotomy? Even if RL and RQ are fundamentally different, should we see a dichotomy?

Quasars, quasi-stellar radio sources, were initially identified, thanks to the precise localization of their radio emission [223]. Only a little later, one realized that in fact the majority of quasars was radio quiet [453]. With more and more radio observations, it seemed as if the radio-to-optical ratio in quasars had a huge spread, and it was discussed whether or not the radio distribution was bimodal (e.g., [105, 149, 155, 258, 490]), see Fig. 3.20. Where does this come from? This question is still with us today, and only slowly can we begin to unravel that mystery while the community is still far from agreeing on a consensus.

An important realization in the early days of radio astronomy was that the radio emission in radio-loud quasars (RLQs)⁴ was due to a pair of highly collimated, relativistically expanding plasma flows, dubbed “jets.” This term goes back to the optical linear “ray” first discovered in M 87 by Curtis [111] (page 31). Baade and Minkowski [26] associated this feature with the newly discovered radio emission in the source, calling it a jet. The structure in M 87 then served as an example to understand the extended radio structure in radio galaxies like Cygnus A and others [218, 388, 558] as an outflow (the “twin-exhaust model” [56]), where the

⁴Note, that given the original meaning of the term “quasar”, the term “radio-loud quasar” is actually a tautology, but we will use it nonetheless given its widespread use.

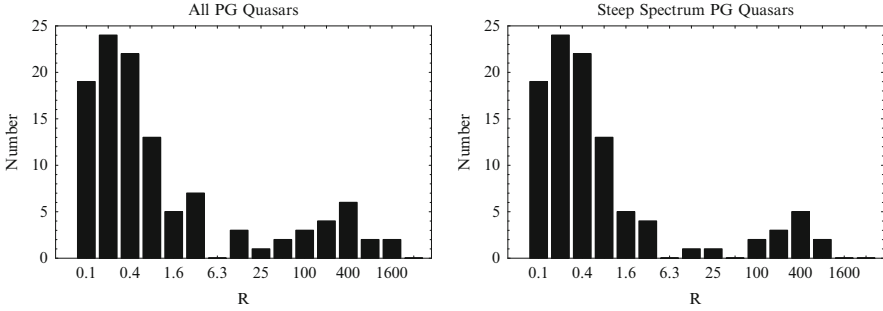


Fig. 3.20 Distribution of the radio-to-optical ratio R for the extensively studied and optically selected PG quasar sample (*left*). The *right panel* is for a subsample where the flat-spectrum sources, which are likely affected by relativistic beaming, are removed. Sources with $R > 10$ are typically considered radio loud, while for $R < 10$, they are typically radio quiet. Flat-spectrum sources around $R \sim 10$ are considered radio intermediate. Figure taken from [149]

big radio lobes were supplied by particles, magnetic field, and energy from a central source [454]. High-resolution very-long baseline interferometry (VLBI) observations then quickly revealed apparent superluminal motion indicating the relativistic nature of these jets (e.g., [60, 101, 456]). This then led to the relativistic jet model by Blandford and others [48, 58]. Hence, the bright radio emission in radio galaxies and quasars was readily understood as jet emission [77], and RLQs and radio galaxies were understood as being the same thing seen from different angles [37].

In the following, unified schemes became very successful [22, 529]. This sorted the zoo of active galactic nuclei (AGNs), of which quasars are an important part, into interrelated classes. However, until today, these schemes are unable to unify radio-loud and radio-quiet objects in simple terms, i.e., there are standard unified schemes for radio-loud and radio-quiet AGNs, but there is essentially no accepted scheme to unify radio-loud with radio-quiet AGNs. Whatever the final solution is, it will have to do with jets, and here, the first question to ask is: are jets in radio-loud objects just stronger or are they completely absent?

Fortunately, the last statement can easily be ruled out. Seyfert galaxies have been considered radio-quiet objects, but like radio-quiet quasars, they are not void of radio emission. Numerous studies of the radio emission in Seyferts have revealed structures akin to collimated outflows ([152, 342, 360, 525, 527, 528] to name just a few). Those outflows strongly interact with the hot gas in the narrow emission-line regions (NLRs) of these AGNs (e.g., [86, 152]) and hence carry collimated kinetic energy. A qualitatively similar picture has been found in radio-quiet quasars [302], and one can find that the power and size of the radio emission as well as the luminosity and size of the NLR [49] increases with the bolometric luminosity of the AGN. In those terms, radio-quiet quasars simply seem to be the more powerful versions of Seyfert galaxies and are not fundamentally different. There is even evidence for relativistic motion and beaming in so-called radio-intermediate quasars

(RIQs) [81, 151]. These are quasars which lack the powerful extended lobes of RLQs, but whose radio core emission is significantly enhanced over those of RQQs. They have been interpreted as beamed radio-quiet sources.

Hence, while it is, of course, always possible that there is also a contribution from star formation in the radio emission of RQQs (e.g., [259, 365, 475])—and sometimes it is difficult to separate the amorphous extended emission of Seyfert-like jets at low resolution from a star-formation region—RQQs and Seyferts are certainly not completely jet-less. This is further supported by the existence of similar radio variability in RLQs and RQQs [39].

What are the main causes for the different jet power?

A preciser question to ask is then: if not the complete absence of jets, what is then the cause for the different types and strengths of jets in RQQs and RLQs? This requires one to understand the basic parameters that drives the evolution of jets.

One commonly quoted parameter that is suspected to drive radio loudness is the spin of the black hole (e.g., [471]). The most compelling observational fact in favor of this scenario is that radio-loud quasars and radio galaxies seem to occur almost exclusively in elliptical galaxies, while radio-quiet AGNs are mainly (but not exclusively) found in spiral galaxies [28, 212]. Wilson and Colbert [560] argued that this is due to the fact that black holes, in ellipticals are rapidly spun up due to mergers. However, for stellar mass black holes spin does not seem to be quite so important for radio loudness [159], and the equation “elliptical = radio loud” may also have to do with black hole mass [335], at least to some degree.

Another important piece to the puzzle of jet efficiency was added in the 1990s when it was realized that jets cannot be viewed independently of their accretion disks. In the standard quasar model, their optical and UV emission is produced by emission from an accretion flow onto the supermassive black hole. That emission also leads to the appearance of the broad and narrow emission lines, seen, e.g., in optical spectra. It was then found that there is a relation between the radio emission and the optical flux [43]. Rawlings and Saunders [428] translated this into a correlation between disk luminosity and jet power in radio galaxies. Falcke et al. [148] then showed a correlation between *bolometric* disk luminosity and radio power in radio-loud and radio-quiet quasars. This would mean that jets and disks are tightly coupled, in what they called the “jet–disk symbiosis” [145, 148]. Within this model, the radio–optical distribution could be understood, if the jet power was directly proportional to the accretion rate (but with a different efficiency for radio-loud and radio-quiet jets).

The main idea here is that the driving parameter for supermassive black holes is the accretion rate \dot{M}_{disk} , which sets the overall power scale and lets one unify black holes as a function of power. Falcke et al. [145, 147] made the utterly simple, yet until today, highly successful Ansatz that the jet power is $Q_{\text{jet}} = q_{\text{jet}} \dot{M}_{\text{disk}}$ essentially for all accretion rates and black hole masses and where the jet efficiency q_{jet} is of order of a few percent [148, 269].

3.9.4 *Microquasars: Inclusion of Stellar Mass Black Holes*

Given this scaling with accretion rate, one would then expect to see also jets and disks at much lower accretion rates in sources with supermassive black holes. After all, quasars are quasars only for a short fraction of the time. Already for some time, it was speculated that LINERs [224, 232] would be low-luminosity AGN (LLAGN) and hence be the less powerful siblings of quasars and Seyfert galaxies. And indeed, many of the weakly active galaxies show compact radio emission in their centers [372–374, 565] which are strong indicators of jet activity from supermassive black holes [144, 153, 371] and are not due to star formation (which was an alternative interpretation of LINERs [510]). The surprise finding, however, was that these radio jets appear to be radio loud rather than radio quiet [231, 374] (when relative rather than absolute measures were applied), with radio cores in elliptical galaxies being slightly more radio loud than radio cores in spiral galaxies [374]. Overall, however, the accretion rate and jet power remained the dominating factor, setting the absolute flux scale.

With the discovery of microquasars, i.e., relativistic jets in stellar mass black holes (X-ray binaries, XRBs) [229, 230, 353], it then actually became possible to expand this scaling with power and mass to an even wider range of parameters. Observations showed that XRBs cycle through a number of accretion states as a function of \dot{M}_{disk} , which are directly related to various jet states [158]. Already early on, it was noted that XRBs manage to switch between radio-loud and radio-quiet states (e.g., [146, 160]) *in the same source*—something that is hardly observable in quasars, given the long viscous timescales of their accretion flows. Another interesting suggestion was that XRBs switch to a radiatively inefficient accretion flow mode below some fraction of the Eddington luminosity [136]. This is something that may also be applicable to LLAGN, explaining their low optical/UV flux [231], and it is something which needs to be taken into account when interpreting radio-optical ratios and radio loudness.

So, how can one hope to get a comprehensive view of what is going on in radio-loud and radio-quiet quasars? Well, one important step is not to talk about quasars alone. For example, when studying the dependence of the radio loudness on other parameters of the AGN, one finds that the observed parameter space of AGN is actually fairly small. The Eddington ratio of quasars is typically in the range of 0.1–1 [483], making mass and luminosity strongly coupled in many quasar surveys. So, one possibility to overcome this problem is to include smaller accreting black holes in the study. As discussed above, stellar mass black hole X-ray binaries (XRBs) share many properties of the central engine. Like in the AGN case, it is generally assumed that the central engine consists of a black hole, an accretion flow, a corona, and often a relativistic jet. If one includes these stellar objects in a global study, one obtains very large parameter spaces, where one can easily find relations that one cannot find in a single class of objects alone. However, when doing so, one has to ensure that one disentangles intrinsic properties of the central black hole and properties of the environment. While we can assume that the former does scale

with black hole mass, it will be impossible to “scale” a binary star into a galaxy that provides the fuel for an AGN.

3.9.5 *Radio Loudness and a Unified View of Black Holes*

So, what is the difference between radio-loud and radio-quiet quasars?

The answer may still not be clear-cut, and there are many pieces in the puzzle one has to put together, sometimes perhaps in a still somewhat speculative way. Nonetheless, in the following, we try to sketch a unified picture on how black holes behave as certain parameters change, based on the analogy between stellar and supermassive black holes. This should, however, be considered a hypothesis to be further tested rather than a fully established paradigm.

Power evolution of black holes in elliptical galaxy. Let us first look at one cycle in the life of a supermassive black hole in an elliptical galaxies and start with a very low accretion rate. In this case, accretion proceeds through a radiatively inefficient accretion flow, fed from the tenuous, hot interstellar medium (ISM) in the center of the galaxy. The galaxy will appear as an inactive elliptical with faint radio emission in the core from a feeble and moderately relativistic, collimated outflow. The radio emission will be similar to what is seen in Sgr A* but is likely too faint to be detected by today’s radio telescopes (but this may change with the SKA in the future). As the accretion rate increases, one gets to see a LINER/LLAGN in an elliptical galaxy with a noticeable radio core in the center. The black hole has a radiatively inefficient accretion flow that—like the jet—produces some nonthermal optical and X-ray continuum, ionizing surrounding gas and producing the LINER spectrum. A sudden increase in accretion rate will lead to a brighter nucleus and the formation of a more powerful and brighter relativistic jet. As the jet ploughs its way through the ISM, compact hot spots will form on the parsec and later on, the kiloparsec scale, making the source appear as gigahertz peaked-spectrum (GPS) and later, as a compact steep-spectrum (CSS) source [389]. When it has further matured, the source will appear as a powerful FRI radio galaxy or as a BL Lac object when seen from within a small angle of the jet axis. Finally, when the accretion rate reaches some fraction (say 10%) of the Eddington rate, the jet will become highly relativistic and unstable with major outbursts as seen in radio-loud quasars and soft state X-ray binaries [323]. Somewhere in the same area of accretion rate, the disk would become fully radiatively efficient and produce the characteristic luminous blue bump of quasars as well as the broad-line region (BLR).

If seen from the side, such a source would be called a radio galaxy if seen face on, it would appear as a blazar. As the accretion rate increases further, the source may move to the left of the hardness–intensity diagram, where jet formation ceases, and the jet might switch off or at least is highly quenched for an expanded period of time. The quasar will become radio quiet, but a faint jet or at least remnants of previous outbursts may still be around.

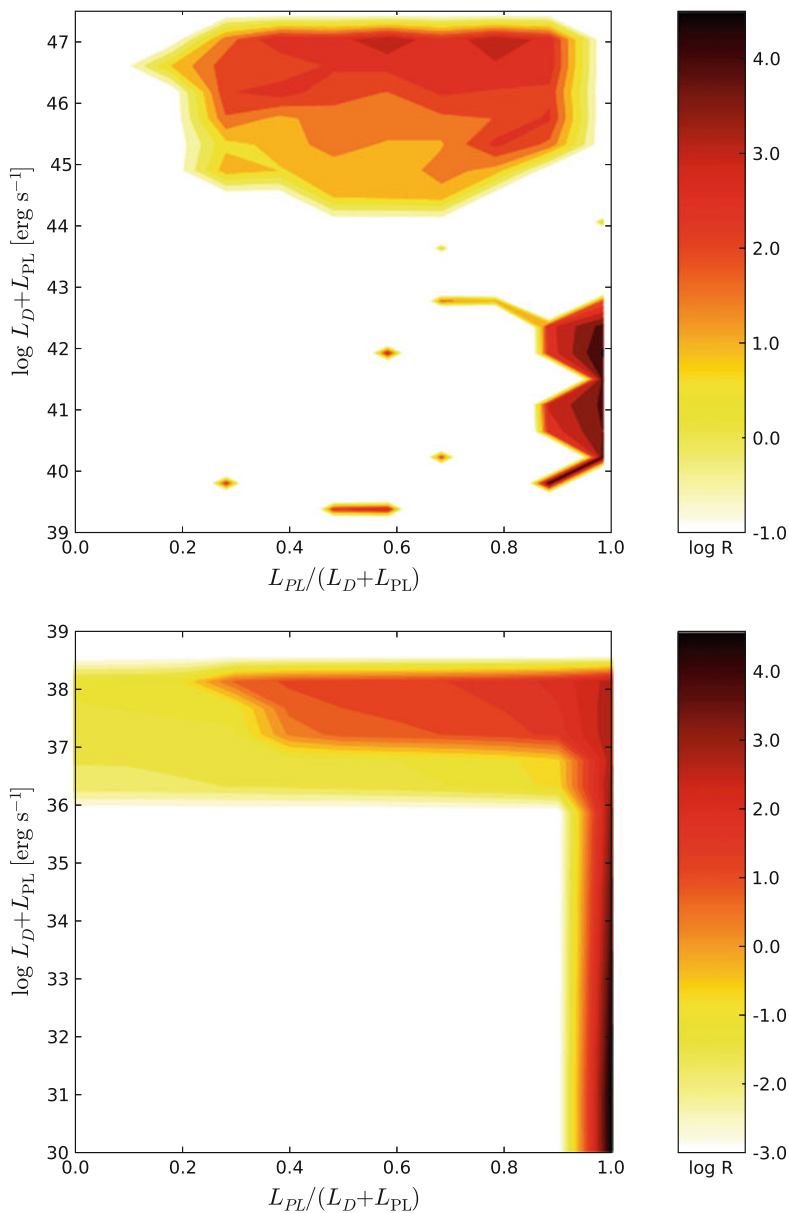


Fig. 3.21 Average radio loudness as a function of the position on the disk-fraction luminosity diagram (DFLD). *Left panel:* SDSS sample together with a low-luminosity sample. *Right panel:* Monte Carlo simulation of 100 XRB outbursts

Power Evolution of Black Holes in a Spiral Galaxy. The evolution in a spiral galaxy would proceed very similar: At low accretion rates, the black hole will look like Sgr A* and become a LINER like M 81 at higher accretion rates. Closer to the Eddington rate, the galaxy will turn into a Seyfert galaxy with a radiatively efficient disk. The jet will switch off when the hysteresis loop in the HID/DFLD (Fig. 3.21) is reached. Since black holes in spirals are typically less massive, the Eddington rate and maximum jet power will never reach values needed to produce jets as seen in powerful radio galaxies that extend far beyond the galaxy. An additional hampering factor is the fact that the ISM in spirals is dense and rich of molecular clouds, making it difficult to drill through. This is especially true if the jet axis is not aligned with the axis of the galaxy disk [370]. In some cases, the jets may point toward the observer or get stuck already on a very small spatial scale and then appear as a radio-intermediate quasar or Seyfert galaxy, like III Zw 2 [81]. For the detectability of large-scale jets, the environment certainly plays a role, which is evident from the fact that such jets are hardly seen from stellar mass black holes.

In addition, there may be secondary factors in determining the radio efficiency. Spin, while likely not being the dominant factor, could well have some influence on jet efficiency and hence further increase the spread between ellipticals and spirals (if it is indeed true that the latter have lower spins). Moreover, as the type of accretion flow does play some role in jet formation—especially the magnetic field content—also the immediate environment could play some role, which is certainly different between spiral and elliptical galaxies. The environment could also play a role in determining on which branch of the hysteresis part in the power evolution of black holes different types of AGN preferentially reside.

So, while not having solved completely the issues of radio loudness, we at least have a few culprits to point at. First of all, radio loudness should always be defined in relative terms, i.e., the radio output relative to proxies of the accretion rate (which may or may not be optical or X-ray emission, depending on the source). Furthermore, empirically, the crucial factor seems to be the change of the disk jet coupling as the accretion flow changes state when the accretion rate changes. Here, magneto-hydrodynamic simulations of disks and jets are making good progress [266, 338] but have not yet tackled state switches. Interestingly, looking at the entire range of states of accreting black holes that we have laid out, radio quietness seems to be more an exception than the rule, when defined in relative terms. This is in stark contrast to the general perception, where it is thought that 90% of AGN are radio quiet. If, however, black holes are indeed mainly radio quiet only at the highest accretion rates, i.e., in those states (e.g., the QSO or the high-soft state) where they are most easily found and not in the states wherein they reside most of the time, our perception in the past might have been severely skewed.

Thank you, Heino and Elmar. We now leave the domain of earthbound observations to move to a waveband that is accessible only from space. In the 1950s and 1960s, it was at all obvious how the sky would have looked in the X-ray domain. Martin Elvis introduces the motivations that drove the early rockets and space experiments. Then, he summarized the main facts derived from high-energy studies. After him, Dirk

Grube will introduce techniques of discovery of new quasars from X-ray surveys. We then go into a more detailed discussion of the spectral features, notably the warm absorber (with Ajit Kembhavi) and the iron $K\alpha$ line. This last feature is very important but nowadays considered to be uncertain since part of the ASCA results obtained in the late 1990s have been challenged by new observations. The topic is discussed by Ajit Kembhavi and Jane Turner.

3.10 X-Rays Properties of Quasars

Dear Martin (*Elvis*), why should we care about X-rays in general, and about X-rays from quasars in particular?

I like to say there are four answers to this question, one each for four different enquirers:

- *Astronomers* should be able to say what is in the night sky. In the optical and infrared bands, the stars dominate the sky. But outside this narrow (2–3-decade wide) range, it is the quasars that dominate—in the radio (~ 5 decades) and at high X-ray and γ -ray energies (>6 decades). It is embarrassing not to know the answer.

Astronomers also want to explain the bright cosmic diffuse X-ray background discovered in the very first rocket experiment in extrasolar X-ray astronomy [191]. Already by 1980, it was clear that the X-ray emission of quasars was likely to be enough to account for the entirety of it. Yet it took until deep *Chandra* observations to establish this firmly in the hard 2–10 keV band [192], though *ROSAT* had nailed this for the soft (0.2–2 keV) band some years earlier [221]. (Seeing Riccardo Giacconi’s name leading both the discovery and the solution paper gives an idea of the determination behind his 2002 Nobel Prize for physics.) That the X-ray background was found within a year of the discovery of quasars themselves is remarkable. How strange that the problem of the X-ray background should be solved by an almost contemporaneous discovery based on radio and optical data, even if it took four decades to prove it.

- *Astrophysicists* want to understand the physics of how quasars work. They are clearly not powered by nuclear fusion, and although gravitational energy released via an accretion disk gives the right energetics, neither the radio nor the high-energy emission comes from the accretion disk. For the radio and γ -rays, we know the process by which the photons are emitted, but not how that process comes to occur: the radio comes from synchrotron emission from a relativistic jet, but that does not tell us how the jet is accelerated. Whatever that process is occurs way down close to the black hole, near where the X-rays come from. The gamma-rays are photons Compton upscattered by the relativistic electrons in the jet, but where do those photons come from? Instead, for the X-rays, we are not even sure of the emission process. The X-rays are thought to be photons from the disk, also upscattered, this time by a hot “corona,” but that is not much more than

a name. We really do not know which of many detailed suggestions is correct. In fact, while we have learned an enormous amount about the behavior of X-rays from quasars in 30 years, we know but little about their origin.

- *Cosmologists* want to understand how the central supermassive black holes in galaxies grow in line with the growth of the formation of stars in the galaxy, as they seem to [163, 185]. This is odd because while supermassive black holes can be as luminous as a whole galaxy when active as quasars, the supermassive black hole is no larger than the black spot on the wing of a ladybug compared to the size of the Earth. How can they influence something so much bigger? Obviously, we need to study how these black holes grow. My former office mate, Andrzej Soltan, showed that most of this growth happened while the black holes were lit up as quasars [477].⁵
- *Physicists* are intrigued by what goes on in the strong gravity near a black hole, as a means to test general relativity and to understand how particles can be accelerated to energies well above what the Large Hadron Collider can produce here on Earth, in beams more tightly focused than a laser. As X-rays from quasars vary very rapidly (see below), we presume that the X-rays are the radiation that comes from nearest the black hole. (The ultraviolet (UV) radiation comes from 10 times or more larger region, for example.) X-rays are then the best way to probe these extreme physics situations.

What do we know about the X-ray properties of quasars?

There are a few basic properties we learn at any waveband: how bright the quasar is (its flux), how the light is distributed in color (its spectrum), and whether the light output changes (its variability). All three are well studied in X-rays.

- X-rays account for $\sim 1\%$ – 10% of the total power output (the “bolometric luminosity”) of quasars. So they are significant but not dominant. Quasars that are strong radio sources (“radio loud”) are a few times stronger in X-rays than the rest (the “radio-quiet” quasars). Presumably, this extra emission is connected to the obvious relativistic jets in radio-loud quasars. A quasar that is more luminous in its optical emission tends to have a lower percentage of its power coming out in X-rays. The thought is that the X-rays come from a hot “corona” that upscatters UV photons from the accretion disk below. The temperature and/or optical depth of this corona would then vary with the luminosity of the disk to produce the observed correlation. We do not know why.
- The X-ray spectra of quasars rise in terms of the power emitted per decade (i.e., in “ $\log \nu f_\nu$ vs. $\log \nu$ ” space, where f_ν is a flux in energy/unit area per second and ν is frequency (or $1/\text{wavelength}$). A rising spectrum is called “hard”), in a roughly straight line from ~ 1 to ~ 100 keV, but somewhere thereafter, they drop

⁵Irritatingly, he did this during that brief time he was sharing an office with me, he even told me what he was doing, and I just did not understand it. Rats. It could have been the Soltan–Elvis argument. I guess it pays to be smart.

sharply. (Such a straight line is called a “power law”, because it is described by the formula $f_\nu \propto \nu^\alpha$, where α is the slope of the power law.) The drop at $\sim 50\text{--}500\text{ keV}$ is thought to be set by the temperature of the upscattering “coronal” gas, but for now, this temperature is so poorly measured that we do not know if they are all the same or if they span a wide range. Something sets the corona temperature and optical depth. We do not know what.

- The X-rays from quasars vary rapidly (minutes to hours), and by huge amounts (factors of 2 or more) so, by the simple “light travel-time” argument, they must be coming from a small region (light-minutes to light-hours across), a size that is not much larger than the black hole. Most of the potential energy available from dropping matter into a black hole is released only in this tiny region. So why do X-rays not dominate the output of quasars, instead of the UV light from further out? We do not know. One possibility is to realize that the light travel time only gives us a size, not a location. Perhaps, the X-rays come from a small region further out. The beginnings of the relativistic jet seem like a plausible location. But we do not know.

Although a power law is a good basic description of a quasar X-ray spectrum, there are so many features imprinted upon it that the naked power law is rarely ever seen. From low energies to high, these features are:

1. *A Soft Excess*: There is often a rapid rise in the spectrum toward lower energies at the lowest X-ray energies (i.e., in the “soft” band below $\sim 1\text{ keV}$). This could be connected to the light produced by the accretion disk [113], or it could be an artifact of light produced nearby and reflected off the accretion disk [194]. We do not know which.
2. *A Cold Absorber*: Quasars commonly have their X-ray spectrum absorbed by cold gas between us and the quasar X-ray source (along our “line of sight”). This is particularly common in less luminous quasars [293, 482].

Matter absorbs X-rays, as is clear from a dentist’s X-ray. The main mechanism is photoelectric absorption, where an X-ray knocks an electron out of an atom. For this “photoionization” to be effective, the energy of the photon needs to be at or just above that needed to knock out the electron. X-rays have energies of the most tightly bound electrons, those in the inner shells around the atomic nuclei. Higher atomic number atoms have more tightly bound electrons, so we can tell which atomic element is absorbing the X-rays from the energy at which we see a drop in the spectrum. As more material piles up, the abundant low atomic number elements absorb all the lower energy X-ray light, then the less common, higher atomic number, elements start to absorb many of the higher energy X-rays.

We see a wide range in the amount of cold-absorbing material, from just detectable to over a 1,000 times larger, so the spectrum we see is cut-off below an energy anywhere from $1/2$ to 10 keV . This absorption was for many years ascribed to a donut-shaped torus of gas so cold that molecules survived in it [276]. This puts the torus far from the black hole, light-months away (see below).

Now though, that simple picture is being replaced with a more complex one. The amount of cold absorber gas (its column density: the number of atoms/unit

area) often varies strongly by factors of 10 or more [442]. These changes occur in a few days or less and so need fast-moving material to cover or uncover the X-ray source. The implied velocities of a few $1,000 \text{ km s}^{-1}$ are too fast for the cold torus, but are similar to those in the region emitting the broad emission lines. The densities and ionization states of the gas also match the broad emission-line clouds, so we are quite confident that these varying cold absorbers let us “X-ray” the broad-line clouds.

The results can be surprising. Maiolino et al. [315] show that clouds have a “cometary” shape, with a sharply defined, small and high column density head, with a larger, less thick tail of more ionized gas. Something is pushing out a tail of material opposite to the direction the cloud is moving.⁶ The obvious idea is that the cloud is moving supersonically through another, hotter and less dense, medium, and a shock forms, sweeping the gas backward. If this is right, then the cloud will be destroyed in just a few months, and so a fresh supply of clouds must be found. The accretion disk is the obvious source for new clouds. (This will be discussed more below.) While we think we know where the rapidly changing absorbing gas lies, for the rest, we do not know.

3. *A Warm Absorber*: Even quasars in which cold gas is not absorbing X-rays often show absorption by warm gas [210]. As a gas is heated up, or is irradiated more intensely, it becomes ionized, stripping the electrons of the lighter, lower atomic number, elements first. This makes the gas ineffective at absorbing lower energy X-rays while still absorbing at higher energies. This leads to a characteristic notch being cut of the spectrum. In quasars without cold absorption, at least 1/2 of all AGNs show warm absorption [436]. High-resolution spectra from *Chandra* and *XMM-Newton* have measured the Doppler shift of this gas, and it is moving toward us, and away from the black hole, at $\sim 1,000 \text{ km s}^{-1}$ (~ 1 million km h^{-1}). This is fast but not extremely fast by the standards of quasars. The location of this warm absorber wind is my candidate for “worst determined number in astronomy.” It is uncertain by a factor of 1 million: from ~ 1 light-day away from the black hole to $\sim 1,000$ light-years away. Confusingly, the only good measurements lie at opposite ends of the scale [46, 277]. Why? We do not know.
4. *Iron emission-line (Fe–K)*: Virtually, every quasar has a strong emission line at 6.4 keV (redshifted down by the redshift of the quasar to a lower observed energy) due to emission from a transition to the innermost shell of the Iron atom, the K-shell. Hence, the line is called “the Fe–K line.” (Atomic physics shows that it is really a set of lines, but X-ray telescopes do not yet have enough resolution to see this level of detail.) The obvious Fe–K line is narrow, though possibly resolved at a width of $\sim 2,000 \text{ km s}^{-1}$. As with warm absorbers, this is fast, but not as fast as other motions in quasars.

Much more spectacular are the “red wings” to the narrow Fe–K line seen in some quasars [502]. If these are Doppler-shifted Fe–K emission then the

⁶Not radially, like the ion tail of a solar system comet, otherwise we would not see an asymmetrical dip.

velocities required are moving away from us at $0.1\text{--}0.3 c$ ($c =$ the speed of light). Or gas emitting the line must be close to the black hole event horizon, so that the gravitational redshift the line suffers coming out of the deep gravity well is large. At this small radius, the orbital velocity is also relativistic, so that there is strong Doppler boosting of the approaching side of the disk, and this produces a strong peak on the blue (higher energy) side of the Fe–K line (see [142] for a review).

The 6.4-keV Fe–K line is emitted not because the gas is hot, but through fluorescence off nearly neutral gas, implying that the main X-ray source is illuminating the accretion disk, the only obvious source of such gas near the black hole. Changes in the continuum should then be reflected in changes in the Fe–K line, but this is not seen in the data. This does not mean the picture has to be wrong. Miniutti and Fabian [351] and others use the distortions of space-time near the black hole and changes in the location of the X-ray source above the disk to reproduce the data well. The prospect of seeing strong gravitational redshifts is exciting. If this model is correct, we can measure the black hole spin [76] and perhaps, test whether the form of the space-time metric agrees with general relativity.

However, others have found this model to be rather fine-tuned. The only alternative model proposed so far notes the low contrast of the Fe–K red wing—a few percent above the continuum in the reddest parts—and suggests that weak curvature in the spectrum can be produced by a population of cold and ionized absorbers (see above) crossing our line of sight and covering the source by varying amounts. Miller et al. [346] show that this model fits the data just as well as the light-bending picture. As both light bending and multiple absorbers are expected, or known, properties of quasars it is not at all clear that Occam’s razor can be used to distinguish these two models. We do not know which is correct.

5. *Compton Hump*: The highest energy feature is a broad hump from ~ 10 to ~ 40 keV, related to the Fe–K line. The cross section for the Fe–K transition is similar to the Thomson cross section for electron scattering, so whenever the Fe–K line is seen, electron scattering must also be important. Because photoelectric absorption has a much higher cross section than electron scattering below about 10 keV, the electron-scattered X-rays are absorbed there, and they only appear once photoelectric absorption tails off at ~ 10 keV. Electron scattering does not depend on energy, until the energy of the photon is enough to impart a substantial recoil velocity in the electron, at which point, the cross section decreases. This is called the Klein–Nishina limit and sets in around 40 keV. The resulting 10–40 keV “Compton humps” are commonly seen in quasars. In principle, Compton humps can be used to measure black hole spin too, but they are hard to measure with current instruments. Compton humps seem to cover a wide range of sizes. We do not know why.

What have we learned?

The above section emphasized what we still do not know about quasars. But this is too negative. In the richness of the phenomenology lies an abundance of raw material from which we can build a more complete quasar model.

One new component, to add to the standard three—black hole, accretion disk, and jet—is already clear: accretion disk winds. Warm absorber winds are common and are also seen in UV absorption lines. The UV lines let us take the observations to much larger samples and higher redshifts, showing that most, and perhaps all, quasars have these winds. We will explain this fourth component of quasars in more detail.

The cold absorbing clouds eclipsing the central X-ray source are already close to resolving the size of the source [443] and are limited only by telescope collecting area. Effectively, this provides micro-arcsecond imaging, that could address the final part of the puzzle—the X-ray source of quasars.

Thank you, Martin.

3.10.1 *Discovering Quasars in the X-ray Domain*

Dear Dirk (Grupe), how efficient have X-ray telescopes been for discovering quasars?

X-ray surveys have been extremely successful in discovering quasars. Surveys can be distinguished between two types, all-sky surveys like the ROSAT All-Sky Survey (RASS, [540]) which cover the whole sky but which are rather shallow and deep surveys like the *Chandra* deep fields (e.g., [72]) which can detect very faint AGN like high-redshift quasars but only cover a tiny part of the sky.

Are X-ray surveys biased toward particular types of quasars?

The RASS which was performed in 1990/1991 in the 0.1–2.4 keV range still is the largest X-ray survey. About half of all of the 150,000 sources detected in the RASS are thought to be AGN. Of the bright X-ray sources which could all be identified by optical spectroscopy, about 1/3 are AGN [52, 457, 511]. As mentioned by Stephens [487] from her study of *Einstein* observed AGN, soft X-ray surveys like the RASS tend to be biased to find NLSy1s. Grupe et al. [201, 202] found that about half of the bright AGN from the RASS are NLSy1s.

Deep X-ray surveys on the other hand focus on a very small portion of the sky but provide very deep exposures to detected even very faint X-ray sources. One of the first deep surveys was the ROSAT survey of the Lockman Hole [220]. The main motivation was to find out the origin of the soft X-ray background. It turned out that the X-ray background could be associated to point sources, preliminarily AGN. The deepest X-ray surveys have been performed by *Chandra* in the 0.5–8 keV band with the *Chandra* Deep Field North and South which both have exposure times of more than 2 Ms each. Due to the superb point spread function of the *Chandra* X-ray

telescope, *Chandra* is able to detect sources with count rates down to one photon a week. The other advantage of the *Chandra* deep surveys is that they are very sensitive toward absorbed quasars. These are intrinsically highly absorbed AGN that cannot be detected at lower energies and surveys like the RASS.

Another survey that has been very successful in detecting obscured quasars is the BAT survey [515]. The Burst Alert Telescope (BAT, [38]) is a wide-field telescope onboard the Gamma-ray burst (GRB) Explorer mission *Swift* [186]. It operates in the 14–195 keV hard X-ray band. While *Swift* is observing a target with its X-ray and UV/Optical telescopes, the BAT monitors an $80^\circ \times 120^\circ$ field of the sky in order to detect GRBs. At the same time, it collects the data in this field. The BAT survey is the deepest hard X-ray all-sky survey ever performed. In the first 22 months of the survey [515], 461 sources were detected of which 266 are Seyferts. Winter et al. [561] found that about a quarter of the BAT survey AGN are “hidden” AGN, so AGN which are highly absorbed. The BAT survey, however, is biased against NLSy1s because of their steep X-ray spectra which makes them very faint at high energies.

What have been the most fruitful quasars surveys conducted in the X-ray band?

All the X-ray surveys described above have their pros and cons. While the RASS was a soft X-ray survey which was extremely sensitive toward finding NLSy1s, it was biased against absorbed AGN. The big advantage of the RASS, although already 20 years old, is the huge number of X-ray sources detected, 150,000 in total. The nature of being an all-sky survey is that the RASS is rather shallow. On the other hand, “pencil-beam” surveys such as the *Chandra* deep fields can detect very faint sources, and these surveys have been very successful in finding the most distant AGN in X-rays. However, the disadvantage is that they only cover a very small region in the sky.

Thank you, Dirk.

Dear Jane (Turner), is there now a well-established X-ray definition for quasars?

In the 1970s, hard X-ray emission was established as a common property of active galactic nuclei [131]. The 2–10-keV band luminosities of AGN were found to predominantly lie in the range $10^{42} - 10^{48} \text{ erg s}^{-1}$, comprising a significant fraction (5–40%: [549]) of the bolometric emission from these objects. The discovery that the X-ray flux varies down to at least kilosecond timescales in local radio-quiet Seyfert galaxies confirmed an origin from a small nuclear region [294, 412]. The X-ray variability timescale increases with increasing source luminosity, as expected given that both quantities should scale with the central source mass. In radio-loud AGN, the X-ray luminosity is, again, an indicator of nuclear activity. However, some of the observed hard X-ray flux may arise from a jet and depending on the orientation of the jet to our line-of-sight, this component may be beamed and difficult to separate from the nuclear flux.

The sky has been well studied in the 2–10-keV band by a combination of shallow, large-area surveys and also deep “pencil-beam” surveys in selected parts of the sky. However, the discovery of many AGN in the IBIS and BAT instrument surveys above 10 keV (e.g., [514]) shows that some active nuclei exist with very high column densities, and therefore, not all AGN will be found by searching the sky below 10 keV. So, a strong 2–10-keV band luminosity is an indication of nuclear activity, but the absence of such does not assure the observer that the nucleus is not active.

Is there an X-ray definitional difference between type-1 and type-2 sources or between radio-quiet and radio-loud quasars?

It is useful to start with a quick overview of X-ray production in AGN. For a thin accretion disk around a supermassive black hole, the disk spectrum has an intensity that peaks in the UV band [464]. It is thought that those inner-disk UV photons are promoted to X-ray energies and that a likely way that this is achieved is via inverse-Compton scattering from a corona of relativistic electrons. The scattering corona may exist on size scales less than a few tens of gravitational radii from the black hole, sandwiching the disk. Some of the X-ray continuum photons may be scattered into the direction of the observer, picking up the spectral imprint from absorption by material along the line of sight. Another possibility is that X-ray photons illuminate the surface of the accretion disk, and some are reflected back into the direction of the observer. The observed spectrum is thought to be the sum of the primary continuum and reprocessed X-rays, and the two are not trivial to separate using X-ray spectra available to date. The imprints of reprocessing are therefore thought to be valuable diagnostics of material in the immediate environs of the black hole.

The Unified Model for AGN posits that any phenomena that are observed in type-2 AGN should also be present in type-1 AGN, modified by a differing viewing angle [22]. This model was initially motivated by observational results such as the optical line properties of AGN. However, the concept has now been extended to the X-ray regime, where AGN whose X-ray emission is absorbed by Compton-thick intervening material are known as type-2, and those without significant absorption being evident are known as type-1.

The term Compton-thick is used mainly by X-ray astronomers, and merits a brief explanation. In gas with a high column density, Compton scattering has a significant effect. For photons in the 2–10-keV band (the best studied X-ray range to date) $h\nu \ll m_e c^2$ and the Compton scattering cross section for free electrons is approximately the energy-independent Thomson cross section σ_T . For gas of solar abundance in which H and He are fully ionized, the dominant scattering is by free electrons, and so the continuum optical depth is $\tau \simeq n_e \sigma_T$, where n_e is the free electron column density (heavier ions also have significant energy-dependent individual scattering cross sections, but their net contribution is rather small). The scattering optical depth has a value unity approximately at $n_H \simeq 1/1.2\sigma_T \simeq 1.25 \times 10^{24} \text{cm}^{-2}$. For solar abundance material, the cross sections for Compton scattering and photoelectric absorption, σ_{pe} , are comparable at 10 keV, and this represents an energy that has been considered as the low threshold for studying the

“Compton-reflected” components of AGNs. For a gas column up to about 10^{25}cm^{-2} , some transmitted radiation is still visible above 10 keV [331].

Although there is often a good correspondence between optical and X-ray classifications for type-1 vs. type-2 AGNs [42], this agreement is not perfect [403]. It has been recently established that some type-1 AGNs (e.g., 1H0419-577 [523]) have large columns of gas obscuring much of the X-ray flux below 10 keV but leaving a direct view of some fraction of nuclear flux through lines of sight that are not obscured by the partial-covering gas. Compton-thick, partial-covering obscuration also exists in sources of high luminosity, as evidenced by the *Suzaku* observations of PDS 456 [432]. Thus, recent results indicate that the Unified Model requires an additional level of complexity, either in the geometry/form of the key absorber (to naturally allow for a range of observed covering fractions) or a consideration of covering fraction as a variable, in addition to source orientation.

Is there any unusual X-ray characteristic involving particular subclasses, for example, narrow-line Seyfert-1 galaxies or blazars?

The X-ray spectra of NLSy1 galaxies appear systematically steeper than the rest of the local Seyfert population, and their X-ray flux variability is more marked on short timescales.

Observations from the *ROSAT* mission were key in revealing an anti-correlation between the soft-band (0.5–2 keV) X-ray photon index and $H\beta$ FWHM [64, 165, 289], revealing systematically steeper spectra for the NLSy1 subclass. Boller et al. [64] also noted that NLSy1s frequently display rapid short timescale variability in the *ROSAT* bandpass. Using ASCA data, studies confirmed this result to extend to the 2–10-keV spectra of NLSy1s (e.g., [300, 522]). Turner et al. [522] also established a correlation between variability measure σ_{rms}^2 and $H\beta$ in the sense that the more variable sources have the narrowest optical line widths. These discoveries were consistent with earlier ideas (based initially on optical data) that the NLSy1 subpopulation were either viewed at a different orientation to BLSy1s [314] or that they might have a relatively central black hole mass or high accretion rate [416]. ASCA and other satellite data have also yielded numerous claims of a huge equivalent width for Fe $K\alpha$ emission in NLSy1s: however, in light of recent progress, it is clear that the interpretation of those spectra must be now rethought in the context of complex reprocessing models.

Radio-loud AGNs have long been known to show systematically weaker and narrower Fe $K\alpha$ emission lines and apparently, weaker Compton reflection components above 10 keV than the radio-quiet AGNs [135, 451], along with a relatively low amplitude of flux variability on short timescales. Interestingly however, recent data have allowed the isolation of X-ray absorption lines [513], indicating reprocessing in a high-velocity outflow for some radio-loud AGNs. At this point, the origin of the apparent systematic differences between these subclasses of AGNs is not well understood, but indications are now that there are differences in circumnuclear conditions, rather than a lack of X-ray reprocessing gas in the radio-loud sources.

Technological advances now enable us to obtain reasonably high-resolution X-ray spectra. We can even measure redshifts in the X-ray. What is the current state of our knowledge about X-ray emission lines in Seyfert galaxies and quasars?

X-ray data carry signatures of circumnuclear reprocessing, and a study of this material offers the best chance to understand importance mechanisms such as the accretion process that fuels AGN and the feedback of material and energy to the host, through winds and jets. While the X-ray emission and reprocessing regions are far too small to be imaged with current X-ray instrumentation, spectroscopy and timing analysis offer ways to probe the reprocessing gas indirectly. The last decade has seen technological improvements in X-ray satellite detectors that have allowed significant progress in understanding the nuclear environs of AGNs. To illustrate what constraints are currently possible, I review the spectral capabilities of the existing X-ray grating instruments; 1999 saw the launch of two new satellites, the *Chandra* X-ray observatory and *XMM-Newton*, each offering grating instruments dispersing X-ray photons onto high-sensitivity focal plane detectors. The *Chandra* and *XMM-Newton* instrument ensembles allow sufficient accumulated counts in grating spectra for the first useful high-resolution studies of AGNs to be conducted.

So, what are the current instrumental capabilities?

Chandra. In addition to the high-resolution X-ray optics for which *Chandra* (see for an overview of the mission and its instruments [551]) is well known, the observatory provides the High Energy Transmission Grating (HETG; [83]) comprising the high-energy grating (HEG) and the medium-energy grating (MEG) assemblies. X-ray photons are dispersed by the gratings by an angle that depends on the photon wavelength. The Advanced CCD Imaging Spectrometer (ACIS) comprises one focal plane instrument for *Chandra*. A micro-channel high-resolution counter (HRC) provides alternative focal plane instrumentation.

HETG is calibrated to an absolute wavelength accuracy that is equivalent to $\sim 100 \text{ km s}^{-1}$, and this gives a typical accuracy to which an AGN outflow velocity can be determined (although one can do a little better when there is very high signal to noise in the features). In more detail, HEG provides spectral resolution FWHM $\Delta\lambda = 0.012 \text{ \AA}$ and energy/wavelength-scale calibration accurate to 0.006 \AA across its effective energy range ($0.8\text{--}8.5 \text{ keV}/16\text{--}1.5 \text{ \AA}$), approximately twice as good as that of the MEG which has FWHM $\Delta\lambda \simeq 0.023 \text{ \AA}$ and calibration accuracy 0.011 \AA over $0.5\text{--}7 \text{ keV}$ ($25\text{--}2 \text{ \AA}$). Aside from HEG, no other grating instrument has any useful sensitivity to photons above 6 keV , and so, HEG is the only instrument for which grating-resolution data can be accumulated in the Fe K region at present. The HEG energy resolution FWHM $\simeq 40 \text{ eV}$ is equivalent to a velocity resolution about $1,900 \text{ km s}^{-1}$ at 6.4 keV (a factor of several improvement over existing CCD instruments). Optionally, observers can instead utilize the single Low Energy Transmission Grating (LETG) whose soft response complements HETG, providing $\Delta\lambda = 0.05 \text{ \AA}$ over $0.07\text{--}6.0 \text{ keV}/175\text{--}2 \text{ \AA}$.

XMM-*Newton* carries a pair of reflection grating spectrometer (RGS) gratings [115]. RGS gratings disperse X-rays onto focal plane CCDs, providing a resolution $\text{FWHM} \simeq 2.9 \text{ eV}$ at 1 keV ($\Delta\lambda \simeq 0.07 \text{ \AA}$). The absolute wavelength calibration for the RGS is 0.008 \AA equivalent to 100 km s^{-1} at about 0.5 keV . XMM-*Newton* also carries both metal oxide semiconductor (MOS) and pn-CCDs covering $0.5\text{--}10 \text{ keV}$ with energy resolution $\text{FWHM} \simeq 130 \text{ eV}$ at 6 keV and $\text{FWHM} \simeq 55 \text{ eV}$ at 1 keV . Useful RGS data can be accumulated over the range $0.4\text{--}2.0 \text{ keV}/31\text{--}6 \text{ \AA}$: data below 0.4 keV are affected by a detector feature, and above 2.0 keV , the effective area falls rapidly to zero. Although offering a lower spectral resolution than the *Chandra* gratings, RGS gratings offer greater effective area. As the finite signal-to-noise is often a limiting factor in error determination for many astrophysical features, there are scientific objectives for which the lower-resolution, high-throughput RGS gratings are better suited than the *Chandra* gratings.

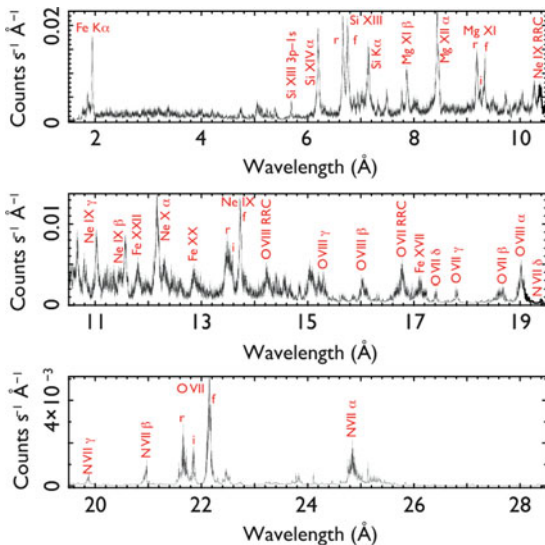
3.10.2 X-Ray Emission and Absorption Lines

What are the emission and absorption features presently detected in X-ray spectra?

Current X-ray grating instruments have improved the soft-band spectral resolution over $0.5\text{--}1 \text{ keV}$ by almost two orders of magnitude over previous CCDs. Consequently, several key diagnostic spectral lines, such as the He-like triplets of O and Ne have become resolvable, allowing component ratios to be used as temperature and density diagnostics of the reprocessing gas. Obscuration of the nuclear emission in type-2 AGN has allowed the most sensitive study of soft X-ray line emission in those AGN (although the same emitting gas surely exists in type-1 AGN but is outshone by the direct view of the continuum emission). Unsurprisingly, the best constraints to date for *absorption* lines have been obtained from long grating exposures of the nearest type-1 AGN. The 900 ks HETG exposure on the type-1 AGN NGC 3783 comprises the deepest single AGN exposure to date with an X-ray grating detector yielding more than 100 line detections [254].

In bright type-2 AGNs such as NGC 1068 (e.g., Fig. 3.22 [138]), Mrk 3 [449] and the Circinus galaxy [452]—HETG and RGS spectra—reveal gas dominated by H-like and He-like species from “light metals” and L transitions of Fe. The emission lines appear to be produced in a plasma typically photoionized by the nuclear radiation (e.g., [206, 264, 449, 452]). The emission lines do not generally show a significant bulk velocity in the galaxy frame—as expected if the gas is observed in regions out of the line of sight and/or distributed around the central source. However, grating observations of absorption features in type-1 AGN typically reveal significant systematic velocity shifts, indicating outflow of the absorbing gas of order a few hundred km s^{-1} , in keeping with the general observation of outflow for lower ionization gas detected in the UV band.

Fig. 3.22 Co-added *Chandra* HETG HEG and MEG grating spectra of NGC 1068 from the 440-ks observational dataset. The principal transitions from H-like and He-like species are noted, along with some radiative recombination continua. This figure has been provided courtesy of Dan Evans. Evans et al. [138] describe the preliminary results from analysis of this spectrum



As only a small percentage of the nuclear flux is reprocessed into emission lines and returned into the observers line of sight, a limiting factor in understanding emission lines is the poor signal-to-noise in many accumulated spectra. This is a particularly acute problem when attempting to split the spectral signal into spatially resolved regions, and consequently, only a handful of bright nearby AGN have been spectroscopically mapped down to the size scale of the optical narrow-line region (NLR). Such analysis has shown the soft X-ray emission of Seyfert-2 galaxies to be morphologically correlated with that of the NLR gas where the latter is traced by the OIII λ 5007 HST images (e.g., [54, 242, 571]). Further, a very simple model where both the optical narrow lines and soft X-ray lines are produced in the same photoionized gas can explain the spectra of some local AGN satisfactorily [54]. Interestingly, radio ejecta are also often found to be spatially correlated with the line-emitting gas, such as in NGC 1068 [78], where the data are consistent with emission from a cone of plasma, irradiated by the central nucleus.

What are the physical parameters and the distance of the X-ray absorbers?

An improved ability to identify individual lines has naturally also led to a major advancement in understanding the X-ray absorbers in type-1 AGN. Most local type-1 AGN shows numerous narrow absorption lines in the soft X-ray regime where the effective area and spectral resolution of various X-ray grating instruments are relatively high. Absorbing zones with $\log \xi < 0$ are commonly found (e.g., [108, 253, 254, 386]) from soft-band lines. Outflow velocities of the low-ionization absorbing zones are typically in the range $100\text{--}2,000 \text{ km s}^{-1}$, and line widths indicate that the gas turbulent velocities are of a similar order. The good quality of the soft-band data has provided a level of detail that has revealed unresolved transition arrays [273, 450, 474] and some dust absorption edges [297], allowing

the first isolation of cool and dusty zones of gas that were previously difficult to distinguish from absorption edges and broadened emission lines.

Gas zones having $\log \xi \gtrsim 4$ are also firmly established in AGN from detection of telltale absorption lines from FeXXV and FeXXVI, these absorption lines have equivalent widths of many tens of eV and likely arise from gas in the range $10^{23} - 10^{25} \text{ cm}^{-2}$ (e.g., [349, 521]). The outflow velocities of the high-column absorbers lie in the range several thousands of km s^{-1} up to relativistic flows. In fact, the range of zones detected in grating data covers the entire range of both ξ and n_{H} to which X-ray observations are sensitive ([62, 63, 336] and references therein). It is worth noting that the extension of the observable bandpass up to several tens of keV courtesy of instruments such as the *Suzaku* PIN have increased the number of cases for the highest column absorbers. In many sources, the broad spectral shape shows that these high-column absorbers cover upward of a few tens of percent of the continuum source, sometimes allowing a significant soft X-ray flux to reach the observer along the unobscured sight line. Of course, absorbers that are Compton-thick lead to an expectation of some accompanying reflection from the same gas, the level of accompanying reflection or reemission from the gas depends critically on ionization state and gas geometry, and work is ongoing to separate these signatures and map the gas. An unambiguous signature of partial-covering absorbing gas would be the detection of saturated line profiles that have nonzero flux in the line core, as observed in UV spectra of AGNs [108]. With these, we could start to separate out the reprocessing signatures from different regions of gas with the ultimate goal of mapping out the source. Unfortunately, as many of the X-ray absorption lines are not resolved even in grating data, X-ray line profiles cannot yet be used to make such a determination. In the meantime, consideration of the detailed timing behavior can help us select between spectroscopically similar solutions [350].

The distance of the absorbers from the ionizing source may be estimated from the value of ionization parameter ξ^7 obtained from model fits to spectra. Based on such estimates, some Compton-thick partial-covering absorbers appear to lie within the BLR [523], while lower column gas generally appears to exist outside the BLR [62], possibly associated with the NLR gas or torus. Other estimates of the location of the gas come from observation of column variations that imply origins typically on the inner edge of the BLR (e.g., [415]). However, such arguments rely on the apparent absorption variations being attributed to obscuration changes from clouds in Keplerian orbits around the central source, which is not yet established. Given the evidence for outflow of the line-of-sight absorber, in type-1 AGNs, and the alignment of the emission with optical NLR gas seen in edge-on sources, it is arguably more interesting to consider the measurements in the context of physical models for large-scale outflows, such as disk winds (e.g., [175, 281, 472, 473]). In the near future, we may be able to use the ensemble of existing data to place interesting constraints on the dominant physics driving in such winds. Important parameters

⁷The ionization parameter introduced here (and defined by (3.1) on page 175) differs from the ionization parameter U that has been defined previously. ξ is customarily defined as proportional to the energy flux divided by the gas density.

such as the mass outflow rate depend critically on the volume filling factor of the gas, which cannot yet be measured directly. However, some estimated limits for the material flow are very interesting: for example, [62] found that for a sample of local AGNs, the median mass outflow rate was about $0.3 M_{\odot} \text{ year}^{-1}$ compared to a median mass accretion rate of only $0.04 M_{\odot} \text{ year}^{-1}$; other studies suggest outflow and accretion rates to be consistent, given the uncertainty in filling factor [94, 336]. As yet, there are too few tightly constrained results from the high-velocity gas zones to draw many global conclusions. However, a recent analysis of PG 1211+143 [413] found a P Cygni signature of high-velocity gas that implied an outflow with solid angle around π steradian. The constraint on global covering allowed [413] to estimate the outflow energetics and to conclude that this zone of gas makes an energetically significant contribution to feedback to the host galaxy.

We now focus our discussion on emission lines detected in the hard X-ray domain and especially on the strongest one, the $K\alpha$ line of iron.

Why is the iron (Fe) $K\alpha$ line so important?

Studies in the hard band concentrate on emission from the K-shell of Fe because Fe has both high abundance and high fluorescence yield, making it the most prominent spectral line in the 2–10-keV band. The Fe $K\alpha$ line is a doublet with components at energies 6.404 and 6.391 keV when produced in neutral gas. These doublet components are currently indistinguishable, even using grating instruments. For ionized material, the binding energies of the inner shells increase with increasing ionization and consequently, emission and absorption features increase in energy. Fe $K\alpha$ emission from ionized gas becomes a complex of permitted, inter-combination, and forbidden transitions (see, e.g., [45, 53, 252]), and some distinction is possible between emission from different ionization states in X-ray spectra. The Fe $K\beta$ line (at 7.06 keV in neutral material), predicted to have 13.5% of the flux of $K\alpha$, is also detectable in bright AGN (e.g., [296, 402]).

X-ray spectral surveys of AGN using HEG have shown that a narrow component of Fe emission is commonly observed at an energy consistent with 6.4 keV, in local AGN [468, 568]. The large numbers of neutral line components detected indicate that reprocessing by low-ionization material is an important constituent of X-ray spectra (confirming previous such indications from data of lower resolution, e.g., [491]). The [468] study showed a mean Fe $K\alpha$ emission line width $FWHM = 2,060 \pm 230 \text{ km s}^{-1}$ for the sample sources and compared these with the optical $H\beta$ line widths, finding no universal location of the Fe $K\alpha$ line-emitting region relative to the optical BLR. Shu et al. [468] concluded that a given source may have contributions to the Fe $K\alpha$ line flux from parsec-scale radii down to half the radius of the BLR location. In the [468] sample, the mean equivalent width was $53 \pm 3 \text{ eV}$; however, observed line equivalent widths are a function of geometry, column density, covering factor, element abundances, and orientation of the line emitter, and so their interpretation is not trivial.

The luminosity of Fe $K\alpha$ emission is observed to be weak in some local Seyfert-type AGN. [437] have argued the observed Fe $K\alpha$ line luminosity to be inconsistent with complex absorption models in some sources, unless the global covering factor

of the absorber(s) is very low. However, the [437] calculation effectively considers the only source of opacity to be the Fe K bound-free transition and neglects the opacity at the line energy: correction to realistic opacity decreases the predicted line flux by a large factor. Contrary to [437], calculations by [346] and [569] that include all sources of line opacity show that Fe $K\alpha$ emission is observed at the luminosity expected in the context of absorption models for all sources observed to date.

Further to the conclusion of the [468] study, some contribution to the narrow Fe $K\alpha$ emission from “close-in” regions such as the accretion disk has been suggested on the basis of variable line flux in some individual sources such as MCG–6–30–15 [298] and Mrk 841 [407]. In addition to these two, narrow, and rapidly variable emission lines were discovered at 5.6 and 6.2 keV in NGC 3516, [518]. In the case of NGC 3516 the lines were initially discussed in the context of velocity-shifted Fe emission from the accretion disk [518], and similar lines found in Mrk 766 were also discussed in the context of an outflow [519]. Further examples of the phenomenon, dubbed “transient Fe lines” (because of their flux variability), soon came from observations of other AGN (e.g., [205, 308, 567]), spawning discussion of other possible origins, such as enhancement of Cr and Mn abundances from spallation of Fe [517].

Are there any luminosity dependences for emission lines?

Early work with low-resolution X-ray spectra (having an effective resolution at 6 keV limited to the equivalent of FWHM $\sim 7,000$ km s⁻¹ or worse) searched for a so-called X-ray Baldwin effect, that is, an anti-correlation between the Fe $K\alpha$ line equivalent width and X-ray luminosity. Several studies claimed evidence for AGN spectral evolution with luminosity, and specifically, attributed that evolution to changes in the profile of an assumed broad Fe emission line (e.g., [240, 245, 368, 401]); further work suggested the spectral evolution to be a function of accretion rate rather than luminosity [55, 561], although a cautionary note was added by [561] who found that the significance of any correlation was a strong function of the sample point binning.

As older data would have been unable to separate blends of narrow Fe lines from different ionization states, [468] revisited the question of any luminosity correlation for Fe $K\alpha$ emission using only HEG data: those authors confirmed found an anti-correlation between the Fe $K\alpha$ line equivalent width and X-ray continuum luminosity; importantly, this was isolated to the narrow core of the Fe $K\alpha$ emission line. Shu et al. [468] speculated that the effect may be related to a decrease of covering factor and/or of the column density of line-emitting gas with increasing X-ray continuum luminosity. Another possibility is that the line-emitting material becomes increasingly ionized as the X-ray luminosity gets larger.

Just a few years ago, X-ray spectroscopy revealed an apparently broad and redshifted line at 6.4 keV. This Fe $K\alpha$ feature was widely interpreted as the signature of the innermost regions of an accretion disk. It was thought to be present in many or most AGNs observed at that time. More recent *Chandra* and *XMM-Newton* X-ray spectra appear to have negated/changed/confused this

picture with many broad FeK α lines, now much less broad or strong. What happened?

That the X-ray spectra of AGNs show marked curvature in the 2–8 keV regime is well established—although the interpretation of this curvature has been the source of much debate (see [516]).

Taking results both from sample studies and across the literature, it appears that models dominated either by blurred reflection *or* by complex absorption provide statistically comparable fits to the *mean* snapshot X-ray spectra of most AGNs over 2–10 keV. However, one must examine the solutions obtained, the spectral variability, and detailed timing behavior. Considering all aspects of source behavior, there is strong evidence for a complex reprocessor whose absorption and scattering/reflection signatures are evident. However, in the opinion of these authors, there is no compelling case that the X-ray spectral signatures we are currently sensitive to are dominated by reprocessing within 20 gravitational radii of the central black hole, as often claimed; $20 r_g$ is not a special radius other than representing the upper limit for which discernible modifications could be measured for strong emission lines in the brightest AGNs using current instrumentation (and assuming no other “confusing” features exist in the X-ray spectrum). As this is a very important issue in AGN research at this time, I discuss the two scenarios in some detail below.

3.10.3 Blurred Reflection and Absorption

The approach of many teams to modeling the curvature observed over 2–8 keV is to use blurred reflection models obtained by convolving reflection spectra from, for example, [446], with the effects of emission from a rotating disk deep in a black hole’s potential well (e.g., [287]).

As AGNs carry unambiguous evidence for absorption, from the detections of numerous absorption lines and edges, especially in grating data, this gas must first be modeled. Proponents of blurred reflection then add to the model a blurred reflection signature to account for curvature in the 6-keV regime. The motivation behind this approach is that the signatures from material within a few tens of gravitational radii might reasonably be expected to be produced in AGNs with measurable general relativistic effects on contributions from reprocessing within $20 r_g$ of the black hole. Solutions obtained from such modeling often require relatively large contributions from very small radii. In principle, if one has a clean view of the reflection spectrum, then the extent of the “red wing” could constrain the inner radius of the emission and thus the black hole spin: if it is found that emission from radii $r < 6 r_g$ is required in the reflection model, then one may interpret the data as favoring an innermost stable circular orbit $r_{\text{ISCO}} < 6 r_g$ and thus indicative of a Kerr metric. Claims for detection of black hole spin have been made in MCG–6-30-15 and IRAS 18325–5926 [243] based on modeling curvature is down to ~ 2 keV as part of the line profile. With the uncertainty and debate on the physical processes that dominate the X-ray spectrum in this energy range (e.g., [347]). Even if a relativistically broadened Fe K line were

the dominant signature in the X-ray spectrum, measurement of spin is degenerate with several other system parameters; consequently, it is not currently possible to constrain the black hole spin in a model-independent way.

Production of the X-ray continuum over an extended corona would not result in disk reflection that was strongly weighted toward small radii, so the size of the X-ray continuum source is also a key issue in assessing the feasibility of the model solutions for blurred reflection. The case has long been made that the rapid variability observed in X-ray light curves of AGN demonstrates, from arguments based upon light-crossing timescales, that the X-ray emitter must be very compact (few hundred light-seconds in diameter for local AGNs; [431]). Questions have been raised, however, as to whether X-ray flux variability should be interpreted in terms of absorption variations rather than intrinsic continuum variations (see below), leaving the X-ray continuum size as an open question. Further, even the assumption of a central placement of the continuum has been questioned, based upon the varying degrees of temporal correlation found in multiwavelength variability campaigns [182].

Arguably, the biggest problem for the blurred-reflection-dominated picture is the lack of any simple correlation observed between continuum and reflection. “Light-bending” models [351] rely on the continuum flux being intrinsically steady and then explain the observed phenomena by invoking changes in the height of the continuum source above the disk. Opponents of this light-bending picture argue that the required variation in continuum placement is ad hoc and might require fine-tuning if it is observed in sample studies that there is generally no line-continuum correlation seen in AGNs. Some other models seek to explain the observed constancy of the red wing in other ways (e.g., [340, 375, 582]), but these may have difficulty reproducing the high flux detected above 10 keV in many *Suzaku* spectra of AGNs: these hard PIN-band spectra indicate solid angles much greater than 2π for blurred reflection (see [516]). Some hard excesses are sufficiently extreme that model fitting disfavors reflection with all reasonable modifications [432, 523] (Fig. 3.23).

X-ray Absorption. Another view is that spectral signatures from complex absorption dominate the X-ray spectra and explain the spectral variability and detailed lag behavior observed in AGNs. Important in the motivation of such a model was the fact that data from several wave bands support the existence of partial-covering absorbers in AGNs. UV spectroscopy reveals multiple zones of gas distinguished by different ionization states, covering fractions, and kinematics [108]. In any case, partial covering by neutral gas and/or ionized absorbing gas has long been suggested as one possible way to explain the curvature in X-ray spectra of AGNs (e.g., [234, 433]), and in early work, the gas was suggested to be consistent with an origin in the optical broad-line region (BLR; [234, 410]). In the context of absorption-dominated models, X-ray spectral variability is often explained by changes in covering or opacity of the gas layers, or a response in gas ionization state as the continuum varies [278, 385]. Further to this, *ROSAT* observations of narrow-line Seyfert-1 galaxies showed some cases of extremely large-amplitude variability, apparently exceeding what might be reasonably expected from variable continuum

processes [65, 71], and arguably favoring X-ray absorption changes as the origin of the observed flux range in at least some AGNs.

A common argument against partial-covering models is based on probability, that is, that to have a covering fraction of order several tens of percent with significant observed variations in covering implies that there must be obscuration from a few clouds subtending a similar transverse size on the sky as the continuum source. Obviously, if the clouds exist as far out as the BLR, then the probability of observing an orbiting cloud cross the line of sight is low. However, the distances estimated for absorbing clouds depend critically on the cloud density assumed. If one assumes a high density for the absorber (e.g., $n > 10^{12} \text{cm}^{-3}$), then the material is indicative of an origin close to the active nucleus, and the probability issue is alleviated.

Another important consideration is accounting for the scattering losses as a large fraction of the continuum can be lost to the observers view via scattering if the gas is Compton thick. Correcting for scattering losses can change the implied covering fraction upward of the fitted value, and this correction *alone* can alleviate any probability concerns [523].

Finally, a compelling case comes from theory. We expect winds to be driven off accretion disks [263] for sources radiating close to the Eddington limit, and it appears likely such winds would extend to relatively close to the black hole (e.g., [414]). The theoretical perspective thus motivates the consideration of absorption-dominated models as signatures of disk winds.

Does the well-studied Seyfert-1 MCG-6-30-15 provide a good case in favor of relativistic accretion disk emission?

Since the *ASCA* satellite era of the 1990s, the Seyfert galaxy MCG–6-30-15 has been the poster child for so-called broad “red wing” on Fe $K\alpha$ emission lines in AGN. The idea is that photons from the peak of the 6.4-keV Fe $K\alpha$ line are shifted to lower energies by strong gravitational effects, forming a red wing on the line profile. Many models for the X-ray spectrum have been built around an interpretation representing “blurred reflection” signatures produced in the innermost accretion disk (e.g., [241, 352, 502, 559]), with some solutions requiring emission down to the innermost stable orbit in the Kerr metric ($1.235 r_g$). The case of MCG–6-30-15 is important because it is cited as a compelling case for dominance by blurred reflection component, with other models being argued (by some) as having been ruled out [139].

Recently, Miller et al. [347] have shown that the substantial X-ray dataset for MCG–6-30-15, comprising *Chandra* HETG, *XMM-Newton* EPIC-pn and RGS, and *Suzaku* XIS and HXD-PIN observations (between them covering the range 0.5–40 keV), could be fitted by an absorption-dominated model with no relativistically blurred emission. The [347] analysis is unique in systematically analyzing this multi-observatory dataset across the whole available energy range: importantly, the model accounts for the spectral variability that takes MCG–6-30-15 from a low, absorbed-looking state to a higher, less absorbed state (a behavior that is common to sources of this class). Some other studies taking a subset of the data have concurred with the conclusions [129]. A key ingredient of the MCG–6-30-15 work was that one of the absorbing zones should be “partial covering,” implying the absorber

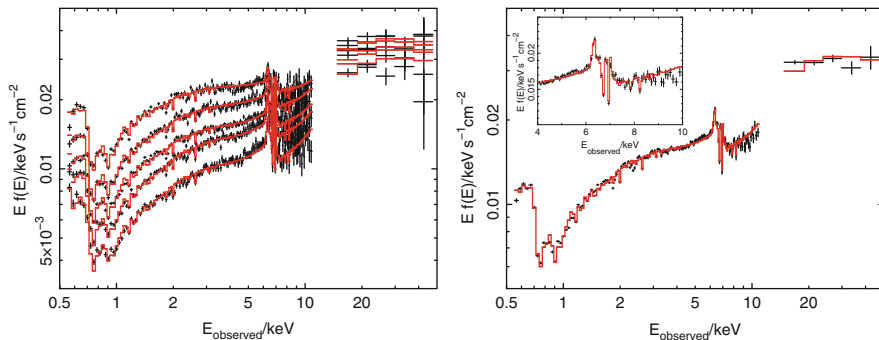


Fig. 3.23 Model fit to the *Suzaku* data of MCG-6-30-15. *Left*: the data are divided into five flux states. *Right*: the mean spectrum is shown with an insert zoom in, showing the 4–10-keV region with linear axes. The model is shown in units of $Ef(E)$; points with error bars show the “unfolded” data. From [346]: reproduced by permission of MNRAS

is clumpy. Grating data clearly show the absorber to be outflowing [297, 572], and [347] suggested the absorbers comprise an accretion disk wind. This work demonstrated that there are no AGNs for which blurred reflection is *required* as an explanation of the spectral form.

As the absorbing gas is expected to be photoionized, we should see recombination and fluorescent emission from the absorber. In principle, we can use the line luminosity to constrain the global covering factor of the absorbing gas (i.e., the fraction of the sky covered by the absorber as seen from the ionizing source). A low line luminosity might imply that the covering factor is small and that our view through an absorber is an unusual and “fortuitous” sight line. As discussed above, [432] have tried to argue that the implied global covering factor would be low for the [347] model; however, as shown by [346] and [569], the calculation of [432] makes poor assumptions that invalidate that conclusion.

Lag Spectra. Detailed timing analysis offers another opportunity for discerning the dominant physics in these systems. The narrow-line Seyfert-1 galaxy 1H0707-495 has previously been identified as showing time lags between flux variations in the soft (0.3–1 keV) and medium-energy (1–4 keV) X-ray bands that oscillate between positive and negative values as a function of the frequency of the mode of variation [143, 581]. At high variability frequencies, the ~ 30 s lag of the soft band relative to the medium has been claimed to arise from the longer light path that a photon reflected from the accretion disk needs to travel with respect to one directly emitted by the primary source [581], while the positive lags at lower frequencies were attributed to an entirely different process. In a review of “Progress in AGN research with XMM-Newton,” [207] suggested that the detection of the positive lag may have settled the issue in favor of a strong dominance by blurred reflection (at least in 1H0707-495), so it is important to examine these data in detail. Unfortunately, the [581] analysis did not include data in the 4–7.5-keV band where their model

predicts the highest fractional contribution from ionized reflection. Consideration of the entire spectrum of lags over 0.3–7.5 keV, and the full frequency range, $10^{-5} \lesssim \nu \lesssim 10^{-2}$ Hz rules out models in which the inner accretion disk makes a significant contribution at both Fe L and Fe K energies and thus rules out the spectral model of [581]. In particular, the lags between the hard and medium bands and between the hard and soft bands are also negative in the same range of frequencies that the lags between medium and soft band are negative. Comparison between the observed lags and those predicted rules out the [581] model at >99.9% confidence [350]. A simple model in which all X-ray bands have differing levels of contribution from a reverberated signal provides a good quantitative description of the large positive lags at low frequencies *and* the high-frequency transition to negative lags and fits the full lag spectra between all bands given the measurement uncertainties. The harder X-ray bands require the longest maximum time lags than softer bands, consistent with a geometry in which reverberation arises from scattering of radiation that is passing through partially opaque material.

As a final note, Titarchuk et al. [512] have pointed out that cataclysmic variable GK Per has characteristically the same spectral signature as an AGN in the Fe K band, presenting a case that demonstrably cannot be an exhibition of general relativistic effects and whose detailed analysis is strongly supportive of reprocessing of X-rays in an outflowing wind.

Thank you, Jane.

3.10.4 *More on X-ray Absorption: The “Warm Absorber”*

Dear Ajit (Kembhavi), the warm absorber has become an important X-ray component of the standard model. What is it and where is it located relative to the accretion disk? What are its currently inferred properties?

The electromagnetic spectrum emitted by some active galactic nuclei (AGN) in the soft X-ray region (about 0.3–1.5 keV), shows prominent and characteristic absorption features. These arise due to the absorption of the X-rays by a gas consisting of atoms of various chemical elements in different states of ionization. The temperature of the gas is about 10^5 K. This temperature is more than that of cold gas which is largely neutral and less than that of a hot gas in which most electrons are stripped from atoms and therefore the gas is called a *warm absorber*. The existence of a warm gas was first proposed by Halpern [215] from X-ray observation of the quasar MR2251-178 with the *Einstein* observatory. This was the second quasar ever to be detected as an X-ray source, and only the third for which parameters defining a spectrum could be estimated. In one of the observations of the quasar, with a detector sensitive in the range from 1.2 to 20 keV, it was found that the spectrum showed absorption due to intervening matter, at the lower end of the energy range. If this absorption were to be due to cold matter, then there should be even greater absorption at energies lower than 1 keV. But simultaneous observation

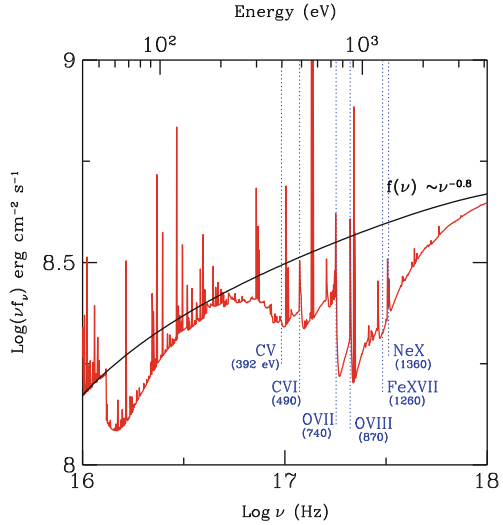
of the quasar with a detector which is sensitive up to ~ 0.1 keV led to higher than expected X-ray counts at low energies. There are different ways in which this excess could be explained, but the data were most consistent with absorption by a warm gas. Such a gas would lead to significant absorption at soft X-ray energies around 0.5–1 keV, but not at lower energies. The ionic species which could do the absorbing at low energies, and which are present in a cold gas at temperatures $\leq 10^4$ K, are largely absent from the warm gas since they undergo further ionization because of the prevailing conditions and the incident radiation.

Halpern's insightful argument were based on very limited observational data but have later been vindicated by many observations by subsequent X-ray missions, which had more sensitive detectors than the ones available to the pioneering observers. Warm absorbers have been found in about half of all active galaxies, mainly Seyfert galaxies of various kinds, observed at X-ray energies, some quasars, and a few blazars. There are reasons to believe that if enough sensitivity were available, essentially all AGN would be detected to have a warm absorber. High-resolution spectra from detectors on the *Chandra* and *XMM-Newton* X-ray satellites have helped identify specific absorption as well as emission features in warm absorbers, and these have led to some understanding of the physical state, distribution, and dynamics of the gas.

The basic physics of the warm gas is quite straightforward. The continuum radiation emerging from the region close to the central engine ionizes a gas through the photoelectric effect. For a given element in a certain stage of ionization, this happens at the threshold energy required to strip an electron from the ion, so that a sharp absorption edge is produced. As the photon energy increases beyond the threshold, the cross section for the process decreases approximately as ϵ^{-3} , where ϵ is the photon energy, producing a broad absorption feature associated with the specific ion. The ionization is followed by recombination of electrons with the ions and associated transitions within the ions, leading to the production of continuous as well as line emission. The atoms can be excited and deexcited by collisions as well, and the relative importance of the radiative and collisional processes depends upon the temperature of the gas and details of the atomic processes. The emitted radiation can either be reabsorbed or escape from the gas, depending on the optical depth of the medium at various photon energies.

Radiation consisting of photons with sufficient energy incident on a gas causes ionization, releasing free electrons into the gas, while the inverse process, recombination, reunites the electrons with the ions. When the source of radiation is in a steady state, or varies sufficiently slowly, then the number of ionizations are balanced by the number of recombinations, establishing an ionization equilibrium, in which the ratio of the number of various ionic species remains constant and depends on various factors mentioned below. The action of the radiation results in the gas reaching a certain temperature, which is determined by a balance between the heating and cooling of the gas. The heating occurs due to the energy of the photoelectrons $\epsilon - \epsilon_0$ introduced into the gas, where ϵ is the energy of the photon causing the ionization and ϵ_0 is the threshold energy for causing the ionization. The electron energy is thermalized due to its interaction with other

Fig. 3.24 A theoretical warm absorber spectrum [92]. The figure was kindly provided by Susmita Chakravorty



particles. Energy can also be gained by the gas through various other processes like thermal bremsstrahlung and at high temperature through the Compton effect. On the other hand, the gas loses energy due to the loss from the medium of the photons released due to recombination-related processes and through other processes like bremsstrahlung and the inverse Compton effect. When the heating and cooling balance each other, thermal equilibrium is reached at some temperature T of the gas. An excellent description of these processes can be found in [406].

The response of a cloud of gas to radiation from the AGN, and the nature of the ionic and thermodynamic equilibrium reached, depends on the spectrum of the radiation, the flux of the ionizing radiation at the cloud and the density and size of the cloud, and the chemical composition of the gas. The dependence on the flux and density can be conveniently encapsulated in an *ionization parameter*, which is proportional to the ratio of the density of the ionizing photons to the density of the gas:

$$\xi = \frac{L_{\text{ion}}}{n_{\text{H}} R^2}, \quad (3.1)$$

where L_{ion} is the ionizing luminosity, R the distance of the cloud from the source of the radiation, and n_{H} is the density of the gas. Various important properties of the gas, like the ratio of different ionization states, depend sensitively on this parameter.

A theoretical spectrum produced by a warm absorber is shown in Fig. 3.24. This is generated by passing radiation with a simple power-law spectrum $L(\nu) \propto \nu^{-0.8}$, with cutoffs at low and high energy, through a cloud of gas with properties indicated in the figure. The chemical composition is taken to be the same as that of the Sun and $N_{\text{H}} = n_{\text{H}} l$, with l the linear size of the medium. Several important absorption features are indicated and labeled, and some emission lines are indicated. The input spectrum is shown as a continuous black line. Such a theoretical spectrum, when

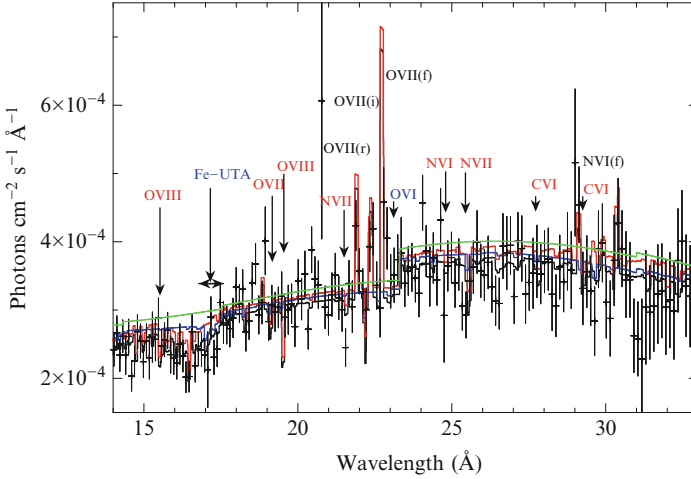


Fig. 3.25 The warm absorber spectrum of the Seyfert-1 galaxy Mrk 704, obtained using the program Cloudy [161] to fit data from XMM-Newton archives. The figure was kindly provided by Sibasish Laha and G. Dewangan

observed by an X-ray detector on board a satellite, presents a different appearance because of the broadening produced in the features due to various effects in the source and the limited and nonuniform sensitivity of the detector. Such an observed spectrum, which is obtained after significant processing of the raw X-ray data, is shown in Fig. 3.25. From observations and theoretical studies, it has been estimated that warm absorbers have a temperature around 10^5 K but could go as high as 10^6 K or as low as 10^4 K. It is difficult to estimate the density directly since it appears through ξ in combination with other quantities. Changing the density does not change the temperature of the warm absorber, unless the density becomes as large as $\sim 10^{14}$ cm^{-3} , when additional effects have to be taken into account. The typical density used while considering warm absorbers is $N_{\text{H}} = 10^9$ cm^{-3} but can span an enormous range around this value. References to the physics of warm absorbers may be found in [62, 92].

When the ionization parameter is increased, the number of ionizing photons available per gas particle goes up, which in general, results in higher ionization and higher temperature. Very useful insight into the nature of equilibrium states of the gas can be obtained by making a plot of the temperature T against ξ/T for equilibrium states obtained for a given gas cloud, for increasing values of ξ . Such a curve is shown in Fig. 3.26, for a gas of hydrogen and helium in the same ratio as the Sun. A point, like the one marked A in the figure, represents an equilibrium state at a temperature T for a specific value of ξ/T , which is proportional to the inverse of the pressure of the gas. If for the same value of pressure, the gas were to have a temperature somewhat greater than at A, then it would be represented by a point vertically above A since constant pressure means constant ξ/T . In this region,

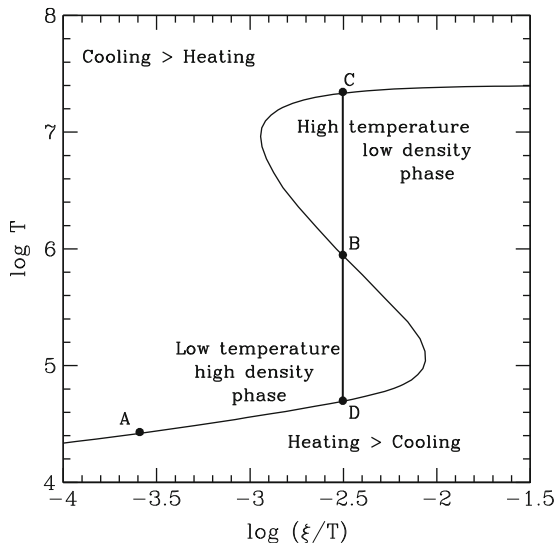


Fig. 3.26 The equilibrium curve for a warm absorber. The figure was kindly provided by Susmita Chakravorty

cooling dominates heating, and the gas cools to the point A, where it is again in equilibrium. Similarly, if the gas were at a temperature lower than at A, it would be heated more than it cools and would again reach the equilibrium temperature at A. The equilibrium at A is therefore stable. This would not be true at a point like B. If the gas were at higher temperature than at B, where the stability curve has a negative slope, it would be in a region where heating dominates, and it would continue to get hotter until it reaches a new equilibrium at C. Similarly, a gas which cools to slightly lower temperature than at B would continue to cool until it reached a new equilibrium at D. Gas in such regions would therefore split into two phases, both at the same pressure, but with one phase having much higher temperature than the other. When the chemical composition is made more realistic, with the addition of heavier chemical elements, amounting to just a percent or so of the total, the equilibrium curve can become much more complex, with a number of wiggles, as a result of which there can be more than two phases of the warm gas. Modeling of data from various sources has required one, two, or even three different phases, but models with a continuous variation of density and temperature are also possible.

Observation shows that the wavelengths of various features detected in warm absorbers are shorter than their laboratory counterparts, and the spectrum is said to be blueshifted. The shift occurs due to the Doppler effect, brought about by the gas causing the absorption moving toward the observer at high velocity. This indicates a general outflow of the warm absorber from the central region. The velocities in the case of active galaxies are generally in the range of hundreds of kilometers per second, while in quasars, they can be much higher and in some cases, are a significant fraction of the speed of light. The outflow is driven by the momentum

provided by the radiation in its interaction with the matter, and the outflow velocities can be different for different phases in the same source. The outflow does not uniformly cover the central source and occupies only a fraction of the volume of space around it. This fraction, known as the volume filling factor, is no more than several percent, can be substantially lower, and can be different for different phases in the same source. The total mass carried away by the flow can be estimated and ranges from a small fraction of the solar mass to several times the Solar mass per year. The AGN itself derives its energy from the gravitational energy released from matter accreting to it. The ratio of the outflowing mass to the mass being accreted can vary from a being much less than unity to several times unity. The kinetic energy of the flow, which can be estimated since the mass outflow rate and the velocity are known, and known, is less than one percent of the total radiant energy emitted by the AGN. Therefore, warm absorber outflows are not important for the overall energetics of the AGN. An excellent source for simple calculations leading to the estimates provided here is [62].

The great unknown in warm absorber physics is the distance of the gas from the central source. If the outflowing gas has to escape from the gravitational field of the black hole, then its observed velocity v_{out} should be greater than the escape velocity at a distance r of the flow from the AGN. This provides a minimum distance from which the flow can take place given by $r_{\text{min}} = 2GM/v_{\text{out}}^2$. The maximum distance of the flow can be estimated from the expectation that the size of an absorbing cloud is smaller than its distance from the central source. Using these arguments, [62] estimate that in the case of AGN, even the minimum distance of the warm absorber is much greater than distance of the broad-line region. In the case of the more luminous quasars, on the other hand, even the maximum estimated distances is substantially closer to the central source than the broad-line region.

While it has been established that warm absorbers occur in a substantial fraction, and possibly all, active galaxies, many of the details of their nature, and whether they have a substantial effect on the larger galaxy remain to be understood.

3.10.5 *More on the Fe K α Line*

Dear Jane (Turner), what fraction of sources now show a broad Fe K α line?

The most recent systematic study of local AGNs was that of [369] based on available XMM-Newton data. It was concluded that a large fraction of local AGN show emission that appeared best-fitted with a blurred reflection model but with a large dispersion in the characteristic radius of emission. However, when testing absorption models, the study did not allow the X-ray absorbers to have covering fractions less than unity nor was it able to test models against the spectral variability of AGN, as has been performed for successful absorption models of many local sources. Once covering fraction is allowed as a free parameter, then absorption-based models are also acceptable fits to the time-averaged X-ray spectra (e.g.,

Mrk 766 [369, 520]). The sample study that would reveal the true fraction of broad Fe emission lines must first account for the absorption signatures in the spectrum. In this author's experience, there are no believable lines with widths of several keV, as often claimed. However, a consensus on the occurrence rate of modestly broadened lines, like that detected over 6.5–7.0-keV band for Mrk 766, would be an interesting and useful study and could be performed using available archived data.

Successful flight of an X-ray calorimeter should resolve the issue by providing unprecedented resolution at 6 keV. The spectral resolution now achievable with calorimeters is $\text{FWHM} \simeq 7 \text{ eV}$. As technology development is still progressing positively for calorimeters, a spectral resolution $\text{FWHM} \simeq 4 \text{ eV}$ is projected at 6 keV for the calorimeters that should fly aboard ASTRO-H and $\text{FWHM} \simeq 2.5 \text{ eV}$ for those on the *International X-ray Observatory* (IXO) (note: at the time of writing, IXO faces an uncertain future based upon the astronomy and astrophysics decadal survey of the National Research Council, National Academy of Sciences).

Can broad Fe $K\alpha$ lines still tell us something important about the inner structure of an AGN?

Detection of discrete absorption lines in most local type-1 AGNs show there to be column densities up into the Compton-thick regime in and out of the line of sight and that the gas has a high global covering fraction. In one example, decomposition of the spectral states of Mrk 766 has isolated the variable and steady signatures of reprocessing, revealing an ionized component of Fe emission dominating the 6.5–7.0-keV band. The flux of the ionized line appeared well correlated with the continuum flux down to tens of ks [348], suggesting an origin for a modest (in strength) ionized component of Fe K emission within light-hours of the central black hole.

Obviously, the signatures of absorption, reflection, and scattering must be properly accounted for in order to extract the fundamental parameters of the system. While reflection signatures are clearly part of the mix, some recent results from reverberation *within* the X-ray bandpass indicate that reprocessing may be dominated by signatures in the regime of a few tens to hundreds of gravitational radii, rather than being dominated by blurred signatures much closer to the black hole event horizon.

Thank you, Jane. Since the Fe $K\alpha$ emission is still a hot and debated issue, we now ask a few questions to Ajit Kembhavi.

Dear Ajit (Kembhavi), where is the iron Fe $K\alpha$ line produced in AGN? In some sources, it shows a strong red asymmetry that has been attributed to gravitationally redshifted emission produced near the inner edge of the accretion disk. Is it possible that it simply arises from Compton downscattering of emission-line photons?

The X-ray spectrum of many Seyfert galaxies contains an emission feature at $\sim 6.4 \text{ keV}$, which is identified to be line emission from iron. This feature provides very important insight into the way the observed spectrum is produced in the region around the center. The line is found to be very broad, and there is a good

case to say that the line originates in a region which is very close to the central supermassive black hole. General relativistic effects due to strong gravity have therefore to be taken into account in explaining the profile of the emission line, and with good data, it will be possible to measure mass and spin of the black hole.

X-rays, which have energy in the keV range, can photoionize an electron from the inner shells of atoms of heavy elements. The atom is then in an excited state and can lose energy when the vacant state is filled by an electron from one of the higher levels, leading to the emission of a photon, which is known as fluorescence. An alternative process, known as the Auger effect, is where the filling of the vacancy is accompanied by the ejection of an electron from a higher shell, and the atom loses energy in a radiationless manner. The fluorescent yield of a shell is a measure of the fraction of time an atom loses energy through the emission of a photon, following ionization from that shell. The intensity of an emission line produced through fluorescence depends on the product of the fluorescent yield for the shell and the abundance of the element. This product is the highest for iron, and therefore, it is the iron fluorescence which is the most important in the X-ray spectra of AGN. The energy of the iron K_{α} varies from 6.4 keV for neutral iron to 6.9 keV for FeXXVI, which is iron with all but one electron removed, with the difference in energy being due to the screening effect of the electrons when they are present.

Iron emission and absorption features were first observed in a few AGNs by early satellites including ARIEL, TENMA, and EXOSAT, but these features were established as being common in the spectra of AGNs through observation by the X-ray satellite GINGA [367]. In these observations, an emission line was found with energy close to 6.4 keV, which is consistent with the feature being the K_{α} line due to fluorescence from cold (neutral) iron. A simple interpretation here would be to say that the emission is produced in transmission, that is, by iron in a gas along the line of sight to the observer. But iron is only a small fraction of such a gas (a few hundredths of one percent of the mass of the gas is in iron), and to produce an emission line with the observed strength would require so much gas that it would produce greater absorption at X-ray energy below 2 keV than is actually observed. The absorption would be less if the gas were ionized, but then the iron would be partially ionized too, and the iron line would have greater energy than is observed. A transmission model is therefore not consistent with observations, and one has to turn to reflection models.

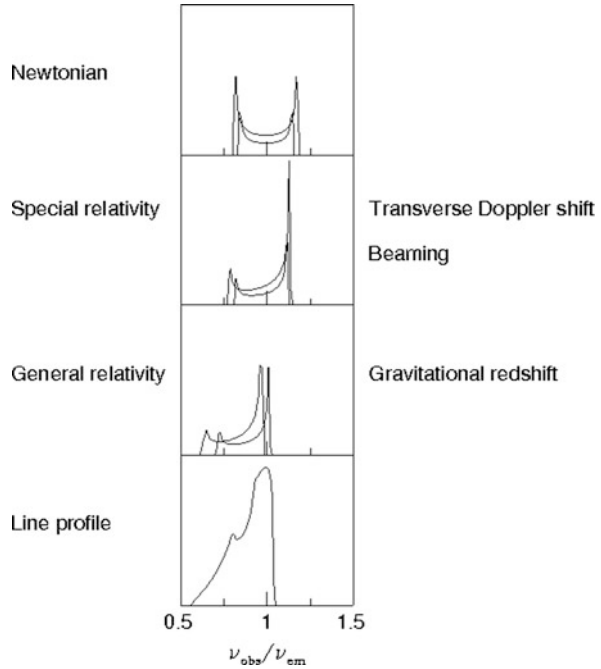
The X-ray emission is thought to arise in a hot gas in a corona around the accretion disk. Photons produced in the optical and ultraviolet region of the spectrum by the accretion disk around the central black hole are boosted to X-ray energy by the electrons in the corona through the inverse Compton effect. This results in X-rays having a power-law spectrum. A fraction of the photons with the power-law spectrum travel to the observer, while others are directed toward the relatively cold accretion disk. Here, they undergo repeated scattering and can emerge from the cold matter they are interacting with, to travel in the direction of the observer. The spectrum of these photons is altered due to the energy loss they suffer in the Compton scattering. Some of the photons which enter the cold matter photoionize iron atoms in the slab, and iron K_{α} lines are produced by fluorescence,

some of which travel toward the observer. So the spectrum that the observer sees is a combination of the original power-law spectrum and the reflected spectrum, which includes the iron line. The spectrum at low energies is also altered by the absorption it undergoes in traveling through partially ionized matter. A simple description of the physics of the iron line and reflection, with references to the original work, can be found in [139, 261].

The iron line produced due to reflection from the accretion disk is very narrow at emission but can be broadened due to various effects. The disk is in rotation around the central black hole, with the rotation speed of an annulus with radius r having the Keplerian value $v = \sqrt{GM/r}$. The radiation emitted from parts of the disk moving away from the observer is found to have lesser photon energy than at emission. The observed wavelength is therefore greater than the emitted wavelength, and the radiation is said to be redshifted. Similarly, radiation emitted from parts of the disk moving toward the observer has higher photon energy, or decreased wavelength, and is said to be blue shifted. The parts of the disk which are closer to the center rotate at a greater velocity, so that the Doppler effect on radiation from the inner region is greater. The rotation results in a two-horned structure for the line profile, as is shown in the upper panel of Fig. 3.24 [139], for emission from two annuli. Such a line profile is obtained for emission from a rotating disk, when the rotation velocity is nonrelativistic, that is, small compared to the speed of light. The X-ray emission occurs from a compact region close to the center, where the gravitational field is strong, the velocities are high, and special relativistic effects become important. This results in increase in the intensity of the radiation from the blueshifted peak, due to the relativistic beaming effect, which makes the blue peak taller than the redshifted peak as shown in the second panel from the top in Fig. 3.24. The high velocities also lead to a transverse Doppler effect, which causes photons to be redshifted to lower energy. A similar effect is produced by gravitational redshift, which causes the photons to lose energy as they move from a region with strong gravity to the distant observer. The magnitude of these effects depends on the radius of the annulus of the accretion disk from which they are emitted, and the effect on radiation from two different annuli is shown in the third panel of Fig. 3.24. The above effects acting together broaden and smear the emission line, as shown in the bottom panel.

How much the line is broadened depends on how close the inner part of the disk gets to the black hole and the inclination of the disk. For a Schwarzschild black hole, which has mass but no spin, the minimum possible radius that the inner part of the disk can reach is $6r_g$, with $r_g = GM/c^2$, where M is the mass of the black hole, G is the gravitational constant, and c is the speed of light. There are no stable orbits at smaller radii, and the matter which enters such a region plunges toward the black hole. If the black hole is spinning, that is, has angular momentum, then the radius of the last stable orbit can be much smaller, that is, the inner part of the disk can be located closer to the black hole, so that gravity is stronger and the rotation speed is higher, which makes the line greatly broadened. The last stable orbit has the smallest radius of about $1.25r_g$ when the black hole has the maximum spin general relativistic considerations permit. The observed breadth of the line should

Fig. 3.27 The broadening of an emission line due to rotation, special relativistic effects and strong gravity [141]



make it possible to estimate the spin of the black hole (Fig. 3.27). Useful reviews and references to the literature on these matters and the observational situation may be found in [139, 141, 435].

A very well-studied AGN for details of the iron line is the Seyfert galaxy MCG-6-30-15, in which the iron emission is particularly strong because the iron abundance is about 2 times the solar value. This galaxy was observed by the X-ray satellite ASCA in a long exposure of about four days with a detector with very good energy resolution [502]. The profile of the line was found to be made up of two parts: a narrow component around 6.4 keV and a broad part extending to lower energies, or redward, of 6.4 keV. The feature was so broad that if the redshift were to be produced due to the Doppler effect alone, then the velocities involved would be as high as $\sim 100,000 \text{ km s}^{-1}$. Detailed modeling showed that asymmetric profile most probably arises from the innermost parts of an accretion disk around a Schwarzschild black hole, the region of emission extending from $6r_g$ to $10r_g$ from the center. The shape of the line has been later studied in great detail by ASCA, as well as later satellites like *Beppo-SAX*, *XMM-Newton*, and *Suzaku* (Fig. 3.28). The observations indicate that the broadening of the line observed requires emission from regions closer to the black hole than $6r_g$, with detailed modeling leading to inner disk radius as small as $2r_g$. Since this is much smaller than radius of the last stable orbit for a non-rotating Schwarzschild black hole, it appears that the black hole must have spin and in fact, must be rotating close to its extremal value. The

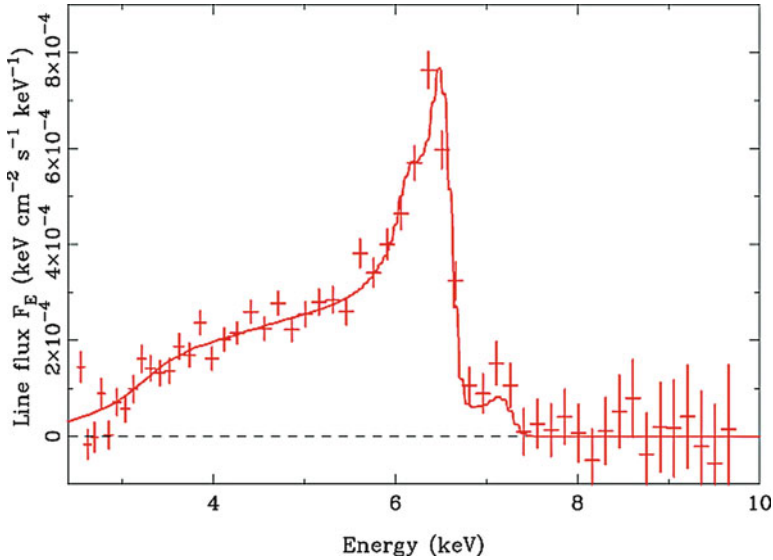


Fig. 3.28 The broad iron line in MCG-6-30-15 obtained from XMM observations [140]

line emission, and other radiation associated with reflection, must therefore arise from a very compact region in which gravity is very strong, and effects which could be traced to light bending in the strong gravitational fields have been seen in the data. However, one cannot yet unambiguously say that black hole spin has been detected. It is possible, for example, to argue that there is no spin, and the emission from the innermost regions arise from matter plunging within the innermost stable orbit of a Schwarzschild black hole.

The possibility that the broad iron line is indicative of a spinning black hole is a very exciting one, but the importance of the conclusion requires that the interpretation is established as being unique to the data. One possible way to explain the shape of the line is through Compton scattering [354, 355]. In this model a narrow iron line is broadened due to repeated Compton scattering by electrons in a cloud surrounding the X-ray source. The cloud is taken to be relatively cool, so that the average energy of the electrons in it about 0.2 keV, which is much less than the energy of the iron line photons. In each scattering therefore, the photons lose energy due to the Compton process, and the asymmetric broad shape extending to low energy can be obtained. The cloud needs to have sufficient density and size (i.e., optical depth) to make repeated scattering possible. It also needs to be highly ionized, as otherwise strong iron absorption features would be produced which are not seen in the data. There are various arguments against such a model which are summarized in [139]. It has recently been proposed by [347] that the line shape could be explained by a complex pattern of absorption produced by multiple absorbers, which are moderately ionized and partially cover the source. Various

arguments have been made against such a model by Reynolds et al. [437], but these have been refuted [346, 569].

Given the observational situation, it seems on balance that iron line observed in MCG–6–30–15, and in other AGN, is indicative of the effects of strong gravity and very likely indicates that there is a spinning black hole at the center of the AGN.

Thank you, Ajit. The last years have seen an impressive increase of γ -ray detections of quasars with Fermi. We have asked Luigi Foschini a short review of the main results achieved until now.

3.11 The γ Ray Domain

Dear Luigi (Foschini), what was the understanding and the expected properties of quasars emitting γ rays before Fermi?

Basically, a large part of all the knowledge in this research field was built on the observations performed by the Energetic Gamma Ray Experiment Telescope (EGRET) onboard the *Compton Gamma Ray Observatory* (CGRO, 1991–2000).⁸ The third EGRET catalogue contained 271 γ -ray sources, detected at energies between 100 MeV and more than 20 GeV [219], but only roughly one third was identified. Among the identified sources, the vast majority was composed of quasars (66), followed by BL Lac Objects (21), 10 generic flat-spectrum radio sources, and 1 radio galaxy.⁹ A very important complement to space-based observations came from the improvement of ground-based Čerenkov telescopes, operating TeV energies, which, during 1990s, made it possible to start detecting several BL Lacs (see [228] for a review). The first quasar, 3C 279 ($z = 0.536$), was detected only in 2008 by MAGIC [16].

From an observational point of view, these sources are characterized by strong variability at almost all the wavelengths,¹⁰ even on very short timescales: from a few minutes in the cases of the BL Lac objects PKS 2155–304 ($z = 0.116$, [14]) and Mrk 501 ($z = 0.034$, [15]) to less than 1 hour for the quasar NRAO 530 ($z = 0.902$, [170]). Almost all the quasars and some BL Lac objects display an ultraviolet thermal bump, while the optical emission is often polarized [173, 316, 555]. The emission lines observed in quasars are strong (equivalent width $EW > 5 \text{ \AA}$, e.g., [408]), and there is a sharp roll off in the distribution of their FWHM at about $2,000 \text{ km s}^{-1}$ [556]. On the other hand, BL Lacs often do not show lines, but when present, they are weak ($EW < 5 \text{ \AA}$) and broad [107]. Observations at radio

⁸Before *CGRO*, only one quasar, namely, 3C 273 ($z = 0.158$), was detected at high-energy γ rays (50–500 MeV) by *COS-B* [501].

⁹Another radio galaxy—NGC 6251 ($z = 0.025$)—was later indicated as counterpart of the γ -ray source 3EG J1621+8203 [168, 359, 366].

¹⁰Indeed, an old classification name for certain quasar was optically violently variable (OVV).

frequencies give similar results: rapid variability (flux, spectrum, polarization), brightness temperature in excess of the Compton limit $T \sim 10^{12}$ K (cf. [429]), and extended structures from pc to kpc scales (e.g., [579]). Sometimes, components moving at superluminal speed can be observed. This effect, known since 1960s [430] and detected for the first time in early 1970s [100], indicates the presence of relativistic motion.

However, specifically in the case of quasars, it often happens that the source is very compact, and therefore, it is not possible to observe significant motion of unresolved components. In this case, the observation of high energy and variable γ rays can give the unequivocal proof of the presence of a relativistic jet viewed at small angles. Indeed, as the γ energy surpasses the sum of two electrons rest energy (2×511 keV), the photon can disappear while generating a electron/positron pair, if it finds another particle or field to interact with,¹¹ in order to save the momentum budget. Therefore, if one detects γ rays with energies greater than several MeV, this means that something hampered the pair production, and this is special relativity in action. Indeed, the Doppler boosting¹² reduces the $\gamma\gamma$ opacity of the source by a factor δ^6 . By using common values for quasars, it is possible to show that a Doppler factor of a few is already sufficient to allow high-energy γ rays to escape (see, e.g., [329] for details in the calculations).

It is worth noting that observations at γ rays are important not only to establish the presence of a jet but also because they are a direct gauge of the bolometric power of the source.

When putting together all the information gathered from multiwavelength observations, the resulting spectral energy distribution (SED) has the characteristic double-humped shape. The component at low frequencies (infrared/X-rays) displays the typical features of the synchrotron emission from relativistic electrons. The higher-energy component is thought to be due to inverse-Compton scattering of the same population of electrons off seed photons from different regions. The frequencies of the two peaks change depending on the bolometric luminosity of the source, forming a “sequence” [172] where the most powerful quasars have the peaks at relatively low frequencies (infrared for synchrotron; MeV–GeV for inverse Compton), and the less luminous BL Lac Objects have instead the peaks at greater frequencies (ultraviolet/X-rays for synchrotron; TeV for inverse-Compton). Radio galaxies have even lower power, and it is not (yet?) known if they form a sequence too. The “sequence” has been recently revised by [189], explaining the observed SED as a function of mass of the central black hole and its accretion rate: the masses are distributed over a range $10^{8-10} M_{\odot}$, although BL Lacs tend to be within $10^{8-9} M_{\odot}$. Most important is the dividing line of the accretion, which is set to $L_{\text{disc}}/L_{\text{Edd}} \sim 10^{-3}$. Below this value are BL Lacs, while quasars display greater values.

¹¹The process with the greater cross section is the photon–photon interaction ($\gamma\gamma$).

¹² $\delta = [\Gamma(1 - \beta \cos \theta)]^{-1}$, where Γ is the bulk Lorentz factor, β is the speed in units of c , and θ is the viewing angle.

The main interpretation of these observational features is that we are observing a relativistic jet at small angles, so that the effects of special relativity play a dominant role in shaping the observed electromagnetic emission. The first pillars of the unified model of active galactic nuclei (AGN) with relativistic jets were set up by Blandford and Rees [57], in their seminal talk given at the “Pittsburgh Conference on BL Lacs.” In the same conference, Ed Spiegel proposed to unify also the names of BL Lac objects and quasars since they share several observational properties due to the presence of the relativistic jet. He proposed to collectively call all these sources *blazars*, which is the contraction of the names BL Lacs and quasars. Barthel [37] proposed the unification of blazars and radio galaxies, on the basis that they are the same type of source—an AGN with relativistic jet—viewed at different angles: small for blazars and large for radio galaxies. Special relativity effects play a dominant role in the former, while in the latter, they are much weaker, and therefore the jet has to compete with the emission from the other AGN components. This scenario was later refined and organized in a unified model by Urry and Padovani [529].

It is worth noting that both blazars and radio galaxies are hosted in elliptical galaxies, and it is believed that BL Lacs are the evolution of quasars. The latter are sources that can be present up to high redshifts and have high accretion rates, while the former have low accretion power and low redshift. Therefore, BL Lacs should be the evolution of the quasars when they are going to finish their fuel [69,90,318].

***Fermi* has a unique spatial resolution. What are other principal observing capability of the observatory? What are the properties of the typical (and less typical) sources detected by *Fermi*? Is *Fermi* simply improving or is it revolutionizing our understanding of quasar γ -ray emission?**

The Large Area Telescope (LAT, [24]) onboard the *Fermi Gamma-ray Space Telescope* is really a jewel of the modern technology. It has improved the flux sensitivity by a factor ~ 30 with respect to CGRO/EGRET and has a much larger field of view (2.4 steradians), which permits to perform an all-sky survey every two orbits (~ 3 h). For the first time, it is possible to monitor in near real time all the sky at γ rays. Also, the spatial resolution improved by roughly one order of magnitude with respect to EGRET, reaching the value of a few arcminutes (at 1 GeV), which is exceptional at γ rays. This performance permitted—for the first time—to resolve at GeV energies a jet from the core at least in a nearby radio galaxy (Centaurus A, 3.7 Mpc, [6]).

The first *Fermi* catalogue,¹³ released after 1 year of operations, contains $\sim 1,500$ sources at $E > 100$ MeV [7], and roughly half of them are still unidentified. In addition to blazars [190], which are still the greatest population of γ -ray sources, there are 11 radio galaxies [5], tens of galactic sources (mainly pulsars), a few nearby starburst galaxies [8,303], two of them detected also at TeV by HESS [13]

¹³At the moment of writing these notes, the second catalogue covering 2 years of operations has not yet been published, but it is forthcoming.

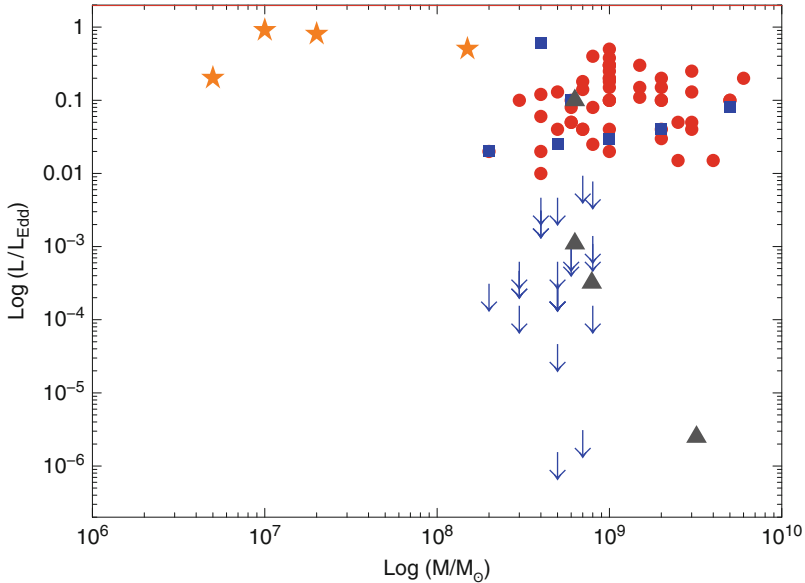


Fig. 3.29 Mass of the central space-time singularity vs. the accretion power (see also [167]). *Red circles* are flat-spectrum radio quasars, while *blue squares* (or upper limits) are BL Lac objects (data from [190]). *Gray triangles* are radio galaxies detected at γ rays ([5]; data on mass and accretion are from [471]). *Orange stars* are NLSy1 from [2]

and VERITAS [11], and a handful of narrow-line Seyfert-1 galaxies (NLSy1s, [2], see also [167] for a review).

The most important discovery is, in my opinion, the γ -ray emission from NLSy1s. The first one was PMN J0948 + 0022 ($z = 0.585$), which was detected at GeV energies during the first months of operations of *Fermi* [3, 169]. A multiwavelength campaign was immediately set up (2009 March–July), during which coordinated variability was detected at all the wavelengths, from radio to γ rays, confirming that the γ rays were indeed emitted by the NLSy1 and that the electromagnetic emission spectrum was dominated by the radiation of a relativistic jet very similar in power and behavior to those in blazars [4]. Later, three more NLSy1s were discovered by analyzing the first year of LAT data [2]. In July 2010, again, the NLSy1 PMN J0948 + 0022 underwent a strong outburst reaching a γ -ray luminosity of $\sim 10^{48}$ erg s^{-1} , at the level of the most powerful quasars, which was preceded by a significant change of the radio polarization angle [171].

However, although the relativistic jets in NLSy1s seem to be very similar to those in blazars, these sources are neither blazars nor radio galaxies. Figure 3.29 shows the mass vs. accretion rate for blazars (cf. [189]) and radio galaxies, together with NLSy1s. It is immediately evident that NLSy1s are the third class of γ -ray emitting AGNs, after blazars and radio galaxies. Other distinctive features are (a) the FWHM distribution of the BLR emission lines, which is different from those of quasars, the latter having a roll off at $\sim 2,000$ km s^{-1} [556], and the former a cutoff

at the same threshold [411]; (b) the extreme compactness of the radio emission, generally confined within a few parsecs or tens of parsecs, despite the extreme power generated at γ rays; (c) last, but not least, the host galaxy of NLSy1s has spiral morphology, while blazars and radio galaxies are hosted in ellipticals. Presently, only one of the four γ -ray NLSy1s has been observed with sufficient resolution to show a spiral morphology (1H 0323 + 342, $z = 0.061$ [21, 580]). The others are quasar-like, but low-resolution observations suggest that they could be hosted in gas-rich disk galaxies, probably as the result of a recent merger [575]. Future works should clarify this issue.

Therefore, this discovery casts severe doubts on the paradigm that linked the presence of relativistic jets to elliptical host galaxies (e.g., [69, 90, 318, 529]). On the other hand, it is worth reminding that such a paradigm is unlikely because it is known that jets are rather ubiquitous, from protostars, to galactic compact objects (cataclysmic variables, neutron stars, stellar mass black holes), to AGNs, and gamma-ray bursts (see, e.g., [166] for a review). Therefore, it would be rather strange that only in AGN that there was a dependence on the host. This was already clear to Roger Blandford in 1978. At the “Pittsburgh Conference on BL Lacs,” when G. Burbidge asked him “Roger, is your model for AO 0235+164 an elliptical galaxy with a black hole at the center?” Blandford replied, “I would say that it is either a galaxy or a protogalaxy. As the continuum emission is proposed to originate in the central 10 pc, I don’t think the nature of the surrounding object is particularly relevant to the model” (see the minutes of the discussion after the talk in [57]).

I think it is too early to say if these or other yet to be done discoveries will revolutionize our knowledge about quasars. My answer would be “yes!” but I am strongly biased by my role in the discovery of γ -ray emission from NLSy1s (*Cicero pro domo sua. . .*). Surely, the data gathered from *Fermi* and the present generation of Čerenkov telescopes (MAGIC, HESS, VERITAS) are raising important questions on present theories, pushing our minds to think more deeply. This is already a great undoubtable success.

Thank you, Luigi.

Dear Yuri (Neshpor), could you please summarize the main γ ray observations carried out by Soviet astronomers?

Search for high-energy ($E > 10^{11}$ eV) gamma radiation of AGN and subsequent study of its variability have been carried out at the Crimean Astrophysical Observatory (CrAO) since 1969 by means of the Cherenkov flashes [485]. Among the first objects studied at CrAO with the Cherenkov γ -telescope of the first generation RChV-1 [485] were active galaxy nuclei BL Lac, OJ 287, and 3C 120. The power spectrum of radiation, the absence of spectral lines, and rapid brightness variations in these objects strongly indicated there is a great number of high-energy particles. However, no statistically significant level of very high-energy gamma fluxes (VHE, $E > 10^{12}$ eV) was found in these objects. Later, a new gamma telescope of the second-generation GT-48 [539] was built in CrAO. The telescope consists of forty-eight 1.2-m mirrors, with total area of 54 m². This was the first stereoscopic device which allowed to register images of the Cherenkov flashes produced both

Table 3.1 Fluxes from γ -ray sources

Name	Distance [kpc]	Log L [erg s^{-1}]	Year of the first observation and observers	Reference
3C66A	1,800,000	46.3	1996 (CrAO)	[377]
IH 1426 + 428	516,000	44.0	2001 (Whipple)	[236]
BLLac	280,000	44.5	1998 (CrAO)	[378]
IES 1959 + 650	192,000	43.8	1999 (Array)	[387]
IES 2344 + 514	176,000	42.5	1997 (Whipple)	[89]
Mrk501	136,000	44.5	1995 (Whipple)	[420]
Mrk421	124,000	44.0	1992 (Whipple)	[417]

by the proton-nuclear component of cosmic rays and by the VHE gamma quanta penetrating into the Earth's atmosphere. Observations with the gamma-telescope GT-48 began in 1989.

Investigation of AGNs in the VHE range, by means of ground-based gamma-ray telescopes, started in the world in 1990s after the orbital observatory EGRET's discovery of γ -ray emission with energy above 100 MeV from a number of AGN. In CrAO, observations of AGNs have been carried out with GT-48 since 1996 and up to date [378, 381, 382, 486]. The results are given in Table 3.1.

In 1996, GT-48 has first registered with high confidence level the VHE gamma emission from AGN 3C 66A [377]. Earlier, up to the end of twentieth century, it was believed that VHE gamma quanta can be detected only from the objects with $z < 0.1$. The distance to the 3C 66A is rather large, $z = 0.444$, and the flux of gamma quanta must be considerably weakened. Therefore, many astrophysicists were skeptical about this result. However, later in 2007–2008 the gamma-telescope VERITAS has registered the flux of gamma quanta with energy $E > 100$ GeV at the significance of 21.2 standard deviations [12].

From observations of Mrk 501 galaxy in 1997 the flux of VHE gamma quanta was shown to be variable on a timescale of a day [251]. Observations of the VHE flux from Mrk 501 galaxy in 1997, 1998, and 2000 with GT-48 showed the annual flux variability [20] and confirmed the presence of a periodic component [274] with period of 23.2 days [379].

In 1998, with GT-48, the VHE gamma-ray emission from BL Lac galaxy was first detected [378]. Later, it was confirmed by observations with the gamma-telescope MAGIC [17]. From 2 years of observations (2000 and 2002) of BL Lac galaxy, we found a positive correlation between the average flux of the VHE gamma quanta during a lunation (moonless period over a month) and the average optical brightness of the object over the same time interval [380]. In observations of Mrk 421 galaxy from December 2 to December 6, 2002, the VHE gamma-ray burst was registered. It has coincided in time with the X-ray burst in the region of 3–25 keV. The significance of the registered VHE gamma-ray emission during the X-ray burst was 5.1 standard deviations [164].

Thank you, Yuri. Space observations have really opened a new world of scientific possibilities also in the IR domain. Quasars are known to be strong emitters in

the mid-far IR since the 1980s when many were detected by IRAS. A major increase occurred recently with the IR observatory Spitzer. We have asked Alberto Franceschini to provide us a panoramic view of the scientific results achieved in this waveband.

3.12 Observations at Infrared Wavelengths

Dear Alberto (*Franceschini*), what are infrared observations teaching us about the properties of active galactic nuclei and quasars?

Our knowledge of the structure and physical properties of active galactic nuclei and quasars has received a dramatic boost by space telescopes observing in the mid and far-infrared. At these wavelengths, the observation from a space platform is made necessary by the complete opacity of the Earth atmosphere. Indeed, if the AGN unification paradigm has some value, we expect strong signatures of the hot dust emission to show up in the mid- and far-IR. As a matter of fact, the circumnuclear dust predicted by the model is illuminated by the intense radiant field of the nuclear source, absorbs the UV photons emitted in the direction of the torus, heats up, and then reradiates this absorbed energy like a blackbody process at the grain equilibrium temperature. The field is so intense that part of the dust grains sublimate, while the other emit at temperatures ranging from several tens to thousands absolute degrees, corresponding to photon wavelengths ranging from a few to several tens of μm .

Already, the first IR space observatory, IRAS, performing a 1-year-long all-sky survey in 1984, revealed intense emissions in the far-IR by Seyfert galaxies and quasars [476]. These results were confirmed by observations at the millimeter with large ground-based mm observatories (SEST, JCMT, IRAM, among others, [19, 50, 391]).

IRAS was a small cooled telescope able to detect only bright local AGNs and the most luminous quasars. Ten years later, the Infrared Space Observatory (ISO) confirmed the IRAS results and detected higher-redshift objects, thanks to a better sensitivity and longer targeted observations. ISO also carried out the first IR spectroscopic observations of cosmic sources. Extensive characterization of IR line emission properties of both local and high-redshift objects was made possible in 2003 with the new-generation observatory *Spitzer* Space Telescope and more recently in 2009, with the first 4-m class telescope in space, *Herschel*.

Thank you, Alberto.

3.12.1 Evidence of a Thick Torus

Dear Alberto, does the observational evidence favor a thick torus of dense molecular gas?

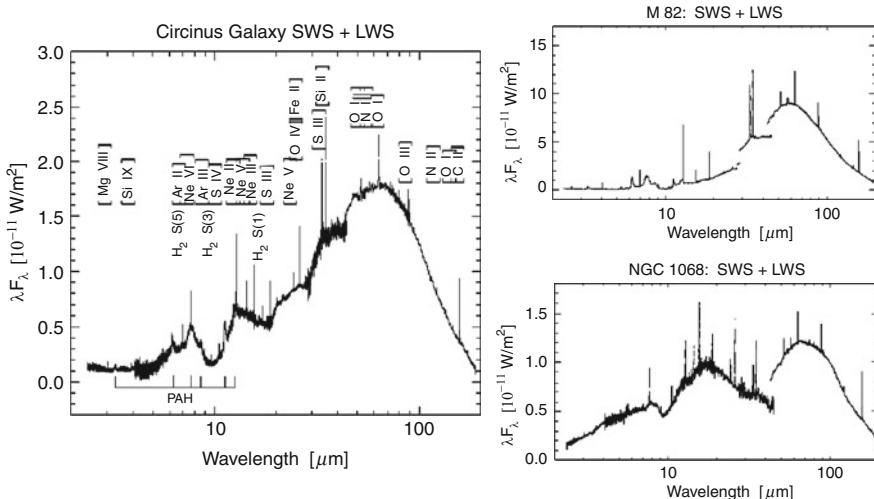


Fig. 3.30 ISO spectra of prototypical IR-bright active galaxies: the starburst galaxy M82, the closeby type-2 AGN NGC 1068, and the heavily extinguished AGN the *Circinus* galaxy. A number of coronal emission lines, PAH emission boundlets at 6–10 μm and many other spectral features are visible [187]

All these observations offered a dramatic evidence for the existence of circumnuclear dust in AGN: all kinds of active galaxies and quasars revealed prominent emission at wavelengths longer than 1 μm . Although being slightly debated originally (one considered possibility was synchrotron radiation, see, e.g., [130]), theoretical astrophysicists soon realized that this intense emission can only be interpreted as dust thermal reradiation. This thermal component was found to be present in all active galactic nuclei and quasars of the radio-quiet category, with the only exception of a few radio-loud sources clearly dominated by synchrotron emission, but these make a small fraction of the quasar population. Figure 3.9 on page 123 shows a composite spectrum of various categories of AGNs: the dust reradiation bump in radio-quiet quasars is clearly seen to peak between 1 and 10 μm or rest frequencies of 10^{13} – 10^{14} Hz. It is also shown that in type-1 quasars, as much as one-third of the bolometric emission emerges in the far-infrared: simple geometrical consideration indicates that this is approximately the sky-covering factor intercepted by the torus of the central power source in luminous type-1 quasars.

At the same time, infrared observations revealed that type-2 AGNs have an even more prominent emissivity in the far-IR, while the optical emission being depressed. In particular, the nuclear emission of the prototype type-2 Seyfert galaxy, NGC 1068 (Fig. 3.30 below), showed extremely red colors from 1 to 30 μm , well fit by hot circumnuclear dust emission [199].

All this confirmed the overall validity of the unification model for local active galactic nuclei, hence the widespread existence of a thick torus of dense molecular gas in all of them (perhaps less evident in the small minority of radiogalaxies).

Can we detect dust signatures in the torus emission spectrum?

This question remained unanswered for long time because, although the broad-band photometric properties of quasars were well established over a large interval of wavelengths (Fig. 3.9 on page 123), the investigation of the detailed spectral features of dust emission and absorption in quasar spectra required the operation of the first IR spectrographs on ISO and later on *Spitzer*.

The first characterization of IR spectra by ISO clearly revealed the occurrence of the silicate absorption features at 9.7 and 18 μm , like shown in the spectrum of the type-2 quasar the *Circinus* galaxy in Fig. 3.30. This was apparent in essentially all spectra of type-2 AGNs and is easily understood if we consider that, according to the unification model, this category of AGNs are observed with inclinations of the observer line of sight intersecting the torus: the silicate grains, present as a major component of the dusty molecular gas, then preferentially absorb photons at these two wavelengths due to the two spectral features present here.

Another aspect of this question concerns the population of type-1 objects: in such case, the observer line of sight is face on to the dusty torus and does not intersect it. Therefore, all photons preferentially absorbed by the torus' silicates at 9.7 and 18 μm are expected to be reemitted by the torus itself in the form of two emission features. While ISO did not have the sensitivity to detect them, the more sensitive *Spitzer* spectrographs eventually identified the 9.7 μm emission in type-1 quasars, which however turned out to be broader than expected (the reason for the ISO non-detection). Again a good, convincing proof of the local general validity of the unification scheme.

Thank you, Alberto.

References

1. Abazajian, K.N., Adelman-McCarthy, J.K., Agüeros, M.A., et al.: The seventh data release of the sloan digital sky survey. *Astrophys. J. Suppl. Ser.* **182**, 543–558 (2009)
2. Abdo, A.A., Ackermann, M., Ajello, M., et al. (*Fermi* Collaboration): Radio-loud narrow-line seyfert-1 as a new class of gamma-ray active galactic nuclei. *Astrophys. J.* **707**, L142–L147 (2009)
3. Abdo, A.A., Ackermann, M., Ajello, M., et al. (*Fermi* Collaboration): *Fermi* large area telescope discovery of gamma-ray emission from a relativistic jet in the narrow-line quasar PMN J0948+0022. *Astrophys. J.* **699**, 976–984 (2009)
4. Abdo, A.A., Ackermann, M., Ajello, M., et al. (*Fermi* Collaboration): Multiwavelength monitoring of the enigmatic narrow-line seyfert-1 PMN J0948+0022 in 2009 march-july. *Astrophys. J.* **707**, 727–737 (2009)
5. Abdo, A.A., Ackermann, M., Ajello, M., et al. (*Fermi* Collaboration): *Fermi* large area telescope observations of misaligned active galactic nuclei. *Astrophys. J.* **720**, 912–922 (2010)
6. Abdo, A.A., Ackermann, M., Ajello, M., et al. (*Fermi* Collaboration): *Fermi* gamma-ray imaging of a radio galaxy. *Science* **328**, 725–729, (2010)
7. Abdo, A.A., Ackermann, M., Ajello, M., et al. (*Fermi* Collaboration): *Fermi* large area telescope first source catalog. *Astrophys. J. Suppl. Ser.* **188**, 405–436 (2010)

8. Abdo, A.A., Ackermann, M., Ajello, M., et al. (*Fermi* Collaboration): Detection of gamma-ray emission from the starburst galaxies M82 and NGC 253 with the large area telescope on *Fermi*. *Astrophys. J.* **709**, L152–L157 (2010)
9. Abdo, A.A., Ackermann, M., Ajello, M., et al.: Multi-wavelength observations of the flaring gamma-ray blazar 3C 66A in 2008 october. *Astrophys. J.* **726**, 43 (2011)
10. Abramowicz, M.A.: Vorticity-free rings orbiting black holes. I – The metric. *Astrophys. J.* **254**, 748 (1982)
11. Acciari, V.A., Aliu, E., Arlen, T., et al. (VERITAS Collaboration): A connection between star formation activity and cosmic rays in the starburst galaxy M82. *Nature* **462**, 770–772 (2009)
12. Acciari, V.A., Aliu, E., Arlen, T., et al. (VERITAS Collaboration): VERITAS observations of a very high energy γ -ray flare from the blazar 3C 66A. *Astrophys. J.* **693**, 104 (2009)
13. Acero, F., Aharonian, F., Akhperjanian, A.G., et al. (HESS Collaboration): Detection of gamma rays from a starburst galaxy. *Science* **326**, 1080–1082 (2009)
14. Aharonian, F., Akhperjanian, A.G., Bazer-Bachi, A.R., et al. (HESS Collaboration): An exceptional very high energy gamma-ray flare of PKS 2155–304. *Astrophys. J.* **664**, L71–L74 (2007)
15. Albert, J., Aliu, E., Anderhub, H., et al. (MAGIC Collaboration): Variable very high energy γ -ray emission from markarian 501. *Astrophys. J.* **669**, 862–883 (2007)
16. Albert, J., Aliu, E., Anderhub, H., et al. (MAGIC Collaboration): Very-high-energy gamma rays from a distant quasar: how transparent is the universe? *Science* **320**, 1752–1754 (2008)
17. Albert, J., Aliu, E., Anderhub, H., et al. (MAGIC Collaboration): *Astrophys. J.* **696**, 2170 (2009)
18. Allen, S.W., Dunn, R.J.H., Fabian, A.C., et al.: The relation between accretion rate and jet power in x-ray luminous elliptical galaxies. *Mon. Not. R. Astron. Soc.* **372**, 21–30 (2006)
19. Andreani, P., Franceschini, A., Granato, G.: Dust emission from quasars and quasar host galaxies. *Mon. Not. R. Astron. Soc.* **306**, 161 (1999)
20. Andreeva, N., Zyskin, Yu.L., Kalekin, O.R., et al: Observations of the gamma-ray flux from the galaxy Mk 501. *Astron. Lett.* **26**, 199 (2000)
21. Antón, S., Browne, I.W.A., Marchã, M.J.: The colour of the narrow line Sy1-blazar 0324+3410. *Astron. Astrophys.* **490**, 583–587 (2008)
22. Antonucci, R.: Unified models for active galactic nuclei and quasars. *Ann. Rev. Astron. Astrophys.* **31**, 473–521 (1993)
23. Antonucci, R.R.J., Miller, J.S.: Spectropolarimetry and the nature of NGC 1068. *Astrophys. J.* **297**, 621 (1985)
24. Atwood, W.B., Abdo, A.A., Ackermann, M., et al. (*Fermi* Collaboration): The large area telescope on the *fermi gamma-ray space telescope* Mission. *Astrophys. J.* **697**, 1071–1102 (2009)
25. Avni, Y., Tananbaum, H.: On the cosmological evolution of the x-ray emission from quasars. *Astrophys. J. Lett.* **262**, L17–L21 (1982)
26. Baade, W., Minkowski, R.: On the indentification of radio sources. *Astrophys. J.* **119**, 215 (1954)
27. Bachev, R., et al.: Average ultraviolet quasar spectra in the context of eigenvector 1: a baldwin effect governed by the eddington ratio? *Astrophys. J.* **617**, 171 (2004)
28. Bahcall, J.N., Kirhakos, S., Saxe, D.H., Schneider, D.P.: Hubble space telescope images of a sample of 20 nearby luminous quasars. *Astrophys. J.* **479**, 642 (1997)
29. Baldwin, J.A.: The Ly- α /H- β intensity ratio in the spectra of QSOs. *Mon. Not. R. Astron. Soc.* **178**, 78P (1977)
30. Baldwin, J.A.: Luminosity indicators in the spectra of quasi-stellar objects. *Astrophys. J.* **214**, 769–684 (1977)
31. Baldwin, J.A., Burke, W.L., Gaskell, C.M., Wampler, E.J.: Relative quasar luminosities determined from emission line strengths. *Nature* **273**, 431 (1978)
32. Baldwin, J., Ferland, G., Korista, K., Verner, D.: Locally optimally emitting clouds and the origin of quasar emission lines. *Astrophys. J.* **445**, 119–122 (1995)

33. Baldwin, J.: The next steps. In "Quasars and Cosmology", ASP Conf. Ser. vol. 162, p. 475, 1999
34. Baldwin, J.A., et al.: The origin of FeII emission in active galactic nuclei. *Astrophys. J.* **615**, 610 (2004)
35. Balmaverde, B., Capetti, A., Grandi, P.: The chandra view of the 3C/FR I sample of low luminosity radio-galaxies. *Astron. Astrophys.* **451**, 35–44 (2006)
36. Balmaverde, B., Baldi, R.D., Capetti, A.: The accretion mechanism in low-power radio galaxies. *Astron. Astrophys.* **486**, 119–130 (2008)
37. Barthel, P.D.: Is every quasar beamed? *Astrophys. J.* **336**, 606–611 (1989)
38. Barthelmy, S.D.: The burst alert telescope (BAT) on the SWIFT midex mission. *Space Sci. Rev.* **120**, 143 (2005)
39. Barvainis, R., Lehar, J., Birkinshaw, M., et al.: Radio variability of radio-quiet and radio-loud quasars. *Astrophys. J.* **618**, 108–122 (2005)
40. Baskin, A., Laor, A.: On the origin of the CIV baldwin effect in active galactic nuclei. *Mon. Not. R. Astron. Soc.* **350**, 31 (2004)
41. Baskin, A., Laor, A.: What controls the CIV line profile in active galactic nuclei? *Mon. Not. R. Astron. Soc.* **356**, 1029–1044 (2005)
42. Bassani, L., Dadina, M., Maiolino, R., et al.: A three-dimensional diagnostic diagram for seyfert-2 galaxies: probing x-ray absorption and compton thickness. *Astrophys. J. Suppl. Ser.* **121**, 473–482 (1999)
43. Baum, S.A., Heckman, T.: Extended optical line emitting gas in powerful radio galaxies – what is the radio emission-line connection? *Astrophys. J.* **336**, 702–721 (1989)
44. Baum, S.A., Zirbel, E.L., O'Dea, C.P.: Toward understanding the fanaroff–riley dichotomy in radio source morphology and power. *Astrophys. J.* **451**, 88 (1995)
45. Bautista, M.A., Kallman, T.R.: Recombination spectra of helium-like ions. *Astrophys. J.* **544**, 581–591 (2000)
46. Bautista, M.A., Dunn, J.P., Arav, N., et al.: Distance to multiple kinematic components of quasar outflows: very large telescope observations of QSO 2359–1241 and SDSS J0318-0600. *Astrophys. J.* **713**, 25 (2010)
47. Becker, R.H., White, R.L., Helfand, D.J.: The FIRST survey: faint images of the radio sky at twenty centimeters. *Astrophys. J.* **450**, 559–577 (1995)
48. Begelman, M.C., Blandford, R.D., Rees, M.J.: Theory of extragalactic radio sources. *Rev. Mod. Phys.* **56**, 255–351 (1984)
49. Bennert, N., Falcke, H., Schulz, H., et al.: Size and structure of the narrow-line region of quasars. *Astrophys. J. Lett.* **574**, L105–L109 (2002)
50. Bertoldi, F., Carilli, C.L., Cox, P., et al.: Dust emission from the most distant quasars. *Astron. Astrophys.* **406**, 55 (2003)
51. Best, P.N., Kauffmann, G., Heckman, T.M., et al.: The host galaxies of radio-loud active galactic nuclei: mass dependences, gas cooling and active galactic nuclei feedback. *Mon. Not. R. Astron. Soc.* **362**, 25 (2005)
52. Beuermann, K., Thomas, H.-C., Reinsch, K., et al.: Identification of soft high galactic latitude RASS x-ray sources. II. Sources with PSPC count rate CR < 0.5 cts/s. *Astron. Astrophys.* **347**, 47 (1999)
53. Bianchi, S., Matt, G., Nicastro, F., et al.: FeXXV and FeXXVI lines from low-velocity, photoionized gas in the X-ray spectra of active galactic nuclei. *Mon. Not. R. Astron. Soc.* **357**, 599–607 (2005)
54. Bianchi, S., Guainazzi, M., Chiaberge, M.: The soft x-ray/NLR connection: a single photoionized medium? *Astron. Astrophys.* **448**, 499–511 (2006)
55. Bianchi, S., Guainazzi, M., Matt, G., Fonseca Bonilla, N.: On the iwawasa-taniguchi effect of radio-quiet AGN. *Astron. Astrophys.* **467**, L19–L22 (2007)
56. Blandford, R.D., Rees, M.J.: A 'twin-exhaust' model for double radio sources. *Mon. Not. R. Astron. Soc.* **169**, 395–415 (1974)
57. Blandford, R.D., Rees, M.J.: Some comments on radiation mechanisms in lacertids. In: Pittsburgh Conference on BL Lac Objects. University of Pittsburgh, Pittsburgh, p. 328–341

- (1978)
58. Blandford, R.D., Koenigl, A.: Relativistic jets as compact radio sources. *Astrophys. J.* **232**, 34 (1979)
 59. Blandford, R.D., Payne, D.G.: Hydromagnetic flows from accretion discs and the production of radio jets. *Mon. Not. R. Astron. Soc.* **199**, 883–903 (1982)
 60. Blandford, R.D., McKee, C.F., Rees, M.J.: Super-luminal expansion in extragalactic radio sources. *Nature* **267**, 211–216 (1977)
 61. Blundell, K.M., Rawlings, S.: The optically powerful quasar E1821+643 is associated with a 300 kiloparsec-scale FR I radio structure. *Astrophys. J.* **562**, 5 (2001)
 62. Blustin, A.J., Page, M.J., Fuerst, S.V., et al.: The nature and origin of seyfert warm absorbers. *Astron. Astrophys.* **431**, 111–125 (2005)
 63. Blustin, A.J., Kriss, G.A., Holczer, T., et al.: The mass-energy budget of the ionised outflow in NGC 7469. *Astron. Astrophys.* **466**, 107–118 (2007)
 64. Boller, T., Brandt, W.N., Fink, H.: Soft x-ray properties of narrow-line seyfert-1 galaxies. *Astron. Astrophys.* **305**, 53 (1996)
 65. Boller, T., Brandt, W.N., Fabian, A.C., Fink, H.H.: ROSAT monitoring of persistent giant and rapid variability in the narrow-line seyfert-1 galaxy IRAS 13224-3809. *Mon. Not. R. Astron. Soc.* **289**, 393–405 (1997)
 66. Boroson, T.A., Green, R.F.: The emission-line properties of low-redshift quasi-stellar objects. *Astrophys. J. Suppl. Ser.* **80**, 109–135 (1992)
 67. Boroson, T.A.: Black hole mass and eddington ratio as drivers for the observable properties of radio-loud and radio-quiet QSOs. *Astrophys. J.* **565**, 78–85 (2002)
 68. Boroson, T.A.: Blueshifted [OIII] emission: indications of a dynamic narrowline region. *Astron. J.* **130**, 381–386 (2005)
 69. Böttcher, M., Dermer, C.D.: An evolutionary scenario for blazar unification. *Astrophys. J.* **564**, 86–91 (2002)
 70. Boyle, B.J., et al.: The 2dF QSO redshift survey – I. The optical luminosity function of quasi-stellar objects. *Mon. Not. R. Astron. Soc.* **317**, 1014–1022 (2000)
 71. Brandt, W.N., Boller, Th., Fabian, A.C., Ruszkowski, M.: ROSAT high-resolution imager monitoring of extreme x-ray variability in the narrow-line quasar PHL 1092. *Mon. Not. R. Astron. Soc.* **303**, L53–L57 (1999)
 72. Brandt, W.N., Alexander, D.M., Hornschemeier, A.E., et al.: The chandra deep field north survey. V. 1 Ms source catalogs. *Astron. J.* **122**, 2810 (2001)
 73. Bridle, A.H., Perley, R.A.: Extragalactic radio jets. *Ann. Rev. Astron. Astrophys.* **22**, 319–358 (1984)
 74. Breedt, E., Arévalo, P., McHardy, I.M., et al.: Long-term optical and x-ray variability of the seyfert galaxy markarian 79. *Mon. Not. R. Astron. Soc.* **394**, 427 (2009)
 75. Breedt, E., McHardy, I.M., Arévalo, P., et al.: Twelve years of x-ray and optical variability in the seyfert galaxy NGC 4051. *Mon. Not. R. Astron. Soc.* **403**, 605 (2010)
 76. Brenneman, L., Reynolds, C.S.: Relativistic broadening of iron emission lines in a sample of active galactic nuclei. *Astrophys. J.* **702**, 1367 (2009)
 77. Bridle, A.H., Perley, R.A.: Extragalactic radio jets. *Ann. Rev. Astron. Astrophys.* **22**, 319–358 (1984)
 78. Brinkman, A.C., Kaastra, J.S., van der Meer, R.L.J., et al.: The soft x-ray spectrum from NGC 1068 observed with LETGS on chandra. *Astron. Astrophys.* **396**, 761–772 (2002)
 79. Brotherton, M.S., Wills, Beverley, J., Steidel, C.C., Sargent, W.L.W.: Statistics of QSO broad emission-line profiles. 2: The CIV wavelength 1549, CIII] λ 1909, and MgII λ 2798 lines. *Astrophys. J.* **423**, 131 (1994)
 80. Brotherton, M.S., Tran, H.D., Becker, R.H., et al.: Composite spectra from the FIRST bright quasar survey. *Astroph. J.* **546**, 775–781 (2001)
 81. Brunthaler, A., Falcke, H., Bower, G.C., et al.: III ZW 2, the first superluminal jet in a seyfert galaxy. *Astron. Astrophys.* **357**, 45 (2000)
 82. Buttiglione, S., Capetti, A., Celotti, A., et al.: An optical spectroscopic survey of the 3CR sample of radio galaxies with $z < 0.3$. II. Spectroscopic classes and accretion modes in radio-

- loud AGN. *Astron. Astrophys.* **509**, 6 (2010)
83. Canizares, C.R., Davis, J.E., Dewey, D., et al.: The chandra high-energy transmission grating: design, fabrication, ground calibration, and 5 years in flight. *PASP* **117**, 1144–1171 (2005)
 84. Capetti, A., Balmaverde, B.: The host galaxy/AGN connection in nearby early-type galaxies. Sample selection and hosts brightness profiles. *Astron. Astrophys.* **440**, 73–84 (2005)
 85. Capetti, A., Balmaverde, B.: The host galaxy/AGN connection in nearby early-type galaxies. A new view of the origin of the radio-quiet/radio-loud dichotomy? *Astron. Astrophys.* **453**, 27–37 (2006)
 86. Capetti, A., Axon, D.J., Macchetto, F., et al.: Radio outflows and the origin of the narrow-line region in seyfert galaxies. *Astron. Astrophys. J.* **469**, 554 (1996)
 87. Carini, M.T., Miller, H.R., Goodrich, B.D.: The timescales of the optical variability of blazars. I – OQ 530. *Astron. J.* **100**, 347 (1990)
 88. Carrasco, L., Dultzin-Hacyan, D., Cruz-Gonzalez, I.: Periodicity in the BL lac object OJ287. *Nature* **314**, 146 (1985)
 89. Catanese, M., Akerlof, C.W., Badran, H.M., et al.: Discovery of gamma-ray emission above 350 GeV from the BL lacertae object IES 2344+514. *Astrophys. J.* **501**, 616 (1998)
 90. Cavaliere, A., D'Elia, V.: The blazar main sequence. *Astrophys. J.* **571**, 226–233 (2002)
 91. Chakrabarti, S.K., Wiita, P.J.: Variable emission lines as evidence of spiral shocks in accretion disks around active galactic nuclei. *Astrophys. J.* **434**, 518 (1994)
 92. Chakravorty, S.: Physics of radiation from AGN. Ph.D. Thesis (2009)
 93. Chand, H., Wiita, P.J., Gupta, A.C.: Probing spectral properties of radio-quiet quasars searched for optical microvariability. *Mon. Not. R. Astron. Soc.* **402**, 1059 (2010)
 94. Chelouche, D., Netzer, H.: Dynamical and spectral modeling of the ionized gas and nuclear environment in NGC3783. *Astrophys. J.* **625**, 95–107 (2005)
 95. Chesnok, N.G., Sergeev, S.G., Vavilova, I.B.: Optical and x-ray variability of seyfert galaxies NGC 5548, NGC 7469, NGC 3227, NGC 4051, NGC 4151, Mrk 509, Mrk 79, and Akn 564 and quasar 1E 0754. *Kinematics and Physics of Celestial Bodies* **25**, 107 (2009)
 96. Cirasuolo, M., Magliocchetti, M., Celotti, A., Danese, L.: The radio-loud/radio-quiet dichotomy: news from the 2dF QSO redshift survey. *Mon. Not. R. Astron. Soc.* **341**, 993–1004 (2003)
 97. Cirasuolo, M., Celotti, A., Magliocchetti, M., Danese, L.: Is there a dichotomy in the radio loudness distribution of quasars? *Mon. Not. R. Astron. Soc.* **346**, 447–455 (2003)
 98. Cleary, K., Lawrence, C.R., Marshall, J.A., Hao, L., Meier, D.: Spitzer observations of 3C quasars and radio galaxies: mid-infrared properties of powerful radio sources. *Astrophys. J.* **660**, 117–145 (2007)
 99. Clements, S.D., Carini, M.T.: Multiband microvariability observations of BL lacertae during the outburst of 1997. *Astron. J.* **121**, 90 (2001)
 100. Cohen, M.H., Cannon, W., Purcell, G.H., et al.: The small-scale structure of radio galaxies and quasi-stellar sources at 3.8 centimeters. *Astrophys. J.* **170**, 207–217 (1971)
 101. Cohen, M.H., Linfield, R.P., Moffet, A.T., et al.: Radio sources with superluminal velocities. *Nature* **268**, 405–409 (1977)
 102. Collin-Souffrin, S., Lasota, J.-P.: The broad-line region of active galactic nuclei revisited. *PASP* **100**, 1041 (1988)
 103. Collin, S.: Systematic effects in measurement of black hole masses by emission-line reverberation of active galactic nuclei: eddington ratio and inclination. *Astron. Astrophys.* **456**, 75–90 (2006)
 104. Condon, J.J.: Radio emission from normal galaxies. *Ann. Rev. Astron. Astrophys.* **30**, 575–611 (1992)
 105. Condon, J.J., Odell, S.L., Puschell, J.J., Stein, W.A.: Radio emission from bright, optically selected quasars. *Astrophys. J.* **246**, 624–646 (1981)
 106. Condon, J.J., Cotton, W.D., Greisen, E.W., et al.: The NRAO VLA sky survey. *Astron. J.* **115**, 1693–1716 (1998)
 107. Corbett, E.A., Robinson, A., Axon, D.J., Hough, J.H.: A seyfert-like nucleus concealed in BL lacertae? *Astrophys. J.* **311**, 485–492 (2000)

108. Crenshaw, D.M., Kraemer, S.B., George, I.M.: Mass loss from the nuclei of active galaxies. *Ann. Rev. Astron. Astrophys.* **41**, 117–167 (2003)
109. Croom, S.M., Smith, R.J., Boyle, B.J., et al.: The 2dF QSO redshift survey – XII. The spectroscopic catalogue and luminosity function. *Mon. Not. R. Astron. Soc.* **349**, 1397–1418 (2004)
110. Croton, D.J., Springel, V., White, S.D.M., et al.: The many lives of active galactic nuclei: cooling flows, black holes and the luminosities and colours of galaxies. *Mon. Not. R. Astron. Soc.* **365**, 11–28 (2006)
111. Curtis, H.D.: Descriptions of 762 nebulae and clusters photographed with the crossley reflector. *Publ. Lick Obs.* **13**, 9–42 (1918)
112. Cutri, R.M., Nelson, B.O., Kirkpatrick, J.D., et al.: The search for red AGN with 2MASS. In: Clowes, R., Adamson, A. Bromage, G. (eds.) *The New Era of Wide Field Astronomy*. San Francisco: ASP. ASP Conf. Ser. **232**, 78–83 (2001)
113. Czerny, B., Elvis, M.: Constraints on quasar accretion disks from the optical/ultraviolet/soft x-ray big bump. *Astrophys. J.* **321**, 305 (1987)
114. de Diego, J.A., Dultzin-Hacyan, D., Ramirez, A., Benitez, E.: A comparative study of the microvariability properties in radio-loud and radio-quiet quasars. *Astrophys. J.* **501**, 69 (1998)
115. den Herder, J.W., Brinkman, A.C., Kahn, S.M., et al.: The reflection grating spectrometer on board XMM-newton. *Astron. Astrophys.* **365**, 7–17 (2001)
116. Denney, K.D., Peterson, B.M., Pogge, R.W., et al.: Reverberation mapping measurements of black hole masses in six local seyfert galaxies. *Astrophys. J.* **721**, 715 (2010)
117. de Vries, W.H., Becker, R.H. White, R.L.: Double-lobed radio quasars from the sloan digital sky survey. *Astron. J.* **131**, 666–679 (2006)
118. de Vries, N., Snellen, I.A.G., Schilizzi, R.T., Mack, K.-H., Kaiser, C.R.: VLBI observations of the CORALZ sample: young radio sources at low redshift. *Astron. Astrophys.* **498**, 641–659 (2009)
119. Dibai, É.A., Pronik, V.I.: A spectrophotometric study of seyfert-galaxy nuclei. *Soviet Ast.* **44**, 952 (1967)
120. Dietrich, M., Hamann, F., Shields, J.C., et al.: Continuum and emission-line strength relations for a large active galactic nuclei sample. *Astrophys. J.* **581**, 912 (2002)
121. Done, C.: Simultaneous multifrequency observations of the seyfert-1 galaxy NGC 4051 – constant optical-infrared emission observed during large-amplitude x-ray variability. *Mon. Not. R. Astron. Soc.* **243**, 713 (1990)
122. Doroshenko, V.T., Sergeev, S.G., Merkulova, N.I., et al.: BVRI CCD-photometry of comparison stars in the neighborhoods of galaxies with active nuclei. I. *Astrophys.* **48**, 156 (2005)
123. Doroshenko, V.T., Sergeev, S.G., Efimov, Yu. S., et al.: Comparison of the x-ray and optical variabilities in the seyfert galaxy 3C 120. *Astron. Lett.* **35**, 361 (2009)
124. Doroshenko, V.T., Sergeev, S.G., Vovk, E.Yu., et al.: X-ray and optical variability of the seyfertn galaxy NGC 7469. *Astron. Lett.* **36**, 611 (2010)
125. Doroshenko, V.T., Sergeev, S.G., Klimanov, S.A., Pronik, V.I., Efimov, Yu. S.: BLR kinematics and Black Hole Mass in Markarian 6. arXiv:1203.2084 (2012)
126. Dultzin-Hacyan, D., Schuster, W.J., Parrao, L., et al.: Optical variability of the seyfert nucleus NGC 7469 in timescales from days to minutes. *Astron. J.* **103**, 1769 (1992)
127. Dultzin-Hacyan, D., Takalo, L.O., Benitez, E., et al.: Microvariability of OJ 287 during a flare. *Rev. Mex. Astron. Astrofis.* **33**, 17 (1997)
128. Dunlop, J.S., McLure, R.J. Kukula, M.J., et al.: Quasars, their host galaxies and their central black holes. *Mon. Not. R. Astron. Soc.* **340**, 1095–1135 (2003)
129. Ebisawa, K., Miyakawa, T., Inoue, H.: X-ray emission and absorption environments in seyfert-1 galaxy MCG-6-30-15. *Bull. Am. Astron. Soc.* **41**, 666 (2010)
130. Edelson, R.A., Malkan, M.A.: Spectral energy distributions of active galactic nuclei between 0.1 and 100 microns. *Astrophys. J.* **308**, 59 (1986)
131. Elvis, M., Maccacaro, T., Wilson, A.S., et al.: Seyfert galaxies as x-ray sources. *Mon. Not. R. Astron. Soc.* **183**, 129–157 (1978)
132. Elvis, M., Wilkes, B.J., McDowell, J.C., et al.: Atlas of quasar energy distributions. *Astrophys. J. Suppl. Ser.* **95**, 1 (1994)

133. Elvis, M.: A structure for quasars. *Astrophys. J.* **545**, 63–76 (2000)
134. Epstein, E.E., Fogarty, W.G., Hackney, K.R., et al.: 3C 120, BL lacertae, and OJ 287: coordinated optical, infrared, and radio observations of intraday variability. *Astrophys. J.* **178**, L51, (1972)
135. Eracleous, M., Sambruna, R., Mushotzky, R.F.: Hard x-ray spectra of broad-line radio galaxies from the rossi x-ray timing explorer. *Astrophys. J.* **537**, 654–666 (2000)
136. Esin, A.A., McClintock, J.E., Narayan, R.: Advection-dominated accretion and the spectral states of black hole x-ray binaries: application to nova MUSCAE 1991. *Astrophys. J.* **489**, 865 (1997)
137. Espey, B.R., Lanzetta, K.M., Turnshek, D.A.: An ionization-dependent baldwin effect? *BAAS25*, 1448 (1993)
138. Evans, D.A., Ogle, P.M., Marshall, H.L., et al.: Searching for AGN outflows: spatially resolved chandra HETG spectroscopy of the NLR ionization cone in NGC 1068. *ASP Conf. Ser.* **427**, 97 (2010)
139. Fabian, A.C., Iwasawa, K., Reynolds, C.S., Young, A.J.: Broad iron lines in active galactic nuclei. *PASP* **112**, 1145–1161 (2000)
140. Fabian, A.C.: A long hard look at MCG-6-30-15 with XMM-newton. *Mon. Not. R. Astron. Soc.* **335**, L1 (2002)
141. Fabian, A.C.: XMM-newton and broad iron lines. *Astron. Nachr.* **88**, 789 (2006)
142. Fabian, A.C.: XMM and broad iron lines. In “XMM-Newton: The Next Decade”, conference held 4th – 6th June (2007) at European Space Astronomy Centre (ESAC), Villafranca del Castillo, Madrid, Spain
143. Fabian, A.C., Zoghbi, A., Ross, R.R., et al.: Broad line emission from iron K- and L-shell transitions in the active galaxy 1H0707-495. *Nature* **459**, 540–542 (2009)
144. Falcke, H.: The silent majority – jets and radio cores from low-luminosity black holes. *Rev. Mod. Astron.* **14**, 15 (2001)
145. Falcke, H., Biermann, P.L.: The jet-disk symbiosis. I. Radio to x-ray emission models for quasars. *Astron. Astrophys.* **293**, 665–682 (1995)
146. Falcke, H., Biermann, P.L.: Galactic jet sources and the AGN connection. *Astron. Astrophys.* **308**, 321–329 (1996)
147. Falcke, H., Biermann, P.L.: The jet/disk symbiosis. III. What the radio cores in GRS 1915+105, NGC 4258, M 81 and SGR A* tell us about accreting black holes. *Astron. Astrophys.* **342**, 49–56 (1999)
148. Falcke, H., Malkan, M.A., Biermann, P.L.: The jet-disk symbiosis. ii.interpreting the radio/uv correlations in quasars. *Astron. Astrophys.* **298**, 375 (1995)
149. Falcke, H., Sherwood, W., Patnaik, A.R.: The nature of radio-intermediate quasars: what is radio-loud and what is radio-quiet? *Astrophys. J.* **471**, 106 (1996)
150. Falcke, H., Gopal-Krishna, Y., Biermann, P.L.: Unified schemes for active galaxies: a clue from the missing fanaroff–riley type I quasar population. *Astron. Astrophys.* **298**, 395 (1995)
151. Falcke, H., Patnaik, A.R., Sherwood, W.: EVN + MERLIN observations of radio-intermediate quasars: evidence for boosted radio-weak quasars. *Astrophys. J. Lett.* **473**, L13 (1996)
152. Falcke, H., Wilson, A.S., Simpson, C.: HST and VLA observations of seyfert-2 galaxies: the relationship between radio ejecta and the narrow-line region. *Astrophys. J.* **502**, 199 (1998)
153. Falcke, H., Nagar, N.M., Wilson, A.S., Ulvestad, J.S.: Radio sources in low-luminosity active galactic nuclei. ii. VLBI detections of compact radio cores and jets in a sample of liners. *Astrophys. J.* **542**, 197 (2000)
154. Fanaroff, B.L., Riley, J.M.: The morphology of extragalactic radio sources of high and low luminosity. *Mon. Not. R. Astron. Soc.* **167**, 31–36 (1974)
155. Fanti, C., Fanti, R., Lari, C., et al.: A search for radio emission from a sample of optically selected quasars. *Astron. Astrophys.* **61**, 487–491 (1977)
156. Faulkner, J., Gaskell, M.: Astronomers licked by QSOs and active galactic nuclei. *Nature* **275**, 91 (1978)
157. Fath, E.A.: The spectra of some spiral nebulae and globular star clusters. *Lick Obs. Bull.* **5**, 71 (1909)

158. Fender, R.P., Belloni, T.M., Gallo, E.: Towards a unified model for black hole x-ray binary jets. *Mon. Not. R. Astron. Soc.* **355**, 1105–1118 (2004)
159. Fender, R.P., Gallo, E., Russell, D.: No evidence for black hole spin powering of jets in x-ray binaries. *Mon. Not. R. Astron. Soc.* **406**, 1425–1434 (2010)
160. Fender, R., Corbel, S., Tzioumis, T., McIntyre, V., Campbell-Wilson, D., Nowak, M., Sood, R., Hunstead, R., Harmon, A., Durouchoux, P., Heindl, W.: Quenching of the radio jet during the x-ray high state of GX 339-4. *Astrophys. J. Lett.* **519**, L165–L168 (1999)
161. Ferland, G., Korista, K.T., Verner, D.A., et. al.: CLOUDY 90: Numerical simulation of plasmas and their spectra. *PASP* **110**, 761 (1998)
162. Ferland, G., Hu, C., Wang, J.-M., et al.: Implications of infalling Fe II-emitting clouds in active galactic nuclei: anisotropic properties. *Astrophys. J. Lett.* **707**, L82 (2009)
163. Ferrarese, L., Merritt, D.: A fundamental relation between supermassive black holes and their host galaxies. *Astrophys. J. Lett.* **539**, 9 (2000)
164. Fidelis, V.V., Eliseev, V.S., Zhogolev, N.A., Nehaj, E.M., Neshpor, Yu.I., Skiruta, Z.N., Fomin, V.P.: The results of observations of crab nebula, galaxies Mk 421 and 1ES 1959+650. In: 28-th All-Russian conference cosmic rays. Moskva. MIFI 105. In Russian. (2004)
165. Forster, K., Halpern, J.P.: Extreme x-ray variability in the narrow-line QSO PHL 1092. *Astrophys. J.* **468**, 565 (1996)
166. Foschini, L.: Jets (relativistic and non) in astrophysics. *Le Stelle*, n. 82, March 2010, [arXiv:1003.4212] (2010)
167. Foschini, L.: Evidence of powerful relativistic jets in narrow-line seyfert-1 galaxies. In: Foschini, L., et al. (eds.) *Narrow-Line Seyfert-1 Galaxies and Their Place in the Universe*, Proceedings of Science **NLS1**, 024 (2011)
168. Foschini, L., Chiaberge, M., Grandi, P., Grenier, I.A., et al.: Investigating the EGRET-radio galaxies link with *INTEGRAL*: the case of 3EGJ1621+8203 and NGC6251. *Astron. Astrophys.* **433**, 515–518 (2005)
169. Foschini, L., Fermi/Lat Collaboration, Ghisellini, G., Maraschi, L., Tavecchio, F., Angelakis, E.: *Fermi*/LAT discovery of gamma-ray emission from a relativistic jet in the narrow-line seyfert-1 quasar PMN J0948+0022. In: Maraschi, L., et al. (eds.) *Accretion and Ejection in AGN: A Global View*, ASP Conference Series, vol. 427, p. 243–248. San Francisco, 2010
170. Foschini, L., Pian, E., Maraschi, L., Raiteri, C.M., Tavecchio, F., et al.: A short hard x-ray flare from the blazar NRAO 530 observed by *INTEGRAL*. *Astron. Astrophys.* **450**, 77–81 (2006)
171. Foschini, L., Ghisellini, G., Kovalev, Y.Y., Lister, M.L., D’Ammando, F., Thompson, D.J., Tramacere, A., et al.: The first gamma-ray outburst of a narrow-line seyfert-1 galaxy: the case of PMN J0948+0022 in 2010 july. *Mon. Not. R. Astron. Soc.* **413**, 1671–1677 (2011)
172. Fossati, G., Maraschi, L., Celotti, A., et al.: A unifying view of the spectral energy distributions of blazars. *Mon. Not. R. Astron. Soc.* **299**, 433–448 (1998)
173. Francis, P.J., Hewett, P.C., Foltz, C.B., et al.: A high signal-to-noise ratio composite quasar spectrum. *Astrophys. J.* **373**, 465–470 (1991)
174. Fu, H., Stockton, A.: FR II quasars: infrared properties, star formation rates, and extended ionized gas. *Astrophys. J.* **696**, 1693–1699 (2009)
175. Fukumura, K., Kazanas, D., Contopoulos, I., Behar, E.: Magnetohydrodynamic accretion disk winds as x-ray absorbers in active galactic nuclei. *Astrophys. J.* **715**, 636–650 (2010)
176. Gallimore, J.F., Axon, D.J., O’Dea, C.-P., et al.: A survey of kiloparsec-scale radio outflows in radio-quiet active galactic nuclei. *Astron. J.* **132**, 546–569 (2006)
177. Garofalo, D., Evans, D.A., Sambruna, R.M.: The evolution of radio-loud active galactic nuclei as a function of black hole spin. *Mon. Not. R. Astron. Soc.* **406**, 975–986 (2010)
178. Gaskell, C.M.: A redshift difference between high and low ionization emission-line regions in QSOs – evidence for radial motions. *Astrophys. J.* **263**, 79 (1982)
179. Gaskell, C.M.: The quasar family – an introduction and taxonomy. *NATO ASIC Proc.* **208**: *Astrophysical Jets and their Engines*, p. 29 (1987)
180. Gaskell, C.M.: Direct evidence of gravitational domination of the motion of gas within one light-week of the central object in NGC 4151 and the determination of the mass of the probable

- black hole. *Astrophys. J.* **325**, 114 (1988)
181. Gaskell, C.M.: Inflow of the broad-line region and the fundamental limitations of reverberation mapping. *ASP Conf. Ser.* **427**, 68 (2010)
 182. Gaskell, C.M.: Off-axis energy generation in active galactic nuclei: explaining broad-line profiles, spectropolarimetric observations, and velocity-resolved reverberation mapping. *Astrophys. J.* submitted [arXiv:1008.1057] (2010)
 183. Gaskell, C.M., Goosmann, R.W.: Line shifts, broad-line region inflow, and the feeding of AGNs. *Astrophys. J.* submitted [arXiv:0805.4258] (2008)
 184. Gear, W.K., Brown, L.M.J., Robson, E.I., et al.: Multifrequency observations of blazars. II – The variability of the 1 micron to 2 MM continuum. *Astrophys. J.* **304**, 295 (1986)
 185. Gebhardt, K., Bender, R., Bower, G., et al.: A relationship between nuclear black hole mass and galaxy velocity dispersion. *Astrophys. J. Lett.* **539**, 13 (2000)
 186. Gehrels, N., Chincarini, G., Giommi, P., et al.: The swift gamma-ray burst mission. *Astrophys. J.* **611**, 1005 (2004)
 187. Genzel, R., Cesarsky, C.J.: Extragalactic results from the infrared space observatory. *Ann. Rev. Astron. Astrophys.* **38**, 761 (2000)
 188. George, I.M., Fabian, A.C.: X-ray reflection from cold matter in active galactic nuclei and x-ray binaries. *Mon. Not. R. Astron. Soc.* **249**, 352 (1991)
 189. Ghisellini, G., Tavecchio, F.: The blazar sequence: a new perspective. *Mon. Not. R. Astron. Soc.* **387**, 1669–1680 (2008)
 190. Ghisellini, G., Tavecchio, F., Foschini, L., et al.: General physical properties of bright Fermi blazars. *Mon. Not. R. Astron. Soc.* **402**, 497–518 (2010)
 191. Giacconi, R., Gursky, H., Paolini, F.R., Rossi, B.B.: Evidence for x rays from sources outside the solar system. *Phys. Rev. Lett.* **9**, 439 (1962)
 192. Giacconi, R., Rosati, P., Tozzi, P., et al.: First results from the x-ray and optical survey of the chandra deep field south, *Astrophys. J.* **9**, 439 (2001)
 193. Gibson, R.R., Brandt, W.N., Schneider, D.P.: Are optically selected quasars universally x-ray luminous? X-ray-UV relations in sloan digital sky survey quasars. *Astrophys. J.* **685**, 773 (2008)
 194. Gierlinski, M., Done, C.: Is the soft excess in active galactic nuclei real? *Mon. Not. R. Astron. Soc.* **349**, L7 (2004)
 195. Goldschmidt, P., Miller, L., La Franca, R., Christiani, S.: The high surface density of bright ultraviolet-excess quasars. *Mon. Not. R. Astron. Soc.* **256**, 65P–68P (1992)
 196. Goldschmidt, P., Kukula, M.J., Miller, L., Dunlop, J.S.: A comparison of the optical properties of radio-loud and radio-quiet quasars. *Astrophys. J.* **511**, 612–624 (1999)
 197. Gopal-Krishna, Y., et al.: Near-infrared and optical imaging of Q2345+007: the largest gravitationally lensed QSO system? *Astron. Astrophys.* **280**, 360 (1993)
 198. Gopal-Krishna, Y., Wiita, P.J., Altieri, B.: Optical microvariability and radio quiet QSOS. *Astron. Astrophys.* **271**, 89 (1993)
 199. Granato, G.L., Danese, L., Franceschini, A.: Thick tori around active galactic nuclei: the case for extended tori and consequences for their x-ray and infrared emission. *Astrophys. J.* **486**, 147 (1997)
 200. Green, R.F., Schmidt, M., Liebert, J.: The palomar-green catalog of ultraviolet-excess stellar objects. *Astrophys. J. Suppl. Ser.* **61**, 305–322 (1986)
 201. Grupe, D.: A complete sample of soft x-ray-selected AGNs. II. Statistical analysis. *Astron. J.* **127**, 1799 (2004)
 202. Grupe, D., Beuermann, K., Mannheim, K., Thomas, H.-C.: New bright soft x-ray selected ROSAT AGN. II. Optical emission line properties. *Astron. Astrophys.* **350**, 805 (1999)
 203. Grupe, D., Komossa, S., Leighly, K.M., Page, K.L.: The simultaneous optical-to-x-ray spectral energy distribution of soft x-ray selected active galactic nuclei observed by swift. *Astrophys. J. Suppl. Ser.* **187**, 64 (2010)
 204. Gu, M.F., et al.: Multi-colour optical monitoring of eight red blazars. *Astron. Astrophys.* **450**, 39 (2006)

205. Guainazzi, M.: The history of the iron K_{α} line profile in the piccinotti AGN ESO 198-G24. *Astron. Astrophys.* **401**, 903–910 (2003)
206. Guainazzi, M., Bianchi, S.: On the origin of soft x-rays in obscured AGN: answers from high-resolution spectroscopy with XMM-newton. *Mon. Not. R. Astron. Soc.* **374**, 1290–1302 (2007)
207. Guainazzi, M.: Progress in AGN research with XMM-newton. *MemSAIt***81**, 226 (2010)
208. Gupta, A.C., Joshi, U.C.: Intra-night optical variability of luminous radio-quiet QSOs. *Astron. Astrophys.* **440**, 855 (2005)
209. Hawkins, M.R.S.: On time dilation in quasar light curves. *Mon. Not. R. Astron. Soc.* **405**, 1940–1946 (2010)
210. Halpern, J.: Variable x-ray absorption in the QSO MR 2251-178. *Astrophys. J.* **281**, 90 (1984)
211. Hamann, F., Ferland, G.: Elemental abundances in quasistellar objects: star formation and galactic nuclear evolution at high redshifts. *Ann. Rev. Astron. Astrophys.* **37**, 487 (1999)
212. Hamilton, T.S.: Quasar radio-loudness and the elliptical core problem. *Mon. Not. R. Astron. Soc.* **407**, 2393–2398 (2010)
213. Haas, M., Klaas, U., Müller, S.A.H., et al.: The ISO view of palomar-green quasars. *Astron. Astrophys.* **402**, 87–111 (2003)
214. Haas, M., Siebenmorgen, R., Schulz, B., Krügel, E., Chini, R.: Spitzer IRS spectroscopy of 3CR radio galaxies and quasars: testing the unified schemes. *Astron. Astrophys.* **442**, L39–L43 (2005)
215. Halpern, J.P.: Variable X-ray absorption in the QSO MR2251-178. *Astrophys. J.* **281**, 90 (1984)
216. Hardcastle, M.J., Evans, D.A., Croston, J.H.: The x-ray nuclei of intermediate-redshift radio sources. *Mon. Not. R. Astron. Soc.* **370**, 1893–1904 (2006)
217. Hardcastle, M.J., Evans, D.A., Croston, J.H.: Hot and cold gas accretion and feedback in radio-loud active galaxies. *Mon. Not. R. Astron. Soc.* **376**, 1849–1856 (2007)
218. Hargrave, P.J., Ryle, M.: Observations of cygnus a with the 5-km radio telescope. *Mon. Not. R. Astron. Soc.* **166**, 305–327 (1974)
219. Hartman, R.C., Bertsch, D.L., Bloom, S.D., et al.: The third EGRET catalog of high-energy gamma-ray sources. *Astrophys. J. Suppl. Ser.* **123**, 79–202 (1999)
220. Hasinger, G., Burg, R., Giacconi, R., et al.: A deep x-ray survey in the lockman-hole and the soft x-ray N-log. *Astron. Astrophys.* **275**, 1 (1993)
221. Hasinger, G., Burg, R., Giacconi, R., et al.: The ROSAT deep survey. I. X-ray sources in the lockman field. *Astrophys. J.* **329**, 482 (1998)
222. Hawkins, M.R.S.: Variability in active galactic nuclei: confrontation of models with observations. *Mon. Not. R. Astron. Soc.* **329**, 76–86 (2002)
223. Hazard, C., Mackey, M.B., Shimmins, A.J.: Investigation of the radio source 3C 273 by the method of lunar occultations. *Nature* **197**, 1037 (1963)
224. Heckman, T.M.: An optical and radio survey of the nuclei of bright galaxies – activity in normal galactic nuclei. *Astron. Astrophys.* **87**, 152–164 (1980)
225. Heckman, T.M., Smith, E.P., Baum, S.A., et al.: Galaxy collisions and mergers – the genesis of very powerful radio sources?. *Astrophys. J.* **311**, 526–547 (1986)
226. Heywood, I., Blundell, K.M., Rawlings, S.: The prevalence of fanaroff–riley type I radio quasars. *Mon. Not. R. Astron. Soc.* **381**, 1093–1102 (2007)
227. Heidt, J., Wagner, S.J.: Statistics of optical intraday variability in a complete sample of radio-selected BL lacertae objects. *Astron. Astrophys.* **305**, 42 (1996)
228. Hinton, J.A., Hofmann, W.: Teraelectronvolt astronomy. *Ann. Rev. Astron. Astrophys.* **47**, 523–565 (2009)
229. Hjellming, R.M., Johnston, K.J.: Radio emission from conical jets associated with x-ray binaries. *Astrophys. J.* **328**, 600–609 (1988)
230. Hjellming, R.M., Rupen, M.P.: Episodic ejection of relativistic jets by the x-ray transient GRO J1655-40. *Nature* **375**, 464 (1995)
231. Ho, L.C.: The spectral energy distributions of low-luminosity active galactic nuclei. *Astrophys. J.* **516**, 672–682 (1999)

232. Ho, L.C., Filippenko, A.V., Sargent, W.L.W.: A search for “dwarf” seyfert nuclei. v. demographics of nuclear activity in nearby galaxies. *Astrophys. J.* **487**, 568 (1997)
233. Ho, L.C., Peng, C.Y.: Nuclear luminosities and radio loudness of seyfert nuclei. *Astroph. J.* **555**, 650–662 (2001)
234. Holt, S.S., Mushotzky, R.F., Boldt, E.A., et al.: X-ray spectral constraints on the broad-line cloud geometry of NGC 4151. *Astrophys. J. Lett.* **241**, L13–L17 (1980)
235. Hooper, E.J., Impey, C.D., Foltz, C.B., Hewett, P.C.: Radio properties of optically selected quasars. *Astrophys. J.* **445**, 62–79 (1995)
236. Horan, D. (The VERITAS Collaboration): Observations of 1H1426+428 with the whipple 10 m imaging atmospheric cherenkov telescope. In: Simon, V., Lorenz, E., Pohl, M., (eds.) *Proc. of the 27th ICRC*, (Hamburg, Germany: IUPAP, 2001) **7**, 2622 (2001)
237. Hu, S.M., Zhao, G., Guo, H.Y., et al.: The optical spectral slope variability of 17 blazars. *Mon. Not. R. Astron. Soc.* **371**, 1243 (2006)
238. Hubble, E.P.: Extragalactic nebulae. *Astrophys. J.* **624**, 321–369 (1926)
239. Ivezić, Ž., Menou, Kristen, Knapp, Gillian R., et al.: Optical and radio properties of extragalactic sources observed by the FIRST survey and the sloan digital sky survey. *Astron. J.* **124**, 2364–2400 (2002)
240. Iwasawa, K., Taniguchi, Y. The x-ray baldwin effect. *Astrophys. J. Lett.* **413**, L15–L18 (1993)
241. Iwasawa, K., Fabian, A.C. Reynolds, C.S., et al.: The variable iron K emission line in MCG-6-30-15. *Mon. Not. R. Astron. Soc.* **282**, 1038–1048 (1996)
242. Iwasawa, K., Wilson, A.S., Fabian, A.C., Young, A.J.: The x-ray nebula around the type-2 seyfert galaxy NGC4388. *Mon. Not. R. Astron. Soc.* **345**, 369–378 (2003)
243. Iwasawa, K., Miniutti, G., Fabian, A.C.: Flux and energy modulation of redshifted iron emission in NGC 3516: implications for the black hole mass. *Mon. Not. R. Astron. Soc.* **355**, 1073–1079 (2004)
244. Jackson, C.A., Wall, J.V.: Extragalactic radio-source evolution under the dual-population unification scheme. *Mon. Not. R. Astron. Soc.* **304**, 160–174 (1999)
245. Jiang, P., Wang, J.X., Wang, T.G.: On the x-ray baldwin effect for narrow Fe K α emission lines. *Astrophys. J.* **644**, 725–732 (2006)
246. Jiang, L., Fan, X., Ivezić, Ž., et al.: The radio-loud fraction of quasars is a strong function of redshift and optical luminosity. *Astrophys. J.* **656**, 680–690 (2007)
247. Jester, S., Schneider, D.P., Richards, G.T., et al.: The sloan digital sky survey view of the palomar-green bright quasar survey. *Astrophys. J.* **130**, 873–895 (2005)
248. Jester, S.: A simple test for the existence of two accretion modes in active galactic nuclei. *Astrophys. J.* **625**, 667–679 (2005)
249. Just, D.: The X-ray properties of the most luminous quasars from the sloan digital sky survey. *Astrophys. J.* **665**, 1004 (2007)
250. Kadler, M., Ros, E., Perucho, M., et al.: The trails of superluminal jet components in 3C 111. *Astrophys. J.* **680**, 867–884 (2008)
251. Kalekin, O.R., et al.: Izvestiya of Russian Akademy Nauk, Fizikal Ser. **63/3**, 604. In Russian. (1999)
252. Kallman, T.R., Palmeri, P., Bautista, M.A., et al.: Photoionization modeling and the K lines of iron. *Astrophys. J. Suppl. Ser.* **155**, 675–701 (2004)
253. Kaspi, S., Smith, P.S., Netzer, H., et al.: Reverberation measurements for 17 quasars and the size-mass-luminosity relations in active galactic nuclei. *Astrophys. J.* **533**, 631–649 (2000)
254. Kaspi, S., Brandt, W.N., George, Ian M., et al.: The ionized gas and nuclear environment in NGC 3783. I. Time-averaged 900 kilosecond chandra grating spectroscopy. *Astrophys. J.* **574**, 643–662 (2002)
255. Kaspi, S., Maoz, D., Netzer, H., et al.: The relationship between luminosity and broad-line region size in active galactic nuclei. *Astrophys. J.* **629**, 61–71 (2005)
256. Kauffmann, G., Heckman, T.M., Best, P.N.: Radio jets in galaxies with actively accreting black holes: new insights from the SDSS. *Mon. Not. R. Astron. Soc.* **384**, 953–971 (2008)
257. Kawaguchi, T., Mineshige, S., Umemura, M., Turner, E.L.: Optical variability in active galactic nuclei: starbursts or disk instabilities? *Astrophys. J.* **504**, 671–679 (1998)

258. Kellermann, K.I., Sramek, R., Schmidt, M., et al.: VLA observations of objects in the palomar bright quasar survey. *Astron. J.* **98**, 1195 (1989)
259. Kellermann, K.I., Fomalont, E.B., Mainieri, V., et al.: The VLA survey of the chandra deep field-south. I. Overview and the radio data. *Astrophys. J. Suppl. Ser.* **179**, 71–94 (2008)
260. Kellermann, K.I., Lister, M.L., Homan, D.C., et al.: Kinematics of AGN and quasar jets. *ASP Conf. Ser.* **402**, 173 (2009)
261. Kambhavi, A., Narlikar, J.V.: Quasars and active galactic nuclei: an introduction. Cambridge University Press, Cambridge (1999)
262. Khachikian, E.E., Weedman, D.W.: A spectroscopic study of luminous galactic nuclei. *Astrophys. J.* **7**, 389 (1971)
263. King, A.R., Pounds, K.A.: Black hole winds. *Mon. Not. R. Astron. Soc.* **345**, 657–659 (2003)
264. Kinkhabwala, A., Sako, M., Behar, E., et al.: XMM-newton reflection grating spectrometer observations of discrete soft x-ray emission features from NGC1068. *Astrophys. J.* **575**, 732–746 (2002)
265. Kinney, A.L., Rivolo, A.R., Koratkar, A.P.: A study of the baldwin effect in the IUE data set. *Astrophys. J.* **357**, 338 (1990)
266. Koide, S., Shibata, K., Kudoh, T.: Relativistic jet formation from black hole magnetized accretion disks: method, tests, and applications of a general relativistic magnetohydrodynamic numerical code. *Astrophys. J.* **522**, 727–752 (1999)
267. Körtling, E.G., Fender, R.P., Migliari, S.: Jet-dominated advective systems: radio and x-ray luminosity dependence on the accretion rate. *Mon. Not. R. Astron. Soc.* **369**, 1451–1458 (2006)
268. Körtling, E.G., Jester, S., Fender, R.: Accretion states and radio loudness in active galactic nuclei: analogies with x-ray binaries. *Mon. Not. R. Astron. Soc.* **372**, 1366–1378 (2006)
269. Körtling, E.G., Jester, S., Fender, R.: Measuring the accretion rate and kinetic luminosity functions of supermassive black holes. *Mon. Not. R. Astron. Soc.* **383**, 277 (2008)
270. Kormendy, J., Fisher, D.B., Cornell, M.E., Bender, R.: Structure and formation of elliptical and spheroidal galaxies. *Astrophys. J. Suppl. Ser.* **182**, 216–309 (2009)
271. Kovačević, J., Popović, L.Č., Dimitrijević, M.S.: Analysis of optical FeII emission in a sample of active galactic nucleus spectra. *Astrophys. J. Suppl. Ser.* **189**, 15 (2010)
272. Kovalev, Y.Y., Aller, H.D., Aller, M.F., Homan, D.C., Kadler, M., Kellermann, K.I., Kovalev, Y.A., Lister, M.L., McCormick, M.J., Pushkarev, A.B., Ros, E., Zensus, J.A.: The relation between AGN gamma-ray emission and parsec-scale radio jets. *ApJ* **696**, L17–L21 (2009)
273. Kraemer, S.B., George, I.M., Crenshaw, D.M., et al.: Simultaneous ultraviolet and x-ray observations of seyfert galaxy NGC 4151. I. Physical conditions in the x-ray absorbers. *Astrophys. J.* **633**, 693–705 (2005)
274. Kranich, D., et al.: In: Proceedings of JCRC. OG2. 1.18, 1999
275. Krishan, V., Wiita, P.J.: Plasma mechanisms for variability in active galactic nuclei. *Astrophys. J.* **423**, 172 (1994)
276. Krolik, J.H., Begelman, M.: Molecular tori in seyfert galaxies – feeding the monster and hiding it. *Astrophys. J.* **329**, 702 (1988)
277. Krongold, Y., Nicastro, F., Brickhouse, N.S., et al.: Toward a self-consistent model of the ionized absorber in NGC3783. *Astrophys. J.* **597**, 832 (2003)
278. Krongold, Y., Nicastro, F., Brickhouse, N.S., et al.: Opacity variations in the ionized absorption in NGC 3783: a compact absorber. *Astrophys. J.* **622**, 842–846 (2005)
279. Kruczek, N.E., Richards, G.T., Gallagher, S.C., et al.: Blueshifting of CIV and the baldwin effect in 18,000 SDSS quasars. *BAAS* **43** (2011)
280. Kukula, M.J., Dunlop, J.S., Hughes, D.H., Rawlings, S.: The radio properties of radio-quiet quasars. *Mon. Not. R. Astron. Soc.* **297**, 366–382 (1998)
281. Kurosawa, R., Proga, D.: Three-dimensional simulations of dynamics of accretion flows irradiated by a quasar. *Astrophys. J.* **693**, 1929–1945 (2009)
282. Kwan, J., Krolik, J.H.: Hydrogen line and continuum emission in quasars. *Astrophys. J.* **233**, L91–L95 (1979)

283. Lacy, M., Laurent-Muehleisen, Sally, A., et al.: The radio luminosity-black hole mass correlation for quasars from the FIRST bright quasar survey and a “Unification Scheme” for radio-loud and radio-quiet quasars. *Astroph. J.* **551**, L17–L21 (2001)
284. Laing, R.A., Riley, J.M., Longair, M.S.: Bright radio sources at 178 MHz – flux densities, optical identifications and the cosmological evolution of powerful radio galaxies. *Mon. Not. R. Astron. Soc.* **204**, 151–187 (1983)
285. Laing, R.A., Bridle, A.H., Parma, P., Murgia, M.: Structures of the magnetoionic media around the fanaroff–riley class I radio galaxies 3C31 and hydra A. *Mon. Not. R. Astron. Soc.* **391**, 521–549 (2008)
286. Laing, R.A., Bridle, A.H.: Jet-environment interactions in FRI radio galaxies. In: “Extragalactic Jets: Theory and Observation from Radio to Gamma Ray” **386**, 70 (2008)
287. Laor, A.: Line profiles from a disk around a rotating black hole. *Astrophys. J.* **376**, 90 (1991)
288. Laor, A., Jannuzi, B.T., Green, R.F., Boroson, T.A.: The ultraviolet properties of the narrow-line quasar IZw1. *Astrophys. J.* **489**, 656 (1997)
289. Laor, A., Fiore, F., Elvis, M., et al.: The soft x-ray properties of a complete sample of optically selected quasars. II. Final results. *Astrophys. J.* **477**, 93 (1997)
290. Laor, A.: On quasar masses and quasar host galaxies. *Astrophys. J. Lett.* **505**, L83 (1998)
291. Laor, A.: On black hole masses and radio loudness in active galactic nuclei. *Astrophys. J. Lett.* **543**, L111 (2000)
292. Laor, A.: Some comments related to AGN radio loudness. [astro-ph/0312417] (2003)
293. Lawrence, A., Elvis, M.: Obscuration and the various types of sefert galaxy. *Astrophys. J.* **256**, 410 (1982)
294. Lawrence, A., Watson, M.G., Pounds, K.A., Elvis, M.: Continuous rapid x-ray variability and spectral changes in NGC4051. *Mon. Not. R. Astron. Soc.* **217**, 685–699 (1985)
295. Lazio, J.: The square kilometre array. Proceedings of “Panoramic Radio Astronomy: Wide-field 1-2 GHz Research on Galaxy Evolution”. In: Heald, G., Serra, P., (eds.) Proceedings of Science: <http://pos.sissa.it/cgi-bin/reader/conf.cgi?confid=89> (2009)
296. Leahy, D.A., Creighton, J.: Montecarlo simulations of x-ray spectra for internally illuminated spherical matter distributions. *Mon. Not. R. Astron. Soc.* **263**, 314 (1993)
297. Lee, J.C., Ogle, P.M., Canizares, C.R., et al.: Revealing the dusty warm absorber in MCG-6-30-15 with the chandra high-energy transmission grating. *Astrophys. J. Lett.* **554**, L13–L17 (2001)
298. Lee, J.C., Iwasawa, K., Houck, J.C., et al.: The shape of the relativistic iron $K\alpha$ line from MCG -6-30-15 measured with the chandra high energy transmission grating spectrometer and the rossi x-ray timing explorer. *Astrophys. J. Lett.* **570**, L47–L50 (2002)
299. Lehto, H.J., Valtonen, M.J.: OJ 287 outburst structure and a binary black hole model. *Astrophys. J.* **460**, 207 (1996)
300. Leighly, K.M.: A comprehensive spectral and variability study of narrow-line sefert-1 galaxies observed by ASCA. I. Observations and time series analysis. *Astrophys. J. Suppl. Ser.* **125**, 297–316 (1999)
301. Leighly, K.M.: Hubble space telescope STIS ultraviolet spectral evidence of outflow in extreme narrow-line sefert-1 galaxies. II. Modeling and interpretation. *Astrophys. J.* **611**, 125–152 (2004)
302. Leipski, C., et al.: The radio structure of radio-quiet quasars. *Astron. Astrophys.* **455**, 161–172 (2006)
303. Lenain, J.-P., Ricci, C., Türler, M., et al.: Seyfert-2 galaxies in the GeV band: jets and starburst. *Astron. Astrophys.* **524**, A72 (2010)
304. Lister, M.L., Cohen, M.H., Homan, D.C., et al.: MOJAVE: Monitoring of jets in active galactic nuclei with VLBA experiments. VI. Kinematics analysis of a complete sample of blazar jets. *Astrophys. J.* **138**, 1874–1892 (2009)
305. Lister, M.L., Homan, D.C., Kadler, M., Kellermann, K.I., Kovalev, Y.Y., Ros, E., Savolainen, T., Zensus, J.A.: A connection between apparent VLBA jet speeds and initial active galactic nucleus detections made by the fermi gamma-ray observatory. *Astrophys. J.* **696**, L22–L26 (2009)

306. Liu, Y., Zhang, S.N.: The lorentz factor distribution and luminosity function of relativistic jets in AGNs. *Astrophys. J.* **667**, 724–730 (2007)
307. Liu, Y., Jiang, D.R., Gu, M.F.: The jet power, radio loudness, and black hole mass in radio-loud active galactic nuclei. *Astrophys. J.* **637**, 669–681 (2006)
308. Longinotti, A.L., Nandra, K., Petrucci, P.O., O’Neill, P.M.: On the variability of the iron K α line in Mrk 841. *Mon. Not. R. Astron. Soc.* **355**, 929–934 (2004)
309. Lusso, E., Comastri, A., Vignali, C., et al.: The x-ray to optical-UV luminosity ratio of x-ray selected type-1 AGN in XMM-COSMOS. *Astron. Astrophys.* **512**, 34 (2010)
310. Ly, C., Walker, R.C., Junor, W.: High-frequency VLBI imaging of the jet base of M87. *Astrophys. J.* **660**, 200–205 (2007)
311. Lyutyi, V.M., Doroshenko, V.T.: Optical variability of the nuclei of the seyfert galaxies NGC 3516 and NGC 5548 on time scales from 20 years to 20 minutes. *Astron. Lett.* **19**, 405 (1993)
312. Lyutyi, V.M., Aslanov, A.A., Khruzina, T.S., et al.: Rapid optical variations in the NGC 4151 nucleus. *Soviet Astr. Lett. (TR: Pisma)* **15**, 247 (1989)
313. Maccarone, T.J., Gallo, E., Fender, R.: The connection between radio-quiet active galactic nuclei and the high/soft state of x-ray binaries. *Mon. Not. R. Astron. Soc.* **345**, L19–L24 (2003)
314. Madau, P.: Thick accretion disks around black holes and the UV/soft x-ray excess in quasars. *Astrophys. J.* **327**, 116–127 (1988)
315. Maiolino, R., Risaliti, G., Salvati, M., et al.: “Comets” orbiting a black hole. *Astron. Astrophys.* **517**, 47 (2010)
316. Malkan, M.A., Moore, R.L.: The ultraviolet excess of quasars. III. The highly polarized quasars PKS0736+017 and PKS1510–089. *Astrophys. J.* **300**, 216–223 (1986)
317. Mangalam, A.V., Wiita, P.J.: Accretion disk models for optical and ultraviolet microvariability in active galactic nuclei. *Astrophys. J.* **406**, 420 (1993)
318. Maraschi, L., Tavecchio, F.: The jet-disk connection and blazar unification. *Astrophys. J.* **593**, 667–675 (2003)
319. Marconi, A., Risaliti, G., Gilli, R., et al.: Local supermassive black holes, relics of active galactic nuclei and the x-ray background. *Mon. Not. R. Astron. Soc.* **351**, 169 (2004)
320. Marscher, A.P., Gear, W.K.: Models for high-frequency radio outbursts in extragalactic sources, with application to the early 1983 millimeter-to-infrared flare of 3C 273. *Astrophys. J.* **298**, 114 (1985)
321. Marscher, A.P., Gear, W.K., Travis, J.P.: Variability of nonthermal continuum emission in blazars. In: “Variability of Blazars”, p. 85 (1992)
322. Marscher, A.: Jets in active galactic nuclei. In: Belloni, T., (ed.) *The Jet Paradigm – From Microquasars to Quasars*, Lecture Notes Physics, vol. 794, 2009, [arXiv:0909.2576]
323. Marscher, A.P., et al.: Observational evidence for the accretion-disk origin for a radio jet in an active galaxy. *Nature* **417**, 625–627 (2002)
324. Marziani, P., Sulentic, J.W., Dultzin-Hacyan, D., et al.: Comparative analysis of the high- and low-ionization lines in the broad-line region of active galactic nuclei. *Astrophys. J. Suppl. Ser.* **104**, 37–70 (1996)
325. Marziani, P., Sulentic, J.W., Zamanov, R., et al.: An optical spectroscopic atlas of low-redshift active galactic nuclei. *ApJS* **145**, 199–211 (2003)
326. Marziani, P., Sulentic, J.W., Zwitter, T., et al.: Searching for the physical drivers of eigenvector 1: influence of black hole mass and eddington ratio. *Mon. Not. R. Astron. Soc.* **345**, 1133–1144 (2003)
327. Marziani, P., Sulentic, J.W., Dultzin, D.: Accretion onto supermassive black holes in quasars: learning from optical/UV observations. In: Kreitler, P.V. (ed) “New Developments in Black Hole Research”, ISBN 1-59454-641-X, p.123. Nova Science Publishers, New York (2006)
328. Massaro, E., Nesci, R., Maesano, M., et al.: Fast variability of BL lacertae at 1 μ m. *Mon. Not. R. Astr. Soc.* **299**, 47 (1998)
329. Mastichiadis, A.: Radiative processes in relativistic outflows. In: Guthmann, A.W., et al. (ed.) *Relativistic outflows in astrophysics. Lect. Not. Phys.* **589**, 1–23 (2002)

330. Matsuoka, K., Nagao, T., Marconi, A., et al.: The mass-metallicity relation of SDSS quasars. *Astron. Astrophys.* **527**, 100 (2011)
331. Matt, G., Pompilio, F., La Franca, F.: X-ray spectra transmitted through compton-thick absorbers. *New Astron.* **4**, 191–195 (1999)
332. Mathews, T.A., Sandage, A.R.: Optical identification of 3C 48, 3C 196, and 3C 286 with stellar objects. *Astrophys. J.* **138**, 30 (1963)
333. Mathews, W.G., Blumenthal, G.R., Grandi, S.A.: Hydrogen line intensities from dense plasmas – application to quasar spectra. *Astrophys. J.* **235**, 971–985 (1980)
334. McLure, R.J., Dunlop, J.S.: The black hole masses of sefert galaxies and quasars. *Mon. Not. R. Astron. Soc.* **327**, 199 (2001)
335. McLure, R.J., Jarvis, M.J.: The relationship between radio luminosity and black hole mass in optically selected quasars. *Mon. Not. R. Astron. Soc.* **353**, L45–L49 (2004)
336. McKernan, B., Yaqoob, T., Reynolds, C.S.: A soft x-ray study of type I active galactic nuclei observed with chandra high-energy transmission grating spectrometer. *Mon. Not. R. Astron. Soc.* **379**, 1359–1372 (2007)
337. Meier, D.L.: The association of jet production with geometrically thick accretion flows and black hole rotation. *Astrophys. J.* **548**, L9–L12 (2001)
338. Meier, D.L., Koide, S., Uchida, Y.: Magnetohydrodynamic production of relativistic jets. *Science* **291**, 84–92 (2001)
339. Merkulova, N.I., Metik, L.P., Pronik, I.I.: Characteristics of the continuum variability of the nucleus of NGC 4151 in the optical from 1989–1996. *Astron. Astrophys.* **374**, 770 (2001)
340. Merloni, A., Malzac, J., Fabian, A.C., Ross, R.R.: On the x-ray spectra of luminous, inhomogeneous accretion flows. *Mon. Not. R. Astron. Soc.* **370**, 1699–1712 (2006)
341. Metcalf, R.B., Magliocchetti, M.: The role of black hole mass in quasar radio activity. *Mon. Not. R. Astron. Soc.* **365**, 101–109 (2006)
342. Middelberg, E.: Motion and properties of nuclear radio components in sefert galaxies seen with VLBI. *Astron. Astrophys.* **417**, 925–944 (2004)
343. Miley, G., De Breuck, C.: Distant radio galaxies and their environments. *Astron. Astrophys. Rev.* **15**, 67–144 (2008)
344. Miller, L., Peacock, J.A., Mead, A.R.G.: The bimodal radio luminosity function of quasars. *Mon. Not. R. Astron. Soc.* **244**, 207–213 (1990)
345. Miller, P., Rawlings, S., Saunders, R.: The radio and optical properties of the $z < 0.5$ BQS quasars. *Mon. Not. R. Astron. Soc.* **263**, 425–460 (1993)
346. Miller, L., Turner, T.J., Reeves, J.: The absorption-dominated model for the x-ray spectra of type I active galaxies: MCG-6-30-15. *Mon. Not. R. Astron. Soc.* **399**, L69–L73 (2009)
347. Miller, L., Turner, T.J., Reeves, J.: An absorption origin for the x-ray spectral variability of MCG-6-30-15. *Astron. Astrophys.* **483**, 437–452 (2008)
348. Miller, L., Turner, T.J., Reeves, J.N., et al.: Variable iron-line emission near the black hole of markarian 766. *Astron. Astrophys.* **453**, 13–16 (2006)
349. Miller, L., Turner, T.J., Reeves, J.N., et al.: The variable x-ray spectrum of markarian 766. I. Principal components analysis. *Astron. Astrophys.* **463**, 131–143 (2007)
350. Miller, L., Turner, T.J., Reeves, J.N., et al.: Spectral variability and reverberation time delays in the suzaku x-ray spectrum of NGC 4051. *Mon. Not. R. Astron. Soc.* **403**, 196–210 (2010)
351. Miniutti, G., Fabian, A.C.: A light bending model for the x-ray temporal and spectral properties of accreting black holes. *Mon. Not. R. Astron. Soc.* **349**, 1435 (2004)
352. Miniutti, G., et al.: Suzaku observations of the hard x-ray variability of MCG -6-30-15: the effects of strong gravity around a kerr black hole. *PASJ* **59**, 315–325 (2007)
353. Mirabel, I.F., Rodriguez, L.F.: A superluminal source in the galaxy. *Nature* **371**, 46 (1994)
354. Misra, R., Kembhavi, A.K.: Broadening of the iron emission line in MCG -6-30-15 by comptonization. *Astrophys. J.* **499**, 205 (1998)
355. Misra, R., Sutaria, F.K.: Comparisons of various model FITS to the iron line profile in MCG -6-30-15. *Astrophys. J.* **517**, 661 (1999)
356. Moderski, R., Sikora, M., Lasota, J.-P.: On the spin paradigm and the radio dichotomy of quasars. *Mon. Not. R. Astron. Soc.* **301**, 142–148 (1998)

357. Morganti, R., Peck, A.B., Oosterloo, T.A., et al.: Is cold gas fuelling the radio galaxy NGC 315? *Astron. Astrophys.* **505**, 559–567 (2009)
358. Morganti, R., Greenhill, L.J., Peck, A.B., et al.: Disks, tori, and cocoons: emission and absorption diagnostics of AGN environments. *New Astron. Rev.* **48**, 1195–1209 (2004)
359. Mukherjee, R., Halpern, J., Mirabal, N., Gotthelf, E.V.: Is the EGRET source 3EGJ1621 + 8203 the radio galaxy NGC6251? *Astrophys. J.* **574**, 693–700 (2002)
360. Mundell, C.G., Wilson, A.S., Ulvestad, J.S., Roy, A.L.: Parsec-scale images of flat-spectrum radio sources in seyfert galaxies. *Astrophys. J.* **529**, 816–831 (2000)
361. Mundell, C.G., Wrobel, J.M., Pedlar, A., Gallimore, J.F.: The nuclear regions of the seyfert galaxy NGC 4151: parsec-scale H I absorption and a remarkable radio jet. *Astrophys. J.* **583**, 192–204 (2003)
362. Murray, N., Chiang, J.: Disk winds and disk emission lines. *Astrophys. J.* **474**, 91 (1997)
363. Murray, N., Chiang, J.: Photoionization of disk winds. *Astrophys. J.* **494**, 125 (1998)
364. Murray, N., Chiang, J., Grossman, S.A., Voit, G.M.: Accretion disk winds from active galactic nuclei. *Astrophys. J.* **451**, 498 (1995)
365. Muxlow, T.W.B., Richards, A.M.S., Garrington, S.T., et al.: High-resolution studies of radio sources in the hubble deep and flanking fields. *Mon. Not. R. Astron. Soc.* **358**, 1159–1194 (2005)
366. Nandikotkur, G., Jahoda, K.M., Hartman, R.C., et al.: Does the blazar gamma-ray spectrum harden with increasing flux? Analysis of 9 years of EGRET data. *Astrophys. J.* **657**, 706–724 (2007)
367. Nandra, K., Pounds, K.A.: GINGA observations of the x-ray spectra of seyfert galaxies. *Mon. Not. R. Astron. Soc.* **267**, 139 (1994)
368. Nandra, K., George, I.M., Mushotzky, R.F., et al.: ASCA observations of seyfert-1 galaxies. II. Relativistic iron $K\alpha$ emission. *Astrophys. J.* **477**, 602 (1997)
369. Nandra, K., O’Neill, P.M., George, I.M., Reeves, J.N.: An XMM-newton survey of broad iron lines in seyfert galaxies. *Mon. Not. R. Astron. Soc.* **382**, 194–228 (2007)
370. Nagar, N.M., Wilson, A.S.: The relative orientation of nuclear accretion and galaxy stellar disks in seyfert galaxies. *Astrophys. J.* **516**, 97–113 (1999)
371. Nagar, N.M., Wilson, A.S., Falcke, H.: Evidence for jet domination of the nuclear radio emission in low-luminosity active galactic nuclei. *Astrophys. J. Lett.* **559**, L87–L90 (2001)
372. Nagar, N.M., Falcke, H., Wilson, A.S., Ho, L.C.: Radio sources in low-luminosity active galactic nuclei. i. VLA detections of compact, flat-spectrum cores. *Astrophys. J.* **542**, 186 (2000)
373. Nagar, N.M., Falcke, H., Wilson, A.S., Ulvestad, J.S.: Radio sources in low-luminosity active galactic nuclei. III. “AGNs” in a distance-limited sample of “LLAGNs”. *Astron. Astrophys.* **392**, 53–82 (2002)
374. Nagar, N.M., Falcke, H., Wilson, A.S.: Radio sources in low-luminosity active galactic nuclei. IV. Radio luminosity function, importance of jet power, and radio properties of the complete palomar sample. *Astron. Astrophys.* **435**, 521–543 (2005)
375. Nayakshin, S., Kazanas, D.: On time-dependent x-ray reflection by photoionized accretion disks: implications for Fe $K\alpha$ line reverberation studies of active galactic nuclei. *Astrophys. J.* **567**, 85–96 (2002)
376. Nesci, R., et al.: Intraday variability of BL lacertae in the great 1997 outburst. *Astron. Astrophys.* **332**, 1 (1998)
377. Neshpor, Yu.I., et al.: Pisma v astronomicheskii zhurnal **24/3**, 167 (1998) (in Russian)
378. Neshpor, Yu.I., et al.: *Astronomicheskii Zhurnal*. **8/4**, 291 (2001) (in Russian)
379. Neshpor, Yu.I., et al.: *Izvestiya of the crimean astrophysical observatory* **99**, 34 (2003) (in Russian)
380. Neshpor, Yu.I., et al.: *Izvestiya of the crimean astrophysical observatory* **99**, 43 (2003) (in Russian)
381. Neshpor, Yu.I., et al.: *Izvestiya of the crimean. Astrophys. Observ.* **103/1**, 27 (2007) (in Russian)
382. Neshpor, Yu.I., Zhovtan, A.V.: *Izvestiya of the crimean astrophysical observatory* **104/1**, 185 (2008) (in Russian)

383. Netzer, H.: Quasar discs. I – The baldwin effect. *Mon. Not. R. Astron. Soc.* **216**, 63 (1985)
384. Netzer, H., Laor, A., Gondhalekar, P.M.: Quasar discs. III – Line and continuum correlations. *Mon. Not. R. Astron. Soc.* **254**, 15 (1992)
385. Netzer, H., Chelouche, Doron, George, I.M., et al.: The density and location of the x-ray-absorbing gas in NGC3516. *Astrophys. J.* **571**, 256–264 (2002)
386. Netzer, H., Kaspi, S., Behar, E., et al.: The ionized gas and nuclear environment in NGC 3783. IV. Variability and modeling of the 900 kilosecond chandra spectrum. *Astrophys. J.* **599**, 933 (2003)
387. Nishiyama, T.: Detection of a new TeV gamma-ray source of BL lac object 1ES 1959+650. In: Dingus, B.L., Kieda, D.B., Salamon, M.H., (eds.) *Proc. of the 26th ICRC*, vol. 3, AIP Conf. Proc. (AIP, Salt Lake City, Utah, 2000), Vol. 516, p. 370 (2000)
388. Northover, K.J.E.: The radio galaxy 3C 66. *Mon. Not. R. Astron. Soc.* **165**, 369 (1973)
389. O'Dea, C.P.: The compact steep-spectrum and gigahertz peaked-spectrum radio sources. *PASP* **110**, 493–532 (1998)
390. Ogle, P., Whysong, D., Antonucci, R.: Spitzer reveals hidden quasar nuclei in some powerful FR II radio galaxies. *Astrophys. J.* **647**, 161–171 (2006)
391. Omont, A., et al.: A 1.2 mm MAMBO/IRAM-30 m survey of dust emission from the highest redshift PSS quasars. *Astron. Astrophys.* **374**, 371 (2001)
392. Onken, C.A., et al.: Supermassive black holes in active galactic nuclei. II. Calibration of the black hole mass-velocity dispersion relationship for active galactic nuclei. *Astrophys. J.* **615**, 645 (2004)
393. Orr, M.J.L., Browne, I.W.A.: Relativistic beaming and quasar statistics. *Mon. Not. R. Astron. Soc.* **200**, 1067–1080 (1982)
394. Osmer, P.S., Shields, J.C.: A review of line and continuum correlations in AGNs. In: “Quasars and Cosmology” **162**, 235 (1999)
395. Osterbrock, D.E., Koski, A.T., Phillips, M.M.: Broad balmer emission lines in radio galaxies. *Astrophys. J. Lett.* **197**, L41 (1975)
396. Osterbrock, D.E.: Spectrophotometry of seyfert-1 galaxies. *Astrophys. J.* **215**, 733 (1977)
397. Osterbrock, D.E.: Observational model of the ionized gas in seyfert and radio-galaxy nuclei. *Proc. Nat. Acad. Sci.* **75**, 540 (1978)
398. Osterbrock, D.E., Ferland, G.J.: *Astrophysics of gaseous nebulae and active galactic nuclei*, 2nd ed. University Science Books, Sausalito, CA (2006)
399. Padovani, P.: The radio loud fraction of QSOS and its dependence on magnitude and redshift. *Mon. Not. R. Astron. Soc.* **263**, 461–470 (1993)
400. Padovani, P.: The microjy and nanojy radio sky: source population and multi-wavelength properties. [arXiv:1009.6116] (2010)
401. Page, K.L., O'Brien, P.T., Reeves, J.N., Turner, M.J.L.: An x-ray baldwin effect for the narrow Fe K α lines observed in active galactic nuclei. *Mon. Not. R. Astron. Soc.* **347**, 316–322 (2004)
402. Palmeri, P., Mendoza, C., Kallman, T.R., et al.: Modeling of iron K lines: radiative and auger decay data for Fe II-Fe IX. *Astron. Astrophys.* **410**, 359–364 (2003)
403. Panessa, F., Bassani, L.: Unabsorbed seyfert-2 galaxies. *Astron. Astrophys.* **394**, 435–442 (2002)
404. Papadakis, I.E., Samaritakis, V., Boumis, P., Papamastorakis, J.: Multi-band optical micro-variability observations of BL lacertae. *Astron. Astrophys.* **397**, 565 (2003)
405. Peacock, J.A., Miller, L., Longair, M.S.: The statistics of radio emission from quasars. *Mon. Not. R. Astron. Soc.* **218**, 265–278 (1986)
406. Peterson, B.M.: *Introduction to active galactic nuclei*. Cambridge University press, Cambridge (1997)
407. Petrucci, P.O.: A rapidly variable narrow x-ray iron line in Mkn 841. *Astron. Astrophys.* **388**, L5–L8 (2002)
408. Pian, E., Falomo, R., Treves, A.: *Hubble Space Telescope* ultraviolet spectroscopy of blazars: emission-line properties and black hole masses. *Mon. Not. R. Astron. Soc.* **361**, 919–926 (2005)

409. Pian, E., Foschini, L., Beckmann, V., et al.: INTEGRAL observations of the blazar 3C 454.3 in outburst. *Astron. Astrophys.* **449**, L21 (2006)
410. Piro, L., Yamauchi, M., Matsuoka, M.: X-ray spectral signatures of very thick cold matter in the spectra of seyfert galaxies. *Nuovo Cimento C. Geophysics Space Physics C* **15**, 811–818 (1992)
411. Pogge, R.: Narrow-line seyfert 1s: 15 years later. *New Astron. Rev.* **44**, 381–385 (2000)
412. Pounds, K.A., Turner, T.J., Warwick, R.S.: Rapid x-ray variability of the seyfert galaxy MCG-6-30-15. *Mon. Not. R. Astron. Soc.* **221**, 7–12 (1986)
413. Pounds, K.A., Reeves, J.N.: Resolving a broad PCygni line profile to quantify the fast outflow in the luminous seyfert galaxy PG1211+143. *Mon. Not. R. Astron. Soc.* **397**, 249 (2009)
414. Proga, D., Stone, J.M., Kallman, T.R.: Dynamics of line-driven disk winds in active galactic nuclei. *Astrophys. J.* **543**, 686–696 (2000)
415. Puccetti, S., Risaliti, G., Fiore, F., et al.: Rapid N_H changes in NGC4151. *Nucl. Phys. B Proc. Suppl.* **132**, 225–228 (2004)
416. Puchnarewicz, E.M., Mason, K.O., Cordova, F.A., et al.: Optical properties of active galaxies with ultra-soft x-ray spectra. *Mon. Not. R. Astron. Soc.* **256**, 589–623 (1992)
417. Punch, M., Akerlof, C.W., Cawley, M.F., et al.: Detection of TeV photons from the active galaxy markarian 421. *Nature* **358**, 477 (1992)
418. Punsly, B.: The redshifted excess in quasar C IV broad emission lines. *Astroph. J.* **713**, 232–238 (2010)
419. Qian, S.J., Quirrenbach, A., Witzel, A., et al.: A model for the rapid radio variability in the quasar 0917 + 624. *Astron. Astrophys.* **241**, 15 (1991)
420. Quinn, J., Akerlof, C.W., Biller, S., et al.: Detection of gamma rays with $E > 300$ GeV from markarian 501. *Astrophys. J. Lett.* **456**, L83 (1996)
421. Racine, R.: Photometry of BL lacertae with a time resolution of 15 seconds. *Astrophys. J. Lett.* **159**, L99 (1970)
422. Ramirez, A., Dultzin, D.: in preparation (2011)
423. Ramirez, A., Dultzin, D., de Diego, J.A.: Optical microvariability in quasars: spectral variability. *Astrophys. J.* **714**, 605 (2010)
424. Ramirez, A., de Diego, J.A., Dultzin-Hacyan, D., González-Pérez, J.N.: Optical variability of PKS 0736+017. *Astron. Astrophys.* **421**, 83 (2004)
425. Ramirez, A., de Diego, J.A., Dultzin-Hacyan, D., González-Pérez, J.N.: Multiband comparative study of optical microvariability in radio-loud versus radio-quiet quasars. *Astron. J.* **138**, 991 (2009)
426. Ramos Almeida, C., Tadhunter, C.N., Inskip, K.J., et al.: The optical morphologies of the 2Jy sample of radio galaxies: evidence for galaxy interactions. *Mon. Not. R. Astron. Soc.* **410**, 1550 (2011)
427. Rani, B., Gupta, Alok C., Joshi, U.C., et al.: Quasi-periodic oscillations of 15 minutes in the optical light curve of the BL lac S5 0716+714. *Astrophys. J. Lett.* **719**, L153 (2010)
428. Rawlings, S., Saunders, R.: Evidence for a common central-engine mechanism in all extragalactic radio sources. *Nature* **349**, 138–140 (1991)
429. Readhead, A.C.S.: Equipartition brightness temperature and the inverse compton catastrophe. *Astrophys. J.* **426**, 51–59 (1994)
430. Rees, M.J.: Appearance of relativistically expanding radio sources. *Nature* **211**, 468–470 (1966)
431. Rees, M.J.: George DARWIN lecture 1976 – quasars and young galaxies. *QJRAS* **18**, 429–442 (1977)
432. Reeves, J.N., et al.: A compton-thick wind in the high-luminosity quasar, PDS 456. *Astrophys. J.* **701**, 493–507 (2009)
433. Reichert, G.A., Mushotzky, R.F., Holt, S.S., Petre, R.: Soft x-ray spectral observations of low-luminosity active galaxies. *Astrophys. J.* **296**, 69–89 (1985)
434. Reiner, M.J., et al.: Solar origin of the radio attributes of a complex type III burst observed on 11 April 2001. *Solar Phys.* **249**, 337 (2008)

435. Reynolds, C.J., Nowak, M.A.: Fluorescent iron lines as a probe of astrophysical black hole systems. *Phys. Rev.* **377**, 389 (2003)
436. Reynolds, C.J.: An x-ray spectral study of 24 type-I active galactic nuclei. *Mon. Not. R. Astron. Soc.* **286**, 513 (1997)
437. Reynolds, C.S.: Constraints on the absorption-dominated model for the x-ray spectrum of MCG-6-30-15. *Mon. Not. R. Astron. Soc.* **397**, L21–L25 (2009)
438. Richards, G.T., Vanden Berk, D.E., Reichard, T.A., et al.: Broad emission-line shifts in quasars: an orientation measure for radio-quiet quasars? *Astron. J.* **124**, 1 (2002)
439. Richards, G.T., Croom, S.M., Anderson, S.F., et al.: The 2dF-SDSS LRG and QSO (2SLAQ) survey: the $z < 2.1$ quasar luminosity function from 5645 quasars to $g = 21.85$. *Mon. Not. R. Astron. Soc.* **360**, 839–852 (2005)
440. Richards, G.T., Strauss, M.A., Fan, X., et al.: The sloan digital sky survey quasar survey: quasar luminosity function from data release 3. *Astron. J.* **131**, 2766–2787 (2006)
441. Richards, G.T., Kruczek, N.E., Gallagher, S.C., Hall, P.B., Hewett, P.C., et al.: Unification of luminous type-I quasars through CIV emission. [2010arXiv1011.2282R] *Astron. J.* 141, article id. 167 (2011)
442. Risaliti, G., Elvis, M., Fabbiano, G., et al.: Rapid compton-thick/compton-thin transitions in the seyfert-2 galaxy NGC1365. *Astrophys. J.* **623**, 93 (2005)
443. Risaliti, G., Elvis, M., Fabbiano, G., et al.: Occultation measurement of the size of the x-ray-emitting region in the active galactic nucleus of NGC1365. *Astrophys. J.* **659**, 111 (2007)
444. Risaliti, G., Salvati, M., Marconi, A.: [O III] equivalent width and orientation effects in quasars. [arXiv:1010.2037] *Mon. Not Royal Astr. Soc.* 411 pp. 2223–2229 (2011)
445. Rokaki, E., Lawrence, A., Economou, F., Mastichiadis, A.: Is there a disc in the superluminal quasars? *Mon. Not. R. Astron. Soc.* **340**, 1298–1308 (2003)
446. Ross, R.R., Fabian, A.C.: A comprehensive range of x-ray ionized-reflection models. *Mon. Not. R. Astron. Soc.* **358**, 211–216 (2005)
447. Rottgering, H.J.A., Braun, R., Barthel, P.D., et al.: LOFAR – opening up a new window on the universe. *ArXiv Astrophysics e-prints arXiv:astro-ph/0610596* (2006)
448. Saikia, D.J., Jamrozy, M.: Recurrent activity in active galactic nuclei. *Bull. Astron. Soc. India* **37**, 63–89 (2009)
449. Sako, M., Kahn, S.M., Paerels, F., Liedahl, D.A.: The chandra high-energy transmission grating observation of an x-ray ionization cone in markarian 3. *Astrophys. J. Lett.* **543**, L115–L118 (2000)
450. Sako, M., Kahn, S.M., Behar, E., et al.: Complex resonance absorption structure in the x-ray spectrum of IRAS 13349+2438. *Astron. Astrophys.* **365**, 168–173 (2001)
451. Sambruna, R.M., Eracleous, M., Mushotzky, R.F.: An x-ray spectral survey of radio-loud active galactic nuclei with ASCA. *Astrophys. J.* **526**, 60–96 (1999)
452. Sambruna, R.M., Netzer, H., Kaspi, S., et al.: High-resolution x-ray spectroscopy of the seyfert-2 galaxy circinus with chandra. *Astrophys. J. Lett.* **546**, L13–L17 (2001)
453. Sandage, A.: The existence of a major new constituent of the universe: the quasistellar galaxies. *Astrophys. J.* **141**, 1560 (1965)
454. Scheuer, P.A.G.: Models of extragalactic radio sources with a continuous energy supply from a central object. *Mon. Not. R. Astron. Soc.* **166**, 513–528 (1974)
455. Scheuer, P.A.G.: Tests of beaming models. In: Zensus, J.A., Pearson, T.J., (eds.) *Proceedings of the Workshop, Pasadena, CA, Oct. 28–30, 1986 (A88-39751 16-90)*, Cambridge University Press, Cambridge pp. 104–113 (1987)
456. Scheuer, P.A.G., Readhead, A.C.S.: Superluminally expanding radio sources and the radio-quiet QSOs. *Nature* **277**, 182–185 (1979)
457. Schwobe, A.D., Hasinger, G., Lehmann, I., et al.: The ROSAT bright survey: II. Catalogue of all high-galactic latitude RASS sources with PSPC countrate $CR > 0.2 \text{ s}^{-1}$. *Astron. Nach.* **321**, 1 (2000)
458. Schneider, D.P., Richards, G.T., Hall, P.B., et al.: The sloan digital sky survey quasar catalog. V. Seventh data release. *Astron. J.* **139**, 2360–2373 (2010)

459. Schmidt, M., Green, R.F.: Quasar evolution derived from the palomar bright quasar survey and other complete quasar surveys. *Astrophys. J.* **269**, 352–374 (1983)
460. Seyfert, C.K.: Nuclear emission in spiral nebulae. *Astrophys. J.* **97**, 28 (1943)
461. Sergeev, S.G., et al.: Lag-luminosity relationship for interband lags between variations in B, V, R, and I bands in active galactic nuclei. *Astrophys. J.* **622**, 129 (2005)
462. Sergeev, S.G., Klimanov, S.A., Okhmat, N.N., Sivtsov, G.A.: *Bulletin of the crimean astrophysical observatory* **106**, 92 (2010)
463. Sergeev, S.G., Klimanov, S.A., Doroshenko, V.T., et al.: Variability of the 3C 390.3 nucleus in 2000–2007 and a new estimate of the central black hole mass. *Mon. Not. R. Astron. Soc.* **410**, 1877 (2011)
464. Shakura, N.I., Syunyaev, R.A.: Black holes in binary systems – observational appearance. *Astron. Astrophys.* **24**, 337–355 (1973)
465. Shemmer, O., Netzer, H.: Is there a metallicity-luminosity relationship in active galactic nuclei? the case of narrow-line seyfert-1 galaxies. *Astrophys. J. Lett.* **567**, L19 (2002)
466. Shi, Y., Ogle, P., Rieke, G.H., et al.: Aromatic features in AGNs: star-forming infrared luminosity function of AGN host galaxies. *Astrophys. J.* **669**, 841–861 (2007)
467. Shields, J.C.: Emission-line versus continuum correlations in active galactic nuclei. In “The Central Engine of Active Galactic Nuclei”, *ASP Conf. Ser.* **373**, 355 (2007)
468. Shu, X.W., Yaqoob, T., Wang, J.X.: The cores of the Fe K α lines in active galactic nuclei: an extended chandra high energy grating sample. *Astrophys. J. Suppl. Ser.* **187**, 581–606 (2010)
469. Sillanpaa, A., Haarala, S., Valtonen, M.J., et al.: OJ 287 – binary pair of supermassive black holes. *Astrophys. J.* **325**, 628 (1988)
470. Sillanpaa, A., Takalo, L.O., Pursimo, T., et al.: Confirmation of the 12-year optical outburst cycle in blazar OJ 287. *Astron. Astrophys.* **305**, L17 (1996)
471. Sikora, M., Stawarz, L., Lasota, J.-P.: Radio loudness of active galactic nuclei: observational facts and theoretical implications. *Astrophys. J.* **658**, 815–828 (2007)
472. Sim, S.A., Long, K.S., Miller, L., Turner, T.J.: Multidimensional modelling of x-ray spectra for AGN accretion disc outflows. *Mon. Not. R. Astron. Soc.* **388**, 611–624 (2008)
473. Sim, S.A., Miller, L., Long, K.S., et al.: Multidimensional modelling of x-ray spectra for AGN accretion disc outflows – II. *Mon. Not. R. Astron. Soc.* **404**, 1369–1384 (2010)
474. Smith, R.A.N., Page, M.J., Branduardi-Raymont, G.: The XMM-newton RGS spectrum of the high luminosity seyfert-1 galaxy markarian 509. *Astron. Astrophys.* **461**, 135–142 (2007)
475. Smolčić, V., et al.: A new method to separate star-forming from AGN galaxies at intermediate redshift: the submillijansky radio population in the VLA-COSMOS survey. *Astrophys. J. Suppl. Ser.* **177**, 14–38 (2008)
476. Soifer, B.T., Neugebauer, G., Houck, J.R.: The IRAS view of the extragalactic sky. *Ann. Rev. Astron. Astrophys.* **25**, 187 (1987)
477. Soltan, A.: Masses of quasars. *Mon. Not. R. Astron. Soc.* **200**, 115 (1982)
478. Sopp, H.M., Alexander, P.: A composite plot of far-infrared versus radio luminosity, and the origin of far-infrared luminosity in quasars. *Mon. Not. R. Astron. Soc.* **251**, 14P–16P (1991)
479. Spergel, D.N., Bean, R., Doré, O., et al.: Three-year wilkinson microwave anisotropy probe (WMAP) observations: Implications for cosmology. *Astrophys. J. Suppl. Ser.* **170**, 377 (2007)
480. Speziali, R., Natali, G.: BVI microvariability in BL lacertae during the summer 1997 outburst. *Astron. Astrophys.* **339**, 382 (1998)
481. Stalin, C.S., Gopal, K., Sagar, R., Wiita, P.J.: Intranight optical variability of radio-quiet and radio lobe-dominated quasars. *Mon. Not. R. Astron. Soc.* **350**, 175 (2004)
482. Steffen, A.T., Barger, A.J., Cowie, L.L., et al.: The changing active galactic nucleus population. *Astrophys. J.* **596**, 23 (2003)
483. Steinhardt, C.L., Elvis, M.: The quasar mass-luminosity plane – I. A sub-eddington limit for quasars. *Mon. Not. R. Astron. Soc.* **402**, 2637–2648 (2010)
484. Steiner, J.E.: A spectrophotometric classification of low-redshift quasars and active galactic nuclei. *Astrophys. J.* **250**, 469 (1981)
485. Stepanian, A.A., et al.: *Izvestiya of the crimean astrophysical observatory* **53**, 29 (1975) (in Russian)
486. Stepanian, A.A., et al.: *Astronomicheskii zhurnal* **79/8**, 702 (2002) (in Russian)

487. Stephens, S.: Optical spectroscopy of x-ray-selected active galactic nuclei. *Astron. J.* **97**, 10 (1989)
488. Stocke, J.T., Morris, S.L., Weymann, R.J., Foltz, C.B.: The radio properties of the broad-absorption-line QSOs. *Astrophys. J.* **396**, 487–503 (1992)
489. Strateva, I.V., Brandt, W.N., Schneider, D.P., et al.: Soft x-ray and ultraviolet emission relations in optically selected AGN samples. *Astron. J.* **130**, 387 (2005)
490. Strittmatter, P.A., Hill, P., Pauliny-Toth, I.I.K., Steppe, H., Witzel, A.: Radio observations of optically selected quasars. *Astron. Astrophys.* **88**, 12–15 (1980)
491. Sulentic, J.W., Marziani, P., Zwitter, T., et al.: On the origin of broad Fe K α and H I H α lines in active galactic nuclei. *Astrophys. J.* **501**, 54 (1998)
492. Sulentic, J.W., Marziani, P.: The intermediate-line region in active galactic nuclei: a region “Praeter Necessitatem”? *Astrophys. J. Lett.* **518**, L9 (1999)
493. Sulentic, J.W., Marziani, P., Dultzin-Hacyan, D.: Phenomenology of broad emission lines in active galactic nuclei. *Ann. Rev. Astron. Astrophys.* **38**, 521–571 (2000)
494. Sulentic, J.W., Zwitter, T., Marziani, P., Dultzin-Hacyan, D.: Eigenvector 1: an optimal correlation space for active galactic nuclei. *Astrophys. J. Lett.* **536**, L5–L9 (2000)
495. Sulentic, J.W., Marziani, P., Zamanov, R., Bachev, R., Calvani, M., Dultzin-Hacyan, D.: Average quasar spectra in the context of eigenvector 1. *Astrophys. J. Lett.* **566**, L71 (2002)
496. Sulentic, J.W., Zamfir, S., Marziani, P., et al.: Radio-loud active galactic nuclei in the context of the eigenvector 1 parameter space. *Astrophys. J.* **597**, L17–L20 (2003)
497. Sulentic, J.W., Stirpe, G.M., Marziani, P., et al.: VLT/ISAAC spectra of the H β region in intermediate redshift quasars. *Astron. Astrophys.* **423**, 121–132 (2004)
498. Sulentic, J.W., Repetto, P., Stirpe, G.M., et al.: VLT/ISAAC spectra of the H β region in intermediate-redshift quasars. II. Black hole mass and eddington ratio. *Astron. Astrophys.* **456**, 929–939 (2006)
499. Sulentic, J.W., Zamfir, S., Marziani, P., Dultzin, D.: Our search for an H-R diagram of quasars. *Rev. Mex. A. A. (Serie de Conferencias)* **32**, 51–58 (2008)
500. Sulentic, J.W., Bachev, R., Marziani, P., et al.: CIV λ 1549 as an eigenvector 1 parameter for active galactic nuclei. *Astrophys. J.* **666**, 757 (2007)
501. Swanenburg, B.N., Hermsen, W., Bennett, K., et al.: *COSB* observation of high-energy gamma radiation from 3C273. *Nature* **275**, 298 (1978)
502. Tanaka, Y., Nandra, K., Fabian, A.C., et al.: Gravitationally redshifted emission implying an accretion disk and massive black-hole in the active galaxy MCG:-6-30-15. *Nature* **375**, 659 (1995)
503. Tananbaum, H., Avni, Y., Branduardi, G., et al.: X-ray studies of quasars with the einstein observatory. *Astrophys. J.* **234**, 9 (1979)
504. Tarter, C.B., Salpeter, E.P.: The interaction of x-ray sources with optically thick environments. *Astrophys. J.* **156**, 953 (1969)
505. Tadhunter, C.N., Morganti, R., di Serego-Alighieri, S., et al.: Optical spectroscopy of a complete sample of southern 2-JY radio sources. *Mon. Not. R. Astron. Soc.* **263**, 999 (1993)
506. Tadhunter, C.N., Morganti, R., Robinson, A., et al.: The nature of the optical-radio correlations for powerful radio galaxies. *Mon. Not. R. Astron. Soc.* **298**, 1035–1047 (1998)
507. Taylor, G.L., Dunlop, J.S., Hughes, D.H., Robson, E.I.: A near-IR study of the host galaxies of radio-quiet quasars, radio-loud quasars and radio galaxies. *Mon. Not. R. Astron. Soc.* **283**, 930–968 (1996)
508. Tchekhovskoy, A., Narayan, R., McKinney, J.C.: Black hole spin and the radio loud/quiet dichotomy of active galactic nuclei. *Astrophys. J.* **711**, 50–63 (2010)
509. Terashima, Y., Wilson, A.S.: Chandra snapshot observations of low-luminosity active galactic nuclei with a compact radio source. *Astrophys. J.* **583**, 145–158 (2003)
510. Terlevich, R., Tenorio-Tagle, G., Franco, J., Melnick, J.: The starburst model for active galactic nuclei – the broad-line region as supernova remnants evolving in a high-density medium. *Mon. Not. R. Astron. Soc.* **255**, 713–728 (1992)
511. Thomas, H.-C., Beuermann, K., Reinsch, K., et al.: Identification of soft high galactic latitude RASS X-ray sources. I. A complete count-rate limited sample. *Astron. Astrophys.* **335**, 467

- (1998)
512. Titarchuk, L., Laurent, P., Shaposhnikov, N.: On the nonrelativistic origin of red-skewed iron lines in cataclysmic variable, neutron star, and black hole sources. *Astrophys. J.* **700**, 1831–1846 (2009)
 513. Tombesi, F., Sambruna, R.M., Reeves, J.N., et al.: Discovery of ultra-fast outflows in a sample of broad-line radio galaxies observed with *suzaku*. *Astrophys. J.* **719**, 700–715 (2010)
 514. Tueller, J., Mushotzky, R.F., Barthelmy, S., et al.: Swift BAT survey of AGNs. *Astrophys. J.* **681**, 113 (2008)
 515. Tueller, J., Baumgartner, W.H., Markwardt, C.B., et al.: The 22 month *swift*-BAT all-sky hard x-ray survey. *Astrophys. J. Suppl. Ser.* **186**, 378 (2010)
 516. Turner, T.J., Miller, L.: X-ray absorption and reflection in active galactic nuclei. *Astron. Astrophys. Rev.* **17**, 47–104 (2009)
 517. Turner, T.J., Miller, L.: Cosmic-ray spallation in radio-quiet active galactic nuclei: a case study of NGC 4051. *Astrophys. J.* **709**, 1230–1237 (2010)
 518. Turner, T.J., Mushotzky, R.F., Yaqoob, T., et al.: Narrow components within the Fe $K\alpha$ profile of NGC 3516: evidence of the importance of general relativistic effects? *Astrophys. J. Lett.* **574**, L123–L127 (2002)
 519. Turner, T.J., Kraemer, S.B., Reeves, J.N.: Transient relativistically shifted lines as a probe of black hole systems. *Astrophys. J.* **603**, 62–66 (2004)
 520. Turner, T.J., Miller, L., Reeves, J.N., Kraemer, S.B.: The variable x-ray spectrum of markarian 766. II. Time-resolved spectroscopy. *Astron. Astrophys.* **475**, 121–131 (2007)
 521. Turner, T.J., Reeves, J.N., Kraemer, S.B., Miller, L.: Tracing a disk wind in NGC 3516. *Astron. Astrophys.* **483**, 161–169 (2008)
 522. Turner, T.J., George, I.M., Nandra, K., Turcan, D.: On x-ray variability in seyfert galaxies. *Astrophys. J.* **524**, 667–673 (1999)
 523. Turner, T.J., Miller, L., Kraemer, S.B., Reeves, J.N., Pounds, K.A.: *Suzaku* observation of a hard excess in 1H 0419 - 577: detection of a compton-thick partial-covering absorber. *Astrophys. J.* **698**, 99–105 (2009)
 524. Ulrich, M.-H., Maraschi, L., Urry, C.M.: Variability of active galactic nuclei. *Ann. Rev. Astron. Astrophys.* **35**, 445–502 (1997)
 525. Ulvestad, J.S., Wilson, A.S.: Radio structures of seyfert galaxies. vii – Extension of a distance-limited sample. *Astrophys. J.* **343**, 659–671 (1989)
 526. Ulvestad, J.S., et al.: A subparsec radio jet or disk in NGC 4151. *Astrophys. J.* **496**, 196 (1998)
 527. Ulvestad, J.S., et al.: Subrelativistic radio jets and parsec-scale absorption in two seyfert galaxies. *Astrophys. J. Lett.* **517**, L81–L84 (1999)
 528. Ulvestad, J.S., Wong, D.S., Taylor, G.B., et al.: VLBA identification of the milliarcsecond active nucleus in the seyfert galaxy NGC 4151. *Astrophys. J.* **130**, 936–944 (2005)
 529. Urry, C.M., Padovani, P.: Unified schemes for radio-loud active galactic nuclei. *PASP* **107**, 803–845 (1995)
 530. Vagnetti, F., Trevese, D., Nesci, R.: Spectral slope variability of BL lacertae objects in the optical band. *Astrophys. J.* **590**, 123 (2003)
 531. Valtaoja, E., Korhonen, T., Valtonen, M., et al.: A 15.7-min periodicity in OJ287. *Nature* **314**, 148 (1985)
 532. Valtonen, M.J., Kidger, M., Lehto, H., Poyner, G.: The structure of the october/november 2005 outburst in OJ287 and the precessing binary black hole model. *Astron. Astrophys.* **477**, 407 (2008)
 533. Valtonen, M.J., Lehto, H.J., Nilsson, K., et al.: A massive binary black-hole system in OJ287 and a test of general relativity. *Nature* **452**, 851 (2008)
 534. Vanden Berk, D.E., Richards, G.T., Bauer, A., Strauss, M.A., Schneider, D.P., Heckman, T.M., York, D.G., Hall, P.B., Fan, X., et al.: Composite quasar spectra from the sloan digital sky survey. *Astron. J.* **122**, 549–564 (2001)
 535. Vanden Berk, D.E., Schneider, D.P., Richards, G.T., et al.: An empirical calibration of the completeness of the SDSS quasar survey. *Astron. J.* **129**, 2047–2061 (2005)

536. Vasudevan, R.V., Fabian, A.C.: Simultaneous x-ray/optical/UV snapshots of active galactic nuclei from XMM-newton: spectral energy distributions for the reverberation mapped sample. *Mon. Not. R. Astron. Soc.* **392**, 1124 (2009)
537. Villata, M., Raiteri, C.M., Kurtanidze, O.M., et al.: The WEBT campaigns on BL lacertae. Time and cross-correlation analysis of optical and radio light curves 1968–2003. *Astron. Astrophys.* **424**, 497 (2004)
538. Visnovsky, K.L., Impey, C.D., Foltz, C.B., et al.: Radio properties of optically selected quasars. *Astrophys. J.* **391**, 560–568 (1992)
539. Vladimirovsky, B.M., Zyskin, Yu.L., Kornienko, A.P., et al.: Design principles and description of the second-generation gamma-telescope GT-48. *Izvestiya of the Crimean Astrophysical Observatory* **91**, 74 (1994) (in Russian)
540. Voges, W., Aschenbach, B., Boller, Th., et al.: The ROSAT all-sky survey bright source catalogue. *Astron. Astrophys.* **349**, 389 (1999)
541. Volonteri, M., Sikora, M., Lasota, J.-P.: Black hole spin and galactic morphology. *Astrophys. J.* **667**, 704–713 (2007)
542. Vol'vach, A.E., Vol'Vach, L.N., Larionov, M.G., et al.: Correlations between the development of a flare in the Blazar 3C 454.3 in the radio and optical. *Astron. Rep.* **52/11**, 867–874 (2008)
543. Vol'vach, A.E., Vol'Vach, L.N., Kardashev, N.S., Larionov, M.G.: Studies of sources from the WMAP catalog. *Astron. Rep.* **52/6**, 429–441 (2008)
544. Vol'vach, A.E., Vol'Vach, L.N., Kut'kin, A.M., et al.: Sub-parsec structure of binary supermassive black holes in active galactic nuclei. *Astron. Rep.* **54/1**, 28–37 (2010)
545. Volvach, A.E., et al., Kinematics and physics of celestial bodies, in press (2011)
546. Wagner, S., Sanchez-Pons, F., Quirrenbach, A., Witzel, A.: Simultaneous optical and radio monitoring of rapid variability in quasars and BL lac objects. *Astron. Astrophys.* **235**, L1 (1990)
547. Wampler, E.J., Gaskell, C.M., Burke, W.L., Baldwin, J.A.: Spectrophotometry of two complete samples of flat radio spectrum quasars. *Astrophys. J.* **276**, 403 (1984)
548. Wang, T.-G., Zhou, Hong-Yan, Wang, Jun-Xian, et al.: Evidence for a population of beamed radio-intermediate quasars. *Astrophys. J.* **645**, 856–860 (2006)
549. Ward, M., Elvis, Martin, Fabbiano, G., et al.: The continuum of type-1 seyfert galaxies. I – A single form modified by the effects of dust. *Astrophys. J.* **315**, 74–91 (1987)
550. Warner, C., Hamann, F., Dietrich, M.: A relation between supermassive black hole mass and quasar metallicity? *Astrophys. J.* **596**, 72 (2003)
551. Weisskopf, M.C., Tananbaum, H.D., Van Speybroeck, L.P., O'Dell, S.L.: Chandra x-ray observatory (CXO): overview. In: Truemper, J.E., Aschenbach, B., (eds.) Society of Photo-Optical Instrumentation Engineers (SPIE) Conference Series, **4012**, 2–16 (2000)
552. White, R.L., Helfand, D.J., Becker, R.H., et al.: Signals from the noise: image stacking for quasars in the FIRST survey. *Astrophys. J.* **654**, 99–114 (2007)
553. Wiita, P.J.: In Blazar Variability Workshop II: Entering the GLAST Era, In: Miller, H.R., Marshall, K., Webb, J.R., Aller, M.F.(eds.) ASP Conf. Ser. vol. 350, p. 183. ASP, San Francisco, 2006
554. Williams, R.: The ionization and thermal equilibrium of a gas excited by ultraviolet synchrotron radiation. *Astrophys. J.* **147**, 556 (1967)
555. Wills, B.J., Netzer, H., Wills, D.: Broad emission features in QSOs and active galactic nuclei. II. – New observations and theory of FeII and HI emission. *Astrophys. J.* **288**, 94 (1985)
556. Wills, B.J., Browne, I.W.A.: Relativistic beaming and quasar emission lines. *Astrophys. J.* **302**, 56 (1986)
557. Wilkes, B.J.: Studies of broad emission line profiles in QSO. I – Observed, high-resolution profiles. *Mon. Not. R. Astron. Soc.* **207**, 73–98 (1984)
558. Wilkinson, P.N., et al.: Radio structure of 3C147 determined by multi-element very long baseline interferometry. *Nature* **269**, 764–768 (1977)
559. Wilms, J., et al.: XMM-EPIC observation of MCG-6-30-15: direct evidence for the extraction of energy from a spinning black hole? *Mon. Not. R. Astron. Soc.* **328**, L27–L31 (2001)

560. Wilson, A.S., Colbert, E.J.M.: The difference between radio-loud and radio-quiet active galaxies. *Astrophys. J.* **438**, 62–71 (1995)
561. Winter, L.M., Mushotzky, R.F., Reynolds, C.S., Tueller, J.: X-ray spectral properties of the BAT AGN sample. *Astrophys. J.* **690**, 1322 (2009)
562. Wisotzki, L., Christlieb, N., Bade, N., et al.: The hamburg/ESO survey for bright QSOs. III. A large flux-limited sample of QSOs. *Astron. Astrophys.* **358**, 77–87 (2000)
563. Worrall, D.M., Birkinshaw, M., Hardcastle, M.J.: The x-ray jet and central structure of the active galaxy NGC 315. *Mon. Not. R. Astron. Soc.* **343**, L73–L78 (2003)
564. Worrall, D.M.: The x-ray jets of active galaxies. *Astron. Astrophys. Rev.* **17**, 1–46 (2009)
565. Wrobel, J.M., Heeschen, D.S.: Radio-continuum sources in nearby and bright e/s0 galaxies – active nuclei versus star formation. *Astron. J.* **101**, 148–169 (1991)
566. Wu, J., Vanden Berk, Daniel, E., et al.: Probing the origins of the C IV and Fe K α baldwin effects. *Astrophys. J.* **702**, 767–778 (2009)
567. Yaqoob, T., George, I.M., Kallman, T.R., et al.: Fe XXV and Fe XXVI diagnostics of the black hole and accretion disk in active galaxies: chandra time-resolved grating spectroscopy of NGC7314. *Astrophys. J.* **596**, 85–104 (2003)
568. Yaqoob, T., Padmanabhan, U.: The cores of the Fe K lines in seyfert-1 galaxies observed by the chandra high energy grating. *Astrophys. J.* **604**, 63–73 (2004)
569. Yaqoob, T., Murphy, K.D., Miller, L., Turner, T.J.: On the efficiency of production of the Fe K α emission line in neutral matter. *Mon. Not. R. Astron. Soc.* **401**, 411–417 (2010)
570. York, D.G., Adelman, J., Anderson, John, E., Jr., et al.: The sloan digital sky survey: technical summary. *Astron. J.* **120**, 1579–1587 (2000)
571. Young, A.J., Wilson, A.S., Shopbell, P.L.: A chandra x-ray study of NGC 1068. I. Observations of extended emission. *Astrophys. J.* **556**, 6–23, (2001)
572. Young, A.J., Lee, J.C., Fabian, A.C., et al.: A chandra HETGS spectral study of the iron K bandpass in MCG -6-30-15: a narrow view of the broad iron line. *Astrophys. J.* **631**, 733 (2005)
573. Young, M., Elvis, M., Risaliti, G.: The fifth data release sloan digital sky survey/XMM-newton quasar survey. *Astrophys. J. Suppl. Ser.* **183**, 17 (2009)
574. Yuan, W., Siebert, J., Brinkmann, W.: Does the optical-to-x-ray energy distribution of quasars depend on optical luminosity? *Astron. Astrophys.* **334**, 498 (1998)
575. Yuan, W., Zhou, H.Y., Komossa, S., et al.: A population of radio-loud narrow-line seyfert-1 galaxies with blazar-like properties? *Astrophys. J.* **685**, 801–827 (2008)
576. Zamanov, R., Marziani, P., Sulentic, J.W., et al.: Kinematic linkage between the broad- and narrow-line-emitting gas in active galactic nuclei. *Astrophys. J.* **576**, L9–L13 (2002)
577. Zamfir, S., Sulentic, J.W., Marziani, P.: New insights on the QSO radio-loud/radio-quiet dichotomy: SDSS spectra in the context of the 4D eigenvector1 parameter space. *Mon. Not. R. Astron. Soc.* **387**, 856–870 (2008)
578. Zamfir, S., Sulentic, J.W., Marziani, P., Dultzin, D.: Detailed characterization of H β emission line profile in low-z SDSS quasars. *Mon. Not. R. Astron. Soc.* **403**, 1759–1786 (2010)
579. Zensus, J.A.: Parsec-scale jets in extragalactic radio sources. *Ann. Rev. Astron. Astrophys.* **35**, 607–636 (1997)
580. Zhou, H.-Y., Wang, T., Yuan, W., et al.: A narrow-line seyfert 1-blazar composite nucleus in 2MASXJ0324+3410. *Astrophys. J.* **658**, L13–L16 (2007)
581. Zoghbi, A., Fabian, A.C., Uttley, P., et al.: Broad iron L line and X-ray reverberation in 1H0707-495. *Mon. Not. R. Astron. Soc.* **401**, 2419–2432 (2010)
582. Życki, P.T.: Modelling the variability of the Fe K α line in accreting black holes. *Mon. Not. R. Astron. Soc.* **351**, 1180–1186 (2004)

Chapter 4

Quasars Classes and Their Relationships

Contributions by Mauro D’Onofrio, Paola Marziani, Jack W. Sulentic, Deborah Dultzin, Yuri Efimov, Martin Gaskell, Marianne Vestergaard, Damien Hutsemékers, Alberto Franceschini, Ari Laor, Dirk Grupe, Sebastian Lipari, Begoña García Lorenzo, Evencio Mediavilla, Todd Boroson, Mike Eracleous, Isabel Marquez-Perez, Elmar Körding, and Heino Falcke

M. D’Onofrio

Dipartimento di Astronomia, Università degli Studi di Padova, Vicolo Osservatorio 3,
I35122 Padova, Italy
e-mail: mauro.donofrio@unipd.it

P. Marziani

INAF, Osservatorio Astronomico di Padova, Vicolo Osservatorio 5, IT35122 Padova, Italy
e-mail: paola.marziani@oapd.inaf.it

J.W. Sulentic (✉)

Instituto de Astrofísica de Andalucía (CSIC), Granada, Spain
e-mail: sulentic@iaa.es

D. Dultzin

Instituto de Astronomía, Universidad Nacional Autónoma de México (UNAM), Apt.do postal
70-264, México, D.F., México
e-mail: deborah@astrocu.unam.mx

Y. Efimov

Crimean Astrophysical Observatory, 98409, Nauchny, Crimea, Ukraine
e-mail: yseyse@mail.ru

M. Gaskell

Departamento de Física y Astronomía, Facultad de Ciencias, Universidad de Valparaíso,
Av. Gran Bretaña 1111, Valparaíso, Chile
e-mail: martin.gaskell@uv.cl

M. Vestergaard

The Dark Cosmology Centre, The Niels Bohr Institute, University of Copenhagen,
Juliane Maries Vej 30, 2100 Copenhagen 0, Denmark

Steward Observatory and Department of Astronomy, University of Arizona, 933 N. Cherry
Avenue, Tucson 85721, Arizona, USA
e-mail: vester@dark-cosmology.dk

D. Hutsemékers

F.R.S. - FNRS, Institute of Astrophysics and Geophysics, University of Liège, Allée du six août
17, B5c, B-4000, Liège, Belgium
email: hutsemekers@astro.ulg.ac.be

A. Franceschini

Dipartimento di Astronomia, Università degli Studi di Padova, Vicolo Osservatorio 3,
I35122 Padova, Italy
e-mail: alberto.franceschini@unipd.it

Most of the questions in this chapter deal with sources that do not show the “classical” broad emission-line spectrum that characterizes the majority of known AGNs at high and low redshift. If that majority represents a “parent population” of AGNs, is the apparent absence of broad lines a result of obscuration, orientation, or different physical conditions? Can all of the subclasses be unified under the AGN umbrella? With the unification scheme set in place and assumed to be fundamentally correct, there are at least four overarching questions: do all type-2 AGNs possess an obscured broad-line region? Or how can we distinguishing type-2 AGNs without a broad-line region if they exist? Where is the low end of quasar activity? The

A. Laor

Technion - Israel Institute of Technology, Physics Department, Technion City, Haifa 32000, Israel
e-mail: laor@physics.technion.ac.il

D. Grupe

The Pennsylvania State University, 525 Davey Lab., University Park, PA 16802, USA
e-mail: grupe@astro.psu.edu

S. Lipari

Observatorio Astronómico de la Univ. Nac. de Córdoba, Laprida 854, X5000BGR, Córdoba, Argentina, and CONICET, Argentina
e-mail: lipari@oac.uncor.edu

B. García-Lorenzo

Instituto de Astrofísica de Canarias, E-38200 La Laguna, Tenerife, Spain
email: garcialorenzo@iac.es

E. Mediavilla

Instituto de Astrofísica de Canarias, E-38200 La Laguna, Tenerife, Spain
e-mail: mediavilla@iac.es

T. Boroson

National Optical Astronomy Observatory, Tucson, AZ, USA
e-mail: tyb@noao.edu

M. Eracleous

Department of Astronomy and Astrophysics and Center for Gravitational Wave Physics, The Pennsylvania State University, 525 Davey Lab., University Park, PA 16802, USA
e-mail: mce@astro.psu.edu

I.M. Pérez

Instituto de Astrofísica de Andalucía (CSIC), Granada, Spain
e-mail: isabel@iaa.es

E. Körding

Radboud Universiteit Nijmegen, Department of Astronomy, IMAPP, The Netherlands
e-mail: elmar.koerding@astro.ru.nl

H. Falcke

Radboud Universiteit Nijmegen, Department of Astronomy, IMAPP, The Netherlands
ASTRON, Dwingeloo, The Netherlands
Max-Planck Institut für Radioastronomie, Bonn, Germany
e-mail: h.falcke@astro.ru.nl

least luminous AGNs are the so-called low-ionization nuclear emission-line regions (LINERs), but it is legitimate to ask if they are all true AGNs. A third question is related to the active nucleus development and evolution: what is the relationship with star formation, especially as occurring in the most extreme episodes? The unification scheme paints a stationary grand view of AGNs. However, as AGNs are born, evolve, and die (perhaps several time thorough repeated duty cycles), an obvious question is how evolution and unification relate. As the most important parameter of unification scheme is an aspect angle, that is, the orientation at which the symmetry axis of the active nucleus is observed, we organize the chapter starting from minority objects that are believed to be observed at a special angle, that is, along (or close to) the symmetry axis, and then moving from unobscured sources (that were most widely discussed in the previous chapter) to type-2 sources that are presumably observed at large inclinations. Afterward, we consider classes of sources that are not framed within the unification scheme: narrow-line Seyfert 1s (NLSy1s), the ultra-luminous infrared galaxies, a special class of type-1 quasars with double-peaked emission-line profiles, and the least luminous AGNs, the LINERs. At the end, we include a discussion on how accretion processes occur in an extremely wide range of masses, from stellar mass black holes to the most massive radio-loud quasars.

4.1 BL Lacs and Blazars

Dear Deborah (*Dultzin*), what are the phenomenological difference between BL Lacs and blazars? So far, they are exclusively radio-loud sources? Do you think we will ever find radio-quiet examples?

BL Lac objects were discovered in the 1970s, they are a special class of radio-loud AGNs with extreme luminosities and variability characteristics. They were named after their prototype: the “variable star” BL Lacertæ. In 1968, the “star” was identified as a bright, variable radio source [266]. A faint trace of a host galaxy was also found by Oke and Gunn [233] who measured the redshift of BL Lacertæ as $z = 0.07$, corresponding to a recession velocity of $21,000 \text{ km s}^{-1}$ with respect to the Milky Way, which reclassified it as an extragalactic object. The extreme luminosities and variability, as well as other properties of BL Lac objects, such as high and variable polarization, are explained if we see a relativistic jet pointing almost in our line of sight, emitting nonthermal (basically, synchrotron and inverse Compton) radiation. There are relativistic effects known as “relativistic beaming” that enhance both the brightness of the emission and amplitude of the variability. Although in these type of objects, we see only a featureless nonthermal optical continuum most of the time, during the minimum brightness stages weak, emission broad lines can be detected.

The term blazar was originally coined in 1978 to denote the combination of both OVV quasars and BL Lac objects. An OVV (optically violent variable) quasar is a type of highly variable, rather rare, bright radio galaxy, whose visible light output can change by 50% in a day. They are similar in appearance to BL Lacs

but generally have a stronger broad emission line and tend to have higher-redshift components. The generally accepted picture is that OVV quasars are intrinsically powerful radio galaxies, also called “flat-spectrum radio sources”, while BL Lac objects are intrinsically weak radio galaxies. In both cases, the host galaxies are giant ellipticals; the viewing angle to the jet in BL Lac objects is thought to be narrower than that to the jet in OVVs ($\sim 15^\circ$). The special jet orientation explains their general peculiar characteristics (e.g., [132, 229, 258, 281]): high observed luminosity, very rapid variation, high polarization (when compared with non-blazar quasars), and the apparent superluminal motions, probably due to relativistic shock fronts, detected along the first few parsecs of the jets in most blazars.

Alternate explanations for the relativistic jet/unified scheme approach which have been proposed include gravitational microlensing (e.g., [211, 237]) and coherent emission from the relativistic jet. Neither of these explains the overall properties of blazars. For example, microlensing is achromatic, that is, all parts of a spectrum will rise and fall together. This is very clearly not observed in blazars. However, it is possible that these processes, as well as more complex plasma physics, can account for specific observations or some details.

And so, to answer the editors’ specific question on the possible existence of “radio-quiet examples” of blazars, my opinion is NO. The essence of the phenomenology is a jet. In many properties though, BL Lac-type objects can be distinguished from OVV quasars (i.e., blazars vs. “pure BL Lac”).

As for the current state of the art, multiwavelength studies of the variability of blazars are crucial in order to understand the physical processes responsible for the emission along the whole spectrum from the radio to MeV and TeV energies. Since the detection of the exceptional 2005 outburst of 3C 454.3 [96, 106, 241], several monitoring campaigns were carried out to follow this source multifrequency behavior [248, 249]. For other sources, such campaigns have also been conducted. These campaigns require the organization of very large amounts of observers both in earth- and space-bound telescopes and have recently yielded impressive results. For the most recent observational results and interpretation, see [1, 2].

The spectral energy distributions (SEDs) of blazars typically show two distinct humps (see the review by Urry et al. [304]). The first peak occurs in the IR-Optical band in the flat-spectrum radio quasars (FSRQs) and in the low-energy-peaked BL Lacs (LBLs), and at UV-X-rays in the High-energy-peaked BL Lacs (HBLs). The second hump peaks at MeV-GeV and TeV energies in FSRQs/LBLs and in HBLs, respectively. In the framework of leptonic models, the first peak is commonly interpreted as synchrotron radiation from high-energy electrons in the relativistic jet, while the second peak is interpreted as inverse Compton (IC) scattering of soft seed photons by the same relativistic electrons. A recent review of the blazar emission mechanisms and energetics is given in [39]. Alternatively, the blazar SED can be explained in the framework of hadronic models, where the relativistic protons in the jet are the primary accelerated particles, emitting gamma-ray radiation by means of photo-pair and photo-pion production (see [217, 218]).

Thank you, Deborah

Dear Yuri (*Efimov*), why is photometric monitoring of blazars so important to understand their physics?

Among AGNs, there is an extremely exotic subclass of objects called “blazars” named after the first detected star like object of this type, BL Lacertæ. Blazars are the most violent and most luminous AGNs in the universe. These objects are thought to be elliptical galaxies with quasar-like centers. The main features of these objects are their extreme variability in brightness and polarization across a broad spectral region from far-UV to radio. These objects are also sources of powerful and variable X- and gamma-ray radiation. High polarization is an important characteristic of the radiation, and it allows us to obtain information about the physical properties of these objects. A great number of high-quality photo-polarimetric observations of BL Lac objects were carried out at the CRAO by Drs. Yu.S. Efimov and N.M. Shakhovskoy starting in the 1970s with the 2.6-m Shajn telescope (PKS 0109+224, AO 0535+15, 3C 345, PKS 0735+178). This work has continued since 1981 with the 1.25-m telescope in UBVRI bands to study the structure and geometry of the regions of jets where the powerful synchrotron radiation arises. From 1994, these observations were performed in the framework of the international program OJ-94. The main targets are OJ 287, S5 0718+71, 3C 66A, Mrk 421, Mrk 501, ON 231, 3C 273, PG 1553+11, H1722+11, and 3C 454.3.

The main achievements of blazar studies at CRAO can be summarized as follows. It is extremely important to know the geometry of the magnetic field in jets. For OJ 287, during its strong flare in the period 1994–1996, the cyclic variations of polarization position angle which can be due to rotation of the polarization plane with the rate of about 5° per day [71]. It indicates the long-lived helical structure of the field in the inner part of the jet. For PKS 0735+178 in 1975–1980, a strong correlation between the total optical flux and polarized flux was found. This correlation shows a constant degree of polarization of a variable source with changing position of the polarization plane [268]. The large variations of the polarization degree (above 30%) and the position angle of polarization in long (months) and short (days) timescales were revealed in some blazars: 3C 345, 3C 371 [68], OJ 287, PKS 0735+178 [267], and 3C 66A [69]. These variations support the shock wave model for blazar jets. The short-term variations of brightness and polarization parameters can be explained by the irregular structure of the flux of relativistic electrons moving along the magnetic field in a jet. A very unique increase of the polarization degree up to 13% was observed in 1998 in blazer ON 231 during its large outburst (by 0.8 mag in V band) in 1998 [70]. Evidences of the wave-shape variations of spectral index in OJ 287 with time were found in 1994–1997 [71]. The investigation of these unique objects is in progress.

Thank you, Yuri. One of the key element of unification is obscuration of the innermost region comprising the BLR by a structure that is often described as torus of dust and gas. We would like to know first what makes a quasar “unobscured” and then the evidence that an obscured population actually exists.

4.2 Unobscured and Obscured Quasars: Where are They?

Dear Martin (*Gaskell*), most type-1 quasars appear to be remarkably little affected by internal obscuration.

The question of how much obscuration there is in AGNs has been a long-standing one. Osterbrock and Parker [234] found that the NLR of NGC 1068 had a steep Balmer decrement. Curiously, they thought that this was intrinsic (they favored a collisional origin) rather than the result of reddening. Joe Wampler demonstrated unambiguously in 1968 from observations of the [SII] lines that there was substantial reddening of the NLR of Seyfert galaxies [320]. He pointed out that “Because the reddening . . . is substantial, it has a profound effect upon the interpretation of the line spectra of Seyfert galaxies.” Joe also showed [319] that the BLR of low-redshift quasars could show a steep Balmer decrement, but he was uncertain whether this was due to radiative transfer effects or reddening. Thus, began a debate over what has become known as “the hydrogen-line problem.” This peaked in the early 1980s, but it continues down to our present day.

I have always considered the question of AGN reddening to be a very important one. The year before I went to Santa Cruz, Chris McKee and Vahé Petrosian published a paper with the simple title, “Are quasars dusty?” [206]. Their conclusion was a firm “no.” Rather than looking at line ratios, they looked at the shape of the UV continuum. The shape of the UV reddening curve in the solar neighborhood was well known at that time: the extinction rose sharply in the UV, and there was a strong dip at $\lambda 2175$. They found no evidence for either in quasar spectra. I repeated this investigation with much better data as part of my Ph.D. thesis, and I put an upper limit on the reddening of typical bright high-redshift AGNs of $E(B - V) \lesssim 0.05$ mag [99].

On the other hand, Bill Keel’s discovery of the orientation difference between low-luminosity type-1 and type-2 [147] suggested that dust *was* significant. When I went to Cambridge, Gianfranco de Zotti and I followed up on Bill’s work. We found [61] that both the colors and Balmer decrements of AGNs varied with orientation in a way that was consistent with varying reddening. A typical low-luminosity AGN would have a reddening of $E(B - V) \sim 0.2$ mag. This was clearly at variance with what I had found earlier from the shape of the UV continuum. For many years, I felt that the resolution of this problem was that low-luminosity AGNs had low reddening, while high-luminosity ones had little or no reddening (we found evidence in [61] for decreasing reddening with increasing luminosity).

A question from Ski Antonucci in 2002 led to the solution to the reddening conundrum. Ski asked me why the reddened spectra of the more edge-on radio-loud AGNs still looked like power laws. I suggested that flat reddening curves in the UV could do the trick. Ski, René Goosmann, and I calculated the reddening curves for a couple of samples of AGNs and found that they had an unprecedented reddening curve that was similar to other reddening curves in the optical but flat in the UV and lacking the “2200 Angstrom” bump [100]. Such a reddening curve can be explained by the selective destruction of small grains in the harsh environments

of an AGN torus. In addition to the flat reddening curve, we found that there was also, as expected, a decrease in reddening with increasing luminosity.

Do we find any evidence for a semi-obscured population that might bridge type-1 sources and the new IR results pointing toward a large population of highly-obscured quasars?

Of course. They seem to be rare, but they are really quite common. The problem is that “semi-obscured” AGNs are always severely underrepresented in samples of AGNs selected in the optical and UV.

Thank you, Martin. Before considering more extensively the type-2 (obscured) quasars, we now briefly discuss a class of sources whose nature is still hotly debated. They are not strictly strongly obscured sources since their optical-UV continuum is, in general, only slightly reddened. However, they show an almost total absorption of their soft X-ray continuum, implying a large column density of absorbing matter along the line of sight. First, Marianne Vestergaard will describe the general phenomenology of absorption lines in quasars; afterward, Damien Hutsemékers will focus on broad absorption line (BAL) QSOs (in this case, the acronym QSOs has survived because these sources were believed until recently to be exclusively radio quiet).

4.3 Phenomenology of Absorption Lines in Quasars

Dear Marianne (Vestergaard), there is a widely adopted criterion to define BAL sources, that is, the so-called BALnicity index. Absorption lines less deep and wide than the typical BAL yielding BALnicity index >0 are also observed. Some of the sources are called “mini-BAL” QSOs. Can you please summarize the phenomenology of these narrow-to-semi-broad absorption lines still believed to be intrinsic to quasars?

Absorption lines in quasar spectra are generated when the light from the quasar passes through gas where the emission at specific wavelengths are absorbed by the particles in the gas and then reemitted in a random direction. The width of the line depends on the density of the gas, the internal kinematics of the gas, and the covering factor. The covering factor (or fraction) reflects the fraction of the (quasar) source that is covered by the absorber.

The absorption lines in quasars are classified according to their widths. Crudely speaking, they are narrow or broad. Strangely enough, they are not also classified according to their strengths (weak or strong), but there is somewhat of a connection there. Instead, we talk about “intrinsic” and “intervening” absorbers. We use the terminology “intervening” as opposed to “external” since the gas must be between the quasar and us to be detected in absorption. By definition, it is “intervening.” By “intrinsic,” we mean that the gas is associated with the quasar and its host galaxy, that is, it is located within the general extent of the galaxy.

The intrinsic absorption lines tend to have an equivalent width, EW, stronger than 1 \AA (e.g., [325]) and be located within $\sim 5,000 \text{ km s}^{-1}$ of the systemic redshift (e.g., [89]; they are also often called “associated”). These absorption lines are typically of the “narrow” category. s BALs are blueshifted relative to the systemic quasar frame (set by the peak of the emission lines). We observe outflow velocities from as little as 0 km s^{-1} up to $60,000 \text{ km s}^{-1}$ which is a significant fraction of light speed, and widths of $10,000\text{--}20,000 \text{ km s}^{-1}$ are not uncommon. To be classified as a bona fide BAL, usually, the velocity width should be larger than $3,000 \text{ km s}^{-1}$ and the blueshifted absorption extrema greater than about $5,000 \text{ km s}^{-1}$ (e.g., [129]).

The narrow absorption lines (NALs) typically have widths less than a few 100 km s^{-1} , so they are rather sharp features in the spectra. They can appear at any location between the systemic velocity of the quasar and $z \approx 0$. As noted, most of the weak NALs ($EW < 1 \text{ \AA}$) are gas clouds unrelated to the quasar located between us and the quasar.

But the situation is not quite as black and white (or “narrow” and “broad”). There are in fact absorption lines that are intermediate in width between the NALs and BALs. They tend to be less deep than NALs but less broad than BALs. They do look like a weaker, lower velocity version of BALs, so their name “mini-BALs” are very appropriate. Just like the BALs, the mini-BALs can start at the emission line peak and extend blueward thereof, or they can be “detached” from the emission peak. The broad-line widths of both BALs and mini-BALs show that the absorber must be associated with the quasar itself. The fact that mini-BALs span similar blueshifts of its maximum absorption depth and are as smooth in the absorption troughs as BALs suggest that both types of absorption lines share a common origin in outflowing dense gas. The difference in widths may be related to the combination of kinematics, column density, and covering factor of the absorber (see, e.g., [11]).

Thank you, Marianne.

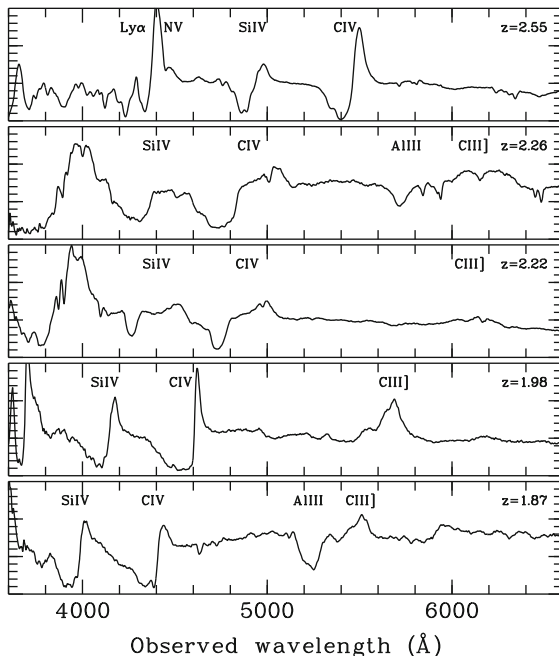
4.3.1 The Broad Absorption Lines QSOs

Dear Damien (*Hutsemékers*), a fraction of quasar spectra show deep absorption troughs in the UV resonance lines of several ionic species. Can you provide a description of the typical spectra of such BAL quasars? Is the BAL appearance a purely high-luminosity, radio-quiet phenomenon? How do BAL QSOs relate to the parent population of quasars?

About 15% of radio-quiet quasars show deep, BALs in the resonance lines of ionized species, such as CIV $\lambda 1550 \text{ \AA}$, SiIV $\lambda 1400 \text{ \AA}$, or NV $\lambda 1240 \text{ \AA}$. Typical spectra of BAL QSOs are illustrated in Fig. 4.1.

The absorption lines appear blueshifted with respect to the corresponding emission lines. They often start close to the emission lines, suggesting they are *intrinsic* to the quasars, as opposed to the narrow *intervening* absorption line systems which come from material disseminated at various redshifts along the line of sight.

Fig. 4.1 Typical spectra of BAL QSOs. The most important emission/absorption lines are indicated, as well as the redshift z of the quasars. These low-resolution spectra were obtained with the EFOSS spectrograph attached to the 3.6-m telescope at the European Southern Observatory, La Silla



Blueshifted absorption is expected if the absorbers are located between the source of continuum and the observer, outflowing from the quasar inner regions. Interpreted in terms of Doppler velocity shifts, absorption is frequently observed at velocities of a few $1,000 \text{ km s}^{-1}$, reaching up to $\sim 60,000 \text{ km s}^{-1}$, that is, $\sim 20\%$ of the speed of light. While intrinsic absorbers are ubiquitous in AGN, high-velocity BAL flows are only observed in quasars, not in low-luminosity AGNs like Seyfert-1 galaxies.

Quasar BALs display a huge variety of shapes. The absorption can be smooth and cut the adjacent emission, forming a *P Cygni-type* profile; it can also be clearly *detached* from the emission line, separated by several thousands km s^{-1} . Some BALs show contiguous absorption, while other ones have several distinct troughs. Although the criteria are somewhat arbitrary, a quasar with contiguous absorption spread on more than $2,000 \text{ km s}^{-1}$ and with a blueward velocity of at least $5,000 \text{ km s}^{-1}$ can be considered as a BAL QSO [325]. Since absorption in high-ionization species like CIV $\lambda 1550 \text{ \AA}$ is required to classify a quasar as a BAL QSO, the detection of BAL QSOs at optical wavelengths is biased toward high redshifts, typically $z \geq 1.5$.

While most BAL QSOs show absorption troughs only in the high-ionization species (HiBALs), approximately 10% of them show *in addition* BALs in low-ionization species such as MgII $\lambda 2800 \text{ \AA}$ or AlIII $\lambda 1860 \text{ \AA}$ (LoBALs), and 2% of them show *in addition* FeII absorption blueward of $\lambda 2800 \text{ \AA}$ (FeLoBALs). More extreme BAL QSOs have been occasionally uncovered in large surveys [127].

It was believed for a long time that BAL QSOs were exclusively radio quiet [285]. The advent of larger, deeper surveys has revealed that many radio-loud BAL quasars do exist, though the incidence of BALs still decreases among the strongest radio sources [17].

Owing to the difficulties in defining robust criteria [264] and achieving complete and unbiased surveys, the exact fraction of BALs among quasars is still poorly known and oscillates between 10 and 40% [6].

Two major interpretations of the BAL phenomenon in quasars have been proposed, usually referred to as *the unification by evolution* and the *unification by orientation* models.

In the first case, the BAL phenomenon represents a step in quasar evolution. Because LoBAL and FeLoBAL quasars apparently contain more dust than non-BAL QSOs, they were considered as young objects emerging from their dust cocoons [317]. Evolutionary sequences such as FeLoBAL \rightarrow LoBAL \rightarrow HiBAL \rightarrow non-BAL were proposed. The fact that some LoBAL QSOs, spatially resolved, appear as young dusty interacting objects, possibly related to ultraluminous infrared galaxies, has provided some support to this scenario [178].

The second model, the most popular, hypothesizes that absorbers are present in all quasars and that the covering factor, that is, the fraction of 4π steradians subtended by the absorbers as seen from the quasar continuum source, is equal to the detection frequency of BALs in quasar spectra, which is of the order of 15%. Only those quasars properly oriented with respect to the observer are thus recognized as BAL QSOs. In this framework, orientation-independent observables are expected to be identical in BAL and non-BAL QSOs. And indeed, apart from subtle differences, important characteristics like emission-line strength and width, or mid-infrared dust emission, appear on average similar in BAL and non-BAL QSOs, suggesting that BAL and non-BAL QSOs are actually drawn from the same parent population [97, 325]. Furthermore, the net polarization measured in the continuum of many BAL QSOs, interpreted in terms of light scattering, indicates that the quasar structure often departs from spherical symmetry. Based on spectropolarimetric observations and theoretical simulations, and assuming the scatterers located in a polar region, a picture then emerged where absorbers are mainly distributed close to the equatorial plane, possibly in a wind issued from the accretion disk [108, 115, 232]. Many variants have been proposed; one of them is illustrated in Fig. 4.2.

The discovery of radio-loud BAL QSOs severely weakened this kind of scenario. Indeed, the radio jets, perpendicular to the equatorial plane, extend over large distances from the quasar core. They can thus be mapped at milliarcsecond scale, providing a direct indication of the orientation of the quasar structure with respect to the line of sight. Contrary to expectations, several BAL QSOs are seen pole-on, and not only edge-on, revealing the existence of polar flows [35, 333].

The BAL phenomenon in quasars thus appears much more complex than depicted by either the *orientation* or the *evolution* unification paradigms, especially when considering the low-ionization or the radio-loud BAL QSOs, whose properties indicate a full range of covering factors and orientations, including both polar and equatorial flows.

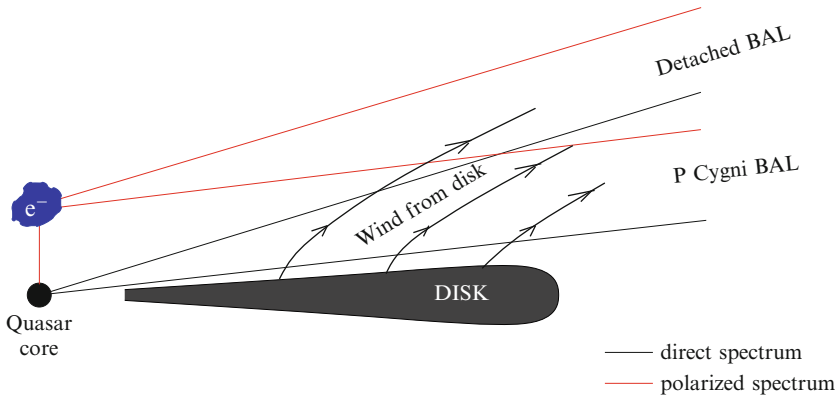


Fig. 4.2 Schematic illustration [161] explaining the polarization properties of a BAL QSO in the framework of the popular *unification by orientation* model. The equatorial wind, represented by the *curved streamlines*, emerges from a geometrically thin accretion disk located in the equatorial plane. At high inclinations (equatorial view) the observer sees a BAL QSO while, at low inclinations (polar view), he sees a non-BAL QSO. A mirror of electrons, located in the polar region, scatters radiation coming from the central regions toward to observer. At high inclinations, both the direct (unpolarized) and scattered (polarized) continua are absorbed in the equatorial wind, assumed to be denser close to the disk. BALs thus appear weaker in the scattered (polarized) spectrum, making the continuum remaining in the BALs more polarized than the adjacent one in the total (direct+scattered) spectrum. Moreover, the direct continuum being more attenuated than the polarized one at high inclinations, the continuum seen by the observer appears more polarized in BAL QSOs than in non-BAL QSOs. When the disk is seen near edge-on, P Cygni-type profiles are observed since the observer sees absorption at all velocities including the low ones near the disk. For less inclined line of sights, detached absorption profiles are observed because the observer misses the low velocity part of the absorption

Fortunately, recent large surveys like the Sloan Digital Sky Survey (SDSS) have uncovered thousands of BAL QSOs [105], allowing meaningful statistical analyses. In parallel, the multiwavelength coverage is definitely increasing for a number of objects, thanks to X-ray and mid- to far-infrared satellites recently launched [97]. This wealth of new data, which only starts to deliver results, should provide us with a better understanding of BAL QSOs, including the role of their outflows in quasar feedback. But it might ultimately appear that, alike the P Cygni line profiles in stars, the BAL *phenomenon* occurs in a wide variety of physically different objects.

Can you please summarize how observations of the BAL profiles might constrain the geometry and dynamics of the BAL gas flow? BALs have long been considered a strong form of evidence favoring outflow motions in the central region of quasars. Do we observe any connection between BALs and BELs (e.g., sources with broad blueshifted/blue-asymmetric emission line)? What are the favored physical mechanisms explaining these outflows?

The BAL profiles depend on the geometry and the kinematics of the flow. Several attempts to retrieve the properties of the flow were thus based on BAL profile analysis.

First, basic arguments, ideally robust, can provide important clues. In particular, photons absorbed in resonance lines are reemitted in all directions, escape the flow, and contribute to the broad emission-line (BEL) profiles. If the flow is spherically symmetric, one expects, for any line of sight, that the number of resonantly scattered photons is equal to the number of absorbed photons, that is, that the equivalent width of the emission line due to resonance scattering is equal to the equivalent width of the absorption line. The fact that in many BAL QSOs the equivalent width of the absorption lines is stronger than the equivalent width of the emission lines suggests that the flow is rarely spherically symmetric, and the covering factor is often much smaller than one [130]. Although departure to spherical symmetry is likely in a majority of BAL wind, it should be pointed out that several mechanisms, as well as models with adequate velocity distributions, can destroy or re-scatter photons and explain, at least in part, the relative weakness of the broad emission lines.

Assuming that BAL flows could be equatorial, polar, or both, axisymmetric models have been considered, including rotating disks and jets. These models can reproduce the observed line profiles. Although some ingredients, like disk rotation, seem important, the parameter space is large and not unique. Many BAL profiles can be reproduced with either polar or disk-like equatorial flows [25]. To break the degeneracy in the parameter space, additional information is needed, like radio maps, which help fix the orientation of the quasar system; spectropolarimetry, which gives a periscopic view of the quasar inner structure (Fig. 4.2); or gravitational microlensing effects, which can provide information on the size and location of the different absorption/emission regions. For instance, the modeling of the $H\alpha$ BEL profiles observed in *both the direct and the polarized light* from a nearby BAL QSO has provided convincing evidence that an outflow is actually launched from a disk with a large rotational velocity [331]. Unfortunately, such observations are still too scarce. Moreover, it should be kept in mind that a unique model may not apply to all BAL QSOs, in particular FeLoBALs [32].

As already mentioned, the contribution of the BAL forming region (BALR) to the BELs depends on the covering factor, which could be as high as 40% on average and strongly vary from one quasar to another. Observations, including spectropolarimetry of BAL QSOs [231] or evidence for $Ly\alpha$ pumping (Fig. 4.3), indicates that BELs are often formed closer to the core than BALs, either in a physically distinct BEL region (BELR)—which may be contiguous to the BALR—or just deeper in the flow. Empirically, some connections are found between BALs and BELs, such as correlations between the minimum outflow velocity (detachment) of the BAL troughs and the width or the strength of the BELs [166, 302]. Moreover, BEL blueshifts, ubiquitous (and unexplained) in non-BAL QSOs, are particularly large in BAL QSO composite spectra [252]. But the exact nature of the relation between BALs and BELs, and/or between the BALR and the BELR, is still largely unknown. More statistical analyses are clearly needed, accounting for differences between BAL QSO subtypes. Spectropolarimetry of non-BAL QSOs to identify the exact contribution of scattered light to the broad emission lines is also mandatory [321].

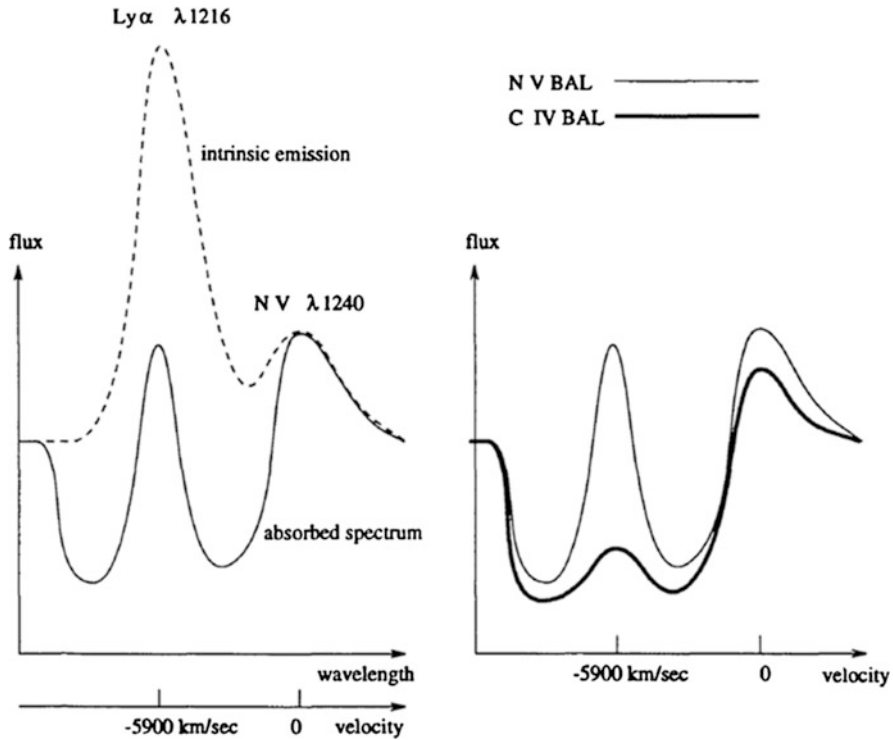


Fig. 4.3 The *ghost of Ly α* (schematic illustration from [10]). Owing to the absorption of photons from the quasar continuum source, NV ions are accelerated outward. As their velocity increases with respect to the core, they absorb bluer photons, according to the Doppler effect. The wavelength separation between Ly α λ 1215 Å and NV λ 1240 Å is 25 Å which corresponds to a Doppler velocity shift of 5,900 km s⁻¹ (left panel). When the NV ions reach the velocity of 5,900 km s⁻¹, they absorb the photons emitted in the intense Ly α emission line in addition to the photons emitted in the continuum. This suddenly increases their outward velocity. Due to Coulomb interactions between ions, all the flow is strongly accelerated, which results in smaller optical depths at velocities close to 5,900 km s⁻¹. This effect manifests itself as a bump at 5,900 km s⁻¹ in the CIV absorption trough, called the *ghost of Ly α* (right panel)

A particularly interesting observational result is the discovery of a structure in CIV BAL profiles, known as the *ghost of Ly α* [10, 157]. The mechanism at the origin of this structure is explained in Fig. 4.3. The existence of this feature demonstrates that BAL outflows accelerate, driven by radiation pressure, and that a significant part of the Ly α BEL is formed closer to the quasar core than the BAL outflow. Unfortunately, the real incidence of the *ghost of Ly α* among BAL QSOs is still unclear [53].

Supported by theoretical models [221, 245], a picture of BAL outflows as radiation-driven winds launched from the accretion disk then emerged, qualitatively explaining many observational facts. Polar flows and electron scattering regions are frequently added to account for the radio and polarimetric observations.

The scattering region may prevent overionization in the wind by shielding the BAL flow from the intense X-ray radiation of the quasar [331]. In this kind of model, the BELs are also formed in the wind.

As a conclusion, we emphasize that current models, although apparently successful, are based on observational results which are still controversial, so that there is still no compelling evidence in favor of a particular model, which in addition might not apply to all BAL QSO subtypes, in particular FeLoBALs.

More information on BAL QSOs can be found in the following conference proceedings [12, 54, 143].

Thank you, Damien.

4.4 Type-2 AGNs

Dear Alberto (*Franceschini*), is there a large population of obscured quasars in the universe? If the answer is “yes,” then what is the evidence for the existence of this population?

The existence of a large population of obscured quasars in the Universe is precisely the expectation of the unification model, an interpretative scheme that has received fair amount of support by observations of nearby sources. Looking in detail at the population statistics, however, there appears to be something that does not fit.

First of all, let us try to estimate the relative fractions of type-1 and type-2 quasars over the total population predicted by the model. This would reflect the sky-covering factor of the torus as viewed by the central source. This fundamental model parameter can in principle be inferred from modelistic analyses of the quasar infrared spectra (see, e.g., [95, 225]): in spite of some unavoidable uncertainties, the spectra seem to indicate large values of the covering factors, which would imply a small fraction of type-1 and a large incidence of type-2 quasars and AGNs. An independent confirmation of this comes from the X-ray background, whose spectral intensity can be explained by assuming a type-2 fraction of 70–80%, as explained below.

On the other hand, observational estimates of the obscured relative to unobscured AGN fractions do not seem to find so many type-2 objects, in general. Optically selected samples of galaxies and AGNs (for example, those based on the revised Shapley–Ames catalogue) typically include a roughly comparable number of AGNs of the two categories.

The most robust constraints have come from far-infrared selected samples, since a far-infrared selection is expected to provide a largely unbiased view with respect to dust extinction and is essentially a selection based on bolometric flux. Rush and collaborators [257] find evidence for a roughly similar number of type-1 and type-2 AGNs in a flux-limited local sample selected from the 12- μm IRAS survey. Remarkably, this statistics was completely confirmed at much fainter flux levels by the European Large-Area ISO Survey (ELAIS), see Fig. 4.4: in a sample of 406 faint

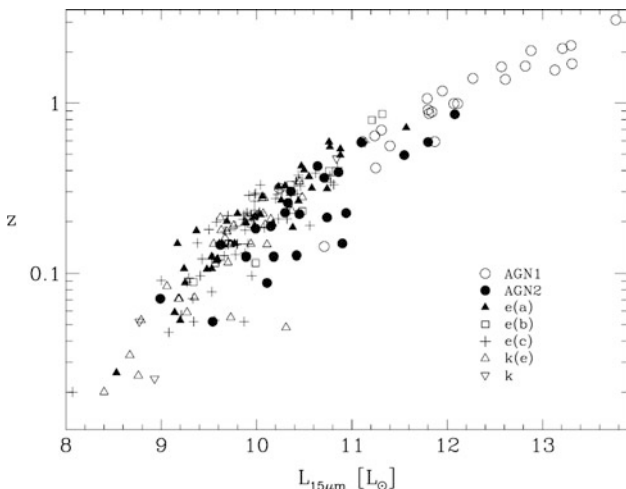


Fig. 4.4 Redshift z vs. luminosity at $15\ \mu\text{m}$ of the ELAIS-S1 spectroscopically identified sources [160]. The various source categories are indicated in the figure label

sources with $15\text{-}\mu\text{m}$ flux $> 0.5\ \text{mJy}$, 332 (82%) sources were optically identified by La Franca et al. [160], of which 25% are AGNs. Among these AGNs, 25 are type-1 (line widths $> 1,200\ \text{km s}^{-1}$) and 23 type-2 (line widths $< 1,200\ \text{km s}^{-1}$), hence again very close to the one to one ratio.

The usual difficulty is to disentangle the narrow-line AGNs from starburst galaxies. La Franca et al. [160] use classical diagnostic line ratios based on $[\text{OIII}]\lambda 5007/\text{H}\beta$ and $[\text{NII}]\lambda 6583/\text{H}\alpha$. Of the starburst galaxy population, approximately half of the sample, 37, have spectra of dust-enshrouded starbursts, 68 are normal spirals, 32 have passive elliptical-like spectra with tiny emission lines, and only 3 are spectra of old stellar populations.

Figure 4.4 illustrates another fundamental limitation of the AGN unification scheme: the most luminous objects ($L_{15\ \mu\text{m}} > 10^{12}\ L_{\odot}$ in the figure) tend to be all type-1 (typically blue, luminous, broad emission-line objects, like the optical quasars), while very luminous type-2 AGNs and quasars are missing.

In conclusion, the lack of type-2 quasars poses a challenge to our understanding: where are they?

The answer to the above question is not univocal, and various physical processes are in operation, two of them in particular. The first one is related with the feedback effect of the luminous central source on the accreting circumnuclear material, in terms of both the radiant and mechanical power. The pressure and heat would quickly get rid of the surrounding gas, and this would be exactly a luminosity-dependent effect. According to this, optically blue, luminous, and broad-line type-1 quasars would be transition objects observed after destruction of the material originally responsible for the object activity [260].

In addition to this “physical,” or intrinsic, bias, there is likely another one operating against the detection of the type-2 quasar population in the optical and related to the presence of optically thick material associated with the nuclear accretion flow. If the optical observations are unsuited for the detection of obscured quasars, far-infrared selection should work much better, as already mentioned.

Indeed, a major discovery of the IRAS mission was the identification of luminous, ultraluminous, and hyperluminous phases in galaxies (respectively LIRGs, with $L > 10^{11} L_{\odot}$; ULIRGs, $L > 10^{12} L_{\odot}$; HyLIRGs, $L > 10^{13} L_{\odot}$), among which the elusive type-2 AGNs and quasars may hide. Together with the optical quasars, these are the most luminous objects in the local universe. The most luminous of these sources, the ULIRGs and HyLIRGs, may represent the long-sought type-2 quasars.

Perhaps, the first luminous type-2 quasar was indeed discovered in the infrared luminous galaxy IRAS 09104+4109, the central galaxy of a high-redshift ($z = 0.44$) cluster: hard X-ray observations by Franceschini et al. [91] have shown this to host a hard X-ray object with unabsorbed broad-band 2–100-keV emission with bolometric flux $L \simeq 2.5 \cdot 10^{46} \text{ erg s}^{-1}$, well within the range of quasar luminosities (Fig. 4.5). The object shows very high-column density of gas. X-ray data also indicate the presence of a huge flow of cooling plasma in the cluster ($\sim 1,000 M_{\odot}$), suggesting a condition of extremely fast mass accumulation that favors the survival of a thick obscuring envelope, which would otherwise be quickly destroyed by the very luminous central source.

Are we talking here about the unification-predicted population of type-2 quasars or a new population of quasars where sources at all orientations are obscured?

Many years after their discovery, the nature, physical, and statistical properties of the LIRGs and ULIRGs still remain rather enigmatic: large gas and dust column densities in the galaxy cores, responsible for the IR emission, prevent a direct observation of the primary energy source. In many cases, these objects appear to be completely covered by the absorbing medium, such that the partial covering with polar holes predicted by the unification scheme does not apply. Hence, the classification tools based on the detection of high-ionization lines emitted by the torus polar regions do not work. At the same time, the IR spectral shapes are highly degenerate with respect to the illuminating source and cannot be conclusively used. A paradigmatic case of such a completely covered, elusive source is the local ULIRG Arp 220: at the current stage, the presence of a completely embedded nuclear AGN contributing to the large IR flux is still strongly debated; you will always find supporters and opposers to such a presence. But no conclusive answer is presently possible.

Spectroscopic observations in the IR and hard X-rays offer in principle opportunities to probe the physical conditions in these obscured active galaxies, while widespread presence of dust makes optical–UV–NIR line diagnostics completely unreliable. The IR spectral domain (10–1,000 μm) includes a number of emission lines produced by atomic and molecular transitions corresponding to wide varieties

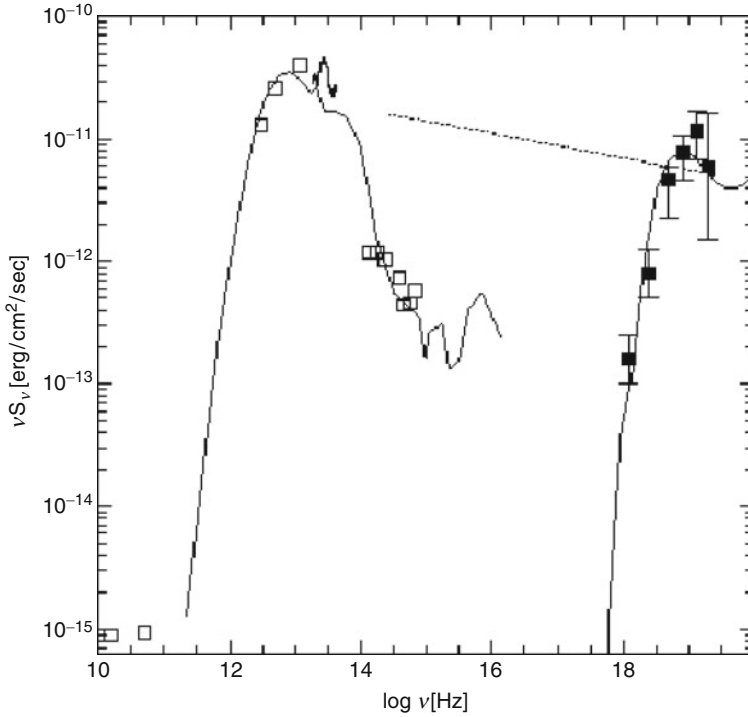


Fig. 4.5 The broad-band spectrum of the type-2 quasar IRAS 09104+4109 over 10 decades in photon energy. The IR and hard X-ray spectra are fitted with an AGN model including a dusty torus responsible for the IR emission with the associated gas photoelectrically absorbing the X-ray photons [91]. The dotted line indicates the average X-ray to IR flux of type-1 AGNs. X-ray datapoints are from BeppoSAX observations

of physical conditions in the plasma and of background spectral shapes. Hence, they offer a powerful tool for diagnosis. In turn, spectra of the X-ray emission looking for high X-ray energy photons and Iron line emission are also used to find signatures of highly energetic processes, implying AGN activity of gravitational origin. Both starburst and AGN activity are found to contribute to the observed luminosities [92, 102, 253, 310]. It is, however, remarkable to notice that some conflicting evidence has been reported about the relative contributions of the two energy sources, stellar and gravitational, in ULIRGs.

On one side, using diagnostics based on IR coronal line intensities (see, e.g., Fig. 3.30), Genzel et al. [102] have performed a systematic investigation of the physical conditions in the heavily extinguished nuclei of LIRGs and ULIRGs. Another used diagnostic tool is based on the ratio of the 7.8 μm line to 6 μm continuum intensity: this quantity is maximum in AGN-dominated sources and minimum in starbursts, again, fairly well effective in distinguishing AGNs from starbursts. Examples of such IR spectra are reported in Fig. 3.30. The result of these

IR spectroscopic analyses was that in the majority of LIRGs and ULIRGs, high-ionization lines are missing; hence, they are mostly powered by star-formation.

Different results come from X-ray spectroscopic investigations. A deep spectroscopic survey with *XMM-Newton* of a complete sample of local ULIRG is reported in [92]: in all sources there is, evidence for thermal emission from hot plasma, likely associated with a nuclear or circumnuclear starburst. At higher energies, typically between 1 and 4 keV rest frame, there is evidence for emissions by high-mass X-ray binaries, hence proportional to the number of newly formed stars and well correlated with the far-IR emission. Finally, in 50% of the sources, there is evidence for photoelectrically absorbed hard X-ray components indicative of deeply buried AGNs. At variance with the results of the mid-IR spectroscopy, these X-ray results show often the presence of buried AGNs (not otherwise evident in the optical or IR) in ultraluminous sources whose bolometric luminosity is dominated by a circumnuclear starburst.

A significant fraction of ULIRGs also exhibit nuclear optical emission-line spectra characteristic of Seyfert galaxies [310], some contain compact central radio sources [277] indicative of an AGN. Soifer et al. [280] have found that several ULIRGs show very compact (100–300 pc or unresolved) structures dominating the mid-IR flux, a fact they interpret as favoring AGN-dominated emission.

The composite nature of ULIRGs is then confirmed, with concomitant starburst and absorbed quasar emissions.

Have we found any transition objects, that is, partially obscured quasars?

A very interesting class of quasars may be likely interpreted as the transition link between the ULIRGs and classical UV-bright quasars: the broad absorption-line (BAL) quasars. These show very BALs, with velocities comparable to or larger than those of the quasar broad emission lines, or several tens of km s^{-1} . The structure of BALs is entirely consistent with the presence in these objects of an intense galactic wind.

BAL quasars make a moderate fraction ($\sim 10\%$) of the optical quasars, but a larger fraction of the radio selected ones [17]. This, together with optical spectral properties, is an indication that BALs are optically depressed by extinction, on average.

There are two competing views for interpreting the BAL phenomenon. The first is that this class corresponds to the fraction of quasars in which the observer’s line of sight is tangential to the molecular torus, and the upper torus shells are being expelled by radiation pressure. This is the “unification by orientation” view. The alternative interpretation that we may indicate as “unification by time” considers the BAL phenomenon as young or recently refueled quasars. Based on radio [17] and far-IR [5] observations, it is very tempting to conclude in favor of the latter interpretation that BAL quasars trace a transient evolutionary phase between an early, dust-obscured phase and the optically bright one.

An evolutionary connection relating ULIRGs and quasars (in which the BAL would make the transition phase) has been suggested by Sanders et al. [260] based on an exhaustive analysis of a complete IRAS-selected ULIRG sample.

It is proposed that ULIRGs represent an initial dust-enshrouded phase of combined quasar and starburst activity. Once the nuclei release their dusty and obscuring envelope, then the AGN starts to dominate the fading starburst, finally becoming an optical quasar. This evolutionary connection was essentially suggested by the analysis of the IR spectra that would evolve from those peaking at $100\ \mu\text{m}$ typical of star-forming galaxies, to warm infrared spectra (with a mid-IR excess over the far-IR emission) comprising a wide variety of AGNs, including powerful radio galaxies and optically selected QSOs.

This evolutionary sequence would be triggered by a galaxy merger, breaking the regular rotation of the interstellar gas disk and concentrating it in the inner galactic region. Eventually, the event would bring to a short quasar phase. Violent relaxation following the merger would bring to a spheroidal galaxy remnant, once the quasar is completely exhausted.

4.4.1 *Dust Obscuration*

Dust obscuration affects many quasars and active nuclei. How does it lead to an unification scheme?

According to current understanding, *galaxy activity* is the consequence of a rapid gas inflow into the nucleus: this suddenly compressed gas is either processed into new stars, or is accreted by the strong gravitational field of a supermassive black hole (BH) present in the nucleus.

These are two profoundly different astrophysical mechanisms for energy production by cosmic sources, the former obtaining radiant flux by thermonuclear burning in stellar cores and the latter extracting vast amounts of power by transformation of the gravitational energy produced by a supermassive collapsed object, like a BH. As we will see, the two phenomena often occur concomitantly in the same source, and we may encounter problems when trying to disentangle them.

An obvious way to do it is to consider the velocity fields in the interstellar medium (ISM) and/or its ionization structure. The presence of a massive BH implies an enormous gravitational force in the nuclear region and very high-velocity fields of the emitting clouds. This is indeed what is observed in *bona fide* quasars, with line widths observed up to several tens thousands km s^{-1} . A purely star-forming cluster, instead, lacks this intense gravitational field, and the velocity components are those typical of the ISM in a normal galaxy (a couple of hundreds km s^{-1} of velocity). A moderate-resolution spectrum of an active source can tell in principle about the physical nature of the emission. Similar considerations apply to the presence of high-ionization lines in quasars and their absence in starburst galaxies.

There is, however, a critical complication: the presence of dust in the circumnuclear region may prevent the direct inspection of the source inner regions. Indeed, the presence of substantial amounts of dust around the optical nuclei of

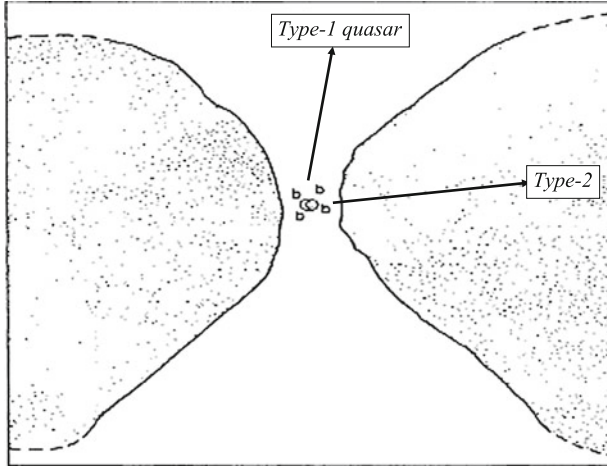


Fig. 4.6 Scheme of a cut through a toroidal structure surrounding the nuclear ionizing continuum source. A polar or an equatorial view would produce a type-1 or a type-2 AGN, respectively, simply due to orientation. From [8]

active galaxies and quasars was suspected soon after the discovery of quasars (e.g., [239, 255]), as we discuss below.

Among AGNs, two main classes of objects have been identified from optical spectroscopic observations: the type-1 AGNs, whose optical spectra show broad permitted (as well as narrow forbidden) lines, and type-2 AGNs showing only narrower emission lines.

The differentiation between type-1 and type-2 AGNs is interpreted as induced by the presence of obscuring material in the nuclear environment, likely associated with the gas flow fueling the AGN: this material acquires a toroidal shape by the presence of residual angular momentum in the accreting gas. As illustrated in Fig. 4.6, the absence of high-velocity lines in narrow-line type-2 objects is interpreted as due to the observer line of sight intersecting the torus and the emission by inner broad-line region (within 0.1 pc of the nucleus) being obscured. For a type-1 object, instead, the observer's line-of-sight remains external to the torus and the inner high-velocity region becomes visible.

This concept has been formalized as the AGN unification model [8], in which the line appearance of an AGN or a quasar is merely an orientation effect, while the intrinsic structure of the object remains the same (Fig. 4.6). The relevance of the orientation effect has been proven by a variety of observational tests, including (a) the linear polarization of some residual scattered broad-line emission in type-2 AGNs (e.g., [9]); (b) the cones of high-ionization narrow-line components, interpreted as due to gas clouds at large distances from the nucleus illuminated by the central nuclear source; and (c) the missing continuum flux in type-2 AGNs inferred from spectroscopic studies. All these facts emphasized the anisotropic

directionality of the ionizing nuclear continuum emission, due to the shadowing effect of the thick dusty torus.

This interpretative scheme has received further support by the consideration that an old problem related with the cosmological photon background observed in X-rays (XRB) by Giacconi and collaborators during the first observations of the X-ray sky [104] could receive an elegant solution within the AGN unification model: if we assume a random sky distribution of AGN inclinations and consider the photoelectric absorption effect as a function of the AGN line-of-sight inclination, then the superposition of both type-1 and type-2 AGNs would easily explain the spectral properties of the background. Contributions to the XRB of 20% by types-1 and 80% by types-2 have been claimed to be roughly consistent with the expected sky-covering fraction of the nucleus by the surrounding torus [47, 186].

Incidentally, the AGN unification scheme, if correct, would have interesting consequences on the problem of disentangling the stellar from the gravitational accretion contributions to the emission by active galaxies. According to the model, although the high-velocity clouds are not visible in type-2 AGNs, AGN emission could still be distinguished from purely starburst activity by the presence of high-ionization emission lines (like OIII, [188]) from clouds illuminated by the high-energy power source along the torus poles, which are free of dust.

In conclusion, the unification scheme appears to explain many observational properties of AGNs and quasars at the current epoch. Circumnuclear dust appears to be a common feature in the population and to deeply influence the quasar phenomenon.

Thank you, Alberto. We now discuss the possibility that some type-2 AGNs might not be obscured type-1 sources.

Dear Ari (Laor), are all Seyfert-2 galaxies properly assumed to be AGNs?

As noted by Osterbrock and Ferland [236] (Chap.13.5, 4th paragraph) when discussing the nature of Seyfert-2 galaxies, “it is clear that the main source of the radiation cannot be hot stars, as in HII regions and planetary nebulae. Radiation from such hot stars will not produce the wide range of ionization observed in NLRG and Seyfert-1 AGNs.” For this reason, the famous Baldwin, Phillips, and Terlevich (BPT) diagrams [14], and their most recent incarnation using the extensive SDSS database ([150] see Fig. 4.14) are so effective in separating which objects have to be powered by a hard ionizing spectrum and cannot be powered by stars. This is also verified by recent photoionization modeling (e.g., [149]).

How do we prove that some of them are the same as type-1 Seyferts (i.e., AGNs)? By the same token, is there evidence that some are not?

The standard obscuration unification scheme, that all type-2 Seyferts are obscured type-1 Seyferts, rests on spectropolarimetry, where the obscured broad lines are detected in scattered polarized light [8]. The scattered broad lines can be detected either from the central source, or from spatially extended emission (e.g., [214]). However, a scattering medium may not be favorably placed with a clear line of

sight, and when the obscuration is extensive enough, scattered light may not be visible. Thus, the absence of evidence for polarized broad lines is not an evidence for the absence of broad lines.

Broad lines may be detectable through other techniques, which rely on piercing through the absorbing material. An absorbing column of $\lesssim 10^{22} \text{ cm}^{-2}$ can be overcome by going to the near IR, which reveals broad permitted lines of H in some objects (e.g., [116]). But this method has a limited success as the absorbing column is typically higher. The most effective technique to pierce the obscuration is through X-ray imaging. The detection of a compact point source inevitably implies accretion onto a massive BH. The X-rays can penetrate columns up to a few $\sim 10^{24} \text{ cm}^{-2}$, above which electron scattering dominates. This is now the most effective method to derive complete samples of AGNs and is implemented on most X-ray telescope (e.g., [133]).

A method which can work at even higher absorbing columns is radio imaging, as neutral gas is completely transparent in the radio, and free-free absorption by ionized gas can be overcome by going to higher frequencies (see an example in [170]). This method is currently limited to mostly RL AGNs [16], and it is clear beyond doubt that extragalactic radio source are AGNs, even if only narrow line are detected. However, most ($\sim 90\%$) AGNs are radio quiet. Since their radio emission is a factor of $\sim 10^3$ weaker than in RL AGNs, they remain mostly undetected in current surveys. The increasing sensitivity, in particular at higher frequencies, of the EVLA and ALMA, will allow the detection of RQ AGNs out to significant z and can thus yield virtually complete samples of AGNs, independent of obscuration. However, to exclude a compact ($< 1 \text{ kpc}$) starburst region, such surveys demand interferometric follow-ups, where a detection of a high surface brightness source ($T > 10^7 \text{ K}$) at mas scale (i.e., pc scale), clearly excludes a stellar origin (e.g., [107]).

In the absence of an absorption-free detection technique, it is impossible to know if some type-2 AGNs do not harbor an obscured type-1 AGN.

The above methods can test if some type-2 AGNs harbor a compact continuum source and are thus powered by accretion onto a massive BH. However, it is still possible that there are two different types of accreting objects, those with broad and narrow lines, that is, type-1 objects, and those with only narrow lines, sometimes termed “true type-2” AGNs, where the accretion onto a massive BH is not associated with the formation of a BLR. Indeed, some type-2 AGNs show a compact X-ray source with no indications of obscuration [109, 162] or show optical variability [134],¹ indicating that we have a clear line of sight to the inner accretion disk, and thus, the BLR is very unlikely to be obscured in such objects. The absence of evidence for a BLR is an evidence of absence in this case. Furthermore, mid-IR observation of some type-2 AGNs indicates that a significant amount of obscuring material does not exist even along other lines of sight [327].

¹Note that in some of the objects where the type-2 identification is based only on the $H\beta$ line, may in fact be type 1.9 Seyferts, that is, Seyferts where a broad component is detected in $H\alpha$ and not in $H\beta$. Seyfert 1.9 objects are clearly not “true type-2” AGNs.

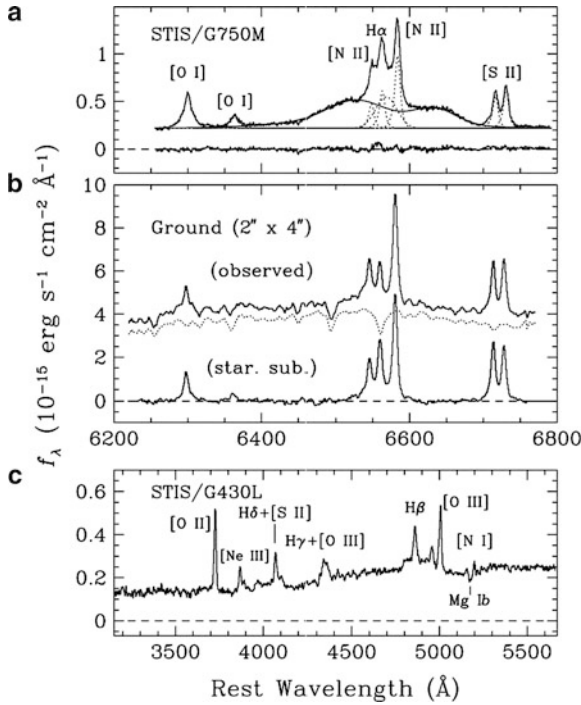


Fig. 4.7 The spectrum of the nucleus of NGC 4450 from the ground and with the HST with a narrow slit (Fig. 1 from [142]). Note that the ground-based spectrum shows only narrow lines, even after careful subtraction of the host galaxy spectrum. The much narrower slit allowed by HST excludes most of the host light and shows the net AGN emission, with a continuum >10 times weaker than the host. This spectrum reveals a very prominent broad $H\alpha$ line, which is completely undetectable in the ground-based spectrum. This object would have been regarded as a “true type-2” AGN, although it is clearly a type-1 AGN. The large width of $H\alpha$ is not unexpected, as the BLR shrinks in size with decreasing luminosity, and the velocity dispersion in the BLR must therefore increase

Why do some accreting objects appear not to harbor a BLR?

Understanding which parameter controls the presence of the BLR is of fundamental importance, as it will provide an important clue to the physical mechanism which generates the BLR. Various suggestions were made, relating to the accretion disk structure [227, 228], an accretion disk wind [56, 72, 73], or it may be due to a maximally detectable line width or maybe a maximal velocity where the BLR can exist [162]. A comparison with observations is discussed in [138]. There are now ongoing searches for “true type-2” (e.g., [272]). Clearly, host dilution is a major limitation in the detection of low-luminosity broad line, and narrow-slit spectroscopy with HST, which rejects most of the host light (see a remarkable demonstration in Fig. 4.7, taken from [142]), is the way to proceed to determine at which M_{BH} and L/L_{Edd} the BLR indeed ceases to exist.

Even if all type-2 AGNs have an obscured BLR, they may not necessarily be identical to type-1 AGNs. The observed ratio of the space density of type-1 and type-2 AGNs is about unity [131]. If all AGNs are identical, this ratio implies a covering factor of obscuring material of about 50%. On the other extreme, type-1 AGNs and type-2 AGNs could be different, where type-1 AGNs may have little or no obscuring material and type-2 may be highly obscured. More likely, there is a distribution of covering factors in AGNs, and objects with larger covering factors of obscuring material are more likely to be detected as obscured. This modification of the pure obscuration unification scheme can be tested by comparing larger scale properties of type-1 and type-2 AGNs, ranging from the NLR properties (e.g., [265]) to the host galaxy properties (e.g., [189]).

Thank you, Ari. We now exit from the dusty cocoon enshrouding the innermost region of quasars to move again into the full light of unobscured sources. Narrow-line Seyfert 1s (NLSy1s) have been believed for long to be peculiar, low-luminosity AGNs. In the framework of unification, they are unobscured sources not unlike the other type-1 quasars. However, NLSy1s possess a property that is not considered in the classification criteria of the unification scheme: they are accreting matter at a lively rate.

4.5 Narrow-Line Seyfert-1 Nuclei

Dear Dirk (*Grupe*), what are narrow-line Seyfert 1s?

Narrow-line Seyfert-1 (NLSy1s) are a special breed of AGNs. While originally they were defined by Osterbrock and Pogge [235] by their widths of their H β line to distinguish between Seyfert 1s and Seyfert 2s in their sample, it turned out over the last 25 years that NLSy1s have a lot of properties that makes them different from the rest of the AGN crowd. Boroson and Green [27] noticed that they generally speaking have very strong optical FeII emission but rather weak [OIII] emission lines. By using a principal component analysis, this led [27] to introduce the “eigenvector 1” relation among AGNs. In a study of ultrasoft X-ray-selected AGNs from *Einstein*, [246] could show that NLSy1s exhibit very steep X-ray spectra, a result that was later confirmed by Boller et al. [24] from ROSAT All-Sky Survey data. Grupe et al. [120, 122] combined the optical and X-ray properties of ROSAT-selected AGNs and found that NLSy1s dominate one extreme in the eigenvector 1 relation: they have the steepest X-ray spectra, strongest FeII emission, and often negligible emission from the NLR. They suggested that one interpretation of the NLSy1s phenomenon is that NLSy1s are AGNs at an early stage of their development. Sulentic et al. [293] interpreted eigenvector 1 as the Eddington ratio L/L_{Edd} in which NLSy1s are AGNs with high L/L_{Edd} . Mathur [202] then also made the connection between NLSy1s and high-redshift quasars which she interpreted both to be young AGNs. Brandt and Gallagher [33] and Boroson [26] suggested that also broad

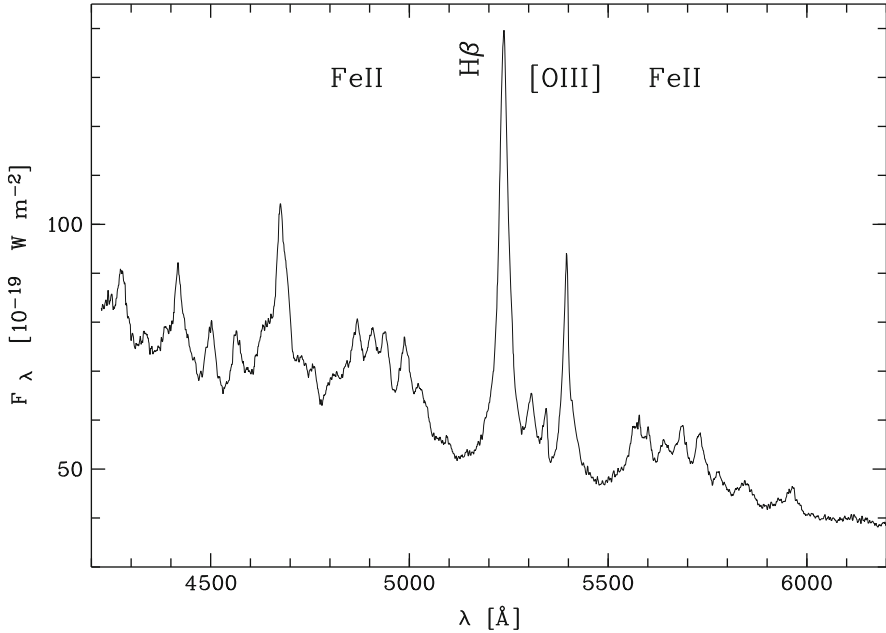


Fig. 4.8 Optical spectrum of the NLSy1 Mrk 478 [120]

absorption-line quasars (BAL QSOs) are high L/L_{Edd} objects, but their difference to NLSy1s is that NLSy1s have much smaller black hole masses than BAL QSOs.

Are NLSy1s truly peculiar?

From their optical spectroscopy study of Mrk 359, Davidson and Kinman [59] noticed that this AGN was quite peculiar: instead of showing only narrow permitted and forbidden lines like a Seyfert-2 galaxy or broad permitted lines and narrow forbidden lines like a classical Seyfert-1 galaxy, its permitted lines were narrow but still significantly broader than its forbidden lines. This at the time made Mrk 359 a peculiar AGN which did not quite fit into the standard Seyfert-1 and 2 classification scheme. In a spectrophotometric study of Seyfert 2s; and narrow-line radio galaxies, Koski [158] noticed that two of the AGNs in the sample were quite peculiar, Mrk 42 and 5C 3.100: from their $H\beta$ line widths, they would be clearly Seyfert 2s, however, their blue continua and their very strong Fe II emission together with their weak forbidden lines placed them into the Seyfert-1 category. The name “narrow-line Seyfert-1 galaxies” (NLSy1s) was introduced by Osterbrock and Pogge [235] in their study of “active galactic nuclei with all properties of Seyfert-1 or 1.5 galaxies but unusual narrow HI lines.” Figure 4.8 shows a typical spectrum of an NLSy1, Mrk 478 [120].

The [OIII]–FeII relation is typically associated with the “eigenvector 1” relation found in AGNs. Boroson and Green [27] studied a sample of 87 Palomar-Green (PG) quasars and performed a principal component analysis (PCA) and found that

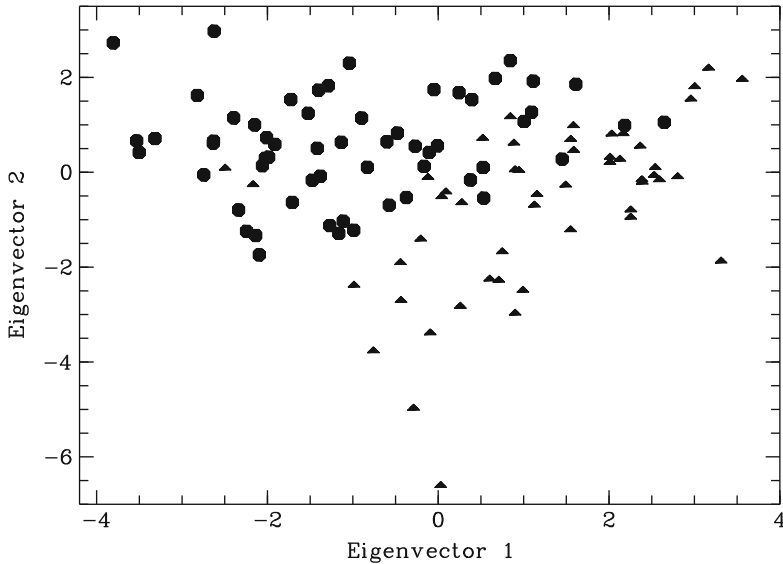


Fig. 4.9 Eigenvector 1 vs. eigenvector 2 in the sample of [126]. A detailed description of this analysis can be found in [119]. NLSy1s and BLSy1s are displayed as *triangles* and *circles*, respectively

the strongest eigenvector, eigenvector 1, correlates strongly with the strength of the optical Fe II blends and anti-correlates with the strength of the [OIII] lines. A well-written description how PCA works can be found in [93]. They noticed that NLSy1s occupy one extreme in the eigenvector 1–eigenvector 2 space. Figure 4.9 displays the eigenvector 1 vs. eigenvector 2 diagram from [119] as an example.

In the following years, it turned out that NLSy1s are not only peculiar at optical wavelengths but also at higher energies. In a sample of 42 Seyfert-1 galaxies observed by the X-ray satellite, *Einstein* [283] discovered that 25% of these were NLSy1s, a percentage that was significantly larger than what was expected from optically selected AGN samples. In a sample of ultrasoft selected AGNs from *Einstein* [246] noticed that about 50% of their Seyfert 1s were NLSy1s. They also found an anti-correlation between the optical permitted line widths and the X-ray spectral slope. This relation was then established by Boller et al. [24] by studying bright AGNs from the ROSAT All-Sky Survey. As we know today, this relation is basically a black hole mass ($\text{FWHM}(\text{H}\beta)$) and accretion ratio (α_X) relation. NLSy1s are therefore Seyfert-1 galaxies with relatively small black hole masses and high accretion ratios close or ever larger than their Eddington limit. The α_X - $\text{FWHM}(\text{H}\beta)$ has been found for soft as well as hard X-ray spectral slopes (e.g., [34, 122, 123, 167]). In all these studies, NLSy1s appear to be the AGNs with the steepest X-ray spectra. Figure 4.10 shows the α_X - $\text{FWHM}(\text{H}\beta)$ relation among the AGNs in the X-ray bright selected sample by Grupe et al. [123] observed by *Swift*.

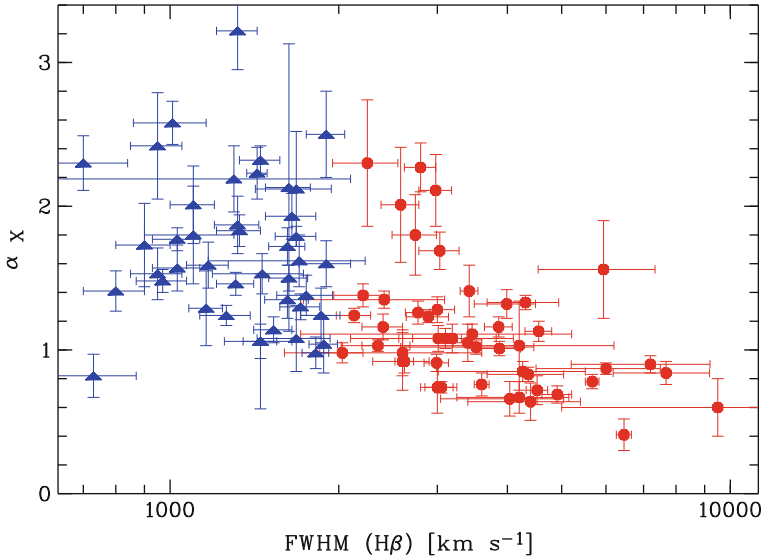


Fig. 4.10 0.2–2.0 keV X-ray spectral α_X vs. $\text{FWHM}(\text{H}\beta)$ of an X-ray-selected sample observed by *Swift* [123]. Narrow-line Seyfert 1s are displayed as *triangles* and broad-line Seyfert 1s as *circles*

As shown by Grupe et al. [123, 126] and Shemmer et al. [269, 270], there is a strong correlation between the X-ray spectral slope α_X and the Eddington ratio L/L_{Edd} .

What is their relationship to the rest of the quasar population?

AGNs display a wide spectrum of black hole masses ranging from about 10^5 to about $10^{10} M_{\odot}$ (e.g., [240, 311]). While quasars with their 10^8 – $10^{10} M_{\odot}$ represent the one extreme, NLSy1s are at the opposite part of the black hole mass spectrum and have black hole masses typically of the order of 10^6 – $10^7 M_{\odot}$. In a matter of fact, as shown in Fig. 4.11, many NLSy1s seem to fall below the well-established $M - \sigma$ relation found for galaxies and AGNs [86, 101, 301], suggesting that they are AGNs where the black hole is still rapidly growing [125, 203]. The relatively low black hole masses have immediate effects on the SED: (1) they can operate easily at high accretion rates resulting in L/L_{Edd} at unity, and (2) due to the $T \propto M^{-1/4}$ relation, their accretion disk temperature is higher than in normal quasars. They show a much weaker accretion disk corona causing the X-ray spectra appear to be steeper. As a result, on the $\alpha_{\text{ox}} - l_{2500\text{\AA}}$ relation, NLSy1s appear to be X-ray weaker than BLSy1s.

As suggested by, for example, [26, 33] BAL quasars and NLSy1s are closely related: both are high Eddington accreting objects but differ in the sizes of their black hole masses. The link between these two groups maybe WPVS 007 which is an extreme NLSy1 [121, 124] which has shown UV properties like a BAL QSO [168]. However, the mass of its central black hole is about a 100 or even a 1,000

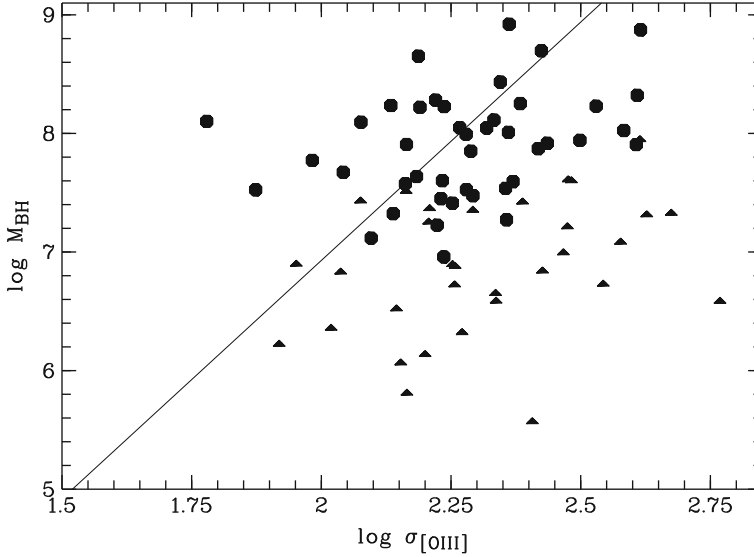


Fig. 4.11 Velocity dispersion $\sigma_{[\text{OIII}]}$ vs. M_{BH} taken from [125]. NLSy1s and BLSy1s are displayed as *triangles* and *circles*, respectively. The *solid line* marks the relation of [301]

times smaller than that of a typical BAL QSO. Support for the BAL QSO—NLSy1 link comes also from the findings of [169] of high-velocity outflows in the X-ray spectra of some NLSy1s.

As suggested by Mathur [202], NLSy1s are related to quasars at higher redshifts. As it has been shown by, for example, [62, 291, 332] from NIR spectroscopy of intermediate redshift quasars, they tend to be high L/L_{Edd} objects that occupy a similar space in the eigenvector 1 parameter space as NLSy1s.

Why have some described NLSy1s as “fledgling quasars”?

One interpretation of the high L/L_{Edd} found in NLSy1s is that they are AGNs in an early stage of their development. While this idea was first suggested by Grupe et al. [118, 120], a more detailed explanation was given by Mathur [202]. The argument that NLSy1s are indeed AGNs at an early stage is supported by the findings of [125] that NLSy1s with high L/L_{Edd} fall significantly below the $M - \sigma$ relation (see above and Fig. 4.11). Especially, those AGNs fall significantly below the $M_{\text{BH}} - \sigma$ relation which have high L/L_{Edd} ratios. These findings have also been supported by Shen et al. [271] who studied the $M_{\text{BH}} - \sigma$ relation in a large sample of quasars in the SDSS [330]. These high L/L_{Edd} NLSy1s are AGNs with rapidly growing black holes in the local universe. NLSy1s are therefore the link between the local to the high-redshift universe, where quasars are expected to accrete at their Eddington limit, just like what NLSy1s do.

Do radio-loud NLSy1s exist?

Historically, radio-loud NLSy1s appeared to be sparse. While about 10–15% of quasars appear to be radio-loud,² only about 7% of NLSy1s are radio loud [156]. Komossa et al. [156] found that radio-loud NLSy1 typically accrete close to or at their Eddington limit and that their black hole masses are at the higher end of the NLSy1 black hole mass spectrum. Similar results were also reported by Whalen et al. [326] who studied a radio-selected sample of NLSy1s. It is still unclear why generally the fraction of radio-loud NLSy1s is low. Most likely, this can be related to their high L/L_{Edd} which causes strong outflows which may prevent a jet being launched. Sulentic et al. [292] put radio loudness also in the context of the eigenvector 1 relation in AGNs and found that radio loudness is mostly seen in AGNs with broad $H\beta$ emission lines. They explained this effect by source orientation. It should also be noted that some radio-loud NLSy1s like PMN J0948+0022 have even been detected in the GeV regime by *Fermi* [3].

What are the physical conditions of the line-emitting gas in the narrow-line Region of NLSy1?

One result of the eigenvector 1 relation is that NLSy1s appear to be AGNs with relatively weak narrow-line region (NLR) emission lines. It is therefore legitimate to ask if the physical properties of the NLR in NLSy1s are different compared with those in BLSy1s. Xu et al. [328] found that while BLSy1s only show NLR electron densities in the order of several 100 cm^{-3} , NLSy1s show a much wider distribution and do show densities as low as a few cm^{-3} . They also found that there is a strong anti-correlation between the NLR electron density and L/L_{Edd} . Again, L/L_{Edd} is the driver. Most likely, the strong outflows seen in NLSy1s are responsible for these observed differences.

Thank you, Dirk.

Dear Sebastian (Lipari), Begoña (García Lorenzo), and Evencio (Mediavilla), what is the role of nuclear and circumnuclear star formation in narrow line-Seyfert 1s?

Lipari [171] found that the prototypes of narrow-line Seyfert-1 AGNs (I Zw 1, Mrk 507, and Mrk 957/5C 03.100) show—in the IR color diagram—composite (i.e., starburst + SMBH) and transition (i.e., between ULIRGs and standard QSOs) properties. Moreover, he found that almost all the NLSy1 of the sample are located in a second sequence of transition AGNs/NLSy1s. This sequence is similar (parallel) to that detected for transition luminous BAL + IR + FeII QSOs but with lower values of $\alpha(60,25)$ and starting in the starburst region (the sequence of transition QSOs start in the area of ultraluminous IR galaxies). Mrk 507 and Mrk 957/5C 03.100 are located in the sequence of transition NLSy1 and inside the starburst area (of this IR diagram).

²We use the definition by Kellermann et al. [148] where AGNs are considered to be radio loud which radio to optical ratio $R > 10$.

Thus, several authors suggested (a) a link between NLSy1s and IR emission + BAL + starburst systems and (b) that composite and transition NLSy1 could be young systems with a very high rate of accretion in their supermassive BH (e.g., [24, 26, 33, 155, 163, 171, 181, 202] and others).

From the theoretical point of view, [181] already studied the main steps for the formation and evolution of the NLR in a strong galactic wind outflow (OF) process, which is associated with a luminous nuclear starburst + AGN. In this evolutionary explosive model, the observed line ratios, FWHM, and size of the NLR evolve on timescale comparable to the timescale for the wind development. This timescales will depend on the rate of energy input, size of the SN region, and on the details of the gas distribution.

From our observational and theoretical results (of IR QSOs and mergers with OF), we suggested that young QSOs/AGNs—with relatively narrow lines—will evolve from narrow-line young BAL + IR + FeII QSOs/AGNs and Sy1 to broad-line standard QSOs/AGNs.

It is possible that FeII might be enhanced by the star-formation activity, in NLSy1s? (since NLSy1s often show very strong Fe II emission)

In our second program of study of AGNs/QSOs, (a) *The Evolution of Composite QSOs, ULIRGs, and the Role of BAL+Fe II+IR QSOs and NLSy1 Galaxies* and (b) *The Explosive and Evolutionary Model for BAL+Fe II+IR QSOs and Narrow Line QSOs+Sy1 Galaxies*, very interesting GMOS-IFU results were obtained in relation with the narrow-line emission (in general) and about strong and extreme FeII in NLSy1s and QSOs. Specially, interesting results were found for the QSO core in the circumnuclear and external regions of the NL-QSO IRAS 04505–2958.

In the explosive and composite model for QSOs/AGNs, the observed properties of some QSOs and AGNs with strong FeII emission can be understood as an evolutionary sequence, in which the observed differences between strong and weak FeII emitters and the observed correlations with FeII are related—at least in part—to evolutionary changes in the SN, compact supernova remnant activity, and the development of the OF plus different type of NLRs.

In the composite model, the BLR and part of the NLR could be produced in compact supernova remnant and super-shells in extended OF processes. The observed emission lines are the product of reprocessing of shock radiation by high-density thin shells, ejecta, and super-shells [296, 298]. In these models, the abundances of the ionized gas emission lines are the abundances of the envelope of the star of SN ejecta and super-shells and not only by the abundances of the ISM.

In addition, Lípari and Lawrence et al. [163, 171] already proposed that the nuclear OF is a main process that could explain some of the FeII correlations and properties, observed in AGNs and QSOs. More recently, using our database of IR QSOs with galactic winds and OF, we found a correlation between the $\text{FeII}\lambda 4570/\text{H}\beta$ vs. velocity of OF (see Fig. 30 of [177]). We suggested that a probable explanation for the link between the extreme FeII emission and the extreme velocity OF is that both are associated to the interaction of the star-formation processes and the AGN that generate extreme explosive and hypernova (HyN) events.

Thus, from our program of observational and theoretical studies (of the evolution of IR QSOs and galaxies), we suggested that at least part of the FeII emission in strong and extreme QSOs and AGNs are associated with OF + shock processes.

A very interesting point about the relation between the explosive model of AGNs–QSOs and the Fe II emission in narrow-line QSOs–Sey1 is the following fact: that the spectra of extreme OF associated with giant SN α /HyN α could generate exactly the FeII spectra of NLSy1 (with even extreme FeII emission, which is not explained using photoionization models). In particular, this OF spectra of SN/HyN are almost the same of the spectra of prototypes of this class, that is, I Zw 1, which is also an extreme FeII emitter; [171]. Figure 25 in [172] shows the spectra of the SN 1998E (Ruiz and Suntzeff, private communication), obtained at CTIO in January 31, 1998, with the 4-m telescope, together with the spectra of IRAS 04505–2958 and I Zw 1. This plot depicts very similar features in the spectra of SN 1998E and IRAS 04505–2958. Moreover, this plot shows that the spectra of SN 1998E and I Zw 1 are almost identical and both with extreme FeII emission.

Moreover, Lípari et al. [184] (their Fig. 14) showed the superposition of the spectrum of the radio HyN type II–L 1979c (observed in June 26, 1979) and Mrk 231. Only using colors it is possible to distinguish each spectrum since they are almost identical. Thus, likely, a more constant OF—rather than a single SN—could explain the very unusual spectra of NLSy1 in general even with extreme FeII emission, like I Zw 1, IRAS 04505–2958 (a NLSy1 with strong FeII) and even Mrk 231 (a QSO with broad H-Balmer lines and extreme FeII).

Therefore, from these results, we are suggesting that at least part of the narrow-, intermediate-, and broad-line emissions are associated with explosive OF processes, that is, in giant SN/HyN + galactic winds + shells.

An interesting point about the GMOS results of the NLR observed in the NL-QSO IRAS 04505–2958 is the fact that we are observing at least 3 different NL emission systems: (a) one strong NL system associated with the H-Balmer lines, in the QSO core, with an intermediate FWHM of 800 km s^{-1} ; (b) a very weak NL emission associated with the lines [SiII] λ 6717+31 and [NiII] λ 6583 (also in the QSO core); and (c) an extended and strong NL system associated with the [OIII] λ 5007 and [OII] λ 3727 emission (in almost all the GMOS field of $20 \cdot 30 \text{ kpc}$).

In addition, Fig. 24 in [172] shows in the FWHM [OIII] λ 5007 map of IRAS 04505–2958: large values of the FWHM of [OIII] λ 5007 in different regions of the shell S3. This result could be explained by the presence of weak OF components in [OIII] (which can not be deblended—from the main emission-line component—using medium-low spectral resolution of GMOS-B600).

A similar GMOS-IFU result was obtained for the NLR associated with the weak [SiII] λ 6717, 6731 and [NiII] λ 6583 emission in Mrk 231, IRAS 17002+5153, and IRAS 07598+6508 [175, 178]. Furthermore, we found for the QSO core of Mrk 231 GMOS spectral evidence of two weak [SiII] narrow emission-line systems clearly associated with low-velocity OF. A simple explanation—already proposed—for these very weak nuclear NLR observed in BAL + IR + FeII QSOs is that the extreme OF + shocks generate a weak NL plus this OF process expel at least part of the gas that generate the standard NLR of AGNs. We even already suggested that

part of the broad line emission region in Mrk 231 is likely generated by an extreme OF process [178, 184].

In conclusion, the OF + shocks processes—associated with explosive events, in composite nuclear regions—could play an important role in the generation of weak narrow-line emission systems and the expulsion of gas that generates the standard narrow-line region observed in evolved AGNs and QSOs (where the dominant source of nuclear energy is the SMBH).

Thanks Sebastian, Begoña, and Evencio. We would like to further discuss with you the interplay between the active nucleus and the surrounding star-forming regions, especially in the most extreme cases. While Alberto Franceschini discussed the connection between ULIRGs and QSOs on the basis of obscuration, we would like now to consider aspects related to the active nucleus evolution. ULIRGs are major mergers—and major merging is a mechanism that is believed to have produced the quasars shining bright at high redshifts. However, the extent to which star formation is affecting the AGN proper is still widely debated. In the most conservative approaches, there is a consensus that circumnuclear star formation can strongly enhance the metal content of the line-emitting gas, but this might be only a part of the story. Extremely strong FeII emitters like IRAS 07598+6508 and Mark 231 (both ULIRGs) pose a challenge to the conventional view of FeII production via photoionization. According to some workers, a non-radiative heating mechanism is necessary to model the FeII spectrum [308]. It would not be surprising if massive star evolution (where the most massive stars are expected to collapse into a black hole yielding hypernovæ) could strongly affect not only the chemical composition but also the AGN gas dynamics.

4.6 The ULIRG–QSO Connection

Dear Sebastian (Lípari), Begoña (García Lorenzo), and Evencio (Mediavilla), what is the connection between quasars (QSOs) and Ultraluminous Infrared Galaxies (ULIRGs)?

An excellent review about the first works in this theme was published by Sanders and Mirabel [259]. About this question, it is interesting to note that our team is working (in the last 25 years) mainly in this field or theme. More specifically, we have 2 main observational and theoretical programs:

1. The Evolution of Composite QSOs, ULIRGs: and the Role of BAL+Fe II+IR QSOs and NLSy1 Galaxies.
2. The Explosive and Evolutionary Model for BAL+Fe II+IR QSOs and Narrow Line QSOs+Sy1 Galaxies.

We have obtained interesting results, about this theme: the connection between QSOs and ULIRGs. More specifically, we have found a evolutionary diagram for QSOs and galaxies, with very interesting possible paths and connections.

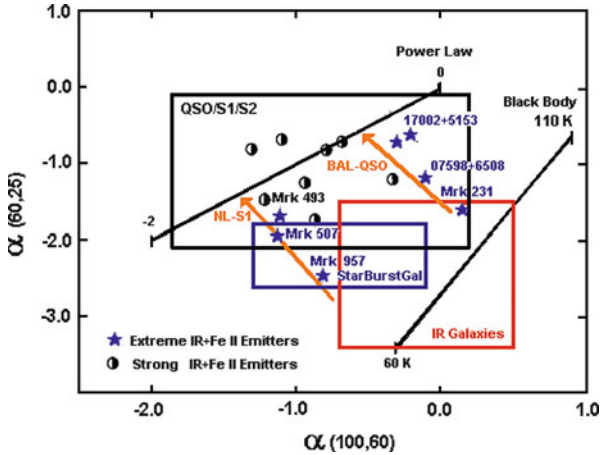


Fig. 4.12 IR color–color diagram of extreme IR + FeII QSOs and AGNs (for a sample of 15 QSOs + AGNs)

Furthermore, these results have important consequences for several main fields of astrophysics, cosmology, and even for theoretical physics: like the nature of dark matter, the origin of cosmic ray with Ultrahigh energy (UHE), etc.

About this general question point (i.e., the evolution and connection between QSOs and ULIRGs), we can summarize the following main results some of them obtained by our team:

First, it is important to note that the IR color–color diagram is an important tool to detect and discriminate different types of activity in the nuclear regions of galaxies. Thus, this diagram is also important for the study of possible links between different phases of ULIRG and QSO evolution. More specifically, using this IR color–color diagram [$\alpha(60, 25)$ vs. $\alpha(100, 60)$] (see Fig. 4.12), Lipari [171] already found that the IR colors of ~ 10 extreme IR + FeII QSOs are distributed between the power law (PL) and the blackbody (BB) regions, that is, the transition area. From a total of ~ 15 IR transitions, IR + FeII QSOs four systems show low-ionization BALs. Therefore, we already suggested that low-ionization BALs + IR + FeII QSOs could be associated with the young phase of the QSO evolution. Figure 4.12 shows—with an orange arrow—this possible evolutive path or connection for BAL + IR + FeII QSOs; in addition, a second path is also showed for narrow-line Seyfert-1 AGNs.

Second, recently, using a more complete database of more than ~ 80 IR mergers and IR QSOs with outflow and galactic winds, we show the IR color diagram of energy distribution for IR mergers and IR QSOs with OF (in Fig. 4.13, and see also [184] their Fig. 15). This new and more complete IR color diagram shows:

1. All the IR mergers with low-velocity OF and starburst are located very close to the BB area.
2. The standard QSOs and radio QSOs are located around the PL region.
3. All the BAL + IR + FeII QSOs are located in the transition region, in a clear first sequence: from Mrk 231 (close to the BB area) to IRAS 07598+6508 to

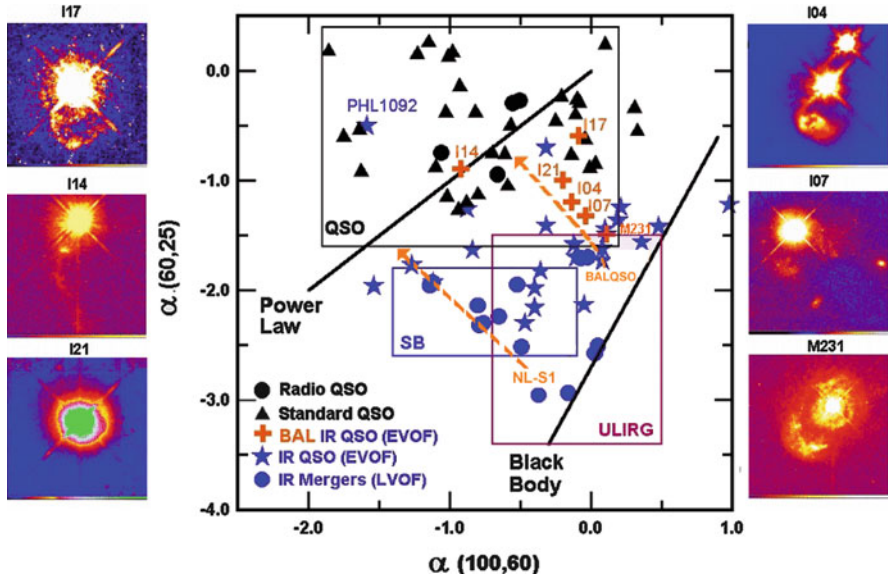


Fig. 4.13 IR color–color diagram of QSOs, mergers, and AGNs (for a sample of ~80 QSOs + mergers + AGNs)

IRAS 04505–2958 to IRAS 21219–1757 to IRAS/PG 17072+5153 and IRAS 14026+4341 (close to the PL area) to standard QSOs.

4. The extreme IR + FeII narrow-line Sy1 AGNs-Galaxies are located also in the transition region, in a second transition sequence. From Mrk 957 (close to the BB area) to Mrk 507 to Mrk 493 to standard QSOs.
5. Using this IR color–color diagram, [184] (their Fig. 15) found the BAL system in IRAS 04505–2958. For the BAL detection, we used the fact that IRAS 04505–2958 is located exactly in the first main sequence of BAL + IR + FeII QSOs: between the BAL QSOs IRAS 07598+6508 and IRAS 21219–1757/IRAS 17072+5153.

We found and suggested that in IRAS 04505–2958, the extreme OF (with hypershells of 50–100 Kpc) generate: (a) the end phase—of the evolution—of the host galaxy (via explosion of hypernovae) and (b) the formation of a young galaxy in the hypershell of this IR QSO.

Another interesting result—which we will consider in detail below—is the detection of a composite nature (i.e., starburst (SB) + supermassive black hole (SMBH)) in the nuclear region of BAL + IR + FeII transition QSOs. Furthermore, we detected that these transition IR QSOs show—almost all—super- and hypergiant symmetric shells, associated with symmetric SN and HyN explosive events (see Fig. 4.13 for details of these shells). It is important to note that these symmetric shells show their center in the nuclear SB regions. In addition, we suggested that these extreme nuclear SBs are originated mainly by the interaction of the

star-formation processes and the very high-density gas of the nuclear accretion disk (around SMBHs).

Can you summarize the observational line of evidence favoring enhanced star-formation activity in AGNs–QSOs? What are the most reliable and widely used tracers of star formation that are relevant for QSOs?

In our observational and theoretical programs of BAL + FeII + IR composite QSOs and extreme IR + FeII NLSy1Gs, clear evidence favoring enhanced star-formation activity in AGNs–QSOs were found. In particular:

1. *Spectral signature of Wolf Rayet in BAL + IR + FeII QSOs (with OF and Shells):* We found for IR mergers and IR QSO spectral features of massive WR stars and OF. Specifically, we detected WR and OF features in the *shells* of Mrk 231 and NGC 5514 plus in the *nuclei* of PG 1535+547, IRAS 01003–2238, and IRAS 22419+6049. WR stars are the progenitors of core-collapse super- and hypernova. Theoretical works suggested that SNe/HyNæ from massive progenitors are probably the only object that could generate the rupture phase of the bubbles, in the QSOs nuclei and in the main knots of the shells [230, 299].
2. *Shells in BAL + IR + FeII QSOs:* In the last years, there is increase observational evidences confirming that galactic OF, BAL processes, super-/hypernova (SN/HyN) explosions and the associated shells play important roles in galaxy and QSO evolution and formation (especially at high redshift, in the young universe; see [172, 178]). Using Gemini, La Palma-WHT, and HST observations, we are studying shells associated to outflowing “shocked” material, mainly associated with enhanced star-formation activity in AGNs–QSOs (these shells have properties very different to rings and arcs associated with tidal tails and loops in galactic collisions). At low z , HST images and 3D spectroscopic data of the interesting class of composite BAL + IR + FeII QSOs show in practically all of these objects “giant and shells with circular-symmetric shape in the external borders (with their centre at the position of the nucleus)”; which are associated with strong OF processes and giant explosive events (see for details [173–175, 178, 182, 184]). Three-dimensional high-resolution spectroscopic data give clear evidences of strong OF processes; mainly from the study of multiple emission line components, kinematics maps, and emission-line ratios plus color maps with structures associated with shocks [173, 174, 176–180, 184]. The presence of multiple concentric expanding supergiant shells in young and composite BAL + IR + Fe II QSOs (especially shells with their center at the position of the nucleus and with highly symmetric circular external borders) could be associated mainly with giant symmetric explosive events [173, 174, 182, 184]. Moreover, only an explosive scenario could explain the exponential shape of the variability curve observed in the BAL system of Mrk 231 [178, 184]. Thus, “circumnuclear and external shells and arcs” could be associated with (a) the final phase of the galactic wind, that is, the blowout of the galactic bubbles [230, 290, 299] and (b) galaxy collisions, that is, tidal tails, rings, loops, etc. For distant QSOs (and even for some nearby QSOs/galaxies), it is difficult to discriminate between

these two types of structures. However, it is well known that the velocity fields of mergers and galaxies in interaction show emission-line components with difference of velocities $\Delta v \approx 500 - 600 \text{ km s}^{-1}$; and in extreme OF, the multiple components show differences of velocities $\Delta v > 700 \text{ km s}^{-1}$. Theoretical results obtained for galactic wind—associated with strong starbursts—show multiple OF components with even $\Delta v > 2,000 \text{ km s}^{-1}$ [290]. This is one of the more clear difference between these two types of shells and arcs.

In conclusion, some of the observational results obtained for *nearby BAL QSOs*, such as extreme IR and FeII emission, strong blue asymmetry/OF in $\text{H}\alpha$, radio quietness, and very weak $[\text{OIII}]\lambda 5007$ emission [29, 171, 182–184, 303], can be explained in the framework of the starburst + AGN + OF scenario.

3. *OF in the nearest extreme BAL + IR + GW + FeII QSOs*: In our study of Mrk 231, and IRAS 0759+6559, we detected typical characteristics of young QSOs with extreme nuclear starburst. In particular, for Mrk 231 we found evidence that the BAL systems are associated with the composite nature of the nuclear regions, that is, OF generated by explosive SN events and the radio jet [178, 184, 247].

For BAL + IR + FeII QSOs, we suggested that these QSOs could be young and composite QSOs at the end phase of an extreme starburst. At the final stage of an “extreme starburst,” that is, type II SN/HyN phase ($[8-60] \cdot 10^6$ year from the initial burst [297, 298], powerful galactic winds, super-/hypergiant galactic shells, BAL systems, extreme FeII emission, large amount of dust, and strong IR emission can appear [181, 182]. The first starburst phase ($[0-3] \cdot 10^6$ yr: dominated by hot main sequence stars with HII regions) is associated with the presence of large amount of dust and extreme IR emission ([297]; Franco 2009, private communication).

4. *Hypernovae in IR QSOs*: We already explained the interesting point that theoretical works suggested that only/mainly type II SN/HyN generates the blowout phase of the supergiant shells and bubbles [230]. However, in dusty nuclear regions of IR QSOs and IR Mergers + shells (with $A_V \sim 10-1,000$ mag; see [102]), the presence of type II SN $\bar{\text{a}}$ /HyN $\bar{\text{a}}$ could be detected only for the nearest IR merger and IR QSO: Arp 220 and NGC 7469. These SN $\bar{\text{a}}$ /HyN $\bar{\text{a}}$ were detected using the largest—very long baseline—radio interferometry (VLBI) array (see [44, 185, 238]).

A very interesting point about the radio SN/HyN found in Arp 220 and NGC 7469 is that almost all these HyN $\bar{\text{a}}$ are of the type IIn (i.e., their progenitors are massive stars, which explode in a dense circumstellar medium generated by their stellar wind). These unusual highly luminous core-collapse radio SN $\bar{\text{a}}$ /HyN $\bar{\text{a}}$ are implying a different stellar initial mass function (with a large number of massive stars) in the nuclei of IR QSOs and mergers.

5. *Hyper-wind and explosive model for Ly α blobs*: In the last decade, very extended blobs—especially in Ly α —has been detected in a variety of high- and low-redshift objects. In addition, the results of the surveys at high z of bright sub-mm source [30, 40, 294] suggest that a high fraction (3/4) of these sources are extended and complex (i.e., showing extended and highly luminous Ly α halos).

Lípari et al. [176] already found that 75% of IR QSOs and mergers (including BAL QSOs) show clear evidence of OF. This value is the same percent (75%) found by Chapman et al. [40, 41] in their study of sub-mm sources, showing extended and highly luminous Ly α halos. Recently, we have started a study of three-dimensional spectroscopic data of high-redshift sub-mm and radio BAL QSOs, using Gemini + GMOS and ESO VLT+VIMOS. Using these GMOS data, we are studying the interesting possibility (already suggested by Lípari and Terlevich [181]) that in sub-mm and radio QSOs—at high redshift—also extreme explosive OF process could play a main role in their evolution.

Furthermore, Lípari et al. [172, 178, 184] suggested that Hyper-wind—associated with HyN generated by the interaction of starburst and SMBH in composite AGNs–QSOs—with hypershells of 50–100 kpc (like those already detected in Mrk 231, IRAS 04505–2958, IRAS 1700+5153, etc.) is a likely explanation for the very extended Ly α blobs, observed at high redshift.

6. *Main Physical consequence of hypernovæ and outflow in IR QSOs (formation and end of galaxies, generation of neutrinos, dark matter, and UHE cosmic rays):*

First, very recently, we found that extreme OF processes could be associated with two main processes in the evolution of QSOs: (a) the formation of companion/satellite galaxies by giant explosions and (b) to define the final mass of the host galaxy, and even if the explosive nuclear outflow is extremely energetic, this process could disrupt an important fraction of the host galaxy.

Second, explosive events associated with HyN α in the nuclei of composite AGNs and in BAL + IR + FeII QSOs is very likely the source of UHE cosmic rays and neutrino/dark matter (see [173, 178]).

Very different types of HyN α could be present in composite QSOs/AGNs and especially in the core of explosive low-ionization BAL + IR + Fe II QSOs. In HyN α , mildly relativistic ejecta is probably the source of ultrahigh-energy (UHE) cosmic-rays (UHECRs) and neutrinos (UHENs). More specifically, ultraenergetic cosmic rays associated with hypernovæ. Recently, using the *Pierre Auger Observatory*, Abraham et al. [4] found that the extremely high-energy CRs are associated with galaxies + AGNs. Two different theories and models could explain these *P. Auger* observations: (a) Obscured and Collimated AGN/Black-Hole and (b) Evolutionary, Explosive, and Composite AGN + starburst model. The production of relativistic electrons is in young SN remnants, and it is believed that remnants simultaneously produce relativistic ions/CRs. In the evolutionary and composite model for AGNs, HyN explosions are a main component; thus, we have suggested that giant HyN explosions and their remnants could be natural candidates for the origin—in AGNs—of UHECRs [174]. In addition, the large duration and very energetic γ -ray bursts are associated mainly with HyN explosions.

From the theoretical point of view, several groups already analyzed the generation of UHECRs and UHENs in:

- *GRBs in general:* In the fireball blast wave scenario for GRB, the waves of ejected relativistic plasma that collide with each other form shocks, which

accelerate UHE particles/CRs and radiate high-energy UV photons (see for references [172, 212]).

- *Hypernovæ, associated with neutron stars in GRB*: In the collapse of neutron star to a black hole (years after the initial SNæ that generate the neutron star), the BH outflow interacts with the original SN remnant through an external shock to form GRB and accelerate UHE particles/CRs and radiate high-energy photons [60, 312–316].
- *Hypernovæ, associated with low-/sub-energetic GRB*: In mildly relativistic HyN ejecta (similar to HyN 1998bw + GRB980425 and HyN 2003lw + GRB031203), the external shock wave—produced by the ejecta—could generate UHE cosmic rays and UHE neutrinos [323, 324].
- *Intergalactic accretion shocks*: Accretion and merger shocks in massive clusters of galaxies could accelerate UHE protons/CRs, which can give rise to neutrinos through *pp* interactions with intercluster gas [145, 219].

Therefore, in the evolutionary, composite, and explosive model for AGNs (and BAL + IR + FeII QSOs), the presence of HyNæ could generate UHECR and UHEN, according to the processes and theoretical studies performed by Wang et al., Vietri and Stella, Dermer and Mitman [60, 313–315, 323, 324]. In the core of composite QSOs and AGNs, different types of HyN could be generated in the accretion regions [45], in particular HyNæ associated with extreme massive stars and neutron stars. In addition, several works suggested that a high percent of core-collapse SN/HyN are associated with mildly relativistic ejecta and GRBs. Thus, in the core of explosive + composite AGNs and BAL + IR + FeII QSOs, different types of HyNæ are one of the main candidates for the origin of UHECRs and UHENs.

7. *Dark matter associated with neutrinos in hypernovæ*: We have explained that several groups already studied theoretically the generation of UHEN and UHECRs in GRBs. More specifically, for the HyN scenario, Wang et al. [323, 324] found that in mildly relativistic ejecta of HyNæ, the UHEN could be generated by the interaction of the HyN UHECR and HyN UV–Optical photons. In addition, in the HyN scenario, Vietri and Stella [314–316] also analyzed the generation of UHEN associated with the collapse of neutron stars to black holes.

On the other hand, in the last decades, a main issue in astrophysics is the search of nonbaryonic massive particles which does not interact strongly with ordinary matter, that is, weakly interacting massive particles (WIMPSs). One of the most attractive candidates for a WIMP are the neutrinos. Because their thermal motion are so significant, particles like massive neutrinos are known as hot dark matter (HDM). Very recently, Lípari et al. [172, 174] proposed that the discovery of different types of giant and extreme—SNæ/HyNæ (which generate UHENs, UHECRs, γ -rays) strongly suggests that these neutrinos—generated by HyNæ—are the probable origin of dark matter.

From the study of HyN 2006gy, Smith et al. [279] proposed that giant—SN/HyN explosions from extreme massive progenitors could be more numerous—especially, in Population III stars, that is, in young objects and

in the early universe—than previously believed. Therefore, it is expected that UHECRs and UHENs (generated by $\text{HyN}\alpha$ in composite + explosive QSOs and AGNs, especially, in BAL + IR + FeII QSOs) play a main role (in general) and especially in the young universe.

Thank you, Sebastian, Begoña, and Evencio. We now move to sources whose relationship with respect to the other type-1 quasars is still a matter of debate. Double-peaked emitters have attracted a lot of attention because of the unusual profile of the Balmer lines.

4.7 Double-Peaked Emitters and the Greater AGN Population

Dear Todd (Boroson), a few type-1 quasars show very broad double-peaked lines. It has been argued that such lines are the signature of either (1) a line-emitting (Keplerian) accretion disk or (2) a binary black hole. Do you agree with either interpretation? If “yes,” then why are sources with double-peaked profiles so rare? If “no,” then what do you think causes the double-peaked structure? Do you think there is evidence for an underlying double-peaked emission-line component in all or most quasars? If “yes,” then why do we not see evidence for it in composite spectra? Or do we?

A few percent of type-1 quasars, the so-called double-peaked emitters, show Balmer lines that have peaks at their blue and red ends, rather than in the center. These lines are quite broad, with widths as large as $15,000\text{--}20,000\text{ km s}^{-1}$ not unusual, and one object, SDSS J0942+0900, having an FWHM over $40,000\text{ km s}^{-1}$. The peaks are generally not sharp but are more like rounded humps. The line profiles are reminiscent of 21 cm HI profiles from rotating galaxy disks, and this similarity has led to the explanation that is currently preferred that the profiles represent emission from the black hole accretion disk. Alternative explanations include the idea that the peaks each represent a black hole in a binary system and the idea that the peaks represent material in a biconical outflow from the central object [103, 287].

These objects are interesting, regardless of the explanation. If we are seeing emission from the accretion disk, then they provide a glimpse of the geometry, kinematics, and radiation transfer at a location we have been unable to probe otherwise. If they are binary black holes, then they give us information about a stage of black hole mergers that has been difficult to model. In either case, one also has to ask why is this phenomenon seen in just a small number of objects.

Monitoring the spectra of these objects provides additional tests for the explanations. The peaks shift in position and relative intensity over timescales of months to years. The details of these shifts provide the strongest argument against the binary black hole explanation, as the shifts are not easily modeled as orbital motion. The strongest argument for the accretion disk explanation is the success of simple models to reproduce the observed line profiles. However, the simple accretion disk

model predicts that the blue peak will always be at least as strong as the red peak, and that is observed not to be true. Thus, the simple models have turned into more complex models, with elliptical disks or perturbing objects invoked.

Although I think that the accretion disk explanation is likely to be correct, a recently studied object, SDSS J1536+0441, has reenergized the discussion [28]. This object has a very strong and sharp blue peak; a less strong, broad peak in the center of the profile; and just a shelf on the red side. This looks different enough from the known and well-studied double-peaked emitters that it might have a different explanation, for example, a binary black hole system in which the accreted black hole is of substantially lower mass than the preexisting one. Given the relative velocity between the two peaks, and making wild guesses at the masses of the two black holes involved, one derives a typical orbital period of around a century. Monitoring of this object for a couple of years now has not shown any significant variation in the spectrum. This has interesting implications for either the disk or the binary explanation, as the relative velocity in either case is due to rotation, and peaks as distinct as the blue one in this object are rarely seen to last more than a few months in the prototypical double-peaked emitters.

This new object has also led to a hybrid explanation that might be a step in the right direction for understanding these objects in general. Tang and Grindlay [295] suggest that both explanations might be true. They argue that it may be the presence of a second, merging black hole that clears out some of the broad-line region material and allows us to see the accretion disk in double-peaked emitters. Tidal forces from the merging black hole on the accretion disk produce the peaks. J1536+0441 would then be an extreme object in that the accretion of the merging black hole is visible; in most cases, the mass of that incoming object is too small. If this is the case, then in most type-1 quasars, that accretion disk is hidden inside the broad-line region, and its emission is reprocessed into a typical, single-peaked line profile.

Thank you, Todd.

Dear Mike (*Eracleous*), are double peakers always radio-loud sources? How many good examples of quasars with double-peaked emission lines are now known?

Double-peaked emission lines were first found in radio-loud AGNs (the prototypes, Arp 102B, 3C 390.3, and 3C 332, are all broad-line radio galaxies). In view of this, the survey of Eracleous and Halpern [74, 75] targeted radio-loud AGNs specifically. But double-peaked emission lines were later discovered in radio-quiet quasars in the SDSS [287] and serendipitously, in LINERs (e.g., [274, 286]) and in hidden Seyfert-1 galaxies observed in polarized light [216, 300]. The total number of such objects known today is about 140. Approximately 15–20% of radio-loud AGNs at $z < 0.4$ turn out to have double-peaked Balmer lines and 3% of all quasars in SDSS in the same redshift range. The fraction of LINERs and Seyfert galaxies with double-peaked Balmer lines is unknown since no systematic survey of these objects, aimed specifically at finding double-peaked lines, has been carried out.

Do you think a line-emitting disk resides in almost every quasar? If yes, then why do we not see a double-peaked signature in ultrahigh S/N composite spectra?

In the context of the current paradigm for the source of the broad emission lines, it is extremely important to understand why we do not see double-peaked lines in many more quasars. If the broad-line region is indeed a disk (as many think), why is it that the line profiles are double-peaked in a small fraction of objects and single-peaked in the majority of cases? This question is indeed very interesting and quite fundamental. We do not yet have a definitive answer, but I suggest possible explanations below.

First, it is important to note that a flat, Keplerian disk will not necessarily give rise to double-peaked line profiles. Double-peaked profiles result in the special case when the ratio of the outer to the inner radius of the line-emitting portion of the disk is small (i.e., using the notation of Fig. 6.9, the ratio of the inner to outer normalized radii is $\xi_2/\xi_1 \lesssim 100$). For larger values of this ratio, the two peaks get so close together that they blend, and the line profile appears single-peaked (see illustrations in [75, 146]). The same effect can also be produced if the line of sight of the observer is close to the axis of the disk (e.g., [52]).

Second, radiative transfer of line photons influences the line profiles quite dramatically by altering the apparent emissivity of the disk. The escape probability of line photons from an outflowing disk atmosphere³ was considered by Chiang and Murray [43, 220], who found that the opacity is anisotropic and depends sensitively on the velocity gradient in the atmosphere projected along the line of sight to the observer. As a result, the disk emissivity does not appear to be axisymmetric; it is suppressed preferentially in the regions of the disk where the projected velocity is large. The consequence is that the wings of the line profile become weaker and the core stronger, thus transforming a double-peaked line into a single-peaked one (see the illustration in Fig. 5 of [220]).

A combination of the geometric and physical effects described above can explain why most quasars have single-peaked emission lines even though these originate in a rotating disk. In this picture, the double-peaked emitters are those objects where the line-emitting skin of the disk has a small optical depth and/or the line-emitting annulus of the disk is narrow. Here, I am resurrecting an old idea by Gregory Shields [273], in which he attributed the broad emission lines of AGNs to material ablated from the accretion disk by radiation pressure. This idea can be tested further by comparing the statistical properties (such as the distribution of shifts, widths, asymmetries) of the line profiles predicted by this model with what is observed (Flohic et al., in preparation).

Thank you, Mike. In addition to your analysis, we can add that double peakers are found to radiate at a low accretion rate; they are probably associated to a late stage

³This is the base of a wind, thought to be emitted by the disks of most quasars and invoked to explain their broad absorption lines.

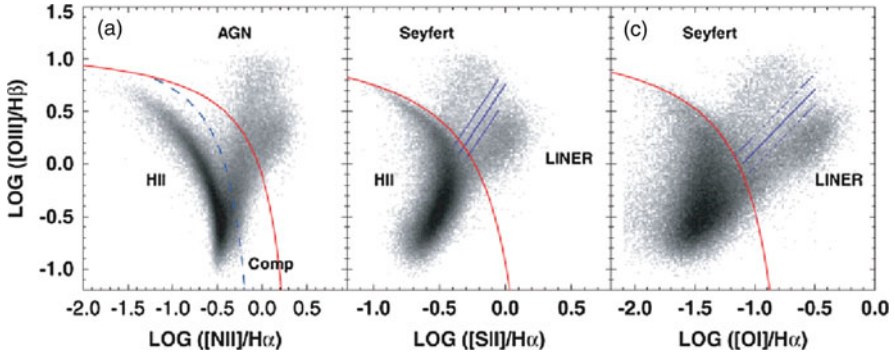


Fig. 4.14 Figure 4 from [150] which shows the different locations of different emission-line galaxies, using various line ratio diagnostics. The initial classification by BPT of the different types of objects was based on other independent criteria, and the regions occupied by the different types in the line ratio plots were based on ~ 100 objects. These SDSS-based plots include $\sim 10^5$ emission-line galaxies, which now clearly marks the exact location occupied by the different types

in the life of AGNs. In the following, we progress considering sources that are at the low end of quasar luminosities and spectroscopic properties. It has been debated for a long time whether LINERs should be considered AGNs at all. We will seek an answer on this issue with the help of Ari Laor and Isabel Marquez-Perez.

4.8 LINERs

Dear Ari (Laor), do you think that LINERs are bona fide AGNs, and if so, how do they relate to Seyfert AGNs?

The prevalence of LINERs in nearby galaxies was discovered by Heckman [135]. Shortly afterward, Ferland and Netzer [85] showed that LINER emission can be produced by low-level AGN emission. However, their high prevalence in nearby galaxies [141] made this interpretation appear unlikely at that time, as it implied BHs are present in a large fraction of galaxies. The seminal discovery of Magorrian et al. [187] that all bulge galaxies likely host a massive black hole led to the obvious interpretation that LINERs are indeed powered by low-level accretion onto the central massive BH. Their non-Seyfert line ratios, that is, their distinct position in the BPT diagrams, may result from a change in the ionizing SED of AGNs at low accretion rates. However, the fact that the line emission originates from the nucleus, where a massive BH resides, does not exclude a different origin. Starbursts do not extend to the LINER region (Fig. 4.14 and [149]), but given the low luminosity, down to a level of a single supergiant star, one may speculate other sources of excitation for the NLR.

Compact UV sources were detected in some LINERs, but their origin, stellar or AGN, was not clear. The detection of significant variability of most of the UV sources [191] excludes the stellar origin. Thus, it is clear that at least some of the LINERs are mini-AGNs. Most likely, the majority, and probably all, are AGN driven.

Some LINERs show a compact radio source. If radio interferometry indicates that the radio source is limited to pc scale, then the source has to be AGN driven, rather than a nuclear starburst which will produce a source not smaller than a fraction of kpc across. Those LINERs which show extended radio jet emission are obviously low-luminosity AGNs. LINERs can be proven to be AGNs also through the detection of a nuclear X-ray point source at the expected luminosity, based on the line luminosity. The ratio of line emission/X-ray emission associated with stellar activity is generally much smaller.

Thank you, Ari.

Dear Isabel (Marquez-Perez), why are LINERs important for understanding AGNs?

Let us first recall that the acronym LINER stands for “low-ionization narrow emission-line regions” which basically means that their optical spectra are characterized by remarkably strong low-ionization emission lines with high-ionization lines that are much fainter (see Fig. 4.15). This distinction is quantified by the position they occupy in diagnostic diagrams using optical [151, 309] or mid-infrared emission-line ratios [19, 58, 256, 276, 278, 288, 289].

They were identified by Heckman [135] and are typically less luminous than Seyferts (Sy) and quasars. While AGNs were widely recognized as sources photoionized by a power-law continuum [128], pioneering work showed that the spectra of LINERs could also be explained in the context of shock ionization [63, 90] and photoionization by post-AGB stars in the case of weak LINERs in ellipticals [21]. LINER nuclei exist in two flavors with type-1 LINERs, showing broad permitted emission lines (about 25% of all LINERs, see [141]). This suggests that type-1 LINERs can be unambiguously connected to the AGN family. The debate is still open with no clear consensus on whether all type-2 LINERs belong to the low-luminosity end of the sequence of AGN phenomena. It is also not clear how important may be the contribution from evolved (post-AGB) stars, low-mass X-ray binaries, or diffuse thermal plasma (see [138] for a full discussion on the topic; see also [76, 207, 282]).

LINERs are found in a large fraction of nearby galaxies. About 40% of galaxies in the Palomar spectroscopic survey (PSS, [141]) fall in this category. There is also compelling evidence that LINERs may host heavily obscured (Compton-thick) AGNs ([112] and references therein) which implies that they may be even more numerous than previously deduced from optical selection. Their study is therefore fundamental for a full understanding of the demography of nearby AGNs.

AGN LINERs are found at the faintest end of the fundamental correlation between mass accretion rate and star-formation rates representing very inefficient accreting systems ([65, 140, 262, 263], but see [226]). Ho [139] place them in

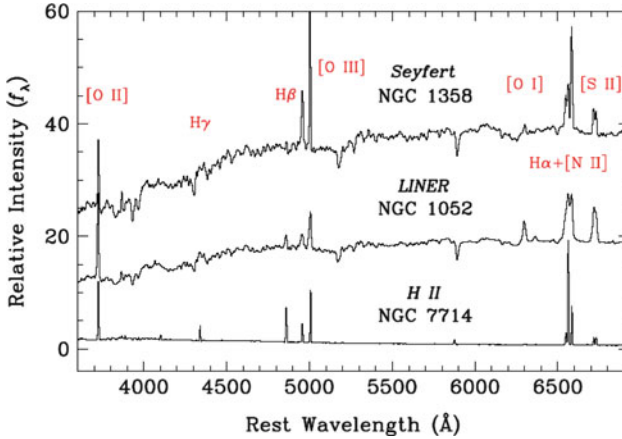


Fig. 4.15 Sample optical spectra of the various classes of emission-line nuclei. Prominent emission lines are identified (from [138])

a sequence of decreasing $L_{\text{bol}}/L_{\text{Edd}}$ ranging from Seyferts to LINERs,⁴ and transition objects, down to passive absorption-line systems. LINERs are therefore important sources for better understanding low-efficiency accretion processes and their connection with stronger AGN activity. Provided (a) that the mass of the central super-massive black hole and the mass of the hosting galaxy are correlated and (b) there exists the expected connection between AGNs with galaxy formation and evolutionary processes; the study of LINERs is of importance for inferring their role as eventual end products in such an evolution scenario (see for instance [322]).

What are the properties of their host galaxies? Are they different than Seyferts’ hosts?

Pioneering work using the Palomar spectroscopic sample (PSS) concluded that LINERs are generally hosted by early-type galaxies (E to Sbc) with morphologies similar to those of Sy [137]. We have reanalysed the PSS sample [197], paying special attention to the environmental status (see below) and confirmed that LINERs are more frequent in earlier-type hosts (from E to S0 and Sab). At variance, the nuclei of spectroscopically classified Sy were almost absent in E and S0 hosts (see Fig. 4.16).

More recent studies have analyzed the properties of AGN hosts by exploiting larger databases from different extragalactic surveys. These generally confirm that LINERs are hosted by early-type galaxies. Within the red galaxy sequence identified in the SDSS, about 30% are LINERs [329]. They are also found more frequently in the red sequence of $z \approx 1$ galaxies in DEEP2 [215]. Among red spiral galaxies

⁴A similar sequence is invoked to explain their generally old stellar populations [23, 261], more evolved central morphologies [144], and richer environments [159] when compared to those of Sy.

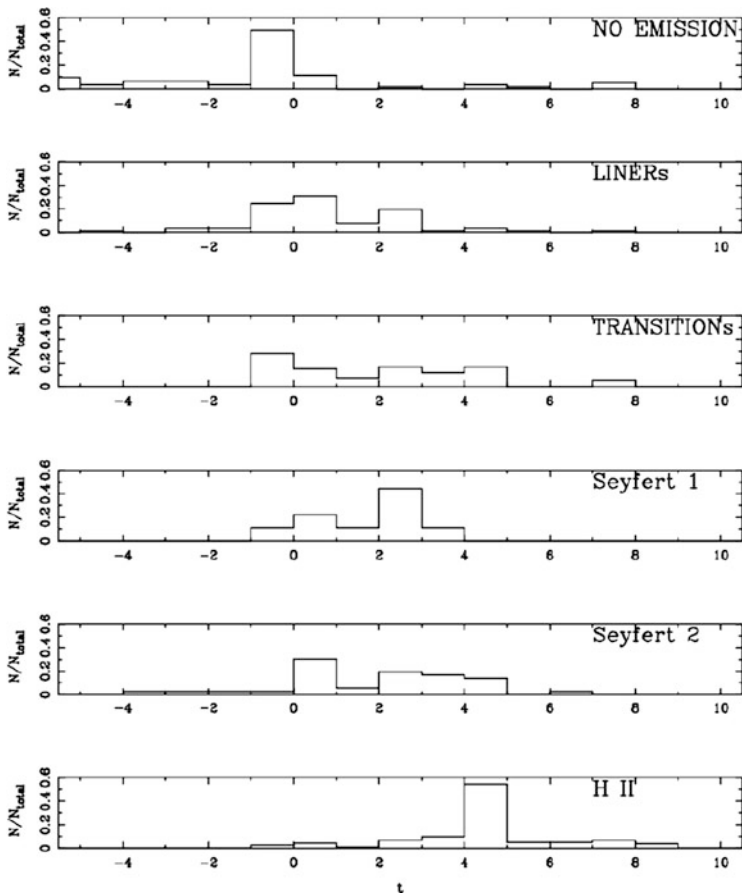


Fig. 4.16 Distribution of morphological types (t) for the various classes of emission-line nuclei in the PSS as analyzed by Márquez et al. [197]. $t(E) < 0, t(S0) = 0, t(Sa) = 1, t(Sb) = 3, t(Sc) = 5, t(Sd) = 7, t(Sm) = 9$

with emission-line spectra in the Galaxy Zoo project, $82 \pm 12\%$ hosts LINER nuclei⁵ [201].

Environmental properties of AGN hosts have long been debated, and controversies still remain concerning both how the environment is described (local density or nearest neighbor) and how to define suitable control samples (see for instance [195–197] and references therein). Ho et al. [140] and Krongold et al. [159] have concluded that LINERs prefer richer environments. On the contrary, the percentage of LINERs in compact groups seems to be quite similar to that of the general

⁵This is in good agreement with the 72% of LINERs that [7] find in a smaller sample of early-type galaxies with ionized gas.

population in PSS [198]. In an attempt to disentangle the effects of host properties from those induced by the close or intermediate environment, we used a distance-limited subsample ($D < 40$ Mpc) selected from the PSS. This provides a good match between active and nonactive galaxies. We classified the objects by estimating the tidal force exerted by the nearest companion (see [307]) which allowed us to define a separate class of isolated galaxies. The main result was that PSS LINERs are very scarce among isolated galaxies [197]. In the same vein, Constantin and Vogeley [49] found that SDSS LINERs are more clustered than Sy galaxies. A very small percentage of LINERs are found in the low-density environments traced by voids [48]. Different pair interaction processes may explain difference in the properties of the brightest neighbors of LINERs and Sy with gas-poorer systems more often involving the former [165].

What do X-ray observations tell us about the nature of LINERs?

X-ray data for low-luminosity AGNs offer the most reliable probe of the high-energy spectrum. In addition to this, the X-ray domain provides many AGN signatures providing one of the most important tools for determining the AGN nature of LINERs. X-ray observations offer one of the best tools to identify AGNs. Early X-ray observations with *Einstein* and ROSAT were limited to soft energies where heavily obscured AGNs are difficult to detect. The ROSAT HRI images showed compact soft X-ray (≤ 2 keV) emission in 70% of LINERs and Sy galaxies [254]. Much progress was made with the advent of *Chandra* and *XMM-Newton*. Different studies carried out in the last decade show that an AGN is present in at least 50% of LINERs.

Calculated X-ray luminosities L_{bol} can be estimated by considering a universal bolometric correction for LINERs, $L_{\text{bol}} \sim L_X$; based on the derived Eddington ratios, it has been concluded that LINERs were the faintest end of the fundamental correlation between mass accretion and star-formation rates, hosting very inefficient accretion processes [65, 77, 88, 140].

Our first effort in this field was focused on analysis of the X-ray properties of 51 LINERs with *Chandra* data. We found that their X-ray morphologies (see Fig. 4.17), spectra, and color-color diagrams together imply that a high percentage of LINER galaxies (at least $\approx 60\%$) may host AGNs [110]. We later updated our sample to include all LINERs from the catalogue by Carrillo et al. [37] with useful observations from *Chandra* and/or *XMM-Newton*, providing the largest sample of LINERs with such data to date [112, 113]. After adding HST optical images and literature data on emission lines, radio compactness, and stellar population results, we concluded that the evidence supports an AGN interpretation for 90% of the sample. The spectral analysis indicates that best fits involve a composite model: (1) an absorbed primary power-law continuum and (2) a soft component below 2 keV described by an absorbed, scattered, and/or thermal component [113]. The most unexpected result relates to the obscuration properties of our LINER sample where about 50% shows evidence of Compton thickness according to the most common tracers (the X-ray spectral index, the $F_X(2-10 \text{ keV})/F([\text{OIII}])$ ratio, and the equivalent width of $\text{FeK}\alpha$ emission line); Compton-thick sources are more common

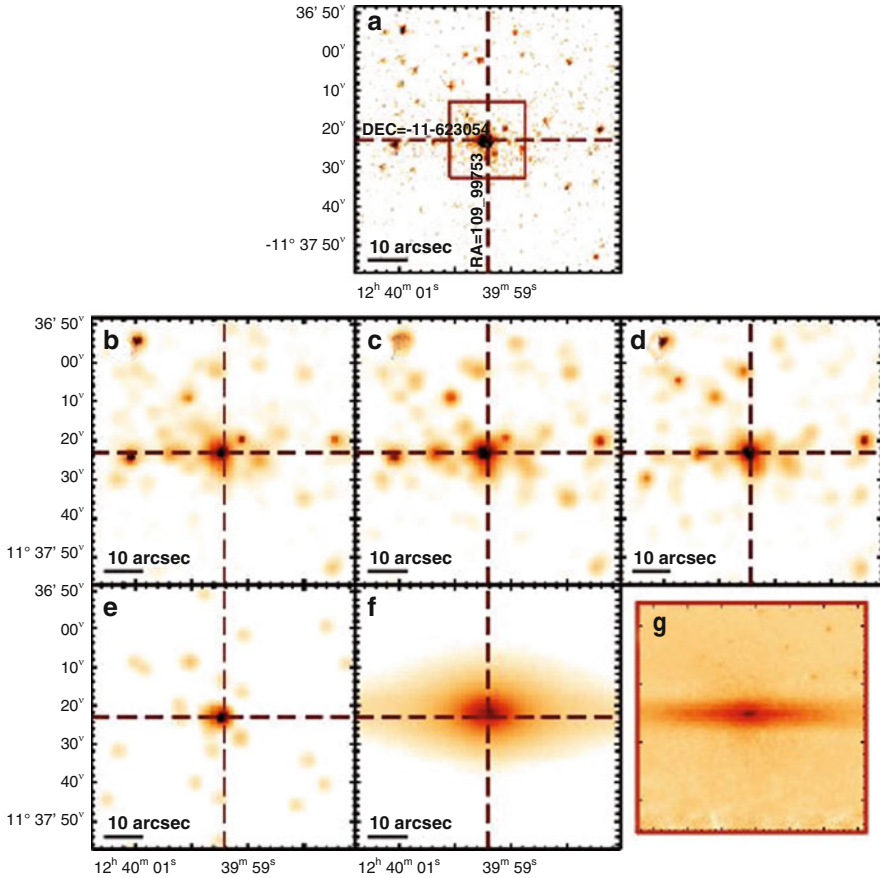


Fig. 4.17 Images of the LINER AGN-candidate NGC 4594. *Chandra*: the *top image* corresponds to the 0.6–8.0 keV band without smoothing; the extraction region is plotted with a *black circle*; the following four images correspond to the X-ray bands 0.6–0.9 (*center-left*), 1.6–2.0 (*center-center*), 4.5–8.0* (*center-right*), and 6.0–7.0 keV (*bottom-left*). The 2MASS image in Ks band is plotted in the *centre-bottom box*. The sharp-divided HST/F814W image (*bottom-right*) shows the *red box* region shown in the *top image*

among LINERs than among Sy [112]. The location and nature of the obscuring matter requires further study. Larger black hole masses and lower Eddington ratios than Sy galaxies have been found consistent with a LINER preference for early-type hosts. It must, however, be noted that once X-ray luminosities are corrected for Compton thickness, LINERs show Eddington ratios overlapping the range of type-2 Sy. Recently, González-Martín et al. [114] have also detected X-ray variability in the type-2 LINER NGC 4102 (from [113]).

What distinguishes LINERs that are not due to nonthermal activity from the LINERs that are believed to be AGNs?

A number of works have shown that a LINER-like spectrum can also arise in a galactic disk (see, for example, [138, 199, 251]). In fact, the contribution from fast shocks in extranuclear LINER emission-line spectra can produce the observed optical line ratios [64] as can ejecta from starburst-driven winds [13] or even a diffuse ionized plasma [46]. The challenge is to determine which sources with a LINER-like spectrum actually harbor a LINER nucleus. A number of diagnostics exist at different wavelengths to make this determination. Detection of broad permitted lines (type-1 LINERs) is a clear indication of an AGN. X-ray properties have also been discussed. The variability at X-ray, UV, and radio frequencies are secure indicators of AGN activity, among others that are briefly discussed below.

Radio Emission: Detection of radio emission can be especially important in sources that are completely obscured in the optical and UV since it becomes possible to detect central engines that are otherwise completely obscured. A VLA survey by Nagar et al. [223] found that 64% LINER 1s and 36% LINER 2s have compact radio cores [222]. When different radio frequencies are available, the resulting radio spectra tend to be flat as is expected when nonthermal processes dominate the emission. Objects bright enough for VLBI observations at 5 GHz were studied by Falcke and Markoff [82] (see also [87]); all showed compact, high-brightness-temperature cores, suggesting that an AGN is responsible for the radio emission. Moreover, the core radio fluxes were found to be variable by a factor of up to a few in about half of the ~ 10 LINERs observed several times during 3 years [224]. A radio survey searching for 1.3-cm water mega-maser emission, an indicator of dense circumnuclear molecular gas only seen in AGNs, detected LINER nuclei at the same rate as type-2 Sy nuclei [31]. A few LINERs show indications of a Seyfert-like ionization cone oriented along their radio axis [200, 243].

IR Emission: Both the overall shape of the continuum and the detection and line ratios of emission lines can be used to reinforce arguments for the existence of a nonthermal component in LINERs. Lawrence et al. [164] found that LINERs are stellar dominated in the range $1\text{--}5\ \mu\text{m}$ but show a strong excess in the range between $10\text{--}20\ \mu\text{m}$, which is interpreted as indicating less hot dust than in Seyferts. At mid-IR frequencies, the unique study done so far by Sturm et al. [288] has shown that two different LINER populations exist: infrared-faint LINERs with LINER emission mostly arising from compact nuclear regions and infrared luminous which often show spatially extended (non-AGN) LINER emission. IR-luminous LINERs show mid-IR SEDs typical of starburst galaxies, while the mid-IR SEDs of IR-faint LINERs are much bluer. The detection of fine-structure emission lines from highly excited gas, such as [OIV], in both populations, suggests the presence of an AGN in a large fraction of IR-bright LINERs as well.

HST Imaging: In more luminous AGNs, the nonstellar nucleus overwhelms the emission from nonnuclear components. This is not the case for LINERs (and other low-luminosity AGNs, LLAGNs) where spatial resolution is of paramount importance for studying the physical processes taking place (see [244]). Several

attempts have been made to detect UV emission from LINERs since stellar contamination from the old population-dominated bulges disappears in the UV. The UV imaging surveys by Barth et al. [15] and Maoz et al. [191] found nuclear UV emission in $\sim 25\%$ of the observed LINERs. About half of them appeared point-like at the resolution of *HST* and thus were good candidate LLAGNs with nonstellar continua. Barth et al. [15] showed that the low UV detection rate is primarily due to dust obscuration of the nuclei. A UV-variability campaign monitored 17 UV-bright LINERs [191] and found that almost all sources varied on either short or long timescales, indicating the presence of an AGN component. In fact, one of the most outstanding results during the last decade has been the discovery that sources with detected radio cores show variability at UV frequencies on timescales of 1 month ([190]; see also [36] for the case of NGC 4278), with some of the UV variable sources also confirmed as X-ray variable [242]. *HST* optical studies [111, 113, 243, 275] have confirmed that almost all the observed LINERs show a nuclear source in addition to an irregular distribution of circumnuclear dust. Dust obscuration can explain the existence of dark-UV LINERs.

Properties of the Ionized Gas: Until new high-resolution X-ray images become available indirect information about the nature of LINERs can be obtained by looking for correlations between lower resolution X-ray properties and higher resolution optical/NIR properties. It is worthwhile to search for the properties of the ionized gas and its relation to the X-ray results. Previous work has shown that the $H\alpha$ morphology of LINERs consists of a point source embedded in an extended structure sometimes clumpy, filamentary, and in some particular cases, with clear indications of nuclear obscuration (similar to what is observed in low luminosity Sy) [42, 57, 243]. STIS spectroscopy [318] demonstrates that at scales of tens of parsecs, the energy source of 13 LINERs is consistent with photoionization by a central nuclear source but with NLR kinematics dominated by outflows.

We made a study of *HST* $H\alpha$ imaging for 32 LINERs [200] in order to characterize the ionized gas in the nuclear regions. An unresolved nuclear component can be identified in 84% of the sources. Extended emission with equivalent sizes ranging from a few tens to hundreds of parsecs is also seen. The morphologies are not homogeneous but can be grouped into three classes: nuclear outflow candidates (42%), core-halo morphologies (25%), and nuclear spiral disks (14%). A size-luminosity relation was found between the equivalent radius of the $H\alpha$ emission and the (2–10 keV) X-ray luminosities. Both ionized gas morphologies and the size-luminosity relation are indistinguishable from those of low-luminosity Sy consistent with a common origin for the NLR of LINERs and Sy. A relation between the soft X-ray and ionized gas morphologies was suggested for the first time in LINERs [200] similar to what has been found for Sy [20].

Thank you, Isabel. Quasars—and especially radio-loud quasars—show several analogies with stellar binary systems hosing a neutron star or a black hole. Since the mid-1990s, there has been a growing discussion dealing with the implications of these binary systems (called “microquasars”) for our understanding of quasars.

4.9 Quasars and Microquasars

4.9.1 *Black Hole X-Ray Binaries*

Dear Elmar (Körding) and Heino (Falcke), why are some binary stars called “microquasars”? How can the analogy help us gain a better understanding of quasars? Are there any radio-quiet stellar analogues of quasars?

Black hole XRBs often show repeated outbursts, during which the XRB changes its luminosity over several orders of magnitude. The typical timescale of such an outburst is of the order of a year, making the evolution of XRBs very well observable. To observe a similar outburst cycle in an AGN, one would need—even for the smallest supermassive black holes—several million years, making them impossible to observe in their entirety. Another benefit of XRBs is that most of the bolometric luminosity is emitted in the X-ray bands. By only observing in the X-rays, one can trace the behavior of nearly all emission components simultaneously. Thus, the evolution of a black hole outburst is best observed in XRBs.

Black hole XRBs can stay for years in quiescence, slowly accumulating matter in their outer accretion disks. Only after a critical mass density is reached an outburst starts, probably triggered by a thermal-viscous instability [94]. During the beginning of the outburst, while the source is still dim, the X-ray spectrum is hard with a typical photon index around 1.8. Hence, the spectrum is nonthermal or at least is not coming from a blackbody. While it rises in luminosity, its hard spectral shape stays basically constant. Once it reaches a luminosity larger than $\sim 30\%$ of the Eddington luminosity, it softens fairly fast (of the order of a week) to a spectrum dominated by blackbody emission [250]. One has therefore defined the so-called spectral states: a source is considered to be in a “hard state” if it has a hard spectrum and is in its “soft state,” when the spectrum is dominated by soft disk photons. In between those two “clean” states, one observes a multitude of intermediate states.

A black hole XRB seems to move through the different accretion states in a predefined order. It starts its outburst in the hard state. Only near the brightest luminosities, it transitions via intermediate states to the soft state. At very late times in the outburst, the source transitions back to the hard state. This transition is at a lower luminosity than the transitions to the hard state. The hysteresis effect can be well demonstrated in a hardness–intensity diagram, where one plots the X-ray spectral hardness (a ratio of the hard flux over the soft flux), against luminosity (see Fig. 4.18). Sources in their hard state are on the right side of the diagram, while sources in their soft state are on the left.

BH XRBs do show jets sometimes during the evolution of the outburst. In the hard state, one observes a flat-spectrum radio core that can sometimes be directly imaged as a compact jet [83, 284]. These types of probably moderately relativistic and stable radio jets are in fact not much different from what one observes in LLAGNs, including sources such as M81 and Sgr A* [78, 80, 208]. During the hard to soft state transition, one usually observes a transient jet: an ejection of jet “blobs”

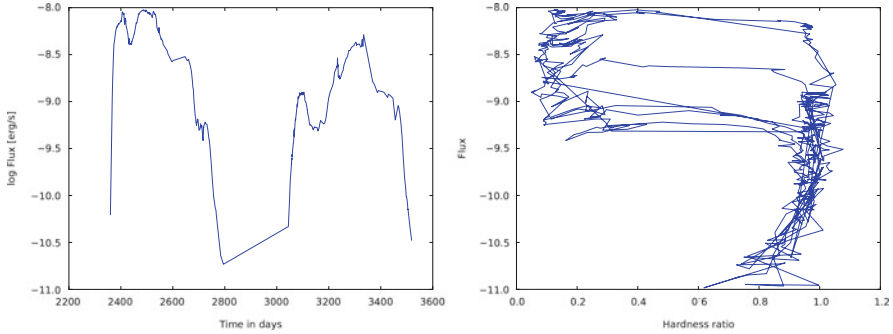


Fig. 4.18 Light curve and hardness–intensity diagram of GX339-4, where we have taken data from [66]. The hard state is found on the *right side* of the hardness–intensity diagram and the soft state on the *left side*. We show several outbursts of the source on the hardness–intensity diagram. In all cases, one can observe the hysteresis effect, only the amplitude varies. The radio jet is active on the right side of the diagram

that can move at relativistic speeds [84]. Finally, in the soft state, one has not yet observed any signature of a jet, neither radio emission nor other signatures of a jet.

For XRBs, we have therefore seen that a single source can change its properties from radio loud to radio quiet in a fairly short time. For a given luminosity, one can observe both possibilities (due to the hysteresis). It is thus not surprising that the distinction between radio-loud and radio-quiet quasars is also not trivial. We note that the spin of the black hole cannot be changed during an outburst. The difference between jet emitting and weak jet sources is therefore—at least for XRBs—not due to the spin.

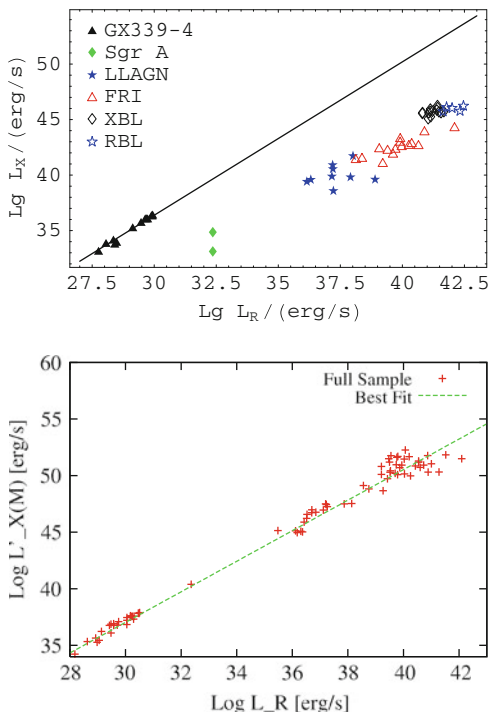
4.9.2 The Fundamental Plane of Black Hole Activity

One of the major results for jets in XRBs research is the radio/X-ray correlation: in many (albeit not all) XRBs, the core-radio flux in its hard state is tightly correlated with the X-ray flux. To a first-order approximation, this correlation seems to be universal for all sources and outbursts [50,51,98]. If one attributes the radio emission to the jet, the correlation indicates a strong coupling between the accretion flow and the power injected into the jet [80, 81, 136, 193].⁶

If one wants to extend this correlation to AGNs, one has to restrict oneself to AGNs that one considers to be in a similar state as those XRBs in their hard state. In a hard state, an XRB shows no strong disk emission, and the X-rays are dominated by a simple power law. If one compares these spectral features with the spectra

⁶Note, however, that at low accretion rates, it is not clear that the X-ray emission comes from the accretion flow or perhaps rather from the jet itself [192, 194].

Fig. 4.19 Radio/X-ray correlation for XRBs and AGNs. *Left panel:* effective “X-ray” emission as a function of the radio luminosity. Besides the radio/X-ray correlation for XRBs, one notices that AGNs are more radio loud for a given X-ray flux. *Right panel:* edge-on projection of the fundamental plane. Plots reproduced from [81, 152] but see also [209] for similar results



of supermassive black holes, it is likely that low-luminosity AGNs are in a similar state as hard state XRBs (for a more detailed discussion see below), but not Seyfert galaxies or quasars, which obviously are in a high accretion state. In contrast to the original radio-loudness discussions, we do *not* look at the extended emission. The extended emission of AGNs is strongly related to the environment of the AGNs and can therefore not be compared to XRBs, where one encounters a wildly different situation. Rather, one has to restrict oneself to the radio cores, that is, the innermost parts of jets, that are mainly dominated by the properties of the central engine.

If one extrapolates the radio/X-ray correlation to AGNs and quasars, one finds that all AGNs are more radio loud for a given X-ray luminosity (see Fig. 4.19) than their XRB counterparts. However, it has been found that the inclusion of the black hole mass as an additional parameter leads to a multivariate correlation between the radio and X-ray luminosities and the black hole masses [81, 209]. Thus, all accreting black holes populate a plane in this parameter space. An edge-on projection of the correlation is shown in Fig. 4.19. In hindsight, this dependence of the radio/X-ray ratio on mass is no surprise, after all were supermassive black holes (i.e., quasars) noted first due to their strong radio emission, while stellar mass black holes (i.e., XRBs) were discovered due to their X-ray emission.

The multivariate correlation can be written as

$$\log L_X \approx 1.4 \log L_R - 0.8M. \quad (4.1)$$

This nonlinear relationship is expected if the radio emission is originating in a scale-invariant conical jet coupled to the accretion disk (e.g., [22, 79]). The X-ray emission can either be explained as inverse-Compton emission from a corona or as synchrotron and synchrotron-self-Compton emission from the jet [194]. Even though the distances of XRBs and AGNs are vastly different, it has been shown that the fundamental plane is not a distance artifact [210].

The scatter in the correlation and the exact fit values depend on the used sample: if one only uses low-luminosity AGNs of LINER type and hard state XRBs, the scatter is roughly consistent with the measurement uncertainties [152]. This supports the idea that AGNs like XRBs have different states. Low-luminosity AGN of LINER type are the best candidates for hard state AGN. If one adds intermediate or soft state objects like Seyferts or FR II Radio galaxies, the scatter around the correlation increases.

The interpretations of the fundamental plane suggest that the accretion rate is correlated with the core-radio emission. K rding et al. [153] investigated this connection further and suggested that the accretion rate can be well estimated from the core-radio emission as

$$\dot{M} = 4 \cdot 10^{14} \text{ g s}^{-1} \left(\frac{L_{8\text{GHz}}}{10^{30} \text{ erg s}^{-1}} \right)^{0.71}. \quad (4.2)$$

This relation is established using hard state black hole and neutron star XRBs, which are probably not strongly affected by relativistic beaming. For any application to high-power AGN, relativistic beaming effects need to be taken into account.

Using this accretion rate measure, we can rewrite the fundamental plane of black hole activity as

$$\frac{L_X}{L_{\text{Edd}}} \propto \left(\frac{\dot{M}}{\dot{M}_{\text{Edd}}} \right)^2. \quad (4.3)$$

Thus, the fundamental plane is simply stating that the X-ray luminosity in units of the Eddington luminosity scales quadratically with the accretion rate in units of Eddington. This is exactly what one expects from inefficient accretion flows.

We note that the presented plane is only valid for sources in the analogue of the hard state found in XRBs, that is, for those sources that are expected to be inefficiently accreting. Radio-loud quasars are typically relativistically beamed which introduces a scatter of several orders of magnitude. Radio-quiet quasars show less radio emission, but compared to quadratic scaling laws of inefficient accreting objects, they are in fact also too X-ray faint (once the source is efficiently radiating, the radiative efficiency cannot increase any further). These effects place the quasars around the fundamental plane, albeit with larger scatter [152].

As the fundamental plane describes the radio emission of a generic black hole of a given accretion rate, it may be a good way to measure radio loudness. A ratio of the radio flux over the expected flux due to the fundamental plane would be a good measure of the jet power with respect to the average jet power observed in the sample used to derive the fundamental plane. Moreover, the fact that both XRBs

and LLAGNs seem to be in a radio-loud state, further strengthens the unification across different mass scales. Of course, an important factor in this radio loudness is the fact that accretion flows become more and more inefficient with decreasing accretion rate, while the jet-related radio emission decreases less rapidly.

Does variability support this view?

To reconfirm that the central engine of XRBs and AGNs are indeed scale invariant, we will present a second correlation connecting both classes of black holes. Besides spectral properties, one can also use variability properties of the X-ray light curves. Since roughly 30 years, it has been shown that the power spectral density (PSD) of the X-ray light curves of AGNs are similar to those of black hole XRBs [204], if one scales the observed frequencies linearly with the black hole mass. Both the PSD of AGNs as well as those of a soft state XRB can be described by a broken power law. At low Fourier frequencies, the PSD can be described as a power law with index ~ -1 which steepens around the characteristic timescale (ν_{hb}) to a power law with index ~ -2 [55, 67, 117]. Uttley and McHardy [305] noted that the correlation between the characteristic timescales and the black hole mass has significant scatter, and there seems to be an indication that the bolometric luminosity influences the characteristic frequencies as well. Also, for XRBs, it has been shown that the variability timescales depend on the accretion rate [306] or on their radio luminosities [213].

Thus, it is likely that also the characteristic timescales do not only depend on the black hole mass but also on the accretion rate. Like the “fundamental plane of black hole activity,” all accreting objects may populate a plane in the space given by the black hole mass, accretion rate, and the characteristic timescales. And indeed, McHardy et al. [205] report the existence of such a plane. In Fig. 4.20, we show an edge-on projection of the variability plane of soft state objects in the left panel. We find

$$\nu_{\text{hb}} \propto \frac{\dot{M}}{M^2} \quad \text{or} \quad M \nu_{\text{hb}} \propto \frac{\dot{M}}{M}. \quad (4.4)$$

The characteristic variability frequency in units of the light-crossing time of the central object depends linearly on the accretion rate in Eddington units and is therefore scale invariant in respect to the black hole mass. In case that the X-ray emission originates from the accretion flow, the correlation suggests that the accretion flow is—at least approximately—scale invariant.

The PSD of hard state X-ray binaries shows more features than those of a soft state object. It is usually fitted by a number of Lorentzians [18]. We argue in [154] that one can identify the characteristic timescale found in AGNs and soft state XRBs with the characteristic frequency ν_l of the lower high-frequency Lorentzian. In Fig. 4.20, a sample of hard state XRBs is shown. To better visualize the behavior in stellar object, the right panel shows only stellar black holes. There seems to be a constant offset between hard state objects and soft state objects. We also show two outbursts of XTE J1550 (1998 and 2000), where the source seem to be in a transition state. It starts off at the hard state scaling and moves toward the soft state scaling. Thus, the frequencies do not only depend on the accretion rates and black hole masses but also on a parameter governing the accretion state of the object.

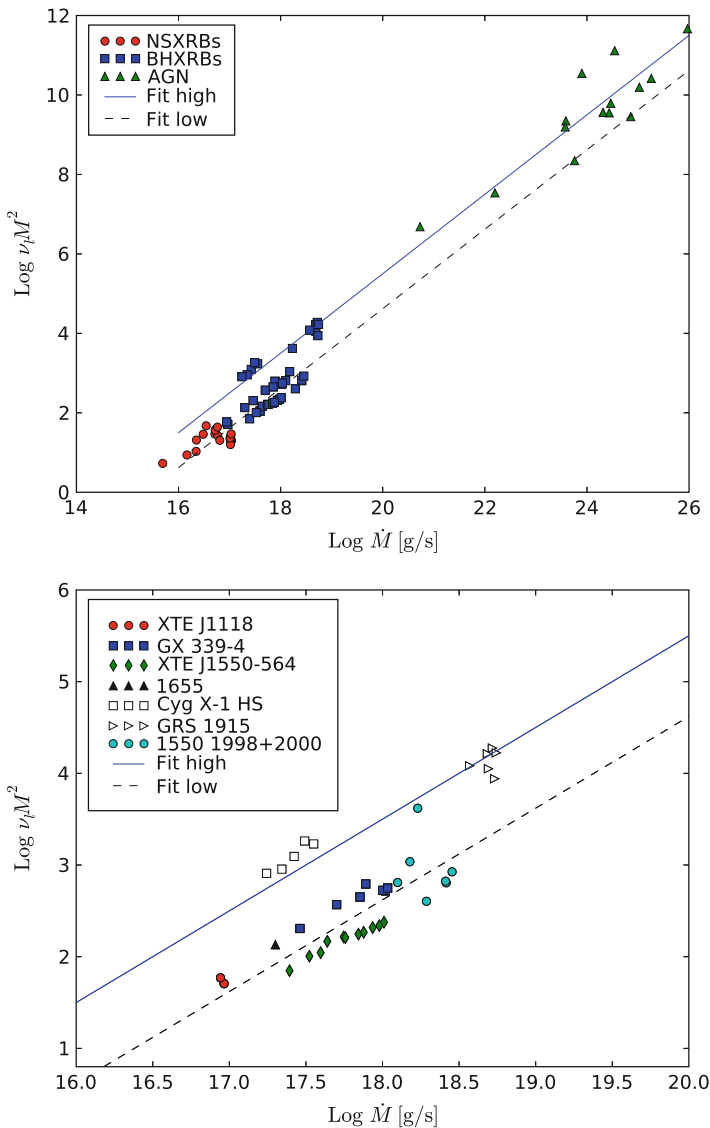


Fig. 4.20 Edge-on projection of the variability plane for AGNs and hard and soft state XRBs. While the *left panel* shows the full correlation the *right panel* zooms in on the XRBs. The linear dependence on the accretion rate is seen both in AGNs alone as well as in hard and soft state XRBs

Besides black holes, one can also add neutron stars with measured frequencies ν_l of the noise components described by the lower high-frequency Lorentzian.

One application of this plane is the estimation of the black hole masses in ultra-luminous X-ray sources. Casella et al. [38] used the variability plane to estimate

the mass of M82 X-1 and NGC 5408 X-1. They conclude that both sources contain black holes of masses between 100 and 1,300 solar masses. While this application is a promising step toward measuring black hole masses using variability timescales, the systematic and statistical uncertainties of the fundamental plane for mass measuring are still very large and only provide an additional argument for the intermediate mass of the object.

Thank you, Heino and Elmar.

References

1. Abdo, A.A., Ackermann, M., Agudo, I., Ajello, M., Aller, H.D., Aller, M.F., Angelakis, E., Arkharov, A.A., Axelsson, M., Bach, U., et al.: The spectral energy distribution of fermi bright blazars. *Astrophys. J.* **716**, 30 (2010)
2. Abdo, A.A., Ackermann, M., Ajello, M., Axelsson, M., Baldini, L., Ballet, J., Barbiellini, G., Bastieri, D., Baughman, B.M., Bechtol, K., et al.: A change in the optical polarization associated with a gamma-ray flare in the blazar 3C 279. *Nature* **463**, 919 (2010)
3. Abdo, A.A., Ackermann, M., Ajello, M., Baldini, L., Ballet, J., Barbiellini, G., Bastieri, D., Bechtol, K., Bellazzini, R., Berenji, B., et al.: Radio-loud narrow-line seyfert-1 as a new class of gamma-ray active galactic nuclei. *Astrophys. J.* **707**, L142 (2009)
4. Abraham, J., Aglietta, M., Aguirre, C., Allard, D., Allekotte, I., Allison, P., Alvarez, C., Alvarez-Muiz, J., Ambrosio, M., Anchordoqui, L., et al.: [the Pierre Auger Collaboration]: Correlation of the highest-energy cosmic rays with nearby extragalactic objects. *Science* **318**, 938–943 (2007)
5. Alexander, D.M., La Franca, F., Fiore, F., Barcons, X., Cileigi, P., Danese, L., Della Ceca, R., Franceschini, A., Gruppioni, C., Matt, G., et al.: The european large-area infrared space observatory survey V: A beppoSAX hard X-ray survey of the S1 region. *Astrophys. J.* **554**, 18 (2001)
6. Allen, J.T., Hewett, P.C., Maddox, N., Richards, G.T., Belokurov, V.: A strong redshift dependence of the broad absorption line quasar fraction. *Mon. Not. R. Astron. Soc.* **410**, 860 (2011)
7. Annibali, F., Bressan, A., Rampazzo, R., Zeilinger, W.W., Vega, O., Panuzzo, P.: Nearby early-type galaxies with ionized gas. IV. Origin and powering mechanism of the ionized gas. *Astron. Astrophys.* **519**, 40 (2010)
8. Antonucci, R.: Unified models for active galactic nuclei and quasars. *Ann. Rev. Astron. Astrophys.* **31**, 473–521 (1993)
9. Antonucci, R.R.J., Miller, J.S.: Spectropolarimetry and the nature of NGC 1068. *Astrophys. J.* **297**, 621 (1985)
10. Arav, N.: The ghost of Ly α as evidence for radiative acceleration in quasars. *Astrophys. J.* **465**, 617 (1996)
11. Arav, N., Korista, K., de Kool, M.: On the column density of agn outflows: the case of NGC 5548. *Astrophys. J.* **566**, 699 (2002)
12. Arav, N., Shlosman, I., Weymann, R.J.: Mass ejection from active galactic nuclei. *ASP Conf. Ser.* **128** (1997)
13. Armus, L., Heckman, T.M., Miley, G.K.: The optical emission-line nebulae of powerful far-infrared galaxies. *Astrophys. J.* **364**, 471 (1990)
14. Baldwin, J.A., Phillips, M.M., Terlevich, R.: Classification parameters for the emission-line spectra of extragalactic objects. *PASP* **93**, 5 (1981)
15. Barth, A.J., Ho, Luis, C., Filippenko, Alexei, V., Sargent, Wallace, L.W.: A search for ultraviolet emission from LINERs. *Astrophys. J.* **496**, 133 (1998)

16. Becker, R.H., White, R.L., Helfand, D.J.: The FIRST survey: Faint images of the radio sky at twenty centimeters. *Astrophys. J.* **450**, 559–577 (1995)
17. Becker, R.H., White, R.L., Gregg, M.D., Brotherton, M.S., Laurent-Muehleisen, S.A., Arav, N.: Properties of radio-selected broad absorption line quasars from the first bright quasar survey. *Astrophys. J.* **538**, 72 (2000)
18. Belloni, T., Psaltis, D., van der Klis, M.: A unified description of the timing features of accreting X-ray binaries. *Astrophys. J.* **572**, 392–406 (2002)
19. Bendo, G.J., uckalew, B.A., Dale, D.A., Draine, B.T., Joseph, R.D., Kennicutt, R.C., Jr., Sheth, K., Smith, J.-D.T., Walter, F., Calzetti, D., Cannon, J.M., et al.: Spitzer and JCMT observations of the active galactic nucleus in the sombrero galaxy (NGC 4594). *Astrophys. J.* **645**, 134 (2006)
20. Bianchi, S., Guainazzi, M., Chiaberge, M.: The soft X-ray/NLR connection: A single photoionized medium? *Astron. Astrophys.* **448**, 499 (2006)
21. Binette, L., Magris, C.G., Stasińska, G., Bruzual, A.G.: Photoionization in elliptical galaxies by old stars. *Astron. Astrophys.* **292**, 13 (1994)
22. Blandford, R.D., Königl, A.: Relativistic jets as compact radio sources. *Astrophys. J.* **232**, 34–48 (1979)
23. Boisson, C., Joly, M., Pelat, D., Ward, M.J.: Stellar populations in active galactic nuclei III. *Astron. Astrophys.* **428**, 373 (2004)
24. Boller, T., Brandt, W.N., Fink, H.H.: Soft X-ray properties of narrow-line seyfert-1 galaxies. *Astron. Astrophys.* **305**, 53 (1996)
25. Borguet, B., Hutsemekers, D.: A polar+equatorial wind model for broad absorption line quasars. I. Fitting the C IV BAL profiles. *Astron. Astrophys.* **515**, 22 (2010)
26. Boroson, T.A.: Black hole mass and eddington ratio as drivers for the observable properties of radio-loud and radio-quiet QSOs. *Astrophys. J.* **565**, 78 (2002)
27. Boroson, T.A., Green, R.F.: The emission-line properties of low-redshift quasi-stellar objects. *Astrophys. J. Suppl. Ser.* **80**, 109 (1992)
28. Boroson, T.A., Lauer, T.R.: A candidate sub-parsec supermassive binary black hole system. *Nature* **703**, 930–938 (2009)
29. Boroson, T.A., Meyers, K.A.: The optical properties of IR-selected and MG II broad absorption line quasars. *Astrophys. J.* 397, 442 (1992)
30. Bower, R.G., Morris, S.L., Bacon, R., Wilman, R.J., Sullivan, M., Chapman, S., Davies, R.L., de Zeeuw, P.T., Emsellem, E.: Deep SAURON spectral imaging of the diffuse Lyman α halo LAB1 in SSA 22. *Mon. Not. R. Astron. Soc.* **351**, 63–69 (2004)
31. Braatz, J.A., Wilson, A.S., Henkel, C.: A survey for H₂O megamasers in active galactic nuclei. II. A comparison of detected and undetected galaxies. *Astrophys. J. Suppl. Ser.* **110**, 321 (1997)
32. Branch, D., Leighly, K.M., Thomas, R.C., Baron, E.: The spectrum of the FeLoBAL quasar FBQS 1214+2803: A resonance-scattering interpretation. *Astrophys. J.* **578**, L37–L40 (2002)
33. Brandt, W.N., Gallagher, S.C.: Observational similarities and potential connections between luminous ultrasoft NLS1s and BALQSOs. *New Astron. Rev.* **44**, 461 (2000)
34. Brandt, W.N., Mathur, S., Elvis, M.: A comparison of the hard ASCA spectral slopes of broad- and narrow-line seyfert-1 galaxies. *Mon. Not. R. Astron. Soc.* **285**, L25 (1997)
35. Brotherton, M.S., De Breuck, C., Schaefer, J.J.: Spectropolarimetry of PKS 0040–005 and the orientation of broad absorption line quasars. *Mon. Not. R. Astron. Soc.* **372**, L58–L62 (2006)
36. Cardullo, A., Corsini, E.M., Beifiori, A., Buson, L.M., Dalla Bontà, E., Morelli, L., Pizzella, A., Bertola, F.: The ultraviolet flare at the center of the elliptical galaxy NGC 4278. *Astron. Astrophys.* **508**, 641 (2010)
37. Carrillo, R., Masegosa, J., Dultzin-Hacyan, D., Ordoñez, R.: A multifrequency catalog of LINERs. *Rev. Mex. Astron. Astrophys.* **35**, 187 (1999)
38. Casella, P., Ponti, G., Patruno, A., Belloni, T., Miniutti, G., Zampieri, L.: Weighing the black holes in ultra-luminous X-ray sources through timing. *Mon. Not. R. Astron. Soc.* **387**, 1707–1711 (2008)

39. Celotti, A., Ghisellini, G.: The power of blazar jets. *Mon. Not. R. Astron. Soc.* **385**, 283 (2008)
40. Chapman, S., Scott, D., Windhorst, R.A., Frayer, D.T., Borys, C., Lewis, G.F., Ivison, R.J.: Further multiwavelength observations of the SSA 22 Ly γ -emitting blob. *Astrophys. J.* **606**, 85 (2004)
41. Chapman, S., Smail, I., Blain, A.W., Ivison, R.J.: A population of hot, dusty ultraluminous galaxies at $z \sim 2$. *Astrophys. J.* **614**, 671 (2004)
42. Chiaberge, M., Capetti, A., Macchetto, F.D.: The hubble space telescope view of LINER nuclei: evidence for a dual population? *Astrophys. J.* **625**, 716 (2005)
43. Chiang, J., Murray, N.: Reverberation mapping and the disk-wind model of the broad-line region. *Astrophys. J.* **466**, 704 (1996)
44. Colina, L., Alberdi, A., Torrelles, J.M., Panagia, N., Wilson, A.S.: Discovery of a bright radio supernova in the circumnuclear starburst of the luminous infrared seyfert-1 galaxy NGC 7469. *Astrophys. J. Lett.* **553**, L19 (2001)
45. Collin, S., Zhan, J.-P.: Star formation and evolution in accretion disks around massive black holes. *Astron. Astrophys.* **344**, 433 (1999)
46. Collins, J.A., Rand, R.J.: Ionization sources and physical conditions in the diffuse ionized gas halos of four edge-on galaxies. *Astrophys. J.* **551**, 57 (2001)
47. Comastri, A., Setti, G., Zamorani, G., Hasinger, G.: The contribution of AGNs to the X-ray background. *Astron. Astrophys.* **296**, 1 (1995)
48. Constantin, A., Hoyle, F., Vogeley, M.S.: Active galactic nuclei in void regions. *Astrophys. J.* **673**, 715 (2008)
49. Constantin, A., Vogeley, M.S.: The clustering of low-luminosity active galactic nuclei. *Astrophys. J.* **650**, 727 (2006)
50. Corbel, S., Fender, R.P., Tzioumis, A.K., Nowak, M., McIntyre, V., Durouchoux, P., Sood, R.: Coupling of the X-ray and radio emission in the black hole candidate and compact jet source GX 339-4. *Astron. Astrophys.* **359**, 251–268 (2000)
51. Corbel, S., Koeding, E., Kaaret, P.: Revisiting the radio/X-ray flux correlation in the black hole V404 Cyg: From outburst to quiescence. *Mon. Not. R. Astron. Soc.* **389**, 1697–1702 (2008)
52. Corbin, M.R.: QSO broad emission line asymmetries: Evidence of gravitational redshift? *Astrophys. J.* **447**, 496 (1995)
53. Cottis, C.E., Goad, M.R., Knigge, C., Scaringi, S.: Searching for the signature of radiative line driving: On the absence of Ly α -NV line-locking features in a large sample of BAL QSOs. *Mon. Not. R. Astron. Soc.* **406**, 2094–2112 (2010)
54. Crenshaw, D.M., Kraemer, S.B., George, I.M.: Mass outflow in active galactic nuclei: New perspectives. *ASP Conf. Ser.* **255** (2002)
55. Cui, W., Zhang, S.N., Focke, W., Swank, J.H.: Temporal properties of cygnus X-1 during the spectral transitions. *Astrophys. J.* **484**, 383 (1997)
56. Czerny, B., Rózańska, A., Kuraszkiewicz, J.: Constraints for the accretion disk evaporation rate in AGN from the existence of the broad line region. *Astron. Astrophys.* **428**, 39 (2004)
57. Dai, H.F., Wang, T.G.: The structure of narrow-line region in LINERs. *Chin. J. Astron. Astrophys.* **8**, 245 (2008)
58. Dale, D.A., Smith, J.D.T., Armus, L., Buckalew, B.A., Helou, G., Kennicutt, R.C., Jr., Moustakas, J., Roussel, H., Sheth, K., Bendo, G.J.: Mid-infrared spectral diagnostics of nuclear and extranuclear regions in nearby galaxies. *Astrophys. J.* **646**, 161 (2006)
59. Davidson, K., Kinman, T.D.: On the possible importance of markarian 359. *Astrophys. J.* **225**, 776 (1978)
60. Dermer, C.D., Mitman, K.E.: External shock model for the prompt phase of gamma ray bursts: implications for GRB source models. *ASP Conf. Ser.* **312**, 301 (2004)
61. de Zotti, G., Gaskell, C.M.: Orientation effects and the reddening of the lines and continua of seyfert galaxies. *Astron. Astrophys.* **147**, 1 (1985)
62. Dietrich, M., Mathur, S., Grupe, D., Komossa, S.: Black hole masses of intermediate-redshift quasars: Near-infrared spectroscopy. *Astrophys. J.* **696**, 1998 (2009)

63. Dopita, M.A., Koratkar, A.P., Allen, M.G., Tsvetanov, Z.I., Ford, H.C., Bicknell, G.V., Sutherland, R.S.: The LINER nucleus of M87: A shock-excited dissipative accretion disk. *Astrophys. J.* **490**, 202 (1997)
64. Dopita, M.A., Sutherland, R.S.: Spectral signatures of fast shocks. II. Optical diagnostic diagrams. *Astrophys. J.* **455**, 468 (1995)
65. Dudik, R.P., Satyapal, S., Gliozzi, M., Sambruna, R.M.: A chandra snapshot survey of infrared-bright LINERs: A possible link between star formation, active galactic nucleus fueling, and mass accretion. *Astrophys. J.* **620**, 113 (2005)
66. Dunn, R.J.H., Fender, R.P., Křiding, E.G., Belloni, T., Merloni, A.: A global study of the behaviour of black hole X-ray binary discs. *Mon. Not. R. Astron. Soc.* **411**, 337 (2011)
67. Edelson, R., Nandra, K.: A cutoff in the X-ray fluctuation power density spectrum of the seyfert-1 galaxy NGC 3516. *Astrophys. J.* **514**, 682–690 (1999)
68. Efimov, Y.S., Shakhovskoy, N.M.: *Izv. Krim. Astrofis. Obs.* **46**, 3 (1972)
69. Efimov, Y.S., Shakhovskoy, N.M.: C 66A: Polarimetry in 1993–2002. In: Astronomy, L.O., Takalo, E., Valtaoja (eds.) *High Energy Blazar. ASP Conf. Ser.*, vol. 299, p. 209 (2003)
70. Efimov, Y.S., Shakhovskoy, N.M.: Optical polarimetry of B2 1219+28 (ON 231) during its great outburst in 1998. *Blazar Data J.*, vol. 1, no. 3 (1998)
71. Efimov, Y.S., Shakhovskoy, N.M., Takalo, L.O., Sillanpää, A.: Photopolarimetric monitoring of OJ 287 in 1994–1997. *Astron. Astrophys.* **381**, 408–419 (2002)
72. Elitzur, M., Ho, L.C.: On the disappearance of the broad-line region in low-luminosity active galactic nuclei. *Astrophys. J. Lett.* **701**, L91 (2009)
73. Elitzur, M., Shlosman, I.: The AGN-obscuring torus: The end of the doughnut paradigm? *Astrophys. J. Lett.* **648**, L101 (2006)
74. Eracleous, M., Halpern, J.P.: Doubled-peaked emission lines in active galactic nuclei. *Astrophys. J. Suppl. Ser.* **90**, 1 (1994)
75. Eracleous, M., Halpern, J.P.: Completion of a survey and detailed study of double-peaked emission lines in radio-loud active galactic nuclei. *Astrophys. J.* **599**, 886 (2003)
76. Eracleous, M., Hwang, J.A., Flohic, H.M.L.G.: An assessment of the energy budgets of low-ionization nuclear emission regions. *Astrophys. J.* **711**, 796 (2010)
77. Eracleous, M., Shields, J.C., Chartas, G., Moran, E.C.: Three LINERs under the chandra X-ray microscope. *Astrophys. J.* **565**, 108 (2002)
78. Falcke, H.: The nuclear jet in m81. *Astrophys. J. Lett.* **464**, L67 (1996)
79. Falcke, H., Biermann, P.L.: The jet-disk symbiosis. I. Radio to X-ray emission models for quasars. *Astron. Astrophys.* **293**, 665–682 (1995)
80. Falcke, H., Biermann, P.L.: The jet/disk symbiosis. III. What the radio cores in GRS 1915+105, NGC 4258, M 81 and SGR A* tell us about accreting black holes. *Astron. Astrophys.* **342**, 49–56 (1999)
81. Falcke, H., Křiding, E., Markoff, S.: A scheme to unify low-power accreting black holes. Jet-dominated accretion flows and the radio/X-ray correlation. *Astron. Astrophys.* **414**, 895–903 (2004)
82. Falcke, H., Markoff, S.: The jet model for Sgr A*: radio and X-ray spectrum. *Astron. Astrophys.* **362**, 113 (2000)
83. Fender, R.P.: Powerful jets from black hole X-ray binaries in low/hard X-ray states. *Mon. Not. R. Astron. Soc.* **322**, 31–42 (2001)
84. Fender, R.P., Garrington, S.T., McKay, D.J., Muxlow, T.W.B., Pooley, G.G., Spencer, R.E., Stirling, A.M., Waltman, E.B.: MERLIN observations of relativistic ejections from GRS 1915+105. *Mon. Not. R. Astron. Soc.* **304**, 865–876 (1999)
85. Ferland, G.J., Netzer, H.: Are there any shock-heated galaxies? *Astrophys. J.* **264**, 105 (1983)
86. Ferrarese, L., Merritt, D.: A fundamental relation between supermassive black holes and their host galaxies. *Astrophys. J. Lett.* **539**, L9–L12 (2000)
87. Filho, M.E., Fraternali, F., Markoff, S., Nagar, N.M., Barthel, P.D., Ho, L.C., Yuan, F.: Further clues to the nature of composite LINER/H II galaxies. *Astron. Astrophys.* **418**, 429 (2004)
88. Flohic, H.M.L.G., Eracleous, M., Chartas, G., Shields, J.C., Moran, E.C.: The central engines of 19 LINERs as viewed by chandra. *Astrophys. J.* **647**, 140 (2006)

89. Foltz, C., Weymann, R.J., Peterson, B.M., Sun, L., Malkan, M.A., Chaffee, F.H., Jr.: C IV absorption systems in QSO spectra – is the character of systems with $Z(\text{abs}) = \text{about } Z(\text{em})$ different from those with $Z(\text{abs})$ much less than $Z(\text{em})$? *Astrophys. J.* **307**, 504 (1986)
90. Fosbury, R.A.E., Mebold, U., Goss, W.M., Dopita, M.A.: The active elliptical galaxy NGC 1052. *Mon. Not. R. Astron. Soc.* **183**, 549 (1978)
91. Franceschini, A., Bassani, L., Cappi, M., Granato, G.L., Malaguti, G., Palazzi, E., Persic, M.: BeppoSAX uncovers a type-2 QSO in the hyperluminous infrared galaxy IRAS 09104+4109. *Astron. Astrophys.* **353**, 910 (2000)
92. Franceschini, A., Braito, V., Persic, M., Della Ceca, R., Bassani, L., Cappi, M., Malaguti, P., Palumbo, G.G.C., Risaliti, G., Salvati, M., Severgnini, P.: An XMM-newton hard X-ray survey of ultraluminous infrared galaxies. *Mon. Not. R. Astron. Soc.* **343**, 1181 (2003)
93. Francis, P.J., Wills, B.J.: Introduction to principal components analysis. *ASP Conf. Ser.* **162**, 163 (1999)
94. Frank, J., King, A., Raine, D.J.: *Accretion Power in Astrophysics: Third Edition*, p. 398. Cambridge University Press, Cambridge (2002)
95. Fritz, J., Franceschini, A., Hatziminaoglou, E.: Revisiting the infrared spectra of active galactic nuclei with a new torus emission model. *Mon. Not. R. Astron. Soc.* **366**, 767 (2006)
96. Fuhrmann, L., Cucchiara, A., Marchili, N., Tosti, G., Nucciarelli, G., Ciprini, S., Molinari, E., Chincarini, G., Zerbi, F.M., Covino, S., et al.: A rapid and dramatic outburst in blazar 3C 454.3 during May 2005. Optical and infrared observations with REM and AIT. *Astron. Astrophys.* **445**, L1 (2006)
97. Gallagher, S.C., Hines, D.C., Blaylock, Myra, Priddey, R.S., Brandt, W.N., Egami, E.E.: Radio through X-ray spectral energy distributions of 38 broad absorption line quasars. *Astrophys. J.* **665**, 157–173 (2007)
98. Gallo, E., Fender, R.P., Pooley, G.G.: A universal radio-X-ray correlation in low/hard state black hole binaries. *Mon. Not. R. Astron. Soc.* **344**, 60–72 (2003)
99. Gaskell, C.M.: The ultra-violet continuum and presence of dust in quasars. *Bull. Am. Astron. Soc.* **11**, 622 (1979)
100. Gaskell, C.M., Goosmann, R.W., Antonucci, R.R.J., Whysong, D.H.: The nuclear reddening curve for active galactic nuclei and the shape of the infrared to X-ray spectral energy distribution. *Astrophys. J.* **616**, 147 (2004)
101. Gebhardt, K., Bender, R., Bower, G., Dressler, A., Faber, S.M., Filippenko, A.V., Green, R., Grillmair, C., Ho, L.C., et al.: A relationship between nuclear black hole mass and galaxy velocity dispersion. *Astrophys. J.* **539**, L13 (2000)
102. Genzel, R., Lutz, D., Sturm, E., Egami, E., Kunze, D., Moorwood, A.F.M., Rigopoulou, D., Spoon, H. W.W., Sternberg, A., Tacconi-Garman, L.E., et al.: What powers ultraluminous IRAS galaxies? *Astrophys. J.* **498**, 579 (1998)
103. Gezari, S., Halpern, J.P., Eracleous, M.: Long-term profile variability of double-peaked emission lines in active galactic nuclei. *Ap. J. Suppl.* **169**, 167–212 (2007)
104. Giacconi, R., Gursky, H., Paolini, F.R., Rossi, B.B.: Evidence for X rays from sources outside the solar system. *Phys. Rev. Lett.* **9**, 439 (1962)
105. Gibson, R.R., Jiang, L., Brandt, W.N., Hall, P.B., Shen, Y., Wu, J., Anderson, S.F., Schneider, D.P., et al.: A catalog of broad absorption line quasars in sloan digital sky survey data release 5. *Astrophys. J.* **692**, 758–777 (2009)
106. Giommi, P., Colafrancesco, S., Cavazzuti, E., Perri, M., Pittori, C.: Non-thermal cosmic backgrounds from blazars: The contribution to the CMB, X-ray and gamma-ray backgrounds. *Astron. Astrophys.* **445**, 843 (2006)
107. Giroletti, M., Panessa, F.: More discoveries of compact radio cores in seyfert galaxies with the EVN. In: *Proceedings of the 10th European VLBI Network Symposium and EVN Users Meeting: VLBI and the new generation of radio arrays*. [arXiv:1012.2665] POS 125, 81 (2010)
108. Glenn, J., Schmidt, G.D., Foltz, C.B.: The polarization and nuclear structure of the broad absorption line QSO CSO 755. *Astrophys. J.* **434**, L47–L50 (1994)

109. Gliozzi, M., Sambruna, R.M., Foschini, L.: A chandra view of naked active galactic nuclei. *Astrophys. J.* **662**, 878 (2007)
110. González-Martín, O., Masegosa, J., Marquez, I., Guerrero, M.A., Dultzin-Hacyan, D.: X-ray nature of the LINER nuclear sources. *Astron. Astrophys.* **460**, 45 (2006)
111. González-Delgado, R.M., Pérez, E., Cid Fernandes, R., Schmitt, H.: HST/WFPC2 imaging of the circumnuclear structure of low-luminosity active galactic nuclei. I. Data and nuclear morphology. *Astron. J.* **135**, 747 (2008)
112. González-Martín, O., Masegosa, J., Márquez, I., Guainazzi, M.: Fitting liner nuclei within the active galactic nucleus family: a matter of obscuration? *Astrophys. J.* **704**, 1570 (2009)
113. González-Martín, O., Masegosa, J., Márquez, I., Guainazzi, M., Jiménez-Bailón, E.: An X-ray view of 82 LINERs with chandra and XMM-newton data. *Astron. Astrophys.* **506**, 1107 (2009)
114. González-Martín, O., Papadakis, I., Braitto, V., Masegosa, J., Marquez, I., Mateos, S., Acosta-Pulido, J.A., Martínez, M.A., Ebrero, J., Esquej, P., et al.: Suzaku observation of the LINER NGC 4102. *Astron. Astrophys.* **527**, 142 (2011)
115. Goodrich, R.W., Miller, J.S.: Polarization clues to the structure of broad absorption line quasi-stellar objects. *Astrophys. J.* **448**, L73 (1995)
116. Goodrich, R.W., Veilleux, S., Hill, G.J.: Infrared spectroscopy of Seyfert-2 galaxies: A look through the obscuring Torus? *Astrophys. J.* **422**, 521 (1994)
117. Green, A.R., McHardy, I.M., Lehto, H.J.: On the nature of rapid X-ray variability in active galactic nuclei. *Mon. Not. R. Astron. Soc.* **265**, 664 (1993)
118. Grupe, D.: PhD Thesis, University of Göttingen (1996)
119. Grupe, D.: A complete sample of soft X-ray-selected AGNs. II. statistical analysis. *Astron. J.* **127**, 1799 (2004)
120. Grupe, D., Beuermann, K., Mannheim, K., Thomas, H.-C.: New bright soft X-ray selected ROSAT AGN. II. Optical emission line properties. *Astron. Astrophys.* **350**, 805 (1999)
121. Grupe, D., Beuerman, K., Mannheim, K., Thomas, H.-C., Fink, H.H., de Martino, D.: Discovery of an ultrasoft transient ROSAT AGN: WPVS 007. *Astron. Astrophys.* **300**, L21 (1995)
122. Grupe, D., Beuermann, K., Thomas, H.-C., Mannheim, K., Fink, H.H.: New bright soft X-ray selected ROSAT AGN. I. Infrared-to-X-ray spectral energy distributions. *Astron. Astrophys.* **330**, 25 (1998)
123. Grupe, D., Komossa, S., Leighly, K.M., Page, K.L.: The simultaneous optical-to-X-ray spectral energy distribution of soft X-ray selected active galactic nuclei observed by swift. *Astrophys. J. Suppl. Ser.* **187**, 64 (2010)
124. Grupe, D., Leighly, K.M., Komossa, S.: First detection of hard X-ray photons in the soft X-ray transient narrow-line seyfert-I galaxy WPVS 007: The X-ray photon distribution observed by swift. *Astron. J.* **136**, 2343 (2008)
125. Grupe, D., Mathur, S.: $M_{\text{BH}} - \sigma$ relation for a complete sample of soft X-ray-selected active galactic nuclei. *Astrophys. J. Lett.* **606**, L41 (2004)
126. Grupe, D., Wills, B.J., Leighly, K.M., Meusinger, H.: A complete sample of soft X-ray-selected AGNs. I. The data. *Astron. J.* **127**, 156–179 (2004)
127. Hall, P.B., Anderson, S.F., Strauss, M.A., York, D.G., Richards, G.T., Fan, X., Knapp, G.R., Schneider, D.P., Vanden Berk, D.E., Geballe, T.R., Bauer, A.E., Becker, R.H., et al.: Unusual broad absorption line quasars from the sloan digital sky survey. *Astrophys. J. Suppl. Ser.* **141**, 267 (2002)
128. Halpern, J.P., Steiner, J.E.: Low-ionization active galactic nuclei – X-ray or shock heated? *Astrophys. J.* **269**, L37 (1983)
129. Hamann, F.: Quasistellar objects: Intrinsic AGN absorption lines. *Encyclopedia Astron. Astrophys.* Available online at <http://eaa.crcpress.com> (2000)
130. Hamann, F., Korista, K.T., Morris, S.L.: On the geometry, covering factor, and scattering-emission properties of QSO broad absorption-line regions. *Astrophys. J.* **415**, 541 (1993)
131. Hao, L., Trauss, M.A., Fan, X., Tremonti, C.A., Schlegel, D.J., Heckman, T.M., Kauffmann, G., Blanton, M.R., Gunn, J.E., Hall, P.B., et al.: Active galactic nuclei in the sloan digital sky survey. II. Emission-line luminosity function. *Astron. J.* **129**, 1795 (2005)

132. Hartman, R.C., Bertsch, D.L., Bloom, S.D., Chen, A.W., Deines-Jones, P., Esposito, J.A., Fichtel, C.E., Friedlander, D.P., Hunter, S.D., McDonald, L.M., et al.: The third EGRET catalog of high-energy gamma-ray sources. *Astrophys. J. Suppl. Ser.* **123**, 79 (1999)
133. Hasinger, G., Miyaji, T., Schmidt, M.: Luminosity-dependent evolution of soft X-ray selected AGN. New chandra and XMM-newton surveys. *Astron. Astrophys.* **441**, 417 (2005)
134. Hawkins, M.R.S.: Naked active galactic nuclei. *Astron. Astrophys.* **424**, 519 (2004)
135. Heckman, T.M.: An optical and radio survey of the nuclei of bright galaxies – stellar populations and normal H II regions. *Astron. Astrophys.* **87**, 142 (1980)
136. Heinz, S., Sunyaev, R.A.: The non-linear dependence of flux on black hole mass and accretion rate in core-dominated jets. *Mon. Not. R. Astron. Soc.* **343**, L59–L64 (2003)
137. Ho, L.C.: Nonstandard central engines in nearby galaxies. *ASP Conf. Ser.* **258**, 165 (2002)
138. Ho, L.C.: Nuclear activity in nearby galaxies. *Ann. Rev. Astron. Astrophys.* **46**, 475 (2008)
139. Ho, L.C.: Radiatively inefficient accretion in nearby galaxies. *Astrophys. J.* **699**, 626 (2009)
140. Ho, L.C., Feigelson, E.D., Townsley, L.K., Sambruna, R.M., Garmire, G.P., Brandt, W.N., et al.: Detection of nuclear X-ray sources in nearby galaxies with chandra. *Astrophys. J.* **549**, L51 (2001)
141. Ho, L.C., Filippenko, A.V., Sargent, W.L.W.: A search for “Dwarf” seyfert nuclei. V. Demographics of nuclear activity in nearby galaxies. *Astrophys. J.* **487**, 568 (1997)
142. Ho, L.C., Rudnick, G., Rix, H.-W., Shields, J.C., McIntosh, D.H., Filippenko, A.V., Sargent, W.L.W., Eracleous, M.: Double-peaked broad emission lines in NGC 4450 and other LINERS. *Astrophys. J.* **541**, 120 (2000)
143. Ho, L.C., Wang, J.-M.: The central engine of active galactic nuclei. *ASP Conf. Ser.* **373** (2007)
144. Hunt, L., Malkan, M.A.: Morphology of the 12 micron seyfert galaxies. I. Hubble types, axial ratios, bars, and rings. *Astrophys. J.* **516**, 660 (1999)
145. Inoue, S., Aharonian, F., Sugiyama, N.: Hard X-ray and gamma-ray emission induced by ultra-high-energy protons in cluster accretion shocks. *Astrophys. J. Lett.* **628**, L9 (2005)
146. Jackson, N., Penston, M.V., Pérez, E.: Quasar H-beta profiles and discs. *Mon. Not. R. Astron. Soc.* **249**, 577 (1991)
147. Keel, W.C.: Inclination effects on the recognition of seyfert galaxies. *Astron. J.* **85**, 198 (1980)
148. Kellermann, K.I., Sramek, R., Schmidt, M., Shaffer, D.B., Green, R.: VLA observations of objects in the palomar bright quasar survey. *Astron. J.* **98**, 1195 (1989)
149. Kewley, L.J., Dopita, M.A., Sutherland, R.S., Heisler, C.A., Trevena, J.: Theoretical modeling of starburst galaxies. *Astrophys. J.* **556**, 121 (2001)
150. Kewley, L.J., Groves, B., Kauffmann, G., Heckman, T.: The host galaxies and classification of active galactic nuclei. *Mon. Not. R. Astron. Soc.* **372**, 961 (2006)
151. Kewley, L.J., Heisler, C.A., Dopita, M.A., Lumsden, S.: Optical classification of southern warm infrared galaxies. *Astrophys. J. Suppl. Ser.* **132**, 37 (2001)
152. Körding, E., Falcke, H., Corbel, S.: Refining the fundamental plane of accreting black holes. *Astron. Astrophys.* **456**, 439–450 (2006)
153. Körding, E., Fender, R.P., Migliari, S.: Jet-dominated advective systems: radio and X-ray luminosity dependence on the accretion rate. *Mon. Not. R. Astron. Soc.* **369**, 1451–1458 (2006)
154. Körding, E., Migliari, S., Fender, R., Belloni, T., Knigge, C., McHardy, I.: The variability plane of accreting compact objects. *Mon. Not. R. Astron. Soc.* **380**, 301–310 (2007)
155. Komossa, S.: Narrow-line seyfert-1 galaxies. *Rev. Mex. Astron. Astrophys.* **32**, 86 (2008)
156. Komossa, S., Voges, W., Xu, D., Mathur, S., Adorf, H.-M., Lemson, G., Duschl, W.J., Grupe, D.: Radio-loud narrow-line type-1 quasars. *Astron. J.* **132**, 531 (2006)
157. Korista, K.T., Voit, G.M., Morris, S.L., Weymann, R.J.: Double troughs in broad absorption line quasars and Ly α -NV line-locking. *Astrophys. J. Suppl. Ser.* **88**, 357–381 (1993)
158. Koski, A.: Spectrophotometry of seyfert-2 galaxies and narrow-line radio galaxies. *Astrophys. J.* **223**, 56 (1978)
159. Krongold, Y., Dultzin-Hacyan, D., Marziani, P.: The close environment of AGN. *Rev. Mex. Astron. Astrophys.* **17**, 105 (2003)

160. La Franca, F., Gruppioni, C., Matute, I., Pozzi, F., Lari, C., Mignoli, M., Zamorani, G., et al.: The nature of the mid-infrared population from optical identifications of the ELAIS-S1 sample. *Astron. J.* **127**, 3075 (2004)
161. Lamy, H., Hutsemekérs, D.: Polarization properties of broad absorption line QSOs: new statistical clues. *Astron. Astrophys.* **427**, 107–123 (2004)
162. Laor, A.: On the nature of low-luminosity narrow-line active galactic nuclei. *Astrophys. J.* **590**, 86 (2003)
163. Lawrence, A., Elvis, M., Wilkes, B.J., McHardy, I., Brandt, N.: X-ray and optical continua of active galactic nuclei with extreme Fe II emission. *Mon. Not. R. Astron. Soc.* **285**, 879 (1997)
164. Lawrence, A., Ward, M., Elvis, M., Fabbiano, G., Willner, S.P., Carleton, N.P., Longmore, A.: Observations from 1 to 20 microns of low-luminosity active galaxies. *Astrophys. J.* **291**, 117 (1985)
165. Lee, J.H., Lee, M.G., Park, C., Choi, Y.-Y.: The nature of the sloan digital sky survey galaxies in various classes based on morphology, colour and spectral features – III. Environments. *Mon. Not. R. Astron. Soc.* **403**, 1930 (2010)
166. Lee, L.W., Turnshek, D.A.: on correlations between the broad absorption lines and adjacent broad emission lines in QSO spectra. *Astrophys. J.* **453**, L61 (1995)
167. Leighly, K.M.: A comprehensive spectral and variability study of narrow-line seyfert-1 galaxies observed by ASCA. II. Spectral analysis and correlations. *Astrophys. J. Suppl. Ser.* **125**, 317 (1999)
168. Leighly, K.M., Hamann, F., Casebeer, D.A., Grupe, D.: Emergence of a broad absorption line outflow in the narrow-line seyfert-1 galaxy WPVS 007. *Astrophys. J.* **701**, 176 (2009)
169. Leighly, K.M., Mushotzky, R.F., Nandra, K., Forster, K.: Evidence for relativistic outflows in narrow-line seyfert-1 galaxies. *Astrophys. J.* **489**, L25 (1997)
170. Levinson, A., Laor, A., Vermeulen, R.C.: Constraints on the Parsec-Scale Environment in NGC 1275. *Astrophys. J.* **448**, 589 (1995)
171. Lípári, S.L.: Galaxies with extreme infrared and Fe II emission. 2: IRAS 07598+6508: A starburst/young broad absorption line QSO. *Astrophys. J.* **436**, 102 (1994)
172. Lípári, S.L., Bergmann, M., Sanchez, S.F., Garcia-Lorenzo, B., Terlevich, R., Mediavilla, E., Taniguchi, Y., Zheng, W., Punsly, B., Ahumada, A., Merlo, D.: GEMINI 3D spectroscopy of BAL + IR + FeII QSOs – II. IRAS 04505–2958, an explosive QSO with hypershells and a new scenario for galaxy formation and galaxy end phase. *Mon. Not. R. Astron. Soc.* **398**, 658 (2009)
173. Lípári, S.L., Bergmann, M., Sanchez, S.F., Terlevich, R., Mediavilla, E., Punsly, B., Garcia-Lorenzo, B., Zheng, W., Sistero, R.: The role of exploding QSOs in explosive models of evolution, formation and end of galaxies. *Bol. Asoc. Argentina Astron. Workshop of Theoretical Astronomy in Argentina*, p. 55 (arXiv: 0707.1493) (2007)
174. Lípári, S.L., Bergmann, M., Sanchez, S., Terlevich, R., Taniguchi, Y., Mediavilla, E., Punsly, B., Garcia, B., Zheng, W., Merlo, D.: Gemini GMOS IFU spectroscopy of IRAS 04505–2958: A new exploding BAL + IR + Fe II QSO. *Bol. Asoc. Argentina Astron. Meeting* **50**, 259 (2007). (arXiv: 0712.0288)
175. Lípári, S.L., Bergmann, M., Taniguchi, Y., Terlevich, R., Mediavilla, E., García-Lorenzo, B., Zheng, W., Sanchez, S.F., Punsly, B., Merlo, D.C.: Gemini 3D-spectroscopy of IRAS 17002+5153 and IRAS 07598+6508: evidence of two new exploding BAL + IR + Fe II QSOs. *Bol. Asoc. Argentina Astron.* **51**, 271 (2008)
176. Lípári, S.L., Mediavilla, E., Díaz, R.J., García-Lorenzo, B., Acosta-Pulido, J., Agüero, M.P., Terlevich, R.: Infrared mergers and infrared quasi-stellar objects with galactic winds – I. NGC 2623: nuclear outflow in a proto-elliptical candidate. *Mon. Not. R. Astron. Soc.* **348**, 369 (2004)
177. Lípári, S.L., Mediavilla, E., Garcia-Lorenzo, B., Díaz, R.J., Acosta-Pulido, J., Agüero, M.P., Taniguchi, Y., Dottori, H., Terlevich, R.: Infrared mergers and infrared quasi-stellar objects with galactic winds – II. NGC5514: two extranuclear starbursts with LINER properties and a supergiant bubble in the rupture phase. *Mon. Not. R. Astron. Soc.* **355**, 641 (2004)

178. Lípári, S.L., Sanchez, S.F., Bergmann, M., Terlevich, R., Garcia-Lorenzo, B., Punsly, B., Mediavilla, E., Taniguchi, Y., et al.: GEMINI 3D spectroscopy of BAL + IR + FeII QSOs – I. Decoupling the BAL, QSO, starburst, NLR, supergiant bubbles and galactic wind in Mrk 231. *Mon. Not. R. Astron. Soc.* **392**, 1295–1338 (2009)
179. Lípári, S.L., Sanchez, S.F., Bergmann, M., Terlevich, R., Punsly, B., Mediavilla, E., Dottori, H., Taniguchi, Y., et al.: Gemini GMOS IFU study of BAL QSOs: decoupling the BAL QSO, starburst, NLR and supergiant bubbles. *Bol. Asoc. Argentina Astron. Meeting* **49**, 267 (2006)
180. Lípári, S.L., Taniguchi, Y., Mediavilla, E., Dottori, H., Terlevich, R., Ajiki, M., et al.: Extreme galactic wind and star formation at low and high redshift. In: Storchi Bergmann, T., Ho, L., Schmitt, H. (eds.) *The Interplay among Black Hole Stars and IGM in Galactic Nuclei*, IAU Symp. No. 222, 529 (2004)
181. Lípári, S.L., Terlevich, R.: Evolutionary unification in composite active galactic nuclei. *Mon. Not. R. Astron. Soc.* **368**, 1001 (2006)
182. Lípári, S.L., Terlevich, R., Díaz, R.J., Taniguchi, Y., Zheng, W., Tsvetanov, Z., Carranza, G., Dottori, H.: Extreme galactic wind and wolf-rayet features in infrared mergers and infrared quasi-stellar objects. *Mon. Not. R. Astron. Soc.* **340**, 289 (2003)
183. Lípári, S.L., Terlevich, R., Macchetto, F.: Extreme optical Fe II emission in luminous IRAS active galactic nuclei. *Astrophys. J.* **406**, 451 (1993)
184. Lípári, S.L., Terlevich, R., Zheng, W., Garcia-Lorenzo, B., Sanchez, S.F., Bergmann, M.: Infrared mergers and infrared quasi-stellar objects with galactic winds – III. Mrk 231: an exploding young quasi-stellar object with composite outflow/broad absorption lines (and multiple expanding superbubbles). *Mon. Not. R. Astron. Soc.* **360**, 416 (2005)
185. Lonsdale, C.J., Diamond, P.J., Thrall, H., Smith, H.E., Lonsdale, C.J.: VLBI images of 49 radio supernovae in Arp 220. *Astrophys. J.* **647**, 185 (2006)
186. Madau, P., Ghisellini, G., Fabian, A.C.: The unified seyfert scheme and the origin of the cosmic X-ray background. *Mon. Not. R. Astron. Soc.* **270**, 17 (1994)
187. Magorrian, J., Tremaine, S., Richstone, D., Bender, R., Bower, G., Dressler, A., Faber, S.M., Gebhardt, K., Green, R., Grillmair, C., Kormendy, J., Lauer, T.: The demography of massive dark objects in galaxy centers. *Astron. J.* **115**, 2285 (1998)
188. Maiolino, R., Rieke, G.H.: Low-luminosity and obscured seyfert nuclei in nearby galaxies. *Astrophys. J.* **454**, 95 (1995)
189. Malkan, M.A., Gorjian, V., Tam, R.: A hubble space telescope imaging survey of nearby active galactic nuclei. *Astrophys. J. Suppl. Ser.* **117**, 25 (1998)
190. Maoz, D.: Low-luminosity active galactic nuclei: Are they UV faint and radio loud? *Mon. Not. R. Astron. Soc.* **377**, 1696 (2007)
191. Maoz, D., Nagar, N.M., Falcke, H., Wilson, A.S.: The murmur of the sleeping black hole: detection of nuclear ultraviolet variability in LINER galaxies. *Astrophys. J.* **625**, 699 (2005)
192. Markoff, S., Falcke, H., Fender, R.: A jet model for the broadband spectrum of XTE J1118+480. Synchrotron emission from radio to X-rays in the Low/Hard spectral state. *Astron. Astrophys.* **372**, L25–L28 (2001)
193. Markoff, S., Nowak, M., Corbel, S., Fender, R., Falcke, H.: Exploring the role of jets in the radio/X-ray correlations of GX 339-4. *Astron. Astrophys.* **397**, 645–658 (2003)
194. Markoff, S., Nowak, M.A., Wilms, J.: Going with the flow: can the base of jets subsume the role of compact accretion disk coronae? *Astrophys. J.* **635**, 1203–1216 (2005)
195. Márquez, I., Masegosa, J.: Feedback between host galaxy and nuclear activity. In: *The Nuclear Region, Host Galaxy and Environment of Active Galaxies* (Eds. Benítez E., Cruz-González I., & Krongold Y.) *Rev. Mex. Astron. Astrof. Conf. Ser.* **32**, 150–154 (2008)
196. Márquez, I., Masegosa, J.: Galaxies hosting AGN activity and their environments. *Astrophys. Space Sci. Proc.* **3**, 119 (2010)
197. Márquez, I., Varela, J., Masegosa, J., del Olmo, A.: AGN in isolated and interacting galaxies in the palomar spectroscopic survey. *ASP Conf. Ser.* **421**, 266 (2010)
198. Martínez, M.A., Del Olmo, A., Coziol, R., Perea, J.: AGN population in compact groups galaxies. *Rev. Mex. Astron. Astrophys.* **32**, 164 (2008)

199. Marziani, P., Keel, W.C., Dultzin-Hacyan, D., Sulentic, J.W.: Multiple high-velocity emission-line systems in the E + S pair CPG 29. *Astrophys. J.* **435**, 668 (1994)
200. Masegosa, J., Márquez, I., Ramirez, A., González-Martín, O.: The nature of nuclear H α emission in LINERs. *Astron. Astrophys.* **527**, 23 (2011)
201. Masters, K.L., Mosleh, M., Romer, A.K., Nichol, R.C., Bamford, S.P., Schawinski, K., Lintott, C.J., Andreescu, D., Campbell, H.C., Crowcroft, B., et al.: Galaxy zoo: passive red spirals. *Mon. Not. R. Astron. Soc.* **405**, 783 (2010)
202. Mathur, S.: Narrow-line seyfert-1 galaxies and the evolution of galaxies and active galaxies. *Mon. Not. R. Astron. Soc.* **314**, L17 (2000)
203. Mathur, S., Grupe, D.: Black hole growth by accretion. *Astron. Astrophys.* **432**, 463 (2005)
204. McHardy, I.: EXOSAT observations of variability in active galactic nuclei. *Mem. Soc. Astron. It.* **59**, 239–259 (1988)
205. McHardy, I.M., Koarding, E., Knigge, C., Uttley, P., Fender, R.P.: Active galactic nuclei as scaled-up Galactic black holes. *Nature* **444**, 730–732 (2006)
206. McKee, C.F., Petrosian, V.: Are quasars dusty? *Astrophys. J.* **189**, 17 (1974)
207. McKernan, B., Ford, K.E.S., Reynolds, C.S.: Black hole mass, host galaxy classification and AGN activity. *Mon. Not. R. Astron. Soc.* **407**, 2399 (2010)
208. Melia, F., Falcke, H.: The supermassive black hole at the galactic center. *Ann. Rev. Astron. Astrophys.* **39**, 309–352 (2001)
209. Merloni, A., Heinz, S., Di Matteo, T.: A fundamental plane of black hole activity. *Mon. Not. R. Astron. Soc.* **345**, 1057–1076 (2003)
210. Merloni, A., Körding, E., Heinz, S., Markoff, S., Di Matteo, T., Falcke, H.: Why the fundamental plane of black hole activity is not simply a distance driven artifact. *New Astron.* **11**, 567–576 (2006)
211. Merrifield, M.R.: Macrolensing, microlensing, and BL Lac objects. *Astron. J.* **104**, 1306 (1992)
212. Meszaros, P., Rezaque, S.: Theoretical Aspects of High Energy Neutrinos and GRB. In: *Energy Budget in the High Energy Universe*. Sato, K., Hisano, J. (Eds.), Singapore, World Scientific, p. 84–93 (2007)
213. Migliari, S., Fender, R.P., van der Klis, M.: Correlation between radio luminosity and X-ray timing frequencies in neutron star and black hole X-ray binaries. *Mon. Not. R. Astron. Soc.* **363**, 112 (2005)
214. Miller, J.S., Goodrich, R.W., Mathews, W.G.: Multidirectional views of the active nucleus of NGC1068. *Astrophys. J.* **378**, 47 (1991)
215. Montero-Dorta, A.D., Croton, D.J., Yan, R., Cooper, M.C., Newman, J.A., Georgakakis, A., Prada, F., Davis, M., Nandra, K., Coil, A.: The DEEP2 galaxy redshift survey: the red sequence AGN fraction and its environment and redshift dependence. *Mon. Not. R. Astron. Soc.* **392**, 125 (2009)
216. Moran, E.C., Barth, A.J., Eracleous, M., Kay, L.E.: Transient and highly polarized double-peaked H α emission in the seyfert-2 nucleus of NGC 2110. *Astrophys. J.* **688**, 31 (2007)
217. Mücke, A., Protheroe, R.J.: A proton synchrotron blazar model for flaring in markarian 501. *Astroparticle Phys.* **15**, 121 (2001)
218. Mücke, A., Protheroe, R.J., Engel, R., Rachen, J.P., Stanev, T.: BL Lac objects in the synchrotron proton blazar model. *Astroparticle Phys.* **18**, 593 (2003)
219. Murase, K., Inoue, S., Nagataki, S.: Cosmic rays above the second knee from clusters of galaxies and associated high-energy neutrino emission. *Astrophys. J.* **689**, L105 (2008)
220. Murray, N., Chiang, J.: Disk winds and disk emission lines. *Astrophys. J.* **474**, 91 (1997)
221. Murray, N., Chiang, J., Grossman, S.A., Voit, G.M.: Accretion disk winds from active galactic nuclei. *Astrophys. J.* **451**, 498 (1995)
222. Nagar, N.M., Falcke, H., Wilson, A.S.: Radio sources in low-luminosity active galactic nuclei. IV. Radio luminosity function, importance of jet power, and radio properties of the complete Palomar sample. *Astrophys. J.* **435**, 521 (2005)
223. Nagar, N.M., Falcke, H., Wilson, A.S., Ho, L.C.: Radio sources in low-luminosity active galactic nuclei. I. VLA detections of compact, flat-spectrum cores. *Astrophys. J.* **542**, 186 (2000)

224. Nagar, N.M., Falcke, H., Wilson, A.S., Ulvestad, J.S.: Radio sources in low-luminosity active galactic nuclei. III. "AGNs" in a distance-limited sample of LLAGNs. *Astron. Astrophys.* **392**, 53 (2002)
225. Nenkova, M., Sirocky, M.M., Ivezić, Ž., Elitzur, M.: AGN dusty tori. I. Handling of clumpy media. *Astrophys. J.* **685**, 147 (2008)
226. Netzer, H.: Accretion and star formation rates in low-redshift type II active galactic nuclei. *Mon. Not. R. Astron. Soc.* **399**, 1907 (2009)
227. Nicastro, F.: Broad emission line regions in active galactic nuclei: the link with the accretion power. *Astrophys. J. Lett.* **530**, L65 (2000)
228. Nicastro, F., Martocchia, A., Matt, G.: The lack of broad-line regions in low accretion rate active galactic nuclei as evidence of their origin in the accretion disk. *Astrophys. J. Lett.* **589**, L13 (2003)
229. Noble, J.C., Carini, M.T., Miller, H.R., Goodrich, B.: The time scales of the optical variability of blazars. IV. OI 090.4. *Astron. J.* **113**, 1995 (1997)
230. Norman, C., Ikeuchi, S.: The disk-halo interaction – superbubbles and the structure of the interstellar medium. *Astrophys. J.* **345**, 372 (1989)
231. Ogle, P.M.: Keck spectropolarimetry of BAL QSOs. Mass ejection from active galactic nuclei. *ASP Conf. Ser.* **128**, 78 (1997)
232. Ogle, P.M., Cohen, M.H., Miller, J.S., Tran, H.D., Goodrich, R.W., Martel, A.R.: Polarization of broad absorption line QSOS. I. A spectropolarimetric atlas. *Astrophys. J. Suppl. Ser.* **125**, 1–34 (1999)
233. Oke, J.B., Gunn, J.E.: The distance of BL lacertae. *Astrophys. J. Lett.* **189**, L5 (1974)
234. Osterbrock, D.E., Parker, R.A.R.: Physical conditions in the nucleus of the seyfert galaxy NGC1068. *Astrophys. J.* **141**, 892 (1965)
235. Osterbrock, D.E., Pogge, R.W.: The spectra of narrow-line seyfert-1 galaxies. *Astrophys. J.* **297**, 166 (1985)
236. Osterbrock, D.E., Ferland, G.J.: *Astrophysics of gaseous nebulae and active galactic nuclei*, 2nd edn. University Science Books, Sausalito, CA (2006)
237. Ostriker, J.P., Vietri, M.: Are some BL Lac objects artefacts of gravitational lensing? *Nature* **318**, 446 (1985)
238. Parra, R., Conway, J.E., Diamond, P.J., Thrall, H., Lonsdale, C.J., Lonsdale, C.J., Smith, H.E.: The radio spectra of the compact sources in arp 220: A mixed population of supernovae and supernova remnants. *Astrophys. J.* **659**, 314 (2007)
239. Penston, M.V., Penston, M.J., Selmes, R.A., Becklin, E.E., Neugebauer, G.: Broadband optical and infrared observations of Seyfert galaxies. *Mon. Not. R. Astron. Soc.* **169**, 357 (1974)
240. Peterson, B.M., Ferrarese, L., Gilbert, K.M., Kaspi, S., Malkan, M.A., Maoz, D., Merritt, D., Netzer, H., et al.: Central masses and broad-line region sizes of active galactic nuclei. II. A homogeneous analysis of a large reverberation-mapping database. *Astrophys. J.* **613**, 682 (2004)
241. Pian, E., Foschini, L., Beckmann, V., Soldi, S., Trler, M., Gehrels, N., Ghisellini, G., Giommi, P., Maraschi, L., Pursimo, T., et al.: INTEGRAL observations of the blazar 3C 454.3 in outburst. *Astron. Astrophys.* **449**, L21 (2006)
242. Pian, E., Romano, P., Maoz, D., Cucchiara, A., Pagani, C., La Parola, V.: Variability and spectral energy distributions of low-luminosity active galactic nuclei: A simultaneous X-ray/UV look with swift. *Mon. Not. R. Astron. Soc.* **401**, 677 (2010)
243. Pogge, R.W., Maoz, D., Ho, L.C., Eracleous, M.: The narrow-line regions of liners as resolved with the hubble space telescope. *Astrophys. J.* **532**, 323 (2000)
244. Prieto, M.A., Reunanen, J., Tristram, K.R.W., Neumayer, N., Fernandez-Ontiveros, J.A., Orienti, M., Meisenheimer, K.: The spectral energy distribution of the central parsecs of the nearest AGN. *Mon. Not. R. Astron. Soc.* **402**, 724 (2010)
245. Proga, D., Stone, J.M., Kallman, T.R.: Dynamics of Line-driven disk winds in active galactic nuclei. *Astrophys. J.* **543**, 686–696 (2000)
246. Puchnarewicz, E.M., Mason, K.O., Cordova, F.A., Kartje, J., et al.: Optical properties of active galaxies with ultra-soft X-ray spectra. *Mon. Not. R. Astron. Soc.* **256**, 589 (1992)

247. Punsly, B., Lipari, S.: Diagnostics of quasar broad absorption line geometry: X-ray observations and two-dimensional optical spectroscopy. *Astrophys. J.* **623**, 101 (2005)
248. Raiteri, C.M., Villata, M., Chen, W.P., Hsiao, W.-S., Kurtanidze, O.M., Nilsson, K., Larionov, V.M., Gurwell, M.A., Agudo, I., Aller, H.D., et al.: The high activity of 3C 454.3 in autumn 2007. Monitoring by the WEBT during the AGILE detection. *Astron. Astrophys.* **485**, L17 (2008)
249. Raiteri, C.M., Villata, M., Larionov, V.M., Pursimo, T., Ibrahimov, M.A., Nilsson, K., Aller, M.F., Kurtanidze, O.M., et al.: WEBT and XMM-newton observations of 3C 454.3 during the post-outburst phase. Detection of the little and big blue bumps. *Astron. Astrophys.* **473**, 819 (2007)
250. Remillard, R.A., McClintock, J.E.: X-ray properties of black-hole binaries. *Ann. Rev. Astron. Astrophys.* **44**, 49–92 (2006)
251. Rich, J.A., Dopita, M.A., Kewley, L.J., Rupke, D.S.N.: NGC 839: Shocks in an M82-like superwind. *Astrophys. J.* **721**, 505 (2010)
252. Richards, G.T., Vanden Berk, D.E., Reichard, T.A., Hall, P.B., Schneider, D.P., SubbaRao, M., Thakar, A.R., York, D.G.: Broad emission-line shifts in quasars: An orientation measure for radio-quiet quasars? *Astron. J.* **124**, 1–17 (2002)
253. Risaliti, G., Gilli, R., Maiolino, R., Salvati, M.: The hard X-ray emission of luminous infrared galaxies. *Astron. Astrophys.* **357**, 13 (2000)
254. Roberts, T.P., Warwick, R.S.: A ROSAT high resolution imager survey of bright nearby galaxies. *Mon. Not. R. Astron. Soc.* **315**, 98 (2000)
255. Rowan-Robinson, M.: On the unity of activity in galaxies. *Astrophys. J.* **213**, 635 (1977)
256. Rupke, D., Veilleux, S., Kim, D.-C., Sturm, E., Contursi, A., Lutz, D., Netzer, H., Sternberg, A., Maoz, D.: Uncovering the active galactic nuclei in low-ionization nuclear emission-line regions with spitzer. *ASP Conf. Ser.*, vol. 373, p. 525 (2007)
257. Rush, B., Malkan, M.A., Spinoglio, L.: The extended 12 micron galaxy sample. *Astrophys. J. Suppl. Ser.* **89**, 1 (1993)
258. Sagar, R., Stalin, C.S., Gopal-Krishna, Wiita, P.J.: Intranight optical variability of blazars. *Mon. Not. R. Astron. Soc.* **348**, 176 (2004)
259. Sanders, D.B., Mirabel, I.F.: Luminous infrared galaxies. *Ann. Rev. Astron. Astrophys.* **34**, 749 (1996)
260. Sanders, D.B., Soifer, B.T., Elias, J.H., Madore, B.F., Matthews, K., Neugebauer, G., Scoville, N.Z.: Ultraluminous infrared galaxies and the origin of quasars. *Astrophys. J.* **325**, 74 (1988)
261. Sarzi, M., Rix, H.-W., Shields, J.C., Ho, L.C., Barth, A.J., Rudnick, G., Filippenko, A.V., Sargent, W.L.W.: The stellar populations in the central parsecs of galactic bulges. *Astrophys. J.* **628**, 169 (2005)
262. Satyapal, S., Dudik, R.P., O'Halloran, B., Gliozzi, M.: The link between star formation and accretion in LINERS: A comparison with other active galactic nucleus subclasses. *Astrophys. J.* **633**, 86 (2005)
263. Satyapal, S., Sambruna, R.M., Dudik, R.P.: A joint mid-infrared spectroscopic and X-ray imaging investigation of LINER galaxies. *Astron. Astrophys.* **414**, 825 (2004)
264. Scaringi, S., Cottis, C.E., Knigge, C., Goad, M.R.: Classifying broad absorption line quasars: metrics, issues and a new catalogue constructed from SDSS DR5. *Mon. Not. R. Astron. Soc.* **399**, 2231–2238 (2009)
265. Schmitt, H.R., Kinney, A.L.: A Comparison between the narrow-line regions of seyfert-1 and seyfert-2 galaxies. *Astrophys. J.* **463**, 498 (1996)
266. Schmitt, J.L.: BL lac identified as a radio source. *Nature* **218**, 663 (1968)
267. Shakhovskoy, N.M., Efimov, Y.S.: Study of the linear polarization of optical emission from BL lac objects. *Izv. Krym. Astrofiz. Obs.* **56**, 39 (1977)
268. Shakhovskoj, N.M., Efimov, Y.S.: In: Proc. All Russian Conference Astrophysics on the threshold of ages. Held at Pushchino Radioastron. Observ. on 17–22 May 2396 1999. Kardashov, N.S., et al. (eds.), pp. 435–442 (in russian) (2001)
269. Shemmer, O., Brandt, W.N., Netzer, H., Maiolino, R., Kaspi, S.: The hard X-ray spectral slope as an accretion rate indicator in radio-quiet active galactic nuclei. *Astrophys. J.* **646**, L29 (2006)

270. Shemmer, O., Brandt, W.N., Netzer, H., Maiolino, R., Kaspi, S.: The hard X-ray spectrum as a probe for black hole growth in radio-quiet active galactic nuclei. *Astrophys. J.* **682**, 81 (2008)
271. Shen, J., Vanden Berk, D.E., Schneider, D.P., Hall, P.B.: The black hole-bulge relationship in luminous broad-line active galactic nuclei and host galaxies. *Astron. J.* **135**, 928 (2008)
272. Shi, Y., Rieke, G.H., Smith, P., Rigby, J., Hines, D., Donley, J., Schmidt, G., Diamond-Stanic, A.M.: Unobscured type-2 active galactic nuclei. *Astrophys. J.* **714**, 115 (2010)
273. Shields, G.A.: The origin of the broad line emission from seyfert galaxies. *Astrophys. J. Lett.* **18**, 119 (1977)
274. Shields, J.C., Rix, H.-W., McIntosh, D.H., Ho, L.C., Rudnick, G., Filippenko, A.V., Sargent, W.L.W., Sarzi, M.: Evidence for a black hole and accretion disk in the LINER NGC 4203. *Astrophys. J.* **534**, L27 (2000)
275. Simões Lopes, R., Storchi-Bergmann, T., de Fátima Saraiva, M., Martini, P.: A strong correlation between circumnuclear dust and black hole accretion in early-type galaxies. *Astrophys. J.* **655**, 718 (2007)
276. Smith, H.A., Li, A., Li, M.P., Köhler, M., Ashby, M.L.N., Fazio, G.G., Huang, J.-S., Marengo, M., Wang, Z., Willner, S., Zezas, A., Spinoglio, L., Wu, Y.L.: Anomalous silicate dust emission in the type-1 liner nucleus of M81. *Astrophys. J.* **716**, 490 (2010)
277. Smith, H.E., Lonsdale, C.J., Lonsdale, C.J.: The starburst-AGN connection. II. The nature of luminous infrared galaxies as revealed by VLBI, VLA, infrared, and optical observations. *Astrophys. J.* **492**, 137 (1998)
278. Smith, J.D.T., Draine, B.T., Dale, D.A., Moustakas, J., Kennicutt, R.C., Jr., Helou, G., Armus, L., Roussel, H., Sheth, K., Bendo, G.J., et al.: The mid-infrared spectrum of star-forming galaxies: global properties of polycyclic aromatic hydrocarbon emission. *Astrophys. J.* **656**, 770 (2007)
279. Smith, N., McCray, R.: Shell-shocked diffusion model for the light curve of SN 2006gy. *Astrophys. J. Lett.* **671**, L17 (2007)
280. Soifer, B.T., Neugebauer, G., Matthews, K., Egami, E., Becklin, E.E., Weinberger, A.J., Ressler, M., Werner, M.W., et al.: High resolution mid-infrared imaging of ultraluminous infrared galaxies. *Astron. J.* **119**, 509 (2000)
281. Stalin, C.S., Gupta, A.C., Gopal-Krishna, Wiita, P.J., Sagar, R.: Intranight optical variability of BL lacs, radio-quiet quasars and radio-loud quasars. *Mon. Not. R. Astron. Soc.* **356**, 607 (2005)
282. Stasińska, G., Vale Asari, N., Cid Fernandes, R., Gomes, J.M., Schlickmann, M., Mateus, A., Schoenell, W., Sodré, L., Jr.: Can retired galaxies mimic active galaxies? Clues from the sloan digital sky survey. *Mon. Not. R. Astron. Soc.* **391**, L29 (2008)
283. Stephens, S.: Optical spectroscopy of X-ray-selected active galactic nuclei. *Astron. J.* **97**, 10 (1989)
284. Stirling, A.M., Spencer, R.E., de la Force, C.J., Garrett, M.A., Fender, R.P., Ogley, R.N.: A relativistic jet from cygnus X-1 in the low/hard X-ray state. *Mon. Not. R. Astron. Soc.* **327**, 1273–1278 (2001)
285. Stocke, J.T., Morris, S.L., Weymann, R.J., Foltz, C.B.: The radio properties of the broad-absorption-line QSOs. *Astrophys. J.* **396**, 487–503 (1992)
286. Storchi-Bergmann, T., Baldwin, J.A., Wilson, A.S.: Double-peaked broad line emission from the LINER nucleus of NGC 1097. *Astrophys. J. Lett.* **410**, L11 (1993)
287. Strateva, I.V., Strauss, M.A., Hao, L., Schlegel, D.J., Hall, P.B., Gunn, J.E., Li, L.-X., Ivezić, Ž., Richards, G.T., et al.: Double-peaked low-ionization emission lines in active galactic nuclei. *Astron. J.* **126** 1720–1749 (2003)
288. Sturm, E., Rupke, D., Contursi, A., Kim, D.-C., Lutz, D., Netzer, H., Veilleux, S., et al.: Mid-infrared diagnostics of LINERS. *Astrophys. J. Lett.* **653**, L13 (2006)
289. Sturm, E., Schweitzer, M., Lutz, D., Contursi, A., Genzel, R., Lehnert, M.D., Tacconi, L.J., Veilleux, S., et al.: Silicate emissions in active galaxies: From LINERs to QSOs. *Astrophys. J. Lett.* **629**, L21 (2005)

290. Suchkov, A., Balsara, D.S., Heckman, T.M., Leitherer, C.: Dynamics and X-ray emission of a galactic superwind interacting with disk and halo gas. *Astrophys. J.* **430**, 511 (1994)
291. Sulentic, J.W., Stirpe, G.M., Marziani, P., Zamanov, R., Calvani, M., Braitto, V.: VLT/ISAAC spectra of the H β region in intermediate redshift quasars. *Astron. Astrophys.* **432**, 121 (2004)
292. Sulentic, J.W., Zamfir, S., Marziani, P., Bachev, R., Calvani, M., Dultzin-Hacyan, D.: radio-loud active galactic nuclei in the context of the eigenvector 1 parameter space. *Astrophys. J.* **597**, L17 (2003)
293. Sulentic, J.W., Zwitter, T., Marziani, P., Dultzin-Hacyan, D.: Eigenvector 1: an optimal correlation space for active galactic nuclei. *Astrophys. J. Lett.* **536**, L5 (2000)
294. Swinbank, A.M., Smail, I., Bower, R.G., Borys, C., Chapman, S.C., Blain, A.W., Ivison, R.J., Howat, S.R., Keel, W.C., Bunker, A.J.: Optical and near-infrared integral field spectroscopy of the SCUBA galaxy N2 850.4. *Mon. Not. R. Astron. Soc.* **359**, 401–407 (2005)
295. Tang, S., Grindlay, J.: The quasar SDSS J153636.22+044127.0: A double-peaked emitter in a candidate binary black hole system. *Astrophys. J.* **704**, 1189–1194 (2009)
296. Tenorio-Tagle, G., Muñoz-Tuñón, C., Pérez, E., Maíz-Apellániz, J., Medina-Tanco, G.: On the ongoing multiple blowout in NGC 604. *Astrophys. J.* **541**, 720 (2000)
297. Terlevich, R., Tenorio-Tagle, G., Franco, J., Boyle, B., Rozyczka, M., Melnick, J.: The starburst model for AGN. In: Rocca-Volmerange, B., Dennefeld, M., Guiderdoni, B., Thanh Van, T. (eds.) *First Light in the Universe: Star or QSOs*, p. 261. Editions Frontieres, Gif-sur-Yvette (1993)
298. Terlevich, R., Tenorio-Tagle, G., Franco, J., Melnick, J.: The starburst model for active galactic nuclei – the broad-line region as supernova remnants evolving in a high-density medium. *Mon. Not. R. Astron. Soc.* **255**, 713 (1992)
299. Tomisaka, K., Ikeuchi, S.: Starburst nucleus – galactic-scale bipolar flow. *Astrophys. J.* **330**, 695 (1988)
300. Tran, H.D.: Hidden double-peaked emitters in seyfert-2 galaxies. *Astrophys. J.* **711**, 1174 (2010)
301. Tremaine, S., Gebhardt, K., Bender, R., Bower, G., Dressler, A., Faber, S.M., Filippenko, A.V., Green, R., Grillmair, C., Ho, L.C., Kormendy, J., Lauer, T.R., Magorrian, J., Pinkney, J., Richstone, D.: The slope of the black hole mass versus velocity dispersion correlation. *Astrophys. J.* **574**, 740 (2002)
302. Turnshek, D.A.: Properties of the broad absorption-line QSOs. *Astrophys. J.* **280**, 51–65 (1984)
303. Turnshek, D.A., Monier, E.M., Sirola, C.J., Espey, B.R.: A hubble space telescope faint object spectrograph survey for broad absorption lines in a sample of low-redshift weak [O iii] quasi-stellar objects. *Astrophys. J.* **476**, 40 (1997)
304. Urry, C.M., Treves, A., Maraschi, L., Marshall, H.L., Kii, T., Madejski, G., Penton, S., Pesce, J.E., Pian, E., Celotti, A., Fujimoto, R., Makino, F., Otani, C., Sambruna, et al.: Multiwavelength monitoring of the BL Lacertae object PKS 2155–304 in 1994 May. III. Probing the inner jet through multiwavelength correlations. *Astrophys. J.* **486**, 799 (1997)
305. Uttley, P., McHardy, I.M.: X-ray variability of NGC 3227 and 5506 and the nature of active galactic nucleus states. *Mon. Not. R. Astron. Soc.* **363**, 586 (2005)
306. van der Klis, M.: A possible explanation for the Parallel Tracks phenomenon in low-mass X-ray binaries. *Astrophys. J.* **561**, 943–949 (2001)
307. Varela, J., Moles, M., Márquez, I., Galletta, G., Masegosa, J., Bettoni, D.: Properties of isolated disk galaxies. *Astron. Astrophys.* **420**, 873 (2004)
308. Véron-Cetty, M.-P., Joly, M., Véron, P., Boroson, T., Lipari, S., Ogle, P.: The emission spectrum of the strong Fe II emitter BAL seyfert-1 galaxy IRAS 07598+6508. *Astron. Astrophys.* **451**, 851–858 (2006)
309. Veilleux, S., Osterbrock, D.E.: Spectral classification of emission-line galaxies. *Astrophys. J. Suppl. Ser.* **63**, 295 (1987)
310. Veilleux, S., Sanders, D.B., Kim, D.-C.: New results from a near-infrared search for hidden broad-line regions in ultraluminous infrared galaxies. *Astrophys. J.* **522**, 139 (1999)

311. Vestergaard, M., Peterson, B.M.: Determining central black hole masses in distant active galaxies and quasars. II. Improved optical and UV scaling relationships. *Astrophys. J.* **641**, 689 (2006)
312. Vietri, M.: Ultrahigh energy neutrinos from gamma ray bursts. *Phys. Rev. Lett.* **80**, 3690 (1998)
313. Vietri, M.: On Particle Acceleration around Shocks. I. *Astroph. J.* 591, 954–961 (2003)
314. Vietri, M., Stella, L.: A new instability of accretion disks around magnetic compact stars. *Astrophys. J.* **503**, 350 (1998)
315. Vietri, M., Stella, L.: A gamma-ray burst model with small baryon contamination. *Astrophys. J. Lett.* **507**, L45 (1998)
316. Vietri, M., Stella, L.: Supranova events from spun-up neutron stars: An explosion in search of an observation. *Astrophys. J. Lett.* **527**, L43 (1999)
317. Voit, G.M., Weymann, R.J., Korista, K.T.: Low-ionization broad absorption lines in quasars. *Astrophys. J.* **413**, 95–109 (1993)
318. Walsh, J.L., Barth, A.J., Ho, L.C., Filippenko, A.V., Rix, H.-W., Shields, J.C., Sarzi, M., Sargent, W.L.W.: Hubble space telescope spectroscopic observations of the narrow-line region in nearby low-luminosity active galactic nuclei. *Astron. J.* **136**, 1677 (2008)
319. Wampler, E.J.: Line intensities in quasi-stellar objects. I. PHL 938, 3c 249.1, and PKS 2251+11. *Astrophys. J.* **153**, 19 (1968)
320. Wampler, E.J.: Reddening in the nuclei of seyfert galaxies. *Astrophys. J. Lett.* **154**, L53 (1968)
321. Wang, H., Wang, T., Yuan, W., Wang, J., Dong, X., Zhou, H.: On the scattering enhancement of NV λ 1240 emission line of quasi-stellar objects. *Astrophys. J.* **710**, 78–90 (2010)
322. Wang, L., Kauffmann, G.: Why are AGN found in high-mass galaxies? *Mon. Not. R. Astron. Soc.* **391**, 785 (2008)
323. Wang, X.-Y., Razzaque, S., Meszaros, P.: On the origin and survival of ultra-high-energy cosmic-ray nuclei in gamma-ray bursts and hypernovae. *Astrophys. J.* **677**, 432 (2008)
324. Wang, X.-Y., Razzaque, S., Meszaros, P., Dai, Z.: High-energy cosmic rays and neutrinos from semirelativistic hypernovae. *Phys. Rev. D* **76**, 083009 (2007)
325. Weymann, R., Morris, S.L., Foltz, C.B., Hewett, P.C.: Comparisons of the emission-line and continuum properties of broad absorption line and normal quasi-stellar objects. *Astrophys. J.* **373**, 23 (1991)
326. Whalen, D.J., Laurent-Muehleisen, S.A., Moran, E.C., Becker, R.H.: Optical properties of radio-selected narrow-line seyfert-1 galaxies. *Astron. J.* **131**, 1948 (2006)
327. Whyson, D., Antonucci, R.: Thermal emission as a test for hidden nuclei in nearby radio galaxies. *Astrophys. J.* **602**, 116 (2004)
328. Xu, D., Komossa, S., Zhou, H., Wang, T., Wei, J.: The narrow-line region of narrow-line and broad-line type-1 active galactic nuclei. I. A zone of avoidance in density. *Astrophys. J.* **670**, 60 (2007)
329. Yan, R., Newman, J.A., Faber, S.M., Konidaris, N., Koo, D., Davis, M.: On the origin of [O II] emission in red-sequence and poststarburst galaxies. *Astrophys. J.* **648**, 281 (2006)
330. York, D.G., Adelman, J., Anderson, J.E., Jr., Anderson, S.F., Annis, J., Bahcall, N.A., Bakken, J.A., Barkhouser, R., Bastian, S., Berman, E., Boroski, W.N., et al.: The sloan digital sky survey: technical summary. *Astron. J.* **120**, 1579 (2000)
331. Young, S., Axon, D.J., Robinson, A., Hough, J.H., Smith, J.E.: The rotating wind of the quasar PG 1700+518. *Nature* **450**, 74–76 (2007)
332. Yuan, M.J., Wills, B.J.: Eddington accretion and QSO emission lines at $z \sim 2$. *Astrophys. J.* **593**, L11 (2003)
333. Zhou, H., Wang, T., Wang, H., Wang, J., Yuan, W., Lu, Y.: Polar outflows in six broad absorption line quasars. *Astrophys. J.* **639**, 716–723 (2006)

Chapter 5

From Observations to Physical Parameters

Contributions by Mauro D’Onofrio, Paola Marziani, Jack W. Sulentic, Greg Shields, Shai Kaspi, Paolo Padovani, Damien Hutsemékers, Ross McLure, Ari Laor, Marianne Vestergaard, Bozena Czerny, Krzysztof Hryniewicz, and Deborah Dultzin

M. D’Onofrio
Dipartimento di Astronomia, Università degli Studi di Padova, Vicolo Osservatorio 3, I35122
Padova, Italy
e-mail: mauro.donofrio@unipd.it

P. Marziani
INAF, Osservatorio Astronomico di Padova, Vicolo Osservatorio 5, IT35122 Padova, Italy
e-mail: paola.marziani@oapd.inaf.it

J.W. Sulentic (✉)
Instituto de Astrofísica de Andalucía (CSIC), Granada, Spain
e-mail: sulentic@iaa.es

G. Shields
Department of Astronomy, University of Texas, Austin, TX 78712-0259, USA
e-mail: shields@astro.as.utexas.edu

S. Kaspi
School of Physics and Astronomy and the Wise Observatory, The Raymond and Beverly Sackler
Faculty of Exact Science, Tel-Aviv University, Tel-Aviv 69978, Israel
e-mail: shai@wise.tau.ac.il

P. Padovani
European Southern Observatory, Karl-Schwarzschild-Str. 2, D-85748 Garching bei München,
Germany
e-mail: ppadovan@eso.org

D. Hutsemékers
F.R.S. - FNRS, Institute of Astrophysics and Geophysics, University of Liège, Allée du six août
17, B5c, B-4000, Liège, Belgium
e-mail: hutsemekers@astro.ulg.ac.be

R. McLure
Institute for Astronomy, Royal Observatory Edinburgh, Blackford Hill, Edinburgh EH9 3HJ, UK
e-mail: rjm@roe.ac.uk

A. Laor
Technion - Israel Institute of Technology Physics Department, Technion City, Haifa 32000, Israel
e-mail: laor@physics.technion.ac.il

Observational measures of AGNs allow us to directly infer some basic physical properties of quasars including (1) physical conditions and chemical abundances in the broad-line emitting gas as well as (2) radius of the line-emitting region,¹ (3) black hole mass, (4) and Eddington ratio. In this chapter, we seek information on how these quantities are measured. One of the surprises of recent times, that would have shocked the discoverers in the 1960s are the large BH masses and high chemical abundances inferred for even some of the highest redshift quasars known. These fundamental physical parameters are the ones that can be connected in a straightforward ways to quantities we measure in the spectra; they are not derived from sophisticated models, but this is not to say that there are no underlying assumptions. These assumptions, however, are rather elementary and probably the most robust ones that can be done, for instance, from nebular physical processes that are common to all photoionized gases. The parameters derived in these ways are more linked to the properties of the line-emitting gas than to the exact nature of the accretion processes around the massive compact object that powers the quasar. We also discuss effects that are likely to be important and that affect the accuracy of the estimated parameters. We start discussing the determination of metallicity. It is potentially a very important parameter that has been determined with high accuracy in other photoionized systems like HII regions and planetary nebulae.

5.1 Chemical Abundances

Dear Greg (*Shields*), what techniques are employed in order to estimate the metallicity in quasars? How do they differ relative to techniques employed for HII regions?

¹Note that in the following, the term “BLR size” will be often used in place of “BLR radius” to indicate the distance of the emitting region to the central continuum source.

M. Vestergaard

The Dark Cosmology Centre, The Niels Bohr Institute, University of Copenhagen, Juliane Maries Vej 30, 2100 Copenhagen 0, Denmark

Steward Observatory and Department of Astronomy, University of Arizona, 933 N. Cherry Avenue, Tucson 85721, Arizona, USA

e-mail: vester@dark-cosmology.dk

B. Czerny

Copernicus Astronomical Center, Bartycka 18, 00-716 Warsaw, Poland bcz@camk.edu.pl

K. Hryniewicz

Copernicus Astronomical Center, Bartycka 18, 00-716 Warsaw, Poland

e-mail: krhr@camk.edu.pl

D. Dultzin

Instituto de Astronomia, Universidad Nacional Autonoma de Mexico (UNAM), Apt.do postal 70-264, Mexico, D.F., Mexico

e-mail: deborah@astroscu.unam.mx

It is difficult to make accurate abundance determinations in AGNs. This is largely because of the high electron density. Even in the NLR, there appears to be a wide range of electron density, extending to more than 10^5 cm^{-3} . This affects the line ratios used to derive the electron temperature, which is needed to calculate the line emissivity used to derive ionic abundance ratios from line-intensity ratios. The most commonly used temperature indicator in nebulae is the [OIII] ratio $I(\lambda\lambda 5, 007, 4, 959)/I(\lambda 4, 363)$. This ratio is affected by density above about $10^{4.5} \text{ cm}^{-3}$, leading to the appearance of a high electron temperature if the density effect is ignored.² As a result, even in the NLR, abundance determinations are difficult.

In the BLR, the situation is even worse. Here, the forbidden lines are not observed at all. The permitted and intercombination lines arise from levels with large excitation potentials, so that the level populations are very sensitive to temperature. In addition, the large optical depths and partial thermalization of the resonance lines affects the emergent intensities. Finally, photoionization modeling has limited ability to constrain abundances because the well-measured ultraviolet lines ($L\alpha$, CIV, CIII], MgII) are also the main coolants for the gas. Their overall intensity is therefore governed by energy conservation in the photoionized gas, rather than abundances. Motivated by these concerns, I looked at deriving abundance ratios for certain chemical elements that have suitable emission lines [158]. The idea was to measure the N/C and N/O abundance ratios from line ratios such as NIV/OIII] and NIII]/CIII] that are only weakly sensitive to temperature. The nitrogen abundance is of interest because the N/O ratio increases with O/H as galactic chemical evolution proceeds. This occurs because nitrogen is largely a “secondary element,” whose production in evolving stars is proportional to the abundance of C and O in those stars. Studies of composition gradients across spiral galaxies indeed show such an increase in N/O with increasing O/H as one goes from the outer disk inward the center. In that early study, I found evidence for N/C ratios several times solar in some QSOs at large redshifts. This implied advanced chemical evolution in these galactic nuclei when the universe was a fraction of its present age. This general approach remains in use ([163], and references therein). Although sensitive to ionizing spectrum, the ratio NV/HeII has been found useful [64]. Various studies have shown that high abundances of nitrogen, and by implication high values of O/H, often occur in quasars out to quite high redshifts. Star formation in the host galaxies of quasars must have started at least 10^8 year before the observed QSO activity to give adequate buildup of the α -elements. Recent studies have looked at trends with luminosity of the quasar or host galaxy, black mass, or star-formation rate.

Another aspect involves the effect of grain formation on the gas-phase abundances and emission-line intensities. As noted above, Seyfert found [FeVII] to be stronger in NGC 1068 than in the planetary nebulae NGC 7027. I interpreted this as a depletion of the gas-phase iron abundance in NGC 7027 by grain formation [157]. It is now clear that refractory elements are often strongly depleted in planetary

²The apparent high temperatures led some early workers to propose that the NLR was largely ionized by shocks.

nebulae and HII regions and of course, also in the interstellar medium. Thus, Seyfert’s remark that [OII], [SII], [NII], and [FeVII] are stronger in NGC 1068 reflects the effects of differences in ionizing spectrum, nitrogen enrichment, and refractory element depletion. The subject of refractory element depletions in the NLR and BLR has been addressed in a number of studies. Gaskell et al. [48] argued against refractory element depletions as strong as occur in planetary nebulae, but recently, [161] proposed that the large range in Fe II strength in AGNs largely results from differing degrees of depletion of iron in the BLR.

Thank you, Greg. We now turn to a parameter that follows from a measurement of time delay and that is in principle independent from the nature of the system. What is needed is a variable, ionizing continuum source, and gas responding from a distant location (i.e., at a distance larger than the size of the continuum-emitting region).

5.2 Reverberation Mapping

Dear Shai (*Kaspi*), broad line region (BLR) radii derived from reverberation mapping can be regarded as “primary” measurements, and these exist for less than 50 largely low z sources. What do these measures tell us about the radius of the BLR in those quasars?

“Reverberation mapping” is a technique to measure the geometry and kinematics of the gas in the broad line region (BLR). These measurements then enable to deduce the mass of the central black hole (BH) in the center of active galactic nuclei (AGNs). The technique is based on the response of the ambient gas in the BLR to changes in the central continuum source. Such response was first used to account for the observations of the apparent expansion of Nova Persei in 1901 [30] and has been proposed to explain the light curves of type I supernovae [111]. The method was first suggested to be used in the analysis of Active Galactic Nuclei (AGNs) light curves by [6], who calculated the response of the line intensity in a spherical distribution of gas. Blandford and McKee [20] were the first to coin the term “reverberation mapping” and put it into mathematical formalism with the fundamental equation that relates the emission line and continuum light curves, $L(v, t)$ and $C(t)$:

$$L(v, t) = \int \Psi(v, \tau) C(t - \tau) d\tau, \quad (5.1)$$

where v is the velocity field of the BLR (which manifest itself in the emission-line profile), and $\Psi(v, \tau)$ is defined from this equation as the transfer function, which holds in it the information about the geometry and kinematics of the BLR. The latter was studied by several authors who showed how $\Psi(v, \tau)$ can be derived from the observed continuum and line light curves and how $\Psi(v, \tau)$ will change for different geometries and kinematics of the BLR (e.g., [72, 131, 189]).

In practice, in order to get the line and continuum light curves, the AGN needs to be monitored frequently over a period of time (from days to years, depending on

the AGN luminosity and variability characteristics). First attempts to carry out AGN reverberation mapping used poorly sampled light curves and low-resolution spectra (e.g., [132] and references therein), thus leading to a collapse of the two-dimensional transfer function, $\Psi(v, \tau)$, into one-dimensional transfer function $\Psi(\tau)$. In fact, this is further collapsed into only one parameter: the time lag between the line light curve and the continuum light curve. The time lag is defined as the centroid of the cross-correlation function between the continuum and line light curves. This centroid is considered as a measure for the size of the BLR, denoted as r_{BLR} .

Over the past quarter of a century, many monitoring campaigns were carried out and enabled the measurement of r_{BLR} in about four dozen AGNs. Some of the notable projects are (1) individual monitoring of Seyfert I galaxies (e.g., Mrk 279, NGC 5548, NGC 4151—[94]—and many more by the “AGN Watch”³ projects, [135]), (2) The Lovers of Active Galaxies (LAG) campaign (e.g., [149]), (3) The Ohio State University monitoring program [139], (4) The Wise Observatory and Steward Observatory 17 Palomar-Green (PG) quasars monitoring program by [77], (5) The Lick AGN Monitoring Project (LAMP; [15]), (6) Michigan-Dartmouth-MIT (MDM) monitoring campaign [36]. For reviews of the subtleties of the reverberation-mapping technique, see [118, 133, 142] and references therein.

5.2.1 Size–Luminosity Relation

Peterson et al. [141] compiled all available reverberation-mapping data, obtained up to then, and analyzed them in a uniform and self-consistent way to improve the determination of the time lags and their uncertainties and derived r_{BLR} for all objects with available data. Kaspi et al. [78] used these size measurements to study the relation between r_{BLR} and the Balmer emission lines, X-ray, UV, and optical continuum luminosities. This relation is a fundamental relation in AGNs studies since both quantities (r_{BLR} and L) are directly obtained from *measurements* with minimum assumptions and models.

Assuming a power-law relation $r_{\text{BLR}} \propto L^\alpha$, [78] find that the mean best-fitting α is about 0.67 ± 0.05 for the optical continuum and the broad H β luminosity, about 0.56 ± 0.05 for the UV continuum luminosity, and about 0.70 ± 0.14 for the X-ray luminosity. They also find an intrinsic scatter of $\sim 40\%$ in these relations.

Bentz et al. [13] used high-resolution images of the central region of 35 of the reverberation-mapped AGNs studied in [78] and accounted for the host-galaxy starlight contamination of the AGN luminosities. Removing the starlight contribution and excluding few points which do not have reliable H β BLR size measurement, they find the size–luminosity relation to be

$$\log(r_{\text{BLR}}) = -21.3_{-2.8}^{+2.9} + 0.519_{-0.066}^{+0.063} \log(\lambda L_\lambda(5100\text{\AA})), \quad (5.2)$$

³<http://www.astronomy.ohio-state.edu/~agnwatch/>

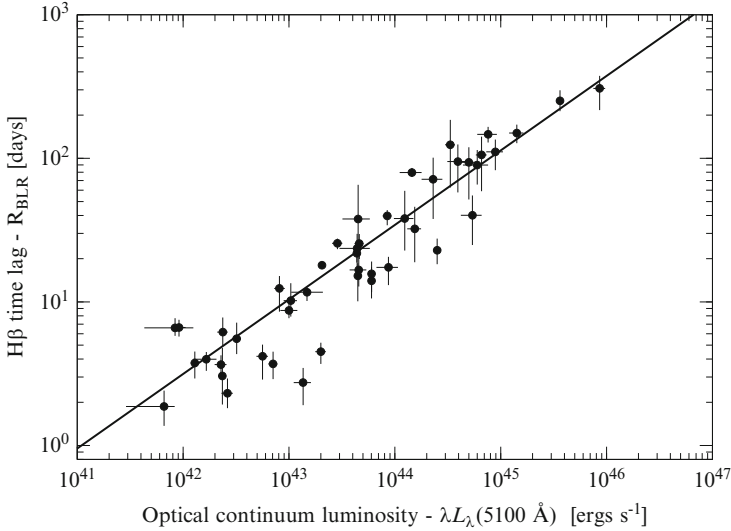


Fig. 5.1 $H\beta$ BLR size plotted vs. the $\lambda L_\lambda(5100 \text{ \AA})$ luminosity. Data points are from [13, 15, 36, 78]. *Solid line* is the current best published estimate for the size–luminosity relation by [13] (it is not a fit to all the shown data points—see [36] for details)

where r_{BLR} measured in days and $\lambda L_\lambda(5, 100^{\circ}\text{A})$ measured in erg s^{-1} (see Fig. 5.1).

5.2.2 Stratification and Keplerian Kinematics of the BLR

In several AGNs, the monitoring projects covered several different lines coming from different ions from the UV to the optical (e.g., $\text{Ly}\alpha$, $\text{CIV}\lambda 1,550$, $\text{MgII}\lambda 2,798$). It was found that the high-ionization lines have smaller r_{BLR} than the low-ionization lines in the same AGN (e.g., [83, 137]). Thus, the high-ionization lines are produced at smaller radii than the low-ionization lines and are closer to the central source. This conclusion is reinforced by the fact that high-ionization lines are also wider than lower ionization lines, placing them closer to the central gravity source (e.g., [100, 162]). Peterson and Wandel [137, 138] show in a few objects, in which each has a few lines with measured r_{BLR} , that there is a tight correlation between the r_{BLR} and the width of the broad lines, V . This correlation has the form of $V \propto r_{\text{BLR}}^{-1/2}$ which is what is expected when the BLR kinematics are Keplerian and are dominated by gravity of a central mass.

Thank you, Shai. We cannot say that all quasar spectra are similar since there is a wide variety of ionization conditions and profile shapes going from NLSy1s to FR-II RL quasars. However, an overall resemblance at high and low luminosity suggests that ionization conditions should not be strongly dependent on luminosity. We will

show below, with the help of Paolo Padovani, that this has a direct implication for the distance of the BLR from the central continuum source.

5.3 An Alternative Method to Estimate the BLR Radius

Dear Paolo (Padovani), early works on black hole mass determination capitalized on the similarity of quasar spectra, and assumed constant physical conditions to derive the radius of the BLR. How do these photoionization methods compare to other methods widely employed in recent times?

The masses of AGN give information about their evolutionary stage and the physical features of the central engine within them. In fact, in the generally accepted framework that the origin of their extraordinary bolometric emission (10^{42} – 10^{48} erg s^{-1}) is the gravitational potential energy of a copious flow of gas into a massive black hole [146], the central mass represents an integrated measure of the past accretion history of the central object.

While nowadays, AGN masses are routinely derived for samples of thousands of sources, in the late 1980s/early 1990s, such estimates were received with a lot of skepticism, to say the least. Some of the early values were actually tied to the first reverberation-mapping measurements, discussed elsewhere in this chapter, which provided estimates of the inner radius r_{in} of the broad line region (BLR) of Seyfert-1 galaxies by studying the response of the emission lines to variations in the optical–UV continuum. The physical conditions of the line-emitting clouds are typically parametrized by an ionization parameter, which describes how many ionizing photons, $Q(H)$, there are per atom and is defined by $U = Q(H)/(4\pi c n r^2)$, where c is the speed of light, n is the particle density of the emitting gas, and r is the distance from the nucleus. At the inner boundaries of the BLR, one can define $(U \times n)_{\text{in}} = Q(H)/(4\pi c r_{\text{in}}^2)$. If this product is shown/assumed to be roughly constant for all AGNs, then $r_{\text{in}} \propto Q(H)^{1/2}$ depends only on the number of ionizing photons, which can be estimated from UV and X-ray data.

Based on the results of [125], Padovani et al. [126, 127] estimated the masses of a number of Seyfert-1 galaxies and quasars, associating r_{in} to the half-width zero intensity (HWZI) of a given BLR line. The HWZI, though somewhat observationally difficult to measure, is physically well defined and represents the maximum cloud velocity v_{max} . Therefore, if the motion is gravitationally bound, it must be associated with the minimum distance from the nucleus. The mass of the central nucleus can then be expressed as $M_{\text{H}} = v_{\text{max}}^2 r_{\text{in}}/2G$,⁴ where v_{max} is the infall velocity of the clouds at distance r_{in} (this would be an upper limit to the mass if the emitting matter were not gravitationally bound).

⁴See elsewhere in this chapter for a full discussion of the assumptions behind the relationship between mass, r_{in} , and v .

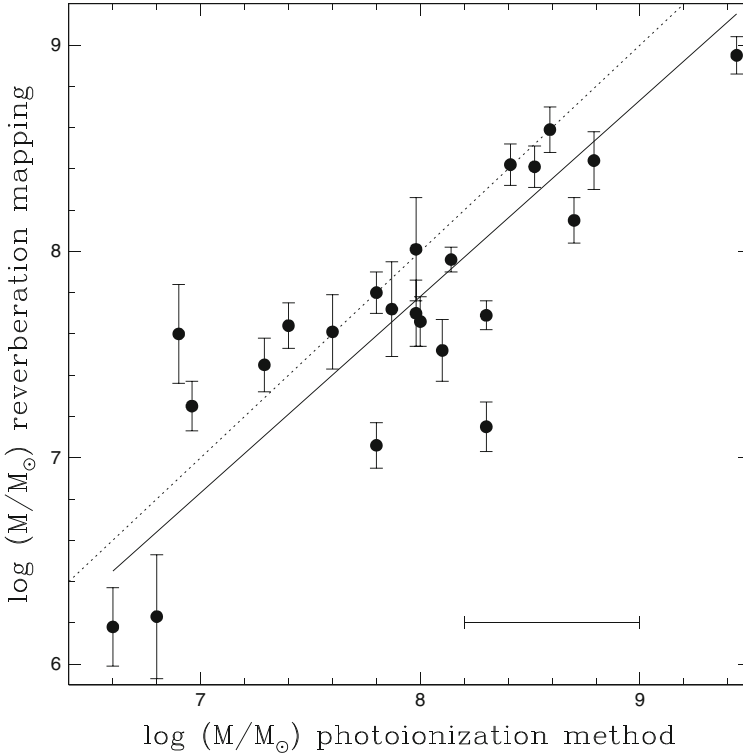


Fig. 5.2 Masses obtained with the reverberation mapping method vs. those derived from the photoionization method. The former values come from [141, 172], and [196], while the latter were derived by [127] and [126]. In both cases, the estimate refers to the $H\beta$ line. Since [126] used a slightly different normalization, their masses have been put on the same scale as [127] by adding 0.1 dex. The dotted line indicates equal masses, while the solid line is the best-fit bisector. The horizontal bar indicates typical errors for the photoionization masses [127]

Figure 5.2 plots masses obtained with the reverberation method vs. those derived from the photoionization method for 23 sources in [127] and [126] with both estimates. Note that while the former are the best values available at present, the latter were derived more than 20 years ago. The two estimates are extremely well correlated ($P > 99.99\%$) with a scatter ~ 0.4 dex. The best-fit bisector slope gives $M_{\text{rev}} \propto M_{\text{phot}}^{0.95 \pm 0.09}$, consistent with a slope of 1. There is a slight offset between the two determinations, with $\log M_{\text{rev}} - \log M_{\text{phot}} = -0.22 \pm 0.08$ and a median difference of -0.18 , which means that current reverberation masses are on average $\sim 60\%$ smaller than the photoionization ones from the 1990s, using the normalization adopted by [127].

The main message is that the product $U \times n$ is indeed roughly constant in the inner regions of the BLR of AGNs and therefore $r_{\text{in}} \propto Q(H)^{1/2} \propto L^{1/2}$ if the shape of the ionizing continuum is independent of luminosity. This allows one to estimate r_{in}

also for objects for which there is no reverberation-mapping determination, which requires a considerable investment of telescope time. Indeed, this is done now routinely through various relationships between r_{in} and $L(H\beta)$, $L_{\lambda}(5100 \text{ \AA})$, and also $L_{\lambda}(1350 \text{ \AA})$ for CIV [174]. Extrapolations at high redshifts, which are also often done, are in my view more problematic for two reasons: (1) all reverberation-mapping determinations have been done at low ($\lesssim 0.3$) redshift, with possibly one exception [79]; (2) no evolution in the physical properties of the BLR across most of the life of the universe is assumed.

Thank you, Paolo. We now consider a fully different method aimed at obtaining the parameter, namely, r_{BLR} . It has a great potential and in one case was used to measure different distances for different parts of the emission-line profiles [165]. It, however, requires a considerable observational effort, comparable to the monitoring performed for reverberation mapping.

5.4 Microlensing

Dear Damien (*Hutsemékers*), in which way can gravitational microlensing help us understand the structure of quasars? Which are the most important results obtain thus far?

When it occurs that a quasar and a foreground galaxy are on the same line of sight, the galaxy can deflect the light from the quasar and act as a gravitational lens for the observer. This usually results in the observation of multiple magnified images of the quasar. The image separation is characterized by the so-called angular *Einstein radius* θ_{E} , which, for the typical case of a lens galaxy at redshift $z_{\text{l}} = 0.5$ and a source quasar at $z_{\text{s}} = 2$, is of the order of $\theta_{\text{E}} \sim 10^{-6} \sqrt{M/M_{\odot}}$ arcsec, where M is the mass of the lens expressed in solar masses M_{\odot} . For a massive galaxy with $M \sim 10^{12} M_{\odot}$, θ_{E} is of the order of a few arcseconds. This is the *macrolensing* regime [154].

When they are close to the line of sight, individual stars in the lens galaxy can also act as gravitational lenses. Much less massive ($M \sim 0.1\text{--}1 M_{\odot}$), they produce sub-images separated by micro-arcseconds, which cannot be resolved with current instrumentation. In this case, one speaks of *microlensing*. The physical scale of the Einstein radius in the quasar plane is $r_{\text{E}} \sim 10^{-2} \sqrt{M/M_{\odot}}$ parsec, with $z_{\text{l}} = 0.5$ and $z_{\text{s}} = 2$. Very interestingly, this radius is comparable to the radius of the continuum-emitting region in quasars. Because the microlensing-induced magnification of a region of radius r depends on the ratio r_{E}/r , the light coming from quasar regions smaller or equal to the continuum-emitting region ($r \lesssim r_{\text{E}} \sim r_{\text{cont}}$) can be significantly amplified, while the light from larger regions ($r \gg r_{\text{E}} \sim r_{\text{cont}}$) is not (e.g., [152]).

Owing to the relative motion observer-lens-source, the stellar microlenses move with respect to the line of sight, producing variations in the observed quasar

continuum flux on timescales of months to years. From a careful measurement of these light variations, the microlensing amplification and then the size of the quasar optical continuum-emitting region can be estimated, at scales far below the spatial resolution reached by current imaging capabilities.

The quasar accretion disk, from which the continuum is thought to originate, has a temperature which depends on the distance to the core, $T \propto r^{-\beta}$, where the parameter β depends on the adopted model. For a Shakura–Sunyaev thin accretion disk, $\beta = 3/4$. According to the Wien’s law, this temperature profile translates, in first approximation, into a wavelength-dependent radius of the continuum-emitting region, $r \propto \lambda^{1/\beta}$. While gravitational microlensing is achromatic, the amplification of the quasar continuum, which depends on r_E/r , changes with the wavelength λ . The measurement of light variations at different wavelengths can thus constrain the temperature profile of the accretion disk [41, 143, 145, 180].

Microlensing can also provide clues to the size and kinematics of the broad emission-line region (BELR). The BELR is larger than the continuum-emitting region, but parts of it can be successively resolved by a moving microlens. If regions of different velocities are successively magnified, time-dependent line profile deformations, characteristics of the BELR kinematics, will be observed in the spectrum of one or another image of the lensed quasar [1, 115]. Moreover, if differences are observed between spectral lines or ions, estimates of the relative sizes of their emitting regions can be derived.

Practically, the measurements are not that simple. First, high-quality long-term (spectro-)photometric observations are required for quasar macro-images separated by typically 1 arcsec. This is still challenging. Second, the microlensing-induced variations must be separated from quasar intrinsic variations, which affect the different macro-images with a time delay. And finally, the microlenses are rarely isolated. The mutual effect of various stellar microlenses results in a magnification of the quasar core and its surroundings by a complex caustic network. Many studies then rely on simulations and statistical methods to extract information on the quasar structure from microlensing events [82].

In spite of these difficulties, a handful of very interesting—although still controversial—results have been recently obtained. Constraints on the temperature profile of the accretion disk have been derived and found compatible [41, 143] or not [19, 46] with the Shakura–Sunyaev thin disk model. X-ray microlensing has been observed, suggesting that the quasar X-ray emission arises from close to the inner edge of the accretion disk [28]. The size of the BELR has been estimated in some quasars and found of the order of one-tenth of a parsec, which is compatible with reverberation mapping measurements [165, 188]. The kinematic structure of the BELR has been partially resolved: the highest velocity components of the broad emission lines were found to originate from the most compact regions in agreement with the virial theorem, while Fe II was found to arise in the outer part of the BELR [164, 165]. Finally, in a lensed broad absorption-line (BAL) quasar, the true absorption- and emission-line profiles have been separated, thanks to a differential microlensing effect, providing evidence that emission lines are indeed reabsorbed in a disklike structure [73].

All these results unfortunately refer to a very small sample of objects and cannot be readily generalized. But they clearly demonstrate the great promise of accurate long-term monitoring of microlensing events to quantitatively probe the quasar inner structure.

Thank you, Damien. We have focused until now on the estimate of r_{BLR} . This parameter is not just interesting for its own sake, but also a fundamental ingredient in the estimation of the central black hole mass.

5.5 Black Hole Mass Estimation

Dear Shai (*Kaspi*), how do we use these measures to develop a method for virial estimation of BH masses for large samples of quasars and especially high-redshift quasars?

To estimate the central masses of AGNs, we assume gravitationally dominated motions of the BLR clouds, which, as seen above, is a valid assumption. As in many other astronomical problems aimed at finding a central mass orbited by a smaller mass, we need to know the distance and velocity of the orbiting mass, and by comparing the gravitational force to the centripetal force (the virial theorem), we can find the central mass. Thus, once r_{BLR} is found from reverberation mapping, the mass of the BH in the center of the AGN can be estimated using

$$M_{\text{BH}} = f G^{-1} r_{\text{BLR}} V^2, \quad (5.3)$$

where V is a measure of the BLR clouds' velocity measured from the line's width, and f is a dimensionless factor which depends on the geometry and kinematics of the BLR. Figure 5.3 shows the mass–luminosity relation for the objects with reverberation-mapping data. The best fit to the data points is $\log(M_{\text{BH}}/10^8) = (0.016 \pm 0.018) + (0.643 \pm 0.017) \log(\lambda L_{\lambda}(5100\text{\AA})/10^{44})$, where M_{BH} measured in M_{\odot} and $\lambda L_{\lambda}(5, 100\text{\AA})$ measured in ergs s^{-1} .

To determine M_{BH} for AGNs which do not have reverberation-mapping data, the “single epoch observation” method is used. By taking one observation of the spectrum of an AGN, the luminosity and line width are measured. Using the luminosity in the r_{BLR} —Luminosity relation described in Sect. 5.2.1, the r_{BLR} for that object is estimated. This r_{BLR} and the measured width of the line are then used in (5.3) to estimate the black hole mass. This method is used on very large samples of AGNs in order to estimate their central black hole mass (e.g., [61, 182, 197]).

The most commonly used line in reverberation-mapping studies is the $\text{H}\beta$ emission line. This is primarily due to its availability in optical spectra of low-luminosity AGNs, and its proximity to the $[\text{OIII}]\lambda\lambda 4959, 5007$ lines which serve to intercalibrate the spectra. Thus, in order to determine M_{BH} , it is best to measure the $\text{H}\beta$ line width and the luminosity at 5100\AA .

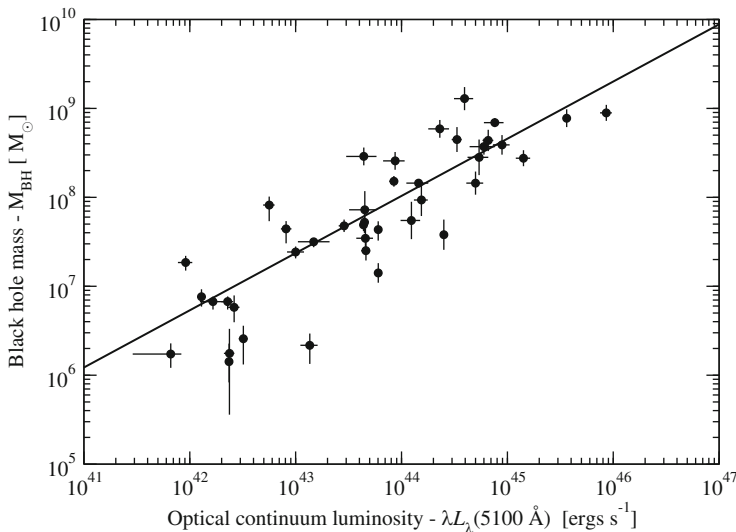


Fig. 5.3 Black hole mass plotted vs. the $\lambda L_{\lambda}(5100 \text{ \AA})$ luminosity. Data points are from [13, 15], and [36]. Solid line is a fit to the data points

For AGNs with redshift above ~ 0.6 , the $H\beta$ emission line is redshifted into IR wavelengths where it is hard or impossible to get a spectrum (e.g., [153]). Thus, different emission lines need to be used, that is, lines in UV wavelength. Only few reverberation-mapping campaigns were carried out for UV lines (see [141] and references therein). Hence, direct size–luminosity relation does not exist for these lines. An indirect method to determine M_{BH} from UV continuum and lines is to use the known relation between M_{BH} , the width of the $H\beta$ emission line, and the optical luminosity in order to find a relation between M_{BH} , the width of the UV emission line, and the UV luminosity. This was suggested in several studies, for example, [104] for $\text{MgII}\lambda 2798$ [174] for $\text{CIV}\lambda 1549$. This method enables to determine M_{BH} for high-redshift quasars based on a single-epoch optical observation which shows the rest-frame UV lines and enables studies of the correlation of M_{BH} with other characteristics of the AGN in a high number of objects.

5.5.1 Difficulties and Uncertainties

The correlation between luminosity and BLR distance suffers from large scatter that hampers accurate black hole mass estimations. What are the most important sources of scatter and uncertainty? What can we do to improve the estimates?

Reverberation-mapping projects are practically very hard to carry out from observational point of view. It is difficult to get spectrophotometric light curves with the appropriate sampling rate and over long enough period of time, in order to clearly detect the time lag between the emission line and the continuum. High signal-to-noise ratio and high-resolution spectra are needed to try two-dimensional reverberation mapping in order to deduce the kinematics of the BLR. Also, the AGN itself needs to “collaborate” and to show significant continuum variation and line response during the period of the monitoring. All these observational limitations are causing the measurement of the time lag itself to be hard, and introduce an uncertainty into the measurement which is not easy to estimate. Improvements in the above observational parameters will yield better observational result and better size–luminosity relation.

The luminosity of AGN is varying over time; thus it is hard to determine the exact luminosity of an object and we need to estimate the average luminosity. Also, the BLR size was found to vary in time, and in some cases to correlate with luminosity within a given object (e.g. [117, 140]). Thus, for a given luminosity in a given AGN, sometimes a different r_{BLR} is found. This is probably an intrinsic characteristic of the AGN, and it produces an intrinsic scatter in the size–luminosity relation which is real and cannot be improved.

Reverberation mapping assumes a simple Keplerian kinematics of the BLR in order to determine the black hole mass. This assumption is surly a simplicity of the reality which is probably much more complicated. Also, the geometry of the BLR is not known, and we must remember that r_{BLR} is only a measure of the BLR size. Different BLR geometries will produce different r_{BLR} , and it could add to the observed scatter in the size–luminosity relation. The kinematics of the BLR is yet unknown, and it could be that different objects have different kinematic patterns. All these factors are affecting the factor f from (5.3). This factor might be different for different object, and it is practically unknown. Thus, our assumption that all AGNs have the same f might be invalid, and this might introduce an extra uncertainty in the mass determination.

While important progress has been made in attempts to extend the optically based size–luminosity relation to UV luminosities and UV broad emission lines using the “single epoch” method, there are still a number of potential problems that need to be addressed (e.g., [9, 95]). Thus, the single-epoch measurements depend on the untested assumption that these extrapolations are valid. Although a posteriori explanations of the physical plausibility of the observed relations can be found, it is quite possible that subtle or strong deviations from the relations occur at high luminosities or redshifts [116].

All these uncertainty factors are leading to a scatter in the size–luminosity relation and even much more scatter in the mass–luminosity relation. It is reasonable to estimate that M_{BH} determination from the reverberation-mapping technique has an uncertainty of about factor of three (e.g., [123]).

Thank you, Shai. Considering that computation of black hole masses have been made in an “industrial” way for samples of thousands of quasars, we would like

to hear the view of Ross McLure who has worked on the determination of M_{BH} in high-redshift quasars.

Dear Ross (McLure), how can one estimate the mass of the black hole assumed to lie at the center of every quasar?

The basic principles behind estimating the mass of a black hole at the center of a quasar, or any galaxy for that matter, are very simple and involve the straightforward application of Newtonian physics. For our purposes, we can regard the central black hole as a simple point mass, and therefore, provided we can observe a test particle in a stable orbit around that point mass, by requiring that the inward pull of gravity is balanced by the centripetal acceleration, we arrive at the equation:

$$M_{\text{bh}} = \frac{r \times V^2}{G}, \quad (5.4)$$

where M_{BH} is the mass of the black hole, r is the radius of our test particle from the black hole, V is the orbital velocity of our test particle, and G is the gravitational constant. Consequently, in principle, all that is required to estimate the mass of a black hole is to measure the radius and velocity of a suitable orbiting body. In reality of course, it is far from straightforward to directly measure these physical parameters in distant galaxies or quasars.

Before proceeding to consider quasars, it is worthwhile considering the process of black hole mass measurement in local, inactive galaxies. Over the last two decades, accurate black hole mass measurements have been obtained for $\simeq 50$ nearby galaxies [50], mostly, thanks to the superb spatial resolution provided by the Hubble Space Telescope (HST). For massive nearby galaxies (i.e., $D \leq 50$ Mpc), it is occasionally possible to resolve large gas disks orbiting the unseen central black hole, allowing a simultaneous measurement of the orbital radius and by taking a spectrum and measuring the Doppler shifts of the gas emission lines, the orbital velocity. Indeed, the most massive black hole mass known in the local universe (M 87, $M_{\text{BH}} = 3 \times 10^9 M_{\odot}$) was first measured using this technique [47].

In contrast to studying the motions of gas, an alternative method for estimating black hole masses in nearby galaxies is to study the influence of the black hole on stellar orbits. Unfortunately, even with HST, it is not possible to study the orbits of individual stars, even in the most nearby galaxies. However, by taking spectra, it is possible to measure the average velocity of the stellar population as a function of position and radius. Armed with this information, detailed, three-dimensional, dynamical models of the stellar orbits can be used to constrain the central gravitational potential and thereby the central black hole mass [50]. Although seemingly less direct, using stellar velocities has the distinct advantage that, unlike gas, stellar orbits are entirely governed by the gravitational potential, and are not subject to complicating physical processes such as outflows and shocks. The ultimate expression of this technique are the detailed observations which have accurately measured the mass of the black hole at the center of our own galaxy. Using high-resolution, near-IR observations to peer through the heavy dust

obscuration at the center of the Milky Way, over the last 15 years, it has been possible to trace the orbits of stars around the unseen dark mass, both confirming that the central object can only be a supermassive black hole, and delivering an accurate measurement of its mass: $4.3 \pm 0.5 \times 10^6 M_{\odot}$ [51, 52].

As the current sample of $\simeq 50$ nearby galaxies with accurate black hole mass measurements was being gradually assembled, tight correlations between black hole mass and the properties of the surrounding stellar bulge (i.e., luminosity, stellar velocity dispersion, and light concentration) were discovered [42, 49, 53, 85, 93]. In fact, it is now clear that all of these separate correlations are proxies for an underlying, approximately linear, correlation between black hole mass and the stellar mass of the surrounding bulge, with most studies converging on a relation of the form: $M_{\text{BH}} \simeq 0.001 M_{\star}$. The unexpected discovery that every local massive galaxy harbors a central black hole with a mass 0.1% of the surrounding stellar bulge had important implications for models of galaxy and quasar evolution. Quite simply, because the black holes at the centers of local massive galaxies can only have assembled their mass through accretion, the profound conclusion is that *every* massive galaxy in the universe is likely to have gone through at least one, and potentially several, quasar epochs in its history. Therefore, it is clearly of great interest to be able to measure the masses of the black holes at the centers of quasars, and to trace how the masses of these black holes evolve with redshift.

Although luminous quasars are too distant to allow direct observation of material orbiting around the central black hole, it turns out that it is possible to obtain a reasonably accurate estimate of the mass of quasar black holes by simply observing their rest-frame optical–UV spectrum. Within the standard model of the structure of the central region of a quasar, the central black hole is surrounded by a hot accretion disk which, in turn, is surrounded by clouds of dense ionized gas in orbit around the black hole. In the UV–optical spectrum of quasars, the radiation emitted by the hot accretion disk can be seen as a blue continuum, and the emission of the hot ionized gas can be seen as a series of strong, broad, emission lines. Due to the Doppler effect, the faster the gas is moving as it orbits the black hole, the broader the emission lines appear. Therefore, by simply measuring the width of the broad emission lines, it is possible to obtain an estimate of the orbital velocity of the broad-line-emitting gas. In order to obtain a black hole mass estimate, however, it is also necessary to get an estimate of the radius of this broad-line gas from the black hole.

In the AGN standard model, the broad-line-emitting gas is ionized by high-energy photons which are emitted by the central accretion disk. Consequently, any variation in the accretion disk output should be reflected by a corresponding variation in the strength of the broad emission lines themselves. Through a series of painstaking observations, whereby the optical spectrum of a quasar is frequently monitored over an extended period of time, it is possible to observe these variations in continuum and emission-line flux. This process, referred to as reverberation mapping [142], allows the time delay, or lag, between the continuum and emission-line variations to be measured. Given that this time delay must be caused by the light travel time between the source of the high-energy photons and the location of the broad-line-emitting gas (the broad-line region, BLR), this provides us with

a direct measurement of the gas radius (i.e., $r_{\text{BLR}} = \Delta t \times c$). When combined with a measurement of the orbital velocity derived from the width of the broad emission lines themselves, we have a measurement of both the physical parameters needed to estimate the mass of the central black hole. As described, this technique is often referred to as a “virial” black hole estimate, simply because it relies on the assumption that the broad-line emitting gas is *virialized*. Within this context, this simply means that the gas is orbiting the central black hole in a stable fashion, solely under the influence of the gravity of the central black hole, and therefore obeys the equation: $M_{\text{BH}} = \frac{r \times V^2}{G}$. It is worth remembering that if, for whatever reason, this is not the case, black hole mass estimates based on the virial assumption could be wildly wrong.

In an ideal world, virial black hole mass estimates would rely on individual reverberation mapping radius measurements. However, unfortunately, it is simply not feasible to obtain orbital radii measurements for large samples of quasars via the reverberation mapping technique. The reason is that the typical broad-line radius for a luminous quasar is $\simeq 100$ light-days, meaning that frequent monitoring over a period of several years is required to obtain an individual reverberation measurement. Consequently, even today, despite years of effort, reverberation mapping time-delay measurements are only available for $\simeq 40$ AGNs [13]. Fortunately, these few objects on their own turn out to be sufficient to allow black hole mass estimates to be derived for tens of thousands of luminous quasars. If the measured time lags for the reverberation-mapped quasars are plotted against a measurement of their optical luminosity, it becomes clear that the two parameters are strongly correlated. Theoretically, this correlation is expected to take the form of $r_{\text{BLR}} \propto L_{\text{opt}}^{0.5}$, because the ionizing flux intercepted by any broad-line-emitting gas cloud will decline with distance following the inverse square law. Indeed, recent studies of the correlation between BLR radius and quasar luminosity do suggest that the correlation is consistent with the simple theoretical expectation [13]. Based on this correlation, it is possible to estimate the radius of the broad-line region for any quasar by simply measuring its optical luminosity. Consequently, armed with the $R - L$ correlation, it is then possible to estimate quasar black hole masses from a single optical spectrum.

So far so good, however, what we would really like is to be able to apply this technique to large samples of quasars spanning a wide range in redshift. In this respect, there is a further, slight complication. The vast majority of the reverberation mapping measurements which have been obtained have been based on the broad hydrogen-beta ($\text{H}\beta$) emission line, at a rest-frame wavelength of 4861 Å. Unfortunately, this emission line is redshifted beyond the reach of optical spectrographs at a redshift of $z \simeq 1$, meaning that it cannot easily be used to estimate the black hole masses of high-redshift quasars. Thankfully, it has proven possible to perform a cross-calibration between the $\text{H}\beta$ emission line and other strong broad emission lines in the rest-frame UV spectrum of quasars, primarily MgII at $\lambda_{\text{rest}} = 2800$ Å [106] and CIV at a $\lambda_{\text{rest}} = 1549$ Å [172]. Using a combination of $\text{H}\beta$, MgII, and CIV, it is then possible to estimate black hole masses for quasars all the way out to a redshift of $z \simeq 5$, from optical spectroscopy alone.

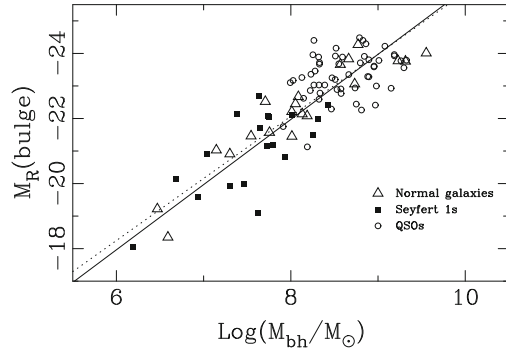
At this stage, it is perhaps worthwhile spending some time considering the assumptions and uncertainties inherent to the virial mass estimator. As previously discussed, the fundamental assumption underlying the virial mass estimator is that the broad emission-line gas is actually *virialized*. In principle, if the gas is far from virial, the black hole mass estimates could be badly wrong, although in practice, there seems to be little evidence that this is the case. Perhaps, the largest uncertainty that we have yet to discuss is the geometry of the broad-line region. Due to a lack of information, the standard assumption to make is that the broad-line-emitting gas clouds orbit around the central black hole with a random, spherical geometry. In this scenario, the typical orbital velocity of the gas should be related to the width of the observed emission lines (as measured by the FWHM—full width at half maximum) in a straightforward fashion: $V_{\text{orb}} \simeq \frac{\sqrt{3}}{2} \times \text{FWHM}$. However, if instead the geometry of the BLR is flattened, or disklike, then the inclination of the observer's line of sight can become very important. Indeed, in this scenario, the FWHM and orbital velocity are related as $V_{\text{orb}} \simeq \text{FWHM}/2 \sin i$, where i is the inclination angle. Therefore, if a spherical geometry is assumed when the actual geometry of the BLR is flattened and viewed close to pole-on ($i \simeq 0^\circ$), the virial black hole mass estimate could be dramatically wrong.

Unfortunately, it is not possible to reliably determine the inclination angle for the bulk of the luminous quasar population. However, for the small subset of quasars which are radio loud, the ratio between core and lobe radio luminosity can provide some measure of inclination. In fact, it has been known for many years that radio-loud quasars do show a correlation between FWHM and $\sin i$ which suggests that the geometry of the BLR is typically flattened [191]. Although the issue of BLR geometry is far from settled, it seems that, averaged over a large sample, the black hole mass estimate is fairly immune to assumed geometry. The likely reason is that the average inclination angle for a suitably large sample should be close to $i \simeq 30^\circ$, meaning that flattened and spherical geometries both predict a very similar relationship between orbital velocity and measured FWHM.

A further uncertainty which has been widely discussed recently is the question of the importance of radiation pressure in the virial mass estimator. In a series of papers [97, 98], it was suggested that for quasars accreting close to the Eddington limit, virial black hole mass estimates could be substantially underestimated if the role of radiation pressure is ignored. Although it is clear that radiation could influence the dynamics of the broad-line region, it is not clear yet that its influence is actually significant. Indeed, based on detailed calculations, a recent paper [120] concludes that the simple virial mass estimate performs well, even when radiation pressure does play an important role.

Within this context, it is clearly worth considering the important question of whether or not virial black hole mass estimates are actually reliable. This question is problematic to address in reality because it is simply not possible to obtain accurate, independent black hole mass measurements of quasars with which to test the virial method. As a consequence, the question of the accuracy of the virial black hole

Fig. 5.4 The bulge luminosity vs. black hole mass relation for AGNs and inactive galaxies [106]. This study demonstrated that based on the virial black hole mass estimator, quasars and Seyfert galaxies follow the same $M_{\text{bh}} - L_{\text{bulge}}$ relation as nearby inactive galaxies with accurate, dynamical black hole mass measurements



mass estimator can only be addressed indirectly. As discussed previously, inactive galaxies in the local universe follow tight correlations between black hole mass and various observational proxies for the mass of their stellar bulge. Through careful observations and analysis, it is possible to obtain measurements of stellar velocity dispersion and bulge luminosity for samples of relatively nearby AGN/quasars, and thereby at least test that the virial black hole mass estimator is consistent with these correlations. Early attempts to perform this consistency check demonstrated that quasar virial black-hole mass estimates are consistent with the local $M_{\text{bh}} - L_{\text{bulge}}$ (Fig. 5.4) [105, 106] and $M_{\text{bh}} - \sigma$ correlations [114, 123] and that, individually, the virial estimator was accurate to within a factor of $\simeq 3$. Although it should always be remembered that these tests have only been performed on a relatively small number of objects, and at relatively low redshift, they do at least provide some confidence that the virial estimator can be used to provide meaningful estimate quasar black hole masses at all redshifts.

In conclusion, it is clear that for any individual quasar, there is plenty of scope for the virial black hole mass estimator to produce an answer which is badly wrong. However, when applied to large samples of quasars, where the different sources of uncertainty effectively average out, there is good evidence that the virial mass estimator provides accurate and unbiased results. Based on this conclusion, several studies have adopted the virial technique [25, 108, 155] to derived black hole mass estimates for tens of thousands of quasars from the Sloan Digital Sky Survey (SDSS). It is from these large-scale studies that we have gained most of our knowledge about the black hole masses of quasars at high redshift.

Does an apparent upper limit to black hole mass make sense? How do we avoid monster black holes which were formed at very high redshift and might have no quiescent counterpart in the local universe?

The large-scale studies performed applying the virial mass estimator to tens of thousands of SDSS quasars [25, 108, 155] demonstrate that there is a well-defined upper limit to the mass of quasar black holes, independent of redshift, at $\simeq 5 \times 10^9 M_{\odot}$. Given this clear observational result, we can ask the straightforward question about

whether this makes any sense, given what we know about supermassive black holes in the local universe. Within our current understanding of galaxy evolution, all of the supermassive black holes we observe as luminous quasars in the distant universe must now be lying dormant at the center of massive galaxies in the local universe. Consequently, we can therefore perform the simple test of hunting for the most massive black holes we can identify in the local universe and checking to see if they are consistent with the most massive black holes we can identify at high redshift.

As discussed earlier, via detailed observations of stellar and gas dynamics, there are now accurate measurements of the mass of $\simeq 50$ dormant supermassive black holes in the local universe. Among the local sample with measured black hole masses, M87 has the most massive black hole with a mass of $3-6 \times 10^9 M_\odot$ [50,92]. On the face of it, this seems in very good agreement with the observed limiting black hole mass among distant, luminous quasars. In principle, it is still possible that more massive black holes do exist locally, given that the cosmological volume within which it is possible to obtain black hole mass measurements is very small. However, it now seems unlikely that this is the case, which can be demonstrated with reference to the well-known scaling relations between black hole mass and galaxy properties. If, for example, we concentrate on the $M_{\text{BH}} - \sigma$ relation, we can calculate that to harbor a dormant black hole of mass $\geq 10^{10} M_\odot$, a local galaxy would need to have a stellar velocity dispersion of $\geq 550 \text{ km s}^{-1}$ [62]. Thanks to the SDSS, we now have a very good idea of the distribution of galaxy stellar velocity dispersions in the local universe, and galaxies with $\sigma \geq 550 \text{ km s}^{-1}$ are incredibly rare [16]. The conclusion from this is that luminous quasars at high redshift, and the properties of local massive galaxies are both consistent with an upper limit to the mass of supermassive black holes of $\simeq 10^{10} M_\odot$.

Although pleasingly consistent, we are now forced to ask the question of why supermassive black holes more massive than $\simeq 10^{10} M_\odot$ do not seem to exist. The basic problem is that, provided that a black hole can be fueled at close to the Eddington limit, the growth in black hole mass is exponential, with a mass doubling time of about 3×10^7 years. Consequently, given that at least some quasars at very high redshift have already assembled a mass of $\simeq 10^9 M_\odot$ [190], and that they are theoretically capable of exceeding a mass of $\simeq 10^{10} M_\odot$ in only $\simeq 10^8$ years, what stops them from doing so? The answer must be that it is not physically possible to continually supply these $\simeq 10^9 M_\odot$ black holes with enough gas to keep them close to the Eddington limit. A black hole of mass $\simeq 10^9 M_\odot$ is required to accrete $\simeq 20 M_\odot$ of material each year to remain at the Eddington limit, and thereby continue exponential mass growth. The fact that $\geq 10^{10} M_\odot$ black holes do not appear to exist in the local universe is probably telling us that it is very difficult to maintain a gas supply of $\geq 10 M_\odot/\text{year}$ for $\geq 10^8$ years.

Thank you Ross.

Dear Ari (*Laor*), what observational properties most closely correlate with black hole mass?

One possible property, already mentioned above, is metallicity. Another property which appears to be strongly correlated with the black hole mass is the radio loudness, as revealed in the PG quasar sample [89] and in the SDSS AGN sample [18].

Why do we not see a clear BH mass–source luminosity correlation among the quasars?

Optically selected samples in fact do show a strong $M_{\text{BH}} - L$ correlation, as they show a small spread in L/L_{Edd} [84], but this is most likely a selection effect. To be optically selected, the AGN needs to outshine the host, that is, there is a lower limit to L/L_{host} . Since the host bulge mass and thus the its luminosity is correlated with M_{BH} [65, 93], the sample selection is therefore equivalent to a lower limit on L/L_{Edd} , which is typically about 0.1. Since there is also an observed upper limit of about unity on L/L_{Edd} , as expected physically, this leaves only a narrow range for L/L_{Edd} in optically selected AGNs.

AGN samples selected at wavelengths where the host contribution is negligible, can detect AGNs to much lower L/L_{Edd} . One band is the radio, where radio-loud AGNs can clearly be detected to $L/L_{\text{Edd}} \ll 10^{-3}$ (e.g., most FR I radio galaxies). Such low L/L_{Edd} objects are commonly termed radio galaxies, as they otherwise look like normal galaxies. In radio-quiet AGNs, the radio to IR luminosity ratio is similar to that in inactive galaxies, but AGNs can be differentiated through their much higher brightness temperature in the radio, revealed through interferometric imaging on mas scale. This technique has not been used yet to form samples of radio-quiet AGNs at low L/L_{Edd} , but it should be feasible now with the EVLA.

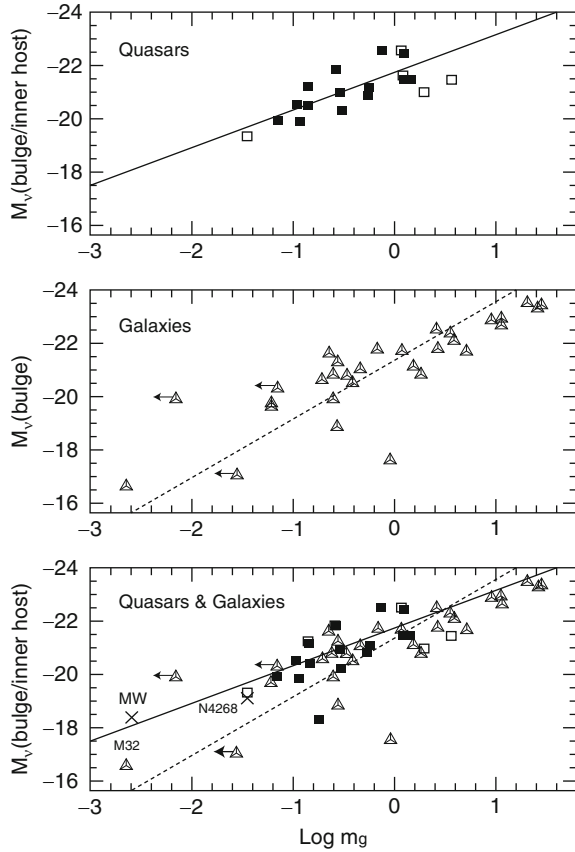
AGNs can outshine the host by a large factor also in the X-ray, which is why X-ray surveys are very efficient in finding AGNs, and start to be diluted by galaxies only at the lowest fluxes of the deepest surveys [66]. These surveys also reveal lower L/L_{Edd} AGNs. AGNs are also revealed through spectroscopic surveys, where AGNs are defined through their narrow emission-line ratios on the BPT diagrams. These surveys can reach extremely low L/L_{Edd} in nearby galaxies, commonly identified as LINERs [68].

Thus, AGNs most likely do not have an intrinsic $M_{\text{BH}} - L$ relation, and the apparent one is a sample selection effect [71].

The lack of $M_{\text{BH}} - L$ relation probably reflects the later stages of AGN life, where M_{BH} has already built up, the accretion rate goes down, and the AGN is on the way to becoming inactive. On the other hand, at the rapid growth stage, the BH may be fed from large-scales interactions/mergers which may occur at rates well above L_{Edd} . The BH then accretes the most it can, and will then shine at L_{Edd} , leading to a tight $M_{\text{BH}} - L$ relation at that growth stage (Fig. 5.5).

Thank you, Ari.

Fig. 5.5 Figure 1 from [88]. The *upper panel* shows in the y-axis, the host galaxy magnitude of a sample of PG quasars measured with HST (see references in [88]). The x-axis is the estimated M_{BH} using the broad $H\beta$ line width and the reverberation-based size of the BLR. The *middle panel* shows the position of the nearby inactive galaxies studied by Magorrian et al. The *lower panel* shows the remarkable match of the positions of the two samples. This provided the first indication that the BLR-based M_{BH} is correct, to a factor of ~ 3



5.5.2 Supermassive Black-Holes and the Host Galaxy Bulge

Dear Marianne (Vestergaard), is there an important relationship between the central black hole mass and the mass of the bulge of the host galaxy?

Yes, this was found some ten years ago [42, 49, 93]. This relationship says that the mass of the central compact object (assumed to be a supermassive black hole) increases with the mass (or the stellar velocity dispersion) in the bulge of the galaxy: large elliptical galaxies have very massive central black holes, while late-type spirals with small bulges have low-mass central black holes. The mass of the black hole, M_{BH} , is determined by characterizing the kinematics (distance and velocity) of stars or gas located very close to the black hole. This requires high spatial resolution and for most, such measurements we need to use the Hubble Space Telescope (e.g., [44]). The velocity dispersion of the stars in the bulge, σ_* , is measured using the width of the stellar absorption lines.

When the relationship is expressed in terms of the bulge mass, M_{bulge} , we observe a linear relation with a slope of about 1.1 (e.g., [65, 96]). In the local universe where this relationship was established, the mass ratio of the black hole to the bulge, $M_{\text{BH}}/M_{\text{bulge}}$, is approximately 0.0014 [65, 86]. A lot of effort has gone into trying to understand both of the $M_{\text{BH}} - \sigma_*$ and the $M_{\text{BH}} - M_{\text{bulge}}$ relations. Some scatter of about 0.3–0.4 dex is seen in the $M_{\text{BH}} - \sigma_*$ relation (e.g., [55, 63, 122]), with elliptical galaxies exhibiting relatively less scatter; the origin of this scatter is not understood. Could this perhaps be due to the fact that individual galaxy types obey their own $M_{\text{BH}} - \sigma_*$ relation in the sense that the slope and the zero point varies according to the galaxy type (elliptical vs. spirals, or even between subclassifications of spirals)? Some studies attempt to illuminate this interesting issue (e.g., [56, 59]) and more are likely underway.

How did this relationship come about? We do not know yet but it seems to argue that somehow, the black hole knows what is going on in the bulge and/or the bulge knows about the black hole. That is, there appears to be a causal connection between gravity on very small central size scales with gravity on a much larger scale. One can perhaps imagine the relationship to result from one of two scenarios, namely, that this relationship is dictated by the initial (or other physical) conditions at the earliest epochs such that M_{BH} and M_{bulge} always grow in synchronization through cosmic history. To ensure this occurs, it has been suggested that energetic feedback from the central black hole helps regulate the rate and duration of both star formation in the bulge and the growth of the black hole itself (e.g., [31, 38, 70]).

On the other hand, we might simply be observing the end result of giga-years of evolution. The question remains—which came first: the black hole or the bulge? Did the black hole form first and through the strength of its gravity assemble the bulge around it to the specifications we see in the local $M_{\text{BH}} - \sigma_*$ relation? Or did the size of the dark matter halo at early epochs dictate the size of the bulge from which the central black hole fragmented or “condensed” out of by a certain fraction? We do not know yet. But one thing is clear, this relationship and how it changes with redshift probably tells us something about how black holes and galaxies form and evolve over cosmic times. For example, do only classical bulges like elliptical galaxies have central massive black holes? Or do only classical bulges have black holes whose mass scales with the bulge mass? If so, do galaxies with small or no bulge—or no classical bulge—have black holes and how massive are they? Can these galaxies not build a black hole or can they not retain them during merger events (e.g., [110, 177])? If these black holes also somehow scale with galaxy properties, then we can compare these relationship with those of classical bulges so to test in which way the bulges and black holes evolve similarly or differently among the individual galaxy types. These issues have naturally sparked a flurry of theoretical studies trying to explain this connection (e.g., [21, 38, 76, 148, 178]).

Or does the relationship actually tell us anything about how black holes and galaxies coevolve? Very recent work seems to suggest that the $M_{\text{BH}} - \sigma_*$ relation we observe locally may simply be a selection effect due to our inability to resolve “the sphere of influence” [10] systematically for lower mass black holes in more distant sources. The “sphere of influence” is the sphere within which the gravity

of the black hole will dominate the dynamics of the surrounding stars to a greater extent than other mass components of the enclosed mass (i.e., gas, stars) at that distance. With increasing distance from the black hole, the stars will increasingly be affected by the gravity of other material, such as gas and stars, and the enclosed mass that we would measure will be larger than the mass of the black hole itself. For these reasons, it is very important that we measure the gas or stellar velocities as close as possible to the black hole. The required high spatial resolution quickly becomes a challenge for more distant sources (see, for example, Fig. 1 of [44]).

Other recent studies suggest that we cannot gain insight into galaxy evolution by studying the $M_{\text{BH}} - \sigma_*$ relation because there is no causal link between M_{BH} and M_{bulge} in the local universe. Peng [128] and Jahnke and Macció [75] suggest that the $M_{\text{BH}} - \sigma_*$ relation can be explained by simply merging hierarchically a random collection of bulges, hosting black holes with a random distribution of masses. That is, there is initially no correlation between M_{bulge} and M_{BH} in these galaxies yet after numerous merger events, the black holes and bulges obey the observed $M_{\text{BH}} - \sigma_*$ relation. If this is true, this would also mean that the feedback processes from the central black hole would not play any role in the making of the $M_{\text{BH}} - \sigma_*$ relation quite contrary to current thinking in the community (e.g., [21, 31, 38, 57]).

This scenario predicts that we see more scatter around the relationship measured at higher redshift.

Interestingly, in this scenario, the physical processes of star formation, black hole accretion, and rearrangement of a fraction of the stars in the initial galaxy disks into the final galaxy bulge are the main origins of the scatter around the $M_{\text{BH}} - \sigma_*$ relation. It also shows that the massive galaxies that have undergone more mergers have relatively smaller scatter and the most massive ones tend to lie above the mean relation defined by the entire sample of $\sim 11,000$ sources [75]. These characteristics are to first order consistent with current observations. Specifically, we see a larger scatter at the low-mass end of the $M_{\text{BH}} - \sigma_*$ relation (e.g., [59]). Obviously, this proposed scenario needs to be tested well and likely, will be so in the future considering the significant ramifications it has for the current $M_{\text{BH}} - \sigma_*$ relation paradigm, potentially rendering a large fraction of current and past studies on the subject irrelevant, uninteresting, or even obsolete.

Can one measure the bulge mass in a quasar?

Yes, but it is not trivial. This can be seen in the study by [187]. M_{bulge} in active galaxies is determined by measuring the velocity dispersion of the stars in the bulge, either the Ca II triplet at $\lambda\lambda$ 8498, 8542, and 8662 Å (e.g., [43, 114, 123, 187]) for $z \lesssim 0.06$ or a broader region of stellar absorption lines (e.g., at λ 3900–4600 Å, 5100–5500 Å [7, 67], or at $\sim 1.5 \mu\text{m}$ [196]) for sources more distant than $z \sim 0.06$ where the CaII triplet lines sit in the water-vapour bands. This requires that we are able to detect these stellar features in the spectra of quasars.

Due to the strong central source in quasars that often outshines the host galaxy, it is either not possible or it is a significant challenge to detect these faint features. The light from the quasar nucleus simply dilutes the absorption features to a strong degree. The stellar absorption features are easier to see for nearby quasars or quasars

with weak nuclear sources compared to the host galaxy. Some astronomers therefore prefer to study quasars where the nuclear source has been weakened internally or externally, for example, by dust and gas extinction (e.g., [27, 67]). Since these quasars are heavily extinguished at blue wavelengths, it is possible that this method selects extreme sources in terms of their intrinsic properties or in their evolution; therefore, care is needed when interpreting the results.

One of the few studies that are able to directly measure the bulge velocity dispersion in bona fide luminous, nonextinguished nearby ($0.15 < z < 0.3$) quasars is that of [193]. The authors corrected off-nuclear spectra for scattered light from the nucleus and measured the widths of the Ca H and K and the MgIb lines, finding the Ca lines most reliable. With the aid of HST imaging of their (PG, PKS, and PHL) quasars, they were able to place their quasars on the fundamental plane (the authors did not determine the M_{BH} values) and found the bulges of both radio-loud and radio-quiet quasars to occupy the region for massive, quiescent ellipticals, although the radio louds tend to be larger and more massive (larger effective radius and bulge velocity dispersion). So it seems safe to conclude that host galaxies of quasars have properties very similar to those of normal, local massive ellipticals.

Astronomers can also use special instrumentation and techniques to limit the amount of nuclear quasar light that makes it into the spectrum used to measure the velocity dispersion of the bulge stars. Watson et al. [187] used the laser guide star adaptive optics on the Gemini North 8-m telescope with the near-infrared integral field spectrometer (IR IFS) which helped these authors obtain a high contrast of the stellar light relative to the quasar light. However, this technique has not been used extensively yet, but it is necessary in order to avoid that our studies and results are subject to potential significant selection effects which will skew our view of the quasar population. This technique allows virtually any relatively bright quasar to be observed.

Dasyra et al. [33] successfully used the widths of CO stellar features in the IR to measure the velocity of these stars. This is convenient when the optical stellar features such as the CaII triplet lines are redshifted into the telluric absorption and emission features which significantly hamper reliable measurements.

Some studies resort to using the velocity of the CO gas in the radio (e.g., [160, 179, 185]) as a proxy for σ_* .

This can be convenient for luminous quasars too distant to observe even the IR stellar CO features. One complication is that we currently do not have a robust way to calibrate the CO gas velocity measurements such that they uniquely reflect the equivalent of the bulge stellar velocities. Ho [69] presents a prescription for obtaining improved $M_{\text{BH}} - M_{\text{bulge}}$ estimates involving the IR luminosity, the CO disk inclination, and a crude relationship between σ_* and the maximum velocity in the CO gas rotation curve. However, the unknown extent and inclination of the CO gas inhibit an accurate correction. Another significant caveat is that it is unclear whether the CO gas is actually virialized at early epochs ($z > 3$) where this method is commonly used. If the line widths do not reflect ordered relaxed motion around the galaxy center, then we cannot use this line emission to estimate M_{bulge} or the dynamical mass of the galaxy.

Is the relation between bulge mass and black hole mass the same as for nonactive galaxies?

Essentially, yes. Again, there are two ways to study this relationship, either as the $M_{\text{BH}} - \sigma_*$ or the $M_{\text{BH}} - M_{\text{bulge}}$ relation. Currently, we see the $M_{\text{BH}} - \sigma_*$ relations are similar but do see some differences for the $M_{\text{BH}} - M_{\text{bulge}}$ relations. I will address each in turn.

For the $M_{\text{BH}} - \sigma_*$ studies where a random value of f is adopted equivalent to an isotropic spherical velocity field, the active galaxies tend to lie just below the $M_{\text{BH}} - \sigma_*$ relation for quiescent galaxies (e.g., [58, 123]) by a small margin of about 0.25 dex. The complication is the unknown kinematic structure of the broad-line region which sets the absolute zero point of the black hole mass scale, that is, the value of f . If one assumes that the black holes in the local active galactic nuclei will not grow significantly in the future, then it is fair to assume that the $M_{\text{BH}} - \sigma_*$ relationships for quiescent and active galaxies, respectively, are very similar. This assumed similarity then allows us to find the average value of f for the current sample of nearby AGNs and quasars. Onken et al. [123] established the value of the f -factor this way and calibrated the zero point of the mass scale for actively accreting black holes. This calibration is still in use.

The assumption that the local active black holes will not grow significantly in the future is not a too unrealistic considering that the local AGNs have Eddington luminosity ratios that are significantly lower than that of quasars (~ 100 – $1,000$ times lower; [141]). The assumption is also thought to be reasonable because active galaxies are hosted by galaxies with properties just like quiescent galaxies and because AGNs in our local universe are much less active than at redshifts of about 2–3. The latter is evident from both space density and luminosity function studies (see, for example, Fig. 11.3 of [134]) which shows that quasar and AGN activity decreases with cosmic time after the quasar epoch, thereby turning active black holes and galaxies into their quiescent counterparts that we observe as normal galaxies locally.

When studying the $M_{\text{BH}} - M_{\text{bulge}}$ relationship we are again facing the challenge of the strong central nuclear source: the host galaxy light is so faint in comparison. This means that special care is needed to limit the spatial extent of the nuclear light both when we observe these sources and also when we measure the luminosity of the host galaxy light. If the spatial resolution is insufficient, it is difficult to separate the nuclear and stellar components, and the host luminosity is easily overestimated. This is likely what happened in the early studies of the $M_{\text{BH}} - M_{\text{bulge}}$ relationship in AGNs (e.g., [181]). In a recent study, [13] did a careful job of modeling simultaneously the two-dimensional stellar light distribution from the host galaxy and the nuclear emission component using a selection of high spatial resolution images from the Hubble Space Telescope and ground-based images of the nearby AGNs with robust mass determinations based on reverberation mapping. This work allows significant progress to be made in our understanding of the nuclear source and its relationship with its host galaxy. The reason is that we now have very good measurements of the bulge luminosities of these sources that are only minimally affected (if at

all) by the nuclear emission component. We can now study and compare the $M_{\text{BH}} - M_{\text{bulge}}$ relations for active and quiescent black holes, respectively. This work is also important because, in addition, it allowed us to properly correct the nuclear luminosity for the unwanted host galaxy contribution. The spectra obtained as part of the monitoring campaigns that mapped out the relationship between the size of the broad-line region and the nuclear luminosity (the $R - L$ relationship) contain sometimes a significant amount of starlight because the objects are nearby and the observing aperture was quite large. This work finally established the *internal* $R-L$ relationship which characterizes the location of the broad emission-line gas that we use to estimate the mass of the black hole.

Bentz et al. [14] find a $M_{\text{BH}} - M_{\text{bulge}}$ relation for the AGNs with a slope of about 0.8 and a scatter of about 0.4 dex. Both the scatter and the slope are somewhat smaller than those of the relationship for quiescent elliptical galaxies [45]; fitting to the [45] data yields a slope between 1.1 and 1.4 depending on the fitting method, and the scatter is ~ 0.7 dex. It is unclear why there is such a large difference in the slope of the two relationships. But the methods that are used to determine the black hole masses of quiescent and active black holes both have uncertainties. For example, if indeed [97] are correct in their suggestion that neglecting radiation pressure on the broad-line gas underestimates the black hole masses, then we might expect the more massive active black holes to be subject to a larger correction. This would make the $M_{\text{BH}} - M_{\text{bulge}}$ relationship steeper. On the other hand, the dataset used to establish the $M_{\text{BH}} - M_{\text{bulge}}$ relationship for quiescent galaxies is not as homogeneous and consistently high quality as the images currently present for the AGNs. Graham [54] carefully updated the quiescent galaxy sample and tried to compensate for the inhomogeneity in the dataset. In doing so, he did find a tighter relationship with a slope of 0.75–0.8. While more work is of course needed to settle the issues related to both active and quiescent black hole masses, it is clear that we really do need to obtain high-quality data and to do actual two-dimensional bulge-disk decompositions in a homogeneous and consistent manner for a large sample of galaxies if we are to make significant progress on understanding these relationships and how they may vary depending on the activity of the black hole.

Moreover, there is an apparent discrepancy between the $M_{\text{BH}} - \sigma_*$ and $M_{\text{BH}} - M_{\text{bulge}}$ for quiescent galaxies which may be due to a bias in the galaxy samples toward sources with large velocity dispersions for their luminosities [17, 90, 171, 199]. This bias may also affect the $M_{\text{BH}} - M_{\text{bulge}}$ relationship for quiescent galaxies.

For active black holes, there are also other uncertainties in the mass estimates such as the unknown velocity structure of the broad-line region and the source inclination, but they are mainly expected to affect the general scatter around the $M_{\text{BH}} - \sigma_*$ and $M_{\text{BH}} - M_{\text{bulge}}$ relationships as opposed to their slopes.

Is it the same for all AGN classes?

Good question! We might expect the relation to depend on the AGN class if indeed the relation depends on the type of quiescent galaxy. We do not have a clear picture of this situation for the AGNs. For one, BL Lac and blazars often have weak or no broad emission lines in their spectra, so it is difficult to determine their black

hole masses using the virial method. But since BL Lac objects appear to reside in host galaxies that fall right on the fundamental plane of quiescent elliptical galaxies [195], it is fair to expect they would obey the $M_{\text{BH}} - \sigma_*$ or $M_{\text{BH}} - M_{\text{bulge}}$ relations in a similar fashion as normal elliptical galaxies. For Seyfert-2 galaxies—the galaxies for which the broad emission-line region if present is not directly visible—we do not yet have a convenient way of independently estimating the black hole mass. So at present, we do not know where these active galaxies would fall in the $M_{\text{BH}} - \sigma_*$ diagram in relation to the other active galaxy classes.

Most of the studies that address the $M_{\text{BH}} - \sigma_*$ relation for active galaxies have targeted Seyfert-1 galaxies (e.g., [43, 114, 123]) because the CaII triplet lines are readily detectable and measurable. For quasars, the powerful nuclear source strongly dilute these features and the large quasar distances often place them in a part of the spectrum that is difficult to observe so often, alternative approaches are applied.

However, since the host galaxies of luminous nearby radio-loud and radio-quiet quasars do lie on the fundamental plane for massive, quiescent ellipticals [193], we expect at least quasars in the nearby universe to fall on the local $M_{\text{BH}} - M_{\text{bulge}}$ relation.

I know of three studies that measure directly the stellar velocity dispersion in the bulge of five nearby PG quasars using both the IR stellar CO absorption lines [33] and Gemini integral field spectroscopy (GIFS; [60, 187]). Three quasars lie on the local relation, while two lie above it; one quasar have improved σ_* measurement based on GIFS, confirming it is an outlier. This is indeed very curious—also in the light of the fact that all studies of the $M_{\text{BH}} - \sigma_*$ relationship at higher redshifts find that quasars fall above the locally defined relationship. That is, their bulge velocity dispersions are relatively lower than the black hole mass compared to local AGNs. It is premature to make conclusions regarding a potential difference in the $M_{\text{BH}} - \sigma_*$ relation for quasars and for Seyfert 1s based on so few objects.

After all, it is unclear whether this is to be expected because luminous quasars have some of the most massive black holes, and a random merger scenario predicts the most massive black holes to lie a little on the high side [75]. One may also wonder if this apparent discrepancy is because a too shallow slope has been assigned the local $M_{\text{BH}} - \sigma_*$ relationship? There has been some debate over which objects should be included and which corrections to apply to the velocity dispersion measurements (e.g., [37, 42, 49]). As a result, the slope has varied between 4 and 5. Graham et al. [56] argue the correct slope should be 5 when all morphological galaxy types are included in the analysis which covers black hole masses between $10^6 M_{\odot}$ and several times $10^9 M_{\odot}$. So to settle the issue of potential differences in the $M_{\text{BH}} - M_{\text{bulge}}$ relationships depending on black hole activity and subtypes of AGNs, we need to first establish the slope, offset, and intrinsic scatter in both quiescent and active galaxies with higher accuracy.

There is, however, one AGN class that may exhibit a real difference. Some studies indicate that a subset of the Seyfert-1 galaxies, known as narrow line Seyfert-1 (NLSy1) galaxies, tend to lie below the $M_{\text{BH}} - \sigma_*$ relation for quiescent (and other active) galaxies [24, 61, 101, 102, 156]. NLSy1 galaxies have broad emission lines that are typically somewhat narrower than other Seyfert-1 galaxies, specifically their

Balmer emission lines have widths less than $2,000 \text{ km s}^{-1}$. The general impression we have of them is that they have highly accreting black holes of lower mass than other Seyfert 1s—by about an order of magnitude [61, 101]. Since the NLSy1s also have luminosities comparable to the Seyfert 1s, this suggests that their Eddington luminosity ratios $L_{\text{BOL}}/L_{\text{Edd}}$ are rather high.

It is most likely the inferred high $L_{\text{BOL}}/L_{\text{Edd}}$ values of NLSy1s that place them below the $M_{\text{BH}} - \sigma_*$ relation. Shen et al. [156] established that for a subset of 900 quasars in the Sloan Digital Sky Survey, the objects with higher $L_{\text{BOL}}/L_{\text{Edd}}$ values lie offset from the $M_{\text{BH}} - \sigma_*$ relation of the objects with lower $L_{\text{BOL}}/L_{\text{Edd}}$ values. This is consistent with the interpretation that black holes in objects with high $L_{\text{BOL}}/L_{\text{Edd}}$ values are still actively accreting and have not yet reached their final mass, while the objects with lower $L_{\text{BOL}}/L_{\text{Edd}}$ values are closer to their final mass since the central engine is fading out as the black hole accretes less and less material.

The reality of this result for NLSy1s has been questioned because the early studies used the width of the [OIII] $\lambda 5007\text{\AA}$ emission line as a proxy for the bulge velocity dispersion; this proxy displays significant scatter with the velocity dispersion [22], and the emission line can be blue asymmetric due to internal (outflow) motions in the narrow-line region (NLR) itself. Such internal motions would tend to broaden the [OIII] line and thereby shift the data points to the right in the $M_{\text{BH}} - \sigma_*$ relation. However, this cannot be the reason based on the results of [156] who analyze the velocity dispersion as measured from template fitting to the stellar features in the spectra.

At the recent conference “NLSy1 galaxies and their place in the Universe” in Milan, April 2011, quite convincing evidence was presented that NLSy1s lie in galaxies with not classical bulges but pseudo-bulges which tend to scatter on and below the $M - \sigma$ relation. This would thus argue that it is the physics of the galaxy (bulge) more than the L/L_{Edd} ratio that determines whether (active or quiescent) galaxies fall on the relationship. Time will show if both play a role here.

Does this ratio depend on redshift?

This is the million dollar question. By investigating the redshift dependence, we can test the hypothesis that the black hole and bulge components always grow in synchronization. If the $M_{\text{BH}}/M_{\text{bulge}}$ ratio stays constant, it would support that hypothesis. If not, we would have to conclude that the $M_{\text{BH}} - \sigma_*$ relation is simply the end product of giga-years of evolution (if indeed the relationship is genuine and not a selection effect). In any event, it is hoped that we can use this ratio and how it varies with redshift to learn more about the evolution of the galaxy and its black hole. For example, does the black hole grow first, followed by the bulge, or viceversa?

A number of studies have addressed this issue, employing different techniques and many report a high $M_{\text{BH}}/M_{\text{bulge}}$ ratio at higher redshift (e.g., [11, 27, 34, 67, 74, 109, 129, 130, 151, 169, 194]); a few find consistency, possibly due to large measurement uncertainties (e.g., [150, 159]) but see also [2] for a different approach.

Intriguingly, based on a large sample of 900 quasars spanning redshifts up to 0.452, [156] did not detect any significant change once the inherent $z-L$ dependence of their dataset is accounted for. Could the apparent redshift dependencies observed be due to selection effects? It is possible: most of the known quasars and active galactic nuclei at higher redshift will tend to be the most luminous and thus the most massive of the population at a given epoch. However, the [169, 194] studies are based on Seyfert galaxies at redshifts of 0.36 and 0.57, respectively, which have lower luminosity than typical quasars and are thus not the most luminous at those epochs, yet these objects still lie above the local $M_{\text{BH}} - \sigma_*$ relation; the authors also use simulations to argue against selection effects. While the uncertainties in the black hole mass estimates (of $\sim 0.3-0.4$ dex; [103, 172, 174]) would seem to make the offset appear worse than it really is, [169] show that increasing the random error on each mass estimate to 0.6 dex (based on [174]) only increases the random error on $\Delta \log M_{\text{BH}}$, the offset in M_{BH} from the local relation, by 0.03 dex to 0.17 dex; thus, the effect is negligible.

Radio measurements of the CO gas in quasars at redshift six (e.g., [179, 185]) also indicate higher black hole masses for a given velocity dispersion as measured from the CO line widths. Taken together, these data would seem to argue that the black hole grew and matured faster than the bulge. Wang et al. [185] estimated the dynamical mass of the detected CO gas by assuming a rotating disk configuration of 2.5 kpc in size inclined on average by 40 degrees to our line of sight (after correcting the CO line width according to [69]). The bulge mass was then estimated as the difference between the CO luminosity inferred gas mass and the dynamical mass. From this, the authors found a $M_{\text{BH}}/M_{\text{bulge}}$ ratio that is 15 times higher than the local ratio—in general agreement with other high- z studies. An interesting observation is that if these systems are to evolve onto the local $M_{\text{BH}} - M_{\text{bulge}}$ relation, then these $z \sim 6$ systems should end up with bulge masses of $10^{12} M_{\odot}$. However, the detected amount of CO gas in these systems would only be able to supply less than 3% of the required mass. This shows that most of the gas needed to build up the stellar bulge has to be assembled at later epochs, for example, through major and minor galaxy mergers. If correct, this is very intriguing. Although cosmological models of the evolution of dark matter halos favor a hierarchical buildup (e.g., [80]), models of galaxy evolution have always favored the (near-) complete build-up of the bulge or the galaxy before the nuclear activity of the black hole turns on (e.g., [57, 70]). When we first mapped out the M_{BH} values of distant quasars, we were struck by the apparent assembly of powerful radio galaxies during epochs as late as redshifts of 3.5–4 (see discussion by [173]). Since radio galaxies are known to be “mis-aligned” radio-loud quasars [4, 8] and the structure of AGNs is relatively similar across the subclasses, it is fair to expect this may be a common scenario [173]. Despite the indications from observations, such an unconventional picture was hard to accept for many scientists at the time. It is interesting that although a universally high $M_{\text{BH}}/M_{\text{bulge}}$ ratio is not widely acknowledged yet due to the many unresolved issues, the paradigm is starting to shift, and more scientists are now more open toward such an interpretation.

However, it is important to remember the caveats (see above discussion). In addition, we only have a CO disk size estimate (~ 2.5 kpc) for a single $z \sim 6$ quasar [179], and the inclinations are also unknown. If the low-velocity CO gas is in fact located at larger distances, the dynamical mass estimate would increase. Yet we may expect that the CO gas is concentrated in the center if the host galaxy has been through one or more gas-rich mergers (e.g., [38, 70]), thereby strongly underestimating the bulge mass and velocity dispersion. Needless to say, we are anxious to know what the situation is in reality as these high-redshift quasars are systems where we can really learn how the first black hole growth and galaxy assembly happened.

Clearly, we still have a way to go before we can confidently declare that we know what the $M_{\text{BH}} - \sigma_*$ and $M_{\text{BH}} - M_{\text{bulge}}$ relations are, how they came about, and whether they change with redshift or galaxy type.

What are the major sources of uncertainty in the black hole mass determinations of quasars?

Let me briefly summarize how we determine M_{BH} because some of the uncertainties also lie in which methods you use and how you measure the important parameters. The uncertainties that affect all methods I will outline thereafter.

M_{BH} estimates in galaxies make use of the virial theorem, that is, $M_{\text{BH}} = rV^2/G$, where V is the velocity of gas or stars at a distance r from the black hole and G is the gravitational constant. In quiescent galaxies, we measure the motion of stars and gas orbiting very close to the black hole. We cannot use this method for quasars due to the strong nuclear source. Instead of attempting to resolve the nuclear regions spatially, we can resolve it temporally.

The most robust mass measurements of active black holes are made using the reverberation mapping (RM or echo-mapping) technique. In this case, the distance r of the broad-line gas is measured by means of the light travel time delays between bursts of continuum emission and the responding broad-line emission, and the gas velocity V is measured from the emission line width. However, this technique is quite resource intensive and is not conveniently applicable to distant quasars. This is because more massive systems (black hole and accretion disk) being larger vary on longer time scales—enhanced by cosmic time dilation—and with smaller amplitudes. With such modulated variations, it is difficult to accurately clock the variations. Instead, we resort to an approximation to the RM method, namely, the single-epoch mass estimates (or sometimes called “the mass scaling relations”).

It turns out that we can actually approximate the virial mass quite well using a single spectrum of a quasar, measuring simply the broad-line width of either $H\beta$, Mg II , or C IV and the continuum luminosity near the emission line (e.g., [103, 107, 172, 174, 175, 198], see also [183]).

Statistically, these mass estimates match the RM masses to within a factor of 2.5–3; this is quite good considering the simple approximation it really is. This method makes use of an important result from reverberation mapping, namely, the radius–luminosity ($r - L$) relationship which shows that the distance to the broad-line gas scales with the square root of the nuclear continuum luminosity [13, 78]. It

is important to use the most recent work of [13]. The earlier incarnations of the r - L relationship [77, 78] neglected to correct for the contribution from the host galaxy to the AGN luminosity measured in the optical spectra which in some objects can be significant. As a result, those early relationships had a steeper slope of 0.6–0.7. When the host galaxy emission is properly corrected for the relationship has a slope of 0.5 [12, 13]. A too steep slope will overestimate the mass of the more massive black holes and underestimate those with low mass of about 10^5 – 10^7 solar masses. One must exercise care when using mass estimates and results from work on this topic as, clearly, not all past work use the appropriate relationship. It gets even more confusing because there are a number of different mass scaling relations from which to estimate the M_{BH} , each with their own calibration. Unfortunately, most of these relationships are not intercalibrated to be on the same mass scale. So it gives a wrong picture when authors compare masses estimated with the different scaling laws because they each have their own zero-point and/or slope in some cases. Apparently unaware of this, a number of authors have compared mass estimates obtained from the individual emission lines ($\text{H}\beta$, Mg II , C IV) based on different calibrations thereby finding that sometimes they give consistent results (e.g., [156, 186]), but just as often that they do not (see, for example, [5, 9, 39, 84, 119, 121, 153]). The discrepancy is often enhanced because authors have to use data that are not obtained at the same time or processed in a homogeneous way (see, for example, discussion in [174]). Dietrich and Hamann [39] make an interesting comparison of some of the mass scaling laws commonly used at that time. Based on these abovementioned comparisons, the general perception in the literature seems to be that Mg II is a good substitute for $\text{H}\beta$ despite the fact that their line widths do not scale one to one—in fact, the slope is tilted toward larger $\text{H}\beta$ line widths (e.g., [183])—and that C IV is a poor and biased mass estimator (but see also [156]).

Briefly speaking, there are two types of uncertainties that are currently present in M_{BH} estimates: those that can be avoided or minimized when care is exercised and those that are a real technical challenge at the present time. Among the former uncertainties are, as mentioned, that we often lack data obtained concurrently across different wavebands or only have limited wavelength coverage. This means that we can only obtain a single broad-line estimate of the mass or that we will have multiple broad-line-based mass estimates that may be affected by source variability, differences in data acquisition and processing, and differences in mass scale zero-point in many cases.

The solution is first to use mass scaling relations that are intercalibrated for all three emission lines. At present, I am only aware of one set of equations (see [174, 175]) for which all three emission lines ($\text{H}\beta$, Mg II , and C IV) are calibrated to be on the same mass scale and are also anchored in the most recent robust RM masses [141]. Next, it is important to use as many measurements as possible for a more accurate estimate of the mass by means of using two or more emission-line estimates or by using spectra obtained at multiple epochs. After all, the RM method also determines the mass from multiple measurements. The broad-line region is a dynamic place, and all the line widths and distances change depending on the luminosity state, the density distribution, the velocity structure, and the variability

status of the broad-line region the instant we obtain our spectrum. The ensemble lines and their measurements will therefore give a better estimate of the black hole mass than a single measurement in a similar way that it is difficult to determine the slope and zero-point of a line with a single datapoint (this is actually what we are doing when estimating the black hole mass). If you have two or three datapoints you are better off, but you get the more precise determination or estimate, the more data points you have. The virial relation diagram of [137] (their Fig. 1) illustrates this point very well: the individual emission-line measurements spread around the fit that yields the black hole mass (through the zero-point), but these measurements also slide up and down the relationship at different epoch, while the slope and zero-point of the relation is constant, as one would expect if it reflects the black hole mass. If we were to pick out an individual measurement and use, that for our estimate, it is clear that we may either slightly over- or underestimate the mass.

Another issue that is now apparent is that the use of spectra with a lower S/N (of about 10–20 per pixel; [35]) will yield not only larger uncertainties but also a systematic bias that is not mitigated by fitting the data with line profile models. This is an important result because this is quite contrary to what has been the common belief until now. The fact that a rather tight $r - L$ relationship (~ 0.11 dex; [136]) is observed when only the highest quality data are used also shows that the largest uncertainties in the mass estimates will ultimately be related to our ability to determine or approximate the velocity dispersion of the broad-line gas that varies. There are two aspects of this issue: how well can we measure the line-of-sight velocity in the data and how does this velocity relate to the intrinsic velocity dispersion that we seek? The former is complicated by the fact that there is no single line width measure or a standard way that line widths are measured. This can lead to sometimes systematic differences between measurements of different authors [35].

The second aspect brings me to the uncertainties that are related to the technical challenges inherent in the method itself or any method relying on dynamics to estimate M_{BH} . The main one is the unknown velocity structure (see, for example, [29, 123, 134]). If the velocities are not isotropic, then our inability to determine accurately the inclination of the central engine relative to our line of sight complicates this issues even further.

We do not have good inclination measurements for most AGNs because the large-scale gas and dust environment in the host galaxy does not necessarily reflect the inclination of the accretion disk in the central engine (e.g., [81]). Only for radio-loud sources—which constitute only about 10% of the quasar population—can we get an indication of the small-scale inclination since the ratio of radio flux density in the lobes relative to the central radio core is a crude measure of inclination (e.g., [191, 192]). In the two extremes, we will see mostly a strong core component for face-on sources and only see double lobe components for sources oriented with the jets in the plane of the sky.

However, using this crude inclination indicator, we now know that there must be a velocity component along the direction of the accretion disk since we see a tendency for broader $H\beta$ lines [191] and broader C IV line bases [176] in more inclined radio-loud AGNs. The fact that face-on sources have broad emission lines

that are (somewhat) wider than the spectral resolution shows that there must also be a velocity component out of the plane of the accretion disk (e.g., [29, 106]). However, there is no simple dependency on source inclination and the line profile shape for a nearby sample of AGNs for which the inclination could be estimated [29]: a particular emission line can be broad due to a mixture of black hole gravity, viewing angle, and the strength of the continuum flux, for instance. We may see the latter in the form of radiation pressure on the broad-line gas which acts to counterbalance the black hole gravity. Marconi et al. [97] show that if at play and corrected for, the scatter in the mass scaling laws will decrease by a factor of ~ 2 ; this is very intriguing. If real and ubiquitous, many mass estimates will increase over the current values. More work is needed to test this hypothesis. One problem we are facing is that to test the reality of radiation pressure, we need an independent measure of the intrinsic—that is, the *true*—black hole mass which we currently do not have a way to determine.

Thank you, Marianne. Efforts to measure M_{BH} are extremely important since the mass can only grow in time—a sort of clock that cannot be turned back—and is therefore related to the evolution of the accretion processes occurring in quasars. Once M_{BH} is known, it is in principle straightforward to derive the Eddington ratio that is directly proportional to the ratio between bolometric luminosity and black hole mass. The Eddington ratio governs the relative balance of gravitational and radiative forces, and is therefore expected to have a pivotal role in the structure of quasars.

5.6 The Eddington Ratio

Dear Ross (McLure), how can the Eddington ratio be determined observationally?

Before proceeding to discuss how the Eddington ratio might be determined observationally, it is worth considering for a moment what the Eddington ratio actually is. The Eddington ratio itself is a unit-less quantity which is the ratio of two different measures of a quasar’s luminosity, and is defined as $L_{\text{bol}}/L_{\text{Edd}}$. In this definition, the numerator (L_{bol}) is the quasar’s bolometric luminosity, which is simply the total luminosity of the quasar, integrated over all wavelengths. The denominator is the quasar’s Eddington luminosity (L_{Edd}) and is defined as the bolometric luminosity of the quasar if it were accreting material at the Eddington limit.

The Eddington limit, in turn, is a theoretic limit, which is defined by the balancing point at which the radiation pressure of the light emitted by the accreting black hole exactly balances its gravitational pull. At this point, higher rates of material accretion are effectively halted because the radiation pressure would overcome the gravitational attraction of the black hole, and at the Eddington limit, the quasar can therefore be thought of as running at *full throttle*. Although the derivation of the Eddington luminosity overly simplifies the physics of accretion (e.g., assuming

spherical geometry) at the centers of quasars, empirically, it does turn out to be a physically meaningful limit. In this scheme, quasars which are completely dormant will have an Eddington ratio of zero, quasars accreting material at the Eddington limit will have an Eddington ratio of one, and any quasars observed to have an Eddington ratio greater than one are referred to as “super-Eddington.” A key point is that the Eddington limit is directly proportional to black hole mass, and therefore, from an observational point of view, the process of determining the Eddington ratio involves measuring the bolometric luminosity and the black hole mass.

Unfortunately, measuring the bolometric luminosity of an individual quasar is far from straightforward. In order to do this properly, multifrequency observations spanning the full range of frequencies over which a quasar radiates (i.e., X-ray through to radio) are required. However, typically you do not have this information available, and all you have is a measurement of the optical luminosity of the quasar. Fortunately, at least as far as luminous broad-line quasars are concerned, their multifrequency spectral energy distributions (SEDs) are very similar in shape. Consequently, by determining the full multifrequency SEDs of a relatively small, but hopefully representative, sample of quasars [147], it is possible to calculate the so-called *bolometric correction factors* which convert between optical and bolometric luminosity. On an individual, object-by-object, basis, these correction factors can be wrong by factors of a few, but in a statistical sense, they should give a reliable estimate of the average bolometric luminosity of a sample of quasars.

In order to estimate a quasar’s Eddington ratio, the second physical parameter we need to measure is the black hole mass. However, when using the virial black hole mass estimator this leads to a major complication. As discussed above, in practice, the virial mass estimator, is largely dependent on a measurement of the quasar’s optical luminosity, that is, $M_{\text{BH}} \propto L_{\text{opt}}^{0.5} \text{FWHM}^2$. At the same time, however, your estimate of the bolometric luminosity is typically also proportional to the optical luminosity, that is, $L_{\text{bol}} \propto L_{\text{opt}}$. Consequently, the two crucial variables in the estimate of the Eddington luminosity are not actually independent, and a correlation between Eddington ratio and quasar luminosity of the form $L_{\text{Edd}} \propto L_{\text{opt}}^{0.5}$ would appear inevitable.

In order to circumvent this problem, it is necessary to break the degeneracy between the bolometric luminosity and black hole mass measurement. In terms of estimating the Eddington ratio for large, statistical, samples of quasars, this is a difficult limitation to overcome, because the virial method is the only technique available for estimating the central black hole masses. However, in principle, it is possible to measure the true bolometric luminosity by compiling the necessary multifrequency observations for each quasar. Traditionally, this has been a close to impossible task; however, with the increasing availability of large-area, multifrequency survey fields (e.g., GOODS, COSMOS), there are now many square degrees of sky over which it is possible to derive individual bolometric luminosity estimates.

What sort of range in Eddington ratio is observed for quasars?

To answer this question, it is first necessary to decide at what luminosity an AGN can be described as a “true” quasar. From a purely observational standpoint for

many years, it was traditional to set the luminosity threshold at an absolute B -band Vega magnitude of $M_B < -23$. An alternative, and perhaps fairer approach, is to base your decision on the bolometric luminosity. For the sake of argument, a perfectly reasonable (if ultimately arbitrary) choice might be to regard everything with $L_{\text{bol}} > 10^{45} \text{ erg s}^{-1}$ ($>10^{38} \text{ W}$) as a quasar. Working from this definition, estimates of the distribution of quasar Eddington ratios show that they typically lie in the range $0.01 < L_{\text{bol}}/L_{\text{Edd}} < 1.0$ [108, 155].

Armed with the observational results, it is worth considering whether or not they make sense within our model of how quasars work. In fact, the lower limit of $L_{\text{bol}}/L_{\text{Edd}} \simeq 0.01$ does make sense from a theoretical perspective, because if the accretion rate, falls much lower than this, the accretion disk is predicted to switch from being radiatively efficient to radiatively inefficient. In a radiatively inefficient accretion flow the gravitational potential energy of the accreted mass is said to be advected straight into the black hole, rather than being converted into radiation, forming a so-called advection dominated accretion flow [113]. In this scenario, the black hole would stop emitting the strong optical continuum and emission lines which are the basis for selecting it as a quasar. Finally, given the simplified nature of the calculation of the Eddington limit, it is interesting to note that the abundance of luminous quasars which have Eddington ratios substantially larger than unity is low [108, 155]. The fact that the Eddington limit appears to be a physically meaningful barrier must be telling us information about the physics of mass accretion, and is certainly relevant to the previous question.

Dear Bozena (*Czerny*) and Krzysztof (*Hryniewicz*), the Eddington ratio or equivalently, the luminosity-to-mass ratio has emerged as one of the most important accretion-related parameters in quasars. How might the Eddington ratio affect the structure and dynamics of the quasar innermost regions?

Eddington ratio is a very simple and a very useful concept. If a spherically symmetric object is a source of radiation and gravity, the radiation pressure acting on a particle decreases the gravitational attraction by the object. The luminosity required to balance the gravity is defined as the Eddington luminosity. Specifically, the definition usually assumes that the atmosphere is fully ionized, the radiation interacts with the plasma only through the electron scattering, and electrons are coupled to protons through Coulomb interaction.

The atmosphere of the body can be static only if the luminosity is lower than the Eddington luminosity; higher luminosity will drive an efficient outflow.

The value of the Eddington luminosity depends only on the mass of the object, not on its radius. Thus, the concept of the Eddington luminosity applies to stars, but it can also be used for accreting black holes. Since the luminosity in this case is related to the accretion rate, we can also define the Eddington accretion rate. Typically, the definition includes the accretion efficiency, but sometimes the efficiency is not included (assumed to be 100%).

Eddington accretion rate is important for estimates of the global evolution of active nuclei. Salpeter timescale is defined as an e-folding rise time of the mass for the accretion rate equal to the Eddington rate ($t_s = M/\dot{M}_{\text{Edd}}$). This timescale

is universal, independent of the black hole mass, and it is of order of 50 million years, assuming 10% efficiency. This means that the growth of the black hole mass typically happens in cosmological timescales.

The assumptions underlying the concept of the Eddington luminosity are not satisfied in the case of objects like active galaxies. AGNs with their rotationally supported accretion disks are not spherical. Super-Eddington accretion rates are possible. Also, for some material (not fully ionized or pair-dominated plasma), the radiatively driven outflow will appear even for low Eddington ratio due to force multiplier, that is, opacity higher than for electron scattering. However, the qualitative trend is likely to be preserved—in case of the accretion rate close or above the Eddington rate, the disk structure becomes modified in comparison to the classical model and radiatively driven outflow likely to develop. Therefore, the Eddington ratio is the key parameter in the description of the accreting black holes. The close similarity between the galactic black holes and active galactic nuclei accreting at the similar Eddington ratio shows that the mass of the central black hole serves mostly just as a linear scaling of the phenomenon in spatial and time domain, while the Eddington ratio determines the proportions between the cold disk and the hot optically thin plasma, and consequently, determines the overall spectral shape of the emitted radiation and the outflow character and intensity.

The observational appearance of an active nucleus depends not only on its Eddington ratio but on the viewing angle, with type-2 objects being an extreme example. However, the Eddington ratio specifies the true (even if obscured) central engine behind the scene.

The dream of a theoretician is thus to have a model of the innermost part of an active nucleus parameterized by the black hole mass, spin, and the Eddington ratio. There is only one caveat: we know that the process is not stationary, and the observations of galactic sources serve as a warning that this non-stationarity imposes an additional complication. In galactic sources, for moderate/high Eddington ratios, the situation close to the black hole is characterized both by the Eddington ratio and a “state.” At the same Eddington ratio, the source may be in a hard state or in the soft state. The same phenomenon is described as the hysteresis effect in transient sources: the transition from the hard state to the soft (disk-dominated) state at the beginning of the outburst happens at higher value of the Eddington ratio, while the transition back to the hard state at the end of the outburst happens at the Eddington ratio by a factor of a few lower. We do not know whether the same phenomenon takes place in AGNs since the determination of the Eddington ratio is accurate within a factor of a few, and the expected timescales of such a transition (a timescale of a day in galactic sources suggests a timescale of a thousand years in AGNs) are so long that the effect, if real, can be only seen statistically.

Nevertheless, it is very important to have large samples of AGNs with determined Eddington ratios in order to study the dependence of the spectral properties on this parameter, including the ranges of expected dispersion. The number of quasars and lower luminosity AGNs available for such studies is rapidly growing, thanks to SDSS. It will serve as a test for future models of the accretion and the accompanying outflow; for the moment, we have very limited understanding of the phenomenon,

with some progress in modeling the optically thick disk, disk winds, and the radiative interaction between the hot X-ray emitting plasma and the disk or the surrounding medium, but no insight in the dynamical coupling between the two media. This last issue limits considerably our theoretical understanding of the trends in the properties in the innermost region with the Eddington ratio. However, both simple intuition and observations suggest that in sources with high Eddington ratios, the inflow is more optically thick (since the amount of inflowing material is higher), and the uncollimated outflow in the form of wind is more efficient, while in the sources with low values of the Eddington ratio, the inflowing material is mostly optically thin and the jet-like collimated magnetically driven outflow seems more important.

5.7 Narrow-Line Seyfert-1 as Extreme Radiators

Phenomenologically, we find narrow-line Seyfert-1 sources and radio-loud quasars at opposite ends of a sequence that appears to be driven by Eddington ratio (and BH mass). The radio-quiet NLSy1s appear to be radiating near the Eddington limit, while some radio louds radiate at less than 1% of L/L_{Edd} . NLSy1 show the narrowest broad lines implying the lowest BH masses, while radio louds (and some quiet) show BH masses ~ 2 dex larger. Does this make sense to you? Many observed properties of quasars appear to be different for sources with lines broader than and narrower than $H\beta$ FWHM = 4,000 km s $^{-1}$ (which corresponds roughly to $L/L_{\text{Edd}} \sim 0.2 \pm 0.1$). Can you envision some fundamental change in BLR structure that might explain the change?

Narrow-line Seyfert-1 galaxies as a class were introduced by [124]. The definition is based on properties of the broad emission lines: a source belongs to this class if the line width of $H\beta$ is lower than 2,000 km s $^{-1}$ and the ratio of the [OIII]/ $H\beta$ lower than 3. The need for a new class was purely observational and restricted to optical range of AGN spectra, and to sources of moderate absolute luminosity (Seyfert galaxies or nearby quasars).

However, further studies soon showed that there is something more deep in this idea than just a convenient spectral classification. A correlation between the width of the $H\beta$ line and the X-ray spectral slope was found (see, for example, [26]). The overall shape of the broad-band spectra of NLSy1 was found to be strangely universal, independent on the source luminosity [32]. The formal principal component analysis indicated that a single parameter catches most of the dispersion in the line and continuum properties of AGNs [23], and the NLSy1 galaxies reside at the extreme side of the trend, with radio-loud sources in the opposite side.

A suggestion of the deeper physical meaning behind this classification came quite early [144]. The NLSy1 galaxies are now broadly considered as high Eddington ratio sources, and their overall broad-band continuum spectral shape shows similarity with the galactic sources in their very high state. The PCA first eigenvector mentioned above is also identified with the Eddington ratio [23]. Radio-loud sources

are thus naturally at the other extreme since the radio-loud sources are shown to be grouping in the fundamental plane, with radio loudness decreasing with the dimensionless accretion rate. However, a few NLSy1 galaxies are known to be radio loud. The most likely explanation is that the emission lines in those sources are narrow not due to high Eddington ratio but due to very low inclination angle. For example, the detection of fast optical variability in RL-NLSy1 galaxy SDSS J094857.3+002225 points to the presence of a jet with a small viewing angle [91].

The connection between the Eddington ratio of the accretion flow and the properties of the BLR is not surprising. Higher luminosity for a given black hole mass implies higher ionization state of the circumnuclear material, and if the broad lines are formed at the specific value of the ionization parameter, BLR must be located further out in such sources. Since the motion of the BLR gas is roughly Keplerian, this means lower velocities and narrower lines than in lower luminosity sources.

However, with simple assumptions, we can go further into quantitative study of the connection between the Eddington ratio, the spectral shape, and the line width.

The radius of the BLR scales with the flux at 5500 Å, which in turn scales with the bolometric luminosity. Therefore, we have a relation:

$$r_{\text{BLR}} \propto (\dot{m}M)^{1/2}. \quad (5.5)$$

The line width, measured as FWHM, can be roughly identified with the Keplerian velocity at this distance:

$$\text{FWHM} \propto \left(\frac{M}{r_{\text{BLR}}} \right)^{1/2} \propto \left(\frac{M}{\dot{m}} \right)^{1/4}. \quad (5.6)$$

The classical blackbody disk emission also peaks at a frequency which depends on the disk parameters exactly in the same way (see, for example, [170]). This explains one puzzle: the universality of the broad-band spectrum of NLSy1 galaxies; since they have the velocities in the range 1,000–2,000 km s⁻¹, their spectra peak at roughly the same frequency, particularly if the range of the mass is rather narrow.

On the other hand, the significant change in the accretion flow pattern, and the relative contribution of the disk and the hot flow should be rather related to the Eddington ratio itself. This change of the pattern, including the change in the level of X-ray emission and X-ray spectral slope, can/should be reflected in the change of the BLR properties through the considerable change of the spectral shape of the irradiating flux.

This means that if such a change happens, let us say, at $\dot{m} = 0.1$ for sources of typical black hole mass $10^7 M_{\odot}$ and the corresponding value of the FWHM is 2,000 km s⁻¹, similar change for quasars with black hole masses $10^8 M_{\odot}$ should take place when the velocity is by a factor $(10^8/10^7)^{1/4} \sim 2$ higher. This is exactly what is seen in the paper by [166] where the classification of low-redshift quasars into type A and type B was introduced, and the limiting velocity was 4,000 km s⁻¹. The

two classes differed with respect to specific line properties as well as in the soft X-ray slopes. In case of even brighter, high-redshift quasars, with typical masses of $3 \times 10^9 M_{\odot}$, this limiting velocity should rise again. The scaling suggested by (5.6) may be too simplistic since the change in the disk temperature itself may additionally affect BLR properties, but the trend is likely to be preserved.

As for the change in the line properties with the transition from A to B sources, or from NLSy1 to BLSy1 sources, its nature is likely to be related with the change of the spectral shape of the radiation. Emission of high Eddington ratio sources is basically soft, while the low Eddington ratio sources have strong hard X-ray component. The line formation, the outflow rate, and the possibility of cloud formation due to thermal instability in the irradiated medium [87] are likely to be strongly affected by such a change. For example, low/high optical depth across the disk wind was used as an explanation of double/single-line profiles by [112].

The contribution to differences may also come from the cold outer disk restructuring, since the outer disk underlying BLR is self-gravitating only at high Eddington ratios [29].

Thank you, Bozena and Krzysztof. We are leaving the realm of physical processes to enter a domain that is influenced by the angle between the axis of symmetry of the quasar and our line of sight. There is no prediction here from the unification scheme for individual quasars; all type-1 quasars are supposed to be observed at an angle between a few degrees and 45–60 degrees. Inferring the aspect angle for each source from an observed orientation indicator is an open problem. An accurate knowledge of the aspect angle will greatly improve the accuracy of M_{BH} and Eddington ratio determinations.

5.8 Orientation Effects on Emission Lines

Dear Deborah (Dultzin), it is widely assumed that the observed properties of quasars depend upon the viewing angle. What are the salient observations that justify this assumption?

The search for a parameter space that might provide spectroscopic unification for all classes of broad-line-emitting AGNs motivated the “three-dimensional eigenvector 1” (3DE1) concept [167]. The 3DE1 parameter space has roots in the PCA analysis of the bright quasar sample (87 sources; [23]) as well as in correlations that emerged from ROSAT measurements of 86 sources [184]. Later, a 4DE1 space was defined [5, 168]. This 4DE1, as defined by the above authors, involves measures of:

1. Full width half maximum of broad $H\beta$ (FWHM $H\beta$).
2. Equivalent width ratio of optical Fe II and broad $H\beta$: $R_{\text{FeII}} = W(\text{FeII}\lambda 4,570) / W(H\beta_{\text{BC}})$.
3. The correlation defined by Wang et al. [184] involving the power-law photon index of the soft X-ray spectra (Γ_{soft}).

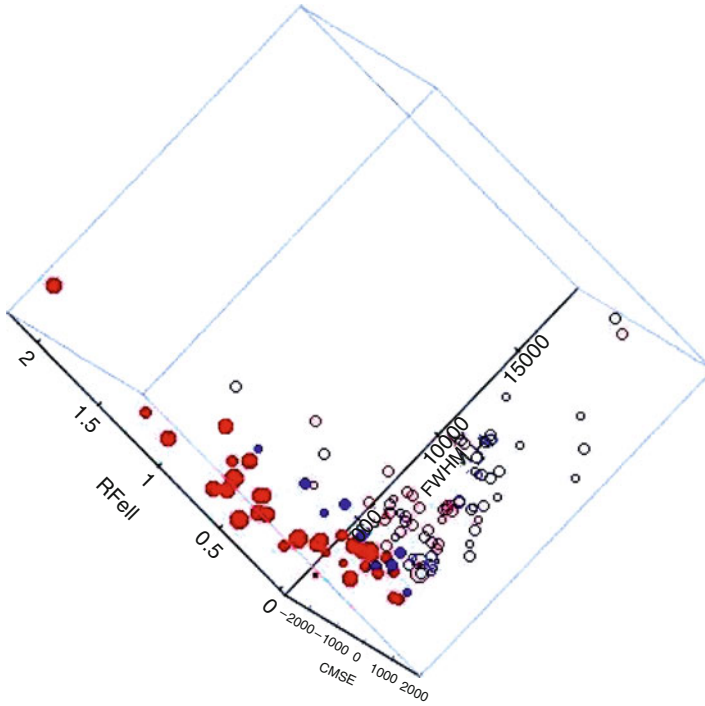


Fig. 5.6 Projection of a three-dimensional plot of the E1 parameter space; “x”-axis shows the R_{FeII} ratio, “y”-axis shows the CIV asymmetry (negative values are blue asymmetries), and “z”-axis shows the FWHM $H\beta$. *Red filled circles* are “Pop. A” RQ objects; *red open circles* “Pop. A” RL objects. *Blue filled and open circles* are “Pop B” RQs and RLs, respectively. The size is related to Γ soft. See text for definitions

4. A detailed measure of (4) C IV $\lambda 1549$ broad-line profile velocity displacement at half maximum ([168] and references therein).

Marziani et al. [99] showed that the observed correlation for radio-quiet sources can be accounted for if it is primarily driven by the ratio of AGN luminosity to black hole mass ($L/M \propto$ Eddington ratio) convolved with source orientation. According to these authors, L/M apparently drives the radio-quiet correlation only for the so-called Population B ($\text{FWHM}(H\beta) \lesssim 4,000 \text{ km s}^{-1}$) objects, which includes narrow-line Seyfert-1 galaxies and can be said to define an AGN “main sequence.” Source orientation plays an increasingly important role as $\text{FWHM}(H\beta_{\text{BC}})$ increases. They also point out that if low-ionization lines like $H\beta$ are emitted in a flattened configuration, then some effect of viewing angle is expected.

In Fig. 5.6, I show a three-dimensional display of the four-dimensional parameter space occupation. It can be clearly seen that the occupation is not randomly distributed, for this reason, [168] refer to a correlation space that might serve as an equivalent to the stellar H–R diagram. But of course, although quasars look like

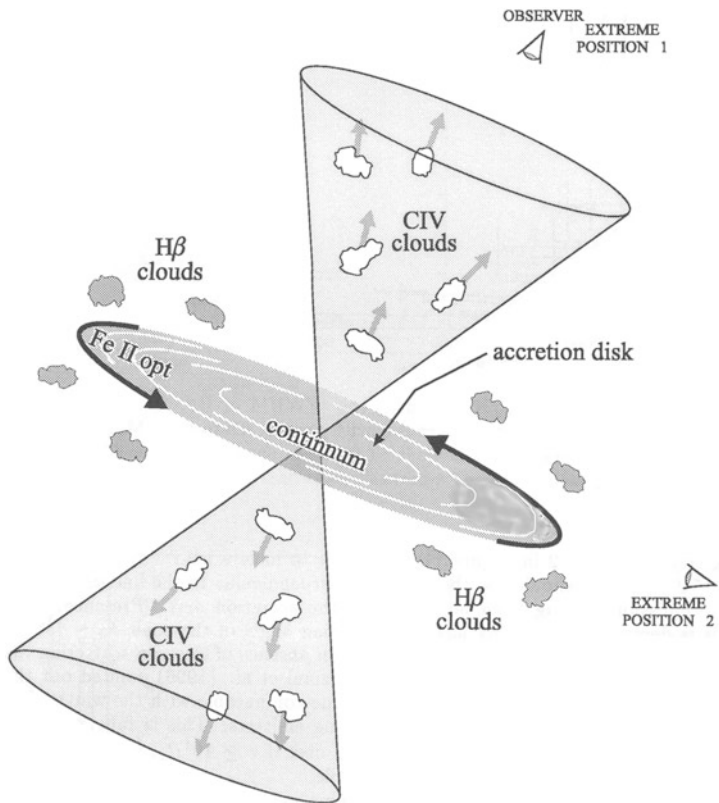


Fig. 5.7 The figure taken from [40] shows a probable geometrical configuration of the innermost emission region of quasars, which is in agreement with the 4DE1 parameter space

stars, they are much more complicated. For one thing, their inner structure is not spherically symmetric, and thus, orientation must play an important role in what we observe. In these figures, we have plotted all sources which have measurements for the four parameters mentioned above. The measurements are all ours (see [168] and references therein), except for Γ_{soft} . Wang et al. [184] used ROSAT data for 86 objects to fit a soft X-ray power law. We are presently preparing a better determination and more rigorous definition using XMM data ([3]).

With a very few exceptions (such as objects with superluminal jets), it is not possible to disentangle the physical from the orientation driving effects that produce the observed 11 main sequence in the 4DE1 space. However, it seems to me, that both drivers complement each other. In Fig. 5.7 (taken from [40]), we show a probable geometrical configuration—albeit simplified—of the innermost BLR of quasars. If we assume that:

- (a) The “soft X excess” has a thermal origin (which we are trying to confirm with the fits to XMM data) probably from the accretion disk (AD).
- (b) The FeII lines are emitted in a high-density medium which can be the AD.
- (c) Balmer lines, particularly $H\beta$, are also emitted either in the outer parts of the AD, or in a flattened configuration of gravitationally bounded clouds.
- (d) In most objects with large enough accretion rates to induce a wind from the AD, the CIV line is emitted from this wind, and is thus dominated by radial motions.

Then, the extreme position 1 for an observer would explain to the observed properties of extreme “Population A” objects. In order to account for the CIV blue asymmetry and/or shift, we have to assume (as it is usually done) that the AD is geometrically thin and optically thick (“opaque”). The extreme line of sight 2 (Fig. 5.7), would explain the observed properties of extreme “Population B” and obviously all in between.

I do want to stress that the above is a simplification, which does not pretend any sort of explanation as to why or how the so-called main sequence can be regarded as an evolutionary sequence or to why most “Pop. B” objects are RL, etc. This is discussed elsewhere in this volume.

Thank you, Deborah. We remind that for Population A sources, we understand NLSy1-like sources with $FWHM(H\beta) \lesssim 4,000 \text{ km s}^{-1}$, and for Population B, all sources that show broader $H\beta$. Along with you, we hope that it will be possible in the future to estimate the parameters discussed in this chapter (M_{BH} , Eddington ratio, orientation, and chemical composition) in an accurate way. These parameters might eventually provide the equivalent of the Hertzsprung–Russell diagram for quasars.

References

1. Abajas, C., Mediavilla, E., Muñoz, J.A., et al.: The influence of gravitational microlensing on the broad emission lines of quasars. *Astrophys. J.* **576**, 640–652 (2002)
2. Adelberger, K.L., Steidel, C.C.: Constraints from galaxy-AGN clustering on the correlation between galaxy and black hole mass at redshift $2 \lesssim z \lesssim 3$. *Astrophys. J.* **627**, L1–L4 (2005)
3. Anguiano, O., Jiménez-Bailón, E., Dultzin, D., Negrete, A., Marziani, P., Sulentic, J.: 3D visualization of evolutionary diagrams for quasars in the parameters space 4DE1. *Rev. Mex. Astron. Astrof. Conf. Ser.* **40**, 42 (2011)
4. Antonucci, R., Hurt, T., Kinney, A.: Evidence for a quasar in the radio galaxy cygnus a from observation of broad-line emission. *Nature* **371**, 313 (1994)
5. Bachev, R., Marziani, P., Sulentic, J.W., et al.: Average ultraviolet quasar spectra in the context of eigenvector 1: a baldwin effect governed by the eddington ratio? *Astrophys. J.* **617**, 171 (2004)
6. Bahcall, J.N., Kozlovsky, B.-Z., Salpeter, E.E.: On the time dependence of emission-line strengths from a photoionized nebula. *Astrophys. J.* **171**, 467 (1972)
7. Barth, A., Ho, L., Sargent, W.L.W.: Stellar velocity dispersion and black hole mass in the blazar markarian 501. *Astrophys. J. Lett.* **566**, L13 (2002)
8. Barthel, P.D.: Is every quasar beamed? *Astrophys. J.* **336**, 606 (1989)
9. Baskin, A., Laor, A.: What controls the CIV line profile in active galactic nuclei? *Mon. Not. R. Astron. Soc.* **356**, 1029 (2005)

10. Batcheldor, D.: The $M_{\bullet} - \sigma^*$ relation derived from sphere of influence arguments. *Astrophys. J. Lett.* **711**, L108 (2010)
11. Bennert, V.N., Treu, T., Woo, J.-H., et al.: Cosmic evolution of black holes and spheroids. IV. The $M_{\text{BH}} - L_{\text{sph}}$ relation. *Astrophys. J.* **708**, 1507 (2010)
12. Bentz, M.C., Peterson, B.M., Pogge, R.W., et al.: The radius-luminosity relationship for active galactic nuclei: the effect of host-galaxy starlight on luminosity measurements. *Astrophys. J.* **644**, 133 (2006)
13. Bentz, M.C., Peterson, B.M., Netzer, H., et al.: The radius-luminosity relationship for active galactic nuclei: the effect of host-galaxy starlight on luminosity measurements. II. The full sample of reverberation-mapped AGNs. *Astrophys. J.* **697**, 160 (2009)
14. Bentz, M.C., Peterson, B.M., Pogge, R.W., Vestergaard, M.: The black hole mass-bulge luminosity relationship for active galactic nuclei from reverberation mapping and hubble space telescope imaging. *Astrophys. J. Lett.* **694**, L166 (2009)
15. Bentz, M.C., Walsh, J.L., Barth, A.J., et al.: The lick AGN monitoring project: broad-line region radii and black hole masses from reverberation mapping of H β . *Astrophys. J.* **705**, 199 (2009)
16. Bernardi, M., Sheth, R.K., Annis, J., et al.: Early-type galaxies in the sloan digital sky survey. II. Correlations between observables. *Astron. J.* **125**, 1849–1865 (2003)
17. Bernardi, M., Sheth, R.K., Tundo, E., et al.: Selection bias in the $M_{\bullet} - \sigma$ and $M_{\bullet} - L$ correlations and its consequences. *Astrophys. J.* **660**, 267 (2007)
18. Best, P.N., Kauffmann, G., Heckman, T.M., et al.: The host galaxies of radio-loud active galactic nuclei: mass dependences, gas cooling and active galactic nuclei feedback. *Mon. Not. R. Astron. Soc.* **362**, 25–40 (2005)
19. Blackburne, J.A., Pooley, D., Rappaport, S., Schechter, P.L.: Sizes and temperature profiles of quasar accretion disks from chromatic microlensing. *Astrophys. J.* **729**, 34 (2011)
20. Blandford, R.D., McKee, C.F.: Reverberation mapping of the emission line regions of Seyfert galaxies and quasars. *Astrophys. J.* **255**, 419 (1982)
21. Booth, C.M., Schaye, J.: Cosmological simulations of the growth of supermassive black holes and feedback from active galactic nuclei: method and tests. *Mon. Not. R. Astron. Soc.* **398**, 53 (2009)
22. Boroson, T.A.: Does the narrow [OIII] λ 5007 line reflect the stellar velocity dispersion in active galactic nuclei? *Astrophys. J.* **585**, 647 (2003)
23. Boroson, T.A., Green, R.F.: The emission-line properties of low-redshift quasi-stellar objects. *Astrophys. J. Suppl. Ser.* **80**, 109–135 (1992)
24. Botte, V., Ciroi, S., Rafanelli, P., Di Mille, F.: Exploring narrow-line seyfert-1 galaxies through the physical properties of their hosts. *Astron. J.* **127**, 3168 (2004)
25. Kelly, B.C., Vestergaard, M., Fan, X., et al.: Constraints on black hole growth, quasar lifetimes, and eddington ratio distributions from the SDSS broad-line quasar black hole mass function. *Astrophys. J.* **719**, 1315–1334 (2010)
26. Brandt, W.N., Mathur, S., Elvis, M.: A comparison of the hard ASCA spectral slopes of broad- and narrow-line seyfert-1 galaxies. *Mon. Not. R. Astron. Soc.* **285**, L25 (1997)
27. Canalizo, G., Wold, M., Lazarova, M., Lacy, M.: Quasar black hole masses from velocity dispersions. *AIP Conf. Ser.* **1053**, 63 (2008)
28. Chartas, G., Kochanek, C.S., Dai, X., Poindexter, S., Garmire, G.: X-ray microlensing in RXJ1131-1231 and HE1104-1805. *Astrophys. J.* **693**, 174–185 (2009)
29. Collin, S., Kawaguchi, T., Peterson, B.M., Vestergaard, M.: Systematic effects in measurement of black hole masses by emission-line reverberation of active galactic nuclei: eddington ratio and inclination. *Astron. Astrophys.* **456**, 75 (2006)
30. Couderc, P.: Les auroles lumineuses des novae. *Annales d’Astrophys.* **2**, 271 (1939)
31. Croton, D., Springel, V., White, S.D.M., et al.: The many lives of active galactic nuclei: cooling flows, black holes and the luminosities and colours of galaxies. *Mon. Not. R. Astron. Soc.* **365**, 11 (2006)
32. Czerny, B., Nikolajuk, M., Rózańska, A., et al.: Universal shape of high accretion rate AGN. *Astron. Astrophys.* **412**, 317 (2003)

33. Dasyra, K., Tacconi, L.J., Davies, R.I., et al.: Host dynamics and origin of palomar-green QSOs. *Astrophys. J.* **657**, 102 (2007)
34. Decarli, R., Falomo, R., Treves, A., et al.: The quasar $M_{BH} - M_{host}$ relation through cosmic time – II. Evidence for evolution from $z = 3$ to the present age. *Mon. Not. R. Astron. Soc.* **402**, 2453 (2010)
35. Denney, K.D., Peterson, B.M., Dietrich, M., et al.: Systematic uncertainties in black hole masses determined from single-epoch spectra. *Astrophys. J.* **692**, 246 (2009)
36. Denney, K.D., Peterson, B.M., Pogge, R.W., et al.: Reverberation mapping measurements of black hole masses in six local seyfert galaxies. *Astrophys. J.* **721**, 715 (2010)
37. de Zeeuw, P.T.: Conference summary. *Coevolution of Black Holes and Galaxies*, 460, 2004
38. Di Matteo, T., Springel, V., Hernquist, L.: Energy input from quasars regulates the growth and activity of black holes and their host galaxies. *Nature* **433**, 604 (2005)
39. Dietrich, M., Hamann, F.: Implications of quasar black hole masses at high redshifts. *Astrophys. J.* **611**, 761 (2004)
40. Dultzin-Hacyan, D., Taniguchi, Y., Uranga, L.: Where is the Ca II triplet emitting region in AGN? In: Gaskell, C.M., Brandt, W.N., Dietrich, M., Dultzin-Hacyan, D., Eracleous, M. (eds.) *Structure and Kinematics of Quasar Broad Line Regions*, ASP Conference Series, vol. 175, pp. 303 (1999)
41. Eigenbrod, A., Courbin, F., Meylan, G., et al.: Microlensing variability in the gravitationally lensed quasar QSO 2237+0305 = the einstein cross. II. Energy profile of the accretion disk. *Astron. Astrophys.* **490**, 933–943 (2008)
42. Ferrarese, L., Merritt, D.: A fundamental relation between supermassive black holes and their host galaxies. *Astrophys. J. Lett.* **539**, 9–12 (2000)
43. Ferrarese, L., Pogge, R.W., Peterson, B.M., et al.: Supermassive black holes in active galactic nuclei. I. The consistency of black hole masses in quiescent and active galaxies. *Astrophys. J. Lett.* **555**, L79 (2001)
44. Ferrarese, L.: Supermassive black hole research in the post-HST Era. In *Hubble's science legacy: future optical-ultraviolet astronomy from space*. ASP Conf. Ser. **291**, 196 (2003)
45. Ferrarese, L., Ford, H.: Supermassive black holes in galactic nuclei: past, present and future research. *Space Sci. Rev.* **116**, 523 (2005)
46. Floyd, D.J.E., Bate, N.F., Webster, R.L.: The accretion disc in the quasar SDSS J0924+0219. *Mon. Not. R. Astron. Soc.* **398**, 233–239 (2009)
47. Ford, H.C., Harms, R.J., Tsvetanov, Z.I., et al.: Narrowband HST images of M87: evidence for a disk of ionized gas around a massive black hole. *Astrophys. J. Lett.* **435**, 27–30 (1994)
48. Gaskell, C.M., Shields, G.A., Wampler, E.J.: Abundances of refractory elements in quasars 1981. *Astrophys. J.* **249**, 443 (1981)
49. Gebhardt, K., Bender, R., Bower, G., et al.: A relationship between nuclear black hole mass and galaxy velocity dispersion. *Astrophys. J. Lett.* **539**, 13–16 (2000)
50. Gebhardt, K., Thomas, J.: The black hole mass, stellar mass-to-light ratio, and dark halo in M87. *Astrophys. J.* **700**, 1690–1701 (2009)
51. Genzel, R., Eisenhauer, F., Gillessen, S.: The Galactic center massive black hole and nuclear star cluster. *Rev. Mod. Phys.* **82**, 3121–3195 (2010)
52. Ghez, A., Salim, S., Weinberg, N.N., et al.: Measuring the distance and properties of the milky way's central supermassive black hole with stellar orbits. *Astrophys. J.* **689**, 1044–1062 (2008)
53. Graham, A.W., Erwin, Peter, Caon, N., Trujillo, I.: A correlation between galaxy light concentration and supermassive black hole mass. *Astrophys. J. Lett.* **563**, 11–14 (2001)
54. Graham, A.W.: The black hole mass – spheroid luminosity relation. *Mon. Not. R. Astron. Soc.* **379**, 711 (2007)
55. Graham, A.W., Li, I.: The $M_{BH} - \sigma$ diagram and the offset nature of barred active galaxies. *Astrophys. J.* **698**, 812 (2009)
56. Graham, A.W., Onken, C.A., Athanassoula, E., Combes, F.: An expanded $M_{BH} - \sigma$ diagram, and a new calibration of active galactic nuclei masses. *Mon. Not. R. Astron. Soc.* **412**, 2211 (2011)

57. Granato, G., De Zotti, G., Silva, L., et al.: A physical model for the coevolution of QSOs and their spheroidal hosts. *Astrophys. J.* **600**, 580 (2004)
58. Greene, J., Ho, L.C.: The $M_{BH} - \sigma^*$ relation in local active galaxies. *Astrophys. J. Lett.* **641**, L21 (2006)
59. Greene, J., Ho, L.C., Barth, A.: Black holes in pseudobulges and spheroidals: a change in the black hole-bulge scaling relations at low mass. *Astrophys. J.* **688**, 159 (2008)
60. Grier, C.J., Watson, L.C., Peterson, B.M., et al.: Investigating the high-luminosity end of the active galaxy $M_{BH} - \sigma^*$ relation. *IAU Symp.* **267**, 204 (2010)
61. Grupe, D., Mathur, S.: $M_{BH} - \sigma$ relation for a complete sample of soft x-ray-selected active galactic nuclei. *Astrophys. J. Lett.* **606**, L41 (2004)
62. Gültekin, K., Richstone, D.O., Gebhardt, K., et al.: The $M - \sigma$ and $M - L$ relations in galactic bulges, and determinations of their intrinsic scatter. *Astrophys. J.* **698**, 198–221 (2009)
63. Gültekin, K.: Determination of the intrinsic scatter in the $M_{BH} - \sigma$ and $M_{BH} - L_{bulge}$ relations. In co-evolution of central black holes and galaxies. *IAU Symp.* **267**, 189 (2010)
64. Hamann, F., Ferland, G.: The chemical evolution of QSOs and the implications for cosmology and galaxy formation. *Astrophys. J.* **418**, 11–27 (1993)
65. Häring, N., Rix, H.-W.: On the black hole mass-bulge mass relation. *Astrophys. J. Lett.* **604**, L89 (2004)
66. Hasinger, G.: Absorption properties and evolution of active galactic nuclei. *Astron. Astrophys.* **490**, 905 (2008)
67. Hiner, K., Canalizo, G., Wold, M., et al.: Investigating the $M - \sigma$ relation of red QSOs. *Bull. Am. Astron. Soc.* **42**, 370 (2010)
68. Ho, L.C., Filippenko, A.V., Sargent, W.L.W.: The influence of bars on nuclear activity. *Astrophys. J.* **487**, 568 (1997)
69. Ho, L.C.: The CO tully-fisher relation and implications for the host galaxies of high-redshift quasars. *Astrophys. J.* **669**, 821 (2007)
70. Hopkins, P.F., Hernquist, L., Cox, T.J., et al.: A unified, merger-driven model of the origin of starbursts, quasars, the cosmic x-ray background, supermassive black holes, and galaxy spheroids. *Astrophys. J. Suppl. Ser.* **163**, 1 (2006)
71. Hopkins, P.F., Hickox, R., Quataert, E., Hernquist, L.: Are most low-luminosity active galactic nuclei really obscured? *Mon. Not. R. Astron. Soc.* **398**, 333 (2009)
72. Horne, K., Peterson, B.M., Collier, S.J., Netzer, H.: Observational requirements for high-fidelity reverberation mapping. *PASP* **116**, 465 (2004)
73. Hutsemekers, D., Borguet, B., Sluse, D., et al.: Microlensing in H1413+117: disentangling line profile emission and absorption in a broad absorption line quasar. *Astron. Astrophys.* **519**, A103 (2010)
74. Jahnke, K., Bongiorno, A., Brusa, M., et al.: Massive galaxies in COSMOS: evolution of black hole versus bulge mass but not versus total stellar mass over the last 9 Gyr? *Astrophys. J. Lett.* **706**, L215 (2009)
75. Jahnke, K., Macció, A.V.: The non-causal origin of the black hole-galaxy scaling relations. [arXiv:1006.0482v1](https://arxiv.org/abs/1006.0482v1) (2010)
76. Johansson, P.H., Burkert, A., Naab, T.: The evolution of black hole scaling relations in galaxy mergers. *Astrophys. J. Lett.* **707**, L184 (2009)
77. Kaspi, S., Smith, P.S., Netzer, H., et al.: Reverberation measurements for 17 quasars and the size-mass-luminosity relations in active galactic nuclei. *Astrophys. J.* **533**, 631 (2000)
78. Kaspi, S., Maoz, D., Netzer, H., et al.: The relationship between luminosity and broad-line region size in active galactic nuclei. *Astrophys. J.* **629**, 61 (2005)
79. Kaspi, S., Brandt, W.N., Maoz, D., et al.: Reverberation mapping of high-luminosity quasars: first results. *Astrophys. J.* **659**, 997–1007 (2007)
80. Kauffmann, G., Haehnelt, M.: A unified model for the evolution of galaxies and quasars. *Mon. Not. R. Astron. Soc.* **311**, 576 (2000)
81. Kinney, A.L.: The tilt of accretion disks in active spiral galaxies. *Adv. Space Res.* **23**, 1089 (1999)

82. Kochanek, C.S.: Quantitative interpretation of quasar microlensing light curves. *Astrophys. J.* **605**, 58–77 (2004)
83. Kollatschny, W.: Accretion disk wind in the AGN broad-line region: spectroscopically resolved line profile variations in Mrk 110. *Astron. Astrophys.* **407**, 461 (2003)
84. Kollmeier, J.A., Onken, C.A., Kochanek, C.S., et al.: Black hole masses and eddington ratios at $0.3 < z < 4$. *Astrophys. J.* **648**, 128 (2006)
85. Kormendy, J., Richstone, D.: Inward bound – The search for supermassive black holes in galactic nuclei. *Ann. Rev. Astron. Astrophys.* **33**, 581–624 (1995)
86. Kormendy, J., Gebhardt, K.: Supermassive black holes in galactic nuclei. *AIP Conf. Proc.* **586**, 363 (2001)
87. Krolik, J.H., McKee, C.F., Tarter, C.B.: Two-phase models of quasar emission line regions. *Astrophys. J.* **249**, 422–442 (1981)
88. Laor, A.: On quasar masses and quasar host galaxies. *Astrophys. J. Lett.* **505**, L83 (1998)
89. Laor, A.: On black hole masses and radio loudness in active galactic nuclei. *Astrophys. J. Lett.* **543**, L11 (2000)
90. Lauer, T., Faber, S.M., Richstone, D., et al.: The masses of nuclear black holes in luminous elliptical galaxies and implications for the space density of the most massive black holes. *Astrophys. J.* **662**, 808 (2007)
91. Liu, H., Wang, J., Mao, Y., Wei, J.: Violent intranight optical variability of a radio-loud narrow-line seyfert-1 galaxy: SDSS J094857.3+002225. *Astrophys. J.* **715**, L113 (2010)
92. Macchetto, F., Marconi, A., Axon, D.J., et al.: The supermassive black hole of M87 and the kinematics of its associated gaseous disk. *Astrophys. J.* **489**, 579–600 (1997)
93. Magorrian, J., Tremaine, S., Richstone, D., et al.: The demography of massive dark objects in galaxy centers. *Astron. J.* **115**, 2285–2305 (1998)
94. Maoz, D., Netzer, H., Mazeh, T., et al.: High-rate active galaxy monitoring at the wise observatory. III – The broad-line region of NGC 4151. *Astrophys. J.* **367**, 493 (1991)
95. Maoz, D.: Comment on: measuring the black hole masses of high redshift quasars. *Astroph/0207295* (2002)
96. Marconi, A., Hunt, L.: The relation between black hole mass, bulge mass, and near-infrared luminosity. *Astrophys. J. Lett.* **589**, L21 (2003)
97. Marconi, A., Axon, D.J., Maiolino, R., et al.: The effect of radiation pressure on virial black hole mass estimates and the case of narrow-line seyfert-1 galaxies. *Astrophys. J.* **678**, 693–700 (2008)
98. Marconi, A., Axon, D.J., Maiolino, R., et al.: On the observed distributions of black hole masses and eddington ratios from radiation pressure corrected virial indicators. *Astrophys. J. Lett.* **698**, 698, 103–107 (2009)
99. Marziani, P., Zamanov, Radoslav, K., et al.: Searching for the physical drivers of eigenvector 1: influence of black hole mass and eddington ratio. *Mon. Not. R. Astron. Soc.* **345**, 1133–1144 (2003b)
100. Mathews, W.G., Wampler, E.J.: Evidence for kinematic variation with ionization level in quasars. *PASP* **97**, 966 (1985)
101. Mathur, S., Grupe, D.: The locus of highly accreting active galactic nuclei on the $M_{BH} - \sigma$ plane: selections, limitations, and implications. *Astrophys. J.* **633**, 688 (2005)
102. Mathur, S., Kuraszkiewicz, J., Czerny, B.: Evolution of active galaxies: black-hole mass-bulge relations for narrow line objects. *New Astron.* **6**, 321 (2001)
103. McGill, K.L., Woo, J.-H., Treu, T., Malkan, M.A.: Comparing and calibrating black hole mass estimators for distant active galactic nuclei. *Astrophys. J.* **673**, 703 (2008)
104. McLure, R.J., Jarvis, M.J.: Measuring the black hole masses of high-redshift quasars. *Mon. Not. R. Astron. Soc.* **337**, 109 (2002)
105. McLure, R.J., Dunlop, J.S.: The black hole masses of seyfert galaxies and quasars. *Mon. Not. R. Astron. Soc.* **327**, 199–207 (2001)
106. McLure, R.J., Dunlop, J.S.: On the black hole-bulge mass relation in active and inactive galaxies. *Mon. Not. R. Astron. Soc.* **331**, 795–804 (2002)

107. McLure, R., Jarvis, M.: Measuring the black hole masses of high-redshift quasars. *Mon. Not. R. Astron. Soc.* **337**, 109 (2002)
108. McLure, R.J., Dunlop, J.S.: The cosmological evolution of quasar black hole masses. *Mon. Not. R. Astron. Soc.* **352**, 1390–1404 (2004)
109. Merloni, A., Bongiorno, A., Bolzonella, M., et al.: On the cosmic evolution of the scaling relations between black holes and their host galaxies: broad-line active galactic nuclei in the zCOSMOS survey. *Astrophys. J.* **708**, 137 (2010)
110. Merritt, D., Milosavljević, M., Favata, M., et al.: Consequences of gravitational radiation recoil. *Astrophys. J.* **607**, L9 (2004)
111. Morrison, P., Sartori, L.: The light of the supernova outburst. *Astrophys. J.* **158**, 541 (1969)
112. Murray, N., Chiang, J.: Photoionized disk winds. Mass ejection from active galactic nuclei. *Astron. Soc. Pac. Conf. Ser.* **128**, 246 (1997)
113. Narayan, R., Yi, I.: Advection-dominated accretion: a self-similar solution. *Astrophys. J. Lett.* **428**, 13–16 (1994)
114. Nelson, C.H., Green, R.F., Bower, G., et al.: The relationship between black hole mass and velocity dispersion in Seyfert-1 galaxies. *Astrophys. J.* **615**, 652–661 (2004)
115. Nemiroff, R.J.: AGN broad emission line amplification from gravitational microlensing. *Astrophys. J.* **335**, 593–605 (1988)
116. Netzer, H.: The largest black holes and the most luminous galaxies. *Astrophys. J. Lett.* **583**, L5 (2003)
117. Netzer, H., Maoz, D.: On the emission-line response to continuum variations in the seyfert galaxy NGC 5548. *Astrophys. J. Lett.* **365**, L5 (1990)
118. Netzer, H., Peterson, B.M.: Reverberation mapping and the physics of active galactic nuclei. In: Maoz, D., Sternberg, A., Leibowitz, E. (eds.) *Astronomical Time Series*, p. 85. Kluwer Academic, Dordrecht (1997)
119. Netzer, H., Trakhtenbrot, B.: Cosmic evolution of mass accretion rate and metallicity in active galactic nuclei. *Astrophys. J.* **654**, 754 (2007)
120. Netzer, H., Marziani, P.: The effect of radiation pressure on emission line profiles and black hole mass determination in active galactic nuclei. *Astrophys. J.* **724**, 318 (2010)
121. Netzer, H., Lira, P., Trakhtenbrot, B., et al.: Black hole mass and growth rate at high redshift. *Astrophys. J.* **671**, 1256 (2007)
122. Nowak, N., Saglia, R.P., Thomas, J., et al.: The supermassive black hole in NGC4486a detected with SINFONI at the very large telescope. *Mon. Not. R. Astron. Soc.* **379**, 909 (2007)
123. Onken, C.A., Ferrarese, L., Merritt, D., et al.: Supermassive black holes in active galactic nuclei. II. Calibration of the black hole mass-velocity dispersion relationship for active galactic nuclei. *Astrophys. J.* **615**, 645 (2004)
124. Osterbrock, D.E., Pogge, R.W.: The spectra of narrow-line seyfert-1 galaxies. *Astrophys. J.* **297**, 166–176 (1985)
125. Padovani, P.: Ionizing photon densities in the broad line regions of active galactic nuclei. *Astron. Astrophys.* **192**, 9–12 (1988)
126. Padovani, P., Rafanelli, P.: Mass-luminosity relationships and accretion rates for seyfert-1 galaxies and quasars. *Astron. Astrophys.* **205**, 53–70 (1988)
127. Padovani, P., Burg, R., Edelson, R.A.: The mass function of seyfert-1 nuclei. *Astrophys. J.* **353**, 438–444 (1990)
128. Peng, C.Y.: How mergers may affect the mass scaling relation between gravitationally bound systems. *Astrophys. J.* **671**, 1098 (2007)
129. Peng, C.Y., Impey, C.D., Ho, L.C., et al.: Probing the coevolution of supermassive black holes and quasar host galaxies. *Astrophys. J.* **640**, 114 (2006)
130. Peng, C.Y., Impey, C.D., Rix, H.-W., et al.: Probing the coevolution of supermassive black holes and galaxies using gravitationally lensed quasar hosts. *Astrophys. J.* **649**, 616 (2006)
131. Perez, E., Robinson, A., de la Fuente, L.: The response of the broad emission line region to ionizing continuum variations. III – an atlas of transfer functions. *Mon. Not. R. Astron. Soc.* **256**, 103 (1992)

132. Peterson, B.M.: Emission-line variability in seyfert galaxies. *PASP* **100**, 18 (1988)
133. Peterson, B.M.: Reverberation mapping of active galactic nuclei. *PASP* **105**, 247 (1993)
134. Peterson, B.M.: An introduction to Active Galactic Nuclei. Cambridge University Press, Cambridge (1997)
135. Peterson, B.M.: The international AGN watch: past, present, and future. In: Structure and Kinematics of Quasar Broad Line Regions, ASP Conf. Ser. **175**, 49 (1999)
136. Peterson, B.M.: Toward precision measurement of central black hole masses. In: Co-Evolution of Central Black Holes and Galaxies. IAU Symp. **268** 151–160 (2010)
137. Peterson, B.M., Wandel, A.: Keplerian motion of broad-line region gas as evidence for supermassive black holes in active galactic nuclei. *Astrophys. J. Lett.* **521**, L95 (1999)
138. Peterson, B.M., Wandel, A.: Evidence for supermassive black holes in active galactic nuclei from emission-line reverberation. *Astrophys. J. Lett.* **540**, L13 (2000)
139. Peterson, B.M., Wanders, I., Bertram, R., et al.: Optical continuum and emission-line variability of Seyfert-1 galaxies. *Astrophys. J.* **501**, 82 (1998)
140. Peterson, B.M., Berlind, P., Bertram, R., et al.: Steps toward determination of the size and structure of the broad-line region in active galactic nuclei. XVI. A 13 year study of spectral variability in NGC 5548. *Astrophys. J.* **581**, 197 (2002)
141. Peterson, B.M., Ferrarese, L., Gilbert, K.M., et al.: Central masses and broad-line region sizes of active galactic nuclei. II. A homogeneous analysis of a large reverberation-mapping database. *Astrophys. J.* **613**, 682 (2004)
142. Peterson, B.M., Bentz, M.C.: Black hole masses from reverberation mapping. *New Astron. Rev.* **50**, 796–799 (2006)
143. Poindexter, S., Morgan, N., Kochanek, C.S.: The spatial structure of an accretion disk. *Astrophys. J.* **673**, 34–38 (2008)
144. Pounds, K.A., Done, C., Osborne, J.P.: RE 1034+39: a high-state Seyfert galaxy? *Mon. Not. R. Astron. Soc.* **277**, L5–L10 (1995)
145. Rauch, K.P., Blandford, R.D.: Microlensing and the structure of active galactic nucleus accretion disks. *Astrophys. J.* **381**, L39–L42 (1991)
146. Rees, M.J.: Black hole models for active galactic nuclei. *Ann. Rev. Astron. Astrophys.* **22**, 471–506 (1984)
147. Richards, G.T., Lacy, M., Storrie-Lombardi, L.J., et al.: Spectral energy distributions and multiwavelength selection of type-1 quasars. *Astrophys. J. Suppl. Ser.* **166**, 470–497 (2006)
148. Robertson, B., et al.: The evolution of the $M_{BH} - \sigma$ relation. *Astrophys. J.* **641**, 90 (2006)
149. Robinson, A.: The LAG spectroscopic monitoring campaign: an overview. In: Reverberation Mapping of the Broad-Line Region in Active Galactic Nuclei, ASP Conf. Ser. **69**, 147 (1994)
150. Salvander, S., Shields, G.A., Gebhardt, K., et al.: The black hole mass-galaxy bulge relationship for QSOs in the sloan digital sky survey data release 3. *Astrophys. J.* **662**, 131 (2007)
151. Schramm, M., Wisotzki, L., Jahnke, K.: Host galaxies of bright high redshift quasars: luminosities and colours. *Astron. Astrophys.* **478**, 311 (2008)
152. Schmidt, R.W., Wambsganss, J.: Quasar microlensing. *Gen. Relat. Gravit.* **42**, 2127–2150 (2010)
153. Shemmer, O., Netzer, H., Maiolino, R., et al.: Near-infrared spectroscopy of high-redshift active galactic nuclei. I. A metallicity-accretion rate relationship. *Astrophys. J.* **614**, 547 (2004)
154. Schneider, P., Ehlers, J., Falco, E.E.: Gravitational Lenses. Springer, Berlin (1992)
155. Shen, Y., Greene, J.E., Strauss, M.A., et al.: Biases in virial black hole masses: An SDSS perspective. *Astrophys. J.* **680**, 169–190 (2008)
156. Shen, J., Vanden Berk, Daniel E., et al.: The black hole-bulge relationship in luminous broad-line active galactic nuclei and host galaxies. *Astron. J.* **135**, 928 (2008)
157. Shields, G.A.: The underabundance of gaseous iron in the planetary nebula NGC 7027. *Astrophys. J.* **195**, 475 (1975)
158. Shields, G.A.: The abundance of nitrogen in QSOs. *Astrophys. J.* **204**, 330 (1976)

159. Shields, G.A., Gebhardt, K., Salvander, S., et al.: The black hole-bulge relationship in quasars. *Astrophys. J.* **583**, 124 (2003)
160. Shields, G.A., Menezes, K.L., Massart, C.A., Vanden Bout, P.: The black hole-bulge relationship for QSOs at high redshift. *Astrophys. J.* **641**, 683 (2006)
161. Shields, G.A., Ludwig, R.R., Salvander, S.: Fe II emission in active galactic nuclei: the role of total and gas-phase iron abundance. *Astrophys. J.* **721**, 1835 (2010)
162. Shuder, J.M.: On the physical conditions and the velocity fields in Seyfert-1 galaxies and QSOs. *Astrophys. J.* **259**, 48 (1982)
163. Simon, L.E., Hamann, F.: Metallicity and far-infrared luminosity of high-redshift quasars. *Mon. Not. R. Astron. Soc.* **407**, 1826 (2010)
164. Sluse, D., Claeskens, J.-F., Hutsemekérs, D., Surdej, J.: Multi-wavelength study of the gravitational lens system RXS J1131-1231. III. Long slit spectroscopy: micro-lensing probes the QSO structure. *Astron. Astrophys.* **468**, 885–901 (2007)
165. Sluse, D., Schmidt, R., Courbin, F., et al.: Zooming into the broad line region of the gravitationally lensed quasar QSO 2237 + 0305 \equiv the Einstein Cross. III. Determination of the size and structure of the CIV and CIII] emitting regions using microlensing. *Astron. Astrophys.* **528**, A100 (2011)
166. Sulentic, J.W., Zwitter, T., Marziani, P., Dultzin-Hacyan, D.: Eigenvector 1: an optimal correlation space for active galactic nuclei. *Astrophys. J. Lett.* **536**, L5 (2000)
167. Sulentic, J.W., Marziani, P., Dultzin-Hacyan, D.: Phenomenology of broad emission lines in active galactic nuclei. *Ann. Rev. Astron. Astrophys.* **38**, 521–571 (2000)
168. Sulentic, J.W., Bachev, R., Marziani, P., et al.: CIV λ 1549 as an Eigenvector 1 parameter for active galactic nuclei. *Astrophys. J.* **666**, 757 (2007)
169. Treu, T., Woo, J.-H., Malkan, M.A., Blandford, R.D.: Cosmic evolution of black holes and spheroids. II. Scaling relations at $z = 0.36$. *Astrophys. J.* **667**, 117 (2007)
170. Tripp, T.M., Bechtold, J., Green, R.F.: Spectral energy distributions of the brightest Palomar-Green quasars at intermediate redshifts. *Astrophys. J.* **433**, 533 (1994)
171. Tundo, E., Mariangela B., Joseph B.H., et al.: On the inconsistency between the black hole mass function inferred from $M_{\bullet} - \sigma$ and $M_{\bullet} - L$ correlations. *Astrophys. J.* **663**, 53 (2007)
172. Vestergaard, M.: Determining central black hole masses in distant active galaxies. *Astrophys. J.* **571**, 733–752 (2002)
173. Vestergaard, M.: Early growth and efficient accretion of massive black holes at high redshift. *Astrophys. J.* **601**, 676 (2004)
174. Vestergaard, M., Peterson, B.M.: Determining central black hole masses in distant active galaxies and quasars. II. Improved optical and UV scaling relationships. *Astrophys. J.* **641**, 689–709 (2006)
175. Vestergaard, M., Osmer, P.S.: Mass functions of the active black holes in distant quasars from the large bright quasar survey, the bright quasar survey, and the color-selected sample of the SDSS fall equatorial stripe. *Astrophys. J.* **699**, 800 (2009)
176. Vestergaard, M., Wilkes, B.J., Barthel, P.D.: Clues to quasar broad-line region geometry and kinematics. *Astrophys. J. Lett.* **538**, L103 (2000)
177. Volonteri, M.: Gravitational recoil: signatures on the massive black hole population. *Astrophys. J. Lett.* **663**, L5 (2007)
178. Volonteri, M., Natarajan, P.: Journey to the $M_{BH} - \sigma$ relation: the fate of low-mass black holes in the Universe. *Mon. Not. R. Astron. Soc.* **400**, 1911 (2009)
179. Walter, F., et al.: Resolved molecular gas in a quasar host galaxy at redshift $z = 6.42$. *Astrophys. J. Lett.* **615**, L17 (2004)
180. Wambsganss, J., Paczynski, B.: Expected color variations of the gravitationally microlensed QSO 2237 + 0305. *Astron. J.* **102**, 864–868 (1991)
181. Wandel, A.: Black holes of active and quiescent galaxies. I. The black hole-bulge relation revisited. *Astrophys. J.* **565**, 762 (2002)
182. Wang, T., Lu, Y.: Black hole mass and velocity dispersion of narrow line region in active galactic nuclei and narrow line Seyfert-1 galaxies. *Astron. Astrophys.* **377**, 52 (2001)

183. Wang, J.G., et al.: Estimating black hole masses in active galactic nuclei using the MgII $\lambda 2,800$ emission line. *Astrophys. J.* **707**, 1334 (2009)
184. Wang, T., Brinkmann, W., Bergeron, J.: X-ray properties of active galactic nuclei with optical FeII emission. *Astron. Astrophys.* **309**, 81–96 (1996)
185. Wang, R., Carilli, C.L., Neri, R., et al.: Molecular gas in $z \sim 6$ quasar host galaxies. *Astrophys. J.* **714**, 699 (2010)
186. Warner, C., Hamann, F., Dietrich, M.: Black hole masses, accretion rates, and narrow line Seyfert 1s. *Astrophys. J.* **596**, 72 (2003)
187. Watson, L.C., Martini, P., Dasyra, K.M., et al.: First stellar velocity dispersion measurement of a luminous quasar host with gemini north laser guide star adaptive optics. *Astrophys. J. Lett.* **682**, L21 (2008)
188. Wayth, R.B., O'Dowd, M., Webster, R.L.: A microlensing measurement of the size of the broad emission-line region in the lensed quasar QSO 2237+0305. *Mon. Not. R. Astron. Soc.* **359**, 561–566 (2005)
189. Welsh, W.F., Horne, K.: Echo images of broad-line regions in active galactic nuclei. *Astrophys. J.* **379**, 586 (1991)
190. Willott, C.J., McLure, R.J., Jarvis, M.J.: A $3 \times 10^9 M_{\text{solar}}$ black hole in the quasar SDSS J1148+5251 at $z = 6.41$. *Astrophys. J. Lett.* **587**, 15–18 (2003)
191. Wills, B.J., Browne, I.W.A.: Relativistic beaming and quasar emission lines. *Astrophys. J.* **302**, 56–63 (1986)
192. Wills, B., Brotherton, M.: An improved measure of quasar orientation. *Astrophys. J.* **448**, L81 (1995)
193. Wolf, M.J., Sheinis, A.: Host galaxies of luminous quasars: structural properties and the fundamental plane. *Astron. J.* **136**, 1587 (2008)
194. Woo, J.-H., Treu, T., Malkan, M.A., Blandford, R.D.: Cosmic evolution of black holes and spheroids. III. The $M_{\text{BH}} - \sigma^*$ relation in the last six billion years. *Astrophys. J.* **681**, 925 (2008)
195. Woo, J.-H., Urry, C.M., Lira, P., van der Marel, R.P., Maza, J.: The fundamental plane evolution of active galactic nucleus host galaxies. *Astrophys. J.* **617**, 903–914 (2004)
196. Woo, J.-H., Treu, T., Barth, A.J., et al.: The lick AGN monitoring project: the $M - \sigma$ relation for reverberation-mapped active galaxies. *Astrophys. J.* **716**, 269–280 (2010)
197. Woo, J., Urry, C.M.: Active galactic nucleus black hole masses and bolometric luminosities. *Astrophys. J.* **579**, 530 (2002)
198. Wu, X.-B., Wang, R., Kong, M.Z., Liu, F.K., Han, J.L.: Black hole mass estimation using a relation between the BLR size and emission line luminosity of AGN. *Astron. Astrophys.* **424**, 793–798 (2004)
199. Yu, Q., Tremaine, S.: Observational constraints on growth of massive black holes. *Mon. Not. R. Astron. Soc.* **335**, 965 (2002)

Chapter 6

Models of Quasars

Contributions by Mauro D’Onofrio, Paola Marziani, Jack W. Sulentic, Julian Krolik, Martin Gaskell, Suzi Collin, Hagai Netzer, Bozena Czerny, Krzysztof Hryniewicz, Luigi Foschini, Michael Eracleous, Daniel Proga, Paolo Padovani, Serguei Komissarov, Isaac Shlosman, and Martin Elvis

M. D’Onofrio

Dipartimento di Astronomia, Università degli Studi di Padova, Vicolo Osservatorio 3, I35122 Padova, Italy

e-mail: mauro.donofrio@unipd.it

P. Marziani

INAF, Osservatorio Astronomico di Padova, Vicolo Osservatorio 5, IT35122 Padova, Italy

e-mail: paola.marziani@oapd.inaf.it

J.W. Sulentic (✉)

Instituto de Astrofísica de Andalucía (CSIC), Granada, Spain

e-mail: sulentic@iaa.es

J. Krolik

Department of Physics and Astronomy, Johns Hopkins University, 3400 N. Charles Street, Baltimore, MD 21218-2686, USA

e-mail: jhk@jhu.edu

M. Gaskell

Departamento de Física y Astronomía, Facultad de Ciencias, Universidad de Valparaíso, Av. Gran Bretaña 1111, Valparaíso, Chile

e-mail: martin.gaskell@uv.cl

S. Collin

LUTH, Observatoire de Paris-Meudon, Section de Meudon, 92195 Meudon, France

e-mail: suzy.collin@obspm.fr

H. Netzer,

School of Physics and Astronomy, Tel Aviv University, Tel Aviv 69978, Israel

e-mail: netzer@wise.tau.ac.il

B. Czerny · K. Hryniewicz

Copernicus Astronomical Center, Bartycka 18, 00-716 Warsaw, Poland

e-mail: bcz@camk.edu.pl; krhr@camk.edu.pl

L. Foschini

Istituto Nazionale di Astrofisica (INAF) - Osservatorio Astronomico di Brera, Via E. Bianchi, 46 - 23807 - Merate (LC) - Italy

e-mail: luigi.foschini@brera.inaf.it

M. Eracleous

Department of Astronomy and Astrophysics and Center for Gravitational Wave Physics, The Pennsylvania State University, 525 Davey Lab., University Park, PA 16802, USA

e-mail: mce@astro.psu.edu

At present, it is believed that all or most galaxies harbor a massive or even supermassive black hole in their nuclei. Sometimes gas finds its way close to and finally into the black hole. This process of accretion is thought to give rise to an active galactic nucleus and in extreme cases, a quasar. The most widely considered model then involves a black hole, an accretion disk, an obscuring torus (for unification), and, for radio-loud sources, very powerful relativistic radio jets. The questions of this chapter will be concerned with the structure and dynamics of the emitting regions and with the relationship to the central black hole parameters.

We choose to focus on a few selected aspects for which the observational data have been extensively reported in previous chapters. The first discussion is on the theory of line formation, followed by an analysis of forces that may shape the profiles of emission lines. Going deeper toward the central black hole, questions address the origin of the thermal component of the continuum.

A major topic are the physical processes that influence the dynamics of outflow and inflow. QSO outflows are extremely important because of their expected effects on the host galaxies. We first discuss winds and go on analyzing relativistic jets, one of the most extreme phenomena in astrophysics (and one that has proved to be among the most difficult to solve). The physical mechanisms that can actualize the accretion paradigm, that is, the very inflow of matter onto the central black hole, need to be well understood before an exhaustive theory of nuclear activity can be formulated. A debated issue is how a molecular torus that is expected to obscure most quasars can preserve a significant geometrical thickness. In the end, we will speak about a phenomenological model that includes the structural elements and dynamical processes discussed in the chapter.

D. Proga

Department of Physics and Astronomy, University of Nevada, Las Vegas 4505, South Maryland Parkway, Las Vegas, Nevada 89154-4002, USA
e-mail: dproga@physics.unlv.edu

P. Padovani

European Southern Observatory, Karl-Schwarzschild-Str. 2, D-85748 Garching bei München, Germany
e-mail: ppadovan@eso.org

S. Komissarov

School of Mathematics, University of Leeds, Leeds, LS29JT, UK
e-mail: serguei@maths.leeds.ac.uk

I. Shlosman

Department of Physics and Astronomy, University of Kentucky, Lexington, KY 40506-0055, USA
e-mail: shlosman@ps.uky.edu

M. Elvis

Harvard Smithsonian Center for Astrophysics, Cambridge MA02138, USA
e-mail: elvis@cfa.harvard.edu

6.1 The Formation of Optical–UV Emission Lines and the AGN Structure

Dear Julian (*Krolik*), what are the major improvements in our understanding of optical–UV line formation that have taken place over the past 30–40 years?

The time span from 40 years ago to the present covers almost the entire history of physical study of atomic emission lines from AGNs, from 1970 to 2010. Undoubtedly, the single greatest achievement in this subject is the solid identification of photoionization as the principal physical mechanism responsible for both the specific ionization states observed in these lines and the energy carried in them. Although this statement is true of both the broad and narrow emission lines, by far, the greatest effort has been expended on the broad lines because their origin is far more difficult to understand. My remarks here will be limited to them.

First proposed by [14], the idea that AGN broad emission lines are both controlled and powered by photoionization was fleshed out by a number of different groups, whose immediate task was to work out its consequences in detail [88, 243, 382]. That is, the first order of business was to provide a quantitative answer to the question: if a strong ionizing spectrum illuminates gas with cosmic abundances, what emission lines emerge, and with what relative strengths? This question also embedded a second: what parameters are most influential in controlling the answer to the first question? This first set of papers demonstrated that the relative fluxes in the strongest UV emission lines could be reproduced, at least approximately, by a pure photoionization model and that the most important parameter governing which lines were seen is the “ionization parameter,” a number describing the ratio of ionizing flux to gas density. “Ionizing flux” in this context means the flux integrated from the H ionization edge at 13.6 eV to roughly X-ray energies, well above the valence-shell ionization edges for the most highly ionized ions seen in the optical–UV spectra. So long as the spectral shape is reasonably smooth (roughly a power law), the integral quantity matters much more than details of its shape. These studies also showed that electron density plays a secondary role. Although it does little to the relative strengths of permitted emission lines, when the electron density exceeds a critical threshold, it can strongly suppress the emitted flux in forbidden and semi-forbidden lines such as [OIII] λ 5007 Å and CIII] λ 1909 Å. These studies were able to identify, within a range of an order of magnitude or two, a mean value of the ionization parameter and electron density consistent with the observed UV emission-line ratios. Combining these two inferred parameters with an individual object’s luminosity yields a characteristic separation between the ionizing photon source and the line-emitting gas that is $\propto L^{1/2}$.

However, this first group of models did not provide a good explanation for the relative fluxes of the Lyman and Balmer lines of hydrogen: they all predicted that Ly α would be much stronger relative to H α and H β than is observed, and that the ratio of H α to H β would be a factor of 2–3 smaller than observed. A partial solution to this problem was provided by removing a limitation of the first generation of photoionization models, their inability to deal with column densities great enough

to make the population of hydrogen excited states significant. Hagai Netzer made the first exploration of this territory [268], examining the consequences of arbitrarily fixed Balmer optical depths; Chris McKee and I [228] showed how to solve self-consistently the hydrogen excited-state population problem and demonstrated the potential of these effects to bring the hydrogen line ratios more closely in line with those observed. These techniques were then melded into complete photoionization models [229], which showed that if there is enough flux in the soft X-ray band to keep the deeper (and therefore only partially ionized) zones of the illuminated gas reasonably warm, Balmer-line optical depths of the sort needed to move closer to the observations would be found. Since that time, far more elaborate and physically complete photoionization codes have been assembled and made available to the astronomical community (Cloudy: [123] and Xstar: [192]).

Further support for the photoionization picture came years later as a result of the “reverberation mapping” campaigns. In these efforts, both the continuum flux and the emission-line fluxes are tracked in time. Because the parameters inferred from photoionization modeling suggested light travel times from the central core of the AGN to the broad emission-line regions of (depending on the luminosity of the object) anywhere from days to years, if photoionization drives the lines, one would expect the line light curves to look like delayed and smoothed versions of the continuum light curves, in which the delay and smoothing times are of order those light travel times. These expectations were clearly vindicated [299], as was the $L^{1/2}$ scaling [33].

A number of loose ends remain, however. Some have to do with whether the photoionization model explains *everything* about the emission lines. There are indications, particularly for Fe II lines, that another mechanism might contribute [74]. Others have to do with moving from a single-zone picture of the emission-line region, so that one works only with mean quantities, to the more physically plausible one of an emission-line region with internal gradients. Because so many free parameters are introduced once one opens up the possibility of multiple subregions, genuine progress in this direction has been very difficult. In principle, reverberation studies might help in this regard because they can be inverted to yield one-dimensional emissivity maps for individual lines. However, the maps given by this method project the emissivity onto paraboloidal surfaces that can span sizable ranges of spherical radius, and a great deal of high-quality data is required to accomplish even this much. Consequently, the only clue derived from reverberation studies about the spatial distribution of the broad emission-line region is the finding that, in a few particularly well-studied objects, the most highly ionized material may be found as much as 10–100 times closer to the central engine than the least-ionized material [63, 227].

The most important unsolved problem, however, is the nature of the line-emitting gas itself. What is its shape in the source? What are its dynamics? What mechanisms produce it? Although most workers in the field routinely describe its state as “cloud-like” because the observed line flux requires that it occupy only a small fraction of the volume enclosed within a sphere whose radius is equal to its distance from the central black hole, it is not at all clear that this is an

appropriate description. Although it might be possible for low-density, much higher temperature gas to provide a transparent pressure-confining medium for “clouds” [226], a variety of hydrodynamical effects due to the motion of the clouds through this medium would make it difficult for them to maintain long-term integrity. In an alternative picture, the line-emitting matter is confined within a thin disk geometry [264]; this would provide an equally valid explanation of the matter’s small volume filling fraction. In this case, however, there are dynamical difficulties in making the gas’s areal covering factor large enough that it intercepts enough of the photoionizing radiation to explain the fairly large equivalent widths of the emission lines. Further complications to all models come from the fact that several forces may all be simultaneously important: gravity, hydrodynamical pressure gradients, and absorption and scattering of the ionizing radiation itself, the last force made significant by the very large opacity per unit mass of photoionized gas.

Thank you, Julian. The previous chapters emphasized a considerable diversity in quasar spectral properties. We would like to discuss with Martin Gaskell the implications for models and especially whether one structural model can explain every quasar.

Dear Martin (Gaskell), can one “answer” fit all lines in a given AGN?

I would now give a qualified “yes” to this question. I now believe that the BLR has a flatten distribution and is self-shielding [145]. A cartoon of this is shown in Fig. 6.1. This produces the strong ionization stratification we observe from reverberation mapping (see [145]). I have shown that this geometry readily produces both the observed profiles, and the right reverberation response [144]. Different lines in a given AGN have different profiles and reverberation responses because they are produced from different ranges of radii. The covering factor probably also varies a little with radius. My “yes” is qualified because this still needs to be confirmed with more detailed modeling.

Does one “answer” describe any specific line in all AGNs? To put it another way—is it safe in 2010 to assume a monolithic (with stratification) region accounting for all broad-line emission?

My own answer to this question now is “yes” because I find (see [144]) that the turbulent “bird’s nest” BLR model of [145] readily produces both the classic “logarithmic” line profile and the disklike line profiles. The key parameter is simply orientation. George Miley spent his 1977–1978 sabbatical in Santa Cruz to look for connections between radio and optical properties of AGNs. A fruit of this was that he and Joe Miller discovered that the Balmer lines were much wider in extended radio sources than in compact radio sources [259]. Although Don Osterbrock had recently published his turbulent disk model of the BLR, and both George and Joe were well aware of the Blandford and Rees orientation proposal, it took a while for the idea of differences in AGNs being a function of orientation to catch on, and neither Blandford and Rees [46] nor Don Osterbrock’s model or any possible role of orientation at all are mentioned in [259]. Proposing that the Miley and Miller correlation of line width with radio type was due to orientation had to wait another

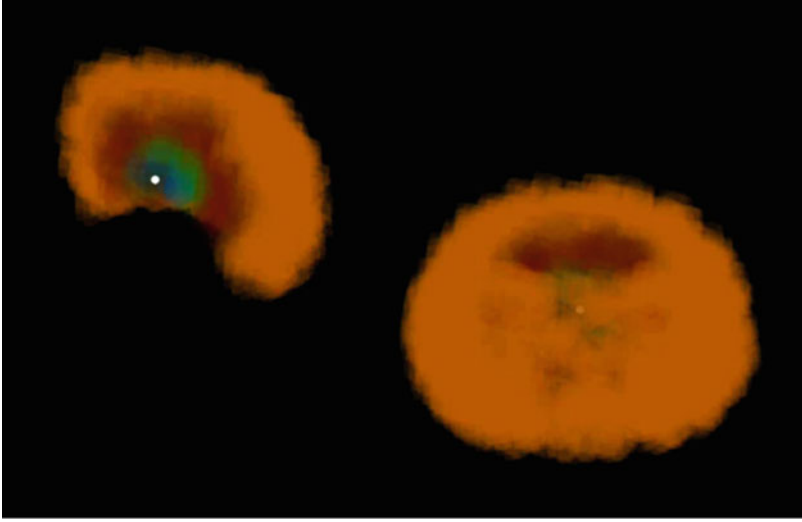


Fig. 6.1 Computer-generated renditions of the appearance of the BLR and clumpy torus of an AGN seen from a “Seyfert 1.9” viewing position (*lower right*) and a cutaway view from the same position (*upper left*). The cut makes a 45 degree angle to the projection of the line of sight onto the equatorial plane. Computer renditions by Daniel Gaskell. Figure from [143]

7 years until [406]. In Fig. 6.2, I show how “logarithmic” line profile and the disklike line profiles can be explained by the same BLR gas distribution. I believe that the differences in line profiles in AGNs are primarily due to differing orientations in different AGNs and to a lesser extent, to luminosity-dependent effects on the effective radii and covering factors.

AGNs with “disklike” line profiles have long presented a special problem. Some AGNs certainly show disklike line profiles with two displaced peaks to the BLR profile of the Balmer lines. The problem is that one peak is often wildly stronger than the other [141]. This led me to propose that these objects have two BLRs each associated with their own black hole [141]. Reverberation mapping observations [95, 285] eventually made the binary black hole model untenable and favored a rotating disk [146]. The disk obviously had to be asymmetric [116, 412], but generating and maintaining the extreme asymmetries in the face of Keplerian shear was a problem.

I have recently proposed that the explanation of the gross asymmetries of the Balmer lines is very simple: they are not primarily due to the disk being asymmetric, but rather to the *continuum emission* being non-axially symmetric [142, 144]. Because of this, one can get one peak to be substantially stronger than another because the continuum source is stronger on the side of the BLR where the strong peak originates. In Fig. 6.3, I show how one of the most extreme $H\beta$ profiles observed can be readily fit with non-axially symmetric illumination. Non-axially

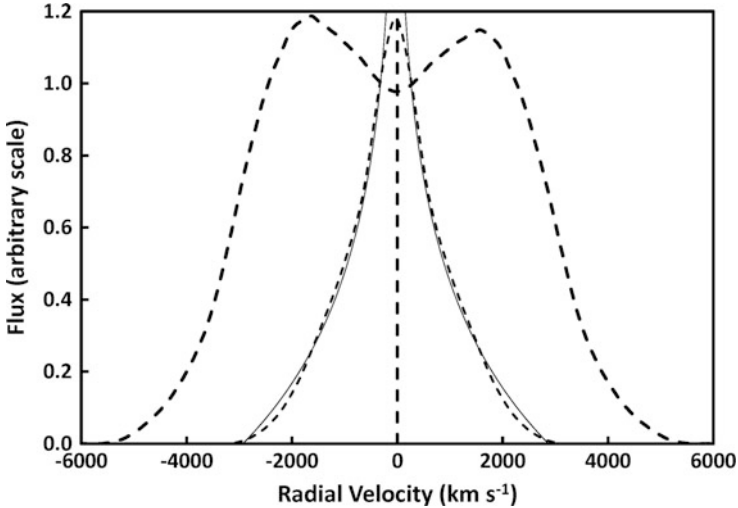


Fig. 6.2 The *dot-dashed line* shows the profile that would arise from a turbulent disk model of [145] if it were centrally illuminated and viewed from 30° off axis (see [144] for details). The profile with short dashes is the same model viewed from face on. The *thin line* superimposed on this is the logarithmic profile of [48]. (Figure taken from [144])

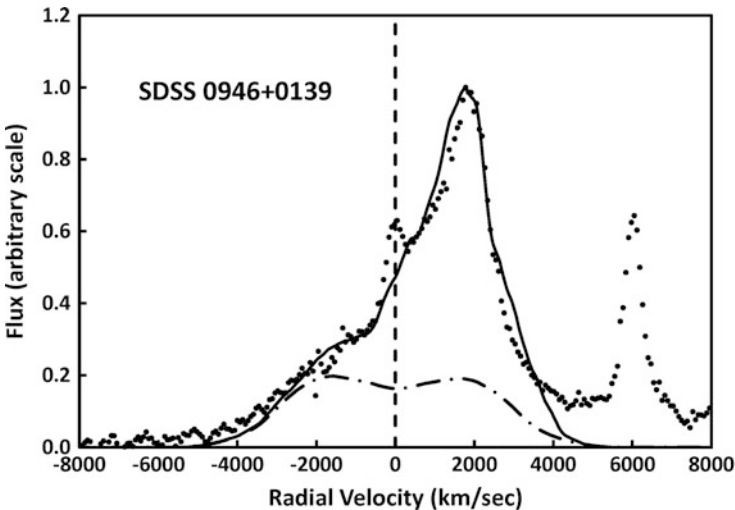


Fig. 6.3 The observed SDSS $H\beta$ profile of SDSS J0946+0139 (*dots*) compared with the off-axis illumination model of [144] (*thick solid line*). The NLR contribution to $H\beta$ to the observed spectrum has not been subtracted. The narrow emission line at $+6,000 \text{ km s}^{-1}$ is $[\text{O III}]\lambda 4959$. The dot-dashed line at the bottom is the same off-axis profile shown in Fig. 6.2 (i.e., with central illumination and viewed from 30° off axis). The thick solid line shows the effect of illuminating the turbulent rotating BLR from an active continuum region located at the inner edge of the $H\beta$ -emitting region. (Figure taken from [144])

symmetric illumination readily explains quite a number of otherwise hard to explain results.

Thank you, Martin. The most credited mechanism for line formation is photoionization of optically thick gas. This basic assumption, supported by several lines of evidence, has been questioned because detailed models cannot account for the intensity of low-ionization lines in the cases of strong Fe II emission. Fe II emission varies widely from source to source but can be strong enough to become determinant in the thermal balance of the BLR as a cooling factor.

Dear Suzy (Collin), in the 1980s, you focussed on low-ionization broad lines and stressed several problems concerning the energy budget of these lines, in particular the strong Fe II emission observed in many quasars. You have pointed out that they might not arise exclusively from gas photoionized by the UV-X-ray continuum. What are alternative solution(s)? You made cogent arguments that implied an accretion disk was needed to account for the low-ionization lines and in particular for Fe II. Is that a true reflection of your work or can you envisage other BLR structures that might account for the Fe II blends? Many of the quasars with strongest Fe II emission show Lorentz-like Balmer line profiles. Are such profiles consistent with an accretion disk origin—assuming, of course, that Fe II and Balmer lines arise in the same clouds?

During the 1970s, photoionization models for explaining the emission lines began to be developed, of the type of those built for planetary nebulae, that is, assuming a stationary medium photoionized and heated by an external UV continuum. The difference with planetary nebulae consisted only in the fact that the UV continuum was a power law and not a blackbody plunging down exponentially at a few tens eV, so several highly ionized species could coexist inside the Strömgen sphere. Another consequence of the power-law continuum is that the completely ionized HII region is surrounded by a weakly ionized “excited HI” region, which is ionized by non-absorbed hard X-rays. This region emits low-ionization lines such as Balmer and Fe II lines, or Balmer continuum. These models did not take into account the effect of a large optical depth and of a high density necessary for the broad-line emission. Kwan and Krolik [229] and Kallman and McCray [193] built the first modern photoionization code adapted for the broad-line region, which takes into account both the line transfer and the collisional excitation. This code was the basis of XSTAR (cf. for instance [27]), while Ferland developed *Cloudy* [122], and Netzer developed ION [274].

All these codes use for the line transfer the so-called escape probability approximation. We showed [68, 69] that this approximation could lead to large errors on the Balmer decrement and on the intensities of other optically thick lines, when the medium is optically thick and inhomogeneous (the first condition leads to the second). It was the reason why later on, we developed with Anne-Marie Dumont the photoionization code *Titan*, which takes into account about the same number of transitions and ions as *Cloudy*, but does not make use of the escape

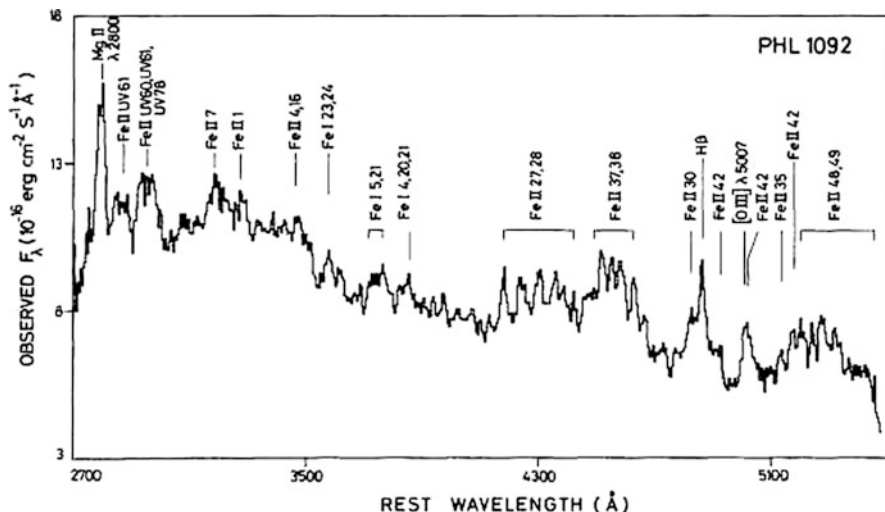


Fig. 6.4 The Fe II spectrum of PHL1092 (from [34])

probability formalism.¹ On the contrary, it performs an exact transfer calculation with the “accelerated lambda iteration” method (cf. [103] and subsequent works). It is specifically aimed at studying the structure and emission of thick and hot X-ray heated media (a description of the code and of the physical processes as well as a user’s guide for the *AstroGrid* version (Virtual Observatory users guide) are available at <http://titan.obspm.fr>).

I became interested by the Fe II problem at the end of the 1970s [75]. For more than 40 years now, strong Fe II emission lines have been observed in active galactic nuclei and quasars. Dozens of papers have been devoted to these observations, and the interest has been renewed recently with the release of data concerning large samples of AGNs, for instance, the SDSS. It was realized that Fe II lines are more intense when the broad lines are narrow, and this was attributed to the difficulty of deblending them. But [50] identified the Fe II line intensities as the eigenvector 1 in their statistical study of Seyfert galaxies, and showed in particular that they are anti-correlated with the line widths and with several other parameters, like the [OIII] intensity and the radio loudness (these results are not understood after 20 years of work). In particular, Fe II is intense in narrow line Seyfert-1 galaxies (NLSy1). As an example, Fig. 6.4 shows a portion of the optical–UV spectrum obtained by [34] of the NLSy1 galaxy PHL1092. In several AGNs, the Fe II spectrum contains as much energy as all other emission lines together, but, as it can be seen on the figure, it is very difficult to determine the intensities of the heavily blended lines.

¹Anne-Marie Dumont has nothing to do with Simone Dumont with whom the previous papers were written.

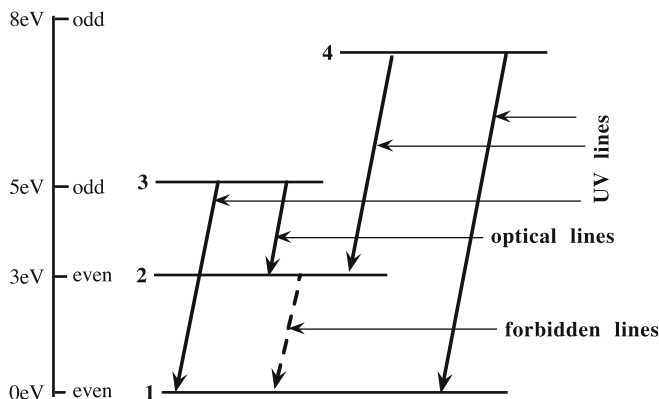


Fig. 6.5 A highly schematized Grotrian diagram of Fe II

The Fe II spectrum is intense for several reasons. First, as the three-dimensional shell is only half-filled, it has more than 10,000 energy levels, and about one million radiative transitions have been listed. Second, since Fe I is easily ionized (ionization potential 7.9 eV), while Fe II is not (ionization potential 16.2 eV), Fe II is very abundant. Finally, a temperature $\sim 5,000$ K is sufficient to excite Fe II.

The Fe II atom is schematized by 4 levels in Fig. 6.5, which shows the different types of transitions occurring in this atom: between odd parity and even parity levels, permitted UV lines around λ 2000–3000 Å, and permitted optical lines in the range 4000–7000 Å including a well-known feature consisting in several multiplets in the range 4500–5300 Å; between the 3 eV even parity levels and the ground level, forbidden optical lines in the range 4000–7000 Å.

Many studies of the Fe II spectrum have been performed in the framework of photoionization models, with ever-improving atomic data and an increasing number of levels [18, 53, 270, 278, 396, 405]. All these computations used the escape probability approximation which is not well adapted to optical permitted Fe II lines whose transfer is strongly linked with that of the optically thick Balmer continuum. Collin-Souffrin et al. [76] and Joly ([187, 188] which include collisional models) had a small number of levels, but they solved the exact line transfer.

Recently, very sophisticated models of the Fe II spectrum were computed. Bruhweiler and Verner [53] succeeded in fitting the UV Fe II spectrum of the NLSy1 IZw 1 (which is not the strongest Fe II emitter) with photoionization models, but they did not consider the optical spectrum. These authors used Cloudy with updated atomic data values for 830 levels for the Fe II atom. Sigut and Pradhan [362] coupled the computation with Cloudy of the structure of the emission region with an exact line transfer of $L\alpha$ aimed at determining accurately the influence of the fluorescence, which requires a thorough treatment of the line transfer, taking into account partial redistribution. They were able to fit the UV lines with those observed in I Zw 1, but it is not clear what they obtained for the optical lines. Using also Cloudy to compute a very large set of models, Baldwin et al. [18] showed that a photoionized medium

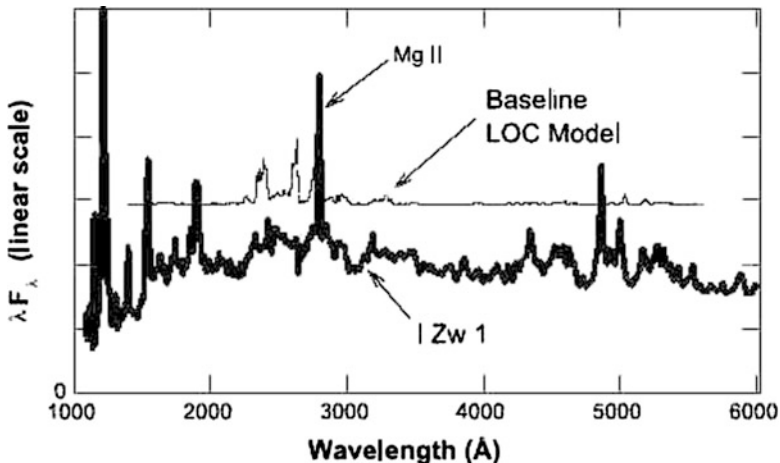


Fig. 6.6 Comparison of the spectrum of I Zw 1 with their best fit model, by [18]. The model is on the same scale as the observed spectrum but has been shifted upward by 1 vertical tick mark. It is clear that the two spectra do not agree

cannot produce both the observed shape and the observed equivalent width of the UV Fe II emission bump, unless there is a micro-turbulent velocity of the order of 100 km s^{-1} or unless the medium is collisionally ionized (see Fig. 6.6). They favored the first solution, but I think that it would necessarily lead to dissipation of the supersonic turbulence, and in fine to mechanical heating of the medium. They noted that in no case the optical–UV Fe II ratio can be reproduced by the models because it “is observed to be considerably higher than is predicted by our (or any other) photoionized models.” Finally, Joly et al. [189] showed that in several strong Fe II emitters, even “hybrid” models including both photoionization and collisional heating do not fit the optical spectra in three strong emitters, and that the source of photoionization must be hidden from the Fe II region.

The problem is indeed more acute concerning the optical Fe II. Let us recall what are the necessary ingredients to produce strong optical lines. If we look at Fig. 6.4, we see that every excitation of levels 3 or 4 from the ground level is followed by cascades giving rise to UV and/or optical photons. When the metastable level 2 is excited, it cannot be radiatively de-excited and becomes therefore strongly overpopulated. Thus, to get a large number of scatterings in order to transform UV lines into optical lines, one needs a large column density of the region containing Fe+ ions. But at the same time, this region should be heated up to at least 5,000 K in order to get collisional excitation up to 5 eV levels. Let us see whether it would be possible to reach these conditions with a photoionization model by playing with the parameters:

- The ionizing–heating continuum: a strong IR and a strong hard X-ray continuum up to γ -rays would provide more heating to the HI* region, but it is not observed.

- The ionization parameter: it is strongly constrained, as it can be neither too high (it would lead to too intense $L\alpha$ emission, etc.) nor too low (it would not provide enough heating).
- The density: a high density would be favorable (to get a large Balmer opacity and to destroy Fe II UV), but it should not be too high (the Balmer and Paschen continua would then be too strong).
- The column density: it should be $\gg 10^{21} \text{ cm}^{-2}$, and it can be arbitrarily large, but this will not increase the amount of Fe II emission above a given limit (since T falls rapidly below the value required for Fe II excitation).
- The turbulent velocity: only a very high nonphysical turbulence would allow an important fluorescence effect, and moreover, it would decrease the line optical thickness too much.
- The iron abundance: its influence is weak, because of the thermostatic effect of FeII; an overabundance of a factor 10 induces less than a factor 2 increase in the total flux.
- The number of levels: it is not important for the total Fe II emission which saturates (again the thermostatic effect).

The conclusion is inevitable: the Fe II emitting region should be heated by an additional non-radiative mechanism. The paper of Baldwin et al. was in this context a great relief for us because Joly and I were claiming since decades that photoionization models could not account for the Fe II optical emission. It was objected that our model atom was not sophisticated enough (it had only 14 levels and did not take into account the very high levels), though from the energetic point of view, this was not important: when there are more levels, the same energy is distributed between them, and the results are not much changed.

What could be the additional heating? There are many possibilities. Let us consider objects with no UV continuum where the Fe II spectrum is very intense. These are cool luminous stars like Miras, with winds and chromospheres; cataclysmic binaries, where it is suggested that Fe II is formed in the accretion disk; novae in which Fe II peaks soon after the outburst, contrary to highly ionized species; symbiotic stars like RR Tel, z Aur/W Cep, where Fe II lines might be formed either in the accretion disk or in the cool component wind; luminous hot stars like PCyg and B[e] supergiants with extreme stellar winds and accretion disks; and some type II supernovae. These stars are all characterized by their variability and by strong outflows where the Fe II region is probably heated by shocks and/or dissipation of supersonic turbulence. It is tempting to compare these properties to those of NLSy1s, which are generally strongly variable and have outflows assessed by the blue asymmetry of $H\beta$ and [OIII]. From the energetic point of view, it is acceptable since the whole power radiated in the Fe II spectrum amounts to only a small fraction of the bolometric luminosity.

More generally, I am convinced that there is a problem with photoionization models for all low-ionization lines. I stressed the problem [64], in answer to [405] who suggested to solve it by assuming a relatively large reddening. But the reddening is small in type-1 AGNs and in quasars ($E(B-V) \leq 0.1$). Later on, we

performed a detailed study of the Seyfert-1 NGC 5548 [104], and we came to the same conclusion on the basis of several observations (EUV and X-ray continuum, variability of lines, and continuum) and a grid of models built with Cloudy: an extra heating mechanism is necessary to account for the low-ionization lines. Even the LOC model (locally optimally emitting clouds [121]) cannot help to solve the problem.

To summarize, the Fe II problem is still unsolved, and it is probably linked with a more general energy budget problem for low-ionization lines. I envisioned the possibility that these lines are emitted by the outer regions of the accretion disk. This would of course produce specific line profiles, but I cannot say that Lorentzian profiles would be favored.

Thank you, Suzy. Considering that important aspects of the formation of emission lines are still debated, we now ask the same question to Hagai Netzer who has been, along with the previous contributors, a pioneer in line formation studies of quasars.

6.2 BLR and NLR Properties

Dear Hagai (*Netzer*), the optical–UV emission-line spectrum is a cornerstone in quasar studies even while IR and X spectroscopy are providing better and better data. What are the major improvements in our understanding of optical–UV line formation that have taken place over the past 30–40 years? After so many years of heroic efforts, do we have a satisfactory view of the broad-line-emitting regions?

Any discussion of AGN emission lines should be divided in two: the understanding of the BLR and NLR physics and the use of the known BLR properties to derive or infer other important properties, such as the BH mass or the structure of the central disk.

Except for the very early papers on the modeling of AGN lines, most other work took into account that the spectrum is very different from what is known from the study of HII regions and planetary nebulae in the Galaxy. Today, we know that there are several reasons for those differences: the gas density, the clouds (or filaments) column density, the SED of the ionizing continuum, and the ionization parameter.

As noted earlier, Davidson and others already established the range of acceptable ionization parameters (hereafter U) in the early 1970s. U as defined today is the ratio of the density of the Lyman continuum photons to the hydrogen density in the gas ([88] defined it somewhat differently). The value of U by itself is not enough for specifying the conditions in the gas. One needs an additional measure of the continuum SED, for example, the mean energy of the ionizing photons. The high density in the BLR was also recognized early on, from the absence of broad forbidden lines and later from the relative intensity of semi-forbidden lines.

The next important development relates to the combination of large column density and high-ionization parameter. Simple arguments show that under such

conditions, most of the Balmer lines will be optically thick, a condition that was not recognized to be of any importance in other nebulae at that time. This would have dramatic effects on the Balmer decrement (the Balmer line ratios) and on other line intensities. My 1975 paper was the first to point this out and later papers by [228], and [244] confirmed this finding for the hydrogen and HeI lines. All BLR models of today take this effect into account albeit with a rather simplified treatment of the (very complicated) radiation transfer. The idea of line emission anisotropy was developed at that time too [126]. The observational and theoretical situation in the late 1970s is reviewed by [89].

The next improvement is the development of several sophisticated photoionization models (e.g., [229, 254]) where all lines are allowed to be optically thick. Interestingly, for some lines, like the hydrogen and iron lines, the effect is very important while for others, like C IV λ 1549 and O VI λ 1035, it is much less so because of the sharp, well-defined creation region [125].

A couple of notable problematic line ratios have been noted as early as 1977. The first is the unusual Ly α /H β ratio first pointed out by [17]. Baldwin realized that typically, $I(\text{Ly}\alpha)/I(\text{H}\beta) \sim 5$, while theoretical calculations suggest 20–40. I consider this problem unsolved even today, although some photoionization codes produce results that are not very different from the observations.

The second major problem is related to Fe II emission lines. Strong optical Fe II bands were observed right from the start, but the $I(\text{Fe II optical})/I(\text{H}\beta)$ line ratio in some objects was so large that no solar abundance photoionization model of the time, could explain it (e.g., [165, 270]). The systematic studies of [278, 405] show a similar, perhaps even more severe problem in UV iron lines. These authors suggested a complicated model where line fluorescence, by the continuum and other Fe II lines, play an important role. The model helped in explaining some features but did not solve the problem partly due to the inadequate atomic data of the time and mostly because of some unknown physics. Later attempts, by Baldwin et al. [18] and others, use more detailed Fe II atomic models based on the same principles, with much improved atomic data and many more levels and lines. Despite these improvements, the main problems remain the same. These problems motivated Collin, Joly, and collaborators [187] to suggest a completely different solution involving mechanical heating of the line-emitting gas, at least the low-ionization gas where Fe II is the most abundant iron ion. This is the first serious attempt to propose that a (large) fraction of the observed broad-line intensity in AGN is due to photoionized gas.

A third central issue is the so-called Baldwin relationship. This is a strong correlation of some line EW with the continuum luminosity. It was first investigated for the C IV λ 1549 line and later in other lines. It seems that the effect is stronger in UV lines and hardly noticeable in optical lines like H β . Suggested explanations range from the dependence of the covering factor of the BLR on source luminosity, a change of mean ionization parameter with L_{bol} , changes in the mean surface temperature of the accretion disk, and even changes in metallicity as a function of L_{bol} . Netzer [271] proposed a more geometrical explanation related to the different orientation of the accretion disk to the line of sight combined with the isotropic

emission of the lines. As in several other cases, the real explanation may involve several of these ingredients.

A major progress in understanding the BLR properties is the realization that the metallicity of this gas is very high, in some cases, up to 4–10 times solar. The method to measure metallicity in the high-density gas was suggested by Hamann [168] and developed further by Hamann and Ferland [170]. Interestingly, the attempt to correlate metallicity with other properties resulted, much later, in a lot of confusion. Hamann and collaborators suggested a strong correlation with L_{bol} , and later with M_{BH} . Shemmer et al. [351] who analyzed the spectrum of high-luminosity AGNs, as well as very low-luminosity but high-metallicity NLSy1s, argued that the fundamental relationship is driven by L/L_{Edd} .

Another interesting, yet not fully understood relationship is the so-called eigenvector 1 sequence. This is an empirical connection between several fundamental properties that was completely unknown in the first two decades of AGN research. It is related to the progress in observing and analyzing large, flux limited, AGN samples. The eigenvector 1 sequence combines several relationships that are clearly revealed by principle component analysis of the spectra of a large number of AGNs. It connects several properties and relationships like the level of ionization of the BLR gas, the FeII/H β line ratio, the X-ray variability, and the soft X-ray continuum slope. It was first pointed out by Boroson and Green [50] in their study of the PG quasar sample and was later studied in great detail by Sulentic, Marziani, Dultzin, and collaborators [379]; by Laor et al. [232]; and by others, most recently by Marziani et al. [252]. There are suggestions that the eigenvector 1 sequence is related to unusual line profiles and thus to the dynamics and the kinematics of the BLR. It is now clear that the main physical drive of these relationships is the normalized accretion rate (L/L_{Edd}), but much of the physics is still missing. The above questions, and others, are related to the fundamental issues of the BLR geometry, the gas distribution, the gas motion, and the gas confinement. Four generic models have been considered for the BLR:

- a) *The cloud model*—This is, in a way, the simplest case. In its simplest form, it assumes a “typical” cloud that represents “typical conditions” (including typical location) in the BLR. Such clouds, unless extremely massive and self-gravitating, must be pressure-supported. It is the only case where photoionization modeling can result in specific and accurate predictions of the emitted emission-line spectrum. The parameters of this model are the gas density, column density, location (or ionization parameter), and chemical composition. An additional property that is usually specified is the pressure (e.g., constant pressure on constant density cloud). Some of the early models of Davidson, Netzer, Ferland, Kwan, and Krolik and others are of this type. The next level of sophistication is to treat an assembly of clouds with a range of conditions and locations. The parametrization in this case includes the variations of the density, column density, and locations of the clouds. The Rees, Netzer, and Ferland [322] model is a good example of this case. Kaspi and Netzer [195] used such a model with an

additional degree of freedom, to try and fit the time-dependent emission-line spectrum of NGC 5548.

- b) *The locally optimized emission-line clouds (LOC) model*—This model, which was suggested and developed by Baldwin, Ferland, and Korista (e.g., [19]), presents a very different view of the BLR. In each location, there is a very large range of density and column density. The emitted spectrum is the result of integrating over all gas components in a certain location and over all locations. The model has been compared, quite successfully, with BLR and NLR observations (e.g., Korista and Goad 2004 [216]). It requires about the same number of free parameters as the multi-cloud model.
- c) *T bloated stars model*—This model is of a completely different type. It assumes that the BLR clouds are the extended envelopes of giant stars that, because of their large size, have typical density and column density of those observed in the BLR. The works of Scoville and Norman [344] and Kazanas [198] were the first to seriously suggest this possibility. Later, more detailed work, by Alexander and Netzer [1, 2], produced real predicted spectra that could be compared with observations. The main features that are very different from the other models are the relatively small number of stars (limited by the mass and the size of the nuclear cluster) and the fact that these “clouds” are self-gravitating; hence, there is no need for confinement.
- d) *Wind models*—Clouds or condensations can be formed out of disk winds and thus be part of an unbound, outflowing cloud system. Blandford et al. [43], Chiang and Murray [61], and others investigated this class of models with little emphasis of the predicted emission-line spectrum. The pure wind aspect of this model requires no confinement since clouds are formed and destroyed all the time. The (more popular) magnetic wind scenario uses magnetic fields as the confining pressure. Some of these models predict BLR clouds are more like long filaments extending along the magnetic field lines. As explained below, there are ways to detect outflow motion from line profile observations and from detailed reverberation mapping studies.

Given the above rather different possibilities, and several of their variants, what can be said about the structure of the BLR? It seems that the answer, or at least part of it, was provided by several detailed X-ray variability studies by Risaliti and collaborators [330]. In a handful of sources, mostly type-2 AGNs, there is evidence for changes in X-ray absorbing column which is most likely due to passing BLR clouds that cross the line of sight to the central X-ray source. The very careful analysis of Maiolino et al. [246] suggests typical column densities of $\text{few} \times 10^{23} \text{cm}^{-2}$, consistent with the predictions of the cloud model. This is the first direct detection of BLR clouds and a clear support for this model.

Can line emission be used to derive other physical properties?

Much of the progress in recent year is due to the use of the known BLR properties to deduce other important physical properties of AGNs. In my opinion, the three most important examples are the deduction of the extreme UV SED, the ability to

measure the typical BLR size and hence the BH mass, and the role of dust in the BLR and the torus.

- a) *The energy budget of AGNs—the far-UV continuum*—A major limitation in measuring the total emitted energy of AGNs, and the shape of the EUV continuum, is the combination of galactic obscuration in low-redshift objects and intergalactic absorption at high redshift. This limits the ability to observe, directly, the SED between about 15 and 100 eV, a spectral region predicted by many accretion disk model, to contain most of the disk emitted energy. A possible way to overcome this difficulty is to use an “energy budget” argument, that is, to combine the photoionization modeling with measured line luminosity and observed emission-line ratios (e.g., the ratio of hydrogen to ionized helium lines, or the total energy emitted by all emission lines). Since basically all of the line energy is due to reprocessing of the Lyman continuum radiation, such methods can be used to derive both the total emitted ionizing energy and the shape of the EUV continuum. The application of this method has been demonstrated by Netzer [272] and several other papers since. This is still an open issue since several direct observation of the part of the continuum that can be observed (10–20 eV), indicate SEDs that are too steep, with not enough energy to explain some of the observations.

There are similar, more recent ideas related to the energy budget of the NLR. They rely on the measured, or the reddening corrected narrow line intensities, e.g., L(O III), and provide useful relationships that allow the use of such intensities to estimate L_{bol} . This is most useful in type-2 sources where the intrinsic optical–UV continuum is obscured.

- b) *The size of the BLR and the mass of the central BH*—Using reverberation mapping (RM) to deduce the “emissivity-weighted BLR size” (r_{BLR}) is an impressive achievement of the last two decades. The first successful measurement were those of [298] and Maoz et al. [62, 248, 300]. The first sample that covered a large enough luminosity range to enable a meaningful $r_{\text{BLR}}-L_{\text{bol}}$ relationship is the one presented in [196]. Additional significant improvements, and more complete samples, were presented recently by [194], and by [33]. The RM measured r_{BLR} can be combined with line width observations, and the assumption of a virialized BLR, to deduce M_{BH} . This is a major achievement of three decades of BLR studies that, currently, is the only reliable way to measure BH mass in intermediate and high-redshift AGNs.
- c) *Dust in the torus, in the outer parts of the BLR, and in the NLR*—The third case is an important example of how to use negative results, in this case, the absence of dust signature in BLR clouds, to derive important quantities. It is related to the understanding that typical galactic dust grains cannot survive in the BLR because their temperature is above the sublimation temperature, a result that is consistent with broad emission-line observations. Barvainis [28] proposed that this is related to the typical BLR size, and Netzer and Laor [276] showed that the outer BLR size, and the torus inner size, are indeed consistent with this prediction. This is now confirmed by direct measurements of the torus

inner dimensions in several AGNs. The understanding that dust is an important ingredient in most NLR clouds (except perhaps in the part called the “coronal line region”) led to an equally important suggestion related to the origin of the very small spread in the value of U across the NLR. Dopita [97] and later Groves and Dopita [166] suggested that radiation pressure on dust grains acts to modify the gas internal pressure such that U is more or less constant regardless of the cloud location and density.

In summary, several of the fundamental questions of the 1970s regarding the BLR, its properties, and composition have been answered using improved observations of large AGN samples and introducing more sophisticated elements into the modeling of the emission line gas. Other problems are still with us, despite much effort by many scientists. The outstanding problems of today are the origin of the BLR gas, its confinement, the total number of BLR clouds (see below), and several unexplained line ratios that are, most probably, related to the inadequate treatment of the line transfer in the high-density large optical depth gas. Most of these are related to global AGN features, rather than individual line properties.

6.3 Radiation Pressure and Irregular Line Profiles

Is radiation likely to have a significant effect on BLR gas motions? Very high spectral resolution observations of optical emission lines reveal that their profiles are smooth down to a $V_r \lesssim 10 \text{ km s}^{-1}$ (e.g., [8]). Can you please review these findings, and how it is possible to understand them in the framework of the current BLR models? Do they support the accretion disk paradigm or are their viable alternatives? What is the role of radiation pressure in the vicinity of the BH?

The motion of ionized clouds of gas, or ionized winds, in the vicinity of the BH and the accretion disk, is determined by various forces:

- a) *Gravity*—The BH gravity dominates the galaxy gravitational field all the way to the “BH sphere of influence.” The radius of this sphere is the boundary of the region where the BH mass is larger than the stellar mass. Since the escape velocity from a large bulge galaxy is about 300 km s^{-1} , the sphere of influence of a $10^8 M_\odot$ BH is roughly 10 pc in radius. This radius is considerably larger than the BLR radius and even the inner boundary of the central torus. Thus, stars should not affect the motion in the BLR. The mass of the accretion disk, assuming a geometrically thin, optically thick disk, is several orders of magnitude smaller than the mass of the BH. Thus, BHs are basically the sole source of gravitational energy in the BLR.

The above is certainly not the case in the NLR. Here, the typical dimensions are several hundred pc to a few kpc, depending on the source luminosity. Stellar mass and cold dark matter mass are more important than the BH mass in shaping the gravitational potential at this region.

- b) *Radiation pressure force*—The radiation pressure force on a gas particle is determined by the momentum delivered to the particle by the radiation field. The total available momentum at a distance r from a point source with a total luminosity L_{bol} is $L_{\text{bol}}/4\pi r^2 c$ where c is the speed of light. The actual momentum delivered to the gas depends on the gas opacity, that is, the fraction of L_{bol} absorbed by the gas. Assuming this fraction is $\alpha(r)$ ($0 \leq \alpha \leq 1$), then the radiation pressure acceleration of a cloud of mass m_c is

$$a_{\text{rad}}(r) = \frac{L_{\text{bol}}\alpha(r)}{m_c 4\pi r^2 c}. \quad (6.1)$$

In the BLR, the most important factors that determine α are the total column density and the level of ionization of the gas. In the NLR, dust opacity can be the dominant factor.

- c) *Drag force*—BLR clouds, NLR clouds, and even disk winds may be subjected to the drag force applied by the (hypothetical) hot, inter-cloud medium. This slows the cloud motion, creates turbulence and instabilities, and can result in the fragmentation of the gas.
- d) *Thermal pressure*—Thermal expansion, due to gas pressure, can also affect the gas and cloud motion.

Putting all of the above together, and ignoring drag force, we can write a general equation of motion for the NLR and BLR gas, provided they are distributed in clumps or condensations throughout the corresponding emission regions:

$$a(r) = a_{\text{rad}}(r) - g(r) - \frac{1}{\rho} \frac{dP_g}{dr}, \quad (6.2)$$

where P_g is the gas pressure and ρ the gas density in g cm^{-3} . Putting the relevant numbers in the above equations suggests that the critical column density in the BLR below which radiation pressure force affects, significantly the cloud dynamics, is about 10^{23}cm^{-2} . Clouds with smaller column densities will not be bound or will spend long periods of time far from the BH moving at velocities that are well below the Keplerian velocity at that location. The motion of clouds with larger columns will be completely virialized.

Acceleration by radiation force was studied, extensively, in the 1970s and 1980s by Mathews, Capriotti, and others [253]. The renewed interest in this idea is mostly due to the important paper of Marconi et al. [249] who reinvestigated this issue with emphasis on the revised RM-based BH mass. The authors re-derived the critical column of 10^{23}cm^{-2} and argued that some BLR clouds, especially those next to a very large L/L_{Edd} source, and very large L_{bol} (i.e., very massive BHs), are strongly affected by radiation pressure force. This can result in a large under-estimation of the BH mass in such systems, up to an order of magnitude in some cases.

A relaxed gravitationally dominated system of clouds will reach virial equilibrium after a few dynamical times. In a spherical virialized system, we expect random

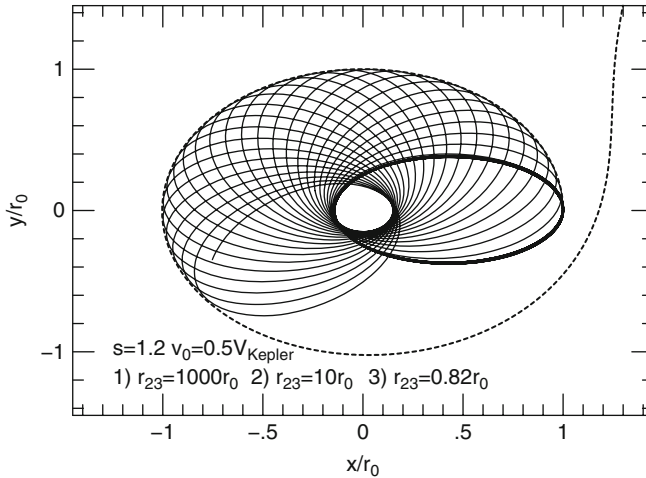


Fig. 6.7 Calculated planar orbits of three clouds with $L/L_{\text{Edd}} = 0.1$ and different column densities. The large column density cloud (*thick line*) moves in a closed elliptical orbit. A smaller column density cloud (*thin line*) moves in a closed rotating orbit and a marginal column density cloud (*dashed line*) escapes the system (from [277])

direction of motion (no infall or outflow), much like the random motion of stars in an elliptical galaxy or stars in a dynamically relaxed stellar bulge. Flat gravitationally dominated systems can be identified by the orderly motion of rotation clouds. In contrast, radiation pressure dominated systems contain a large outward velocity component, or in extreme cases, gas outflow.

The motion of intermediate column ionized BLR clouds has been studied in the 1970s and 1980s and also very recently by Netzer and Marziani [277]. The combined influence of gravity and radiation pressure force results in open planar orbits (because of the conservation of angular momentum). Several such examples are shown in Fig. 6.7. It seems that the orbit shapes, and hence the resulting line profile shapes, depend mostly on L/L_{Edd} of the source.

Can these suggestions be tested observationally? There are various ways to test which of the terms in the equation of motion dominate clouds and gas motion. Gravitationally dominated relaxed systems are likely to show no net inward or outward motion. Outflowing, radiation pressure dominated systems can sometime be identified by line asymmetry. For example, a combination of outflow plus central obscuration that prevent some of the emission from the back side from reaching the observer will be identified by blue asymmetry in the line profiles. There are quite a few well-documented cases of clear blue asymmetry in broad emission lines, mostly in the profiles of C IV $\lambda 1549$ in high-luminosity AGNs and in NLSy1s. In some of these cases, the entire line seems to be shifted to the blue compared with the systemic velocity. These seem to be the most promising candidates, although clear theoretical predictions are not yet available.

Reverberation mapping provides an additional powerful way to distinguish random motion from expansion. The former is characterized by a contribution of both near-side and far-side clouds to the blue and red wings of the profile. Thus, the response time of the blue and the red wings to continuum source variations is identical. The latter case of expansion distinguishes near-side approaching gas contributing mostly to the blue wing, from far-side receding gas, contributing mostly to the red wing. High-precision RM could identify this by measuring a shorter lag in the blue wing of an emission line. There are very few cases where the blue and red wings of $H\alpha$, $H\beta$, and $C\text{ IV } \lambda 1549$ *do not* respond together to continuum source variations. This is a strong indication that radiation pressure force does not dominate the cloud motion in most BLRs.

The situation in the NLR may be different since, in many sources, there are indications of gas outflow in this region. The evidence is obtained from line profile observations of several objects. There are very few models that fully address this issue. The reason is the various complications associated with the special location and properties of the NLR gas. The location is such that gravity is controlled by the stellar mass. Thus, the simple identical dependence of $a_{\text{rad}}(r)$ and $g(r)$ on r^2 found in the BLR cannot be applied to the NLR gas. Also, dust is clearly more important in the NLR, increasing the cloud opacity by several orders of magnitudes. Finally, the NLR is known to be associated with the central radio source, suggesting the motion of fast particles, and shock waves, play an important role in this region.

There are two other ways to test, observationally, the relative importance of radiation pressure acceleration, and gravity, in the BLR. The first is a simple and direct measurement of the column density of the BLR clouds. Recent work by [328], [246], and others show that some of the observed X-ray variability mostly in type-2 sources is due to the passing of a large clump of gas in front of the central X-ray source. Careful modeling of several of these events led to the conclusion that they are moving inside the “typical” BLR radius, and their column density is $\text{few} \times 10^{23} \text{cm}^{-2}$, that is, large enough to prevent the gas dynamics to be dominated by radiation pressure force.

Another test suggestion by Netzer [275] is to compare BH mass determination in type-1 AGNs by using the RM method, with BH mass determination in type-2 sources using the $M - \sigma_*$ method. As noted by Marconi et al. [249], the former will be biased toward small masses if radiation pressure is important. The latter is not affected by the condition in the BLR and is determined by the bulge properties. Such an experiment can be done on several large samples of similar properties (i.e., L_{bol}) type-1 and type-2 AGNs from the SDSS sample. It indicates that, for such low-luminosity sources, radiation pressure force does not influence much the BH mass determination in type-1 sources. This suggests that the typical column density of BLR clouds is larger than about 10^{23}cm^{-2} .

Do smooth line profiles require a very large number of BLR clouds?

The suggestion by Arav et al. [8] to use high-resolution line profile observations to estimate the number of BLR clouds, or to set a limit on this number, provides a real observational test for some of the basic assumptions of the cloud model. The idea

is very simple. The emitted line profile from a single cloud can be predicted, given the known conditions in the gas. Many of those individual profiles, when combined, form the observed line profile. The larger the number of the clouds is, the smoother the profile. A small number of clouds would show clear features in the profile. Observing the same profile twice, and cross-correlating (CC) the two datasets (e.g., part of the red wing of the line) will show, in such a case, a clear CC signal. A very large number of clouds will produce very smooth profiles and no CC signal. The resolution of present-day instruments can easily approach 1 km s^{-1} , providing a powerful tool to count BLR clouds. What is the line profile of an individual BLR cloud? Considering hydrogen Balmer lines, the thermal line width is of order 10 km s^{-1} . Micro-turbulence in the gas, of order of the sound speed, are quite likely. For hydrogen, this, again, is similar to the thermal width. For metal lines, it can easily double or triple the thermal width. Can high-velocity turbulent affect the cloud interior? This question has never been answered properly, but models assuming turbulence of hundreds and even thousands km s^{-1} are still consistent with the observed line ratios. Likely causes for such turbulence are the magnetic pressure and magnetic energy associated with the (hypothetical) magnetic cloud confinement. Finally, the Balmer lines, and many metal lines, are known to be optically thick with significant optical depth. This would mean that individual line photons will only escape the gas when their frequency takes them far from the line center. The increase in line width is roughly by a factor of $\sqrt{\ln \tau}$ where τ is the line optical depth. This frequency shift for Balmer lines emitted in a stable, non-turbulent medium, translates to about 40 km s^{-1} . If the medium is turbulent and the optical depth is very large, this shift is 3–4 times the turbulent velocity. The work of Arav et al. considered various possibilities for the individual line widths. It then assumes several possible cloud distributions based on assumed kinematics and used numerical simulations to compare the resulting profiles with the observations. The clouds were chosen randomly, and the calculated profiles were cross-correlated with those observed. Under such conditions, several clouds can have very similar line-of-sight velocities, and at the same time, some velocity bands may be hardly populated. Under such conditions, the number of clouds required to fit the very smooth profiles observed in some objects (e.g., NGC 4151), were huge, $few \times 10^7$. Figure 6.8 illustrates some of these issues.

Can cloud numbers be estimated from other considerations? This is rather simple given the known BLR size, if the typical dimensions of the clouds and the total BLR covering factor are known. Assume N_{col} is the column density, n_e the gas density, and C_f is the covering factor. RM studies suggests that for $\text{H}\beta$,

$$r_{\text{BLR}}(\text{H}\beta) \simeq 0.1 \left[\frac{L_{5100}}{10^{46} \text{ergs}^{-1}} \right]^{0.6 \pm 0.1} \text{ pc}. \quad (6.3)$$

This would give the following approximation to the number of BLR clouds:

$$n_c = \frac{4C_f r_{\text{BLR}}^2}{(N_{\text{col}}/n_e)^2}. \quad (6.4)$$

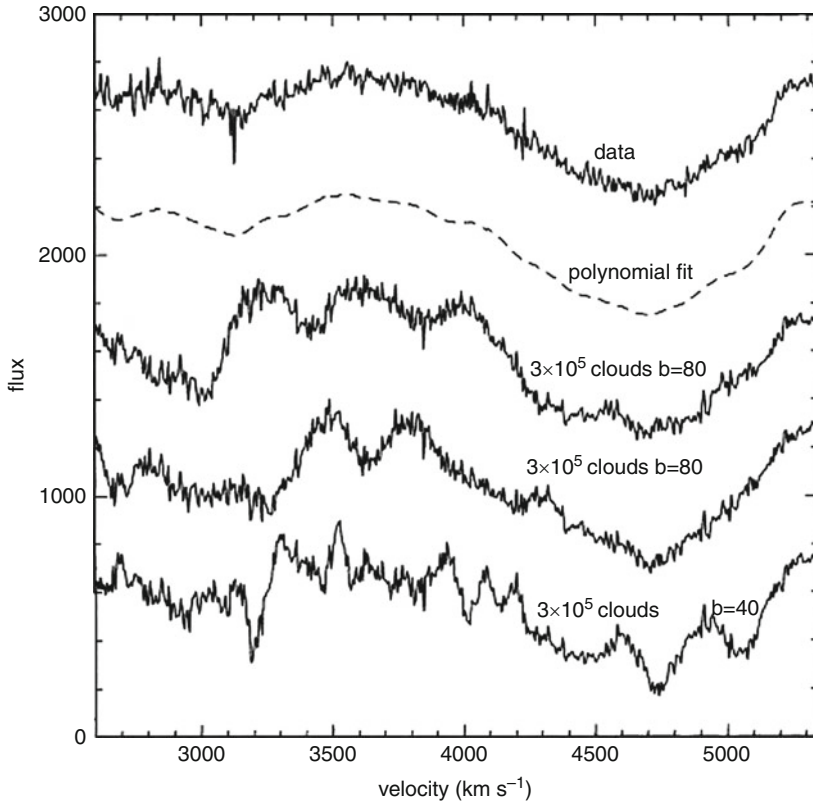


Fig. 6.8 A comparison between the observed H α line profile in NGC 4151 (*top curve*) and several simulated profiles that assume $3 \cdot 10^5$ clouds. The intrinsic (individual cloud) line widths (the b parameter given in units of km s^{-1}) are noted next to each plot (Fig. 8 from [9])

Assume $N_{\text{col}} = 10^{23} \text{cm}^{-2}$, $n_e = 10^{10} \text{cm}^{-3}$ and $C_f = 0.1$, we get for low-luminosity source like NGC 4151, $n_c = \text{few} \times 10^6$. For a high-luminosity AGN, the number is $\text{few} \times 10^8$. For NGC 4151, the number found by Arav et al. as the minimum required to explain the smooth H α profiles is about an order of magnitude larger.

What can result in line profiles that are smoother than those simulated by Arav et al.? The most promising explanation is based on the assumption of ordered cloud motion. Here, each cloud has a somewhat different velocity, and the velocities of all clouds in a certain location are highly correlated. In this case, the total number of clouds could be only several times larger than the one obtained by dividing the observed FWHM to the typical FWHM of an individual cloud (i.e., several thousands clouds). Clouds moving in an ordered flat rotating system around the central source will produce a disklike smooth profile even if their number is not large. Pure outflow or pure inflow are other possibilities where the numbers need

not be very large. Finally, bloated stars with large cometary tails can exhibit very broad profiles resulted from high-velocity internal motion in each atmosphere and/or cometary tail.

Thank you, Hagai. We will treasure your answers and the ones of the previous contributors for the final chapter where we will attempt to assess the state of the art of BLR studies. We now focus on one of the possible origins of emission lines mentioned earlier. The accretion disk is believed to contribute to the typical quasar continuum with a broad thermal feature mainly in the UV, but it could be also a significant source of line emission.

6.4 Line and Continuum Emission from an Accretion Disk

Dear Suzy (Collin), with Dumont, you published an interesting series of papers around 1990 about line and continuum emission from accretion disks. What were the reasons to shift to accretion disk studies at this time, and were they related to the line spectrum?

I have been always worried by the fact that the broad Balmer lines did not have absorption components (this is not the case for resonance lines like $L\alpha$ and $CIV \lambda 1549$). On the one hand, Balmer lines are optically thick in the “standard model” of the BLR; on the other hand, the coverage factor of the continuum source should be larger than 0.1 for the clouds to capture enough ionizing radiation. This implies that the broad-line clouds, at least those emitting the Balmer lines, should not be located on the line of sight of the central source, unless Balmer lines would be partly absorbed. As a consequence, the clouds should be confined in a quite flattened system (but not completely flattened), and we should be looking close to its perpendicular direction. The most natural idea for this system was an “accretion disk,” warped or “flaring.”

This is what we wrote in 1988 in our review with J.-P. Lasota [78]. We proposed that broad emission lines can be separated into two distinct systems: the “high-ionization lines” (HILs) like $L\alpha$ or CIV , and the “low-ionization lines” (LILs) like the Balmer lines. HILs would be emitted by low-pressure optically thin “clouds” illuminated by a rather soft continuum radiation; LILs would be produced by a high-pressure optically thick medium, illuminated mainly by hard X-rays, possibly the outer region of an accretion disk. However, we showed that this version of the photoionization model of the broad-line region was still unable to provide a consistent explanation of the unusual intensities of the iron ($FeII$) lines in strong optical $Fe II$ emitters [73].

HILs and LILs do not have exactly the same kinematics. HILs are sometimes blueshifted with respect to LILs. Quasars BALs with P Cygni profiles in the UV assess the presence of a highly ionized wind on the line of sight which should contribute to the emission, and blue wings of HILs display also absorption

components in some Seyfert-1 nuclei. Thus, Collin et al. [72] proposed a dynamical model accounting for these two components. HILs would be produced in the vicinity of shocks in the wind, and LILs would be produced in the outer part of the accretion disk as a result of energy reflected from the flow above the disk. This model solved the well-known cloud confinement problem by gravitational confinement for the LILs and by postulating a transient cloud population for the HILs.

But since this time, there were many studies of the variability of the line profiles, from which emerges a more complex model where LILs could be produced also partly in a wind. And finally, it is surprising to notice that after 50 years of studies of the line emission—which is after all the most prominent spectral characteristics of quasars and type-1 AGNs—and 30 years of detailed reverberation mapping studies, the kinematics of the BLR is still unknown or is a matter of debate, and one does not know for sure whether the emissive gas is infalling, outflowing, or rotating. And that the very nature of the BLR is absolutely not understood: is it made of bloated stars, of gas ripped off from the disk, or on the contrary, of a condensed portion of the accretion flow?

To come back to accretion disks, the idea that a fraction of the emission lines were emitted by the accretion disk began to grow in my mind. I published the first paper of a series [65], where I showed that, if the outer parts of the disk (at $r \geq 100r_g$ where $r_g = 2GM/c^2$ is the gravitational radius) were illuminated by the central UV continuum, it would be heated and could emit both spectral lines and the “5 μ -bump” which was not explained. Later, it was followed by several other papers published with Anne-Marie Dumont ([71] and the subsequent papers), where we studied in a simplified way the structure of the irradiated atmosphere of the disk and its emission. In particular, we showed that the line should not necessarily display double-peaked profiles if the line emissivity was still high at large radii.

A subject on which I had to fight to impose my views was the origin of the variable optical–UV continuum: I proposed [66] that it was radiation reprocessed in the atmosphere of the accretion disk irradiated by the central X-ray source. It could explain the good correlation with very small time lags between the optical and UV continuum variations, which could not be accounted by dynamical perturbations, whose propagation time was too long. Though the X-ray luminosity did not dominate the bolometric luminosity, the contribution of the reprocessed optical–UV radiation was in agreement with the observations. In particular, it explained why the observed continuum hardens when it brightens. And finally, I predicted that a good correlation should exist between the variability of the X-ray and optical fluxes (it was not yet observed at this time). Later on, Rokaki et al. [335, 336], showed that the observed X-ray and optical continuum and line variability in Seyfert-1 nuclei, in particular in NGC 5548, agreed well with this scenario.

In our series about the line emission from accretion disks, Anne-Marie Dumont and myself had overlooked an important issue: the accretion disk begins to be gravitationally unstable at a typical radius of $1,000r_g$ (locally, not totally unstable, i.e., the mass of the disk at this radius is much smaller than the mass of the black hole). But we have used in our computation the “standard disk” model of Shakura and Sunayev which is not valid in the case of gravitational instability. So I began

to wonder about the structure and the emission of the disk at these large distances. With Huré et al. ([182] and subsequent papers), using a set of molecular opacities, we found that the disk becomes dominated by its local gravity at a radius of the order of $1,000r_g$, with a temperature of a few hundreds to a few thousands degrees. Owing to the gravitational instability, the disk is broken into pieces which, if they do not collapse, could constitute the clouds, giving rise to the broad lines, as they “see” the central UV-X continuum. I have often been impressed by the fact that many people ignore this and imagine that the accretion disk can have an infinite extension. Actually, these outer parts of the disk located between the “real” disk at $r = 10-1,000r_g$ and emitting the “UV bump,” and the torus² at $r \geq 10^5 r_g$, constitute a “no man’s land” whose structure is completely unknown. How are the mass and the angular momentum transported in this part of the disk? Is it this part of the disk which emits the continuum above 1μ whose origin is yet not understood? And if it is the case, what is the source of energy? It could be simply radiative heating by the central parts of the disk, but it requires a strong warping.

Finally, the ultimate consequence of the disk instability is to give rise to clumps which, if they are massive enough, could collapse and form stars. With Zahn ([79] and subsequent works) we showed on the basis of semi-analytical computations that stars could indeed form in the outer parts of the disk. They should then accrete matter and evolve very quickly toward massive stars which explode as supernovae. We proposed that these supernovae could explain the rapid metal enrichment of the BLR in distant quasars. But, most important in my opinion, we proposed also that the massive young stars in the galactic center could be the result of the existence of an accretion disk a few million years ago, when Sgr*A was much more active than presently. This suggestion was ignored, or attributed later to other people. It is shown now with numerical simulations that this scenario is quite plausible and would probably explain the presence of the cluster of massive stars very close to the nucleus of several nearby galaxies (like M31).

Thank you, Suzy.

6.4.1 The Accretion Disk–BLR Relationship

Dear Bozena (Czerny) and Krzysztof (Hryniewicz), part of the current paradigm sees much of broad-line emission arising from or near an accretion disk. Initially, the BLR was often modeled as a quasi-spherical distribution of line-emitting clouds. Why has that model been discarded? Do you think that a line-emitting disk is essential or can you envision other geometries for the BLR? What are the strongest theoretical arguments in favor of a line-emitting accretion disk?

²Another paradigm, presently challenged

The extreme line width of the emission lines in active galaxies can be only explained as the dynamical effect of the emitter motion, so the idea of the BLR clouds was formulated already in 1970s [269]. Since the geometry of the cloud setup was unknown, the early approach assumed a spherical distribution of the clouds (e.g., [273]). At present, it is generally believed that BLR clouds are actually some form of continuous or clumpy winds related to an optically thick accretion disk. The exact form of this geometry is still unknown, although several observational campaigns lasting several years were devoted to the monitoring of the line response (particularly $H\beta$) to the change of the continuum, in hope that the reverberation will give the possibility to map the BLR. This goal was not achieved, but the by-product of the monitoring was a discovery of the universal BLR size–luminosity relation which is of enormous importance and serves nowadays as a basic method in determining the black hole mass.

However, certain constraints on the BLR geometry were found. The observed line luminosity implies that a significant fraction of the nuclear emission ($>10\%$) is intercepted by BLR. On the other hand, those clouds are almost never seen in absorption. Only occasionally, there were reports of the sudden temporary increase in the absorption column toward the nucleus seen in X-ray emission which implies that usually those clouds are not located along the line of sight. Since the broad line objects are viewed face-on in respect to the accretion disk and the dusty molecular torus (likely a disk extension), thus the BLR must be located not too far from the equatorial plane of the system. On the other hand, only part of the BLR is likely to be located very close to the disk surface. As argued by [72], the broad lines can be divided into high ionization lines (HIL), like C IV, and low ionization lines, like $H\beta$ and Mg II (LIL). LIL come from the region of higher density, and HIL come from less dense plasma, more distant from the disk surface, and they may be somewhat displaced with respect to LIL indicating outflow.

The connection of the disk with at least part of the BLR is expected. Lines form due to irradiation, and the disk surface in active galaxies is irradiated either directly or through scattering, by the X-ray and UV emission generated in the inner $10R_g$. The disk, according to theoretical models, is relatively geometrically thin, and the disk thickness does not rise with the radius in the inner, radiation pressure dominated part. Thus, the irradiation likely becomes important in the disk outer region, where the radiation pressure stops to dominate, and the flaring disk becomes exposed to direct irradiation (see, for example, [239] and the references therein). This happens roughly at $10^4 r_g$, where the Keplerian velocities are about $3,000 \text{ km s}^{-1}$ and the detail values depend on the Eddington ratio.

In addition, likely, support for the direct connection between the cold disk and the BLR comes from the consideration of the true Seyfert-2 objects, that is, those which intrinsically seem not to have a BLR. Those sources have rather low Eddington ratios, below 0.001, and at such low luminosities, the cold disk in significant part of the flow (or entirely) is replaced with a hot optically thin flow of the ADAF/RIAF type, and the disappearance of the cold disk and BLR match in the parameter space [85]. Inner hot flow cannot provide the BLR material since the accompanying outflow, even if efficient, does not cool fast enough [54].

This connection does not yet restricts the BLR geometry automatically. As soon as the disk becomes irradiated, a strong wind rises from the disk surface (e.g., [263, 313]). This wind itself may be optically thick in the radial direction, thus shielding the disk at larger radii from irradiation. Such a picture was discussed in detail, for example, by [136], and [107] in his global quasar geometry. Thus, the range of the disk radii illuminated by the central source is determined by the local wind outflow rate, which is rather difficult to predict theoretically. The extension of the irradiated disk is also difficult to determine observationally. Line emission from a disk belt should lead to a double profile, but such a profile is rarely seen (in some radio galaxies or as a variable part of the line profile). This means that the contribution of the kinematic component from the outflowing material as well as from distant material is important. In quasars, HIL lines are somewhat blueshifted thus clearly implying outflow, but LIL lines or in general lines in the lower luminosity AGNs do not show such a shift. The two statements are not in contradiction if the clouds are outflowing as well as inflowing, and such a “boiling” model for a BLR was suggested by the inflow of Fe II emitting clouds [124]. Inflowing/outflowing cloud model for a BLR was considered as early as in 1980s by [368]; also, Chris Done discussed such a model in the context of the warm absorber. Observational considerations suggest that the dispersion part to the Keplerian velocity field is at the level of 0.1 [77]. This explains why some trends between the line width and the inclination of the source are seen [280], but the trend is not strong enough to prevent the use of the line width for black hole mass determination, without a priori knowledge of the system inclination. However, in cases of very low inclination angle sources, the error may be considerable [77]. In our recent paper [86], we showed that the scaling of the BLR radius combined with the standard accretion disk theory implies the universal disk effective temperature of 1,000 K at the inner edge of the BLR, and this in turn points toward the role of the dust in the disk atmosphere in launching a “failed wind.” If this picture is correct, it opens possibilities of quantitative modeling of the BLR.

Thank you, Bozena and Krzysztof. Double-peaked profiles (especially in the Balmer lines) have been considered as compelling evidence of line emission from a weakly relativistic disk. Reality appears to be more complex than the predictions of models, so that we would like to discuss more deeply what double-peaked profiles tell us about accretion disks.

6.4.2 Double-Peaked Profiles and Accretion Disk Line Emission

Dear Mike (*Eracleous*), the current paradigm sees much of the broad-line emission arising from or close to an accretion disk. Double-peaked emission lines in some sources have been interpreted as an accretion disk signature. Do you remain an advocate of this interpretation?

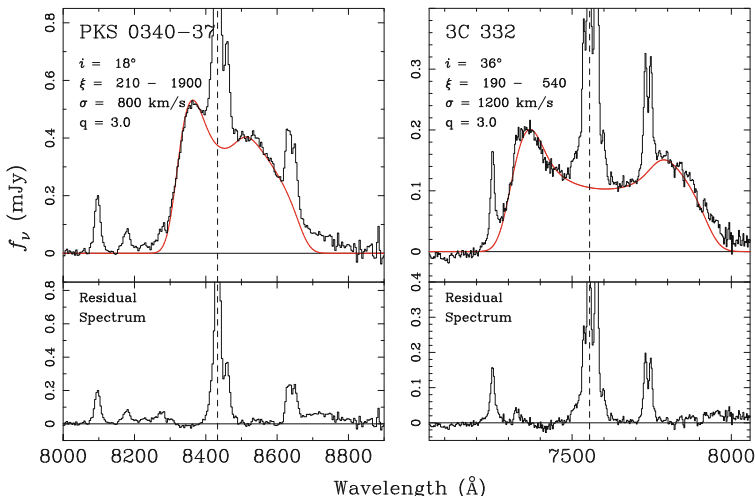


Fig. 6.9 Two examples of double-peaked H α lines found in radio-loud AGNs (from [113]). The wavelength scale is in the frame of the observer. The upper panels show the spectra after subtraction of the continuum, with a model attributing emission to a relativistic, circular, Keplerian disk has been overplotted for comparison (*solid, red line*, with model parameters given in the upper left corner of the frame). In this model, the line-emitting region of the disk lies between radii ξ_1 and ξ_2 ($\xi \equiv r/r_g$, where r_g is the gravitational radius, defined in Sect. 6.4.2). The observer’s line of sight makes an angle i with the axis of the disk, whose emissivity profile varies with radius as ξ^{-q} . The lines are assumed to be broadened by local turbulence which produces a velocity dispersion σ . The lower panels show the residuals after subtraction of the model from the spectrum

Double-peaked Balmer emission lines were noticed in the spectra of active galactic nuclei (AGNs) close to 30 years ago (the earliest report I am aware of was published in 1983 by [371]). Examples of such line profiles are shown in Figs. 6.9 and 6.10, which also illustrate their variety (sometimes the peaks are well separated from each other, while in other cases, they are close enough together that they blend with the narrow H α + [NII] narrow-line complex and take the form of shoulders). Many more examples can be seen in the papers dedicated to finding such “double-peaked emitters” [112, 113, 377].

A number of interpretations have been discussed in the literature since then (see Sect. 6.4.2), many of which have focused on explaining the double-peaked profiles. The interpretation that I find most appealing and I favor attributes the origin of the lines to the photoionized skin of the accretion disk that surrounds the central black hole. The line-emitting region is an annulus between a few hundred and a few thousand gravitational radii from the center (the gravitational radius is $r_g \equiv M_{\text{BH}}/c^2$, with M_{BH} the mass of the black hole). Models for the line profiles based on this scenario were developed by [59, 60] and later extended by other authors (see Sect. 6.4.2). These models can fit about half of the observed profiles very well (see the examples in Fig. 6.9). The remaining profiles can be fitted with more sophisticated models that invoke a perturbed accretion disk (discussed in

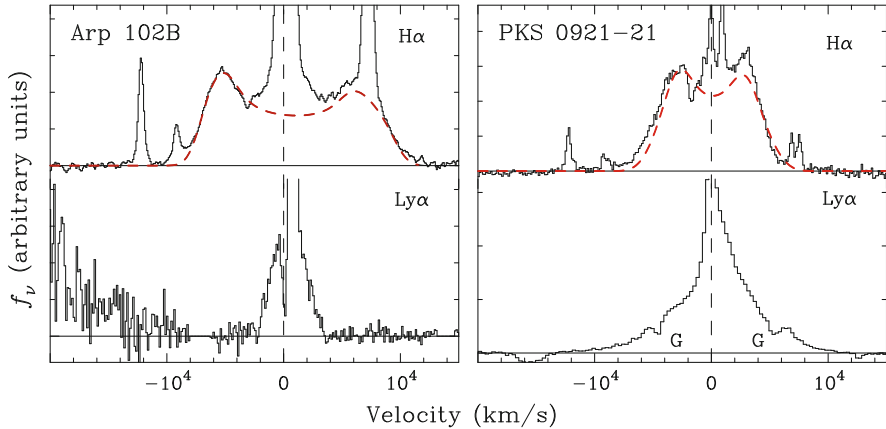


Fig. 6.10 Comparison of the $H\alpha$, $MgII$, and $Ly\alpha$ line profiles of two AGNs with double-peaked Balmer lines. Notice that, even though $H\alpha$ is double-peaked and “boxy”, $Ly\alpha$ is single-peaked and has a smaller width at half-maximum. The $Ly\alpha$ spectra were obtained with the *Hubble Space Telescope*, while the $H\alpha$ spectra were obtained from the ground within two weeks of the UV spectra. The red, dashed lines in the top two panels show a disk model that describes the $H\alpha$ profile. The absorption lines marked with a “G” in the $Ly\alpha$ spectrum of PKS 0921–021 arise in the interstellar medium of the Milky Way

Sect. 6.4.2). The appeal of the disk interpretation comes not only from the fact that it provides good fits to the line profiles but also because it has a complete physical model [70, 101, 102, 335] associated with it that explains all of the other properties of double-peaked emitters.

What do you think about an alternative interpretation of double peakers that interprets them as the signature of binary black holes?

A number of interpretations for double-peaked profiles, other than emission from an accretion disk, have been advanced. Emission from a binary black hole is one such interpretation (e.g., [32, 141]). Other interpretations include emission from a biconical outflow (e.g., [411]) and emission from a spherical distribution of clouds that is illuminated anisotropically by two biconical beams of ionizing radiation (e.g., [163]). All of the above interpretations have been tested observationally and rejected because they cannot explain the properties and variability of double-peaked emission lines as well as the accretion disk scenario. The spherical, anisotropically illuminated region scenario is not physically sound because it invokes clouds in randomly inclined, *crossing*, Keplerian orbits. Such clouds would collide with each other, and the system would be destroyed in a few dynamical times.

A very important test for all of the above scenarios is afforded by the reverberation mapping campaigns on the double-peaked emitters 3C 390.3 and Arp 102B (see [95, 285, 346, 347, 350]). These campaigns showed that the two peaks of the Balmer lines respond in concert to changes in the ionizing continuum. The delays between continuum and line variations range between approximately 20 and 60 days. Such

behavior is incompatible with both the binary black hole scenario and the biconical outflow scenario. Furthermore, the binary black hole scenario implies that the two peaks of the Balmer profiles should move in velocity on timescales of decades as the two black holes and their emitting regions orbit each other (the binary periods are expected to be on the order of a century). However, this behavior is not observed (see the study of [114] and the variability data in [151,236]), which leads to unreasonable values for the masses of the hypothesized binaries.

Finally, another test that disfavors all of the above alternatives and reinforces the appeal of the disk interpretation is based on UV spectroscopy of double-peaked emitters with the *Hubble Space Telescope* [115, 167]. The UV spectra show the profile of the Ly α and other UV lines to be quite different from those of the Balmer lines: Ly α is single-peaked when the Balmer lines are double-peaked, as illustrated in Fig. 6.10. This is not compatible with the binary black hole and biconical outflow scenarios which invoke a separate emission region for each peak in the Balmer profiles. In fact, this difference was *predicted* by [70,335]. This comes about because in the innermost parts of the disk where the velocities are highest, the density and column density are so high that Ly α photons are trapped by resonance scattering and then “destroyed” by collisional de-excitation.

Are there physical or empirical motivations driving several proposed refinements of accretion disk models, for example, elliptical disks, disk warping, and nonuniform illumination of the disk? Do they provide an advance in the interpretation of observed profiles?

The simplest version of the disk model, the static, axisymmetric disk cannot explain all of the observed double-peaked profiles nor can it account for their variability. These two factors have motivated the development of more sophisticated models for the line profiles, which are inspired by dynamical models for non-axisymmetric and time-dependent disks. Examples include spiral arms triggered by self-gravity or an external perturbation, an eccentricity induced by an external massive perturber (an idea borrowed from cataclysmic variables, e.g., [240]), irradiation-induced warping (e.g., [247,307]), and small-amplitude, stochastic perturbations caused by star-disk collisions (e.g., [413]), vorticity (e.g., [24, 186, 297]), or self-gravity (e.g., [164]).

Model line profiles from an elliptical disk were developed by [116] and used by [116, 377] to fit the observed double-peaked profiles that could not be described by the simpler, axisymmetric models. This illustrates that the disks have non-axisymmetric perturbations, although they need not be elliptical. The same model was also used by [375] to describe the variable double-peaked H α profile of NGC 1097, while [376] tested the elliptical disk model and a model of a disk with a 1-arm spiral against the variable H α profile of NGC 1097 and found the latter to be preferable.

Major advances came about with the combination of the above models with longtimes series of spectra that capture the variability of double-peaked lines on timescales from a few months to 30 years. These longtime series allow one to study the changing structure of the line-emitting region and in the context of the disk interpretation, probe disk perturbations. This type of work on double-peaked

emitters was begun by [159, 279], and the most recent results were presented by [130, 151, 190, 236]. The study of the large-amplitude, long-term (several years to decades) profile variations suggests that large-scale, non-axisymmetric perturbations are common in disks. In particular, Lewis et al. [236] suggested that the perturbations are best described by nonsteady spiral arms. The study of small-amplitude variability of the line profiles by [130] suggests that this is best explained by shortlived, self-gravitating clumps in the disk. Thus, a number of clues point to self-gravity as the cause of profile variability.

In my opinion, the next major advance will come from extending such variability studies to AGNs with single-peaked emission lines. If double-peaked emitters are connected to the greater population of AGNs as I suggested in Sect. 4.7, then the lessons we have learned from studying them should have much wider applicability. In other words, these unusual line profiles can reveal phenomena that are not easily recognized in the more common cases.

Thank you, Mike. The continuum of (unobscured) quasars is very particular if compared to the ones of stars; emission extends from radio to the γ -ray domain and is very far from the slightly deformed blackbody of ordinary stars peaked at well-defined wavelengths. At the same time, it is clear that the quasar continuum is not a simple power law. It has features that may help or complicate its interpretation. The enormous range of frequency over which especially radio-loud quasar emit invoked particular nonthermal processes. The physical mechanisms operating in the continuum region remain hotly discussed, with significant differences expected for radio-quiet and radio-loud sources. We will start with the interpretation of the FUV ionizing continuum, to progress with the more exotic processes that are expected to give rise to the radio and high-energy photons.

6.5 Origin of the Continuum

Dear Julian (Krolik), reverberation mapping techniques exploit the emission-line response to continuum variations. The underlying assumption is that the line-emitting gas is photoionized by a continuum source surrounding the central black hole. What are the current ideas about the origin of the ionizing continuum and of continuum variations?

As discussed in the context of black holes as “prime movers” for AGNs, there is a strong consensus identifying accretion onto supermassive black holes as the key mechanism of energy generation in these systems. An immediate consequence of that identification is the prediction that most of their light output should emerge in the UV.

Wherever matter and radiation can interact and exchange energy sufficiently strongly, that is, wherever the density and optical depth are large enough, the matter and radiation reach a state of thermal equilibrium; both distribution functions are

thermal and share a common temperature. Just such a state should be reached in the accretion flows of AGNs. If the mass accretion rate is high enough to supply the power that is required, its total optical depth (predominantly due to Thomson scattering) is expected to remain large at least until the flow approaches the innermost stable circular orbit (ISCO). This large scattering optical depth enhances the effective path length travelled by photons as they diffuse out of the matter, so that the smaller absorptive opacity created by the free–free process can be effective. Thus, the spectrum radiated from the accretion flow is expected to be, at least to a rough approximation, a superposition of local blackbodies. Because the greatest part of the energy comes from the deepest part of the potential from which radiation is effective (somewhere near the ISCO, with “somewhere” subject to the uncertainties discussed in Sect. 6.10.2), the crudest zeroth-order prediction of the spectrum is that of a single blackbody, radiating with the temperature of the ISCO region. That temperature would then be defined by

$$L \sim 2\pi r_{\text{ISCO}}^2 \sigma T^4. \quad (6.5)$$

The factor of 2 comes from the fact that a disk has a top and a bottom surface.

It is convenient to rewrite the luminosity in Eddington units both because it is hard to imagine how the luminosity could exceed that value by a large factor and because the importance of electron opacity makes it a characteristic scale for all relativistic accretion dynamics. In addition, it is natural to scale the radiating area to the gravitational length-scale r_g . In those units, we find that

$$T \sim 10^6 (A_{\text{rad}}/r_g^2)^{-1/4} L_{46}^{-1/4} (L/L_E)^{1/2} \text{ K}, \quad (6.6)$$

where the luminosity L has been scaled in units appropriate to quasars, $10^{46} \text{ erg s}^{-1}$. Because the radiating area in most cases is $\sim O(10)r_g^2$, the characteristic temperature is a bit smaller than 10^6 K . To the degree that the accretion is sub-Eddington, it is still lower. The energy equivalent of 10^5 K is $\simeq 10 \text{ eV}$; in other words, the peak of the spectrum should fall in the UV or EUV.

Thus, the simplest possible application of accretion disk theory points to a spectrum in which photons near the ionization edge of H are a dominant part of the emitted radiation. Fortunately, in equally crude terms, that is exactly what is observed.

In addition, however, all accreting black hole systems, whether of stellar mass scale or galactic mass scale, seem to have the ability to radiate a significant part of their total power in hard X-rays. Exactly how the energy for this “coronal” emission is removed from the optically thick, quasi-thermal disk body and dumped into much lower density, much lower optical depth matter is not well understood, although the importance of magnetic stresses in the disk makes it natural to ascribe this energy transfer to some mechanism associated with magnetic fields. Nonetheless, if one assumes that it happens, and the coronal region is close to the quasi-thermal disk, a natural story emerges for the radiation mechanism responsible for these X-rays.

Relatively low energy photons (~ 10 eV in AGNs) stream out of the disk; as they pass through the much hotter nearby corona, they are inverse Compton scattered; if the temperature of the coronal electrons is ~ 100 keV, the photon energy is, on average, multiplied by a factor of order unity each time it is scattered. All it takes to move $\sim 10\%$ of the emergent light power from the UV to the X-ray band is for the typical number of scatters to be $\sim O(1)$ because those few photons scattered more times, so that they are boosted into X-rays, are multiplied in energy by $\sim O(100)$.

The combination of this coronal process (whose results are universally seen in AGN spectra) and the disk’s thermal emission (likewise universally seen) forms a very natural explanation for the source of the ionization radiation. The principal missing link in our understanding is how the energy for the coronal region is conveyed there from the disk.

Our understanding of continuum variability is as yet in a primitive state. Given the reliance of any accretion at all upon the existence of well-developed MHD turbulence in the disk, it is natural to attribute the origin of variability to that turbulence. However, we do not as yet have a good description of the statistical properties of the turbulence, and we have even less knowledge of how dynamical fluctuations are translated into variations in light output. The principal statement we can make with confidence on the latter score is that heat is carried from the disk interior to the surface primarily by radiative diffusion [176], and as a result, variability on timescales shorter than a photon diffusion time (generically $\sim [O(10)\Omega]^{-1}$, for local orbital frequency Ω) in the local emitted flux should be weak.

To date, there are only two published studies on how fluctuations driven by MHD turbulence might relate to light variability: [341] and [281]. The earlier of these two efforts focussed on thermal emission and the latter on coronal. For a variety of reasons, the power spectrum of fluctuations for the coronal emission is more readily estimated from simulation data, and the simulations do predict a power law not too dissimilar from the one that is observed. These are, however, still very preliminary results; over the next few years, there will likely be more thorough efforts to derive the radiative properties of disks driven by MHD turbulence.

Thank you, Julian.

6.5.1 Accretion Disk Structure and Continuum Emission

Dear Bozena (Czerny) and Krzysztof (Hryniewicz), hot gas in an accretion disk is believed to emit part of the quasar continuum and to give rise to a distinctive optical–UV feature called the “big blue bump.” What are the expected observable features of an accretion disk spectrum? How does accretion disk structure depend on accretion rate? At very low accretion rates, the gas is believed to enter a very low-efficiency accretion mode. Are such advection-dominated accretion flows relevant for quasars? What happens if

the accretion material becomes overabundant? Is there a physical limit above which accretion becomes impossible?

Apart from the broad emission lines, the profound big blue bump is the notable feature in the quasar continuum. Its broad-band shape in some quasars and a bright quasar composite by [132] can be very well fitted by the simplest classical disk model of Shakura–Sunyaev or its relativistic version by Novikov–Thorne [87, 215]. This is in a close analogy with the galactic sources—they also occasionally show disk-dominated spectra, with only weak hard X-ray tail. Such spectra are seen when the accretion rate is high (soft state) but the Comptonization is not too strong (e.g., very high state). Some departure from the black-body emission is expected and models based on more advanced radiative transfer in a hydrogen disk atmosphere were statistically tested for quasars from SDSS survey [90]. The model spectra are frequently bluer than the observed ones, but the discrepancy is satisfactorily explained by the presence of the intrinsic reddening.

The disk continuum emission was theoretically predicted to be present in the IR as well. The recent study of the polarized emission revealed this component, buried in the starlight and warm dust emission, and the spectrum of this component is rising toward shorter wavelengths, as expected from the Shakura–Sunyaev model [203].

Therefore, the overall disk continuum matches well the observed shape of the big blue bump which provides a strong support for its disk origin. However, some aspects of the disk fitting to the big blue bump are still puzzling.

At the shortest wavelengths, the quasar spectra roll off too quickly shortward from the Ly α . In other (high redshift) quasars, the continuum extends very far into UV, with a slope of ~ 1 , and the resulting spectrum is much broader than expected from the simplest disk model. Both issues are likely to be resolved by the specific properties of the intrinsic extinction (large grains and/or nano-diamonds).

Next issue is the lack of spectral features in the observed quasar spectra. The computations of the disk spectra including the bound-free transitions usually predict absorption edges, most notably the Balmer and the Lyman edge. Those edges are expected to be partially smeared due to the disk Keplerian motion, but they still should be visible. However, Lyman edge is never seen in the data; however, a slope of the spectrum changes there, as well as the level of polarization. This indicates the (expected) role of the electron scattering/Comptonization in the disk atmosphere, or in the surrounding fully ionized plasma. Also, the buried Balmer-edge signatures were detected in a few quasars with the use of the best telescopes—VLT and Keck [204]. Therefore, the disk interpretation of the big blue bump is not questioned much nowadays.

The classical disk models are expected to work for moderate Eddington ratios. Above ~ 0.3 Eddington ratio, the theory predicts the increasing role of advection, and more general, slim-disk models apply. Observations suggest that in addition, a significant Comptonization in a moderately hot plasma takes place, shaping the spectra observed in NLSy1 (steep power law in the soft X-ray band). The origin of this Comptonizing plasma is unknown, with disk corona inflow or outflow the most plausible possibilities. Slim-disk models can be used even for extremely

super-Eddington accretion rates (there are no formal limits for the accretion rate), and they predict that disk luminosity then saturates at about 10 Eddington luminosities due to photons being trapped by the inflowing plasma. However, quasars do not seem to accrete significantly above the Eddington rate, either due to lack of material or inflow/outflow balance. Highly super-Eddington accretion may take place early in the life of a growing black hole, but during this process, the black hole is likely completely buried in the surrounding material and thus observationally not recognized as a quasar.

At very low Eddington rates (the extreme case is Sgr A*), there is no cold disk, and the inflowing plasma is optically thin. The early models of such flow postulated low radiative efficiency of such accretion (ADAF, RIAF); at present, the radiative efficiency is still under discussion and likely, to be much higher than expected previously.

At intermediate Eddington rates, we thus have a transition from the cold disk flow to hot flow, and this transition likely happens at ~ 0.001 . The theory is poorly understood; some attempts on prediction of disk evaporation/condensation are being made since 1990s. The description is based on electron conduction and radiative processes, without satisfactory description of the ions, and the role of the magnetic field.

Objects with inner hot flow instead of an inner cold disk should show no big blue bump component. Radio galaxies are likely to be in this category. Spectra of radio-quiet as well as radio-loud quasars, as best seen in quasar composites, are dominated by the big blue bump so the optically thin flow model cannot apply. There are alternative models to the classical disk [67, 183], but they assume the presence of numerous clouds of considerable optical depth, and then, those models are quite similar to a turbulent disk.

Thank you, Bozena and Krzysztof.

Dear Luigi (Foschini), can you please summarize the main aspects of γ -ray production in quasars? To what extent is every quasar a γ -ray emitter?

The most common scenario is that named “leptonic” [46]: a population of relativistic electrons is collimated (likely by a magnetic field) and pushed outward, forming a jet extending from the poles of the central supermassive space-time singularity.³ When moving in a magnetic field, the relativistic electrons generate synchrotron radiation, the low-energy hump of the SED. The same electrons transfer part of their energy to low-energy seed photons (i.e., they cool themselves), which in turn are boosted to high-energy γ rays. If the seed photons are the same generated by synchrotron emission, then the process is named synchrotron self-Compton (SSC). If the seed photons are coming from other regions of the AGN, external to the jet, like the accretion disk, the broad-line region (BLR) or the molecular torus, then the process is collectively called external Compton (EC). See [155] for a recent update on the blazar models and the different components.

³How the jet is triggered is one of the main unknown of the modern astrophysics.

Ghisellini et al. [152] proposed a theoretical explanation of the observed blazar sequence based on the impact of the environment nearby the central black hole on the cooling of electrons. Quasars, which are rich of optical photons (high accretion rate, strong and broad emission lines), offer the proper environment for a fast cooling, and therefore, they are the most powerful object. The γ -ray hump is then basically generated by EC, and the seed photons mainly come from the BLR [129, 158, 305, 383], although some researchers suggest that the region where most of the dissipation occurs could be at larger distances, and the seed photons are those from the molecular torus [250, 365].

The case of BL Lac objects is different: the accretion rate is small, and then, there is low power to ionize the nearby gas. The environment is thus poor of photons, and electrons are not able to cool efficiently. The main mechanism to generate γ rays is SSC, and therefore, the blazar emits low power, but it is able to produce photons of very high energy (in the TeV range). See [158] for a recent summary of the properties of γ -ray bright blazars.

The emission of γ rays from radio galaxies could be different, because the jet is observed at large angles (tens of degrees). Georganopoulos and Kazanas [148] proposed the model of the “decelerating jet,” where the γ rays are produced by the electrons of the jet base, still moving at high speed, which in turn interact with the low-energy photons produced in the deceleration zone. Ghisellini et al. [157] proposed instead the “spine-layer” model, where the jet is composed by an inner and fast spine and an external slower layer. The relative motion of the two component generates the observed high-energy γ rays.

Therefore, every AGN with relativistic jet should be a γ -ray emitter, in a way or another, although it is not easy to estimate the fraction of jetted AGNs with respect to the whole population. The common wisdom says that jets are present in $\sim 10\%$ of AGNs, but it is expected that this fraction could change depending on the redshift (see [399]).

Thank you, Luigi. We now enter into the discussion of a dynamical process that is probably very important in the evolution of the quasar and of its environment. The existence of outflowing gas in various dynamical and physical conditions is supported by a large body of evidence, most of it discussed in the previous chapters. What are the physical processes that make possible outflows from quasars? It is possible to build models on the basis of our present knowledge of the geometry and dynamics of the outflowing gas? These are the questions underlying the dialog that follows.

6.6 QSO Outflows

Dear Daniel (Proga), what do we know about quasar outflows?

All astrophysical objects appear to have some sort of an outflow. In some cases, the outflow can be barely noticeable, that is, its density is very low so that relatively few

particles can escape, and they do so without interacting with other particles. It is akin to a process familiar to us from our daily experience, namely, evaporation. Planetary atmospheres are perhaps the best-studied astrophysical objects with weak outflows. One could push the above generalization farther and claim that all objects in the universe lose matter, however minuscule. Examples range from eroding mountains (e.g., see pictures of the Monument Valley), to black holes (the famous Hawking radiation - we shall remember that $E = mc^2$), and to the entire galaxies.

If an outflow is weak, then its effects become obvious and significant only if it lasts for a very long time, unless of course the source of the outflow is a small mass object. Evaporation is a specific example of a process where few particles have enough kinetic energy to “break free” and escape an object. As the energy of the particles and their density increase, some of them will collide and energize their surroundings. As a result, the outer layers of the object or even the object as a whole will expand. A high rate of mutual interactions will lead to thermalization in which particle properties follow a Maxwell–Boltzmann distribution. This is again a common situation and corresponds to so-called thermal expansion. We can observe and experience, for example, in the Monument Valley, by taking an old-fashioned hot air balloon ride.

My main point above is that the physical mechanisms that produce nonrelativistic quasar outflows could be the very mechanisms that produce outflows from much less exotic, well-known objects.

6.6.1 Three Main Driving Mechanisms

In the simplest terms, to produce a quasar outflow, there must be a force or forces that can overcome gravity. In the quasar context, the force candidates appear highly restricted as the gravity is due to that of a black hole. However, we should keep in mind that quasar outflows likely originate far from the black hole. After going through a list of all known forces, three contenders pose as prominent:

1. The gradient of gas pressure (a.k.a thermal expansion).
2. The radiation force (which results from gradient of radiation pressure).
3. The Lorentz force.

There are two classes of magnetically driven winds:

1. Magnetocentrifugal winds, where the dominant contribution to the Lorentz force is the magnetic tension.
2. Magnetic pressure-driven winds where the dominant contribution to the Lorentz force is the magnetic pressure.

From various observations and experiments (at the laboratory but also at home), we know that each of these forces can produce a wind (e.g., rotating a bead on a wire is very helpful to understand magnetocentrifugal winds). Therefore, the task at hand is to explain why each could operate in quasars. However, this is quite simple.

What we know about quasars for certain is that they are very powerful sources of radiation. This radiation is produced by an accretion disk surrounding a black hole. Keep in mind that, the disk and black hole are at the center of a galaxy (we will return to this later). Thus, in a quasar, there is a lot of radiation which is produced in matter-rich environment (as in that of the accretion disk, stars, and ISM of the host galaxy). We then have a complete recipe for thermal expansion, that is, a source of energy (radiation) heating uniformly up gas (radiation comes from the center), leading to strong gas pressure gradients and hence expansion. Photons carry with them not only energy but also momentum. Therefore, as photons interact with matter, they will share their momentum as well as their energy, and this leads to a radiation force.

To argue for the Lorentz force, we must use less direct arguments; specifically, we recall that the ISM in the Milky Way and other galaxies is magnetized and that stars (including the Sun) also have magnetic fields. Therefore, it is very likely that matter in quasars is magnetized as well.

However, are any of these forces strong enough to produce a quasar outflow? Clues for this question can be found in the observational properties of the outflows themselves. Therefore, let me briefly present some of these properties.

6.6.2 *The Quasar Outflows*

The most dramatic evidence for well-organized outflows in quasars is broad absorption lines (BALs). BALs are almost always blueshifted relative to the emission-line rest frame. Employing the Doppler effect, one can deduce that BALs indicate the presence of fast outflows moving from the active nucleus, with velocities as large as $0.2 c$ (e.g., [390]). Using the data from the Sloan Digital Sky Survey (SDSS), Reichard et al. [323] showed that about 15% of SDSS QSOs have BALs. However, observations of blueshifted C IV emission lines visible in BAL QSOs and many other SDSS quasars hint that winds are even more common [235, 326].

BALs are observed mostly in the UV. There are also examples of X-ray BALs. In particular, Chartas et al. [57] discovered a very broad absorption line in the X-ray spectrum of PG 1115+80. Other evidence for outflows include narrow absorption lines (NALs). The UV spectra of some quasars show NALs that are blueshifted by as much as $\sim 50,000 \text{ km s}^{-1}$ [169, 331]. NALs are found much more commonly in the UV spectra of Seyfert galaxies than in those of quasars, but in Seyfert galaxies, the lines are blueshifted by only several 100 km s^{-1} [83]. Like BALs, NALs are observed not only in the UV but also in X-rays. For example, [191] observed NALs due to highly ionized species in a high-resolution X-ray observation of the Seyfert galaxy NGC 5548 obtained by *Chandra*. The prominent broad emission lines (BELs) in the UV from H α , OVI, NV, CIV, and SiIV are the defining feature of quasars, for example, [44, 287], and they may be associated with outflows, specifically with the base of a disk wind [51, 264]. As shown by [264], the BELs

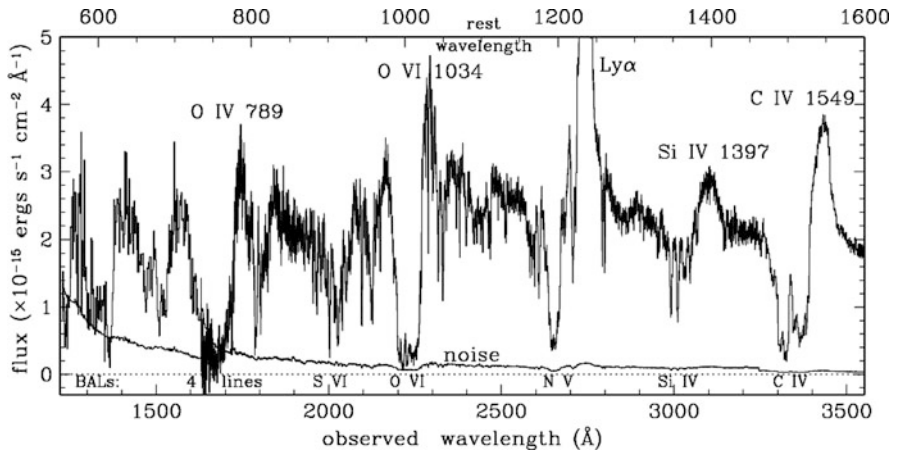


Fig. 6.11 Example of a UV spectrum of a BAL quasar. HST and ground-based observations of PG 0946+301 (taken from [11])

could be formed in regions where the outflow expansion velocity is low compared to the rotational velocity.

Figure 6.11 shows an example of an ultraviolet spectrum of a BAL quasar. It is very likely that the continuum radiation of this and other systems was produced by a thermal source: we believe that it is an accretion disk producing radiation as a multi-temperature blackbody emitter. However, the observed spectra are far from smooth as they often show many broad absorption and emission lines. The presence of the BALs themselves strongly indicates that substantial momentum is transferred from a powerful radiation field to the gas. Consequently, radiation pressure due to spectral lines has been considered by many researchers (e.g., [12,93,100,264,360]).

A crucial clue to the origin of AGN outflows, supporting radiation driving, comes from the discovery of line locking in BAL quasar spectra [131], in which the outflow is continuously accelerated by photons of one specific emission line. Weymann et al. [404] discovered that a composite spectrum of their BAL quasar sample shows a double trough in the C IV $\lambda 1549$ BAL, separated in velocity space by the NV $\lambda 1240$ -Ly α splitting $\sim 5,900$ km s $^{-1}$ (see also [217]). In fact, Arav and Begelman [10] showed that an absorption hump in the C IV $\lambda 1549$ BAL is “the ghost of Ly α ” due to the modulation of the radiation force by the strong emission in Ly α .

Spectral lines are not the only source of opacity in quasars: dust is another one. Therefore, radiation pressure due to dust has been also considered (e.g., [345,398]). However, dust grain cannot survive near quasars because of the strong radiation field. Consequently, radiation driving on dust can be important on parsec scales and produces only slow outflows.

A viable model for quasar outflows must answer the following questions:

- Where does the outflow originate?
- What is its geometry and internal structure?

- What controls the outflow ionization and thermal state?
- What controls the dynamics of the outflow?
- What are the relationships among different types of AGNs and outflows (e.g., what drives very fast UV absorbing winds and what drives very fast X-ray absorbing winds)?

How is it possible to prevent the overionization of the outflow?

The ionization balance is a key constraint on any model of the origin of AGN outflows. On the one hand, we observe very high luminosities in X-rays and in the UV. On the other hand, we observe spectral lines from moderately and highly ionized species. It is straightforward to show that the strong quasar incident continuum is likely to lead to highly ionized gas which would produce few spectral lines. Generally, two mechanisms have been proposed to resolve the so-called overionization problem: (a) the AGN outflows have filling factors less than one and consist of dense clouds, and (b) the filling factors are ~ 1 , but the outflows are shielded from the powerful radiation by some material located between the central engine (CE) and the outflow (e.g., [222]). In this context, thermal driving is unlikely in BAL outflows, because the high thermal energy needed to drive a fast wind requires temperatures that would make the wind fully ionized.

6.6.3 Line-Driven and Magnetic Disk Winds

As I mentioned above, quasar radiation is produced by an accretion disk. It is therefore natural to assume that the mass outflows originate from the disk itself. Such models for BAL QSOs have been proposed by several authors. For example, Murray et al. [264] studied a wind arising from a relatively small distance from the CE ($\sim 10^{16}$ cm). Their model requires the local disk radiation to launch gas from the atmosphere of the disk and the central radiation to accelerate the gas in the radial direction to high velocities. A key ingredient in this model (that solves the overionization problem) is that the CE radiation is attenuated by some gas located between the CE and wind. Murray et al. [264] named this gas “hitchhiking” gas and gave plausible arguments its the existence.

Other models of radiation-driven outflows in quasars propose that the radiation force accelerates a wind that has been launched and kept at a low-ionization state by *some other* mechanisms. For example, the [93] model supposes first that the wind is launched from a large distance ($\sim 10^{18}$ cm) from the CE. Because the disk is cool at these radii, the gas is not lifted from the disk by radiation pressure but rather by some alternative mechanism. Once the gas is high enough above the disk, the radiation force due to the CE accelerates the gas to high velocity. The gas is not overionized in this model due to a small filling factor caused by strong magnetic fields which confine the dense clouds. However, de Kool and Begelman [93] hinted that even in this case, there is a need for some shielding of clouds.

Line-Driven Disk Winds. Our understanding of how radiation pressure due to lines (referred to as “line driving”) produces powerful, high-velocity winds is based on studies of winds in hot stars (e.g., [55, 318, and references therein]). The key element of the [55] model is that the momentum is extracted most efficiently from the radiation field via line opacity. Castor et al. [55] showed that the radiation force due to lines, $F^{\text{rad},l}$, can be stronger than the radiation force due to electron scattering, $F^{\text{rad},e}$, by up to a few orders of magnitude (i.e., $F^{\text{rad},l}/F^{\text{rad},e} > \text{a few } 10^3$). Thus, even a star that radiates at $\sim 0.05\%$ of its Eddington limit, L_E , can have a fast wind. I note here that radiation pressure due to dust is invoked in this context for a very similar reason, that is, compared to electron scattering, the dust opacity can be up to 500 times higher.

To apply LD stellar wind models to quasars, one has to take into account at least two important differences:

1. The difference in geometry—stellar winds are to a good approximation spherically symmetric, whereas winds in AGNs likely arise from disks and are therefore axisymmetric or even non-axisymmetric.
2. The difference in the spectral energy distribution—hot stars radiate mostly in the UV (the UV luminosity, L_{UV} , accounts for most of the total luminosity, L), whereas AGNs radiate strongly both in the UV and X-rays (L_{UV} and L_X are comparable). The latter difference has two important consequences for UV line driving: not all AGN radiation contributes to driving, and even worse, the very X-rays that do not contribute to UV line driving can ionize the gas and reduce the number of transitions that can scatter the UV photons (for a fully ionized gas, $F^{\text{rad},l} = 0$).

The consequences of this difference in geometry have been studied using two-dimensional axisymmetric numerical HD simulations (e.g., [296, 308, 316, 317]). These simulations were applied to CVs which, similar to hot stars, radiate mostly in the UV. In CV disk wind models, the force exerted on the disk material is a result of the absorption and scattering of line radiation due to the disk and white dwarf radiation. In this sense, it is an extension of the [55] model where the force is exerted on the stellar material as a result of the line absorption and scattering of continuum radiation from the star.

To apply the LD disk wind model developed for CVs to AGNs, one should at least take into account the difference in the spectral energy distribution between AGNs and CVs, photoionization, and effects of optical depth on the continuum photons. Proga et al. [315] and Proga and Kallman [313] attempted just that using simulations that follow (a) a hot and low-density flow with negative radial velocity in the polar region; (b) a dense, warm, and fast *equatorial* outflow from the disk; (c) a transitional zone in which the disk outflow is hot and struggles to escape the system (this zone does the job of the “hitchhiking” gas in the [264] model). Figure 6.12 illustrates the density and ionization structure of the wind solution found by [313] (see also [367]).

In short, the concept of line-driven disk winds has been supported by detailed simulations. Now, it is important to make a direct comparison with observations.

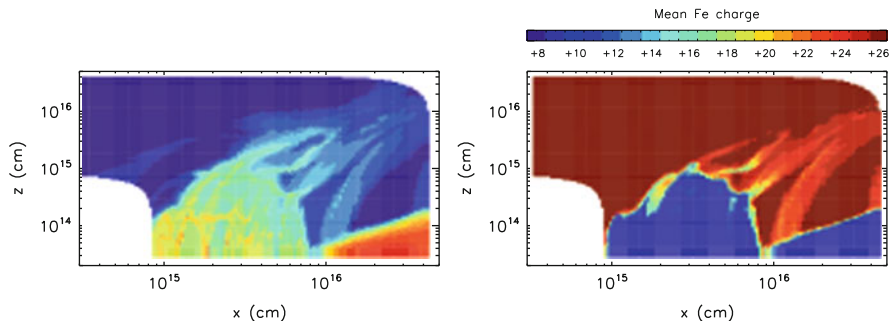


Fig. 6.12 Density (*left*; high density in red, low density in blue) and mean Fe ionization state (*right*) for a snapshot of a two-dimensional disk wind simulation from [313]. The accretion disk is assumed to be geometrically thin and lies in the xy -plane, while the primary X-ray source is assumed to be centrally located. The computational domain extends from $r \sim 9 \cdot 10^{14} - 4 \cdot 10^{16}$ cm, and the model is axisymmetric (about the z -axis) and symmetric under reflection in the disk plane. Note the logarithmic axes (taken from [367])

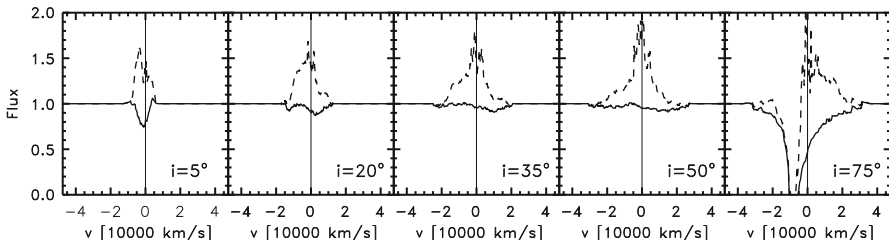


Fig. 6.13 Theoretical profiles of CIV $\lambda 1549 \text{ \AA}$ based on the wind model of [313] as a function of inclination angle, i (see bottom right corner of each panel for the value of i). The solid lines show the profiles due to the absorption only, whereas the dashed lines show the profiles due to the absorption and emission (the line source function includes resonance scattering and thermal emission). Note the sensitivity of the lines on the inclination angle. The zero velocity corresponding to the line center is indicated by the vertical line (taken from [314])

For example, synthetic line profiles can be computed based on the simulations and tested against observed profiles. As shown by PK, the synthetic line profiles show a strong dependence on inclination angle: the absorption forms only when an observer looks at the CE through the fast wind (i.e., $i \geq 60^\circ$ as shown in Fig. 6.13). This i dependence can explain why only 15% of QSOs have BALs. The model also predicts high column densities, strong X-ray absorption for the inclination angles at which strong absorption lines form (e.g., [342,367]). This trend is consistent with the observational result that BAL QSOs are underluminous in X-rays compared to their non-BAL QSO counterparts (e.g., [52, 162]).

Magnetic Disk Winds. It is quite possible that the different parts of the disk can produce different types of outflows, if any. For example, radiation pressure can drive a wind from a UV part of the disk and maybe from the innermost part where X-rays are produced, provided there is enough X-ray line opacity. Thermal driving is

likely important at large radii, provided enough radiation from the central part can reach the outer part in order to heat it (e.g., [98]). These two types of winds can be modified or replaced by a magnetically driven wind.

Undoubtedly, magnetic fields are essential to the existence and evolution of accretion disks because the so-called magnetocentrifugal instability (MRI) is almost certainly responsible for angular momentum transport in accretion disks [16]. It is likely that the fields play an important role in producing winds as shown by many (e.g., [4, 45, 51, 110, 118, 135, 214, 220, 290, 373, 394, and references therein]). To understand MHD winds, we may need models that compute the disk's internal structure as well. Simulations of the disk structure show that it is complex and turbulent (e.g., [16, 41, 176, 260, 312, 389]). This complexity is one of the main reasons why such studies only recently became feasible. It will still take a while before we are in a position to rigorously test radiative properties of magnetized disks.

Blandford and Payne [45] showed that the centrifugal force can drive a wind from the disk if the poloidal component of the magnetic field, \mathbf{B}_p , makes an angle larger than 30° with respect to the normal to the disk surface. Generally, magneto-centrifugal disk winds require the presence of a sufficiently strong, large-scale, ordered magnetic field, threading the disk with a poloidal component at least comparable to the toroidal magnetic field, $|B_\phi/B_p| \lesssim 1$. Several groups have numerically studied outflows using this mechanism (e.g., [197, 222, 290, 394]). An important feature of magnetocentrifugal winds is that they require some assistance to flow freely and steadily from the surface of the disk and to pass through a slow magnetosonic surface [45]. Magnetocentrifugal wind models, while able to predict the geometry and kinematics of the winds, must assume rather than calculate a mass-loss rate. Consequently, they are less amenable to observational testing.

Magnetic winds do not require radiation pressure and thus can be important in both low-luminosity systems such as young stellar objects and in systems with strong radiation field such as quasars that can potentially overionize the gas [214, 220, 290, 394, and references therein]. In the context of AGN outflows, models usually rely on the effects of magnetic fields as well as on line driving [93, 118, 119, 214, 310].

One of the differences between magnetocentrifugal and radiation-driven disk winds is that the former corotate with the disk, at least close to the disk, whereas the latter do not. A key parameter shaping the total line profile made up of both scattered emission and absorption is the ratio of the expansion velocity to the rotational velocity (e.g., [311]). Corotating winds conserve specific angular velocity of the gas, and therefore have a higher rotational velocity than those which do not corotate but instead conserve specific angular momentum of the gas. The former also have higher terminal velocities due to the stronger centrifugal force. Additionally, in corotating winds, the rotational velocity is comparable to the terminal velocity, while in non-corotating winds, the rotational velocity decreases asymptotically to zero with increasing radius, resulting in their having a much lower terminal velocity [309]. We therefore expect that we can distinguish these two kinds of winds based on their line profiles. For example, highly rotating winds should produce emission lines

much broader than slowly rotating winds if we see the disk edge-on. Line absorption should also be changed by the corotation. One should hope that synthetic line profiles predicted by models of magnetocentrifugal winds will soon be computed so that we will be able to compare these two types of winds.

Wind corotation depends on the strength of poloidal magnetic field, B_p . For a relatively weak B_p , a wind may corotate only very close to the disk and be driven by the magnetic pressure instead of the magnetic tension. In particular, the toroidal magnetic field can quickly build up inside the disk due to the differential rotation so that $|B_\phi/B_p| \gg 1$. In such a case, the magnetic pressure of the toroidal field can give rise to a self-starting wind (e.g., [82, 291, 355, 373, 391]). This makes distinguishing between magnetic and non-magnetic winds difficult, because winds driven by the magnetic pressure will not corotate with the disk and consequently may have the kinetic properties similar to radiation-driven winds.

Thank you, Daniel for your extensive account on winds in quasars. Now, we switch to a particular form of outflow—collimated relativistic outflows—and the processes that make possible their remarkable radio emission.

6.7 Interpretation of Radio Emission

6.7.1 Superluminal Motions

Dear Paolo (Padovani), superluminal motion observed in radio-loud quasars is usually explained through the assumption of ejection at relativistic speed. Can you please review the phenomenology of superluminal motion and its fundamental interpretation? Is this the only line of evidence that points toward relativistic motions in quasars?

The term “superluminal motion” describes proper motion of source structure (traditionally mapped at radio wavelengths) that, when converted to an apparent speed v_a , gives $v_a > c$. This phenomenon occurs for emitting regions moving at very high (but still subluminal) speeds at small angles to the line of sight [321].

The geometry of the phenomenon is shown in Fig. 6.14. Consider a blob moving at speed v along a direction forming an angle θ with the line of sight. The blob is observed first at position A and then after a time t , at position B . During that time, the source has moved by vt . But photons emitted at B are closer to the observer by $vt \cos \theta$, and the difference in arrival time is $\Delta t = t_A - t_B = t(1 - v/c \cos \theta)$. The source appears to have moved on the plane of the sky by $\Delta r = vt \sin \theta$, which means the apparent velocity $v_a = \Delta r/\Delta t = \beta_a c$ is related to its true velocity, $v = \beta c$, and the angle to the line of sight by $\beta_a = \beta \sin \theta / (1 - \beta \cos \theta)$. For $v > 1/\sqrt{2}c \simeq 0.7c$ or $\theta > \arcsin[0.5/(\Gamma^2 - 1)]$, where $\Gamma = (1 - \beta^2)^{-1/2}$ is the Lorentz factor, β_a is > 1 . That is, one observes superluminal motion for speeds larger than $\sim 70\%$ the speed of light ($\Gamma > \sqrt{2}$) for some orientations or for some angles larger

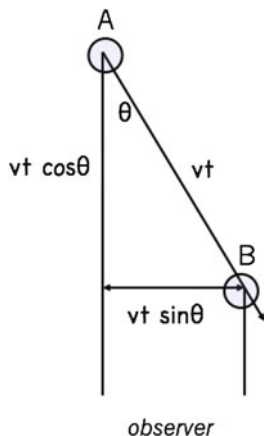


Fig. 6.14 Geometry of superluminal motion. See text for details

than a value which depends on Γ . Plainly speaking, relativistically moving sources “run after” the photons they emit, strongly reducing the time interval separating any two events in the observer’s frame and giving the impression of faster than light motion. The apparent velocity reaches a maximum value $\beta_{a,\max} = \sqrt{\Gamma^2 - 1}$ for $\cos \theta = \beta$ or $\sin \theta = \Gamma^{-1}$. This implies a minimum value for the Lorentz factor $\Gamma_{\min} = \sqrt{\beta_a^2 + 1}$. For example, if one detects superluminal motion in a source with $\beta_a \sim 5$, the Lorentz factor responsible for it has to be at least 5.1, equivalent to $v \sim 0.98c$. Note that superluminal speeds are possible even for large angles to the line of sight: for example, sources oriented at $\theta \sim 50^\circ$ can have $\beta_a \gtrsim 2$ if $\Gamma \gtrsim 5$.

Detection of superluminal motion does not necessarily imply that the source of radiation is moving. The tip of a rotating beam of light moves faster than the speed of light at a distance $> c/\omega$, where ω is the angular speed. If the beam ionizes material that then reemits the radiation, the observer will detect superluminal motion even though the ionized material is not moving at all. This simple model would predict, on average, a similar number of expansions and superluminal contractions, that is, $\beta_a < 0$.

Observed apparent speeds can be quite large: [237] have shown that in their complete AGN sample, the distribution of maximum speeds peaks at ~ 10 with a very small tail extending up to $\beta_a = 50.6 \pm 2.1$, which means that typically $\Gamma \gtrsim 10$, but some jets need to have $\Gamma \gtrsim 51$. The shape of the distribution rules out a single value for Γ since in that case, the distribution should peak at $\beta_a \sim \Gamma$ and drop off sharply at smaller values, against what is observed. In less than 2% of the cases studied by [237], $\beta_a < 0$, but these are explained by a variety of possible observational effects.

Note that what is actually measured is the apparent transverse velocity μ . The intrinsic velocity is then given by $v_a = \mu D$, where D is the distance of the source. This has led some researchers to suggest that v_a appears to be larger than the

speed of light because the distance is wrong and overestimated, which questions the “standard” cosmological interpretation of redshift. However, the discovery that galactic microquasars can also display superluminal motion (e.g., [293]) has provided clear evidence for the occurrence of the superluminal effect, because the galactic nature of the source allowed a reliable estimation of its distance to be made.

There are many other arguments, which strongly suggest the presence of relativistic motion in quasars. These involve the so-called Doppler factor $\delta = [\Gamma(1 - \beta \cos \theta)]^{-1}$, which is typically > 1 for relativistic speeds. For $\delta > 1$, in fact, $\Gamma \gtrsim 0.5\delta$ (because $\delta_{\max} \sim 2\Gamma$). This evidence has been reviewed, for example, by [153] and [393]. I highlight here the most significant points:

1. γ -ray variability. Powerful and variable γ -ray sources such as the blazars detected at GeV and TeV energies *are bound* to have relativistic motion in their inner regions for the reason that otherwise the γ -rays produced in such sources, which are characterized by large luminosity to size ratios, would generate electron positron pairs through annihilation with softer (e.g., X-ray) radiation, and there would be no γ -ray emission at all. The fact that we do observe these sources in the γ -ray band means that relativistic motion is present, and therefore, δ has to be > 1 . This has the effect of artificially boosting the observed powers and decreasing the variability timescales, thereby relaxing the constraints on the intrinsic luminosity to size ratio. In other words, these sources are not as luminous and compact as they seem. Indeed, all γ -ray sources in [96] turn out to have $\delta > 1$, with $\langle \delta \rangle > 4$.
2. Synchrotron self-Compton arguments. The smooth, nonthermal radio-through-infrared continuum emission in radio-loud AGNs is most likely of synchrotron origin, that is, emission from relativistic electrons moving in a strong magnetic field. Some of the synchrotron photons will be inverse Compton scattered to higher energies by the relativistic electrons, which is known as the synchrotron self-Compton (SSC) process. In many cases, the synchrotron radiation density inferred from the observed radio power and angular sizes predicts SSC X-rays well in excess of the observed X-ray flux. The true synchrotron photon density must then be lower than observer’s infer by assuming isotropy. The strong anisotropy and shortened timescales caused by relativistic beaming can account naturally for this, and a lower limit to δ can again be set, with $\langle \delta \rangle > 5.5$ and 1.3, respectively, for the radio quasars and BL Lacertae objects in [153].
3. Population statistics. According to unified schemes low- and high-power radio galaxies (the so-called Fanaroff–Riley type I and II) are respectively BL Lacertae objects and flat-spectrum radio quasars with their jets at relatively large angles with respect to the line of sight. Given the luminosity function (LF) of these misaligned populations, one can predict the LF of the aligned ones and at the same time, constrain the beaming parameters, including the Lorentz factors. It turns out that this hypothesis can explain very well the observed LFs. Moreover, as for the distribution of superluminal speeds, a single Γ value is ruled out, and instead, a distribution of Γ ’s is required, with $n(\Gamma) \propto \Gamma^{-2.3}$, $\langle \Gamma \rangle \sim 11$ and $n(\Gamma) \propto \Gamma^{-4}$, $\langle \Gamma \rangle \sim 3 - 7$ for radio quasars and BL Lacertae objects, respectively, with angles $\lesssim 15 - 20^\circ$.

In recent years, a possible inconsistency in this scenario has been found. Namely, the detection of very fast γ -ray variability in the TeV band for some BL Lac objects (e.g., Mrk 501 and PKS 2155-304) implies $\Gamma \approx 50$ (e.g., [154]). However, radio observations of these sources show evidence only for moderate, if any, superluminal motion, with $\beta_a = 4.4 \pm 2.9$ for PKS 2155-304 [303] and $\beta_a < 1$ for other TeV sources [161]. These two constraints together would imply that the jet makes a very small angle w.r.t. the line of sight (since $\beta_a \rightarrow 0$ for $\theta \rightarrow 0$, independently of Γ), which is inconsistent with other properties (e.g., the ratio between core and extended radio flux, which is also an orientation indicator, and population statistics). Possible solutions to this problem include (a) a structured jet with a fast spine surrounded by a slower external layer, which ties in with very long baseline interferometry (VLBI) observations of limb brightening [156, 161]; (b) a decelerating jet with a fast initial part, responsible for the γ -ray emission, which slows down over a length of ≈ 0.1 pc and then produces the radio emission [149, 303]. In both cases, a consistency between γ -ray and radio data is preserved by assuming that the jet structure is more complicated than previously assumed.

Thank you, Paolo.

Dear Serguei (Komissarov), relativistic ejections give rise to structures on scales of tens of kiloparsecs and even larger. Extended radio-emitting structures are certainly one of the most spectacular signatures of nuclear activity. Another impressive characteristic is the radio-emitting plasma high degree of collimation that justifies the term “jet.” How relativistic, collimated ejections are made possible is still a conundrum. Which are the physical mechanisms likely to be responsible for jet formation and collimation? Is there a complete physical model?

Let it be said in a few words: it is still premature to claim that we fully understand the origin of cosmic jets in general and relativistic AGN jets in particular. However, a consensus has been reached by now that (1) they are produced in systems involving disk accretion onto a compact central object, (2) they are powered by the rotational energy of the disk or/and the central object, (3) this energy is tapped by means of magnetic torques, (4) the magnetic field also plays an important role in the jet collimation and acceleration. This consensus is built upon the results of theoretical studies and numerical simulations, and on the circumstantial observational evidence, but we are still lacking is a direct observational confirmation. Moreover, many aspects of the theory are still under scrutiny.

Indeed, the original phenomenological definition of AGN jets was based on their appearance as geometrically narrow fine structures connecting an AGN with extended regions of radio-emitting plasma. The term jet, as opposite to say “filament,” however, implied from the start the interpretation that the underlying phenomenon involved a flow of plasma, produced somewhere in the galactic center. Nowadays, nobody questions this interpretation because the supporting evidence in its favor is quite overwhelming. So we are dealing with collimated outflows. Not all astrophysical outflows are collimated, the best studied counterexample being the solar wind. On the other hand, jets are not unique to AGNs but also found in other

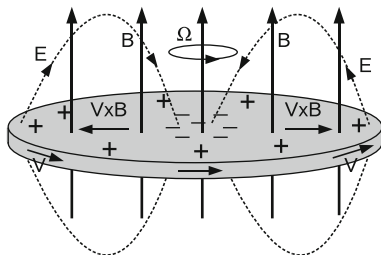


Fig. 6.15 Electrodynamics of the Faraday disk

astronomical objects, such as newly formed stars, or X-ray binary stellar systems. In all such cases, there is also strong evidence for disk accretion onto a compact central object, like a young star, or a supermassive black hole. Thus, the observations give us a hint that accretion disks are essential components of “cosmic jet engines.” This makes perfect sense, as whenever such a flattened structure is present, it introduces a preferred direction along the disk normal, and if collimated outflows are produced by such an engine, they are likely to be aligned with this direction. This simple idea is consistent with the fact that cosmic jets most often come in pairs.

The accretion disks can also be a source of power for the jets. Ultimately, this is the gravitational energy of accreting gas, conveniently converted into the disk rotational energy. There are many examples in engineering where rotational energy is converted in other useful forms. For example, in dynamo engines, it is used to generate electricity. Interestingly, we now believe that this is exactly what is happening in “cosmic jet engines”—the rotational energy is first transformed into the electromagnetic one and then, at least partly, into the kinetic energy of cosmic jets. Accretion disks are also extremely rapidly rotating objects, particularly geometrically thin disks, which rotate with the speed which is only about $\sqrt{2}$ below the local escape speed from the gravitational “trap” of the central object. Such a rapid rotation makes the disk normal even more special.

In order to understand, how the combination of rotation and magnetic field can drive an outflow, consider first the basic principle of the Faraday disk, the prototype dynamo engine (see Fig. 6.15). The free charges of the disk are subject to the Lorentz force, $f = q\mathbf{v} \wedge \mathbf{B}$, where q is the electric charge, \mathbf{v} is the rotational velocity of the disk, imparted on the charges, and \mathbf{B} is the magnetic field. This force points along the disk radius and hence causes a radial separation of electric charges on the disk surface. The separated charges create an electric field. The corresponding electric potential difference between the disk edge and its center means that we have got a “battery.” Connect it via conducting wires to an electric fan, and it will drive a flow of air.

It is obvious now that a magnetized accretion disk can operate, at least in principle, as a Faraday disk. What is left to do is to figure out the natural counterparts to the other components of the electric circuit, considered in the above example. First, we notice that the magnetic field can play the role of conducting wires.

Indeed, the Lorentz force allows free motion of charged particles only along the magnetic field lines and makes them to gyrate in the plane normal to the magnetic field. The next question then is how to fill the disk magnetosphere with charged particles. First, they can be lifted from the disk surface by the electric field. If only this mechanism is operated then the magnetosphere would be electrically charged and extremely rarefied as even a tiny amount of charges would be sufficient to effectively screen the component of electric field along the magnetic field, thus efficiently regulating the outflow of charges from the disk. The magnetic energy would be many orders of magnitude above the rest mass energy of the charges, a configuration which is in the realm of relativistic physics. The charges can also be created “in situ” via the two-photon reaction, leading to production of electron–positron pairs. This mechanism requires high energy γ -ray photons, which can be emitted from active regions on the disk surface. The outcome is still expected to be a relativistic magnetosphere. Finally, the charges can be lifted from the surface via thermal effects. If the surface of the disk is heated to high temperature, the charged particles of both signs can leave the surface because of their thermal motions. This is what occurs in the Sun. This is how the solar corona at the base of the solar wind is created. Explosive eruptions in active regions is another mechanism of particle supply into the Sun’s magnetosphere. In fact, these processes are so effective that the Sun’s magnetosphere is nonrelativistic—the rest mass energy dominates the magnetic one.⁴

In any case, the component of electric field along the magnetic field is effectively killed, but the normal component is preserved and forces the particles to move with the drift speed $\mathbf{v} = -c(\mathbf{E} \wedge \mathbf{B})/B^2$, where c is the speed of light. In steady state, this leads to rotation with the same frequency as the disk at the foot point of the magnetic field line. In the rotating frame, the electric field vanishes, and this fact allows us to describe the magnetic field as rotating with the disk. Moreover, the forces acting on charged particles in this frame are the gravity force, the gas pressure, and the centrifugal force. The centrifugal force and the gas pressure drive charged particles away from the disk, whereas the gravity force pulls them back. At the surface of the accretion disk, these three forces must balance each other, but along the magnetic field line diverging from the axis of rotation, the centrifugal force increases with the distance, whereas the gravity force decreases. Thus, somewhere along such a field line, there is a point where the centrifugal force alone balances gravity. This equilibrium point is unstable—as the disk tries to build up a static corona, it supplies gas beyond this equilibrium point and the centrifugal force takes over and drives an outflow! Because of the importance of the centrifugal force, such disk winds are called centrifugal too.

When we discuss collimated outflows, it is important to make a distinction between jets and plumes, and between subsonic and supersonic jets. Sometimes they have very similar appearance. For example, on a quiet cold winter day, the smoky

⁴This suggests that the relativistic AGN jets do not originate directly from accretion disks but from their central black holes.

hot air coming from a chimney can produce a spectacularly long thin straight plume. This flow is driven by the buoyancy force, and it is confined by the surrounding air. Its kinetic energy is tiny compared to its thermal energy. Should the atmosphere suddenly disappear, the plume appearance would change dramatically. It would spread out in a horizontal layer. Subsonic jets, that is, jets whose speed is below the speed of sound, are similar to plumes in many respects. They do not have to be driven by buoyancy, but they still need external medium to stop them from spreading, and their kinetic energy is still low compared to their thermal energy. When a subsonic jet enters low-pressure environment, it not only spreads out but also slows down. Plumes and subsonic jets are also subject to boundary instabilities that lead to turbulence, slowdown, and effective mixing with the external gas.

Supersonic jets are very different. They can be described as self-sustained collimated flows. Even when they enter vacuum, their spreading is rather limited. Indeed, they begin to expand transversely with the speed close to the speed of sound, c_s , but keep moving forward with the original speed v . As the result, they open up only by the angle $\theta \sim c_s/v = 1/M$, called the Mach angle. ($M = v/c_s$ is called the Mach number.) The overall flow speed increases and so does the kinetic energy of the flow, at the expense of its thermal energy. The boundary instabilities are much less destructive as the sound waves generated at the boundary have trouble penetrating the jet, particularly when its opening angle is higher than the Mach angle. Unless supersonic jets are forced to interact strongly with their environment, they remain collimated and transport their energy without losses. This is the main reason why the supersonic jet model has been so popular in the theory of cosmic jets.

By strong interactions, I mean the interactions which lead to strong shock waves. These waves can move much faster than the sound speed and can penetrate supersonic jets even when they originate at the jet boundary. At shocks, a fraction of the jet kinetic energy dissipates, and it is very tempting to identify such localized dissipation sites with bright “knots” and “spots” characteristic for the AGNs and other cosmic jets. When the interaction is too strong, the initially supersonic jets can become subsonic, with a dramatic change in their properties. This is very much like what we observe in the low power Fanaroff–Riley type I radio sources on kiloparsec scales. On the contrary, in the powerful Fanaroff–Riley type II radio sources, jets seem to remain supersonic all the way to the most remote parts of the radio source, where they are terminated via direct collision with dense external gas at the so-called leading “hot spot.” Thus, the observations suggest that theorists should look for ways of producing supersonic jets. Once they have been produced, they can take care of themselves.

Careful theoretical analysis and numerical simulations show that centrifugal outflows do become supersonic (to be more precise superfast magnetosonic as in magnetized plasma, the role of sound waves is played by the so-called fast magnetosonic waves) when they are allowed to expand. This naturally occurs in outflows into vacuum or when the pressure of the surrounding confining medium decreases with the distance, which is the case in most astrophysical problems. Such medium can also help to collimate the outflow. Imagine a bunch of magnetic field lines emerging from the central part of an accretion disk or indeed the central

compact object. In the absence of confining medium, the bunch expands laterally until it fills the whole space, and the magnetic field strength becomes independent of the polar angle. In the presence of such a medium, which could be a disk corona, it spreads until its magnetic pressure equals to the pressure of this medium, $p = B^2/8\pi$. If $p \propto r^{-b}$ ($b > 0$), then $B \propto r^{-b/2}$, where r is the distance from the origin of the bunch. Because of the magnetic flux conservation $B\varpi_j^2$, where ϖ_j is the radius of the bunch, is constant, and this gives us $\varpi_j \propto r^{b/4}$. Thus, unless $b > 4$, the bunch becomes progressively more collimated. The external pressure can be magnetic in origin as well (see Fig. 6.16).

The electric currents flowing out from the disk create an azimuthal component of the magnetic field, and so it becomes twisted. This does not only increase the total magnetic pressure but also leads to the emergence of a new force, the magnetic hoop stress. The ultimate effect of this stress on the flow geometry is its axial compression. This is often described as self-collimation.

As you may have noticed already, most of the above analysis does not make much use of the disk geometry and, in fact, could be applied equally well to a rotating magnetized star. Without flat geometry, the self-collimation becomes the only strong candidate for collimation mechanism, and it may work quite well for nonrelativistic outflows, with the rotational axis providing the preferred direction [49]. For relativistic magnetically driven outflows, however, this mechanism becomes much less effective, as yet another force comes into play, the electric force, and this force almost balances the hoop stress. Under such circumstances, the external confinement becomes the main collimating factor. Without it, the outflow remains uncollimated. This is why we have pulsar winds and not pulsar jets. On the other hand, the external confinement/collimation of relativistic flows does not have to continue until the jet becomes superfast magnetosonic in order to prevent the total loss of collimation in the regime of free expansion. Indeed, given the jet speed v_j , the speed of lateral expansion has to be below $(c^2 - v_j^2)^{1/2}$ in order to keep the total speed below the speed of light. As the result, the angle of spreading is bound to be below $1/\Gamma_j$, where $\Gamma_j = (1 - v_j^2)^{-1/2}$ is the jet Lorentz factor. However, the external confinement may still be required for effective magnetic acceleration of relativistic jets.

The process of magnetic acceleration can be described as a conversion of the jet Poynting flux into its kinetic energy. In the nonrelativistic limit, this conversion is almost completed when a flow becomes superfast magnetosonic. However, in the ultra-relativistic limit, this is no longer the case. Even if at this point the flow speed is already very close to the speed of light, the Lorentz factor is still well below the value corresponding to the full conversion of magnetic energy. Most of the accelerations has to proceed further out, where it becomes rather delicate. Indeed, in the superfast-magnetosonic regime, the centrifugal force is no longer that important, and it is the magnetic pressure associated with the azimuthal component of magnetic field which is now the main driving force. The azimuthal component is also the main energy carrier. At first sight, this does not look to be a problem. We know, for example, that the gas pressure is very effective in acceleration of

expanding supersonic flows. Yet, consider a sideways expansion of a relativistic jet with azimuthal magnetic field. If the expansion is radial, then the magnetic flux conservation yields $B \propto \varpi_j^{-1}$, and the magnetic energy density $\propto B^2 \varpi_j^2$ is constant. Hence, there is no conversion of magnetic energy!

In order to break this deadlock, the jet expansion has to be non-radial. That is the jet boundary may well expand radially, but inside of it, the separation between stream lines has to increase faster compared to the streamline radius. In fact, this is exactly what the magnetic self-collimation is arranging, as it tries to turn the flow surfaces into cylinders near the jet axis. Although always operating, the process of self-collimation becomes increasingly slower for higher fast-magnetosonic Mach number. (In the relativistic theory, this Mach number is $M = v_j \Gamma_j / c_f \Gamma_f$, where c_f is the fast-magnetosonic speed and Γ_f is the corresponding Lorentz factor.) The “contraction” of inner streamlines upsets the force balance across the jet and invites outer streamlines to join the inner ones. However, this “invitation” travels very slow, at the local Mach angle to the streamlines, and arrives at the boundary well downstream of the starting point. Hence, one can divide the flow into the axial region where the self-collimation and magnetic acceleration remain relatively effective and the outer region where they are not. Along the dividing surface the opening angle of streamlines equals to the local Mach angle. Inside this surface, the causal communication is established on the length scales below the jet length, whereas outside of it, much longer distance may be required. As the flow accelerates, the Mach number increases, the Mach angle becomes smaller, and the acceleration region progressively narrower. This negative effect can be reduced if the external pressure forces the jet itself to become progressively narrower. For this to be effective, the pressure has to decline not faster than r^{-2} . In this case, the acceleration proceeds until the flow kinetic energy is about the same as the remaining magnetic energy [211, 212, 242, 397]. Once this has been achieved, the jet Lorentz factor Γ and opening angle θ satisfy the condition $\Gamma\theta \leq 1$ [212]. If the pressure gradient is steeper, the jet shape is conical, the acceleration effectively freezes out at much lower Γ , and the flow remains magnetically dominated, with only a small fraction of magnetic energy converted into the kinetic one. The close connection of this acceleration mechanism with collimation is the reason behind its name, the “collimation acceleration.”

Interestingly, there is a significant body of observational evidence in support of the collimation acceleration of AGN jets. First, they often show progressive collimation, the M87 jet being the most spectacular example [38]. Second, if their acceleration was much faster, as for example, in pure hydrodynamic models, the jets would reach their high terminal speeds very close to the active nucleus and up-scatter its soft radiation to high energies. We would then be able to detect this emission with the available instruments, but we do not [364]. The much slower collimation acceleration seems to explain why. The VLBI observations provide direct evidence of prolonged acceleration in some AGN jets, though this acceleration can also be explained by the bulk curvature of these jets [178]. Finally, the AGN jets satisfy the constraint $\Gamma\theta \leq 1$ [319]. There are also few problems. For example, the model predicts almost purely azimuthal magnetic field, whereas the observed

polarization of synchrotron emission from these jets suggests a more complicated magnetic field structure [210,401]. The model predicts almost equipartition between the magnetic field and the kinetic energy, whereas the theory of MHD shocks shows that in such a case, shock dissipation is rather inefficient [200]. Observations also suggest continuous dissipation and efficient in situ acceleration of relativistic electrons, whereas the model is adiabatic and moreover, the particle acceleration at strongly magnetized shocks seems to be rather problematic [370].

Another limitation of the model is that it is built on the simplifying assumption of axisymmetry. This assumption is particularly restrictive when it comes to the issue of stability, as non-axisymmetric modes of various global instabilities can be quite destructive. However, recent three-dimensional numerical simulations show that this does not always have to be the case [255]. In fact, the development of such modes requires causal connectivity across the flow. This condition may be satisfied near the central engine, where the outflow is still in the subfast-magnetosonic regime, but the strong poloidal magnetic field in this region damps the instabilities. Further out, where the magnetic field is basically in the form of azimuthal loops, which may slip away from the axis without much of a resistance, the instabilities could be slow globally because the causal connectivity across the jets is already rather poor, particularly if the jet is freely expanding. In the causally connected core, however, they can develop quite rapidly, leading to slippage of magnetic loops, turbulence, and magnetic dissipation. The irregular structures observed in the central regions of both the observed and the simulated three-dimensional jets seem to support this idea. The magnetic dissipation may not only explain the observed emission from the jets but can also play an active role in the jet acceleration [99]. Essentially, the magnetic energy is converted into heat, which then partially converted into the kinetic energy as the jet expands. The surface modes can also result in turbulent boundary layers at the jet interface with the confining external medium. γ -ray emission and pair production can also play an important role in the interaction between the AGN jets and their surrounding. In the so-called “photon bredding” mechanism, this interaction results in efficient conversion of the jet kinetic energy into γ -ray emission [372]. These issues, are beyond the boundaries of the “standard model,” which we have described here, and they will be central in future studies of the AGN jet physics.

6.7.2 *Blandford–Znajek Mechanism*

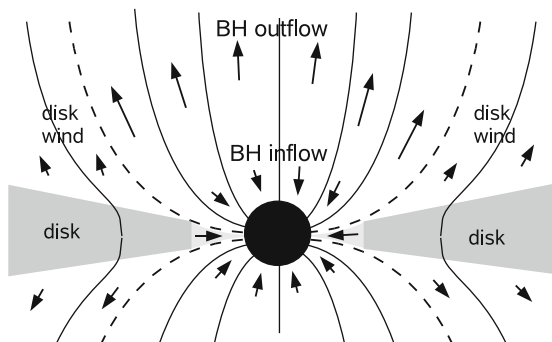
Dear Serguei (Komissarov), is the so-called Blandford–Znajek mechanism fully satisfactory? If not, what are its shortcomings? Chris Reynolds put forward an hypothesis that has become known as the “Reynolds’ conjecture”: in radio-loud quasar, the accreting gas and the black hole are spinning in opposite directions. Is this conjecture likely to be proved true? How does it explain the difference between radio-quiet and radio-loud AGNs?

The Blandford–Znajek mechanism is now widely accepted as the most promising way of producing highly relativistic jets from AGNs. Its power depends mainly on the black hole mass, spin, and accumulated magnetic flux. This magnetic field is of external origin, and it is delivered to the black hole by the accretion disk, but how exactly this is done is not clear. It is expected that close to the black hole, the disk spin is either parallel to the black hole spin (the prograde disk case) or antiparallel to it (the retrograde case). In the latter case, the inner boundary of the disk can be much further out from the black hole. This significantly decreases the accretion power and may also strongly increase the power of the Blandford–Znajek mechanism. It is possible that the retrograde case corresponds to radio-loud AGNs, and the prograde case to radio-quiet ones. This idea is quite attractive, but further research is needed to check its validity.

Going into more details, astrophysical black holes are rather simple highly symmetric “objects” which are described by only three parameters, mass, spin, and electric charge. It is highly unlikely that astrophysical black holes have significant electric charge, and this leaves us with only two parameters. This is the case of a Kerr black hole, which in the case of vanishing spin reduces to a Schwarzschild black hole. Since a black hole has mass, it also has energy, according to the Einstein’s $E = Mc^2$. For a spinning black hole, a fraction of this energy can be extracted, which is accompanied by a reduction of its spin. This is why this energy is called the rotational energy. This possibility is rooted in the peculiar properties of the so-called ergoregion, which surrounds the black hole horizon. In particular, inside the ergoregion, both massive and massless particles can have negative total energy, including the rest mass energy of massive particles. When such a particle is swallowed by the black hole, the hole’s energy is reduced. But in order to be pushed into an orbit with negative total energy in the first place, the particle has to interact with another particle and pass to it its energy excess. This second particle, may have positive total energy and escape from the ergosphere, carrying away the black hole energy. This is called the Penrose process [295]. In fact, energy is not an invariant quantity, and we always have to specify the locally inertial frame in which it is measured. Here, we mean the observer located far away (“at infinity”) from the black hole and at rest relative to it. Moreover, by the energy, we mean the integral of geodesic motion which equals to the particle energy as measured by this observer when the particle escapes to infinity, hence the name “energy at infinity.” In fact, geodesic orbits of particles with negative energy at infinity never cross the ergosphere, the outer surface of the ergoregion, never mind escaping to infinity. In cases like this, the energy at infinity is identified with the same integral of geodesic motion as for the particles which can escape to infinity. Local fiducial observers, which orbit the black hole and measure properties of particles as they are about to disappear into the black hole, always measure positive total energy for such particles, but this energy is not the energy at infinity.

The Blandford–Znajek mechanism [47, 208] is an electromagnetic version of the Penrose process. In flat space-time, a stationary distribution of electric charges creates a stationary electric field, whereas a stationary distribution of electric current creates a stationary magnetic field. It turns out that in the curved space-time of

Fig. 6.16 The central engine of an AGN. The inner region of the accretion disk, shown in a different shade, is the plunging region. The dashed magnetic field line separated the disk magnetosphere (or corona) from the black hole (BH) magnetosphere



general relativity, this clear division between electrostatics and magnetostatics does no longer exist. In particular, a static distribution of electric currents in static space-time can generate not only magnetic but also a divergence-free electric field. This is exactly what occurs when a Kerr black hole is placed into a uniform magnetic field of external origin in such a way that the black hole spin is aligned with the magnetic field [400]. A quadrupole-like electric field is generated, as if the black hole horizon was a rotating magnetized conducting sphere. This property suggested to [47] that spinning black holes could operate as cosmic batteries and drive magnetized outflows in the fashion similar to neutron stars and accretion disks.

However, both the charged particles and the electromagnetic waves cannot be emitted from the event horizon—at the horizon they can only move inward. Thus, instead of a single outgoing wind, the black hole magnetosphere has to support two winds, with the inner wind blowing into the black hole (see Fig. 6.16). This ingoing wind plays the role of the particle with negative energy at infinity of the Penrose process [209, for example]. It is easy to see now, that the space at the base of these two oppositely directed winds must be rather empty, and in fact, plasma has to be continuously supplied into this region by some other processes. The black hole magnetic field effectively shields this region from potentially plasma-rich surrounding, and the pair creation is the only robust mechanism for this plasma supply. This is why we expect the black hole magnetospheres to be relativistically magnetized and drive relativistic outflows.

The power of the Blandford–Znajek process can be estimated via

$$L_{BZ} \simeq \left(\frac{2}{3c} \right) \frac{\Psi \Omega_h^2}{4\pi} \quad (6.7)$$

[23]. In this expression, Ψ is the total magnetic flux threading the black hole, $\Omega_h = f(a)c^3/GM$, where $f(a) = 0.5a/(1 + \sqrt{1 - a^2})$ is its angular velocity, $a = Jc/GM^2$ is the dimensionless spin parameter, M is the black hole mass, and J is its angular momentum. It turns out that for a given black hole mass its angular velocity is bound to be below the limit corresponding to $a = 1$. Black holes can spin up very close to this maximal rate in the process of disk accretion, via accumulating

the high angular momentum of swallowed gas. A merger of binary black holes is another possible way of producing very rapid rotation.

Kerr black holes cannot have magnetic field of their own, but can become magnetized when placed into the magnetic field of external origin. The interstellar magnetic field is too weak for any significant effect, but if the black hole is surrounded by an accretion disk, the magnetic field can be much stronger. First, the accretion flow can advect the interstellar magnetic field toward the black hole, strongly amplifying it in the process. Second, the turbulent motions and differential rotation of accretion disk can generate its own magnetic field. The effectiveness of these processes determines how powerful the relativistic jets from black holes can be. Unfortunately, this is one of the more difficult issues in the theory of AGNs. Although there are many interesting theoretical models, and in spite of very impressive recent numerical simulations, we have not reached yet full understanding of the physics of magnetic fields in accretion disks.

The specific angular momentum (per unit mass) of Keplerian orbits increases outward. Thus, in order to accrete, the gas of accretion disks has to lose its angular momentum. In the classical theory of turbulent accretion disks, this is achieved via friction between faster rotating inner parts of the disk and its slower rotating outer parts. The origin of this friction is turbulent viscosity. The outward transport of angular momentum inside the disk is followed by “viscous” dissipation and heating. The heat can then be radiated away. In the simple model of the magnetic field transport in viscous accretion disks, some external magnetic field, say the field of interstellar origin, is advected inward by the mean flow and also diffuses away due to the turbulent magnetic diffusivity. The overall efficiency of inward transport is then determined by the magnetic Prandtl number, $Pr = \mu/\eta$, which is the ratio of the turbulent viscosity μ and the turbulent magnetic diffusivity η . This model is attractive by its simplicity, but the reality can be more complicated [29, 334, 369].

Normally, the accretion disk does not continue all the way down to the event horizon of the central black hole but terminates somewhere between the so-called marginally stable and marginally bound orbits. Inside the inner boundary, the disk flow is no longer determined by slow viscous transport. Instead, the disk gas plunges rapidly into the black hole (see Fig. 6.16). This purely general relativistic effect completely outplays the turbulent diffusion and the magnetic field is also pulled into the black hole. As the result, the magnetic flux, which would otherwise spread over the inner gap of the accretion disk, becomes trapped in the black hole ([325], see Fig. 6.16). The trapping effect increases the magnetic flux accumulated by the black hole and hence the power of the Blandford–Znajek jets, with larger plunging region, resulting in higher trapped flux. For prograde disks, the size of the plunging region decreases with the black hole spin, and the flux trapping effect is cancelled by the explicit dependence of the Blandford–Znajek luminosity on the spin (see (6.7)). However, for retrograde disks, it is the other way around, and the two factors work hand in hand in increasing the luminosity with spin [139].

Some AGNs are strong sources of radio emission, while most are not [120, 199]. Because the radio emission, particularly from the large-scale radio lobes, is a good

indicator of the AGN jet power, this division suggests a significant diversity in the ability of AGNs to produce jets. Since the radio-loud and the radio-quiet AGNs are very similar in many other respects, this division, however, is hard to explain. Equation (6.7) suggests that the explanation can be based on the black hole spin. Namely, most of AGN black holes are slowly rotating, whereas a small fraction of them are rotating rapidly [261,407]. Accretion disks can both spin up and spin down black holes, quite efficiently, depending on whether they are prograde or retrograde. Thus, the “spin paradigm” implies that AGN black holes accrete episodically with random orientation of angular momentum of accreting gas. In this case, the black hole mass grows linearly with the number of episodes, whereas its mean angular momentum only as the square root of them, resulting in decreasing mean angular momentum per unit mass. In some fortunate cases, however, the number of prograde accretion episodes may be significantly higher than on average, resulting in rapidly rotating black hole. Mergers of binary supermassive black holes, which are expected to form during galactic merges, is another way of producing rapidly rotating black holes. During such a merger, some of the orbital angular momentum of the binary is transformed into the angular momentum of the resulting solitary black hole [407].

From a purely theoretical viewpoint, one can split black hole/accretion disk systems into two groups, depending on whether the accretion disk is prograde or retrograde. Indeed, intermediate orientations are forbidden, thanks to the relativistic Bardeen–Peterson effect [21]. If this factor is important, then AGNs should also split into two clearly different groups, and the observed division into radio-loud and radio-quiet objects seems to be the only obvious suspect. However, in order to make the next step, one needs a plausible mechanism which would explain how exactly these two divisions could be related.⁵ The flux trapping effect seems to provide such a mechanism, as this has been recently illustrated with simplified models of relativistic accretion disks [139]. The result is the “spin anti-alignment paradigm,” where radio-loud AGNs are associated with rapidly rotating black holes with retrograde accretion disks, and radio-quiet ones with black holes with prograde disks.⁶

In general, the “anti-alignment paradigm” has a number of attractive features and has a potential to resolve several long-standing issues in the astrophysics of AGNs. In particular, it provides a very plausible alternative explanation to the observed rarity of radio-loud AGN and their cosmological evolution. Indeed,

⁵I myself wondered back in late 1990s if the orientation of the disk spin could be behind the radio-loud and radio-quiet division and even discussed this idea with Sam Falle, Roger Blandford, and few other colleagues. However, I did not have any clear mechanism in mind. Moreover, the analysis of [338] indicated that retrograde disks were unstable. Finally, the black hole spin paradigm seemed to be a good alternative. In the end, I gave up on this idea. Later, [202] pointed to a flaw in the analysis by [338] and found that prograde disks were in fact stable.

⁶ I am not sure who exactly proposed this paradigm in the first place. This could have been Chris Reynolds indeed, as the question suggests, but as far as I know, in the scientific literature, this idea first floated in [140].

prograde systems are self-sustained, whereas in a retrograde system, the black hole spin decreases until the system becomes prograde. A prograde system may also become retrograde, but only if the angular momentum of accreting gas changes dramatically. This, however, may require a major event like a galactic merger. In the violent early Universe such merges were quite common, and hence, one would expect a large fraction of retrograde systems. At present, however, the galactic merges are much less frequent, resulting in much smaller fraction of retrograde systems. This agrees, at least qualitatively, with the fact that in the early universe powerful radio sources were much more common. It is still very early days, and further research is needed to test this idea against observations. The model predicts that the disks of radio-loud AGNs are truncated far away from the black hole, and that on average, they are significantly less luminous than the disks of radio-quiet AGNs. Apparently, both these predictions can be tested observationally.

There is a number of theoretical issues related to the anti-alignment paradigm, which are yet to be resolved. First, in the toy models explored in [139, 325], the magnetic field strength is completely independent on the mass accretion rate, suggesting that the accretion power and the jet power are uncorrelated, in conflict with the observations [348]. Second, the actual amount of trapped magnetic flux depends on the total available flux in problem, which is just a free parameter in the models. As things stand, a prograde systems with larger imposed total flux could produce more powerful jets than retrograde systems with small imposed flux. Third, it is hard to see how a strong variability of central engine, which is required to explain the observations of AGNs, can naturally arise in this model. Finally, the direct numerical simulations of magnetized accretion disks seem to support a different trend [384], though the setup of these simulations is rather different.

In disks with magnetically driven wind, the disk angular momentum can also be carried away by this wind. Thus, the turbulent viscosity may not always be needed to sustain accretion [39,42]. Moreover, a strong magnetic field can actually suppress the turbulence and hence the outward diffusion of magnetic field. This could result in a much higher magnetic flux accumulated by the black hole and hence much more powerful Blandford–Znajek jets. In addition, the lower dissipation in such disks would lead to a lower disk luminosity [39]. This could be another way to explain the origin of radio-loud AGNs.

6.7.3 *Where is the Jet Launched?*

How does the region of jet formation compare in size to the black hole and to other structures believed to lie close to the center of quasars, like the accretion disk?

The first issue here is where the relativistic jets of AGNs originate from, black holes or accretion disks? As I have already mentioned, it seems unlikely that these jets

come directly from accretion disks. First, the escape speed from the disk surface is only a fraction of the speed of light, with the exception of the very inner regions of prograde disks of very rapidly rotating black holes. Second, their magnetospheres can be relatively easily loaded with substantial mass from the disk surface. On the other hand, the black hole magnetospheres are expected to be very rarefied and highly relativistic, perhaps even more relativistic than this is suggested by the relatively low observed Lorentz factors of AGN jets. Thus, the relativistic AGN jets most likely come directly from their black holes. The numerical simulations of disk accretion onto black holes support this general conclusion [23, 255, 256].

The second issue is how far away these jets become relativistic and collimated. The characteristic length scale here is the so-called light cylinder radius, ϖ_{LC} . This is defined as the cylindrical radius at which the magnetic field line rotates with the speed of light. If the field lines were straight, then the centrifugal force would accelerate charged particles to very high Lorentz factors already at this point, as this is sometimes claimed in the literature. However, they are not. At the light cylinder, the azimuthal component of magnetic field generated by the poloidal electric currents is already of the same order as the poloidal component, even in the limit where the particle inertia is negligible. As the result, the magnetic field lines are trailing spirals, and the angular velocity of the outflowing plasma is below that of the magnetic field. Although the linear outflow speed becomes comparable to the speed of light at the light cylinder, the Lorentz factor is still close to unity. If we ignore the particle interaction with the photons produced by the accretion disk, then beyond the light cylinder, the Lorentz factor grows as $\Gamma \sim (\varpi/\varpi_{\text{LC}})$ [37, 81, 212]. However, the Compton scattering introduces a drag force, and the actual growth rate can be slower.

Different field lines of the black hole magnetosphere may rotate with different angular velocities, but under the typical conditions, this is approximately one half of the angular velocity of the black hole. In this case,

$$\varpi_{\text{LC}} \simeq 2 \frac{c}{\Omega_{\text{h}}} = (2/f(a))r_{\text{g}}, \quad (6.8)$$

where $r_{\text{g}} = GM/c^2$ is the gravitational radius. For $a = 1$, this gives us $\varpi_{\text{LC}} \simeq 4r_{\text{g}}$, which is rather small indeed. However, even in this case, in order to reach $\Gamma \sim 10$, the jet has to expand beyond $\varpi = 40r_{\text{g}}$. For the collimation half-opening angle of one degree, this gives the “optimistic” distance from the black hole $z \sim 2.3 \cdot 10^3 r_{\text{g}}$. Thus, the jets do not emerge from the very vicinity of the event horizon already with very high Lorentz factors, contrary to how this is sometimes presented. At least, not according to our current understanding of their origin.

Thank you, Serguei for your very detailed discussion of the region closest to the event horizon of the central black hole. Inflow has been historically more difficult to detect than outflow. On the theoretical point of view, the main difficulty has been to explain the loss of angular momentum needed for the gas to reach the central parsec

of the active nucleus. We are very eager to ask several question on the physical processes that might help solve this issue. We will then discuss more in detail the structure of the accretion flow within the central parsec and especially how it might depend on parameters related to the circumnuclear environment like the accretion rate.

6.8 Mechanisms of Black Hole Accretion

Dear Isaac (*Shlosman*), please summarize the principal physical mechanisms that stimulate accretion of gas onto the black hole in a galactic nucleus. What happens when the accretion rate is low? Can a quasar ignite if the accretion material is overabundant? What are the relevant timescales of the fueling process? While the entire quasar process involves the hypothesis of accretion/inflow, most of the direct evidence involves collimated and uncollimated outflows. Where are the observational evidences for AGN inflows?

We review a number of outstanding issues about QSOs: the principal physical mechanisms that stimulate accretion of gas onto the supermassive black holes in galactic nuclei, what happens when the accretion rate is low, can a quasar ignite if the accretion material is overabundant, what are the relevant timescales of the fueling process, and the difficulties in detecting the inflows towards the black holes in active galactic nuclei.

Fifty years of QSO research have broadened our horizons and introduced new physical processes and exotic objects into mainstream science. But they have been insufficient in explaining fully how do QSOs operate and what is their role in the general framework of structure formation and evolution in the universe. The origin of QSOs and their central engines—the supermassive black holes (SMBHs), remains one of the hottest topics of frontline astrophysical research. Probably, one of the main accomplishments of this research is our understanding that QSOs are part of a wide class of objects called active galactic nuclei (AGNs)—all powered by accretion⁷ onto the SMBHs (e.g., [241, 337, 410]). The efficiency of this process in releasing radiative or mechanical energies, however, varies profoundly, depending on a number of factors and especially on the rate of accretion. We discuss this in Sect. 6.9, on modes of disk accretion.

Of special interest is the question of what is the source of fuel which powers AGNs in general and QSOs in particular. Because the accreting material is difficult to observe, as we discuss below in Sect. 6.9, it may be wiser to ask what are the possible mechanisms that can deliver fuel to the central SMBHs. Then, based on a specific mechanism, one can identify the reservoir of an available fuel. We review these options in Sects. 6.8.1 and 6.8.2.

⁷Accretion is growth by gravitational attraction of matter.

Outstanding issues with QSOs (and AGNs) are numerous and many lie well outside the scope of this review which focuses narrowly on a number of questions. We do not discuss such issues as the SMBHs mergers and the associated phenomena, efficiency of rotational energy extraction from SMBHs by the Blandford–Znajek [47] mechanism, Eddington ratio of radiation energy outputs and spin for various classes of AGNs (e.g., [363, 366]), jet collimation, etc. Furthermore, although we do survey the modes of accretion, we pass over an important question of the duration of individual accretion events.

6.8.1 Accretion Drivers: Small Scales

Because the accreting matter is expected to have at least some angular momentum, it cannot fall onto the SMBH radially but will form an accretion disk around it. The radial and vertical structures of such a disk depend on kinetic and hydrodynamic properties of the inflowing gas and its ability to dissipate energy. In the likely presence of magnetic fields, either dragged in or generated locally, the situation is complicated further by the laws of magnetohydrodynamics (MHD). In all cases, the main issue is how the accreting gas can get rid of its angular momentum—the options are quite limited. Among these possibilities are *local* hydrodynamical (and magnetohydrodynamical), magnetic or gravitational viscosities (torques), or *global* magnetic and gravitational torques. The former torques are associated with various types of viscosity, such as turbulent and MHD ones. Clearly, molecular viscosity is by far too weak to have any effect on the angular momentum redistribution in the disk.

Do local and nonlocal viscosities provide efficient magnetic brakes?

Let us define the region dominated by the SMBH gravity, so-called radius of influence $R_i \sim 7M_{\text{BH},8}/v_{250}^2$ pc, where $M_{\text{BH},8}$ is the mass of the SMBH in units of $10^8 M_\odot$, and v_{250} is the circular velocity in the external (galactic) potential in units of 250 km s^{-1} . Within this region, it becomes increasingly improbable (with progressively smaller R) that the gas gravity plays any role in being the source of viscosity. The situation can be entirely different at $R \gg R_i$, and we address this in the next section. Within R_i , however, local and large-scale magnetic fields can dominate and serve as the source of local and global viscosities. If the coefficient of viscosity is defined in terms of the α -parameter [349], the timescale of such viscosity-controlled inflow is $t_\alpha \sim 3\alpha^{-1}v_{250}T_{100}^{-1}R_{i,7}$ Gyr, where $T_{100} \equiv T/100 \text{ K}$ is the gas temperature, $R_{i,7} \equiv R_i/7$ pc, and v is the circular velocity in the disk plane at R . This timescale is too long, if T of the flow stays well below the virial temperature. The alternatives to such a cold flow are discussed in Sect. 6.9.

Although $\alpha \lesssim 1$, its exact value is a major uncertainty. Balbus and Hawley ([15]; see also [56, 395]) have suggested that magnetic stresses in the accretion disk

generate the local viscosity⁸ via growing magnetic torques—so-called magneto-rotational instability or MRI. In MRI, the coupling between adjacent radii is established by the growing magnetic field, B , and the energy source is that of a differentially rotating (sheared) disk. While the physics of the MRI has still a number of caveats, it looks very promising as the trigger of angular momentum flow at smaller radii. Massive numerical simulations are currently underway to fully understand its nonlinear phase (e.g., [40]).

Magnetic fields can brake the inner accretion disk via large-scale gravitational torques as well. If the B lines are oriented perpendicular to the disk plane and anchored in its weakly ionized gas, they will torque the disk, resulting in the loss of gas angular momentum [45]. Furthermore, when the magnetic lines are inclined by more than 30° to the rotation axis, the (clumpy) molecular disk gas will be flung out along the lines and accelerated centrifugally, triggering an MHD wind from the accretion disk. The generalized Blandford and Payne model [45] of such hydromagnetically driven disk winds can nicely reproduce the observed shapes of the broad emission lines in AGNs and hence reveal the kinematics of the gas flow [51, 110]. The accretion rate, \dot{M} , driven by the angular momentum loss from the disk by such a torque can be estimated from $\dot{M} R v \sim B_A^2 R_A^3$, where the circular velocity, v , and radius R are calculated at the base of the wind in the disk, and the subscript A refers to the Alfvénic radius, $R_A \sim 3R$, in the wind [110].

We note that around R_i , local gravitational instabilities can contribute to the development of turbulence in the disk (e.g., [292]). The condition for the onset of this type of (gravitational) viscosity is related to the dominant opacity in the disk. If the cooling is inefficient, the local gravitational instability can heat up the gas, and an energy balance is possible when the disk remains close to the marginal gravitational stability. These local torques will transfer angular momentum as well.

Where should a black hole look for the source of fuel?

If accretion within R_i is driven most efficiently by local and global magnetic torques, what is the source of the accreting gas? It can come from local sources, like inner bulge stellar mass loss (e.g., [207]), or from more distant ones, like gas infall from the halo gas or beyond (e.g., [339]). A number of ambiguities are brewing here. First, the spin orientation of the SMBH (e.g., [288]) and the $M_{\text{BH}} - \sigma$ relation, where σ is the stellar dispersion velocity in the bulge [128, 147] appear not to correlate with the disk properties but rather with those of the spheroidal component, like the bulge in disk galaxies and the galaxy itself in ellipticals. On the other hand, it is the disk which is the reservoir of gas which is supposed to feed the SMBH. So the absence of a direct correlation between the galactic disks and the central SMBHs is strange. However, this issue is open to caveats, and one can in principle argue that the dark matter (DM) halo controls the disk growth ([109]; see also [127]).

⁸The proposed mechanism is essentially nonviscous but can be defined in terms of effective viscosity.

Second, the acclaimed $M_{\text{BH}} - \sigma$ is based on σ of the inner bulge. Bulges have been originally thought to be supported by stellar velocity dispersions to some degree. These classical bulges are parts of the spheroidal component [218]. However, a substantial fraction of galactic disks host a different type of a bulge, the so-called pseudo-bulge [219]. Pseudo-bulges are rotationally supported, are disk-like, and form as a result of the vertical buckling instability in stellar bars (e.g., [80, 320]). Moreover, these disk-like bulges can continuously grow because the buckling instability is a recurrent one [251]. Hence, it appears that bulges are also made by the disks. Even in the best resolved Milky Way bulge, the fraction of the classical bulge has been substantially downgraded to less than 8% of the total mass in the bulge [352]. How does this paradigm shift about the bulges relate to $M_{\text{BH}} - \sigma$?

Third, AGNs are often accompanied by an elevated rate of circumnuclear star formation (e.g., [184, 185, 374]) and the claim is that mass loss from these stars can feed the SMBHs (e.g., [402]). However, in this scenario, the problem is simply shifted from the AGN feeding to starburst feeding. What is the source of this circumnuclear gas?

6.8.2 Accretion Drivers: Large Scales

One can make a general statement regarding disk galaxies: they lack low angular momentum gas. So the origin of cold nuclear and circumnuclear gas accumulation must be explained when such gas is detected. This explanation will necessarily involve the mechanism(s) to transport the fuel from larger radii, unless of course it is produced locally. It seems, however, that local sources are inadequate for fueling the QSOs [358]. On large scales, only one mechanism can extract angular momentum from the gas—gravitational torques. Those can arise because of a number of reasons: spontaneous bar instability (a Maclauren sequence-type instability) and induced bars⁹ (via interactions, mergers, and by the [natural or induced] prolateness of a DM halo). We first discuss the theoretical and computational results, then turn to observations.

Which are the main gravitational torques?

Torques from Stellar Bars. The bar instability has been detected in numerical simulations as a robust one (e.g., [177]). Unlike spiral arms, the bar instability is not exactly a density wave as it traps the stars and gas that make up the bar. Most importantly, bars are strongly nonlinear perturbations kept intact by their self-gravity. The associated timescale for extraction of angular momentum, J , from the galactic disk is given by $t_J \sim (M_h/M_d)(\Sigma/\delta\Sigma)^2/t_{\text{dyn}}$, where $M_h \sim M_d$, are DM halo (within the disk radius) and disk masses, Σ and $\delta\Sigma$ are the disk surface density and its perturbation density, and $t_{\text{dyn}} \sim 10^8$ years is the dynamical time in the disk-

⁹Spontaneous and induced bars can be accompanied by $m = 1, 2$, and 3 spiral perturbations.

halo system within the inner 10 kpc [356]. As $\delta\Sigma \sim \Sigma$, for the bar, it underlines the dramatically short timescale, $\sim \text{few} \times t_{\text{dyn}}$, for J redistribution by the bar, by far stronger than by spiral arms. The original idea that the bar instability is damped by the massive DM halos [289] has not been justified. On the contrary, more massive halos lead to a more massive and longer stellar bars, as the disk is an emitter of J , while the DM halo is its sink (e.g., [13, 92]). Bars can be induced by galaxy interactions [35, 150, 283], and no known dynamical and morphological differences exist between spontaneous and induced bars.

The gravitational torques applied by the bar onto the gas can rapidly move it inward due to J loss, but not by more than a factor of ~ 10 in radius, due to the weakening of the torque [357]. These massive gas inflows result in gas accumulation in the nuclear rings [343], typically positioned between few 100 pc and 1.5 kpc from the center [230]. Nuclear rings are well-known sites of starburst activity (e.g., [106, 173, 174, 206]).

Mergers cause extreme perturbations of a disk-halo system and induce substantial gravitational torques which excite lower order resonances and trigger the radial gas inflow. When the gas accumulates within the central kpc or so, it becomes self-gravitating and rotationally supported, so it is prone to cascading gravitational instabilities [358, 359]. Of course the gas inflow can be triggered by the internal bar instability as well, but this process will be milder.

Torques from Nested Bars. These gravitational instabilities come in the form of gaseous or gaseous/stellar nested bars. Nested bars are ubiquitous in disk galaxies [117, 133, 230, 358]), and both stellar (Fig. 6.17) and gaseous/stellar nested bars have been observed, as predicted. For the purpose of fueling the SMBHs and even for their formation, the inner (nuclear) gaseous bar is of the utmost importance. The difference between nested bars induced by mergers [175, 181, 332] and forming as a result of the spontaneous bar instability [111, 359] is mostly in the timescale for gas accumulation in the central kpc. The formation of the primary (large-scale) bars in interactions and mergers can be somewhat accelerated compared to the intrinsic instability. The formation of nuclear (small-scale) bars can be accelerated substantially. We note that gaseous nuclear bars and not their stellar counterparts have been proposed as the prime mechanism of fueling the AGN activity.

What are the characteristic features of gaseous nuclear bars? Here we focus on theoretical and numerical issues, while observations are discussed in Sect. 6.8.2. We first point out that gaseous bar can best be described as transient. In a moderately strong bar, a healthy fraction of the orbits are irregular (or chaotic). Such orbits are not closed and are intersecting. This is of little concern to stars but leads to dramatic consequences for the gas because of shocks and catastrophic loss of angular momentum. Hence, we do not expect that gaseous bars live sufficiently long to attain any definitive morphology. Moreover, their pattern speed, Ω_s , is expected to increase substantially over a fraction of a tumbling period of the bar, approximated well by $\Omega_s \sim a^{-1}$, where a is the semimajor axis of a bar which shrinks quickly with time.

Torques from Prolate Dark Matter Halos. Numerical simulations of DM halos have shown that the high-redshift halos are formed universally triaxial, flattened



Fig. 6.17 Optical image of NGC 5850 galaxy with double bars (credit: Jeff and Paul Neumann/Adam Block/NOAO). *Arrows* show the position angle of the nuclear stellar bar

along the total angular momentum axis, and equatorially prolate (e.g., [3]). At low redshifts, the input from indirect observations reveals that the nearby halos appear axisymmetric due to the action of baryons [36]. So this discussion is limited to high z halos only. Equatorial prolateness of DM halo is a major source of gravitational torques on galactic disks and, therefore, can trigger a substantial radial inflow of the gas. Numerical simulations exhibit a strong *outer* spiral arm activity and *transient* gas-rich stellar bars. These bars appear to come and go as they interact strongly with and are destroyed by asymmetric halos [175].

Torques will be amplified dramatically if the triaxial halos have flat density (harmonic) cores (see [333] on their origin) because this eliminates most of the regular orbits [109]. The gas cannot populate intersecting orbits, which will induce shocks and the subsequent gas collapse to the center. The gas cannot reside on highly eccentric loop orbits either, and the result is essentially the same. As the central mass builds up, in the form of an SMBH and a galactic bulge, progressively less eccentric loop orbits will appear in these harmonic cores, allowing the galactic disk to grow from inside out and possibly in tandem with the SMBH [109, 175].

Do observations provide clear-cut constraints?

Observational evidence of linking galactic bars with starburst activity in the central kpc is substantial, but that linking nested bars with AGN activity is circumstantial. There are a number of difficulties on the way to resolving this issue. The main difficulty lies in recognizing gaseous bars per se—basically, no such survey has been conducted so far. Even strong stellar nuclear bars have been missed—the most

famous case is probably that of NGC 1068 [387], but also NGC 1566 and even our neighbor NGC 4321 (M100). Nested bars with nuclear gaseous bar have been detected only in serendipitous objects, for example, in ESO 97-G13 the Circinus galaxy [245], IC 342 [238], NGC 6946 [20], NGC 2273 [301], Maffei 2 [257], and others.

Second, the lifetime of nuclear gaseous bars is expected to be very short, from a fraction of a crossing time of the central few hundred pc to a few crossing times. The main reason for this timescale is that the gaseous bars have a tendency to self-destruct—strong barlike potential leads to an increasing number of irregular (intersecting) trajectories and these cannot sustain gas due to shocks.

Third, morphology of central kpc in galaxies is the most confusing and does not really correlate with that of the galaxy as a whole because of several centers of star formation, dust obscuration, overwhelming intensity of the Seyfert or QSO nuclei, etc. Moreover, gas unlike stars has no independent source of energy, and so its observed spatial distribution is often biased in favor of the distribution of young massive stars which affect its energy balance. The properties of the cold (molecular and atomic) gas in galactic centers are only now being mapped at sufficient resolution, and their velocity maps are complex and difficult to decipher.

Fourth, due to very different timescales of central, intermediate, and outer regions in galaxies, there is a time offset or delay between the cause and response in the galactic centers. This issue complicates establishment of a clear correlation between stellar and gas morphologies and the AGN activity. Lastly, the cold gas in galaxies is clumpy on various spatial scales, plausibly leading to an intermittent inflow, which can wash out the above correlations.

The crucial role of gravitational torques is to move the cold gas to smaller radii, down to the central regions, where other mechanisms, such as magnetic torques, discussed in Sect. 6.8.1, can take over. There is no deficiency of cold gas on galactic scales and beyond, and there is an ample evidence that mergers and strong galaxy encounters accelerate the formation of cold molecular gas in galactic disks.

6.9 Modes of Disk Accretion

Varying Accretion Rate: From Too Little to Too Much. The QSOs illuminate our universe as a result of radiation emitted by the accreting material before it crosses the point of no return at the horizon of the SMBHs. The luminosity of QSOs and other AGN depends on their rate of accretion, which in turn depends on the conditions in the accretion disk. If the gas falling into the SMBH is able to cool down efficiently, a lot of radiation will be released. On the other hand, if the gas is accreted hot, the QSO will be dim or not visible at all. Furthermore, some of the photons can have difficulty in escaping from the region, especially if the accretion rate is high. All this creates a range of possibilities. What are the known options?

Accretion via Cold Thin Disks. The most popular accretion disk model is the one which deals with sufficiently dense gas able to cool down well below the virial temperature in the region (e.g., [349]). This model is attractive because it is compatible with the observed infrared excess observed in QSOs, can explain the source of cold gas clouds deep inside the potential well of the SMBH, formation of double-peaked emission-line profiles, and many other observed properties of QSOs. There is a direct evidence for geometrically thin cold disks in NGC 4258 and other galaxies from the detected masers.

A strong argument in favor of a cold thin disk in QSOs follows from understanding the origin of clumpy material in the broad emission-line regions of these objects (and in some other AGNs as well). These clouds are best explained as being photoionized at a characteristic distances of ~ 1 pc by the UVX continuum radiation from a much smaller source. Physical conditions in these clouds have been tightly constrained by the observed relative line ratios. The peaks of these line profiles appear to be blueshifted with respect to QSO rest frames, which indicates the prevalence of the outflowing clumpy gas. The high-ionization (say CIV) lines are also systematically blueshifted with respect to the low-ionization (say MgII) lines.

The source of the cold, $\sim 10^4$ K, gas in this outflow is most probably the underlying thin and cold accretion disk. Due to the radial gradient of the photospheric temperatures of such disks, a range of radii will always exist where the disk atmosphere will become unstable. It will be driven away by radiation pressure in the UV resonance lines of the CNO elements, as first shown by [360] for line-driven disk winds. An alternative to such radiation-driven wind is hydromagnetically driven wind described in Sect. 6.8.1. This MHD wind can also take the excess of angular momentum from the disk, thus driving its accretion flow.

Accretion via ADAFs, CDAFs and ADIOS. CDAFs The diametrically opposite model to that of a cold accretion disk, is a model where the gas heats up to a virial temperature (via shock) and is accreted adiabatically (e.g., [258]). The cold, geometrically thin accretion disks radiate their excess energy locally, at each radius. However, other options have been explored as well, when the locally dissipation generated energy in the disk is advected inward and is not immediately radiated away. Such disks, with the cooling time exceeding that of radial inflow time, are called advection-dominated accretion disks (ADAFs, e.g., [265]). They will be substantially underluminous compared to the geometrically thin, cold disks. ADAF mode of accretion would explain why many AGNs found in the gas-rich environments are heavily dimmed compared to QSO-type objects. The ADAF disks will be geometrically thick and may have different temperatures for ions and electrons, unless fast collective instabilities in such a plasma equalize them.

Dimming accretion disks in AGNs can be obtained by additional means. An accretion disk can be “cooled” down by generating a wind with a substantial mass flow compared to the accretion flow, hereafter adiabatic inflow–outflow solution (ADIOS, [42]). Or energy can be stored in the inflow and circulated outward prior to crossing the SMBH horizon (convection-dominated accretion flow, CDAF (e.g., [266])). Hence, at least four realistic solutions or accretion modes are seriously

considered at present. Moreover, it is completely plausible that these modes all are implemented by nature to power the AGN zoo. It also seems that the QSOs and their scaled down version Seyfert nuclei are the most efficient ones in extracting the energy from accretion flows and host a geometrically thin disk, as discussed in Sect. 6.8.1.

The accretion rate onto the SMBH can be arbitrarily high. When the rate exceeds that of the Eddington accretion rate, $\dot{M}_E = 0.2M_{\text{BH},8} M_\odot \text{ year}^{-1}$, the optical depth in the accreting material leads to the trapping of radiation, which is dragged downstream by the flow [30]. The efficiency of extracting the energy from the flow goes down unless a preferential channel for energy release can be maintained.

While accretion rate onto the SMBH can exceed \dot{M}_E , what happens when the liberated luminosity tends to the Eddington luminosity, $L_E = 1.3 \times 10^{46} M_{\text{BH},8} \text{ erg s}^{-1}$? Common sense tells that this radiative feedback should cut off the accretion. In other words, the accretion is self-regulated. However, there are caveats. When the radiative force competes with the local gravity, a novel phenomenon can occur, resembling a phase transition. It has a counterpart in the physics of fluids, where it has been discovered empirically. We shall discuss it now briefly.

How do accretion disks behave close to the Eddington limit?

Take a box of sand in a “hydrostatic” equilibrium and push (from underneath) a pressurized air through it. As long as the gravity exceeds the upward drag imposed on the sand particles by the air, they will remain homogeneous. When the vertical drag force approaches the gravitational forces (in analogy with the Eddington radiative force), one expects the sand particles to be pushed up and away. Instead, as shown in numerous experiments, air bubbles appear and move through the sand, effectively leading to the formation of an inhomogeneous, two-phase substance. Moreover, no “mass loss” of sand has been detected. The properties of the sand under these conditions resemble a fluid, and this phenomenon has been named a “fluidized bed.” The result remains unchanged when the pressurized air pushed through the sand is replaced by water. The principle of the fluidized bed is used in operating the fluidized bed reactors. Current attempts to understand the dynamic behavior of fluidized beds are based on chaotic dynamics (e.g., [91]).

Conditions in the accreting matter close to the Eddington limit, L_E , resemble those in the fluidized bed. If one replaces the air by radiation, a crucial question is if photon bubbles will form, as speculated by [306]. Whether this is a mere analogy or such a process actually operates in the brightest AGN is an open question. Begelman [31] has investigated the linear regime of such a “photon bubble” instability and found that strong density inhomogeneities will develop on scales much smaller than the characteristic disk thickness. This allows the photons to escape from a disk at much higher rate than is predicted by theoretical models of accretion disks. This rate can exceed that of the critical Eddington rate by a factor of up to ~ 100 . Such process can be driven, for example, by periodic shock patterns in the magnetized disk atmospheres. What is not clear is whether it is possible to have photon bubbles with non-leaky boundaries. In other words, what is the effective mean free path of these bubbles? Is the magnetic field necessary and/or sufficient condition for this?

Are there alternative options? If such mildly super-Eddington objects exist in AGNs, they may be some QSOs and Seyfert nuclei. What are the observable features of these objects and how can they be distinguished from the “conventional” AGNs?

Our current understanding is that the mass accretion rate is a crucial parameter that determines the emerging luminosity of AGNs, but it appears to be not the sole parameter which is responsible for this. While the high rates of mass accretion onto the SMBHs can sustain the most powerful of AGNs, the QSOs, the efficiency of the process may vary as some fraction of photons can be trapped by the flow and dragged across the horizon. Although an SMBH can be fed at an arbitrarily high rate, the emerging luminosity will saturate somewhere at the level of $\sim 1\text{--}100 L_E$. In this regime, the disk appears to be able to cool and remain geometrically thin.

Somewhere below the Eddington mass accretion rate, the mode of accretion is switching from geometrically thin disk to one of the thick disk and underluminous solutions, ADAF, CDAF or ADIOS. CDAFs When and under what conditions this change occurs is a matter of further theoretical analysis and of observational input.

Thank you, Isaac.

6.10 Relativistic Accretion Disk Theory

Dear Julian (*Krolik*), a few years before the astronomical consensus for black holes as the central element in quasars jelled, a basic theory of black hole accretion was constructed by Novikov and Thorne and Shakura and Sunyaev [284, 349]. This theory made a number of plausible simplifying assumptions (time steadiness, prompt radiation of heat generated locally, azimuthal symmetry) to permit application of energy and angular momentum conservation. With one heuristic guess (that all stresses in the accreting matter ceased at the ISCO), the theory predicted the radial profile of surface brightness. With another, (that there is a constant ratio between the angular momentum transporting stress in the disk and its pressure), it predicted the radial profile of surface (mass) density. How has that theory held up? In particular, have these two heuristic guesses been vindicated?

The answer to this question naturally divides into two parts: whether there is a constant ratio between stress and pressure, and whether the guessed boundary condition is correct.

6.10.1 *The Nature of Internal Stress in Disks*

Guessing the ratio between stress and pressure was necessary because the theory lacked any specific mechanism to drive accretion. That is, for matter to accrete, some

process must remove its angular momentum, thereby allowing it to drift inward, but in the early 1970s, no one had even the faintest idea what that mechanism might be. Because the orbital frequency declines outward, there is shear between adjacent rings of orbiting gas, and it was vaguely supposed that some sort of friction akin to viscosity might lead to a stress coupling those rings, but actual atomic viscosity was quickly seen to be so weak in this context that its action would be hopelessly inadequate. Because the pressure of the gas has the same units as stress, Shakura and Sunyaev guessed that the magnitude of whatever caused this stress would have a typical magnitude comparable to the pressure. To symbolize this relation, they wrote

$$\int dz \langle T_{r\phi} \rangle = \alpha \int dz \langle p \rangle, \quad (6.9)$$

where the averaging was over both time and azimuthal angle. Although this dimensional argument did not imply that α need be a constant, whether as a function of location or time or object, the simplicity of the relationship led to many papers making that assumption. In addition, the intuitive analogy to viscosity likewise led many to refer to “viscous” accretion disks with “kinematic shear viscosity coefficients” $\nu = \alpha c_s h$, where c_s and h are the local speed of sound and disk thickness.

In the early 1990s, Steven Balbus and John Hawley proposed [15] that the actual mechanism creating angular momentum transport in accretion disks is MHD turbulence, stirred by the “magnetorotational instability,” a dynamical instability that sets in whenever the matter in the disk is a good electrical conductor, and the orbital frequency declines outward. The magnitude of this stress is $B_r B_\phi / 4\pi$, where B_r and B_ϕ are the radial and azimuthal components of the local magnetic field. When the orbital frequency declines outward, orbital shear automatically correlates the turbulence so that $\langle -B_r B_\phi \rangle > 0$; the mean angular momentum flow is then always outward. Thus, in this picture, the stress is not “viscous” by any stretch of the word: it involves magnetic fields, not randomly diffusing atoms, and does not directly lead to local entropy production.

Although there is no direct observational evidence in favor of this mechanism, the intervening years have seen an enormous effort to simulate its operation numerically. These efforts have in general seen success, in the sense that the nonlinear saturation amplitude of the magnetorotational instability appears generally to be large enough to account for the stress required in accretion disks (an excellent review of the early work can be found in [16]).

One consequence of this deeper understanding of accretion disk stress is the recognition that the “ α parameter,” the ratio between stress and pressure, is by no means a constant. It varies chaotically in time at any single location by factors of several. Averaged over local temporal fluctuations, it increases systematically by ~ 100 or more from the disk midplane to its surface. Interpreted in its original sense as the ratio between vertically integrated stress and vertically integrated pressure, its mean value appears to vary only slowly as a function of radius deep inside the disk,

far from either its inner or its outer boundary, but can change drastically near the boundary.

Another success of the MHD picture has been to clarify the internal structure of disks. By carefully tracking where dissipation of the turbulence creates heat, where the heat is used to create photons, and how the photons diffuse to the surface, it has been possible to solve for the vertical profiles of gas density, temperature, and magnetic field intensity [176]. Because magnetic fields are generally buoyant relative to matter, disks are nearly always magnetically dominated in the regions several scale heights above the midplane where the disk photosphere is located (this is why the α parameter systematically increases rapidly with height from the midplane).

A major challenge for this program, however, is a quantitative determination of the saturated magnetic field strength. The essential difficulty in doing so stems from the nature of turbulence: it couples large scales, where the motions are stirred, to small scales, where the turbulent energy is dissipated into heat. Because the physical mechanisms responsible for dissipation act on tiny length scales, no numerical simulation of the foreseeable future can hope to resolve both the stirring scale and the physical dissipation scale; instead, simulators either rely on numerical dissipation at the grid scale to substitute for physical dissipation or assume phenomenological resistivity and shear viscosity, many orders of magnitude larger than anything realistic in order to resolve the dissipation scale. A generic problem with either approach is that when the numerical dissipation scale is too close in magnitude to the stirring scale, the rate at which turbulent energy (mostly magnetic) is dissipated is overestimated, depressing the saturation level of the field. Even the most highly resolved simulations suffer from this problem (e.g., [354]). In addition, there are indications that the character of the turbulence may depend upon the relative magnitude of the resistivity and the fluid shear viscosity, the Prandtl number of the plasma; if so, the saturation amplitude may also depend on this quantity [134].

6.10.2 *Stress at the ISCO?*

The original basis of the “zero-stress” assumption was that inward mass flow in the disk depends on a slow process of angular momentum transport, whereas inward mass flow inside the ISCO does not require any angular momentum loss because all bound orbits lead quickly to the event horizon. Consequently, for a fixed mass accretion rate, the mass inventory in the stable orbit region outside the ISCO should always be much larger than in the plunging region inside. In such a situation, one might find it hard to imagine how the low-mass “tail” could exert much force on the much larger mass “dog.”

An important consequence of the “zero-stress” boundary condition is a simple prediction of the radiative efficiency of black hole accretion. If all dissipated heat is radiated locally, the binding energy of matter orbiting at the ISCO is simply the binding energy of a test-particle orbit there. Furthermore, if there are no stresses

from that radius inward, matter flows from the ISCO to the event horizon without any change in its energy or angular momentum. Consequently, the net energy lost to the outside world is exactly the binding energy of a test-particle orbit at the ISCO. For prograde orbits, this energy increases from 0.057 of the rest mass for non-spinning black holes to 0.42 for maximally spinning black holes.

However, even at the time it was first proposed, the “zero-stress” assumption was questioned on the basis that its plausibility would be severely undercut if magnetic fields were important [386]. Because magnetic fields can be stretched parallel to themselves with no diminution of intensity, there is no particular reason for the field strength to drop across the ISCO. Thus, if they are important outside the ISCO, they could continue to be important near it and inside.

With the recognition that MHD turbulence is central to accretion, these questions were revived [137, 223]. As these papers pointed out, not only might the magnetic field continue to be important as the flow approaches and crosses the ISCO, its relative importance might increase dramatically because the gas density and pressure would drop sharply as the inward flow accelerates across the ISCO. Although qualitative analytic arguments like these suggest that the magnetic stress near the ISCO could be sizable, quantitative calculation of its magnitude requires numerical simulation of the MHD turbulence across a range of radii in the disk, and all of this needs to be done in a general relativistic context.

Attempts to solve this problem began in 2003 [94, 138]. In the current state of the art, it is possible to solve the equations of fully three-dimensional MHD in the Kerr metric appropriate to the vicinity of a rotating black hole. However, it is not yet possible to compute accurately the gas’s equation of state, leading to significant uncertainty about the gas’s dynamics. In addition, the strength of magnetic effects near the ISCO scales with the general strength of magnetic effects elsewhere in the disk, so accurate determination of the magnetic field intensity is essential. The numerical difficulties mentioned in Sect. 6.10.1 regarding the nonlinear saturation amplitude of the turbulence consequently come to the fore in this context.

As a result, considerable controversy divides the different groups active in this area (e.g., [282, 294]), but all agree that there are magnetic stresses near the ISCO at some level. The controversy (as of 2010) centers on whether the general level of magnetic stress in the inner disk depends on magnetic topology, and on whether the advocates of relatively weak stresses have used adequate resolution in their simulations. Given that poor resolution tends to bias the result to weaker field strengths (and more complicated magnetic topologies demand finer resolution), it may be a good bet that, as increased computing power permits improved resolution, the importance of near-ISCO magnetic effects will rise.

To the degree that trans-ISCO magnetic stresses are large, they increase the radiative efficiency η . Any such adjustment will affect the argument mentioned in the historical section (Sect. 2.7), as well as the required mass budget for feeding quasars. It will also affect estimates of the spin distribution of quasar black holes because it will alter the relationship between spin and η . In addition, because the extra light generation takes place over the very small area just outside the black hole’s event horizon, the surface temperature is relatively high; consequently, much

of the additional light should appear at relatively short wavelengths. At such time as disk atmosphere models become reliable enough to be compared in detail with quasar spectra, this point will also become important.

Thank you, Julian. We have a few more questions for you. The major enigma here is related to the aspect of the structure that is believed to obscure most quasars and change them from type-1 to type-2.

6.11 The Obscuring Torus

Is the torus a necessary part of the standard model? What supports the vertical thickness of the torus? Is the torus likely to be clumpy or smooth? Is there any observational way to distinguish between a clumpy and a smooth torus?

Is the torus present in all AGNs?

In 1985, Ski Antonucci and Joe Miller made a dramatic discovery [6]: that many of the contrasts in phenomenology between “type-1” and “type-2” Seyfert galaxies could be attributed to their intrinsic anisotropy. Both types of Seyfert galaxies have optical spectra exhibiting strong emission lines in transitions such as [OIII]5007 and the Balmer lines. The “type-2” variety show little else unusual in the optical, UV, or soft X-ray bands (they can be bright in hard X-rays but that was not known until later). On the other hand, “type-1” Seyferts look just like quasars whose “volume knob” has been turned down. They have strong optical and UV emission lines broadened by thousands of km/s; unlike galaxies, their continuum flux is generally stronger in the UV than in the visible band; and they are very bright in both soft and hard X-rays. They differ from quasars only in that their luminosities are smaller by an order of magnitude or two. Prior to Antonucci and Miller’s work, many people thought that the two types of Seyfert galaxies were intrinsically entirely different.

The drama and scope of that 1985 paper were that, with a single observation, its authors were able to demonstrate that the nearest and brightest type-2 Seyfert galaxy, NGC 1068, *must* be intrinsically a type-1, but we have the misfortune to look at it from the wrong direction. In other words, they showed that, unlike stars, which are extremely round, and look very much the same from all directions, AGNs can look very different from different viewing angles. It was natural, of course, to guess that this discovery could be generalized to *all* Seyfert galaxies, and to suppose that they are all in fact the same sorts of systems, but seen from different points of view.

The agent of anisotropy Antonucci and Miller posited was a toroidally shaped belt of very optically thick gas and dust wrapped around the galactic nucleus outside the regions responsible for producing the optical to X-ray continuum and the broad emission lines, but inside the region where the narrow emission lines are made. If our line of sight runs through the torus, direct light from the nucleus is thoroughly blocked. On the other hand, if our line of sight goes through the hole in the torus, it is almost—but crucially, not quite—transparent. Antonucci and Miller’s

discovery rested on the fact that there is ionized gas in and above the hole. Although this gas is optically thin, those photons that are scattered toward observers near the equatorial plane acquire a net polarization because this structure is far from circularly symmetric when projected on the sky plane. In other words, observers unable to see the nucleus directly can see the nucleus in reflected light, with the reflected signal identifiable by its polarization.

Since that time, a great deal of evidence has been found that generalizes this picture from the single Seyfert galaxy for which it was first suggested to Seyfert galaxies as a whole, as well as to other classes of active galaxies such as radio galaxies [25]. Images of nearby active galaxies show “ionization cones,” bicones of ionized gas centered on the galactic nucleus, bright in narrow emission lines. If the obscuration really is toroidal, it would naturally collimate the ionizing spectrum of the central active nucleus into exactly such a shape. Although type-2 Seyfert galaxies are quite weak in soft X-rays (i.e., a few keV), where the K-shell photoionization optical depth of the obscuring gas is capable of absorbing nearly all the continuum, they frequently strengthen dramatically at energies a few times larger, where the opacity is much less. All Seyfert galaxies and quasars exhibit strong IR continua with quasi-thermal peaks near $10\ \mu$, just as would be predicted if a torus at radii $\sim 1\text{--}10\ \text{pc}$ from an AGN absorbs most of its power output and reradiates it thermally from its dust grains.

For many years, however, there were questions about whether this schema could be extended up the luminosity scale to quasars. Until roughly 10 years ago, there were no known examples of type-2 quasars, a fact suggesting to some that perhaps quasars did not possess this sort of obscuration; on the other hand, it was also recognized that this very obscuration would make type-2 quasars so faint and indistinctive that they would be exceedingly difficult to find. Thanks to the statistical power of the Sloan Digital Sky Survey, we now know that, at least for quasars at modest redshifts ($z \sim 0.5$), type-2 quasars are, in fact, numerous [324], although their fraction in the population may be smaller by a factor of a few at the higher luminosities of quasars than at the lower luminosities of Seyfert nuclei [22, 160, 233, 388, 392].

Now that quasars are seen not to differ qualitatively in this aspect of their phenomenology from the lower luminosity Seyfert galaxies, it is natural to suppose that they also share in the possession of obscuring tori. That they should do is also suggested by several other points. All quasars have bright infrared continua, very similar in shape to those of Seyfert galaxies. Placing the origin of that IR continuum in dust reradiation by an obscuring torus would be a very natural explanation. In fact, the relative share of the infrared continuum in the bolometric luminosity of type-1 quasars has been used to estimate the fraction of solid angle occupied by their tori [388]. High-resolution optical imaging of a small number of type-2 quasars has revealed biconical reflection features analogous to the ionization cones seen in type-2 Seyfert galaxies [409]. Lastly, and perhaps the most powerful argument of all, in the few type-2 quasars for which optical spectropolarimetry has been obtained, one sees polarized spectra [408] identical in character to those on whose basis the entire obscuring torus picture was invented in the first place.

What supports the torus?

At least half of all Seyfert galaxies are seen as type-2 [171]. Presumably, that means that at least half of the solid angle around Seyfert nuclei is obscured. However, such a thick shape for the toroidal obscuration poses a severe dynamical problem.

When a fluid orbits in a gravitational potential, its angular momentum supports it against gravity in the radial direction, while its pressure supports it against the vertical component of gravity. If its vertical thickness h is small compared to the radius r of its orbit, $h \sim (c_s/v_{\text{orb}})r$, where c_s is the effective sound speed (i.e., including magnetic and radiation pressure as appropriate) and v_{orb} is the orbital velocity. At $\sim 1\text{--}10$ pc from the central black hole (the typical distance of obscuring tori, as measured, for example, in systems possessing H₂O 22 GHz masers: [213]), orbital speeds are $\sim 100\text{--}1,000$ km s⁻¹. For pressure to support the torus against gravity strongly enough to make the structure geometrically thick, c_s must be comparable to v_{orb} . If that is a conventional thermal sound speed, a temperature $\sim 10^6$ K or even greater is implied. The problem is that molecular gas and dust cannot survive such high temperatures.

Numerous solutions to this problem have been proposed. Mitch Begelman and I [225] suggested that the gas and dust might be strongly clumped, and these clumps, although containing gas at only $\sim 300\text{--}1,000$ K, might move with Mach numbers ~ 30 , fast enough to rise high above the midplane of the torus. However, if the torus is opaque on most lines of sight, these clumps would necessarily collide with other clumps at least once an orbit. When they do, unless something special happens, much of their kinetic energy would be immediately dissipated. In desperation, we suggested that they might be so strongly magnetized that the collisions would be highly elastic. Since then, a number of other candidate solutions to this problem have been created. One proposal is that the system is not quasi-stationary at all; instead, magnetic forces steadily propel the gas and dust around and outward at similarly supersonic speeds [214]. Yet another idea [224, 302, 353, 385] is that the outward radiation flux of the AGN (perhaps augmented by local starlight) would be capable of levitating the gas. In my opinion (and this is an area where the arguments are strong enough only to support opinions), this last class of ideas is the best of the candidates; it is therefore worthwhile to expand upon it briefly.

Radiation forces can be described compactly in terms of the radiation flux:

$$\mathbf{F}_{\text{rad}} = \kappa \rho \mathcal{F} / c, \quad (6.10)$$

where ρ is the local mass density and κ is the opacity per unit mass, that is, the total photon-material cross section per unit mass. The radiation flux \mathcal{F} is a directional moment over the angular distribution of the radiation. If the intensity (energy flux per solid angle and per photon energy) is $I_\epsilon(\Omega)$,

$$\mathcal{F} \equiv \int d\Omega \int d\epsilon I_\epsilon \hat{\mathbf{n}}(\Omega), \quad (6.11)$$

where Ω denotes solid angle and $\hat{\mathbf{n}}$ is the unit vector pointing in any given direction. When there is an isotropic point source of light with luminosity L at the origin, $\mathcal{F} = L/(4\pi r^2)\hat{\mathbf{r}}$ at any radius r from the center. The most natural standard of comparison for the importance of radiation forces is, of course, the force of gravity. In the case of an isotropic point source, the ratio between the two is

$$\frac{|\mathbf{F}_{\text{rad}}|}{|\mathbf{F}_{\text{grav}}|} = \frac{\kappa L}{4\pi c GM}. \quad (6.12)$$

Because the opacity is dominated by Thomson (sub-relativistic electron) scattering in most regions of AGNs, there is a natural scale for luminosity called the ‘‘Eddington luminosity’’ $L_E = 4\pi c GM/\kappa_T \simeq 1.4 \times 10^{38} (M/M_\odot) \text{ erg s}^{-1}$ at which radiation forces balance gravity.

In order to comply with mass limits on nuclear black holes, typical AGN luminosities in Eddington units cannot be less than ~ 0.01 and are likely at least an order of magnitude larger, so that radiation forces in most parts of their structures are noticeable, but not controlling. However, the opacity per unit mass for mid-infrared light striking dust grains is 10–30 times greater than κ_T . Empirically, we see that the infrared luminosity of AGNs is large enough that if, as seems likely, it is produced by dust reprocessing in obscuring tori, most of the radiation flux must pass through these dusty zones. Consequently, the characteristic ratio of radiation forces to gravity in tori should be $\sim O(1)$. This is the key reason why infrared radiation support almost certainly must play a significant role in keeping the tori geometrically thick.

Is the torus likely to be clumpy or smooth?

The previous subsection presented the principal dynamical argument for strong clumping in the torus but also a possible countervailing argument: to the extent that radiation supports its cool, dusty material, the need for highly supersonic motions of small clumps is reduced. Although the observed inhomogeneity of interstellar gas in our own Galaxy certainly makes clumping in AGN tori plausible, no one has yet suggested a particular mechanism for sustaining density inhomogeneities in the specific context of obscuring tori. Instead, the arguments raised on its behalf have all been based on reasoning backward from observations. In addition to the dynamical argument already discussed, a second such comes from observations of the detailed character of the mid-infrared continuum created when the dust in the torus reprocesses the intrinsically higher energy AGN spectrum.

In order to adequately obscure the central nucleus over the majority of solid angle, the mean optical depth along ray paths within $\sim 45^\circ$ of the equatorial plane must be large for all frequencies from the near-IR through few keV X-rays. If the dust/gas ratio is similar to what we see in our own Galaxy, such large column densities of gas imply that even in the mid-infrared, these rays are optically thick. When the gas and dust are distributed smoothly, the optical depth as a function of direction must likewise vary smoothly; when they are strongly clumped, the optical depth can fluctuate as a function of direction. In the midplane, where the mean

optical depth must be very large, these fluctuations are unlikely to create transparent lines of sight; however, far from the plane, particularly near and above the angle at which the mean direction becomes optically thin, these fluctuations can produce larger effects. Their general sense is to roughen the border between the infrared phenomenology of obscured and unobscured AGNs [180, 267]. Smooth transfer models of the infrared continuum tend to predict that it is “cooler” in obscured AGNs than in unobscured; that is, the radiation tends to emerge at somewhat longer wavelengths, is a somewhat smaller fraction of the total reprocessed power, and is more likely to display absorption features such as the ones near $10\ \mu$ due to Si bending modes in dust grains. To the degree that all these trends map precisely onto obscured/unobscured distinctions, smooth models are favored; to the degree that these trends are not precisely followed across the obscured/unobscured divide, greater clumping may be required. To my mind, the data in hand do not yet permit a clear statement of where we stand [26, 172, 179, 361, 378].

Thank you, Julian. Now, it is the time to consider the structural elements and the physical processes described earlier altogether and to join them to build (or at least to try to build) a self-consistent model that might account for the quasar inner working.

6.12 A Quasar Model

Dear Martin (*Elvis*), about 10 years ago, you proposed a model for unifying structure in the central regions of quasars. Can you give us a summary of this model and tell us about any modifications that you have introduced over the past 10 years?

High-energy physics has a “standard model” of the elementary particles that was created in 1967 [403] and has explained all the data since. Quasars¹⁰ have followed a similar path starting around the same time, but their standard model is now, I believe, yielding to a more advanced and complete one.

Within a decade of their discovery, the quasar standard model was in place. It consists of three elements (Fig. 6.18): (1) a supermassive black hole [241], surrounded by (2) an accretion disk [349], with (3) a relativistic jet [321] originating from just a few Schwarzschild radii. This model successfully accounts for the total power output of a quasar, from gravitational energy released by infall, the maximum temperature of the optical emission from the thermalization of this emission in the

¹⁰For simplicity, I will use “quasar” for all forms activity associated with a supermassive black hole at the center of a galaxy. In the research literature, no single term spans this range, though “active galactic nuclei” comes close, with “quasar” being reserved for objects above an arbitrary luminosity threshold. To me, this is not a useful division, and “quasar” is a short, memorable, term that serves well.

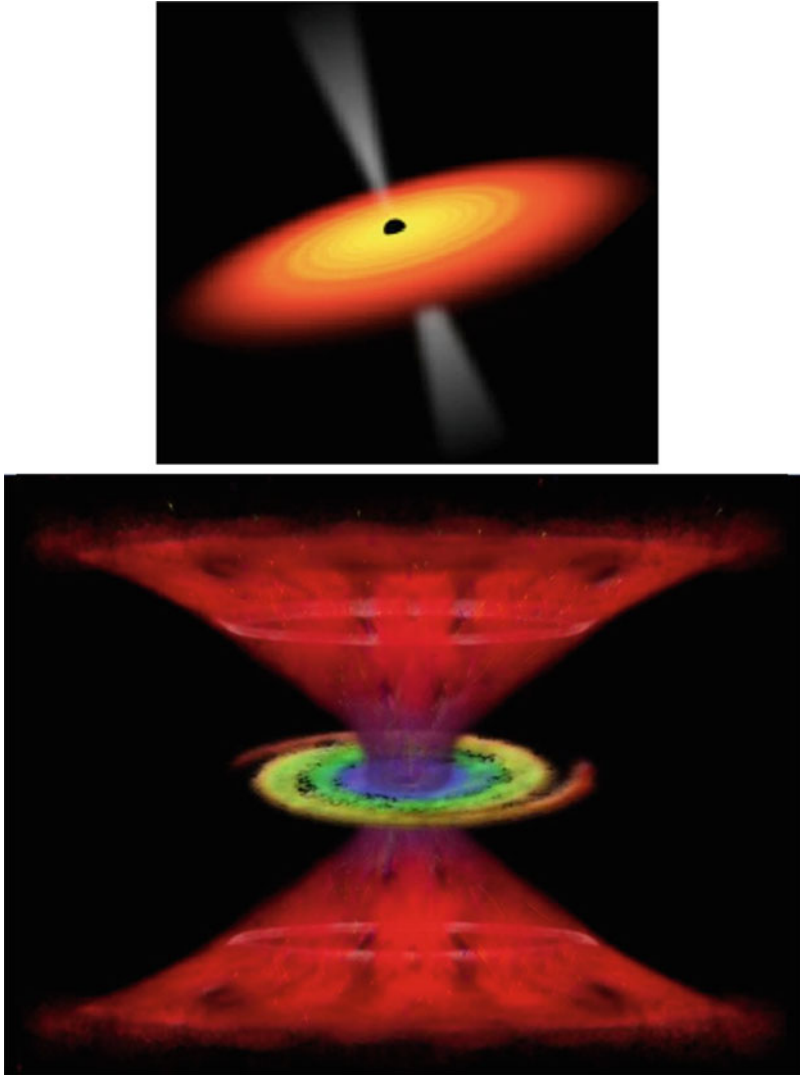


Fig. 6.18 *Top*: the standard model of a quasar: supermassive black hole, accretion disk, and relativistic jet. *Bottom*: funnel-shaped wind proposed by Elvis in 2000 [107]

disk, and the phenomenology of apparent superluminal motion, rapid variability, and polarization of the radio emission in objects where the jet is pointing almost directly at us.

This is all well and good, but there was a great deal unaccounted for. The model does not predict any of the broad or narrow atomic emission and absorption lines, yet they are so characteristic of quasars that they were the reason for their discovery. Clearly, something is missing from the picture. The standard model also

failed to predict the maximally hot dust ($\sim 1,500$ K) found in ever better infrared observations from the ground and space.

Most remarkably perhaps, the model does not predict strong high-energy X-ray emission from quasars. Yet within 5 years of the last defining paper of the standard model [349], data from the Ariel V Sky Survey demonstrated that X-rays were a normal feature of AGNs. This work was the centerpiece of my Ph.D. thesis at Leicester University [108]. A year later, the 100 times more powerful imaging *Einstein Observatory* found that luminous AGNs—quasars—were also X-ray sources [381].

The quasar standard model clearly had major gaps. For the next 4 decades, we have been trying to discover what the missing elements of the quasar model are. While I would have been horrified in 1978 to learn that it would take so long, at this point, I believe we have captured most of them. Surprisingly, the X-ray emission of quasars is still the weakest link.

Accretion disk winds provide a unifying model for all the atomic emission and absorption features in quasars. While numerous pieces of this model were advocated beforehand (notably by [264] and [286]), I was the first to push the idea that *every* feature could be explained this way [107].

My 2000 paper proposed that a wind is ejected vertically at $\sim 1,000$ km s⁻¹ from a narrow zone on the accretion disk outside the region where the strongest UV and optical continuum originates. This wind is then accelerated radially by UV line driving [264], as in O-stars [231], up to velocities of $0.1c$ or so.

The result is a funnel-shaped wind (Fig. 6.18). When viewed through the vertical part of the wind, we see the warm absorbers. Embedded in the warm absorber gas are cooler clouds in pressure equilibrium, and these produce the higher ionization broad emission lines (e.g., C IV, OVI, HeII). Viewed down the radial flow direction, the wind produces the broad absorption lines, seen in the same high-ionization lines, in about $\sim 15\%$ of quasars [286]. From above, where no wind lies between us and the central continuum source, no absorption is seen. As the wind continues outward, it creates the narrow emission-line region (NLR), eventually becoming visible in high-resolution optical and Chandra images as a bicone structure called the “extended narrow emission-line region” (ENLR). Outside the narrow wind-producing part of the disk, gas is still ejected, but fails to reach escape velocity. Here lies the region producing the low-ionization broad emission lines (MgII, Fe II, [72]).

How has this idea fared in the following decade? Pretty well. The outflow of the X-ray warm absorbers and their unity with the UV absorbers was initially hotly contested, but quickly became established with Chandra and XMM high-resolution spectra [83, 221, 262]. The idea that the ENLR was a hollow bicone, rather than the illumination of a preexisting interstellar medium in the host galaxy by a collimated light source, was also quickly established by Hubble STIS spectroscopy of some canonical objects [84]. The puzzle of why the wind zone should be so thin was solved in 2004 by applying O-star theory ([55], CAK) to the winds, although our paper describing how this works was delayed 6 years in publication [327]! The key is that line driving is extremely sensitive to the ionization state of the gas. The great insight of CAK was that the initial momentum absorbed by the gas must be enough

to accelerate the gas to a new velocity, where the lines are Doppler-shifted to a fresh, unabsorbed, section of the continuum, so that the acceleration can continue. Below this threshold no wind forms. Hence, the onset and turnoff of the wind are sudden and occur at specific radii. This is just what the observations were telling us.

One new development, which complements the Elvis model, is the discovery of high-ionization winds at high velocities, a few tenths c , in several quasars. At this ionization level, only electron scattering remains to accelerate the gas. This condition is the same as the Eddington limit—that electron scattering force overcomes that of gravity. And the quasars that have these fast, highly ionized, winds are indeed radiating at their Eddington limits (e.g., [58, 304]). In lower Eddington ratio quasars, any such gas will be accelerated but will not reach escape velocity. An example of this is found in NGC 1365 [329]. These failed winds do provide a means of reducing the X-ray flux along the disk plane by scattering them at large angles, and this enables efficient line-driven acceleration in the warm absorber/high-ionization broad-line region [264, 327].

A second new aspect of disk winds is the realization that beyond some radius, the disk has not become hot enough for dust accreting into it from the host interstellar medium to be destroyed. If this dusty gas were ejected from the disk, it would be efficiently accelerated by the remaining central continuum source because of the high cross section of dust (Fig. 6.19). This would create a third, dusty, wind from the disk [105].

6.12.1 *Parsing the Torus, Dissecting the Donut*

The dominant new idea to arise after the standard model was that quasars contain a flattened obscuring region that hides the central continuum and broad emission-line producing region but does not cover the NLR [7, 234], that is, a torus.

If the obscuring region is aligned with the radio jet, as is clearly the case in radio galaxies [5], then the same picture can unite the jet-dominated blazars and the large double-lobed radio galaxies [25]. The populations of radio galaxies and blazars fit this model well [393].

This was put together into a neat model by [225] who proposed that there is a cold torus containing molecular gas beginning at the radius where the hottest dust can just survive [28] and extending outward. The torus has a large-scale height, producing a donut-like shape. This one idea can explain four things at once: (1) the various types of quasar, in the correct ratio of type-1 (those with obvious broad emission lines) and type-2 (which do not show these broad lines), [201]; (2) the existence of the “hidden” broad-line region found in polarized light [7]; (3) the shape of the bi-conical ENLR, via collimation of the continuum by the torus (e.g., [380]); (4) the existence of the characteristic maximally hot dust in quasars. This makes a very appealing and elegant concept. It also makes a compelling graphic. The image in the review by [393] has been reproduced countless times. Like many powerful images, it looks right, and this has led many to accept this “donut” picture of the quasar torus with little critical thought.

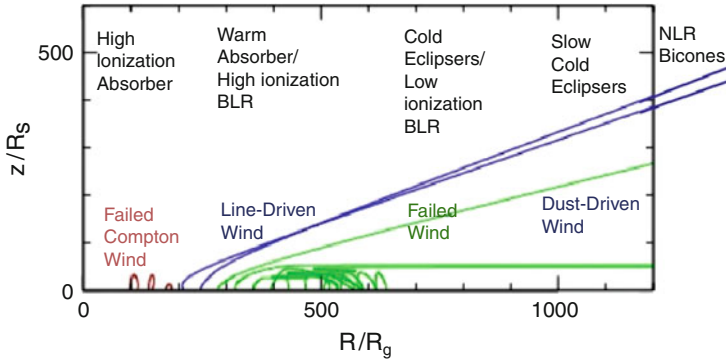


Fig. 6.19 The three ways in which photons can transfer momentum to atoms produce an alternation of winds and failed winds in quasars. Together, they explain all the atomic absorption and emission features of quasars. Note that the two axes scale are *linear* in Schwarzschild radii

Unfortunately, for elegance, reality turns out to be more complicated. There is no single torus that can explain all the obscuration in quasars. There are obscurers on both larger and smaller scales than the donut, and the obscurers on the dust sublimation radius scale of the donut may well be in a wind, rather than a static donut. This is just as well because the theoretical difficulties of maintaining a large-scale height in cold gas are many. Even Mitch Begelman, one of the creators of the idea, says that it is held up “by the power of pure thought.”

Larger scale obscurers must be present because they align with the disks of the host galaxies. This has been shown in a long series of papers (e.g. [234]). Instead, the quasar accretion disk is randomly aligned with these galaxy disks, as the radio jets do not align with the host disks [205], and it is hard to make the jets and the accretion disk not share an axis. The scale of the host disk obscurer is not obvious. To reach alignment with the black hole spin axis, it must lie within the black hole sphere of influence, which is ~ 30 light-years, so a larger scale is likely. A candidate for this obscurer is seen in the molecular disks on scales of ~ 100 light-years in several nearby objects. A notable example is the prototype “type-2” object (narrow lines only), NGC1068, for which the donut torus was first invented. NGC 1068 shows a CO disk mostly aligned with the host, but slightly warped up to cross our line of sight to the inner nucleus [340].

The smaller scale obscurers must also be present because they move rapidly across the X-ray source. As these obscurers lie in the broad-line region, they may not be dusty, but they certainly affect the X-ray classification of their quasars.

A dusty wind from the outer accretion disk produces obscurers on intermediate scales, where the hot dust emission comes from.

These three obscuring regions together account for all the instances of obscuration seen in quasars. While not as neat as the donut torus, it is still quite an economical picture and uses elements that are well established from other observations.

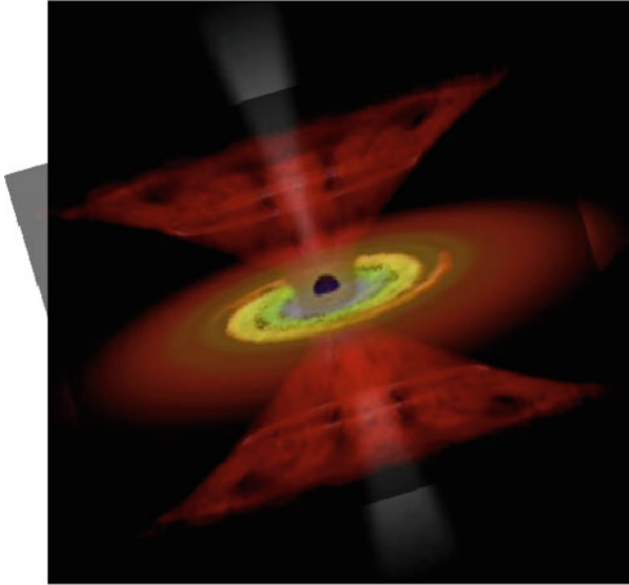


Fig. 6.20 A new standard model of a quasar: supermassive black hole, accretion disk, and relativistic jet and winds

In retrospect, it is not surprising that a single explanation did not work. The level of obscuration seen in quasars spans at least a factor of 1,000 in column density of obscuring material—roughly the difference between a thin sheet of paper and a brick. To make these all from a single structure was a demanding task.

Can we speak of a new quasar standard model? What remains to be understood?

With the addition of disk winds to the standard model of quasars, we have solved most of the puzzles concerning the origin of the wide variety of atomic features: broad and narrow, emission and absorption, as well as forming a more nuanced model of what causes obscuration in quasars. That all three ways in which photons can impart momentum to matter can and do produce a wind, and that the zones in which they are ineffective also produce observable signatures, is rather elegant (Fig. 6.20).

A wide range of observations went into producing this synthesis. It is somewhat paradoxical that absorption of the X-ray continuum—cold, warm, and highly ionized—should be so important. The paradox is that the most poorly understood component that remains is the X-ray continuum source itself. Observations of eclipses of the X-ray source by cold matter may be the best way to attack this question in the near future.

Thank you, Martin.

References

1. Alexander, T., Netzer, H.: Bloated stars as AGN broad-line clouds: the emission line spectrum. *Mon. Not. R. Astron. Soc.* **270**, 781–803 (1994)
2. Alexander, T., Netzer, H.: Bloated stars as AGN broad-line clouds: the emission-line profiles. *Mon. Not. R. Astron. Soc.* **284**, 967–980 (1997)
3. Allgood, B., Flores, R.A., Primack, J.R., Kravtsov, A.V., Wechsler, R.H., Faltenbacher, A., Bullock, J.S.: *Mon. Not. R. Astron. Soc.* **367**, 1781 (2006)
4. Anderson, J.M., Li, Z.-Y., Krasnopolsky, R., Blandford, R.D.: Magnetocentrifugal winds in three dimensions: a nonaxisymmetric steady state. *Astrophys. J.* **653**, L33–L36 (2006)
5. Antonucci, R.R.J.: Optical polarization position angle versus radio source axis in radio galaxies. *Nature* **299**, 605 (1982)
6. Antonucci, R.R.J., Miller, J.S.: Spectropolarimetry and the nature of NGC 1068. *Astrophys. J.* **297**, 621–632 (1985)
7. Antonucci, R.R.J., Miller, J.S.: Spectropolarimetry and the nature of NGC 1068. *Astrophys. J.* **297**, 621 (1985)
8. Arav, N., Barlow, T.A., Laor, A., Blandford, R.D.: Keck high-resolution spectroscopy of MRK 335: constraints on the number of emitting clouds in the broad-line region. *Mon. Not. R. Astron. Soc.* **288**, 1015–1021 (1997)
9. Arav, N., Barlow, T.A., Laor, A., Sargent, W.L.W., Blandford, R.D.: Are AGN broad emission lines formed by discrete clouds? Analysis of keck high-resolution spectroscopy of NGC 4151. *Mon. Not. R. Astron. Soc.* **297**, 990–998 (1998)
10. Arav, N., Begelman, M.C.: Modeling the double-trough structure observed in broad absorption line QSOs using radiative acceleration. *Astrophys. J.* **434**, 479–483 (1994)
11. Arav, N., Korista, K.T., de Kool, M., Junkkarinen, V.T., Begelman, M.C.: Hubble space telescope observations of the broad absorption line quasar PG 0946+301. *Astrophys. J.* **516**, 27–46 (1999)
12. Arav, N., Li, Z.Y., Begelman, M.C.: Radiative acceleration in outflows from broad absorption line quasi-stellar objects. 2: Wind Models”, *Astrophys. J.* **432**, 62–74 (1994)
13. Athanassoula, E., Misiriotis, A.: Three models with different halo central concentrations. *Mon. Not. R. Astron. Soc.* **330**, 35 (2002)
14. Bahcall, J.N., Kozlovsky, B.: Some models of the emission-line region of 3c 273. *Astrophys. J.* **155**, 1077 (1969)
15. Balbus, S.A., Hawley, J.F.: A powerful local shear instability in weakly magnetized disks. I - Linear analysis. II - Nonlinear evolution. *Astrophys. J.* **376**, 214–233 (1991)
16. Balbus, S.A., Hawley, J.F.: Instability, turbulence, and enhanced transport in accretion disks. *Rev. Modern Phys.* **70**, 1–53 (1998)
17. Baldwin, J.A.: The Ly-alpha/H-beta intensity ratio in the spectra of QSOs. *Mon. Not. R. Astron. Soc.* **178**, 67P–74P (1977)
18. Baldwin, J.A., Ferland, G.J., Korista, K.T., Hamann, F., LaCluyzé, A.: The origin of Fe II emission in active galactic nuclei. *Astrophys. J.* **615**, 610–624 (2004)
19. Baldwin, J., Ferland, G., Korista, K., Verner, D.: Locally optimally emitting clouds and the origin of quasar emission lines. *Astrophys. J.* **455**, L119 (1995)
20. Ball, R., Sargent, A.I., Scoville, N.Z., Lo, K.Y., Scott, S.L.: The molecular bar and star formation in the nucleus of NGC 6946. *Astrophys. J.* **298**, L21–L25 (1985)
21. Bardeen, J.M., Petterson, J.A.: The lense-thirring effect and accretion disks around kerr black holes. *Astrophys. J.* **195**, L65 (1975)
22. Barger, A.J., Cowie, L.L., Mushotzky, R.F., Yang, Y., Wang, W., Steffen, A.T., Capak, P.: The cosmic evolution of hard x-ray-selected active galactic nuclei. *Astron. J.* **129**, 578–609 (2005)
23. Barkov, M.V., Komissarov, S.S.: Stellar explosions powered by the blandford–znajek mechanism. *Mon. Not. R. Astron. Soc.* **385**, L28–L32 (2008)

24. Barranco, J.A., Marcus, P.S.: Three-dimensional vortices in stratified protoplanetary disks. *Astrophys. J.* **623**, 1157 (2005)
25. Barthel, P.D.: Is every quasar beamed? *Astrophys. J.* **336**, 606–611 (1989)
26. Baum, S.A., Baum, S.A., Gallimore, J.F., O’Dea, C.P., Buchanan, C.L., Noel-Storr, J., Axon, D.J., Robinson, A., Elitzur, M., Dorn, M., Staudaher, S., Elvis, M.: Infrared diagnostics for the extended 12 μm sample of seyferts. *Astrophys. J.* **710**, 289–308 [arXiv: 0912.3545] (2010)
27. Bautista, M.A., Kallman, T.R.: The XSTAR atomic database. *Astrophys. J. Suppl.* **134**, 139 (2001)
28. Barvainis, X.: Hot dust and the near-infrared bump in the continuum spectra of quasars and active galactic nuclei. *Astrophys. J.* **320**, 537 (1987)
29. Beckwith, K., Hawley, J.F., Krolik, J.H.: Transport of large-scale poloidal flux in black hole accretion. *Astrophys. J.* **707**, 428–445 (2009)
30. Begelman, M.C.: Can a spherically accreting black hole radiate very near the eddington limit. *Mon. Not. R. Astron. Soc.* **187**, 237 (1979)
31. Begelman, M.C.: Super-eddington fluxes from thin accretion disks? *Astrophys. J.* **568**, L97 (2002)
32. Begelman, M.C., Blandford, R.D., Rees, M.J.: Massive black hole binaries in active galactic nuclei. *Nature* **287**, 307 (1980)
33. Bentz, M.C., Peterson, B.M., Netzer, H., Pogge, R.W., Vestergaard, M.: The radius-luminosity relationship for active galactic nuclei: the effect of host-galaxy starlight on luminosity measurements. II. The full sample of reverberation-mapped AGNs. *Astrophys. J.* **697**, 160–181 (2009)
34. Bergeron, J., Kunth, D.: An extreme Fe II emitter – the narrow quasar PHL 1092. *Astron. Astrophys.* **85**, L11 (1980)
35. Berentzen, I., Athanassoula, E., Heller, C., Fricke, K.J.: *Mon. Not. R. Astron. Soc.* **347**, 220 (2004)
36. Berentzen, I., Shlosman, I.: Growing live disks within cosmologically assembling asymmetric halos: washing out the halo. *Astrophys. J.* **648**, 807 (2006)
37. Beskin, V.S., Kuznetsova, I.V., Rafikov, R.R.: On the MHD effects on the force-free monopole outflow. *Mon. Not. R. Astron. Soc.* **299**, 341–348 (1998)
38. Biretta, J.A., Junor, W., Livio, M.: Evidence for initial jet formation by an accretion disk in the radio galaxy M87. *New Astron. Rev.* **46**, 239–245 (2002)
39. Bogovalov, S.V., Kel’Ner, S.R.: Dissipationless disk accretion. *Astron. Rep.* **49**, 57–70 (2005)
40. Blaes, O.: Accretion disks in AGNs. In: Ho, L.C., Wang, J.-M. (eds.) *The Central Engine of AGN*. ASP Conf. Ser. vol. 373, p. 75. ASP, San Francisco (2007)
41. Blaes, O., Hirose, S., Krolik, J.H.: Surface structure in an accretion disk annulus with comparable radiation and gas pressure. *Astrophys. J.* **664**, 1057–1071 (2007)
42. Blandford, R.D., Begelman, M.C.: On the fate of gas accreting at a low rate on to a black hole. *Mon. Not. R. Astron. Soc.* **303**, L1–L5 (1999)
43. Blandford, R.D., Emmering, R.T., Shlosman, L.: A non-starburst model for AGN broad emission lines. In: Filippenko, A.V. (ed.) *Relationships between active galactic nuclei and starburst galaxies*. ASP Conf. Ser. vol. 31, p. 443, 1992
44. Blandford, R.D., Netzer, H., Woltjer, L.: *Active Galactic Nuclei*. Berlin, Springer (1990)
45. Blandford, R.D., Payne, D.G.: Hydromagnetic flows from accretion discs and the production of radio jets. *Mon. Not. R. Astron. Soc.* **199**, 883–903 (1982)
46. Blandford, R.D., Rees, M.J.: Some comments on radiation mechanisms in Lacertids. In: *Proceedings of the Pittsburgh conference on BL lac objects*, Pittsburgh, PA, pp. 328–341. University of Pittsburgh, Pittsburgh, PA. 24–26 April 1978
47. Blandford, R.D., Znajek, R.L.: Electromagnetic extraction of energy from kerr black holes. *Mon. Not. R. Astron. Soc.* **179**, 433–456 (1977)
48. Blumenthal, G.R., Mathews, W.G.: Theoretical emission line profiles in QSOs and seyfert galaxies. *Astrophys. J.* **198**, 517 (1975)
49. Bogovalov, S., Tsinganos, K.: On the magnetic acceleration and collimation of astrophysical outflows. *Mon. Not. R. Astron. Soc.* **305**, 211–224 (1999)

50. Boroson, T.A., Green, R.F.: The emission-line properties of low-redshift quasi-stellar objects. *Astrophys. J. Suppl.* **80**, 109–135 (1992)
51. Bottorff, M., Korista, K.T., Shlosman, I., Blandford, D.R.: Dynamics of broad emission-line region in NGC 5548: hydromagnetic wind model versus observations. *Astrophys. J.* **479**, 200–221 (1997)
52. Brandt, W.N., Laor, A., Wills, B.J.: On the nature of soft x-ray weak quasi-stellar objects. *Astrophys. J.* **528**, 637–649 (2000)
53. Bruhweiler, F., Verner, E.: Modeling Fe II emission and revised Fe II (UV) empirical templates for the seyfert-1 galaxy I Zw 1. *Astrophys. J.* **675**, 83 (2008)
54. Cao, X.: On the disappearance of broad-line region in low-luminosity active galactic nuclei: the role of the outflows from advection dominated accretion flows. arXiv 1009.5043 (2010)
55. Castor, J.I., Abbott, D.C., Klein, R.I.: Radiation driven stellar winds in of stars. *Astrophys. J.* **195**, 157–174 (1975)
56. Chandrasekhar, S.: *Hydrodynamic Hydromagnetic Stability*. Clarendon Press, Oxford (1981)
57. Chartas, G., Brandt, W.N., Gallagher, S.C.: XMM-newton reveals the quasar outflow in PG1115+080. *Astrophys. J.* **595**, 85–93 (2003)
58. Chartas, G., Brandt, W.N., Gallagher, S.C., Garmire, G.P.: CHANDRA detects relativistic broad absorption lines from APM 08279+5255. *Astrophys. J.* **579**, 169 (2002)
59. Chen, K., Halpern, J.P.: Structure of line-emitting accretion disks in active galactic nuclei – ARP 102B. *Astrophys. J.* **344**, 115 (1989)
60. Chen, K., Halpern, J.P., Filippenko, A.V.: Kinematic evidence for a relativistic keplerian disk – ARP 102B. *Astrophys. J.* **339**, 742 (1989)
61. Chiang, J., Murray, N.: Reverberation Mapping and the Disk-Wind Model of the Broad-Line Region. *Astrophys. J.* **466**, 704 (1996)
62. Clavel, J., Boksenberg, A., Bromage, G.E., Elvius, A., Penston, M.V., Perola, G.C., Santos-Lleo, M., Snijders, M.A.J., Ulrich, M.H.: The ultra-compact broad emission line region in NGC4151. *Mon. Not. R. Astron. Soc.* **246**, 668 (1990)
63. Clavel, J., Reichert, G.A., Alloin, D., Crenshaw, D.M., Kriss, G., Krolik, J.H., Malkan, M.A., Netzer, H., Peterson, B.M., Wamsteker, W., Altamore, A., Baribaud, T., et al.: Steps toward determination of the size and structure of the broad-line region in active galactic nuclei. I – an 8 month campaign of monitoring NGC 5548 with IUE. *Astrophys. J.* **366**, 64–81 (1991)
64. Collin-Souffrin, S.: The energy puzzle of the broad line region in quasars. *Astron. Astrophys.* **166**, 115 (1986)
65. Collin-Souffrin, S.: Line and continuum radiation from the outer region of accretion discs in active galactic nuclei. I – Preliminary considerations. *Astron. Astrophys.* **179**, 60 (1987)
66. Collin-Souffrin, S.: On the origin of the optical and UV continuum in active galactic nuclei. *Astron. Astrophys.* **249**, 344 (1991)
67. Collin-Souffrin, S., Czerny, B., Dumont, A.-M., Zycski, P.T.: Quasi-spherical accretion of optically thin clouds as a model for the optical/UV/soft x-ray emission of AGN. *Astron. Astrophys.* **314**, 393 (1996)
68. Collin-Souffrin, S., Delache, P., Frisch, H., Dumont, S.: Hydrogen line spectrum in quasars. I – Approximation procedures for line transfer versus an exact treatment. *Astron. Astrophys.* **104**, 264 (1981)
69. Collin-Souffrin, S., Dumont, S.: The emission spectrum of active galactic nuclei. I – Computational methods. *Astron. Astrophys.* **166**, 13 (1986)
70. Collin-Souffrin, S., Dumont, A.M.: Emission spectra of weakly photoionized media in active nuclei of galaxies. *Astron. Astrophys.* **213**, 29 (1989)
71. Collin-Souffrin, S., Dumont, A.M.: Line and continuum emission from the outer regions of accretion discs in active galactic nuclei. II – Radial structure of the disc. *Astron. Astrophys.* **229**, 292 (1990)
72. Collin-Souffrin, S., Dyson, J.E., McDowell, J.C., Perry, J.J.: The environment of active galactic nuclei. I – A two-component broad emission line model. *Mon. Not. R. Astron. Soc.* **232**, 539–550 (1988)
73. Collin-Souffrin, S., Hameury, J.-M., Joly, M.: Thick Compton-heated media - A solution for the Fe II problem in active galactic nuclei? *Astron. Astrophys.* **205**, 19 (1988)

74. Collin, S., Joly, M.: The Fe II problem in NLS1s. *New Ast. Revs.* **44**, 531–537 (2000)
75. Collin-Souffrin, S., Joly, M., Heidmann, N., Dumont, S.: Formation of permitted lines in the spectrum of type-1 seyfert galaxies and quasars – Fe II lines, preliminary discussion. *Astron. Astrophys.* **72**, 293 (1979)
76. Collin-Souffrin, S., Joly, M., Pequignot, D., Dumont, S.: The emission spectrum of active galactic nuclei. II – High column density photoionization models and low ionization lines. *Astron. Astrophys.* **166**, 27 (1986)
77. Collin, S., Kawaguchi, T., Peterson, B.M., Vestergaard, M.: Systematic effects in measurement of black hole masses by emission-line reverberation of active galactic nuclei: Eddington ratio and inclination. *Astron. Astrophys.* **456**, 75 (2006)
78. Collin-Souffrin, S., Lasota, J.-P.: The broad-line region of active galactic nuclei revisited. *Publ. Astron. Soc. Pacific* **100**, 1041 (1988)
79. Collin, S., Zahn, J.-P.: Star formation and evolution in accretion disks around massive black holes. *Astron. Astrophys.* **344**, 433 (1999)
80. Combes, F., Debbasch, F., Friedli, D., Pfenniger, D.: Box and peanut shapes generated by stellar bars. *Astron. Astrophys.* **233**, 82 (1990)
81. Contopoulos, I., Kazanas, D.: Toward resolving the crab σ -problem: a linear accelerator? *Astrophys. J.* **566**, 336–342 (2002)
82. Contopoulos, J.: A simple type of magnetically driven jets: an astrophysical plasma gun. *Astrophys. J.* **450**, 616–627 (1995)
83. Crenshaw, D.M., Kraemer, S.B., Boggess, A., Maran, S.P., Mushotzky, R.F., Wu, C.C.: Intrinsic absorption lines in seyfert-1 galaxies. I. Ultraviolet spectra from the hubble space telescope. *Astrophys. J.* **516**, 750–768 (1999)
84. Crenshaw, D.M., Kraemer, S.B., Hutchings, J.B., Bradley, L.D., II, Gull, T.R., Kaiser, M.E., Nelson, C.H., Ruiz, J.R., Weistrop, D.: A kinematic model for the narrow-line region in NGC 4151. *Astron. J.* **120**, 1731–1738 (2000)
85. Czerny, B., Rózańska, A., Kuraszkiewicz, J.: Constraints for the accretion disk evaporation rate in AGN from the existence of the broad line region. *Astron. Astrophys.* **428**, 39 (2004)
86. Czerny, B., Hryniewicz, K.: The origin of the broad line region in active galactic nuclei. *Astron. Astrophys.* **525**, L8 (2011)
87. Czerny, B., Hryniewicz, K., Nikolajuk, M., Sadowski, A.: Constraints on the black hole spin in the quasar SDSS J094533.99+100950.1 *MNRAS* **415**, 2942 (2011)
88. Davidson, K.: Photoionization and the emission-line spectra of quasi-stellar objects. *Astrophys. J.* **171**, 213 (1972)
89. Davidson, K., Netzer, H.: The emission lines of quasars and similar objects. *Rev. Modern Phys.* **51**, 715–766 (1979)
90. Davis, S.W., Woo, J.-H., Blaes, O.M.: The UV continuum of quasars: models and SDSS spectral slopes. *Astrophys. J.* **668**, 682 (2007)
91. Daw, A., Deluca, E.E., Golub, L.: Observations and interpretation of soft x-ray limb absorption seen by the normal incidence x-ray telescope. *Astrophys. J.* **453**, 929 (1995)
92. Debattista, V.P., Sellwood, J.A.: Dynamical friction and the distribution of dark matter in barred galaxies. *Astrophys. J.* **493**, L5 (1998)
93. de Kool, M., Begelman, M.C.: Radiation pressure–driven magnetic disk winds in broad absorption line quasi-stellar objects. *Astrophys. J.* **455**, 448–455 (1995)
94. De Villiers, J., Hawley, J.F.: A numerical method for general relativistic magnetohydrodynamics. *Astrophys. J.* **589**, 458–480 (2003)
95. Dietrich, M., Peterson, B.M., Albrecht, P., Altmann, M., Barth, A.J., Bennie, P.J., Bertram, R., Bochkarev, N.G., Bock, H., Braun, J.M., Burenkov, A., et al.: Steps toward determination of the size and structure of the broad-line region in active galactic nuclei. XII. Ground-based monitoring of 3C 390.3. *Astrophys. J. Suppl.* **115**, 185 (1998)
96. Dondi, L., Ghisellini, G.: Gamma-ray-loud blazars and beaming. *Mon. Not. R. Astron. Soc.* **273**, 583–595 (1995)
97. Dopita, M.A., Groves, B.A., Sutherland, R.S., Binette, L., Cecil, G.: Are the narrow-line regions in active galaxies dusty and radiation pressure dominated? *Astrophys. J.* **572**, 753–761 (2002)

98. Dorodnitsyn, A., Kallman, T., Proga, D.: An axisymmetric, hydrodynamical model for the torus wind in active galactic nuclei. *Astrophys. J. Lett.* **675**, L5–L8 (2008)
99. Drenkhahn, G.: Acceleration of GRB outflows by poynting flux dissipation. *Astron. Astrophys.* **387**, 714–724 (2002)
100. Drew, J.E., Boksenberg, A.: Optical spectroscopy of two broad absorption line QSOs and implications for spherical-symmetric absorbing wind models. *Mon. Not. R. Astron. Soc.* **211**, 813–831 (2008)
101. Dumont, A.M., Collin-Souffrin, S.: Line and continuum emission from the outer regions of accretion discs in active galactic nuclei – part IV – line emission. *Astron. Astrophys.* **229**, 313 (1990)
102. Dumont, A.M., Collin-Souffrin, S.: Line and continuum emission from the outer regions of accretion discs in active galactic nuclei. V – detailed computational results. *A&A S.* **83**, 71 (1990)
103. Dumont, A.-M., Collin, S.: Codes for optically thick and hot photoionized media – radiative transfer and new developments. In: Gary Ferland and Daniel Wolf Savin (eds.) *Spectroscopic Challenges of Photoionized Plasmas*, San Francisco, Astronomical Society of the Pacific, ASP Conf. Ser. vol. 247, p. 231, 2001
104. Dumont, A.-M., Collin-Souffrin, S., Nazarova, L.: NGC 5548, a case study for active galactic nuclei. Inconsistencies of photoionized models for the BLR. *Astron. Astrophys.* **331**, 11 (1998)
105. Elitzur, M., Ivezić, Z.: Dusty winds- I. Self-similar solutions. *Mon. Not. R. Astron. Soc.* **327**, 403 (2001)
106. Elmegreen, B.G.: Starbursts by gravitational collapse in the inner lindblad resonance rings of galaxies. *Astrophys. J.* **425**, L73 (1994)
107. Elvis, M.: A structure for quasars. *Astrophys. J.* **545**, 63–76 (2000)
108. Elvis, M., Maccacaro, T., Wilson, A.S., Ward, M.J., Penston, M.V., Fosbury, R.A.E., Perola, G.C.: Seyfert galaxies as x-ray sources. *Mon. Not. R. Astron. Soc.* **183**, 129 (1978)
109. El-Zant, A., Shlosman, I., Begelman, M.C., Frank, J.: Galaxy formation in triaxial halos: black hole-bulge-dark halo correlation. *Astrophys. J.* **590**, 641 (2003)
110. Emmering, R.T., Blandford, R.D., Shlosman, I.: Magnetic acceleration of broad emission-line clouds in active galactic nuclei. *Astrophys. J.* **385**, 460–477 (1992)
111. Englmaier, P., Shlosman, I.: Dynamical decoupling of nested bars: self-gravitating gaseous nuclear bars. *Astrophys. J.* **617**, L115 (2004)
112. Eracleous, M., Halpern, J.P.: Completion of a survey and detailed study of double-peaked emission lines in radio-loud active galactic nuclei. *Astrophys. J.* **599**, 886 (2003)
113. Eracleous, M., Halpern, J.P.: Doubled-peaked emission lines in active galactic nuclei. *Astrophys. J. Suppl.* **90**, 1 (1994)
114. Eracleous, M., Halpern, J.P., Gilbert, A.M., Newman, J.A., Filippenko, A.V.: Rejection of the binary broad-line region interpretation of double-peaked emission lines in three active galactic nuclei. *Astrophys. J.* **490**, 216 (1997)
115. Eracleous, M., Lewis, K.T., Flohic, H.M.L.G.: Double-peaked emission lines as a probe of the broad-line regions of active galactic nuclei. *New Ast. Rev.* **53**, 133 (2009)
116. Eracleous, M., Livio, M., Halpern, J.P., Storchi-Bergmann, T.: Elliptical accretion disks in active galactic nuclei. *Astrophys. J.* **438**, 610 (1995)
117. Erwin, P., Sparke, L.S.: Double bars, inner disks, and nuclear rings in early-type disk galaxies. *Astron. J.* **124**, 65 (2002)
118. Everett, J.E.: Radiative transfer and acceleration in magnetocentrifugal winds. *Astrophys. J.* **631**, 689–706 (2005)
119. Everett, J.E., Königl, A., Arav, N.: Observational evidence for a multiphase outflow in quasar FIRST J1044+3656. *Astrophys. J.* **569**, 671 (2002)
120. Falcke, H., Sherwood, W., Patnaik, A.R.: The nature of radio-intermediate quasars: what is radio-loud and what is radio-quiet? *Astrophys. J.* **471**, 106 (1996)
121. Ferguson, J.W., Korista, K.T., Baldwin, J.A., Ferland, G.J.: Locally optimally emitting clouds and the narrow emission lines in seyfert galaxies. *Astrophys. J.* **487**, 122 (1997)

122. Ferland, G.J.: Hazy, A Brief Introduction to Cloudy 06.02. University of Kentucky Internal Report (2006)
123. Ferland, G.J.: Numerical simulations of photoionized plasmas: applications to astrophysical and laboratory environments. *Astrophys. J.* **331** (2010)
124. Ferland, G.J., Hu, Chen, Wang, J.-M., Baldwin, J.A., Porter, R.L., van Hoof, P.A.M., Williams, R.J.R.: Implications of infalling Fe II-emitting clouds in active galactic nuclei: anisotropic properties. *Astrophys. J.* **707**, L82 (2009)
125. Ferland, G., Netzer, H.: Application of line transfer calculations to active nuclei and novae. *Astrophys. J.* **229**, 274–290 (1979)
126. Ferland, G.J., Shields, G.A., Netzer, H.: Asymmetries of the emission lines of QSOs, Seyfert galaxies, and novae. *Astrophys. J.* **232**, 382–388 (1979)
127. Ferrarese, L.: Beyond the bulge: a fundamental relation between supermassive black holes and dark matter halos. *Astrophys. J.* **578**, 90 (2002)
128. Ferrarese, L., Merritt, D.: A fundamental relation between supermassive black holes and their host galaxies. *Astrophys. J.* **539**, L9–12 (2000)
129. Finke, J.D., Dermer, C.D.: On the break in the *Fermi* large area telescope spectrum of 3C454.3. *Astrophys. J.* **714**, L303–L307 (2010)
130. Flohic, H.M.L.G., Eracleous, M.: Interpreting the variability of double-peaked emission lines in active galactic nuclei with stochastically perturbed accretion disk models. *Astrophys. J.* **686**, 138 (2008)
131. Foltz, C.B., Weymann, R.J., Morris, S.L., Turnshek, D.A.: The complex absorption spectrum of the broad absorption line QSO1303+308. *Astrophys. J.* **317**, 450–459 (1987)
132. Francis, P.J., Hewett, P.C., Foltz, C.B., Chaffee, F.H., Weymann, R.J., Morris, S.L.: A high signal-to-noise ratio composite quasar spectrum. *Astrophys. J.* **373**, 465–470 (1991)
133. Friedli, D.: Secondary bars and triaxial bulges within primary bars. In: Buta, R., Crocker, D.A., Elmegreen, B.G. (eds.). *Barred Galaxies*. ASP Conf. Ser. vol. 91, p. 378. Astronomical Society of the Pacific, San Francisco (1996)
134. Fromang, S., Papaloizou, J., Lesur, G., Heinemann, T.: MHD simulations of the magnetorotational instability in a shearing box with zero net flux. II. The effect of transport coefficients. *AAp* **476**, 1123–1132 (2007)
135. Fukumura, K., Kazanas, D., Contopoulos, I., Behar, E.: Magnetohydrodynamic accretion disk winds as x-ray absorbers in active galactic nuclei. *Astrophys. J.* **715**, 636–650 (2010)
136. Gallagher, S.: Stratified quasar winds: integrating x-ray and infrared views of broad absorption-line quasars. In: 37th COSPAR Scientific Assembly, **37**, 963 (2008)
137. Gammie, C.F.: Efficiency of magnetized thin accretion disks in the Kerr metric. *Astrophys. J. Lett.* **522**, L57–L60 (1999)
138. Gammie, C.F., McKinney, J.C., Tóth, G.: HARM: a numerical scheme for general relativistic magnetohydrodynamics. *Astrophys. J.* **589**, 444–457 (2003)
139. Garofalo, D.: The spin dependence of the Blandford–Znajek effect. *Astrophys. J.* **699**, 400–408 (2009)
140. Garofalo, D., Evans, D.A., Sambruna, R.M.: The evolution of radio-loud active galactic nuclei as a function of black hole spin. *Mon. Not. R. Astron. Soc.* **406**, 975–986 (2010)
141. Gaskell, C.M.: Quasars as supermassive binaries. In: Proc. 24th Liège Int. Astrophys. Colloq., Quasars and Gravitational Lenses Cointe-Ougree: Univ. Liège, p. 473 (1983)
142. Gaskell, C.M.: Accretion disks and the nature and origin of AGN continuum variability. *Rev. Mex. Astron. Astrofis. Conf. Ser.* **32**, 1 (2008)
143. Gaskell, C.M.: What broad emission lines tell us about how active galactic nuclei work. *New Astron. Rev.* **53**, 140 (2009)
144. Gaskell, C.M.: Off-axis energy generation in active galactic nuclei: explaining broad-line profiles, spectropolarimetric observations, and velocity-resolved reverberation mapping. arXiv:1008.1057 (2010)
145. Gaskell, C.M., Klimek, E.S., Nazarova, L.S.: NGC 5548: the AGN energy budget problem and the geometry of the broad-line region and torus. arXiv:0711.1025 (2007)

146. Gaskell, C.M., Snedden, S.A.: The optical case for a disk component of BLR emission. In: Gaskell, C.M., Brandt, W.N., Dietrich, M., Dultzin-Hacyan, D., Eracleous, M., (eds.) *Structure and Kinematics of Quasar Broad Line Regions*. ASP Conf. Ser. vol. 175, p. 157. Astronomical Society of the Pacific, San Francisco (1999)
147. Gebhardt, K., Bender, R., Bower, G., Dressler, A., Faber, S.M., Filippenko, A.V., Green, R., Grillmair, C., Ho, L.C., Kormendy, J., Lauer, T.R., Magorrian, J., Pinkney, J., Richstone, D., Tremaine, S.: A Relationship between nuclear black hole mass and galaxy velocity dispersion. *Astrophys. J. Lett.* **539**, L13–L16 (2000)
148. Georganopoulos, M., Kazanas, D.: Decelerating flows in TeV blazars: a resolution to the BL lacertae–FR I unification problem. *Astrophys. J.* **594**, L27–L30 (2003)
149. Georganopoulos, M., Perlman, E.S., Kazanas, D.: Is the core of M87 the source of its TeV emission? implications for unified schemes. *Astrophys. J.* **643**, L33–L36 (2005)
150. Gerin, M., Combes, F., Athanassoula, E.: The influence of galaxy interactions on stellar bars. *Astron. Astrophys.* **230**, 37 (1990)
151. Gezari, S., Halpern, J.P., Eracleous, M.: Long-term profile variability of double-peaked emission lines in active galactic nuclei. *Astrophys. J. Suppl.* **169**, 167 (2007)
152. Ghisellini, G., Celotti, A., Fossati, G., Maraschi, L., Comastri, A.: A theoretical unifying scheme for gamma-ray bright blazars. *Mon. Not. R. Astron. Soc.* **301**, 451–468 (1998)
153. Ghisellini, G., Padovani, P., Celotti, A., Maraschi, L.: Relativistic bulk motion in active galactic nuclei. *Astrophys. J.* **407**, 65–82 (1993)
154. Ghisellini, G., Tavecchio, F.: Rapid variability in TeV blazars: the case of PKS 2155–304. *Mon. Not. R. Astron. Soc.* **386**, L28–L32 (2008)
155. Ghisellini, G., Tavecchio, F.: Canonical high-power blazars. *Mon. Not. R. Astron. Soc.* **397**, 985–1002 (2009)
156. Ghisellini, G., Tavecchio, F., Chiaberge, M.: Structured jets in TeV BL lac objects and radiogalaxies. Implications for the observed properties. *Astron. Astrophys.* **432**, 401–410 (2005)
157. Ghisellini, G., Tavecchio, F., Chiaberge, M.: Structured jets in TeV BL lac objects and radiogalaxies – implications for the observed properties. *Astron. Astrophys.* **432**, 401–410 (2005)
158. Ghisellini, G., Tavecchio, F., Foschini, L., Ghirlanda, G., Maraschi, L., Celotti, A.: General physical properties of bright Fermi blazars. *Mon. Not. R. Astron. Soc.* **402**, 497–518 (2010)
159. Gilbert, A.M., Eracleous, M., Filippenko, A.V., Halpern, J.P.: Accretion disk models and long-term variability of double-peaked balmer line profiles in AGNs. In: Gaskell, C.M., Brandt, W.N., Dietrich, M., Dultzin-Hacyan, D., Eracleous, M. (eds.) “Structure and Kinematics of Quasar Broad Line Regions”, ASP Conf. Ser. vol. 175, p. 189. ASP, San Francisco
160. Gilli, R., Comastri, A., Hasinger, G.: The synthesis of the cosmic x-ray background in the chandra and XMM-newton era. *AAp* **463**, 79–96 (2007)
161. Giroletti, M., Giovannini, G., Feretti, L., Cotton, W.D., Edwards, P.G., Lara, L., Marscher, A.P., Mattox, J.R., Piner, B.G., Venturi, T.: Parsec-scale properties of markarian 501. *Astrophys. J.* **600**, 127–140 (2004)
162. Giustini, M., Cappi, M., Vignali, C.: On the absorption of x-ray bright broad absorption line quasars. *Astron. Astrophys.* **491**, 425–434 (2008)
163. Goad, M., Wanders, I.: The effect of a variable anisotropic continuum source upon the broad emission line profiles and responses. *Astrophys. J.* **469**, 113 (1996)
164. Goodman, J., Tan, J.C.: Supermassive stars in quasar disks. *Astrophys. J.* **608**, 108 (2004)
165. Grandi, S.A.: Fe II emission in quasars. *Astrophys. J.* **251**, 451–464 (1981)
166. Groves, B.A., Dopita, M.A., Sutherland, R.S.: Dusty, radiation pressure-dominated photoionization. I. model description, structure, and grids. *Astrophys. J. Suppl. Ser.* **153**, 9–73 (2004)
167. Halpern, J.P., Eracleous, M., Filippenko, A.V., Chen, K.: Hubble space telescope ultraviolet spectrum of ARP 102B, the prototypical double-peaked emission-line AGN. *Astrophys. J.* **464**, 704 (1996)
168. Hamann, F.: Metal abundances and ionization in quasar intrinsic absorbers. *Astrophys. J. Suppl. Ser.* **109**, 279 (1997)

169. Hamann, F., Barlow, T.A., Cohen, R.D., Junkkarinen, V., Burbidge, E.M.: Ionization and abundances in intrinsic QSO absorption-line systems. In: Arav, N., Shlosman, I., Weymann, R. (eds.) *Mass Ejection from Active Galactic Nuclei*. ASP Conf. Ser. vol. 128, p. 187. ASP, San Francisco (1997)
170. Hamann, F., Ferland, G.: Elemental abundances in quasi-stellar objects: star formation and galactic nuclear evolution at high redshifts. *Ann. Rev. Astron. Astrophys.* **37**, 487–531 (1991)
171. Hao, L., Strauss, M.A., Fan, X., Tremonti, C.A., Schlegel, D.J., Heckman, T.M., Kauffmann, G., Blanton, M.R., Gunn, J.E., Hall, P.B., Ivezić, Ž., Knapp, G.R., Krolik, J.H., et al.: Active galactic nuclei in the sloan digital sky survey. II. Emission-line luminosity function. *Astron. J.* **129**, 1795–1808 (2005)
172. Hao, L., Weedman, D.W., Spoon, H.W.W., Marshall, J.A., Levenson, N.A., Elitzur, M., Houck, J.R.: The distribution of silicate strength in spitzer spectra of AGNs and ULIRGs. *Astrophys. J. Lett.* **655**, L77–L80 (2007)
173. Heller, C., Shlosman, I.: Fueling nuclear activity in disk galaxies: starbursts and monsters. *Astrophys. J.* **424**, 84 (1994)
174. Heller, C., Shlosman, I.: Dynamical effects of nuclear rings in disk galaxies. *Astrophys. J.* **471**, 143 (1996)
175. Heller, C., Shlosman, I., Athanassoula, E.: Structure formation inside triaxial dark matter halos: galactic disks, bulges, and bars. *Astrophys. J.* **671**, 226 (2007)
176. Hirose, S., Krolik, J.H., Stone, J.M.: Vertical structure of gas pressure-dominated accretion disks with local dissipation of turbulence and radiative transport. *Astrophys. J.* **640**, 901–917 (2006)
177. Hohl, F.: Numerical experiments with a disk of stars. *Astrophys. J.* **168**, 343 (1971)
178. Homan, D.C., Kadler, M., Kellermann, K.I., Kovalev, Y.Y., Lister, M.L., Ros, E., Savolainen, T., Zensus, J.A.: MOJAVE: Monitoring of jets in active galactic nuclei with VLBA experiments. VII. Blazar jet acceleration. *Astrophys. J.* **706**, 1253–1268 (2009)
179. Hönig, S.F., Kishimoto, M.: The dusty heart of nearby active galaxies. II. From clumpy torus models to physical properties of dust around AGN. *AAp* **523** A27 (2010)
180. Hönig, S.F., Kishimoto, M., Gandhi, P., Smette, A., Asmus, D., Duschl, W., Polletta, M., Weigelt, G.: The dusty heart of nearby active galaxies. I. High-spatial resolution mid-IR spectro-photometry of seyfert galaxies. *AAp* **515**, A23 (2010)
181. Hopkins, P.F., Quataert, E.: How do massive black holes get their gas? *Mon. Not. R. Astron. Soc.* **407**, 1529–1564 (2010)
182. Hure, J.-M., Collin-Souffrin, S., Le Bourlot, J., Pineau des Forets, G.: Structure of the outer regions of accretion discs in active galactic nuclei. *Astron. Astrophys.* **290**, 19 (1994)
183. Ishibashi, W., Courvoisier, T.J.-L.: X-ray power law spectra in active galactic nuclei. *Astron. Astrophys.* **512**, 58 (2010)
184. Jogee, S., Kenney, J.D.P., Smith, B.J.: A gas-rich nuclear bar fueling a powerful central starburst in NGC 2782. *Astrophys. J.* **526**, 665 (1999)
185. Jogee, S., Shlosman, I., Laine, S., Englmaier, P., Knapen, J.H., Scoville, N., Wilson, C.D.: Gasdynamics in NGC 5248: Fueling a circumnuclear starburst ring of super-star clusters. *Astrophys. J.* **575**, 156–177 (2002)
186. Johnson, B.M., Gammie, C.F.: Vortices in thin, compressible, unmagnetized disks. *Astrophys. J.* **635**, 149 (2005)
187. Joly, M.: The Fe II spectrum of seyfert-1 galaxies and quasars. *Astron. Astrophys.* **102**, 321 (1981)
188. Joly, M.: Formation of low ionization lines in active galactic nuclei. *Astron. Astrophys.* **184**, 33 (1987)
189. Joly, M., Véron-Cetty, M., Véron, P.: BLR: non-radiative heating in strong Fe II emitters. 2007. In: Ho, L.C., Wang, J.-M. (eds.) *The Central Engine of Active Galactic Nuclei*. Proceedings of the conference held 16–21 October, 2006 at Xi'an Jiaotong University, Xi'an, China. ASP Conference Series vol. 373, p. 376, 2007

190. Jovanović, P., Popović, L.Č., Stalevski, M., Shapovalova, A.I.: Variability of the $H\beta$ line profiles as an indicator of orbiting bright spots in accretion disks of quasars: a case study of 3C 390.3. *Astrophys. J.* **718**, 168 (2010)
191. Kaastra, J.S., Mewe, R., Liedahl, D.A., Komossa, S., Brinkman, A.C.: X-ray absorption lines in the seyfert-1 galaxy NGC5548 discovered with chandra-LETGS. *Astron. Astrophys.* **354**, L83–L86 (2000)
192. Kallman, T., Bautista, M.: Photoionization and high-density gas. *Astrophys. J. Suppl.* **133**, 221–253 (2001)
193. Kallman, T.R., McCray, R.: X-ray nebular models. *Astrophys. J. Suppl.* **50**, 263 (1982)
194. Kaspi, S., Brandt, W.N., Maoz, D., Netzer, H., Schneider, D.P., Shemmer, O.: Reverberation mapping of high-luminosity quasars: first results. *Astrophys. J.* **659**, 997–1007 (2007)
195. Kaspi, S., Netzer, H.: Modeling variable emission lines in active galactic nuclei: method and application to NGC 5548. *Astrophys. J.* **524**, 71–81 (1999)
196. Kaspi, S., Smith, P.S., Netzer, H., Maoz, D., Jannuzi, B.T., Giveon, U.: Reverberation measurements for 17 quasars and the size-mass-luminosity relations in active galactic nuclei. *Astroph. J.* **533**, 631–649 (2000)
197. Kato, S.X., Kudoh, T., Shibata, K.: 2.5-dimensional nonsteady magnetohydrodynamic simulations of magnetically driven jets from geometrically thin disks. *Astrophys. J.* **565**, 1035 (2002)
198. Kazanas, D.: On the nature of emission-line clouds of quasars and active galactic nuclei. *Astrophys. J.* **347**, 74–86 (1989)
199. Kellermann, K.I., Sramek, R., Schmidt, M., Shaffer, D.B., Green, R.: VLA observations of objects in the palomar bright quasar survey. *Astron. J.* **98**, 1195–1207 (1989)
200. Kennel, C.F., Coroniti, F.V.: Confinement of the crab pulsar's wind by its supernova remnant. *Astrophys. J.* **283**, 694–709 (1984)
201. Khachikian, E.Y., Weedman, D.W.: An atlas of seyfert galaxies. *Astrophys. J.* **192**, 581 (1974)
202. King, A.R., Lubow, S.H., Ogilvie, G.I., Pringle, J.E.: Aligning spinning black holes and accretion discs. *Mon. Not. R. Astron. Soc.* **363**, 49–56 (2005)
203. Kishimoto, M., Antonucci, R., Blaes, O., Lawrence, A., Boisson, C., Albrecht, M., Leipski, C.: The characteristic blue spectra of accretion disks in quasars as uncovered in the infrared. *Nature* **454**, 492 (2008)
204. Kishimoto, M., Antonucci, R., Boisson, C., Blaes, O.: The buried balmer-edge signatures from quasars. *Mon. Not. R. Astron. Soc.* **354**, 1065 (2004)
205. Kinney, A.L., Schmitt, H.R., Clarke, C.J., Pringle, J.E., Ulvestad, J.S., Antonucci, R.R.J.: Jet directions in seyfert galaxies. *Astrophys. J.* **537**, 152 (2000)
206. Knapen, J.: Rings and bars: unmasking secular evolution of galaxies. In: Block, D.L., Freeman, K.C., Puerari, I. (eds.) *Galaxies and Their Maskst*. Springer, New York. arXiv:1005.0506 (2010)
207. Knapen, J.H., Beckman, J.E., Shlosman, I., Mahoney, T.J. (eds.): The central kpc of starbursts and AGN: the la palma connection. *ASP Conf. Ser.* vol. 249 (2001)
208. Komissarov, S.S.: Electrodynamics of black hole magnetospheres. *Mon. Not. R. Astron. Soc.* **350**, 427–448 (2004)
209. Komissarov, S.S.: Blandford–znajek mechanism versus penrose process. *J. Korean Phys. Soc.* **54**, 2503 (2009)
210. Komissarov, S.S.: Magnetic acceleration of relativistic jets. ArXiv e-prints, 1006.2242 (2010)
211. Komissarov, S.S., Barkov, M.V., Vlahakis, N., Königl, A.: Magnetic acceleration of relativistic active galactic nucleus jets. *Mon. Not. R. Astron. Soc.* **380**, 51–70 (2007)
212. Komissarov, S.S., Vlahakis, N., Königl, A., Barkov, M.V.: Magnetic acceleration of ultrarelativistic jets in gamma-ray burst sources. *Mon. Not. R. Astron. Soc.* **394**, 1182–1212 (2009)
213. Kondratko, P.T., Greenhill, L.J., Moran, J.M.: Discovery of water maser emission in five AGNs and a possible correlation between water maser and nuclear 2–10 keV luminosities. *Astrophys. J.* **652**, 136–145 (2006)

214. Königl, A., Kartje, J.F.: Disk-driven hydromagnetic winds as a key ingredient of active galactic nuclei unification schemes. *Astrophys. J.* **434**, 446–467 (1994)
215. Koratkar, A., Blaes, O.: The ultraviolet and optical continuum emission in active galactic nuclei: the status of accretion disks. *Publ. Astron. Soc. Pacific* **111**, 1–30 (1999)
216. Korista, K.T., Goad, M.R.: What the optical recombination lines can tell us about the broad-line regions of active galactic nuclei. *Astrophys. J.* **606**, 749–762 (2004)
217. Korista, K.T., Voit, G.M. Morris, S.L., Weymann R.J.: Double troughs in broad absorption line quasars and Ly α -N V line-locking. *Astrophys. J. Suppl.* **88**, 357–381 (1993)
218. Kormendy, J., Illingworth, G.: Rotation of the bulge components of disk galaxies. *Astrophys. J.* **256**, 460 (1982)
219. Kormendy, J., Kennicutt, R.C.: Secular evolution and the formation of pseudobulges in disk galaxies. *Ann. Rev. Astron. Astrophys.* **42**, 603 (2004)
220. Krasnopolsky, R., Li, Z.-Y., Blandford, R.: Magnetocentrifugal launching of jets from accretion disks. I. Cold axisymmetric flows. *Astrophys. J.* **526**, 631–642 (1999)
221. Kriss, G.A.: FUSE and the astrophysics of AGN and QSOs. In: Sonneborn, G., et al. (eds.) *Astrophysics in the Far Ultraviolet: Five Years of Discovery with FUSE*. ASP Conference Series, vol. 348, p. 499 2006
222. Krolik, J.H.: *Active Galactic Nuclei: From the Central Black Hole to the Galactic Environment*. Princeton University Press, Princeton, NJ (1999)
223. Krolik, J.H.: Magnetized accretion inside the marginally stable orbit around a black hole. *Astrophys. J. Lett.* **515**, L73–L76 (1999)
224. Krolik, J.H.: AGN obscuring tori supported by infrared radiation pressure. *Astrophys. J.* **661**, 52–59 (2007)
225. Krolik, J.H., Begelman, M.: Molecular tori in seyfert galaxies – feeding the monster and hiding it. *Astrophys. J.* **329**, 702–711 (1988)
226. Krolik, J.H., McKee, C.F., Tarter, C.B.: Two-phase models of quasar emission line regions. *Astrophys. J.* **249**, 422–442 (1981)
227. Krolik, J.H., Horne, K., Kallman, T.R., Malkan, M.A., Edelson, R.A., Kriss, G.A.: Ultraviolet variability of NGC 5548 – dynamics of the continuum production region and geometry of the broad-line region. *Astrophys. J.* **371**, 541–562 (1991)
228. Krolik, J.H., McKee, C.F.: Hydrogen emission-line spectra in quasars and active galactic nuclei. *Astrophys. J. Supp.* **37**, 459–483 (1978)
229. Kwan, J., Krolik, J.H.: The formation of emission lines in quasars and seyfert nuclei. *Astrophys. J.* **250**, 478–507 (1981)
230. Laine, S., Shlosman, I., Knapen, J.H., Peletier, R.F.: Nested and single bars in seyfert and non-seyfert galaxies. *Astrophys. J.* **567**, 97 (2002)
231. Lamers, H.J.G.L.M., Cassinelli, J.P.: *Introduction to Stellar Winds*. Cambridge University Press, Cambridge (1999)
232. Laor, A., Fiore, F., Elvis, M., Wilkes, B.J., McDowell, J.C.: The soft x-ray properties of a complete sample of optically selected quasars. II. Final results. *Astrophys. J.* **477**, 93 (1997)
233. Lawrence, A.: The relative frequency of broad-lined and narrow-lined active galactic nuclei – implications for unified schemes. *Mon. Not. R. Astron. Soc.* **252**, 586–592 (1991)
234. Lawrence, A., Elvis, M.: Obscuration and the various types of seyfert galaxy, *Astrophys. J.* **256**, 410 (1982)
235. Leighly, K.M.: Hubble space telescope STIS ultraviolet spectral evidence of outflow in extreme narrow-line seyfert-1 galaxies. II. Modeling and interpretation. *Astrophys. J.* **611**, 125–152 (2004)
236. Lewis, K., Eracleous, M., Storchi-Bergmann, T.: Long-term profile variability in active galactic nucleus with double-peaked balmer emission lines. *Astrophys. J. Suppl.* **187**, 418 (2010)
237. Lister, M.L., Cohen, M.H., Homan, D.C., Kadler, M., Kellermann, K.I., Kovalev, Y.Y., Ros, E., Savolainen, T., Zensus, J.A.: 2009 MOJAVE: Monitoring of jets in active galactic nuclei with VLBA experiments. VI. Kinematics analysis of a complete sample of blazar jets. *Astron. J.* **138**, 1874–1892 (2009)

238. Lo, K.Y., Berge, G.L., Claussen, M.J., Heiligman, G.M., Leighton, R.B., Masson, C.R., Moffet, A.T., Phillips, T.G., Sargent, A.I., Scott, S.L., Wannier, P.G., Woody, D.P.: Aperture synthesis observations of CO emission from the nucleus of IC 342. *Astrophys. J.* **282**, L59–L63 (1984)
239. Loska, Z., Czerny, B., Szczerba, R.: Irradiation of accretion discs in active galactic nuclei due to the presence of a warm absorber. *Mon. Not. R. Astron. Soc.* **355**, 1080–1090 (2004)
240. Lubow, S.: Dynamics of eccentric disks with application to superhump binaries. *Astrophys. J.* **401**, 317 (1992)
241. Lynden-Bell, D.: Galactic nuclei as collapsed old quasars. *Nature* **223**, 690 (1969)
242. Lyubarsky, Y.E.: Transformation of the poynting flux into kinetic energy in relativistic jets. *Mon. Not. R. Astron. Soc.* **402**, 353–361 (2010)
243. MacAlpine, G.M.: Photoionization models for the emission-line regions of quasi-stellar and related objects. *Astrophys. J.* **175**, 11 (1972)
244. MacAlpine, G.M.: Possible collisional enhancement of He I at 5876 Å in seyfert galaxies and QSOs. *Astrophys. J.* **204**, 694–698 (1976)
245. Maiolino, R., Alonso-Herrero, A., Anders, S., Quillen, A., Rieke, M.J., Rieke, G.H., Tacconi-Garman, L.E.: Discovery of a nuclear gas bar feeding the active nucleus in circinus. *Astrophys. J.* **531**, 219–231 (2000)
246. Maiolino, R., Risaliti, G., Salvati, M., Pietrini, P., Torricelli-Ciamponi, G., Elvis, M., Fabbiano, G., Braito, V., Reeves, J.: “Comets” orbiting a black hole. *Astron. Astrophys.* **517**, A47 (2010)
247. Maloney, P.R., Begelman, M.C., Pringle, J.E.: Radiation-driven warping: the origin of WARPS and precession in accretion disks. *Astrophys. J.* **472**, 582 (1996)
248. Maoz, D., Netzer, H., Leibowitz, E., Brosch, N., Laor, A., Mendelson, H., Beck, S., Almozino, E., Mazeh, T.: High-rate spectroscopic active galactic nucleus monitoring at the wise observatory. I. markarian 279. *Astrophys. J.* **351**, 75–82 (1990)
249. Marconi, A., Axon, D.J., Maiolino, R., Nagao, T., Pastorini, G., Pietrini, P., Robinson, A., Torricelli, G.: The effect of radiation pressure on virial black hole mass estimates and the case of narrow-line seyfert-1 galaxies. *Astrophys. J.* **678**, 693–700 (2008)
250. Marscher, A., Jorstad, S.G., D’Arcangelo, F.D., Smith, P.S., Williams, G.G., Larionov, V.M., Oh, H., Olmstead, A.R., Aller, M.F., Aller, H.D., McHardy, et al.: The inner jet of an active galactic nucleus as revealed by a radio-to- γ -ray outburst. *Nature* **452**, 966–969 (2008)
251. Martinez-Valpuesta, I., Shlosman, I., Heller, C.H.: Evolution of stellar bars in live axisymmetric halos: recurrent buckling and secular growth. *Astrophys. J.* **637**, 214 (2006)
252. Marziani, P., Sulentic, J.W., Negrete, C.A., Dultzin, D., Zamfir, S., Bachev, R.: Broad-line region physical conditions along the quasar eigenvector 1 sequence. *Mon. Not. R. Astron. Soc.* **409**, 1033–1048 (2010)
253. Mathews, W.G.: Radiative acceleration of gas clouds near quasi-stellar objects and seyfert galaxy nuclei. *Astrophys. J.* **189**, 23–32 (1974)
254. Mathews, W.G., Ferland, G.J.: What heats the hot phase in active nuclei? *Astrophys. J.* **323**, 456–467 (1987)
255. McKinney, J.C., Blandford, R.D.: Stability of relativistic jets from rotating, accreting black holes via fully three-dimensional magnetohydrodynamic simulations. *Mon. Not. R. Astron. Soc.* **394**, L126–L130 (2009)
256. McKinney, J.C., Gammie, C.F.: A measurement of the electromagnetic luminosity of a kerr black hole. *Astrophys. J.* **611**, 977–995 (2004)
257. Meier, D.S., Turner, J.L., Hurt, R.L.: Nuclear bar catalyzed star formation: ^{13}CO , C^{18}O , and molecular gas properties in the nucleus of maffei 2. *Astrophys. J.* **675**, 281 (2008)
258. Meszaros, P., Ostriker, J.P.: Shocks in spherically accreting black holes – a model for classical quasars. *Astrophys. J.* **273**, L59 (1983)
259. Miley, G.K., Miller, J.S.: Relations between the emission spectra and radio structures of quasars. *Astrophys. J. Lett.* **228**, L55 (1979)
260. Miller, K.A., Stone, J.M.: The formation and structure of a strongly magnetized corona above a weakly magnetized accretion disk. *Astrophys. J.* **534**, 398–419 (2000)

261. Moderski, R., Sikora, M., Lasota, J.-P.: On the spin paradigm and the radio dichotomy of quasars. *Mon. Not. R. Astron. Soc.* **301**, 142–148 (1998)
262. Monier, E.M., Mathur, S., Wilkes, B., Elvis, M.: Discovery of associated absorption lines in an x-ray warm absorber: hubble space telescope faint object spectrograph observations of MR 2251-178. *Astrophys. J.* **559**, 675 (2001)
263. Murray, N., Chiang, J.: Photoionized disk winds. In: *Mass Ejection from Active Galactic Nuclei*. Astronomical Society of the Pacific Conference Series, vol. 128, p. 246, 1997
264. Murray, N., Chiang, X., Voit, M.: Accretion disk winds from active galactic nuclei. *Astrophys. J.* **451**, 498–509 (1995)
265. Narayan, R., Yi, I.: Advection-dominated accretion: a self-similar solution. *Astrophys. J.* **428**, L13 (1994)
266. Narayan, R., Igumenshchev, I.V., Abramowicz, M.A.: Self-similar accretion flows with convection. *Astrophys. J.* **539**, 798 (2000)
267. Nenkova, M., Sirocky, M.M., Nikutta, R., Ivezić, Ž., Elitzur, M.: AGN dusty tori. II. Observational implications of clumpiness. *Astrophys. J.* **685**, 160–180 (2008)
268. Netzer, H.: Physical conditions in active nuclei-I. The balmer decrement. *Mon. Not. R. Astron. Soc.* **171**, 395–406 (1975)
269. Netzer, H.: On the profiles of the broad lines in the spectra of QSOs and seyfert galaxies. *Mon. Not. R. Astron. Soc.* **181**, 89–92 (1977)
270. Netzer, H.: Excitation of MG II and Fe II lines in quasars and seyfert galaxies. *Astrophys. J.* **236**, 406–418 (1980)
271. Netzer, H.: Quasar discs. I – The baldwin effect. *Mon. Not. R. Astron. Soc.* **216**, 63–78 (1985)
272. Netzer, H.: The far-ultraviolet continuum of quasars and the universe at z greater than 4. *Astrophys. J.* **289**, 451–456 (1985)
273. Netzer, H.: AGN emission lines. 20. Saas-Fee Advanced Course of the Swiss Society for Astrophysics and Astronomy: Active Galactic Nuclei, pp. 57–160. Springer, Berlin (1990)
274. Netzer, H.: X-ray lines in active galactic nuclei and photoionized gases. *Astrophys. J.* **473**, 781 (1996)
275. Netzer, H.: Accretion and star formation rates in low-redshift type II active galactic nuclei. *Mon. Not. R. Astron. Soc.* **399**, 1907 (2009)
276. Netzer, H., Laor, A.: Dust in the narrow-line region of active galactic nuclei. *Astrophys. J.* **404**, L51–L54 (1993)
277. Netzer, H., Marziani, P.: The effect of radiation pressure on emission line profiles and black hole mass determination in active galactic nuclei. *Astrophys. J. ApJ* **724**, 318 (2010)
278. Netzer, H., Wills, B.J.: Broad emission features in QSOs and active galactic nuclei. I – New calculations of Fe II line strengths. *Astrophys. J.* **275**, 445–460 (1983)
279. Newman, J.A., Eracleous, M., Filippenko, A.V., Halpern, J.P.: Measurement of an active galactic nucleus central mass on centiparsec scales: results of long-term optical monitoring of ARP 102B. *Astrophys. J.* **485**, 570 (1997)
280. Nikolajuk, M., Czerny, B., Ziolkowski, J., Gierlinski, M.: Consistency of the black hole mass determination in AGN from the reverberation and the x-ray excess variance method. *Mon. Not. R. Astron. Soc.* **370**, 1534–1540 (2006)
281. Noble, S.C., Krolik, J.H.: GRMHD prediction of coronal variability in accreting black holes. *Astrophys. J.* **703**, 964–975 (2009)
282. Noble, S.C., Krolik, J.H., Hawley, J.F.: Dependence of inner accretion disk stress on parameters: the schwarzschild case. *Astrophys. J.* **711**, 959–973 (2010)
283. Noguchi, M.: Gas dynamics in interacting disc galaxies – fuelling of nuclei by induced bars. *Astron. Astrophys.* **203**, 259 (1988)
284. Novikov, I.D., Thorne, K.S.: Astrophysics of black holes. In: Dewitt, C., Dewitt, B.S. (eds.) *Black Holes (Les Astres Occlus)*, pp. 343–450. Gordon and Breach, New York (1973)
285. O’Brien, P.T., Dietrich, M., Leighly, K., Alloin, D., Clavel, J., Crenshaw, D.M., Horne, K., Kriss, G.A., Krolik, J.H., Malkan, M.A., Netzer, H., Peterson, B.M.: Steps toward determination of the size and structure of the broad-line region in active galactic nuclei. XIII. Ultraviolet observations of the broad-line radio galaxy 3C 390.3. *Astrophys. J.* **509**, 163 (1998)

286. Ogle, P.M., Cohen, M.H., Miller, J.S., Tran, H.D., Goodrich, R.W., Martel, A.R.: Polarization of broad absorption line QSOS. I. A spectropolarimetric atlas. *Astrophys. J. Suppl.* **125**, 1 (1999)
287. Osterbrock, D.E.: *Astrophysics of Gaseous Nebulae and Active Galactic Nuclei*, Chap. 11. University Science Books, Mill Valley (1989)
288. Osterbrock, D.E., Shuder, J.M.: Emission-line profiles in seyfert-1 galaxies. *Astrophys. J. Suppl.* **49**, 149 (1982)
289. Ostriker, J.P., Peebles, P.J.E.: A numerical study of the stability of flattened galaxies: or, can cold galaxies survive? *Astrophys. J.* **186**, 467 (1973)
290. Ouyed, R., Pudritz, R.E.: Numerical simulations of astrophysical jets from keplerian disks. II. Episodic outflows. *Astrophys. J.* **484**, 794–809 (1997)
291. Ouyed, R., Pudritz, R.E.: Numerical simulations of astrophysical jets from keplerian disks. II. Episodic outflows. *Astrophys. J.* **484**, 794 (1997)
292. Paczynski, B.: A model of selfgravitating accretion disk. *Acta Astron.* **28**, 91 (1978)
293. Paredes, J.M.: *Stellar radio astrophysics*. EAS Publication Series, vol. 15, 187–206 (2005)
294. Penna, R.F., McKinney, J.C., Narayan, R., Tchekhovskoy, A., Shafee, R., McClintock, J.E.: Simulations of magnetized discs around black holes: effects of black hole spin, disc thickness and magnetic field geometry. *Mon. Not. R. Astron. Soc.* **408**, 752–782 (2010)
295. Penrose, R.: Gravitational collapse: the role of general relativity. *Rivista del Nuovo Cimento*, Numero Speciale I, 252 (1969)
296. Pereyra, N.A., Kallman, T.R., Blondin, J.M.: Hydrodynamical models of line-driven accretion disk winds. *Astrophys. J.* **477**, 368–378 (1997)
297. Petersen, M.R., Stewart, G.R., Julien, K.: Baroclinic vorticity production in protoplanetary disks. II. Vortex growth and longevity. *Astrophys. J.* **658**, 1252 (2007)
298. Peterson, B.M.: Emission-line variability in seyfert galaxies. *PASP* **100**, 18 (1988)
299. Peterson, B.M.: Reverberation mapping of active nuclei. *Adv. Space Res.* **21**, 57–66 (1998)
300. Peterson, B.M., Korista, K.T., Wagner, R.M.: Continuum and emission-line variability of the seyfert galaxy arakelian 120 – analysis of a large database. *Astron. J.* **98**, 500–512 (1989)
301. Petitpas, G.R., Wilson, C.D.: Molecular gas in candidate double-barred galaxies. I. The diverse morphology and dynamics of NGC 2273 and NGC 5728. *Astrophys. J.* **575**, 814 (2002)
302. Pier, E.A., Krolik, J.H.: Radiation-pressure-supported obscuring tori around active galactic nuclei. *Astrophys. J. Lett.* **399**, L23–L26 (1992)
303. Piner, B.G., Edwards, P.G.: The parsec-scale structure and jet motions of the TeV blazars 1ES 1959+650, PKS 2155-304, and 1ES 2344+514. *Astrophys. J.* **600**, 115–126 (2004)
304. Pounds, K.A., Reeves, J.N., King, A.R., Page, K.L., O'Brien, P.T., Turner, M.J.L.: A high-velocity ionized outflow and XUV photosphere in the narrow emission line quasar PG1211+143. *Mon. Not. R. Astron. Soc.* **345**, 705 (2003)
305. Poutanen, J., Stern, B.: GeV breaks in blazars as a result of gamma-ray absorption within the broad-line region. *Astrophys. J.* **717**, L118–L121 (2010)
306. Prengergast, K.H., Spiegel, E.A.: Photon bubbles. *Comm. Astrophys. Space Sci.* **5**, 43 (1973)
307. Pringle, J.E.: Self-induced warping of accretion discs. *Mon. Not. R. Astron. Soc.* **281**, 357 (1996)
308. Proga, D.: Comparison of theoretical radiation-driven winds from stars and discs. *Mon. Not. R. Astron. Soc.* **304**, 938–946 (1999)
309. Proga, D.: Winds from accretion disks driven by radiation and magnetocentrifugal force. *Astrophys. J.* **538**, 684–690 (2000)
310. Proga, D.: Numerical simulations of mass outflows driven from accretion disks by radiation and magnetic forces. *Astrophys. J.* **585**, 406–417 (2003)
311. Proga, D.: On resonance-line profiles predicted by radiation-driven disk-wind models. *Astrophys. J.* **592**, L9–L12 (2003)
312. Proga, D., Begelman, M.C.: Accretion of low angular momentum material onto black holes: two-dimensional magnetohydrodynamic case. *Astrophys. J.* **592**, 767–781 (2003)

313. Proga, D., Kallman, T.: Dynamics of line-driven disk winds in active galactic nuclei. II. Effects of disk radiation. *Astrophys. J.* **616**, 688 (2004)
314. Proga, D., Kurosawa, R.: Outflows from AGN: their impact on spectra and the environment. In: Maraschi, L., Ghisellini, G., Della Ceca, R., Tavecchio, F. (eds.) *Accretion and Ejection in AGN: A Global View*, Como, Italy. ASP Conf. Ser. (arXiv:1002.4667)
315. Proga, D., Stone, J.M., Kallman, T.: Dynamics of line-driven disk winds in active galactic nuclei. *Astrophys. J.* **543**, 686–696 (2000)
316. Proga, D., Stone, J.M., Drew, J.E.: Radiation-driven winds from luminous accretion discs. *Mon. Not. R. Astron. Soc.* **295**, 595–617 (1998)
317. Proga, D., Stone, J.M., Drew, J.E.: Line-driven disc wind models with an improved line force. *Mon. Not. R. Astron. Soc.* **310**, 476–482 (1999)
318. Puls, J., Vink, J.S., Najarro, F.: Mass loss from hot massive stars. *Astron. Astrophys. Rev.* **16**, 209–325 (2008)
319. Pushkarev, A.B., Kovalev, Y.Y., Lister, M.L., Savolainen, T.: Jet opening angles and gamma-ray brightness of AGN. *Astron. Astrophys.* **507**, L33–L36 (2009)
320. Raha, N., Sellwood, J.A., James, R.A., Kahn, F.D.: A dynamical instability of bars in disk galaxies. *Nature* **352**, 411 (1991)
321. Rees, M.J.: Appearance of relativistically expanding radio sources. *Nature* **211**, 468 (1966)
322. Rees, M.J., Netzer, H., Ferland, G.J.: Small dense broad-line regions in active nuclei. *Astrophys. J.* **347**, 640–655 (1989)
323. Reichard, T.A., Richards, G.T., Hall, P.B., Schneider, D.P., Vanden Berk, D.E., Fan, X., York, D.G., Knapp, G.R., Brinkmann, J.: Continuum and emission-line properties of broad absorption line quasars. *Astron. J.* **126**, 2594 (2003)
324. Reyes, R., Zakamska, N.L., Strauss, M.A., Green, J., Krolik, J.H., Shen, Y., Richards, G.T., Anderson, S.F., Schneider, D.P.: Space density of optically selected type-2 quasars. *Astron. J.* **136**, 2373–2390 (2008)
325. Reynolds, C.S., Garofalo, D., Begelman, M.C.: Trapping of magnetic flux by the plunge region of a black hole accretion disk. *Astrophys. J.* **651**, 1023–1030 (2006)
326. Richards, G.T., Vanden Berk, D.E., Reichard, T.A., Hall, P.B., Schneider, D.P., SubbaRao, M., Thakar, A.R., York, D.G. et al.: Broad emission-line shifts in quasars: an orientation measure for radio-quiet quasars? *Astron. J.* **124**, 1–17 (2002)
327. Risaliti, G., Elvis, M.: Anon-hydrodynamical model for acceleration of line-driven winds in inactive galactic nuclei. *Astron. Astrophys.* **516**, 89 (2010)
328. Risaliti, G., Elvis, M., Bianchi, S., Matt, G.: Chandra monitoring of UGC 4203: the structure of the x-ray absorber. *Mon. Not. R. Astron. Soc.* **406**, L20–L24 (2010)
329. Risaliti, G., Elvis, M., Fabbiano, G., Baldi, A., Zezas, A.: Rapid compton-thick/compton-thin transitions in the seyfert-2 galaxy NGC 1365. *Astrophys. J. Lett.* **623**, L93–L96 (2005)
330. Risaliti, G., Salvati, M., Elvis, M., Fabbiano, G., Baldi, A., Bianchi, S., Braito, V., Guainazzi, M., Matt, G., Miniutti, G., Reeves, J., Soria, R., Zezas, A.: The XMM-newton long look of NGC 1365: uncovering of the obscured x-ray source. *Mon. Not. R. Astron. Soc.* **393**, L1–L5 (2009)
331. Rodriguez Hidalgo, P., Hamann, F., Hall, P.: The extreme high-velocity outflow in quasar PG0935+417. *Mon. Not. R. Astron. Soc.* **411**, 247 (2010)
332. Romano-Diaz, E., Shlosman, I., Heller, C., Hoffman, Y.: Disk evolution and bar triggering driven by interactions with dark matter substructure. *Astrophys. J.* **687**, L13 (2008)
333. Romano-Diaz, E., Shlosman, I., Hoffman, Y., Heller, C.: Erasing dark matter cusps in cosmological galactic halos with baryons. *Astrophys. J.* **685**, L105 (2008)
334. Rothstein, D.M., Lovelace, R.V.E.: Advection of magnetic fields in accretion disks: not so difficult after all. *Astrophys. J.* **677**, 1221–1232 (2008)
335. Rokaki, E., Boisson, C., Collin-Souffrin, S.: Fitting the broad line spectrum and UV continuum by accretion discs in active galactic nuclei. *Astron. Astrophys.* **253**, 57 (1992)
336. Rokaki, E., Collin-Souffrin, S., Magnan, C.: NGC5548 – a perfect laboratory for testing AGN models. *Astron. Astrophys.* **272**, 8 (1993)

337. Salpeter, E.E.: Accretion of interstellar matter by massive objects. *Astrophys. J.* **140**, 796 (1964)
338. Scheuer, P.A.G., Feiler, R.: The realignment of a black hole misaligned with its accretion disc. *Mon. Not. R. Astron. Soc.* **282**, 291 (1996)
339. Schinnerer, E., Boker, T., Emsellem, E., Lisenfeld, U.: Molecular gas dynamics in NGC 6946: a bar-driven nuclear starburst “Caught in the Act”. *Astrophys. J.* **649**, 181 (2006)
340. Schinnerer, E., Eckart, A., Tacconi, L.J., Genzel, R., Downes, D.: Bars and warpstraced by the molecular gas in the seyfert-2 galaxy NGC 1068. *Astrophys. J.* **533**, 850 (2000)
341. Schnittman, J.D., Krolik, J.H., Hawley, J.F.: Light curves from an MHD simulation of a black hole accretion disk. *Astrophys. J.* **651**, 1031–1048 (2006)
342. Schurch, N.J., Done, C., Proga, D.: The impact of accretion disk winds on the x-ray spectra of active galactic nuclei. II. Xscort + hydrodynamic simulations. *Astrophys. J.* **694**, 1–11 (2009)
343. Schwarz, M.P.: On the relationship between lenses and inner rings in spiral galaxies. *Astron. Soc. Australia Proc.* **6**, 202 (1985)
344. Scoville, N., Norman, C.: Broad emission lines from the mass-loss envelopes of giant stars in active galactic nuclei. *Astrophys. J.* **332**, 163–171 (1988)
345. Scoville, N., Norman, C.: Stellar contrails in quasi-stellar objects: the origin of broad absorption lines. *Astrophys. J.* **451**, 510–524 (1995)
346. Sergeev, S.G., Pronik, V.I., Peterson, B.M., Sergeeva, E.A., Zheng, W.: Variability of the broad balmer emission lines in 3C 390.3 from 1992 to 2000. *Astrophys. J.* **576**, 660 (2002)
347. Sergeev, S.G., Pronik, V.I., Sergeeva, E.A.: Arp 102B: variability patterns of the H α line profile as evidence for gas rotation in the broad-line region. *Astron. Astrophys.* **356**, 41–49 (2000)
348. Serjeant, S., Rawlings, S., Lacy, M., Maddox, S.J., Baker, J.C., Clements, D., Lilje, P.B.: The radio-optical correlation in steep-spectrum quasars. *Mon. Not. R. Astron. Soc.* **294**, 494 (1988)
349. Shakura, X., Sunayev, R.: Black holes in binary systems. Observational appearance. *Astron. Astrophys.* **24**, 337 (1973)
350. Shapovalova, A.I., Burenkov, A.N., Carrasco, L., Chavushyan, V.H., Doroshenko, V.T., Dumont, A.M., Lyuty, V.M., Valdés, J.R., Vlasuyk, V.V., Bochkarev, N.G., et al.: Intermediate resolution H β spectroscopy and photometric monitoring of 3C 390.3. I. Further evidence of a nuclear accretion disk. *Astron. Astrophys.* **376**, 775–792 (2001)
351. Shemmer, O., Netzer, H., Maiolino, R., Oliva, E., Croon, S., Corbett, E., di Fabrizio, L.: Near-infrared spectroscopy of high of redshift active galactic nuclei. I. A Metallicity-accretion rate relationship. *Astrophys. J.* **614**, 547–557 (2004)
352. Shen, J., Rich, R.M., Kormendy, J., Howard, C.D., De Propriis, R., Kunder, A.: Our milky way as a pure-disk GalaxyA challenge for galaxy formation. *Astrophys. J.* **720**, L72 (2010)
353. Shi, J., Krolik, J.H.: Radiation pressure-supported active galactic nucleus tori with hard x-ray and stellar heating. *Astrophys. J.* **679**, 1018–1028 (2008)
354. Shi, J., Krolik, J.H., Hirose, S.: What is the numerically converged amplitude of magnetohydrodynamics turbulence in stratified shearing boxes? *Astrophys. J.* **708**, 1716–1727 (2010)
355. Shibata, K., Uchida, Y.: A magnetodynamic mechanism for the formation of astroph. Jets. II – Dynamical processes in the accretion of magnetized mass in rotation. *Publ. Astron. Soc. Jpn.* **38**, 631–660 (1986)
356. Shlosman, I.: Induced starburst and nuclear activity: faith, facts, and theory. In: Sulentic, J., Keel, W., (eds.) *IAU Colloq. 124 on Paired and Interacting Galaxies*, p. 689. MSFC, NASA (1990)
357. Shlosman, I., Begelman, M.C.: Evolution of self-gravitating accretion disks in active galactic nuclei. *Astrophys. J.* **341**, 685 (1989)
358. Shlosman, I., Begelman, M.C., Frank, J.: The fuelling of active galactic nuclei. *Nature* **345**, 679–686 (1990)
359. Shlosman, I., Frank, J., Begelman, M.C.: Bars within bars – a mechanism for fuelling active galactic nuclei. *Nature* **338**, 45 (1989)

360. Shlosman, I., Vitello, P., Shaviv, G.: Active galactic nuclei – internal dynamics and formation of emission clouds. *Astrophys. J.* **294**, 96–105 (1985)
361. Siebenmorgen, R., Haas, M., Krügel, E., Schulz, B.: Discovery of 10 μm silicate emission in quasars. Evidence of the AGN unification scheme. *AAp* **436**, L5–L8 (2005)
362. Sigut, T.A.A., Pradhan, A.K.: Predicted Fe II emission-line strengths from active galactic nuclei. *Astrophys. J. Suppl.* **145**, 15 (2003)
363. Sikora, M.: Radio bimodality: spin, accretion mode, or both? *Astron. Nach.* **330**, 291 (2009)
364. Sikora, M., Begelman, M.C., Madejski, G.M., Lasota, J.-P.: Are quasar jets dominated by poynting flux? *Astrophys. J.* **625**, 72–77 (2005)
365. Sikora, M., Stawarz, Ł., Moderski, R., Nalewajko, K., Madejski, G.M.: Constraining emission models of luminous blazar sources. *Astrophys. J.* **704**, 38–50 (2009)
366. Sikora, M., Lukasz, S., Lasota, J.-P.: Radio-loudness of active galaxies and the black hole evolution. *NewAstron. Rev.* **51**, 891 (2008)
367. Sim, S.A., Proga, D., Miller, L., Long, K.S., Turner, T.J.: Multidimensional modelling of x-ray spectra for AGN accretion disc outflows – III. Application to a hydrodynamical simulation'. *Mon. Not. R. Astron. Soc.* **408**, 1396–1408 (2010)
368. Smith, M.D., Raine, D.J.: Wind interactions above accretion discs – a model for broad-line regions and collimated outflow. *Mon. Not. R. Astron. Soc.* **212**, 425 (1985)
369. Spruit, H.C., Uzdensky, D.A.: Magnetic flux captured by an accretion disk. *Astrophys. J.* **629**, 960–968 (2005)
370. Sironi, L., Spitkovsky, A.: Particle acceleration in relativistic magnetized collisionless electron-ion shocks. *Astrophys. J.* **726**, 75 (2011)
371. Stauffer, J., Schild, R., Keel, W.: ARP 102B – a new and unusual broad-line galaxy. *Astrophys. J.* **270**, 465 (1983)
372. Stern, B.E., Poutanen, J.: Radiation from relativistic jets in blazars and the efficient dissipation of their bulk energy via photon breeding. *Mon. Not. R. Astron. Soc.* **383**, 1695–1712 (2008)
373. Stone, J.M., Norman, M.L.: Numerical simulations of magnetic accretion disks. *Astrophys. J.* **433**, 746–756 (1994)
374. Storchi-Bergmann, T., Gonzalez-Delgado, R.M., Schmitt, H.R., Cid-Fernandez, R., Heckman, T.: Circumnuclear stellar population, morphology, and environment of seyfert-2 galaxies: an evolutionary scenario. *Astrophys. J.* **559**, 147 (2001)
375. Storchi-Bergmann, T., Eracleous, M., Ruiz, M.T., Livio, M., Wilson, A.S., Filippenko, A.V.: Evidence for a precessing accretion disk in the nucleus of NGC 1097. *Astrophys. J.* **489**, 87 (1997)
376. Storchi-Bergmann, T., Nemmen da Silva, R., Eracleous, M., Halpern, J.P., Wilson, A.S., Filippenko, A.V., Ruiz, M.T., Smith, R.C., Nagar, N.M.: Evolution of the nuclear accretion disk emission in NGC 1097: getting closer to the black hole. *Astrophys. J.* **598**, 956–968 (2003)
377. Strateva, I.V., Strauss, M.A., Hao, L., Schlegel, D.J., Hall, P.B., Gunn, J.E., Li, L.-X., Ivezić Ž., Richards, G.T., Zakamska, N.L., Voges, W., Anderson, S.F., Lupton, R.H., Schneider, D.P., Brinkmann, J., Nichol, R.C.: Double-peaked low-ionization emission lines in active galactic nuclei. *Astron. J.* **126**, 1720–1749 (2003)
378. Sturm, E., Hasinger, G., Lehmann, I., Mainieri, V., Genzel, R., Lehnert, M.D., Lutz, D., Tacconi, L.J.: Mid-infrared spitzer spectra of x-ray-selected type-2 QSOs: QSOs are not ultraluminous infrared galaxies. *Astrophys. J.* **642**, 81–86 (2006)
379. Sulentic, J.W., Marziani, P., Dultzin-Hacyan, D.: Phenomenology of broad emission lines in active galactic nuclei. *Ann. Rev. Astron. Astrophys.* **38**, 521–571 (2000)
380. Tadhunter, C., Tsvetanov, Z.: Anisotropic ionizing radiation in NGC5252. *Nature* **341**, 422(1989)
381. Tananbaum, H., Avni, Y., Branduardi, G., Elvis, M., Fabbiano, G., Feigelson, E., Giacconi, R., Henry, J.P., Pye, J.P., Soltan, A., Zamorani, G.: X-ray studies of quasars with the einstein observatory. *Astrophys. J.* **234**, 9 (1979)
382. Tarter, C.B., Tucker, W.H., Salpeter, E.E.: The interaction of X-ray sources with optically thin environments. *Astrophys. J.* **156**, 943 (1969)

383. Tavecchio, F., Ghisellini, G., Bonnoli, G., Ghirlanda, G.: Constraining the location of the emitting region in *Fermi* blazars through rapid γ -ray variability. *Mon. Not. R. Astron. Soc.* **405**, L94–L98 (2010)
384. Tchekhovskoy, A., Narayan, R., McKinney, J.C.: Black hole spin and the radio loud/quiet dichotomy of active galactic nuclei. *Astroph. J.* **711**, 50–63 (2010)
385. Thompson, T.A., Quataert, E., Murray, N.: Radiation pressure-supported starburst disks and active galactic nucleus fueling. *Astrophys. J.* **630**, 167–185 (2005)
386. Thorne, K.S.: Disk-accretion onto a black hole. II. Evolution of the hole. *Astrophys. J.* **191**, 507–520 (1974)
387. Thronson, H.A., Jr., Hereld, M., Majewski, S., Greenhouse, M., Johnson, P., Spillar, E., Woodward, C.E., Harper, D.A., Rauscher, B.J.: Near-infrared image of NGC 1068 – bar-driven star formation and the circumnuclear composition. *Astrophys. J.* **343**, 158–168 (1989)
388. Treister, E., Krolik, J.H., Dullemond, C.: Measuring the fraction of obscured quasars by the infrared luminosity of unobscured quasars. *Astrophys. J.* **679**, 140–148 (2008)
389. Turner, N.J., Stone, J.M., Krolik, J.H., Sano, T.: Local three-dimensional simulations of magnetorotational instability in radiation-dominated accretion disks. *Astrophys. J.* **593**, 992–1006 (2003)
390. Turnshek, D.A.: BAL QSOs – observations, models and implications for narrow absorption line systems. In: Blades, J.C., Turnshek, D.A., Norman, C.A. (eds.) *QSO Absorption Lines: Probing the Universe*, pp. 17–46. Cambridge University Press, Cambridge (1988)
391. Uchida, Y., Shibata, K.: Magnetodynamical acceleration of CO and optical bipolar flows from the region of star formation. *Publ. Astron. Soc. Jpn.* **37**, 515–535 (1985)
392. Ueda, Y., Akiyama, M., Ohta, K., Miyaji, T.: Cosmological evolution of the hard X-ray active galactic nucleus luminosity function and the origin of the hard X-ray background. *Astrophys. J.* **598**, 886–908 (2003)
393. Urry, C.M., Padovani, P.: Unified schemes for radio-loud active galactic nuclei. *PASP* **107**, 803–845 (1995)
394. Ustyugova, G.V., Koldoba, A.V., Romanova, M.M., Chechetkin, V.M., Lovelace, R.V.E.: Magnetocentrifugally driven winds: comparison of MHD simulations with theory. *Astrophys. J.* **516**, 221–235
395. Velikhov, E.P.: *Sov. Phys. JETP* **9**, 995 (1959)
396. Verner, E.M., Verner, D.A., Korista, K.T., Ferguson, J.W., Hamann, F., Ferland, G.J.: Numerical simulations of Fe II emission spectra. *Astrophys. J. Suppl.* **120**, 101 (1999)
397. Vlahakis, N., Königl, A.: Magnetic driving of relativistic outflows in active galactic nuclei. I. Interpretation of parsec-scale accelerations. *Astrophys. J.* **605**, 656–661 (2004)
398. Voit, G.M., Weymann, R.J., Korista, K.T.: Low-ionization broad absorption lines in quasars. *Astrophys. J.* **413**, 95–109 (1993)
399. Volonteri, M., Haardt, F., Ghisellini, G., Della Ceca, R.: Blazars in the early Universe. *Mon. Not. R. Astron. Soc.* **416**, 216 (2012)
400. Wald, R.M.: Black hole in a uniform magnetic field. *Phys. Rev. D* **10**, 1680–1685 (1974)
401. Wardle, J.F.C.: Magnetic fields in AGN. In: Zensus, J.A., Taylor, G.B., Wrobel, J.M. (eds.) *IAU Colloq. 164: Radio emission from galactic and extragalactic compact sources*. ASP Conf. Ser. **144**, 97 (1998)
402. Weaver, K.A.: X-ray properties of the central kpc of AGN and starbursts: the latest news from chandra. In: Knapen, J.H., Beckman, J.E., Shlosman, I., Mahoney, T.J. (eds.) *The Central Kpc of Starbursts AGN: The La Palma Connection*. ASP Conf. Ser. **249**, 389 (2001)
403. Weinberg, S.: A model of leptons. *Phys. Rev. Lett.* **19**, 1264 (1967)
404. Weymann, R.J., Morris, S.L., Foltz, C.B., Hewett, P.C.: Comparisons of the emission-line and continuum properties of broad absorption line and normal quasi-stellar objects. *Astrophys. J.* **373**, 23–53 (1991)
405. Wills, B.J., Netzer, H., Wills, D.: Broad emission features in QSOs and active galactic nuclei. II – New observations and theory of Fe II and H I emission. *Astrophys. J.* **288**, 94–116 (1985)
406. Wills, B.J., Browne, I.W.A.: Relativistic beaming and quasar emission lines. *Astrophys. J.* **302**, 56 (1986)

407. Wilson, A.S., Colbert, E.J.M.: The difference between radio-loud and radio-quiet active galaxies. *Astrophys. J.* **438**, 62–71 (1995)
408. Zakamska, N.L., Schmidt, G.D., Smith, P.S., Strauss, M.A., Krolik, J.H., Hall, P.B., Richards, G.T., Schneider, D.P., Brinkmann, J., Szokoly, G.P.: Candidate type II quasars from the sloan digital sky survey. III. Spectropolarimetry reveals hidden type I nuclei. *Astron. J.* **129**, 1212–1224 (2005)
409. Zakamska, N.L., Strauss, M.A., Krolik, J.H., Ridgway, S.E., Schmidt, G.D., Smith, P.S., Heckman, T.M., Schneider, D.P., Hao, L., Brinkmann, J.: Type II quasars from the sloan digital sky survey. V. Imaging host galaxies with the hubble space telescope. *Astron. J.* **132**, 1496–1516 (2006)
410. Zeldovich, Ya.B.: *Dokl. Akad. Nauk SSSR* **155**, 67. English translation in *Sov. Phys. Dokl.* **9**, 195 (1964)
411. Zheng, W., Binette, L., Sulentic, J.W.: A double-stream model for line profiles. *Astrophys. J.* **365**, 115 (1990)
412. Zheng, W., Veilleux, S., Grandi, S.A.: 3C 390.3 – Modeling variable profile humps. *Astrophys. J.* **381**, 41 (1991)
413. Zurek, W.H., Siemiginowska, A., Colgate, S.A.: Star-disk collisions and the origin of the broad lines in quasars. *Astrophys. J.* **434**, 46 (1995)

Chapter 7

Quasars in the Cosmic Environment

Contributions by Mauro D’Onofrio, Paola Marziani, Jack W. Sulentic, Deborah Dultzin, Gordon Richards, Johan Knapen, Isaac Shlosman, Raffaella Morganti, Renato Falomo, Mike Hawkins, Alfonso Cavaliere, Ross McLure, Greg Shields, Hagai Netzer, Daniel Proga, Alberto Franceschini, Xiaoui Fan, and Martin Elvis

M. D’Onofrio

Dipartimento di Astronomia, Universit’ a degli Studi di Padova, Vicolo Osservatorio 3,
I35122 Padova, Italy
e-mail: mauro.donofrio@unipd.it

P. Marziani

INAF, Osservatorio Astronomico di Padova, Vicolo Osservatorio 5, IT35122 Padova, Italy
e-mail: paola.marziani@oapd.inaf.it

J.W. Sulentic (✉)

Instituto de Astrofísica de Andalucía (CSIC), Granada, Spain
e-mail: sulentic@iaa.es

D. Dultzin

Instituto de Astronomia, Universidad Nacional Autonoma de Mexico (UNAM), Apt.do postal
70-264, Mexico, DF, Mexico
e-mail: deborah@astrocu.unam.mx

G. Richards

Department of Physics, Drexel University, 3141 Chestnut Street, Philadelphia, PA 19104 USA
e-mail: gtr@physics.drexel.edu

J. Knapen

Instituto de Astrofísica de Canarias, E-38200 La Laguna, Tenerife, Spain

Departamento de Astrofísica, Universidad de La Laguna, E-38205 La Laguna, tenerife, Spain
e-mail: jhk@iac.es

I. Shlosman

Department of Physics and Astronomy, University of Kentucky, Lexington,
KY 40506-0055, USA
e-mail: shlosman@ps.uky.edu

R. Morganti

Netherlands Institute for RadioAstronomy (ASTRON), Postbus 2, 7990 AA, Dwingeloo,
The Netherlands

Kapteyn Astronomical Institute, University of Groningen, P.O. Box 800, 9700 AV Groningen,
The Netherlands

e-mail: morganti@astron.nl

R. Falomo

INAF-Osservatorio Astronomico di Padova, Vicolo Osservatorio 2, I35122 Padova, Italy
e-mail: renato.falomo@oapd.inaf.it

We now consider the environment of quasars in the widest possible sense, from the circumnuclear regions to very large scales of hundreds of kiloparsecs. The circumgalactic environment of nearby quasars has been widely studied since the late 1960s in an attempt to test its influence on the triggering of nuclear activity. The underlying hypothesis is that gravitational perturbations might ease the infall of matter toward the nucleus, providing accretion material for the central black hole. This implies large-scale gas motions toward the nucleus that should be detectable. On the other hand, after a quasar is born, its metabolic activity will bring it to an eventual demise, as accreting black holes spew gas and radiation around themselves, ultimately creating a hollow space devoid of accretion fuel. The complex interplay between the quasar energetic output and its environment (commonly known as feedback) produces a rich phenomenology that has been a subject of intense study in the last few years, but that remains difficult to evaluate in distant quasars.

Several questions are devoted to the birth and evolution of quasars. Since massive black holes are now found at redshifts $\gtrsim 6$, the birth of the first quasars is expected to occur at a very early age of the Universe, possibly affecting also the early protogalactic spheroids—another manifestation of feedback processes.

M. Hawkins · R. McLure
Institute for Astronomy (IfA), University of Edinburgh, Royal Observatory, Blackford Hill,
Edinburgh EH9 3HJ, UK
e-mail: mrsh@roe.ac.uk; rjm@roe.ac.uk

A. Cavaliere
Dipartimento di Fisica, Università di Tor Vergata, via Ricerca Scientifica 1, 00133 Roma, Italy
e-mail: cavaliere@roma2.infn.it

G. Shields
Department of Astronomy, University of Texas, Austin, TX 78712-0259, USA
e-mail: shields@astro.as.utexas.edu

H. Netzer
School of Physics and Astronomy, Tel Aviv University, Tel Aviv 69978, Israel
e-mail: netzer@wise.tau.ac.il

D. Proga
Department of Physics and Astronomy, University of Nevada, Las Vegas 4505, South Maryland
Parkway, Las Vegas, Nevada 89154-4002, USA
e-mail: dproga@physics.unlv.edu

A. Franceschini
Dipartimento di Astronomia, Università degli Studi di Padova, Vicolo Osservatorio 3,
I35122 Padova, Italy
e-mail: alberto.franceschini@unipd.it

X. Fan
Steward Observatory and Department of Astronomy, University of Arizona, 933 N. Cherry
Avenue, Tucson 85721, Arizona, USA
e-mail: fan@as.arizona.edu

M. Elvis
Harvard Smithsonian Center for Astrophysics, Cambridge MA02138, USA
e-mail: elvis@cfa.harvard.edu

We then turn our attention to the most luminous quasars when considering their utility as cosmological probes. Fainter AGNs can be observed and studied locally, but the situation at high redshift is yet unclear. The utility of quasars as cosmological probes is obvious if we can observe unobscured examples and samples over a very large z range. They offer the possibility to search for and quantify evolution in the Universe—for comparison with predictions of standard cosmological model.

7.1 The Environment Around Quasars and AGNs

Dear Deborah (*Dultzin*), the environment of low-redshift AGNs can be studied in a relatively straightforward way on scales ~ 100 kpc. What techniques are employed in such studies? How does the environment of Seyfert galaxies compare to that for normal and star-forming galaxies? How does environment affect the observed properties of AGNs?

In my opinion, one of the outstanding problems in the understanding of the active galactic nuclei (AGNs) phenomenon is the feeding process (or processes) of the central supermassive black hole. The gas fueling (or feeding) may be promoted from extragalactic to galactic, and nuclear proper scales. The main proposed mechanism to induce gas inflow to the center of galaxies, on the extragalactic scales, consists of interactions with other galaxies (e.g., [11]). Although any other non-axisymmetric potential may contribute. Among many other confusions in the literature, is the definition of *nuclear activity* because some authors include both nonthermal (properly AGNs) activity as well as nuclear/circumnuclear starburst (hereafter SB) activity. I will try to be specific, although it is not always possible. Low Ionization Nuclear Emitting Regions (LINERs) are easy to observe; however the nature of the dominating emission mechanism is not yet well established (e.g., [93, 175, 206]). And then, there are so-called transition objects with spectral features of both AGN and SB combined. The first to propose a starburst-AGN connection were Perry and Dyson in 1985 [238]. An excellent recent review on this topic can be found in [285].

The first studies of the extragalactic influence on AGNs were devoted to investigate the difference in the environment between active and nonactive galaxies, without distinction of type of activity (e.g., [46–48]). But soon, it became clear that it was necessary to distinguish between type-1 and type-2 AGNs (and even starburst or enhanced Star-forming activity). More recently, the importance of distinguishing between close (<100 kpc) and large-scale environment has become clear. The first studies were affected by the lack of clear definitions, statistical biases, and also biases introduced by sample selection effects. All these methodological problems have yielded contradictory results that can be found in the literature over more than 20 years (from [282] to [168]).

In my opinion, the first study which got rid of many of these biases was done by [188, 189], although their sample is still biased toward low-galactic latitude

objects. In addition, their study was based on computer-aided measurements on the plates. In other cases, even worse, on printed enlargements [246]. Another problem was the use of the Shane and Wirtanen counts to provide an estimate of the number of optical companions expected by chance alignment with background (or foreground) galaxies. Several improvements were reported in the study by Dultzin-Hacyan et al. [59], such as the determination of the number density, that goes into the formula for the predicted number of background galaxies within each area. The determination was made directly from the DSS plates using faint object classification and analysis system (FOCAS; [136]) counting galaxies in regions of one square degree surrounding each galaxy. In that work, the background densities between samples are statistically equal (according to a Mann–Whitneys U test). The authors identified all galaxies with at least one companion within three times the diameter of the galaxy ($3D_S$). The search was performed automatically on the DSS with FOCAS and was limited to galaxies that could be unambiguously distinguished from stars by the FOCAS algorithm. This procedure reduces to a minimum several bias present in previous works. Another important methodological improvement of that work was the definition of control samples of nonactive galaxies which matched the distribution of Seyfert-1 and Seyfert-2 galaxies in all respects except that they do not have an active nucleus. In order to achieve this, two control samples were defined, one for each type of Seyfert galaxies, because both the Hubble type and redshift distributions of the two types of Seyfert galaxies differ. Absolute magnitude distributions were not matched since this would introduce a bias (e.g., [54]). However, they did match the diameters distribution. Both the Seyfert and control samples were complete (in volume) to a confidence level of up to 97%.

Finally, Koulouridis et al. [170] measured all the distances to the claimed companions of Seyferts using the exact same samples of [59] extended as explained below, in order to study the three-dimensional environment of Seyfert-1 and 2 galaxies. Based on their own spectroscopic observations of all projected neighbors within a $100 h^{-1}$ kpc radius and down to $m_B \sim 18.5$. In order to enlarge the original sample, they also used the CfA2 and Sloan Digital Sky Survey (SDSS) galaxy catalogues which cover a large solid angle of the sky. In addition, they also studied the large-scale environment of Seyfert-1 and Seyfert-2 galaxies, and also found a difference, although in the opposite sense: with Seyfert-1 preferring more overdense regions than Seyfert 2s. However, since the same difference is present in their respective control samples, they concluded that it is not related to their nuclear activity but rather to the different morphological types of their host galaxies. Indeed, they verified that Seyfert-2 AGNs are hosted in later type galaxies, which was noticed by [291] and later confirmed by several authors (e.g., [59, 200, 201]), which are known to be less clustered than earlier type galaxies (e.g., [312]). Summarizing their results, they conclude that although Seyfert-2 galaxies reside in less dense large-scale environments with respect to Seyfert-1 galaxies, they do have close ($D \leq 75 h^{-1}$ kpc, $\Delta v < 600 \text{ km s}^{-1}$) companions much more frequently.

In [169], a three-dimensional study of the local environment of bright IRAS galaxies was performed to further investigate the connection between AGNs and SB galaxies.

For a detailed account of a historical development of techniques that got rid of many different biases, see Dultzin-Hacyan et al. [59] and more recently, Sorrentino et al. [279]. From the statistical point of view [279], have made the comparison of the environment of AGNs, SFGs, and normal galaxies, for a complete sample of 1829 Seyfert galaxies (725 Sy1s and 1,104 Sy2s) and 6,061 SFGs from the fourth data release (DR4) of the SDSS. This study confirms the results found by [59] and by [169, 170]. The authors state that for close systems (<100 kpc), they find a higher fraction of Sy2 compared to Sy1s in agreement; with moreover, the frequency of Sy2s is similar to that of SFGs.

These statistical results are at odds with the simpler version of the so-called unified scheme (hereafter UM, [4]) for ANG that states that the difference between type-1 and type-2 objects can be explained by inclination/obscuration effects only. An alternative (but including) model which is able to explain these results is the evolutionary model [58, 173, 174] to which I shall refer in more detail below. The fact that the results present a problem for the simplest formulation of the unification paradigm does not imply that the unification schemes are totally incorrect. Orientation of the host galaxy as well as evolution should play their role.

A complementary approach has been the investigation of the incidence of nuclear activity in a well-defined sample of interacting galaxies such as close isolated pairs. Since 1999, we focused on the sample of isolated mixed-morphology (E+S) pairs studied by Hernández-Toledo et al. [113, 114], obtained from the Catalogue of Isolated Pairs in the northern hemisphere (KPG; [141]). These pairs are a unique laboratory to study the effect of tidal forces in triggering nuclear activity because they are relatively simple systems where a gas-rich galaxy interacts with a gas-poor one. In such systems, a clean interpretation of the origin and evolution of the gaseous component is possible. E+S pairs minimize the role of the relative orientation of pair component spin vectors in driving interaction-induced effects (e.g., [146]). Since the late-type spiral component is the primary source of gas in a mixed pair, it is therefore expected to be the site of all or most star formation and nuclear activity, although recent results have shown evidence of star formation and AGN activity in a non-negligible fraction of the early-type components of the pairs [53, 112].

In a recent review paper, Dultzin et al. [58] results are presented and discussed from high-resolution, long-slit, spectroscopy data taken at the SPM Observatory at Baja California (for details, see [91]) for the spiral components of 105 mixed-morphology pairs. There is little doubt that these systems are physical pairs [83–85, 113, 114]. The fraction of optical pairs in the sample has been estimated to be 10% [113, 114]. We have reevaluated the statistical completeness for the pair (E+S) sample. The V/V_{\max} test suggests that this sample is complete (in the magnitude interval 13.5–15.5) to a 90% level. The main result from this analysis is that 40% of the spiral galaxies in those pairs show the presence of an AGN. This fraction of AGNs was compared to the fraction in the AMIGA sample of isolated galaxies is, which is 20%, according to Varela et al. [301]. In addition, the sample of spirals in isolated (E+S) pairs also shows a clear connection between the separation of the pair and nuclear activity (Fig. 7.1), with AGNs being closer to their neighbors

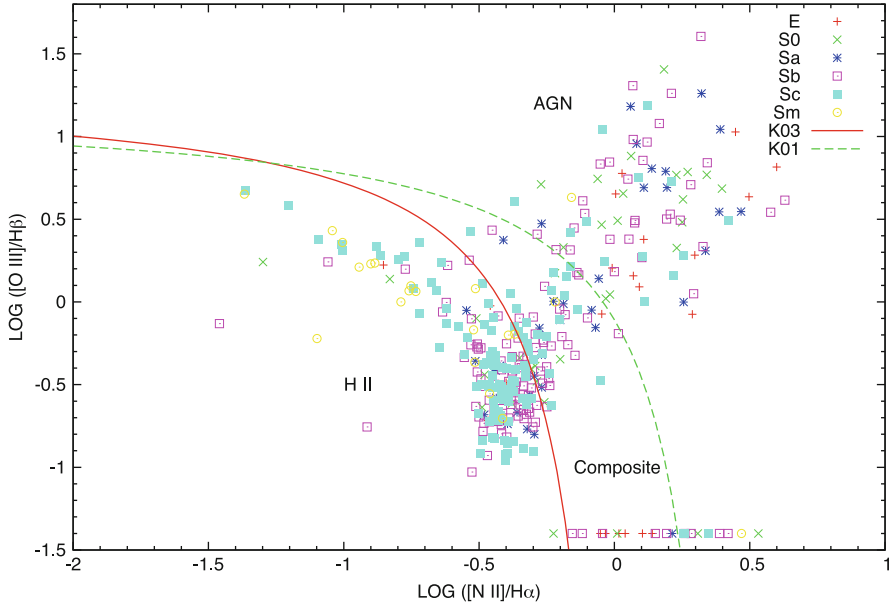


Fig. 7.1 Diagnostic Baldwin, Phillips, and Terlevich (BPT; [9, 309]) diagram of the galaxies with emission-line nuclei in the SDSS (DR7) sample of isolated close (<100 kpc) pairs. The Kewley et al. [149] “maximum starburst line” and the Kauffmann et al. [145] classification lines are shown as *dashed and solid lines*, respectively (see [148] for definitions of maximum starburst (or HII) and composite occupation regions). Different morphological types of the host galaxy are given by different symbols

than star-forming nuclei. These results provide direct evidence of the influence of interaction on the onset and evolution of nuclear activity.

The most striking result, however, is that only a single one, out of the 39 clear-cut AGNs in their sample, is of type-1. This result is again, at odds with the simplest formulation of the unified model (UM). As stated above, this model postulates that type-1 and type-2 Seyferts are intrinsically the same kind of objects, with the only distinction of the orientation of the line of sight of the observer: an Seyfert-2 is observed when our line of sight crosses a putative “obscuring torus” that hides the region where the broad emission lines are produced. A 2.6% frequency of type-1 activity is too low to be explained with an obscuration/orientation effect alone. Interestingly [203], found a similar result from a study of Seyferts in compact groups of galaxies: a deficiency of broad-line AGNs.

But the dynamics of interactions are so much more complicated in these groups that we have continued to study paired galaxies. Studies based on spiral–spiral pairs have shown that starburst and possibly AGN activity in galaxies may be triggered by interactions. Keel et al. [147] studied a sample of 56 nearby spirals in pairs vs a control sample of 86 galaxies and found that interactions induce an enhancement of

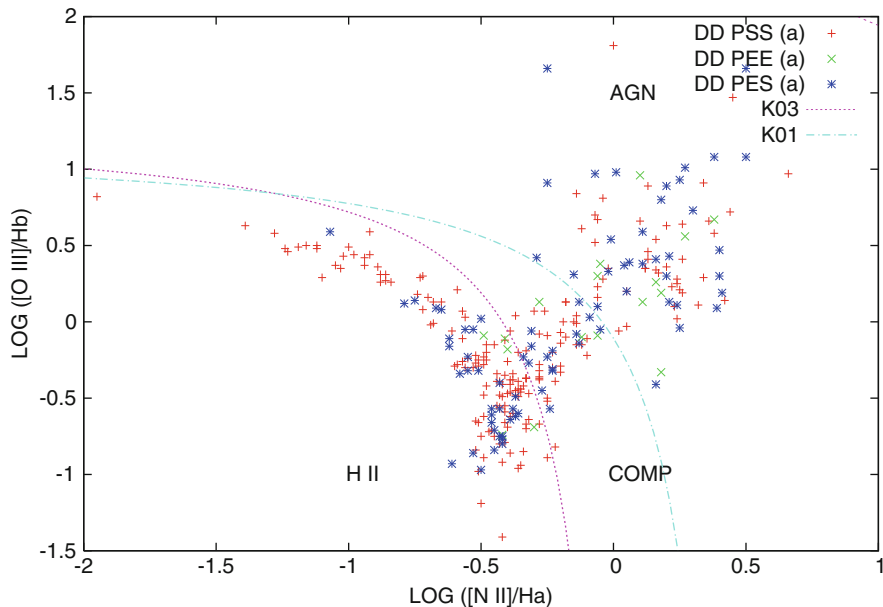


Fig. 7.2 Diagnostic diagram for the Karachentseva sample of isolated emission-line nuclei of galaxies

the level of nuclear activity. Furthermore, they also found a significant fraction of Seyfert or Seyfert-like type nuclei. However, these studies have searched for activity without distinguishing between thermal (starburst, hereafter SB) and nonthermal (properly an AGN) activity. Thus, these studies have not addressed the incidence of type-1 vs type-2 AGNs in pairs of galaxies.

We have recently studied a much larger sample of all the of isolated pairs (as defined by [141]) of all morphological types (S+S, S+E, and E+E extracted from the SDSS (DR7)) and two control samples of isolated galaxies: the one defined by Karachentsev and Karachentseva [142], with similar criteria of the ones used by Karachentsev to define isolated pairs, and another taken from [301], who uses a more rigorous definition in terms of the quantitative value of the tidal force (no relevant difference is found between the two samples, by the way).

The results [112] with respect to the *incidence* (i.e., frequency) of activity are very different depending on morphology (see their Table 1), with a surprisingly high number of 60% for E+E pairs and 20% (no difference with respect to isolated galaxies) for S+S pairs. It remains to be untangled what are the respective roles of bulge mass, gas content, and separation between the closely paired galaxies. *But the fact of the lack of Seyferts type-1 remains unchanged.* Figures 7.1–7.3, show ionization diagnostic diagrams known as “BPT” [9] for the we studied as compared to the same diagrams for isolated galaxies. Separation by morphological types is indicated.

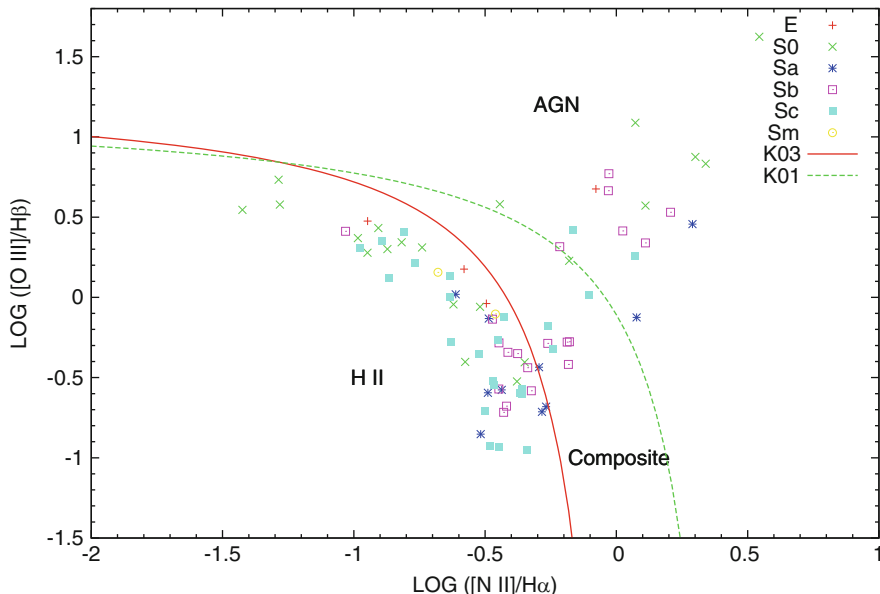


Fig. 7.3 Diagnostic diagram for the Varela sample of emission-line isolated galaxies

All these facts may naturally follow from an *evolutionary scenario*. Such scenario was proposed by [287] for the effects of galaxy interactions to induce a nuclear SB and subsequently, a Seyfert Nucleus. The scenario was further developed by [173, 175], linking the evolution of a nuclear SB induced by the interaction to the formation of a type-2 AGNs and ultimately, to a type-1 AGNs (see [285] for a review and the first observational evidence to support the feeding of the SMBH at hundred of parsec scales).

In the last scenario, besides the possible obscuring/inclination effects present at any of the evolutionary phases, the onset of both nuclear activity and enhanced nuclear star formation is a consequence of the infall of large amounts of gas toward the nucleus, induced by strong tidal forces during the interaction with a nearby companion of similar mass, and follow four distinct phases:

- (a) In the early stages of the interaction, a strong starburst dominates the emission during a first phase of the evolution.
- (b) As more material falls into the innermost regions, the onset of nonthermal activity begins. At first, not only the nonthermal power is low but also the nuclear region (including any broad-line clouds present) is fully obscured and only a type-2 AGN could be observed at this second phase. During this stage, there is a high probability for the detection of the nearby companion.
- (c) As even more material keeps falling, the accretion rate gradually increases, and only a partial obscuration is expected as the spherical distribution of dust flattens

out to form a torus, such that both broad- and narrow-line AGNs can be observed during this third phase.

- (d) In the final stages, most of the dust is either destroyed or swept away by both the winds of massive stars and the AGN itself, and a naked type-1 AGN neatly emerges at the fourth and final phase of this evolutionary scenario. After a timescale of 10^9 year, the evidence of possible past interactions can be erased, either through the completion of a merging event or through the dissolution of an unbounded interacting pair. In order to explain why type-2 AGNs are often found in interacting systems while type-1 AGNs are rarely found with companions, the evolution toward the final fourth phase should take about this long.

At least qualitatively, the described evolutionary scenario naturally accounts for the main statistical properties of the nuclear emission found in previous studies and the results from the present sample of spirals in isolated (E+S) galaxy pairs, implying that interactions play a key role in the triggering and evolution of nuclear activity.

Can the results obtained for nearby AGNs be extended to distant quasars? What recent studies have focused on environments of quasars?

It is obvious that the problem becomes more complicated both from the theoretical and observational point of views; however a similar evolutionary scenario has been proposed and seems to explain many existing observations.

From the theoretical point of view, the luminosity of quasars is so much higher than the effects of a strong wind from the accretion disk and therefore feedback effects have to be included in an evolutionary model. Recently, Menci et al. [214] introduced a new scenario, in which the absorption properties of an AGN depend both on the orientation to the line of sight and on the time needed to sweep the central regions of galaxy disks. On the basis of galaxy interactions as triggers for AGN accretion and on expanding blast waves as a mechanism to propagate outward the AGN energy injected into the interstellar medium, one may expect that X-ray-selected, moderately obscured quasars are caught at a later stage of feedback activity than highly obscured, Compton thick quasars. Martinez-Sansigre et al. [202] report *Spitzer* (IR orbital observatory) spectra dominated by AGN continuum but showing PAHs (complex molecules present in starburst regions) features in emission in samples of ultra luminous infrared galaxies (ULIRGs, see below) and radio-selected obscured quasars at $z \sim 2$. Lacy et al. [183] find evidence for dust-obscured star formation in the spectra of type-2 quasars (my bold characters). All these findings are in general agreement with the evolutionary scenario.

From the observational point of view, the study of high-redshift AGNs which are fainter in optical light is complicated by obscuration and requires a multifrequency approach. X-Rays, IR, and radio frequencies are less affected by obscuration. We are also dealing with objects at different cosmological evolutionary stages. An extreme example of obscuration in the local universe is represented by LIRGs and ULIRGs. With bolometric energy outputs rivaling bright quasars, luminous infrared galaxies

(LIRGs) and ULIRGs are some of the most extreme objects in the universe (for a review, see [262]). These powerful objects provide the opportunity for probing one possible final stage of interaction: a merging process, that is, the existence of a dust-enshrouded double AGN within the envelope of the host galaxy merger (e.g., [321] and references therein).

Counterparts at relative high z of the local universe ULIRGs have been discovered over the last few years: an increasing number of interacting and disturbed molecular gas-rich galaxy systems, showing both coeval powerful starburst (SB) and quasar activity. Reference [163] discovered the first and unambiguous example of an active SMBH pair separated by $d \approx 1.4$ kpc in the center of the ULIRG NGC 6240. For many other cases, see [239] and references therein.

In all the cases reported (see, for example, [242] and references therein), one AGN or both, are type-2 quasars (my bold characters), which is what we expect in this still obscured phase of evolution according to the evolutionary scenario described above.

Thank you, Deborah. Environmental studies provide circumstantial evidence, as they cannot offer a view of the proximate regions of the central black hole, where infall of accretion material should actually occur. In the previous chapter, Isaac Shlosman already reviewed several mechanisms that can in principle be able to drive a flow toward the active nucleus. Here, we would like to review the direct evidence in favor of infall, as well as analyze in more detail the physical processes and their actual applicability in the AGN context. We start from the scale of the BLR, and we progress to larger and larger scales.

7.2 The Observational Evidence of Infall from the Circumnuclear Environment

Dear Gordon (Richards), while the entire quasar process involves the hypothesis of accretion/inflow, most of the direct evidence involves collimated and uncollimated outflows. Where are the observational evidences for AGN inflows?

Since quasars are clearly accreting matter, it makes sense to consider the possibility of an inflowing contribution to the BELR. Some recent evidence of inflows/redshifted gas comes from Hu et al. [124, 125] who found that Fe II appears to be redshifted with respect to $H\beta$. Ferland et al. argue that this makes sense if we are seeing the shielded side of the infalling high column density “clouds” [75]. Indeed [88], has argued that the C IV blueshifts may be due to *infalling* gas—contrary to our discussion above. While we find an (outflowing) wind explanation for C IV more convincing, that certainly does not preclude an inflowing component of the BELR.

It is also been noted [288] that radio-loud quasars tend to have redward asymmetric $H\beta$ lines. While this red asymmetry may or may not indicate an inflowing

component, the observation that $H\beta$ tends to be redward asymmetric when CIV is systemic, but not when CIV is blueshifted, argues for different locations/kinematics for the high-ionization and low-ionization emission-line gas [205, 288]. In general, the BELR gas is thought to be too far from the black hole for the redward asymmetries to be due to a significant *gravitational* redshift, but that possibility has certainly been considered [38, 241].

Overall, the idea of an infalling component is interesting and deserves further study. However, one has to consider the angular momentum problem: it is already difficult enough to shed the angular momentum of the accreting material without invoking another infalling component. In addition, if the infalling component is related to the accretion disk itself, it is worth remembering that it can be dangerous to interpret velocities as being related to distance for a flattened, rotating distribution (i.e., a disk) since the observed velocity distribution of an emission line has a complex spatial dependence in the disk (e.g., [123], their Fig. 1). Nevertheless, the subject of inflows is clearly ripe for further investigation.

Thank you Gordon. We now leave the BLR context, and ask Johan Knapen on the evidence of infall and fueling on larger spatial scales.

Dear Johan (Knapen), observational evidence for infall is important in the quasar context because it might ultimately provide evidence for the fuel needed to sustain the activity. Please review the observational evidence for infalling matter on all spatial scales (i.e., from tens of kpc down to less than 1 pc)? How well do the observations support the accretion scenario? What is still missing? How might future instrumentation improve our ability to test the accretion scenario?

Observational evidence for infall is important in the quasar context because it might ultimately provide evidence for the fuel needed to sustain the activity. Here, I review the observational evidence for infalling matter in active galaxies, with a particular emphasis on the smallest observable scales. I consider indirect and direct evidence for inflow in active galaxies and review what we know in this context about the host galaxies of both low- and high-luminosity AGNs. Finally, I describe the prospects of using the upcoming observing facilities to study the details of inflow into the black hole regions of AGNs.

How does the fuelling of active nuclei occur?

Most galaxies are thought to contain supermassive black holes in their centers [165], and such black holes have long been considered to lie at the origin of nonstellar nuclear activity (e.g., [12, 193]). Material falling into the zone of influence of the black hole is used as fuel for the active galactic nucleus (AGN). At the extreme end of the spectrum of nuclear activity are luminous quasars, which may need up to $10 M_{\odot} \text{ year}^{-1}$ of fuel to be powered. This is not at all a large quantity of fuel, not even over relatively long lifetimes of quasar activity of up to say 10^8 year . The problem is not the amount of fuel that is available in a quasar host galaxy, but how to get it to the compact inner region near the black hole. And a second, related, problem is how to fine-tune the small amount of material that reaches the black

hole so that the black hole growth leads to the observed constant ratio between the masses of the black hole and its surrounding bulge.

The main problem in transporting gaseous material inward in galaxies is that this gas is usually in rotation, and thus needs to lose significant quantities of angular momentum. This can be achieved by shocks, and relevant shocks can be set up relatively easily by non-axisymmetries in the disk, in the form of bars and interactions, but also of less prominent actors such as spiral arms or ovals/lenses (e.g., [34, 157, 268]). This has led to the idea that bars, or nested bars, may be related to fueling AGNs and/or stellar circumnuclear activity in the form of starbursts [275], although statistical evidence from observations that this is indeed a direct relation has been hard to come by (see next section). For the relation between interactions and starburst or AGN activity, the situation is not much different (see below), although one is often led to believe that the fact that extreme starbursts, such as ULIRGs, are almost all interacting or merging is indicative of the *rule*, rather than the *exception* (see [159]).

For high-luminosity AGNs, such as the QSOs that are the subject of this book, the situation is slightly different, mainly because their host galaxies tend to be massive ellipticals rather than the spirals which define the hosts of less luminous AGNs such as Seyferts (e.g., [60]). Rotation plays a much reduced role in massive ellipticals, but the fuel which falls into the zone of influence of the black hole and powers the AGN must still fall in to very small scales, just like in the AGNs hosted by spiral disks. Infall must still play a role. In addition, inflow on much larger scales must have played a significant role in the early universe, where both the merger rate and the AGN fraction were much higher than they are in the present-day universe. During the galaxy assembly phase, the frequent interactions and mergers are presumed to have caused high gas accretion rates. How much of this material was available for AGN fueling, and on what timescales, is much less clear.

I will now review observational evidence for infall of material mainly into the central regions of galaxies. I will discuss direct and indirect measurements of inflow right below and afterward, show how they might be applicable to low- and high-luminosity AGNs. In the next chapter I will introduce some of the future observational facilities that might shed further light on the issues discussed here. Related previous reviews include those by [111, 154, 274].

What are the main lines of observational evidence indicating gas inflow?

Indirect Evidence: There are a number of pieces of indirect evidence for radial gas inflow in galaxies, most of which concern barred galaxies. With indirect, I mean in this context that the inflow itself has not been observed, but the effects resulting from this inflow have. Typically, this is in a statistical sense.

Perhaps, the most comprehensive evidence comes from surveys of the molecular gas distribution in barred vs non-barred galaxies, which can easily be transformed into a mass concentration index. This has been done by Sakamoto et al. [260] for a sample of 10 barred and 10 non-barred galaxies, and afterwards, by Sheth et al. [272] who collected CO observations of 29 barred and 15 non-barred galaxies.

These studies concluded that the barred galaxies have, in a statistical sense, more concentrated CO emission and thus, presumably, molecular hydrogen. Several caveats can be highlighted, though. Firstly, the effect is purely statistical, and the scatter is very large. Secondly, these studies assume that the X -factor, which is used to transform CO luminosity into molecular hydrogen mass, is constant among galaxies (in particular, from barred to non-barred) and within them (central kiloparsec vs. further out), which it may not be. Thirdly, as pointed out by Komugi et al. [164], the effect of bulges, measured through varying Hubble types, on the central gas concentration may be more important than that of bars.

Further indirect evidence comes from the increase in star formation in the central regions of barred galaxies compared to non-barred galaxies. This is seen from a variety of observations, such as the central concentration of PAH emission [249], the shapes of profiles of $H\alpha$ emission [135], or the properties of HII region populations [3], which all show differences between barred and non-barred galaxies compatible with enhanced star formation in the central regions of barred galaxies, which comes about as a result of gas being transported from the disk to the center under the influence of the bar.

In addition, there is a lot of work, going back to papers by Hummel [126] or Hawarden et al. [109], showing that nuclear starbursts seem to occur preferentially in barred host galaxies (see review by [154], which also points out some possible caveats and exceptions). The occurrence of rings in barred galaxies (e.g., [24]) is often seen in conjunction with all this, but as [155] and [35] have shown, nuclear rings hardly show any preference for barred galaxies, and as many as 20% occur in non-barred hosts. This does not invalidate that rings are connected to inflow, but does show that only a little of it is needed.

The conclusion is that there is a significant amount of indirect evidence that bars indeed cause an inflow of gas toward the central regions of galaxies. As a proof of concept, this is useful, but it is less so for AGN fueling. The scales considered so far are of 100s of pc to a kpc, very far removed from where an AGN needs its fuel delivered, and star formation rather than nonstellar activity may result.

Direct Evidence: In recent years, there has been a steady stream of papers announcing the observation of gas inflow in local galaxies, often moderate AGNs. I review these under the heading “Direct Evidence,” even though often, the observation is still of phenomena such as spiral arm streaming, which may be at least one step away from observing the inflowing gas itself. This research activity is due mostly to new instrumentation, and in particular to high-spatial resolution integral field spectroscopy on large telescopes, which allows one to study the two-dimensional velocity distribution in regions relatively close to the nuclei of galaxies.

As examples, we cite the work by Fathi et al. [74] and Storchi-Bergmann et al. [286] who report gas streaming motions along nuclear spiral arms in the LINER/Seyfert-1 and LINER (respectively) hosts NGC 1097 and NGC 6951 from GMOS integral field spectroscopy on the Gemini telescopes. In the case of the latter galaxy, they use these observations to estimate a mass inflow rate of ionized gas of $\sim 3 \times 10^{-4} M_{\odot} \text{ year}^{-1}$, claimed to be roughly enough to power the LINER.

Fathi et al. [73] confirm from high-resolution Fabry–Perot observations that gas spirals into the nuclear starburst region of M83 from its outer regions. Riffel et al. [255] used Gemini to study the Seyfert host NGC 7582, and found evidence for both outflow, due to feedback from the AGN activity, and inflow which traces the feeding of the Seyfert nucleus. Van de Ven and Fathi [300] model the gas inflow in, again, NGC 1097, reaching the conclusion that the resulting inflow rate is comparable to that needed to fuel the black hole (though noting the difference in scale of several orders of magnitude). Davies et al. [50], who used the SINFONI on the ESO VLT to observe, once more, NGC 1097, also distinguish between the inflow rate as measured along the nuclear spiral arms, and the much smaller net inflow or accretion rate of gas which reaches the central regions of tens of pc.

This is an important distinction, because in both bar and spiral streaming, only a small fraction of the observed flow (and even inflow) is in fact *net* inflow. Most of the gas mass seen to be flowing in at a certain position along the spiral arm or in the bar is canceled in its effects by gas flowing out elsewhere. In the case of bars, this is simply because bar orbits are elongated, hence by definition, gas on bar orbits exhibits radial inflow roughly half the time—the *net* inflow is much smaller than the observed motion.

Concluding this section, we may state that the various observations lead to inflow estimates that are compatible with what is needed to fuel the moderate starburst or AGN activity in the nucleus. But we are still, in spite of the good angular resolution, orders of magnitude away from black hole accretion scales, we still trace mostly projected inflow rather than net inflow, and we are still limited to nearby and relatively low-luminosity AGN.

How are the host galaxies of low-luminosity AGNs affected?

AGNs of the Seyfert and LINER variety occur preferentially in disk galaxies. Much of the study into the relationships between the AGNs and their hosts has focused on statistical studies of non-axisymmetries in the hosts. As indicated earlier, such non-axisymmetries in the gravitational potential can lead to loss of angular momentum in the rotating gas, which will move to smaller radii and may eventually become available for fueling of the nuclear activity.

The most prominent causes, and observational tracers, of non-axisymmetry are galactic bars and interactions, although spiral arms, ovals, and lenses can also lead to inflow at a generally more reduced level. As proposed in detail by Shlosman et al. [274, 275], a system of nested bars can, in principle, be invoked to solve the fueling problems of AGNs because it would allow the gas to flow inward to the very small radii at which it can get captured by the black hole and transformed into luminosity.

Attempting to establish whether AGN host galaxies are, for instance, more often barred or interacting depends critically on comparison with a control sample which must statistically be as equal as possible to the AGN sample in all properties, *except* the presence of nuclear activity (see [188] for an early overview). After discarding studies without a proper control sample, we find that there is not, in general, strong evidence for an excess of either bars, or interactions, among low-luminosity AGN hosts.

Do bars matter?

The fraction of barred galaxies among Seyfert hosts has been studied by many authors, starting with Adams [1]. Most of the older work is plagued by imperfections such as the absence of a properly matched control sample or the use of nonoptimal methods to decide whether a galaxy is barred or not (as reviewed by [154]).

When high-quality near-infrared (NIR) images are used to find properly defined bars in carefully matched samples of active and nonactive galaxies, the results are not overwhelming. Mulchaey and Regan [221], for instance, found no difference in bar fraction, whereas [161], and [185] found a slightly higher bar fraction among the Seyfert galaxies (4/5 of which were found to be barred vs. 3/5 of the nonactive galaxies) but because the samples were not very large this result is barely significant statistically.

Hao et al. [103] reexamined this issue using a much larger sample selected from the SDSS of over 1,000 galaxies for which [10] had earlier determined whether or not they have a bar. Using the SDSS spectroscopy, Hao et al. correlated the presence of AGN and starburst activity with that of a bar. Reporting bar fractions of 50%, 47%, and 29% (no uncertainties given) for AGNs, starburst, and nonactive galaxies, respectively, Hao et al. qualitatively confirm the excess of bars among AGN hosts reported by [161] and [185], but find that the starburst hosts show an equally large excess (the latter have long been known to be preferentially barred, as reviewed by [154]). Hao et al. [103] recognize that their bar determination is based on optical and not NIR imaging (which partly explains their relatively low bar fractions) but note that this should not have changed the relative bar fractions in active vs. nonactive galaxies.

There is thus evidence for a slight excess of bars among low-luminosity AGN hosts as compared to nonactive galaxies, which may well be indicative of the presence of a nonaxisymmetric component in the gravitational potential, leading to angular momentum loss and thus inflow of disk gas. There is, however, no one-to-one correlation between the presence of a bar and that of Seyfert activity, and many Seyfert hosts are not barred. Also, secondary agents will be needed to transport the material further in than the roughly 1-kpc radius region where inflow due to large bars slows down (and where, as a consequence, circumnuclear star-forming rings exist; [35]). Smaller bars may facilitate this second stage of inflow [275], although observations of nested bars have not yet shown that these occur significantly more often in Seyfert hosts than in nonactive galaxies [185].

Are gravitational interactions among galaxies relevant?

Although the extreme and very rare galaxies with the highest star-formation rates, in particular the ULIRGs almost without exception show distorted morphology indicative of interactions or mergers, it is not clear whether in general galaxies with enhanced star formation in the nuclear region (often referred to as starbursts, but see [159]) occur in response to galaxy–galaxy interactions (as reviewed by [154] and [159]).

Of the low-luminosity AGNs, a number of rather spectacular Seyfert galaxies are obviously interacting or in an advanced stage of merging (e.g., NGC 2992 or the ULIRG Mrk 273). But searches for either the numbers of companion galaxies to Seyfert and nonactive galaxies or the fractions of AGNs and nonactive galaxies in different environments have not yielded unambiguous evidence for a statistical connection between the occurrence of Seyfert activity and interactions (see references in reviews by [188] and [154]). Newer results, based partly on the SDSS, including galaxies at higher AGN luminosity and/or larger distance (up to a redshift of around unity), also generally fail to find evidence for a connection between interactions or even an excess of close companions and AGN activity (e.g., [87, 97, 191, 240, 250], but see [166]).

The conclusion is that although in individual cases low-luminosity AGN activity can most certainly occur in interacting or merging galaxies, there is no evidence that these two phenomena are causally connected.

What are the properties of the host galaxies of high-luminosity AGNs?

For several reasons, the study of the host galaxies of QSOs is much harder than that of Seyfert or LINER hosts. Firstly, the contrast between the luminosity of the AGNs and its host galaxy is much higher in QSOs, and secondly, QSOs are much rarer in the local universe which means in practice, that those studied are at larger distances. These two factors alone make it very hard to observe the hosts and have led to the use of the Hubble Space Telescope (HST) for the most relevant studies (see below). In addition, thirdly, the host galaxies of QSOs tend to be of earlier morphological type, often massive ellipticals (e.g., [60]). This implies that studies must focus more on the structural properties than on particular components (such as bars) of the galaxies and that any handle on observing inflow becomes much more indirect and thus difficult.

Various groups have used the HST to image the host galaxies of QSOs (e.g., [7, 56, 60, 176, 208, 210, 236, 254]). The factors listed in the previous paragraph imply that these studies cannot go much further than determining the most basic of the structural parameters of the hosts, such as luminosity and size, but the consensus is that the hosts of luminous QSOs tend to be massive ellipticals, relatively undisturbed, and not significantly different, as far as can be ascertained, from comparable nonactive galaxies. These results are mainly based on the middle part of the host galaxies; the faint outer parts, where tidal features might be found, being too faint to observe; and the bright inner parts being contaminated by the QSO emission.

Whereas these results can be used to constrain many different aspects of AGN physics and galaxy evolution, and although they are incredibly difficult to obtain, they shine very little light on the main issue discussed here: inflow of matter to the nuclear region. What is clear is that the role of clearly identifiable agents such as bars, rather than prominent in many low-luminosity AGNs, is very much reduced or even negligible in the high-luminosity QSOs. The fraction of the host mass involved in the nuclear activity is very small though, and black hole growth may even be determined by the mass-loss rate of evolved stars in gas-poor central regions [144].

Considering in addition that QSO-type activity is exceedingly rare among galaxies in the nearby universe, we should hardly be surprised if it may turn out that we cannot identify tangible statistical links between gas inflow in the inner regions and high-luminosity AGN activity.

Concluding, the AGN fueling problem is not whether enough gaseous fuel is available in a host galaxy but how to get this material near enough the center. To move so far in, gas must lose significant amounts of angular momentum, which can be achieved by non-axisymmetries in the gravitational potential such as bars, or by interactions. Because star formation in the central region of a galaxy may precede, or coincide with, the nonstellar activity, these issues are related directly to both cosmological and secular evolution of galaxies.

There are various pieces of evidence that confirm that indeed inflow occurs in galaxies, and that this is often under the influence of bars. Direct links to AGN activity are much harder to identify, though. There is some evidence that low-luminosity AGN hosts are more often barred than otherwise similar but nonactive galaxies, but the effect is statistical and at a rather low significance level. There is no evidence that AGN activity is statistically connected to galaxy–galaxy interactions.

The host galaxies of high-luminosity AGNs, powerful QSOs, for instance, tend to be massive ellipticals that appear to be identical in their structural properties to nonactive comparison galaxies. There is no observational evidence for inflow in such powerful AGNs, and for reasons outlined above, it will not be trivial at all to uncover such evidence in future.

Future facilities will allow us to observe the morphology and kinematics and deduce the physical properties of the surroundings of AGNs with unprecedented angular resolution, of typically 10 mas, and across most of the optical to radio wavelength domain. This should allow us to reach the BLR in nearby, mostly low-luminosity AGNs and in the nearest cases of luminous QSOs, maybe the outer edge of the region where the black hole extends its influence. In addition, very deep infrared imaging with the next-generation space telescope should shine light on whether mergers and interactions are responsible for cold gas inflow into forming galaxies at high redshifts. The observational future in this area of astrophysics is thus very exciting.

Thank you, Johan. Having heard the answer of an observational astronomer, we know turn the same questions to a theorist.

Dear Isaac (Shlosman), where is the inflow? How can we trace it?

According to the AGN paradigm, they are powered by accretion onto the SMBHs at the rate of $\dot{M} \sim 1 \eta_{0.1}^{-1} L_{46} \text{ M}_{\odot} \text{ year}^{-1}$, where $\eta_{0.1} \equiv \eta/0.1$ is the efficiency of converting the accretion energy into radiation and $L_{46} \equiv L/10^{46} \text{ erg s}^{-1}$ is the accretion luminosity. Half a century into AGN research, we have identified some of the motions in the region as outflows (winds), and a solid theoretical base exists to understand the physical mechanisms which trigger and maintain these outflows. We still have no *direct* evidence for the inflows on smallest spatial scales, $\lesssim R_i$ (see Sect. 6.8.1 and below), although evidence for outflows on such scales is plentiful. Why is this so? Why is it so much more difficult to observe the inflow itself?

Where are the inflows or outflows in correspondence of the broad-line regions and of the molecular torus?

For a long period of time, we have been aware of large velocities, $\sim 10^3\text{--}10^4\text{ km s}^{-1}$, associated with the AGNs and especially with QSOs, in the region which is responsible for the formation of emission lines of H and the CNO gas. Over time, the observed broad emission-line region has been considered as gravitationally confined, inflow and/or outflow dominated, and each of these possibilities had many followers. Unfortunately, *the signatures of an inflow on scales $\lesssim 1\text{ pc}$ have “evaporated” under scrutiny.* It is probably the detection of broad absorption line (BAL) throughs in the QSO PHL 5200 [194] and others, blueshifted of up to $\sim 0.2c$, which has clearly and unequivocally identified them with massive outflows. It was not clear, however, whether the BAL QSOs are mere curiosity or these winds are characteristic of all AGNs. Presently, the outflow signatures in AGNs are ubiquitous and are not limited to absorption only but are prominent also in the emission lines.

On spatial scales just outside the broad emission-line regions, $\gtrsim 1\text{ pc}$, lies colder obscuring material known as the torus—a geometrically and optically thick configuration of dusty molecular gas. Original analysis of dynamics of these tori has been based on the model of a net slow inflow driven by cloud–cloud collisional viscosity [172]. Stirring of the torus by supernovae and stellar processes has been found insufficient, and viscous collisional heating has been postulated for preventing the torus from collapsing to a thin disk. Despite subsequent numerical work advancing the idea of a stellar feedback origin of the torus in the region of 1-pc, it appears to contradict observations of a much smaller torus confined to the region around $\sim 1\text{ pc}$ from the SMBH. Analysis of the data, supplemented by radiative transfer in the clumpy medium, in tandem with a hydromagnetically driven disk wind currently provide the best explanation for the origin of the torus [63, 119].

To summarize, the early claims that the most prominent features of AGNs characterize the accretion flows onto the SMBH were not confirmed by later analysis, which indicated that the broad emission and absorption lines are signatures of outflows. Moreover, even the region of the obscuring torus appears to be dominated by an outflow. Yet, as we shall argue below, the inflows have been detected on larger scales.

How can we trace the inflow from the largest to the smallest scales?

Given the estimates for accretion rates onto the SMBHs in QSOs, how is it possible to hide such massive inflows? For hints, we look at the available evidence for inflows associated with star formation, where accretion rates are in the range of $\dot{M} \sim 10^{-5\text{--}4} M_{\odot} \text{ year}^{-1}$, for massive stars. While this rate is much lower than that anticipated in the QSOs, the star formation regions are much closer to us, $\sim 1\text{ kpc}$ or even less and so can be resolved much better spatially. Are inflows observed in the star-forming regions?

The answer is positive, but *only* on the largest scales, those corresponding to molecular cloud core outskirts, $\sim 0.01\text{--}1\text{ pc}$. Still rare, these inflows have been observed through Doppler spectroscopy of molecular lines, such as optically thick lines of CO and CS [225], in the form of double-peaked line profiles, or as

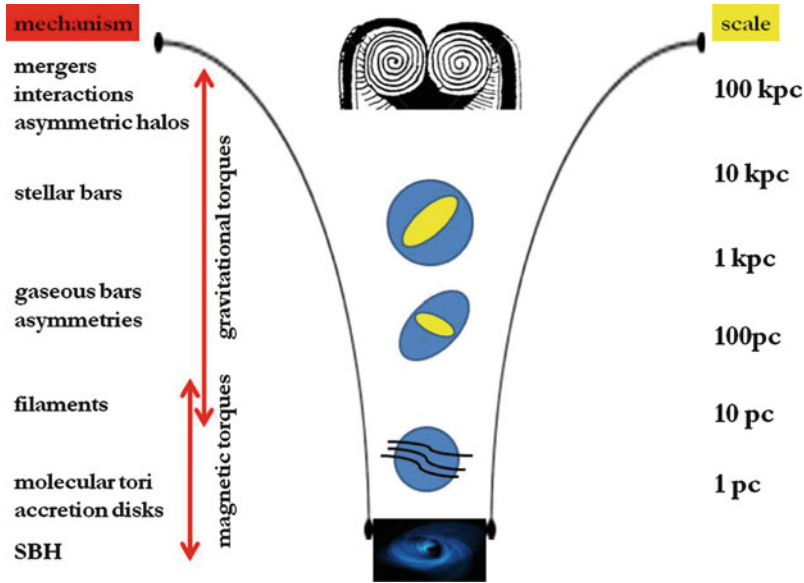


Fig. 7.4 Schematic representation of dominant mechanisms triggering gas inflows toward the SMBH and corresponding spatial scales

blue-skewed single lines (e.g., [319]). This “infall asymmetry” forms when the foreground collapsing gas that has sufficient optical depth has a lower excitation temperature than the background gas. For consistency, maps in optically thick and thin lines are required to differentiate between infall, rotation, and bipolar outflows. For the nearby star-forming complexes, the resolution is $\sim 0.007 - 0.02$ pc at a distance of 140 pc. Such spatial resolution is not achievable yet in AGNs, for example, SINFONI—NIR adaptive optics integral field spectrograph provides a peak spatial resolution of $0.05''$ at $2 \mu\text{m}$ (\sim few pc for nearby AGNs) and intermediate spectral resolution of $\sim 100 \text{ km s}^{-1}$ —insufficient to measure the much smaller infall velocities. Double peaks in molecular gas have been observed in AGNs as well but have been interpreted as due to rotation, for example, in Arp 220, or outflows.

We have separated the spatial scales into four characteristic scales and list them with short commentaries, starting from large scales and down to the smallest ones (see also Fig. 7.4).

Largest Scales, $\gtrsim 1$ kpc: Inflows have been observed triggered by stellar bars and strong interactions and mergers which frequently generate bars and substantial distortions in the disk (e.g., [158]). The concurrent star formation ranges from an elevated rate in the galactic disk as a whole to the starburst rate in the central region.

Intermediate Scales, ~ 50 pc–1 kpc: Inflows, when observed, are associated with stellar or gaseous bars and multiple spiral arms (e.g., [137–139, 160, 264]). Potential errors in estimating the inflow rates here lie in associated noncircular motions in the

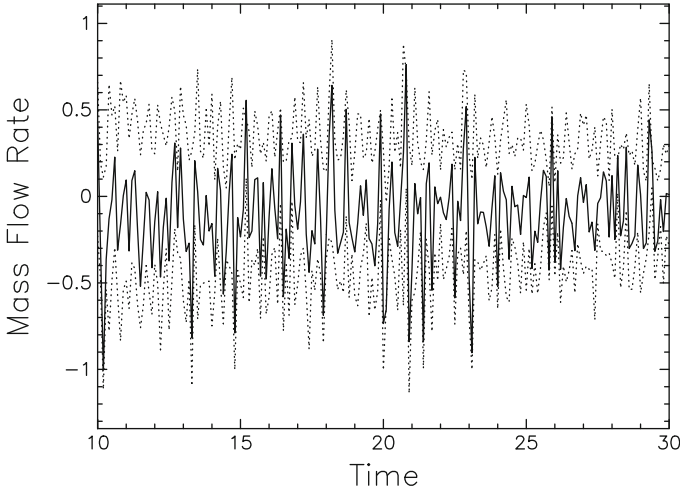


Fig. 7.5 Time evolution of the gas inflow (*negative*) rate (in $M_{\odot} \text{ year}^{-1}$) across the nested bars interface, $R \sim 1$ kpc, which is the corotation of the nuclear bar and the ILR of the large-scale bar. *Upper dotted line*: Flow rate within $\pm 45^{\circ}$ of the major axis of the large-scale bar. *Lower dotted line*: Flow within $\pm 45^{\circ}$ of the minor axis of the primary bar. *Solid line*: Total flow across the nested bars interface. Time is given in units of dynamical time, $t \sim 4.7 \times 10^7$ years (from [276])

gas. These estimates are often taken at face value, although numerical simulations have shown that an inflow along a particular direction is associated with an outflow along other directions [276]. Hence, the net inflow can be very sensitive to these details. Moreover, when noncircular motions on larger scales interact gravitationally with those on smaller scales, chaotic motions develop (Fig. 7.5). High inflow velocities detected at some positions are not representative of the overall flow in the region.

On these scales, starbursts are often observed in the nuclear rings which are positioned inside the inner Lindblad resonance of the large-scale bars. These rings are clear signatures of recent inflows from large scales.

Small Scales, $R_i \sim 50$ pc: Detections of inflow are very scarce and contradictory (e.g., [222] for NGC 1068) and superposed on molecular gas rotation (e.g., [117]) and turbulent motions (e.g., [36] for the galactic center). Filaments have been observed, including in the galactic center, and appear confined by magnetic fields (e.g., review by [298]). Starbursts in some Seyfert-2 nuclei have been detected, and some indication exists that this could be the tail of the nuclear starbursting ring distribution (e.g. [156]). This strengthens the explanation of nuclear starbursts as by-product of radial gas redistribution driven by mechanisms discussed in Sect. 6.8. The mass loss from these stars can in principle be part of the (processed) fuel for less luminous AGNs but hardly for QSOs. Nuclear stellar disks on these scales have been predicted [273] and detected [65].

Smallest Scales, $\lesssim R_i$: With one exception ([16] for Arp 151), no direct detections of inflows have been reported. Bentz et al. claim a signature of radial inflow in the broad-line region, based on the (one-dimensional) time lag of the $H\beta$ emitting gas variability. This result must be verified by means of full two-dimensional reverberation mapping. In a number of AGNs, maser emission points to a disk rotation (e.g., [62,96,115]). In addition, cold winds provide circumstantial evidence for the underlying cold accretion flows.

Thank you, Isaac. We now turn our discussion to the effect of outflows from quasars on their environment.

7.3 Evidence of Feedback

7.3.1 Interplay Between Radio Jet and the Environment

Dear Raffaella (*Morganti*), how might radio ejecta affect the interstellar medium of the host galaxy? Can the results obtained from nearby AGNs be extrapolated to luminous quasars?

Different diagnostics (e.g., kinematics and ionization of the gas) have already shown that, on scales from tens to hundreds of kpc, relativistic plasma jets can have an impact on the surrounding ISM. This is one of the reason why in recent years, the interest in AGNs has spread to a wider community: the realization that feedback effects associated with AGN-induced outflows can represent an important process in galaxy evolution ([55, 277] see also [26] for an overview). They can affect the clearing of the circumnuclear regions and halting the growth of the super massive black holes, regulating the correlations found between the black hole mass and the host galaxies bulge properties and preventing the formation of too many massive galaxies in the early universe.

In many powerful radio galaxies, the extended emission lines show highly perturbed kinematics in the regions along the radio axis (see, for example, [280] and references therein). In high- z radio galaxies, high velocity gradients are observed in the $Ly\alpha$ halos (see e.g. [227, 303] and references therein). Using integral field spectroscopy, extended, kpc-sized outflows of ionized gas corresponding to significant fractions of the interstellar medium have been observed in massive galaxies (see [227] and [226] for an overview). The large line widths (FWHM $\sim 800 - 1,000 \text{ km s}^{-1}$) suggest that the gas is very turbulent (see [227] and Fig. 7.6). A “cocoon” of hot, over-pressurized gas inflated by the radio jet may be the main driver of accelerating and ionizing the dense and warm gas we observe in the optical line emission. This perturbed, wide region is also seen in the results of numerical simulations (see for example [171] and reference therein) showing how the passage of the jet creates a large cocoon of shocked ambient gas.

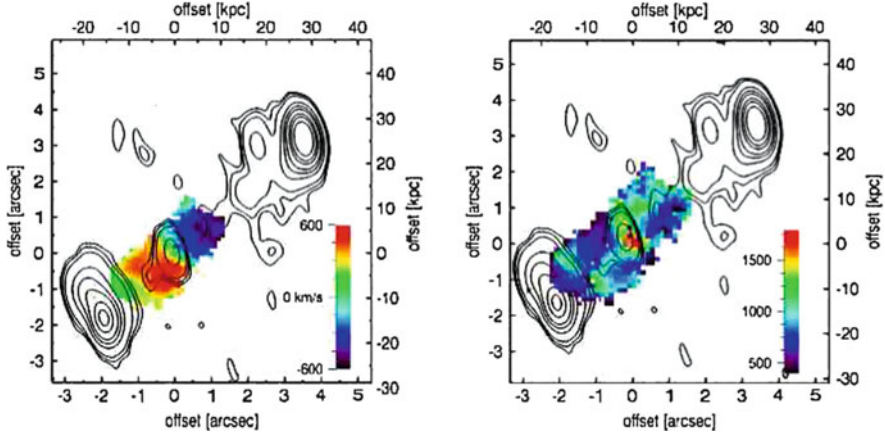


Fig. 7.6 Velocity map (*left*) and map of the line widths obtained from [OIII] $\lambda 5007$ A emission lines in the radio galaxy MRC0406–244 at $z = 2.42$. Color bar shows the relative velocities and FWHM in km s^{-1} the contours indicate the 1.4 GHz morphology. From [227]

This interaction appears to be even more relevant during the early stages of the evolution of the radio source, that is when the jet is interacting with the natal cocoon of gas deposited in the inner regions during the triggering event, often considered a merger and/or interaction (see, for example, [120] and references therein). Numerical simulation also show the highly complex interplay between a newly born radio jet and the rich and clumpy surrounding ISM (see for example, [262, 290, 308] and references therein).

Other extreme examples of interaction between the radio plasma and ISM are the X-ray cavities in the hot gas that are hollowed out by the expanding radio lobes (see, for example, [211], see also Fig. 7.7). The existence and the characteristics of such cavities show that the radio emission can prevent the hot gas from cooling and forming stars. These studies already illustrate that the impact of radio plasma jets is not only limited to their (often) very collimated structures but that the effect extends to the surrounding gas by the impinging of the jet in the ISM.

The cold gas component is also playing an important role. Surprisingly, fast (from 800 to $2,000 \text{ km s}^{-1}$) and massive outflows have been discovered in neutral hydrogen (H I, detected in absorption against the strong continuum source) in a number of nearby powerful radio galaxies [218, 219, 231], see Fig. 7.8. Only in a couple of cases the exact location of the outflow could be identified. At least in these cases, H I outflows occur at the location of a radio-jet hot spot at kpc distance from the nucleus (IC 5063 and 3C 305, see [217, 218] see also below). This suggests that the fast H I outflows are driven by the interactions between the expanding radio jets and the gaseous medium enshrouding the central regions. The associated mass outflow rates are up to $50 M_{\odot} \text{ year}^{-1}$, which is two orders of magnitude larger than similar fast outflows detected in the ionized gas in these systems, indicating that AGN feedback may be dominated by the cold and neutral component of the ISM.

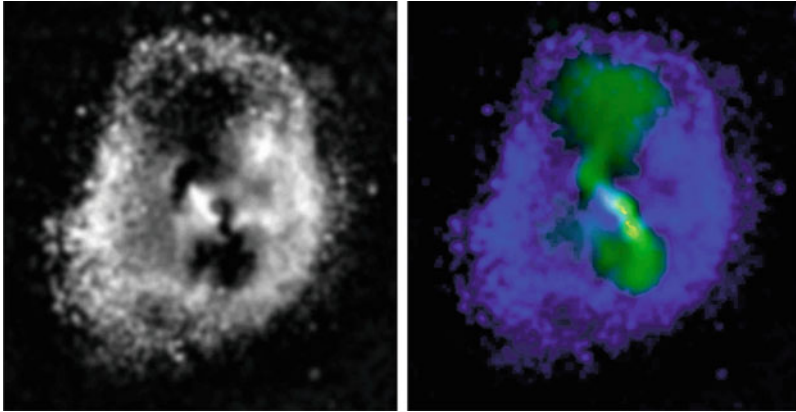


Fig. 7.7 *Left:* image of the X-ray emission in Hydra A. The cavities are clearly visible. *Right:* composite color image of Hydra A that illustrates the close connection between the observed, large X-ray cavity system (shown in blue) and the low-frequency, 330-MHz radio emission (shown in green). The 330-MHz radio data are from [186]. The 1.4-GHz VLA image of Hydra A is also shown in the core in yellow. From [317]

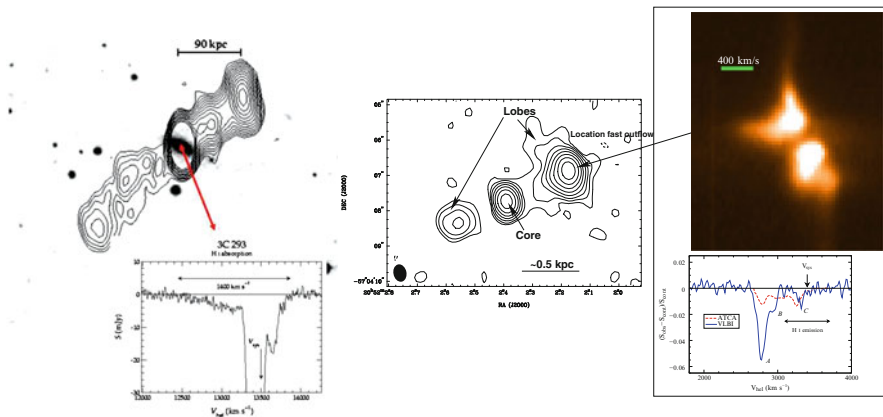


Fig. 7.8 Two examples of fast outflows detected in atomic neutral hydrogen—*Left:* HI absorption profile detected against the nuclear regions of the radio galaxy 3C 293. The outflow is detected as the faint but broad wing blueshifted with respect to the systemic velocity and with velocity reaches $\sim 1,500 \text{ km s}^{-1}$ (FWZI). The short vertical line indicates the systemic velocity. *Right:* Radio continuum image of IC 5063 with a comparison between the width of the HI absorption (bottom plot) and that of the ionized gas (top; from the [OIII] $\lambda 5,007 \text{ \AA}$). The first order similarity between the amplitude of the blueshifted component is clearly seen

Moreover, these outflow rates are comparable to the lower end of gas outflow rates associated with starburst-driven superwinds in ULIRGs, [259], which means that studies of the neutral—and possibly also the molecular—gas in radio galaxies are likely to reveal the main missing component of AGN feedback processes. Interesting

are the results on molecular gas that are also beginning to show also there the presence of very massive gas outflow (see the case of Mrk 231 [79]).

Finally, it is worth making a remark about “positive” feedback. Jet–ISM interaction can, in principle, also provide the mechanism for the triggering of star formation. Current theoretical models suggest that radio source shocks propagating through the clumpy ISM/IGM trigger the collapse and/or fragmentation of overdense regions, which may then subsequently form stars (e.g., [81, 213] and references therein).

Jet-induced star formation is considered to be particularly important for high- z radio galaxies where some examples have been found (see [216] for a review). As mentioned above, there are many examples found in the nearby universe of gas shocked by the interaction with the radio jet. However, there are not many cases of jet-induced star formation known at low- z . Nevertheless, the few cases known are ideal for study the details of such interaction (e.g., Cen A, Minkowski object, [39, 230]).

Thank you, Raffaella.

7.3.2 *Feedback Due to Quasar Winds*

Dear Daniel (*Proga*), what is the feedback of quasars on their host galaxies?

The central location of quasars in their host galaxies and the fact that they can produce a large amount of energy imply that quasars can play a dominant role in determining the physical conditions of matter, not only in the quasar vicinity but also on galactic and even intergalactic scales (e.g., [13, 31, 67, 151, 224, 281] and references therein). There is an abundance of observational evidence supporting this idea. For example, as I mentioned earlier in this book, the presence of (BELs), (BALs), mini-BALs, narrow emission lines (NELs), and narrow absorption lines (NALs) in quasar spectra indicate that quasar continuum radiation affects the quasar’s immediate environment. In addition, the tight correlation between the mass M of the central BH in a galactic nucleus and the velocity dispersion σ of the galaxy’s bulge or spheroid, the so-called $M_{\text{BH}} - \sigma_*$ relation [89, 128, 293], can be explained by feedback between quasars and the infalling material from large distances. This feedback can quench both BH accretion and star formation in the galaxy when the BH reaches a certain mass. Quasars could provide such feedback precisely because they are very powerful sources of energy and momentum (e.g., [18, 32, 66, 151, 224, 277, 281]).

Most studies of quasar feedback have been concerned with order of magnitude estimates of the one or two most important physical processes under some restrictive assumptions regarding geometry and microphysics. This is understandable because the problem is complex and includes local and global processes that are often coupled in a nonlinear way. In addition, some key physical processes, such as

the thermodynamics and the radiative properties of accretion flows, are still poorly understood.

The most advanced studies of feedback effects were carried out by [19, 55, 281]. These studies used computer simulations of merging galaxies within which local and global processes were linked. This was possible because they adopted relatively crude phenomenological realizations of star formation; of radiative cooling in a complex, multiphase medium; and of quasar accretion and feedback and because they limited spatial resolution to about 10 parsecs. The main result of these simulations is that the $M_{\text{BH}}-\sigma_*$ relation can be well reproduced and that the relation is insensitive to the assumed gas fraction.

It has been argued that these results suggest that the feedback regulating BH accretion operates on local scales, comparable to the BH's accretion radius or even closer in, rather than solely on the global scales usually considered [13, 32, 224]. It is also possible that the insensitivity to gas fraction occurs because the gas mass is somehow “maximized” on the scales where the accretion rate is determined [13]. Thus, on these scales, quasar feedback can be much more important than that due to stars. If this is correct for state-of-the-art models, the key feedback processes represent “subgrid” physics. This is a serious limitation of current cosmological models of quasar feedback because they cannot be directly related to quasar physics.

The capability of outflows to quench star formation depends not only on their power but also on their geometry (e.g., [233, and references therein]). The reason being that the outflow energy needs to be delivered to the regions where the stars are to form. For this purpose, powerful relativistic jets are ineffective because they channel energy in the direction perpendicular to the galactic disk. Quasar disk winds are much better candidates in this regard, especially if they are equatorial. However, we still do not know if they are strong and persistent enough to deliver energy over large radii. More specific answers require multidimensional simulations following physics on small scales (as in that referred to as “subgrid” in big galaxy simulations).

Such simulations have recently been attempted and highlight the risk of neglecting small-scale physics. For example [179], measured and analyzed the energy, momentum, and mass feedback efficiencies due to radiation emanating from a quasar in relatively large-scale outflows. These measurements were based on a large set of axisymmetric and time-dependent radiation-hydrodynamical simulations presented in [180] and a smaller set of fully three-dimensional simulations presented in [178]. The simulations followed the dynamics of gas under the influences of the quasar radiation and the gravity of the central $10^8 M_{\odot}$ black hole on scales of ~ 0.01 to ~ 10 pc (i.e., outside the computational domain of [245]’s simulations). The maximum momentum and mass feedback efficiencies found in our models are $\sim 10^{-2}$ and $\sim 10^{-1}$, respectively. However, the large-scale outflows are much less important energetically: their thermal and kinetic powers in units of the radiative luminosity are $\sim 10^{-5}$ and $\sim 10^{-4}$, respectively. These energy feedback efficiencies are significantly lower than 0.05, the value required in some cosmological and galaxy merger simulations. If correct (dust was not included in these simulations), the revised figures could have significant implications for the mass growth of black holes. More work is needed to be decisive, as the simulations also did not consider

the innermost parts of the accretion and outflow where radiation and matter interact most strongly. The feedback from this region could have efficiencies significantly larger than those found by [179]. The inclusion of disk winds such as those modeled by [245] in the fully three-dimensional case is in order but not yet feasible.

For now, we can try to gain some insights from one-dimensional models. For example, [32] showed that mechanical feedback (including energy, momentum, and mass) is necessary for models to produce systems having duty cycles, central black hole masses, X-ray luminosities, optical light profiles, and E+A spectra in accord with the broad suite of modern observations of massive elliptical systems. Generally, they illustrate how complex the galaxy evolution and formation are: a variety of feedback mechanisms is required to meet all of the major observational constraints (see also [233]).

The departing message is, that quasars continue to be fascinating despite their being much less exotic (a very subjective term). Now at the 50-year mark since their discovery, they still come across as mysterious due to their internal complexity and unclear web of connections with their host galaxies. The connection of special interest is the nonrelativistic outflow.

Thank you, Daniel. A better knowledge of quasar host galaxies seems to a necessary step to evaluate the relation between a quasar and its environment.

7.4 Quasars from Well Dressed to Naked

Dear Renato (*Falomo*), the nature and the morphology of the galaxies hosting QSO are poorly known since only recently, it has been possible to develop techniques for removing the outshining light of the nuclei. Could you please review for us the results that have been obtained up to now in this research area? What are the developments foreseen for the next future? Up to which redshift do you believe we can obtain a reliable decomposition of nuclear and host galaxy light?

In recent years, it has become clear that supermassive black holes are ubiquitous in nearby galaxies. The black hole masses are correlated with the properties of the surrounding galaxy bulge, namely, luminosity or mass (via velocity dispersion). The cosmic history of black hole growth also appears to trace the cosmic star-formation rate, at least from redshift 0 to $z \sim 1 - 2$, establishing another connection between black hole and galaxy properties. These discoveries have changed our view of AGNs.

Accretion onto a central black hole now appears to be a common phase in the evolution of normal galaxies. Furthermore, supermassive black holes (SMBH) may well have a period of maximum growth (maximum nuclear luminosity) contemporaneous with the bulk of the initial star formation in the bulge. This has led to a renewed interest in AGN properties, especially regarding the host

galaxies. Studies of the coevolution of SMBH and their host spheroids are obviously critical to understanding how and when galaxies in the local universe formed and evolved. The last 10 years have yielded considerable progress in characterizing AGN host galaxies. Observationally, one needs excellent spatial resolution and a stable point spread function (PSF), in order to minimize the contamination of the weak host galaxy nebulosity by the strong central point source. One also needs the largest possible telescope throughput to detect the low surface-brightness emission at large galaxy radii. Also, there are strong selection effects, for example, the more luminous the active galactic nucleus, the more difficult the determination of the host galaxy properties. The contrast becomes formidable at high redshift because of the redshift–luminosity correlation induced in flux-limited samples and the fast surface brightness dimming (with redshift) of the extended emission. At low redshifts, a major contribution to our knowledge of active nuclei host galaxies has been provided by images from the HST. At higher redshift ($z > 1$), HST observations have been complemented by significant contributions from 8-m class ground-based telescopes under superb seeing conditions. The use of adaptive optics in large telescopes, which can deliver diffraction-limited images, promises to yield uniquely important results for the highest redshift sources.

Comparisons of host galaxies of AGNs at high- and low-redshift constrain host galaxy evolution, which can then be compared to the evolution of normal galaxies. Several groups have recently published new and interesting results in this area, which allow comment on scenarios for galaxy-black hole coevolution. Most recently, the world’s most powerful telescopes have been used to measure stellar velocity dispersions in the host galaxies. This allows for a direct study of the fundamental plane of AGN host galaxies, and even the evolution of the mass-to-light ratio of AGN hosts.

The Characterization of the Host Galaxies. From the observational point of view, the image of a quasar is composed by a central bright unresolved source (with a shape that depends on the PSF) and a surrounding nebulosity (the host galaxy). The relative strength of these two components and their spatial extension make the objects resolved or not depending on the instrument capabilities. In Fig. 7.9, we show an example of low-redshift quasars imaged by HST.

The detection and characterization of the host galaxies of high-redshift quasars is more challenging since the quasar luminosity overwhelms the extended emission from the galaxy, especially in optical imaging, corresponding to rest-frame UV emission. Furthermore, the host galaxy surface brightness decreases rapidly with redshift. In order to cope with these difficulties, imaging with high spatial resolution and S/N together with a well-defined PSF are essential. Figure 7.10 provides an example of a typical photometric analysis performed on quasar images. Systematic reliable studies of the host galaxies of $z > 1$ quasars have thus become available, thanks to the use of NIR imaging, where the nucleus-host luminosity ratio is more favorable, allowing to detect the old stellar population at high redshift.

Beyond $z \sim 2$, detecting the host galaxies becomes extremely difficult, even with the state-of-art observational techniques. Only a small number of objects have

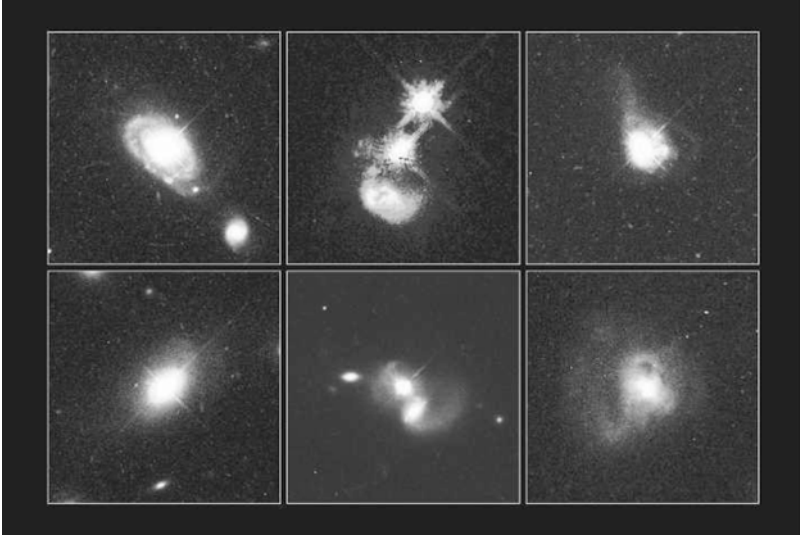


Fig. 7.9 Images of low-redshift QSO host galaxies as observed by Hubble Space Telescope. A large variety of galaxies may host active quasars: from normal spiral and elliptical galaxies to interacting and merging systems

been reported to be resolved [42, 68, 69, 236, 254, 267, 304] mainly following three different approaches:

1. Observations from space [176], provide an excellent narrow PSF but are usually limited by the small collecting area of the HST.
2. The extended emission from the host galaxies is naturally magnified in gravitationally lensed quasars [236]. The drawback in this approach is that the PSF of the lensed targets is difficult to characterize, and the lens galaxy may contaminate the emission from the quasar host, making its detection extremely uncertain.
3. Ground-based imaging with adaptive optics (AO) [42, 68, 69] usually satisfies the severe constrains in the spatial resolution required to disentangle the extended emission of the host galaxies from the nuclear one.

The Morphology of the Host Galaxies. What type of galaxies host luminous quasars has been a subject of many papers as soon as it was realized that the QSO phenomenon occurs in nuclei of galaxies. Since lower luminosity nuclear activity (such as that observed in Seyfert galaxies) is seen in spiral galaxies, it was argued that quasars may also be hosted in spiral galaxies. On the other hand, radio-loud extragalactic sources are mainly associated with massive elliptical galaxies. This has led to suggest that radio-loud quasars (RLQ) host are elliptical, while radio-quiet quasars (RQQ) reside in spirals. The characterization of the right morphology of the host galaxies is a difficult task, and only using an adequate spatial resolution it is possible to properly disentangle the two components and derive the host

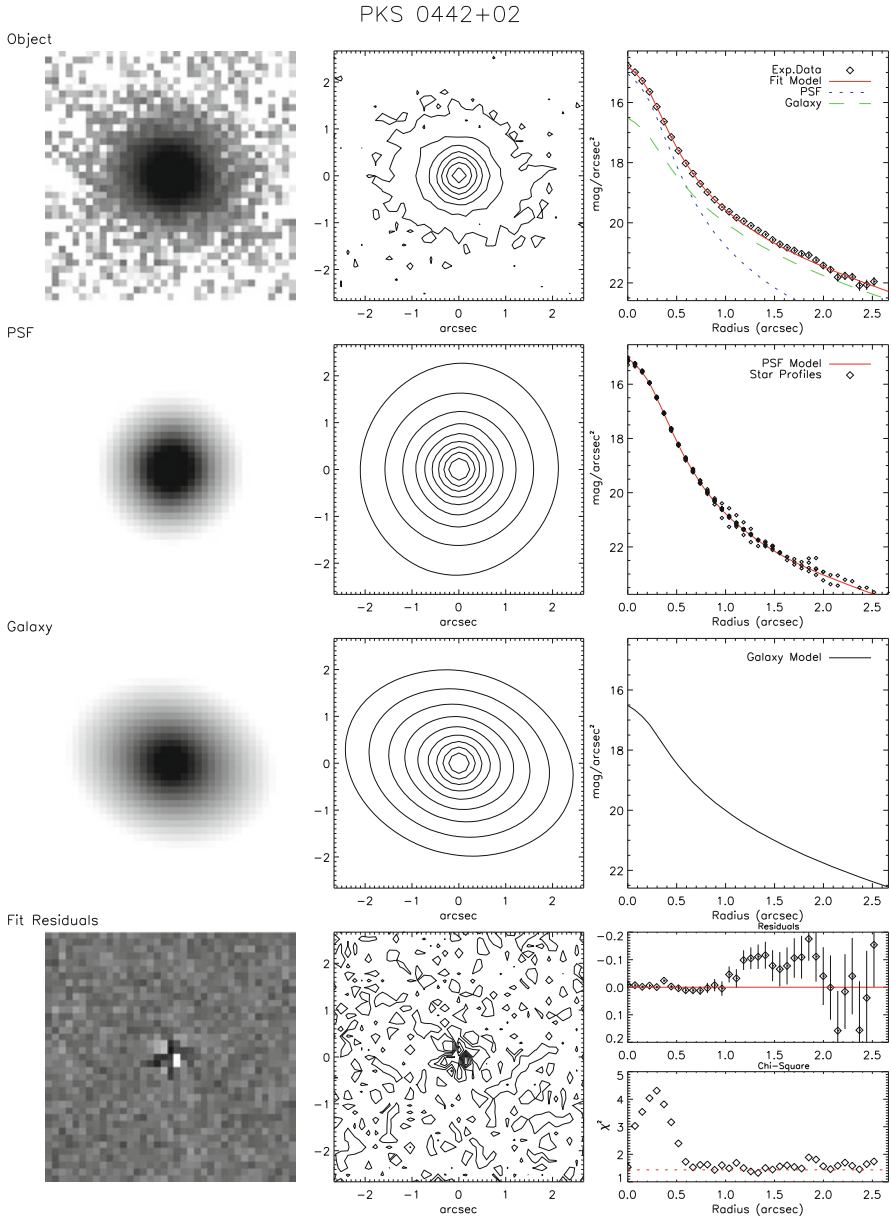


Fig. 7.10 The decomposition of the image of a quasar into two components: the bright nucleus (described by the PSF) and the surrounding host galaxy. For the first three rows, *left, middle, and right panels* give the gray scale image, contour plot and average brightness profile of the object (*top*), point source (*middle*), and host galaxy (*bottom*). In the last row, the residual of the best fit is shown

morphology. It has become clear using HST observations that both type of galaxies (elliptical and spirals) may host in their center the QSO phenomenon (see Fig. 7.9). However, it turns out also that RLQ are almost uniquely hosted in ellipticals, while RQQ may be found both in ellipticals and in disk galaxies. Also, in the latter case, however, the host have a conspicuous bulge component. This led to argue that in all cases, the QSO phenomenon is associated with massive bulges.

Stellar Population. Their stellar populations are believed to be relatively old, especially in *very luminous* AGNs compared to their inactive counterparts [60,228]. However, there is some imaging and spectroscopic evidence for relatively young-/intermediate-age stellar populations in some low-redshift AGN host galaxies and even in apparently quiescent ellipticals [127, 128, 130, 145, 167, 247].

What is the ratio luminosity/mass of the host galaxies?

Several studies carried out at low redshift [17, 190, 278] and high redshift [129, 237, 316, 323] have shown that powerful radio emission is almost ubiquitously linked with massive and luminous ellipticals. Indeed, the global photometric and structural properties of radio galaxies are identical to those of non-radio early-type galaxies of similar mass (or luminosity).

Cosmic Evolution of Host Galaxies. Given the above premises, it is therefore of interest to compare the cosmic evolution of RLQ host luminosity with that of radiogalaxies (RG). Willott et al. [316] present a compilation of K band magnitudes of various samples of radio galaxies. The trend in luminosity of this dataset of radio galaxies is very similar to that exhibited by the host of RLQ (see Fig. 7.11). This remarkable similarity is suggestive of a common origin of the parent galaxies and also emphasizes that both types of radio-loud galaxies follow the same evolutionary trend of inactive massive spheroids.

This has important implications for theories of the structure formation in the universe. In particular, hierarchical merging scenarios predicting a substantial mass reduction at early epochs [143], as well as those models predicting a late merging and assembly period for local massive spheroids, have difficulties in explaining the existence of a substantial population of massive, passive (red and dead) early-type galaxies at high redshift (e.g., [25, 45, 192, 207, 234]). Only the most recent hierarchical models (e.g., [21, 44, 52, 94]) which take into account the influence of the central supermassive black hole (AGN feedback, e.g. through heating of gas in massive halos by AGN energetic) do in fact agree reasonably well with the observed stellar mass function and allow for the existence of massive early-type galaxies out to $z \sim 4$.

What is in your view, the BH mass—host galaxies connection?

Many pieces of evidence suggest that supermassive black holes (BHs) and their host galaxies share a joint evolution throughout cosmic time. In particular:

1. The evolution of the quasar luminosity function [41, 61, 80] closely matches the trend of the star-formation density through cosmic ages [195].
2. Massive black holes are found in virtually all massive spheroids [165].

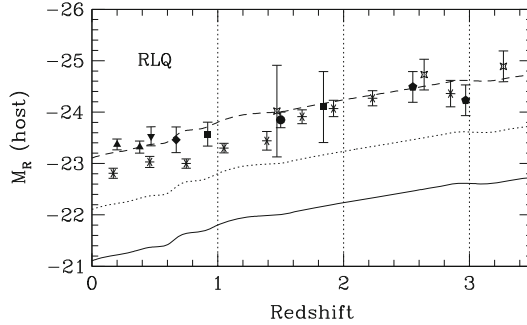


Fig. 7.11 The evolution of radio-loud quasar host luminosity compared with that expected for massive ellipticals (at M^* , M^*-1 and M^*-2 ; *solid, dotted, and dashed* line) undergoing passive stellar evolution [23]. The host galaxy of the RLQ at z are shown as *filled points*. HST data for lensed hosts by [236] (*open stars*). RG are shown by *asterisk*. Each point is plotted at the mean redshift of the sample with error bars representing the 1σ dispersion of the sample. In the case of individual objects, the uncertainty of the measurement is given. See [69] for details

3. Their mass M_{BH} is tightly correlated with the large-scale properties (stellar velocity dispersion, σ_* ; luminosity, L_{host} ; mass, M_{host}) of their host galaxies (see for a review [77, 98]).

When and how these relations set in and which are the physical processes responsible of their onset are still open questions, despite the large efforts perfused both from a theoretical [121, 152, 199, 256, 277, 320] and an observational point of view [209, 235, 236, 261, 318].

Probing BH–host galaxy relations at high redshift is extremely challenging. Direct measurements of M_{BH} from gaseous or stellar dynamics require observations capable to resolve the BH sphere of influence, which are feasible only for a limited number of nearby galaxies. The only way to measure M_{BH} in distant ($>$ few tens of Mpc) galaxies is to focus on type-1 AGNs, where M_{BH} can be inferred from the width of emission lines Doppler-broadened by the BH potential well and from the AGN continuum luminosity [302], assuming the virial equilibrium. Quasars represent therefore the best tool to probe M_{BH} at high redshift, thanks to their huge luminosity. Indeed, wide-field spectroscopic surveys allowed the estimate of M_{BH} in several thousands of objects [181, 182, 269]. Preliminary studies suggest that, for a given galaxy mass, black holes in high- z AGNs are more massive than their low- z counterparts [209, 235, 236]. In Fig. 7.12, we show the comparison of the evolution of the ratio $\Gamma = M_{\text{BH}}/M_{\text{host}}$ from various sources (see [51]). All together, these data depict an increase of Γ with z .

What are the perspective for the future of host galaxies studies?

Resolving and measuring properties of the host galaxy around a bright nucleus depends on how well the nuclear light can be characterized in an image. The effective limits are thus given by a combination of contrast between nucleus and host galaxy brightness, PSF width, and the precision to which the PSF shape can

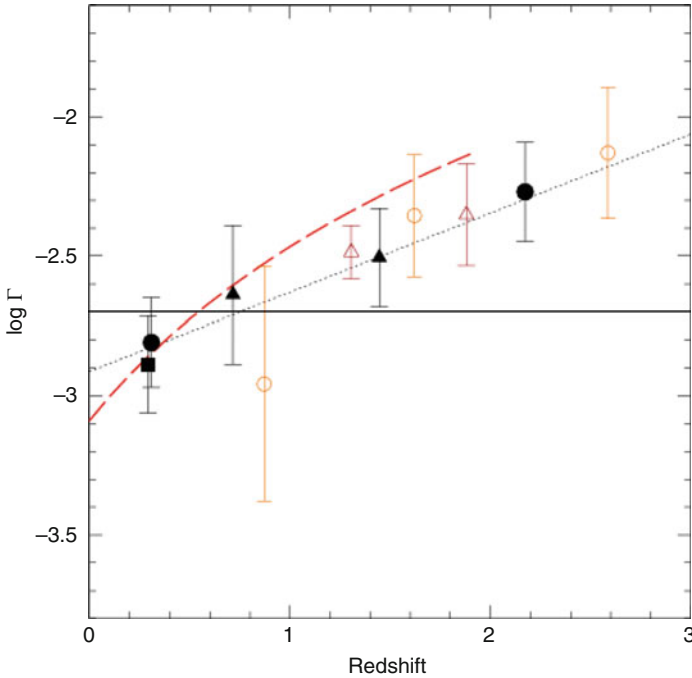


Fig. 7.12 The average values of Γ for the quasars [51] (filled symbols), together with the linear best fit (dotted line). Also shown [209] (dashed line). The average Γ values of the 51 lensed and non-lensed quasars from [235, 236] (empty circles) and of the 89 AGNs from [215] (empty triangles). The horizontal solid line represents the constant $\Gamma = 0.002$ case

be characterized. Moreover, since it is of mandatory importance to be able to characterize the host galaxies of quasars at high redshift, it becomes extremely important to reach resolution of about 10 mas or better in the near-IR and beyond. Such resolution together with adequate sensitivity are required to properly characterize the properties of galaxies with apparent size of 0.1 – 0.2 arcsec. These conditions are not reachable with present instrumentation but could become available before the end of this decade with the begin of operation of JWST and with the next generation of extremely large telescopes as TMT and E-ELT equipped with near-IR adaptive optics cameras.

Thank you, Renato.

Dear Michael (Hawkins), do naked quasars exist or are they always hosted in the nucleus of a galaxy? The quasar images by Magain et al. appear to show a naked quasar—what is your opinion and do you know of other cases? One case in the SDSS archive turned out to be a supernova, but this does not seem to be the case for the Magain et al.’s object.

The term “naked quasar” has been used in more than one context in the literature. The standard model for AGNs includes a supermassive black hole fueled by an

associated accretion disk. Surrounding this is a dusty torus, restricting the view of the nucleus from certain directions. Further out are high-velocity highly ionized gas clouds forming what is known as the broad-line region, and the entire structure is surrounded by low-excitation low-velocity gas, the narrow-line region. In the class of AGNs known as Seyfert-2 galaxies, the nucleus is obscured by the dusty torus, and only the narrow-line region is visible. The obscuration of the nucleus implies that these objects have very faint continua and consequently, are not seen to vary in brightness. However, Hawkins [110] reported a class of AGNs where although the broad-line region was not seen, the quasar nucleus was bright in continuum light and varied strongly. The conclusion was that these quasars lack a broad-line region and are the end point of a sequence of AGNs with progressively weaker broad lines.

The term “naked quasar” was used in a different context by Magain et al. [197] to describe a quasar which appeared not to possess a host galaxy but was being fueled by a nearby gas cloud. They make a strong case that any host galaxy must be very much fainter than normal, and that the nearby gas cloud is a plausible source of fuel for a supermassive black hole to manifest itself as a quasar nucleus. The main problem with this picture is the mechanism by which the gas cloud was captured from a nearby galaxy and more generally, how the black hole grew to its present size. Another possibility is that the AGN resides in a dark galaxy where no significant star formation has taken place. This would help to explain how the gas cloud was captured, or provide a source of gas itself.

Thank you, Michael. When asking this question we intended the meaning of Magain et al. [197]. This discovery of a “naked quasar” is not yet fully understood—and the challenge is indeed to understand how a black hole can remain active outside of its host galaxy. We will return on this issue in the final chapter, but in the meantime, we can reassert that the overwhelming majority of quasars is born at the center of their host galaxy and will reside there. This leads to the question of how quasar are born, will grow, and eventually die.

7.5 Quasar Birth and Evolution

Dear Alfonso (*Cavaliere*), what are the principal drivers of quasar birth and evolution?

We have seen in Sect. 2.9 that to feed quasar-like outputs, substantial accretion onto a SMBH is required. Key conditions are constituted by a rich stockpile of baryons surrounding the very nucleus and by some agency, inducing them to shed out their specific angular momentum. In fact, most of the latter ($j = v R \sim 3 \times 10^{28} \text{ cm}^2/\text{s}$ is to drop by factors 10^{-4} down to values $c r_s \sim 3 \times 10^{24}$) has to be lost or transferred out for securing inflow from kpc distances toward the SMBH, and hit the tiny target constituted by the last stable orbit at $r_s \sim$ light-hours.

Such a feat implies in turn three main steps: sufficient matter from the reservoir has to enter the hole’s sphere of attraction inside some 10 pc; thence, the baryons are

to collect into an accretion disk of sub-parsec size, sufficiently dense for switching on viscous dissipation mainly from small-scale magnetic fields; finally, the baryons within have to spiral in to r_s , to eventually plunge into the gravitational horizon.

A generic condition for breaking angular momentum conservation is constituted by azimuthal asymmetries in the inner gravitational potential of the host galaxy induced by dynamical events. Their strengths range up from secular disk instabilities in spirals, to encounters of the host with a companion galaxy in a group, up to major mergers, and to the chaotic collapses of baryons and DM together in the cosmic ratio ≈ 0.16 . The latter build up and mix the bulk of a massive spheroid to a virialized velocity dispersion σ on a dynamical time $t_d = R/\sigma \sim 10^{-1}$ Gyr. I think the full range of dynamical events to be effective in kindling or rekindling nuclear activity at levels that range from weak AGNs to bright QSOs.

As to the origin of their evolution, let me argue that the formation of surrounding galactic “halos” must be the main driver, based upon a couple of straight indications. The first is based on comparing the timescales:

$$\eta t_E \approx 40 \text{ Myr} \gg t_{ev} \sim \text{several Gyrs} < t_o = 13.7 \text{ Gyr}, \quad (7.1)$$

that show the single SMBH growth scale to constitute just a fleeting flash on the scale of the observed evolution, itself considerably shorter than the universe age. To me, this cogently indicates that some grand coordinator is needed for organizing all those flashes into a coherent demographic pattern on a timescale nested, as it were, in between the vastly different scales ηt_E and t_o .

As a second indication, I stress that the evolutionary span of several Gyrs is what is taken by the formation of host halos all the way from small spheroidal up to the giant galaxies approaching $10^{13} M_\odot$. Their typical formation epochs are given (with considerable variance) by the hierarchical sequence $M_h \sim M_c(z) = 10^{15} (1 + z)^{-6/(n+3)} M_\odot$, with the index $n \approx -2 \div -1.5$ provided by the power spectrum of the initial CDM density perturbations; the range $10^{11} \div 10^{13} M_\odot$ spans formation epochs from $z \approx 7$ to 2.5. Indeed, at the upper end, we now observe intensely star-forming galaxies out to $z \approx 7 - 8$ [20]; at the lower end, star formation had to be terminated by $z \approx 3$ in big spheroids for them to passively become “red and dead” by $z \approx 2$ as observed.

Can we estimate at which cosmic epoch we expect to find the first luminous quasars? What is the estimated length of a cycle of quasar activity?

The answers must consider the times taken by quasars to fully shine within their halos; conceivably, they lagged by quite some while behind the first blue/UV forming stars.

To begin with, similar sets of emission lines observed in QSOs and in local Seyferts witness to previous generations of stars having substantially enriched with metals the gas stockpile for accretion. This is because stars form already during the halo collapse on a timescale $t_d \sim 10^2$ Myr, while SMBHs take longer times $\eta t_E \ln(M_f/M_i) = 6 \times 10^2$ Myr to exponentiate from $M_i = 10^2$ up to $M_f = 10^8 M_\odot$. In addition, their first emissions in the O/UV must fight against

the thick dust produced by the first and fast stellar generations [37]. The picture is consistent with the highest known quasar redshifts in the range $z = 6 - 7$, lying considerably below the values $z \approx 7 - 8$ currently being observed (or inferred) for galaxies.

Thus, in a forming halo, the QSO and the stars live through a hectic and competitive coevolution: the stars are fast to provide evolved abundances but also to enshroud a nascent QSO undercovers that obscure its UV/O and return FIR/sub-mm emissions; eventually, the mature powerful QSO will break through the clouds in full shine. On the other hand, the previously hidden output had to heat up the covering dust; the reprocessed power can account for many a sub-mm source observed with SCUBA and currently scanned by *Herschel* [187].

In a nutshell, the first observable lights after the dark ages of the universe were conceivably switched on by old good stars, while they obscured the young nuclear sources by their dust, before the latter gave way to fancy bright quasars.

But as the latter approach their peak activity, they strike back by sweeping the residual gas out of their accretion reservoir with the feedback due by their radiation, and/or by heating up the baryons throughout the galactic bulge. Thus, they quench off not only their own activity but also the very star formation in the spheroids, leaving them to redden with the tinge of the small, cold, and long-lived stars. Direct evidence of fast outflows has been observed around several quasars ([310] and refs. therein), while massive outflows have been recently caught from favorable broad CO lines [79].

Thus, at $z \approx 6.5$, the duty cycle $\delta t/t$ ranges from close to unity for the entire SMBH activity, to a few times $\eta t_E/t \sim 10\%$ for the final spike of optical shine.

How might we recognize quasars undergoing their first episode of activity? Are galaxy nuclei that host quasars likely to experience multiple episodes of quasar activity?

The first episode of activity is due to involve dust-enshrouded sources bright in the sub-mm band, as discussed above. This is to be followed by bright O/UV emissions up to some $\sim 10^{47}$ erg/s; pinpointing SMBHs already grown up to $M_{\text{BH}} \sim$ a few $10^9 M_{\odot}$, and yet with high Eddington ratios around unity would be telling.

As to the recurrent activity we mentioned before, I added that the best evidence is perhaps provided by the numerous galaxy clusters that feature a so-called cool core, that is, their intra-cluster medium observed in X-rays features a temperature peak declining toward the center by a factor around 3. These limited drops associated to high densities and short radiative cooling times $t_c \sim 0.3$ Gyr, require intermittent energy injections by central AGNs on comparable timescales and spreading out to several tens of kpcs, if these cores are to be stabilized against runaway cooling.

High-redshift ($z \sim 4 \div 6$) quasars have been found with estimated black hole masses $M_{\text{BH}} \sim 10^{9.5} M_{\odot}$, yet today, local AGNs show much lower estimated masses. Where are the monsters of the past hiding?

Truly supermassive relics approaching $M_{\text{BH}} \approx 5 \times 10^9 M_{\odot}$ have been reliably unveiled at the center of rare local large ellipticals such as M 87, NGC 4649, and

NGC 7052 and other red and dead, inactive (or feebly active) galaxies including the bright central giants in galaxy clusters [5, 49]; so within 10^2 Mpc, we know directly where the high-mass end of the relic SMBH distribution is located. At the other end, small specimens of order $10^6 M_\odot$ have been detected in the bulges of several spirals such as M 31, at our own galactic center with impressive precision from single orbiting stars, and even in dwarf ellipticals as M 32.

Firm detections now are in the tens, most based on gas circulation or on star velocity dispersions σ_* within the central bulge. They give rise to the famous, steep correlation $M_{\text{BH}} - \sigma_c^n$ with a debated exponent from $n \approx 5$ to ≈ 4 [78, 89].

This constitutes a tantalizing, direct link of the SMBHs with their hosts, so many efforts (recounted in detail elsewhere in this volume) are being devoted to extend the sampling to other inactive galaxies with slow progress. In currently active galaxies, on the other hand, the velocities can be measured much farther out basing on the width of the emission lines; but pinpointing the related sizes requires calibration with long reverberation mapping and delicate scalings outward (see [263] for a recent review).

As the data body slowly grows, signs of the correlation evolving toward high z loom out, yet are not fully agreed upon. On the other hand, the whole of these findings has produced a local relic mass distribution that invites comparisons with the statistics of distant quasars and closer AGNs that I may touch upon later on.

Black hole growth and massive baryonic spheroid development may occur in parallel. How do quasars relate to dark matter halos? Do we expect any difference with respect to baryonic structures?

Toward focusing these complex issues, I shall indulge in a bit of modeling taking up from [27, 28]. Consider first the conditions prevailing earlier than $z \approx 3$, when the galactic DM halos collapse hierarchically with the baryons following suite and striving to keep up with their cosmic fraction 0.16. As long as this is replenished during the collapse and the associated rounds of major mergers, the SMBHs can accrete up to some tens of $M_\odot \text{ year}^{-1}$ in the Eddington regime and grow up while producing outputs up to some $10^{47} \text{ erg s}^{-1}$. But the baryons within kpc scales are sensitive to the energy fed back from the rising activity and so reach the verge of outright ejection. Stability requires the binding energy to balance the energy deposited over a dynamical time in the surrounding gas, to imply $5 \cdot 10^{-2} L t_d \lesssim G M_h m / 2 R$.

When halo quantities are used to scale $t_d \propto R/\sigma$, $M_h/R \propto \sigma^2$, $m \propto M_h$, the balance results in the steep correlation $M_{\text{BH}} \propto \sigma^5$ pointed out by [277] or equivalently, $M_{\text{BH}} \propto M_h^{5/3}$; the normalization turns out to be consistent with the observed ratio $M_{\text{BH}}/M_b \approx 10^{-3}$ to the bulge mass but evolves strongly to early z as $(1+z)^{5/2}$.

Yet a number of questions arise: what about optical depths $\propto \rho R \propto \sigma/R$ replacing the deposited energy fraction at a sharp 5%, so flattening the correlation toward σ^4 ? Is it not the above evolution $M_{\text{BH}}/M_h \propto (1+z)^{5/2} M_h^{2/3}$ too strong for having long eluded detection? Should not we look for BHs fueling from smaller regions than the full halo, like the baryonic bulge or the central sphere of influence?

But then, how would we understand the evidence of feedback being effective on scales out to 10^2 kpc, as we mentioned earlier in connection with galaxy clusters? Such issues are still debated both in the context of modeling and as possible sources of observational bias. Here, it suffices to say that the feedback balance discussed above may be taken as a simple baseline to calibrate more sophisticated models (see [95]).

The other building block toward understanding the QSO luminosity functions at high- z concerns their relationship to the forming halos, to provide the source function S in the spirit of (eq. 2.1). On taking up parallel formation of massive BH and host spheroids (with $M_h \gtrsim 10^{11} M_\odot$ so as to contain some $10^{10} M_\odot$ of gas), the straight link obtains

$$N(L, t) dL = \delta t \partial N(M_h, t) \partial t_+ dM_h. \quad (7.2)$$

Here, on the rhs, the halo forming rate is expressed as the positive time change of the mass distribution and has been computed by [29] from Press and Schechter to yield $N(M_h, t)/t_+$ with $t_+ = 1.5 t (M_c/M_h)^{(n+3)/3}$. The amplitude is weighted low by the short duty cycle specific to optical visibility, that is, $\delta t/t \approx$ a few times $\eta t_E/t$ in the last spike of SMBH growth discussed above. As a result, consistent with the high- z data, the LF is expected to undergo negative density evolution toward the past, when fewer halos formed exceeding $M_h \approx 10^{11} M_\odot$ (see Fig. 7.13). A steep power-law shape arises from the high end of the mass distribution stretched out by the feedback balance that yields the scaling $L \propto M_h^{5/3}$ (cfr. Fig. 7.14).

On the other hand, for decreasing $z < 3$, such an evolution is expected to saturate and reverse. This is because a supply-limited regime sets in; here, the key role in driving accretion is left to encounter with companions experienced by the host galaxy especially in a small group, while its baryon stockpile is no longer replenished and peters out.

Such conditions may be focused on representing the output in the form:

$$L \propto f m(t), \quad (7.3)$$

split into the residual gas mass $m(t)$ that decreases and yields the trend, and the fluctuating fraction $f \equiv \Delta m/m \approx \Delta j/j$ destabilized by losses of angular momentum upon stochastic interactions; the detailed fractions follow a steep decline beyond the average value $\langle f \rangle \approx 10^{-1}$. The gas, once destabilized, is partly funneled down to rekindle the nuclear SMBH, while a larger amount hangs over at a wider range to kindle circumnuclear starbursts.

The related decrease of $m(t)$ averages to $dm/dt = -\langle f \rangle m/\tau$ from interactions recurring in a small galaxy group on the timescale $\tau \approx 1/n \Sigma V \propto (1+z)^{-3/2}$ set by the galaxy cross section Σ , their density n , and the velocity dispersion V , to yield $\tau = \tau_o t/t_o$ for $z \gtrsim 1$. So the trend comes to $m \propto t^{-\langle f \rangle t_o/\tau_o} \approx t^{-1.5 \div -2}$, given that $\tau_o \approx 1$ Gyr obtains from scaling to virialized groups with overdensities about 200 the timescale of 200 Gyr derived from the census by [292] of local galaxies with persisting marks of interactions.

Fig. 7.13 To illustrate the birth of early quasars in galactic halos with masses exceeding $10^{11} M_{\odot}$, from a distribution like Press and Schechter’s. Such halos first form when $M_c(t)$ crosses that limit, at a rate initially growing rapidly, then declining

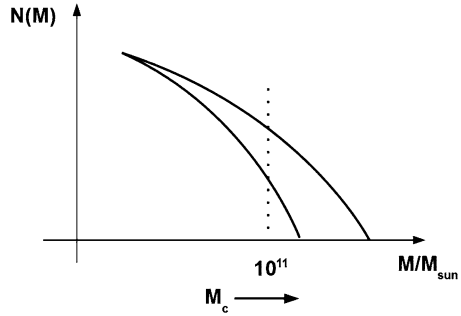
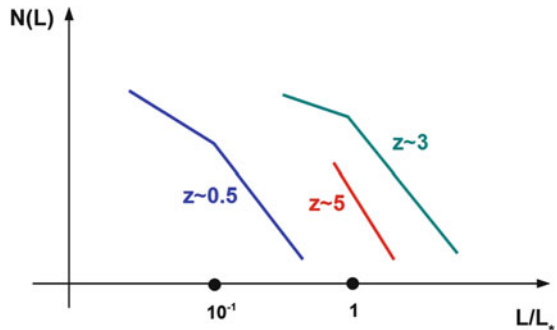


Fig. 7.14 A schematics of complex LF evolution to high- z from AGNs toward QSOs, including a sequence of DE, LE, and negative DE. $L_* \sim 10^{45}$ erg/s in the blue band, bolometric correction 10



As a result, all luminosities scale down out to a retreating break $L_b(t) \propto m(t)$ in the LF. Fainter than this, the LF features a shape governed by $N(L) \propto 1/\dot{L} \propto L^{-1}$ as we discussed apropos of (2.1); while the bright end of the LF steepens to $L^{-2.5 \div -3}$, related to the dropping statistics of stronger interactions causing large mass inputs. In other words, and consistently with the data, luminosity evolution takes place above the break $L_b(t)$, as illustrated in Fig. 7.14; meanwhile, some density evolution is to occur as the sites conducive to such interactions dwindle later than $z \approx 2.5$, the typical epoch for small group formation.

Later still, even the weak encounters dwindle and peter out when the host galaxy finds itself located in a larger and thinner group or cluster and worse, out in the field. Then the stage is taken by localized minor events such as internal disk instabilities or cannibalism from a retinue of satellite galaxies; these provide last bits of accretion dominated by faint events and producing a steep LF, best observable in X-rays [106, 184].

I hope that the above models helped us to see through the complex observational behavior of the LF and focus why my picture envisages two populations of sources corresponding to the QSOs and the AGNs (see also [105]). The picture bases on broadly the same SMBHs being fueled after two distinct accretion regimes related to their changing environment: feedback-controlled replenishment of gas during halo formation yields powerful sub-mm sources and eventually, optically bright QSOs; weaker AGNs mainly fueled by scanty reactivations of large preformed SMBHs,

with a sprinkle of less-massive BHs and halos belated after their typical epoch. The so-called narrow-line Seyfert-1, in particular, may constitute instances of late yet substantially growing BHs under Eddington accretion (see [289] for a recent survey).

The end result is a multitude of relic SMBHs hosted in most local spheroids, fueled ever more sparingly and intermittently to low $L \ll 10^{45}$ erg/s and with decreasing duty cycles $\delta t/t \sim 10^{-2}$. Let me stress that such a 2-population picture turns out to be in tune with the two-stage perception of the halo formation process that is currently taking hold from observations and fresh views at updated simulations (see [37, 309]). Here, the halos are held to form by fast bulk collapses and related mergers, followed by slow inside-out growth of the outskirts, to yield early spheroids and later disks with different mass ratios as illustrated in Fig. 7.15. In the quasar context, the bulk collapses provide early large inputs of fuel, while the outskirts provide limited but longer-lived gas reservoirs, as necessary to sustain in a “downsizing” manner not only the star formation in blue galaxies but also AGN activities when tapped by diverse processes like minor mergers, cannibalism, bar, or secular instabilities. The evolutionary upshot of all that is a fast rise in cosmic time of the QSOs culminating at $z \approx 2.5$, then going over into the slow fall and branching diversity of the AGNs.

Specific lines of evidence corroborate this 2-population picture: the divide at a power around $L \sim 10^{45}$ erg/s; the Eddington or sub-Eddington regime governing many QSOs or AGNs, respectively; the LFs featuring different slopes and modes of evolution as illustrated in Fig. 7.15. Add the information from the bimodal blazars, a class of activity in the form of a relativistic collimated jet blazing at us; these come in two flavors: the high- z , strongly evolving flat-spectrum radio quasars apparently give way to a steady population of BL Lac objects below $z \approx 1$. Converging spectral signs (strong/weak emission lines and “big blue bump”) relate the former to presence of abundant, the latter to dearth of gas surrounding the SMBH.

The blazar spectra go from the radio band to X and hard γ rays and are dominated by nonthermal, minimally reprocessed photons, except for optically thin inverse Compton radiation. At the other extreme, narrow-lined AGNs (the so-called type-2 AGNs) lack broad lines emitted at a closer range from the BH, to be likely obscured by a surrounding torus seen edge on as predicated by the unified model of the AGNs discussed elsewhere in this book. On this line, obscuration in soft and hard X-rays up to Compton-thick sources is expected and is increasingly found in many AGNs. Such objects conceivably provide the missing sources to fill in the cosmic X-ray background at energies above a few keVs and may also fill up the estimated local density of black hole mass estimated at $4 \pm 1 \cdot 10^5 M_{\odot}/\text{Mpc}^3$ of BH masses, especially at the low end of their distribution (see [263]).

Is the X-ray emission from quasars powerful enough, and quasars numerous enough, to account for the cosmic X-ray background?

The AGNs at $z \lesssim 1$ largely outnumber the bright distant QSOs, and come very close to fill out the CXRB at keV energies: a result that rounded up the saga opened by R. Giacconi with his discovery of the CXRB [90] together with the first stellar

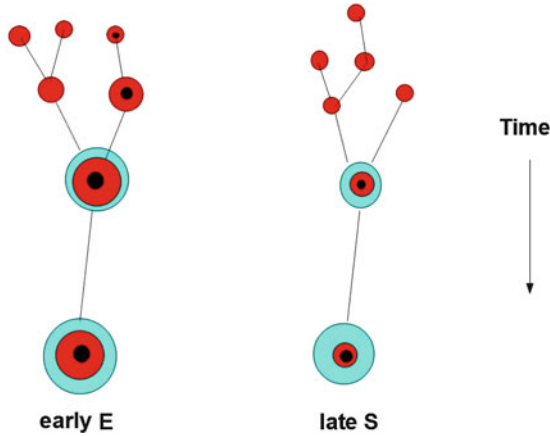


Fig. 7.15 A cartoon illustrating the two-stage galaxy formation. *Left:* Early collapse and major mergers of comparable clumps of DM and baryons form large spheroidal halos; a central BH grows, and its accretion produces enough power and feedback as to eventually sweep the spheroid clear of cold gas, starve itself to death, and terminate star formation. Thereafter, the outskirts slowly grow and add a limited mass amount. *Right:* smaller spheroids grow later substantial outskirts, including a disk that contains enough gas to feed continuing star formation and prolonged if intermittent AGN activity

X-ray source and contributing to his Nobel Prize 2002 in physics. Around 10 keV, the AGNs may account for even more than 1/2, provided the obscured ones compete or dominate by a factor of a few, itself larger than unveiled to now. Toward 30 keV where most of the CXRB energy resides, the main contributors are still actively chased and may require considerable progress beyond the present instrumentation in the hard X ray band.

Thank you, Alfonso. We now focus on the development of BHs at the earliest cosmic epochs.

7.6 Black Hole Growth and Extremely Large Black Holes

7.6.1 Primordial (Seed) Black Holes

Dear Ross (McLure), are galaxies, and quasars, seeded by primordial black holes or are all black holes likely a product of secular evolution?

In general, it is a very difficult task to determine what the initial conditions of black hole growth are, simply because the supermassive black holes that we observe as luminous quasars in the distant universe have already grown by many orders of magnitude from their initial seed black holes, effectively “washing out” the initial

conditions. Perhaps, the tightest observational constraints we can place on the early growth of the supermassive black holes come from studying the black hole masses of the luminous SDSS quasars which have been identified at $5.5 < z < 6.5$, many of which have virial black hole mass estimates $\geq 10^9 M_\odot$ [177, 313]. Since their discovery, the key question has been whether or not it is possible to actually grow a black hole from a given seed mass to $\geq 10^9 M_\odot$ within one Gyr of the Big Bang. In fact, if we make the standard assumptions that we are restricted to Eddington-limited accretion and a radiation efficiency of $\simeq 10\%$ (i.e., a mass doubling time of $\simeq 3 \times 10^7$ years), then it is *just possible* to grow from a seed mass of $\simeq 10 M_\odot$ (plausible for a massive supernovae in the local universe) to a mass of $\simeq 10^9 M_\odot$ within one Gyr. Although possible, this situation is slightly uncomfortable to say the least, and it is interesting to explore possibilities which do not require such “fine-tuning.” For example, two obvious mechanisms by which black hole growth can be accelerated are super-Eddington accretion rates and significant amounts of black hole merging. Another mechanism is to start off with a seed black hole which is significantly more massive. Indeed, one likely source of seed black holes for the luminous $z \simeq 6$ SDSS quasars is supernovae of ultralow metallicity Population III stars, which are predicted to produce black holes with masses of $\simeq 100 M_\odot$. Although starting with a $\simeq 100 M_\odot$ seed black hole does allow a mass of $\simeq 10^9 M_\odot$ to be reached $\simeq 100$ Myrs quicker, the timing is still somewhat uncomfortable.

Of course, the process as discussed so far is purely secular, but the accreting gas must first be transported into the black hole’s sphere of influence, and galaxy merging is the most likely mechanism at high redshift. However, interestingly, it appears that a key aspect of the merging process is that it is sufficiently chaotic to ensure that the angular momentum of the central black hole is kept low at all times [153]. If this is not the case, the central black hole will be “spun-up” increasing its radiative efficiency and slowing down the black hole’s growth to a point where achieving a mass of $\simeq 10^9$ within a Gyr is no longer possible.

An alternative path to building supermassive black holes quickly at high redshift are variations on the so-called “direct collapse” scenario, which can remove the need for a seed black hole produced by an early supernova entirely. In this scenario, low-metallicity gas in pre-galactic halos either directly collapses to form a $\simeq 20 M_\odot$ black hole which can rapidly grow to $10^3 - 10^6 M_\odot$ via super-Eddington accretion [14], or mergers between gas-rich protogalaxies can form massive, unstable, gas disks which can directly collapse to form supermassive black holes of mass $10^7 - 10^8 M_\odot$ [212]. Either way, starting off with a direct collapse scenario would allow plenty of time to reach a final mass of $\simeq 10^9 M_\odot$ by $z \simeq 6$ via “normal” Eddington limited accretion.

Naively, one would expect to see the most luminous quasars at low- z , that is, in the local universe since present-day quasars should possess the largest BH masses. Why do we no longer see very luminous quasars in the local universe?

One of the most fundamental observational facts regarding luminous quasars is that their space density evolves rapidly with increasing redshift. Although the space density of luminous quasars is very low locally, they were significantly more

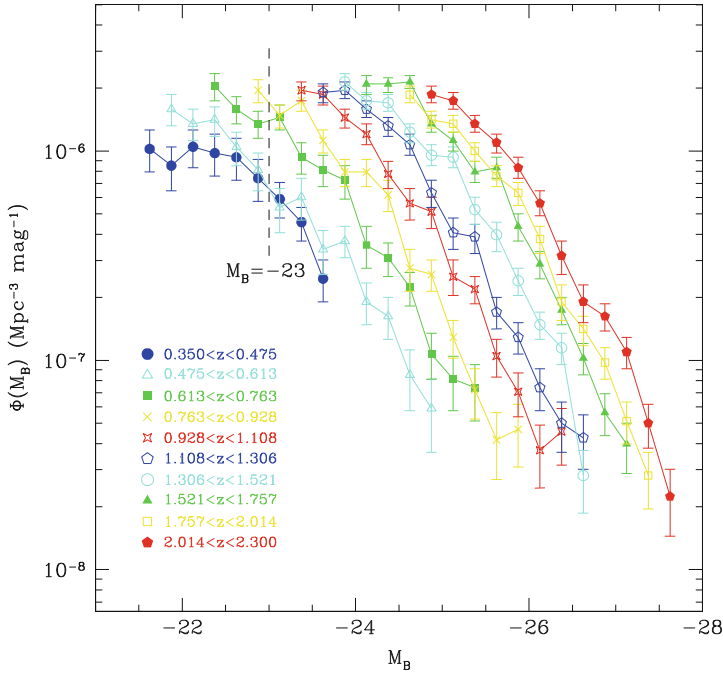


Fig. 7.16 Evolution of the optically selected quasar luminosity function in the redshift interval $0.35 < z < 2.30$ from [22]

numerous in the early history of the universe, reaching a peak during the so-called “quasar epoch” at redshift $z \simeq 2.5$. This fact can easily be seen by considering the optically-selected quasar luminosity function (Fig. 7.16, [22]), which is defined as the number of quasars per unit volume, per unit magnitude.

If we consider the number density of very luminous quasars, say $M_B < -26$ for the sake of argument, you can see from Fig. 7.16 that even during the quasar-epoch these objects were comparatively rare, with a number density of $\simeq 10^{-6} \text{Mpc}^{-3}$. So partly, the absence of these objects locally is simply a question of cosmological volume. In fact, given this peak number density, it is interesting to calculate how many of these truly luminous quasars we might expect to see in the local universe. Of course, defining what constitutes the “local” universe is always somewhat arbitrary, but again, for the sake of argument, we can define the local universe as the cosmological volume contained within a redshift of $z \leq 0.1$. Using this definition, the volume of the local universe is $\simeq 3 \times 10^8 \text{Mpc}^3$. Therefore, if the number density of luminous quasars had stayed as it was at the peak of the quasar epoch, observing over the whole night sky, we might expect to see a few hundred $M_B < -26$ quasars with $z \leq 0.1$. The fact that there are no such luminous quasars within $z \leq 0.1$ confirms that the number density of luminous quasars has dramatically evolved over the last 10 Gyrs.

The form of the observed evolution is traditionally discussed in terms of either luminosity or density evolution, and it is worth considering both in turn. In the simplified picture of pure luminosity evolution, a given fraction of the high-redshift galaxy population are active as quasars, and remain so within the intervening redshift interval (e.g., $0 < z < 2.5$), while the remainder of the galaxy population never become quasars. Given the evidence we now have of supermassive black holes being ubiquitous in local massive galaxies, this now seems somewhat unlikely, but it is still interesting to consider it as a possibility. In this model, the apparent lack of luminous quasars locally is caused by the fading of each quasar over time, due to lack of fuel and/or decreasing radiative efficiency. In fact, although highly simplified, the evolution of the optically selected quasar luminosity function can be reasonably well explained by luminosity evolution, at least qualitatively. This can actually be seen in Fig. 7.16, where pure luminosity evolution would manifest itself in a simple horizontal shift of the luminosity function with redshift. However, quantitatively, pure luminosity evolution cannot match the evolution of the luminosity function in detail [41], and makes the incorrect prediction that low-redshift Seyfert galaxies should harbor black holes as massive as those found in luminous quasars at redshift $z \simeq 2.5$.

The alternative extreme form of evolution to be considered is pure density evolution, which corresponds to shifting the luminosity functions in Fig. 7.16 vertically. In this model, instead of quasars having a long active lifetime, their lifetime is short compared to the age of the universe (sometimes referred to as quasars having a short “duty cycle”). In this scenario, the rarity of luminous quasars locally is due to the number of quasars being triggered into life dropping as a function of time, most likely because the number of galaxy–galaxy mergers is much less locally than in the early universe. Although pure density evolution does have the advantage of predicting large numbers of dormant black holes in the local universe, it cannot accurately account for the observed evolution of the quasar luminosity function either because it severely overpredicts the numbers of luminous quasars we should see locally. The fundamental reason for this is that, between $z = 2.5$ and $z = 0$, the evolution of the brightest quasars has been more dramatic than the evolution of the fainter quasar population. An alternative way of stating this is to say that the form of the evolution appears to be luminosity-dependent density evolution (LDDE), whereby the evolution of the quasar population is a combination of both luminosity and density evolution [41].

In summary, the rarity of very luminous quasars in the local universe is due to a number of factors. Partly, it is because the observable volume in the local universe is relatively small, partly it is because the amount of fuel available to fuel quasars in the local universe is significantly less than it was at high redshift, and partly it is because the merging events which are most likely responsible for triggering quasars into life, are much less frequent in the local universe than at high redshift.

Thank you, Ross.

Dear Hagai (Netzer), is there likely to be an upper limit for central black hole masses in quasars? Why do we not observe black hole masses of 10^{12} solar

masses at any redshift? The masses of super massive BHs in the local universe depend on the initial masses of seed BHs in the early universe, at $z = 10\text{--}20$, and the details of their growth. The first depend on various processes, or possibilities, that are not fully understood. The second, on the more general issue of galaxy evolution.

So how did the first (seed) BHs in the early universe form?

There are three processes that are thought to produce seed BHs, of various sizes and masses, in the early universe. The first is the formation and evolution of the first stars, occasionally refer to as POPIII stars. These are thought to be formed as early as $z = 20 - 40$ out of the primordial gas and hence contain no metals. Numerical calculations suggest typical masses of $100 - 1,000 M_{\odot}$, extremely short (several Myr) evolution, and several ways of producing BHs with masses (here after M_{seed}) that are approximately half the initial mass. Many BHs of this type are likely to be present in the earlier galaxies, some at regions that contain enough cold gas to continue their growth immediately after their formation.

The second class of seed BHs is speculated to result from the direct collapse of a very massive cloud of dense gas. Such clouds are speculated to exist in the centers of protogalaxies. Unlike enriched gas clouds, very low-metallicity gas clouds do not fragment and retains their original mass and temperature. The process of direct collapse involves various instabilities and the formation of supermassive stars at the final stage. Such stars evolve and produces BHs that continue to accrete from the surrounding gas. The evolution ends up with the formation of seed BHs with masses in the range of $10^4 - 10^5 M_{\odot}$.

The third scenario for the formation of seed BHs involves stellar dynamical processes. Such processes are the results of dynamical interactions in dense stellar systems. Here, again, the end results is a population of seed BHs with typical masses of $1,000 - 2,000 M_{\odot}$.

7.6.2 *Black Hole Growth Through Galaxy Evolution*

The later stages of BH growth are related to the evolution of their host galaxy. The rate of growth depends on the type and the rate of galaxy mergers (and hence BH merger), the availability of gas in the vicinity of the BH, and the physical processes that determine the minimum and the maximum growth rate.

It is thought that most of the mass of the supermassive BHs in the local universe is due to direct accretion onto the BH. There are several ways to describe this growth. The first is a “linear growth” resulting from the assumption of

$$\dot{M} = \alpha, \tag{7.4}$$

where $\alpha = L_{\text{bol}}/\eta c^2$ and η is the mass-to-luminosity conversion efficiency (in the range 0.04–0.4). Such growth may last for short or long periods, depending

on the gas supply. This is a somewhat hypothetical case since no known physical process can explain a constant gas supply over a long period of time when the BH mass steadily increase.

An alternative assumption is that the accretion rate is proportional to the mass of the BH

$$\dot{M} = \beta M. \quad (7.5)$$

The initial mass in this process is the above M_{seed} , the growth is exponential, and the simple solution for the characteristic growth time is

$$t_{\text{grow}} = \frac{1}{\beta} \simeq 4 \times 10^8 \frac{\eta}{1 - \eta} \frac{1}{L/L_{\text{Edd}}} \ln \frac{M_{\text{BH}}}{M_{\text{seed}}} \frac{1}{f_{\text{act}}}, \text{ year} \quad (7.6)$$

where f_{act} is the fraction of the time when the BH is active (the BH “duty cycle”). Such a growth phase is expected in cases where there is a natural upper limit to the accretion rate. This can be related to the Eddington luminosity, for example, an upper limit of $L/L_{\text{Edd}} \simeq 1$. Such a limit will force the conditions of (7.5) over a long period of time. The typical, e-folding time (sometimes referred to as the “Salpeter time”) in this case, assuming $\eta = 0.1$ is about 4×10^7 years.

The second way to grow more massive BHs is through the merger of two smaller BHs during the process of galaxy merger. In most such cases, one of the merging holes is considerably smaller than the other, that is, the process does not add much to the total BH mass. Moreover, some of those events are likely to end up with the ejection of the lighter BH from the system.

We can use simple arguments, based on the current understanding and current observations of galaxy evolution, to estimate the maximum BH mass after 13 Gyrs. A fundamental point in the calculation is the ratio of BH growth rate to star-formation rate (SFR). Theoretical and numerical calculations show that, under no circumstances, BH growth is faster (in absolute numbers) than the (time averaged) growth of the stellar mass in its host. To illustrate this, we can use numbers obtained from the observations of the most massive, most luminous AGNs that are located in galaxies with extremely high SFR. Here, the growth rate of the BH, and of the stellar mass, are close to their maximum. The observations of such systems that usually found at $z = 2 \div 3$, an epoch of intense SF activity, show SFR of $10^3 M_{\odot}$ per year and a growth of the BH by about $100 M_{\odot}$ per year, that is, a 1:10 ratio. In addition, the duty cycle of a typical SF event (several Myr) is much longer than the duty cycle of BH activity. This is easily estimated by noting that, at any redshift, the number of SF galaxies is 10 or more times larger than the number of fast accreting BHs (not counting BHs in LINERs that are more numerous but with much slower growth rate). Thus, the mean accumulated mass by accreting BHs is at least 100 times slower than the mean accumulated stellar mass. In fact, these numbers only apply to the largest BHs, and the ratio is more like 1:1,000 in smaller systems. Since the stellar mass of the largest known galaxies is $few \times 10^{12} M_{\odot}$, the largest BHs of today are of order $10^{10} M_{\odot}$. In short, even if BH accretion proceeds at its highest

allowed rate, there is simply not enough cold gas in its vicinity and not enough time to grow from $M_{\text{seed}} \sim 10^2 - 10^5 M_{\odot}$, to much beyond $10^{10} M_{\odot}$ in 13 Gyrs.

Thank you, Hagai. It is perhaps simplistic to think that very high- z quasars will look the same as the quasars observed at $z \approx 2 - 3$. The fraction of obscured quasars should increase, and so most of them will be shrouded by a thick cocoon of gas and dust. Very high SFRs are also expected in primordial quasars. Their presence should be detectable only through FIR/submm spectroscopy.

7.7 Dust-Enshrouded Quasars

Dear Alberto (Franceschini), what is the cosmological relevance of the dust-enshrouded quasar population, that is, of the quasars at the galaxy formation epoch? What are the likely implications of an obscured population on the IRLF for quasars and for those concerning the history of radiant energy production by cosmic sources?

Cosmological surveys in the optical, X-ray and, more recently, in the IR have shown that, while quasars and ULIRGs make a tiny fraction of the galaxy population at the present cosmic time, they are major components of the universe during past cosmic epochs, as a consequence of a very fast evolution with redshift (for both luminosities and spatial densities) observed in all wavebands.

Recent systematic observations carried out with space IR observatories in particular (*Spitzer* and *Herschel*) have demonstrated that IR-luminous objects (LIRGs and ULIRGs) dominate the cosmic scene at redshift $z > 1$ (corresponding to the first half of the Hubble time): evidently, the existence of such luminous sources has something to deal with the formation and early evolution of galaxies and quasar nuclei. A second remarkable result concerns the similarities identified in the evolution rates of quasars and galaxies as a function of redshift and source luminosity (e.g., [82, 322]), showing that the two processes followed very similar paths, at least on statistical grounds.

It would be essential to prove the relationship of star formation and quasar activity in the single objects. Indeed the physical characterization of the luminous high-redshift objects is one of the key themes of observational cosmology today. Let us illustrate our current understanding with a few important results. Alexander et al. [2] have combined an extremely deep hard X-ray survey by *Chandra* with a map obtained with the sub-millimetric telescope JCMT: a substantial fraction ($\sim 40\%$) of the faint IR sources at high redshifts appear to host an AGN, some of which are luminous type-2 quasars. From a comparison of the X-ray to bolometric luminosity ratio, it is argued that in almost all cases, these AGN components are significant but not dominant, the AGN contribution to the total flux being $< 20\%$. The conclusion of these studies is that star formation appears to dominate the bolometric output of the majority of the ultraluminous IR sources at high redshifts, but many of them reveal the presence of a concomitant AGN.

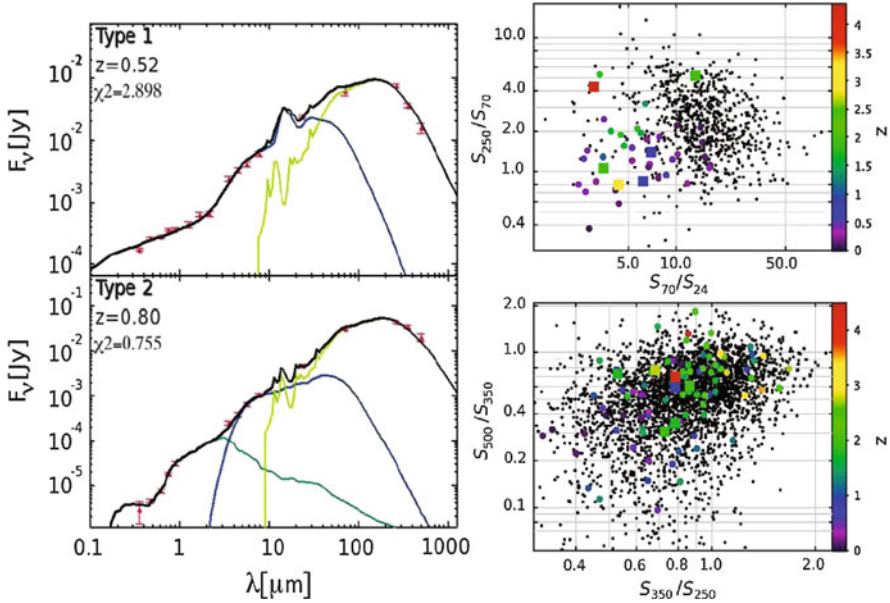


Fig. 7.17 *Left:* The broad-band spectra of a type-1 and a type-2 quasar, including *Herschel* sub-mm observations. *Right top:* mid- and far-IR colors for quasars (large colored symbols) compared with those of normal galaxies (in black). *Right bottom:* same for sub-mm colors. Taken from [108]

A second remarkable results, coming from recent observations with the *Herschel* space observatory by [108], is illustrated in Fig. 7.17. While the mid-IR colors of high-redshift quasars show the contribution of hot AGN dust emission, the sub-mm colors are exactly consistent with those of the host galaxy and demonstrate that the total radiant energy by high-redshift quasars is still largely contributed by stellar emission in the host galaxy (shown as a green line in the spectra of Fig. 7.17, the blue line is the AGN contribution).

In summary, luminous AGNs and starburst galaxies are frequently found associated with each other at high redshifts, both of them dust-obscured. Main phases of stellar formation and quasar gravitational accretion are dust-enshrouded and well visible in the infrared. All this is qualitatively consistent with the observed tight correlation between the nuclear supermassive black hole and the host galaxy masses in all luminous galaxies, as found by [198].

If it exists, at what redshift does this obscured population become important, given that we observe completely unobscured type-1 quasars out to $z > 6$?

Observations of the (~ 40) most distant quasars at $z \sim 6$ with current large millimetric telescopes have detected dust emission in approximately 30% of them [311]. Molecular line emissions are also detected in many objects, proving that active star formation has preceded or is ongoing in the host galaxies. Interesting to mention that a very deep investigation with *Spitzer* of the most distant $z \sim 6$ quasars has

found only two objects with some indication of a lack of hot dust emission, perhaps suggestive of a first generation of quasars born in dust-free environments, too young to have formed a detectable amount of hot dust [133].

However, we cannot exhaustively answer the question of how star formation relates with quasar activity at such high redshifts, as we currently lack the sensitivity needed to observe effectively in the far-IR.

What we can certainly say is that the quasar phenomenon and the stellar activity that has accompanied it have taken place over a large fraction of the Hubble time, and only in the last billions of years it has faded significantly.

Thank you, Alberto.

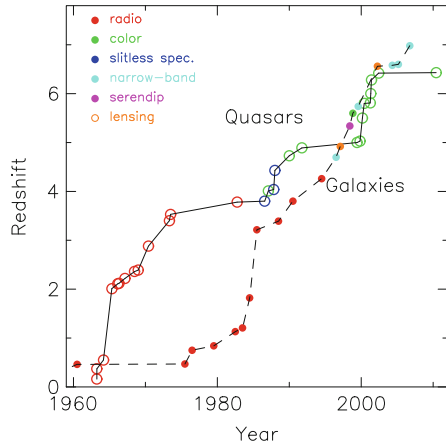
7.8 High-Redshift QSOs

Dear Xiaoui (*Fan*), what are the principal discovery techniques employed by quasar hunters at high redshift? Can one technique find all of the quasars that exist in any given volume? How many quasars are now known with $z > 6$? How do we search for quasars beyond $z \sim 6.5$?

Quasars are discovered using a wide range of search methods, based on their unique spectral and temporal properties. They include radio selection (using which the first quasars were discovered), X-ray selection, infrared selection, optical color selection, optical slitless spectroscopy, optical variability, and (lack of) proper motion. They are also found in general spectroscopic surveys and as serendipity discoveries in observations for other purposes. Most of these techniques can be applied to high redshift, and quasars at $z > 4$ are discovered by the majority in this list. However, they all suffer from some form of selection biases, resulting in the survey either completely misses, or is biased against quasars with certain properties. Osmer [232] gave a modern review of this subject with a detailed discussion on selection effects. Different survey methods also have vastly different efficiencies, in the sense of the survey speed, and the success rate of spectroscopic identification.

Figure 7.18 presents the record of the highest redshift quasars and galaxies discovered over the last 50 years, labeled by their selection techniques. At the highest redshift, quasar density is so low that only possible way is to carry out wide area surveys of sufficient depth to cover large enough volume in order to establish a sample of rare quasars. Therefore, in the last 20 years, surveys of the most luminous quasars are dominated by large projects using wide-field optical imaging and spectroscopy. The best examples are the 2dF quasar survey (2QZ [43]) and the quasar survey in the SDSS [266], which discovered 25,000 and 100,000 quasars, respectively. However, optical surveys can be severely biased: based on AGN unification model, a large fraction of quasars are obscured. Optical selection will miss these obscured sources and is only sensitive to type-1 quasars. They also tends to bias against quasars that are modestly reddened due to foreground dust or have weak emission lines. Surveys based on optical colors are not complete in

Fig. 7.18 The highest redshift quasars and galaxies known, as a function of discovery years. Different selection techniques are labeled with different symbols



certain redshift range, where quasar colors are similar to those of stars or compact galaxies. For example, the SDSS color selection is very inefficient in finding quasars at $z \sim 2.5 - 3$ where quasar locus crosses stellar locus in color space. As shown in [252], some of these selection effect can be carefully corrected for when deriving statistical properties. But some, such as obscuration, are difficult to correct.

Most of the highest redshift quasars are selected using the Lyman break technique. At $z > 3$, the IGM intervening absorption systems in quasar spectrum, first Ly α forest and then Lyman Limit Systems, which has the rest-frame $\lambda < 1216 \text{ \AA}$, are redshifted into the optical wavelength and cause a large continuum break in the quasar spectral energy distribution. High-redshift quasar surveys look for this continuum break using multicolor photometry. At $z \sim 6$, quasars appear as *i*-dropout objects in wide-field imaging surveys and can only be detected in the reddest z -band ($\lambda \sim 9,000$) in commonly used photometric systems. Figure 7.19 presents moderate resolution spectroscopy of a sample of 19 quasars at $z \sim 7$ from the SDSS sample [72]. As of fall 2010, there have been about 30 quasars discovered at $z > 6$, 60 at $z > 5.5$ and over one hundred at $z > 5$. Most of them are discovered using data from wide-field multicolor imaging surveys such as the SDSS high-redshift quasar survey (e.g., [72, 132]), the Canadian–French High- z Quasar Survey (CFHQS, e.g., [315]) and the UKIDSS Infrared Deep Sky Survey (UKIDSS, e.g., [220]). Currently, the highest redshift quasars is at $z = 6.44$, discovered in CFHQS [314]. Spectra in Fig. 6.8 shows strong redshift evolution of the transmission of the IGM: transmitted flux is clearly detected in the spectra of quasars at $z < 6$ and blueward of the Ly α emission line; the absorption troughs deepen for the high-redshift quasars, and complete Gunn–Peterson absorption begins to appear along lines of sight at $z > 6.1$. These spectra also exhibit strong metal emission lines, suggesting a rapid chemical enrichment in the quasar immediate environment.

Redshift of 6.5 is the limit of CCD-based photometry. At $z > 7$, Lyman moves to $\sim 1 \mu\text{m}$. Quasars disappear from optical surveys all together. Wide-field near-IR survey is needed. A number of ambitious surveys are being carried out or in the

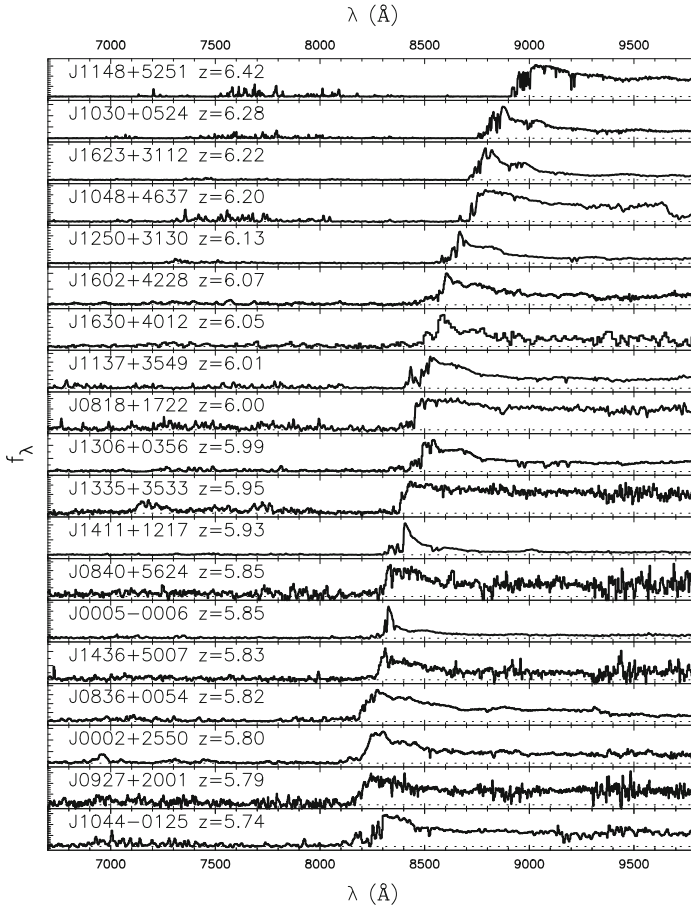


Fig. 7.19 Moderate resolution spectra of 19 quasars at $z = 5.7 - 6.4$ selected from the SDSS sample. Adapted from Fan et al. [72]

planning stage. These include the Panoramic Survey Telescope and Rapid Response System—Panstarrs-PS1 survey, which is using a dedicated 1.8-m telescope and a 7-deg² wide-field camera with good 1 μ m response (thick, deep depletion CCD chips) to carry out a survey of 30,000 deg² down to 21 mag in Y_{AB} ($\lambda \sim 1\mu$ m) and is sensitive to quasars at $z \sim 7$; the UKIDSS surveys is continuing to use its YJHK photometry to search for $z > 7$ quasars, as the survey area increases; the Visible and Infrared Survey Telescope for Astronomy—VISTA—which is a 4-m wide-field near-IR survey telescope, that is planning on a number of tiered surveys in YJHK bands with one of the main goals being the discovery of $z > 7$ quasars. Over longer term, ground-based LSST survey and ultimately, space-based projects, such as *Euclid*, JANUS, and WFIRST, will finally be sensitive to discover a large number of quasars at $7 < z < 10$.

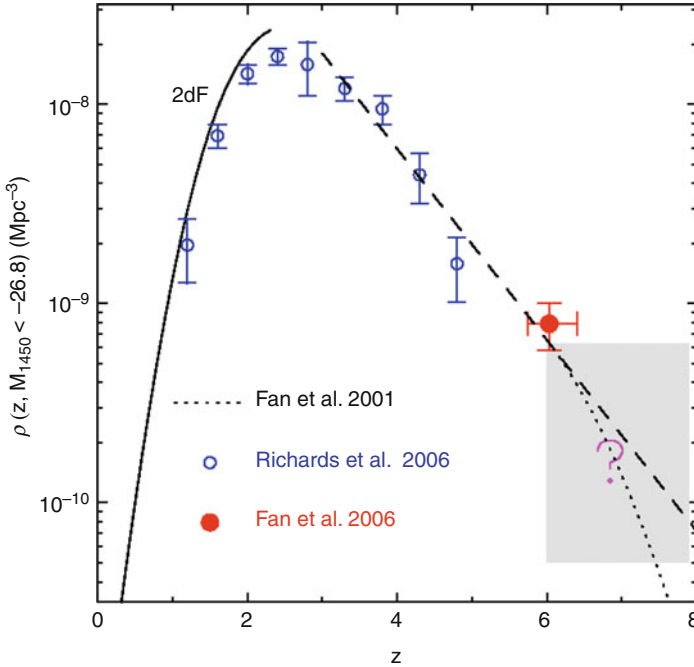


Fig. 7.20 Evolution of number density of luminous quasars as a function of redshift. The SDSS survey established the fundamental sample of $z \sim 6$ quasars. It is uncertain whether quasar evolution will continue its low-redshift trends at $z > 7$. Adapted from [71]

One of the key issue, however, is whether the luminous quasars such as those discovered by the SDSS and other surveys at $z \sim 6$, continue to exist at $z > 7$. The density of luminous quasars is a strong function of redshift: it peaks at $z \sim 2 - 3$ and declines exponentially toward lower and higher redshift (e.g., [22, 265]). This exponential decline continues to the highest redshifts. Figure 7.20 [71] presents the density evolution of luminous quasars at $M_{1450} < -26.7$. The comoving density of luminous quasars at $z \sim 6$ is ~ 40 times smaller than that at $z \sim 3$, as we close in to the epoch of the formation of first supermassive black holes in the universe.

The spectral energy distributions of luminous quasars show little evolution out to high redshift. There is growing evidence from emission-line ratio measurements that quasar broad emission-line regions have roughly solar or even higher metallicities at $z > 4$. Optical and infrared spectroscopy of some $z \sim 6$ quasars indicates a lack of evolution in the spectral properties of these luminous quasars. Figure 7.21 shows the composite of our $z \sim 6$ quasar spectra: it is almost identical to the low- z composite, both in terms of the spectral slope and emission-line strength. Will this trend continue? The black hole mass estimates of the $z \sim 6$ SDSS quasars ranging from several times $10^8 M_{\odot}$ to several times $10^9 M_{\odot}$. Assuming continuous Eddington accretion from a seed black hole of $100 M_{\odot}$, the formation redshift for seed black holes must be at $z > 10$. Even with continuous accretion, black holes

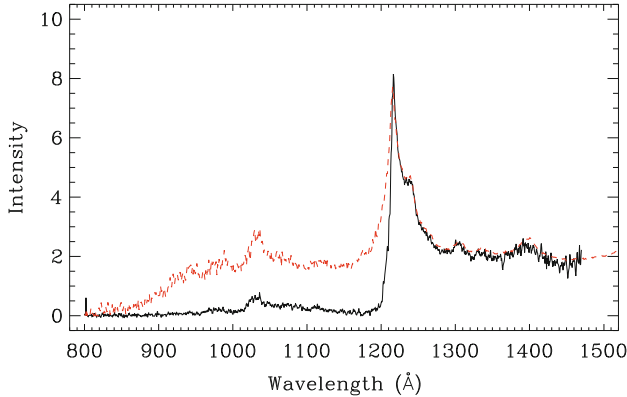


Fig. 7.21 The composite spectrum of $z \sim 6$ quasars (*solid line*). For comparison, we also plot the low-redshift quasar spectral composite from [299]. The effective redshift in the 1000–1500 Å range in the Vanden Berk et al. composite is about 2. The quasar intrinsic spectrum redward of $\text{Ly}\alpha$ emission shows no detectable evolution up to $z \sim 6$, in terms of both the continuum shape and emission-line strengths. On the blue side of $\text{Ly}\alpha$ emission, the strong IGM absorption at $z \sim 6$ removes most of the quasar flux. Adapted from [71]

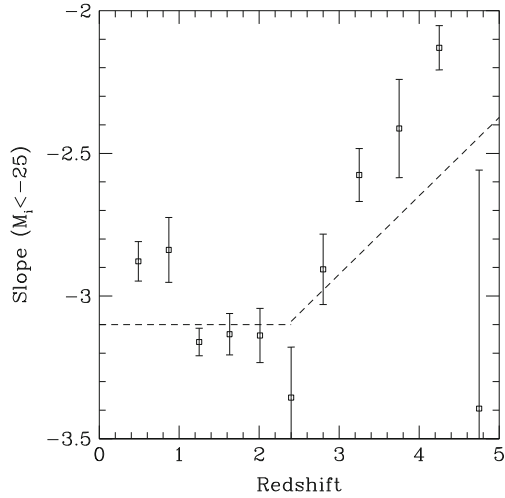
in the most luminous quasars barely had enough time growing. While there are various ways of accreting faster than Eddington, the fact that the highest redshift quasars sit right at the threshold of the re-ionization epoch simply indicate that the initial growth of those BHs have to be very efficient and very early on. We are at the threshold of the earliest generation of quasars. Any discovery of quasars at $z > 7$, or the lack of, will provide powerful constraint to the formation of the first supermassive black holes in the universe.

7.9 The Optical Luminosity Function of QSOs and Its Evolution

What is the current state of our knowledge about the optical luminosity function (OLF) of quasars. Is there a faint end cutoff? How does the OLF change as a function of redshift? Do we know anything about the faint end ($L_{\text{bol}} \leq 10^{44} \text{ erg s}^{-1}$) beyond $z \sim 1$?

There is a long history of studying the OLF of quasars. OLF is usually fitted as a double power law (Fig. 7.22), which is parameterized by its bright-end slope, faint-end slope, and characteristic or break luminosity. Early efforts focused on both determining the overall density and parameterizing the evolution of the shape of OLF, that is, whether it can be best fit as a pure density evolution, pure luminosity function, or a mixture of both—LDDE. It was proven to be a difficult job because of

Fig. 7.22 Slope of the OLF as a function of redshift determined from the SDSS sample. The slope of the luminosity function significantly flattens with redshift at $z > 3$. The *dashed line* shows the best-fit constant slope for $z \leq 2.4$ and the best-fit redshift-dependent slope for $z > 2.4$. Adapted from [253]

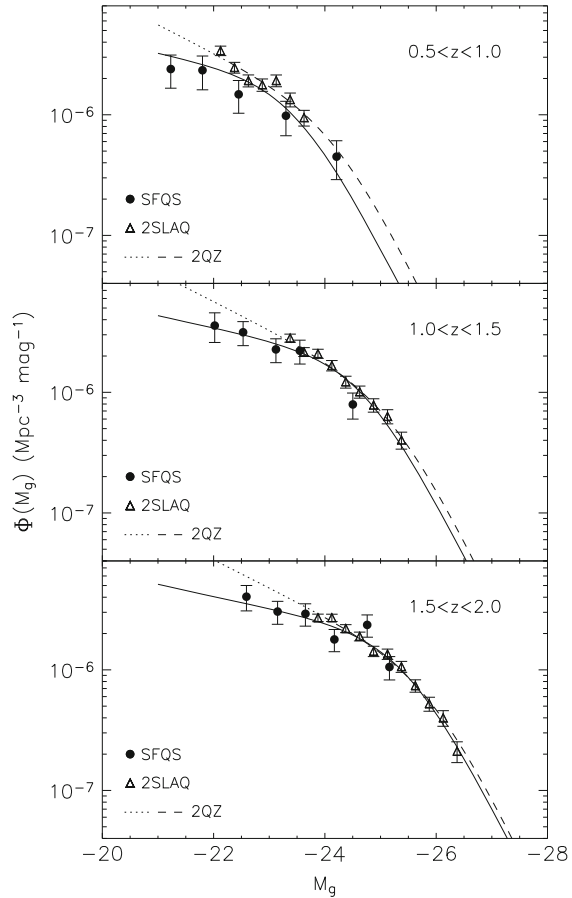


the challenges in observing faint quasars and accurately accounting selection effect at these levels.

The overall evolution of the most luminous quasars has already been described in the previous section and presented in Fig. 7.20. Those measurements are made using large area color-selected quasar surveys such as the 2dF quasar survey (2QZ, [43]) and SDSS [253], which are best in probing the rarest and most luminous objects. They also go to sufficient depth to measure the slope of bright-end slope of OLF. Using the SDSS sample, Richards et al. [253] show that there is strong evolution in the bright-end slope of OLF: it is considerably shallower at low redshift, while the slope at $z < 3$ significantly steeper, fully consistent with measurements from other low-redshift quasar surveys such as the 2QZ. This result could still be affected by selection effect at the faint limit of the SDSS but was later confirmed by a number of deeper optical quasar surveys. It implies an evolution in the accretion and growth of quasars as a function of redshift and can be compared with detailed simulations. The fact bright-end slope is evolving also indicates that a pure density or luminosity evolution model will not apply to all redshifts.

A number of recent surveys (e.g., [41, 134]) targeted quasars significantly deeper than those in 2QZ and in SDSS in order to probe the evolution of faint-end QLF. Figures 7.23 and 7.24 presents results from a survey using data from the SDSS deep equatorial stripe [134]. It is evident that the characteristic luminosity of quasars decreases toward higher redshift, consistent with “cosmic downsizing” of quasar activity. It should be noted, however, that at even lower luminosities, survey for type-1 AGNs begin to be affected by host galaxy contribution and associated selection effect; furthermore, there appear to exist a correlation between fraction of obscured AGNs and luminosity, in the sense that objects with low bolometric luminosity are more obscured (e.g., [122]). Therefore, OLF will present a partial picture of AGN evolution; the limitation is especially evident at low luminosities. Hao et al.

Fig. 7.23 Evolution of faint quasar luminosity function from SDSS faint quasar survey ([134]), comparing with results from 2QZ [22] and 2SLAQ [251]. There is a clear evolution in the characteristic luminosity, consistent with cosmic downsizing. Adapted from [134]



[104] measured luminosity function of local Seyfert-1 galaxies selected from their emission lines in the SDSS galaxy redshift survey, and found that it continue to rise towards the detection limit of $M_B \sim -14$, or $L_{\text{bol}} \sim 10^{42}$ erg s^{-1} , with no apparent cutoff.

Recent efforts to extend searches for quasars at $z \sim 6$ to lower luminosities, using deeper imaging data from SDSS deep stripe [132] and CFHQZ [315] also allowed determination of the shape of quasar OLF at the highest redshift end. Combined with bright-end density from the SDSS main survey (e.g., [71]) the OLF at $z \sim 6$ is characterized by a relatively steep slope with a tentative detection of the LF break at $M_{1450} \sim -25.5$ (Fig. 7.23). It is intriguing that the bright-end slope appears to have steepened again, comparing to the values at $z \sim 4$ (Fig. 7.21). The relatively bright break in the LF also have strong implication in designing future quasar surveys: the total number of expected quasars will be significantly overestimated if one assumes a pure power law down to low luminosities.

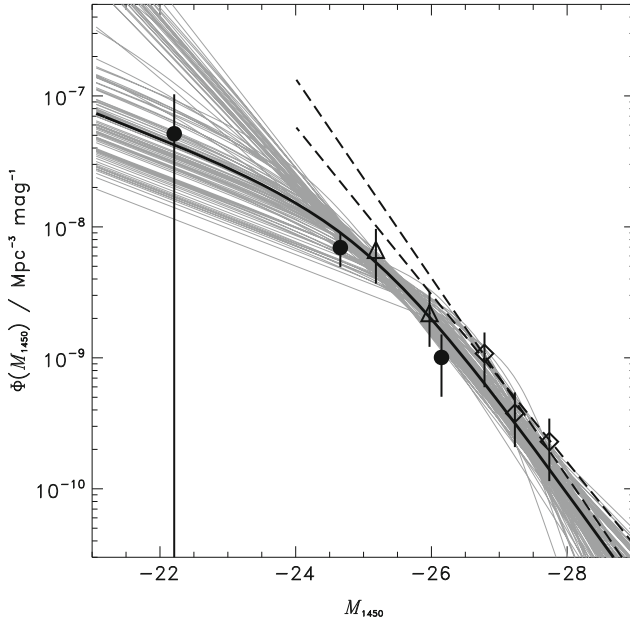


Fig. 7.24 Luminosity function of quasars at $z \sim 6$, combining results from the SDSS main survey [71], SDSS deep survey [132] and CFHQS [315]. Adapted from [315]

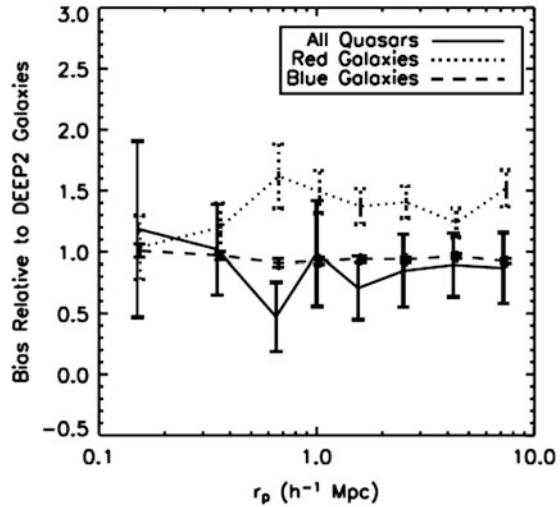
Thank you, Xiaoui. Deborah Dultzin introduced at the beginning of the chapter the environmental properties of quasars and AGN at low redshift. Now, we would like to learn more about the environment of distant quasars. Do quasar clustering properties provide information on the large scale distribution of baryonic and dark matter?

7.10 QSO Large-Scale Environment and Clustering

Dear Massimo (Stiavelli), you studied the large-scale environment of high-redshift quasars. Did you find important difference with low- z quasars?

An old area of research that might experience a new surge thanks to the new facilities is the study of quasar environments. The theoretical bias is that quasar will be some of the earliest structures to become nonlinear and as such they are expected to be very biased. However, theory also predicts that the earliest nonlinearities are somewhat diluted by subsequent mergers as the probability of merging with average halos is much larger than that of merging with other extreme structures. Thus, over time the most extreme nonlinearities will become more normal and less extreme [257, 294]. Moreover, a natural prediction is that with decreasing redshift older quasars will turn off by ending up in massive, gas-poor galaxies, and new

Fig. 7.25 Bias relative to DEEP2 galaxies from [33]. All SDSS QSOs (*solid line*) are clustered like the blue galaxies in the DEEP2 sample (*dashed line*) rather than the more clustered red galaxies (*dotted line*)



quasars will turn on in newly assembled gas-rich galaxies. A simple consequence of this observation is that quasars should become progressively less biased at decreasing redshift.

Observations of five quasar fields at $z = 6$ shows that two of them are surrounded by overdensities of *i*-dropouts, while two of them are in underdense regions [150]. Unfortunately, the number of objects involved is modest and the statistical significance of this result is modest. A possible interpretation of this result is that quasars do indeed sit in overdensities, but their radiative feedback quenches star formation in their neighborhood. The size of the quenched region depends on the on-time of the quasar. Evidence supporting this scenario has been provided by *Subaru* observations [297] showing that for CFHQS J2329–0301 a region devoid of any *i*-dropout surrounds the quasar and is in turn encircled by a ring of *i*-dropouts. The higher sensitivity afforded by JWST will enable us to achieve higher statistical significance on the immediate quasar neighborhood by probing deeper in the luminosity function. At the same time, probing a larger region around the quasar to a shallower but still adequate depth will become less prohibitive.

Quasars at low redshift are not particularly located in clusters of galaxies, and this is in good agreement with the general theoretical argument outlined earlier. Clustering studies show quasars to be clustered more like the blue galaxy population rather than the red [33] (see also Fig. 7.25) and also that radio-loud galaxies are more clustered than quasars [57]. There have also been studies of clustering of obscured and unobscured quasars and the evidence so far is that they are comparably clustered, with perhaps a hint of obscured quasars being more clustered than their unobscured counterparts [116]. A more quantitative comparison between theory and observations would require a better understanding of the galaxy–black hole interaction which has implications on quasar duty cycles and lifetime as quasars should turn off at the same time that the host galaxy moves to the red sequence.

7.11 What Are Quasars Telling Us on Structure Formation?

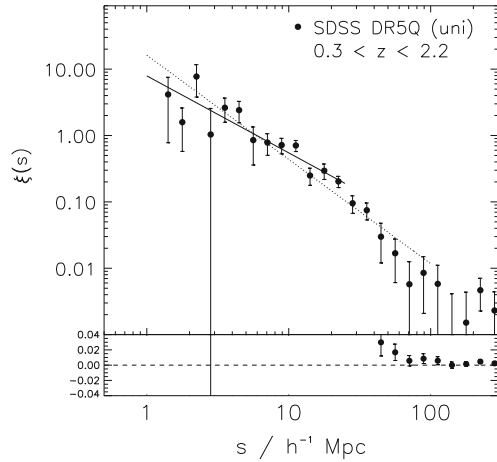
Quasars are great potential probes for structure formation. Unfortunately, selection of quasar samples can be biased. A pillar of quasar studies has traditionally been X-ray observations. However, this field seems in a difficult state at this moment as the preeminent X-ray mission understudy, the International X-ray Explorer (IXO) has not been ranked at the top by the US National Academy Decadal Survey ASTRO2010. The lack of a high-sensitivity wide-field X-ray telescope is also hampering efforts to find more distant quasars. This will change once eRosita [244] will be operational, but one would hope for further efforts in the area of wide-field X-ray telescope as finding quasars at $z > 7$ might be the key to address some fundamental questions on the initial growth of massive black holes.

Availability of statistically meaningful samples of quasars at high redshift would enable us to probe the earliest epochs of quasar growth. The existence of massive black holes already at redshift 6 puts pressure on most formation scenarios as these objects would require constant growth at the Eddington rate from the earliest redshifts if they started out from a stellar mass black hole as in the classical model for black hole growth [118]. Two scenarios have been proposed to address this issue, but they both have weaknesses [100]. In one scenario, the black hole growth is kick started by the massive remnants left by Population III stars [196]. The gain of two orders of magnitude in mass shortens the process by a few Salpeter times, making the process more plausible. The main difficulty of this scenario is that merger of halos with massive black holes can lead to ejection of both blackholes due to gravitational wave kick [306, 307]. The main issue is then whether the remnants of the earliest Population III stars can grow sufficiently before the first major merger as to be safe against ejection. This may well be possible given their small numbers and isolated environments [295]. The second scenario is based on the idea that a $10^8 M_{\odot}$ halo could collapse monolithically to form a supermassive black hole of $M_{\odot} 10^3 - 10^4$ [14]. The main problem of this scenario is that the gas in such halo would need to have primordial composition to avoid fragmentation. This favors certain scenario for Lyman–Werner feedback quenching Population III formation in mini-halos as well as an isolated location to avoid contamination by winds in neighboring halos [140, 296]. Both these factors tend to favor a preferential location in voids which appears to be at odds with the findings on high- z quasar environments.

In principle, the two scenarios might be tested by studying the faint-end luminosity function of quasars and mini-quasars at the very high redshift, although this is going to be challenging. Telling apart these scenarios would provide a good probe of our models of Population III formation by providing constraints for the formation of Population III in mini-halos, the Lyman–Werner background onset, and the survivability of halos with pristine chemical composition.

Quasars are also considered one of the premier tools for quenching star formation in galaxies at late times, moving objects from the blue to the red sequence. While we do not know if they are the only factor at play in this transition, the existence of mass

Fig. 7.26 The SDSS quasar redshift-space 2-point correlation function. The *solid line* shows the best-fit single power-law model over $1 - 25.0 h^{-1}$ Mpc; the *dotted line* shows the best-fit single power-law model over $1 - 100 h^{-1}$ Mpc. The real-space correlation length is $\sim 5 h^{-1}$ Mpc. Adapted from [258]



correlations between black holes and spheroids is suggestive that such an interplay must be in action at least to some extent. The basic idea of mutually constrained growth of galaxies and black holes goes back several years [277], but it is not yet well understood.

Thank you, Massimo.

Dear Xiaoui (Fan), on what scales do quasar cluster? Is there any evidence of quasar clustering evolution with redshift? Do quasars in galaxy clusters differ from quasars in less dense galactic environment? Have quasars been found in the nearest massive clusters like Virgo and Coma? If so, how do those quasars compare with the general population (in terms of, for example, L_{bol})?

Quasar clustering traces the underlying dark matter distribution. They should show similar large-scale structure as galaxies with similar masses to their host galaxies. However, because of the low spatial density of quasars, early measurements based on small-area survey were dominated by shot noise. Again, the era of large-area quasar surveys, in particular, SDSS and 2dF, made accurate measurements of quasar clusterings, such as 2-point correlation function, possible. Figure 7.26 presents the 2-point correlation function measured in the SDSS at $z < 2.9$, using a sample of $\sim 30,000$ quasars covering over $4,000 \text{ deg}^2$ [258]. It shows the usual power-law shape over the range of $\sim 1 h^{-1}$ to $25 h^{-1}$ Mpc in comoving units. The real-space correlation length is $\sim 5 h^{-1}$ Mpc, with a power-law slope of ~ 1.9 . Therefore, on average, the correlation scale for quasars at $z \sim 1 - 2$ is comparable to that of $z \sim 0$ galaxies. Because perturbation is expected to grow between the average redshift of 1.3 in the SDSS sample, the large clustering strength of quasars implies that they are biased tracer of mass distribution ($z \sim 0$ galaxies are only slightly biased): the best-fit value is $b \sim 2$ for the entire SDSS sample. This can be directly compared with simulation; the quasar dark matter halo has an average mass of $\sim 2 \times 10^{12} h^{-1} M_{\odot}$. The clustering scale, which is determined by mass scale, can then be combined

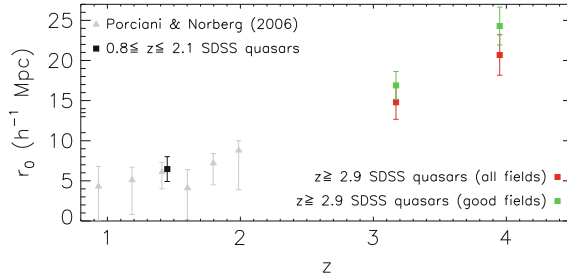


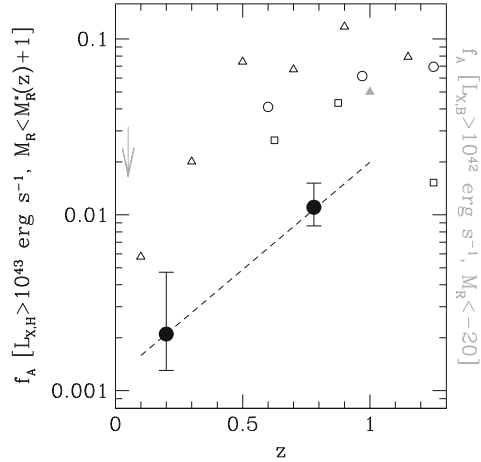
Fig. 7.27 The evolution of the comoving correlation length r_0 as a function of redshift. *Triangles* represents 2dF data from [243]; *black points* are for SDS quasars at $z < 2.1$, while *red and green squares* are for SDSS quasars at $2.9 < z < 3.5$ and $z > 3.5$. There is a strong evolution of quasar clustering, indicating that high-redshift quasars are highly biased systems. Adapted from [270]

with quasar density to constrain the duty cycle and average lifetime of quasars. While this constraint is only mildly sensitive to quasar clustering and has large uncertainty, it is broadly consistent with an average lifetime of quasar being at the order of Eddington time ~ 40 million years. Shen et al. [271] further subdivided the SDSS sample into bins with different physical properties. They found evidence that more luminous quasars are more strongly clustered, and radio-loud quasars are more strongly clustered, implying higher mass among these subsamples.

Clustering of high-redshift quasars is even more difficult to measure: high-redshift quasar pairs are extremely rare due to the reduced spatial density. Large-scale clustering was hinted in earlier results, but the first detailed measurement was again achieved by the SDSS survey. Shen et al. [270] used $\sim 4,400$ quasars at $2.9 < z < 5.4$ over $\sim 4,000 \text{ deg}^2$ to derive the correlation function of high-redshift quasars. Their results are summarized in Fig. 7.27. Correlation length of quasars at $z > 2.9$ is considerably larger than that at low redshift: it is $\sim 15 \text{ h}^{-1} \text{ Mpc}$ for the entire sample and $\sim 24 \text{ h}^{-1} \text{ Mpc}$ for the subsample at $z > 3.5$. This demonstrates that high-redshift quasars are strongly biased system; they also reside in the most massive dark matter halos at high redshift. The effective bias is ~ 10 for such objects. Given our understanding of dark matter clustering in a ΛCDM universe and its redshift evolution, quasar clustering provides a unique way to provide the properties of quasar hosts, in particular their halo mass, and the average duty cycle or quasar lifetime.

Although at high-redshift quasars are highly clustered with correlation length comparable to current day galaxy clusters, few quasars have been discovered in center of mature massive clusters at low redshift. Popular models of quasar formation suggest that quasar activity is triggered by large-scale gaseous interaction in galaxies that provide the fuel for black hole accretion, such as during major galaxy merger. At low redshift, merger rate is much reduced. At the center of virialized clusters, there is little fresh gas to feed quasar activity; there is also little star formation and gas accretion among cluster member galaxies: the same physics that is causing density–morphology relation at low redshift is starving quasar

Fig. 7.28 Evolution of AGN fraction in clusters at $z \sim 0 - 1.3$ (*solid points*). It is consistent with a power-law increase $f_A \propto (1+z)^{5.3}$. *Open symbols* represents AGN fractions in field galaxies. Adapted from [204]



activity. This is another manifestation of the close connection between the growth of galaxies and their central black holes. However, low-level AGN activity, traced by X-ray emission, does exist in quasar environment. Martini [204] (Fig. 7.27) presents recent X-ray survey of AGNs in cluster environment from $z \sim 0$ to > 1 . He found that at both low and high redshift, the AGN fraction in clusters is consistently about one order of magnitude lower than that among field galaxies; however, the *absolute* fraction does grow considerably from $z \sim 0$ to $z \sim 1$ (Fig. 7.28), following the general trend observed in the field galaxies. This is an example of quasar/galaxy coevolution, with the link likely to be the gas supply that is required for both star formation and black hole growth.

Thank you, Xiaoui. We know after your discussion that quasars do not look at all like standard candles since their luminosity is spread over many orders of magnitude. In addition, they are anisotropic and variable sources, often in an unpredictable way. Nonetheless, we also know that the universe is filled with accreting black holes that appear as quasars. Will we ever be able to exploit quasars for constraining the properties of the early universe and the major cosmological parameters? In the following, we will discuss a few sparse topics that are however at the frontier in quasar research. First, we will consider quasars at the reionization epoch; then how distant quasars might be able to lead to fundamental physical and cosmological parameter estimates, including the fine structure constant. Two main aspects of this broad issue are considered: the constraints imposed by the metal enrichment of high- z quasars and the possibility of measuring the quasar luminosity in a way not dependent on redshift.

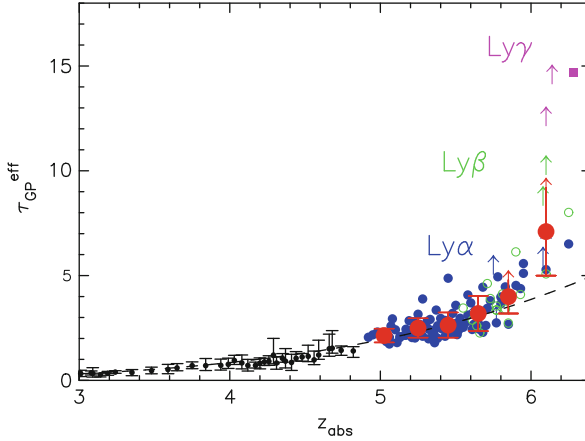


Fig. 7.29 Evolution of Gunn–Peterson optical depth as a function of redshift. The *dash line* is for a redshift evolution of $\tau_{\text{GP}} \propto (1+z)^{4.3}$. At $z > 5.5$, the best fit evolution has $\tau_{\text{GP}} \propto (1+z)^{10.9}$, indicating an accelerated evolution. The *large open symbols* with error bars are the average and standard deviation of optical depth at each redshift. The sample variance increases also increases rapidly with redshift. Adapted from [72]

7.12 QSOs as Cosmological Probes

Dear Xiaoui (*Fan*), the most distant quasars are potentially valuable cosmological probes. Some of them were shining before the epoch at which re-ionization was completed and their continuum shortward of $\text{Ly}\alpha$ appears to be fully absorbed (the so-called Gunn–Peterson effect). Did quasar provide a significant contribution to the reionization process?

Gunn and Peterson [99] first proposed using $\text{Ly}\alpha$ resonance absorption in the spectrum of distant quasars as a direct probe to the neutral hydrogen density in the IGM at high redshift. For objects beyond re-ionization, neutral hydrogen in the IGM creates complete Gunn–Peterson absorption throughs in the quasar spectrum blueward of $\text{Ly}\alpha$ emission. Observations of the Gunn–Peterson effect directly constrain the evolution of neutral hydrogen fraction and the ionization state of the IGM.

Fan et al. [72] measured the evolution of Gunn–Peterson optical depths along the line of sight of the nineteen $z > 5.7$ quasars from the SDSS (Fig. 7.29). We found that at $z_{\text{obs}} < 5.5$, the optical depth can be best fit as $\tau \propto (1+z)^{4.3}$, while at $z_{\text{obs}} > 5.5$, the evolution of optical depth accelerates: $\tau \propto (1+z)^{10}$. There is also a rapid increase in the variation of optical depth along different lines of sight: $\sigma(\tau)/\tau$ increases from $\sim 15\%$ at $z \sim 5$, to $> 30\%$ at $z > 6$, in which τ is averaged over a scale of ~ 60 comoving Mpc.

Assuming photoionization equilibrium and a model of IGM density distribution, one can convert the measured effective optical depth in Fig. 7.29 to IGM properties,

such as the level of UV ionizing background and average neutral fraction. We find that at $z > 6$, the volume-averaged neutral fraction of the IGM has increased to $> 10^{-3.5}$, with both ionizing background and neutral fraction experiencing about one order of magnitude change over a narrow redshift range, and the mean-free-path of UV photons is shown to be < 1 physical Mpc at $z > 6$. These results are consistent with conditions expected at the end of re-ionization, during the transition from the percolation, or overlap, stage to the post-overlap stage of re-ionization, as suggested by numerical simulations.

Quasars and AGNs are effective emitters of UV photons. Luminous quasar density declines exponentially toward high redshift: it is ~ 40 times lower at $z \sim 6$ than at its peak at $z \sim 2.5$. However, quasars have a steep luminosity function at the bright end—most of the UV photons come from the faint quasars that are currently below the detection limit at high redshift. Jiang et al. [131] recently determined the bright-end luminosity function of quasars at $z \sim 6$ using a sample of faint quasars. Based on the derived luminosity function, we find that the quasar—AGN population cannot provide enough photons to ionize the intergalactic medium (IGM) at $z \sim 6$ unless the IGM is very homogeneous and the luminosity at which the QLF power law breaks is very low.

Due to the rapid decline in the AGN populations at very high- z , most theoretical models assume stellar sources re-ionized the universe. However, despite rapid progress, there is still considerable uncertainty in estimating the total UV photon emissivity of star-forming galaxies at high redshift, especially the IMF and the UV escape fraction from dwarf galaxies. Given these uncertainties, the current data are consistent with star-forming galaxies, in particular, relatively low luminosity galaxies, as being the dominant sources of reionizing photons, although more exotic sources, such as high-redshift mini-quasars, cannot yet be ruled out as minor contributors of re-ionization budget.

Over the next decade, observations of quasars and galaxies at $z > 7$ from large ground-based surveys as well as from JWST and ALMA, and direct detection of 21-cm radiation from high-redshift neutral hydrogen will likely reveal the history of re-ionization at $z \sim 7 - 15$, during the peak of re-ionization era at the end of cosmic dark ages (Fig. 7.30).

Thank you, Xiaoui.

Dear Greg (Shields), the α -elements (O, Ne, Mg, Si, S) are mainly produced in type II supernovæ on relatively short timescales (0.1 Gyr), while the Fe-peak elements are produced in SNe Ia with a longer timescale estimated to be 0.3–1.0 Gyr through chemo-dynamical modeling of galaxies. The recent discovery of a quasar at $z = 3.9$, with $\text{Fe/O} = 2.5$ solar already poses a challenge to Λ CDM models. Also, it is well known that several quasars have been found at $z > 6$ with strong FeII UV emission. The strength of their FeII emission demands at least a solar $[\text{Fe/Mg}]$ abundance ratio, and the highest redshifts imply an age of the universe of ≈ 0.8 Gyr ($H_0 \approx 65 \text{ km s}^{-1} \text{ Mpc}^{-1}$, $\Omega_M \approx 0.3$). Is it possible to estimate reliable timescales for metal and especially for iron enrichment in quasars? Do you think that a discrepancy between the time

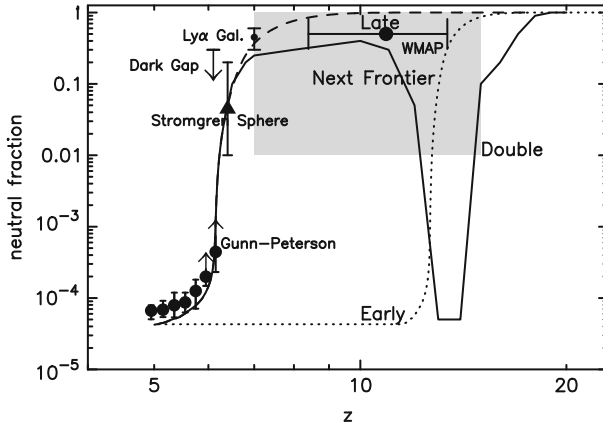


Fig. 7.30 The volume-averaged neutral fraction of the IGM vs. redshift using various techniques. The *dash line* shows the fiducial model of Gnedin ([92]) with late re-ionization at $z = 6 - 7$, the *solid line* shows an idealized model with double re-ionization as described in [30], and the *dotted line* illustrates the model with early re-ionization at $z \sim 14$. Adapted from [70]

needed for Fe enrichment and the presumed age of the universe might arise in the near future, if more quasars with similar Fe II properties are discovered at similar or even higher redshift?

Iron abundances in high-redshift QSOs are potentially interesting as constraints on the early chemical evolution of galaxies and on cosmological parameters (see review by [102]). The $z = 3.91$ quasar that you refer to, APM 08279+5255, was argued to have Fe/O of 2–5 times solar by [107] on the basis of a strong $K\alpha$ absorption edge at energies corresponding to FeXV to FeXVIII. Most of the Fe production over the history of a normal stellar population comes from SN Ia, giving a delay of order 1 billion years [101]. In contrast, the α -elements can reach high abundance in only $\sim 10^8$ year. Friaca et al. [86] computed chemical evolution models for massive elliptical galaxies indicating that Fe/O would only reach 2 times solar at about 1.3 Gyr after the start of star formation. For a standard concordance cosmology ($H_0 = 71$, $\Omega_M = 0.27$, $\Omega_\Lambda = 0.73$), the age of the universe at redshift 3.9 is 1.6 Gyr. So there is not really a conflict, as long as star formation began in earnest within a few hundred million years of the Big Bang. Even at redshift 6, the universe was 1 Gyr in the standard model, so that there is time for the Fe/Mg to reach roughly solar values.

One might see in this the potential for a stringent test of cosmology, if a reliable value for Fe/O of at least 3 times solar is found in an object with a redshift of 4 or greater. Such measurements will be challenging. As emphasized by Friaca et al. and earlier authors, absolute abundances in AGNs are difficult to measure. Relative abundances may be more promising, including Fe/O. The measurement of Fe column density in APM 08279+5255 relies on a pretty clear Fe $K\alpha$ feature, but the oxygen edge is redshifted to fairly low photon energies. Even when good

column densities are available for both Fe and O, there is the question of ionization correction and geometry. Hasinger et al. computed photoionization models that supported their result. My own examination of a few high-ionization parameter models with the Cloudy program [76] suggest that if FeXVII and FeXVIII are indeed the dominant ions of Fe, then most of the oxygen will be totally stripped of electrons, with a fraction of OVIII around 10–30%. An uncertainty in the ionization correction for Fe/O of only a factor of two will weaken applications to cosmology. There is also the matter of geometrical complexity. Reports of bizarre abundances based on the UV BALs of BAL QSOs now appear to result from incomplete covering of the continuum source by the absorbing material. This can cause saturated absorption lines of different elements to appear to have similar, modest optical depths, leading to erroneous column densities. The X-ray absorption in APM 08279+5255 is attributed to the BAL outflow in this object [107], and geometrical complications may be an issue. Given these uncertainties, caution seems in order regarding cosmological conclusions from current QSO iron abundances. Friaca et al. do make a case that certain nonstandard models of cosmology may already be inconsistent with the results for APM 08279+5255. However, all of this assumes that the abundances in QSOs reflect normal stellar evolution processes. In fact, the amount of mass involved in the BLR and the BAL outflows is small. Exotic processes that might affect abundances locally in AGNs include accretion onto stars trapped in the AGN accretion disk and undergoing rapid growth and evolution [6].

What about other ways to measure the iron abundance in QSOs?

The Fe⁺ ion is complex, and the physics of iron emission in AGNs may not be fully understood. Recent models including pumping by L α have achieved Fe II intensities closer to those observed, but extreme objects such as I Zw 1 still pose a challenge. Observed optical Fe II intensities, expressed as equivalent width or flux relative to H β , differ by more than an order of magnitude among QSOs. This variation is unlikely to result from the iron abundance. If there is depletion into grains in the BLR, then we must treat the gas-phase abundance as a lower limit until the depletion is understood. On the other hand, if unknown excitation processes explain the highest intensities of Fe II as in I Zw 1, then iron abundances may be overestimated. For now, I am inclined to reserve judgment on iron abundances from the optical and UV multiplets of Fe II, at the level of accuracy needed to test cosmology.

Another approach is to use the [FeVII] optical lines from the NLR, as discussed above. Although [229] proposed that the Fe⁺⁶/Ne⁺⁵ ratio should be a useful ratio because of similar ionization potentials, photoionization models indicate that these ions can come from substantially different zones in the ionization structure. Nevertheless, one can hope to constrain a photoionization model with multiple observed ions, and I suspect that the ionization correction uncertainty for Fe/Ne can be better than a factor of two. For high-redshift objects, [FeVII] λ 6086 may be challenging to observe. However, it could be used for lower redshift objects as a double check on Fe abundances obtained from X-ray features and from the Fe II emission lines in the optical and UV. Confirmation of high Fe abundances in

low-redshift objects would be interesting for chemical evolution studies and could lend greater confidence to high-redshift determinations relevant to cosmology.

Thank you, Greg.

Dear Michael (*Hawkins*), high-redshift quasars can be useful cosmological probes. They can even be used for testing the actual constancy of some of the fundamental physical constants, like the fine structure constant. How can quasars be useful for cosmology and for fundamental physics?

Quasars have an important property which makes them exceptionally useful for cosmological studies and some tests of fundamental physics. Their great luminosity and compact size mean that they can be used as light sources with some reasonably well-defined characteristics at very large distances or equivalently at early epochs in the universe. Perhaps, the greatest drawback of quasars as cosmological tools is their unsuitability as standard candles. Quasars have a huge range in luminosity, and although there are correlations such as the Baldwin effect between luminosity and emission-line strength which might be used as a measure, the scatter is too great to be useful for most purposes.

Notwithstanding this, quasars have played a major role in cosmological investigations. Although quasars do not make good standard candles, they have been used with good results to measure clustering on large scales. For example, the 2QZ quasar survey [40] measured the two-point correlation function for a sample of some 22,000 quasars to derive measures of the evolution of large-scale structure. Perhaps, the greatest uncertainty is the extent to which quasars are unbiased tracers of mass.

One of the most fruitful areas of cosmological research involving quasars has been the analysis of the absorption-line systems seen in quasar spectra produced by intervening galaxies and gas clouds and in particular, the dense pattern of absorption lines seen beyond the quasar Lyman α line. These lines are Lyman α absorption by gas clouds along the line of sight to the quasar and have been used to measure large-scale structure and evolution at high redshift [248].

Gravitational lens systems where a quasar image is split into two or more images have provided useful laboratories for a number of projects. Of particular interest for cosmology is a method for measuring the Hubble constant independently of the cosmic distance ladder. The method is based on the idea that changes in brightness of the quasar will be seen at different times in the two images, depending on the respective light travel times. These will differ, typically by a few light-months, as the light paths corresponding to the two images will not be the same. The calculation of the Hubble constant relies on modeling the matter distribution producing the lensing, which requires an estimation of the lensing galaxy's redshift and mass distribution. There are a number of lensed systems where modeling can be attempted, and a measure for H_0 obtained. The usefulness of these measures is limited by the accuracy of the mass model, and the fact that the time delays in individual systems appear to vary somewhat presumably due to small changes in path length associated with microlensing.

In addition to their use in cosmological projects, quasars have also been used to address questions in fundamental physics. The ratio of the wavelength of spectral

lines is a measure of the fine structure constant α , and quasars with their many absorption systems provide an excellent way of computing the value of α at different cosmic epochs and in different directions in space. Early results implied that α was increasing with time [223], but these results have since been challenged, and the group have now changed their claim to a model where α has different values in different directions.

Thank you Michael.

Dear Martin (*Elvis*), quasars have been discovered up to $z > 6$ at bright magnitudes. The type Ia SNe that have been famously used to establish cosmic acceleration are, in comparison, much dimmer sources, and even the most recent studies employ SNe only up to redshift $z \approx 1.9$. Why then have quasars never been used as standard candles?

First, quasars span an enormous range of intrinsic luminosity, at least 6 decades. This is comparable to the range of main sequence stars from O-giants to M-dwarfs. To be useful as standard candles requires some way of scaling these luminosities to a standard value, and the scaling parameter must itself be independent of distance. This is not a killer as the same type of scaling is applied to SNe, despite the lack of a physical theory for these scaling laws.

There are some ways a similar scaling might be done for quasars.

The Eddington limit is one possibility that could apply to populations in a narrow redshift band. Quasars clearly know about the Eddington limit [162], so the relation of distance to redshift could be tweaked to make the brightest quasars at any redshift be radiating exactly at this limit. This method assumes we can measure the mass of the black hole in each quasar, else we do not know where to put the limit. To be useful, the scaling must be accurate to a few percent, certainly $<10\%$. Measuring the total power of a quasar to this accuracy is not easy, and worse, current mass estimation methods are uncertain by at least a factor of 2. Moreover, it seems that the most massive quasars at any redshift fall short of the Eddington limit by a factor of several, even while lower mass quasars at the same redshift hit the limit [283].

The quasar mass-luminosity plane offers a variant on this method. Although not parallel to the $L = L_{\text{Edd}}$ line, the locus of quasars is tightly clustered around a ridge line with just a factor of 2 or so spread. Given that quasars vary by a factor of two, and the spectroscopic observations giving the black hole mass followed the photometric ones giving the luminosity by a year or more, the intrinsic spread must be considerably smaller [284]. Why this is so, we don’t know. It could well be that simultaneous measurements would give a ridge line sufficiently narrow to be useful as a standard candle.

Failing that can we use any spectroscopic signature [8] showed that the equivalent width of the CIV broad emission line (i.e., its strength relative to the local continuum) declines slowly as luminosity increases. CIV equivalent width could thus be used as a proxy for luminosity, while the line itself gives the redshift. As a result, this “Baldwin effect” has been extensively investigated for use as a standard candle. So far, however, the weakness of the decline and the spread in equivalent

width for objects of the same redshift and luminosity have proven too great to make the method useful.

Reverberation mapping gives the linear size of the broad emission-line region in light-days. If we could spatially resolve the broad-line region, we would have a size in arcseconds. The ratio would then determine the distance to the quasar in physical units (cm, Megaparsecs). The easily determined redshift would then give the Hubble constant, H_0 . We explored this idea in [64]. The angular scale of the hydrogen $H\beta$ emitting broad-line region is derivable from reverberation mapping sizes and turns out to be ~ 0.1 milliarcsec. This size does not shrink with redshift as beyond a redshift of ~ 2 angular sizes grow and because the brightest high-luminosity quasars have larger broad-line regions as $L^{1/2}$ [15].

The right way to make this measurement is with “imaging reverberation mapping” so that exactly the same gas is used to give both the angular and linear sizes. With this technique, the structure of the broad emission-line region can be fully determined in all three spatial and all three velocity components. For those of us who have struggled to understand quasar structure, it will be like looking up the answers in the back of the book.

The current and upcoming generation of optical interferometers that are sensitive enough to detect quasars (VLT-I, Keck-I, Magdalena Ridge) have baselines of a few 100 m, which gives about 1 milliarcsecond resolution in the near-IR (JHK bands, $1\text{--}2\mu\text{m}$), where they work well. So the prospect is not too far beyond present capabilities to imagine in a next-generation interferometer. Longer baselines of a few km may be possible, for example, at Domes A or B in Antarctica. At the shorter UV wavelengths, an interferometer only needs a few 100-m baselines to image the broad emission-line region but has to be in space to avoid atmospheric absorption. The “Stellar Imager” concept would do just that but is currently not an approved mission.

Thank you, Martin.

References

1. Adams, T.F.: A survey of the seyfert galaxies based on large-scale image-tube plates. *Astrophys. J. Suppl.* **33**, 19–34 (1977)
2. Alexander, D.M., Bauer, F.E., Brandt, W.N., Hornschemeier, A.E., Vignali, C., Garmire, G.P., Schneider, D.P., Chartas, G., Gallagher, S.C.: The chandra deep field north survey. XIV. X-ray-detected obscured AGNs and starburst galaxies in the bright submillimeter source population. *Astron. J.* **125**, 383 (2003)
3. Alonso-Herrero, A., Knapen, J.H.: Statistical properties of circumnuclear H II regions in nearby galaxies. *Astron. J.* **122**, 1350–1364 (2001)
4. Antonucci, R.: Unified models for active galactic nuclei and quasars. *Ann. Rev. Astron. Astrophys.* **31**, 473 (1993)
5. Ascaso, B., Aguerrí, J.A.L., Varela, J., Cava, A., Bettoni, D., Moles, M., D’Onofrio, M.: Evolution of BCG structural parameters in the Last 6 Gyr: Feedback processes versus merger events. *Astrophys. J.* **726**, 69 (2011)

6. Artymowicz, P., Lin, D.N.C., Wampler, E.J.: Star trapping and metallicity enrichment in quasars and active galactic nuclei. *Astrophys. J.* **409**, 592–603 (1993)
7. Bahcall, J.N., Kirhakos, S., Saxe, D.H., Schneider, D.P.: Hubble space telescope images of a sample of 20 nearby luminous quasars. *Astrophys. J.* **479**, 642–658 (1997)
8. Baldwin, J.: Luminosity indicators in the Spectra of quasi-stellar objects. *Astrophys. J.* **214**, 679 (1977)
9. Baldwin, J.A., Phillips, M.M., Terlevich, R.: Classification parameters for the emission-line spectra of extragalactic objects. *Publ. Astron. Soc. Pacific* **93**, 5–19 (1981)
10. Barazza, F.D., Joglee, S., Marinova, I.: Bars in disk-dominated and bulge-dominated galaxies at $z \sim 0$: New insights from ~ 3600 SDSS galaxies. *Astrophys. J.* **675**, 1194–1212 (2008)
11. Barnes, J.E., Hernquist, L.: Formation of dwarf galaxies in tidal tails. *Nature* **360**, 715–717 (1992)
12. Begelman, M.C., Blandford, R.D., Rees, M.J.: Theory of extragalactic radio sources. *RvMP*, **56**, 255–351 (1984)
13. Begelman, M.C., Nath, B.B.: Self-regulated black hole accretion, the $M - \sigma$ relation and the growth of bulges in galaxies. *Mon. Not. R. Astron. Soc.* **361**, 1387–1392 (2005)
14. Begelman, M., Volonteri, M., Rees, M.J.: Formation of supermassive black holes by direct collapse of pre-galactic halos. *Mon. Not. R. Astron. Soc.* **370**, 289–298 (2006)
15. Bentz, M.C., Peterson, B.M., Netzer, H., Pogge, R.W., Vestergaard, M.: The radius-luminosity relationship for active galactic nuclei: The effect of host-galaxy starlight on luminosity measurements II. The full sample of reverberation-mapped AGNs. *Astrophys. J.* **697**, 160–181 (2009)
16. Bentz, M.C., Walsh, J.L., Barth, A.J., Baliber, N., Bennert, N., Canalizo, G., Filippenko, A.V., Ganeshalingam, M., Gates, E.L., Greene, J.E., Hidas, M.G., Hiner, K.D., et al.: First results from the lick AGN monitoring project: The mass of the black hole in Arp 151. *Astrophys. J.* **689**, L21 (2008)
17. Bettoni, D., Falomo, R., Fasano, G., Govoni, F., Salvo, M., Scarpa, R.: The fundamental plane of radio galaxies. *Astron. Astrophys.* **380**, 471 (2001)
18. Blandford R.D.: Origin and evolution of massive black holes in galactic nuclei. In: *Galaxy Dynamics*. Merritt D.R., Valluri M., Sellwood J.A. (eds.) *Astron. Soc. Pac.*, San Francisco, ASP Conf. Ser. **182**, 87
19. Booth, C.M. Schaye, J.: Cosmological simulations of the growth of supermassive black holes and feedback from active galactic nuclei: Method and tests. *Mon. Not. R. Astron. Soc.* **398**, 53 (2009)
20. Bouwens, R.J., Illingworth, G.D., Oesch, P.A., Stiavelli, et al.: Discovery of $z \sim 8$ galaxies in the hubble ultra deep field from ultra-deep WFC3/IR observations. *Astrophys. J.* **709**, L133–L137 (2010)
21. Bower, R.G., Benson, A.J., Malbon, R., Helly, J.C., Frenk, C.S., Baugh, C.M., Cole, S., Lacey, C.G.: Breaking the hierarchy of galaxy formation. *Mon. Not. R. Astron. Soc.* **370**, 645–655 (2006)
22. Boyle, B.J., Shanks, T., Croom, S.M., Smith, R.J., Miller, L., Loaring, B., Heymans, C.: The 2dF QSO redshift survey – I. The optical luminosity function of quasi-stellar objects. *Mon. Not. R. Astron. Soc.* **317**, 1014–1022 (2000)
23. Bressan, A., Granato G.L., Silva, L.: Modelling intermediate age and old stellar populations in the infrared. *Astron. Astrophys.* **332**, 135 (1998)
24. Buta, R., Combes, F.: Galactic rings. *Fundam. Cosmic Ph.* **17**, 95–281 (1996)
25. Cassata, P., Vanzella, E., Pozzetti, L., Cristiani, S., Fontana, A., Rodighiero, G., Mignoli, M., Zamorani, G.: Old galaxies in the young universe. *Nature* **430**, 184 (2004)
26. Cattaneo, A., Faber, S.M., Binney, J., Dekel, A., Kormendy, J., Mushotzky, R., Babul, A., Best, P.N., Brügggen, M., Fabian, A.C., Frenk, C.S., Khalatyan, A., Netzer, H., Mahdavi, A., Silk, J., Steinmetz, M., Wisotzki, L.: The role of black holes in galaxy formation and evolution. *Nature* **460**, 213–219 (2009)
27. Cavaliere, A., Vittorini, V.: Supermassive black holes in galactic nuclei. *Astrophys. J.* **570**, 114–118 (2002)

28. Cavaliere, A., Vittorini, V.: The fall of the quasar population. *Astrophys. J.* **543**, 599–610 (2000)
29. Cavaliere, A., Colafrancesco, S., Scaramella, R.: The mass distribution of groups and clusters of galaxies. *Astrophys. J.* **380**, 15–23 (1991)
30. Cen, R.: The universe was reionized twice. *Astrophys. J.* **591**, 12 (2003)
31. Ciotti L. Ostriker J.P.: Cooling flows and quasars: Different aspects of the same phenomenon? I. Concepts. *Astrophys. J.* **487**, L105 (1997)
32. Ciotti, L., Ostriker, J.P., Proga, D.: Feedback from central black holes in elliptical galaxies. III. Models with both radiative and mechanical feedback. *Astrophys. J.* **717**, 708–723 (2010)
33. Coil, A.L., Hennawi, J.F., Newman, J.A., Cooper, M.C., Davis, M.: The DEEP2 galaxy redshift survey: Clustering of quasars and galaxies at $z=1$. *Astrophys. J.* **654**, 115–124 (2007)
34. Combes, F., Gerin, M.: Spiral structure of molecular clouds in response to bar forcing – A particle simulation. *Astron. Astrophys.* **150**, 327–338 (1985)
35. Comerón, S., Knapen, J.H., Beckman, J.E., Laurikainen, E., Salo, H., Martínez-Valpuesta, I., Buta, R.J.: AINUR: Atlas of images of NUClear rings. *Mon. Not. R. Astron. Soc.* **402**, 2462–2490 (2010)
36. Contini, M., Goldman, I.: Spectra from the shocked nebulae revealing turbulence near the galactic centre. *Mon. Not. R. Astron. Soc.* **411**, 792–806 (2011)
37. Cook, M., Lapi, A., Granato, G.L.: Two-phase galaxy formation. *Mon. Not. R. Astron. Soc.* **397**, 534–47 (2009)
38. Corbin, M.R.: Relativistic effects in the QSO broad-line region. *Astrophys. J.* **485**, 517 (1997)
39. Croft, S., van Breugel, W., de Vries, W., Dopita, M., Martin, C., Morganti, R., Neff, S., Oosterloo, T., Schiminovich, D., Stanford, S.A., van Gorkom, J.: Minkowski’s object: A starburst triggered by a radio jet, revisited. *Astrophys. J.* **647**, 1040–1055 (2006)
40. Croom, S.M., Boyle, B.J., Shanks, T., Smith, R.J., Miller, L., Outram, P.J., Loaring, N.S., Hoyle, F., da Ângela, J.: The 2dF QSO redshift survey – XIV. Structure and evolution from the two-point correlation function. *Mon. Not. R. Astron. Soc.* **356**, 415–438 (2005)
41. Croom S.M., Richards G.T., Shanks T., Boyle B.J., Strauss M.A., Myers A.D., Nichol R.C., Pimblet K.A., et al.: The 2dF-SDSS LRG and QSO survey: The QSO luminosity function at $0.4 < z < 2.6$. *Mon. Not. R. Astron. Soc.* **399**, 1755–1772 (2009)
42. Croom, S.M., Schade, D., Boyle, B.J., Shanks, T., Miller, L., Smith, R.J.: Gemini imaging of QSO host galaxies at $z \sim 2$. *Astrophys. J.* **606**, 126 (2004)
43. Croom, S.M., Smith, R.J., Boyle, B.J., Shanks, T., Miller, L., Outram, P.J., Loaring, N.S.: The 2dF QSO redshift survey – XII. The spectroscopic catalogue and luminosity function. *Mon. Not. R. Astron. Soc.* **349**, 1397 (2004)
44. Croton, D.J., Springel, V., White, S.D.M., De Lucia, G., Frenk, C.S., Gao, L., Jenkins, A., Kauffmann, G., Navarro, J.F., Yoshida, N.: The many lives of active galactic nuclei: cooling flows, black holes and the luminosities and colours of galaxies. *Mon. Not. R. Astron. Soc.* **365**, 11–28. Erratum: *Mon. Not. R. Astron. Soc.* **367**, 864 (2006)
45. Daddi, E., Renzini, A., Pirzkal, N., Cimatti, A., Malhotra, S., Stiavelli, M., Xu, C., Pasquali, A., Rhoads, J.E., Brusa, M., di Serego Alighieri, S., et al.: Passively evolving early-type galaxies at $1.4 \lesssim z \sim 2.5$ in the hubble ultra deep field. *Astrophys. J.* **626**, 680 (2005)
46. Dahari, O.: Companions of seyfert galaxies – A statistical survey. *Astron. J.* **89**, 966–974 (1984)
47. Dahari, O.: Companions of seyfert galaxies. II. *Astron. J.* **90**, 1772–1782 (1985)
48. Dahari, O.: The nuclear activity of interacting galaxies. *Astrophys. J.* **57**, 643–664 (1985)
49. Dalla Bontà, E., Ferrarese, L., Corsini, E.M., Miralda-Escudé, J., Coccatto, L., Sarzi, M., Pizzella, A., Beifiori, A.: The high-mass end of the black hole mass function: Mass estimates in brightest cluster galaxies. *Astrophys. J.* **690**, 537–559 (2009)
50. Davies, R.I., Maciejewski, W., Hicks, E.K.S., Tacconi, L.J., Genzel, R., Engel, H.: Stellar and molecular gas kinematics of NGC 1097: Inflow driven by a nuclear spiral. *Astrophys. J.* **702**, 114–128 (2009)

51. Decarli, R., Falomo, R., Treves, A., Kotilainen, J., Labita M., Scarpa, R.: The quasar $M_{\text{BH}} - M_{\text{host}}$ relation through cosmic time – II. Evidence for evolution from $z = 3$ to the present age. *Mon. Not. R. Astron. Soc.* **402**, 2453 (2010)
52. De Lucia, G., Springel, V., White, S.D.M., Croton, D., Kauffmann, G.: The formation history of elliptical galaxies. *Mon. Not. R. Astron. Soc.* **366**, 499–509 (2006)
53. de Mello, D.F., Sulentic, J.W., de Souza, R.E.: Star Formation in interacting galaxies. *RMxAC* **4**, 140 (1996)
54. De Robertis, M.M., Yee, H.K.C., Hayhoe, K.: A CCD study of the environment of seyfert galaxies. II. Testing the interaction hypothesis. *Astrophys. J.* **496**, 93 (1998)
55. Di Matteo, T., Springel, V., Hernquist, L.: Energy input from quasars regulates the growth and activity of black holes and their host galaxies. *Nature* **433**, 604–607 (2005)
56. Disney, M.J., Oyce, P.J., Blades, J.C., Boksenberg, A., Crane, P., Deharveng, J.M., Macchetto, F., Mackay, C.D., Sparks, W.B., Phillipps, S.: Interacting elliptical galaxies as hosts of intermediate-redshift quasars. *Nature* **376**, 150–153 (1995)
57. Donoso, E., Li, C., Kauffman, G., Best, P.N., Heckman, T.M.: Clustering of radio galaxies and quasars. *Mon. Not. R. astron. Soc.* **407**, 1078–1089 (2010)
58. Dultzin, D., Krongold, Y., González, J.J., Hernández-Toledo, H.: Does close interaction between galaxies induce nuclear activity? *ASP Conf. Ser.* **421**, 115 (2010)
59. Dultzin-Hacyan, D., Krongold, Y., Fuentes-Guridi, I., Marziani, P.: The close environment of seyfert galaxies and its implication for unification models. *Astrophys. J.* **513**, L111–L114 (1999)
60. Dunlop, J.S., McLure, R.J., Kukula, M.J., Baum, S.A., O’Dea, C.P., Hughes, D.H.: Quasars, their host galaxies and their central black holes. *Mon. Not. R. Astron. Soc.* **340**, 1095–1135 (2003)
61. Dunlop, J.S., Peacock J.: The redshift cut-off in the luminosity function of radio galaxies and quasars. *Mon. Not. R. Astron. Soc.* **247**, 19 (1990)
62. Elitzur, M.: The obscuring torus in AGN. *New Astron. Rev.* **50**, 728–731 (2006)
63. Elitzur, M., Shlosman, I.: The AGN-obscuring torus: The end of the “Doughnut” paradigm? *Astrophys. J.* **648**, L101–L104 (2006)
64. Elvis M., Karovska, M.: Quasar parallax: A method for determining direct geometrical distances to quasars. *Astrophys. J.* **581**, 67 (2002)
65. Emsellem, E., Greusard, D., Combes, F., Friedli, D., Leon, S., Pécontal, E., Wozniak, H.: Dynamics of embedded bars and the connection with AGN. I. ISAAC/VLT stellar kinematics. *Astron. Astrophys.* **368**, 52–63 (2001)
66. Fabian A.C.: The obscured growth of massive black holes. *Mon. Not. R. Astron. Soc.* **308**, L39 (1999)
67. Fabian, A.C., Celotti, A., Erlund, M.C.: Radiative pressure feedback by a quasar in a galactic bulge. *Mon. Not. R. Astron. Soc.* **373**, L16 (2006)
68. Falomo R., Kotilainen J.K., Scarpa R., Treves A.: VLT adaptive optics imaging of QSO host galaxies and their close environment at $z \sim 2.5$: Results from a pilot program. *Astron. Astrophys.* **434**, 469 (2005)
69. Falomo R., Treves A., Kotilainen J.K., Scarpa R., Uslenghi M.: Near-infrared adaptive optics imaging of high-redshift quasars. *Astrophys. J.* **673**, 694 (2008)
70. Fan, X., Carilli, C.L., Keating, B.: Observational constraints on cosmic reionization. *Ann. Rev. Astron. Astrophys.* **44**, 415 (2006)
71. Fan, X., Hennawi, J.F., Richards, G.T., Strauss, M.A., Schneider, D.P., Donley, J.L., Young, J.E., Annis, J., Lin, H., Lampeitl, H., Lupton, R.H., et al.: A Survey of $z > 5.7$ quasars in the sloan digital sky survey. III. Discovery of five additional quasars. *Astron. J.* **128**, 515–522 (2004)
72. Fan, X., Strauss, M.A., Richards, G.T., Hennawi, J.F., Becker, R.H., White, R.L., Diamond-Stanic, A.M., Donley, J.L., Jiang, L., Kim, J.S., Vestergaard, M., et al.: A survey of $z \sim 5.7$ quasars in the sloan digital sky survey. IV. Discovery of seven additional quasars. *Astron. J.* **131**, 1203–1209 (2006)

73. Fathi, K., Beckman, J.E., Lundgren, A.A., Carignan, C., Hernandez, O., Amram, P., Balard, P., Boulesteix, J., et al.: Spiral inflow feeding the nuclear starburst in M83, observed in H α emission with the GH α FaS fabry-perot interferometer. *Astrophys. J.* **675**, L17–L20 (2008)
74. Fathi, K., Storchi-Bergmann, T., Riffel, R.A., Winge, C., Axon, D.J., Robinson, A., Capetti, A., Marconi, A.: Streaming motions toward the supermassive black hole in NGC 1097. *Astrophys. J.* **641**, L25–L28 (2006)
75. Ferland, G.J., Hu, C., Wang, J.-M., Baldwin, J.A., Porter, R.L., van Hoof, P.A.M., Williams, R.J.R.: Implications of infalling Fe II-emitting clouds in active galactic nuclei: Anisotropic properties. *Astrophys. J.* **707**, L82–L86 (2009)
76. Ferland, G.J., Korista, K.T., Verner, D.A., Ferguson, J.W., Kingdon, J.B., Verner, E.M.: CLOUDY 90: Numerical simulations of ionized plasmas and their spectra. *Pub. Astron. Soc. Pacific* **110**, 761 (1998)
77. Ferrarese, L.: Observational evidence for supermassive black holes. In: Haardt, F., Gorini, V., Moschella, U., Colpi, M. (eds.) *Joint Evolution of Black Holes and Galaxies*, pp. 1–62. Taylor & Francis, New York (2006)
78. Ferrarese, L., Merritt, D.: A fundamental relation between supermassive black holes and their host galaxies. *Astrophys. J.* **539**, L9–L12 (2000)
79. Feruglio, C., Maiolino, R., Piconcelli, E., Menci, N., Aussel, H., Lamastra, A., Fiore, F.: Quasar feedback revealed by giant molecular outflows. *Astron. Astrophys.* **518**, L155–L159 (2010)
80. Fontanot, F., Cristiani S., Monaco P., Nonino M., Vanzella E., Brandt, W.N., Grazian, A., Mao, J.: The luminosity function of high-redshift quasi-stellar objects. A combined analysis of GOODS and SDSS. *Astron. Astrophys.* **461**, 39 (2007)
81. Fragile, P.C., Murray, S.D., Anninos, P., van Breugel, W.: Radiative shock-induced collapse of intergalactic clouds. *Astrophys. J.* **604**, 74–87 (2004)
82. Franceschini, A., Hasinger, G., Miyaji, T., Malquori, D.: On the relationship between galaxy formation and quasar evolution. *Mon. Not. R. Astron. Soc.* **310**, L5–L9 (1999)
83. Franco-Balderas, A., Dultzin-Hacyan, D., Hernández-Toledo, H.M.: BVRI surface photometry of mixed morphology pairs of galaxies. Interactions, mergers and nuclear activity. In: Mújica, R., Maiolino, R. (eds.) *Multiwavelength AGN Surveys. Proceedings of the Guillermo Haro Conference 2003*, pp. 395–396. World Scientific Publishing Co., Singapore (2004)
84. Franco-Balderas, A., Hernández-Toledo, H.M., Dultzin-Hacyan, D., García-Ruiz, G.: BVRI surface photometry of mixed morphology pairs of galaxies. I. The first data set. *Astron. Astrophys.* **406**, 415–426 (2003)
85. Franco-Balderas, A., Hernández-Toledo, H.M., Dultzin-Hacyan, D., Rosado, M.: BVRI surface photometry of mixed morphology pairs of galaxies. III. The third data set. *Rev. Mex. Astron. Astrof.* **41**, 483–505 (2005)
86. Friaca, A.C.S., Alcaniz, J.S., Lima, J.A.S.: An old quasar in a young dark energy-dominated universe? *Mon. Not. R. Astron. Soc.* **362**, 1295–1300 (2005)
87. Gabor, J.M., Impey, C.D., Jahnke, K., Simmons, B.D., Trump, J.R., Koekemoer, A.M., Brusa, M., Cappelluti, N., Schinnerer, E., Smolčić V., Salvato, M., Rhodes, J.D., Mobasher, B., Capak, P., Massey, R., Leauthaud, A., Scoville, N.: Active galactic nucleus host galaxy morphologies in COSMOS. *Astrophys. J.* **691**, 705–722 (2009)
88. Gaskell, C.M.: Inflow of the Broad-Line Region and the Fundamental Limitations of Reverberation Mapping. In: *Accretion and Ejection in AGN: a Global View*. L. Maraschi, G. Ghisellini, R. Della Ceca, and F. Tavecchio. (eds), p.68, (2009)
89. Gebhardt, K., Bender, R., Bower, G., Dressler, A., Faber, S.M., Filippenko, A.V., Green, R., Grillmair, C., Ho, L.C., et al.: A relationship between nuclear black hole mass and galaxy velocity dispersion. *Astrophys. J.* **539**, L13–L16 (2000)
90. Giacconi, R., Gursky, H., Paolini, F., Rossi, B.: Evidence for X-rays from sources outside the solar system. *Phys. Rev. Lett.* **9**, 439 (1962)
91. González, J.J., Krongold, Y., Dultzin, D., Hernández-Toledo, H.M., Huerta, E.M., Olguín, L., Marziani, P., Cruz-González, I.: Induced activity in mixed-morphology galaxy pairs. *Rev. Mex. Astron. Astrophys. Conf. Ser.* **32**, 170–172 (2008)

92. Gnedin, N.Y.: Reionization, sloan, and WMAP: Is the picture consistent? *Astrophys. J.* **610**, 9 (2004)
93. González-Martín, O., Masegosa, J., Márquez, I., Guerrero, M.A., Dultzin-Hacyan, D.: X-ray nature of the LINER nuclear sources. *Astron. Astrophys.* **460**, 45–57 (2006)
94. Granato, G.L., De Zotti, G., Silva, L., Bressan, A., Danese, L.: A physical model for the coevolution of QSOs and their spheroidal hosts. *Astrophys. J.* **600**, 580–594 (2004)
95. Granato, G.L., Silva, L., Lapi, A., Shankar, F., De Zotti, G., Danese, L.: The growth of the nuclear black holes in submillimetre galaxies. *Mon. Not. R. Astron. Soc.* **368**, 72 (2006)
96. Greenhill, L.J., Booth, R.S., Ellingsen, S.P., Herrnstein, J.R., Jauncey, D.L., McCulloch, P.M., Moran, J.M., Norris, R.P., Reynolds, J.E., Tzioumis, A.K.: A warped accretion disk and wide-angle outflow in the inner parsec of the circinus galaxy. *Astrophys. J.* **590**, 162–173 (2003)
97. Grogin, N.A., Conselice, C.J., Chatzichristou, E., Alexander, D.M., Bauer, F.E., Hornschemeier, A.E., Jogee, S., Koekemoer, A.M., Laidler, V.G., Livio, M., Lucas, R.A., Paolillo, M., Ravindranath, S., Schreier, E.J., Simmons, B.D., Urry, C.M.: AGN host galaxies at $z \sim 0.4 - 1.3$: Bulge-dominated and lacking Merger-AGN connection. *Astrophys. J.* **627**, L97–L100 (2005)
98. Gültekin, K., Richstone, D.O., Gebhardt, K., Lauer, T.R., Tremaine, S., Aller, M.C., Bender, R., Dressler, A., Faber, S.M., et al.: The $M-\sigma$ and $M-L$ relations in galactic bulges, and determinations of their intrinsic scatter. *Astrophys. J.* **698**, 198–221 (2009)
99. Gunn, J.E., Peterson, B.A.: On the density of neutral hydrogen in intergalactic space. *Astrophys. J.* **142**, 1633 (1965)
100. Haiman, Z.: The origin and detection of high-redshift supermassive black holes. *AIP Conf. Proc.* **1294**, 215–224 (2010)
101. Hamann, F., Ferland, G.: The chemical evolution of QSOs and the implications for cosmology and galaxy formation. *Astrophys. J.* **418**, 11–27 (1993)
102. Hamann, F., Ferland, G.: Elemental abundances in quasi-stellar objects: Star formation and galactic nuclear evolution at high redshifts. *Ann. Rev. Astron. Astrophys.* **37**, 487–531 (1999)
103. Hao, L., Jogee, S., Barazza, F.D., Marinova, I., Shen, J.: Bars in starbursts and AGNs – A quantitative reexamination. In: Jogee, S., Marinova, I., Hao, L., Blanc, G.A. (eds.) *Galaxy Evolution: Emerging Insights and Future Challenges*. Proceedings of a conference held 11–14 November 2008 at the University of Texas, Austin, Texas, USA; ASP Conference Series vol. 419, pp. 402–409. Astronomical Society of the Pacific, San Francisco (2009)
104. Hao, L., Strauss, M.A., Fan, X., Tremonti, C.A., Schlegel, D.J., Heckman, T.M., Kauffmann, G., Blanton, M.R., Gunn, J.E., Hall, et al.: Active galactic nuclei in the sloan digital sky survey. II. Emission-line luminosity function. *Astron. J.* **129**, 1795–1808 (2005)
105. Hasinger, G.: Absorption properties and evolution of active galactic nuclei. *Astron. Astrophys.* **490**, 905–922 (2008)
106. Hasinger, G., Miyaji, T., Schmidt, M.: Luminosity-dependent evolution of soft X-ray selected AGN. New chandra and XMM-newton surveys. *Astron. Astrophys.* **441**, 417–434 (2005)
107. Hasinger, G., Scharrel, N., Komossa, S.: Discovery of an ionized Fe K edge in the $z = 3.91$ broad absorption line quasar APM 08279+5255 with XMM-Newton. *Astrophys. J.* **573**, L77–L80 (2002)
108. Hatziminaoglou, E., Omont, A., Stevens, J.A., Amblard, A., Arumugam, V., Auld, R., Aussel, H., Babbedge, T., Blain, A., Bock, J., Boselli, A., Buat, V., Burgarella, D., et al.: HerMES: Far infrared properties of known AGN in the HerMES fields. *Astron. Astrophys.* **518**, L33 (2010)
109. Hawarden, T.G., Mountain, C.M., Leggett, S.K., Puxley, P.J.: Enhanced star formation – The importance of bars in spiral galaxies. *Mon. Not. R. Astron. Soc.* **221**, 41P–45P (1986)
110. Hawkins, M.R.S.: Naked active galactic nuclei. *Astron. Astrophys.* **424**, 519–529 (2004)

111. Heckman, T.M.: The Co-evolution of galaxies and black holes: Current status and future prospects. In: Co-evolution of central black holes and galaxies. IAU Symposium, vol. 267, pp. 3–14 (2010)
112. Hernández-Ibarra, F., et al.: Induced Nuclear Activity in Galaxy Pairs, *Revista Mexicana de Astronomía y Astrofísica*, **40**, 58 (2011)
113. Hernández Toledo, H.M., Dultzin-Hacyan, D., Gonzalez, J.J., Sulentic, J.W.: Statistical properties of the emission in mixed-morphology (E+S) pairs. I. Optical results. *Astron. J.* **118**, 108–125 (1999)
114. Hernández Toledo, H.M., Dultzin-Hacyan, D., Sulentic, J.W.: Statistical properties of the emission in mixed-morphology (E+S) pairs. II. MIR/FIR results. *Astron. J.* **121**, 1319–1335 (2001)
115. Herrnstein, J.R., Greenhill, L.J., Moran, J.M.: The warp in the subparsec molecular disk in NGC4258 as an explanation for persistent asymmetries in the maser spectrum. *Astrophys. J.* **468**, L17 (1996)
116. Hickox, R.C., Myers, A.D., Brodwin, M., et al.: Clustering of obscured and unobscured quasars in the bootes field: Placing rapidly growing black holes in the cosmic web. *Astrophys. J.* **731**, 117 (2011)
117. Hicks, E.K.S., Davies, R.I., Malkan, M.A., Genzel, R., Tacconi, L.J., Müller Sánchez, F., Sternberg, A.: The role of molecular gas in obscuring seyfert active galactic nuclei. *Astrophys. J.* **696**, 448–470 (2009)
118. Hills, J.G.: Possible power source of Seyfert galaxies and QSOs. *Nature*, **254**, 295–297 (1975)
119. Ho, L.C.: Nuclear activity in nearby galaxies. *Ann. Rev. Astro. Astrophys.* **46**, 475 (2008)
120. Holt, J., Tadhunter, C.N., Morganti, R.: Fast outflows in compact radio sources: Evidence for AGN-induced feedback in the early stages of radio source. *Mon. Not. R. Astron. Soc.* **387**, 639–659 (2008)
121. Hopkins, P.F., Hernquist, L., Cox, T.J., Robertson, B., Krause, E.: A theoretical interpretation of the black hole fundamental plane. *Astrophys. J.* **669**, 45–66 (2007)
122. Hopkins, P.F., Richards, G.T., Hernquist, L.: An observational determination of the bolometric quasar luminosity function. *Astrophys. J.* **654**, 731 (2007)
123. Horne, K., Marsh, T.R.: Emission line formation in accretion discs. *Mon. Not. R. Astron. Soc.* **218**, 761–773 (1986)
124. Hu, C., Wang, J.-M., Ho, L.C., Chen, Y.-M., Bian, W.-H., Xue, S.-J.: $H\beta$ profiles in quasars: Evidence for an intermediate-line region. *Astrophys. J. Lett.* **683**, L115–L118 (2008)
125. Hu, C., Wang, J.-M., Ho, L.C., Chen, Y.-M., Zhang, H.-T., Bian, W.-H., Xue, S.-J.: A systematic analysis of Fe II emission in quasars: Evidence for inflow to the central black hole. *Astrophys. J.* **687**, 78–96 (2008)
126. Hummel, E.: The radio continuum properties of spiral galaxies. *Astron. Astrophys.* **93**, 93–105 (1981)
127. Hyvönen, T., Kotilainen, J.K., Falomo, R., Örndahl, E., Pursimo, T.: The stellar content of low redshift BL Lacertae host galaxies from multicolour imaging. *Astron. Astrophys.* **476**, 723–734 (2007)
128. Hyvönen, T., Kotilainen, J.K., Reunanen, J., Falomo, R.: The stellar content of low redshift radio galaxies from near-infrared spectroscopy. *Astron. Astrophys.* **499**, 417–425 (2009)
129. Inskip, K.J., Best, P.N., Longair, M.S., Röttgering, H.J.A.: HST and UKIRT imaging observations of $z \sim 1$ 6C radio galaxies – II. Galaxy morphologies and the alignment effect. *Mon. Not. R. Astron. Soc.* **359**, 1393–1414 (2005)
130. Jahnke K., Kuhlbrodt B., Wisotzki L.: Quasar host galaxy star formation activity from multicolour data. *Mon. Not. R. Astron. Soc.* **352**, 399 (2004)
131. Jiang, L., Fan, X., Annis, J., Becker, R.H., White, R.L., Chiu, K., Lin, H., Lupton, R.H., Richards, G.T., Strauss, M.A., Jester, S., Schneider, D.P.: A survey of $z \sim 6$ quasars in the sloan digital sky survey deep stripe. I. A flux-limited sample at $z_{AB} < 21$. *Astron. J.* **135**, 1057–1066 (2008)

132. Jiang, L., Fan, X., Bian, F., Annis, J., Chiu, K., Jester, S., Lin, H., Lupton, R.H., Richards, G.T., Strauss, M.A., Malanushenko, V., Malanushenko, E., Schneider, D.P.: A survey of $z \sim 6$ quasars in the sloan digital sky survey deep stripe. II. Discovery of six quasars at $z_{AB} > 21$. *Astron. J.* **138**, 305–311 (2009)
133. Jiang, L., Fan, X., Brandt, W.N., Carilli, C., Egami, E., Hines, D.C., Kurk, J.D., Richards, G.T., Shen, Y., Strauss, M.A., Vestergaard, M., Walter, F.: Dust-free quasars in the early universe. *Nature* **464**, 380 (2010)
134. Jiang, L., Fan, X., Cool, R.J., Eisenstein, D.J., Zehavi, I., Richards, G.T., Scranton, R., Johnston, D., Strauss, M.A., Schneider, D.P., Brinkmann, J.: A spectroscopic survey of faint quasars in the SDSS deep stripe. I. Preliminary results from the Co-added catalog. *Astron. J.* **131**, 2788–2800 (2006)
135. James, P.A., Bretherton, C.F., Knapen, J.H.: The $H\alpha$ galaxy survey. VII. The spatial distribution of star formation within disks and bulges. *Astron. Astrophys.* **501**, 207–220 (2009)
136. Jarvis, J.F., Tyson, J.A.: FOCAS – Faint object classification and analysis system. *Astron. J.* **86**, 476–495 (1981)
137. Jogee, S., Kenney, J.D.P., Smith, B.J.: A Gas-rich nuclear bar fueling a powerful central starburst in NGC 2782. *Astrophys. J.* **526**, 665 (1999)
138. Jogee, S., Scoville, N., Kenney, J.D.P.: The central region of barred galaxies: Molecular environment, starbursts, and secular evolution. *Astrophys. J.* **630**, 837–863 (2005)
139. Jogee, S., Shlosman, I., Laine, S., Englmaier, P., Knapen, J.H., Scoville, N., Wilson, C.D.: Gasdynamics in NGC 5248: Fueling a circumnuclear starburst ring of super-star clusters. *Astrophys. J.* **575**, 156–177 (2002)
140. Johnson, J., Greif, T., Bromm, V.: Occurrence of metal-free galaxies in the early Universe. *Mon. Not. R. Astron. Soc.* **388**, 26–38 (2008)
141. Karachentsev, I.D.: Catalogue of isolated pairs of galaxies in the northern hemisphere. *Soobshcheniya Spetsial'noj Astrofizicheskoy Observatorii* **7**, 1 (1972)
142. Karachentsev, I.D., Karachentseva, V.E.: Type and shape differences for isolated and paired galaxies. *Soviet Astron.* **18**, 428 (1975)
143. Kauffmann, G., Haehnelt M.: A unified model for the evolution of galaxies and quasars. *Mon. Not. R. Astron. Soc.* **311**, 576 (2000)
144. Kauffmann, G., Heckman, T.M.: Feast and famine: Regulation of black hole growth in low-redshift galaxies. *Mon. Not. R. Astron. Soc.* **397**, 135–147 (2009)
145. Kauffmann, G., Heckman, T.M., Tremonti, C., Brinchmann, J., Charlot, S., White, S.D.M., Ridgway, S.E., Brinkmann, J., Fukugita, M., Hall, P.B., Ivezić, Ž., Richards, G.T., Schneider, D.P.: The host galaxies of active galactic nuclei. *Mon. Not. R. Astron. Soc.* **346**, 1055–1077 (2003)
146. Keel, W.C.: Dynamical segregation of direct and retrograde orbits in binary disk galaxies. *Astrophys. J.* **375**, L5–L7 (1991)
147. Keel, W.C., Kennicutt, R.C., Jr., Hummel, E., van der Hulst, J.M.: The effects of interactions on spiral galaxies. I – Nuclear activity and star formation. *Astron. J.* **90**, 708–730 (1985)
148. Kewley, L.J., Groves, B., Kauffmann, G., Heckman, T.: The host galaxies and classification of active galactic nuclei. *Mon. Not. R. Astron. Soc.* **372**, 961–976 (2006)
149. Kewley, L.J., Heisler, C.A., Dopita, M.A., Lumsden, S.: Optical classification of southern warm infrared galaxies. *Astrophys. J. Suppl.* **132**, 37–71 (2001)
150. Kim, S., Stiavelli, M., Trenti, M., et al.: The environments of high-redshift quasi-stellar objects. *Astrophys. J.*, **695**, 809–817 (2009)
151. King, A.: Black holes, galaxy formation, and the $M_{\text{BH}} - \sigma$ relation. *Astrophys. J.* **596**, L27 (2003)
152. King, A.: The AGN-starburst connection, galactic superwinds, and $M_{\text{BH}} - \sigma$. *Astrophys. J. Lett.* **635**, L121 (2005)
153. King, A.R., Pringle, J.E., Hofmann, J.A.: The evolution of black hole mass and spin in active galactic nuclei. *Mon. Not. R. Astron. Soc.* **385**, 1621–1627 (2008)
154. Knapen, J.H.: Fuelling starbursts and AGN. *ASSL* **319**, 189–206 (2004)

155. Knapen, J.H.: Structure and star formation in disk galaxies. III. Nuclear and circumnuclear H α emission. *Astron. Astrophys.* **429**, 141–151 (2005)
156. Knapen, J.H.: Rings and bars: Unmasking secular evolution of galaxies. In: Block, D.L., Freeman, K.C., Puerari, I. (eds.) *Galaxies and their Masks*. pp. 201–220. Springer, New York (2010)
157. Knapen, J.H., Beckman, J.E., Heller, C.H., Shlosman, I., de Jong, R.S.: The central region in M100: Observations and modeling. *Astrophys. J.* **454**, 623–642 (1995)
158. Knapen, J.H., Beckman, J.E., Shlosman, I., Mahoney, T.J. (eds.): The central Kpc of starbursts and AGN: The La Palma connection. *ASP Conf. Ser.* **249** (2001)
159. Knapen, J.H., James, P.A.: The H α galaxy survey. VIII. Close companions and interactions, and the definition of starbursts. *Astrophys. J.*, **698**, 1437–1455 (2009)
160. Knapen, J.H., Sharp, R.G., Ryder, S.D., Falc3n-Barroso, J., Fathi, K., Guti3rrez, L.: The central region of M83: massive star formation, kinematics, and the location and origin of the nucleus. *Mon. Not. R. Astron. Soc.* **408**, 797–811 (2010)
161. Knapen, J.H., Shlosman, I., Peletier, R.F.: A subarcsecond resolution near-infrared study of seyfert and “Normal” galaxies. II. Morphol. *Astrophys. J.* **529**, 93–100 (2000)
162. Kollmerier, J., Onken, C.A., Kochanek, C.S., Gould, A., Weinberg, D.H., Dietrich, M., Cool, R., Dey, A., Eisenstein, D.J., Jannuzi, B.T., Le Floch, E., Stern, D.: Black hole masses and eddington ratios at $0.3 < z < 4$. *Astrophys. J.* **648**, 128 (2006)
163. Komossa, S., Burwitz, V., Hasinger, G., Predehl, P., Kaastra, J.S., Ikebe, Y.: Discovery of a binary active galactic nucleus in the ultraluminous infrared galaxy NGC 6240 using chandra. *Astrophys. J.* **582**, L15–L19 (2003)
164. Komugi, S., Sofue, Y., Kohno, K., Nakanishi, H., Onodera, S., Egusa, F., Muraoka, K.: Molecular gas distribution in barred and nonbarred galaxies along the hubble sequence. *Astrophys. J.S.* **178**, 225–246 (2008)
165. Kormendy, J., Richstone, D.: Inward bound—the search for supermassive black holes in galactic nuclei. *Ann. Rev. Astron. Astrophys.* **33**, 581–624 (1995)
166. Koss, M., Mushotzky, R., Veilleux, S., Winter, L.: Merging and clustering of the swift BAT AGN sample. *Astrophys. J.* **716**, L125–L130 (2010)
167. Kotilainen, J.K., Falomo, R.: The optical-near-infrared colour of the host galaxies of BL lacertae objects. *Astron. Astrophys.* **424**, 107 (2004)
168. Koulouridis, E., Chavushyan, V.H., Plionis, M., Dultzin, D., Krongold, Y., Goudis, C., Chatzichristou, E.: The environment of Sy1, Sy2 bright IRAS galaxies: the AGN/starburst connection. *Mem. Soc. Astron. Italiana* **79**, 1185 (2008)
169. Koulouridis, E., Chavushyan, V., Plionis, M., Krongold, Y., Dultzin-Hacyan, D.: A three-dimensional study of the local environment of bright IRAS galaxies: The active galactic nucleus-starburst connection. *Astrophys. J.* **651**, 93–100 (2006)
170. Koulouridis, E., Plionis, M., Chavushyan, V., Dultzin-Hacyan, D., Krongold, Y., Goudis, C.: Local and large-scale environment of seyfert galaxies. *Astrophys. J.* **639**, 37–45 (2006)
171. Krause, M., Gaibler, V.: Physics and fate of jet related emission line regions. In: Antonuccio-Delogu, V., Silk, J. (eds.) *AGN Feedback in Galaxy Formation*. In: *AGN Feedback in Galaxy Formation*, V. Antonuccio-Delogu and J. Silk (eds). Cambridge University Press, ISBN: 9780521192545, p. 183–193 (2010)
172. Krolik J.H., Begelman, M.: Molecular tori in seyfert galaxies – Feeding the monster and hiding it. *Astrophys. J.* **329**, 702 (1988)
173. Krongold, Y., Dultzin-Hacyan, D., Marziani, P.: The circumgalactic environment of bright IRAS galaxies. *Astrophys. J.* **572**, 169–177 (2002)
174. Krongold, Y., Dultzin-Hacyan, D., Marziani, P.: An evolutionary sequence for AGN. *ASP Conf. Ser.* **290**, 523 (2003)
175. Krongold, Y., Dultzin-Hacyan, D., Marziani, P., de Diego, J.A.: The circum-galactic environment of LINERs. *Rev. Mex. Astron. Astrof.* **39**, 225–237 (2003)
176. Kukula, M.J., Dunlop, J.S., McLure, R.J., Miller, L., Percival, W.J., Baum, S.A., O’Dea, C.P.: A NICMOS imaging study of high-z quasar host galaxies. *Mon. Not. R. Astron. Soc.* **326**, 1533–1546 (2001)

177. Kurk, J.D., Walter, F., Fan, X., Jiang, L., Riechers, D.A., Rix, H.-W., Pentericci, L., Strauss, M.A., Carilli, C., Wagner, S.: Black hole masses and enrichment of $z \sim 6$ quasars. *Astrophys. J.* **669**, 32–44 (2007)
178. Kurosawa, R., Proga, D.: Three-dimensional simulations of dynamics of accretion flows irradiated by a quasar. *Astrophys. J.* **693**, 1929–1945 (2009)
179. Kurosawa, R., Proga, D., Nagamine, K.: On the feedback efficiency of active galactic nuclei. *Astrophys. J.* **707**, 823–832 (2009)
180. Kurosawa, R., Proga, D.: On the large-scale outflows in active galactic nuclei: Consequences of coupling the mass supply rate and accretion luminosity. *Mon. Not. R. Astron. Soc.* **397**, 1791–1803 (2009)
181. Labita, M., Decarli, R., Treves, A., Falomo, R.: Downsizing of supermassive black holes from the SDSS quasar survey. *Mon. Not. R. Astron. Soc.* **396**, 1537 (2009)
182. Labita, M., Decarli, R., Treves, A., Falomo, R.: Downsizing of supermassive black holes from the SDSS quasar survey – II. Extension to $z \sim 4$. *Mon. Not. R. Astron. Soc.* **399**, 2099–2106 (2009)
183. Lacy, M., Sajina, A., Petric, A.O., Seymour, N., Canalizo, G., Ridgway, S.E., Armus, L., Storrie-Lombardi, L.J.: Large amounts of optically obscured star formation in the host galaxies of some type-2 quasars. *Astrophys. J.* **669**, 61 (2007)
184. La Franca, F., Fiore, F., Comastri, A., Perola, G.C., Sacchi, N., Brusa, M., Cocchia, F., Feruglio, C., Matt, G., Vignali, C., et al.: The hard X-ray luminosity function of AGNs up to $z = 4$: More absorbed AGNs at low luminosities and high redshift. *Astrophys. J.* **635**, 864–79 (2005)
185. Laine, S., Shlosman, I., Knapen, J.H., Peletier, R.F.: Nested and single bars in seyfert and Non-seyfert galaxies. *Astrophys. J.* **567**, 97–117 (2002)
186. Lane, W.M., Clarke, T.E., Taylor, G.B., Perley, R.A., Kassim, N.E.: Hydra A at low radio frequencies. *Astron. J.* **127**, 48–52 (2004)
187. Lapi, A., and the Herschel-ATLAS Collaboration: Herschel-ATLAS galaxy counts and high redshift luminosity functions: The formation of massive early type galaxies. *Astrophys. J.* **742**, 24, (2011)
188. Laurikainen, E., Salo, H.: Environments of seyfert galaxies. II. Statistical analyses. *Astron. Astrophys.* **293**, 683–702 (1995)
189. Laurikainen, E., Salo, H., Teerikorpi, P., Petrov, G.: Environments of seyfert galaxies. I. Construction of the sample and selection effects. *Astron. Astrophys. Suppl.* **108**, 491–508 (1994)
190. Ledlow, M.J., Owen, F.N.: A 20 cm Survey of abell clusters of galaxies. V. Optical observations and surface photometry. *Astron. J.* **110**, 1959 (1995)
191. Li, C., Kauffmann, G., Heckman, T.M., White, S.D.M., Jing, Y.P.: Interactions, star formation and AGN activity. *Mon. Not. R. Astron. Soc.* **385**, 1915–1922 (2008)
192. Longhetti, M., Saracco, P., Severgnini, P., Della Ceca, R., Mannucci, F., Bender, R., Drory, N., Feulner, G., Hopp, U.: The Kormendy relation of massive elliptical galaxies at $z 1.5$: Evidence for size evolution. *Mon. Not. R. Astron. Soc.* **374**, 614–626 (2007)
193. Lynden-Bell, D.: Galactic nuclei as collapsed old quasars. *Nature* **223**, 690–694 (1969)
194. Lynds, C.R.: A quasi-stellar source with a rapidly expanding envelope. *Astrophys. J.* **147**, 396 (1967)
195. Madau, P., Pozzetti, L., Dickinson, M.: The star formation history of field galaxies. *Astrophys. J.* **498**, 106
196. Madau, P., Rees, M.J.: Massive black holes as population III remnants. *Astrophys. J.* **551**, L27–L30 (2001)
197. Magain, P., Magain, P., Letawe, G., Courbin, F., Jablonka, P., Jahnke, K., Meylan, G., Wisotzki, L.: Discovery of a bright quasar without a massive galaxy. *Nature* **437**, 381–384 (2005)
198. Magorrian, J., Tremaine, S., Richstone, D., Bender, R., Bower, G., Dressler, A., Faber, S.M., Gebhardt, K., Green, R., Grillmair, C., et al.: The demography of massive dark objects in galaxy centers. *Astron. J.* **115**, 2285 (1998)

199. Malbon, R.K., Baugh, C.M., Frenk, C.S., Lacey, C.G.: Black hole growth in hierarchical galaxy formation. *Mon. Not. R. Astron. Soc.* **382**, 1394–1414 (2007)
200. Malkan, M.A., Gorjian, V., Tam, R.: A hubble space telescope imaging survey of nearby active galactic nuclei. *Astrophys. J.S* **117**, 25 (1998)
201. Márquez, I., Masegosa, J.: Feedback between host galaxy and nuclear activity. *RMxAC* **32**, 150–154 (2008)
202. Martínez-Sansigre, A., Lacy, M., Sajina, A., Rawlings, S.: Mid-infrared spectroscopy of high-redshift obscured quasars. *Astrophys. J.* **674**, 676–685 (2008)
203. Martínez, M.A., del Olmo, A., Coziol, R., Focardi, P.: Deficiency of broad-line AGNs in compact groups of galaxies. *Astrophys. J.* **678**, L9–L12 (2008)
204. Martini, P.: The evolution of AGN in groups and clusters. *AIP Conf. Proc.* **1201**, 115 (2009)
205. Marziani, P., Sulentic, J.W., Dultzin-Hacyan, D., Calvani, M., Moles, M.: Comparative analysis of the high- and low-ionization lines in the broad-line region of active galactic nuclei, *ApJS*, **104**, 37–70 (1996)
206. Masegosa, J., Márquez, I., Ramirez, A., González-Martín, O.: The nature of nuclear H α emission in LINERs. *Astron. Astrophys.* **527**, A23 (2011)
207. McCarthy, P.J., Le Borgne, D., Crampton, D., Chen, H.-W., Abraham, R.G., Glazebrook, K., Savaglio, S., Carlberg, R.G., Marzke, R.O., Roth, K., et al.: Evolved galaxies at $z > 1.5$ from the gemini deep deep survey: The formation epoch of massive stellar systems. *Astrophys. J.* **614**, L9 (2004)
208. McLeod, K.K., McLeod, B.A.: NICMOS observations of low-redshift quasar host galaxies. *Astrophys. J.* **546**, 782–794 (2001)
209. McLure, R.J., Jarvis, M.J., Targett, T.A., Dunlop, J.S., Best, P.N.: On the evolution of the black hole: Spheroid mass ratio. *Mon. Not. R. Astron. Soc.* **368**, 1395 (2006)
210. McLure, R.J., Kukulka, M.J., Dunlop, J.S., Baum, S.A., O’Dea, C.P., Hughes, D.H.: A comparative HST imaging study of the host galaxies of radio-quiet quasars, radio-loud quasars and radio galaxies – I. *Mon. Not. R. Astron. Soc.* **308**, 377–404 (1999)
211. McNamara, B.R., Nulsen, P.E.J.: Heating hot atmospheres with active galactic. *Nuclei. Ann. Rev. Astron. Astrophys.* **45**, 117–175 (2007)
212. Mayer, L., Kazantzidis, S., Escala, A., Callegari, S.: Direct formation of supermassive black holes via multi-scale as inflows in galaxy mergers. *Nature* **466**, 1082–1084 (2010)
213. Mellema, G., Kurk, J.D., Röttgering, H.J.A.: Evolution of clouds in radio galaxy cocoons. *Astron. Astrophys.* **395**, L13–L16 (2002)
214. Menci, N., Fiore, F., Puccetti, S., Cavaliere, A.: The blast wave model for AGN feedback: Effects on AGN obscuration. *Astrophys. J.* **686**, 219–229 (2008)
215. Merloni, A., Bongiorno, A., Bolzonella, M., Brusa, M., Civano, F., Comastri, A., Elvis, M., Fiore, F., Gilli, R., Hao, H., Jahnke, K., Koekemoer, A.M., Lusso, E., Mainieri, V., Mignoli, M., Miyaji, et al.: On the cosmic evolution of the scaling relations between black holes and their host galaxies: Broad-line active galactic nuclei in the zCOSMOS survey. *Astrophys. J.* **708**, 137–157 (2010)
216. Miley, G., De Breuck, C.: Distant radio galaxies and their environments. *Astron. Astrophys. Rev.* **15**, 67–144 (2008)
217. Morganti, R., Holt, J., Saripalli, L., Oosterloo, T.A., Tadhunter, C.N.: IC 5063: AGN driven outflow of warm and cold gas. *Astron. Astrophys.* **476**, 735–743 (2007)
218. Morganti, R., Oosterloo, T.A., Tadhunter, C.N., van Moorsel, G., Emonts, B.: The location of the broad H i absorption in 3C 305: clear evidence for a jet-accelerated neutral outflow. *Astron. Astrophys.* **439**, 521–526 (2005)
219. Morganti, R., Tadhunter, C.N., Oosterloo, T.A.: Fast neutral outflows in powerful radio galaxies: A major source of feedback in massive galaxies. *Astron. Astrophys.* **444**, L9–L13 (2005)
220. Mortlock, D.J., Patel, M., Warren, S.J., Venemans, B.P., McMahon, R.G., Hewett, P.C., Simpson, C., Sharp, R.G., Burningham, B., Dye, S., Ellis, S., Gonzales-Solares, E.A., Huélamo, N.: Discovery of a redshift 6.13 quasar in the UKIRT infrared deep sky survey. *Astron. Astrophys.* **505**, 97–104 (2009)

221. Mulchaey, J.S., Regan, M.W.: The fueling of nuclear activity: The bar properties of seyfert and normal galaxies. *Astrophys. J.* **482**, L135–L137 (1997)
222. Müller Sánchez, F., Davies, R.I., Genzel, R., Tacconi, L.J., Eisenhauer, F., Hicks, E.K.S., Friedrich, S., Sternberg, A.: Molecular gas streamers feeding and obscuring the active nucleus of NGC 1068. *Astrophys. J.* **691**, 749–759 (2009)
223. Murphy, M.T., Webb, J.K., Flambaum, V.V.: Further evidence for a variable fine-structure constant from Keck/HIRES QSO absorption spectra. *Mon. Not. R. Astron. Soc.* **345**, 609–638 (2003)
224. Murray, N., Quataert, E., Thompson, T.A.: On the maximum luminosity of galaxies and their central black holes: Feedback from momentum-driven winds. *Astrophys. J.* **618**, 569 (2005)
225. Myers, P.C., Evans, N.J., Ohashi, N.: Observations of infall in star-forming regions. In: Mannings, V., Boss, A.P., Russell, S.S. (eds.) *Protostars & Planets IV*. p. 217. University of Arizona, Tucson (2000)
226. Nesvadba, N.P.H.: Giant outflows in $z \sim 2$ radio galaxies: The smoking gun of AGN feedback in the early universe. [arXiv:0906.2900] (2009)
227. Nesvadba, N.P.H., Lehnert, M.D., De Breuck, C., Gilbert, A.M., van Breugel, W.: Evidence for powerful AGN winds at high redshift: Dynamics of galactic outflows in radio galaxies during the “Quasar Era”. *Astron. Astrophys.* **491**, 407–424 (2008)
228. Nolan, L., Dunlop, J., Kukulka, M., Hughes, D., Boroson, T., Jimenez, R.: The ages of quasar host galaxies. *Mon. Not. R. Astron. Soc.* **323**, 308 (2001)
229. Nussbaumer, H., Osterbrock, D.E.: On the forbidden emission lines of iron in Seyfert galaxies. *Astrophys. J.* **161**, 811 (1970)
230. Oosterloo, T.A., Morganti, R.: Anomalous HI kinematics in centaurus A: Evidence for jet-induced star formation. *Astron. Astrophys.* **429**, 469–475 (2005)
231. Oosterloo, T.A., Morganti, R., Tzioumis, A., Reynolds, J., King, E., McCulloch, P., Tsvetanov, Z.: A strong jet-cloud interaction in the seyfert galaxy. *Astron. J.* **119**, 2085 (2000)
232. Osmer, P.S.: The evolution of quasars. In: Ho, L. (eds.) *Coevolution of Black Holes and Galaxies*. p. 324. Cambridge University Press, Cambridge (2009)
233. Ostriker, J.P., Choi, E., Ciotti, L., Novak, G.S., Proga, D.: Momentum driving: which physical processes dominate active galactic nucleus feedback? *Astrophys. J.* **722**, 642–652 (2010)
234. Papovich, C., Moustakas, L.A., Dickinson, M., Le Floc'h, E., Rieke, G.H., Daddi, E., Alexander, D.M., Bauer, F., Brandt, W.N., Dahlen, T., Egami, E., Eisenhardt, P., Elbaz, D., Ferguson, H.C., et al.: Spitzer observations of massive, red galaxies at high redshift. *Astrophys. J.* **640**, 92–113 (2006)
235. Peng, C.Y., Impey, C.D., Ho, L.C., Barton, E.J., Rix, H.-W.: Probing the coevolution of supermassive black holes and quasar host galaxies. *Astrophys. J.* **640**, 114 (2006)
236. Peng, C.Y., Impey, C.D., Rix, H.-W., Kochanek, C.S., Keeton, C.R., Falco, E.E., Lehár, J., McLeod, B.A.: Probing the coevolution of supermassive black holes and galaxies using gravitationally lensed quasar hosts. *Astrophys. J.* **649**, 616–634 (2006)
237. Pentericci, L., McCarthy, P.J., Roettgering, H.J.A., Miley, G.K., van Breugel, W.J.M., Fosbury, R.: NICMOS observations of high-redshift radio galaxies: Witnessing the formation of bright elliptical galaxies? *Astrophys. J. Suppl.* **135**, 63 (2001)
238. Perry, J.J., Dyson, J.E.: Shock formation of the broad emission-line regions in QSOs and active galactic nuclei. *Mon. Not. R. Astron. Soc.* **213**, 665–710 (1985)
239. Piconcelli, E.: Revealing AGN pairs in galaxy collisions. In: *Active Galactic Nuclei 9: Black Holes and Revelations*, Conference held 24–27 May, 2010 at Aula Magna dell'Università, di Ferrara (2010)
240. Pierce, C.M., Lotz, J.M., Laird, E.S., Lin, L., Nandra, K., Primack, J.R., Faber, S.M., Bamby, P., Park, S.Q., Willner, S.P., Gwyn, S., Koo, D.C., et al.: AEGIS: Host galaxy morphologies of X-ray-selected and infrared-selected active galactic nuclei at $0.2 \leq z < 1.2$. *Astrophys. J.* **660**, L19–L22 (2007)
241. Popovic, L.C., Vince, I., Atanackovic-Vukmanovic, O., Kubicela, A.: Contribution of gravitational redshift to spectral line profiles of seyfert galaxies and quasars. *Astron. Astrophys.* **293**, 309–314 (1995)

242. Polletta, M.D.C., Wilkes, B.J., Siana, B., Lonsdale, C.J., Kilgard, R., Smith, H.E., Kim, D.-W., Owen, F., Efstathiou, A., Jarrett, T., Stacey, G., Franceschini, A., et al.: Chandra and spitzer unveil heavily obscured quasars in the chandra/SWIRE survey. *Astrophys. J.* **642**, 673–693 (2006)
243. Porciani, C., Norberg, P.: Luminosity- and redshift-dependent quasar clustering. *Mon. Not. R. Astron. Soc.* **371**, 1824 (2007)
244. Predehl, P., et al.: eRosita on SRG. In: Proceedings of the SPIE **7732**, 77320U-77320U-10 (2010)
245. Proga, D., Kallman, T.: Dynamics of line-driven disk winds in active galactic nuclei. II. Effects of disk radiation. *Astrophys. J.* **616**, 688–695 (2004)
246. Rafanelli, P., Violato, M., Baruffolo, A.: On the excess of physical companions among seyfert galaxies. *Astron. J.* **109**, 1546–1554 (1995)
247. Raimann, D., Storchi-Bergmann, T., Quintana, H., Hunstead, R., Wisotzki, L.: Stellar populations in a complete sample of local radio galaxies. *Mon. Not. R. Astron. Soc.* **364**, 1239 (2005)
248. Rauch, M.: The Lyman alpha forest in the spectra of QSOs. *Ann. Rev. Astron. Astrophys.* **36**, 267–316 (1998)
249. Regan, M.W., Thornley, M.D., Vogel, S.N., Sheth, K., Draine, B.T., Hollenbach, D.J., Meyer, M., Dale, D.A., Engelbracht, C.W., Kennicutt, et al.: The radial distribution of the interstellar medium in disk galaxies: Evidence for secular evolution. *Astrophys. J.*, **652**, 1112–1121 (2006)
250. Reichard, T.A., Heckman, T.M., Rudnick, G., Brinchmann, J., Kauffmann, G., Wild, V.: The lopsidedness of present-day galaxies: Connections to the formation of stars, the chemical evolution of galaxies, and the growth of black holes. *Astrophys. J.*, **691**, 1005–1020 (2009)
251. Richards, G.T., Croom, S.M., Anderson, S.F., Bland-Hawthorn, J., Boyle, B.J., De Propriis, R., Drinkwater, M.J., Fan, X., Gunn, J.E., et al.: The 2dF-SDSS LRG and QSO (2SLAQ) Survey: the $z < 2.1$ quasar luminosity function from 5645 quasars to $g = 21.85$. *Mon. Not. R. Astron. Soc.* **360**, 839 (2005)
252. Richards, G.T., Fan, X., Newberg, H.J., Strauss, M.A., Vanden Berk, D.E., Schneider, D.P., Yanny, B., Boucher, A., Burles, S., Frieman, J.A., Gunn, J.E., Hall, P.B., et al: Spectroscopic target selection in the sloan digital sky survey: The quasar sample. *Astron. J.* **123**, 2945 (2002)
253. Richards, G.T., Strauss, M.A., Fan, X., Hall, P.B., Jester, S., Schneider, D.P., Vanden Berk, D.E., Stoughton, C., et al.: The sloan digital sky survey quasar survey: Quasar luminosity function from data release 3. *Astron. J.* **131**, 2766 (2006)
254. Ridgway, S.E., Heckman, T.M., Calzetti, D., Lehnert, M.: NICMOS imaging of the host galaxies of $z \sim 2 - 3$ radio-quiet quasars. *Astrophys. J.* **550**, 122–141 (2001)
255. Riffel, R.A., Storchi-Bergmann, T., Dors, O.L., Winge, C.: AGN-starburst connection in NGC7582: Gemini near-infrared spectrograph integral field unit observations. *Mon. Not. R. Astron. Soc.* **393**, 783–797 (2009)
256. Robertson, B., Hernquist, L., Cox, T.J., Di Matteo, T., Hopkins, P.H., Martini, P., Springel, V.: The evolution of the $M_{\text{BH}} - \sigma$ relation. *Astrophys. J.* **641**, 90 (2006)
257. Romano-Diaz, E., Shlosman, I., Trenti, M., Hoffman, Y.: The dark side of QSO formation at high redshift. *Astrophys. J.* **736**, 66 (2011)
258. Ross, N.P., Shen, Y., Strauss, M.A., Vanden Berk, D.E., Connolly, A.J., Richards, G.T., Schneider, D.P., Weinberg, D.H., Hall, P.B., Bahcall, N.A., Brunner, R.J.: Clustering of low-redshift ($z \leq 2.2$) quasars from the sloan digital sky survey. *Astrophys. J.* **697**, 1634–1655 (2009)
259. Rupke, D.S., Veilleux, S., Sanders, D.B.: Keck absorption-line spectroscopy of galactic winds in ultraluminous infrared galaxies. *Astrophys. J.* **570**, 588–609 (2002)
260. Sakamoto, K., Okumura, S.K., Ishizuki, S., Scoville, N.Z.: Bar-driven transport of molecular gas to galactic centers and its consequences. *Astrophys. J.* **525**, 691–701 (1999)
261. Salvander, S., Shields, G.A., Gebhardt, K., Bonning, E.W.: The black hole mass-galaxy bulge relationship for QSOs in the sloan digital sky survey data release 3. *Astrophys. J.* **662**, 131 (2007)

262. Sanders, D.B., Mirabel, I.F.: Luminous infrared galaxies. *Ann. Rev. Astron. Astrophys.* **34**, 749 (1996)
263. Shankar, F.: The demography of supermassive black holes: Growing monsters at the heart of galaxies. *New Astron. Rev.* **53**, 57–77 (2009)
264. Schinnerer, E., Böker, T., Emsellem, E., Lisenfeld, U.: Molecular gas dynamics in NGC 6946: A bar-Driven nuclear starburst Caught in the act. *Astrophys. J.* **649**, 181–200 (2006)
265. Schmidt, M., Schneider, D.P., Gunn, J.E.: Spectroscopic CCD surveys for quasars at large redshift. IV. Evolution of the luminosity function from Quasars detected by their Lyman-alpha emission. *Astron. J.* **110**, 68 (1995)
266. Schneider, D.P., Richards, G.T., Hall, P.B., Strauss, M.A., Anderson, S.F., Boroson, T.A., Ross, N.P., Shen, Y., Brandt, W.N., Fan, X., Inada, N., Jester, S., Knapp, G.R., Krawczyk, C., et al.: The Sloan Digital Sky Survey Quasar Catalog. V. Seventh data release. *Astron. J.* **139**, 2360–2373 (2010)
267. Schramm, M., Wisotzki, L., Jahnke, K.: Host galaxies of bright high redshift quasars: Luminosities and colours. *Astron. Astrophys.* **478**, 311–319 (2008)
268. Schwarz, M.P.: How bar strength and pattern speed affect galactic spiral structure. *Mon. Not. R. Astron. Soc.* **209**, 93–109 (1984)
269. Shen, Y., Greene, J.E., Strauss, M.A., Richards, G.T., Schneider, D.P.: Biases in virial black hole masses: An SDSS perspective. *Astrophys. J.* **680**, 169–190 (2008)
270. Shen, Y., Strauss, M.A., Oguri, M., Hennawi, J.F., Fan, X., Richards, G.T., Hall, P.B., Gunn, J.E., Schneider, D.P., Szalay, A.S., Thakar, A.R., Vanden Berk, D.E., Anderson, S.F., Bahcall, N.A., Connolly, A.J., Knapp, G.R.: Clustering of high-redshift ($z \geq 2.9$) quasars from the Sloan Digital Sky Survey. *Astron. J.* **133**, 2222–2241 (2007)
271. Shen, Y., Strauss, M.A., Ross, N.P., Hall, P.B., Lin, Y.-T., Richards, G.T., Schneider, D.P., Weinberg, D.H., Connolly, A.J., Fan, X., Hennawi, J.F., Shankar, F., Vanden Berk, D.E., Bahcall, N.A., Brunner, R.J.: Quasar clustering from SDSS DR5: Dependences on physical properties. *Astrophys. J.* **697**, 1656–1673 (2009)
272. Sheth, K., Vogel, S.N., Regan, M.W., Thornley, M.D., Teuben, P.J.: Secular evolution via Bar-driven gas inflow: Results from BIMA SONG. *Astrophys. J.* **632**, 217–226 (2005)
273. Shlosman, I., Begelman, M.C.: Evolution of self-gravitating accretion disks in active galactic nuclei. *Astrophys. J.* **341**, 685–691 (1989)
274. Shlosman, I., Begelman, M.C., Frank, J.: The fuelling of active galactic nuclei. *Nature* **345**, 679–686 (1990)
275. Shlosman, I., Frank, J., Begelman, M.C.: Bars within bars – A mechanism for fuelling active galactic nuclei. *Nature* **338**, 45–47 (1989)
276. Shlosman, I., Heller, C.: Nested bars in disk galaxies: No offset dust lanes in secondary nuclear bars. *Astrophys. J.* **565**, 921 (2002)
277. Silk, J., Rees, M.J.: Quasars and galaxy formation. *Astron. Astrophys.* **331**, L1–L4 (1998)
278. Smith, E.P., Heckman, T.M.: Multicolor surface photometry of powerful radio galaxies. II – Morphology and stellar content. *Astrophys. J.* **341**, 658 (1989)
279. Sorrentino, G., Radovich, M., Rifatto, A.: The environment of active galaxies in the SDSS-DR4. *Astron. Astrophys.* **451**, 809–816 (2006)
280. Solórzano-Iñárrrea, C., Tadhunter, C.N.: INTEGRAL spectroscopy of three powerful radio galaxies: jet-cloud interactions seen in three dimensions. *Mon. Not. R. Astron. Soc.* **340**, 705–721 (2003)
281. Springel, V., Di Matteo, T., Hernquist, L.: Modelling feedback from stars and black holes in galaxy mergers. *Astrophys. J.* **620**, L79 (2005)
282. Stauffer, J.R.: A nuclear spectroscopic survey of disk galaxies. II – Galaxies with emission lines not excited by stellar photoionization. *Astrophys. J.* **262**, 66–80 (1982)
283. Steinhardt C., Elvis, M.: The quasar mass-luminosity plane – I. A sub-Eddington limit for quasars. *Mon. Not. R. Astron. Soc.* **402**, 2637 (2010)
284. Steinhardt, C.L., Elvis, M.: The quasar mass-luminosity plane – III. Smaller errors on virial mass estimates. *Mon. Not. R. Astron. Soc.* **406**, L1–L5 (2010)

285. Storchi-Bergmann, T.: Observational overview of the feeding of active galactic nuclei. *Rev. Mex. Astron. Astrof. Conf. Ser.* **32**, 139–146 (2008)
286. Storchi-Bergmann, T., et al.: Nuclear spirals as feeding channels to the supermassive black hole: The case of the galaxy NGC 6951. *Astrophys. J.* **670**, 959–967 (2007)
287. Storchi-Bergmann, T., et al.: Circumnuclear stellar population, morphology, and environment of seyfert-2 galaxies: An evolutionary scenario. *Astrophys. J.* **559**, 147–156 (2001)
288. Sulentic, J.W., Marziani, P., Dultzin-Hacyan, D.: Phenomenology of broad emission lines in active galactic nuclei. *Ann. Rev. Astron. Astrophys.* **38**, 521–571 (2000)
289. Sulentic, J., Marziani, P., Stirpe, G., Zamfir, S., Dultzin, D., Calvani, M., Repetto, P., Zamanov, R.: Constraining quasar structural evolution with VLT/ISAAC. *The Messenger* **137**, 30–33 (2009)
290. Sutherland, R.S., Bicknell, G.V.: Interaction of jets with the ISM of radio galaxies. *Astrophys. Space Sci.* **311**, 293–303 (2007)
291. Terlevich, R., Melnick, J., Moles, M.: Starburst models for AGNs. *IAU Symp.* **121**, 499 (1987)
292. Toomre, A.: Mergers and some consequences. In: Tinsley, B.M., Larson, R.B. (eds.) *Galaxies and Stellar Populations*. pp. 401–426. Yale University Obs, New Haven (1977)
293. Tremaine, S., Gebhardt, K., Bender, R., Bower, G., Dressler, A., Faber, S.M., Filippenko, A.V., Green, R., Grillmair, C., Ho, L.C., Kormendy, J., Lauer, T.R., Magorrian, J., Pinkney, J., Richstone, D.: The slope of the black hole mass versus velocity dispersion correlation. *Astroph. J.* **574**, 740–753 (2002)
294. Trenti, M., Santos, M.R., Stiavelli, M.: Where can we really find the first stars' remnants today? *Astrophys. J.* **687**, 1–6 (2008)
295. Trenti, M., Stiavelli, M.: Distribution of the very first population III stars and their relation to bright $z\sim 6$ quasars. *Astrophys. J.* **667**, 33–48 (2007)
296. Trenti, M., Stiavelli, M., Shull, M.J.: Metal-free gas supply at the edge of reionization: Late-epoch population III star formation. *Astrophys. J.* **700**, 1672–1679 (2009)
297. Utsumi, Y., Goto, T., Kashikawa, N., Miyazaki, S., Komiyama, Y., Furusawa, H., Overzier, R.: A large number of $z\lesssim 6$ galaxies around a QSO at $z=6.43$: Evidence for a protocluster? *Astrophys. J.* **721**, 1680–1688 (2010)
298. Vallee, J.P.: Cosmic magnetic fields – as observed in the Universe, in galactic dynamos, and in the Milky Way. *New Astron. Rev.* **48**, 763 (2004)
299. Vanden Berk, D.E., Richards, G.T., Bauer, A., Strauss, M.A., Schneider, D.P., Heckman, T.M., York, D.G., Hall, P.B., Fan, X., Knapp, G.R., Anderson, S.F., Annis, J., Bahcall, N.A., et al.: Composite quasar spectra from the sloan digital sky survey. *Astron. J.* **122**, 549–564 (2001)
300. van de Ven, G., Fathi, K.: Kinematic analysis of nuclear spirals: Feeding the black hole in NGC 1097. *Astrophys. J.* **723**, 767–780 (2010)
301. Varela, J., Moles, M., M árquez, I., Galletta, G., Masegosa, J., Bettoni, D.: Properties of isolated disk galaxies. *Astron. Astrophys.* **420**, 873–879 (2004)
302. Vestergaard, M.: Determining central black hole masses in distant active galaxies. *Astrophys. J.* **571**, 733–752 (2002)
303. Villar-Martín, M., Vernet, J., di Serego Alighieri, S., Fosbury, R., Pentericci, L., Cohen, M., Goodrich, R., Humphrey, A.: Giant low surface brightness haloes in distant radio galaxies: USS0828+193. *Mon. Not. R. Astron. Soc.* **336**, 436–444 (2002)
304. Villforth, C., Heidt, J., Nilsson, K.: Quasar host galaxies in the FORS deep field. *Astron. Astrophys.* **488**, 133–143 (2008)
305. Veilleux, S., Osterbrock, D.E.: Spectral classification of emission-line galaxies. *Astroph. J. Suppl. Ser.* **63**, 295 (1987)
306. Volonteri, M.: Formation of supermassive black holes. *Astron. Astrophys. Rev.* **18**, 279–315 (2010)
307. Volonteri, M., Gültekin, K., Dotti, M.: Gravitational recoil: effects on massive black hole occupation fraction over cosmic time. *Mon. Not. R. Astron. Soc.* **404**, 2143–2150 (2010)
308. Wagner, A.Y., Bicknell, G.V.: Relativistic jet feedback in evolving galaxies. *Astrophys. J.* **728**, 29 (2011)

309. Wang, J., Navarro, J.F., Frenk, C.S., White, S.D.M., Springel, V., Jenkins, A., Helmi, A., Ludlow, A., Vogelsberger, M.: Assembly history and structure of galactic cold dark matter halos. *Mon. Not. R. Astron. Soc.* **413**, 1373–1382 (2011)
310. Wang, J.X., Wang, T.G., Tozzi, P., Giacconi, R., Hasinger, G., Kewley, L., Mainieri, V., Nonino, M., Norman, et al.: Relativistic outflow in CXOCDFS J033260.0–274748. *Astrophys. J.* **631**, L33–L36 (2005)
311. Wang, R., Carilli, C.L., Neri, R., Walter, F., Bertoldi, F., Cox, P.: The nature of the millimeter bright quasars at $z \sim 6$. In: Wang, W., Yang, Z., Luo, Z., Chen, Z. (eds.) *The Starburst-AGN Connection. Proceedings of the conference held 27–31 October 2008, at Shanghai Normal University, Shanghai, China. ASP Conf. Ser.* **408**, 452 (2009)
312. Willmer, C.N.A., da Costa, L.N., Pellegrini, P.S.: Southern sky redshift survey: Clustering of local galaxies. *Astron. J.* **115**, 869–884 (1998)
313. Willott, C.J., McLure, R.J., Jarvis, M.J.: A $3 \times 10^9 M_{\text{Solar}}$ black hole in the quasar SDSS J1148+5251 at $z = 6.41$. *Astrophys. J. Lett.* **587**, L15–L18 (2003)
314. Willott, C.J., Albert, L., Arzoumanian, D., Bergeron, J., Crampton, D., Delorme, P., Hutchings, J.B., Omont, A., Reylé, C., Schade, D.: Eddington-limited accretion and the black hole mass function at redshift 6. *Astron. J.* **140**, 546–560 (2010)
315. Willott, C.J., Delorme, P., Reylé, C., Albert, L., Bergeron, J., Crampton, D., Delfosse, X., Forveille, T., Hutchings, J.B., McLure, R.J., Omont, A., Schade, D.: The canada-france high- z quasar survey: Nine new quasars and the luminosity function at redshift 6. *Astron. J.* **139**, 906–918 (2010)
316. Willott, C.J., Rawlings, S., Jarvis, M.J., Blundell, K.M.: Near-infrared imaging and the K- z relation for radio galaxies in the 7C redshift survey. *Mon. Not. R. Astron. Soc.* **339**, 173 (2003)
317. Wise, M.W., McNamara, B.R., Nulsen, P.E.J., Houck, J.C., David, L.P.: X-ray supercavities in the hydra a cluster and the outburst history of the central galaxy’s active nucleus. *Astrophys. J.* **659**, 1153 (2007)
318. Woo, J.-H., Treu, T., Malkan, M.A., Blandford, R.D.: Cosmic evolution of black holes and spheroids. III. The $M_{\text{BH}} - \sigma_*$ relation in the last six billion years. *Astrophys. J.* **681**, 925 (2008)
319. Wu, Y., Henkel, C., Xue, R., Guan, X., Miller, M.: Signatures of inflow motion in cores of massive star formation: Potential collapse candidates. *Astrophys. J.* **669**, L37 (2007)
320. Wyithe, J.S.B., Loeb, A.: Constraints on the process that regulates the growth of supermassive black holes based on the intrinsic scatter in the $M_{\text{bh}} - \sigma_{\text{sph}}$ relation. *Astrophys. J.* **634**, 910 (2005)
321. Younger, J.D., Hayward, C.C., Narayanan, D., Cox, T.J., Hernquist, L., Jonsson, P.: The merger-driven evolution of warm infrared luminous galaxies. *Mon. Not. R. Astron. Soc.* **396**, L66–L70 (2009)
322. Zheng, X.Z., Bell, E.F., Somerville, R.S., Rix, H.-W., Jahnke, K., Fontanot, F., Rieke, G.H., Schiminovich, D., Meisenheimer, K.: Observational constraints on the Co-evolution of supermassive black holes and galaxies. *Astrophys. J.* **707**, 1566 (2009)
323. Zirm, A.W., van der Wel, A., Franx, M., Labbé, I., Trujillo, I., van Dokkum, P., Toft, S., Daddi, E., Rudnick, G., Rix, H.-W., Röttgering, H.J.A., van der Werf, P.: NICMOS imaging of DRGs in the HDF-S: A relation between star formation and size at $z \sim 2.5$. *Astrophys. J.* **656**, 66–72 (2007)

Chapter 8

The Future of Quasar Studies

Contributions by Mauro D’Onofrio, Paola Marziani, Jack W. Sulentic, Suzy Collin, Alberto Franceschini, Martin Elvis, Shai Kaspi, Marianne Vestergaard, Paolo Padovani, Johan Knapen, and Isaac Shlosman

M. D’Onofrio

Dipartimento di Astronomia, Università degli Studi di Padova, Vicolo Osservatorio 3,
I35122 Padova, Italy
e-mail: mauro.donofrio@unipd.it

P. Marziani

INAF, Osservatorio Astronomico di Padova, Vicolo Osservatorio 5, IT35122 Padova, Italy
e-mail: paola.marziani@oapd.inaf.it

J.W. Sulentic (✉)

Instituto de Astrofísica de Andalucía (CSIC), Granada, Spain
e-mail: sulentic@iaa.es

S. Collin

LUTH, Observatoire de Paris-Meudon, Section de Meudon, 92195 Meudon, France
e-mail: suzy.collin@obspm.fr

A. Franceschini

Dipartimento di Astronomia, Università degli Studi di Padova, Vicolo Osservatorio 3,
I35122 Padova, Italy
e-mail: alberto.franceschini@unipd.it

M. Elvis

Harvard Smithsonian Center for Astrophysics, Cambridge MA02138, USA
e-mail: elvis@cfa.harvard.edu

S. Kaspi

School of Physics and Astronomy and the Wise Observatory, The Raymond and Beverly Sackler
Faculty of Exact Science, Tel-Aviv University, Tel-Aviv 69978, Israel
e-mail: shai@wise.tau.ac.il

M. Vestergaard

The Dark Cosmology Centre, The Niels Bohr Institute, University of Copenhagen, Juliane Maries
Vej 30, 2100 Copenhagen 0, Denmark

Steward Observatory and Department of Astronomy, University of Arizona, 933 N. Cherry
Avenue, Tucson 85721, Arizona, USA
e-mail: vester@dark-cosmology.dk

P. Padovani

European Southern Observatory, Karl-Schwarzschild-Str. 2, D-85748 Garching bei München,
Germany
e-mail: ppadovan@eso.org

How will quasar studies be pursued in the near future? Starting from a summary of past achievement, we ask questions on expected instrumental and computational advancements that can shape quasar research in a foreseeable way. There is excitement due to the planned large new-generation telescopes, ground-based and in space. New surveys will lead to an order-of-magnitude increase of known quasars. How will the redshift frontier (presently at $z \approx 6.5 - 7$) be pushed ahead? Will the planned X-ray missions lead to the revelation of the black hole event horizon in the closest active nuclei? No doubt reverberation mapping will be pursued with better data and more extended coverage but will we be able to resolve the emitting region structure before optical and IR interferometers reach a sufficient resolving power? In the end, the one major goal is to provide the final proof of the basic aspects of the accretion paradigm.

8.1 The Past Achievements

Dear Suzy (Collin), what are your main feelings about the evolution of quasar knowledge? Do you think there has been a steady progress?

I was very fortunate to participate since the beginning in this long “saga” of quasars and AGNs, which is still continuing, though I may have contributed little to it. All along my scientific life, I was indeed fascinated by the way this field developed. More than any other subjects, it allowed to observe that research is not “a long quiet river” but on the contrary, that it evolves in a nonlinear and erratic way, full of mistakes and of dead ends, and that it can give rise to passionate controversies, in particular when observations are pushed to their limits. I have seen how some ideas that presently are taken for granted had great difficulties to emerge and to gain credence and are then often not attributed to their promoters, in particular if these are not well known. On the contrary, other ideas had almost the status of paradigms during 20 or more years and were then completely abandoned (like the UV continuum interpreted as synchrotron radiation in radio-quiet quasars and Seyfert nuclei, which was reinterpreted in the 1980s as thermal disk emission; it proves that we see sometimes in the observations what we are prepared to see!). Some ideas were on the contrary premonitory, like quasars as nuclei of galaxies, or the prediction by Martin Rees of “superluminal motions” ([54] and subsequent

J. Knapen
Instituto de Astrofísica de Canarias, E-38200 La Laguna, Tenerife, Spain

Departamento de Astrofísica, Universidad de La Laguna, E-38205 La Laguna, Tenerife, Spain
e-mail: jhk@iac.es

I. Shlosman
Department of Physics and Astronomy, University of Kentucky, Lexington, KY 40506-0055,
USA
e-mail: shlosman@ps.uky.edu

papers), which were observed later and were not understood during several years. And of course, the black hole model took so much time to be accepted.

Thus, more than in other fields, progresses in AGN science relied most on observations (i.e., spatial missions, detectors, large telescopes, now big surveys), and theories went after. Observations were sometimes due to chance and not anticipated, like the discovery of quasars themselves: for instance, how long would we have waited for it, if 3C273 had not displayed this small redshift, allowing Maarten Schmidt to recognize the Balmer spectrum? A good example was also “reverberation mapping.” It was undertaken after Blandford and McKee [8] have proposed the method to obtain kinematical informations on the BLR. It was very clever, but it did not work because it would have required both very short time intervals between the observations and very long monitoring. This is not achieved yet, but it will be perhaps in the future. However, who could have guessed that it would lead to the determination with a good accuracy of the masses of the central black holes? And that these measurements would lead to a relationship between the size of the BLR and the luminosity, which could be used to deduce the mass of thousands of quasars? And was it predictable that these black hole masses could then be compared to the dispersion velocities in the host galaxies, and would lead to the discovery of a tight relation between the mass of the central black hole and the mass of the bulge?

On the contrary, some observations have been made with a given purpose and pursued until the purpose was reached. The best example in my opinion is the long-lasting study of proper motions of the stars in the galactic center, which allowed to measure the mass of the central black hole by Eckart and Genzel [17]. At this time, a majority of people thought that SgrA* did not contain a massive black hole because it was not “active” in the classical sense, that is, not associated with a strong infrared or X-ray source. Another well-targeted study was the polarimetric observation of the type-2 Seyfert NGC 1068, which opened the “unified scheme” era (Antonucci and Miller [1]).

Thus it was observations that impulsed new fields. For instance, the presence of massive black holes in the center of most galaxies (predicted by Soltan many years before [60] and promoted by Rees [55]), changed our vision of galaxy evolution in a new and non-expected way. To end with an anecdote, I remember I was attending a seminar on galaxy formation and evolution by a well-known scientist at the end of the 1980s, and I asked him: “You have not spoken at all of quasars and massive black holes, why?” The answer was: “they have nothing to do with the subject.”

Thank you, Suzy. We now leave the realm of the past, and we move forward a little bit in the future. The following questions are asked to people personally involved in the development of a new generation of instruments expected to come into use within this decade or at the beginning of the next. Key spectral ranges in the study of high- z quasars will be in the IR, sub-mm, and X-ray domain. We start considering two telescopes: the likely heir of HST that will operate mainly in the IR spectral region, and a survey telescope (LSSTs) expected to vastly increase the number of known quasars.

8.2 Future Observational Prospects

8.2.1 Visual–Near IR

Dear Massimo (*Stiavelli*), what progress in the study of quasars will come with JWST?

Quasars are very luminous objects, and for this reason, they are easy to identify up to very high redshift. Unfortunately, they are also rare, and finding bright ones has often required selection over very large areas of the sky. For this reason, instruments with a small field of view have been traditionally devoted to in depth study of a few objects rather than to the search of new ones. This is going to be true largely also for the study of bright quasars with James Webb Space Telescope (JWST).

The study of quasar host galaxies has greatly benefited from the high angular resolution of the Hubble Space Telescope [2]. However, Hubble’s coronagraphs have been limited in their performance, and most studies have avoided their use. JWST will dramatically change this. The near-infrared camera (NIRCam), the mid-infrared instruments (MIRI), and the tunable filter imager (TFI) all have advanced coronagraphic capabilities that should enable the study of host galaxies down to relatively small angular distances from the quasar, thanks to their suppression exceeding 10^{-4} contrast. This is particularly true for the MIRI phase-mask coronagraph and for the TFI nonredundant mask (NRM) that do not have a minimum working radius. The TFI-NRM will not be straightforward to use for extended sources but it remains very promising.

Direct imaging of host galaxies up to $z \simeq 6$ and beyond will provide us with a direct way to prove the galaxy mass–black hole mass relation [21, 22], if only photometrically. There are examples of objects where star formation in a galaxy or black hole growth (as estimated through accretion) are decoupled [27]. We do not know whether this is a generic property or an exception and whether the correlation between masses is established through a deterministic process or statistically. There is also evidence for this relation evolving with redshift [65, 70], but this evidence is at this stage very preliminary. Exploring the host galaxies in the most distant quasars will provide us with a significant lever arm to understand the origin of this correlation.

Thanks to the near-infrared spectrograph (NIRSpec), JWST will also be able to extend the sample of AGNs with masses derived on the basis of time delays (reverberation mapping) and perhaps simultaneous measurement of the galaxy velocity dispersion. This should enable us to extend the study of black hole mass vs. spheroid mass correlation at least to redshift 1.

In the recent years, an important field of research has been that of obscured active galactic nuclei (AGNs) and ultra-luminous infrared galaxies (ULIRGs). Extreme X-ray to optical ratio objects (EXOs [37], see Fig. 8.1) have been identified and interpreted as obscured AGNs. JWST’s sensitivity at mid-IR wavelength should enable major progress in this area with access to line diagnostics, such as PAH features, that should clarify whether the energy source in any given object is

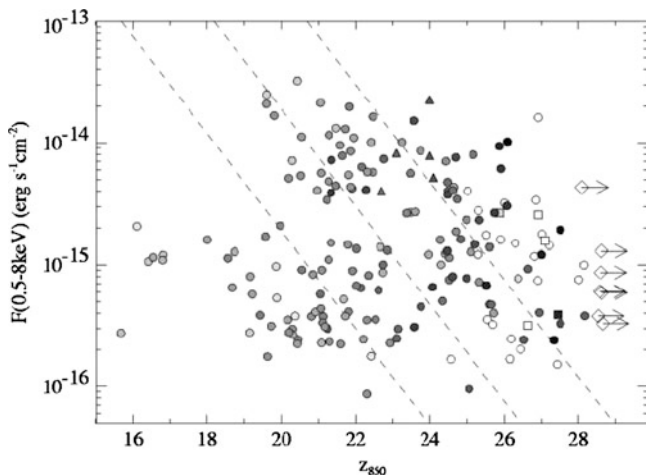


Fig. 8.1 X-ray flux in the 0.5–8 KeV band vs. z_{850} from [37]. The symbol shading illustrates the $z_{850} - K$ color, light to dark representing 0–5. The square symbols with arrows represent a sample of EXOs

primarily accretion or star formation. Some of the targets for this observations might be provided by future X-ray missions, and in this case, spectroscopy with JWST might also be crucial to identify the redshift.

Finally, it is worth noting that the combination of field of view and sensitivity of JWST will enable us to search for fainter quasars at high redshift, constraining the faint end of the luminosity function.

What can we expect for quasar studies from the next generation of large, ground-based telescopes?

The large synoptic survey telescope (LSST) is a future facility that will be very effective in finding new bright quasars. Progress on the study of quasar evolution requires us to find objects at $z > 6$. LSST will be a major asset in this regard particularly if its Y-band sensitivity proves as good as planned, given that this band is essential to detect dropout candidates at redshift 7. LSST will also prove invaluable to extend quasar samples at $z \leq 6$ to lower luminosities and to provide unique variability data on all AGNs. ESO's VISTA is also very interesting because it enables large-area searches in the near-IR which is essential to find quasars at $z > 7$.

The 30-m class telescopes on the ground, which we will indicate with ELT, and ALMA share the small field of JWST combined to significant capabilities for in-depth studies. For these observatories, better suited to in-depth studies, quasars will be interesting per se but will also continue to be fundamental as bright beacons, allowing studies of the evolution of intervening structures along the line of sight. The classic study of absorption systems will receive a boost from the extra sensitivity allowed by ELTs, by increasing the number of lines of sight that can be observed by going to lower and lower mass AGNs, and by measuring fainter lines for bright quasars [53, 67]. A development in this area is probably going to also be

the derivation of tighter constraints on the evolution of the fine structure constant α [71] or lack thereof.

The most challenging application of quasars as probe is the measurement of Λ based on the direct measurement of acceleration. This requires exquisite wavelength calibration accuracy and stability over a few decades, and it may well prove beyond our capabilities in the near future.

Large ground-based telescopes of the next generation will also enable the measurement of velocity dispersion of distant quasar host galaxies, thanks also to active optics-driven spectrographs. Combined with black hole masses from reverberation mapping obtained through a combination of space and ground-based observatories and longer timescales probed over time for the most massive black holes, one will be able to map with increasing confidence the evolution of the black hole mass vs. sigma relation. Another angle on this problem will be provided by the study of more extensive samples of galaxies provided by LSST coupled to wide-areas spectroscopic followups capable to extend in luminosity and redshift that can be done today with the Sloan digital sky survey (SDSS) [28].

A classic feature of quasar studies of the past was the differentiation between radio-loud and radio-quiet objects. Unfortunately, as our capability of finding quasars to higher and higher redshift has improved, radio facilities have been incapable of surveying large portions of the sky to the sensitivity of interest so that we do not know much about the evolution of the fraction of radio-loud quasars up to redshift 6. Improvements will be brought about by the extended VLA (EVLA). On the longer term, this field will benefit from the square kilometer array (SKA). SKA is not a survey instrument, but its great sensitivity should make it possible to target individual quasars. An open issue is whether or not the ratio of radio-loud to radio-quiet quasars number densities changes with redshift. There are some intriguing hints on this from the discovery of a radio-loud $z \sim 6$ quasar from the FIRST radio survey. This observation has either been very lucky or could indicate that radio-loud quasars are more common at $z \sim 6$. Clearly, it is hard to do statistics on one object, and more data would be highly desirable. I expect that this issue will be explored with future radio telescope such as SKA.

Thank you, Massimo.

8.2.2 IR–mm Domain

Dear Alberto (Franceschini), what future improvements can we expect for IR and mm observations of quasars?

I expect three major steps forward to be made by future facilities. The first of these to come will be the Atacama large millimetric array (ALMA), the first planetary-scale astronomical facility (with contributions by all important worldwide national communities and agencies). ALMA enormous spatial resolution, sensitivity, and spectroscopic capabilities will make a full revolution in astronomy and will allow

detection and characterization of dusty and gaseous media in cosmic sources at any redshifts. We can just imaging some of the potential breakthroughs that ALMA will make possible. The environment of the highest redshift quasars will be investigated with unprecedented sensitivity and spatial resolution (better than HST in the optical), establishing how dust is spatially distributed, either spread over the host galaxy on a large galactic scale or centrally peaked in the nuclear region. This will illuminate on how the earliest dust produced in the universe has originated. And the same will be possible, and easier, for quasars at lower redshifts, allowing to discriminate how much of the dust is illuminated by the central power source and how much by young stars in the host galaxy. The spectroscopic capabilities of ALMA will be used in the atmospheric transmission wavebands to detect a variety of atomic (e.g., redshifted OI $63\ \mu\text{m}$, OIII $88\ \mu\text{m}$, CII $158\ \mu\text{m}$ among others) and molecular species (CO in particular) that will be exploited as diagnostics of the physical conditions in the quasar/host-galaxy media. At the same time, ALMA spectral-imaging capability will be used for in-depth investigations of the dynamical and kinematic structure of the diffuse media.

In time order, a second potentially critical development will be offered by the Japan–ESA collaboration SPICA for a cooled 4-m class IR telescope in space. SPICA’s specific feature, compared to other facilities like JWST and *Herschel*, will be a unique sensitivity in the range from a few μm to $200\ \mu\text{m}$, thanks to a cooling system able to maintain the whole telescope assembly at few Kelvin degrees. This will make possible spectral surveys of high-redshift quasars and galaxies being performed to very faint flux limits and good spatial resolution (few arcsec). At these wavelengths SPICA will exploit the detection of a rich variety of atomic, ionic, and molecular lines for physical analyses, completely unaffected by dust absorption. Measurements of these spectral lines will allow us to determine the properties of the primary photon energy source and finally, discriminate how much is coming from young stars or from a deeply dust-embedded AGN.

Finally, decisive progress in our understanding of the quasar phenomenon inside highly opaque media will be made possible by the next generation of the very high-energy X-ray observatories (like ESA’s IXO): the photoelectric absorption becomes negligible at high X-ray energies. Our Fig. 4.5 in Chap. 4 illustrates that even a Compton-thick AGN buried inside a high column density cocoon leaves trace emission above 10 KeV. Current X-ray observatories (*XMM-Newton* and *Chandra*) barely detect photons above 5 KeV, but IXO (or similar future facilities) will deploy large grazing-incidence mirrors effective up to energies of several tens kilo electron volt. The currently unresolvable problem of discriminating the relative roles of gravitational accretion and stellar activity during the main phases of AGN and galaxy formation will then be effectively addressed by a combined effort in the IR (SPICA) and X-rays (IXO or similar).

Thank you, Alberto. Every quasar emits in the hard X-ray domain—and hard X-ray photons are not absorbed in obscured quasars. It is therefore not surprising that several space-based X-ray observatories are being planned to replace XMM-Newton and Chandra.

8.2.3 X-Ray

Dear Martin (*Elvis*), X-ray surveys have become a major tool to identify distant quasars. What is to come?

Breakthrough advances from the two premier X-ray observatories now operating—NASA’s *Chandra* X-ray Observatory [72] and ESA’s *XMM-Newton* [31]—have become almost routine over the past decade. With these telescopes, in the 50 years since the Giacconi et al., rocket flight, the sensitivity of X-ray observations has improved a billion-fold (10^9 times). This is equivalent to going from naked eye to Hubble Deep Field observations but in 40 years rather than 400. (Both *Chandra* and *XMM* were launched in 1999.) Similarly, X-ray spectroscopy has improved in resolution 400-fold since the early proportional counter days of *Uhuru* and *Ariel V*. The area of sky covered by X-ray imaging detectors (their “field of view”) is usually larger than most optical imagers: ~ 15 arcmin for *Chandra* and ~ 30 arcmin for *XMM*. In one respect, X-ray astronomy has always beaten optical astronomy: timing to milliseconds is inherent in most X-ray detectors, and the poorest time resolution is still better than 1 s. Instead virtually all optical detectors expose for minutes to hours and can see no changes on shorter timescales.

Nonetheless, X-ray instrumentation is still far behind that in the optical and other wavelength bands in most respects:

1. The effective collecting area of these observatories is not much bigger than a dinner plate (*Chandra*) or a serving dish (*XMM*), compared with the dining table size of even small professional optical telescopes and the swimming pool size of VLT or Keck. X-ray spectrometers have even less area, just a few square centimeters—espresso cup size. As X-ray photons from quasars are at least a 1,000 times less numerous than optical ones, this is a major disadvantage. Most of the famous images from *Chandra* (<http://chandra.si.edu>) take a week or more to acquire (typically 1 Msec). The faintest sources yield 1 photon every other day. While this is a tribute to the low background in *Chandra*’s ACIS instrument, it is clearly preventing much deeper or wider surveys being undertaken because of the prohibitive time needed to carry them out.
2. The spectral resolving power ($\lambda/\Delta\lambda$, where λ is the X-ray wavelength) of the best X-ray spectrometers is ~ 400 at ~ 1 keV, while a value of 1,000 is unremarkable in the optical, and 20,000 is not unusual. This limits the measurement of Doppler shifts, or line widths, to $\sim 1,000$ km s $^{-1}$ or greater, which prevents us measuring the widths of lines of X-ray hot gas, which are a factor ~ 10 smaller. In the soft X-ray region (< 2 keV), the number of atomic transitions is huge, and so multiple lines often appear within a single resolution element. This “line blending” is severe in quasar warm absorbers [40].
3. The sharpest X-ray images, that is, the best angular resolution ones, come from *Chandra* and have $\sim 1/2$ arcsec widths. By comparison, Hubble produces 0.1 arcsec images. This factor 5 means images 25 times the number of pixels per square arcsecond, a substantial difference. Adaptive optics (AO) imaging on



Fig. 8.2 Five missions to be launched by 2015: (left to right) ASTROSAT, eROSITA, NuSTAR, GEMS, ASTRO-H

large ground-based telescopes is now making even better images of quasars [61], while near-IR interferometry is beginning to do an order of magnitude better still [36].

4. New optical and infrared telescopes dedicated to wide-field work are starting to produce deep images of the whole sky: Pan-STARRS [32], UKIDSS, and VISTA in the near-infrared [41]. The much larger optical survey telescope LSST is the #1 priority of the NSF for ground-based US astronomy for the next decade.

Each of these challenges can be addressed by new X-ray technologies, but the immediate prospects are limited. Five small X-ray telescopes will be launched in the next decade, each specializing in a different area (Fig. 8.2):

1. *ASTROSAT (India)*: Launch: Late 2011, early 2012. Main strength: Timing, broad-band (0.5–200 keV) sensitivity
2. *NuSTAR (USA)*: Launch: Early 2012. Main strength: first imaging telescope above 10 keV; Hundred times more sensitive in this band than preceding instruments
3. *eROSITA/Spectrum-X (Germany/Russia)*: Launch: 2013. Main strength: 4 year all-sky survey up to 10 keV with CCD energy resolution (resolving power ~ 10)
4. *GEMS (USA)*: Launch: 2014. Main strength: first X-ray polarimetry mission. Factor 100 or more greater sensitivity to polarization than previous (1970s) technology
5. *ASTRO-H (Japan)*: Launch: 2015. Main strength: high-resolution spectroscopy ($\Delta E \sim 2$ eV), esp. at the 6.4 keV Fe–K line, where its resolving power will be $\sim 3,000$

This is an impressive list and guarantees a vibrant decade in X-ray astronomy, not least in studies of quasars. Missing from this list, however, are large-area, wide-field, and high angular resolution.

Large area, combined with good spectral resolving power ($\sim 4,000$), was expected to come from the *International X-ray Observatory (IXO)*, a joint NASA–ESA project. However, IXO, though highly praised, was not rated highly enough in the 2010 decadal review (*New Worlds, New Horizons* [7]) to allow for a start on it before 2020, at the earliest. (Once started, a large mission like IXO would take nearly a decade before it flies.)

Recovering from this setback may require a rethinking of how the instruments were packaged. IXO had a 3-decade wide band of sensitive spectroscopic instruments, equivalent to covering the UV to the mid-infrared in a single telescope. It is rare that a hot, unobscured UV target is also a source of strong cool dust emission, which is characteristic of mid-IR targets. For similar reasons, it is rare for a strong sub-keV source to also be bright above 10 keV, where many obscured sources shine out strongly. Splitting these capabilities among separate, specialized, spacecraft may be the more efficient way to go. NASA may strengthen its Explorer series of small astronomy satellites [20] as this was the #2 recommendation of the decadal committee, among the large space-based programs which would enable this approach.

Many of the ideas floated, and proposed, after the decadal report follow this logic. For example, *Gravitas* would concentrate on the 1–10 keV band for large-area CCD-level spectroscopy [69]; WHIMEx and *Pharos* [10, 19] ignore the >1-keV band but give large areas for high resolving power ($\sim 4,000$) in the decade below that energy.

A wide-field 0.5–10 keV survey matched to the new optical surveys is also not in the program for now. The *Wide-Field X-ray telescope* (WFXT, [44]) could reproduce a month-long deep *Chandra* survey in a few hours but to get enough collecting area, the total cost of the mission is too high, well beyond that of a NASA Explorer or ESA M-class mission. The same fate overtook *EXIST*, a sensitive all-sky survey and variability monitor at 10 to ~ 100 keV, that could also study the highest redshift ($z > 8$) γ -ray bursts in detail [25].

Most surprising of all, to an outside observer, is the total lack of plans for any successor to the sub-arcsecond angular resolution of *Chandra*. Four of the five missions now readying for launch have arcminute level imagers, while eROSITA reaches ~ 15 arcsec. IXO was to have an angular resolution of 5 arcsec, WFXT about 2 arcsec. Why this reticence about following up the spectacular, and physically revealing, sub-arcsecond *Chandra* imaging? If the *Chandra* optics had been perfect, they would have had 20-marcsec resolution, so better imaging is allowed by physics. At first there was a psychological barrier: all of the above missions were planned before *Chandra* was launched, and the power of its imaging abilities could only be guessed. *Chandra*’s mirrors cost 200 M USD to produce, more in 2012 dollars, and they are heavy—*Chandra* was the heaviest payload launched by the Space Shuttle except for the *Compton Gamma-Ray Observatory* [43]. Scaling them up seemed to be prohibitively expensive and possibly not even feasible with current rockets. Meanwhile, lower cost but lower resolution optics were already feasible, as had been well demonstrated by the ASCA satellite [64].

But why not treat *Chandra* as an existence proof that high-resolution optics are possible and begin a major program to find a lighter, cheaper way of making such optics larger? Any such mirror must use much thinner shells than the ~ 1 -cm-thick *Chandra* ones, and will have a larger diameter, so is unlikely to be made of complete almost cylinders. Instead, partial arcs would be employed, as on the Japanese ASCA and *ASTRO-H* missions. While the mirrors need not be as thin as the ones planned for IXO, they will still be floppy and liable to bend, which would ruin their image quality. One concept, proposed as the core of the *Generation-X* concept [9],

is “active X-ray optics.” Estimates are that such optics could produce 1/10 arcsec or better images. With this resolution and large area, we should be able to witness the initial rapid growth of supermassive black holes at redshifts of ~ 10 . Several approaches to active X-ray optics are possible, but using large numbers of thin piezoelectric actuators deposited on the backs of every shell is currently the most promising [56].

How about higher angular resolution? Like any electromagnetic wave, X-rays can produce interference fringes [10], but practical X-ray interferometers have not been built. One concept, a telephoto design, seems closest to being buildable and could give milli-arcsecond imaging, though the area, and field of view, may be small in a practicable design [75].

To actually image the event horizon in quasars needs 0.1- μ arcsec imaging. For now, this is infeasible. Indirect methods, using the cold absorber clouds to eclipse the X-ray source, can have this effective resolution. The repeated one-dimensional scans that the eclipses provide give us a “poor man’s imager” and if the clouds behave as we hope, may allow tomographic reconstruction of the size and shape of the X-ray source and of the region emitting the general relativistically broadened Fe–K line, assuming that is the correct interpretation of the “red wings.” This method can be exploited with just arcminute telescopes but needs a large collecting area, such as *Gravitas* can provide. Higher spectral resolution may pick out individual clumps of Fe–K emitting gas as they orbit the black hole [68]. A large-area mirror imaging onto a microcalorimeter array might achieve this at moderate cost, if it can be made extremely light, as seems possible [18].

Thank you, Martin. In the coming years, it will remain difficult or impossible to spatially resolve the broad-line-emitting regions. The indirect techniques described in the previous chapters will be most likely farther pursued.

8.3 Reverberation Mapping

Dear Shai (*Kaspi*), are there more results to come from reverberation mapping? Does reverberation mapping have a real capability to resolve the structure of the BLR? Reverberation studies and perhaps other arguments have convinced us that the Balmer lines are reliable virial BH mass estimators. We measure the FWHM of a Balmer line and combine it with the size–luminosity relation (and a poorly known geometric factor f) to obtain a BH mass estimate. How can we improve this procedure? What are the most reasonable estimates of f ? What happens to FWHM if the Balmer lines are composite?

Current reverberation mapping studies cover the luminosity range of $\sim 10^{42}$ – 10^{46} erg s $^{-1}$. Since the full AGN luminosity range is four orders of magnitude larger than this range and span the range 10^{40} – 10^{48} erg s $^{-1}$, there is an essential need to carry out reverberation mapping studies for lower- and higher-luminosity AGNs.

Hopefully, such broadening of the luminosity range will help to better define the size–luminosity relation.

Quasars of the highest luminosities (with bolometric luminosity, $L_{\text{bol}} \approx 10^{47} - 10^{48} \text{ erg s}^{-1}$) are expected to harbor some of the most massive BHs known, with $M_{\text{BH}} \gtrsim 10^9 M_{\odot}$. Reverberation mapping of these high-luminosity quasars is an ambitious task and there are many difficulties: for example, the timescale of variations is of order of years, monitoring periods of decades are needed, the monitored lines are in the rest-frame UV, smaller intrinsic variability amplitude of the continuum, high-redshift sources are fainter, and hence more difficult to observe. Due to all of these possible problems, no reverberation measurements exist for AGNs with $L \gtrsim 10^{46} \text{ erg s}^{-1}$, and several attempts at such measurements have so far not been successful (e.g., [66, 74]).

Kaspi et al. [34] report on a campaign to monitor several high-luminosity quasars. After 5 years of monitoring, they found a tentative time lag between the C IV line and the continuum in S5 0836 + 71 to be 595_{-110}^{+86} days, which is 188_{-37}^{+27} days in the quasar rest frame. Combining this with the mean FWHM of about $9,700 \text{ km s}^{-1}$ and using equation 5 of [33] the central mass of S5 0836+71 is estimated to be $\sim 2.6 \times 10^9 M_{\odot}$. This is the highest mass directly measured for a BH in an AGN using reverberation mapping so far.

Reverberation mapping of low-luminosity AGNs might be considered fairly easy due to the short timescales involved and the expected high-amplitude variability. However, as these objects are of low luminosity, there is a need of a 3–10-m class telescopes in order to carry out reverberation mapping campaigns for such objects (e.g., the candidate AGNs with intermediate-mass BH from the sample by [24]). So far no reverberation mapping campaigns for AGNs with optical luminosity $L_{\alpha} 10^{42} \text{ erg s}^{-1}$ were carried out successfully.

The one exception is NGC 4395 ($\lambda L_{\lambda}(5100 \text{ \AA}) = 5.9 \times 10^{39} \text{ erg s}^{-1}$) in which [52] measured the BLR size of its C IV emission line to be 1 ± 0.3 light-hour. This is consistent with the size expected from extrapolating the $r_{\text{BLR}} - L$ relation to lower luminosities. However, two optical campaigns to determine the H β time lag of NGC 4395 were so far unsuccessful due to bad weather [15].

Until recently, only four AGNs had measured C IV reverberation time lags: NGC 3783, NGC 5548, NGC 7469, and 3C 390.3 (see [51], for a summary). NGC 4395 is four orders of magnitude lower in luminosity than those four AGNs, and S5 0836 + 71 is three orders of magnitude higher. Thus, a preliminary C IV-size–UV-luminosity relation over seven orders of magnitude in luminosity can be determined. Figure 8.3 shows the data for the above six objects with the best fit for the size–luminosity relation:

$$\log(r_{\text{BLR}}/10) = (0.17 \pm 0.04) + (0.52 \pm 0.04) \log(\lambda L_{\lambda}(1,350 \text{ \AA})/10^{43}), \quad (8.1)$$

where r_{BLR} measured in days and $\lambda L_{\lambda}(1,350 \text{ \AA})$ measured in erg s^{-1} (see [35] for details).

Thank you, Shai.

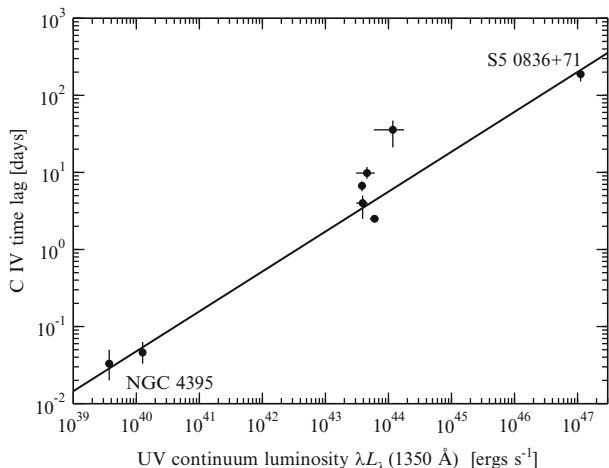


Fig. 8.3 Size–luminosity relationship based on the C IV emission line and the UV continuum. *Solid line* is the linear fit to the data

8.3.1 Two-Dimensional Reverberation Mapping and Structure of the BLR

Dear Marianne (Vestergaard), does two-dimensional reverberation mapping have a real capability to resolve the structure of the BLR?

Yes, very much so. It is actually the whole essence of the technique. In reverberation monitoring campaigns, we observe the response of the line-emitting gas to a continuum burst. It is delayed due to the light travel time of the photons from the continuum region to the BLR, which contains the line-emitting gas. The observed emission-line light curve can be described as

$$L(V_{\text{LOS}}, t) = \int \Psi(V_{\text{LOS}}, \tau)C(t - \tau)d\tau, \tag{8.2}$$

where $C(t)$ is the continuum luminosity at time t , V_{LOS} is the line-of-sight velocity of the gas, and the transfer function Ψ is the observed response of the broad line gas to a delta function continuum outburst [50]. This transfer function is a two-dimensional function of both time and LOS velocity, also referred to as the “velocity-delay map.” As one may imagine, this map depends on the structure and dynamics of the BLR as well as the inclination of the BLR to the line of sight. Therefore, by inverting this problem and deconvolving the continuum and emission-line light curves, one can indeed directly derive the velocity delay map (the two-dimensional transfer function) and thus obtain the structure and dynamics of the BLR. However, this requires both very high time sampling in the light curves and high-quality data. The majority of the monitoring campaigns to

date unfortunately do not have sufficient time sampling to achieve this goal. The reason is that when the community started to monitor AGNs, it was convinced that the BLR was much larger than we now know to be the case (about 10 times larger), so the time sampling of early campaigns was too coarse. This means that the campaigns were unable to resolve anything but the mean line response (i.e., delays as a function of line-of-sight velocity remained unresolved), and the extracted RM results were quite uncertain, especially for the lower luminosity sources containing the smallest BLRs. We are in the process of obtaining better monitoring data for many of these affected sources (e.g., [12, 14]). The Lick AGN Monitoring Project is also performing RM of low-luminosity AGN with lower-mass black holes, which is also of interest in this context (e.g., [5]). We have learned much in the past 20 years since the first campaigns, about how to do this well. As Shai Kaspi describes above, the observations are nontrivial due to the required high quality controls needed to ensure good measurements of the RM response. Keith Horne and collaborators have made extensive simulations showing that even quite complex dynamical and geometrical structures can be recovered from velocity-delay maps through maximum entropy methods (e.g., [29] and Prof. Horne’s web site; though see also [39] for recovering the transfer function with regularized linear inversion). Much work has gone into these simulations in recent years to determine the data quality required to recover high-fidelity velocity-delay maps (see [30]). A couple of recent monitoring campaigns with high-cadence observations show velocity-resolved time lags in the emission-line responses [4, 13], demonstrating the data necessary for producing successful two-dimensional reverberation mapping results are in hand and the goal of recovering high-fidelity velocity-delay maps within reach (e.g., [6]). It is interesting to note that so far we see diverse kinematic signatures, including Keplerian rotation, outflowing, and inflowing gas, suggesting that there is no universal velocity structure in AGNs. Unless, of course, a given source exhibits all these characteristics at different times. What remains to be seen is how these velocity fields may change with time and how the specific velocity field and its variations affect the black hole mass estimates. Overall, this means that we are entering a new era where we can soon uncover the much desired structure and dynamics of the BLR. This is very exciting news!

Thank you, Marianne.

Dear Shai (Kaspi), how reverberation mapping can lead to a reconstruction of the quasar central engine spatial structure and kinematics?

The initial goal of the reverberation mapping technique [8] is to study the geometry and kinematics of the BLR. This was not yet achieved due to poor spectroscopic data and insufficient time sampling. More detailed information on BLR geometry and kinematics in AGNs can be obtained by studying line profile variations. Various researchers computed two-dimensional echo images for specific gas motions in the BLR: outward-moving gas clouds, inward falling clouds, circulating gas clouds in a plane, or clouds orbiting in randomly inclined orbits (e.g., [30, 49, 73]).

Several studies attempted two-dimensional reverberation mapping on actual data. So far, none of them resulted with a conclusive result about the BLR kinematics, although the results give some additional information to the simple determination of a time lag. Kollatschny [38] used the monitoring data of Mrk 110 to study the variations in the line profiles and produced time delay vs. velocity maps. These maps resemble a disk transfer-function maps and show that the outer line wing respond before the inner line profile. Bentz et al. [6] used the monitoring data of Arp 151 and find that there is a deficit of prompt response in the Balmer-line cores but strong prompt response in the red wings. Comparison with simple models identifies two classes that reproduce these features: free-falling gas and a half-illuminated disk with a hot spot at small radius on the receding lobe.

Thus, with recent improved sensitivity of optical telescopes and the accumulated experience from previous mapping campaigns, combined with monitoring baselines of several months, daily sampling, and homogeneous data with high signal-to-noise ratios, it is becoming possible to obtain the crucial information about the geometry and kinematics of the BLR gas.

How can estimations of black hole masses be improved?

One of the uncertainty factors when estimating M_{BH} is the parameter f in (5.3). As mentioned, this factor depends on the geometry and kinematics of the BLR and simple models of BLR morphologies yield f parameters of the order of unity. To better estimate this factor [46] used 16 AGNs which have both mass estimates from reverberation mapping and mass estimates from velocity dispersions and the $M_{\text{BH}} - \sigma_*$ relation. The best estimate for the f parameter they find in order to reconcile between the two mass estimates is $f = 5.5$. To improve on this result, one needs more objects with these two mass estimates. A different approach can materialized once the geometry and kinematic of the BLR will be found from two dimensional reverberation mapping. Once this will be determined, the factor f will be derived directly and reliably from the known geometry and kinematic.

Broad lines can show inflections and asymmetries that may indicate a composite nature of the emitting region, likely connected to a complex structure and kinematics of the emitting region even for the same ionic species (e.g., [42, 45, 63]). This pose a problem for reverberation mapping studies which, as described above, assume simple kinematic structure and use a simple measurement of the line's FWHM. To overcome part of this problem, reverberation mapping studies measure the FWHM of the lines from the RMS spectrum of all spectra taken in the observing campaign. This ensures that the corresponding r_{BLR} is matched to the variable part of the emission line that had produced the time lag and ignores the velocities in the line profile that did not contribute to the line variability and to the estimate of r_{BLR} . Indeed, for the single-epoch measurement of M_{BH} this problem poses a challenge. This could only be solved probably when good enough statistics be gathered on the composite nature of the emitting region.

8.3.2 *Dust Reverberation Mapping*

IR emission in AGNs is considered to be from the alleged torus region which is at distances larger than the BLR from the BH. Thus, IR reverberation mapping might reveal the distance of the torus from the BH. Only a few IR monitoring campaigns were carried out in the past 2 decades (e.g., [11, 23, 59]). Recently, Suganuma et al. [62] monitored the optical and IR emission in four additional objects and determined time lags. Together with previous results, they are able to construct the torus size–luminosity relation for ten objects. They find the torus size to strongly correlate with the optical luminosity (the time lag is consistent with the square root of the luminosity) and that it weakly correlates with the mass of the BH.

8.3.3 *X-Ray FeK α Reverberation Mapping*

Several studies suggested the application of the reverberation mapping technique to the broad 6.4-keV FeK α line seen in the X-ray band (e.g., [57]). This line is considered to emerge from the accretion disk in the very close vicinity of the BH, and using reverberation mapping will allow the measurement of the disk’s size. So far, several attempts to apply this method did not produce significant results (e.g., [3] and references therein), implying either on the complicated connection between the broad 6.4-keV FeK α line flux and the X-ray continuum, or on the fact that the X-ray data obtained so far were not sufficient for reverberation mapping.

In summary, over the past two and a half decades, reverberation mapping of AGNs have yield measurements of the BLR size in about four dozen AGNs in the luminosity range $\sim 10^{42} - 10^{46} \text{ erg s}^{-1}$. This enables to establish a scaling relation between the BLR size and luminosity in AGNs which, in turn, allows to estimate the BH mass in AGNs. Using reverberation mapping of different emission lines implies about the radial ionization stratification of the BLR (higher ionized species emits from inner BLR) and that motion of the gas in the BLR are virial and primarily orbital. Current BLR studies should aim at broadening the luminosity range to all AGNs, and first steps toward low- and high-luminosity AGNs are being taken. Two-dimensional reverberation mapping is a promising direction which will produce information about the geometry and kinematics of the BLR. Reverberation mapping in the IR enables measurement of the dusty region in AGNs (torus) which seems to surround the BLR. On the other hand, reverberation mapping of the inner accretion disk, using X-ray observations, is still to be proven feasible.

Thank you, Shai. The LSST and other new telescopes and instruments will make available an impressive amount of data. These data should be made easily accessible to be exploited by the widest possible community of astronomers.

8.4 Digital Observatories

Dear Paolo (Padovani), there are now more than 160,000 quasars and AGNs in catalogues. Which new surveys will further increase this number in the near future and by how much? How will the Virtual Observatory and the data archives help us manage these new data? What other advancements in our understanding of AGNs can we expect from new astronomical facilities?

The number of known AGNs since the discovery of quasars has been growing enormously. Figure 8.4 plots the number of entries in all Véron-Cetty and Véron catalogues over the years, starting from the first one in 1984, which included 2,800 sources, to the latest one in 2010, which contains almost 170,000 objects. The number of AGNs has increased steadily by a factor ~ 60 in the past 27 years. The pace changed dramatically around the year 2000, switching from a rate of ~ 900 per year to $\sim 15,000$ per year starting with the 10th edition (2001), when the first release of the 2dF quasar catalogue was included. The 11th edition (2003), which had the final 2dF release and the first SDSS catalogue, continued the trend, which has not slowed down since.

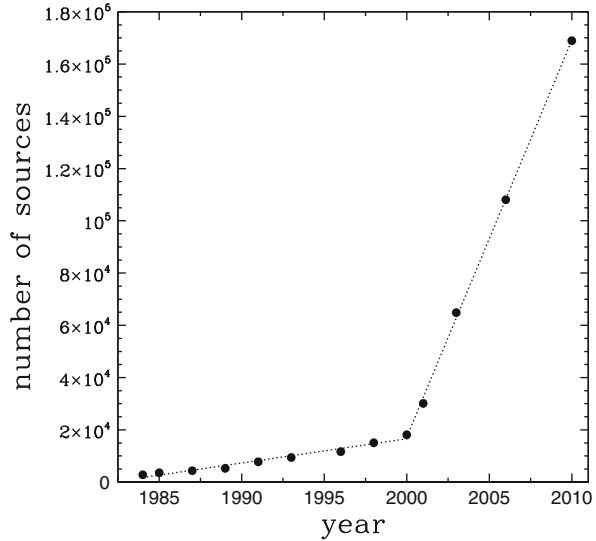
What is the total number of AGNs in the universe? Padovani [47] estimates $\approx 2 \times 10^4 \text{ deg}^{-2}$ radio-quiet AGNs (broad- and narrow-lined), based on radio data supported by X-ray considerations, with radio-loud ones, making up a very small minority. This translates to ≈ 800 million AGNs over the whole sky, which means that there is plenty of room for improvement!

What is in store for the future? A naive extrapolation of the trend in Fig. 8.4 would suggest a doubling of the number of known AGNs in the next 10 years, thereby reaching the $\sim 320,000$ level by 2020. This is likely to be a severe underestimate: X-ray, optical, infrared, and radio surveys will produce in the next few years catalogues containing *millions* of *potential* AGNs. I highlight here some of these surveys, with no presumption of completeness, as there are many more (which are either smaller or not dedicated to AGNs):

- X-ray surveys are currently revealing the largest surface density of AGNs. The number counts in [26] indicate $\sim 2,000 \text{ deg}^{-2}$ of unabsorbed AGNs down to the faintest *Chandra* limits, to be compared, for example, with $\sim 80 \text{ deg}^{-2}$ for one of the deepest optically selected quasar samples ($g \sim 22$; [58]). Future large-area surveys include those with eROSITA,¹ to be launched in 2012 and

¹<http://www.mpe.mpg.de/heg/www/Projects/EROSITA/main.html>.

Fig. 8.4 The number of AGNs in the Véron-Cetty and Véron catalogues over the years. The two *dotted lines* are linear fits to the points before and after 2000, with slopes of ~ 922 and $\sim 15,184$ AGN/year, respectively



which are expected to detect ≈ 2 million AGNs and in the more distant future (pending approval), those with the WFXT,² which should reveal more than ten million AGNs.

- Optical surveys will catch up with the X-ray ones, thanks to the Panoramic Survey Telescope and Rapid Response System,³ which from Hawaii will survey about 3/4 of the sky down to $R_{\text{mag}} \sim 26$ during 10 years of operation and the LSST,⁴ which will be located in Chile and will provide a survey of about half the sky down to $R_{\text{mag}} \sim 27.5$ during 10 years of operation. LSST, which should begin operations in 2018, is expected to detect 20–80 million AGNs through their colors and variability. One of the four telescopes making up Pan-STARRS has already started operations in 2010. Despite its somewhat brighter magnitude limit, PAN-STARRS should detect a similar number of AGNs as LSST, given its larger survey area, but on a shorter timescale, as PAN-STARRS is already being built.
- The Wide-field Infrared Survey Explorer⁵ mission is using a 40-cm space telescope to perform an all-sky survey, covering at least 95% of the sky, at four infrared wavelengths: 3.3, 4.7, 12, and 23 μm . WISE will deliver all-sky catalogues of half a billion objects in these four bands, which should include

²<http://wfxt.pha.jhu.edu>.

³<http://pan-starrs.ifa.hawaii.edu>.

⁴<http://www.lsst.org>.

⁵<http://wise.ssl.berkeley.edu>.

millions of potential AGNs (based on previous infrared missions). *Euclid*⁶ will provide near-infrared spectra for tens of millions of galaxies selected in the *H*-band ($H_{AB} < 22$), including ≈ 1 million AGNs. *Euclid* is being evaluated along with two other missions by the European Space Agency for a possible launch in 2017–2018.

- Deep ($f_r < 100 \mu\text{Jy}$ at 1.4 GHz) radio surveys are also revealing large surface densities of AGNs: the VLA *Chandra* deep field south (CDFS) survey has reached ~ 520 radio-quiet AGNs deg^{-2} [48], almost exactly in between optical and X-ray surveys. Classical radio-loud quasars, being intrinsically radio powerful, are basically nonexistent below 1 mJy. Future surveys will detect huge numbers of radio-quiet AGNs in the radio band bypassing the problems of obscuration, which plague the optical and the soft X-ray bands. For example, the Evolutionary Map of the Universe,⁷ which will use the new Australian Square Kilometer Array Pathfinder,⁸ will survey 3/4 of the sky down to a flux density similar to that of the VLA-CDFS ($f_r \sim 50 \mu\text{Jy}$). With a likely start of operations in 2013, the EMU catalogue should be available to the astronomical community by around 2015 and will contain around 70 million sources. Out of these, ≈ 14 million should be (radio-quiet) AGNs, extrapolating from the results of the VLA-CDFS. Many other radio telescopes are currently under construction in the lead up to the Square Kilometer Array,⁹ which will revolutionize astronomy by extending well into the *nano Jansky* regime with unprecedented versatility.

First, science with $\sim 10\%$ SKA should be near the end of this decade. Location will be in the southern hemisphere, either Australia or South Africa. Many surveys are being planned with the SKA, possibly comprising an all-sky (as visible from its southern location) $1\text{-}\mu\text{Jy}$ survey at 1.4 GHz and an HI survey out to redshift ~ 1.5 , which should include one billion galaxies. Note that a $1\text{-}\mu\text{Jy}$ survey covering $\sim 150 \text{deg}^2$ might detect ≈ 1 million radio-quiet AGNs, while a half-sky one could get to the 140 million level, that is, $\approx 1/6$ of all AGNs!

These huge numbers of AGNs go beyond anything we have seen so far and will present big identification problems. That is, how will we be able to get counterparts for all these sources in other bands to properly classify them? For example, the identification of broad-lined, type-1 AGNs in X-ray surveys normally requires an optical classification or at a minimum, the presence of an unabsorbed X-ray spectrum and an X-ray luminosity $> 10^{42} \text{erg s}^{-1}$ [26]. In both cases, there is an obvious need for spectroscopy. How will we manage that for millions of sources? The largest spectroscopic survey available to date is the SDSS (<http://www.sdss.org>), which in its Data Release 7 includes 121,000 quasars with $i < 19.1$ (20.2 for objects likely at $z > 2.3$). *Euclid* will obtain spectra for ≈ 1 million AGNs, but

⁶<http://sci.esa.int/euclid>.

⁷<http://www.atnf.csiro.au/people/morris/emu>.

⁸<http://www.atnf.csiro.au/projects/askap>.

⁹<http://www.skatelescope.org>.

these will have $H_{AB} < 22$, so overlap with other surveys will not be guaranteed. In any case, future X-ray, optical, and radio surveys will produce AGNs in the tens of millions. Photometric redshifts are now derived routinely, but they have limitations beyond a certain magnitude/redshift. But much more than redshift is needed: Padovani et al. [48] have shown that proper classification of faint radio sources requires a variety of multiwavelength data, including optical morphology and power, X-ray data, near-IR colors, and far-IR data. This means that the SKA pathfinders, like EMU, will need many complementary data at other wavelengths to classify their radio sources, which will not be available for all of them. The situation for the SKA will be even worse [47]. A likely scenario, then, is one where complete identification programs will be carried out on relatively small areas of the sky through dedicated surveys in bands complementary to the one where the sample was originally defined. In parallel, we will need to extract as much information as possible from whatever data will be available on large areas. The radio band is then likely to lead the way in extragalactic astronomy in terms of survey depth and areas in the near future.

Non-survey telescopes will also provide major breakthroughs in our understanding of AGNs. It is impossible to cover here all of them and the AGN-relevant science they will produce (which takes up many pages in many large documents!). A (small) selection includes the Atacama Large Millimeter Array,¹⁰ which will soon study molecular absorption lines in the obscuring regions of AGNs and will trace the kinematics of the molecular gas and probe the physical and chemical conditions in their central regions, and the James Webb Space Telescope,¹¹ which will study in the IR the role of black holes in galaxy evolution, especially at early times, the power source of quasars, and will discover many high-redshift (>6 and up to 20!) objects. Moreover, three very large telescopes are being planned: the European Extremely Large Telescope (42 m),¹² the Thirty Meter Telescope,¹³ and the Giant Magellan Telescope (25 m).¹⁴ These will revolutionize AGN research by allowing, among other things, study of supermassive black holes down to the low mass end ($\sim 10^6 M_{\odot}$) out to the Virgo cluster, very detailed studies of intrinsically weak sources, and identification of extremely faint and distant objects.

Note that even if we had unlimited access to telescope time to secure spectra for all the sources we wanted, this might not be enough to classify all objects. We are in fact reaching fainter and fainter sources, routinely beyond the typical identification limits of 8/10 m telescopes ($R_{\text{mag}} \approx 26$ for a 10 h exposure in the case of strong emission lines), which makes “classical” identification problematic. Very large telescopes will obviously have less problems but on relatively small areas. Managing all these new data will also not be easy. In fact, it could well be impossible

¹⁰<http://www.eso.org/sci/facilities/alma>.

¹¹<http://www.stsci.edu/jwst>.

¹²<http://www.eso.org/sci/facilities/eelt>.

¹³<http://www.tmt.org>.

¹⁴<http://www.gmto.org>.

if we do not succeed in putting this huge amount of new information together in a coherent and relatively simple way.

All of the above calls for innovative solutions. For example, the observing efficiency can be increased by a clever preselection of the targets, which will require some pre-characterization of the sources before hand, so that less time is “wasted” on sources which are not of the type under investigation. One can expand this concept even further and provide a statistical identification of astronomical sources by using all the available, multiwavelength information without the need for a spectrum (assuming the relevant data is there). And finally, easy and clever access to all astronomical data worldwide would certainly help in dealing with this data explosion and would allow astronomers to take advantage of it in the best of ways.

The name of the solution is the Virtual Observatory (VO). The VO is an innovative system, which allows users to interrogate multiple data centers in a seamless and transparent way, to utilize at best astronomical data. New science is being enabled, by moving Astronomy, beyond “classical” identification with the characterization of the properties of very faint sources by using all the available information. All this requires good communication, that is, the adoption of a common language between data providers, tool users, and developers. This is being defined using new international standards for data access, interoperability, and mining protocols under the auspices of the International Virtual Observatory Alliance,¹⁵ a global collaboration of the world’s astronomical communities.

After a few years of development, the VO is now entering an operational phase. The most important standards have been specified, VO-tools¹⁶ are now quite robust and are being used by astronomers for their daily research work, and more and more data are being delivered through VO interfaces and protocols.

A possible vision for a future with ever larger amounts of data might be as follows: huge surveys, more complex instruments, and larger telescopes will make data reduction (almost) become a thing of the past for the typical astronomer. Most astronomers, therefore, will only deal with catalogues and already processed (so-called science-ready) data. All of these data will need to be well-described and interoperable; otherwise, it will be impossible to make sense of them. Data providers not conforming to this model will be quickly weeded out and go extinct, as their data will not be used and funding agencies will stop supporting them. And perhaps, nobody will remember what the VO was, although everybody will be using it!

Thank you, Paolo. Along with the revelation of the black hole event horizon, one of the major tenets of the accretion paradigm is the inflow of matter. Until now, we miss direct evidence confirming this process.

¹⁵<http://ivoa.net>.

¹⁶<http://www.euro-vo.org/pub/fc/software.html>.

8.5 The Detection of Infalling Matter and the Accretion Scenario

Dear Johan (*Knapen*), can you please mention some future observational prospects concerning the revelation of infall motions?

The future for direct observations of inflow into the central regions QSOs is most interesting. Important improvements in observing infrastructure will become available in the next decade or so, but the problem with observing QSO fueling remains twofold: the high angular resolution needed to detail processes close to the black hole, and the huge contrast between the emission from the QSO itself and that from its surroundings. Perhaps, the most promising approach would be to try and observe the gas flows around the QSO. This reduces the contrast problem as QSOs have relatively little radio line emission, but the resolution problem remains.

To illustrate this, one should contrast the angular resolution to be achieved with new facilities such as the enhanced version of the multi-element radio-linked interferometer network (e-MERLIN), the ALMA, the SKA, or the optical extremely large telescope/Giant Segmented Mirror Telescope, which is in all cases of the order of 10 mas. The very nearest QSOs in the 2003 study by Dunlop et al. [16] have a redshift of just over 0.1, which indicates a distance of several 100 Mpc. At 200 Mpc, 1 mas corresponds roughly to 1 pc in scale, so all these new facilities will allow us to reach spatial scales of a couple of parsecs, across optical, near-IR, mm, and radio wavelengths—an astounding improvement over current capabilities.

This should allow us to study $z \sim 0.1$ QSOs at similar physical scales as the nearby AGNs discussed in Sect. 7.2. But even though the black holes in QSOs are more massive, and thus the Eddington and AGN radii larger than in the nearby low-luminosity AGNs being studied at present, the inflow that can be studied with the new facilities occurs at scales at best comparable to that at which the black hole influence starts to become the dominant factor.

In nearby AGNs, on the other hand, the improved spatial resolution should allow the detailed study of the physics occurring in the sphere of influence of the massive black hole. In fact, at a distance of 20 Mpc, the spatial resolution of the suite of new facilities (around 10 mas) corresponds to the size of the broad-line region in AGNs, which is around a parsec. Studying morphology, kinematics, and physical properties, all based on data from across the wavelength range, will revolutionize our understanding of AGNs. Although these “local” AGNs do not include many QSOs, the understanding of the detailed physics gained by studying local AGNs can be extrapolated to their more energetic QSO counterparts. Studying gas flows at scales of a few pc around massive QSOs at substantial redshifts will open up another hitherto unexplored region of parameter space. Gas flows in the vicinity of the AGNs will be observed and modeled, and parallels can be drawn to flows currently being observed in more nearby but less luminous AGNs. The actual inflow into the accretion zone, however, will still be mostly beyond reach and will have to be modeled in detail using the new observations as invaluable constraints.

On the other hand, inflow at larger scales, for instance related to cold gas coming into the host galaxies by mergers or interactions in the early Universe, will be reachable by detailed observations primarily at infrared to radio wavelengths, with, for example, the *James Webb space Telescope*, ALMA, or the SKA. At the high spatial resolution offered, we will be able to construct detailed maps of the distribution and kinematics, as well as of the physical properties, of the cold gas in the outskirts of statistically meaningful samples of AGNs and non-AGNs at intermediate and even high redshifts. This should lead to an understanding of not just AGN fueling but also the related more general issue of galaxy formation and evolution.

Dear Isaac (*Shlosman*), what are the most outstanding issues to test concerning the accretion scenario of quasars?

Dramatic progress has occurred since the detection of first QSOs, which includes the basic understanding of their energy source as an accretion process onto an SMBH, the collimated and uncollimated outflows associated with these objects and manifesting themselves in broad emission and absorption lines, and the ever-growing role of the SMBH feedback onto the galaxy evolution.

The list of outstanding issues is long as well. It includes detection of accretion flows on smallest spatial scales, inside r_1 (the radius of influence of the central supermassive black hole, see Sect. 6.8.1), and understanding the prevailing mode of accretion there. Do ADAFs, CDAFs, and ADIOS exist in nature? If yes, what is the critical accretion rate for this switch between modes? Has it anything to do with the conditions at the outer “boundary” of AGNs? Verifying the role of magnetic fields in this region is crucial as well. Especially important is to understand the magnetic collimation process at the base of the jets, the role of the magnetic reconnection, and the efficiency of rotational energy extraction from the black hole via the Blandford–Znajek mechanism.

On scales beyond r_1 and within the central kpc, it is important to obtain evidence for the distribution of molecular gas and the strength of gravitational torques. Magnetic torques can also be important in the inner parts of this region.

It is natural that star formation at some level will be associated with inflows, especially within the inner few 100 pc. In this sense, nuclear star formation can be a by-product of the large-scale gas flow toward the center. It is entirely possible that some of the processed gas by stars will rejoin the main inflow and contribute to the AGN fueling. But the stellar role must be quantified in this process.

Thank you, Isaac.

References

1. Antonucci, R.R.J., Miller, J.S.: Spectropolarimetry and the nature of NGC 1068. *Astrophys. J.* **297**, 621 (1985)
2. Bahcall, J., Kirhakos, S., Saxe, D.H., Schneider, D.P.: Hubble space telescope images of a sample of 20 nearby luminous quasars. *Astrophys. J.* **479**, 642–658 (1997)

3. Ballantyne, D.R., Turner, N.J., Young, A.J.: X-ray reflection from inhomogeneous accretion disks. II. Emission-line variability and implications for reverberation mapping. *Astrophys. J.* **619**, 1028 (2005)
4. Bentz, M.C., Walsh, J.L., Barth, A.J., Baliber, N., Bennert, V.N., Canalizo, G., Filippenko, A.V., Ganeshalingam, M., Gates, E.L., Greene, J.E., Hidas, M.G., Hiner, K.D., Lee, N., et al.: The lick AGN monitoring project: Broad-line region radii and black hole masses from reverberation mapping of H β . *Astrophys. J.* **705**, 199 (2009)
5. Bentz, M.C., Walsh, J.L., Barth, A.J., Yoshii, Y., Woo, J.-H., Wang, X., Treu, T., Thornton, C.E., Street, R.A., Steele, T.N., Silverman, J.M., et al.: The lick AGN monitoring project: Reverberation mapping of optical hydrogen and helium recombination lines. *Astrophys. J.* **716**, 993 (2010)
6. Bentz, M.C., Horne, K., Barth, A.J., Bennert, V.N., Canalizo, G., Filippenko, A.V., Gates, E.L., Malkan, M.A., Minezaki, T., Treu, T., Woo, J.-H., Walsh, J.L.: The lick AGN monitoring project: Velocity-delay maps from the maximum-entropy method for Arp 151. *Astrophys. J.* **720**, L46 (2010)
7. Blandford, R.D.: National research council (U.S.). Committee for a decadal survey of astronomy and astrophysics: New Worlds, new horizons in astronomy and astrophysics. National Academies Press, Washington (2010)
8. Blandford, R.D., McKee, C.F.: Reverberation mapping of the emission line regions of seyfert galaxies and quasars. *Astrophys. J.* **255**, 419 (1982)
9. Brissenden R.J.V., Generation-X team: The generation-X Vision mission study and advanced mission concept. AAS, High Energy Astrophysics Division (HEAD) meeting, vol. 10, p. 37 (2008)
10. Cash, W.: WHIMEX: An explorer for high resolution X-ray spectroscopy of the intergalactic medium. AAS Meeting **217**, 433 (2011)
11. Clavel, J., Wamsteker, W., Glass, I.S.: Hot dust on the outskirts of the broad-line region in Fairall 9. *Astrophys. J.* **337**, 236 (1989)
12. Denney, K.D., Watson, L.C., Peterson, B.M., Pogge, R.W., Atlee, D.W., Bentz, M.C., Bird, J.C., Brokofsky, D.J., et al.: A revised broad-line region radius and black hole mass for the narrow-line seyfert-1 NGC4051. *Astrophys. J.* **702**, 1353 (2009)
13. Denney, K.D., Peterson, B.M., Pogge, R.W., Adair, A., Atlee, D.W., Au-Yong, K., Bentz, M.C., Bird, J.C., et al.: Diverse kinematic signatures from reverberation mapping of the broad-line region in AGNs. *Astrophys. J.* **704**, L80 (2009)
14. Denney, K.D., Peterson, B.M., Pogge, R.W., Adair, A., Atlee, D.W., Au-Yong, K., Bentz, M.C., Bird, J.C., Brokofsky, D.J., Chisholm, E., et al.: Reverberation mapping measurements of black hole masses in six local seyfert galaxies. *Astrophys. J.* **721**, 715 (2010)
15. Desroches, L.-B., Filippenko, A.V., Kaspi, S., Laor, A., Maoz, D., Ganeshalingam, M., Li, W., Moran, E.C., Swift, B., Bentz, M.C., et al.: Multiwavelength monitoring of the dwarf seyfert-1 galaxy NGC 4395. III. optical variability and X-Ray/UV/Optical correlations. *Astrophys. J.* **650**, 88 (2006)
16. Dunlop, J.S., McLure, R.J., Kukula, M.J., Baum, S.A., O'Dea, C.P., Hughes, D.H.: Quasars, their host galaxies and their central black holes. *Mon. Not. R. Astron. Soc.* **300**, 1095–1135 (2003)
17. Eckart, A., Genzel, R.: Observations of stellar proper motions near the galactic centre. *Nature* **383**, 415 (1996)
18. Elvis M.: The extreme physics explorer. *SPIE* **6266**, 20 (2006)
19. Elvis, M., Fiore, F.: Pharos collaboration: Pharos: A high resolution intergalactic explorer for the soft X-ray. *Bull. Am. Astron. Soc.* **203**, 563 (2003)
20. Elvis, M., Beasley, M., Brissenden, R., Chakrabarti, S., Cherry, M., Devlin, M., Edelman, J., Eisenhardt, P., Feldman, P., Ford, H., Gehrels, N., Golub, L., Marshall, H., Martin, C., Mather, J., et al.: A vigorous explorer program. An activities/program white paper submitted to the Astro2010 NAS/NRC decadal review of astronomy and astrophysics. [arXiv:0911.3383] (2009)

21. Ferrarese, L., Merritt, D.: A fundamental relation between supermassive black holes and their host galaxies. *Astrophys. J.* **539**, L9–L12 (2000)
22. Gebhardt, K., Bender, R., Dressler, A., et al.: A relationship between nuclear black hole mass and galaxy velocity dispersion. *Astrophys. J.* **539**, L13 – L16 (2000), see also errata in *Astrophys. J.* **555**, L75–L75 (2001)
23. Glass, I.S.: Infrared variability of the seyfert galaxy NGC 3783. *Mon. Not. R. Astron. Soc.* **256**, 23 (1992)
24. Greene, J.E., Ho, L.C.: Active galactic nuclei with candidate intermediate-mass black holes. *Astrophys. J.* **610**, 722 (2004)
25. Grindlay, J., Gehrels, N., Bloom, J., Coppi, P., Soderberg, Al., Hong, J., Allen, B., Barthelmy, S., Tagliaferri, G., Moseley, H., et al.: Overview of EXIST mission science and implementation. *SPIE* **7732**, 59 (2010)
26. Hasinger, G., Miyaji, T., Schmidt, M.: Luminosity-dependent evolution of soft X-ray selected AGN. New Chandra and XMM-Newton surveys. *Astron. Astrophys.* **441**, 417–434 (2005)
27. Heckman, T.: The co-evolution of galaxies and black holes: Current status and future prospects. *Proc. IAU* **5**, 3–14 (2010)
28. Heckman, T.M., Kauffmann, G., Brichmann, J., Charlot, S., Tremonti, C., White, S.D.M.: Present-day growth of black holes and bulges: The sloan digital sky survey perspective. *Astrophys. J.* **613**, 109–118 (2004)
29. Horne, K.: Echo mapping problems maximum entropy solutions. *ASP Conf. Ser.* **69**, 23 (1994)
30. Horne, K., Peterson, B.M., Collier, S.J., Netzer, H.: Observational requirements for high-fidelity reverberation mapping. *PASP* **116**, 465 (2004)
31. Jansen, F., Lumb, D., Altieri, B., Clavel, J., Ehle, M., Erd, C., Gabriel, C., Guainazzi, M., Gondoin, P., Much, R., et al.: XMM-Newton observatory. I. The spacecraft and operations. *Astron. Astrophys.* **365**, L1 (2001)
32. Kaiser, N., Burgett, W., Chambers, K., Denneau, L., Heasley, J., Jedicke, R., Magnier, E., Morgan, J., Onaka, P., Tonry, J.: The pan-STARRS wide-fieldoptical/NIR imaging survey. *SPIE* **7733**, 12 (2010)
33. Kaspi, S., Smith, P.S., Netzer, H., Maoz, D., Jannuzi, B.T., Giveon, U.: Reverberation measurements for 17 quasars and the size-mass-luminosity relations in active galactic nuclei. *Astroph. J.* **533**, 631–649 (2000)
34. Kaspi, S., Maoz, D., Netzer, H., Peterson, B.M., Vestergaard, M., Jannuzi, B.T.: The relationship between luminosity and broad-line region size in active galactic nuclei. *Astroph. J.* **629**, 61–71 (2005)
35. Kaspi, S., Brandt, W.N., Maoz, D., Netzer, H., Schneider, D.P., Shemmer, O.: Reverberation mapping of high-luminosity quasars: First results. *Astrophys. J.* **659**, 997–1007 (2007)
36. Kishimoto, M., Hönl, S.F., Antonucci, R., Kotani, T., Barvainis, R., Tristram, K.R.W., Weigelt, G.: Exploring the inner region of type-I AGNs with the Keck interferometer. *Astron. Astrophys.* **507**, 57 (2009)
37. Koekemoer, A.M., Alexander, D.M., Bauer, F.E., et al.: A possible new population of sources with extreme X-Ray/Optical ratios. *Astrophys. J.* **600**, L123–L126 (2004)
38. Kollatschny, W.: Accretion disk wind in the AGN broad-line region: Spectroscopically resolved line profile variations in Mrk 110. *Astron. Astrophys.* **407**, 461 (2003)
39. Krolik, J.H., Done, C.: Reverberation mapping by regularized linear inversion. *Astrophys. J.* **440**, 166 (1995)
40. Krongold, Y., Nicastro, F., Brickhouse, N.S., Elvis, M., Liedahl, D.A., Mathur, S.: Toward a self-consistent model of the ionized absorber in NGC 3783. *Astrophys. J.* **597**, 832–850 (2003)
41. Lawrence, A., Warren, S.J., Almaini, O., Edge, A.C., Hambly, N.C., Jameson, R.F., Lucas, P., Casali, M., Adamson, A., Dye, S., Emerson, J.P., Foucaud, S., et al.: The UKIRT infraredDeep sky survey (UKIDSS). *Mon. Not. R. Astron. Soc.* **379**, 1599–1617 (2007)
42. Marziani, P., Sulentic, J.W., Stirpe, G.M., Zamfir, S., Calvani, M.: VLT/ISAAC spectra of the H β region in intermediate-redshift quasars. III. H β broad-line profile analysis and inferences about BLR structure. *Astron. Astrophys.* **495**, 83 (2009)

43. McDowell, J.C.: Jonathan's Space report. URL:<http://www.planet4589.org/space/jsr/jsr.html> (access in 2011)
44. Murray, S., Giacconi, R., Ptak, A., Rosati, P., Weisskopf, M., Borgani, S., Jones, C., Pareschi, G., Tozzi, P., Gilli, R., Campana, S., Paolillo, et al.: The wide field X-ray telescope mission – a digital sky survey in X-rays. *AIP Conf. Proc.* **1248**, 549 (2010)
45. Netzer, H., Trakhtenbrot, B.: Cosmic evolution of mass accretion rate and metallicity in active galactic nuclei. *Astrophys. J.* **654**, 754 (2007)
46. Onken, C.A., Ferrarese, L., Merritt, D., Peterson, B.M., Pogge, R.W., Vestergaard, M., Wandel, A.: Supermassive black holes in active galactic nuclei. II. Calibration of the black hole mass-velocity dispersion relationship for active galactic nuclei. *Astrophys. J.* **615**, 645 (2004)
47. Padovani, P.: The microJy and NanoJy radio sky: Source population and multi-wavelength properties. *Mon. Not. R. Astron. Soc.* **411**, 1547 (2011)
48. Padovani, P., Miller, N., Kellermann, K.I., Mainieri, V., Rosati, P., Tozzi, P.: The VLA survey of the CDFS. V. Evolution and luminosity functions of sub-mJy radio sources and the issue of radio emission in radio-quiet quasars. *Astrophys. J.* **740**, 20 (2011)
49. Perez, E., Robinson, A., de la Fuente, L.: The response of the broad emission line region to ionizing continuum variations. III – an atlas of transfer functions. *Mon. Not. R. Astron. Soc.* **256**, 103 (1992)
50. Peterson, B.M.: The central black hole and relationships with the host galaxy. *New Astron. Rev.* **52**, 240 (2008)
51. Peterson, B.M., Ferrarese, L., Gilbert, K.M., Kaspi, S., Malkan, M.A., Maoz, D., Merritt, D., Netzer, H., Onken, C.A., Pogge, R.W., Vestergaard, M., Wandel, A.: Central masses and broad-line region sizes of active galactic nuclei. II. A homogeneous analysis of a large reverberation-mapping database. *Astrophys. J.* **613**, 682–699 (2004)
52. Peterson, B.M., Bentz, M.C., Desroches, L.-B., Filippenko, A.V., Ho, L.C., Kaspi, S., Laor, A., Maoz, D., Moran, E.C., Pogge, R.W., Quillen, A.C.: Multiwavelength monitoring of the dwarf seyfert-1 galaxy NGC 4395. I. A reverberation-based measurement of the black hole mass. *Astrophys. J.* **632**, 799; Erratum: (2006); *Astrophys. J.* **641**, 638 (2005)
53. Prochaska, J.X., Chen, H.-W., Howk, J.C., Weiner, B.J., Mulchaey, J.: Probing the intergalactic medium-galaxy connection toward PKS 0405–123. I. Ultraviolet spectroscopy and metal line systems. *Astrophys. J.* **617**, 718–745 (2004)
54. Rees, M.J.: Studies in radio source structure-I. A relativistically expanding model for variable quasi-stellar radio sources. *Mon. Not. R. Astron. Soc.* **135**, 345 (1967)
55. Rees, M.J.: Galaxies and their nuclei. *R. Soc. Lond. Proc. Ser. A* **400**, 183 (1985)
56. Reid, P.B., Davis, W., O'Dell, S., Schwartz, D.A., Tolier-McKinstry, S., Wilke, R.H.T., Zhang, W.: Generation-X mirror technology development plan and the development of adjustable X-ray optics. *SPIE* **7437**, 48 (2009)
57. Reynolds, C.S., Young, A.J., Begelman, M.C., Fabian, A.C.: X-Ray iron line reverberation from black hole accretion disks. *Astrophys. J.* **514**, 164 (1999)
58. Richards, G.T., Croom, S.M., Anderson, S.F., Bland-Hawthorn, J., Boyle, B.J., De Propriis, R., Drinkwater, M.J., Fan, X., Gunn, J.E., et al.: The 2dF-SDSS LRG and QSO (2SLAQ) survey: The $z < 2.1$ quasar luminosity function from 5645 quasars to $g = 21.85$. *Mon. Not. R. Astron. Soc.* **360**, 839–852 (2005)
59. Sitko, M.L., Sitko, A.K., Siemiginowska, A., Szczerba, R.: Multifrequency observations of the optically active radio-quiet quasar GQ Comae. II – Ultraviolet, optical, and infrared continuum variability. *Astrophys. J.* **409**, 139 (1993)
60. Soltan A.: Masses of quasars. *Mon. Not. R. Astron. Soc.* **200**, 115 (1982)
61. Storchi-Bergmann, T., Lopes, R.D., Simões, McGregor, P.J., Riffel, Rogemar A., Beck, T., Martini, P.: Feeding versus feedback in NGC4151 probed with Gemini NIFS – II. Kinematics. *Mon. Not. R. Astron. Soc.* **402**, 819 (2010)
62. Suganuma, M., Yoshii, Y., Kobayashi, Y., Minezaki, T., Enya, K., Tomita, H., Aoki, T., Koshida, S., Peterson, B.A.: Reverberation measurements of the inner radius of the dust torus in nearby seyfert-I galaxies. *Astrophys. J.* **639**, 46 (2006)

63. Sulentic, J.W., Zwitter, T., Marziani, P., Dultzin-Hacyan, D.: Eigenvector 1: An optimal correlation space for active galactic nuclei. *Astrophys. J. Lett.* **536**, L5 (2000)
64. Tanaka, Y, Inoue, H., Holt S.S.: The X-ray astronomy satellite ASCA. *Proc. Astron. Soc. Jpn.* **46**, L37 (1994)
65. Treu, T. Woo, J.-H., Malkan, M.A., Blandford, R.D.: Cosmic evolution of black holes and spheroids. II. Scaling relations at $z = 0.36$. *Astrophys. J.* **667**, 117–130 (2007)
66. Trevese, D., Paris, D., Stirpe, G.M., Vagnetti, F., Zitelli, V.: Line and continuum variability of two intermediate-redshift, high-luminosity quasars. *Astron. Astrophys.* **470**, 491 (2007)
67. Tumlinson, J., Malec, A.L., Carswell, R.F., Murphy, M.T., Buning, R., Milutinovic, N., Ellison, S.L., Prochaska, J.X., Jorgenson, R.A., Ubachs, W., Wolfe, A.M., et al.: Cosmological concordance or chemical coincidence? Deuterated molecular hydrogen abundances at high redshift. *Astrophys. J.* **718**, L156–L160 (2010)
68. Turner, T.J., Miller, L., George, I.M., Reeves, J.N.: Evidence for orbital motion of material close to the central black hole of Mrk 766. *Astron. Astrophys.* **445**, 59 (2006)
69. Nandra, K.P., Barret, D., Fabian, A.C., Jonker, G., et al.: First GRAVITAS science workshop. http://www.mpe.mpg.de/gravitas/workshop_2010 (2010)
70. Wang, R., Carilli, C.L., Neri, R., et al.: Molecular gas in $z \sim 6$ Quasar host galaxies. *Astrophys. J.* **714**, 699–712 (2010)
71. Webb, J.K., Murphy, M.T., Flambaum, V.V., Curran, S.J.: Does the fine structure constant vary? A third quasar absorption sample consistent with varying α . *Astrophys. Space Sci.* **283**, 565–575 (2003)
72. Weisskopf, M.C., Brinkman, B., Canizares, C., Garmire, G., Murray, S., Van Speybroeck, L.P.: An overview of the performance and scientific results from the chandra X-ray observatory. *ASP Conf. Ser.* **114**, 1 (2002)
73. Welsh, W.F., Horne, K.: Echo images of broad-line regions in active galactic nuclei. *Astrophys. J.* **379**, 586 (1991)
74. Welsh, W., Robinson, E.L., Hill, G., Shields, G., Wills, B., Brandt, N., Eracleous, M., Kollatschny, W., Horne, K., Gallo, L.: The HET echo mapping project. *AAS* **32**, 1458 (2000)
75. Willingale R.: X-ray interferometry. In 50 years of space science at leicester. http://www.star.le.ac.uk/conf50/talks/S05P_1115_Dick_Willingale.pdf (2010) (access July 2010)

Chapter 9

Fifty Years of Quasars: Current Impressions and Future Perspectives

Contributions by Jack W. Sulentic, Paola Marziani, and Mauro D’Onofrio

There are more things in heaven and earth, Horatio,
Than are dreamt of in your philosophy.
Hamlet, Act 1, Scene 5

This final chapter summarizes discoveries and accomplishments recounted by the contributors. It is an attempt to answer the question posed at the outset: have we made real progress in understanding the quasars? We will then devote a few pages on speculating how the first of next 50 years may look for quasar research.

9.1 Summary of Achievements

Contributors to the previous chapters describe an impressive body of research carried out over the past 50 years. One can argue that there is now considerable evidence supporting the hypothesis that the quasar phenomenon is driven by accretion onto a supermassive object. Hard X-ray emission may be the most direct signature of that accretion process and perhaps the only universal property shared

J.W. Sulentic (✉)
Instituto de Astrofísica de Andalucía (CSIC), Granada, Spain
e-mail: sulentic@iaa.es

P. Marziani
INAF, Osservatorio Astronomico di Padova, Vicolo Osservatorio 5, IT35122 Padova, Italy
e-mail: paola.marziani@oapd.inaf.it

M. D’Onofrio
Dipartimento di Astronomia, Università degli Studi di Padova, Vicolo Osservatorio 3,
I35122 Padova, Italy
e-mail: mauro.donofrio@unipd.it

by all types of AGN. This possibility brings us closer to an operational definition of the quasar phenomenon and therefore may answer the question posed in the Introduction.

If the overarching question of this chapter is: “Has there been real progress in our understanding of quasars since their discovery?” As far as the wealth of *data* collected in every accessible band of the electromagnetic spectrum is concerned, our response must be strongly affirmative. As far as our *understanding* is concerned we offer a more cautious affirmation with challenges and areas of uncertainty addressed later in the chapter. Progress does not necessarily mean a paradigm shift, and we have seen the black hole + accretion disk paradigm grow in acceptance since the 1970s.

We identify four areas where quasar research has grown perhaps much beyond what were plausible expectations 4–5 decades ago:

- Discovery of a large population of unobscured quasars now extending to $z \approx 7$ coexisting with a probably larger population of obscured quasars.
- Evidence that virtually all [20] quasars are hosted by a galaxy, suggesting that all or most (massive) galaxies pass through a cycle (or cycles) of quasar activity.
- Multiwavelength observations probing ever deeper into the central engine.
- Evidence for the self-similarity of accretion processes.

Perhaps one might put a question mark after each of the four areas Do they encompass the advances of this 50-year period? Have all yielded fundamental breakthroughs in our understanding? Certainly, there would be a wide range of opinions. There are areas where even the basic observational and/or theoretical interpretations are still open. In our opinion these include:

- Origin and composition of relativistic radio jets and by extension, the origin of the radio-loud vs. radio-quiet quasar dichotomy.
- Origin and number of components contributing to the quasar continuum—especially for radio-quiet sources.
- Structure and kinematics of the broad-line-emitting region.
- Feedback processes into the quasar. host galaxy.

Some areas involving more circumstantial evidence have grown in strength and credibility:

- Role of the large-scale environment in triggering nuclear activity.
- Inflow of accreted material toward the active nucleus.
- Nature of the central massive object usually assumed to be a black hole.
- Quest for the equivalent of an “H–R” diagram for quasars.

Most of these issues were already discussed in the late 1960s but are still debated today. The editors, not unlike notary registrars, can only state the reasons why a consolidated vision on these issues has not yet emerged. Notary registrars are however famously shortsighted. So we will soon shed the black robes and discuss achievements and problems along with some foreseeable but hypothetical developments (Sect. 9.5).

9.2 Areas of Major Achievements

9.2.1 *A Large Population of Quasars and Unification*

Developments over the past decades have changed our view of quasars. Until the mid-1980s, quasars involved a few hundreds distant peculiar sources. Even then, there was discussing of orientation unification to explain why many Seyfert-2 galaxies showed no broad lines except (sometimes) in polarized light. Since then, the number of quasars has grown exponentially. In addition to the multitude of type-1 sources, now extending to $z \approx 7.05$, results from *Chandra* and *Spitzer* imply a large population of heavily obscured quasars at high redshift. Quasars can account for most of the previously unresolved diffuse X-ray background.

The unification schemes discussed in Chap. 4 are thought to apply to the vast majority of quasars. Two basic processes lie behind orientation unification: relativistic beaming and obscuration (Chaps. 3 and 4). Superluminal motions are understood in terms of matter moving at relativistic speed—radio synchrotron outflow or ejection. Spectropolarimetric observations of hidden/scattered broad-line emission and soft X-ray absorption support the presence of a thick circumnuclear structure often called the “obscuring torus” [1]. Present-day instrumentation (i.e., the MIDI VLTI interferometer) is on the verge of resolving this obscuring structure in nearby AGNs [15, 52].

However, there is more to the story than simple unification which paints a static picture and ignores the diversity among unobscured quasars. NGC 4151—low luminosity Seyfert nucleus—has been observed to change from type-1 to (almost) type-2 [38]. Some Seyfert-2 sources show no evidence of a BLR even in polarized light. Evolution is not included in the unification scheme. Nuclear activity can coexist with high star-formation rates, and there may be a temporal sequence linking very luminous star-forming systems (the ultraluminous IR galaxies, ULIRGs) to the emergence of a quasar (Chap. 4). The role of environment in triggering nuclear activity is also not considered in unification schemes. We think to have learned how to recognize fledglings quasars as well as quasars that are dying, but unification is not yet able to take such considerations into account.

9.2.2 *A Universe Filled with Quasars*

The overall quasar evolution scenario described by contributors to Chap. 7 is quite simple. A quasar is likely born when accreted gas falls onto a massive object at the center of the host galaxy, possibly following a merger event. Quasars were most luminous at $z \approx 2.0$ – 2.5 when the universe was about one quarter its present age after which a decline set in. Outflows associated with nuclear activity may have eventually deprived quasars of accreting material, leading to death by “starvation.” The merger rate appears to decrease strongly for $z \lesssim 2$, and the

probability of obtaining abundant accretion fuel decreases accordingly. Outflows and decreasing merger rates explain the somewhat counterintuitive result that the most massive galaxies—the ones in the local Universe—do not host luminous quasars. Their black holes are very massive, but their accretion rates are very small (e.g., Messier 87).

If quasar activity is a stage in the life of massive galaxies (lasting perhaps $\sim 10^8$ year), then most galaxies today should harbor an extinguished black hole, as proposed in the late 1960s [18]. The quest for exhausted quasars became serious in the 1980s. Since a luminous active nucleus is absent, it becomes possible to study the distribution of stars and gas near the black hole. In the early 1990s, HST observations resolved gas motions in the nucleus of Messier 87 [19] where a black hole was found with mass similar to those of luminous quasars at $z \approx 2$. A circle was closed.

9.2.3 Probing Deep

Techniques have been developed to probe what is still spatially unresolved and time-delay effects have proven especially fruitful. Continuum variability in the optical and UV have been attributed to reprocessing of high-energy radiation (see review by M.-H. Ulrich and collaborators [54]). Measures of line response to continuum changes—in the UV, optical, and more recently in the IR—have led to a wealth of information. Reverberation mapping is probing gas at less than 10^4 gravitational radii. As pointed out in Chaps. 5 and 8, the potential of two-dimensional reverberation mapping has yet to be fully exploited.

9.2.3.1 What Is the $K\alpha$ Line Telling Us?

Observations of the $K\alpha$ line in the mid-1990s were hailed as near proof of the existence of accretion disks which would be tantamount to proof of the existence of black holes. A broad “relativistic” FeK signature appeared to be a common feature in AGN shortly after ASCA came into operation [12, 49]. More recent X-ray spectroscopy with *Chandra* and *Newton* have not confirmed this relativistic broad $K\alpha$ profile in many sources [13], although it remains prominent in prototypical MCG-06-30-15. The broader redshifted component is observed in 20–40% of the 150 AGN observed with XMM. The broadened feature appears to be most convincing in NLSy1-like sources (high accreting Population A quasars in the four-dimensional eigenvector 1 framework). Radio-loud quasars and other Population B sources (sources with $L/L_{\text{Edd}} \lesssim 0.15$) show a hard X-ray power law with little or no $K\alpha$ emission. If the relativistic Fe $K\alpha$ feature is an accretion disk signature, and if accretion disks are found in all type-1 AGN, then why do we not see it more often? Or at least more often in a highly accreting quasar subclass?

9.2.4 *Self-Similarity of Accretion Processes*

One of the most intriguing relations found in the past decade connects supermassive black holes to stellar-mass black holes in X-ray binary systems (XRBs). The stellar/AGN black hole analogy gained momentum with the discovery that some stellar sources possess highly relativistic jets not unlike their extragalactic counterparts [28]. The analogy XRB/quasar is reinforced by the linear relation (in log scale) between black hole mass, X-ray luminosity, and radio luminosity defining the so-called “fundamental plane of black hole activity” [26]. The correlation between radio and X-ray luminosity is consistent with current ideas about continuum formation in radio-loud quasars.

How far can this analogy be pursued? This question brings us to one of the unsolved problems in quasar research connected with the origin of the radio-power difference between radio-quiet (RQ) and radio-loud (RL) quasars. The 90% of quasars comprising the RQ majority are not radio silent. Nonthermal cores have been detected in several RQ quasars. On the other hand, RQ AGNs appear to follow the same radio-FIR correlation as normal star-forming galaxies where the radio emission should be related to star death. The problem is compounded by the unclear origin of X-ray emission from RQ quasars. We were reminded in Chap. 4 that quasars and XRB involve different accretion states. The analogy appears to hold for the low (or hard in terms of X-ray spectral shape) state in accreting systems—especially at the very low accretion rates typical of LINERs. It is difficult to say whether the analogy can be extended to highly accreting systems that are, incidentally, almost all radio quiet.

We note that this contextualization of LINERs agrees with the conclusion that emerged from Chap. 4: the wide majority of LINERs are AGNs. However, their low luminosity makes it possible that different ionization mechanisms are at work in different sources. A few sources show a LINER-like spectrum outside of the nucleus and likely associated with shocks produced by the collision of molecular clouds.

9.3 The Weak Points or Some Questions That Remain for the Editors and Probably Many Readers as Well

9.3.1 *The Nature of Radio Jets and the RL–RQ Dichotomy*

An important and still debated issue involves whether relativistic plasma is only composed by leptons (i.e., electrons or positrons) or if it also includes baryons which might yield a “heavy” jet. It remains open whether real progress has been made in modeling radio jets—most notably, through magnetohydrodynamic simulations.

The work of Blandford and Znajek [7] suggested that electromagnetic extraction from the spin of a black hole might be a suitable mechanism for powering and

collimating radio jets (Chap. 6). RL quasars might arise only surrounding the most rapidly spinning black holes. A more recent analysis suggests that the jet might instead be powered by rotational energy from the inner accretion disk gas—perhaps removing the need for a rapidly spinning black hole [6].

A question that can be addressed with observations involves what makes RQ and RL sources so different in terms of radio power. Is there a dichotomy? RL quasars have been interpreted as sources at the high end of a continuous distribution of radio power in quasars. In this view, they are not fundamentally different (in structure and kinematics) from RQ quasars. The alternate view interprets RL sources as fundamentally different in host galaxy properties and/or black hole properties such as mass and spin.

The problem is entangled with issues about quasar evolution. RL quasars appear to host the more massive black holes and to accrete at low Eddington ratios. Yet, FR II are the parent population of RL quasars so, if black hole spin rules jet power, then they should have the most rapidly spinning black holes. This is the contrary of what is expected on the basis of elementary considerations. Classical double-lobe FR II morphology indicates a very evolved system whose spin is unlikely to be high. Fledgling quasars are predominantly RQ and accreting closer to the Eddington limit (likely corresponding to the soft state of stellar mass BH). NLSy1s are probably experiencing an early accretion episode (first duty cycle?), so that their black holes may be consistently spun up. But only a few NLSy1s are RL with relativistic jets, as we were reminded in Chap. 3. Contributors to Chap. 4 note that the disk-jet coupling may change when the accretion rate changes, but this would make the existence of RL sources radiating close to the Eddington limit impossible at all.

In summary, we still do not have consistent answers to several basic questions. Radio loudness, as an electromagnetic phenomenon, how does it relate to black hole mass, black hole spin, or accretion disk angular momentum? Does accretion efficiency also play a role?

9.3.2 *The Origin of Continuum Emission in Radio-Quiet Quasars*

The mechanism underlying production of the nonthermal continuum in RL quasars is fairly well understood. Radio photons produced via the synchrotron process are converted into much higher energy photons via inverse Compton scattering. There is still some debate whether the seed photons of X-ray emission are the ones emitted in the radio jet, but the scheme outlined above provides a nice explanation for the spectral energy distribution of the most extreme nonthermal sources, blazars. An explanation of continuum production in RQ sources is more problematic. There is evidence of a thermal component that is especially strong in the optical/UV range, the *big blue bump* suggested to be a signature of a

geometrically thin, optically thick accretion disk [22, 23]. Moreover a soft X-ray excess is frequently observed whose origin is not completely understood, as remarked in Chap. 3. The relevance of nonthermal emission in RQ sources is unclear. The coming upgrades of VLA and MERLIN will allow deeper studies of radio cores in RQ quasars that may provide an improvement in our understanding.

9.3.3 *The Broad-Line-Emitting Region(s)*

Several contributors addressed key points about our understanding of BLR structure. A general consensus has emerged on some basic aspects. Most contributors agree that broad-line emission primarily arises in a photoionized medium ([35], Chap. 6). Non-radiative heating is, however, apparently necessary to explain ultra-strong Fe II emitters that are relatively rare and peculiar sources. There is not yet a consensus on the main emitting components within the broad line region. Models that have gained credibility in the past decades assume an accretion disk and an associated wind or outflow. Double-peaked emitters often cited as evidence for accretion disk emission appear to be rare and very low accretors. Generally speaking, there is a danger and intellectual fallacy in using a few rare sources with unusual properties to establish phenomenological commonalities. At present, this is a danger we cannot overcome in several fields of quasar research, especially in the ones involving accretion disks, black hole spin, binary black holes, and observations of the $K\alpha$ line profile. Double-peaked emitters look more like old starving sources in the fading stage of AGN activity (Chaps. 3 and 5). Models of line-emitting accretion disks with associated wind components have been moderately successful in accounting for more common single-peaked line profiles, although the frequency of Lorentz profiles among low-ionization lines pose a challenge for disk models. An elegant experiment attempted to resolve discrete emitting clouds in two sources [2, 3]. These very high S/N spectra yielded a negative result—profiles are smooth and can be accounted for only by a continuous medium or by a very large number of discrete gas clouds. On the other hand, discrete clouds have been seen passing in front of the active nucleus [21].

The Editors limit themselves to two considerations:

1. Observational evidence supports a role for gravitation (i.e., virial broadening low-ionization broad lines) and radiation pressure (probably driving the outflow in part of the high-ionization line-emitting gas).
2. It is very unlikely that the same structure of the line-emitting regions is present in NLSy1-like sources (Pop. A or Pop. 1, respectively, in [9, 45]) and in sources with broader line profiles. Intriguingly, the FWHM limit separating Pop. A and B ($\text{FWHM } H\beta \approx 4,000 \text{ km s}^{-1}$) corresponds to $L/L_{\text{Edd}} \approx 0.15$ where gravitational and radiative forces might be in balance.

9.3.4 *Feedback and the Joint Evolution of Quasars and Their Host Galaxies*

The radiant energy released by an active nucleus may have a dramatic effect on surrounding regions. There is little doubt about this—as reviewed in Chap. 7 and as well shown by ionization maps [46]—but can the mechanical and radiative output of the active nucleus affect the entire bulge of a host galaxy? This question has arisen in the last 10–15 years. Just a few years ago, a paper dealing with the observational evidence of feedback noted that *this process is poorly understood, and compelling observational evidence for its mere existence is still missing* [41].

There are recent claims that the black hole might drive large-scale molecular outflows of the kind revealed by Herschel. We quote the press release reporting this finding:

[...] these outflows are robbing the galaxy of the raw material it needs to make new stars. If the outflows are powerful enough, they could even halt star formation altogether.¹

Where is the direct evidence? The energetic output of quasars can exceed the binding energy of a massive bulge or of an elliptical galaxy. Winds and relativistic jets leave signatures on large scales, but how determinant are they of the evolution (both chemical and dynamical) of the host galaxy? One can, for example, consider feedback produced by radio jets—which in turns depend on the composition of the jet. Collimated outflows may be easily disrupted by interstellar molecular clouds, and even if an expanding cocoon sweeps through the interstellar medium of the host galaxy or into the intra-cluster medium, its effect on dense molecular clouds and on star formation is not obvious. A myriad of theoretical and observational approaches are currently tackling the feedback phenomenon. They may lead to a consistent scenario fully supported by the observations within this decade.

The $M_{\text{BH}}-M_{\text{bulge}}$ correlation was unknown when the first 25 years of quasar research were reviewed [51]. Part of the importance of the $M_{\text{BH}}-M_{\text{bulge}}$ correlation involves the expectation of coeval evolution for bulges and SMBHs through feedback. There are continuous claims of new circumstantial evidence that this occurs even at the earliest epochs, that is, when galaxies were still forming. Is the $M_{\text{BH}}-M_{\text{bulge}}$ relation a solid starting point? It is still debated whether the correlation might be due to a selection effect. Resolving the sphere of influence of a supermassive black hole is still beyond present-day instrumental capabilities. Perhaps, only the most massive black holes have been measured up till now and a much broader range of black hole masses exists for a given bulge mass. Taken at face value the $M_{\text{BH}}-M_{\text{bulge}}$ correlation represents the final stage of a complex evolutionary process in the local universe [59]. Recent large surveys suggest a significant evolution of the correlation with cosmic time [27].

¹ESA—Space Science News: Raging storms sweep away galactic gas, May 9, 2011.

It is difficult to undervalue the broader significance of feedback studies: they could lead to a “grand scenario” encompassing galaxy formation and evolution, including the role of nuclear activity in these large-scale processes. However, it seems safe to point out that the jury is still out on the issue of black hole and host galaxy coevolution and especially on the $M_{\text{BH}}-M_{\text{bulge}}$ correlation.

9.4 Areas Supported by Partial or Inconclusive Evidence

9.4.1 *The Quasar Environment*

Environmental studies—discussed in Chap. 7—have proved only partly satisfactory. There is plenty of evidence that gravitational interactions between two gas-rich galaxies can lead to a strong enhancement of their global and nuclear star formation. Despite a considerable effort started in the early 1970s, it is unclear whether this conclusion applies to nuclear activity. At low redshift, there is evidence that type-2 AGN are strongly affected, in a similar manner to star-forming galaxies (Chap. 4), while type-1 sources do not seem to be affected at all. At intermediate- to high-redshift quasars follow the large-scale distribution of galaxies. However, as reminded in Chap. 7, quasars appear to cluster more like the star-forming galaxies providing some indirect evidence in favor of a role for gravitational interactions.

9.4.2 *The Smoking Gun of Infall*

There is a long-standing joke in this field that the AGN process is thought to be driven by infall (accretion), but all we ever see is evidence for outflow! Where is the evidence for infall? There are well-understood theoretical scenarios reviewed in Chap. 6 that explain how gas in a galaxy disk might dissipate angular momentum and fall into the galaxy nucleus. The evidence of outflow is abundant on several scales. Outflows are revealed on the scale of the BLR and NLR via high ionization line blueshifts, warm absorbers, BALs (as reviewed in Chap. 3), and even on larger scales by atomic neutral hydrogen and molecular outflows (Chap. 7). Infall has been more elusive to track in part because the most interesting region is the one closest to the nucleus and also because the evidence connecting merger/interaction processes to large-scale flows of matter is still indirect. The hope of detecting actual molecular gas inflow rests on the improved spatial resolution of ALMA that will allow us to study the molecular gas geometry and kinematics with an angular resolution of about 10 mas.

9.4.3 *Is It Really a Black Hole?*

Circumstantial evidence is considered overwhelming that the central massive object in quasars involves a supermassive black hole. The definition of event horizon occurring at $1 r_g$ requires the mass of a black hole to satisfy the condition $M_{\text{BH}}/r_g \gtrsim 6.7 \cdot 10^{27} \text{ g cm}^{-1}$. In luminous Seyfert-1 galaxies, the central mass can be $\sim 10^8 M_\odot$ within a BLR radius on the order of 1 light-month. The resulting $M_{\text{BH}}/r_{\text{BLR}} \sim 10^{24} \text{ g cm}^{-1}$ is far less than the M_{BH}/r requirement for a black hole. Time responses for lines of different width are roughly consistent with a Keplerian trend, that is, with a “point-like” mass concentration relative to the BLR radius. The currently most compelling observations of resolved velocity structures come from H₂O megamasers. Recent work sets lower limits to the density of central object between $10^9 M_\odot \text{ pc}^{-3}$ and $6 \cdot 10^{10} M_\odot \text{ pc}^{-3}$, ruling out in most cases a cluster of stars or stellar remnants as the central object [11, 16].

It is therefore reasonable to talk about “compact massive objects” at the center of AGNs. This would be a proper, observation-bounded definition. Demonstrating that matter is actually falling onto a black hole is equivalent to showing that the massive compact object has an event horizon [34], that is, is not bounded by a hard surface (like neutron stars and white dwarves) or that a photon falling toward the event horizons shows higher and higher redshift. The first condition is tested for stellar mass black holes. Binary systems in which one component exceeds the Chandrasekhar limit are often X-ray underluminous with respect to systems where the compact component is a neutron star. Unfortunately, such tests are not feasible for quasars since there is no supermassive star to compare with supermassive black holes. The second line of investigation is also very difficult to carry out. Even if redshifted X-ray features have been cited as evidence for gravitational infall of matter onto the supermassive black hole [39], the interpretation is much less than conclusive.

9.4.4 *The Quest for an H–R Diagram*

It is difficult to understate the importance of the principal component analysis (PCA) approach introduced into quasar in the early 1990s [8]. We have advanced from relations involving tens of sources to multivariate correlation analysis of large datasets. The discovery of the two main eigenvectors was pivotal to our understanding that the most important factor governing the appearance of quasar spectra is likely the Eddington ratio. However, we cannot as yet connect measured broad-line parameters to physical parameters. Most present-day estimations of M_{BH} , Eddington ratio, metallicity, and the orientation parameter believed to be important for quasars discussed in Chap. 5 are still plagued by poor accuracy.

The quest for relations with a role equivalent to the stellar H–R diagram is clearly a complex one. The obvious remark is that active nuclei do not have spherical

symmetry, are separated into radio loud and radio quiet, and more parameters are therefore involved than for stars. The major inconvenience is however that the search for an H–R diagram of quasars is linked to the structure and dynamics of the broad-line-emitting region.

Empirically, even if the underlying process is the same, it is not justified to combine in an indiscriminate way spectra from large quasar surveys as it is not justified to average together stellar spectra of different spectral type. Inconclusive or erroneous evidence might result from a careless averaging of spectra. Sources are so different that an understanding of this difference lies at the heart of understanding quasar structure and physics.

9.5 The Future: Peering into the First of the Next 50 Years

The discovery of quasars was an example of how technological development can facilitate an important scientific advance. At the time of their discovery, observational research on quasars was difficult for astronomers outside the US and USSR since they lacked the large apertures and instrumentation necessary for spectroscopic observations. The last 50 years have seen a great change with surveys like SDSS, providing a rich database of 100,000+ quasar spectra that is accessible to all. The contributors to Chap. 8 reviewed major instrumental advancements that are planned for the next decades.

Empirical and theoretical studies of stars evolved much more in synchronism as the name “Hertzsprung–Russell diagram” implies. Yet it was not until 30 years after the introduction of the H–R contextualization that the underlying energy production mechanism in stars was understood. An energy generation mechanism for quasars was suggested soon after their discovery, although our ability to connect physical properties like mass and luminosity to spectroscopic measures is still rudimentary. One can argue that we have only primitive ideas about BLR structure and kinematics. This may be due in part to the nonuniform way that quasars research has proceeded. This historical thread can be evaluated by examining the “hits” one finds when using NED to search for papers related to the ~ 100 brightest quasars. One finds a disproportionate number of papers measuring radio and high-energy X-ray (and now γ -ray) flux measurements. RL quasars generally yield more “hits” including many flux measures and two-dimensional maps of ever greater sensitivity and resolution. But RL quasars are only $\approx 10\%$ of the quasar population. Observations of RL quasars are strongly overrepresented in the HST archive. Part of this may be best explained by psychologists—anyone who has seen high-resolution radio images of FR II sources cannot help but be intrigued and attracted to this area of study. Quasars were discovered as radio sources, and we watched them fall into a minority population relatively rapidly, yet we still do not understand the RL–RQ dichotomy.

The most surprising result of a NED search involves emission-line spectroscopy. In many sources with hundreds of “hits,” one finds typically 2–3 papers involving

optical–UV spectroscopy. Many of the spectra date from the pre-CCD discovery epoch. These spectra offer us a direct sight line into structure and kinematics on scales of $\sim 1,000$ Schwarzschild radii (1 light-month in Seyfert nuclei). This is a resolution we will never achieve in direct imaging except for a few nearby AGNs. Yet it has been little exploited (beyond [8]) in the past 20–30 years. In fact, it is well known that only a handful of people work on moderate/high S/N and resolution spectroscopy of quasars. The reasons for this include (1) the idea that all quasar spectra are self similar and/or (2) that interpretation of the spectra in terms of sources structure and evolution, convolved with orientation effects, represents an intractable problem.

It is hoped that this book will help to dispel these notions and encourage a new generation of researchers to enter the field. Databases like SDSS can be both a blessing and a danger in connection with this hope. SDSS provides spectra for 100,000+ quasars, so surely, someone may think that we need no more spectroscopic data and can simply build our models using this enormous resource. This might even be possible if all quasar spectra are the same. Unfortunately, they are not the same. Only the brightest few hundreds of SDSS spectra show a continuum S/N > 20 –30. Noisier spectra do not enable the kinds of line studies necessary to advance our understanding of BLR structure. The most clear evidence that not all quasar spectra are self similar involves the Population A–B separation mentioned earlier. Essentially, all broad lines (and some narrow, as well as continuum properties) are different for Pop. A and B quasars. Exploration of these differences likely hold important clues, if not the key, to understanding the internal structure and kinematics of quasars.

Technology now makes it much easier to obtain more and better spectra that will enable focused studies in the future. The VLT/ISAAC spectrum of a high-redshift quasar ($z \approx 3.7$; Fig. 9.1) shows that is now possible to achieve IR coverage of the $H\beta$ spectral range with S/N $\gtrsim 20$ –30 and resolution (1 – 10 \AA) comparable to the best optical spectra. It will become easier to obtain spectra of this kind in the coming years and thus easier to obtain accurate black hole masses for high- z quasars. IR spectra of this quality were unthinkable just 15 years ago, and at present, they are available for only ~ 100 sources. These spectra allow one to extend eigenvector 1-type analyses that have been so fruitful for the interpretation of low-redshift quasars (as emphasized in Chaps. 3 and 5) to $z \approx 4$.

9.5.1 Do We Really Need to Find More Quasars?

Generally speaking, there is a danger and intellectual fallacy in using a few rare sources with unusual properties to establish phenomenological commonalities. At present, this is a danger we cannot overcome in several fields of quasar research, especially in the ones involving accretion disks, black hole spin, binary black holes, and observations of the $K\alpha$ line profile.

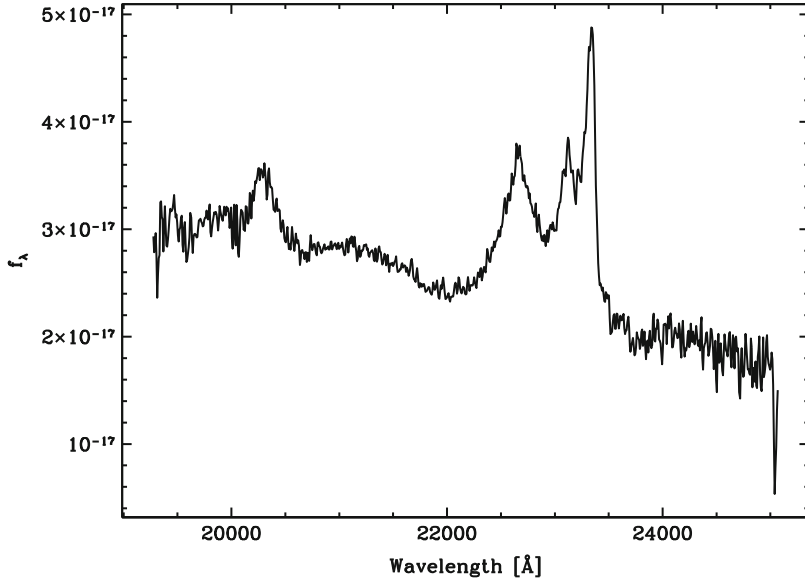


Fig. 9.1 VLT/ISAAC spectrum of the high- z quasar H0055–2659. Abscissa is observed wavelength, and ordinate is observed specific flux in units $\text{erg s}^{-1} \text{cm}^{-2} \text{\AA}^{-1}$. Note that the H β spectral range is shifted into the IR K -band because of the large redshift

One might think that more than 160,000 quasars already represent a formidable sample and that no new surveys are needed. The need for new deeper surveys is made obvious by examining the limits of the SDSS quasar sample that represents a large fraction of presently known quasars. The upper panel of Fig. 9.2 shows the redshift–magnitude diagram for a subset of SDSS quasars [43]. The three lines show the expected apparent magnitude as a function of redshift for three fixed values of absolute i -band magnitude: $M_{i'} = -23.3$ refers to the conventional luminosity limit separating quasars from luminous Seyfert-1 nuclei, $M_{i'} = -25.8$ corresponds to luminous quasars, and $M_{i'} = -29.0$ to the absolute magnitude of the most luminous known quasars. The somewhat irregular shape of the curves reflects a K -correction that includes the effect of emission lines. It is clear that we miss an increasing fraction of quasars with increasing redshift. At redshift $\gtrsim 1$, it is almost impossible to detect sources with luminosity typical of local luminous Seyfert-1 nuclei; at redshift $\gtrsim 3$, only the most luminous quasars are detected. The lower panel of Fig. 9.2 shows the $M_{i'}$ vs. z plane. The line at $m_{i'} \approx 20.2$ roughly corresponds to the completeness limit of the SDSS survey. A magnitude limit of $m_{i'} \approx 19.1$ (roughly corresponding to Johnson B magnitude $m_B \approx 18.3$) would miss the majority of the quasars discovered by the SDSS. These data allow us to define a volume-limited sample as indicated by the shaded box in Fig. 9.2. At $z \approx 1$, it is already impossible to sample the optical luminosity function below $M_{i'} \approx -24$.

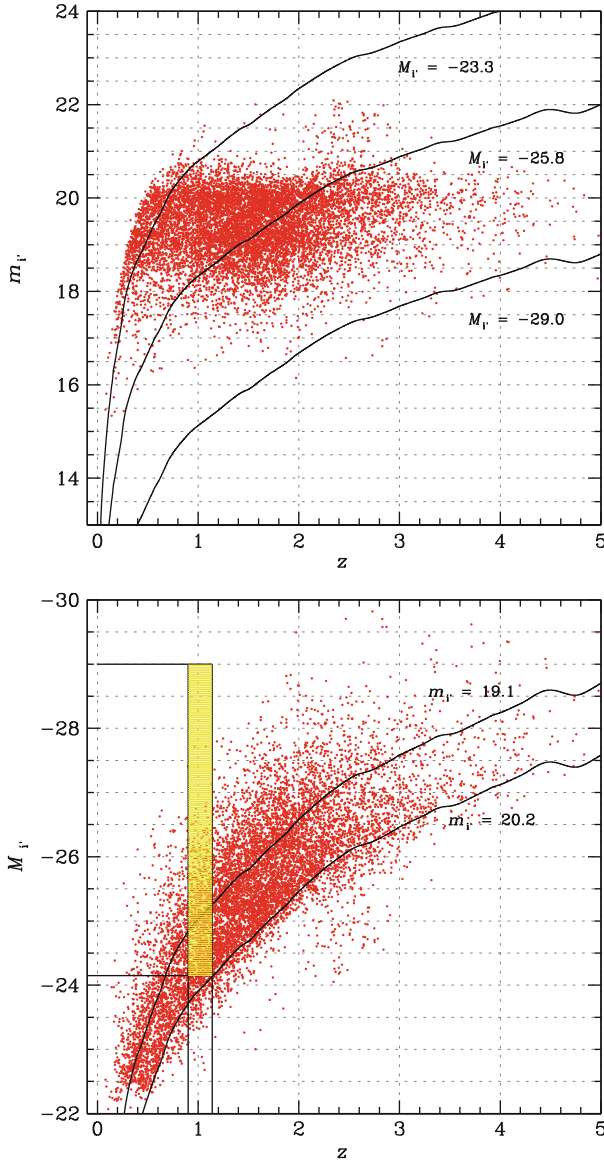


Fig. 9.2 *Upper panel:* apparent i' magnitude of quasars vs. redshift in the SDSS-based catalogues of Schneider et al. [43]. Datapoints (red dots) refer to a random restriction to 10,000 quasars (1/10 of the catalog size) for clarity. The curves refer to three values of absolute i' magnitude: $M_{i'} = -23.3$, the conventional luminosity limit separating quasars from luminous Seyfert-1 nuclei; $M_{i'} = -25.8$, representative of luminous quasars; and $M_{i'} = -29.0$, indicative of the most luminous quasars known in the universe. *Lower panel:* absolute i' magnitude of quasars vs. redshift for the same sample of the previous figure. The curves are computed for two limiting magnitudes $m_{i'} = 19.1$ and $m_{i'} = 20.2$. The K -correction has been computed following the prescription of [40]. The shaded box identifies an example of volume-limited between $0.9 \leq z \leq 1.1$. The limits in luminosity sampling of quasars increase strongly with redshift. Only the high end of the quasar luminosity function can be sampled at high- z , even with relatively deep surveys

The increase in minimum detectable luminosity with z is of great importance for studies of quasar evolution. At redshift $z \approx 1$ and beyond, we do not know whether a low-luminosity quasar population exists that is equivalent to what we observe locally. Relatively massive low-accreting black holes are not observable, and they are obviously important for analyzing any systematic evolution in Eddington ratio with redshift. In addition, the revelation of distant, faint quasars is a necessary condition in the study of the black hole/host galaxy relation outside of the local universe and of any bulge/black hole coevolution. Of course, these studies are feasible only with telescopes of large collecting area. It is possible that we have enough quasars to provide a detailed understanding of broad-line physics/kinematics/geometry, but we lack many of the quasars needed to make them effective cosmological probes.

9.5.2 *Toward a Deeper Physical Understanding*

Spectroscopic investigations will remain the key for our attempts to understand quasar structure and physics. The “old school” approach based on optical and UV data will remain the backbone for interpretation of unobscured quasars. The trend is toward an increasing spectral multiplexing capability (for example, sampling the entire “visual” range from 3000 to 10000 Å). Simultaneity of observations in different bands is a requirement that has been met only at the expense of large organizational efforts, but that is needed to draw reliable inferences especially at low- z where timescales can be as short as a few days in the optical and UV domains. We know already that BLR differences (as well as the population A–B distinction) likely reflect differences in Eddington ratio, with a role for black hole mass, metallicity, and evolutionary state. Thus, we are on the threshold of linking quasar empiricism and quasar physics as was accomplished for stars in the early twentieth century. The larger obscured population demands new approaches based on radio, IR, and X-ray spectroscopy.

A discussion of quasars in more physical terms may also be driven by expected improvements in resolving power and collecting area. Radio observations will benefit from a tenfold increase in sensitivity expected for existing arrays in the next few years (i.e., the eVLA); this improvement parallels the introduction of CCDs in optical astronomy. Much higher sensitivity will be achieved with SKA in the 2020s. Resolving power will reach $10 \mu\text{arcsec}$, thanks to radio space interferometric missions scheduled to become operational in the next few years (*RadioAstron*, VSOP-2). Even if radio VLBI satellites planned for launch in the near future will not resolve the shadow of the black hole (at radio frequencies plasma effects may defocus the image even if the resolution of VSOP-2 [$20 \mu\text{arcsec}$] is in principle sufficient to partly resolve the region [14, 47]), they will nevertheless provide maps of radio jets with unprecedented resolution which may permit tests and refinement of the Blandford–Znajek model. Perhaps, detection of the black hole event horizon will come later. Hopes are based on the development of space-based X-ray interferometry missions like MAXIM or *Constellation-X* (presently under

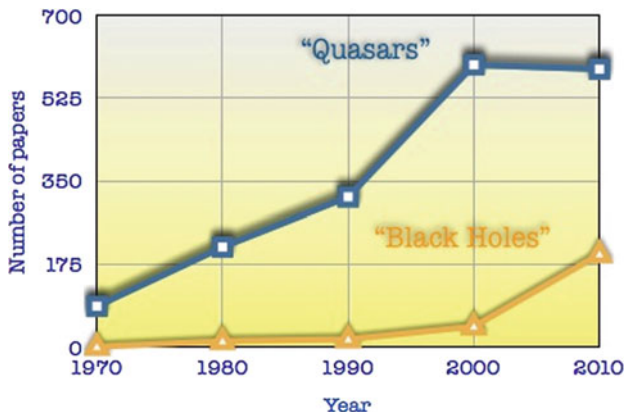


Fig. 9.3 Number of papers (as of June 2011) containing the word black hole (*orange*) or quasars (*blue*) as a function of time

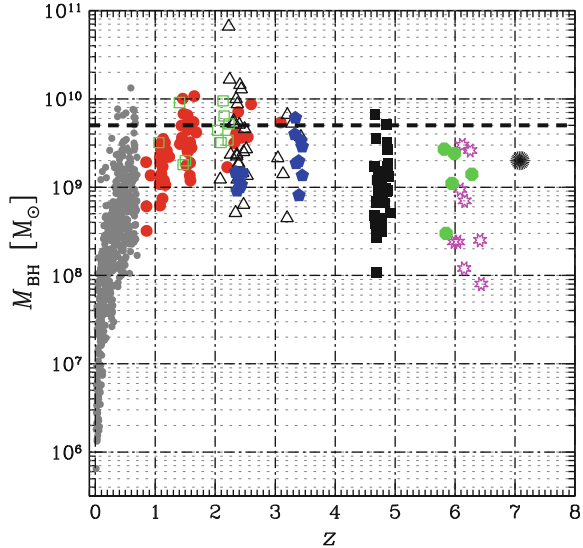
study). Gravitational waves from spaceborne interferometers (LISA) might allow us to detect merging of supermassive black holes at the earliest cosmic epochs, perhaps solving one of the hottest problems involving the growth of massive black holes from primordial seeds. By the time we reach $z \approx 7$, however, we speak of rest-frame spectra fully shifted beyond $1 \mu\text{m}$, in the IR. How lucky we are to find unobscured quasars even at $z \approx 7$ (probably, other discoveries will follow the recent one): it means we can see directly into the central regions over most of the age of the universe. The observations suggest that the fraction of obscured quasars likely increases with redshift; they will be identified with diagnostics involving IR lines and molecular emission features.

As a consequence of deeper physical understanding and broadening observational perspectives the very word quasar may pass into history. A simple ADS count of the numbers of papers containing “quasar,” “QSO,” or “quasi stellar” object in their titles indicate that the number of papers as a function of time is probably reaching a saturation level. On the converse, the word “black hole” (in the quasar context, that is, whenever the three terms listed above and “AGN” were found in the abstract) in titles of papers has grown from 0 in 1970 to almost 200 in 2010 (Fig. 9.3). After all, the acronym quasar refers to an historically delimited period when quasars indeed appeared stellar. Like “compact,” the term quasar depends on instrumental resolving power. It is curious that black hole has become of so frequent usage, while the nature of the central massive object is not yet fully proved.

9.5.3 The New Redshift Frontier

In the course of the last 50 years, no quasar with a systemic blueshift has been ever identified. Quasar light has been found to be gravitationally lensed by intervening galaxies; several cases are known of lensed high- z quasars where the lensing galaxy

Fig. 9.4 M_{BH} vs. z for a low- z sample (grey dots [60]) and several intermediate- to high- z samples. Red circles: [25]; open triangles: [44]; open squares: [10]; filled pentagons: [36]; filled squares: [50]; open starred octagons: [58]; filled octagons: [17]; large spot at $z \approx 7$: the high- z quasar whose discovery was announced in late June 2011 [31]. The dashed line marks $M_{\text{BH}} = 5 \cdot 10^9 M_{\odot}$. After [24]



is at $z \sim 1$ (e.g., [37]). Host galaxies of quasars are revealed up to $z \approx 2$ in the NIR, according to reports in Chap. 7. Intervening $\text{Ly}\alpha$ absorptions are interpreted as due to neutral gas in discrete clouds at various distance between the quasar and the Earth. Supported by these lines of evidence, the wide majority of astronomers agree that the quasar redshift is cosmological and use it routinely as a distance estimator.

At present, only a few tens of quasars are found above $z \approx 6$ with the current record holder at $z = 7.08$ [31]. This recent discovery presumably opens the new era of IR discovery of high- z quasars. Twenty-five years ago, when the record-holding quasar was at $z \approx 3.5$ [51], it was believed that very few quasars could exist beyond $z \approx 4$. Since then surveys discovered a significant population of more distant quasars even if there is now compelling evidence that the (type-1) quasar population is rapidly declining from a maximum around $z \approx 2$ – 2.5 . We call the evidence compelling because it comes from radio, optical, and X-ray surveys independently—as noted in Chap. 8. Redshift higher than 6.5 remain an uncharted territory. Conventional expectations mirror the ones of 25 years ago: very few quasars will likely be found. A temporary standoff is due to the lack of wide-field IR surveys. $\text{Ly}\alpha$ and all of the UV emission-line spectra typical of quasars are shifted into the IR and quasars at $z \gtrsim 6$ – 7 , cannot be discovered with the filters employed by SDSS. What will we see beyond $z \approx 6.5$? Certainly ground and space IR surveys will increase the number of quasars known near the present limit. These surveys will be much more critical for cosmology than 25 years ago.

An example of state-of-the-art investigation close to the redshift frontier involves a diagram showing black hole mass computations as a function of redshift (Fig. 9.4, cf. [50]). Here, the M_{BH} determination is based upon either $\text{H}\beta$ ($z \lesssim 3.8$) or Mg II ($z \gtrsim 3.8$). At redshift $z \gtrsim 0.9$, the $\text{H}\beta$ observations come from IR spectra that

roughly match the resolution and S/N of spectra obtained with optical spectrometers (a large, low- z flux-limited SDSS sample [60] is also shown in Fig. 9.4). As noted in Chap. 5 of this book, $H\beta$ and $Mg\ II$ widths are likely good estimators of the virial broadening and are therefore a preferred choice in M_{BH} computations. Most sources in the range $1 \lesssim z \lesssim 2.5$ were selected from the brightest quasars in the ESO Hamburg survey and are the most luminous quasars known in that redshift range. Observations at very high redshift refer to much more distant quasars, and sources with $M_{BH} \lesssim 10^8 M_{\odot}$ are simply not detected. We must restrict our attention to the high-end of the mass distribution when we discuss Fig. 9.4. The interesting aspect is that, at $z \gtrsim 3$, the mass of the most massive black holes appears to consistently decrease, suggesting a “turnover” in the high-mass end of the quasar mass distribution. More data are needed to confirm this trend—and to fully appreciate its meaning for quasar evolution and for cosmology—but Fig. 9.4 already indicates that the bulk of growth in (at least some) quasars can occur at very early cosmic ages.

9.5.4 Moore’s Law in Quasar Astronomy

Next-generation telescopes will lead to an increase in the number of known quasars by a factor 10^3 . The planned missions eROSITA and WFXT—a Wide-Field X-ray instrument—are expected to detect $>10^7$ X-ray AGNs over more than $10,000 \text{ deg}^2$ of sky. We can estimate a lower limit to the number of detectable quasars from an estimate of the number of galaxies in the visible universe. We simply count the galaxies detected in the HDF, in the same way, done by undergraduate students in their Astronomy Lab classes. The resulting number is $\sim 10^{11}$ and is obviously a lower limit since the HDF misses all sources whose light is shifted into the IR. If we assume that 1 out of 100 galaxies shines with an active nucleus, we conclude that $\sim 10^9$ AGNs might be detectable (cf. Sect. 8.4). Even after the surveys planned for this decade, we will still be at least two orders of magnitude below this limit.

The number of known quasars has grown exponentially up till now—an exponential law nicely fits the total numbers of quasars in the 13 editions of the Véron-Cetty and Véron catalogues shown in Chap. 8 of this book [55]. The exponential growth in quasar numbers brings to mind Moore’s law of exponential growth in computer performance (more rigorously, in surface density of transistors in microprocessors [30]). Clearly, progress in astronomy means more than an improvement in computing power—it means also enhancing multiplexing ability (and curiously growth in the number of pixels in CCDs also appears to follow Moore’s law [33]) as do increasing spatial resolution, light-gathering power, and detector dynamic range. A related issue is the availability (or better the easy *mining*) of astronomical data even those of observations from times that will become more and more a distant past. At present, connecting data from different wavebands (say a radio map, a radio spectrum, and an optical spectrum of a low- z RL quasar) still requires a painstaking effort. As pointed out in Chap. 8, several ongoing projects

will ease these tasks. It is not unconceivable that, in a not too distant future, all astronomical observations might be available in a global, multifrequency, virtual observatory. It is simply reassuring to learn that any instrumental improvement and any further growth in the number of known quasars will be supported by an increase in computing power since the Moore's law of computers is predicted to remain valid for at least this decade.

9.5.5 Quasars, the Foundations of Cosmology and Fundamental Physics

Two frontier fields among the ones summarized in this chapter may be conducive to new physics: imaging within a few gravitational radii of the central mass and the revelation of quasars at redshifts much beyond the current limit. The Ly α forest has already been used to trace baryonic acoustic oscillations, that is, large-scale, overdense regions associated with primordial density fluctuations [4, 42]. Intergalactic absorption lines were used to place an upper limit on the change in the fine-structure constant with cosmic time [32, 53, 57]. Positions of unresolved cores of RL quasars are being used to build more and more precise astrometric reference frames [29]. Observations of high-redshift quasars have been used to constrain the image blurring arising from quantum gravity effects [48]. As the accuracy improves some effects related to cosmology may emerge. High expectations focus on obtaining redshift independent estimates of quasar luminosities, for example, monitoring quasars to derive the reverberation time delay τ that, if assumed $\propto \sqrt{L}$, will yield a distance measurement just computing the ratio τ/\sqrt{F} , where F is the observed flux [56]. This challenge is closely related to many major aspects of quasars research and will require a better understanding of the structure in the line-emitting region. As pointed out in Chap. 8 and by one of the editors elsewhere [5], quasar properties depend strongly on Eddington ratio, and once M_{BH} is known with good accuracy, the luminosity can be estimated, but we stop here our speculations. We express our confidence that improvements in our understanding of quasars will drive a better understanding of the universe as a whole.

References

1. Antonucci, R.R.J., Miller, J.S.: Spectropolarimetry and the nature of NGC 1068. *Astrophys. J.* **297**, 621–632 (1985)
2. Arav, N., Barlow, T.A., Laor, A., Blandford, R.D.: Keck high-resolution spectroscopy of MRK 335: Constraints on the number of emitting clouds in the broad-line region. *Mon. Not. R. Astron. Soc.* **288**, 1015–1021 (1997)
3. Arav, N., Barlow, T.A., Laor, A., Sargent, W.L.W., Blandford, R.D.: Are AGN broad emission lines formed by discrete clouds? Analysis of keck high-resolution spectroscopy of NGC 4151. *Mon. Not. R. Astron. Soc.* **297**, 990–998 (1998)

4. Balbi, A., Bennett, C.L., Bucher, M., Burigana, C., Coles, P., D'Onofrio, M., Durrer, R., Mather, J., Naselsky, P., Perrotta, F., Popa, L.A., Spergel, D., Subramanian, K., Vittorio, N.: Astrophysical cosmology. In: D' Onofrio, M., Burigana, C. (eds.) Questions of Modern Cosmology, pp. 203–300. Springer, Berlin (2009)
5. Bartelmann, M., Bennett, C.L., Burigana, C., Chiosi, C., D'Onofrio, M., Dressler, A., Gioia, I., Hasinger, G., Macias-Perez, J.F., Madau, P., Marziani, P., Mather, J., Matteucci, F., Olive, K., Peacock, J., Reich, W., Robitaille, P.-M., Rowan-Robinson, M., Steigman, G., Steinmetz, M., Sulentic, J.W., Turatto, M., White, S.D.M.: Fundamental cosmological observations and data interpretation. In: D' Onofrio, M., Burigana, C. (eds.) Questions of Modern Cosmology, pp. 7–202. Springer, Berlin (2009)
6. Blandford, R.D., Payne, D.G.: Hydromagnetic flows from accretion discs and the production of radio jets. *Mon. Not. R. Astron. Soc.* **199**, 883–903 (1982)
7. Blandford, R.D., Znajek, R.L.: Electromagnetic extraction of energy from kerr black holes. *Mon. Not. R. Astron. Soc.* **179**, 433–456 (1977)
8. Boroson, T.A., Green, R.F.: The emission-line properties of low-redshift quasi-stellar objects. *Astrophys. J. Suppl. Ser.* **80**, 109–135 (1992)
9. Collin, S., Kawaguchi, T., Peterson, B.M., Vestergaard, M.: Systematic effects in measurement of black hole masses by emission-line reverberation of active galactic nuclei: Eddington ratio and inclination. *Astron. Astrophys.* **456**, 75 (2006)
10. Dietrich, M., Mathur, S., Grupe, D., Komossa, S.: Black hole masses of intermediate-redshift quasars: Near-infrared spectroscopy. *Astrophys. J.* **696**, 1998–2013 (2009)
11. Greene, J.E., Peng, C.Y., Kim, M., Kuo, C.-Y., Braatz, J.A., Violette Impellizzeri, C.M., Condon, J.J., Lo, K.Y., Henkel, C., Reid, M.J.: Precise black hole masses from megamaser disks: Black hole-bulge relations at low mass. *Astroph. J.* **721**, 26–45 (2010)
12. Halpern, J.P.: Seeing and believing. *Nature* **375**, 633 (1995)
13. Jiménez-Bailón, E., Piconcelli, E., Guainazzi, M., Schartel, N., Rodríguez-Pascual, P.M., Santos-Lleó, M.: The XMM-Newton view of PG quasars. II. Properties of the Fe $K\alpha$ line. *Astron. Astrophys.* **435**, 449–457 (2005)
14. Kamenno, S., Tsuboi, M., Murata, Y., Doi, A., Asaki, Y., Mochizuki, N., Hagiwara, Y.-A., Kino, M., Nagai, H., Asada, K., Inoue, M., Sudou, H., Sawada-Satoh, S.: VSOP-2: A space VLBI mission to image central engines and jet launching regions. *COSPAR* **38**, 2272 (2010)
15. Kishimoto, M., Hönig, S.F., Antonucci, R., Barvainis, R., Kotani, T., Tristram, K.R.W., Weigelt, G., Levin, K.: The innermost dusty structure in active galactic nuclei as probed by the Keck interferometer. *Astron. Astrophys.* **527**, A121 (2011)
16. Kuo, C.Y., Braatz, J.A., Condon, J.J., Impellizzeri, C.M.V., Lo, K.Y., Zaw, I., Schenker, M., Henkel, C., Reid, M.J., Greene, J.E.: The megamaser cosmology project. III. Accurate masses of seven supermassive black holes in active galaxies with circumnuclear megamaser disks. *Astroph. J.* **727**, 20 (2011)
17. Kurk, J.D., Walter, F., Fan, X., Jiang, L., Riechers, D.A., Rix, H.-W., Pentericci, L., Strauss, M.A., Carilli, C., Wagner, S.: Black hole masses and enrichment of $z \sim 6$ SDSS quasars. *Astrophys. J.* **669**, 32–44 (2007)
18. Lynden-Bell, D.: Galactic nuclei as collapsed old quasars. *Nature* **223**, 690–694 (1969)
19. Macchetto, F., Marconi, A., Axon, D.J., Capetti, A., Sparks, W., Crane, P.: The supermassive black hole of M87 and the kinematics of its associated gaseous disk. *Astrophys. J.* **489**, 579 (1997)
20. Magain, P., Letawe, G., Courbin, F., Jablonka, P., Jahnke, K., Meylan, G., Wisotzki, L.: Discovery of a bright quasar without a massive host galaxy. *Nature* **437**, 381–384 (2005)
21. Maiolino, R., Risaliti, G., Salvati, M., Pietrini, P., Torricelli-Ciamponi, G., Elvis, M., Fabbiano, G., Braitto, V., Reeves, J.: “Comets” orbiting a black hole. *Astron. Astrophys.* **517**, A47 (2010)
22. Malkan, M.A.: The ultraviolet excess of luminous quasars. II – Evidence for massive accretion disks. *ApJ* **268**, 582–590 (1983)

23. Malkan, M.A., Sargent, W.L.W.: The ultraviolet excess of seyfert-1 galaxies and quasars. *ApJ* **254**, 22–37 (1982)
24. Marziani, P., Sulentic, J.W.: Estimating black hole masses in quasars using broad optical and UV emission lines. *New Astron. Rev.* **56**, 49–63 (2012)
25. Marziani, P., Sulentic, J.W., Stirpe, G.M., Zamfir, S., Calvani, M.: VLT/ISAAC spectra of the H β region in intermediate-redshift quasars. III. H β broad-line profile analysis and inferences about BLR structure. *Astron. Astrophys.* **495**, 83–112 (2009)
26. Merloni, A., Heinz, S., di Matteo, T.: A fundamental plane of black hole activity. *Mon. Not. R. Astron. Soc.* **345**, 1057–1076 (2003)
27. Merloni, A., Bongiorno, A., Bolzonella, M., Brusa, M., Civano, F., Comastri, A., Elvis, M., Fiore, F., Gilli, R., Hao, H., Jahnke, K., Koekemoer, A.M., Lusso, E., Mainieri, V., Mignoli, M., Miyaji, T., Renzini, A., Salvato, M., et al.: On the cosmic evolution of the scaling relations between black holes and their host galaxies: Broad-line active galactic nuclei in the zCOSMOS survey. *Astrophys. J.* **708**, 137–157 (2010)
28. Mirabel, I.F., Rodríguez, L.F.: A superluminal source in the galaxy. *Nature* **371**, 46–48 (1994)
29. Moór, A., Frey, S., Lambert, S.B., Titov, O.A., Bakos, J.: On the connection of the apparent proper motion and the VLBI structure of compact radio sources. *AJ* **141**, 178 (2011)
30. Moore, G.E.: Cramming more components onto integrated circuits. *Electron. Mag.* **38**, 19 (1965)
31. Mortlock, D.J., Warren, S.J., Venemans, B.P., Patel, M., Hewett, P.C., McMahon, R.G., Simpson, C., Theuns, T., Gonzales-Solares, E.A., Adamson, A., Dye, S., Hambly, N.C., Hirst, P., Irwin, M.J., Kuiper, E., Lawrence, A., Rottgering, H.J.A.: A luminous quasar at a redshift of $z = 7.085$. *Nature* **474**, 616–619
32. Murphy, M.T., Webb, J.K., Flambaum, V.V., Dzuba, V.A., Churchill, C.W., Prochaska, J.X., Barrow, J.D., Wolfe, A.M.: Possible evidence for a variable fine-structure constant from QSO absorption lines: Motivations, analysis and results. *Mon. Not. R. Astron. Soc.* **327**, 1208–1222 (2001)
33. Myhrvold, N.: Moore’s Law Corollary: Pixel Power. *New York Times*, 7 June (2006)
34. Narayan, R.: George darwin lecture: Evidence for the black hole event horizon. *Astron. Geophys.* **44**, 060000–6 (2003)
35. Netzer, H.: AGN emission lines. 20. Saas-fee advanced course of the Swiss Society for Astrophysics and Astronomy: Active galactic nuclei, pp. 57–160. Springer, Berlin (1990)
36. Netzer, H., Lira, P., Trakhtenbrot, B., Shemmer, O., Cury, I.: Black hole mass and growth rate at high redshift. *Astrophys. J.* **671**, 1256–1263 (2007)
37. Ofek, E.O., Rix, H.-W., Maoz, D.: The redshift distribution of gravitational lenses revisited: Constraints on galaxy mass evolution. *Mon. Not. R. Astron. Soc.* **343**, 639–652 (2003)
38. Penston, M.V., Perez, E.: An evolutionary link between Seyfert I and II galaxies? *Mon. Not. R. Astron. Soc.* **211**, 33P–39P (1984)
39. Reeves, J.N., Pounds, K., Uttley, P., Kraemer, S., Mushotzky, R., Yaqoob, T., George, I.M., Turner, T.J.: Evidence for gravitational infall of matter onto the supermassive black hole in the quasar PG 1211+143? *Astrophys. J.* **633**, L81–L84 (2005)
40. Richards, G.T., Strauss, M.A., Fan, X., Hall, P.B., Jester, S., Schneider, D.P., Vanden Berk, D.E., Stoughton, C., et al.: The sloan digital sky survey quasar survey: Quasar luminosity function from data release 3. *Astron. J.* **131**, 2766 (2006)
41. Schawinski, K., Thomas, D., Sarzi, M., Maraston, C., Kaviraj, S., Joo, S.-J., Yi, S.K., Silk, J.: Observational evidence for AGN feedback in early-type galaxies. *Mon. Not. R. Astron. Soc.* **382**, 1415–1431 (2007)
42. Schlegel, D., Abdalla, F., Abraham, T., Ahn, C., Allende Prieto, C., Annis, J., Aubourg, E., Azzaro, M., Baltay, S.B.C., Baugh, C., Bebek, C., Becerril, S., Blanton, M., Bolton, A., Bromley, B., et al.: The BigBOSS experiment. *arXiv:1106.1706* (2011)
43. Schneider, D.P., Richards, G.T., Hall, P.B., Strauss, M.A., Anderson, S.F., Boroson, T.A., Ross, N.P., Shen, Y., Brandt, W.N., Fan, X., Inada, N., Jester, S., Knapp, G.R., Krawczyk, C., et al.: The sloan digital sky survey quasar catalog. V. Seventh data release. *Astron. J.* **139**, 2360–2373 (2010)

44. Shemmer, O., Netzer, H., Maiolino, R., Oliva, E., Croom, S., Corbett, E., di Fabrizio, L.: Near-infrared spectroscopy of high-redshift active galactic nuclei. I. A metallicity-accretion rate relationship. *Astrophys. J.* **614**, 547–557 (2004)
45. Sulentic, J.W., Marziani, P., Dultzin-Hacyan, D.: Phenomenology of broad emission lines in active galactic nuclei. *Ann. Rev. Astron. Astrophys.* **38**, 521–571 (2000)
46. Tadhunter, C., Tsvetanov, Z.: Anisotropic ionizing radiation in NGC5252. *Nature* **341**, 422–424 (1989)
47. Takahashi, R.: Shapes and positions of black hole shadows in accretion disks and spin parameters of black holes. *Astrophys. J.* **611**, 996–1004 (2004)
48. Tamburini, F., Cuofano, C., Della Valle, M., Gilmozzi, R.: No quantum gravity signature from the farthest quasars. *Astron. Astrophys.* **533**, A71 (2011)
49. Tanaka, Y., Nandra, K., Fabian, A.C., Inoue, H., Otani, C., Dotani, T., Hayashida, K., Iwasawa, K., Kii, T., Kunieda, H., Makino, F., Matsuoka, M.: Gravitationally redshifted emission implying an accretion disk and massive black-hole in the active galaxy MCG:-6-30-15. *Nature* **375**, 659–661 (1995)
50. Trakhtenbrot, B., Netzer, H., Lira, P., Shemmer, O.: Black hole mass and growth rate at $z = 4.8$: A short episode of fast growth followed by short duty cycle activity. *Astroph. J.* **730**, 7 (2011)
51. Trimble, V., Woltjer, L.: Quasars at 25. *Science* **234**, 155–161 (1986)
52. Tristram, K.R.W., Raban, D., Meisenheimer, K., Jaffe, W., Röttgering, H., Burtscher, L., Cotton, W.D., Graser, U., Henning, T., Leinert, C., Lopez, B., Morel, S., Perrin, G., Wittkowski, M.: Parsec-scale dust distributions in seyfert galaxies. Results of the MIDI AGN snapshot survey. *Astron. Astrophys.* **502**, 67–84 (2009)
53. Tzanavaris, P., Webb, J.K., Murphy, M.T., Flambaum, V.V., Curran, S.J.: Limits on variations in fundamental constants from 21-cm and ultraviolet quasar absorption lines. *Phys. Rev. Lett.* **95**, 041301 (2005)
54. Ulrich, M.-H., Maraschi, L., Urry, C.M.: Variability of active galactic nuclei. *Ann. Rev. Astron. Astrophys.* **35**, 445–502 (1997)
55. Véron-Cetty, M.-P., Véron, P.: A catalogue of quasars and active nuclei: 13th edition. *Astron. Astrophys.* **518**, A10 (2010)
56. Watson, D., Denney, K.D., Vestergaard, M., Davis, T. M.: A new cosmological distance measure using AGN. **740**, L49 (2012)
57. Webb, J.K., Murphy, M.T., Flambaum, V.V., Dzuba, V.A., Barrow, J.D., Churchill, C.W., Prochaska, J.X., Wolfe, A.M.: Further evidence for cosmological evolution of the fine structure constant. *Phys. Rev. Lett.* **87**, 091301 (2001)
58. Willott, C.J., Delorme, P., Reylé, C., Albert, L., Bergeron, J., Crampton, D., Delfosse, X., Forveille, T., Hutchings, J.B., McLure, R.J., Omont, A., Schade, D.: The canada-france high- z quasar survey: Nine new quasars and the luminosity function at redshift 6. *Astron. J.* **139**, 906–918 (2010)
59. Woo, J.-H., Treu, T., Malkan, M.A., Blandford, R.D.: Cosmic evolution of black holes and spheroids. III. The $M_{\text{BH}}-M_{\text{bulge}}$ relation in the last six billion years. *Astrophys. J.* **681**, 925–930 (2008)
60. Zamfir, S., Sulentic, J.W., Marziani, P., Dultzin, D.: Detailed characterization of $H\beta$ emission line profile in low- z SDSS quasars. *Mon. Not. R. Astron. Soc.* **403**, 1759 (2010)

Index

- Abramowicz, Marek, 122
- Absolute magnitude, 102, 107, 561
- Absorption lines, 223, 224
 - intergalactic, 567
 - molecular, 540
 - stellar, 25
- Accretion disk, 154, 251, 350, 354, 385, 386, 552, 554, 560
 - Fe K α emission, 168, 536, 552
 - ablation, 257
 - atmosphere, 128, 361
 - column density, 367
 - continuum emission, 360
 - geometrically thick, 122
 - geometrically thin, 227
 - geometrically thin, optically thick, 54, 161, 296, 354, 555
 - geometrically thin, optically thin, 135
 - instability, 117
 - line emission, 255, 256, 360
 - models, 59, 338, 353, 367, 404
 - off-axis illumination, 99
 - optically thick, 363
 - paradigm, 6, 550
 - Shakura–Sunyaev model, 54, 296, 361, 371, 398, 404, 406, 407, 416
 - structure, 122, 129, 138, 179, 182, 239, 349, 360, 363, 404
 - temperature, 296, 325
 - theory, 364, 369, 406
 - thermal emission, 30, 124, 370
 - wind, 128, 129, 226, 229, 239, 257, 364, 416, 447, 555
 - X-ray illumination, 161
- Accretion rate, 8, 60, 99, 100, 108, 134, 146, 149–151, 153, 162, 167, 168, 185, 187, 240, 242, 243, 259, 269, 270, 306, 321, 324, 328, 351, 369, 373, 397, 399, 403, 406, 408, 446, 450, 483, 543, 552, 553
 - for massive stars, 456
 - super-Eddington, 322, 372, 405, 479
- Adaptive optics, 526, 528
- Advection dominated accretion flow (ADAF), 363, 372, 404, 406, 543
- Advection dominated inflow-outflow solution (ADIOS), 404, 406, 543
- AGNs
 - first use of term, 28, 57
 - total number, 537
 - type-1, 100, 110, 165, 166, 179, 192, 231, 233, 236, 357, 361, 417, 447, 469, 491, 539, 552
 - type-1 and type-2, 112, 161, 162, 164, 222, 230, 236–240, 441, 443, 446, 557
 - type-2, 60, 230, 446
- α_{ox} parameter, 124, 129, 243
- AM 2230-284, 65
- Ambartsumian, Viktor, 28, 45
- Anglo-Australian observatory (AAO), 24, 40
- Angular momentum, 395, 400, 412, 554
 - of accreting gas, 393, 394
 - conservation, 356, 472
 - in a wind, 380
 - excess, 404
 - extraction, 400
 - of gas in a galaxy disk, 557
 - loss, 399, 407, 452, 453, 455, 471, 475
 - by a companion black hole, 138
 - problem in AGNs, 449
 - transfer to radio jet, 138
 - transport, 16, 362, 380, 393, 398, 407, 408
- Anisotropic emission, 350, 383, 410
- Annihilation, 383

- Antonucci, Robert, 34, 100
 APM 08279+5255, 501
 Ariel V observatory, 41, 43, 44
 Arp 102B, 47, 256, 366
 Arp 151, 535
 Arp 220, 252, 457
 Arp 227, 62
 Arp Atlas, 62
 Atacama large millimeter array (ALMA), 238,
 500, 525–527, 540, 542, 543, 557
- Baade, Walter, 1, 147
 Back hole
 mass, 304
 Baldwin effect, 40, 125, 126, 503, 504
 X-ray, 168
 Baldwin, Jack, 29
 Balmer continuum, 346
 Balmer decrement, 17, 19, 37, 222, 344, 350
 Balmer lines, 3, 99, 100, 127, 128, 247, 255,
 256, 291, 341, 344, 358, 360, 410,
 531
 optical depth, 350, 358
 profile, 257, 342, 364, 366, 367
 BALnicity index, 223
 Bar instability, 400, 401
 Barred galaxies, 450
 molecular distribution, 450
 Bars, nested, 403
 Baryonic acoustic oscillation (BAO), 567
 Begelman, Mitch, 418
 Big blue bump, 17, 151, 371, 372, 477, 554
 BL Lacertae objects, 33, 42, 49, 60, 97, 118,
 120, 122, 123, 132, 151, 184–189,
 219–221, 312, 373, 383, 384, 477,
 554
 Black body, 55, 266, 344, 368, 371, 376
 disk emission, 324
 Black hole, 254, 552, 554, 558, 560, 563, 564
 binary, 138, 255, 256, 342, 366, 367, 555,
 560
 ergosphere, 391
 extinguished, 552
 event horizon, 51, 158, 391, 409, 522, 541,
 558
 imaging, 531
 fundamental plane of BH activity, 267–270,
 272, 553
 gravitational field, 354
 growth, 77, 243, 524, 526, 531
 in XRBs, 269
 Kerr, 169, 391–393, 409
 magneto-sphere, 392, 396
 mass, 8, 16, 23, 31, 33, 52, 100, 133, 149,
 187, 241–243, 245, 263, 268, 270,
 271, 288, 297, 299, 307, 312, 363,
 523, 534, 553, 554, 556
 density, 53
 as a function of z , 565
 limit, 413, 482
 in non-active galaxies, 300
 range, 219, 243
 turnover, 566
 uncertainty, 315, 535
 virial, 303, 304, 316, 320
 in XRBs, 270
 $M_{\text{BH}} - M_{\text{bulge}}$ correlation, 34, 52, 113, 258,
 308, 311, 312, 469, 523, 524, 556,
 557
 in NLSy1s, 244
 $M_{\text{BH}} - \sigma_*$ relation, 307, 309, 313, 462,
 469, 535
 merging, 255, 256, 393, 479
 potential well, 169
 as power source, 54, 58, 77, 550, 558
 primordial seed, 478, 564
 Schwarzschild, 181, 183, 391
 sphere of influence, 309, 450, 469, 479,
 542, 543
 spin, 77, 108, 147, 153, 158, 169, 182,
 322, 390, 391, 394, 409, 418, 479,
 553–555, 560
 as driver of radio loudness, 149
 stellar mass, 553, 558
 supermassive, 6, 9, 58, 121, 134, 141, 149,
 150, 155, 161, 180, 301, 338, 397,
 403, 405, 414, 419, 449, 464, 468,
 479, 523, 556, 558
 in XRBs, 266
 black hole
 mass, 27
 Blandford, Roger, 33, 394
 Blandford–Znajek mechanism, 391, 543, 554
 Blazars, 121, 123, 151, 174, 184, 186, 187,
 220, 221, 312, 373, 383, 477
 Blueshift, systemic of quasars, 77
 Blurred reflection, 169, 171, 172
 Bolometric correction, 124, 320
 Bolometric luminosity, 155, 491
 Braccisi, Alessandro, 23
 Bremsstrahlung, 95, 175
 Bridgman, Percy, 63
 Brightness temperature, 132, 140, 185, 306
 Broad absorption line (BAL), 224, 227–229,
 250, 251, 253, 254, 257, 375, 376,
 379, 543
 blueshift, 224, 375

- FeLoBAL, 228, 230
- ghost of Ly α , 229
- HiBAL, 225, 226
- incidence, 226
- line locking, 376
- LoBAL, 225, 226, 249, 253
- mini, 224
- polarization, 227
- profile, 223, 225, 227, 228, 234, 251, 252, 360
- relation to emission lines, 228
- X-ray, 375
- Broad absorption line (BAL) QSOs, 224–230, 234, 241, 243–247, 249, 251–253, 255, 296, 375–377, 456, 502, 557
- Broad line region (BLR), 15, 30, 33, 95, 98, 100, 127, 151, 167, 222, 239, 289, 363, 534, 536, 555, 558
 - absence, 239
 - clouds, 30, 33, 297, 355–357, 555
 - motion, 356
 - column density, 167, 352, 355–358
 - density, 17, 55, 96, 349
 - difference between population A and B, 563
 - formation, 136, 238
 - geometry, 33, 303, 363
 - geometry and kinematics, 535
 - hidden, 100, 551
 - high ionization, 32, 99
 - inclination, 533
 - ionization stratification, 292, 536
 - kinematics, 32, 239, 292, 297, 523, 534–536, 550, 559
 - light travel time, 533
 - low ionization, 99
 - models, 350, 352, 364
 - obscuration, 221, 238, 240
 - Osterbrock’s turbulent disk model, 34, 99, 341
 - outflow, 34, 99, 534, 557
 - physical conditions, 96
 - produced by supernova remnants, 246
 - radius, 96, 290, 354, 536, 558
 - radius–luminosity relation, 292, 297, 299, 531, 536
 - refractory element depletions, 290
 - size, 55, 239, 291, 307, 353, 523, 532, 534–536
 - structure, 33, 111–113, 157, 293, 325, 341, 342, 352, 363, 531, 533–536, 550, 559, 560
 - velocity dispersion, 239
 - velocity field, 290, 534
 - X-ray absorption, 157, 166
- Brown, Hanbury, 73
- Bulge, 25, 474, 556
 - escape velocity, 354
 - of host galaxies of quasars, 556
 - luminosity, 301, 311
 - mass, 304, 307, 399, 400, 445, 474
 - of the Milky Way, 400
 - pseudo-bulge, 400
 - structure, 399, 400
 - velocity dispersion, 399
- Bulk velocity, 164
- Burbidge, Geoffrey, 2, 74
- Burbidge, Margaret, 2
- Burst alert telescope (BAT), 160
- 3C 48, 2, 4, 45, 63, 120
- 3C 66, 121
- 3C 66A, 189, 221
- 3C 120, 48, 188
- 3C 175, 136
- 3C 273, 2–4, 21, 35–37, 41, 45, 61, 63, 74, 75, 105, 111, 184, 221, 523
- 3C 274, 62
- 3C 275, 62
- 3C 279, 184
- 3C 293, 461
- 3C 305, 460
- 3C 332, 256
- 3C 343.1, 64, 70
- 3C 345, 22, 221
- 3C 390.3, 47, 256, 366, 532
- 3C 454.3, 138, 220, 221
- 5C 3.100, 241, 245
- C IV, 129, 144, 302
- Ceccarelli, Maurizio, 23
- Centaurus A, 2, 20, 41, 132, 139, 186, 462
- Central compact massive object, 558
- Charge-coupled device (CCD), 4, 35, 119, 487, 529, 530, 563, 566
- Chemical abundances, 95, 177, 288, 328, 350, 558, 563
- Chemical enrichment, 290, 362, 487, 498, 500, 501
- Circinus galaxy, 164
- Clustering
 - of quasars, 496, 497
 - at high redshift, 497
- Clusters of galaxies, 2
 - catalogs
 - Abell, 2, 43
 - Zwicky, 2
- Cohen, Ross, 32

- Cold dark matter, 57, 472
 Collisional excitation, 37, 95, 96, 344
 Color, 121, 525
 of AGNs, 222, 538
 IR, 485, 525, 540
 of Mrk 231 and HyNæ, 247
 of quasar candidates, 101
 of quasars, 102–104, 115, 122
 of stars, 36, 107
 sub-mm, 485
 Color-color diagram, 262
 IR, 249
 Color-magnitude diagram, 61
 Column density, 113, 156, 223, 224, 347–349,
 351, 352, 355, 501
 Comoving volume, 53
 Compact groups, 261
 Compton hump, 158
 Compton reflection, 158, 162
 Compton scattering, 121, 123, 154, 161, 175,
 183, 370, 396
 Compton thickness, 161, 171, 179, 259, 262
 Continuity equation, 56
 Continuum, 291, 353, 487, 550, 553
 IR, 411
 non-thermal, 30, 54, 64, 555
 polarization, 226, 227
 thermal, 555
 UV excess, 4, 19, 54, 63
 variability, 32, 370, 532, 552
 Convection-dominated accretion flows
 (CDAF), 404, 406, 543
 Corona, 150, 154–156, 161, 170, 180, 243, 370
 solar, 36
 Corotation, 381
 Correlation function, 291, 496, 497, 503
 Cosmic age, 566
 Cosmic microwave background (CMB), 18, 55
 Cosmic rays, 189, 253
 Cosmology
 Λ CDM, 6, 526
 big bang, 9, 55, 72, 114, 479, 501
 steady state, 2, 73
 Coulomb interaction, 229
 Covering factor
 in BAL QSOs, 223, 224, 226, 228
 of the BLR, 167, 341, 342, 350, 358
 of obscuring material, 240
 of obscuring torus, 60, 191, 230
 of X-ray absorber, 172
 of X-ray emitting gas, 168
 Crab Nebula, 22
 Crimean Astrophysical Observatory, 7, 46, 120
 Cherenkov γ -telescope, 188
 Critical density, 111
 Crossley telescope, 36
 Cygnus A, 2, 13, 147
 Cyosmic downsizing, 491

 Dark age, 500
 Dark energy, 56
 Dark matter, 56, 118, 253, 254, 308, 315, 354,
 399, 401, 474, 493, 496, 497
 Decadal review 2010, 179, 529
 Demography of quasars, 57
 Density evolution, 481
 Density perturbation, 472
 Diagnostic diagrams, 258, 259
 of BPT, 237, 258, 445
 Dibai, Ernst, 34
 Disk-jet coupling, 153
 Disk-wind model, 32, 99
 Distance, 269, 565
 angular, 524
 comoving radial, 6, 7
 of quasars
 independent of redshift, 567
 Distance indicator, 4
 Distance scale, 61
 Doppler boosting, 158
 Doppler effect, 72, 78, 181, 229, 301,
 375
 Doppler redshift, 61
 Double-peaked profiles, 105, 219, 255–257,
 364, 366, 404
 Dust, 190–192, 222, 226, 230–233, 235, 240,
 252, 264, 265, 354, 364, 417, 418,
 486, 527
 absorption edges, 165
 circumnuclear, 34, 191, 235, 237
 cocoon, 484
 emission, 191, 226, 530
 grains, 190, 222, 354, 411, 414
 opacity, 355
 reddening, 37
 Dust/gas content, 100
 Duty cycle, 219, 473, 481, 483, 494
 Dynamo engine, 385

 Eddington limit, 171, 244, 245, 303, 305, 319,
 321, 323, 378, 405, 417, 479, 504,
 554
 Eddington luminosity, 59, 60, 269, 311,
 319–321, 405, 483
 Eddington ratio, 33, 100, 113, 143, 145, 240,
 243, 244, 262, 263, 288, 319–326,

- 328, 363, 371, 398, 417, 473, 554,
 558, 563, 567
- Eigenvector 1, 106, 112, 113, 126, 130, 242,
 244, 245, 345, 351, 560
- 4D, 107, 109, 147, 325, 552
- Eigenvector 2, 106, 242
- Einstein radius, 295
- Einstein, Albert, 391
- Einstein-de Sitter Universe, 79
- Electron density, 47, 96, 245, 289, 339
 in radio jets, 140
- Electron scattering, 17, 54, 158, 238, 321, 322,
 371, 417
- Electron temperature, 289
- Elliptical galaxies, 307, 466, 501
- Emission lines, 2, 54, 94, 97, 98, 218, 220,
 228, 260, 293, 344, 559
- blueshift, 32, 33, 99, 227, 228
- broad, 3, 19, 34, 40, 45, 55, 57, 128, 182,
 259, 535
- Ca II, 97
- coronal, 15, 36, 37, 191
- C IV, 32, 125, 129, 144, 292, 302, 316–318,
 328, 356, 357, 404, 416, 448, 449,
 504, 532
- blueshift, 129–131, 144, 375, 448
- Doppler broadening, 469
- Fe II, 30, 37, 96, 97, 100, 246, 247, 296,
 328, 340, 344, 345, 348, 350, 351,
 364, 448, 500, 502
- Fe K α , 52, 93, 157, 162, 167, 168, 179,
 262, 501, 531, 552, 555, 560
- in GK Per, 173
- line profile, 169, 171, 178, 179, 181
- forbidden, 5, 15, 37, 95–97, 111, 127, 167,
 236, 241, 289, 339, 346, 349
- H α , 48, 357, 359
- H β , 48, 294, 298, 316–318, 328, 339, 350,
 357, 358, 448, 502, 555, 560, 561,
 565, 566
- high ionization, 259
- blueshift, 34, 40, 99, 128
- internal shifts, 127, 128
- IR, 232
- Ly α , 93, 96, 228, 229, 252, 292, 367, 376,
 565
- Ly α /H α problem, 339
- Ly α forest, 487, 503, 565, 567
- Mg II, 292, 317, 565, 566
- multiple components, 251
- narrow, 111, 245
- O III, 48, 237, 247, 314
- permitted, 4, 15, 339
- profile, 52, 98–100, 123, 187, 228, 256,
 257, 356, 358, 534, 535
- variability, 361, 535
- single peaked, 257
- Environment, 69, 260–262, 550, 551
- of AGNs, 153, 261, 268, 441
- of galaxies, 6
- of LINERs, 261
- of quasars, 441, 462, 527
- of Seyfert galaxies, 441, 442
- Equation of state, 77, 409
- Equivalent width, 15, 54, 96, 125, 127, 129,
 167, 168, 228, 262, 325, 341, 347,
 502, 504, 505
- Euclidean universe, 139
- European extremely large telescope (EELT),
 525, 540, 542
- European large area ISO survey (ELAIS), 230
- European southern observatory (ESO), 40,
 225, 253, 403, 525, 566
- EVLA, 142, 238, 306
- Evolution, 248
- of AGNs, 219, 248, 260
- of BAL QSOs, 226
- of galaxies, 6, 25, 523, 540, 543, 557
- of the host galaxy, 250
- of massive stars, 248
- of quasars, 17, 27, 55, 247, 249, 251, 253,
 525, 551, 554, 563, 566
- in density, 57, 475, 476, 489, 490
- in luminosity, 57, 476, 481, 491
- of quasars and their host galaxies, 556
- spectral, 168
- of ULIRGs, 249
- Explosive model, 246, 248, 254
- Extreme X-ray-to-optical objects, 524
- Emission lines
- broad, 93
- Fanaroff–Riley, 383, 387
- Fanaroff–Riley I, 134–137, 139, 143–145, 554,
 559
- Bondi accretion, 138
- Fanaroff–Riley II, 134, 136, 138, 554
- Fe II, 296
- Feedback, 167, 227, 231, 308, 309, 338, 405,
 447, 452, 456, 459, 461–464, 468,
 473, 475, 476, 494, 543, 550, 556,
 557
- Lyman-Werner, 495
- Filling factor, 377
- Fine structure constant, 526, 567

- First Texas Symposium on Relativistic
 Astrophysics, 76
 Fluorescence, 51, 96, 158, 167, 180, 346, 348,
 350
 Formation
 of bars, 401
 of cold molecular gas, 403
 of cosmic structures, 57
 of galaxies, 25, 57, 260, 523, 527, 543, 557
 of host halos, 472
 of quasars, 251
 Fourier analysis, 122
 Fowler, William A., 27
 Friedmann-Robertson-Walker models, 55
 Fueling, 59, 397, 400, 401, 441, 450, 474, 542,
 543

 Galactic bubbles, 251
 Galactic superwind, 461
 Galactic wind, 166, 234, 246, 247, 252
 Galaxy zoo project, 261
 γ -ray, 154, 184, 390, 559
 astronomy in Soviet Union, 189
 Doppler boosting, 185
 emission mechanisms, 186, 373
 from NLSy1s, 187, 188
 variability, 383
 γ -ray bursts, 253, 530
 Giacconi, Riccardo, 154, 477
 Giant Magellan Telescope, 540
 Giant Segmented Mirror Telescope, 542
 Gravitational collapse, 27, 74, 76, 235, 248,
 254, 362
 Gravitational force, 74, 182, 567
 Gravitational lensing, 295, 503
 with quasar as lens, 40
 Gravitational radius, 361, 365, 396
 Gravitational redshift, 52, 77, 158
 of Fe K α line, 158, 181
 Greenstein, Jesse, 2
 Gunn-Peterson effect, 487, 499

 1H 0419-577, 162
 H 1722+11, 221
 H₂O megamasers, 558
 Halo collapse, 472
 Hawking radiation, 374
 H β , 298
 Hertzsprung–Russell diagram, 107, 559
 for quasars, 107, 328, 550, 558
 Hierarchical merging, 468, 472

 Host galaxies
 of AGNs, 5, 34, 60, 240, 260, 416, 442,
 449, 452, 453, 464, 465
 of BL Lacs, 219, 220, 313
 CO rotation curve, 310
 contribution to nuclear spectrum, 116, 239,
 309, 312, 317
 of LINERs, 260, 261, 263, 265
 of NLSy1s, 314
 of quasars, 52, 132, 146, 289, 313, 375,
 400, 450, 451, 454, 462, 464, 466,
 469, 485, 494, 496, 527, 550, 554,
 556
 alignment with accretion disk, 418
 CO gas content, 316
 HST observations, 454
 imaging, 524
 mass, 253
 stellar mass growth, 483
 velocity dispersion, 526
 of radio loud AGNs, 133
 of radio-loud quasars, 554
 of Seyferts, 33
 Hot spot, 134, 387
 accretion disk, 535
 Hoyle, Fred, 2, 34, 73
 Hoyle-Narlikar theory of gravity, 79
 Hubble constant, 6, 7, 13, 61, 79, 503, 505
 Hubble deep field (HDF), 566
 Hubble distance, 75
 Hubble law, 4, 79
 Hubble space telescope (HST), 165, 239, 251,
 262–265, 300, 307, 310, 376, 454,
 465, 468, 523, 527, 552, 559
 Hubble time, 484
 Hubble, Edwin, 94
 Hydra A, 461
 Hypernovae, 246–248, 250, 252–254

 I-band dropout technique, 494
 IC 1767, 65
 IC 342, 403
 IC 5063, 460
 Image dissector scanner (IDS), 24, 29, 39
 Image reduction and analysis facility (IRAF),
 98
 Infall, 108, 557, 558
 of matter toward the central black hole, 542
 velocity of clouds, 293
 Inflow, 456, 543
 in AGNs, 449, 450
 Innermost stable circular orbit (ISCO), 169,
 369, 406, 408, 409

- Integral field spectroscopy, 451, 457, 459
 Interstellar medium (ISM), 22, 36, 112, 235, 290, 366, 416, 447, 459, 556
 Ionization cones, 236, 264, 411
 Ionization parameter, 55, 95, 96, 113, 166, 175, 176, 293, 339, 348–351, 502
 Ionization potential, 346
 IR observations, 190
 IRAS 01003-2238, 251
 IRAS 04505–2958, 250
 IRAS 04505-2958, 246, 247, 253
 IRAS 0759+6559, 252
 IRAS 07598+6508, 247, 249
 IRAS 09104+4109, 233
 IRAS 14026+4341, 250
 IRAS 18325-5926, 169
 IRAS 21219-1757, 250
 IRAS 22419+6049, 251
 I Zw 1, 30, 153, 245, 247, 346, 347, 502

 J1536+0441, 256
 James Webb space telescope (JWST), 470, 494, 500, 524, 525, 527, 540, 543

 K correction, 561
 Keplerian orbits, 366
 Keplerian kinematics, 52, 257, 364, 365, 371, 534, 558
 Keplerian orbits, 292, 299, 393
 Keplerian rotation, 181
 Keplerian velocity, 355, 363, 364
 Klein-Nishina limit, 158
 Kormendy, John, 34
 Kraft, Robert, 39

 Large synoptic survey telescope (LSST), 523, 525, 526, 529, 537, 538
 Lick Observatory, 24, 25, 27, 28, 30, 32, 35–40, 126
 AGN monitoring project (LAMP), 291, 534
 Light curves, 116, 119
 Light cylinder, 396
 Lindblad resonance, 458
 Locally optimally emitting cloud model, 96, 349
 Lookback time, 6
 Lorentz distribution, 185, 270, 271, 389
 line profiles, 555
 Lorentz factor, 381, 383, 388, 396
 Lorentz force, 374, 385
 Low frequency Array (LOFAR), 142

 Low-ionization nuclear emitting regions (LINERs), 60, 150, 219, 256, 258–265, 269, 306, 441, 483, 553
 as AGNs, 258, 262
 radio, 259, 264
 type-1, 259, 264
 X-ray, 259, 262, 265
 morphology, 262
 Luminosity function, 19, 56, 104, 143, 311, 383, 468, 475, 480, 481, 490–492, 494, 495, 500, 525, 561, 562
 Ly α halos, 252, 459
 Ly α /H α problem, 339
 Lynden-Bell, Donald, 16

 M 31, 15, 27, 362, 474
 M 32, 474
 M 33, 51
 M 81, 153, 266
 M 82, 51, 191, 272
 M 83, 452
 M 87, 1, 2, 4, 5, 62, 139, 142, 147, 300, 389, 473, 552
 radio jet, 68
 M 100, 403
 Mach angle, 387
 Magnetic field, 13, 20, 22, 45, 140, 148, 221, 352, 372, 375, 377, 380, 381, 383, 385, 386, 388, 390, 472, 543
 Magnetic pressure, 374
 Magnetic reconnection, 543
 Magneto-hydrodynamics (MHD), 370, 398, 409, 553
 Major atmospheric gamma-ray imaging Cherenkov (MAGIC), 184, 188, 189
 Malmquist bias, 8
 Markarian, Benjamin, 45
 Markarian galaxies, 48
 Masers, 404, 459
 Mass-luminosity plane of quasars, 504
 Massive compact halo object (MACHO), 115
 Matthews, Thomas, 75
 Maxwell-Boltzmann distribution, 374
 MCG 8–11-11, 44
 MCG-06-30-15, 168, 169, 171, 182–184, 552
 Merger, 137, 249, 253, 306, 448, 477, 482, 493
 rate, 497
 velocity field, 252
 Micro-quasars, 150
 Micro-variability, 8, 113, 120–122
 Microlensing, 117, 118, 220, 228, 295, 296, 503

- Milky Way, 2, 20, 21, 27, 75, 94, 219, 301, 349, 366, 375, 413
- Miller, Joe, 29, 39, 100
- Mini-quasars, 45
- Minkowski
metric, 79
- Minkowski, Rudolf, 1, 17, 147
- Moore's law, 566
- Mrk 3, 164
- Mrk 6, 47, 48
- Mrk 42, 241
- Mrk 79, 119
- Mrk 110, 535
- Mrk 231, 247, 251
- Mrk 273, 454
- Mrk 279, 291
- Mrk 359, 241
- Mrk 421, 189, 221
- Mrk 478, 241
- Mrk 493, 250
- Mrk 501, 184, 189, 221, 384
- Mrk 507, 245, 250
- Mrk 704, 176
- Mrk 766, 168, 179
- Mrk 841, 168
- Mrk 957, 250
- MR 2251-178, 173
- Mueller, Fred, 35
- Multi element radio linked interferometry (MERLIN), 555
- Naked quasars, 58, 471
- Narrow absorption lines (NALs), 224, 375, 462
- Narrow line region (NLR), 15, 34, 96, 98, 165, 166, 222, 240, 245–247, 258, 265, 289, 353, 354, 357, 417, 557
- interaction with radio jet, 148
- physical conditions, 96
- produced by supernova remnants, 246
- reddening, 222
- refractory element depletions, 290
- Narrow Line Seyfert 1s (NLSy1s), 99, 162, 187, 188, 240, 241, 243–248, 251, 292, 314, 323–325, 356, 554, 555
- connection to high-*z* quasars, 240, 244
- in eigenvector 1, 242, 244, 323
- metallicity, 351
- prevalence, 242
- radio-loud, 245
- relativistic jets, 187
- X-ray, 124, 159, 160, 162, 240, 242, 244, 371
- NASA Astrophysics Data System (ADS), 29
- Neutron star, 22, 188, 254, 271, 392, 558
- NGC 315, 137
- NGC 526a, 44
- NGC 1068, 13–15, 94, 100, 164, 191, 222, 289, 410, 458, 523
- NGC 1097, 367, 451
- NGC 1275, 48, 49
- NGC 1365, 417
- NGC 1566, 403
- NGC 2273, 403
- NGC 2639, 66, 70
- NGC 2992, 454
- NGC 3227, 48
- NGC 3516, 32, 67, 168
- NGC 3615, 16
- NGC 3628, 66
- NGC 3783, 44, 164, 532
- NGC 4051, 119
- NGC 4102, 263
- NGC 4151, 5, 32, 41, 46–49, 94, 132, 291, 551
- NGC 4258, 404
- NGC 4395, 532
- NGC 4450, 239
- NGC 4472, 62
- NGC 4649, 473
- NGC 5128, 77
- NGC 5408, 272
- NGC 5514, 251
- NGC 5548, 31, 46, 48, 49, 115, 121, 291, 349, 361, 375, 532
- NGC 5985, 67
- NGC 6251, 13, 14, 184
- NGC 6946, 403
- NGC 6951, 451
- NGC 7027, 94, 289
- NGC 7052, 474
- NGC 7468, 49
- NGC 7469, 46, 48, 252, 532
- NGC 7582, 44, 452
- NGC 7603, 80
- Obscuring torus, 6, 59, 221, 236, 237, 338, 410, 411, 456, 536
- absence in low-luminosity radio galaxies, 135
- distance from black hole, 536
- IR observational evidence, 190
- size–luminosity relation, 536
- vertical thickness, 410
- X-ray absorption, 156
- OJ 287, 120, 121, 188, 221
- Oke, Bev, 36
- ON 231, 221

- Oppenheimer, J. Robert, 76
 Optical depth, 17, 30, 96, 155, 161, 325, 340, 344, 348
 Optically violently variable (OVV) quasars, 184, 219, 220
 OQ 172, 40
 Orientation, 105, 144, 160, 167, 218, 222, 226, 227, 234, 236, 245, 318, 341, 350, 444, 447, 551, 558, 560
 effect on quasar spectra, 112, 236, 326, 328
 of host galaxies, 222, 443
 of radio jet, 33, 220
 Osterbrock, Donald E., 17, 25, 30, 34, 55, 126, 222, 237, 341
 Outflow, 31, 33, 34, 99, 108, 111, 164, 177, 224, 225, 227, 228, 230, 245, 246, 251–253, 265, 375, 456, 534, 543, 551, 556, 557
 biconical, 255, 367
 in BLR, 128, 555
 collimated, 148, 151, 386, 556
 driven by radiation pressure, 229
 early observation, 30
 mass rate, 167
 models, 377
 molecular, 556, 557
 in NLSy1s, 245
 non-relativistic, 464
 of HI, 460
 radio, 2
 relativistic, 551
 reprocessing, 162
 in stars, 348
 in sub-mm and radio-loud quasars, 253
 velocity, 70, 163, 224, 376, 387

 PAH emission features, 145, 524
 Pair production, 185, 390
 Palomar observatory, 43
 Panoramic survey telescope & rapid response system (Pan-STARRS), 529, 538
 Particle acceleration, 20, 22, 63
 P Cygni line profile, 167, 227
 PDS 456, 162
 Peebles, Philip J.E., 57
 Penrose process, 391
 Penrose, Roger, 391
 PG 1115+80, 375
 PG 1211+143, 167
 PG 1427+480, 111
 PG 1535+547, 251
 PG 1553+11, 221
 PG 1700+518, 111, 247, 253

 PG 17072+5153, 250
 Phillips, Mark M., 30
 PHL 1092, 345
 PHL 5200, 30, 456
 Photoionization, 17, 248, 259, 265, 339, 344, 347, 378, 555
 code
 Cloudy, 176, 340, 344, 346, 349
 Titan, 344
 ION, 344
 XSTAR, 344
 equilibrium, 95, 499
 models, 95, 96, 237, 289, 339, 340, 344, 346–348, 350, 351, 353, 360, 502
 Photoionization method, 31, 34, 293, 294
 Photometric observations, 49, 118, 120
 Photon density, 383
 PKS 0735+178, 221
 PKS 0921-021, 366
 PKS 2155–304, 184
 PKS 2251+11, 24
 Planetary nebulae, 94
 Plasmoids, 61
 PMN J0948+0022, 187, 245
 Point spread function (PSF), 465, 466, 469
 Population A, 130, 324, 328, 552, 555, 560, 563
 Population B, 131, 144, 147, 324, 326, 328, 552, 555, 560, 563
 Population III stars, 479, 495
 Post-AGB stars, 259
 Principal component analysis (PCA), 106, 107, 241, 325
 Pulsars, 18

 Q1548+115, 40
 Quasar-galaxy connection, 62, 71, 80
 Quasars
 catalogues, 537
 ejection, 72
 light density, 53
 local hypothesis, 20
 obscured, 223, 232
 rest frame, 99
 type-1, 191, 192, 219, 222, 223, 231, 240, 255, 325, 486
 type-1 and type-2, 230, 410, 485
 type-2, 192, 230–233, 447, 484

 Radiation pressure, 130, 355, 374
 Radiation transfer, 255, 350, 456
 Radiative cooling, 463

- Radio core, 141
- Radio-FIR correlation, 145, 553
- Radio galaxy, 62, 64, 151, 219
 - definition, 28
- Radio interferometry, 41, 93
- Radio-intermediate quasars, 146
- Radio isophotes, 64, 71
- Radio jet, 33, 48, 111, 131, 132, 139, 149, 150, 160, 226, 259, 267, 417, 418, 460, 550, 553, 554, 556, 563
 - cocoon, 459
 - collimation, 388
 - formation, 140, 153, 395
 - induced star formation, 462
 - interaction with the ISM, 134, 460, 462
 - relativistic, 148, 338, 393
 - in XRBs, 266
- Radio-loud AGNs, 6, 8, 112, 113, 131, 222, 256, 318, 365, 383, 390, 391, 395
 - fraction, 104
- Radio-loud/radio-quiet dichotomy, 144, 146, 147, 151, 550, 553, 559
- Radio-loud quasars, 130, 131, 143, 144, 147, 526, 554
- Radio morphology, 51, 132
- Radio sources
 - as colliding galaxies, 74
 - compact, 13, 18, 20, 51, 150, 259, 341
- Radio-quiet AGNs, 6, 112, 131, 148, 162, 395, 537, 539
- Radio-quiet quasars, 191
- Recombination, 95, 165, 174
- Reddening curve, 222
- Redshift, 2, 75, 77, 93, 564
 - cosmological, 75
 - intrinsic, 63, 70
 - non-cosmological, 20
 - quantization, 81
 - Karlsson, 65, 80
- Redshift-distance relation, 2
- Rees, Martin, 33, 341, 522
- Relativistic beaming, 33, 148
- Reverberation mapping, 32, 115, 117, 290, 291, 293, 295, 297, 299, 301, 302, 311, 316, 341, 352, 353, 357, 361, 366, 368, 474, 505, 522, 526, 531, 532, 534–536
 - 2D, 99, 299, 459, 533–536, 552
 - dust, 536
 - Fe K α , 536
 - imaging, 505
- Ring, 251
- Robinson, Lloyd, 29, 38
- Röntgensatellit (ROSAT), 262
 - all-sky survey (RASS), 159, 242
- Ryle, Martin, 44, 73
- S5 0836+71, 532
- Sagittarius A, 52, 153, 266, 372, 523
- Salpeter timescale, 321, 483
- Salpeter, Edwin E., 16
- Sandage, Allan, 5, 19, 75
- Scalar field, 76
- Schmidt, Maarten, 2, 4, 36, 523
- Science-ready data, 541
- SDSS J0946+0139, 343
- SDSS J1536+0441, 256
- Secular evolution, 455
- Seyfert galaxies, 4, 5, 14, 17, 19, 26, 27, 47–49, 57, 67, 97, 102, 117, 120, 132, 160, 163, 179, 256, 291, 304, 345, 375, 410, 411
 - analogy with planetary nebulae, 94
 - continuity with quasars, 5, 17
 - definition, 5
 - discovery as X-ray sources, 41, 44
 - morphology, 453, 454
 - radio emission, 33, 132
 - reddening, 222
 - type-1, 34, 171, 237, 445, 561
 - type-1 and type-2, 54, 97, 410, 444
 - type-2, 34, 412
- Seyfert, Carl, 1
- Shane telescope, 36, 37
- Shock front, 220, 387
- Shock heating, 348, 404
- Shock theory, 390
- Shocks, 157, 247, 248, 251, 253, 254, 264, 387, 553
 - in blazars, 221
 - in a disk atmosphere, 405
 - due to a companion black hole, 138
 - ionization via, 259
 - in NLR, 289
 - in supernova remnants, 246
- Sloan digital sky survey (SDSS), 101–103, 130, 306, 345, 371, 442, 479, 486, 487, 537, 559–562
- Soft X-ray excess, 156, 555
- Solar corona, 17
- Soltan argument, 155
- Sound speed, 358, 387, 412
- Space observatory
 - Ariel V, 416
 - ASCA, 93, 162, 182, 530
 - ASTRO-H, 529, 530
 - ASTROSAT, 529

- Chandra*, 93, 139, 157, 159, 160, 163, 164, 169, 171, 262, 375, 416, 484, 527, 528, 530, 537, 551, 552
- Compton γ -ray observatory, 530
- Constellation-X, 564
- EGRET, 189
- Einstein*, 242, 262
- energetic X-ray imaging survey telescope (EXIST), 530
- eROSITA, 529, 537, 566
- Euclid*, 539
- Fermi*, 139, 184, 186
- GEMS, 529
- GINGA, 180
- Gravitas*, 530
- Herschel*, 190, 473, 484, 485, 527, 556
- IRAS, 169, 190, 230, 232, 234, 442
- ISO, 190, 192
- IXO, 529
- MAXIM, 563
- NuSTAR, 529
- Radioastron, 139, 563
- ROSAT, 162
- SAS-3, 44
- Spitzer*, 145, 190, 192, 447, 484, 485, 551
- Suzaku, 162, 166, 170, 172, 182
- VSOP-2, 563
- XMM-Newton, 93, 139, 157, 163, 164, 169, 172, 176, 178, 182, 183, 234, 262, 328, 416, 527, 528, 552
- Spectral energy distribution (SED), 30, 31, 54, 100, 108, 114, 115, 118, 123–125, 129, 185, 220, 258, 264, 320, 349, 352, 353, 372
- ionizing, 127–129
- Spectropolarimetry, 25, 228, 411
- Spiral galaxies
- arms, 367, 368, 400–402, 450–452, 457
- Square kilometer array (SKA), 142, 151, 526, 539, 540, 542, 543, 563
- Standard candles, 96, 504
- Star formation, 132, 145, 150, 219, 245, 246, 251, 289, 308, 400, 403, 443, 447, 451, 455–457, 462–464, 468, 471–473, 477, 484, 485, 494, 498, 501, 524, 525, 556, 557
- in barred galaxies, 451
- circumnuclear, 245, 248
- induced by jet, 462
- nuclear, 446, 543
- quenching, 463, 495
- radio emission, 149
- rate (SFR), 259, 262, 453, 483, 551
- Starburst, 250
- Starburst galaxies, 252, 258, 441, 446, 447, 450, 458
- Stellar mass loss, 399
- Sternberg astronomical institute (SAI), 32, 46
- Steward observatory, 4
- meeting on Seyfert galaxies in 1968, 16
- Strömgren length, 33
- Strömgren sphere, 95
- Structure function, 49, 117
- Superluminal motion, 139, 148, 220, 381–384, 415, 522
- Supernovae, 2, 16, 22, 36, 74, 100, 117, 126, 132, 290, 348, 362, 479
- Supernova remnants, 246
- Supersonic flow, 388
- Supersonic jets, 387
- Suprathermal electrons, 16
- Surface brightness, 52, 62, 65, 134, 145, 238, 350, 406, 465
- Surface density, 400, 537, 566
- Survey, 160, 559, 561, 562, 565, 566
- BAT, 160
- bright quasar survey (BQS), 104
- 3C, 3, 145
- Canadian-French High-z Quasar Survey (CFHQS), 487
- CDFN, 159
- CDFS, 159, 539
- Chandra*, 530, 539
- color based, 102, 486, 491
- 2dF, 486, 537
- FIRST, 143, 526
- forthcoming, 522, 537
- Euclid*, 539
- radio, 539
- SKA, 539
- WISE, 538
- at high z , 252
- of high- z quasars, 527
- IR, 190, 230, 523
- optical, 529, 538
- Palomar-Green, 101, 102, 241
- Palomar spectroscopic survey (PSS), 259, 260
- of quasars, 150, 486
- radio, 40, 264, 539, 540
- RASS, 159, 240
- two microns sky survey (2MASS), 145, 263
- UKIDSS, 529
- University of Michigan Curtis Schmidt, 101
- UV excess, 101
- X-ray, 159, 160, 167, 234, 528–530, 537, 539

- Seyfert galaxies
 continuity with quasars, 12
- Synchrotron radiation, 13, 30, 54, 62, 72, 74, 77, 124, 132, 154, 185, 191, 220, 269, 372, 383, 390, 522, 551, 554
- Synchrotron self-Compton (SSC), 73, 373, 383, 554
- Sydney survey
 UKIDSS, 487
- Thermalization, 96, 289, 374, 414
- Thirty meter telescope, 540
- Thomson scattering, 129, 369
- Tidal tails, 251
- Timescale, 246, 265, 538, 563
 of black hole activity, 270
 of blazar variability, 221
 of variation in high-luminosity quasars, 532
- Tonantzintla observatory, 121
- Trimble, Virginia, 6
- Turbulence, 108, 348, 365
- Uhuru, 41, 43, 45, 528
- Ultra-luminous IR galaxies (ULIRGs), 226, 232–234, 245, 246, 248, 447, 448, 453, 484, 524, 551
 relation to QSOs, 248
- Unidentified high galactic latitude sources (UHGLS), 43
- Unification, 8, 17, 59, 60, 161, 186, 191, 192, 218, 230–232, 235–237, 443, 551
- Variability, 46, 47, 49, 54, 117, 188, 219, 221, 251, 265, 272, 525, 530, 532, 538
 inter-night, 50
 intra-day, 120
 intra-night, 50
 long term, 22, 121
 optical photometric, 114, 119
 radio, 138
 timescale, 13, 16, 18, 114, 162
- Variable mass hypothesis, 80
- Velocity dispersion, 472
 of the broad line gas, 318
 of galaxies, 475
 in the NLR, 47
 stellar, 53, 97, 111, 301, 304, 305, 307, 309, 313, 314, 400, 462, 464, 465, 474, 524
- Very large array (VLA), 143, 526, 539, 555
- Very large telescope (VLT), 253, 371, 452, 528, 551, 560
- Very long baseline interferometry (VLBI), 51, 139–141, 264, 389, 563
- Virgo cluster, 61, 540
- Virial equilibrium, 355
- Virial temperature, 31
- Virial theorem, 296, 297, 316
- Virtual observatory (VO), 537, 541
- Viscosity
 friction, 407
 molecular, 398
 turbulence, 16, 393, 395, 398
- Visible and infrared survey telescope for astronomy (VISTA), 488, 525, 529
- Wampler, Joe, 24, 25, 29, 35, 55, 125, 222
- Warm absorber, 154, 157, 166, 173–175, 177, 178, 364, 416, 417, 528, 557
- Weinberg, Steven, 55
- Westinghouse SEC vidicon, 38
- White dwarfs, 558
- White hole, 53
- Whitford, Albert, 36
- Wide-field IR survey explorer (WISE), 538
- Wide field X-ray telescope (WFXT), 530
- Wien's law, 296
- Wind, 31, 99, 129, 226–230, 246, 252, 264, 378, 379, 416, 417, 556
- Wolf-Rayet stars, 100, 251
- Woltjer, Lodewijk, 6
- WPVS 007, 243
- X-ray, 44, 60, 69, 72, 95, 119, 124, 143, 164, 167, 169, 173, 262, 268, 269, 417, 528, 553
 absorption, 162, 234, 352, 379
 absorption lines, 162, 164, 166, 169, 170, 179
 astronomy, 41, 529
 background, 21, 44, 60, 154, 159, 230, 237, 477, 551
 blurred reflection, 169, 171, 179
 burst, 189
 cavities, 460
 cold absorber, 156
 continuum, 129, 151, 161, 168, 170, 223, 349, 419, 536
 correlation with radio, 267, 268
 emission lines, 97, 164, 167, 168
 filament, 66
 hard, 160, 232, 242, 265, 552

- imaging, 528, 531
- instrumentation, 163, 528, 531
- interferometers, 563
- morphology, 265
- optics, 531
- partial covering, 171
- polarimetry, 529
- selected AGNs, 240
- soft, 242, 528
- spectra, 160, 163, 164, 168, 178, 179, 233, 234, 243
- spectral index, 262
- spectral hardness, 266
- spectral slope, 124, 242
- spectral variability, 171
- spectroscopy, 528, 552, 563
- telescopes, 41, 159, 163, 180, 238, 495, 525, 527, 528
 - forthcoming, 522, 529, 531, 538, 566
 - timing, 528
 - variability, 119, 155, 156, 160, 170, 263–265, 270, 271, 351, 352
- X-ray binaries (XRBs), 41, 150, 234, 259, 266, 270, 385
 - analogy with AGNs, 150, 266, 553
- X-ray Bright Optically Normal galaxies (XBONGs), 102
- X-ray galaxies, 43

- Yerkes observatory, 39

- Zasov, Anatoly, 34
- Zel'dovich, Yakov Borisovich, 16